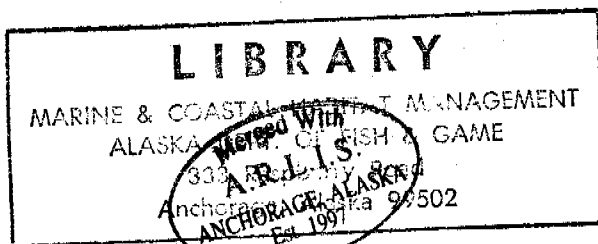


Environmental Assessment of the Alaskan Continental Shelf

Annual Reports of Principal Investigators
for the year ending March 1978

Volume XI. Hazards



U.S. DEPARTMENT OF COMMERCE
National Oceanic and Atmospheric Administration



U.S. DEPARTMENT OF THE INTERIOR
Bureau of Land Management

DATE DUE

NOV 2 1974			

Demco No. 62-0549

VOLUME I RECEPTORS -- MAMMALS
BIRDS

VOLUME II RECEPTORS -- BIRDS

VOLUME III RECEPTORS -- BIRDS

VOLUME IV RECEPTORS -- FISH, LITTORAL, BENTHOS

VOLUME V RECEPTORS -- FISH, LITTORAL, BENTHOS

VOLUME VI RECEPTORS -- MICROBIOLOGY

VOLUME VII EFFECTS

VOLUME VIII CONTAMINANT BASELINES

VOLUME IX TRANSPORT

VOLUME X TRANSPORT

VOLUME XI HAZARDS

VOLUME XII HAZARDS

VOLUME XIII DATA MANAGEMENT

ARLIS
Alaska Resources
Library & Information Services
Anchorage, Alaska

GC
85.2
.A4
E57
1978
v.11

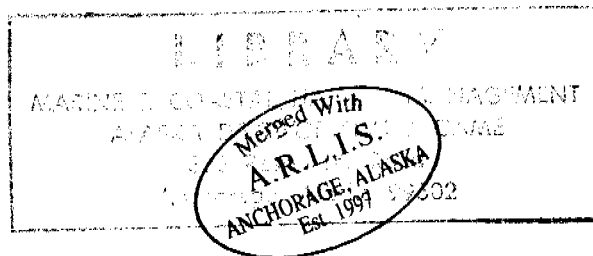
Environmental Assessment of the Alaskan Continental Shelf

Annual Reports of Principal Investigators
for the year ending March 1978

Volume XI. Hazards

Outer Continental Shelf Environmental Assessment Program
Boulder, Colorado

October 1978



U.S. DEPARTMENT OF COMMERCE
National Oceanic and Atmospheric Administration

U.S. DEPARTMENT OF INTERIOR
Bureau of Land Management

ARLIS
Alaska Resources
Library & Information Services
Anchorage, Alaska

DISCLAIMER

The National Oceanic and Atmospheric Administration (NOAA) does not approve, recommend, or endorse any proprietary product or proprietary material mentioned in this publication. No reference shall be made to NOAA or to this publication furnished by NOAA in any advertising or sales promotion which would indicate or imply that NOAA approves, recommends, or endorses any proprietary product or proprietary material mentioned herein, or which has as its purpose an intent to cause directly or indirectly the advertised product to be used or purchased because of this publication.

ACKNOWLEDGMENT

These annual reports were submitted as part of contracts with the Outer Continental Shelf Environmental Assessment Program under major funding from the Bureau of Land Management.

HAZARDS

Contents

<u>RU #</u>	<u>PI - Agency</u>	<u>Title</u>	<u>Page</u>
059	Nummedal, D. - Dept. of Geology et al. Univ. of S.C. Columbia, SC	Oil Spill Vulnerability of the Beaufort Sea Coast	1
087	Martin, S. - Dept. of Ocean- ography Univ. of WA Seattle, WA	The Interaction of Oil with Sea Ice in the Arctic Ocean	8
088	Kovacs, A. - Cold Regions Weeks, W. Research & Engineering Lab. Hanover, NH	Dynamics of Near-shore Ice	11
	Page, F. - Dartmouth College Hanover, NH	Geochemistry of Subsea Permafrost at Prudhoe Bay, Alaska (M.A. Thesis)	23
098	Pritchard, R. - Polar Science Center Univ. of WA Seattle, WA	Dynamics of Near Shore Ice	39
105	Sellmann, P. - CRREL et al. Hanover, NH	Delineation and Engineering Characteristics of Perma- frost beneath the Beaufort Sea	50
204	Hopkins, D. - US Geological Hartz, R. Survey (USGS) Menlo Park, CA	Offshore Permafrost Studies, Beaufort Sea	75
205	Barnes, P. - USGS Reimnitz, E. Menlo Park, CA	Marine environmental problems in the ice covered Beaufort Sea shelf and coastal regions	148

<u>RU #</u>	<u>PI - Agency</u>	<u>Title</u>	<u>Page</u>
206	Gardner, J. - USGS et al. Menlo Park, CA	Distribution of Grain Size, Total Carbon, Heavy and Light Minerals, Clay Mineralogy, and Inorganic Geochemistry, Outer Continental Shelf, Southern Bering Sea	300
208	Dupré, W. - Dept. of Geology Univ. of Houston Houston, TX	Yukon Delta Coastal Processes Study	384
210	Lahr, J. - USGS et al. Menlo Park, CA	Earthquake Activity and Ground Shaking in and along the Eastern Gulf of Alaska	447
251	Pulpan, H. - Geophysical Inst. Kienle, J. Univ. of Alaska Fairbanks, AK	Seismic and Volcanic Risk Studies, Western Gulf of Alaska	475
253	Osterkamp, T. - Geophysical Inst. Harrison, W. Univ. of Alaska Fairbanks, AK	Subsea Permafrost: Probing, Thermal Regime and Data Analysis	570
271	Rogers, J. - Geophysical Inst. Morack, J. Univ. of Alaska Fairbanks, AK	Beaufort Seacoast Permafrost Studies	651

ANNUAL REPORT
April 18, 1978
OCS RESEARCH UNIT # 59

"Oil Spill Vulnerability of the Beaufort Sea Coast"

Dag Nummedal, Principal Investigator
Ian A. Fischer and Jeffrey S. Knoth, Co-Investigators

I. Objectives

A. Project Objectives

1. To characterize the morphology of the barrier islands and the mainland shoreline.
2. To assess the retention potential for spilled hydrocarbons within the coastal environment.

B. Report Objectives

Summarize all available data on coarse-grained (sand and gravel) transport along the Beaufort beaches.

Coastal Research Division
Department of Geology
University of South Carolina
Columbia, S. C. 29208

II. Field Studies - Field observations of the surf zone. At 5 different days during August 1977, measurements were made of breaker conditions at selected sites along the coast. Two sets of observations, Aug. 8 and 10, were taken during a northeast storm at Pt. Barrow. The measurements are thought to be representative of energy levels occurring a few days every open-water season. Measurements at Pt. Barrow on Aug. 7 and along the western shore of Prudhoe Bay on Aug. 5 are typical of the majority of the days during summer.

The following parameters were measured in the surf as outlined:

Wave height (H_b): measured by sighting along a graduated measurement rod on the horizon.

Wave orthogonal angle (α_b): measured by protractor; angle is relative to the local shoreline trend.

Wave period (T): determined by measuring the average period of ten successive breakers.

Longshore current velocity (V): measured by timing the drift of a neutrally buoyant float along a pre-determined distance of beach.

Wind speed (W): measured by hand-held anemometer.

Wind direction (S): determined by Brunton compass.

The longshore wave energy flux and sediment transport rate are calculated by the following equations (these are the metric equivalents to eqs. 4-35 and 4-40 in the Shore Protection Manual, Coastal Engineering Research Center, 1973):

$$P_{1s} = 2.784 \times 10^{-2} H_b^{5/2} \sin 2\alpha_b \quad (1)$$

where the longshore energy flux, P_{1s} , has the dimension Joules per meter per second. H_b is measured in centimeters and α_b in degrees. The sediment transport rate is calculated by:

$$Q_s = 1.277 \times 10^3 P_{1s} \quad (2)$$

where Q_s has the dimension cubic meters per year.

All field observations and calculations based on equations 1 and 2 are

Table 1. Surf zone parameters and longshore transport rates for the Beaufort Coast of Alaska. Measurements during August 1977.

Station	Date	Time ADT ¹	Wave Hgt (cm)	Orthogonal angle (deg.)	Period (S)	Longshore current vel. (cm/s) ²	Wind speed (km/h)	Wind direction (deg.)	Longshore energy flux (J/m/s) ²	Sediment transport rate (m ³ /day) ²
Prudhoe Bay										
BE 48	Aug. 5	1540	12	65°	1.35	+22	32	40	10.6	37
BE 51a	Aug. 5	1730	12	110°	1.70	-14	0	--	-8.9	-31
Be 51b	Aug. 5	1800	14	145°	1.70	-10	0	--	-19.1	-67
Pt. Barrow										
BE 86	Aug. 8	1015	65	115°	3.2	-96	38	80	-725	-2539
BE 86	Aug. 10	----	75	120°	3.6	-114	64	115	-1173	-4107
BE 87	Aug. 8	----	70	115°	3.1	-122	38	80	-873	-3056
BE 87	Aug. 10	----	50	110°	3.6	-78	67	115	-316	-1105
BE 88	Aug. 8	1120	50	110°	3.2	-116	37	80	-316	-1105
BE 88	Aug. 10	----	45	115°	3.3	-140	67	115	-289	-1012
BE 89	Aug. 8	----	30	125°	3.5	-90	37	80	-129	-451
BE 89	Aug. 10	----	20	105°	3.1	-36	57	110	-24.8	-87
BE 90	Aug. 8	1240	8	93°	2.4	0	37	80	-.52	-1.8
BE 90	Aug. 10	----	8	92°	1.6	0	57	110	-.35	-1.2
BE 91a	Aug. 8	1500	20	75°	2.8	+75	48	80	24.9	87
BE 91a	Aug. 10	----	25	80°	3.4	65	--	--	29.7	103
BE 91b	Aug. 8	1515	30	111°	2.9	-77	32	80	-91.7	-321
BE 91b	Aug. 10	----	25	110°	3.0	-34	--	--	-55.9	-195
BE 91c	Aug. 8	1545	25	80°	2.7	55	41	80	27.9	104
BE 91d	Aug. 8	1600	35	105°	3.3	-58	45	80	-100.7	352
Plover Point & Spit										
BE 84a	Aug. 7	2050	5	120°	1.5	-6	9	25	-1.3	-4.71
BE 84a	Aug. 8	1340	40	105°	2.8	-44	48	80	-140	-492
BE 84a	Aug. 10	----	45	115°	3.5	-72	64	115	-289	-1012
BE 84b	Aug. 7	2100	22	90°	2.0	-1	9	25	.03	.13
BE 84b	Aug. 10	----	55	70°	3.8	124	38	80	401	1405
BE 85	Aug. 8	1350	45	105°	3.0	-55	64	115	-188	-660
BE 85	Aug. 10	----	60	110°	3.7	-84	38	80	-498	-1744
BE 85	Aug. 8	1400	58	108°	3.0	-34	38	80	-418	-1465

¹ ADT: Alaska Daylight Time

² Negative values refer to currents (transport) to the left. Positive values indicate movement to the right.

summarized in Table 1. Figures 1 and 2 present graphically the variability in transport rates around the cusped foreland of Pt. Barrow.

III. Results and Interpretation.

A. Results. - The rate of longshore movement of coarse-grained beach material (sand and gravel) is found to range from essentially zero up to 4100 cubic meters per day. The average rate along the Beaufort shore of Plover Spit and Pt. Barrow during August 8 and 10, is 1663 cubic meters per day. The storm maintained essentially undiminished vigor for about 3 days. Thus, this storm alone could have moved about 5000 cubic meters to the west past Pt. Barrow. The dramatic decrease in transport rate between stations BE 88 and BE 89 is in excellent accord with the morphology: a series of recurved beach ridges on the west-northwest side of Pt. Barrow attest to a rapid transport from the beaches further east, at least for the last few years.

Few littoral wave observations have previously been made along the Beaufort Coast. The ones that exist, however, demonstrate fair agreement with the ones presented above. Dygas and Burrell (1975) report on wave conditions and calculated sediment transport rates for the mainland shore at Oliktok Point during the summers of 1971 and 1972. The relatively sheltered location of Oliktok Point and the apparent absence of any high-energy events during their 1971 field season produced quite moderate transport rates compared to those encountered at Pt. Barrow during a storm (Table 2). The maximum recorded wave height reached 32 cm, the maximum transport rate was 384 m³/day. Since Dygas and Burrell's (1975) transport estimates were based on the rating curve presented in Technical Memorandum No. 4 (Coastal Engineering Research Center, 1966), their rates are lower than what is presented in this report based on the same field data. As explained by Galvin and Vitale (1976), the relationship

between longshore sediment transport rates and the longshore component of wave energy flux to be used in the field should be based on field observations only. Thus, by excluding wave tank data used in T.M. 4 (Coastal Engineering Research Center, 1966), the updated Shore Protection Manual (Coastal Engineering Research Center, 1973) recommends using a rating curve which gives a higher transport rate for a given energy flux than was the case with the old version. The new rating curve is equation 2 in this paper.

Observations by Short (1973) along the outer beaches of the Jones Islands, during the 1972 open-water season, indicate a westward transport along the outer beaches of about 10^4 cubic meters of sediment. Most of this transport appears to have occurred during September, a period of unusually high easterly waves.

IV. Summary

Measurements of littoral process variables along the mainland and island shores of the Beaufort Coast of Alaska are much too sparse to permit an evaluation of the spatial and temporal variations of beach sediment transport.

Data presented in this report and those obtained by Short (1973), however, are suggestive of a typical annual net transport rate of about 10^4 cubic meters to the west along the seaward beaches of the Beaufort barriers.

Data obtained by Dygas and Burrell (1975) suggest that annual transport rates along the mainland shore near Oliktok Point are somewhat less, perhaps of the order of some thousand cubic meters per year. The direction of net transport along the mainland shore is highly dependent on location.

For purposes of perspective, these transport rates of the Arctic should be compared to typical rates of a few hundred thousand cubic meters,

generally to the south, along the east coast of the United States (Wiegel, 1964). Nummedal and Stephen (1978) have calculated rates ranging up to 1.4 million cubic meters to the west along the Malaspina Foreland.

Table 2. Summary of littoral observations at Oliktok Point, 1971 (From Dygas & Burrell, 1975).

	Northwest-facing shore	Northeast-facing shore
Mean wave height (cm)	5.8 - 32.2	
Period (s)	1.3 - 3.6	
Longshore currents (cm/s)	0 - 75.5	0 - 58.0
Longshore component of wave energy flux (J/m/s)	1 - 110	0.2 - 21.2
Longshore sediment transport rate ¹ (m ³ /day)	3.5 - 384	.7 - 74

1

Recalculated from data in Dygas and Burrell (1975) according to the revised rating curve presented in the Shore Protection Manual (Coastal Engineering Research Center, 1973) and given in this paper as equation 2.

REFERENCES CITED

- Coastal Engineering Research Center, 1966, Shore Protection Planning and Design: C.E.R.C. Tech. Memo. no. 4.
- Coastal Engineering Research Center, 1973, Shore Protection Manual: Government Printing Office, Washington, D. C.
- Dygas, J. A., and Burrell, D. C., 1975, Dynamic sedimentological processes along the Beaufort Sea coast of Alaska: in Assessment of the Arctic Marine Environment, Hood, D. W. and Burrell, D. C., (eds.), Occasional Pub. No. 4, Institute of Marine Science, University of Alaska, Fairbanks, p. 189 - 203.
- Galvin, C. J., Jr., and Vitale, P., 1976, Longshore transport prediction - SPM 73 equation: Proceedings of the 15th Coastal Engineering Conference, v. II, p. 1133-1148.
- Nummedal, D., and Stephen, M. F., 1978, Wave climate and littoral sediment transport, northeast Gulf of Alaska: Jour. Sedimentary Petrology, v. 48, p. 359-371.
- Short, A. D., 1973, Beach dynamics and nearshore morphology of the Alaskan Arctic coast: Ph.D. dissertation, Louisiana State University, Baton Rouge, La., 140 p.
- Wiegel, R. L., 1964, Oceanographical Engineering: Prentice-Hall, Inc., New Jersey, 532 p.

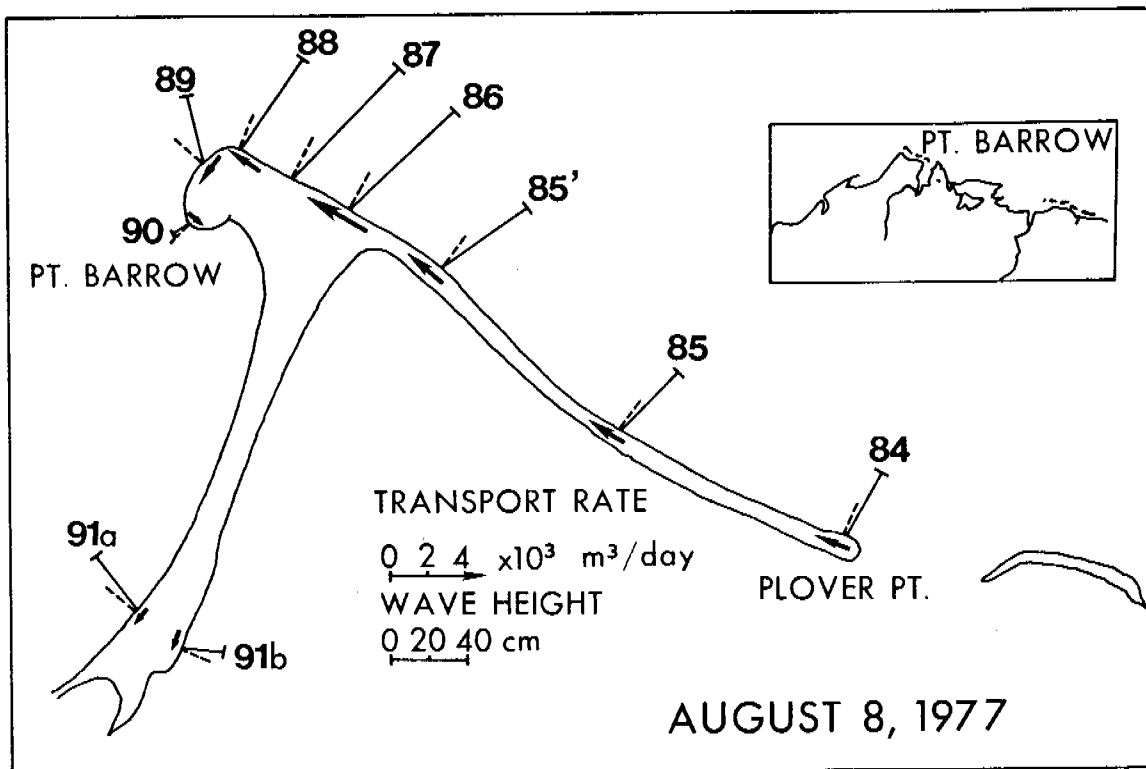


Figure 1. Wave parameters and sediment transport rates along the Pt. Barrow beaches on August 8, 1977.

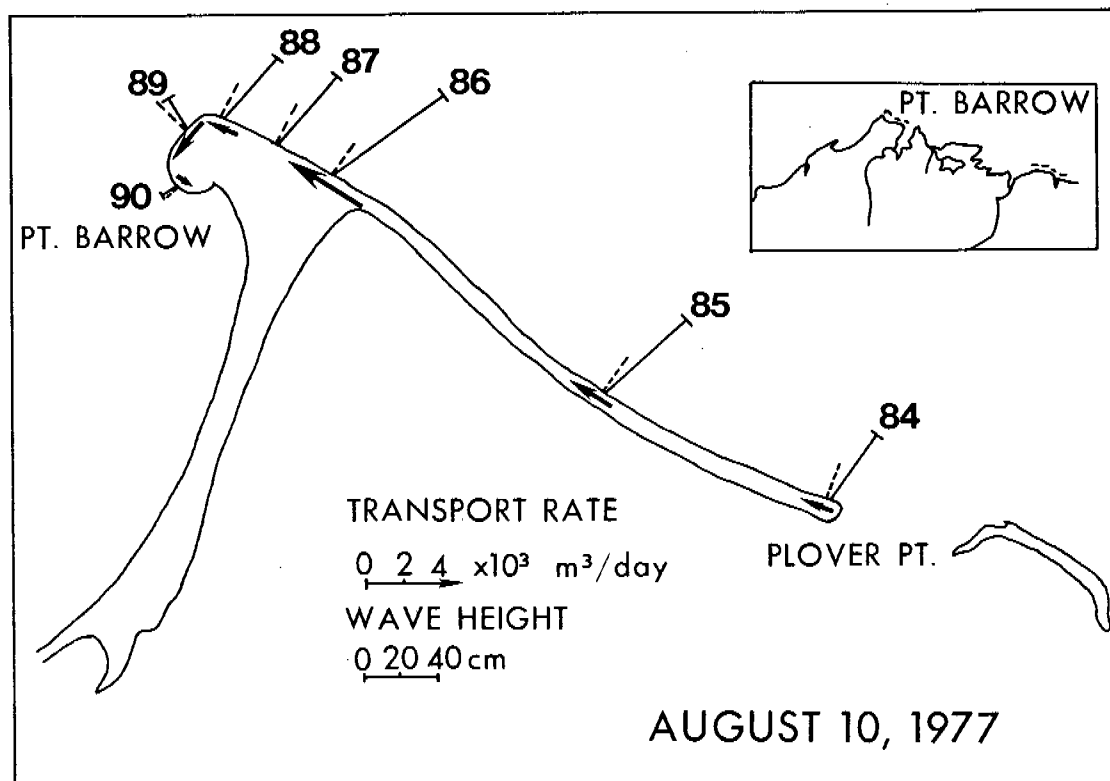


Figure 2. Wave parameters and sediment transport rates along the Pt. Barrow beaches on August 10, 1977.

ANNUAL REPORT

Contract #03-5-022-67
Research Unit #87
Reporting Period:
1 April 1977 - 1 April 1978
Number of Pages: 3

THE INTERACTION OF OIL WITH SEA ICE IN THE ARCTIC OCEAN

Seelye Martin
Department of Oceanography
University of Washington
Seattle, Washington 98195

22 February 1978

Because we are leaving on 3 March 1978 for a field trip in Norton Sound, Kotzebue Sound, and the Chukchi Sea off of Cape Lisburne, we are submitting our annual report early. The results of the forthcoming field traverse will be submitted in our next field report.

I. Summary of Objectives:

Our purpose is to understand from laboratory experiments and field traverses how oil and sea ice would interact in an arctic oil spill.

II. Publications and Reports:

During the past year, we have submitted the following material for publication:

1. "Data Report on the March 1977 field traverse of BLM/NOAA Task Order Contract No. 03-5-022-67, Task Order No. 6, R.U. #87" by Seelye Martin and Peter Kauffman (available from the Environmental Data Service).

2. "A Laboratory Study of the Dispersion of Crude Oil within Sea Ice Grown in a Wave Field", by Martin, Kauffman, and Welander, to appear in the Proceedings of the 27th Alaska Science Conference, 1978.

3. "The Behavior of the Bouchard #65 Oil Spill in the Ice-covered Waters of Buzzards Bay", by Deslauriers and Martin, to appear in the Proceedings of the 1978 Offshore Technology Conference, 1978. (Note: the author was employed as a consultant to ARCTEC for part of the preparation of this report.)

4. We have also prepared a 7 minute film under the present contract entitled "The Buzzards Bay Oil Spill", which will be submitted with this report. The film shows both aerial and surface footage of how oil interacted with the sea ice in the Buzzards Bay spill.

III. Field Work:

Our field work during the past year took place on the fast ice offshore of Prudhoe Bay during March 1977. Our results are available in the above Field Report by Martin and Kauffman. To summarize, the cores which we took from the traverse were very similar to those reported on in our 1977 annual report. As far as describing the small-scale entrainment of oil by sea ice, our 1977 annual report remains correct. As a related part of this experiment, Dr. Thomas Grenfell of the Department of Atmospheric Sciences, University of Washington, accompanied us on some of the traverses and took measurements with his underwater spectrophotometer. His work will be published within the year.

IV. Laboratory Work:

Our major laboratory effort is to develop a model for oil entrainment in grease and pancake ice; forms of ice which are important in the lee shore regions of Norton and Kotzebue Sound. Also, the laboratory pancake work is a rough model of how oil might spread in a field of larger floes. Some of this work will be published in the Proceedings of the 27th Alaska Science Conference, 1978; the rest is in preparation.

In a related ONR study, we find that grease ice is a slurry of sea water and small ice platelets measuring 1-2 mm in diameter. Our experiments show that the slurry is a non-Newtonian fluid analogous to human blood, where the sea water corresponds to plasma, and the ice platelets to red blood cells. At high shear rates, both the platelets and the cells move independently. At low shear rates in blood, the red blood cells aggregate together yielding a viscosity increase; at low shear rates in grease ice, the ice crystals 'sinter' or pressure melt together into clumps, also yielding a viscosity increase. At very low shear rates, there is a point where the slurry moves as a solid rather than as a liquid, so that a 'yield stress' characterizes grease ice.

Our work suggests that oil will collect in the grease ice at the point of transition from a liquid to a solid. In lease areas such as Norton and Kotzebue Sound, satellite photographs show that the grease ice forms in long narrow Langmuir-like plumes parallel to the wind. These plumes absorb the energy of the bi-directional wind-wave field. We suspect from our experiments that oil spilled in these areas will be driven into the Langmuir plumes by the circulation, and collect in bands parallel to the grease ice.

To examine this idea further, during our forth-coming field experiment, we plan low-level helicopter flights over regions of grease ice formation, during which we will film the grease ice in an attempt to look at wave attenuation. We also plan to take ice cores downwind of the regions of grease ice generation to see if the wind drives the grease ice under the pack ice. Evidence that grease ice is driven under the pack ice will suggest that spilled oil might behave in a similar manner.

V. Summary of Fourth Quarter Activities:

A. Field and laboratory activities:

1. Field traverse planned for period 3-27 March, 1978.
2. A student, Ms. Jane Bauer, is on a SURVEYOR cruise in Bristol Bay during 13-28 February to examine and photograph the forms of ice which occur at the edge of the pack.
3. Laboratory activities have consisted of two grease ice experiments, the usual massive preparation for the field traverse, and attendance at the Second Barrow Synthesis meeting.

B. Problems: no unusual problems.

ANNUAL REPORT

R.U. #88: Dynamics of Near-Shore Ice

P.O.: 01-5-022-1651

Reporting Period: 1 April 1977 to
30 March 1978

No. of Pages: 12

DYNAMICS OF NEAR-SHORE ICE

Principal Investigators: A. Kovacs and W. Weeks

Cold Regions Research and Engineering Laboratory
Hanover, New Hampshire 03755

16 March 1978

I. SUMMARY OF OBJECTIVES, CONCLUSIONS AND IMPLICATIONS WITH RESPECT TO
OCS OIL AND GAS DEVELOPMENT

The purpose of this project is to:

- a. study the motion of the fast ice and near-shore sea ice north of Prudhoe Bay and in the vicinity of the Bering Strait,
- b. make observations on major ice deformation features that occur near the edge of the pack ice/fast ice boundary,
- c. explore the use of an airborne pulsed radar system to measure the thickness of sea ice,
- d. study the internal structure of near-shore sea ice,
- e. characterize the spatial and temporal variations in sea ice pressure ridging via the use of laser profilometry and side-looking airborne radar (SLAR).

At the present time our results (discussed more fully later in this report) suggest the following:

- a. during the time period March-May 1976 fast ice motions within the barrier islands are small,
- b. fast ice motions outside the barrier islands increase with increasing distance from shore,
- c. the fast ice/pack ice boundary may be located a considerable distance offshore from the 18 m depth contour, where it is usually assumed to be located,
- d. locally-formed multiyear pressure ridge systems are a major hazard to offshore development in water depths in excess of 18 m,
- e. impulse radar systems can quite effectively obtain sea ice thickness information when operated from a helicopter,

- f. large areas of fast ice show the same crystal orientation [The orientation is believed to be controlled by the current direction under the ice. The orientation makes the ice properties directionally dependent.]
- g. remote sensing studies of ice deformation show a general decrease in the amount of pressure ridging as one moves to the west from Barter Island and/or further north away from the edge of the fast ice.

II. INTRODUCTION

A. General Nature and Scope of Study.

The present program can be considered to be split into three main sub-projects:

1. The Narwhal Island Program

The purpose of this program is to obtain detailed quantitative information on the movement and deformation of both the near-shore pack ice and the fast ice along the coast of the Beaufort Sea (with particular emphasis on the region north of Prudhoe Bay). Using this same field site studies have also been carried out on the nature of the ridge systems located near the edge of the fast ice, on lateral variations in the thickness of first and multiyear ice, and on the internal structure of sea ice.

2. The Bering Strait Program

This program is focused on one task; measuring the flux of sea ice through the Bering Strait in specific and developing theoretical models for the motion of ice through straits in general.

3. The Remote Sensing Program

This program attempts both to gather remote sensing data using a

laser profilometer, a SLAR system and standard mapping cameras and to utilize this data to study the nature of pressure ridging and ice conditions along the coast of the Beaufort and Chukchi Seas. Studies have also been made of the nature of the radar return from sea ice.

B. Specific Objectives

See previous section.

C. Relevance to Problems of Petroleum Development

A knowledge of motion, deformation and physical characteristics of both the near-shore pack ice and the fast ice is essential to adequately designing and estimating the hazards associated with a variety of engineering options that may be considered for offshore operations in the near coastal areas of the Beaufort and Chukchi Seas (e.g. construction of gravel islands, structural platforms, causeways, reinforced ice platforms, buried pipelines, or the utilization of the ice sheet itself to carry large, long-term loads). The present program contributes directly to the solution of this general class of engineering problems in that it will provide much of the geophysical and engineering data upon which sound engineering and regulatory decisions can be made. The Narwhal Island area that is being studied is currently being considered by the petroleum companies because it possesses favorable geologic structures and is a natural extension of the known Prudhoe Bay field. It is also a portion of the coming lease sale (December 1979).

Our interest in observing and in developing methods to predict the drift of pack ice through the Bering Strait is, as mentioned earlier, linked to the fact that ice flow through the Straits would be a key mechanism in dispersing an oil spill occurring along the coastal areas of the Beaufort and Chukchi Seas. We also believe that a knowledge of the ice conditions in the Strait

is essential to developing an adequate ice forecasting model for the Chukchi and Bering Seas. Such a model is required to predict the trajectories of potential oil spills.

The remote sensing program provides the basic information on the distribution of ice types and features and in particular ridges that will be required as one aspect of a risk analysis for the construction of an offshore drilling platform sited on the edge of the Arctic Ocean.

III. CURRENT STATE OF KNOWLEDGE

There has never been a comparable study of the motion of near-shore fast and pack ice as has been carried out at Narwhal Island. The closest study is that of the University of Washington (R.U. #98) using drifting data buoys employed on the ice north of the Alaskan coast. These buoys are located further offshore than our study area. However, this data set will definitely prove to be useful to us in analyzing our results. The oil companies have also carried out studies of the motion of the fast ice in the vicinity of our operation. However, their results have not been made available to OCS program.

The Bering Strait Program is also quite different than existing programs. The most similar programs are R.U. #250 which uses a radar system to study the formation of near-shore ridges near Barrow, and the Japanese program using radar to study ice motion along the coast of Hokkaido. Neither of these efforts is focused on the problem of the passage of sea ice through restricted channels.

The laser profilometer program is the only such program currently underway. In the past there have been laser flights in the area of the Mackenzie

Delta carried out by the Beaufort Sea Program. This data will be most useful to us in making regional comparisons of ridging intensities.

IV. STUDY AREAS

Our detailed observations have been made at two principal locations; the Narwhal Island - Cross Island region north of Deadhorse and the Bering Strait between Wales and Little Diomed Island. Our observations of ridging have included most of the Beaufort Sea coast and our remote sensing studies have ranged by Kaktovik on the Beaufort Sea to Point Lay on the Chukchi Sea.

V. RESULTS

1. Published reports (DB indicates availability in the OCS Data Bank)
 - a) Kovacs, A. (1976) Grounded ice in the fast ice zone along the Beaufort Sea Coast of Alaska. CRREL Report 76-32, 21 pp.(DB)
 - b) Kovacs, A. and Gow, A.J. (1976) Some characteristics of grounded floebergs near Prudhoe Bay, Alaska. CRREL Report 76-34, 10 pp.; also available in Arctic 29 (3), 169-73 (1976).
 - c) Weeks, W.F., Kovacs, A., Mock, S.H., Tucker, W.B., Hibler, W.D. and Gow, A.J. (1977) Studies of the movement of coastal sea ice near Prudhoe Bay, Alaska. Journal of Glaciology, Vol. 19, No. 81, p. 533-46 (DB).
 - d) Kovacs, A. (1977) Sea ice thickness profiling and under-ice oil entrapment. Offshore Technology Conference Paper OTC 29-49, (DB).
 - e) Schwarz, J. and Weeks, W.F. (1977) Engineering properties of sea ice. Journal of Glaciology, Vol. 19, No. 81, p. 499-531 (DB).
 - f) Gow, A.J. and Weeks, W.F. (1977) The internal structure of fast ice near Narwhal Island, Beaufort Sea, Alaska. CRREL Report 77-29, 8 p. (DB).
 - g) Sohdi, D.S. (1977) Ice arching and the drift of pack ice through restricted channels. CRREL Report 77-18, 14 p. (DB).

- h) Kovacs, A. (1977) Iceberg thickness profiling. In "Conference on Port and Ocean Engineering under Arctic Conditions" Memorial University of Newfoundland, St. Johns. (DB).

2. Completed reports currently in press

- a) Kovacs, A. Radar profile of a multiyear pressure ridge. Arctic.
- b) Kovacs, A. Iceberg thickness and crack detection. Proceed. First Internat. Conf. on Iceberg Utilization. Pergamon Press.
- c) Tucker, W.B., III, Weeks, W.F., Kovacs, A. and Gow, A.J., (1977) Near shore ice motion at Prudhoe Bay, Alaska. AIDJEX Sea Ice Symposium. Univ. of Washington Press.
- d) Weeks, W.F., Tucker, W.B. III, Frank, M. and Fungcharoen, S. (1977) Characterization of the surface roughness and floe geometry of the sea ice over the continental shelves of the Beaufort and Chukchi Seas. AIDJEX Sea Ice Symposium. Univ. of Washington Press.
- e) Weeks, W.F. and Gow, A.J. Preferred crystal orientations in the fast ice along the margins of the Arctic Ocean. Journal of Geophysical Research (Oceans and Atmospheres).
- f) Kovacs, A. and Morey, R.M. Radar anisotropy of sea ice due to preferred azimuthal orientation of the horizontal c-axes of ice crystals. Journal of Geophysical Research.
- g) Kovacs, A. Some problems associated with radar sea ice profiling. Cold Regions Research and Engineering Laboratory Tech. Note, 6 p.
- h) Kovacs, A. Remote detection of water under ice covered lakes on the North Slope. Cold Regions Research and Engineering Laboratory Report.

3. Reports currently in preparation

- a) Tucker, W.B., Weeks, W.F. and Frank, M. Sea ice ridging on the Alaskan continental shelf during 1976.
- b) Kovacs, A., Tucker, W.D. and Weeks, W.F. The Narwhal Island ice movement experiment.

VI. CONCLUSIONS

A. Narwhal Island

- a) Laser observations of fast ice motion at sites close to Narwhal Island show long term changes in the distance to targets located

on the ice that are believed to be primarily the result of the thermal expansion of the sea ice. The main ice motion was outward normal to the coast (in the least-constrained direction). The maximum movement was approximately 3 m with short term changes of 30 cm. Larger movements (up to 60 m) were associated with the formation of cracks and ridges within the fast ice.

- b) Radar observations of fast ice sites further off-shore from the barrier islands do not permit the study of small motions (as do the laser records) because of insufficient measurement resolution. However, these records show many larger events with the standard deviation of the motion measured parallel to the coast increasing systematically with distance off-shore reaching a value of ± 6.6 m at 31 km. The ice motions show short term displacements of as much as 12 m at the sites furthest from the coast. The observations also show systematic changes in line length (up to 6 m over a distance of 30 km) that are believed to be the result of thermal expansion of the ice. Correlations between the wind and the ice movement are only appreciable for movements normal to the coast.
- c) Radar targets located within the pack ice showed large short term movements (up to 2.7 km) but negligible net motion along the coast. There was no significant correlation between the motion of the pack and the local wind suggesting the models for predicting coastal ice movement in the Beaufort Sea during the March-June time period can only succeed if they are handled

as part of a regional model which incorporates the lateral transfer of stress through the pack ice.

- d) Off-shore from Narwhal and Cross Islands the fast ice/pack ice boundary was usually located (during March-May 1976) in 30 to 35 m of water as opposed to 18 m of water where the boundary has been observed at sites further west along the Alaskan coast.
- e) The large grounded multiyear shear ridge formations that were studied along the Beaufort Sea coast in the Harrison Bay/Prudhoe Bay area must be considered as formidable obstacles in the development of off-shore operations in this region. In the design of off-shore drilling structures significant consideration must be given to not only the forces which can develop when these formations are pushed against the structures, but also to the potential for ice piling up and overriding them. The inner edges of the multiyear shear ridge formations studied north of Cross Island were found to be as high as 12.5 m and to be grounded along the ~ 15 m depth contour. This depth is significantly less than the ~ 19 m contour previously considered to be the water depth at which grounded shear ridges begin to form. The grounded ice formations studied formed in the fall of 1974 and remained through August 1976. However, they were not present in November 1976.
- f) The dual antenna impulse radar system was highly effective in determining the thickness of both first-year and multiyear

sea ice from the air. Good agreement was achieved between calculated and observed ice thicknesses and representative cross-sections of both ice types were obtained. These cross sections reveal characteristic undulating bottom relief in both ice types which could trap significant amounts of oil as the result of an under-ice spill. Preliminary estimates of the entrapped volume of oil are 0.03 m^3 of oil per square meter of ice area for first year ice and 0.3 m^3 of oil per square meter for multiyear ice.

- g) Our observations coupled with published U.S. and Russian results show that very large areas (tens of kilometers) of sea ice have sufficiently similar c-axes orientations to act as a large single crystal. Because of this, off-shore structures may have to be designed for "hard-fail" ice strengths which are 2 to 6 times the strength values normally used. The Russian theory that such orientations are aligned parallel to the magnetic field is shown to be doubtful. The orientation is probably related to the current direction.

B. Bering Strait

- a) The radar system was installed at Top Camp at Tin City on the Bering Strait and is now operating at 50 KW power output.
- b) The theory of the flow of granular media through chutes and hoppers has been applied with considerable success to ice motion through the Bering Strait. There is good correspondence between observed arching and lead patterns and those predicted

by theory. In addition values determined via the theory for the angle of internal friction of pack ice (≈ 30 to 35°) and the cohesive strength ($\approx 2000 \text{ N/m}^3$) are similar to values obtained by other approaches. It is estimated that if the wind velocity parallel to the Bering Strait exceeds $\approx 6 \text{ m/s}$, there will be ice flow through the Strait.

C. Remote Sensing

- a) During the 1975-76 ice season the heaviest ridging occurred at Barter Island and there was a general decrease in the intensity of the ridging as one moves further west into the Chukchi Sea. Ridging also decreases as one moves further offshore. Individual frequency profiles fall off in an exponential manner as ridge height increases. There is no decrease in frequency at low ridge heights as has been suggested from the analysis of sonar profiles.
- b) Analysis of SLAR imagery shows that the area of ridged ice decreases in a linear manner as one moves away (North) from the coast. There is no obvious break corresponding to the boundary of the so-called shear zone.
- c) The most common shape of multiyear ice floes is roughly circular. The largest length to width ratio observed was just over 5. The distribution of floe diameters shows an exponential decrease as floe size increases. The largest floe diameter observed was 3600 m.

- d) Although there have been many studies of the engineering properties of sea ice, there still is considerable uncertainty concerning the appropriate values to use in offshore design. This comment is particularly true of the mechanical properties where both the basic experimental measurements and their interpretation are not well resolved.

VII. SUMMARY OF 4th QUARTER OPERATIONS

During this quarter time has been devoted to the following subjects:

- a) Report Writing
Work is continuing on the final Narwhal Island paper and on the laser profilometer study of ridging.
- b) Field preparations are being made for 1) the spring observational program on shore ice piling (Kovacs) and 2) the spring study of ice crystal orientations between Kotzebue Sound and Demarcation Bay (Weeks and Gow).
- c) A visit was made to Tin City to repair the radar unit. The problem was found to be one that could not be handled in the field. The equipment was returned to the factory, repaired and is now in transit back to the field.
- d) Weeks attended the Barrow OCS meeting and chaired the Panel on "Environmental Hazards to Offshore Operations Along the Coast of the Beaufort Sea." A 22 page report on this subject has just been completed and sent to Weller.
- e) Tucker is currently in the field on a remote sensing exercise (NASA) along the Beaufort Coast. Gow and Weeks leave for Kotzebue on 24 March and Kovacs goes to Deadhorse in mid-April.

GEOCHEMISTRY OF SUBSEA PERMAFROST
AT PRUDHOE BAY, ALASKA

A Thesis
Submitted to the Faculty
in partial fulfillment of the requirements for the
degree of
Master of Arts

by

Frederick W. Page

Some basis for the research described herein was performed under
research units 88, 105, 204, and 473 managed by OCSEAP/NOAA and
primarily funded by BLM.

DARTMOUTH COLLEGE
Hanover, New Hampshire

June 1978

Examining Committee:

RC Reynolds Jr
Chairman

Charles L. Drake

James F. Hornig

Agua Pythe
Dean of Graduate Studies

Abstract

The objectives of this study were to define the salinity and chemical composition of the interstitial water in sediment samples from Prudhoe Bay, Alaska; to gain insight into the processes which may have affected the composition of the pore water; to provide information useful in understanding the engineering properties of the sediments; and to provide additional information on the distribution of ice-bonded permafrost under the shallow coastal waters of the Beaufort Sea.

A total 14 sea water and 96 sediment samples were collected from 5 boreholes during the spring of 1977. The samples were analyzed using standard analytical techniques. Sediment analyses included determinations of moisture content, organic carbon content, and calcium carbonate content. Interstitial and sea water analyses included pH, electrical conductivity, alkalinity, and the determinations of the sodium, potassium, calcium, magnesium, chloride, and sulfate ion concentrations. The salinity, ionic balance, and freezing point of the water were calculated.

The sediments under Prudhoe Bay consist of a thin layer of Holocene to late Pleistocene marine muds overlying late Pleistocene glacial and fluvial gravels. The muds contain higher amounts of calcium carbonate and organic carbon than the underlying gravels. On land, a thin layer of sand,

silt, and peat veneer the gravel deposits. Water and organic carbon contents in this surficial layer of sediment are much higher than those encountered offshore.

In early spring, the salinity of the sea water at distances of more than 10 kilometers from shore is generally 1 to 1.5 parts per thousand (p.p.t.) less saline than normal sea water. Close to shore, where sea ice is frozen directly to, or is located near, the sea bottom, or where circulation with more open water is restricted, the salinity of the sea water is much higher (up to 57.3 p.p.t.). These brines probably result from salt exclusion during the formation of sea ice. Calculated freezing points indicate that the temperature of these brines should be close to -2.95°C whereas the water further offshore should have a temperature of -1.8°C . All of the sea water samples contain proportionately more calcium and potassium, and less sulfate and alkalinity, than normal sea water.

In the marine sediments, the interstitial water had a composition similar to that for normal sea water, suggesting that sea water had either infiltrated into, or been deposited with, the sediments. In mildly reducing sediments, relatively more potassium, calcium, and bicarbonate (alkalinity), and less sulfate, were found in the interstitial water than in normal sea water. In the pore water of more strongly reducing sediments, relatively more potassium and bicarbonate, and less calcium, magnesium,

and sulfate, were found than in normal sea water. These variations in composition are thought to result from a combination of oxidation of organic matter, cation exchange reactions, dissolution, precipitation, and/or recrystallization of calcium and/or calcium-magnesium carbonates, weathering of potassium-rich minerals, and reduction of sulfate by bacteria.

On land, the salinity of the interstitial water varies from 0.5 to 12.5 p.p.t. The lowest salinities (less than 1.5 p.p.t.) are encountered in the upper 2 to 3 meters of the sediment column, where calcium, sulfate, and bicarbonate ions predominate the composition of the interstitial water. This layer of sediment is probably characterized by annual freezing and thawing, leaching, weathering, and the infiltration of fresh water from the surface. Below a depth of about 3 meters, the salinity gradually increases with depth and the composition of the pore water becomes progressively more like that of normal sea water.

Temperature data obtained from the U.S. Geological Survey indicate that permafrost conditions may exist at most of the sites examined. In the boreholes drilled offshore, a partially frozen layer of non-bonded sediments was encountered near the surface of the sea bed. This frozen layer passed laterally into more bonded sediments closer to shore. Concentrated brines were found in the sediments immediately beneath the frozen layer and are thought to

result from brine exclusion during the freezing of the interstitial water. Ice-bonded permafrost was encountered in 2 of the boreholes at depths of approximately 30.5 and 62 meters below the sea ice surface, and at distances of 1.0 and 3.2 kilometers from land, respectively. On land, ice crystals and ice lenses were found in the upper 3 meters of the sedimentary column and most of the sediments were ice-bonded.

Acknowledgments

This study is part of the Outer Continental Shelf Environmental Assessment Program (OCSEAP) which is supported by the Bureau of Land Management through an interagency agreement with the National Oceanographic and Atmospheric Administration (NOAA). I wish to thank Dr. Iskandar K. Iskandar and Dr. Robert C. Reynolds, Jr.; this study could not have been done without their support and guidance. I am also indebted to Dr. Jerry Brown for providing valuable resource material, for aid in planning the field portion of this study, and for technical review of this manuscript; to Paul V. Sellmann for collecting the sediment and sea water samples and for technical review of this manuscript; to Edwin J. Chamberlain for providing the results of the grain size analyses and for collecting the sediment and sea water samples; to Dr. David M. Hopkins and Roger Hartz of the U.S. Geological Survey for providing copies of the borehole logs; and to B. Vaughn Marshall and Dr. Arthur H. Lachenbruch of the U.S. Geological Survey for permission to use the temperature data. And finally, I dedicate this thesis to my loving wife, Nancy, who tolerated a long absence while the field work was being conducted and who provided constant support and encouragement.

Table of Contents

	Page
Abstract	ii
Acknowledgments	vi
Table of Contents	vii
List of Figures	ix
List of Tables	xi
Introduction	1
Site Characteristics	6
Geography	6
Climate	11
Geology	13
Late Quaternary Geological and Climatological History	14
Hydrology	18
Oceanography	21
Sea Ice	24
Sample Collection and Analytical Methodology	28
Sample Collection	28
Sample Preparation and Laboratory Analyses	29
Sediment Analyses	35
Sample Notation	37
Results and Discussion	39
Sediment Characteristics	39
Lithology and Stratigraphy	39
Moisture Content	46

	Page
Calcium Carbonate Content	49
Organic Carbon Content	50
Sea Water and Interstitial Water Chemistry	52
pH	52
Salinity and Conductivity	55
Temperature and Calculated Freezing Points	58
Ionic Balance	66
Ionic Ratios	69
Sodium to Chloride Ratio	69
Other Ionic Ratios	71
Comparison with other Studies	89
Summary and Conclusions	96
Appendix	101
References Cited	104

List of Figures

	Page
Figure 1. Physiographic units of the North Slope of Alaska (from Walker, 1974).	7
Figure 2. Reconstruction of sea-level history for the continental shelf of western and northern Alaska. Width of boxes indicates uncertainty of age and height indicates uncertainty of position of sea level. Down-pointing arrows mark maximum possible position of sea level whereas up-pointing arrows mark minimum possible position of sea level. After Hopkins in Beaufort Sea Synthesis Report, Weller et al., editors, 1977.	17
Figure 3. Map of Prudhoe Bay, Alaska, showing locations of sample collection sites. PB1-3 are from Iskandar et al. (in press); -226, 191, 481, 964, and 3370 are from Osterkamp and Harrison (1976); and PB5-9, PH25, and PH27 are holes drilled and sampled during the spring of 1977. Depth contours are in meters below mean sea level.	20
Figure 4. Filtering centrifuge apparatus.	30
Figure 5. Apparatus used for calcium carbonate determinations.	36
Figure 6. Preliminary log of borehole PB5 (Courtesy of Dr. D.M. Hopkins and Roger Hartz, U.S.G.S.).	40
Figure 7. Preliminary log of borehole PB6 (Courtesy of Dr. D.M. Hopkins and Roger Hartz, U.S.G.S.).	41
Figure 8. Preliminary log of borehole PB7 (Courtesy of Dr. D.M. Hopkins and Roger Hartz, U.S.G.S.).	42, 43
Figure 9. Preliminary log of borehole PB8 (Courtesy of Dr. D.M. Hopkins and Roger Hartz, U.S.G.S.).	44
Figure 10. Preliminary log of borehole PB9. (Hole drilled by R&M Engineering).	45

Figure 11. Temperature and calculated freezing points as a function of depth for borehole PB5 (Temperature data courtesy of B.V. Marshall and Dr. A.H. Lachenbruch, U.S.G.S.).	62
Figure 12. Temperature and calculated freezing points as a function of depth for borehole PB6 (Temperature data courtesy of B.V. Marshall and Dr. A.H. Lachenbruch, U.S.G.S.).	63
Figure 13. Temperature and calculated freezing points as a function of depth for borehole PB7 (Temperature data courtesy of B.V. Marshall and Dr. A.H. Lachenbruch, U.S.G.S.).	64
Figure 14. Temperature and calculated freezing points as a function of depth for borehole PB8 (Temperature data courtesy of B.V. Marshall and Dr. A.H. Lachenbruch, U.S.G.S.).	65
Figure 15. Sodium ion concentration as a function of chloride ion concentration.	72
Figure 16. Chloride, sodium, potassium, and salinity as a function of depth for borehole PB8.	84
Figure 17. Calcium, magnesium, sulfate, and alkalinity as a function of depth for borehole PB8.	85
Figure 18. Conductivity as a function of depth for PB3 and PB7. Data for PB3 from Iskandar et al. (in press).	93
Figure 19. Chloride ion concentration as a function of depth for PB3 and PB7. Data for PB3 from Iskandar et al. (in press).	95

List of Tables

	Page
Table 1. Selected sediment characteristics, Prudhoe Bay, Alaska.	47,48
Table 2. Selected interstitial and sea water analyses.	53,54
Table 3. Chemical analyses of interstitial and sea water samples from Prudhoe Bay, Alaska; in parts per thousand.	67,68
Table 4. Summary of the ionic balances in all interstitial and sea water samples.	70
Table 5. Selected ionic ratios, by weight.	73,74
Table 6. Summary of the sea water ionic ratios.	75
Table 7. Summary of the interstitial water mean ionic ratios in different holes from Prudhoe Bay, Alaska.	77
Table 8. Sea water ionic concentrations for PB3, PB7, and PB8.	90
Table 9. Interstitial water ionic concentrations and ratios for PB3 and PB7.	92

Introduction

Permafrost is defined as any earth material that is continuously below a temperature of zero degrees Celsius for a period of two or more years (National Academy of Sciences, 1976). This definition is based solely on temperature without regard to the amount or the state of any moisture present, or to the lithologic character of the material. Examples of permafrost could be an ice-bonded sand, a brine-saturated silt, or a cold, dry granite.

Although permafrost is defined on the basis of temperature, researchers have frequently added the terms "ice-bonded" or "ice-rich" to more fully describe the state and amount of the moisture present. Bonded, or ice-bonded, permafrost is material in which the soil particles are bound together by interstitial ice. Ice-rich permafrost denotes material which has a considerable volume of ice. Sediments that contain ice wedges or ice lenses would be examples of the latter type. In recent years, it has also become customary to distinguish between permafrost that exists in the marine environment and that which occurs on land. Terms such as "offshore permafrost" and "subsea permafrost" have been used.

All permafrost can be classified into two types, depending on its equilibrium with its present physical-chemical environment (MacKay, 1972). "Equilibrium

permafrost," as its name implies, is permafrost that is in equilibrium with its environment. It is essentially stable in its present spatial distribution. "Disequilibrium permafrost" is not, and it can be further subdivided on the basis of whether it is expanding ("aggrading") or contracting ("degrading") in area or in thickness. A common term for degrading disequilibrium permafrost is the term "relict permafrost." Relict permafrost results when the physical-chemical processes are slow in changing the distribution of permafrost that was formed under a former, more severe climate to its new equilibrium distribution (National Academy of Sciences, 1976).

Since 1968, when oil was discovered at Prudhoe Bay, Alaska, interest in the exploration and development of potential petroleum reserves in the offshore environment has increased. By 1972, results from drilling and geophysical exploration had shown that the prospects of finding oil were excellent. In response to this, the Department of Interior published tentative schedules for leasing offshore lands and, in 1974, the Bureau of Land Management requested that the National Oceanographic and Atmospheric Administration (NOAA) initiate an environmental assessment program for the northeastern Gulf of Alaska. This program was expanded in 1975 to encompass other areas of the Alaskan continental shelf including the Beaufort Sea. These studies were initiated to establish a basis for predicting and assessing

the environmental impact of petroleum development.

The objectives of the Outer Continental Shelf Environmental Assessment Program (OCSEAP), as it is called, are the following:

- 1- to describe the distribution and abundance of major biological components of the marine ecosystem for predicting qualitatively the possible impacts of major accidents
 - 2- to establish the baseline levels of major contaminants in the natural environment
 - 3- to provide improved circulation models for the Alaskan shelf and new insights into the dynamics of ice movement and other pollutant transport mechanisms
 - 4- to fill in some of the major gaps in understanding the systematic effects of target pollutants on selected arctic and subarctic biota
- and 5- to improve capabilities for assessing hazards that the Alaskan marine environment presents to development.

It is under this last objective that research on subsea permafrost is being conducted.

Permafrost poses a number of hazards to the exploration and development of petroleum reserves in the offshore environment. Among these are:

- 1- ruptured pipelines and well casings, and damage to drilling and production structures, resulting from differential freezing and thawing
- 2- blowouts and fires caused by the presence of "gas hydrates." These solid compounds of gas (mainly methane) and ice produce a sudden evolution of gas upon heating known as a "gas kick." This kick must be contained during drilling operations.
- 3- corrosion and weakening of metals in drilling

and production structures, and in pipelines, well casings, etc., due to the concentrated brines often associated with permafrost

and 4- erroneous interpretation of seismic data due to the increased seismic velocity of ice-bonded sediments. This may cause offshore production and distribution facilities to be improperly designed.

To help cope with these problems and to form a basis for environmental decisions and regulations, present studies on permafrost are aimed at:

1- developing maps portraying the occurrence of offshore permafrost including the depth to the ice-bonded permafrost table and the thickness of the ice-bonded permafrost layer

2- determining the properties of subsea permafrost including its engineering characteristics

and 3- developing models for predicting the occurrence of both relict and equilibrium permafrost.

This latter objective involves evaluating the relationship between permafrost and various factors including temperature, water and ice content, mass transfer processes such as subsurface fluid migration, sedimentation rates and erosion, past climatological and geological history, terrestrial heat flow, depth of burial, properties of the sediment, and salinity and chemical composition of the interstitial water.

The objectives of the present study are related to these latter two factors, i.e., the salinity and chemical composition of the interstitial water. They are:

1- to define the salinity and chemical composition of the interstitial water in an area where other detailed studies are being conducted. These

studies will form a basis for evaluating any models that are developed to predict the occurrence of subsea permafrost

2- to gain insight into the processes which may have affected the chemical composition and salinity of the interstitial water

and 3- to confirm the presence of ice-bonded permafrost in boreholes drilled in Prudhoe Bay.

ANNUAL REPORT

Contract: 03-50-022-67, No. 5
Research Unit: 98
Reporting Period: 1 April 1977-
31 March 1978
Number of Pages: 9

DYNAMICS OF NEAR SHORE ICE

Robert S. Pritchard
Research Scientist

Polar Science Center
Division of Marine Resources
University of Washington
Seattle, Washington 98195

March, 1978

CONTENTS

	Page
I. Summary	1
II. Introduction	1
III. Current State of Knowledge	3
IV. Study Area	3
V. Sources, Methods and Rationale of Data Collection	4
VI. Results	4
VII. Discussion	4
VIII. Conclusions	7
IX. Summary of Fourth Quarter Operations	7
Figure 1. Monthly Displacements of Chukchi Sea Ice Cover - 1977	5
Table I. Positions of Drifting Buoys Deployed over Continental	9

I. Summary

The objective of the work reported is to study the dynamics of the near shore ice on the continental shelf of the Beaufort and Chukchi Seas. Specifically, Chukchi Sea ice motions are presented from March to September 1977, and the deployment of additional buoys in March 1978 is discussed.

Drift of the Chukchi Sea ice cover during March-September 1977 is generally northward. At this time, the observed ice motions could not advect oil or other pollutants spilled in the ice into the Bering Sea. Instead it is conjectured that this ice eventually entered the transpolar drift stream.

The ice drift data presented in this report add to our knowledge of the arctic environment. The data provide an example of the large-scale transport of oil spilled in ice. But there are other benefits also. The data can be correlated with atmospheric conditions by using a plastic sea ice model. This model has been shown to simulate ice dynamics accurately, and can be used to determine ice motions that occurred for the period when barometric pressure maps are available. Furthermore, this same model, if chosen properly, can help predict loads that could be exerted on marine structures operating in these waters. These problems of ascertaining motions and loads are currently of importance to the petroleum development of the arctic offshore.

Also, an array of buoys were deployed successfully in March 1978 on the continental shelf of the Beaufort and Chukchi Sea from Cape Lisbourne to east of Point Barrow. These drifting buoys are expected to determine the near shore motions that might be the cause of frequent polynyas and leads in this region that are attractive habitat for migrating mammals and birds.

II. Introduction

A. General Nature and Scope of Study

The purpose of this project is to determine from drifting buoys and model calculations the large-scale behavior of the ice cover in the Beaufort and Chukchi Seas. The work during the past year has been limited to observations of ice motion by buoys deployed on and drifting with the ice cover. One set of six buoys were deployed in March 1977 to determine the general motion of the Chukchi Sea ice cover through the summer melt season (into September 1977). It is expected that this motion can be correlated with the position of the ice edges to determine the relative importance of dynamic and thermodynamic

effects in causing the ice edge to move. Knowledge of this motion will also allow future testing of ice model performance in this region. At this same time, two additional buoys were deployed near Prudhoe Bay in the Beaufort Sea to help determine motion over the continental shelf in this region. Another set of four data buoys were deployed in March 1978 over the continental shelf in the Beaufort and Chukchi Seas from east of Point Barrow to Cape Lisbourne. This region is of special interest because large recurring leads and polynyas seem to provide ideal habitat for migrating mammals and birds.

B. Specific Objectives

The specific objectives of this report are (1) to present the motions observed throughout the Chukchi Sea during March-September 1977 and (2) to describe the March 1978 deployment of buoys over the continental shelf from Barrow to Lisbourne.

C. Relevance to Problems of Petroleum Development

Observations of ice motions are relevant to problems of petroleum development for two broad reasons: (1) the ice cover will serve as a carrier of any petroleum products spilled in either the Beaufort or Chukchi Sea so that ice trajectories serve as the first estimate of the paths to be taken by the oil; and (2) the ice motion is an observable quantity that may be compared with simulated values to test the performance of an ice dynamics model which in turn may be used to determine a range of ice motions in a variety of environmental conditions. Although observed motions are limited by the short life of the OCSEA Program, the data must be acquired and related to atmospheric conditions (work performed during AIDJEX and other efforts have proved that winds provide the primary driving force over much of the Arctic ice cover). By using the data to prove that a mathematical ice dynamics model can simulate ice motions accurately, the historic atmospheric surface pressure maps provide a long-term (since 1946) statistical basis for defining mean and extreme conditions.

The ice motion data in the Chukchi Sea (both area wide and over the continental shelf) is particularly important because of its proximity to the Bering Sea which is a rich ecosystem that must be protected from pollution because of its high biological productivity. Since there are known to be breakouts of

Chukchi Sea ice into the Bering Sea, an understanding of this dynamic condition is needed.

III. Current State of Knowledge

Air droppable buoys (ADRAMS) have been developed to the point where they may be purchased as off-the-shelf items at reasonable cost (\$5,000) and be expected to provide data for the design life of batteries. In addition, a barometer (cost \$2,500) may be added to sense the surface pressure. Data transmission currently uses the Random Access Measurement System (RAMS) aboard the NIMBUS satellite. There is no way to sense ocean currents with these buoys. This shortcoming may be circumvented when currents are necessary if personnel can be set down on the ice. In this case a spar buoy can be deployed utilizing the same tracking and data transmission system.

The buoys purchased during FY 1978 represent the third set deployed as part of OCSEAP. The first set provided drift data in the southern Beaufort Sea in conjunction with the AIDJEX project during October 1975 - December 1976. Four of these buoys were spar buoys with ocean current meters on them. These trajectories were reported in the 1977 Annual Report, Vol. XVI, by Untersteiner and Coon (RU 98). The second set were deployed in the Chukchi Sea during March 1977 - September 1977 and trajectories are reported in the OCSEAP Principal Investigators Reports of January-March 1978. The third set has just been deployed (March 1978) and trajectories will be reported at a later date. Other ice drift data are available in the central Arctic from Russian drifting stations and from the drift of ice island T-3. Furthermore, a set of 17 RAMS buoys are presently being deployed on the continental shelf in the eastern Canadian Basin as part of a Canadian program. Except for a few isolated drift stations and buoys, this represents the current extent of knowledge of ice drift from surface-based sensors. Some additional work has been done to determine ice drift from LANDSAT imagery, but there are few useful data sets available.

IV. Study Area

Beaufort and Chukchi Seas.

V. Sources, Methods and Rationale of Data Collection

The buoys and sensors used in this work and the rationale for their choice is unchanged from last year. The description remains unchanged from that found in the OCSEAP Annual Report for 1977 [Untersteiner and Coon, RU 98].

VI. Results

Positions of the eight buoys deployed in March 1977 (six in the Chukchi Sea and the remaining two near Prudhoe Bay) have been edited and interpolated to determine daily values. These results were presented by A. S. Thorndike in a report entitled "Measurements of Sea Ice Motion, January 1977 to September 1977" in the OCSEAP Principal Investigators' Reports of January-March 1978. In addition to these daily positions, the trajectory of each buoy is presented graphically. In addition, trajectories of all buoys in the Chukchi Sea (two of which were deployed as part of AIDJEX) are superposed on one map presented as Figure 1. On this chart monthly displacements are used to compose each trajectory. This same presentation was used in the Beaufort Sea Synthesis Report to describe ice trajectories in the Beaufort Sea [OCSEAP, Special Bulletin No. 15]. For the presentation of Chukchi Sea ice drift we have used different symbols to identify displacements during different months for all buoys in an attempt to clarify the history of the observed motions. The trajectory of the buoy located nearest the Bering Strait is for March only. Its displacement is too small to show clearly which symbol is appropriate.

Initial positions of the four buoys deployed in March 1978 are shown in Figure 1. The solid circle indicates the buoy that contains a barometer. Initial positions and early drift of these buoys are indicated in Table 1.

VII. Discussion

In trajectories in the Chukchi Sea during 1977 (Figure 1) all were northward during spring and summer months, except during March when small motions occurred toward the Bering Strait. This motion is thought to be typical of the Chukchi Sea from this time of year. A few weeks prior to the deployment there was motion to the south (seen by NOAA satellites), but there were no quantitative observations. This knowledge is important to indicate where oil would be advected by the ice cover if it was spilled. During this time period

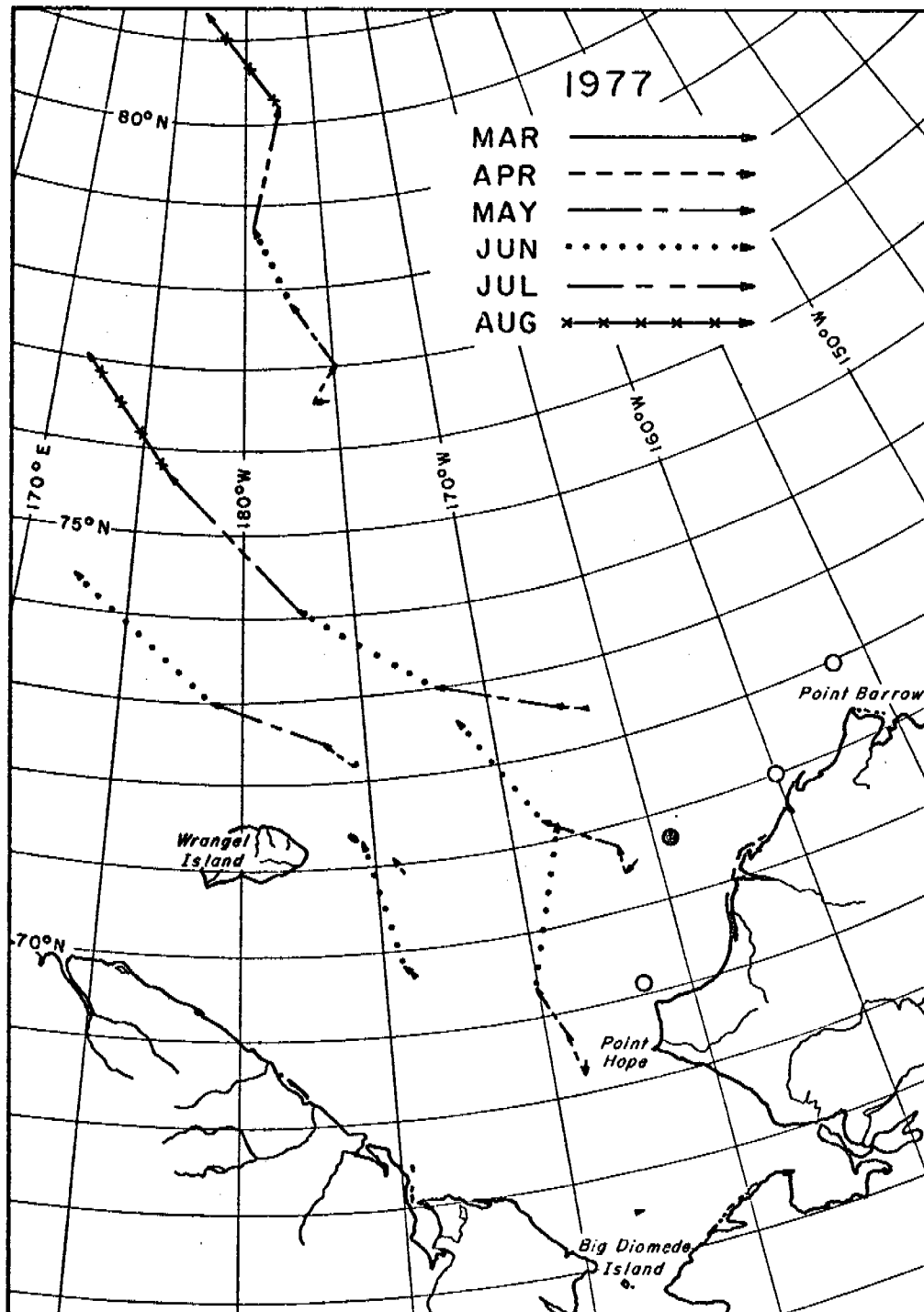


Figure 1. Monthly Displacements of Chukchi Sea Ice Cover - 1977

the drift data demonstrate that there would be no transport of oil from the Chukchi Sea into the Bering Sea (this statement assumes that the oil is spilled at least 80 km north of the Bering Strait, the southernmost site of observations). Also it appears that the Chukchi Sea ice cover drifted far enough to the west that it would eventually enter the transpolar drift stream and not enter the Beaufort Gyre--although this is conjecture.

During the coming spring and summer (March-September 1978) the drift of ice over the continental shelf of the Chukchi Sea will be observed. This information will be important for determining how far south oil can be advected from the Beaufort Sea near Barrow south into the Chukchi Sea.

Ice motions provide a hazard both because the ice can advect oil in and under it and because the mobile ice can apply large loads on marine structures operating in the area. The data base on ice motions in the Arctic is small, but growing. We must continue to expand this data base by deploying arrays of buoys in the future. Our aims in this program must remain as stated last year: to increase geographic coverage, to obtain data at different times of the year, to determine season-to-season and year-to-year variability, and to understand what causes the variability. This last problem must be addressed primarily by continuing to develop mathematical models of the atmosphere, ice and ocean that allow simulation of the ice dynamics. In this task the ice motions observed by drifting buoys serve to test performance of the models. The models, with proven performance, can then be used to simulate a range of conditions anticipated over the producing lifetime of the Alaska offshore petroleum fields.

As part of the continuing buoy deployment program it shall be necessary to monitor barometric pressure and ocean currents. In addition, thought should be given to measuring surface winds. Also, there is at present a severe shortage of data on ocean currents in regions where ice dynamics is of interest. Since ocean currents are capable of moving the ice just as effectively as winds, this shortcoming is a serious problem. An understanding of the near shore ice dynamics must eventually rest upon simultaneous wind, ice drift and ocean current measurements. The barometric pressure is necessary to help determine widespread geostrophic flow in the atmosphere; and it is this average, not the local winds, that controls motion of the ice cover. Our understanding of the averaging effects of the ocean is less complete, but the physics of the ice behavior requires a similar relationship.

VIII. Conclusions

Drift of the ice cover in the Chukchi Sea during March-September 1977 has been determined. The generally northward motion would have precluded oil spilled on or in the ice from being transported into the Bering Sea at this time. However, earlier motions to the south have not been determined. By using an appropriate ice model these motion observations can be correlated with the motions determined by radar transponder at the Bering Strait and with the wind and current fields to aid our understanding of the ice dynamics.

More data on ice drift are needed to extend temporal and spatial coverage. These additional buoy arrays should be deployed each year to assess year-to-year variability. Times and locations of deployment as well as the sensors included on each buoy, should be coordinated with modeling and other projects in OCSEAP.

The deployment of four buoys in the continental shelf area of the Chukchi Sea was successful. All sensors are functioning accurately. In addition, the decision to attempt to find the one buoy stranded near Karluk Island from the 1977 deployment was wise since the buoy was retrieved at nominal cost to OCSEAP.

IX. Summary of Fourth Quarter Operations

A. Field Activities

The array of buoys over the continental shelf of the Chukchi Sea was deployed between March 12-15, 1978. Early positions and drift are presented in Table 1. Mr. Pat Martin, a consultant from Martin Marine, performed the work with the help of OCSEAP and NARL support personnel. Nominal initial locations of these buoys are shown in Figure 1 as circles near the Alaska coast of the Chukchi Sea. The buoy with a pressure sensor is shown shaded. The performance of all sensors has been tested by telephone communications with NASA. The barometer was checked against NWS readings at Barrow and the manufacturer's calibration found accurate.

The buoys were purchased with parachutes so that they could be dropped from a fixed wing aircraft without landing on the ice. However, good weather and ice conditions coupled with availability of the NARL Cessna 180 permitted the deployment party to land. Parachutes were removed and turned over to OCSEAP for use with future programs.

With the agreement of Dr. Gunter Weller, another attempt was made to retrieve a buoy deployed during 1977 that was known to be located at the landward edge of Karluk Island. Mr. Martin did locate the buoy, returning it to OCSEAP. It is hoped that this buoy can be repaired and used for future programs.

Two important milestones for this project have now been met. These are (1) contract and purchase of buoys, February 1978; and (2) deployment of buoys, March 1978.

B. Problems Encountered/Recommended Changes

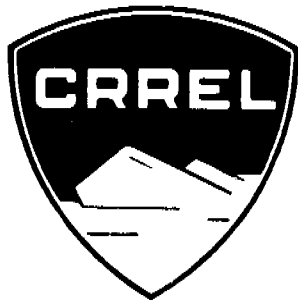
There were no important problems encountered in this field program.

Table I. Positions of Drifting Buoys Deployed over Continental Shelf of Chukchi Sea during March 1978

Date	Time GMT	Buoy Identifier	Latitude (°N)	Longitude (°W)
12 Mar	2004	0413	71.98	156.45
12 Mar	2004	1003	71.05	159.77
12 Mar	2004	0425*	70.72	164.38
16 Mar	0304	0413	71.86	156.75
15 Mar	2100	1003	70.76	160.62
15 Mar	2100	0425	70.64	164.23
18 Mar	--	1301	69.2 †	166.5 †
30 Mar	0736	0413	71.79	158.57
30 Mar	0737	1003	70.45	162.64
30 Mar	0737	0425	70.22	165.64
30 Mar	0739	1301	68.58	167.66

* Buoy number 0425 contains a barometer.

† This is an estimated position. This buoy was deployed on 15 March. However, a party working in the area on 17 March found the buoy and retrieved it. Fortunately, the buoy was redeployed on 18 March in the same region by this party.



Contract no. - 01-5-022-2313
Research Unit no. - RU105
Reporting period - 1 April 1977 -
31 March 1978
Number of pages - 24

ANNUAL REPORT

DELINEATION AND ENGINEERING CHARACTERISTICS OF
PERMAFROST BENEATH THE BEAUFORT SEA

Principal Investigators:

P. V. Sellmann
E. Chamberlain

Associate Investigators:

S. Arcone
S. Blouin
A. Delaney
I. Iskandar
F. Page

1 April 1978

CORPS OF ENGINEERS, U.S. ARMY
COLD REGIONS RESEARCH AND ENGINEERING LABORATORY
HANOVER, NEW HAMPSHIRE

Approved for public release; distribution unlimited.

I. SUMMARY

The objective of CRREL's subsea permafrost program is to obtain specific information on the distribution and engineering characteristics of permafrost beneath the Beaufort Sea. Observations include determinations of subsea sediment temperature, type, ice content, and chemical composition. These data, coupled with geophysical studies and results from other Beaufort Sea geological studies, are being used jointly to ascertain subsea permafrost distribution. This report includes a summary of the spring 1977 field program and a general summation of the results from two years of field study in the Prudhoe Bay area.

The 1977 field study produced six additional drilled and sampled holes plus 27 probe sites which yielded both material property and temperature data (Fig. 1). The field observations and the results of laboratory analyses of the samples help to demonstrate the complex nature of subsea permafrost.

Thermal data from the probe and drill holes indicate that permafrost exists in all of the sites examined. In water depths greater than 1.5 m, evidence of ice-bonded sediment was found in drill holes PB-2, PB-3, PB-6 and PB-7, and probe holes PH-26 and PH-27 (Fig. 1). In water shallower than 1.5 m, ice-bonded sediment below the seasonally frozen zone is common (Osterkamp and Harrison, 1976).

The new probe used during the 1977 field season was extremely helpful in characterizing material properties and providing thermal data. The combined data helped to define areas where sediments are seasonally frozen as well as perennially ice-bonded. The profiles shown in Figure 2, which summarizes the results of several of the OCSEAP projects, help to illustrate the variation in the position of ice-bonded sediment with distance from shore along the Prudhoe study line. The extreme variability in the position of the bonded sediment appears, in part, to be related to the properties of the sediments in the area. Some sediments are very coarse-grained and were possibly undersaturated prior to inundation, providing an opportunity for very rapid movement of salty water into the sediment. In other areas, such as north of Reindeer Island, the sediment is fine-grained and may greatly reduce the rate of salt transport.

The pore water chemistry studies coupled with the thermal data provided extremely good control on the position of ice-bonded sediment. Calculated freezing point values for the pore water and the measured thermal data helped to confirm the position of the ice-bonded sediments indicated in Figure 2a.

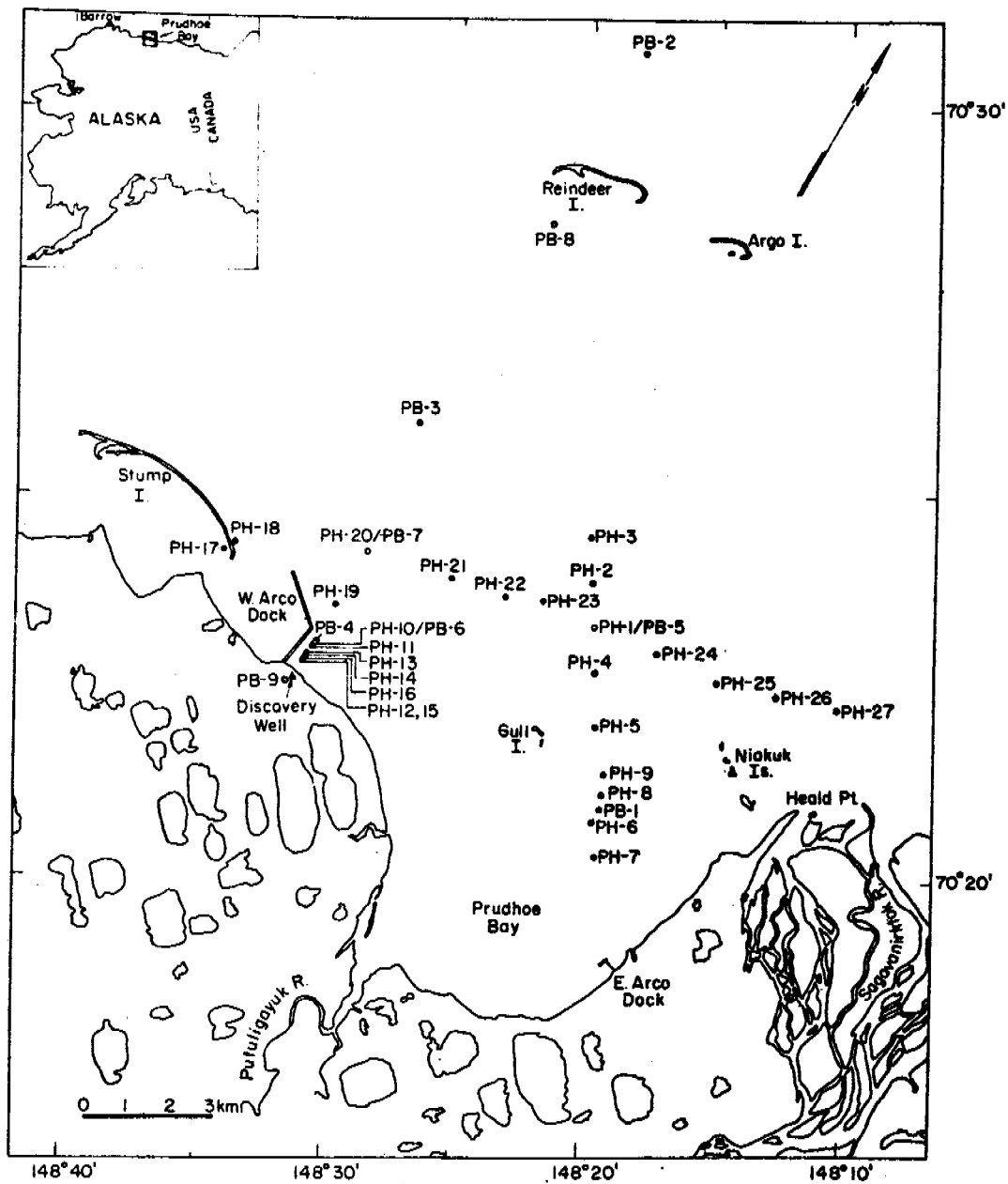


Figure 1. Site locations in Prudhoe Bay, Alaska. PB indicates drill holes; open circles indicate holes drilled during the 1977 season (PB 5-9) and closed circles indicate holes drilled during the 1976 season (PB 1-4). PH indicates probe holes.

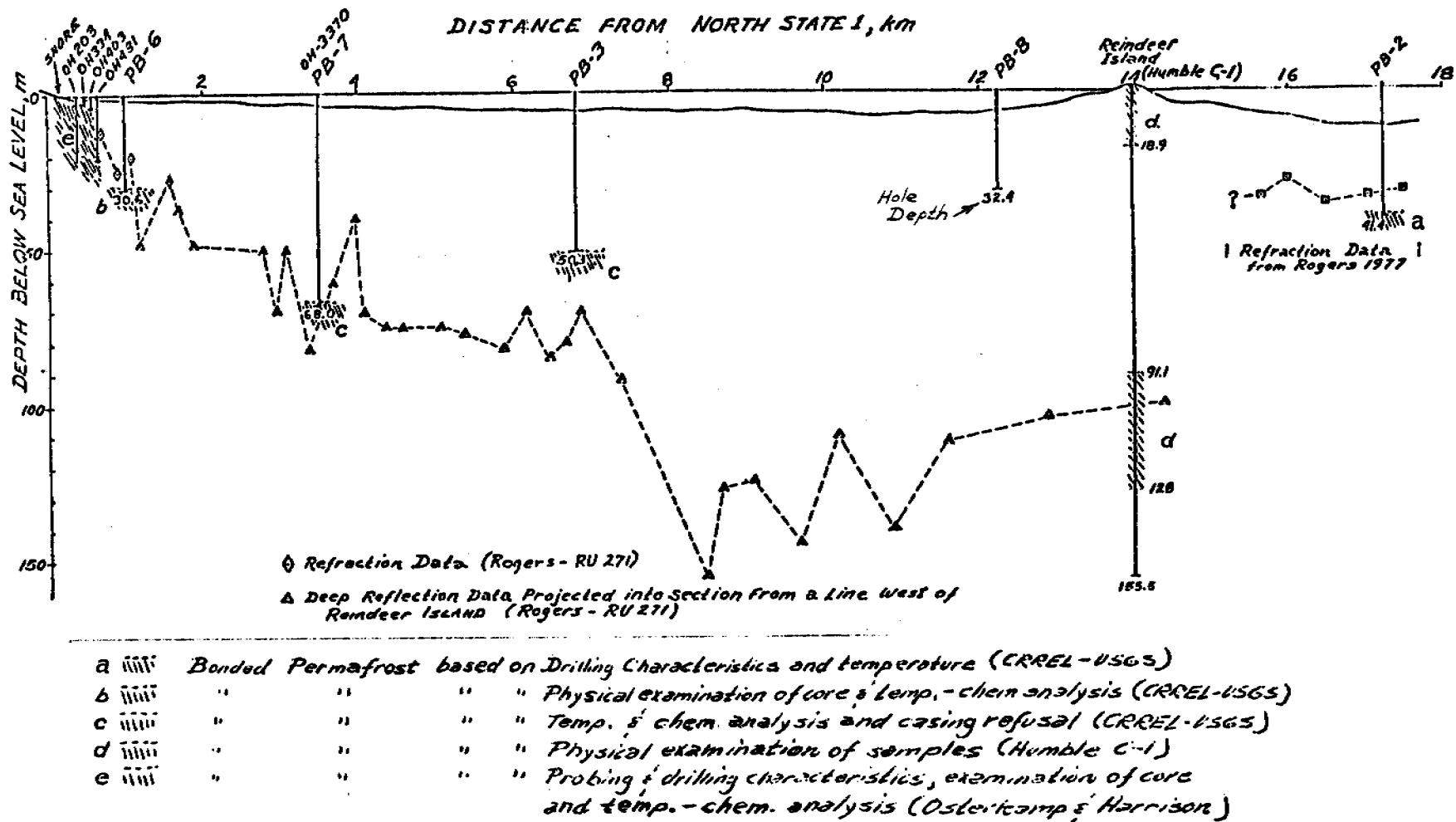


Figure 2. Summary of results of several OCSEAP studies.

- a. Position of ice-banded sediments, along the Prudhoe study line from the West ARCO dock through Reindeer Island.

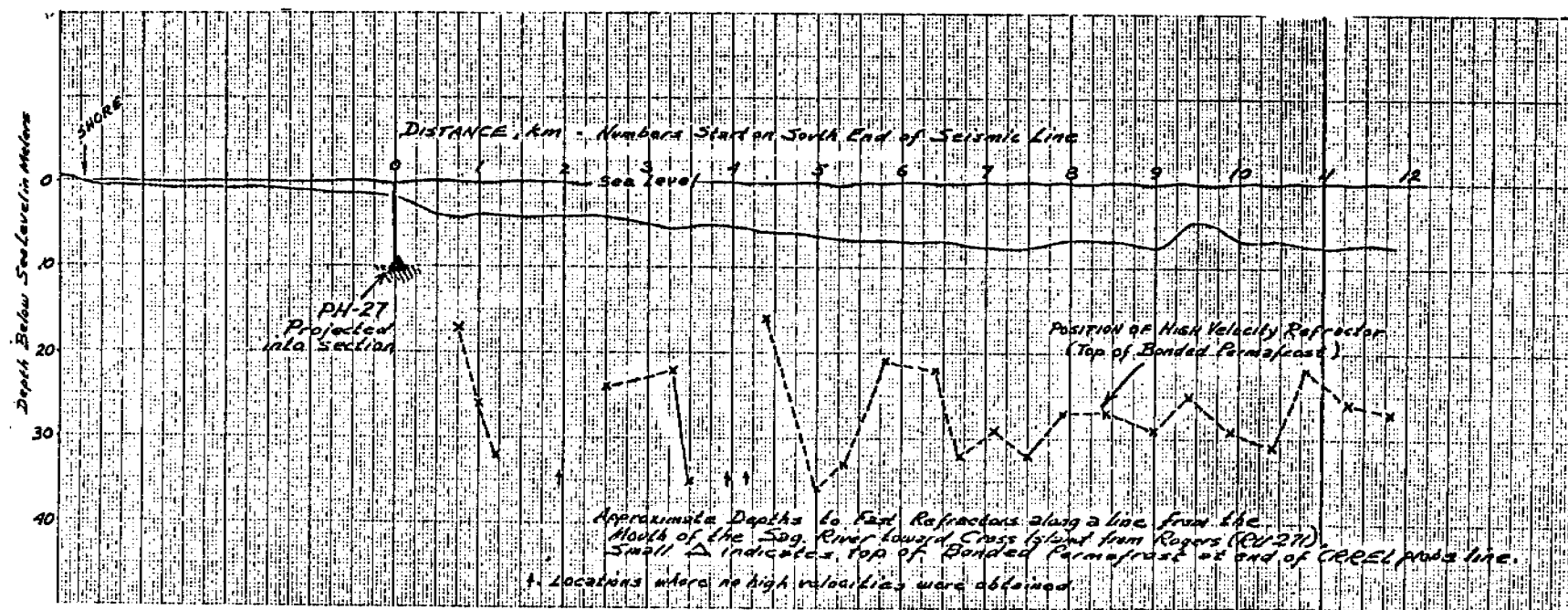


Figure 2. (cont'd.)

b. Position of bonded permafrost off the Sagavanirktok River Delta.

The greatest variation in the chemistry of the pore water (salinity) takes place in the fine-grained material located near the surface of the sea bed. These variations are probably related to salt enrichments caused by the formation of both sea and interstitial ice and may also be related to large seasonal changes in sea water chemistry to which the sediments are exposed. Below the upper few meters of sediment the chemical composition of the pore water is fairly uniform with depth.

The most significant results to date from the engineering property studies appear to be the laboratory confirmation of the existence of overconsolidated clay-rich sediment in the study area. The occurrence and distribution of these stiff clays are of importance in 1) design and location of offshore structures, 2) determining the types of techniques required for emplacing facilities and pipelines into the bed, and 3) determining excavation modes required when attempting to utilize gravels that can occur under the clays.

The variable depth to ice-bonded permafrost will also require detailed evaluation when specific designs are proposed for facilities that could cause thaw of these sediments and possible associated settlement.

II. INTRODUCTION

CRREL's major involvement in the BLM-NOAA-OCSEAP subsea permafrost program was designed to provide samples and data necessary for characterizing the engineering, thermal and chemical properties, history, and distribution of subsea permafrost in an offshore environment considered to be fairly typical of much of this eastern Alaska Beaufort Sea coast. This was accomplished through joint study with the USGS and University of Alaska OCS projects, and Robert Lewellen's ONR subsea permafrost studies, which were previously based at Barrow. This year's efforts concluded CRREL's two-year field study at Prudhoe Bay, which consisted of drilling, sampling and probing programs. The work since the completion of the spring 1977 program has comprised chemical and engineering tests and analyses in the CRREL laboratory. This work is essentially completed. Major reporting has been completed with all reports in final draft form except one covering the remaining engineering property analysis.

The field program, which involved rotary drilling, drive sampling and shallow probing using the spring ice cover as a stable platform, was covered in our 1977 operational report (Sellmann et al., 1977). The results of this effort, combined with results of the other OCSEAP projects, can provide a basis for extrapolating some general facts concerning offshore permafrost from the Prudhoe area to other areas along the Beaufort Sea coast. New work that is just being undertaken will involve

examination and evaluation of commercially acquired seismic data to obtain additional information on the upper surface of bonded permafrost.

The specific objectives of this program are listed below and remain essentially the same as those stated in last year's report. The only significant change is the transition from the drilling program to the pilot study of offshore seismic data.

- a. Drill and sample subsea permafrost in Prudhoe Bay, and provide access holes for USGS temperature logging.
- b. Conduct laboratory studies to establish engineering properties of samples obtained.
- c. Conduct a chemical analysis of the pore water extracted from designated sediment samples.
- d. Evaluate and obtain additional engineering and thermal data from the subsea sediments through development and use of probing techniques.
- e. Examine commercial seismic data to provide more regional information on the position of the top of bonded permafrost.

The irregular distribution and unknown thaw consolidation characteristics of the bonded subsea permafrost will require continual consideration and understanding of permafrost for every offshore development project. This would be increasingly important for those projects that can in some way alter the thermal setting and cause thawing of the sediment. The results of this and other subsea permafrost projects hopefully will provide the basis for development of appropriate constraints and guidelines and will provide some background data for industry-sponsored, site-specific investigations undertaken at least when each major offshore development activity is planned.

III. CURRENT STATE OF KNOWLEDGE

The current state of knowledge of the U.S. Beaufort Sea has an extremely limited base. The existing data are based on several recent and fairly local studies. The NOAA program has provided some detailed data from Prudhoe Bay which is in part summarized in Figure 2. These data conceivably provide some indication of the types of conditions that can be anticipated along the eastern Alaska portion of the Beaufort coastline. Additional probing work undertaken by Osterkamp and Harrison helps to establish some control west of this area but is restricted to observations at a few study sites (see their annual report). The only other known non-industry data are available from the Navy (ONR) program conducted near Barrow by Lewellen.

Industry activities have resulted in several holes through subsea permafrost in this region, although the data from these activities are not generally available.

The existing NOAA and past ONR studies indicate permafrost is widespread on the continental shelf, and a summary of this information is provided in the OCSEAP Synthesis Report.

This year's study at Prudhoe indicates that bonded sediments can occur at depths of as little as 10 m below the seabed in water 2 m deep. Bonded sediment at shallow depths of 20-30 m below the sea bed in water depths greater than 2 m also appear to be confirmed by a seismic study conducted by Rogers (RU271) and our hole north of Reindeer Island. These results indicate that increased depth to bonded permafrost with increased water depth can not be assumed, particularly in areas of extremely variable lithology.

IV STUDY AREA

The sites for the 1977 drill program were selected jointly by USGS and CRREL personnel. They were situated in areas where obvious gaps existed in data from previous drilling activities. The probe sites were selected based on an attempt to obtain data from most of the depositional environments in the Prudhoe Bay area. Probe data were collected along three lines normal to the coast. The shortest, most western line was off Stump Island; the middle line was part of the line off the west ARCO dock; and the third line extended offshore east of Gull Island. A long line was also established normal to these from Stump Island to the Sagavanirktok River delta along the 2-m bathymetric contour. The locations of the drill and probe sites are given in Tables I and II along with information on ice thickness, water depth, and maximum depth of penetration.

Information has also been compiled on the distribution of commercially available seismic data. This information is being used to determine which areas along the coast will be examined as part of the new study employing seismic data to delineate the top of bonded permafrost.

V. SOURCES, METHODS AND RATIONALE OF DATA COLLECTION

The 1977 field program drilling and sampling operation was similar to last year's, covered in the annual report. The details of sampling techniques and procedures used this season are covered in CRREL Special Report 77-41, entitled 1977 CRREL-USGS Subsea Permafrost Program, Beaufort Sea, Alaska--Operational Report. All sampling was done using drive sampling techniques in both fine- and coarse-grained material. The most significant difference over the previous year's operation, and the factor that permitted deeper sampling, was the use of an air-driven

TABLE I

DATA FOR 1977 PRUDHOE BAY CRREL-USGS DRILL LOCATIONS

<u>Hole</u>	<u>General Location</u>	<u>Latitude</u>	<u>Longitude</u>	<u>Ice Thickness (m)</u>	<u>Water Depth (m)</u>	<u>Hole Depth (from ice surface) (m)</u>
PB-5	2.8 km NE of Gull Island	70°23.3'	148°19.7'	1.50	1.75	11.8
PB-6	1.0 km NE of Discovery Well	70°23.05'	148°30.6'	1.80	1.85	8.2
PB-6A	1.0 km NE of Discovery Well	70°23.05'	148°30.6'	1.80	1.85	30.6
PB-7	3.5 km NE of Discovery Well	70°24.25'	148°28.5'	1.81	2.86	68.0
PB-8	1.3 km SW of Reindeer Island	70°28.5'	148°21.6'	2.18	6.98	32.4
PB-9*	0.3 km SW of Discovery Well	70°22.55'	148°31.6'	land	land	19.1

* PB-9 was drilled and sampled by R&M Engineering and is located on land.

TABLE II.

DATA FOR 1977 PRUDHOE BAY CRREL PROBE LOCATIONS

<u>Hole</u>	<u>General Location</u>	<u>Latitude</u>	<u>Longitude</u>	<u>Ice thickness (m)</u>	<u>Water depth (m)</u>	<u>Maximum penetration (m)</u>
PH-1	2.8 km NE of Gull Island	70°23.3'	148°19.7'	1.83	1.98	11.8
PH-2	3.7 km NE of Gull Island	70°23.85'	148°19.8'	1.83	3.15	12.3
PH-3	4.7 km NNE of Gull Island	70°24.4'	148°19.85'	1.52	3.23	12.9
PH-4	1.9 km NE of Gull Island	70°22.7'	148°19.7'	1.52	1.52	13.3
PH-5	1.4 km E of Gull Island	70°21.9'	148°19.6'	0.90	0.90	7.5
PH-6	3.3 km SSE of Gull Island	70°20.7'	148°19.7'	1.75	2.93	14.1
PH-7	2.6 km SSE of Gull Island	70°20.3'	148°19.5'	1.60	2.43	15.1
PH-8	2.6 km SE of Gull Island	70°21.2'	148°19.3'	1.50	1.69	10.3
PH-9	2.2 km SE of Gull Island	70°22.55'	148°31.9'	1.28	1.28	15.4
PH-10	1.0 km NE of Discovery Well	70°23.05'	148°30.6'	1.68	2.12	11.3
PH-11	0.8 km NE of Discovery Well	70°22.95'	148°30.8'	1.68	1.73	12.3
PH-12	0.5 km NE of Discovery Well	70°22.85'	148°31'	0.91	0.91	1.3
PH-13	.63 km NE of Discovery Well	70°22.95'	148°30.9'	1.56	1.56	8.4
PH-14	.57 km NE of Discovery Well	70°22.9'	148°30.9'	1.53	1.53	12.2
PH-15	0.5 km NE of Discovery Well	70°22.85'	148°31'	0.69	0.69	1.2
PH-16	0.54 km NE of Discovery Well	70°22.87'	148°31'	1.35	1.35	9.9
PH-17	0.12 km inland from Stump Is.	70°22.25'	148°34.1'	0.91	0.91	4.5
PH-18	0.12 km seaward from Stump Is.	70°24.3'	148°33.7'	1.83	1.94	11.3
PH-19	2.0 km NE of Discovery Well	70°23.5'	148°29.75'	1.80	1.95	10.6
PH-20	3.5 km NE of Discovery Well	70°24.25'	148°28.5'	1.80	2.06	11.1
PH-21	4.2 km NW of Gull Island	70°23.9'	148°25.3'	1.70	1.88	8.3
PH-22	3.3 km NW of Gull Island	70°23.65'	148°23.2'	1.85	2.17	10.9
PH-23	3.2 km N of Gull Island	70°23.6'	148°21.7'	1.60	2.13	11.2
PH-24	3.2 km NW of Niakuk Island	70°22.9'	148°17.3'	1.80	2.03	10.7
PH-25	1.5 km N of Niakuk Island	70°22.6'	148°15'	1.80	2.00	11.6
PH-26	1.9 km NE of Niakuk Island	70°22.4'	148°12.7'	1.80	1.83	10.0
PH-27	2.5 km NE of Heald Point	70°22.2'	148°10.4'	1.65	1.89	14.6

casing hammer and larger, heavy duty casing. The casing hammer and larger casing were used to replace the drop-hammer in the deeper holes. The hammer was rated at 1356 N-m₃ (1000 ft-lb)₃ of energy per blow and 300 blows/min, and required a 7.08-m³/min (250-ft³/min), 6.89 x 10⁷-Pa (100-psi) air compressor for its air supply. This hammer was adapted to the existing drill rig. The new casing was 11.4 cm (4-1/2 in.) O.D. by 9.5 cm (3-3/4 in.) I.D. flush-joint. This additional equipment greatly improved the drilling operation.

The sample-handling and field logging were also similar to last year's program, with the exception that all samples collected for chemical analysis were shipped directly to CRREL's laboratory in Fairbanks for initial processing and chemical analysis. This was done to avoid temperature fluctuations and reduce the time between sampling and analysis.

All drilled holes on completion were cased with 5-cm (PVC) casing for thermal logging purposes. The measurements were made at these sites by USGS personnel using a thermistor probe. Results of this study are covered by USGS reports.

Results of the experimental probe program initiated during 1976 were successful enough to encourage further probe development and an expanded field program during this year. The probe equipment used this year was designed for rapid acquisition of engineering data, including thermal profiles. The primary testing mode used with this penetrometer device was static, although dynamic capability was included. The testing equipment was housed completely in a 1.52 x 2.59 m (5 x 8 1/2 ft) building mounted on a ski base. Time-consuming anchor setting was eliminated by parking the tractor on the ski extensions, providing needed reaction force. The small enclosure contained all the equipment for electrical data acquisition. The penetration resistances of the casing and probe string were plotted independently as a function of depth on an X-YY recorder. Temperature data were obtained through the probe string after the fluid-filled column came to equilibrium, which usually required approximately 6 to 8 hours. For additional details see the 1977 Operational Report.

Sediment samples from holes PB-5 through PB-9 were shipped to the CRREL laboratory in Fairbanks for preliminary chemical analysis. Interstitial water was extracted from each of the sediment samples by centrifugation (2000 rpm for 15 minutes), using commercially available filtering centrifuge tubes. The water was analyzed immediately for conductivity, alkalinity and pH. Moisture contents were also determined for the sediment. The interstitial water and sediment samples were then transported to Hanover for further analysis.

In Hanover, analysis of both the extracted water and sea water samples included determination of sodium, potassium, calcium, and magnesium by atomic adsorption spectrophotometry, chloride by wet chemical titration, and sulfate after the method described in Scheide and Durst, 1977 (Analytical Letters, V.10, no.1, p. 55-65). The sediment samples were analyzed for organic carbon and calcium carbonate content, and gross mineralogy was determined by X-ray diffraction. The moisture and organic carbon contents were determined during both the chemical and engineering property studies and the results were in good agreement.

The engineering tests performed included strength, consolidation and index property determinations. The strength tests were standard undrained, unconsolidated triaxial compression tests conducted at in situ confining pressures. The index property determinations included determinations of water content, grain size, density, organic content, specific gravity and Atterburg limits. Standard consolidation tests were performed on the fine-grained samples to determine maximum past stress. Details concerning the methods employed for the above tests were given in past technical reports on this project.

A collection of plots indicating the distribution of offshore seismic data has been assembled. Several study areas were selected and a limited number of processed records have been received.

VI and VII RESULTS AND DISCUSSION

The results of almost all aspects of the 1977 field program have been covered in several formal reports:

- 1) Geochemistry of subsea permafrost at Prudhoe Bay, Alaska, MA Thesis, Dept. of Earth Sciences, Dartmouth College by F.W. Page (1978) (CRREL Report, in preparation).
- 2) Field methods and preliminary results from subsea permafrost studies in the Beaufort Sea, Alaska (extended abstract), Symposium on Permafrost Field Methods and Permafrost Geophysics, Oct. 1977, Saskatoon, Saskatchewan, by P.V. Sellmann et al. (1977).
- 3) Subsea penetrometer studies at Prudhoe Bay, Alaska, CRREL report (in review), S. Blouin et al. (1978).

Additional reporting on the previous year's study was compiled in a CRREL report entitled:

Engineering properties of subsea permafrost in the Prudhoe Bay region of the Beaufort Sea- Obtained from samples acquired during the 1976 field season, by E.W. Chamberlain et al. (1978).

The following discussion summarizes the results to date but does not include detailed listing of all data. Preprints of the reports mentioned above and those referenced last year are available upon request.

Sediment Distribution: The sediment distribution patterns were much the same as those observed in last year's work, with generally fine-grained surface sections over more coarse-grained sediments. Discussion of drill hole lithology and geology will be covered by the USGS work unit.

Engineering Probe Study: The point resistance data obtained from the static penetrometer tests provided considerable information on sediment type, vertical distribution, and strength of the subsea sediments in the area. This was confirmed by comparison of point resistance plots with adjacent drill hole logs.

The point resistance is defined as the point load divided by the projected area of the 2 1/2-in.-diameter point. The point resistance varied in the fine-grained material from a few hundred pascals (at times insufficient to keep the point from advancing under the weight of the column) to 13.7×10^5 Pa (200 psi). The point resistance in the coarse grained material varied continuously and often dramatically, with values as low as 27.5×10^5 Pa (400 psi) and commonly varying upward to 393×10^5 Pa (5700 psi), the capacity of the equipment when the standard point was used. The loose silty sand and fine-grained material in general would tend toward the lower end of the spectrum while dense, coarse gravel would lie toward the upper end. Material identification was aided greatly by the shape of the probe curves, with the coarser material developing very distinctive, irregular saw-tooth-shaped curves.

The distribution of frozen material could also be strongly inferred based on both the probe and thermal data. Both seasonally and perennially ice-bonded sediment were located. In the frozen soil it was observed that slight changes in penetration rate caused changes in load. This was not observed in the unfrozen materials and may be related to highly strain-rate-dependent strength characteristics of ice-bonded soils.

Seasonally frozen sediments were encountered in PH-12, -13, -14, -15, -16 and possibly -11. Deeper bonded permafrost was detected in PH-4, -5, -9, -26 and -27, and possibly at the bottom of PH-25. The coldest bed temperatures were encountered at PH-12 and -15, the furthest shoreward sites. Penetration at these two sites was not possible, with

refusal occurring just below the bed in this very cold, well-bonded sediment. Seaward of these sites it was possible to penetrate the frozen bed, with penetration resistance decreasing with increasing ice thickness and distance from shore, all parameters indicating warmer bed temperatures. This probe indicates that seasonally frozen sediments are absent seaward of the zone where some water exists below the ice. However, chemical analysis of interstitial water samples and thermal data from PB5-8 indicates that seasonal ice can occur in the near bed sediments much further offshore. The amounts of interstitial ice apparently are not adequate to change the sediment properties so that they could be detected by the probe. Measured temperatures in probe holes where there appears to be little question of ice-bonded permafrost were as low as -3.25°C to -3.5°C , with -2.5°C obtained at one of the questionable locations.

In the casing load study it was difficult to separate the influence of the load on the oversized casing shoe from additional load that may have resulted from collapse of soil on the casing string. A test at PH-3 was conducted without the casing shoe using a point of the same diameter [5.72 cm (2-1/4 in.)] as the casing string. In this test a significant portion of the total load on the string was needed to advance the casing. Even though a majority of the 9.75 m (32 ft) penetration was through fine grained material having almost no point resistance, the casing resistance built steadily to almost $40 \times 10^3 \text{ N}$ (9000 lb) before the point reached refusal in a gravel layer. The average shear resistance over the entire casing length was about 0.23 bar (3-1/3 psi). At many of the probe sites in areas free of bonded sediment, the soil profiles seem ideally suited for end-bearing piles founded on dense gravels. The single test at PH-3 suggests significant bearing could be generated by the side friction shear component as well.

Bonded Permafrost (Drill Holes): Permafrost temperatures were obtained in all drill and probe holes. In PB-6, ice-bonded sediments were obtained near the bottom of this 30.6-m hole. Casing refusal occurred at the base of PB-7 at approximately 68 m below sea level, suggesting that the ice-bonded permafrost interface was encountered. The occurrence of an ice-bonded interface near the base of both of these holes was confirmed by examination of both the chemical data from interstitial pore water samples and the thermal data. Calculated freezing points for the interstitial water indicate that the sediment should contain some ice in the pores near the depth where the bonded samples were obtained in PB-6 and near the point where refusal was encountered in PB-7. The minimum temperature obtained at depth in the drilled holes was -2.5°C from the bottom of PB-6. The temperature

data from the apparently bonded sediment from both the probe and drilling data indicate that temperatures range from -2.5°C to -3.5°C , although the chemistry data indicate that ice may occur in the pores at higher temperatures.

The summary of information concerning the position of bonded permafrost is shown in Figure 2, with bonded sediments as close as 10 m from the bed off the Sagavanirktok delta.

Chemistry Section: The sediments in Prudhoe Bay generally consist of a thin layer of marine muds overlying glacial and fluvial gravels. The muds are calcareous and have higher interstitial water and organic carbon contents than the gravels. On land, the gravels are overlain by sands and silts which contain large amounts of peat. Water and organic carbon contents in these sediments were much higher than those found offshore.

During the early spring of 1977, the salinity of the sea water in Prudhoe Bay varied from 33.5 to 57.3 parts per thousand (p.p.t.). The higher salinities were found near the shore where sea ice is frozen directly to, or is located near, the sea bed, or where circulation with more open water is restricted. These brines probably resulted from salt exclusion during the formation of sea ice. Further offshore, lower salinities were encountered which were approximately 1.0 to 1.5 p.p.t. less saline than normal sea water.

The in situ temperature of the Prudhoe Bay sea water samples was inferred to vary from -3.0°C to -1.75°C , based on the calculated freezing points of the water. The lower temperatures were encountered in the brines near the shore, whereas the higher temperatures were from water collected further offshore.

Compositionally, sodium, magnesium, and chloride ions in the sea water samples were present in the same proportions as for normal sea water. Calcium and potassium appeared to be enriched relative to the chloride ion concentration by about 6 and 18%, respectively, whereas alkalinity and sulfate were both depleted by about 12 to 13%.

The salinity of the interstitial water was highest near the shore where concentrated brines were infiltrating into the surficial layer of sediments. Highly saline water was also encountered immediately below sediments near the surface of the sea bed in which some of the interstitial water was frozen. Elsewhere, lower salinities were encountered which were usually within 5 p.p.t. of the salinity for normal sea water.

In the mildly reducing sediments of PB5, PB6 and PB7, proportionately more potassium, calcium, and alkalinity, and less sulfate and magnesium are found than in normal sea water. These changes in the interstitial water composition are thought to result from oxidation of organic carbon, cation exchange reactions, dissolution of calcium carbonate, weathering of potassium-rich minerals, reduction of sulfate by bacteria, and possibly replacement of magnesium for calcium in calcium carbonate. In more strongly reducing sediments (PB8), proportionately more potassium and alkalinity and less calcium, magnesium, and sulfate are found than in normal sea water. These variations may be due to the recrystallization of calcium carbonate to dolomite and the precipitation of calcium and/or calcium-magnesium carbonate, in addition to most of the other mechanisms given above.

On land (PB9), the salinity of the interstitial water varied from 0.5 to 12.5 p.p.t. In the peat layer located in the upper 2 to 3 m of the sediment column, salinity was less than 1.5 p.p.t. and the composition of the water was predominated by calcium, bicarbonate and sulfate ions. This layer is probably characterized by freezing and thawing, leaching, weathering, and the infiltration of fresh water from the surface. Below a depth of about 3 m the salinity gradually increased with depth and the composition of the interstitial water became progressively more like that of normal sea water.

In boreholes PB5-8 evidence of frozen water was found in most of the sediments located near the surface of the sea bed (Fig. 3). This partially frozen layer of sediments appeared to be up to 4 m thick in one hole. Because the sediments lacked visible ice crystals and because resistance to penetration during either drilling operations or penetration tests was not markedly different from unfrozen sediments, it is inferred that the sediments located near the surface of the sea bed were only partially frozen. Penetration tests in shallower water (less than 1.5 m) however, indicated that the sediments there were bonded to a much greater degree, as mentioned in the probe section. Concentrated brines found immediately beneath the partially frozen layer are thought to result from salt exclusion during the freezing of the interstitial water, which was also suggested by the probe study.

Engineering Properties:

Some of the most important engineering properties for sites PB-5, PB-7 and PB-8 are shown in Figures 4-7. Figure 4 shows the water content by weight, compressive strength, and grain size profiles for site PB-5. It can be seen that to a depth of approximately 8 m the sediments are dominated by non-plastic silts having high moisture contents, and

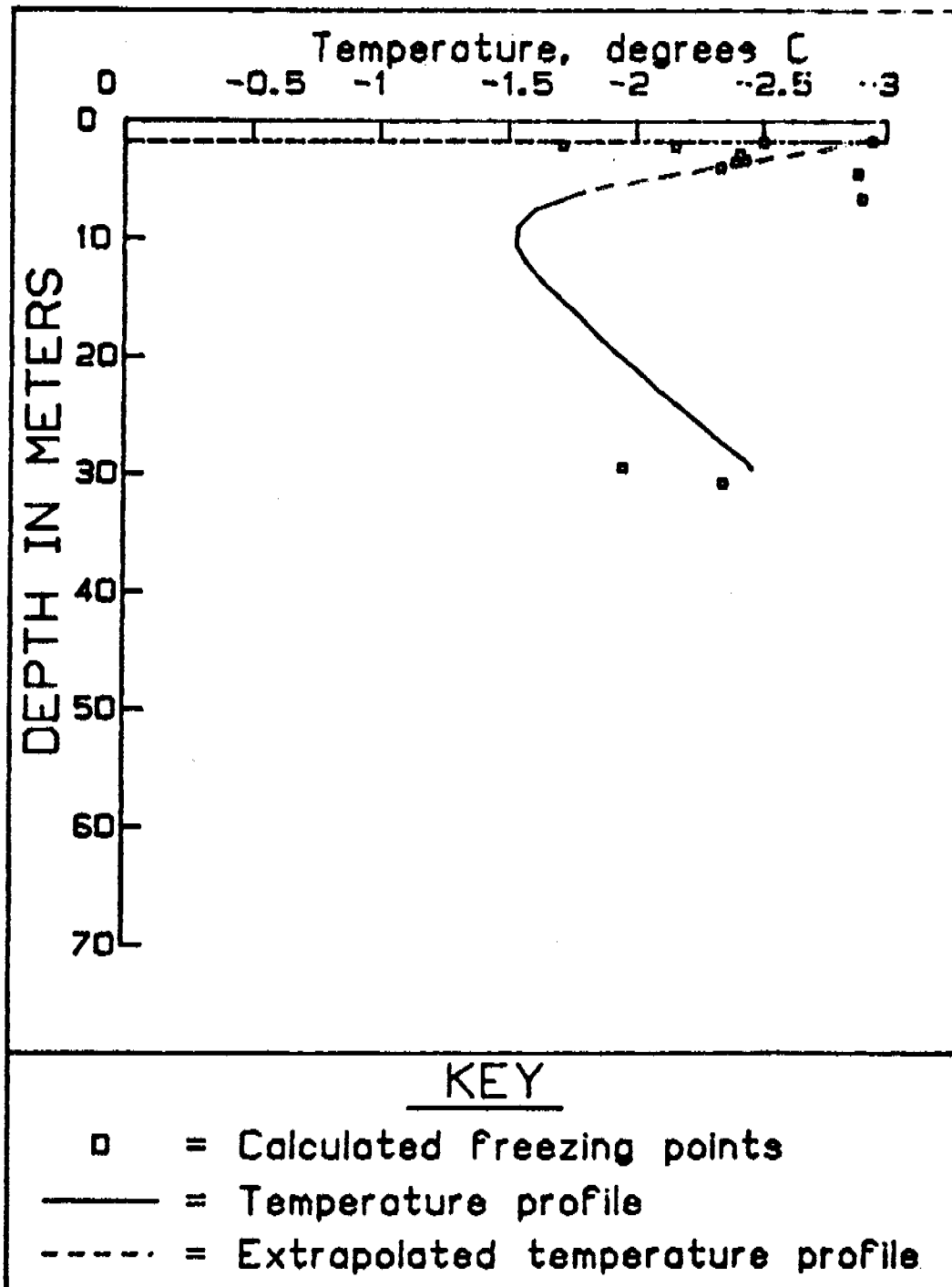


Figure 3. Temperature and calculated freezing points as a function of depth for borehole PB5 (Temperature data courtesy of B.V. Marshall and Dr. A.H. Lachenbruch, U.S.G.S.).

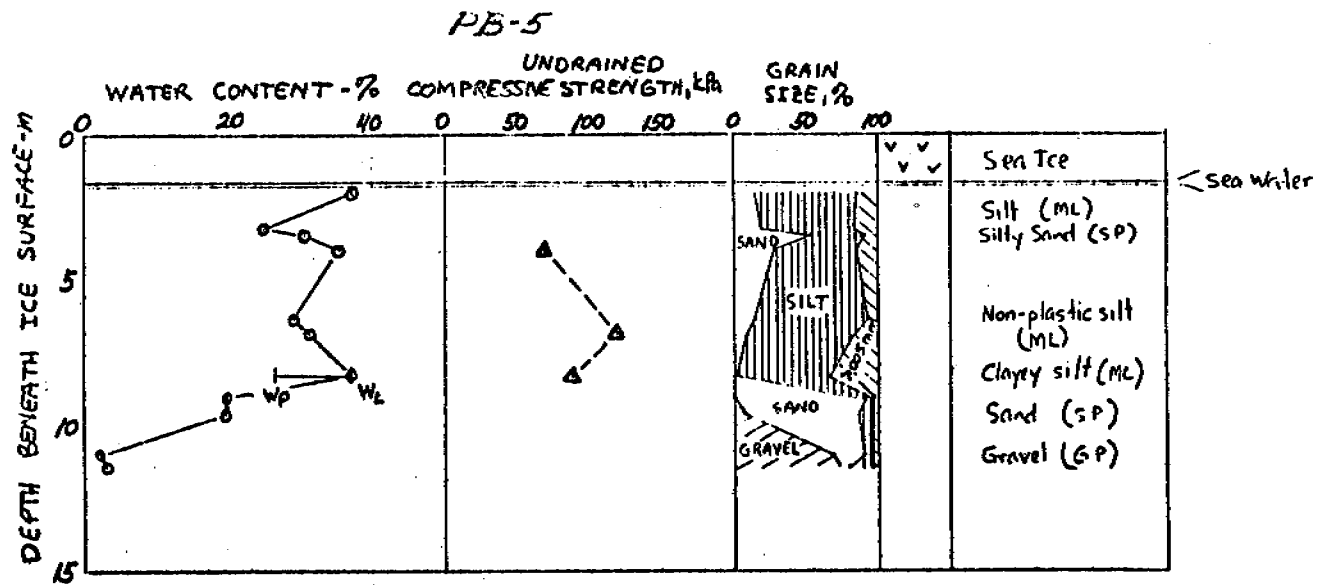


Figure 4. Geotechnical Description and Laboratory Test Results for Site PB-5.

PB-6

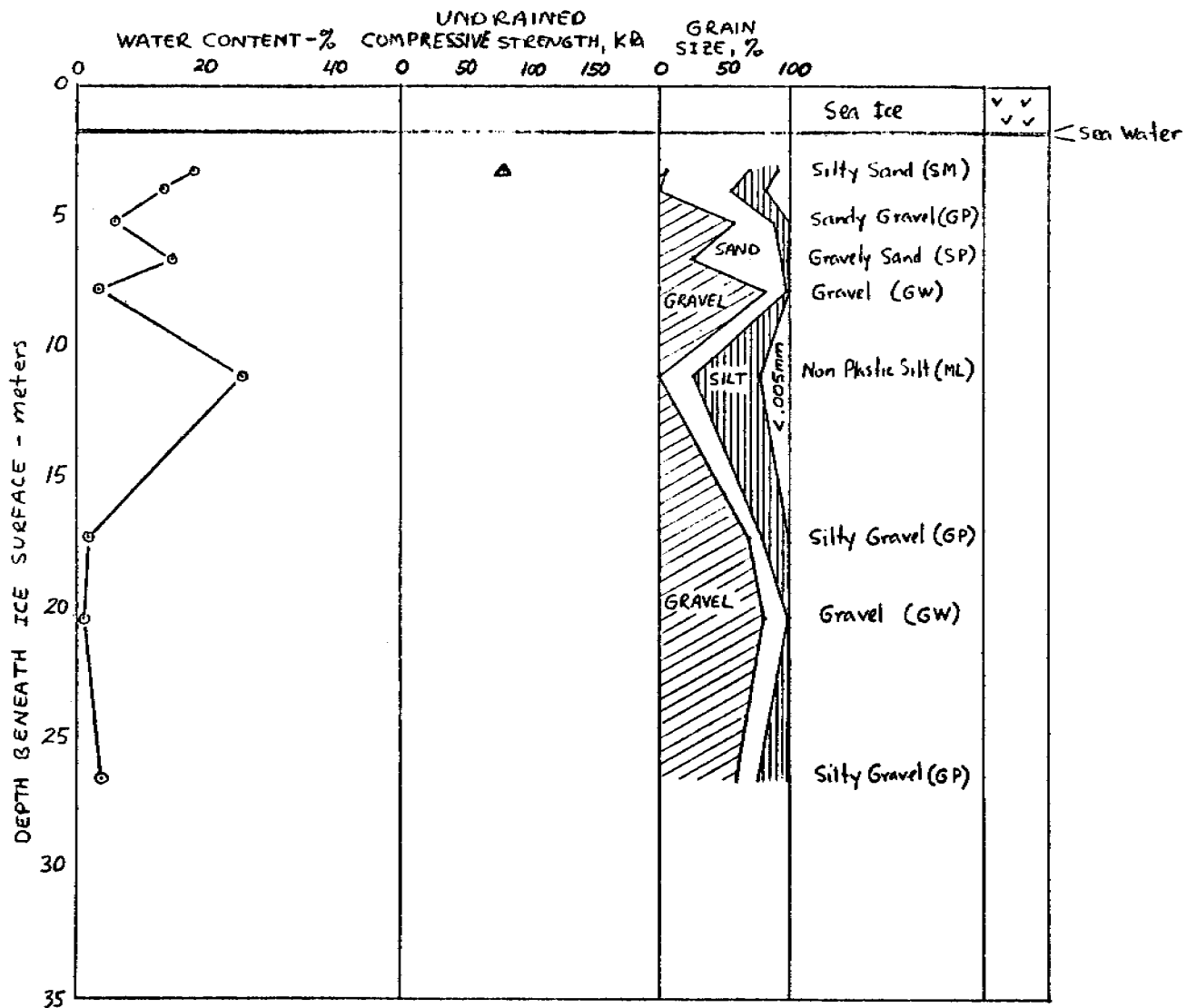


Figure 5. Geotechnical Description and Laboratory Test Results for Site PB-6.

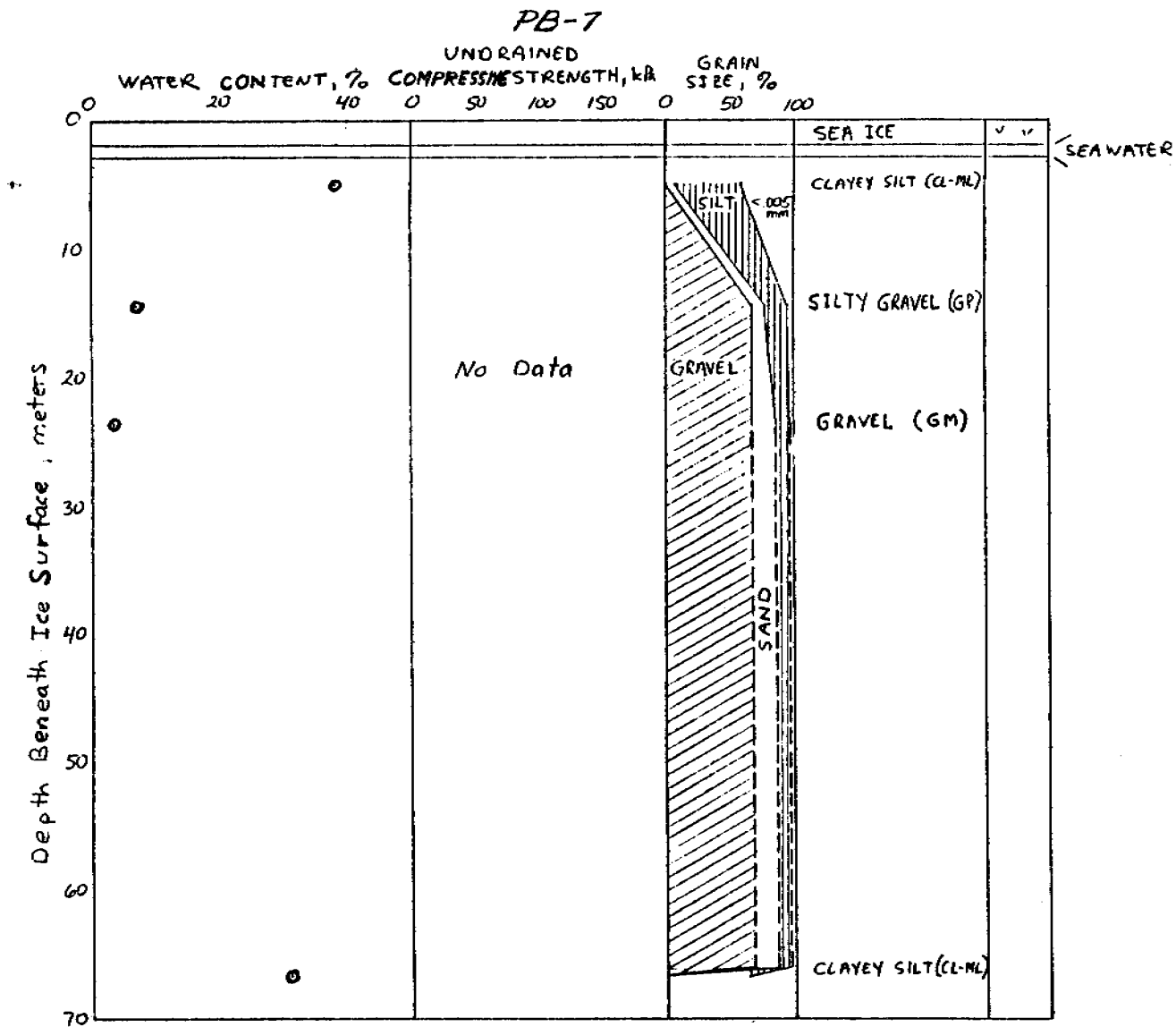


Figure 6. Geotechnical Description and Laboratory Test Results for Site PB-7.

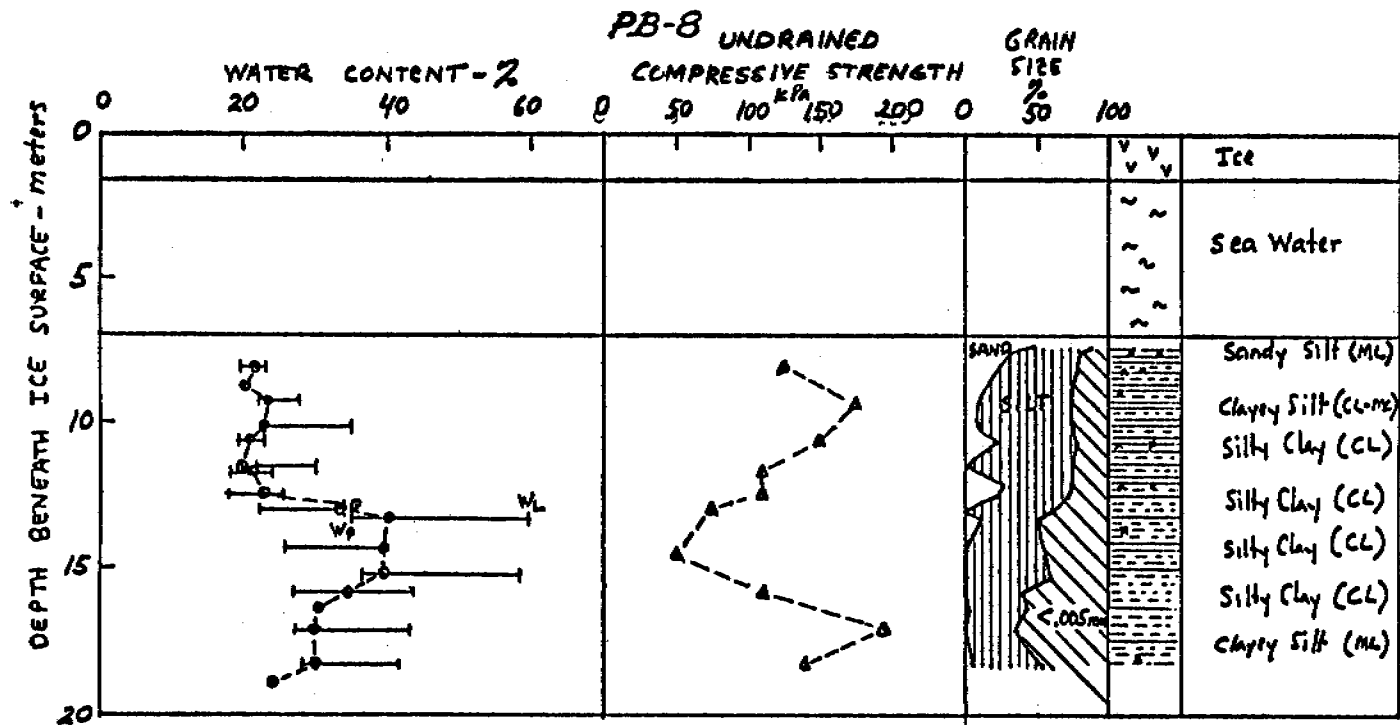


Figure 7. Geotechnical Description and Laboratory Test Results for Site PB-8

at approximately 8 m in depth a band of clayey silt occurs that has a plasticity index of 10%. The compressive strengths range from 60 to 120 kPa. Immediately below the band of clayey silt are sands, and at 10 to 11 m in depth relatively clean gravels were encountered. The fine-grained portion of this section is soft and will not provide good foundation conditions for some types of facilities and structures. This material, however, which is approximately 6 m thick, could probably be easily penetrated by piles or hydraulically excavated to the sands and gravels below, which appear to be very dense and strong. Strength tests were not conducted on the sands and gravels because of the difficulty in obtaining undisturbed samples. The stronger sands and gravels appear to provide adequate strength from the probe studies for pile foundations.

At site PB-6 (Figure 5), very little fine-grained silt or clay was encountered. The upper 2 m of this section is dominated by a silty sand. A single strength test for this material showed a compressive strength of approximately 80 kPa. Below 4 m depth dense sands and gravels were encountered, the exception being at 11 m depth where a dense non-plastic silt layer was observed. Little difficulty should be encountered in founding engineering structures at this site based on the soil properties observed in the section sampled.

Figure 6 shows that the soil profile at site PB-7 is dominated by gravel with the exception of soft clayey silt in the upper 3 m. No strength data are available for this site because of the difficulty in obtaining undisturbed samples. A single consolidation test conducted on a sample from a depth of 5 m indicates that the site is normally consolidated and that considerable deformation would occur if this site were loaded by some types of structures. Any structure, with the possible exception of gravity structures, may need to be founded on the dense sands and gravels below the 10 m depth.

Site PB-8 (Figure 7) shows the most complicated engineering property profile. At this site, silts and clays dominate the upper 12 m of the section. The upper half of these fine-grained sediments is highly overconsolidated and has compressive strengths in the range of 110 to 175 kPa. The next 2 m is normally consolidated and has a water content approximately double (40 versus 22%) that of the overconsolidated sediments above. As can be seen in Figure 7, the compressive strength falls to 50 kPa in this region. In the lower 4 m of this fine-grained section, the water content falls to approximately 24% and the strength increases to values like those observed in the upper half. Consolidation tests reveal that the lower 4 m of sediments are moderately to highly overconsolidated. Although it is not shown here, these sediments overlie dense sands and gravels. Access to the sands and gravels for founding structures or for borrow material may be restricted by the fine-grained

8. These fine-grained sediments cover coarser dense sand and gravels interspersed occasionally with finer-grained soils. The sands and gravels appear to be good material for providing borrow or for founding some types of structures. However, access to the sands and gravels is restricted by the finer-grained soils.

9. The probe study provided much rapid and detailed information on material type and distribution as well as thermal data useful in establishing the distribution of shallow frozen sediments.

10. The pore water chemistry data coupled with the thermal data are extremely useful for confirming the position of the zone where ice can occur in the pores (Fig. 3).

11. In general, the salinity of the interstitial water is close to that of normal sea water and is fairly uniform with depth. The largest variations are encountered close to shore, where highly saline sea water (about 60 p.p.t.) infiltrates into the surface layer of sediments. These brines form as a result of salt exclusion during the formation of sea ice. Other large variations in salinity are associated with the partial freezing of the interstitial water in sediments located near the surface of the sea bed.

IX. SUMMARY OF 4TH QUARTER OPERATIONS

A. Field Activities

1. The OCSEAP's Workshop at Barrow, Alaska, was attended. Primary activity related to the workshop involved efforts directed to updating the subsea permafrost section. No field activities were undertaken during this period.

2. NA.

3. This period was spent completing all aspects of the analysis and reporting on the probe study, chemical analysis and all aspects of the 1976 program. Analysis of samples from the 1977 program was undertaken on a continuous basis during this period and is essentially complete. All methods employed for both engineering property studies have been covered in other OCSEAP reporting.

4. No new field data were collected during this quarter.

5. Milestone charts -- Activities have slipped on the seismic data study by approximately three months. This was largely due to an

sediments above. Because of the very stiff nature of the upper half of these sediments, mechanical or mechanically aided rather than pure hydraulic excavation techniques would probably have to be employed.

One of the major problems that can not be generalized is the position of the ice-bonded sediments and their potential degree of thaw consolidation. The proximity of ice-bonded sediments must be considered in any situation where development is proposed. Only the properties and characteristics of the unfrozen sediments are discussed above.

VIII. CONCLUSIONS

1. Temperatures below 0°C were present in all 9 drill holes and 31 probe holes examined during the 1976 and 1977 spring field programs.

2. Ice-bonded sediments were encountered locally in the upper 10 m of sediment, in water depths of 2 m off the Sagavanirktok delta.

3. Seasonally frozen bed sediments appear to be widely distributed, as indicated by the probe, chemistry and thermal data. The degree of bonding is related to the sea bed temperature and is greatest in shallow water areas (< 2 m).

4. The position of the bonded permafrost interface is extremely variable, as would be anticipated in a marginal permafrost zone. The distribution of bonded sediments is strongly related to engineering properties, primarily grain size and degree of initial ice saturation, as well as other factors such as water depth and transgressive and preinundation history of the area.

5. It is not inconceivable that ice-bonded sediments can occur locally nearer the surface of the sea bed with increasing distance from shore (Figure 2a).

6. Fine-grained sand, silt and clay sediments occur near the sea bed to beyond Reindeer Island, and are as great as 10 m in thickness. With the exception of sites PB-2 (seaward of Reindeer Island) and PB-8 (shoreward of Reindeer Island) these fine-grained sediments are soft and are of low bearing capacity.

7. Shallow, highly overconsolidated marine clays occur seaward and slightly shoreward of Reindeer Island in areas we have studied. If the freeze-thaw mechanism is responsible for their formation, they could be found in many shallow water areas (< 2 m water depth) where fine-grained marine sediments occur.

almost 3-month delay in transfer of funds for this project. Additional delay resulted from an attempt to complete all remaining analysis of data and reporting from the 1977 field season.

B. No Significant Problems other than the delay in seismic study; as the drilling program activities are completed full attention will be directed to the seismic study.

Annual Report Task D-9

Research Unit #204

April 1977 to March 1978

OFFSHORE PERMAFROST STUDIES, BEAUFORT SEA

D. M. Hopkins and R. W. Hartz
U.S. Geological Survey
345 Middlefield Road
Menlo Park, CA 94025

TABLE OF CONTENTS

Summary	-----
Introduction	-----
Data Gathering	-----
Results	-----
Summary of Fourth Quarter Operations	-----
Appendices:	
I. Foraminifera	
II. Ostracodes	
III. Marine Amphipod	
IV. A) Final Report on Pollen from Borehole PB-2	
B) Modern Pollen Rain on the Chukchi and Beaufort	
Sea Coasts, Alaska	
V. Offshore Cross-sections	
VI. Thermal Profiles	
VII. Radiocarbon Dates	
VIII. Condensed Boring Logs	
IX. The Flaxman Formation of Northern Alaska:	
Evidence for an Arctic Ice Shelf?	
X. Quarterly Reports, April 1976 to December 1977	

Annual Report Task D-9
R.U. 204

OFFSHORE PERMAFROST STUDIES, BEAUFORT SEA

D.M. Hopkins and R.W. Hartz
U.S. Geological Survey
345 Middlefield Road
Menlo Park, CA 94025

SUMMARY

Our main objective in this study is to obtain direct knowledge of offshore permafrost by drilling and thermally instrumenting boreholes in the Prudhoe Bay area. Utilizing sea ice as a drilling platform, four boreholes were drilled and cored during the spring of 1977.

During 1977 drilling operations intact ice-bonded cores were recovered for the first time and it was established that ice-bonded permafrost is likely to be present within a few meters below the sea bottom at points as much as 17 km offshore. The 1977 boreholes also provide evidence of rapid thermokarst subsidence following initial submergence and they establish that Prudhoe Bay is the remnant of an ancient thaw lake that once extended to Gull Island Shoal.

The report presents detailed data on stratigraphy, fossil content, radiocarbon dates, pollen chronology, and geothermal profiles.

INTRODUCTION

Research of the past decade has shown that both ice-bonded permafrost and permafrost consisting of brine-soaked sediments below 0°C extends far offshore on the continental shelf of the Beaufort Sea. However, little was known of its distribution, thickness, state, and temperature under subsea influences.

The ever increasing development of offshore oil and gas resources in such a unique environment as the Beaufort Sea requires that we gain a more thorough understanding of offshore permafrost if disaster situations are to be avoided during exploration.

Our study undertakes to obtain direct knowledge of offshore permafrost based on thermally instrumented boreholes in the Prudhoe Bay area, and on the study of cores and cuttings from those boreholes. The study is a joint effort of the Geological Survey and R. I. Lewellen of Arctic Research Inc. (R.U. 204) and the Cold Regions Research and Engineering Laboratories (CRREL) (R.U. 105). It is closely coordinated with permafrost-probe and modeling studies at the University of Alaska, Fairbanks (R.U. 253, 255, and 256), seismic refraction studies at the University of Alaska, Anchorage (R.U. 271), and a study oriented toward development of a predictive model for distribution of offshore permafrost at the Institute of Arctic and Alpine Research (INSTAAR), University of Colorado.

DATA GATHERING

Four boreholes were completed offshore and one onshore in the Prudhoe Bay area during the spring of 1977 (fig. 1). Borehole P.B.-5 was placed on Gull Island Shoal; a second, P.B.-6, was drilled near the elbow of ARCO's west dock; a third, P.B.-7, was located approximately 3 km offshore and at 68 meters - it was the deepest borehole in our program; the fourth hole, P.B.-8, was located just south of Reindeer Island. Engineering probes, developed by Scott Blouin and Don Garfield (CRREL) (R.U. 104) provided supplementary information on stratigraphy and geothermal temperatures at about 27 sites. One onshore auger-hole provided additional stratigraphic data.

Core recovery was a major objective in the 1977 borehole program, it was important to obtain intact core material for use in engineering tests, geochemical analyses, geochronological analyses, and stratigraphic interpretation. In a few boreholes, cores were attempted continuously through the upper marine muds and fine sands, but in general cores were extracted at intervals ranging from 0.5 to 6.0 m. Drill cuttings ("wash samples") were monitored continuously and collected in the intervals that were not cored. The cores were photographed and divided in the field with splits apportioned to CRREL and the USGS. All wash samples were retained by the Geological Survey. Engineering tests, geochemical analyses, and granulometric analyses were conducted by CRREL (see 1978 Annual Report R.U. 104).

Wash samples and cores retained by the Geological Survey were used for stratigraphic, paleontological, geochronological, and paleoecological studies. Radiographs were taken of all fine-grained cores in order to define the nature of stratification and the distribution of fossil mollusks and ice-rafted pebbles. The cores were then washed for pebbles and fossils.

Paleontological studies include the identification of foraminifera (Appendix I), ostracodes (Appendix II), a marine amphipod (Appendix III), and pollen (Appendix IV). Stratigraphic studies are summarized in the offshore cross-sections (Appendix V) showing the distribution of sediments and permafrost in the Prudhoe Bay area.

Upon completion of boreholes PB-5, PB-6, PB-7, and PB-8, plastic pipe was installed and filled with non-freezing fluid. Downhole temperatures were observed immediately following drilling operations; the boreholes were allowed time to return to a state of thermal equilibrium, and were then revisited to measure equilibrium temperatures. The results of geothermal studies are presented in Appendix VI.

Once again in 1977, material suitable for radiocarbon-dating proved to be scarce, but samples were collected and dates are in progress. An anomalous radiocarbon date from borehole PB-2, drilled in 1976, has been re-examined and the results are presented in Appendix VII.

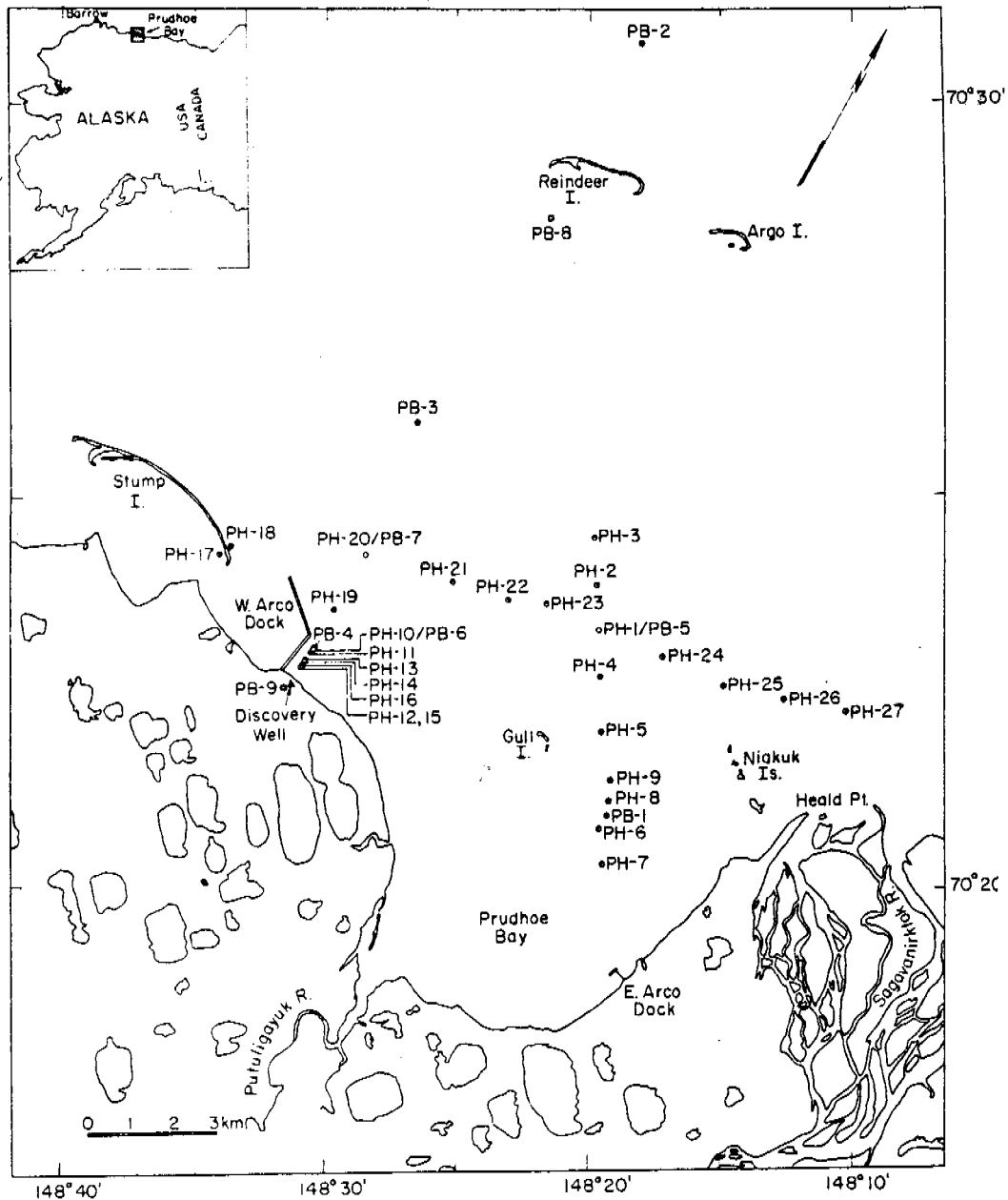


Figure 1. Map of site locations in Prudhoe Bay, Alaska. PB indicates locations of drill holes; open circles (PB 5-9) indicate holes drilled during the 1977 season; closed circles (PB 1-4) indicate holes drilled during the 1976 season. Ph indicates probe locations.

Geochronological analyses based on racemization ratios for amino acids in mollusk shells is underway, and results should be forthcoming.

RESULTS

The major conclusions with regard to the history and stratigraphy of the Prudhoe Bay area are best summarized in Hopkins 1977 Annual Report RU 204. Briefly, most of the Prudhoe Bay boreholes penetrate a Holocene marine mud from 5 to 10 meters thick underlain by Holocene beach deposits 1 to 2 meters thick. The basal beach deposits indicate the transgression of the early Holocene shoreline from 9,000 to 10,000 years ago. The marine section is underlain by late Wisconsin outwash composed of interbedded sand and gravel. Below the glacial outwash is a thick section of alluvial sands and gravels of probable mid-Wisconsin age (Appendix VIII).

During the 1976 drilling program borehole PB-2 encountered a stiff overconsolidated marine clay 3 km seaward of Reindeer Island. Initially we thought that overconsolidation had occurred as Reindeer Island migrated landward. In order to determine the relationship between the barrier island and the overconsolidated clay borehole PB-8 was located 1.7 km inland from Reindeer Island. Overconsolidated clay was encountered again in PB-8 and thus its origin has been reconsidered (Appendix IX).

Highlights of the study thus far are summarized in the R.U. Quarterly Reports (Appendix X).

SUMMARY OF FOURTH QUARTER OPERATIONS

A. Ship and laboratory activities

- 1) No cruises
- 2) D. M. Hopkins, R. W. Hartz, R. E. Nelson, Peggy Smith
- 3) Laboratory activities: Hand-picked samples for radiocarbon dates. Mollusks submitted for amino-acid racemization.
Interpreted pebble lithology in marine clay section of PB-7 and PB-2.
Hand-picked samples for identifiable seeds and insects.
- 4) Field activities: D. M. Hopkins and R. W. Hartz attended the Beaufort Sea synthesis meeting at Barrow in January 1978.

Appendix I. Foraminifera

SPECIES	LOCATION											
	Mf 4148	Mf 4149	Mf 4325	Mf 4326	Mf 4328	Mf 4150	Mf 4151	Mf 4329	Mf 4152	Mf 4153	Mf 4154	Mf 4155
<i>Elphidium clavatum</i> Cushman	50	32		1					6	8	3	
<i>Elphidium orbiculare</i> (Brady)	50	55	66	35	87	27	55	66	26	97	46	9
<i>Elphidiella groenlandica</i> (Cushman)		.2		2	6	13	6					4
<i>Elphidium</i> spp.		.5								12		
<i>Pseudopolymorphina</i> spp.			3	13	5	10	13		4	6	4	10
<i>Reophax</i> sp.				2	2							
<i>Elphidium incertum</i> (Williamson)				3	3	5	23		2	9	16	19
<i>Buccella frigida</i> (Cushman)				2	9			6	8	3	4	10
<i>Quinqueloculina arctica</i> (Cushman)					1	4						
<i>Quinqueloculina</i> sp.					.6							
<i>Discorbis</i> sp.							2					
<i>Cassidulina teretis</i> Tappan								6				
<i>Elphidium bartletti</i> Cushman								6	2	6	4	3
<i>Cassidulina islandica</i> Norvang									1			4
<i>Lagena gracillima</i> (Sequenza)									.4			
Total %	100	100	100	99	99	99	99	99	99	99	99	99
Total #	12	48	46	16	3	94	26	31	52			
Ostracods	7	19	58	32	12	24	43	9	4	11	0	7
Mega-fossil	x	x	x	x	x	x	x	x	x	x	x	x
Plant	x	x	x	x	x	x	x	x	x	x	x	x
Chara												1
Diversity	2	6	5	9	6	4	5	7	6	6	5	5

SPECIES	LOCATION									
	Mf 4156	Mf 4330	Mf 4157	Mf 4158	Mf 4159	Mf 4160	Mf 4161	Mf 4162	Mf 4163	Mf 4164
<i>Buccella frigida</i> (Cushman)	1								33	
<i>Elphidiella groenlandica</i> (Cushman)	2									
<i>Elphidium bartletti</i> Cushman	2									
<i>Elphidium incertum</i> (Williamson)	39	1	3	3						
<i>Elphidium orbiculare</i> (Brady)	56	8	5	6	7				67	
<i>Elphidium</i> spp.	2	3								
<i>Pseudopolymorphina</i> spp.	2									
<i>Trochammina nana</i> (Brady)	5									
Total %	99	0	0	0	0	0	0	0	0	0
Total #	39	3	0	0	0	0	0	0	3	0
Megafossil	x	x	x	x	x	x	x			
Plant	x	x		x	x	x	x			x
Ostracod	95	25	2	1	1				x	
Diversity	8	3	2	0	0	0	0	0	2	0

SPECIES \ LOCATION		LOCATION																							
		Mf 4165	Mf 4333	Mf 4166	Mf 4167	Mf 4334	Mf 4168	Mf 4170	Mf 4169																
<i>Buccella frigida</i> (Cushman)		3	10	5	5	7	4																		
<i>Elphidium incertum</i> (Williamson)		38	18	17	3	15	33																		
<i>Elphidium orbiculare</i> (Brady)		55	61	62	60	78	99	6																	
<i>Pseudopolymorphina</i> spp.		3	3	2	4		2																		
<i>Silicosigmolina groenlandica</i> (Cushman)		2																							
<i>Elphidiella groenlandica</i> (Cushman)				1	2			5																	
<i>Elphidium bartletti</i> Cushman				1																					
<i>Elphidium clavatum</i> Cushman			7	13	25																				
<i>Quinqueloculina artica</i> (Cushman)			3	2				2																	
<i>Trochammina nana</i> (Brady)				1	2																				
<i>Elphidium</i> spp.								49																	
<i>Elphidiella</i> sp.					4																				
<i>Globulina</i> sp.			7																						
Total %		99	99	99	99	99	99	99	99	99	99	99	99	99	99	99	99	99	99	99	99	99	99	99	99
Total #		45	138	29	71	21	45	20	7																
Megafossil		x		x	x			x																	
Plant		x	x	x	x	x	x	x	x																
Diatom																									
Ostracod		95	97	33	35	35	63	3	1																
Diversity		5	7	9	8	3	6	2	1																

mf number	diversity	#/100 gms	water depth → increasing	interpretations
4191	11	3178		middle - inner neritic slight fluctuations of depth
4192	13	1558		
4193	18	3094		
4194	12	2962		
4195	13	1076		
4196	13	8970		
4197	12	596		
4198	14	2583		
4199	15	1574		
4200	13	842		
4201	12	684		
4202	16	1499		
4203	16	2490		
4204	14	3742		
4205	14	2607		
4206	13	2430		
4207	12	2230		
4208	16	511		
4209	15	5088		
4210	15	555		
4211	16	1607		
4212	10	616		
4213	14	3600		
4214	13	2792		
4215	12	2408		
4216	14	925		
4217	16	3212		
4218	14	2128		
4219	14	985		
4220	10	137		
4221	13	287		
4222	6	28		
4223	10	153		
4224	9	91		
4225	7	50		
4226	8	97		
4227	8	78		
4228	13	115		
4229	8	35		
4230	12	318		
4231	12	391		
4232	11	902		
4233	9	62		
4234	11	783		
4235	9	158		
4236	9	51		
4237	7	14		
4238	10	66		
4239	8	24		
4240	8	55		
4241	14	183		
4242	11	75		
4243	10	89		
4244	12	143		
4245	11	343		
4246	14	380		
4247	16	546		
4248	11	107		
4249	14	99		
4250	6	26		
4251	4	10		
4252	5	7		
4253	9	56		
4254	8	28		

Unconformity

middle - inner neritic
Floxman formation

Atlantic faunas appears in this interval
last glacial phase

REPORT ON REFERRED FOSSILS

6 XX

XX
7

STRATIGRAPHIC RANGE

SHIPMENT NUMBER A-77-38M-G

GENERAL LOCALITY

REGION

QUADRANGLE OR AREA

DATE RECEIVED

KINDS OF FOSSILS

STATUS OF WORK

REFERRED BY

DATE REPORTED

REPORT PREPARED BY

Mf 4231 (field no. PB 8 - WS 20.21)

Benthic foraminifers:

- CASSIDULINA ISLANDICA Norvang
- ELPHIDIELLA GROENLANDICA (Cushman)
- ELPHIDIUM BARTLETTI Cushman
- ELPHIDIUM CLAVATUM Cushman
- ELPHIDIUM ORBICULARE (Brady)
- ENTOSOLENIA sp.
- LAGENA GRACILLIMA (Seguenza)
- PSEUDOPOLYMORPHINA spp.

Ostracods

- Megafossil fragments
- Plant fragments

Age and Comments: The oldest foraminiferal deposit in PB-6 occurs in Mf 4163. This fauna represents shallow nearshore marine conditions. Below this the sediment is composed of outwash or beach gravels without any marine fauna. Above this the microfauna disappears but the megafauna continues to indicate nearshore marine or beach conditions. The microfauna is reestablished in Mf 4158 and increases in number of individuals and diversity as the water depth increases toward the top of this borehole. Although representative of shallower conditions, the depth trends in PB-6 are nearly identical to those seen in PB-1 (E&R dated 02/10/77); outwash gravels, short marine transgression, beach, and followed by marine transgression.

This pattern is repeated in PB-5. The lowest samples, Mf 4155 to Mf 4329, are indicative of increasing water depths from inner neritic to middle neritic (not greater than 25-30 m). This sequence is interrupted by a sandy interval (9.85 to 8.85 m) which probably represents

Continued in A-77-38M, Part H @

REPORT ON REFERRED FOSSILS

XX

1 XX


 STRATIGRAPHIC
RANGE

Pleistocene to Holocene

SHIPMENT
NUMBER

A-77-38M-H

GENERAL
LOCALITY

Alaska

REGION

Arctic Coast

QUADRANGLE
OR AREA

Prudhoe Bay 1:80,000

DATE
RECEIVED

06/07/77

KINDS OF
FOSSILS

Microfossils - Benthic Foraminifera

STATUS
OF WORK

Complete

REFERRED
BY

David M. Hopkins, Alaskan Branch

DATE
REPORTED

03/20/78

REPORT
PREPARED BY

Kristin McDougall

Continued from A-77-38M, Part G

Age and comments (continued):

a nearshore sand correlative to the beach sands and gravels in PB-1 and PB-6. Above this the marine microfauna progresses from an inner neritic assemblage, Mf 4150, to middle neritic assemblage, Mf 4326. Above this the diversity and number of individuals declines because of shallower water depths due to the construction of the Gulf Island Shoal.

Borehole PB-7 again demonstrates the same depth trends as in PB-1, 5, and 6. In this borehole the oldest sample, Mf 4169, lies above the beach gravels and represents a very nearshore faunal assemblage. The fauna becomes more abundant and diverse as the water depth increases from inner neritic, Mf 4169, to middle neritic (not greater than 25-30 m), Mf 4166. Water depths appear to decrease slightly above this (Stump Island Shoal?)

Borehole PB-8 cannot yet be correlated with the other boreholes. The microfauna in the upper part of PB-8, Mf 4171 to Mf 4199, represents a Holocene fauna similar to the other boreholes. Water depths of inner to middle neritic are suggested. The middle neritic depths are favored because several species typical of ***deeper*** water are present including a planktic foraminifer.

There may be an unconformity (paraconformity) at approximately 13.50 m. The fauna undergoes several changes below Mf 4200: (1) decreased diversity; (2) decreased number of individuals per 100 gms; and (3) changes in species dominance. Also, in this lower group of samples are several new species. Gudina (1976) finds such species as GORDIOSPIRA ARCTICA Cushman present, in late Pleistocene deposits in Eastern Siberia. These are Atlantic species which she believes penetrated the Arctic Ocean during the last glacial. If this is correct the lower samples in PB-8, Mf 4201 to Mf 4231, represent the last glacial and the penetration of Atlantic species probably via Greenland and Canada @

Other borehole data that was submitted was not capable of being reproduced. Further details may be obtained from the author.

Appendix II. Ostracodes

STRATIGRAPHIC RANGE	Holocene	SHIPMENT NUMBER	A-76-47M
GENERAL LOCALITY	Alaska	REGION	North Slope
QUADRANGLE OR AREA	Beechey Point C-3 quad.	DATE RECEIVED	10/76
KINDS OF FOSSILS	Ostracodes	STATUS OF WORK	Complete
REFERRED BY	David M. Hopkins	DATE REPORTED	11/7/77
REPORT PREPARED BY	Ellen Compton, Tom Cronin, Joe Hazel		

This report covers samples from three boreholes drilled offshore in the Prudhoe Bay area of Alaska in the Beaufort Sea. The holes were drilled in connection with offshore permafrost studies (Task D-9).

Borehole PB-1. Lat. 70 deg. 20.9 min. N., Long. 148 deg. 19.3 min. W. 13 feet of water and 4.5 feet of ice were penetrated above the sediment-water interface. In the following lists the numbers of identifiable valves for each species is indicated to the left of the name of the taxon. Depths in the borehole are given after the sample numbers.

PB-1 WS 17.2 - 18

- 65 HETEROCYPRIDEIS SORBYANA (Jones, 1856)
- 2 CYTHEROMORPHA MACCHESNEYI (Brady & Crosskey, 1870)
- 22 PARACYPRIDEIS PSEUDOPUNCTILLATA Swain 1963

PB-1 WS 18-19

- 318 HETEROCYPRIDEIS SORBYANA (Jones, 1856)
- 34 CYTHEROMORPHA MACCHESNEYI (Brady & Crosskey, 1870)
- 17 PARACYPRIDEIS PSEUDOPUNCTILLATA Swain 1963
- 1 LOXOCONCHA VENEPIDERMOIDEA Swain 1963

PB-1 WS 19-19.5

- 100 HETEROCYPRIDEIS SORBYANA (Jones, 1856)
- 37 PARACYPRIDEIS PSEUDOPUNCTILLATA Swain 1963
- 12 CYTHEROMORPHA MACCHESNEYI (Brady & Crosskey, 1870)

PB-1 WS 19.5-20

- 15 PARACYPRIDEIS PSEUDOPUNCTILLATA Swain, 1963
- 2 CYTHEROMORPHA MACCHESNEYI (Brady & Crosskey, 1870)
- 32 HETEROCYPRIDEIS SORBYANA (Jones, 1856)

PB-1 WS 20-20.5

- 89 HETEROCYPRIDEIS SORBYANA (Jones, 1856)
- 39 PARACYPRIDEIS PSEUDOPUNCTILLATA Swain 1963
- 7 CYTHEROMORPHA MACCHESNEYI (Brady & Crosskey, 1870) @

STRATIGRAPHIC
RANGESHIPMENT
NUMBER

A-76-47M

GENERAL
LOCALITY

REGION

QUADRANGLE
OR AREADATE
RECEIVEDKINDS OF
FOSSILSSTATUS
OF WORKREFERRED
BYDATE
REPORTEDREPORT
PREPARED BY

- PB-1 WS 20.5-21
 19 PARACYPRIDEIS PSEUDOPUNCTILLATA Swain 1963
 91 HETEROCYPRIDEIS SORBYANA (Jones, 1856)
 12 CYTHEROMORPHA MACCHESNEYI (Brady & Crosskey, 1870)
 1 RABILIMIS SEPTENTRIONALIS (Brady, 1866)
- PB-1 WS 21-21.5
 32 HETEROCYPRIS SORBYANA (Jones, 1856)
 5 CYTHEROMORPHA MACCHESNEYI (Brady & Crosskey, 1870)
 1 PARACYPRIDEIS PSEUDOPUNCTILLATA Swain, 1963
- PB-1 WS 21.5-22
 4 CYTHEROMORPHA MACCHESNEYI (Brady & Crosskey, 1870)
 10 HETEROCYPRIDEIS SORBYANA (Jones, 1856)
 2 EUCYTHERIDEA BRADII (Norman, 1863)
- PB-1 WS 23-25
 23 PARACYPRIDEIS PSEUDOPUNCTILLATA Swain, 1963
 10 HETEROCYPRIDEIS SORBYANA (Jones, 1856)
 6 CYTHEROMORPHA MACCHESNEYI (Brady & Crosskey, 1870)
 1 LOXOCONCHA VENEPIDERMOIDEA Swain, 1963
- PB-1 WS 25-27
 14 HETEROCYPRIDEIS SORBYANA (Jones, 1856)
 7 LOXOCONCHA VENEPIDERMOIDEA Swain, 1963
 3 LOXOCONCHA sp. 1
 10 CYTHEROMORPHA MACCHESNEYI (Brady & Crosskey, 1870)
 43 PARACYPRIDEIS PSEUDOPUNCTILLATA Swain, 1963
- PB-1 GS1a 26-26.5
 47 HETEROCYPRIDEIS SORBYANA (Jones, 1856)
 1 CYTHEROMORPHA MACCHESNEYI (Brady & Crosskey, 1870)
 2 PARACYPRIDEIS PSEUDOPUNCTILLATA Swain 1963
- PB-1 GS4 plus-minus 32
 21 PARACYPRIDEIS PSEUDOPUNCTILLATA Swain, 1963
 5 LOXOCONCHA sp. 1 (= L. ELLIPTICA Brady 1868?)
 13 HETEROCYPRIS SORBYANA (Jones, 1856)
 2 CYTHEROMORPHA MACCHESNEYI (Brady & Crosskey, 1870)
 1 CANDONA cf. C. CANDIDA (O.F. Muller) @

STRATIGRAPHIC
RANGE

GENERAL
LOCALITY

QUADRANGLE
OR AREA

KINDS OF
FOSSILS

REFERRED
BY

REPORT
PREPARED BY

SHIPMENT
NUMBER A-76-47M

REGION

DATE
RECEIVED

STATUS
OF WORK

DATE
REPORTED

All the assemblages in this hole indicate very nearshore marginal marine conditions. The dominance of HETEROCYPRIDEIS SORBYANA, the small assemblage size, and the consistent presence of PARACYPRIDEIS PSEUDOPUNCTILLATA, and CYTHEROMORPHA MACCHESNEYI suggest reduced salinity. The presence of the fresh water genus CANDONA in PB1 GS4 at 32 feet lends strength to such an interpretation.

Borehole PB-2. Lat. 70 deg. 36.6 min. N., Long. 148 deg. 26.6 min. W. 6 ft. of ice and 39 feet of water, 1.5 miles north of Reindeer Island.

PB-2 WS 43.8 - 48.8

- 13 RABILIMIS SEPTENTRIONALIS (Brady, 1866)
- 3 PARACYPRIDEIS PSEUDOPUNCTILLATA Swain, 1963
- 1 NORMANICYTHERE LEIODERMA (Norman, 1868)
- 4 HETEROCYPRIDEIS SORBYANA (Jones, 1856)
- 3 CYTHERETTA TESHEKPUKENSIS Swain, 1963
- 1 CYTHEROPTERON MONTROSIENSE Brady, Crosskey, & Robertson 1874
- 7 EUCYTHERIDEA BRADII (Norman, 1863)

PB-2 WS 45.8 - 47

- 3 HETEROCYPRIDEIS SORBYANA (Jones, 1856)
- 3 RABILIMIS SEPTENTRIONALIS (Brady, 1866)
- 1 EUCYTHEREDIA BRADII (Norman, 1863)
- 2 NORMANICYTHERE LEIODERMA (Norman, 1868)
- 1 CYTHERETTA TESHEKPUKENSIS Swain 1963

PB-2 Clay bit 49.7

- 5 RABILIMIS SEPTENTRIONALIS (Brady, 1866)
- 2 PALMANELLA LIMICOLA (Norman, 1865)
- 5 EUCYTHERIDEA BRADII (Norman, 1863)
- 6 HETEROCYPRIDEIS SORBYANA (Jones, 1856)
- 2 CYTHERETTA TESHEKPUKENSIS Swain, 1963
- 1 CYTHERETTA EDWARDSI of Swain (1963)
- 1 *ACANTHOCYTHEREIS* DUNELMENSIS s.l. @

STRATIGRAPHIC
RANGESHIPMENT
NUMBER

A-76-47M

GENERAL
LOCALITY

REGION

QUADRANGLE
OR AREADATE
RECEIVEDKINDS OF
FOSSILSSTATUS
OF WORKREFERRED
BYDATE
REPORTEDREPORT
PREPARED BY

- PB-2 GS3 50?
 2 RABILIMIS SEPTENTRIONALIS (Brady, 1866)
 7 HETEROCYPRIDEIS SORBYANA (Jones, 1856)
 2 CYTHEROMORPHA MACCHESNEYI (Brady & Crosskey, 1870)
 32 PARACYPRIDEIS PSEUDOPUNCTILLATA Swain, 1963
 4 LOXOCONCHA VENEPIDERMOIDEA Swain, 1963
 1 LOXOCONCHA sp. 1 (= L. ELLIPTICA Brady, 1868?)
- PB-2 GS 03e 51
 2 CYTHERETTA TESHEKPUKENSIS Swain, 1963
 1 PARACYPRIDEIS PSEUDOPUNCTILLATA Swain, 1963
 44 RABILIMIS SEPTENTRIONALIS (Brady, 1866)
- PB-2 GS 04b 54
 2 RABILIMIS MIRABILIS (Brady, 1868)
 1 KRITHE GLACIALIS Brady, Crosskey & Robertson, 1874
- PB-2 GS 04e 56
 1 KRITHE sp.
- PB-2 GS 05b 57
 10 RABILIMIS MIRABILIS (Brady, 1868)
 9 CYTHEROPTERON MONTROSIENSE Brady, Crosskey & Robertson, 1874
 2 KRITHE GLACIALIS Brady, Crosskey & Robertson, 1874
- PB-2 GS 05c 58
 4 RABILIMIS MIRABILIS (Brady, 1868)
 3 CYTHEROPTERON MONTROSIENSE Brady, Crosskey & Robertson, 1874
 1 KRITHE cf. K. GLACIALIS
- PB-2 GS 05e 58
 18 KRITHE GLACIALIS Brady, Crosskey & Robertson, 1874
 2 CYTHEROPTERON MONTROSIENSE Brady, Crosskey & Robertson, 1874
 10 RABILIMIS MIRABILIS (Brady, 1868)
- PB-2 Clay bit 58-60
 1 RABILIMIS MIRABILIS (Brady, 1868)
- PB-2 GS 06x 62
 1 KRITHE GLACIALIS Brady, Crosskey & Robertson, 1874 @

STRATIGRAPHIC RANGE	SHIPMENT NUMBER	A-76-47M
GENERAL LOCALITY	REGION	
QUADRANGLE OR AREA	DATE RECEIVED	
KINDS OF FOSSILS	STATUS OF WORK	
REFERRED BY	DATE REPORTED	
REPORT PREPARED BY		

- PB-2 Clay bit 68 (65.8)
RABILIMIS MIRABILIS (Brady, 1868)
- PB-2 GS 8A 71
2 RABILIMIS MIRABILIS (Brady, 1868)
1 KRITHE GLACILIS Brady, Crosskey & Robertson, 1874
- PB-2 GS 8E 72
3 KRITHE GLACIALIS Brady, Crosskey & Robertson, 1874
1 RABILIMIS MIRABILIS (Brady, 1868)
- PB-2 Clay bit/core 72.9
8 KRITHE GLACIALIS Brady, Crosskey & Robertson, 1874

The assemblages from 43.8 feet through 51 feet in this bore hole are more diverse and more equitable than those of PB-1. They indicate shallow, marginal marine environments like those of PB-1 but the presence of NORMANICYTHERE LEIODERMA, CYTHEROPTERON MONTROSIENSE and *ACANTHOCYTHEREIS* DUNELMENSIS s.l., and the higher species diversity, suggest near normal marine salinities (28-35 PPT). At 54 feet (PB-2-GS 04b) KRITHE GLACIALIS and RABILIMIS MIRABILIS occur. Based on known modern occurrences their presence suggests more open marine, deeper water conditions, and these kinds of assemblages prevail through the rest of the fossiliferous part of the bore hole. The deepest sample containing ostracodes is at 72.9 feet.

Bore hole PB-3. Lat. 70 deg. 25.8 min. N., Long. 148 deg. 26.6 min. W. 5.5 feet of ice and 24 feet of water, halfway between the ARCO causeway and Reindeer Island.

- PB-3 GS 1B 24
30 HETEROCYPRIDEIS SORBYANA (Jones, 1856)
14 RABILIMIS SEPTENTRIONALIS (Brady, 1866)
10 CYTHEROMORPHA MACCHESNEYI (Brady & Crosskey, 1870)
10 PARACYPRIDEIS PSEUDOPUNCTILLATA Swain, 1963
1 PALMANELLA LINICOLA (Norman, 1865)
2 CYTHEROPTERON MONTROSIENSE Brady, Crosskey & Robertson, 1874
26 EUCYTHERIDEA BRADII (Norman, 1863) @

STRATIGRAPHIC
RANGESHIPMENT
NUMBER

A-76-47M

GENERAL
LOCALITY

REGION

QUADRANGLE
OR AREADATE
RECEIVEDKINDS OF
FOSSILSSTATUS
OF WORKREFERRED
BYDATE
REPORTEDREPORT
PREPARED BY

PB-3 GS 3y 25

- 5 HETEROCYPRIDEIS SORBYANA (Jones, 1856)
- 5 RABILIMIS SEPTENTRIONALIS (Brady, 1866)
- 1 CYTHERETTA TESHEKPUKENSIS Swain, 1963
- 7 EUCYTHERIDEA BRADII (Norman, 1863)

PB-3 B2b Depth not specified

- 8 HETEROCYPRIDEIS SORBYANA (Jones, 1856)
- 3 CYTHERETTA? TESHEKPUKENSIS Swain, 1963
- 2 CYTHERETTA? EDWARDSI of Swain, 1963
- 19 RABILIMIS SEPTENTRIONALIS (Brady, 1966)
- 8 PARACYPRIDEIS PSEUDOPUNCTILLATA Swain, 1963

PB-3 GS 3x 30

- 3 HETEROCYPRIDEIS SORBYANA (Jones, 1856)
- 14 PARACYPRIDEIS PSEUDOPUNCTILLATA Swain, 1963
- 2 CYTHERETTA sp. (juv.)
- 1 CYTHERETTA EDWARDSI of Swain
- 13 RABILIMIS SEPTENTRIONALIS (Brady, 1866)
- 3 - EUCYTHERIDEA BRADII (Norman, 1863)

PB-3 GS 4x 32

- 9 HETEROCYPRIDEIS SORBYANA (Jones, 1856)
- 2 CYTHERETTA EDWARDSI of Swain
- 3 CYTHERETTA sp. juv.
- 8 CYTHEROMORPHA MACCHESNEYI (Brady & Crosskey, 1870)
- 10 PARACYPRIDEIS PSEUDOPUNCTILLATA Swain, 1963
- 1 EUCYTHERE(sp. 1)DECLIVIS (Norman)
- 17 RABILIMIS SEPTENTRIONALIS (Brady, 1866)
- 2 EUCYTHERIDEA BRADII (Norman, 1863)

PB-3 GS 05B Depth not specified

- 12 CYTHEROMORPHA MACCHESNEYI (Brady & Crosskey, 1870)
- 17 HETEROCYPRIDEIS SORBYANA (Jones, 1856)
- 10 PARACYPRIDEIS PSEUDOPUNCTILLATA Swain, 1963
- 1 RABILIMIS SEPTENTRIONALIS (Brady, 1866)

CONTINUED IN PART A. 3

STRATIGRAPHIC RANGE		SHIPMENT NUMBER	A-76-47MA
GENERAL LOCALITY	Alaska	REGION	North Slope
QUADRANGLE OR AREA	Beechey Point C-3 Quad.	DATE RECEIVED	10/76
KINDS OF FOSSILS	Ostracodes	STATUS OF WORK	Complete
REFERRED BY	David M. Hopkins	DATE REPORTED	11/7/77
REPORT PREPARED BY	Ellen Compton, Tom Cronin, Joe Hazel		

CONTINUED FROM A-76-47M.

PB-3 GS 05x 35

- 1 CYTHEROMORPHA MACCHESNEYI (Brady & Crosskey, 1870)
- 3 HETEROCYPRIDEIS SORBYANA (Jones)
- 47 PARACYPRIDEIS PSEUDOPUNCTILLATA Swain, 1963
- 1 RABILIMIS SEPTENTRIONALIS (Brady, 1866)
- 1 CYTHEROPTERON MONTROSIENSE Brady, Crosskey & Robertson, 1874
- 2 PALMANELLA LIMICOLA (Norman, 1965)
- 3 EUCYTHERIDEA BRADII (Norman, 1963)
- 2 CYTHERETTA TESHEKPUKENSIS Swain, 1963

PB-3 06A Depth not specified

- 17 HETEROCYPRIDEIS SORBYANA (Jones, 1856)
- 2 CYTHEROMORPHA MACCHESNEYI (Brady & Crosskey, 1870)
- 1 CYTHEROPTERON MONTROSIENSE Brady, Crosskey & Robertson, 1874
- 1 CYTHERETTA sp. juv.
- 1 CYTHERETTA TESHEKPUKENSIS Swain, 1963
- 35 EUCYTHERIDEA BRADII (Norman, 1963)
- 54 PARACYPRIDEIS PSEUDOPUNCTILLATA Swain, 1963

PB-3 GS 06x 39

- 40 PARACYPRIDEIS PSEUDOPUNCTILLATA Swain, 1963
- 1 RABILIMIS SEPTENTRIONALIS (Brady, 1966)
- 1 CYTHEROMORPHA MACCHESNEYI (Brady & Crosskey, 1870)
- 11 HETEROCYPRIDEIS SORBYANA (Jones, 1856)
- 10 EUCYTHERIDEA BRADII (Norman, 1863)
- 1 CYTHEROPTERON MONTROSIENSE Brady, Crosskey & Robertson, 1874

PB-3 WS 40-40.5

- 1 RABILIMIS SEPTENTRIONALIS (Brady, 1866)
- 2 EUCYTHERIDEA BRADII (Norman, 1863)
- 1 PARACYPRIDEIS PSEUDOPUNCTILLATA Swain, 1963 @

XX

REPORT ON REFERRED FOSSILS

2 XX

STRATIGRAPHIC
RANGE

SHIPMENT
NUMBER

A-76-47MA

GENERAL
LOCALITY

REGION

QUADRANGLE
OR AREA

DATE
RECEIVED

KINDS OF
FOSSILS

STATUS
OF WORK

REFERRED
BY

DATE
REPORTED

REPORT
PREPARED BY

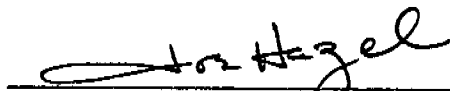
The assemblages in this bore hole are like those of PB-1 and indicate brackish water conditions. @



Ellen Compton



Tom Cronin



Joe Hazel

Appendix III. Marine Amphipod

July 22, 1977

Dr. David M. Hopkins
Alaskan Geology Branch
US Geological Survey
345 Middlefield Road
Menlo Park, California 94025
USA

Dear David:

Thank you very much for the letter which arrived a few days ago. Yes, I know well about the mammoths. I have also once payed my ~~res~~ respect to the first one found, the one which is stuffed at the Leningrad Museum. - I will be very interested to know the results of dating of the present material.

I have thought very much, now one way, now another, about the naming in your report of this piece of amphipod. For a definite identification as far as to species, you certainly need much more of a specimen than a tail end, generally also for an identification to genus. This tail end is indeed very suggestive of Onisimus affinis, a species occurring in the topical part of the Arctic Ocean, but since no other parts of the specimen are available for an examintation doubts still adhere to the identification. I am not sure that I am prepared to publish it as definite. Not even the genus is definitely ascertained. If your report says "a marine amphipod, possibly Onisimus cf. affinis Hansen, 1886" it may be better. Or what do you say?

This adhering uncertainty does not affect the paleogeographic evidence, though, so far as I can see. The only amphipods I have found in Alaskan lakes (fresh water) is Gammarus lacustris, Bontoporeia affinis and Gammaracanthus loricatus. Another species, not yet found on the Northern Slope, but which could be expected since it has been found in north-western Canada, is Hyaella azteca. They all have quite different tail ends than the one you sent. - Onisimus and related genera are known as entirely marine. Many of the members may occur very close to the coast, and in the shallow lagoons, at the northern Alaskan coast for instance, salinity generally varies considerably throughout the year - but no one knows as yet how settled these amphipods are in the lagoons. Thus, the inference will under all circumstances be that we are dealing with a marine amphipod, possibly inhabiting or periodically invading coastal, inshore waters.

I wish you a successful field trip. I am going to the Limnological Congress in Copenhagen in August, after which I will attend the post-congress excursion to western Greenland. I will be back here at the end of August.

Best regards,

W. G. S. S.

Appendix IV. A) Final Report on Pollen from Borehole PB-2

B) Modern Pollen Rain on the Chukchi and Beaufort
Sea Coasts, Alaska

FINAL REPORT ON POLLEN FROM BOREHOLE PB-2

Robert E. Nelson
Branch of Alaskan Geology
U. S. Geological Survey
Menlo Park, California 94025

and

Dept. of Geological Sciences*
University of Washington
Seattle, Washington 98195

Borehole PB-2, drilled near Prudhoe Bay in 1976 (see Figure 1), was sampled at eighteen (18) levels between core depths of 48.3 and 74.0 feet (see Figure 2). These samples, after being analysed for paleomagnetism (Hillhouse, 1977), were forwarded to me for palynological study. This report is a sequel to, and revision of, the Preliminary Report on the pollen from sediments obtained by this borehole (Nelson, 1977). Methodology utilized in the study was outlined in the previous report and need not be repeated here.

Counting has been completed for all samples submitted from PB-2 at this time, including additional counting on samples covered in the previous report, and several samples of modern marine sediment from nearby sites have also been analysed. This more recent work necessitates a revision of the conclusions put forth in the Preliminary Report.

MODERN SEDIMENTS

Four samples of surficial (uppermost 5 cm., mixed) sediment from relatively shallow (less than 20 m.) water on the Beaufort Sea Continental Shelf have been processed and analysed for pollen content. The samples were from core tops donated by Dr. Peter Barnes, Office of Marine Geology, U. S. Geological Survey, Menlo Park. Location of the cores, numbered V-1, V-12, V-13, and V-17, showing their position relative to both the coastline and PB-2, are shown in Figure 1.

* Please use this address for any correspondence.

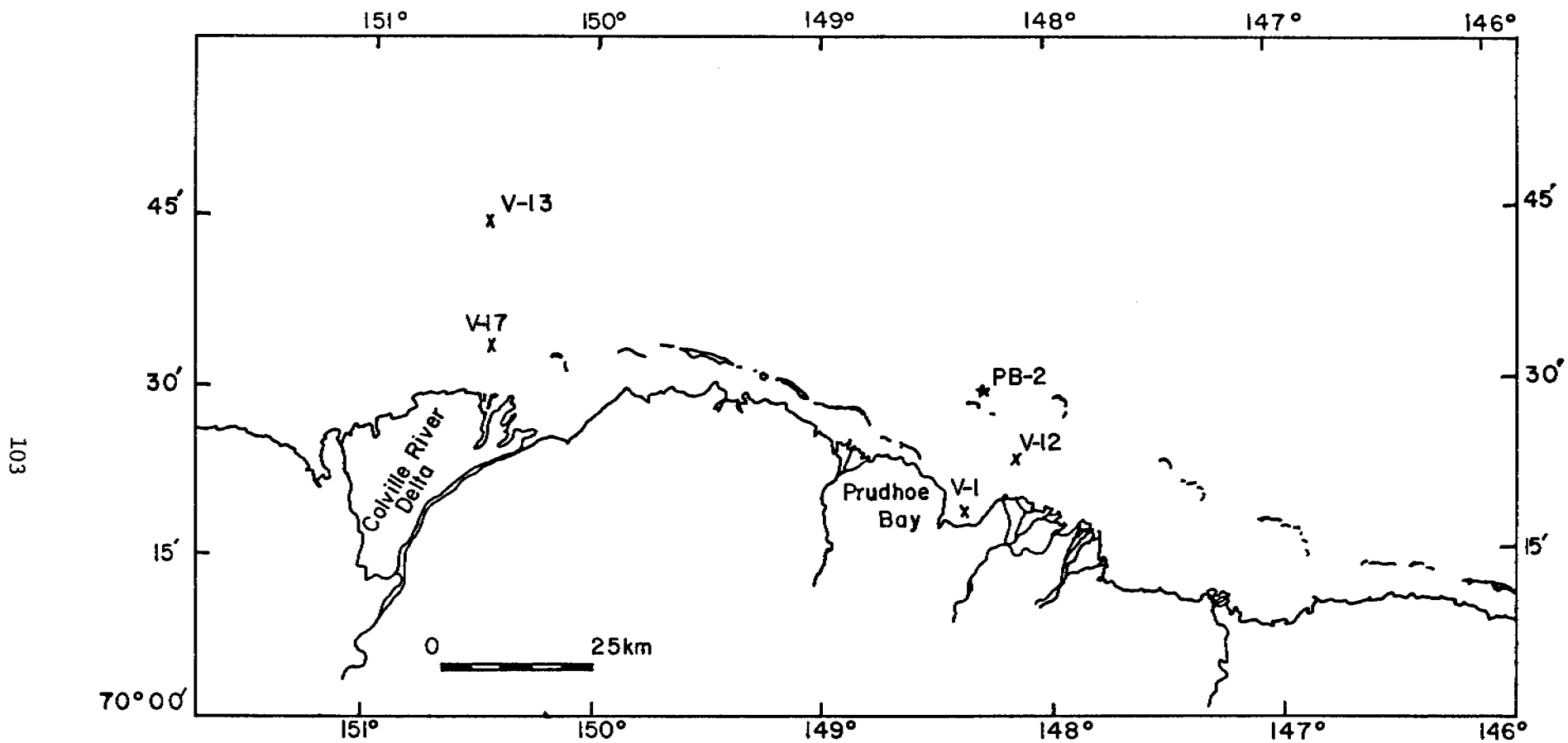
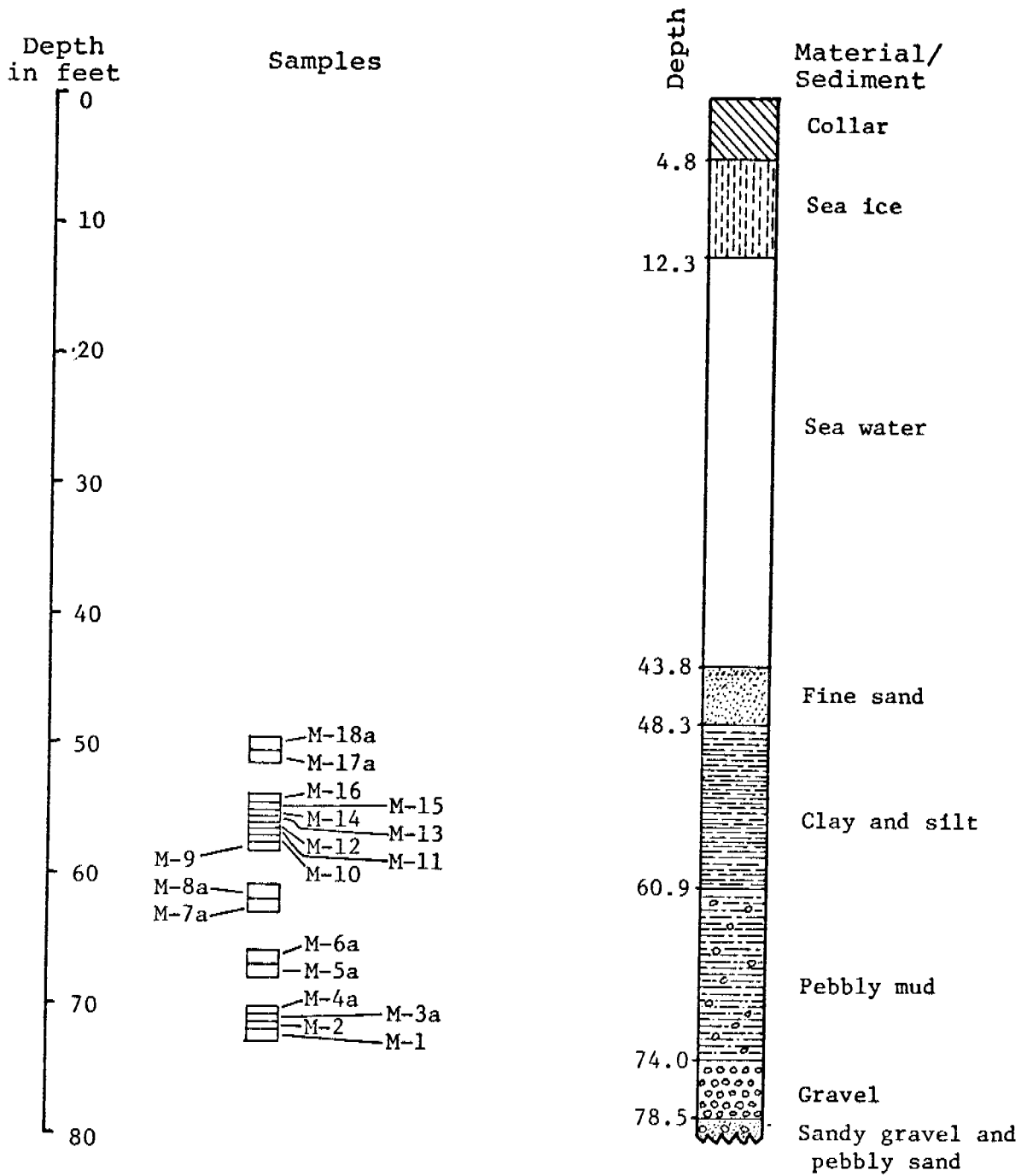


Figure 1

Coastline map of the Prudhoe Bay - Colville River Delta area, showing location of borehole PB-2 as well as of modern surface samples reported in this study.

FIGURE 2

Stratigraphy of the upper portion of borehole PB-2, showing location of samples analysed for pollen content.



Processing of the core tops followed similar procedures as for the material from PB-2. Results of pollen analysis of the modern sediments are shown in Figure 3a.

The four modern pollen spectra are reasonably consistent internally and show that pollen content of modern sediments in this area is dominated by sedges (Cyperaceae). Sedge pollen accounts for about half the total pollen encountered in these sediments. Grass (Gramineae) pollen is typically less than 10% of the total, while alder (Alnus) and birch (Betula) account for 5-10% and 10-15% respectively.

Spruce (Picea) pollen is present in variable amounts in the modern sediments, but the two samples that appear anomalously high (V-1 and V-13) may be reasonably explained. Sample V-1, from the center of Prudhoe Bay, is from a restricted embayment where free circulation of marine waters is probably limited. Terrestrial modern pollen samples from the Prudhoe Bay area (see accompanying report, "Modern Pollen Rain on the Chukchi and Beaufort Sea Coasts", in this volume) are also anomalously high in spruce pollen, and contain significant amounts of pine pollen as well. As neither spruce nor pine are present on the Arctic Coastal Plain of Alaska, this implies that local pollen production in the Prudhoe Bay area is very low. The high amounts of Artemisia (sage) pollen present in V-1 is probably derived from Artemisia arctica, which grows in abundance in the Sagavanirktok River delta.

The 10.5% spruce and 5% pine found in sample V-13 are most probably related to the distance of this site from the coastline. Both pine and spruce pollen tend to be hydraulically favored over denser types in long-distance transport, as was found by Heusser and Balsam (1977) in their study of pollen in sediments in the northeastern Pacific Ocean basin. In sample V-13, many of the grains of both pine and spruce pollen showed considerable abrasion and corrosion, further supporting the hypothesis that they were derived from distant sources. While it

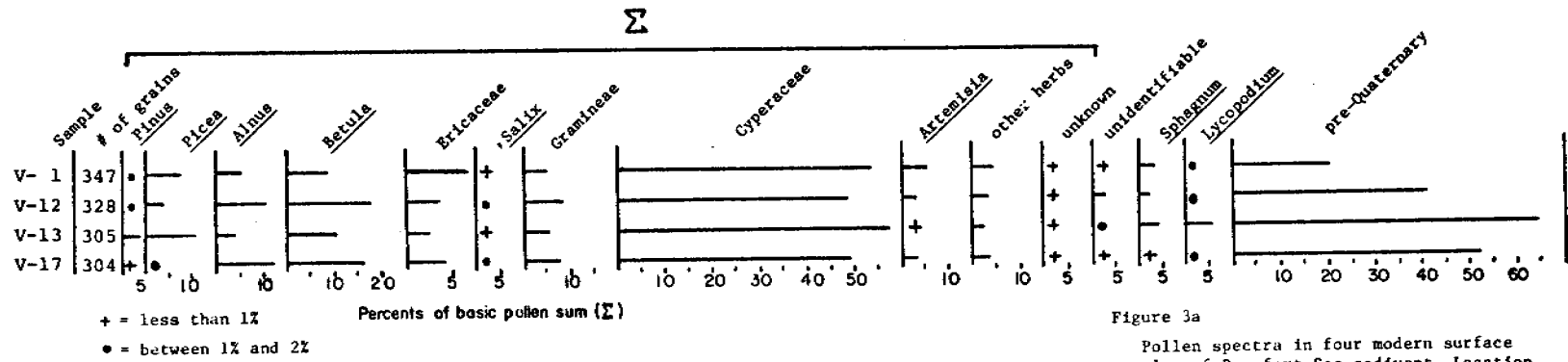


Figure 3a
Pollen spectra in four modern surface samples of Beaufort Sea sediment. Location of samples shown in figure 1.

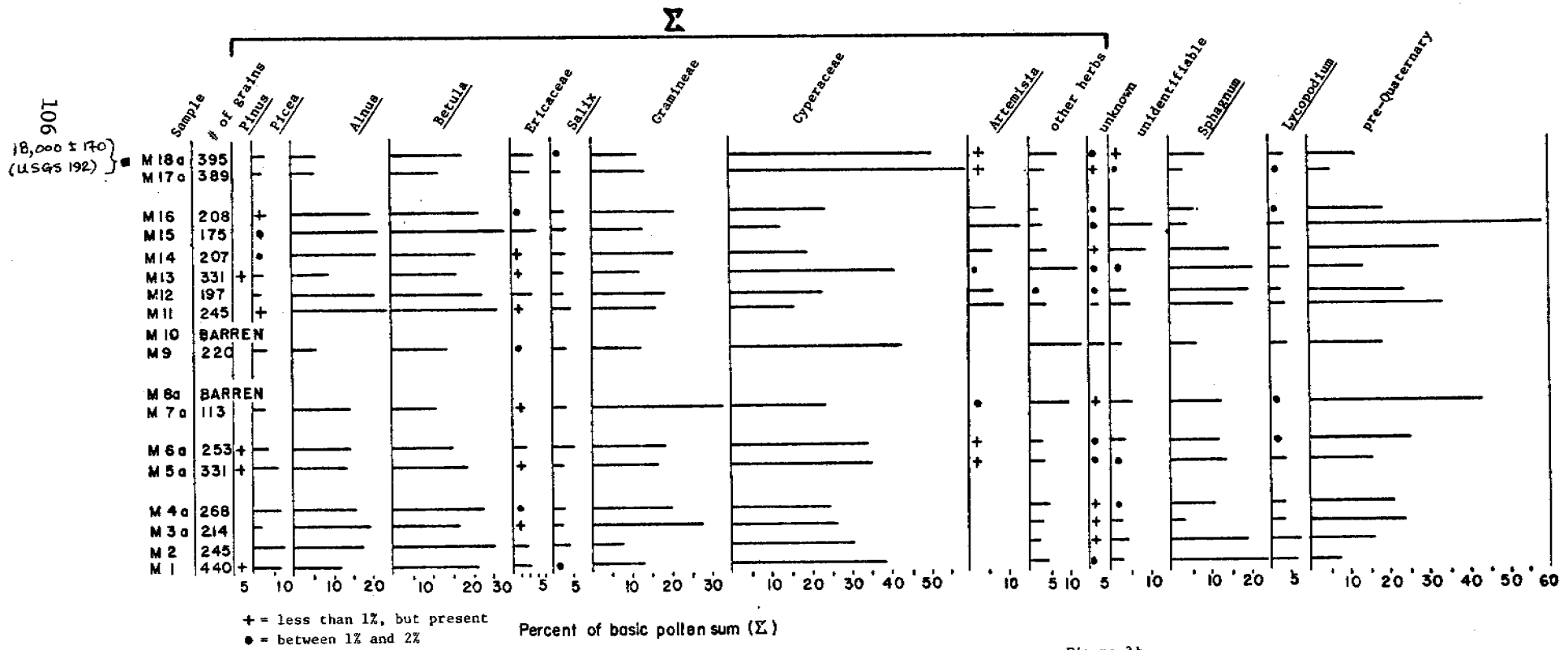


Figure 3b
Pollen diagram for the upper portion of borehole PB-2. All percentages expressed as percents of the basic pollen sum (Σ). (Analysis by R. E. Nelson)

is possible that marine currents may have transported some of these grains from Mackenzie River sources, this hypothesis cannot be tested with the data at hand.

Overall, however, the modern samples are surprisingly consistent internally. In addition to the generalities (with exceptions) noted above, it should also be mentioned that Sphagnum accounts for no more than 5% of the basic pollen sum (Σ) in any of the modern samples, nor do the combined herb taxa for all herbs not specifically mentioned on the diagram by name. Salix (willow) is consistently less than 2% in all samples.

POLLEN FROM PB-2

A diagram showing the pollen encountered in all samples analyzed from PB-2 is presented here as Figure 3b.

In general, the pollen content from the upper two samples from PB-2, M-17a and M-18a, is remarkably similar to that of the modern samples. The only significant difference between them is a much higher ratio of reworked, pre-Quaternary pollen and spores in the modern samples. Samples M-17a and M-18a could, then, suggest deposition during a time when terrestrial vegetation in the region (i.e., Arctic Coastal Plain) was much the same as it is at present. Alternatively, as suggested by D. M. Hopkins (oral comm., 7 March, 1978), they could represent reworking of more recent pollen from overlying sediments by bioturbation. Mud lumps in the overlying fine sands, as reported by Barnes (1977), would seem to support this hypothesis.

The bioturbation suggestion also seems to be supported by the pollen content of the lower samples in this section. Major differences between the modern pollen spectra and the remainder of the PB-2 materials indicate that this portion of the core may well have been deposited during a period of greater warmth than the present.

Alder in the PB-2 material is typically 15-20% of the total Quaternary

pollen content, roughly twice the concentrations found in modern samples. Similarly, birch typically comprises 20 to 30% of the fossil spectra, but only 10 to 20% in the modern. The higher grass:sedge ratios in the fossil material may be related to greater warmth or greater aridity, and the consistently important Artemisia in samples M-11 through M-16 would seem to suggest greater aridity than at present. My experience with Artemisia in the Arctic indicates that it is typically found on dryish, sandy sites with deep thaw and good drainage. The greater effective aridity indicated by the relatively high Artemisia in this section of PB-2 might be a product of decreased precipitation, or of increased summer warmth, causing deeper thaw and better soil drainage.

Also indicative of greater warmth, though not of greater aridity, in the fossil material is the surprising abundance of Sphagnum in almost all samples. Lycopodium (clubmoss) is also typically better represented in the fossil than in the modern samples. Spruce is more abundant in the lower part of the core than in either the upper part or in modern samples. This is a strange anomaly if this part of the core represents postglacial sedimentation, since spruce was virtually eliminated from the unglaciated portion of Interior Alaska during the last (Wisconsin) glaciation. Salix (willow) is slightly but consistently higher in the fossil samples than in modern spectra, but this small difference is not in itself indicative of any significant climatic shifts.

Reworked, pre-Quaternary taxa encountered in the PB-2 materials include Sequoia and Aquilapollenites, as reported in the Preliminary Report, and also Wodehouseia, Azonia, Tasmanites, cf. Podocarpus, Fibulapollis, and Cicatricosisporites, as well as a number of taxa that were presumed reworked but not identified. Most of these unidentified taxa were primitive, thick-walled trilete spores, unlike any forms that would be expected in a modern Arctic plant.

The radiocarbon age of $18,000 \pm 170$ years (USGS 192) from the same level as sample M-18a is obviously in error. It is inconceivable that full-glacial vegetation on the Arctic Coastal Plain should be similar to that of the modern day, as Colinvaux (1964) has argued. Fine detrital coal is abundant in pollen preparations from all horizons examined, however, and it is therefore a possibility that the sample is considerably younger than indicated by this age determination.

The pollen evidence, though, seems to indicate that it may be more likely that the opposite case is true, i.e., the units I have examined are of pre-Wisconsinan age, contaminated with more recent carbon at their contact with the overlying Holocene marine sands.

Livingstone, in his two classic papers on Holocene palynology from the Alaskan Arctic (Livingstone, 1955; 1957), shows alder pollen reaching modern levels only about half-way through the Holocene at Umiat, which geographically lies well within the modern distributional limits for alder. Moreover, both his Chandler Lake and Umiat diagrams show a major period (his Pollen Zone II) where birch was a major component of the vegetation and alder was apparently rare, which preceded the alder maximum of the latter half of Holocene time.

In the PB-2 materials, by contrast, birch and alder follow approximately parallel courses throughout the section. An increase in alder is typically accompanied by an increase in birch pollen, throughout the section, and almost always at concentrations in excess of modern values. In Chandler Lake, Livingstone (1955) had no values for alder that were significantly above modern ones anywhere in his core, although he did note a tendency for alder to decline slightly in the upper part of his core there.

Colinvaux (1964), in presenting pollen data from ten radiocarbon-dated samples from the Arctic Coastal Plain, found only a trace of alder pollen in

samples from either Barrow or Umiat that were over 8,000 years old. His evidence also parallels that of Livingstone, in that there was at least a detectable period prior to the advent of significant amounts of alder in the vegetation, when birch was common in the virtual absence of alder.

In short, the bulk of the sediments in borehole PB-2 that have been analysed for pollen content show pollen spectra that are unlike either those of the modern day or those recorded from Holocene deposits elsewhere on the Coastal Plain. The possibility that this part of the core represents extremely rapid deposition at the height of the postglacial thermal maximum seems both geologically and palynologically unrealistic.

We are thus left with the tentative conclusion that these sediments in fact represent deposits of a period predating the last glacial maximum. While it is perhaps possible that this could be a mid-Wisconsin interstadial time, it would seem more likely, in view of all the evidence, that these are most probably deposits from the Sangamon (Pelukian) or an earlier interglacial. Work presently being done with Sangamonian marine sediments collected from coastal bluffs during the 1977 field season should help to further clarify the situation.

REFERENCES CITED

- Barnes, P. W., 1977: Core Radiography, Appendix I to Offshore Permafrost Studies, Beaufort Sea, by D. M. Hopkins and others, p. 413-414 in Environmental Assessment of the Alaskan Continental Shelf, Annual Reports of Principal Investigators for the year ending March, 1977, vol. 16: Hazards (Boulder, Colorado: Outer Continental Shelf Environmental Assessment Program, March, 1977)
- Colinvaux, Paul A., 1964: Origin of Ice Ages: Pollen Evidence from Arctic Alaska. Science, vol. 145, No. 3633, p. 707-708, August 14, 1964
- Heusser, Linda, and William L. Balsam, 1977: Pollen Distribution in the Northeast Pacific Ocean. Quaternary Research, vol. 7 no. 1, p. 45-62, January, 1977
- Hillhouse, Jack, 1977: Paleomagnetism of Marine Section of Borehole PB-2, Appendix II to Offshore Permafrost Studies, Beaufort Sea, by D. M. Hopkins and others, p. 415-416 in Environmental Assessment of the Alaskan Continental Shelf, Annual Reports of Principal Investigators for the year ending March, 1977, vol. 16: Hazards (Boulder, Colorado: Outer Continental Shelf Environmental Assessment Program, March, 1977)

- Livingstone, D. A., 1955: Some pollen profiles from Arctic Alaska.
Ecology, vol. 36, no. 4, p. 587-600, October, 1955
- , 1957: Pollen Analysis of a valley fill near Umiat, Alaska.
American Journal of Science, vol. 255, p. 254-260, April, 1957
- Nelson, R. E., 1977: Preliminary Report on Pollen from Borehole PB-2,
Appendix VI to Offshore Permafrost Studies, Beaufort Sea, by D. M. Hopkins
and others, p. 426-431 in Environmental Assessment of the Alaskan
Continental Shelf, Annual Reports of Principal Investigators for the year
ending March, 1977, vol. 16: Hazards (Boulder, Colorado: Outer Continental
Shelf Environmental Assessment Program, March, 1977)

* * *

MODERN POLLEN RAIN ON THE CHUKCHI AND BEAUFORT SEA COASTS, ALASKA

by

Robert E. Nelson
Branch of Alaskan Geology
U. S. Geological Survey
345 Middlefield Road
Menlo Park, California 94025

and

Dept. of Geological Sciences
University of Washington
Seattle, Washington 98195 *

INTRODUCTION

Little has been done in the line of Quaternary palynology on the Arctic Coastal Plain of Alaska since the early studies of Livingstone (1955; 1957) and Colinvaux (1964). Even less has been done with regard to modern pollen studies, which are a necessary prerequisite to understanding fossil pollen spectra.

This study is the initial product of an attempt to gather together sufficient modern pollen data from the Arctic Coastal Plain to give depth and meaning to studies of fossil pollen floras in this region. While the sampling of coastal environments is neither ecologically nor geographically exhaustive, it is hoped that this preliminary report may provide both some insight into modern pollen rain here as well as impetus for further work.

Most of the samples used in this study were collected from coastal bluffs underlain by sandy or gravelly deposits of the last (Sangamon) interglacial high sea level stand. This porous substrate, compounded by the topographic relief of the coastal bluffs, has resulted in more xeric conditions along the coast than probably exist even one kilometer inland. Whether this significantly affects the pollen rain can only be determined by further sampling inland from the coast.

SAMPLE COLLECTION AND PROCESSING

The samples utilized in this study were collected during the course of

* Please use this address for any correspondence.

geological field investigations along the Chukchi and Beaufort Sea coasts of northern Alaska during the summers of 1976 and 1977. Moss polsters were collected by hand and then sealed in sterile plastic sample bags; surficial algal muds from dry pond bottoms were scraped from the upper 5 mm of sediment, placed in sterile sample bags and sealed.

In the laboratory, about 5 ml of each sample was placed in a plastic 15 ml centrifuge tube and covered with a 5% solution of KOH. Samples were then placed in a boiling water bath for 15 minutes, after which they were mixed to within 1 cm of the top of the centrifuge tube with distilled water. The samples were then centrifuged at approximately 5000 rpm for one minute, and the supernatants decanted and discarded. Samples were washed once with distilled water, then filtered through a 180-micron or 250-micron sieve in order to remove coarse debris. The fine residue was washed with 10% HCl to remove carbonates, then treated with 48% HF in a hot water bath for 30 minutes to remove silicates. Residues remaining after the HF treatment were washed with glacial acetic acid and then acetolysed 3 to 4 minutes. Final residues were mounted in glycerine jelly beneath 22 x 30 mm coverslips, and counted at a magnification of 200x.

In general, one entire slide was counted to obtain a satisfactory count of pollen grains, although it was occasionally necessary to count a second slide. The number of grains counted in each sample is shown in Table I. Percentages of total pollen (exclusive of spores) for Picea (spruce), Alnus (alder), Betula (birch), Gramineae (grasses), Cyperaceae (sedges), and Salix (willow) are shown in Figure 1; percentages for other taxa accounting for more than 1% of the total pollen (included in "others" in Figure 1) are enumerated in Table I.

DISCUSSION

Extraordinarily high spruce pollen content makes two samples stand out immediately in Figure 1, samples 77-ANr-1 and 77-ANr-2d, from the Prudhoe Bay area. Moriya (1976) also detected a surprisingly high (7.5%) percentage of spruce in his

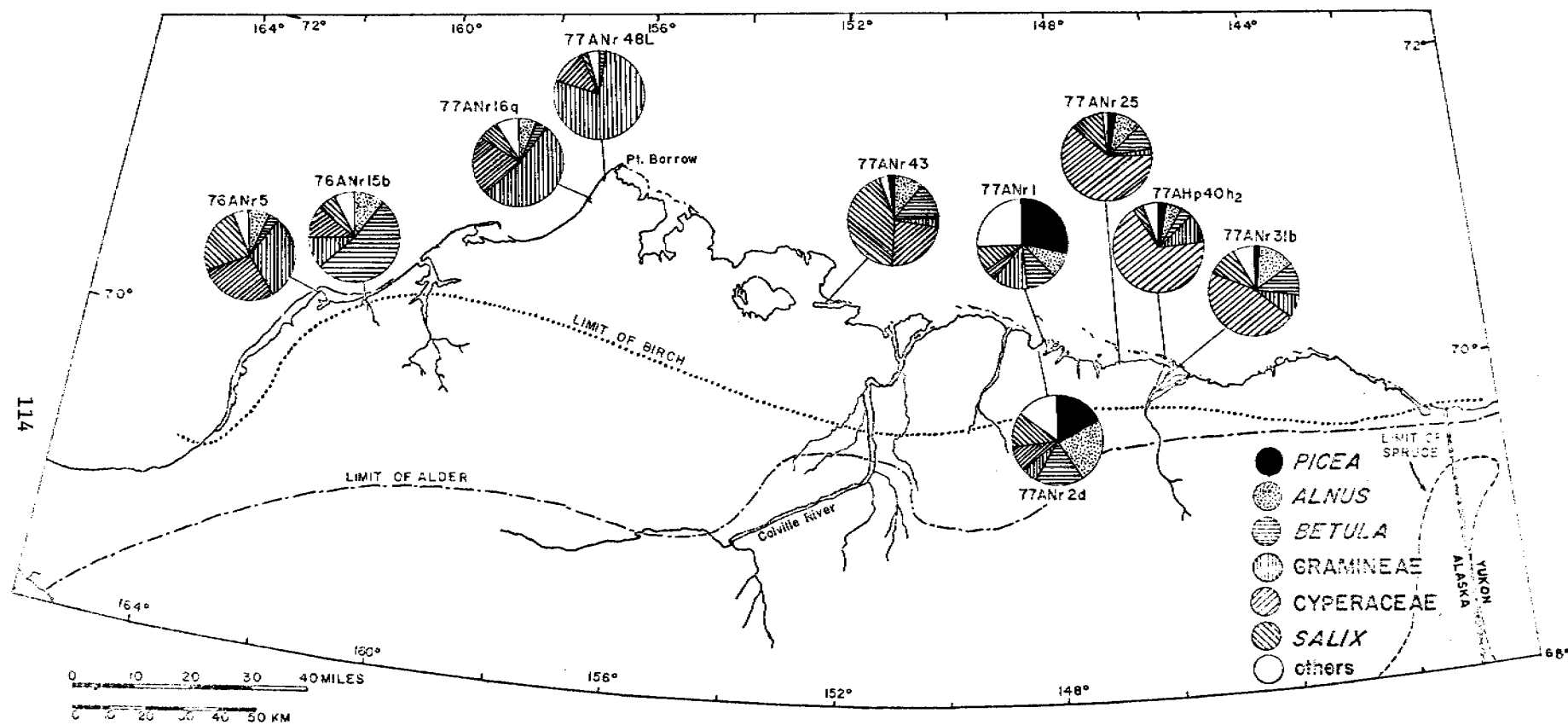


Figure 1

Index map showing location and major pollen taxa of samples reported in this study. Also shown are modern distributional limits for spruce (*Picea glauca*), alder (*Alnus crispa*) and birch (*Betula nana*). Distribution limits taken from Hulten (1968) and Viereck and Little (1972), modified for birch to include plants growing at sample site 76ANr15b.

TABLE I

Sample No.	Grains Counted	Sample Type	Dominant Surrounding Vegetation	Other taxa*
76 ANr 5	423	moss polster	sedges locally dominant, some grasses and prostrate willows	Ericaceae (2.4%) Saxifragaceae (1.2%)
76 ANr 15b	322	moss polster	<u>Dryas</u> , grasses, <u>Eriophorum</u> ; prostrate willows common to locally abundant; <u>Betula nana</u> uncommon but not rare	Ericaceae (2.2%)
77 ANr 16q	250	moss polster	<u>Carex-Eriophorum</u> meadow with admixed Gramineae, prostrate willows and <u>Petasites frigidus</u>	Ericaceae (1.6%) Oxyria-type (2.4%) (Polygonaceae)
77 ANr 48L	399	moss polster	dry tundra, moss from the bottom of a dry depression, surrounded by grasses with some <u>Salix</u> , sedges, <u>Saxifraga</u> and Caryophyllaceae	Ericaceae (1.7%)
77 ANr 43	351	surface mud, dry pond	<u>Carex-Eriophorum</u> meadow with some grasses; abundant prostrate willows beyond 5 meters	Ericaceae (1.4%)
77 ANr 1	192	moss polster	Ground only about 50% covered by vegetation. In order of abundance, <u>Dryas</u> , Gramineae, <u>Artemisia arctica</u> . About 10% other herbs	<u>Pinus</u> (5.2%) Ericaceae (7.8%) <u>Artemisia</u> (4.2%) other Compositae (1.6%) Saxifragaceae (1.6%) Rosaceae (3.1%)
77 ANr 2d	346	moss polster	moist tundra dom. by <u>Carex</u> and <u>Eriophorum</u> , with grasses and prostrate willows, <u>Pedicularis</u> and other herbs	<u>Pinus</u> (1.4%) Ericaceae (2.6%) Rosaceae (3.2%) <u>Polygonum bistorta</u> type (2.6%) Scrophulariaceae (1.2%)
77 ANr 25	186	surface mud, dry pond	drained thaw lake basin, wet tundra dominated by <u>Carex</u> and <u>Eriophorum</u> , some prostrate willows	none
77 ANr 31b	245	surface mud, dry pond	sedges, some grasses and occasional prostrate willows	<u>Artemisia</u> (2.0%)
77 AHp 40h ₂	179	moss polster	dry tundra, dominated by very short <u>Carex</u> , <u>Eriophorum</u> , some <u>Cladonia</u> and short grass. <u>Cardamine</u> , <u>Papaver</u> , and <u>Taraxacum</u> on bluff faces	<u>Artemisia</u> (1.7%)

* Taxa present in amounts exceeding 1% of total pollen, in addition to taxa shown in Figure 1.

Table showing additional data for samples reported in this study.

sample from a polygon fill at Prudhoe Bay. That pine should constitute over 5% of sample 77-ANr-1 is even more surprising, since the nearest pines to Prudhoe Bay are jack pine (Pinus banksiana) in the central Yukon Territory, and lodgepole pine (P. contorta) in southeastern Alaska, both over 1,000 km distant. The nearest spruce to Prudhoe Bay lies some 150 km to the south.

Both samples 77-ANr-1 and 77-ANr-2d were taken from areas near the Sagavanirktok River main channel, however, and it is possible that some of the conifer pollen in them may be redeposited from older deposits or areas with higher percentages of modern conifer pollen further to the south. Pollen of Sequoia type was found in both samples, in addition to a few primitive trilete spores probably derived from Tertiary or Cretaceous strata over which the river flows upstream from my sample sites. Moriya's sample (1976, p. 345) was collected from a depth of 5 cm and thus may not reflect represent modern pollen rain, but rather that of some time in the recent past (probably since 1900).

The high spruce content in the Prudhoe Bay samples is also interesting from another standpoint: is pollen production in the Prudhoe Bay area really lower (by as much as an order of magnitude) than elsewhere along the Beaufort Sea coast, or is some strange circumstance of atmospheric circulation concentrating the southerly storm winds, with their content of forest-zone pollen, such that they are directed directly over the Prudhoe Bay area ?

It would seem most likely that a combination of these two factors is involved, but absolute pollen influx studies, using pollen traps monitored over a number of years in numerous localities, would be necessary to determine the relative importance of each factor. Such a detailed study is beyond the scope of our work, but may well provide an interesting project for future work.

Also worthy of note with regard to spruce pollen is its failure to account for as much as 1% of the total pollen in any of the samples from Barrow southwards along the Chukchi coast, as far as Icy Cape, including the two spectra Livingstone

(1955) published for the Barrow area. Only five grains were found in the four samples I have counted along this coastal stretch, out of a total of 1,396 pollen grains. It would seem to follow, then, that fossil spectra from this same area that show significant amounts of spruce would imply either northward movement of the spruce treeline or a shift in the southerly storm winds.

Sample 76-ANr-15b, taken several miles inland from the Chukchi coast along the Nokotlek River, represents pollen rain at the geographical distribution limit for dwarf birch (Betula nana). Although neither Hulten (1968) nor Viereck and Little (1972) show dwarf birch extending this far towards the coast in this area, I found a number of individuals growing at or near the site where this sample was collected. The high (53.7%) percentage of birch in this sample is thus understandable.

The relatively high percentages of grass pollen in samples 77-ANr-16q and 77-ANr-48L (53.6% and 79.2%, respectively) are consistent with values reported by Livingstone (1955) for two samples from near Barrow (41% and 49%), although it is most probably overrepresented in my sample 48L. Livingstone's samples also showed 5% and 10% alder at Barrow, whereas sample 77-ANr-48L contains less than 1% alder. This is at least in part a product of the overrepresentation of grass pollen in this sample.

The three easternmost samples analysed, 77-ANr-25, 77-AHp-40h₂, and 77-ANr-31b, are dominated by sedge pollen, even though this area is where both dwarf birch and alder distribution limits most closely approach the sample sites. Local pollen production in this area might therefore be relatively high compared to the other sited studied.

SUMMARY

Spruce pollen is found in abnormally high concentrations in modern pollen samples from the Prudhoe Bay area, although some of this may be due to reworking

of extralocal and/or fossil pollen by flooding of the Sagavanirktok River. Spruce pollen is present in only minute traces in coastal samples between Icy Cape and Point Barrow.

Birch pollen can represent more than half the total pollen present in samples taken at its distribution limit, yet drops to no more than 10% a few tens of kilometers beyond its distribution limit. Grass seems to be slightly more important than sedge along the Chukchi coast, whereas the opposite tends to be true along the Beaufort Sea coast of Alaska. Alder pollen is variable, but tends to decrease in importance with greater distance beyond its distribution limit. Sedge is particularly important along the eastern part of the Beaufort coast, at least as far as the mouth of the Canning River, the furthest east that samples have been taken.

Sphagnum does not account for more than 2% of total pollen and spores in any of the samples studied, except for the two Prudhoe Bay samples. Implications of this are discussed in the section regarding spruce content in those two samples.

ACKNOWLEDGMENTS

This work could not have been done without the tactical support of the United States Naval Arctic Research Laboratory (NARL) at Barrow, Alaska, and their assistance is gratefully acknowledged. Peggy A. Smith aided greatly in collection of materials in the field, and Mia La Londe processed some of the samples in the laboratory. Dr. Matsuo Tsukada brought the Moriya book to my attention, and Yoriko Tsukada assisted with translation of the passage relating to the Prudhoe Bay sample.

REFERENCES CITED

- Colinvaux, Paul A., 1964: Origin of Ice Ages: Pollen evidence from Arctic Alaska. Science, vol. 145, No. 3633, p. 707-708; August 14, 1964
- Hulten, Eric, 1968: Flora of Alaska and Neighboring Territories. Stanford, California: Stanford University Press, 1008 pages
- Livingstone, D. A., 1955: Some pollen profiles from Arctic Alaska. Ecology, vol. 36, no. 4, p. 587-600; October, 1955

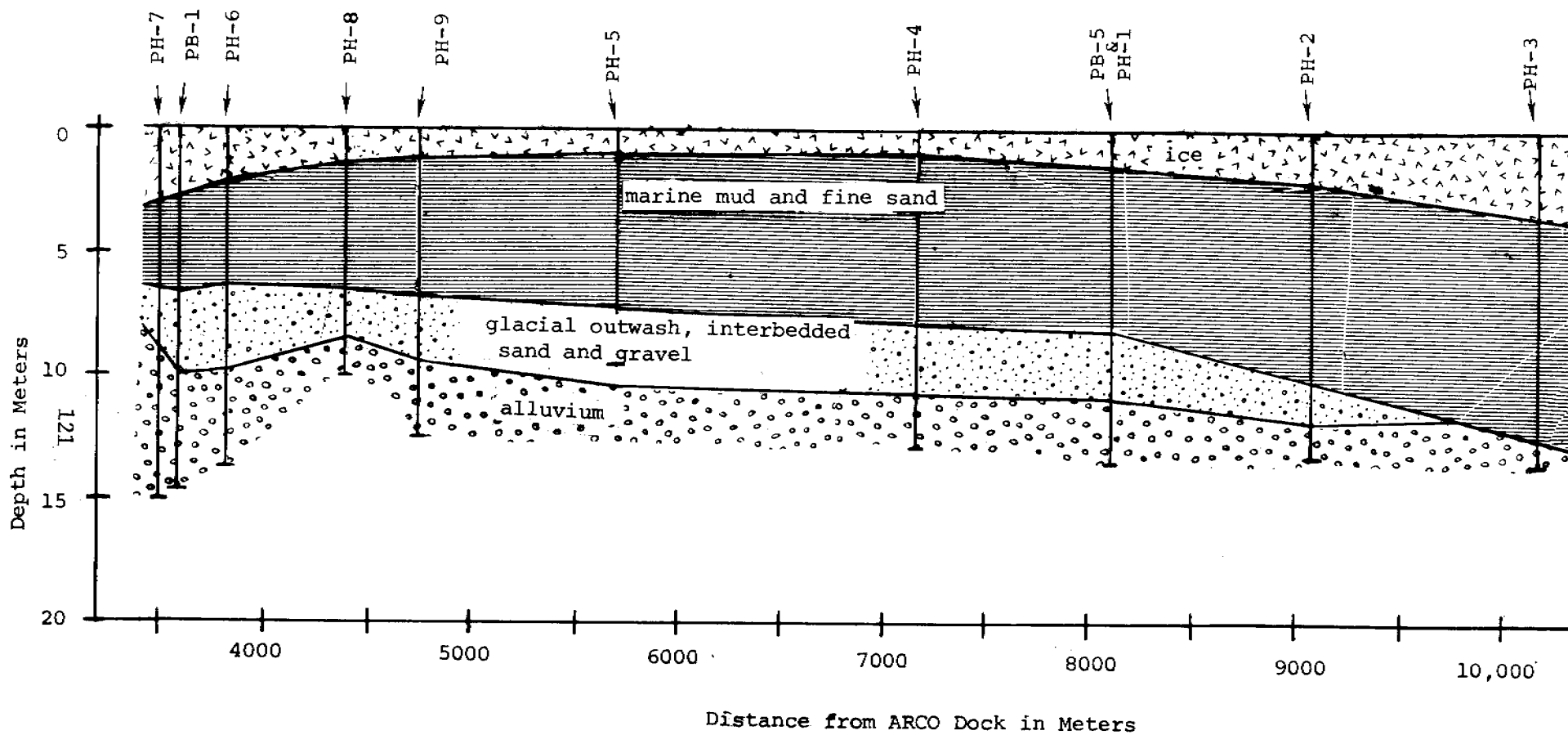
Livingstone, D. A., 1957: Pollen analysis of a valley fill near Umiat, Alaska.
American Journal of Science, vol. 255, p. 254-260; April, 1957

Moriya, Kikuo, 1976: Flora and Palynomorphs of Alaska. Tokyo: Kodansha Company;
366 pages (in Japanese)

Viereck, Leslie A., and Elbert L. Little, Jr., 1972: Alaska Trees and Shrubs.
Washington, D. C.: Forest Service, U. S. Department of Agriculture: Agriculture
Handbook No. 410; 265 pages

Appendix V. Offshore Cross-sections

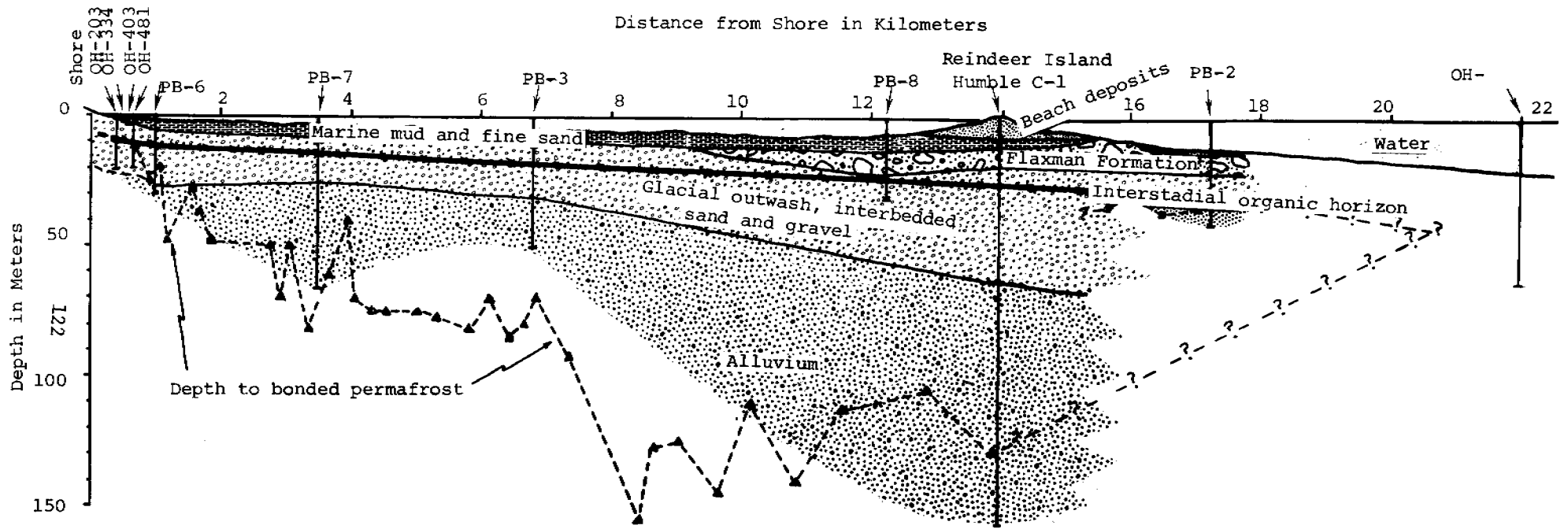
Cross Section based on Engineering Probes



PH = Engineering Probe

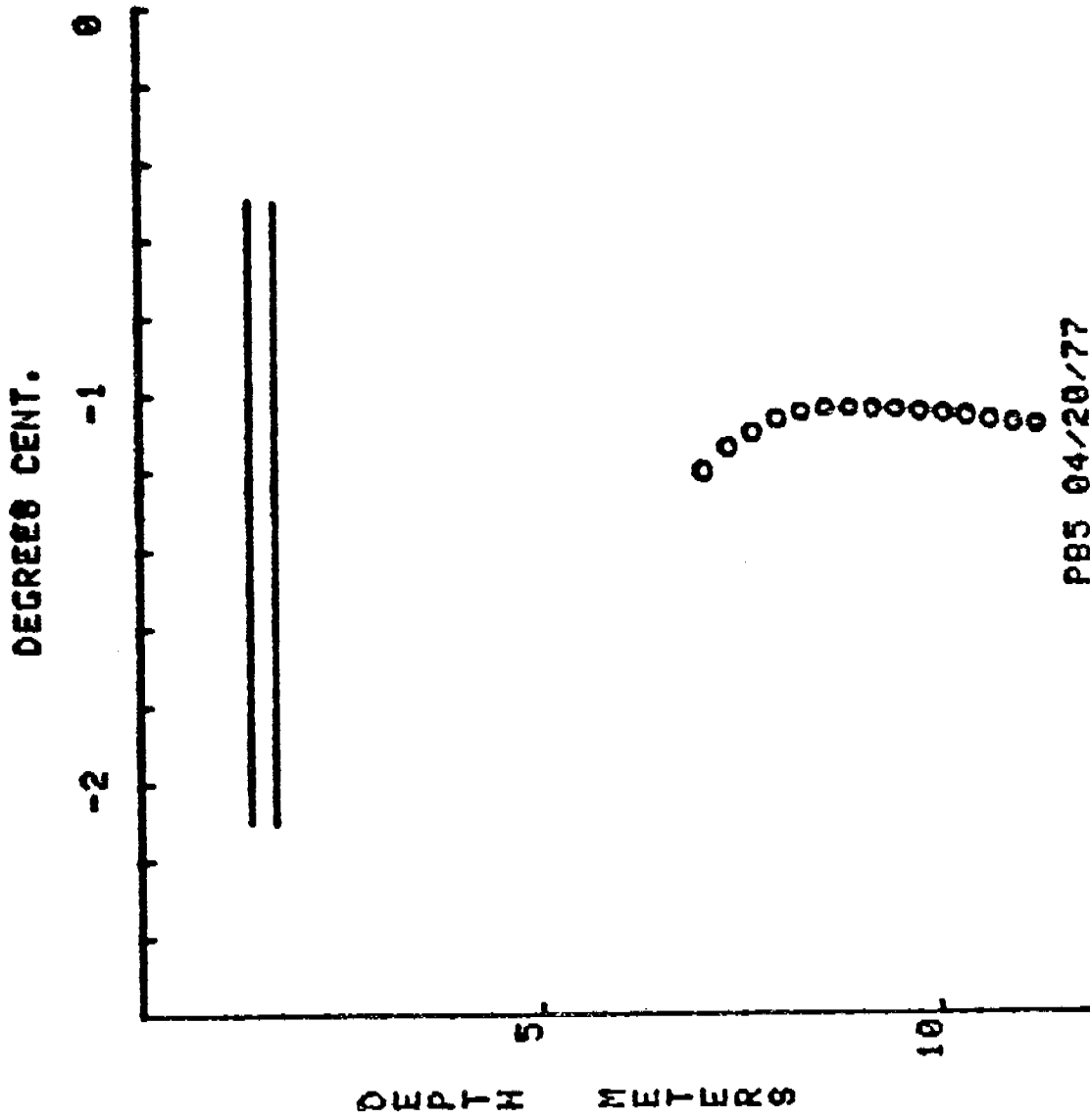
PB = Borehole

Cross Section of Prudhoe Bay based on Boreholes



Appendix VI. Thermal Profiles

Appendix Thermal Data.

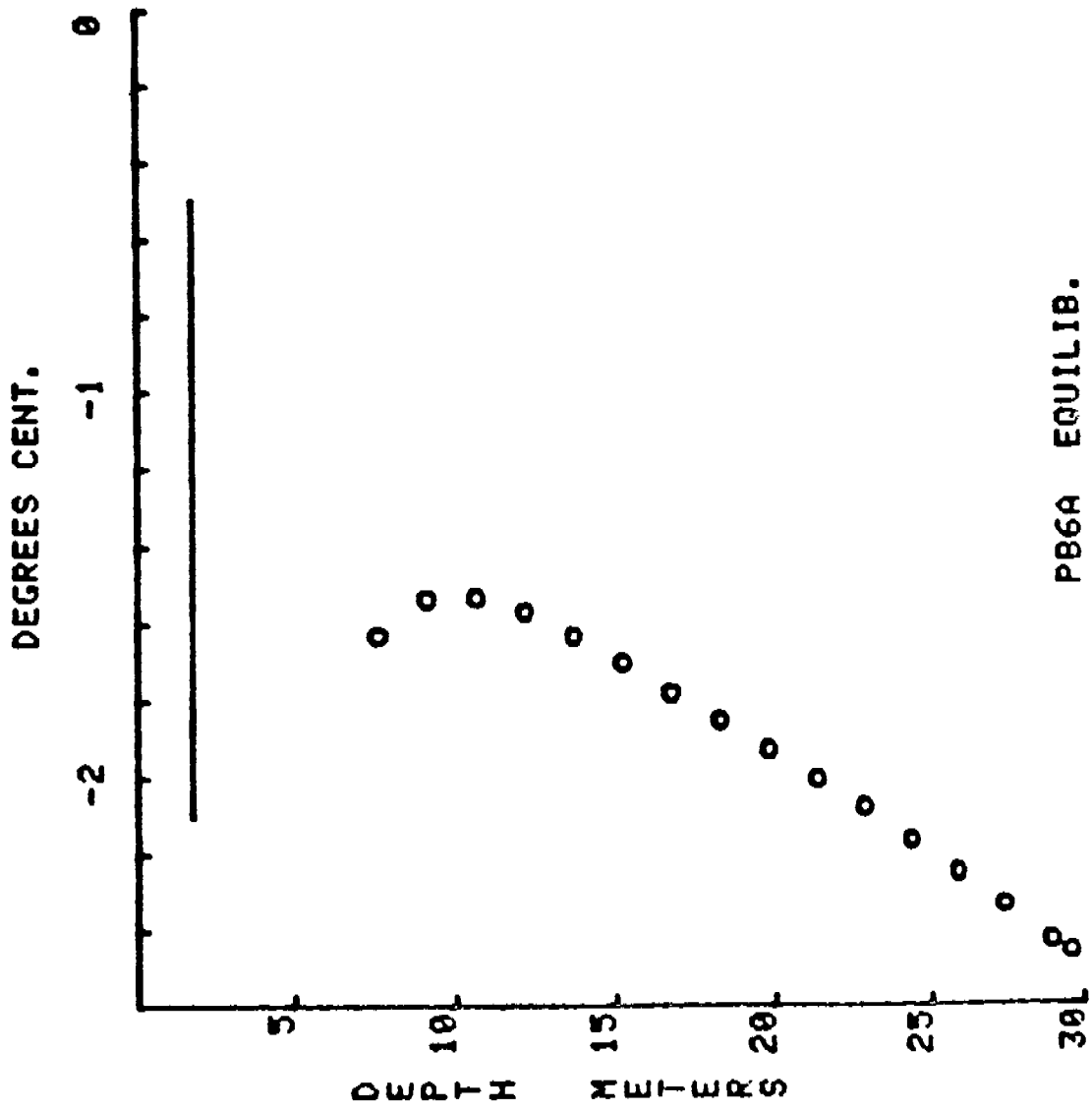


P85 04/20/77

Appendix Thermal Data.

PB5	DEPTH(M)	TEMP(C)
	-7.04	-1.2025
	-7.35	-1.1399
	-7.65	-1.1008
	-7.96	-1.0686
	-8.26	-1.0476
	-8.56	-1.0399
	-8.87	-1.0406
	-9.17	-1.0420
	-9.48	-1.0441
	-9.78	-1.0497
	-10.09	-1.0546
	-10.39	-1.0616
	-10.70	-1.0707
	-11.00	-1.0805
	-11.31	-1.0826

Appendix . Thermal Data.

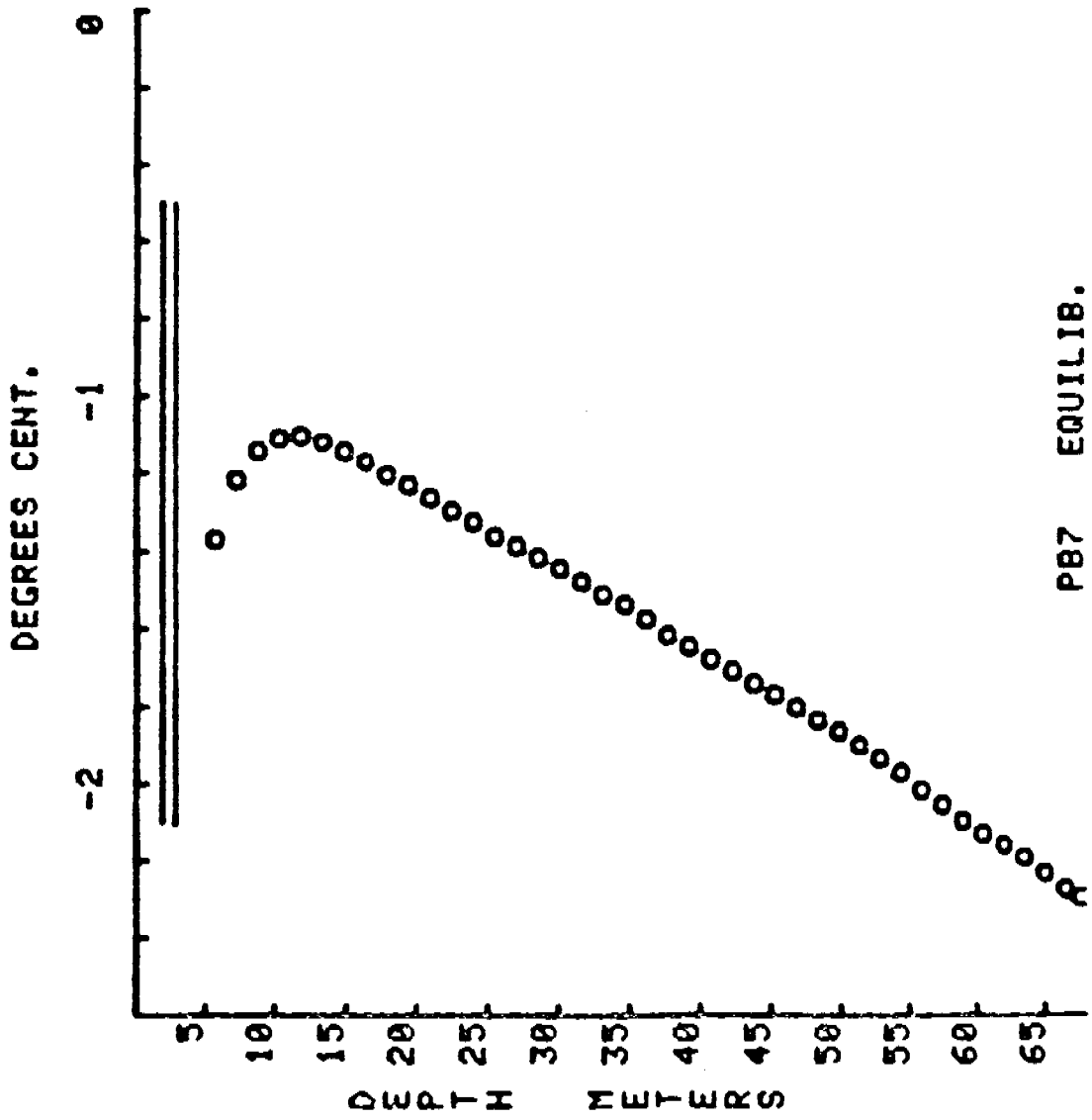


Appendix Thermal Data.

	DATA
X	-1.631
	-1.536
	-1.534
	-1.57
	-1.632
	-1.703
	-1.781
	-1.852
	-1.93
	-2.009
	-2.083
	-2.168
	-2.255
	-2.338
	-2.433
	-2.46
Y	-7.62
	-9.14
	-10.67
	-12.19
	-13.72
	-15.24
	-16.76
	-18.29
	-19.81
	-21.34
	-22.86
	-24.38
	-25.91
	-27.43
	-28.96
	-29.6

PB6A - EQ. TEMPS.

Appendix Thermal Data.

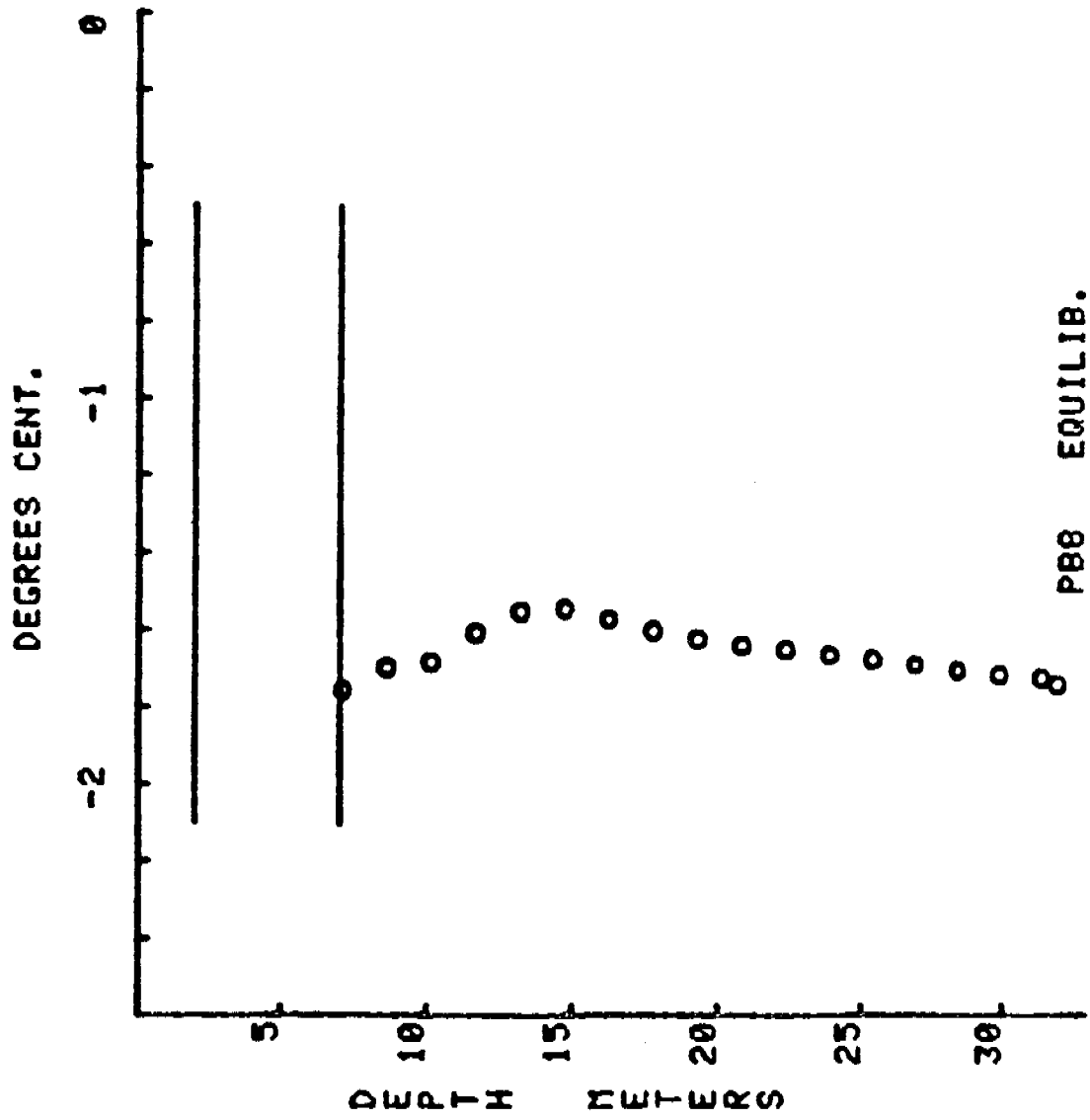


Appendix Thermal Data.

X	Y	DATA
-1.371	-5.7	-34.47
-1.217	-7.22	-55.99
-1.142	-8.75	-57.52
-1.109	-10.27	-59.04
-1.116	-11.8	-60.56
-1.143	-13.32	-62.09
-1.169	-14.84	-63.61
-1.203	-16.37	-65.14
-1.229	-17.89	-66.66
-1.262	-19.42	-67.76
-1.295	-20.94	
-1.326	-22.46	
-1.361	-23.99	
-1.388	-25.51	
-1.416	-27.04	
-1.445	-28.56	
-1.478	-30.08	
-1.511	-31.61	
-1.536	-33.13	
-1.575	-34.66	
-1.615	-36.18	
-1.646	-37.7	
-1.679	-39.23	
-1.71	-40.75	
-1.743	-42.28	
-1.771	-43.8	
-1.804	-45.32	
-1.837	-46.85	
-1.868	-48.37	
-1.905	-49.9	
-1.938	-51.42	
	-52.94	

PB7 EQUILIBRIUM TEMPERATURES

Appendix Thermal Data.



Appendix Thermal Data.

	DATA
X	-1.757
	-1.7
	-1.686
	-1.689
	-1.553
	-1.547
	-1.572
	-1.602
	-1.624
	-1.641
	-1.655
	-1.667
	-1.68
	-1.693
	-1.71
	-1.721
	-1.728
	-1.747
Y	-7.11
	-8.63
	-10.16
	-11.68
	-13.21
	-14.73
	-16.25
	-17.78
	-19.3
	-20.83
	-22.35
	-23.87
	-25.4
	-26.92
	-28.45
	-29.97
	-31.49
	-32.07

PB8 -- EQUIL. TEMPS.

Appendix VII. Radiocarbon Dates

March 6, 1978

Information bearing on interpretation of radiocarbon date USGS-192
(Top of marine clay, Borehole PB-2)

This sample was collected in water about 13 m deep but sample itself lies at -14 m. The foram fauna is rich and implies open shelf conditions well removed from the shoreline, although faunal sequence indicates that water was shoaling from previous greater depths and shoreline was nearer than it had been previously. It seems conservative to estimate that water over the sample site was at least 4 m deep and that relative sea level of the time was no lower than -10 m.

Nature of the carbon.--Sample contained abundant forams, rare mollusks, a very few ostracodes, abundant swigs, seeds, and bits of plant tissue, abundant palynomorphs, and some coal. The mollusks, forams, and ostracodes are seemingly indigenous and lived contemporaneous with deposition. The coal and a minor part of the palynomorphs are obviously redeposited from Tertiary sediments on the mainland to the south.

The twigs, seeds, and plant tissue and most of the palynomorphs may represent contemporary material blown over ice in winter or washed in during summer, or they may represent redeposited ancient material derived by erosion of ancient peat in coastal bluffs.

The pollen spectrum includes much spruce, alder, and sphagnum, all palynomorphs representing species present during Holocene time and during the last interglacial but absent from Alaska 18,000 years ago. The pollen spectrum includes little or no Artemesia, although Artemesia generally constitutes 10-15% of 18,000 year-old pollen spectra in Alaska.

Coastal bluffs of the Beaufort Sea expose thick peat, but the peat is mostly Holocene in age. Gravel pits and other boreholes suggest that 18,000 years ago, the Prudhoe Bay area was a glacial outwash fan with sparse vegetation and certainly no substantial peat marshes nor even a continuous turf. Interglacial peats would have been buried, presumably below the level of shoreline bluffs.

Radiocarbon analysis.--A bulk sample was submitted. Separate analyses of carbon content at CRREL indicate about 1.5% organic carbon at this level.

Sample was first leached with acid, which should remove all forams and mollusk shells as well as any limestone or dolomite that might have been present. Sample was then combusted. Steve has had analytical labs determine total organic carbon in another bulk sediment sample and established that yield from his combustion process is incomplete when sediment samples are being burned. A sample determined by Analytical Labs to contain 3.8% carbon lost only 1.0 to 1.5% of its total weight upon combustion in the radiocarbon lab. Thus, radiocarbon lab recovered only about a quarter or a third of the most easily combusted carbon. This suggests that coal in the sample tended to remain uncombusted and that the yield to the radiocarbon line tended to come only from the fresh plant tissue.

It seems, then, that radiocarbon age determination USGS-192 is probably based entirely on fresh plant tissue. If the sample is not entirely contemporary with the sediment, then it must be a mixture of contemporary material and redeposited interglacial material older than the range of radiocarbon dating.

Attached chart shows the effects upon the apparent age of varying mixtures of dead material and material contemporary with the sample. For example, if the sample were modern, 89.5% of the plant material in the sample would be redeposited dead carbon (or if the sample were ancient, 10.5% modern contaminants would give an apparent age of 18,000 years). If the sample were 8,000 years old (as would be suggested by its present position below sea level), then it would be contaminated by 78% dead carbon.

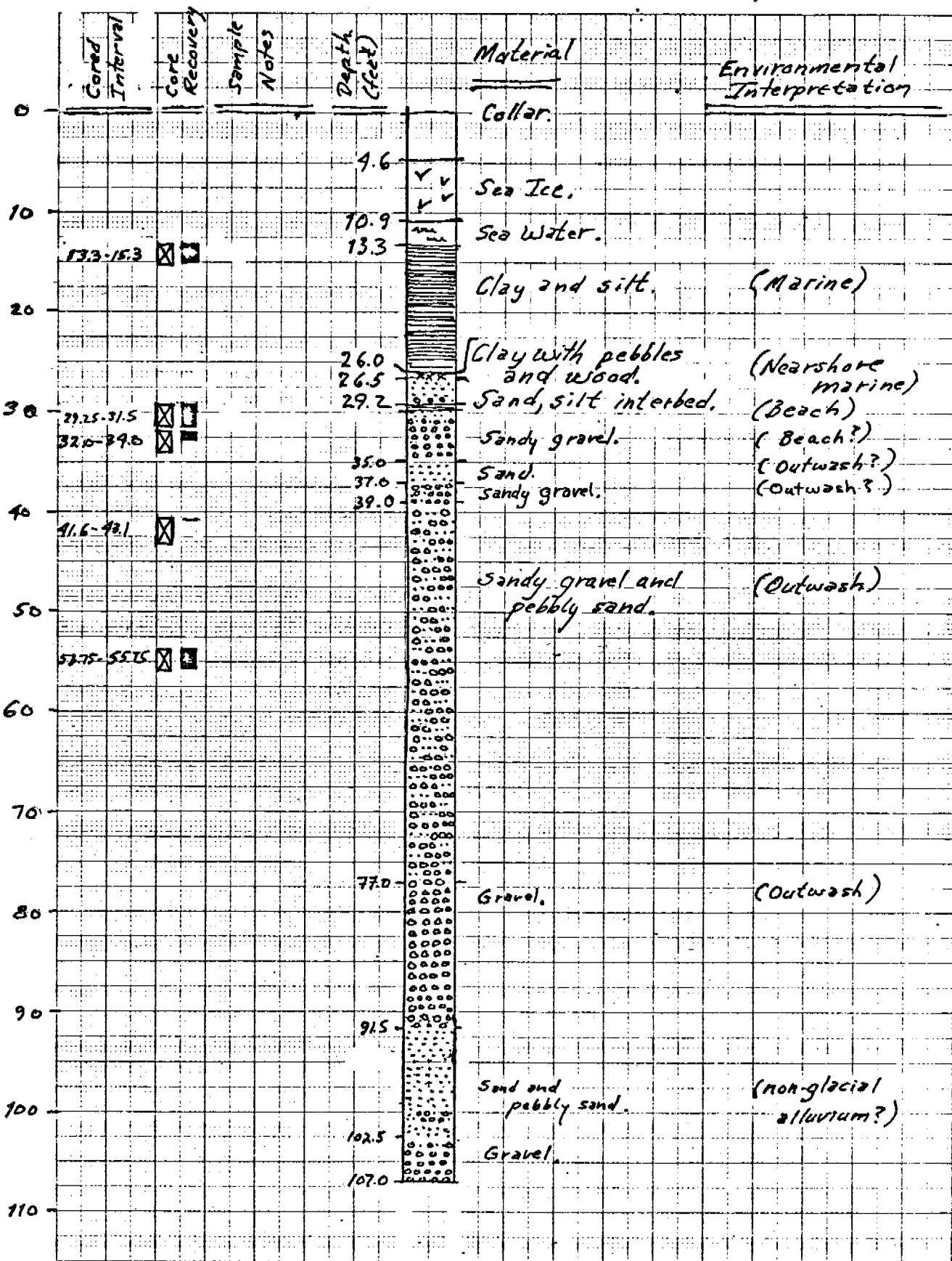
D. M. Hopkins

cc: Bob Nelson
Steve Robinson

Appendix VIII. Condensed Boring Logs

461510

K-E 10 X 10 TO THE CENTIMETER 10 X 25 CM.
KEUPPEL & ESSER CO. MADE IN U.S.A.

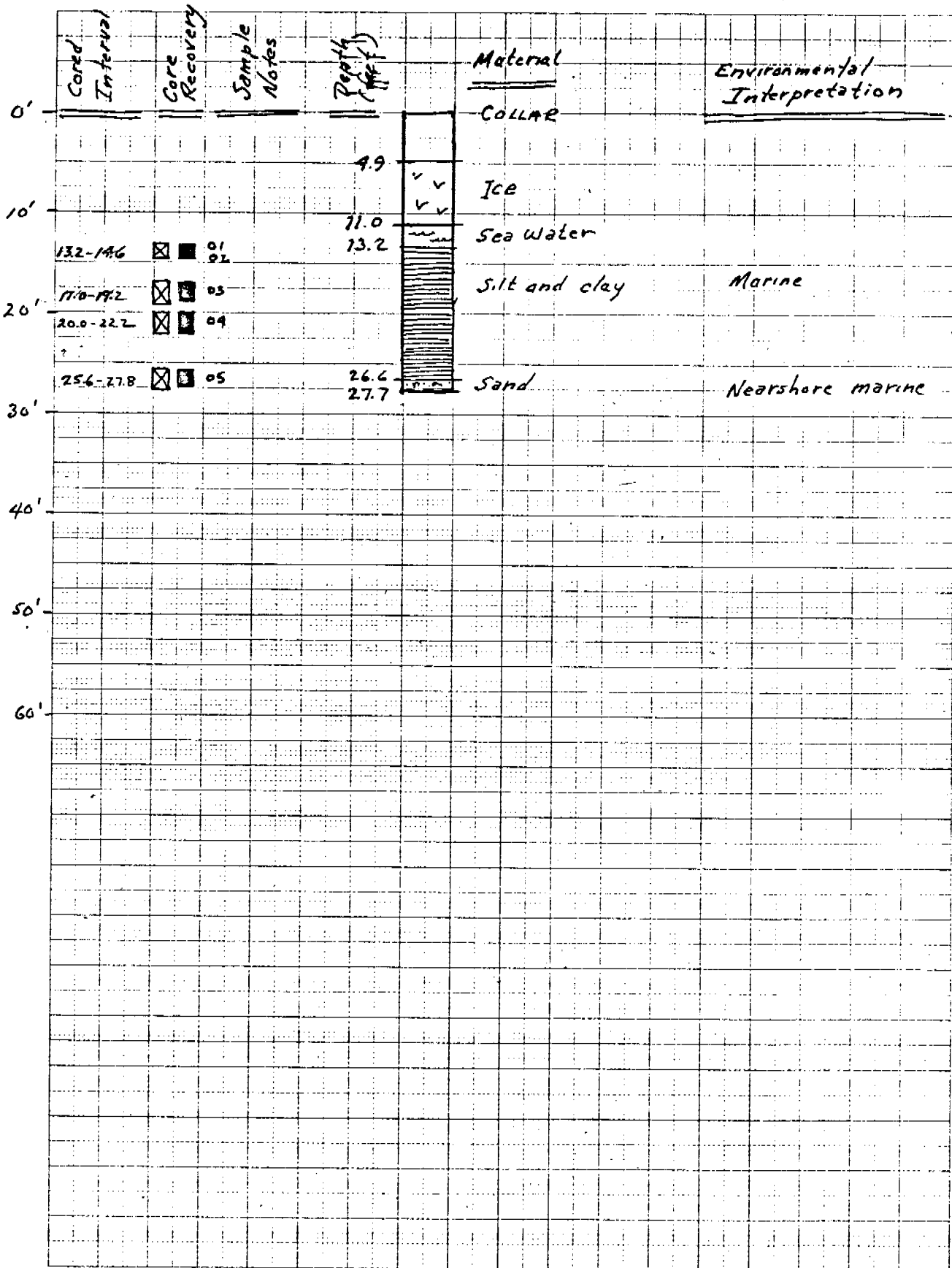


BOREHOLE PB-1A

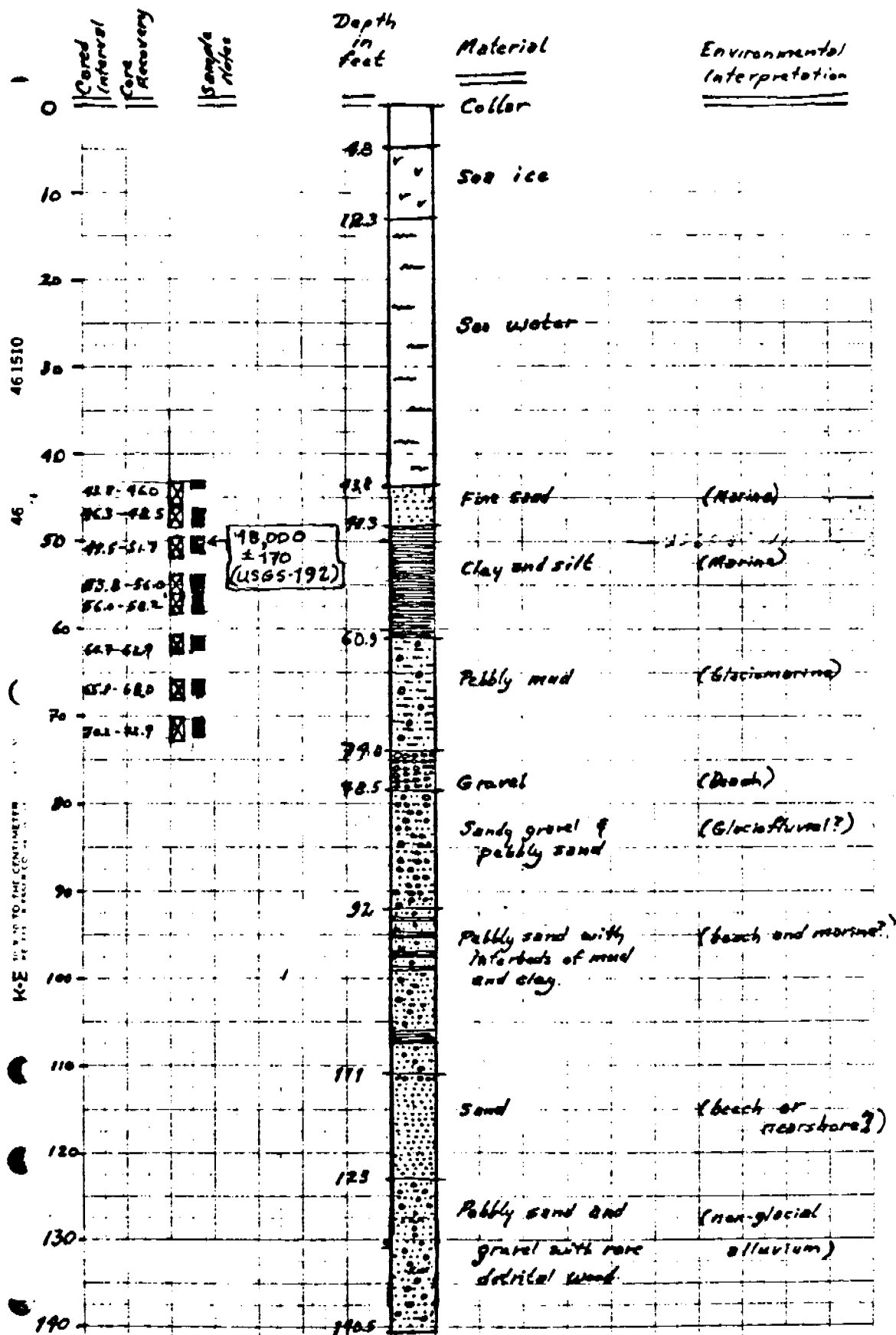
LAT. 10° 20.7' N
LONG. 198° 19.3' W

461510

10 X 10 TO THE CENTIMETER 18 X 25 CM
KEUFFEL & ESSER CO. MADE IN U.S.A.

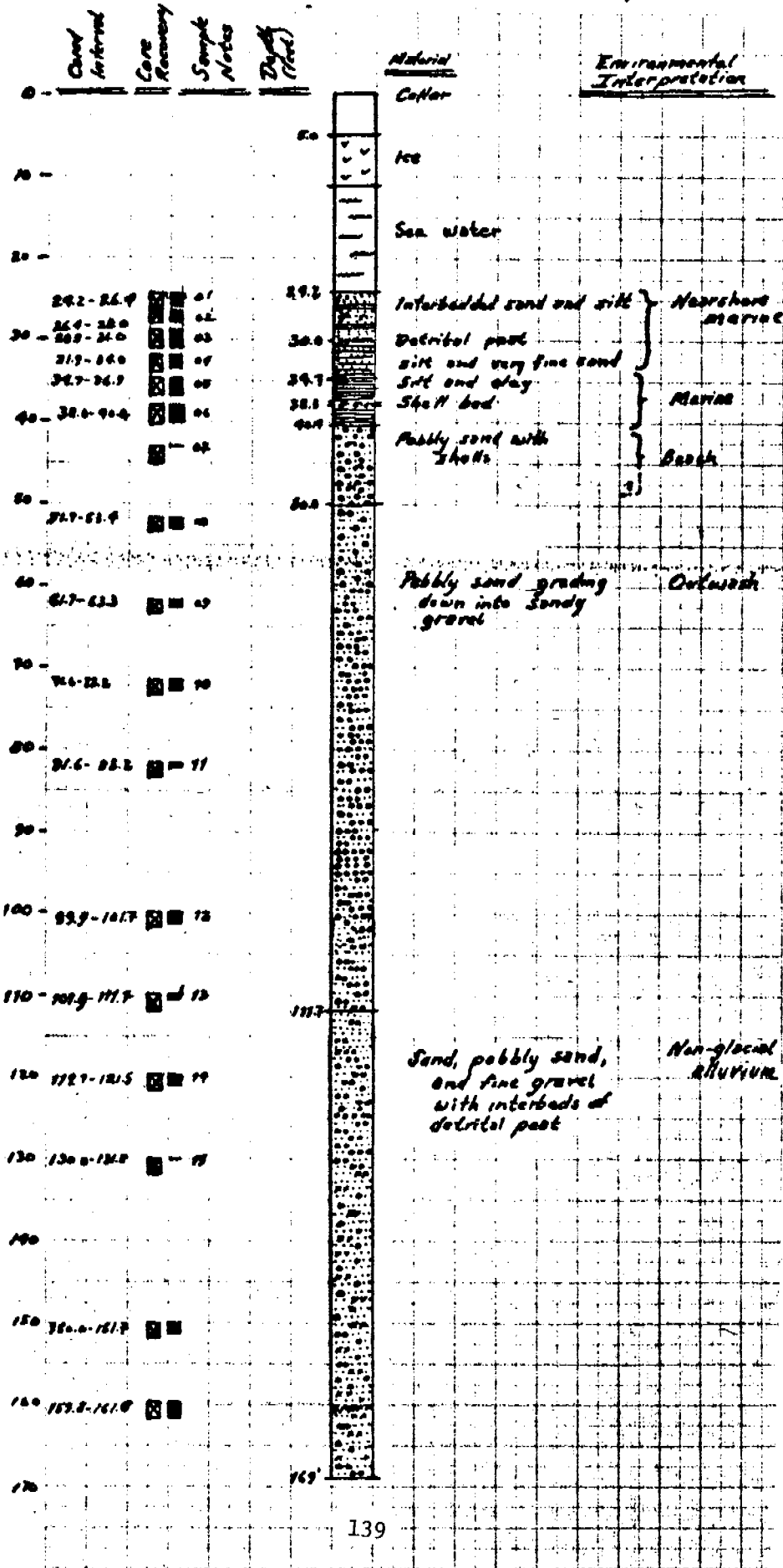


BOREHOLE PB-2

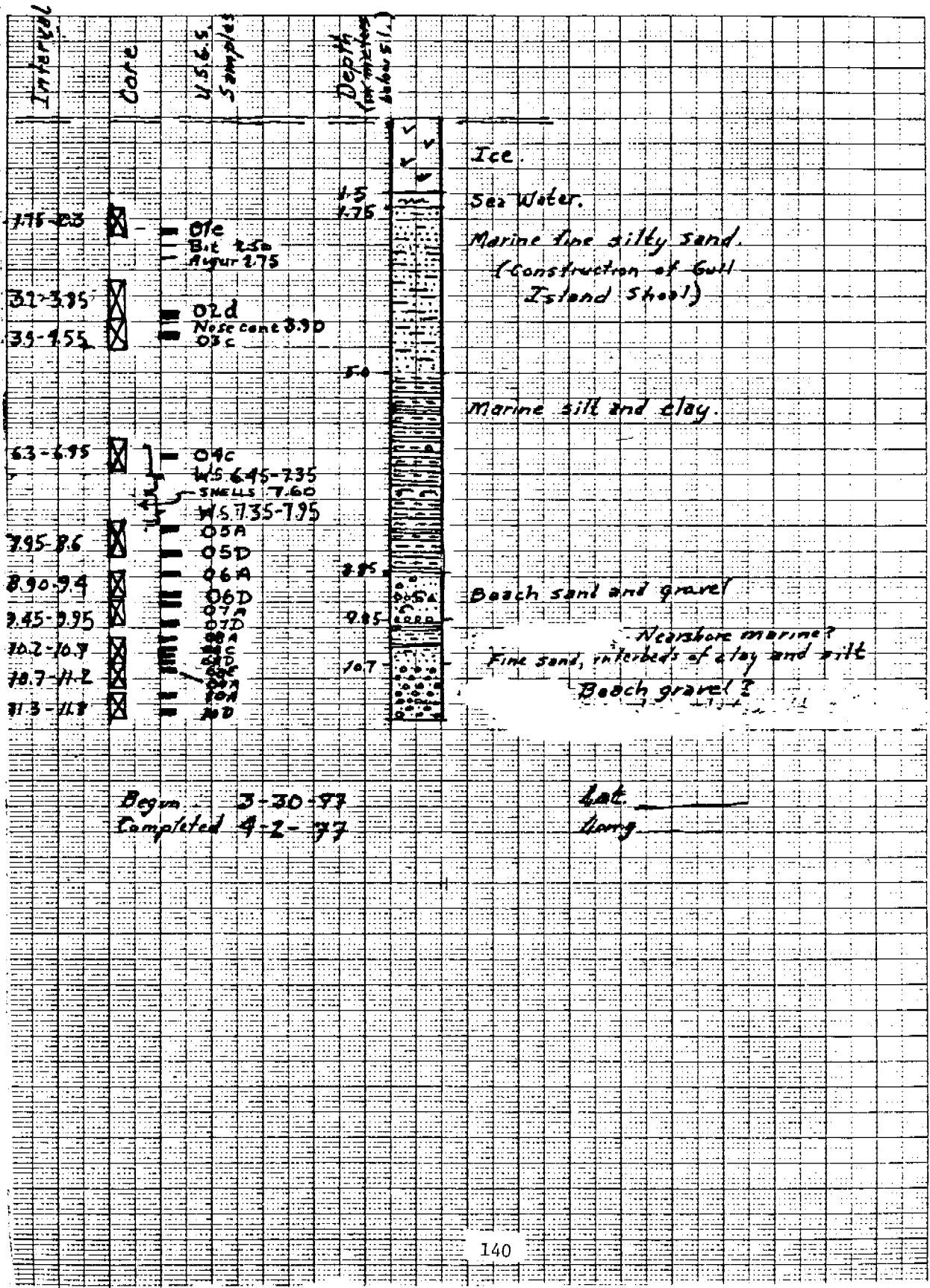


BOREHOLE PB-3

Lat. 70° 40' 00" N
Long. 148° 26.6' W



BOREHOLE PB-5



K·E 10 X 10 TO THE CENTIMETER 18 X 25 CM.
 KEUFEL & ESSER CO. MADE IN U.S.A.

461510

SUMMARY LOG: BOREHOLE PB-6/6A

CORE NO.	INTERVAL (Meters below sea level)	Graphic	U.S.G.S. Samples	Depth of Lithologic Change	NOTES	Interpretation
					Ice	
					Water	
01	1.85-2.50		0601c	1.80		
02	2.50-3.20		0601b	1.85		
03	3.25-3.85		0601a		Medium sand and thin beds of fine silty sand	Holocene Nearshore(?) sand
04	3.85-4.50		0600b			
05	4.50-5.15		0600a	4.80		
06	5.15-5.60		060c		Pebble gravel, interbeds of pebbly sand	Holocene Beach gravel
			W.S. 6.45-6.05			
			W.S. 6.05-6.45			
07	6.65-7.15		060c			
			W.S. 6.9-7.5			
08	7.35-8.10					Holocene Beach gravel?
			W.S. 8.75-11.10			
09	11.10-11.65		060c	10.50	Fine sand grading down into clay	Holocene offshore and beach? or Holocene flow lake?
			W.S. 12.0-14.2	11.90	Interbedded medium sand and coarse silty gravel	
10	14.15-14.70			14.75		
			W.S. 15.40-16.30			
			W.S. 16.30-17.25			
11	17.25-17.75		11A		Coarse, clean, well-rounded gravel; no organic remains	Late Wisconsin glacial outwash
			W.S. 18.45-19.40			
			W.S. 19.45-20.30			
12	20.30-20.85					
			W.S. 21.55-22.45			
			W.S. 22.45-23.30			
			W.S. 24.3-25.4			
			W.S. 25.40-26.45	26.0		
13	26.45-26.95		DBA		Gravel, possibly with plant remains	
			W.S. 27.7-28.6			
			W.S. 28.6-29.0	29.0		
14	29.55-30.10		14A	29.5		
15	30.10-30.55		15A		Coarse pebbly sand, fine sand, and pebble gravel	Mid-Wisconsin alluvium

SUMMARY LOG: BOREHOLE PB-7

CORE NO.	Interval (Meters below seabed)	Graphic	G.S.G. Samples	Depth of Sample Change	Notes	Lab. Comp.
					Ice	
				1.81	Water	
01	2.25-3.50	X	01A 01D WS 2.75-5.00	2.25	Interbedded sandy silt and silty clay	Holocene marine sand
02	4.95-5.40	X	02A 02B WS 5.10-5.123 5.05 WS 5.12-6.50 BSM Sample 6.50 02D WS 6.50-7.90		Pebbly sand	Holocene Beach
03	6.60-7.10	X	03A WS 6.65-7.95 7.90		Sandy gravel	
04	7.40-9.95	X	04 WS 7.75-8.35 WS 8.35-9.00 05 WS 9.00-9.6	7.40	Angular, silty gravel, in beds of sand. Vent. faun.	Idkiliik (Lab. Wisconsin) outwash
05	8.75-9.45	X	05 WS 9.4-10.2			
06	10.2-10.7	X	06D			
07	11.25-11.55	X	07			
08	14.25-14.75	X	08A WS 15.10-16.35		Sand with detrital silt - green. Some. Dated at 24,000 years in 04-1990	
09	17.15-17.65	X	09 WS 18.20-19.40 WS 19.40-20.75		Coarse gravel	
10	20.25-20.75	X	10A 10B WS 21.25-21.75 WS 21.75-22.50		Very coarse gravel sand matrix	
11	23.25-23.75	X	11A 11B WS 24.75-25.50 WS 25.50-26.75		Coarse gravel	
12	26.53-26.97	X	12A 12B WS 27.10-28.02 WS 28.02-28.53 WS 28.53-28.85		Interbedded coarse gravel and sand	
13	29.25-29.97	X	13 WS 30.45-31.10 WS 31.10-31.70 WS 31.70-32.70 WS 32.70-32.85		Upward fine sequence sandy gravel	
14	32.45-32.76	X	14 WS 33.25-33.66 WS 33.66-35.06 WS 35.06-35.67 WS 36.00-36.61 WS 36.61-37.25 WS 37.25-37.85		Interbedded sand gravel w/ organic thin out	
15	38.25-39.25	X	15A	142	Organic silt	
					Coarse gravel	
					Interbedded coarse sand & coarse sand	
					Sand w/ organic	
					Organic sandy silt (silty)	
					Coarse gravel, slightly sand & organic	
					Slightly sandy coarse gravel	

461510

10 X 10 TO THE CENTIMETER 10 X 2 CM
K&E MODEL & DESIGN CO. SAN FRANCISCO

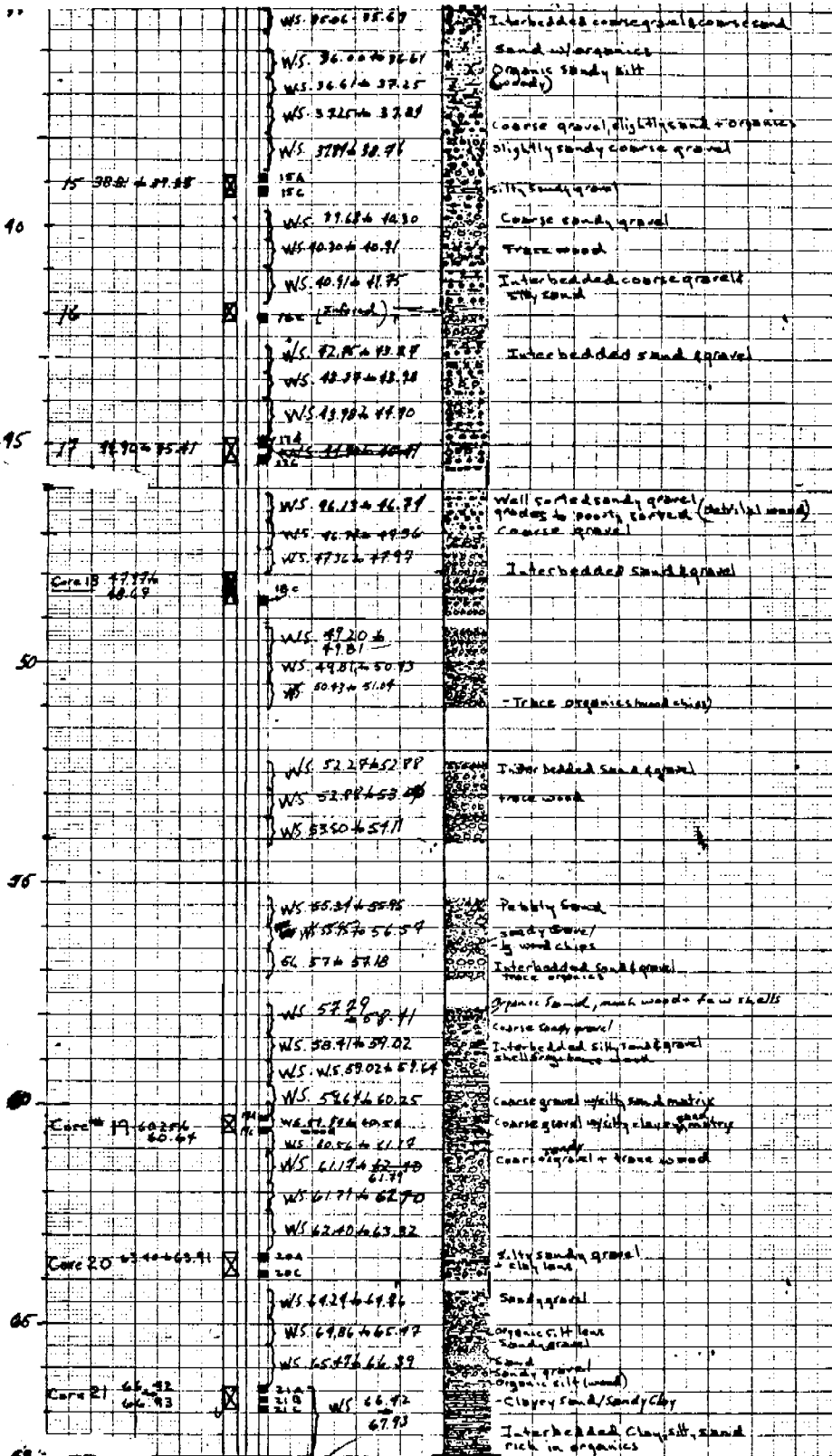
461510

10 X 7 TO THE CENTIMETER 10 X 2 CM
K&E MODEL & DESIGN CO. SAN FRANCISCO

10 X 10 TO THE CENTIMETER
K&E
K&E
K&E

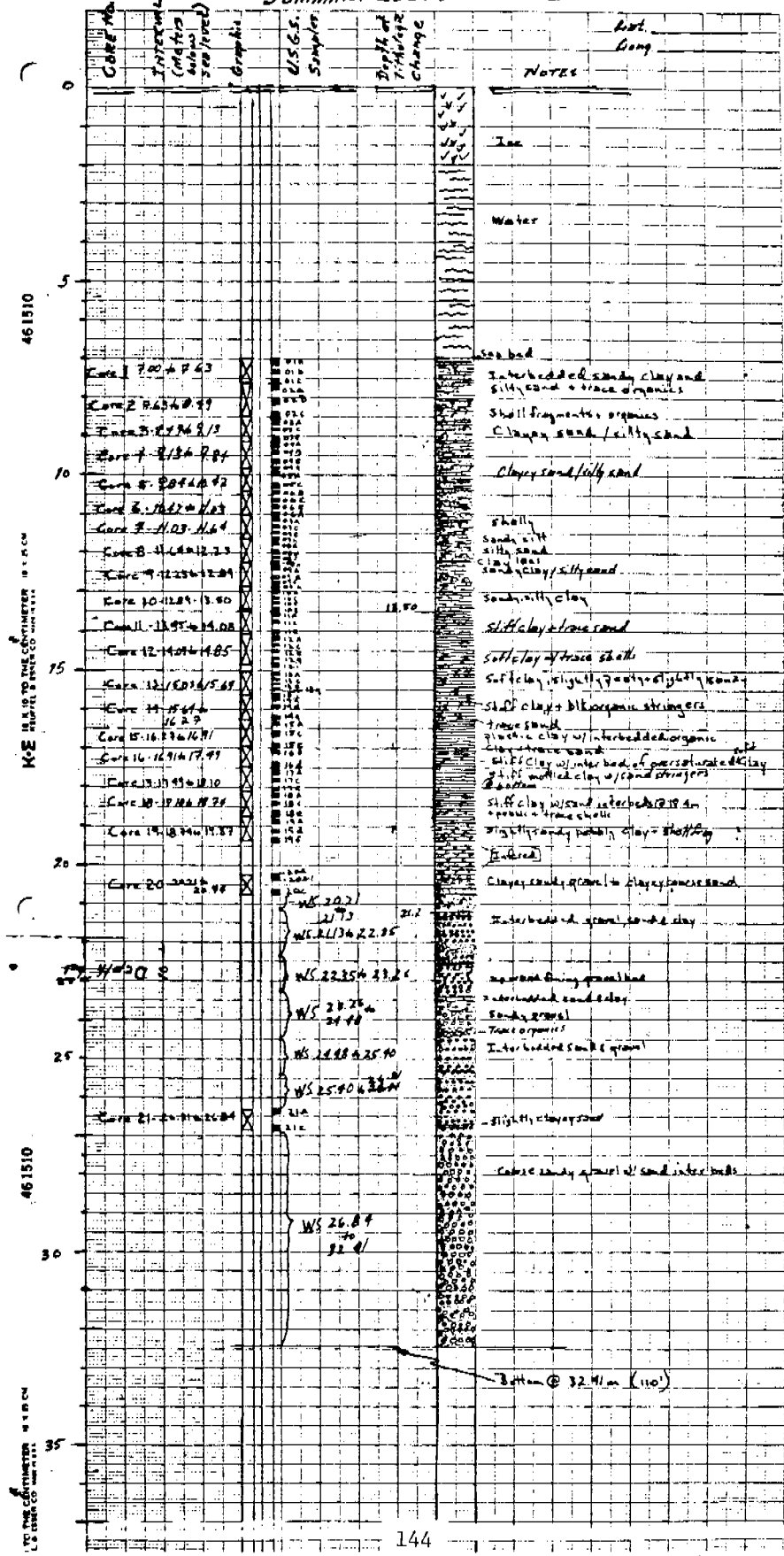
461510

10 X 10 TO THE CENTIMETER
K&E
K&E
K&E



Bottom @ 69.93 m (225')

SUMMARY LOG: BOREHOLE FB-8



Appendix IX. The Flaxman Formation of Northern Alaska:
Evidence for an Arctic Ice Shelf?

THE FLAXMAN FORMATION OF NORTHERN ALASKA:
EVIDENCE FOR AN ARCTIC ICE SHELF?

David M. Hopkins, U.S. Geological Survey, Menlo Park, CA 94025,
Kristin McDougall, U.S. Geological Survey, Menlo Park, CA 94025, and
Robert E. Nelson, University of Washington, Seattle, WA 98195

The Flaxman Formation (including some deposits described by Black, 1964, as the "Skull Cliff Unit of the Gubik Formation") is a sheet of bedded sandy silt and clay containing dropstone pebbles. The formation underlies the northernmost Arctic coastal plain of Alaska and extends to the outer Beaufort Sea shelf. It is well exposed in coastal bluffs, crops out widely on the shelf, and has been penetrated and sampled in two offshore boreholes near Prudhoe Bay.

In coastal exposures, the Flaxman Formation consists mostly of compact, dark grey, bedded sandy silt containing striated glacial erratic dropstones probably derived from the Amundssen Gulf region of Canada. East of the Colville River, this facies seems to lack megafauna, but farther west, it has yielded whale remains and marine mollusks near Lonely and five species of marine mollusks near Cape Simpson.

Outcrops on the seafloor consist of tough, overconsolidated clay commonly covered by lag gravel of Canadian lithology. The two offshore boreholes penetrated lag gravel of Canadian lithology underlain by overconsolidated marine silt and clay in which the few stones are of Brooks Range origin and then beach gravel and glacial outwash of Brooks Range lithology. Pollen and foraminiferal analyses indicate that the silt and clay in the boreholes were deposited during the last interglacial. We believe that the Flaxman Formation includes a Sangamon interglacial marine member and an overlying glaciomarine member of Wisconsinan age. Erratic boulders of Canadian lithology are also found in the deposits of a middle Pleistocene marine terrace west of the Colville River, but these evidently record one or more earlier cycles of glaciomarine deposition in Arctic Alaska.

Hughes, Denton, and Groswald (1977) noted that the presence of Canadian erratics in the Alaskan Flaxman Formation seemed supportive of their concept of an ice shelf covering the Arctic basin. The apparent presence of Wisconsinan glaciomarine sediments on the shelf and low-lying shores of the Beaufort Sea indeed suggests sedimentation in a marginal moat isostatically depressed by a grounded ice shelf, but if the shelf covered the entire abyssal Arctic Ocean, reduced salinities and a lack of marine life would be expected. A more local ice shelf covering the MacKenzie Bight seems more consistent with our present limited knowledge.

Appendix X. Quarterly Reports

April-June, 1977	Vol. 2, p. 441
July-September 1977	Vol. 3, p. 522
October-December, 1977	Vol. 2, p. 318

ANNUAL REPORT

Contract: RK6-6074
Research Unit: 205
Reporting period: April, 1977 -
March, 1978
Number of Pages: 17
4 Attachments

Marine environmental problems in the ice covered
Beaufort Sea shelf and coastal regions

Peter Barnes

Erk Reimnitz

Pacific-Arctic Branch of Marine Geology
345 Middlefield Road
Menlo Park, California 94025

April 1, 1978

TABLE OF CONTENTS

I. Summary of Objectives, conclusions and implications.....

II. Introduction

 A. General nature and scope of study.....

 B. Specific objectives.....

 C. Relevance to problems of petroleum development.....

III. Current state of knowledge.....

IV. Study area.....

V. Sources, methods and rationale of data collection.....

VI, VII, and VIII - Results, Discussion, COncclusions

 (As attachments to report)

 A. Storm Surges of the Alaskan Beaufort Sea

 B. Ice Gouge Characteristics: Their Changing Patterns from 1975 to 1977, Beaufort Sea, Alaska

 C. Character of Ice Gouging in the Chukchi Sea

 D. Stamukhi Shoals of the Arctic - Some Examples from Alaska

IX. Needs for further study.....

 Table I.....

X. Summary of fourth quarter operations.....

XI. Bibliography and references.....

I. Summary of objectives, conclusions and implications with respect to OCS oil and gas development.

The present investigation is an expansion and intensification of our earlier studies on the marine geology and modern sedimentary environment off arctic Alaska with emphasis on rates and processes. In particular we have concentrated on phenomena involving ice and its unique influence on the shelf and inshore environment. The marine environment of the arctic shelf poses special problems to offshore development. Faulting, tectonic activity and sea floor instability are environmentally of lower concern in the Beaufort Sea, when compared to processes involving sea ice and low temperatures. Seven years of study have provided a basic understanding of this unique marine geologic environment. However, many important aspects have yet to be addressed. For example, the major processes involved in ice gouging of the sea floor are reasonably understood, including distribution, densities, gouge trends, rates of gouging, depths of reworking and the variability of gouge formation from year to year. Critical questions regarding the interaction of the stamukhi with the continental margin, the distribution and character of gouging in this zone, the time of formation and the year to year stability of the stamukhi zone. Neither are the effects of the stamukhi zone on oceanographic circulation, sediment disruption and dispersal, and the shelf profile understood.

Another area where we have poor understanding involves coastal zone processes. The spring flooding of the sea ice with river water is reasonably well known as a phenomenon but the intensity of the associated processes of transport, scour and ice movement are only poorly understood. Rates of coastal erosion are known to be significant, but the fate of these erosional products, their relationship to river input, and the growth and maintenance of the barrier islands need to be assessed. Inside the 2-m bench were ice rests on the bottom at the end of the winter, a unique sedimentary environment exists where tides and surges set up significant currents and cause vertical fluctuations in the ice cover. In addition, conductive heat transfer through the grounded ice makes this an area of differing permafrost character.

The third year of field work and subsequent laboratory and office work has resulted in the following tentative conclusions regarding the arctic nearshore environment.

Preliminary analysis of a series of 60 vibracores taken in the nearshore area between the Sagavanirktok River and the Colville River shows five different environments. Lagoonal and bay sediments are indistinctly laminated sandy silts and clays. Cores in the vicinity of the barrier islands are sands and gravels with an abundance of depositional sedimentary structures. Offshore shoals are characterized by clean well-laminated sands underlain by finer material on the ridge flanks. Off the Colville delta layered sands, silts and peats are replaced seaward beyond 5 m by disrupted or poorly laminated muds, probably related to strudel and ice gouge reworking. The absence of

gravels except in the immediate vicinity of the coastal bluffs and barrier islands is of significance to offshore development.

Re-examination of two precisely controlled side-scan sonar survey lines first established in 1973 and subsequently resurveyed in 1975, 1976, and 1977 indicated that the inner shelf between 5 and 15 m of water depth is completely reworked to depths averaging 20 cm in periods between 50 and 100 years. Gouge trends appear to be consistent within any one year but show differences from year to year. Furthermore, trends are related to bathymetry and sea-floor relief. Gouging north of Oliktok is apparently "steered" by the orientation of shoals. Gouging is expected to be more intense further seaward within the stamukhi zone.

Detailed bathymetry in the vicinity of the new causeway and in the entrance channel to Prudhoe Bay shows several significant changes. The Prudhoe Bay entrance channel is migrating shoreward at 1-2 m per year and may be influenced by seasonal infilling and erosion resulting from channel restriction by ice growth. Coastal retreat in this area is also averaging 1-2 m per year. It is apparent from this study that the construction of features like the new causeway will affect the patterns of erosion and deposition but to an unknown extent.

Surficial and cross-sectional observations of temperature, salinity and turbidity from several years of data indicate that central Harrison Bay may contain a slug of cold saline water related to the process of brine formation during the freezing of the 2 m seasonal ice cover. If this proves to be the case, then pollutants entering this area may be entrained in an area of sluggish circulation and mixing.

Currents measured just west of the Sagavanirktok River in Stefansson Sound indicated a net drift of 3.75 cm/sec at 330° with a mean current speed of 12.78 cm/sec at 1 m off the bottom. During the 53 day record in August and September of 1976, a warm brackish water mass was associated with easterly currents while colder more saline waters were found when westerly currents dominated the system. Attempts to quantify the winter inshore current regime have only resulted in lost equipment.

A zone of grounded shear and pressure ridges - the stamukhi zone - develops each year between the moving polar pack ice and the stationary fast ice. The stamukhi zone, as mapped, essentially follows the 15-20 m isobaths and is controlled by the coastal promontories and by offshore shoals. After the development of the innermost early winter stamukhi, additional stamukhi are formed seaward, generally in an accretionary manner. The existence of grounded ridges in a stamukhi zone acts to shield the inner shelf from ice forces. It is in these stamukhi that the energy of the winter Arctic Ocean is expended on the continents rather than in the swash zone of lower latitude shelves. The early winter zone of ice ridging will probably be another hindrance to offshore development in the near future due to technological limitations of working in zones of intensive sea-ice ridging.

Sonographs obtained in the eastern Chukchi Sea reveal a character of ice-gouged microrelief that is similar to the Beaufort Sea shelf.

Ice gouging is extensive at least as far south as Cape Prince of Wales shoal and into water depths of at least 60 m, but is unevenly distributed. Analysis of gouges shows that the density of ice gouges increases with increasing latitude, increased slope gradients, and decreasing water depth. Densities of over 200 gouges per square kilometer of trackline values higher than $50/\text{km}^2$ were encountered at water depths over 50 m. No ice gouges were observed in water depths exceeding 58 m. Saturation ice gouge densities (greater than $300/\text{km}^2$) occur along the eastern side of Barrow sea valley and the northeast flank of Hanna Shoal. A maximum incision depth at 4.5 m was encountered in the 35-40 m depth interval. Individual ice gouge events wider than 100 m were found, mostly produced by multi-keeled ice fragments. The dominant linear trend (azimuth) of gouge furrows shows no preferred orientation on the Chukchi Sea shelf. Only locally does bathymetric control of the trend of gouges appear. The occurrence of current-produced bedforms within individual ice gouges suggests an interaction between slow-moving grounded or gouging ice keels and swift currents. In other cases, current-produced bedforms, interpreted as being in equilibrium with existing flow regimes, lie adjacent to ice gouges, suggesting contemporary ice gouging to water depths of at least 43 m. Due to generally higher current velocities in the Chukchi Sea, development may prove more difficult here than it will be in the Beaufort Sea.

Studies of suspended particulate matter during both the winter and summer show significant differences between the two seasons. In winter (March) low, oceanic, suspensate values contain less than 25% mineral matter, even in very shallow water. During summer (August, September), inner-shelf values of suspended matter are not especially reflective of stream discharge, except in the vicinity of the Colville River, which apparently dominates the suspended particulate transport regime. By September it is difficult to observe any influence of rivers other than the Colville between the Canning River and Cape Halkett. The concentrations in summer are an order of magnitude higher (or more) than in winter, confirming that this is the season of maximum particulate transport.

A study of the bathymetry, geology, and water characteristics of the Kogru River, a large elongate embayment of the coast, indicates that the origin of this admittedly lake-like feature may have been oversimplified in the past. For one, it is too deep and a morphologic misfit in comparison to the adjacent tundra. It does appear that the Kogru River area is near a significant facies change in the Pleistocene Gubic formation, and may mark the boundary between the readily available gravel to the east and a paucity to the west.

Diving observations of areas of sonograph anomalies called "funny bottom" led to some surprises. The marine encrusted boulder patch inside Karluk Island in Stefansson Sound is apparently a lag deposit from the Gubic formation which may correlate with the Flaxman boulders. Abundant marine growth and a lack of Sagavanirktok River sediments in this area is puzzling. In another area of the lagoon, a dense field of polychaete worm tubes was responsible for "funny bottom" on the sonograph records. Observations in the channel east of Flaxman Island

indicate a closed 10.5 m actively deepening scour depression. A source for the strong currents at this depth and for observed ice gouges in the bottom of the depression is puzzling.

Studies of the morphologic change of 3 offshore islands over a 28 year period shows significant changes. The islands are being transposed landward at about 5 m per year as semi-isolated cells. Accretion is most rapid on the western spits although the overall change in subareal volume of the islands is negligible within the analysis error. Ice push on the seaward facing beaches is apparently a factor in bringing material to the islands from depths of several meters. Most push features are confined to within 100 m of the shoreline. These studies suggest that if the islands were used as gravel borrow sites they would not replenish themselves.

Nearsurface thermoprobe measurements and interstitial salinity determinations in the upper 2 m of the sea floor indicated that the extreme range for these parameters as well as the greatest seasonal variation occurs inside the 2 m isobath. Values from deeper water depths on the open shelf suggest a less variable regime. Clearly sub-sea permafrost is influenced by the presence of salt and inshore of the 2 m bench; brine exclusion during ice formation is also a factor.

Sediment transport and water movement near the seabed is directed out of Harrison Bay and to the west as determined from the release of bottom drifters off the Colville River. The bulk of drifter returns came within 45 days from the Pitt Point region. This is equivalent to a minimum net current of about 3 cm/sec. The implication is that pollutants adhering to suspended sediments in Harrison Bay will normally be partially flushed from the bay to the west.

A study of the 1970 storm surge based on a survey of linear driftwood deposits found on the coastal plain shows that the areas flooded range in width from 20 m to 5000 m on delta plains and in height from about 1.5 m to over 3 m above normal sea level. Variations in height are related to coastline configuration, with maximum runup occurring at the heads of shallow embayments. Major causeways, like major headlands, will cause water to pile up which in turn could cause the causeways to be washed away by wave and current action or destroyed by ice during a future major surge. Our search for evidence on surges similar to the one in 1970 indicates that such surges may be expected only once every 25 to 100 years. We also believe that there has been no surge higher than that of 1970 for several hundred years.

In the area where previous work on ice dynamics and ice zonation suggested the possible existence of a shoal, open water conditions in 1977 allowed us to map a 17 km long, continuous linear shoal 4-10 m high. While the bathymetry might indicate a drowned barrier island/lagoon system as the origin for the feature, the continuous grinding action of ice on the crest of the shoal does not allow long-term preservation of such a feature within the stamukhi zone. We believe that the shoal is maintained, if not built; by ice-bottom interaction. Ice gouge distribution, extremely dense on the seaward flank, is almost totally lacking on the landward side. This suggests

that the shoal plays a role in offshore development and construction.

II. Introduction

A. General nature and scope of study

Arctic shelves, where ice is present seasonally for part of the year, comprise 25% of the world's shelves. Yet the interaction of ice in the regime of sedimentary processes on arctic shelves is poorly understood. Investigation of the continental shelf and shores of the Chukchi and Beaufort Seas was initiated in 1970. The primary goal of this program has been to understand the processes that are unique to arctic shelves and their sedimentary environment where sea ice plays an important if not dominant role.

B. Specific objectives

Many questions have been raised on the basis of our past investigations, and apparently hold the key to an understanding of the seasonal cycle in the marine environment. It is these tasks that we address in our current research.

1) Process of ice gouging - in particular the repetitive rates of gouging, seasonal distribution, and the extent to which it occurs outside the area of our past investigations. The ice bottom interaction in the stamukhi zone where the bulk of oceanic energy is expended on the continent needs special emphasis.

2) Shelf sediment transport regime - including ice rafting, river effluents and reworking and resuspension of bottom materials by ice and benthos.

3) The fast-ice zone; its undersurface morphology and its influence on nearshore current circulation, bedforms, sediment transport, permafrost, and on river discharge.

4) The stamukhi between the coastal ice and the offshore pack ice, and its influence and/or relationship to a) bathymetry, b) thermal effects on the sea floor, c) ice gouging, d) winter current regime, e) tides, and f) sediment transport.

5) An estimation of coastal erosion and its relationship to the formation of offshore islands, submerged shoals, and the stability of the coastal marine environment.

6) Inner shelf oceanography, and its relationship to the sedimentary environment. This includes upwelling in the coastal zone, the dispersal of highly saline (60 ‰) and cold (-5°C) water generated in the shallow embayments, lagoons, and river mouths during the winter, and the possibility of anchor ice formation and ice rafting as factors in the sedimentary environment.

7) A study of the apparent lack of deltaic sedimentation near

river mouths in the arctic, and the unique marine aspects of arctic rivers in general.

8) Outlining the Pleistocene stratigraphy and geologic history of the shelf as an aid to determining a sea level curve for the Beaufort Sea.

9) Delineation of sediment character on the inner shelf from a correlation of available seismic reflection records, samples and drill hole data.

C. Relevance to problems of petroleum development

The character of the arctic continental shelf and coastal area, with its year round and seasonal sea ice and with its permafrost, faces the developer with many special problems. The interaction of the arctic shelf with the arctic pack ice takes the form of ice gouging and the formation of a large stamukhi zone each winter.

Oil drilling and production during the next several years will probably not extend into the stamukhi zone seaward of the seasonal fast-ice zone. Of critical concern are the ice gouge and strudel scour effects on structures and pipelines. A similar emphasis has been taken by the Canadian Beaufort Sea Project in their more advanced state of knowledge and readiness to lease their outer continental shelf lands (Milne and Smiley, 1976). Any structure which is to be mated with the ocean floor requires data concerning the strength and character of the ocean floor. Furthermore, foundation materials in the form of gravels will be needed for work pads offshore. In addition, the offshore drilling operation may encounter permafrost which could be substantially altered during the process of pumping hot oil up to the sea floor or along the sea floor in gathering and transportation pipelines.

III. Current state of knowledge

The current state of general knowledge has been excellently summarized in the Arctic Institute of North America's 1974 publication: The Coast and Shelf of the Beaufort Sea. The bulk of background geologic material for the Alaskan Beaufort shelf has been summarized in articles by Reimnitz, Barnes, Naidu, Short, Walker and others, in this same volume. The Beaufort Sea synthesis volume contains a very useful summary of the current state of knowledge. References to more recent material may be found in the Results and Discussion sections below and in the appended reports. The interested reader is also directed to the comprehensive series of reports resulting from the Canadian Beaufort Sea Project.

Briefly, results to date have clearly established drifting ice as a major influence on the marine geologic and sedimentologic environment of arctic shelves (best summarized in Reimnitz and Barnes, 1974; Barnes and Reimnitz, 1974; and in the 1976 and 1977 Annual Reports).

Major boundaries exist which are related to inner shelf sea ice zonation (Fig. 1). Inside the 2 m contour, ice rests on the bottom at the end of the seasonal growth and generally remains stable and undisturbed through the winter. Seaward from this bottom fast ice, a zone of relatively undisturbed, floating fast ice as much as 2 m thick extends offshore to where it meets the moving ice of the polar pack. At this juncture, shear and pressure ridges develop which are grounded, forming the stamukhi zone. Each of these zones apparently has distinctive sedimentologic, permafrost, morphologic and ice gouge characteristics.

A rudimentary framework for the processes and related sedimentologic record over the major ice zones can be established (Fig. 2) which relates the relative importance of ice and water as dynamic agents affecting the sea bottom. The major processes involved in each ice zone are:

Bottom fast ice zone:

1) River overflow onto the sea ice and subsequent drainage through strudle holes and cracks causes sea-floor scour depressions and initiates sub-ice sediment transport.

2) Sub-ice tidal and storm surge currents act to maintain and perhaps enlarge tidal channels in lagoons and bays.

3) Storm surges raise sea level as much as 3 m, erode beaches, coastal bluffs, and islands and inundate the coastal plains.

4) Wave action modifies beaches and coasts during the open water season.

5) Ice-push acts on exposed parts of coasts and offshore islands.

6) Add-freezing of sediments and lowering of sediment temperatures occurs where sea ice is in contact with the bottom.

Floating fast ice zone:

1) Waves and currents result in moderate reworking of the bottom sediments.

2) Ice gouging occurs in exposed areas primarily in winter but to a lesser extent during summer.

3) Bioturbation and sedimentation are most dominant in this zone throughout the year.

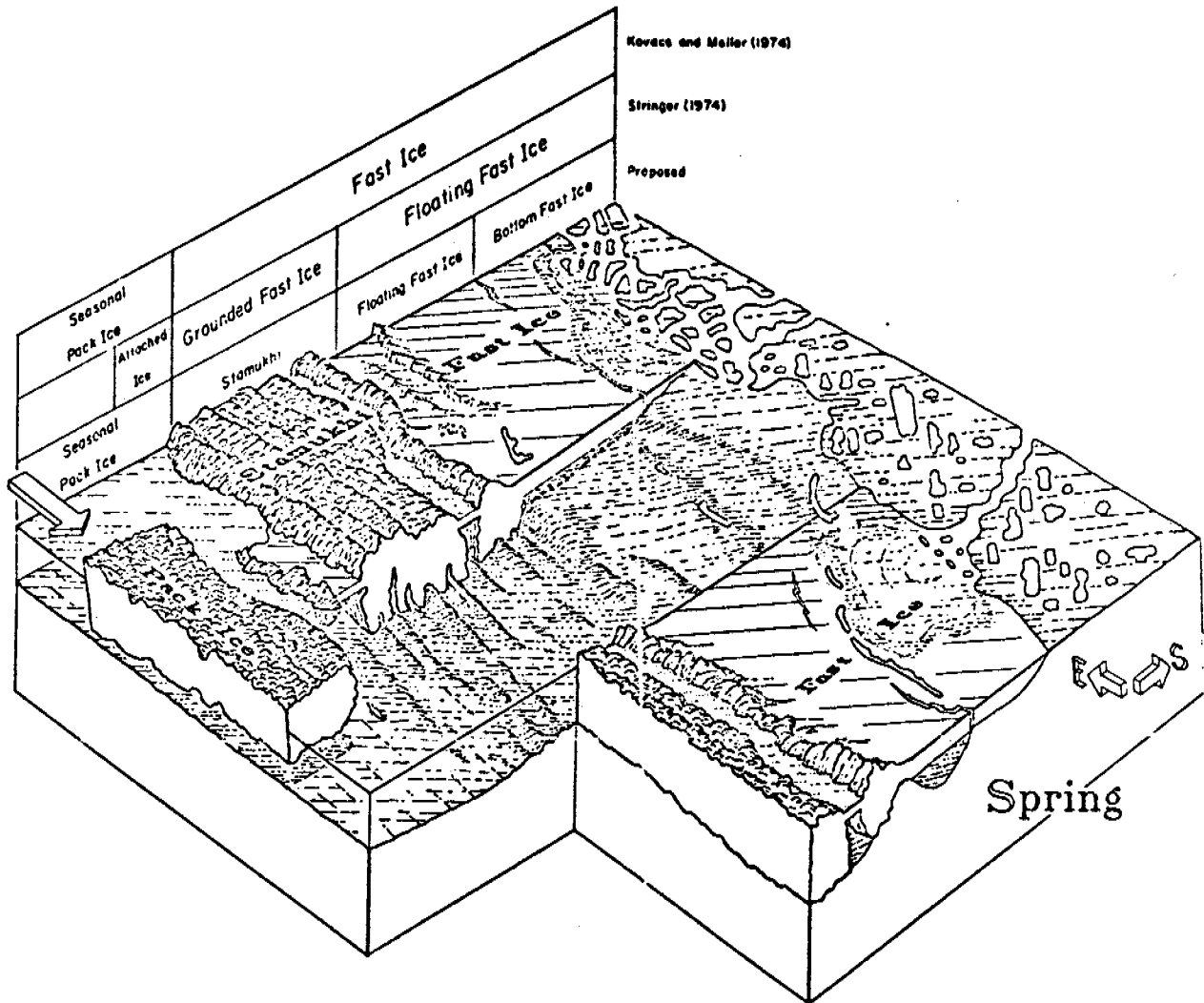


Figure 1. Diagram of an idealized cross-section of the fully developed ice zonation along the Alaskan Beaufort Sea coast at the time of maximum ice growth in spring. Drawing by Tau Rho Alpha.

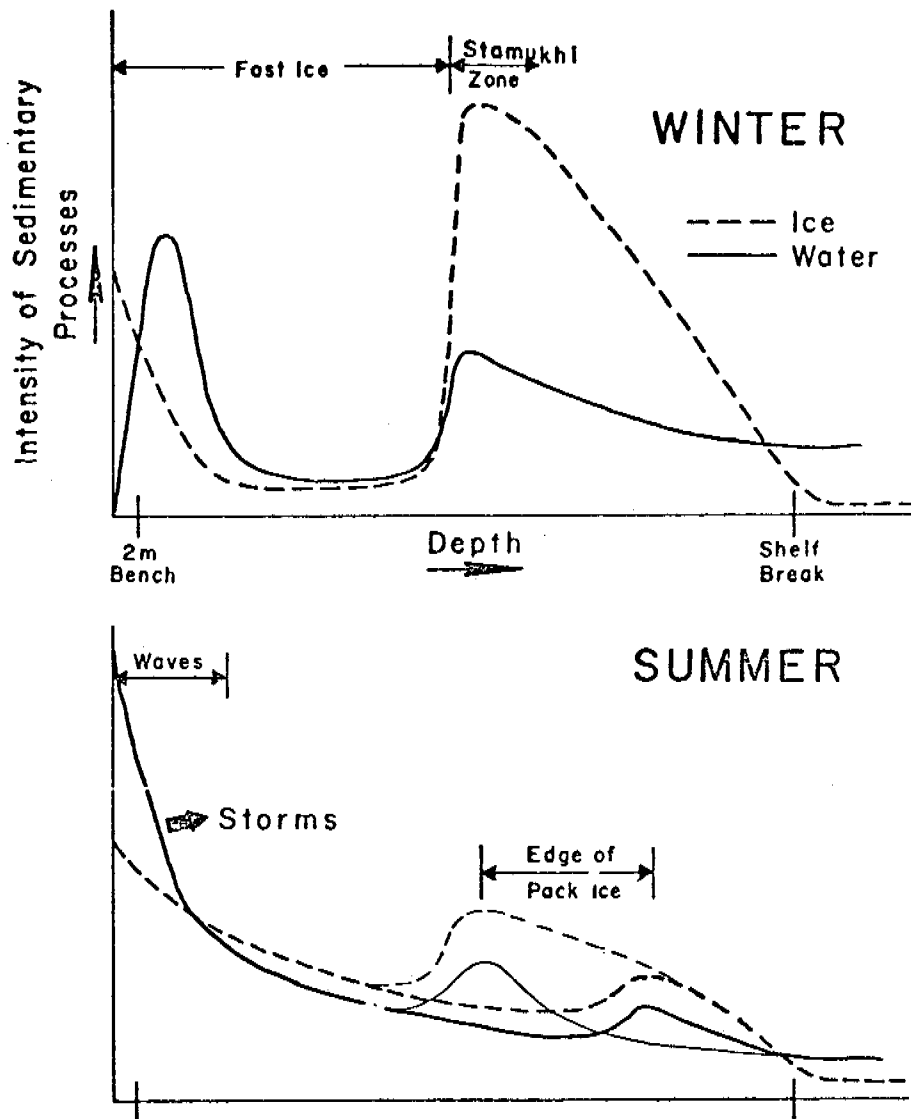


Figure 2. Conceptual model of the relative importance of ice and water as process agents on the bottom sediments of the arctic shelf off northern Alaska.

Stamukhi zone:

1) Ice gouging of bottom reworks sediments to depths in excess of 25 cm in less than 100 years, maximum gouge incisions are probably in excess of 2 m, obliterating sedimentary structures.

2) Current transport and scour are associated with grounded keels of ice.

3) Control of inner shelf ice character results from coastal configuration and distribution and orientation of submerged shoals. Creation or maintenance of these shoals by ice-related processes.

IV. Study Area

The primary study area includes the Beaufort Sea shelf between Barter Island on the east and Point Barrow on the west, with emphasis on an inshore segment between Flaxman Island and Cape Hallett. The width of the shelf in this area is variable, ranging from 55 km in the east to 110 km in the west. The adjacent land is a broad, flat coastal plain composed mainly of Quaternary deposits of silts, sands and gravels. In much of the area, the coast is being eroded by the sea at a rapid rate forming coastal bluffs as much as 6 m high. The line of bluffs is interrupted by low mud flats at the mouths of major rivers. Much of the coast is marked by islands at varying distances from the shore. Most of the islands are less than 3 m in elevation, narrow, and comprised of sand and gravel. Others are capped by tundra and are apparently erosional remnants of the inundated coastal plain. Coast-parallel shoals are also a feature of the inner shelf.

The shelf is generally rather flat and remains shallow for a considerable distance from shore. Off the Colville River the 2 m isobath is up to 12 km from shore. The shelf break lies at depths of 50 to 70 m. The shallowness of the shelf break and the presence of elevated Pleistocene beach lines suggests a broad regional uplift. The Holocene marine sediments on the inner shelf are generally 5 to 10 m thick.

The rivers flood in early June, delivering 50 to 80% of the yearly runoff in a 2-3 week period. The bulk of sediment input from rivers is associated with this flood. Initial flooding seaward of the river delta occurs on top of the unmelted sea ice, although the influx of warmer water eventually leads to ice-free areas off the deltas early in the sea-ice melt season. River drainage basins are located in the Brooks Range and the eastern rivers drain directly into the ocean while the western rivers meander across the broad coastal plain. The rivers are navigable only for vessels with extremely shallow draft.

Sea ice is a ubiquitous feature in the study area. New ice starts to form in late September and grows to a thickness of 2 m through the winter, welding older ice into more or less solid sheets. Where forces are sufficient, ice fractures and piles into hummocks and ridges. By

June, sea-ice melting is well underway and usually sometime in July enough ice has melted so that the protected bays and lagoons are free of ice, and waves and wind-driven currents are present. Ice remains on the shelf in the study area throughout the summer. Its location and concentration depend on the degree of melting and winds. The prevailing northeasterly wind tends to carry drifting summer ice away from the shore while the westerlies pile ice against the coast. Ice commonly remains grounded throughout the summer on many of the shoals on the inner shelf.

Currents and waves are a function of the winds during the open-water season. Waves are generally poorly developed due to the limited fetch which results from the presence of ice during most of the summer. Water circulation is dominated by the prevailing northeasterly winds which generate a westerly flow to the surface waters on the inner shelf. In winter currents under the ice are generally sluggish although restrictions of the tidal prism by ice at tidal inlets and on the broad, shallow, 2-m bench causes significantly higher velocities.

V. Sources, methods and rationale of data collection

Equipment operated routinely from the R/V KARLUK includes bottom sampling and coring gear, water salinity, -temperature, and -turbidity sensors, fathometers, a high and medium resolution seismic system, and a side-scan sonar. Precision navigation is maintained to 3 m accuracy with a range-range system. Near Prudhoe Bay, a seismic refraction system has been used (in cooperation with the Institute of Geophysics of The University of Alaska) to search for high-velocity layers that may be related to permafrost.

Topical problems have been investigated using current meters implanted on the inner shelf near Prudhoe just off the Colville River. Special techniques include (a) repetitive sonar and fathometer surveys of ice gouges, (b) diving observations and bottom photography, (c) measurements of sediment thicknesses within ice gouges by combined use of narrow beam echo sounder, and (d) a near-bottom tow package incorporating sub-bottom profiler and television, (4) near-surface stratigraphic studies using a vibracorer capable of obtaining 2-m long cores and (f) detailed surveys of bathymetry in river and lagoonal channels and in the vicinity of manmade structures. Coastal observations of rates of bluff erosion and the distribution and elevation of storm surge strand lines was carried out by helicopter.

The past and present status of data and product submission to NOAA-BLM-OCSEAP is given in the table on the following page.

VI, VII, VIII. Results, Discussion and Conclusions - (As attachments to report)

- A. Storm Surges of the Alaskan Beaufort Sea
- B. Ice Gouge Characteristics: Their Changing Patterns from 1975 to 1977, Beaufort Sea, Alaska

R,U. 205 Barnes, Reimnitz
 Product Submission Status
 REPORTS TO NOAA-BLM

Data Products	Sept. 1978	June 1978	April 1978	Dec. 1977	Sept. 1977	June 1977	Apr. 1977	Feb. 1977	Dec. 1976	Sept. 1976	June 1976	Apr. 1976	Dec. 1975	Sept. 1975	Other Sources of Data (Numbers refer to references on p. 16)
<u>Non Digital</u>															
-core descriptions						x									0 0
-acoustic profiles w/nav.							x			x	x				0 0 (8)
<u>Digital</u>															
-water temp./sal.										x	x				
-current meter										x	x	x			0 0 (2)
-nephelometer															Lost equipment
<u>Summary Products</u>															
1. Ice gouge maps								x							x (4, 6, 14, 17)
2. Evaluation of ice hazards										x	x	x	x		x 0 0 (5, 6, 7, 10, 12, 14, 16, 18)
3. Offshore gravel resources										x	x				x (1, 17)
4. Holocene marine sediments													x		(1, 6, 7, 15)
5. Bottom currents and processes													x	x	x 0 0 (1, 4, 7, 16, 18)
6. Sediment transport regime													x		x x (1, 17, 18)
7. Interpretation of stamukhi															x (6, 10, 11, 17)
8. Coastal erosion and delta progradation															x x 0 0 (3, 9, 17, 18)
<u>Additional Information</u>															
1. Sediment distribution and character															x 0 0 (1, 15)
2. Charts															x 0 0
3. Oceanographic															0 0 (2, 18)
4. Engineering properties															x (1, 6, 15, 18)
5. Chukchi Sea Studies															x (13)
6. Fresh water resources															x (3, 12)
7. Sediment interstitial salt, sea floor temp.															x (15)
8. Diving Observations															x 0 0 (6, 15)

x - data or information submitted
 0 - work in progress or planned for this period

C. Character of Ice Gouging in the Chukchi Sea

D. Stamukhi Sohals of the Arctic - Some Examples from Alaska

IX. Needs for further study

The interdisciplinary meeting held in Barrow during January outlined the present needs for additional information. The primary emphasis as relates to our study includes the following: recurrence rates and intensity of ice gouging in the stamukhi zone; evaluation of the presence or absence of gas-charged sediments on the inner shelf and if present, their relationship to permafrost; determination of the rates of sediment migration along the mainland coast; assessing the character of ice sediment interaction in the vicinity of the 2-m bench, as related to sub-ice current scour, oil entrapment and sediment stability; and an assessment of the Holocene stratigraphy for clues as to sea level history, gravel sources, and engineering character.

X. Summary of 4th Quarter Operations

A. Ship or Laboratory Activities

1. Ship or field trip schedule- Peter Barnes and Erk Reimnitz attended the Beaufort Sea synthesis meeting at Barrow on 23-27 January, 1978.

2. Personnel involved in project:

Peter Barnes	Project Chief - Geologist	U.S.G.S., Marine Geology
Erk Reimnitz	Principal Investigator-Geologist	" " "
Larry Toimil	Co-Investigator-Geologist	" " "
Douglas Maurer	Physical Science Technician	" " "
David McDowell	Physical Science Technician	" " "

3. Methods

Efforts this quarter have been primarily aimed at data compilation, data reduction, and report writing. Significant project efforts during the quarter were:

- a) description and characterization of core samples, photography, radiography, sediment casts, sampling, radio-carbon dating
- b) preparation of the annual report
- c) preparation and editing of the earth-science section of the Beaufort Sea Synthesis report
- d) preparation and planning for spring and summer field efforts
- e) computer compilation of bathymetry and precision-navigation data
- f) compilation of ice gouge data from test lines

4. Data collected or analyzed:

DATA TYPE	Km of record or number of samples analyzed
Side-scan sonar	80 km
Bathymetry profiles	200 km
High-resolution seismic profiles	10 km
Vibracores	33

REFERENCES

1. Barnes, P.W., and Reimnitz, Erk, 1974, Sedimentary processes on arctic shelves off the northern coast of Alaska, in Reed and Sater, eds.: The Coast and Shelf of the Beaufort Sea, The Arctic Inst. of N. Am., Arlington, Va., p. 439-576.
2. Barnes, P.W., and Garlow, R., 1975, Surface Current Observations-Beaufort Sea, 1972, U.S. Geol. Survey open-file report 75-691, 3 p. and map.
3. Barnes, P.W. and Reimnitz, Erk, 1976, Flooding of sea ice by rivers of northern Alaska; in ERTS-1, A New Window on Our Planet, R.W. Williams, Jr., and W.D. Carter, eds., U.S. Geol. Survey Prof. Paper 929, p. 356-359.
4. Reimnitz, Erk, Barnes, P.W., and Alpha, T.R., 1973, Bottom features and processes related to drifting ice on the arctic shelf, Alaska: U.S. Geol. Survey Misc. Field Studies Map MF-532.
5. Reimnitz, Erk and Barnes, P.W., 1976, Influence of sea ice on sedimentary processes off northern Alaska: in ERTS-1, A new window on our planet, Williams, R.S., Jr., and Carter, W.D., eds., U.S. Geol. Survey Prof. Paper 929, p. 360-362.
6. Reimnitz, Erk and Barnes, P.W., 1974, Sea ice as a geologic agent on the Beaufort Sea shelf of Alaska: in Reed, and Sater, eds., The coast and shelf of the Beaufort Sea, The Arctic Inst. of North America, Arlington, Virginia, p. 301-351.
7. Grantz, Arthur, Barnes, P.W., Eittreim, S.L., Reimnitz, Erk, Scott, E.W., Smith, R.A., Stewart, George, and Toimil, L.J., 1976, Summary of sediments, structural framework, petroleum potential, environmental conditions, and operational considerations of the United States Beaufort Sea, Alaska area: U.S. Geol. Survey open-file report 76-830, 32 p., 3 figs., 1 table.
8. Reimnitz, Erk, 1976, High resolution seismic profiles, Beaufort Sea, 1975: U.S. Geol. Survey open-file report 76-747, 3 plates.
9. Barnes, P.W., Reimnitz, Erk, Smith, Greg, and Melchior, John, 1977, Bathymetric and shoreline changes, northwestern Prudhoe Bay, Alaska, U.S. Geol. Survey open-file report No. 77-161, 8 p.
10. Reimnitz, Erk, Toimil, L.J., and Barnes, P.W., 1977, Arctic continental shelf processes and morphology related to sea ice zonation, Beaufort Sea Alaska: AIDJEX Bull.v36, p.15-64.

11. Reimnitz, Erk, Toimil, L.J., and Barnes, P.W., 1977, Stamukhi zone processes: Implication for developing the arctic offshore area: Offshore Technology Conference. Houston, Tex., Proceedings v. 3, p. 513-518.
12. Harden, Deborah, Barnes, P.W., and Reimnitz, Erk, 1977, Distribution and character of nalds in northeast Alaska: Arctic v. 30, p. 28-40.
13. Toimil, L.J., and Grantz, Arthur, 1976, Origin of a bergfield at Hanna Shoal, northeastern Chukchi Sea and its influence on the sedimentary environment: AIDJEX Bull., no. 34, p. 1-42.
14. Reimnitz, Erk, Barnes, P.W., Toimil, L.J., and Melchior, John, 1977, Ice gouge recurrence and rates of sediment reworking, Beaufort Sea, Alaska: Geology, v. 5, p. 405-408.
15. Reimnitz, Erk, Maurer, D.K., Barnes, P.W., and Toimil, L.J., 1977, Some physical properties of shelf surface sediments, Beaufort Sea, Alaska: Open-File Report No. 77-416, 8 p.
16. Aagaard, Knut, Atlas, R., Barnes, P.W., Callay, R.J., Craig, P., Harrison, W.D., Pritchard, R. S., Lowry, L. Martin, Seelye, Nummedal, Dag, Schell, D.M., and Wisemann, W.J. 1977, Spills transport and effects of oil: in G. Weller, D. Norton and T. Johnson, eds; Beaufort Sea Synthesis Report - Environmental impacts of OCS development in Northern Alaska; Outer Continental Shelf Environmental Assessment Program, Arctic Project - Special Bull. no. 15, p. 179-187.
17. Hopkins, D.M., Barnes, P.W., Biswas, N.N., Cannon, J.K., Chamberlain, Edwin, Dygas, J., Harrison, W.D., Naidu, .S., Nummedal, Dag, Rogers, J.C., Sellmann, P.V., Vigdorichik, Michael, Wiseman, W.J., and Osterkamp, T.E., 1977, Earth Science Studies: in G. Weller, D. Norton and T. Johnson eds: Beaufort Sea synthesis Report - Environmental impacts of OCS development in Northern Alaska; Outer Continental Shelf Environmental Assessment Program, Arctic Project - Special Bull. no. 15, p. 43-72.
18. Barnes, P.W., Reimnitz, Erk, Drake, D.E. and, Toimil, L.J., 1977, Miscellaneous hydrologic and geologic observations on the inner Beaufort Sea shelf, Alaska: U.S. Geol. Survey open-file report 77-477, 95 p.

Storm surges in the Alaskan Beaufort Sea

by

Erk Reimnitz and Douglas K. Maurer.

Introduction

A large percentage of the world's human population is concentrated on low coastal plains or deltas fringing the oceans. As a result of this and the fact that extreme storms, tidal waves, and floods occur; there is a long record of major catastrophes for man in terms of lost lives and property. The North Slope of Alaska fringes the sea with a very low, tundra-covered coastal plain and numerous low deltas, thus storm surges can inundate extensive areas. Until recently, the North Slope was an undeveloped area; therefore, no long term written record exists which might document catastrophes in this region. Since the nation is now looking at the North Slope and continental shelf as a source for future energy, we should be aware of the consequences of potential catastrophes in this area.

In the Fall of 1970, westerly gale force winds occurred in the Canadian and Alaskan Beaufort Sea resulting in a surge reported to have been up to 3 m high (Anon., 1971a; Reimnitz, et al., 1972; Lewis and Forbes, 1975; Dygas and Burrell, 1976b). This is an order of magnitude higher than normal flood tide. Recurrence intervals for similar events range from 25 to 50 years (Anon., 1971a). The first author observed considerable amounts of driftwood during the storm, while in transit on a small vessel from Point Barrow to Prudhoe Bay. Much of this driftwood was deposited on land and formed a rim that roughly marks the storm surge level. This rim can still be seen from low-flying aircraft.

During August, 1977, we used one and a half days of helicopter time for a reconnaissance survey of the configuration and elevation of this driftwood line from Cape Halkett to the Canning River (Fig. 1). The purpose of this report is to present the results of this survey together with other observations related to the 1970 storm surge and other surges. We will also briefly discuss the marine geological consequences of storm surges in the Beaufort Sea.

Field methods and their limitations

The driftwood line was sketched from an altitude of 500 feet on 1:63,360 scale topographic sheets, wherever it was adequately defined. 35 mm color photographs were taken at the same time and later used to resolve some uncertainties in the sketch of the driftwood line. In some areas one pass with the aircraft was not sufficient to make an accurate sketch. For this reason the lines in maps 1 through 5 contain local errors but provide a general configuration of the driftwood line. Along with color photography we used color IR photography to enhance differences in vegetation between the low-lying terrain which had been inundated by salt water in 1970, and the higher terrain.

The flight was interrupted at a number of places in order to inspect material contained in the driftwood line and to measure the elevation of the line above sea level. In general we chose sites where the driftwood line was well defined within 200-300 m of the open ocean. This limit was dictated by the pole-and-horizon method (Emery, 1961), used for elevation measurements. In view of other limitations to the approach, the technique is sufficiently accurate (± 10 cm). No tide gauge was in operation nearby during the period of the survey (August 14 and 15), but the weather was very calm and steady. We believe sea level was within ± 20 cm of its mean. Beach features related to the sea-level were noted at each site so that we could monitor the onset of any anomalous events.

Driftwood, in fact, does not mark the highest water level of a surge. It may lie higher or lower than the storm surge level, and we will briefly consider the two extremes.

1) On a steeply sloping land surface, oriented normal to deep water wave orthogonals, and with deep water close by, there is a considerable wave run-up. Here the driftwood comes to rest at an elevation representing the sum of storm surge height and maximum wave height. Due to the shallowness of the inner shelf in the study area, and due to the presence of ice which reduces the fetch, we estimate that the driftwood was not more than .5 m above the storm surge level at the sites studied. Moreover, the barrier islands with steep foreshores were entirely awash during the storm and therefore the driftwood came to rest during surge recession. We have found some clear evidence for this at Cross Island which we will present later.

2) On a gently sloping land surface with shallow water offshore, there is essentially no wave run-up. Here the largest trees, often with branches and other irregularities, may have .5 m or more draft. They therefore run aground far short of the extreme landward position of the water line and act as fences for smaller debris, which causes formation of a distinct driftwood line.

The latter conditions applied to much of the driftwood on the mainland (Fig. 2). Here the measured surge elevations generally underestimated the true surge height. The values for the offshore islands, many of which were entirely awash, also may be too low in general. It is important to keep these limitations in mind in planning for coastal installations. Some discrepancies between the surge height as measured and the surge heights as inferred from other observations will be discussed later.

Background Information

The shelf of the Beaufort Sea in the study area (Fig. 1) is shallow, with the 20 m isobath about 30 to 35 km from the mainland shore and the relief is gentle (Carsola, 1954; Barnes and Reimnitz, 1974; Reimnitz and Barnes, 1974). The shelf has a nearly complete sea ice cover for nine months of the year. Astronomical tides have an average range of only 15 cm, and on a day-to-day basis they are overshadowed by the effects of wind. Easterly wind is most common, causing low water

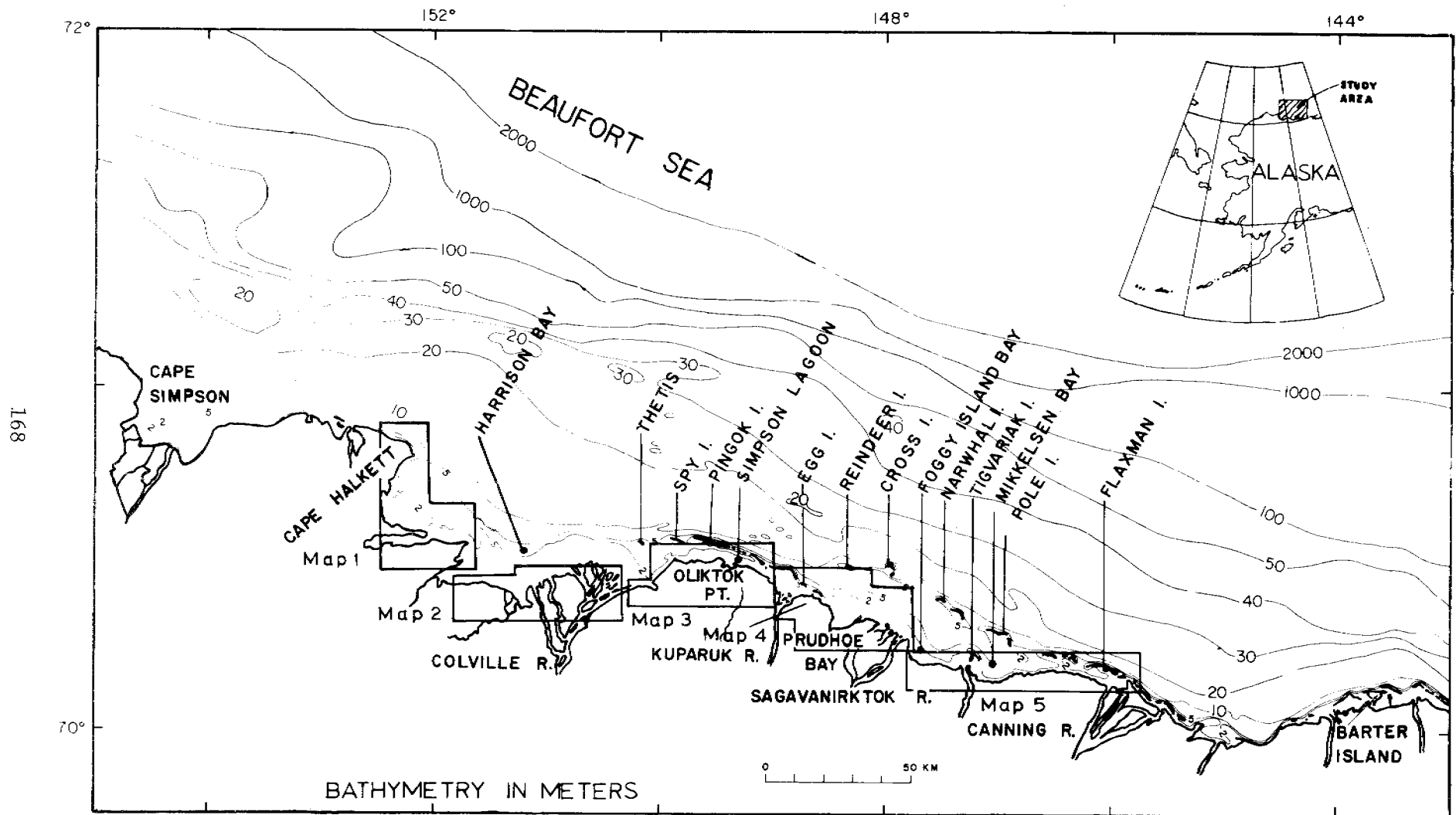


Figure 1.- Location map showing regional bathymetry and delineating map areas 1 through 5.

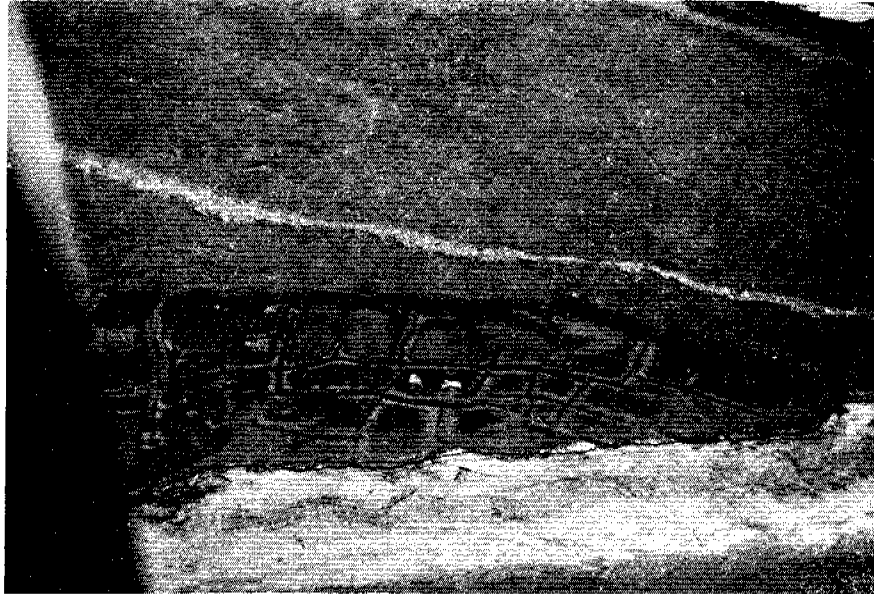


Figure 2.- Aerial view of well defined driftwood line on tundra surface with imperceptible slope. Distance across photograph is about 100 m.



Figure 3.- Large pieces of sea ice driven onto islands by storm surge of September 1970, with keels deeply imbedded into island surface.

levels, while westerly wind causes a rise in water level (Short, 1973). The most severe storms bring westerly winds which generally occur during September or October.

Coastal navigators are well aware of the simple relationship between wind direction and water level and therefore read the wind rather than the tide tables. Ice is also moved onshore by westerlies and offshore by easterlies.

The sea level fluctuates with the tides regardless of the presence of an ice cover. Only within the shallow areas of the bottom-fast ice zone landward of the tidal cracks does the sea level remain constant under most conditions (Reimnitz, et al., in press). It has been noted, but is not well understood, that meteorologic tides, even surges, can occur in the middle of the winter in the presence of a nearly complete ice cover (Zubov, 1945, Henry, 1975, and Brian Mathews, personal commun.).

The September 13, 1970 storm reached its peak during the afternoon when northwesterly winds of 80 km/hr were observed at the Oliktok DEW-line site. According to Dygas and Burrell (1976b) the winds were gusting to almost 130 km/hr. At Deadhorse, some distance inland, peak wind velocities apparently reached only approximately 46 km/hr. (U.S. Dept. of Commerce). This wind activity could be expected, because in the presence of a surface cold front, winds over the water may be two to four times stronger than those reported inland (Burns, 1973). In the area off Cape Halkett the first author estimated westerly winds at 130 km/hr (70 knots), and wave heights of about 3 m. The waves were relatively small due to the presence of scattered burgy bits along the coast and due to the fact that 1/10 to 6/10 of the sea surface 20 km seaward was covered by sea ice (Atmospheric Environment Service, Canada). The Canadian ice chart for the Beaufort Sea on 24 September, 1970, showed that, probably as a result of the storm, pack ice had replaced most of the water of the inner shelf (A.E.S., Canada).

Spy Island (Fig. 1), observed through binoculars from Oliktok (Dygas, personal commun.), was marked by a line of foam from breaking waves, and large chunks of ice could be heard pounding the island which is 5 km from the observation point.

After the storm subsided all the islands between Oliktok and Prudhoe Bay were marked by large ice chunks (Fig. 3). The tundra surface around the Oliktok DEW-line site had been inundated, but the roads, pads, and runway remained above water. Two members of a shore navigation station who had been camping east of Oliktok Point, almost lost their lives trying to wade across the flooded land to higher ground. Coastal erosion along the west side of the Point endangered the fuel storage tanks at the Point and waves and currents removed several hundred meters of road leads across the tundra. The land area around Bud Helmericks' settlement on the Colville Delta was entirely submerged. Only the pads on which the living quarters and hangar are built remained above water (personal commun.). According to Helmericks, the flood level was 1.5 m above the river level. Due to the high water, the lake which provides the settlement's fresh water supply, turned to unusable

salt water. A cabin built by Helmericks on the highest part of Thetis Island in Harrison Bay (Fig. 1), and all materials lying around the cabin, were washed away. Only one plank was found later. An Eskimo cabin on Cross Island was damaged. According to Helmericks the cabin was built around the turn of the century but Abraham Stein (a native of the area) claimed it was built about 1930. Some planks known to have been part of the cabin are now lying east of the cabin at a relatively low level. The cross after which Stockton (1890) named the island is still standing and the year 1889 is carved on it. According to Helmericks, wood chips from the construction and carving were lying around the base of the cross before the 1970 storm, but the wood chips were carried away and the island surface was reshaped by currents during the storm. The settlement at Beechy Point in Simpson Lagoon was awash during the flood, and some small boats were carried away. A large barge broke loose in the Prudhoe Bay area and came to rest nearly 1 m above sea level at the eastern part of the Sagavanirktok Delta. Some of the lighter barges used in Prudhoe Bay, which were secured for the winter next to the causeway, were set on top of the causeway (personal commun., James Lowe, Supt. of the Sealift operation). These barges require four feet of water to float and the causeway is six to seven feet above sea level, therefore, the minimum surge height required to lift the barges onto the causeway would have to be ten to eleven feet (± 3 m). Along the open coast the height of the storm surge was estimated to be approximately 3 m (Reimnitz, et al., 1972; Dygas and Burrell, 1976).

In the Canadian sector of the Beaufort Sea, where the pack ice front at the time of the storm was more than 150 km from the coast, nearly optimum conditions for the generation of a surge and waves existed (Anon., 1971b). A rise in water level was observed at Herschel Island more than five hours prior to the storm. At Shingle Point the winds were only 8-15 km/hr (5-10 mph) from the southwest. Five minutes later they were gusting in excess of 110 km/hr (70 mph) from the northwest (Anon., 1971b). The observed surge height was 2.4 m (Anon., 1971b), but locally it might have been up to 3 m (Lewis and Forbes, 1975). Deep water waves of up to 9 m were noted. Pack ice, including many remnants of multi-year floes and one ice island, were driven into Babbage Bight. The ice island grounded at 11 m water depth with its surface up to 12 m above sea level (Kovacs and Mellor, 1971), suggesting considerable surge height and driving forces. Damage reported from the Canadian coast was considerable, including bluff erosion (up to 12 m) at Tuktoyaktuk (Anon., 1971b).

Observations of interest to the sedimentologist are the large amounts of sediment which were in suspension in the shallow waters. For example, the tugboat Radium Dew, anchored behind Escape Reef near Shingle Point, reported waves breaking over the wheelhouse coating the tug with mud. Buildings at Tuktoyaktuk, 200 to 30 m from shore were coated in frozen mud (Anon., 1971b). The entire sandspit at Nicholson Peninsula DEW-line site was awash and marked by 1 m breakers. As a result of the washover, the spit was 30 m narrower after the storm.

Some information on storm surges is available for the Chukchi Sea, mainly from observations and recordings at Barrow (Hume and Schalk, 1967). But the setting at Barrow is very different from that of the

Beaufort Sea coast in general, and surges recorded at Barrow do not appear on the records at Oliktok or in Canada (Mathews, personal commun.). Thus the Beaufort Sea surge of 1970 was not an unusual event at Barrow, and the Barrow storm surge of October 1963, which flooded much of the Naval Arctic Research Laboratory area (Hume and Schalk, 1967), was about .5 m below the level of the 1970 surge on the Colville Delta (Helmericks, personal commun.) and was comparable to the normal spring flood stage of the Colville River.

Results

Configuration of driftwood line.- The driftwood line, where it could be easily mapped from the air, is shown on maps 1 through 5. These maps are keyed to boxes on Figure 1. The elevation of the tundra surface, as shown on U.S.G.S. topographic sheets, is too high, especially along Simpson Lagoon, where discrepancies of up to 4 m are found (Lewellen, 1977). Thus it is not possible to read the elevation of the driftwood line directly from the maps.

The distance of the driftwood line from the shore varies from 20 m to about 5000 m on the Kuparok and Colville Deltas. But on the deltas the lines are difficult to trace, because a well defined shoreline is so far away and the driftwood is scattered about widely. Storm surges also interact with river floods. These floods, which are occasionally enhanced by ice jams during the river break-up, mix wood freshly brought down from the interior with wood from the sea. The driftwood line on the delta plains therefore is dashed. In many localities two or even three distinct driftwood lines could be identified from the air (Fig. 4). The second highest line could, in some cases, be related to a westerly storm of August 1975, but no attempt was made to map this event. It was .7 to 1.2 m lower than the 1970 surge. Materials set adrift during positive storm surges are moving eastward along the coast. Therefore westward facing slopes, often oriented at right angles to the general trend of the coast, intercept more wood than land surfaces sloping northward toward the open sea (Fig. 5). Coastal depressions which open westward to the sea, as the creek valley in Figure 4, often have well defined driftwood lines on opposing slopes and generally catch abnormally large amounts of flotsam.

Elevation of driftwood line.-The elevation of the highest driftwood line shows large variations, ranging from about 1.4 m to 3.4 m above sea level (Fig. 6). We were able to read the elevation of the flotsam above sea level to the nearest centimeter, but have rounded the values off to the nearest decimeter. At a number of stations we either have doubts about the elevation readings given in Figure 6, or we know of discrepancies between our measurements and other information. We will discuss these problems, proceeding along the coast from west to east.

The value of 1.4 m at the Colville River delta is probably too low because it was referenced to an elevated sea surface from the dynamic and steric contribution (fresh water) of the river. The 2.1 m value for Thetis Island is also too low because the cabin of Helmericks, located on ground equally as high as that on which the highest driftwood was found, was washed away in 1970. Furthermore, for neighboring Spy



Figure 4.- Two driftwood lines at different elevations, paralleling a westward-opening drainage. The higher line records the 1970 storm surge, and about 1 m lower is an accumulation dating a 1975 storm.

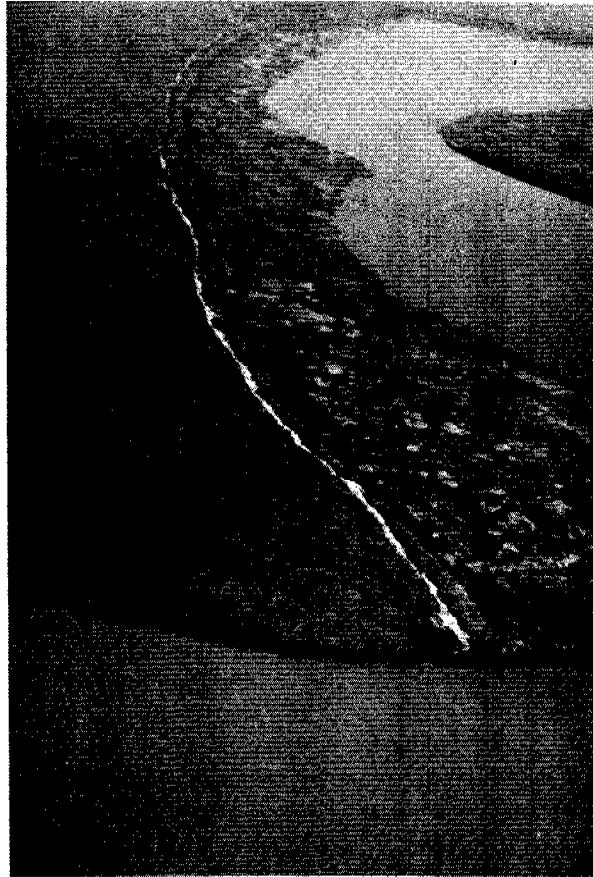


Figure 5.- Driftwood line on westerly slope, facing into the surface drift of the 1970 storm surge. Opposite side of estuary lacks driftwood. White driftwood line parallels linear relief feature, separating surfaces with differing morphologies.

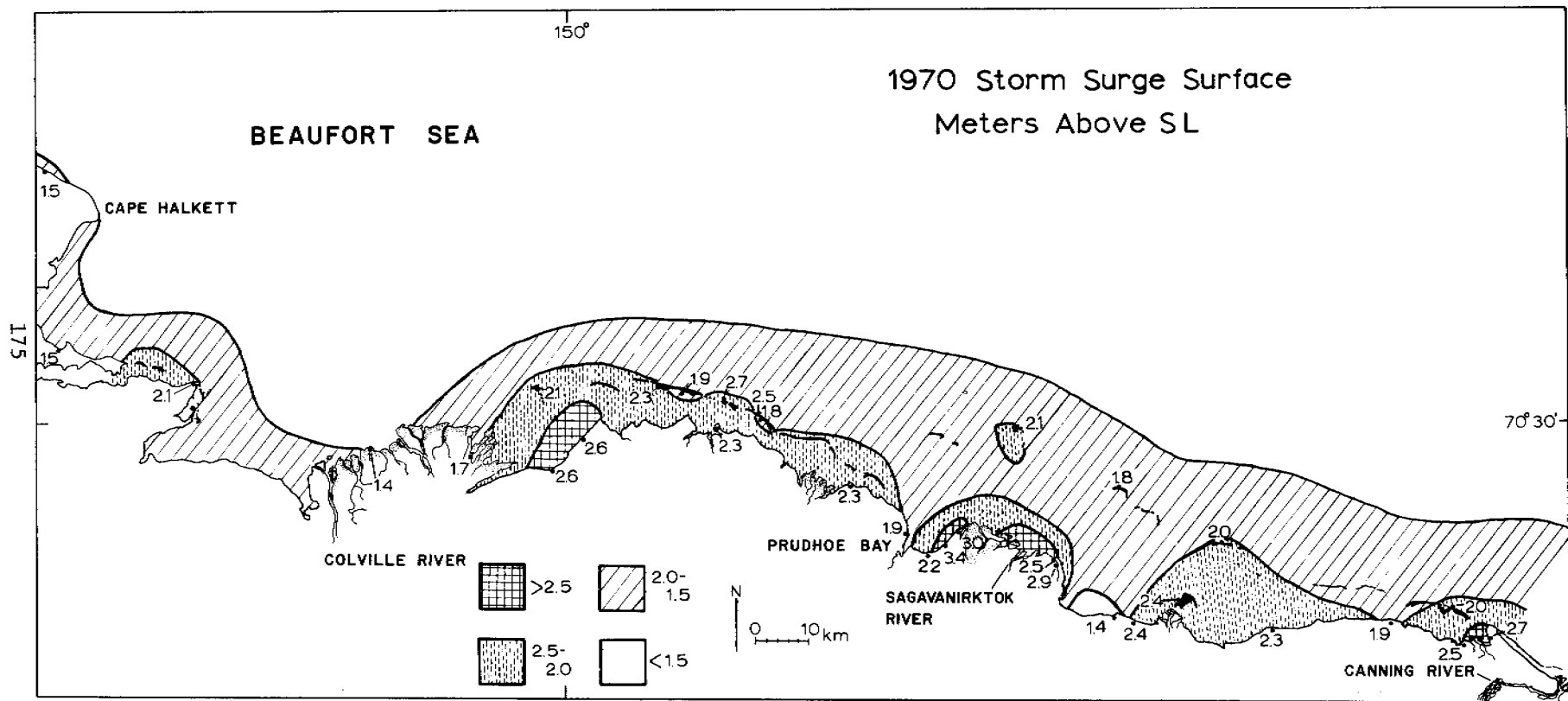


Figure 6.- Height of 1970 storm surge above mean sea level, as measured from the elevation of driftwood found on the mainland and islands. Note pile-up of water on the east side of shallow embayments and the lagoon near the Canning River.

Island, Reimnitz et al. (1972) reported an elevation slightly above 3 m. This estimate was made by referencing the flotation line of stranded bergy bits to sea level and allowing for the effects of a seaway during the grounding. This was probably compensated for largely by the fact that up to 1.5 m of ice keels were buried in the island surface. A surge height of 3 m for this area would also be in line with an eye witness estimate (Dygas and Burrell, 1976). On the tundra-capped part of Cottle Island we made one stop for elevation measurements. There a well-developed driftwood line on the seaward side was less than 100 m distant from an equally pronounced accumulation on the lagoon side. The elevations were 2.5 and 1.8 m, respectively. The difference is due either to high wave run-up on the seaward side and protection on the lagoon side, or to a later time of deposition of the materials on the lagoon side. On Cross Island we measured the height of a natural accumulation of driftwood at 2.05 m, but a still higher accumulation is present which we suspect has been piled up by man. In any case, the small Eskimo hut (40 to 70 years old) on the island, which was severely damaged during the storm, would have been submerged at least .8 to .9 m. None of the lumber found as far as 1 km distant from the hut, and clearly identifiable as a part of it, now lies more than 1.2 m above normal sea level. We do not have a good explanation for this. On the east side of Prudhoe Bay we found the highest driftwood, 3.4 m. We were doubtful about this reading because the wood was found only a few meters inland from the edge of a near vertical, westward-facing bluff. However, this elevation measurement is supported by eye witness accounts from personnel of Arctic Marine Freighters at the East Dock nearby (about 3 m). Driftwood found on Narwhal Island was measured at heights up to 1.8 m above sea level. Viewed from the air, the highest part of the island, at 2.5 m, shows traces of what appear to be current-produced bedforms. Therefore we believe that the island may have been overtopped during the 1970 storm. Also, the 2 m value measured on the highest part of Pole Island, may well be conservative. Lastly, a reading of 1.85 m was obtained on a driftwood line on the mainland coast near the west tip of Flaxman Island, where a gravel storm berm on the present beach is up to .3 m higher.

Configuration of sea surface during the 1970 surge.- The elevation of the sea surface during the 1970 storm surge was contoured in Figure 6, based on our measurements on land and on the islands. Along the shores this surface may be .5 to 1 m in error. These errors are inherent in the driftwood line and its relationship to mean sea level, as previously discussed. The offshore extent of the surface higher than 1.5 m is arbitrary, but it is known that storm surge amplitudes decrease rapidly with distance from the coast (Henry, 1975).

Vegetation patterns related to the driftwood line.- Summer ground observations made locally during the first three seasons after the storm suggested that the tundra vegetation was killed as far inland as the driftwood line. Locally there are patches of vegetation with different color intensities near the shore than those landward of the driftwood lines, as for example in Figure 7. But today, about eight years after tundra vegetation was inundated by salt water, salt-burn patterns cannot be used to map the extent of inundation.



Figure 7.- Black-and-white print of color infra-red photo showing faint driftwood line trending from the left lake to lower left of photo. Region with dark patches of vegetation does not coincide with area inundated by saltwater in 1970. Tire tracks on beach give scale.



Figure 8.- Close-up view of driftwood deposited by the 1970 storm surge. Note barrel for scale. Smooth well drained slope leading to higher ground on right lacks evidence of higher surges, and should preserve such records for at least 100 years, but probably 200 to 300 years.

Composition of the driftwood line.- The wood in the highest driftwood line is generally sound, giving evidence for a slow rate of decay (Fig. 8). Most of the wood has probably gone through a number of cycles of drift and rest, and 95% of it appears to be fresh enough to be set adrift again. Logs up to 45 cm in diameter and 10 m long are mixed with small trunks, branches, and sticks (Fig. 8). Logs more than 15 cm in diameter and stumps do not originate in drainage basins of Alaska's North Slope because they do not grow at this latitude and elevation. We believe that most of this material comes from the drainage basin of the Mackenzie River and not from the Yukon or other rivers draining to the Bering and Chukchi Seas. This belief is based partly on findings by Giddings (1952), who studied driftwood in the Canadian Arctic and on the predominance of westerly coastal currents. Much of the large lumber on the beaches and in the high driftwood line has been notched or chipped with crude tools. We believe that most of these marks are more than thirty or forty years old because the coast today is not inhabited by natives as it was in the past. Along with the natural wood, the high driftwood line also contains varying amounts of milled lumber, pallets, treated pilings, and other debris. The ubiquitous oil drum is present in many places, but under favorable conditions it moves with a strong wind on flat terrain, and therefore is not a good indicator of the extent of flooding. Small amounts of glassware, jars, bottles, and light bulbs, are also found in the high driftwood line, together with an occasional plastic item. Materials in direct contact with the tundra surface are slowly being incorporated into the vegetative mat. Only rarely during bluff erosion are tundra slabs ripped off and incorporated into the driftwood line.

Older surges and the extreme event.- Old and rotten wood can also be found within the areas flooded in 1970. The largest logs seem to last the longest, and thus we commonly found surfaces of old logs barely protruding above the tundra mat, so rotten that they no longer supported the weight of a man. Nowhere did we find such materials at elevations above those of the 1970 surge, but in some places rotten wood was found coincident with the 1970 driftwood line. It always is very distinct from the driftwood moved by the 1970 storm surge. In areas where much driftwood collects, very old events, with all components decomposed, might be expected to show up as linear accumulations of compost, perhaps marked by different vegetation. We found no such evidence.

In most places studied, the land slopes imperceptibly, and therefore evidence for an "extreme event" ranging up to 1 m higher than the 1970 surge, might be found over a very wide area. In such areas, evidence for still higher surges is difficult to obtain. We found one location where the detection of a very high surge was facilitated by a smooth, well-drained, relatively steep slope leading to higher ground a short distance from the beach (Fig. 8). This location is at the mouth of the Canning River (Fig. 6), where at 2.7 m elevation, the driftwood line is relatively high, and where much driftwood accumulates. This eastern end of the long lagoon system acts like a natural trap for driftwood. This would also have been true in the past, but we found no evidence for surges higher than the one of 1970.

Discussion

Surge surface height.- The variations in the height of the surge surface are considerable. But they follow a predictable pattern based on model studies (Henry and Heaps, 1976). Shallow embayments open in the direction of the wind forcing the surge show maximum run-up. On the other hand, major promontories provide shelter and therefore show little surge run-up on their lee sides. In the study area (Fig. 6) a major pile-up of water occurred on the southeast corner of Harrison Bay, in the southeast corner of Prudhoe Bay, and at the eastern end of the long lagoon ending at the Canning River (Leffingwell Lagoon). The positive bulge off the eastern Sagavanirktok Delta may be explained in terms of water piling up against Point Brower, a high promontory east of the Delta. In the southwestern sectors of Harrison, Prudhoe- and Foggy Bays (east of the Sagavanirktok River), the water level remained relatively low. We expected to find evidence for a pile-up of water in the eastern end of Simpson Lagoon which apparently did not occur.

Recurrence of major surges.- Historical evidence suggests that storm surges of the magnitude of the 1970 event do not occur often. In the Mackenzie Delta area, the winds recorded during the September 1970 storm have a return period of 40 to 50 years (Anon., 1971a). Although this was the worst storm in the memory of even the oldest residents of Tuktoyaktuk, there was another severe storm on September 9, 1944 (Anon., 1971b). Lucy Ahvakana, a native from Beechey Point near Prudhoe Bay, estimated that it had been 25 years since the last similar storm (personal commun., 1970). This was confirmed by Bud Helmericks of the Colville Delta, who said that according to natives there was a similar storm in the early forties (pers. commun., 1978). R.F. Henry searched the historical records of the Mackenzie Bay area and found mention of two earlier surges: 1905 and 1929 (pers. commun.). From Bud Helmericks' observations on Cross Island, mentioned earlier, one could conclude that there has not been a surge of the 1970 amplitude since 1889, when the cross was erected.

Based on observations on weathering characteristics of wood used in native cabins, abandoned boats, day beacons, and other markers, and a comparison with driftwood found in the highest deposits, we estimate that the 1970 surge has not been exceeded for 50 to possibly 100 years.

Geologic effects of storm surges.- Shoreline erosion is a major contributor to the sediment budget of Arctic shelves, and this contribution may be larger than that of the rivers. Dygas and Burrell (1976a) show that along Simpson Lagoon the average yearly erosion rate is 1.4 m, but rates of up to 40 m have been documented in a single season (Short, 1973). The long-term averages generally are the result of short-term severe events (Dygas and Burrell, 1976a), when as much as 20 years of normal sediment transport can be affected (Hume and Schalk, 1967). Since bluff retreat is largely a result of thermal erosion of ice-bonded sediments, and this in turn requires an overtopping of the narrow beaches to bring the sea water in contact with the bluffs, a westerly wind is most efficient. A thermo-erosional niche (Fig. 9), extending as much as 10 m into the bluff is formed, triggering slumping

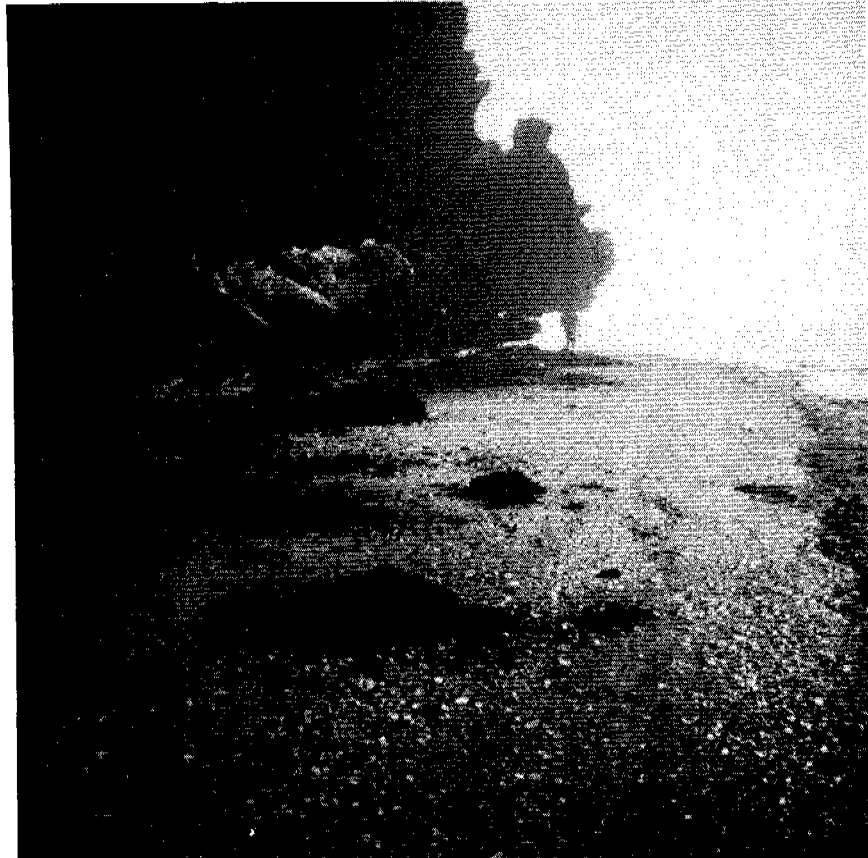


Figure 9.- Thermo-erosional niche resulting from minor surge in 1972.
The sea overtopped the beach and undermined the coastal plain up to 5m.

and solifluction. During strong easterly winds, on the other hand, sea level is lowered, occasionally exposing 40 m or more of lagoon floor (Lewellen, 1977). At these times bluff erosion does not contribute to the sediment supply.

The reports of bluff retreat during the 1970 storm in the Canadian sector of the Beaufort Sea, the size reduction of a spit, and especially the mud coating of buildings far inland and of a tug at anchor (mentioned earlier), all point to the dynamic processes which occur during westerly storms. Thus it is not surprising to find that bluff erosion along Simpson Lagoon, where many data points are available (Dygas and Burrell, 1976a), is higher on the west side of promontories than on their east side. There is ample evidence that the net longshore transport, and the direction of island migration is to the west (Short, 1973, Dygas and Burrell, 1976a). However, during the extreme events, when tremendous amounts of sediment are introduced into the sea and concentrations of suspended matter are extremely high near shore, the transport is in the opposite direction, to the east.

Ice gouging is very effective during westerly storms, bringing pack ice against the coast where it runs aground. This causes ice gouging and bulldozing of sediments toward the east, opposite to the general direction of ice drift (Reimnitz and Barnes 1974). The 1970 storm, which brought growlers and bergy bits up to the highest parts of the barrier islands (Fig. 3), produced gouges leading up to areas normally exposed above sea level (Reimnitz, et al., 1972). Due to strong currents during these times, the gouges are being filled at the same rate at which they are produced (Reimnitz et al., 1972). Depressions up to 1.5 m deep, resulting from the melting of the ice above sea level, were found on the islands in following years (Short, 1973). These depressions attest to the depth of gouges made in shallow regions of the shelf. If the fetch and the resulting waves are large, as they were in Canada during the storm, long continuous gouges probably would not form because the ice is pounding in the sea and impacting the bottom at regular intervals. As the fetch decreases with the advancing pack ice front, the resulting gouges will become increasingly linear and regular. The process of ice gouging in a strong current results in winnowing and re-suspension of shelf sediment, as discussed by Reimnitz and Barnes (1974). Vibracores, which we obtained recently, show that periods of slow deposition of mud were interrupted by a number of severe events of current winnowing, when clean, ripple-bedded sand units of 10 or more centimeters in thickness formed, 20 or more kilometers from shore. Such sand units may represent storm surges of the 1970 magnitude.

Major changes in the size and configuration of barrier islands and bars seem to occur during the major storm surges. Argo and Reindeer Islands, charted in 1970 as single islands, now are double islands, probably breached during the storm. Gravel-filled drums which serve as foundations for a day beacon on Spy Island, seem to have originally been flush with the top of the island but they are now exposed up to 50 cm. This exposure, together with the extensive overwash deposits along the south side of the island, suggest that island migration occurs in steps related to major storms. Barnes, et al., (1977) detected an anomalous

seaward migration of the east end of Stump Island over a 20-year period and related this to the widening of the narrow funnel-like end of Simpson Lagoon during a westerly storm. The highest surfaces of all barrier islands in the area show the effects of current shaping.

Recent findings by Sallenger in the northern Bering Sea indicate that under otherwise similar conditions, a cold temperature storm surge may have very different effects on the coastline than a warm temperature surge. The cold temperature storm surge was accompanied by beach accretion which Sallenger attributes to the possible effects of the formation of an icefoot during that time (Pers. commun.).

Storm Surge Scenario.- For the developer of offshore- and shoreline facilities required for petroleum exploration and production it would be useful to simulate the course of events that might be triggered by a major storm surge.

Open water conditions are a requisite for the generation of a major surge, since transmission of wind stress to the water is inhibited by the presence of shorefast ice. A severe westerly storm is the second requisite. A combination of these two factors restricts the time frame to the months of September and October. The pack ice edge during this time may be somewhere on the midshelf. There may be little or no warning of the storm, and wind velocity may increase from light to gale force within just minutes, as was reported in Canada. However, the water may start to rise before a change in local wind regime occurs. Maximum wave size will be reached within a few hours of the onset of the westerly storm, as the fetch is later restricted by the encroachment of pack ice on the inner shelf region. Swift easterly currents of 2 to 3 knots should be anticipated in the shallow regions of the shelf. Most positively buoyant items below the surge level will be picked up by the seas and moved eastward and onshore at a rapid rate. These items include boats, barges, fuel containers, lumber, and buildings, as well as driftwood. The greatest danger to artificial structures probably lies in the encroachment of pack ice. Solid fields of pack ice exert tremendous pressures, but even individual growlers, rolling and pounding with the waves, will act as huge battering rams exerting thousands of tons of force on any fixed structures. Such rams might impact the bottom to greater depths than the depths of incision of long, continuous ice gouges, and thereby endanger buried pipelines.

Major surges inundate rather extensive coastal regions. Because roads leading to causeways, and the causeways themselves, may be flooded, land-based relief and rescue operations using vessels such as small tugs, will be difficult. Vessels navigating in coastal waters generally rely on radar for positioning. A flooded coastline will be hard to recognize and navigation during the time of a surge will be difficult. Causeways at right angles to the force of the storms, such as the present West Dock, will probably be either breached or destroyed, just as the road at Oliktok Point was destroyed. The gravel fill of the West Dock might well plug the 1-m deep entrance channel to Prudhoe Bay. Similar to the effects of major promontories, causeways would initially cause a pile-up of water, and therefore cause an abnormal inundation of the adjacent land.

Natural hazards are one of the main causes of oil spills, and the likelihood of a spill is great during a storm surge. The oil could cover regions as extensive as those shown in maps 1 through 5. In any case, the intrusion of salt water would make the lakes within those areas useless to man. Up to five years is required to restore them to normal freshness.

Winter storm surges.- Most major surges occur during open water conditions where 2 to 3/10 ice cover may be considered open water (Henry and Heaps, 1976). But, winter surges, which occur during times of complete ice cover, have also been reported. Zubov (1945) describes an unusual rise in water level to 1.25 m above normal at Cape Cheliuskin in late January (p. 253). He also describes a "roller" of 1 to 2 m height (p. 254), moving into a bay in January and breaking up the 1 m ice cover which was complete. Furthermore he reports that "wind-driven fluctuations of sea level on the Severnaya Dvina did not cease throughout the winter, while the entire sea was solidly covered with ice" (p. 335). Winter storm surges have not always shown a correlation with storms. Henry (1975) recorded two surges of about 1 m height in the Canadian sector of the Beaufort Sea during the winter of 1973/1974; one in November and another in January. Only the November surge was associated with local strong westerly winds (Henry and Heaps, 1976). These winter surges were recorded on three tide gauges; two onshore, and one offshore. The observation that offshore levels seem to be comparable to onshore levels under the fast ice cover is of extreme interest (Henry and Heaps, 1976), as it suggests driving mechanisms other than wind for some of the reported winter surges.

Murphy Clark of CATCO Inc. at Prudhoe Bay (who has had ten years of winter experience on the fast ice regions working with Rolligons and other heavy equipment) noted that flooding of extensive areas of fast ice along the coast and in lagoons does occur occasionally (pers. commun.). We must assume that this flooding affects only the bottom-fast ice, which is not free to lift off the sea floor immediately with a rising water level. This phenomenon is commonly observed during surface flooding of fast ice by rivers, where only the floating fast ice rises to the top of the flood waters.

Driftwood certainly would not be moved by such winter surges, and most other summer-surge related processes, such as bluff erosion, will not occur. But since winter sub-ice processes have been largely ignored, and their potential is even rejected by some, we will briefly discuss one aspect of winter surges that the sedimentologist should consider. Lack of documentation, however, makes this purely speculative.

In lagoon and bay entrances where an ice canopy restricts cross sections, high flow velocities might be anticipated during winter surges. Ice coring data obtained in May and June, 1969, when the fast ice thickness is still near its maximum, indicated that the ice in the entrance channel to Prudhoe Bay was abnormally thin due to turbulence, and that at the shoalest point there was over 40 cm of water below the ice (Barnes et al., 1976). This leads to the conclusion that surges should affect Prudhoe Bay throughout the winter.

Brian Mathews operated a bubbler-type tide gauge at Oliktok during the winter of 1973. Three surges were recorded during January and February with heights of 94 cm, 140 cm, and 69 cm. He provided us with the 140 cm surge record, which lasted from January 8 through January 10. The trace was truncated at 140 cm height and the surge may have peaked at 160 cm. The pressure rise to 140 cm occurred over an 18 hour period.

In attempting to calculate flow velocities in the Prudhoe Bay channel during the surge recorded at Oliktok, we proceeded as follows:

Based on an ice growth curve for the region (Schell, 1974), the ice thickness at that time was estimated to be approximately 1.1 m. The area lying within the 1.1 m isobath of Prudhoe Bay, determined from U.S. Coast and Geodetic Survey smooth sheet #7857, is $15.6 \times 10^6 \text{ m}^2$. The channel crosssection was calculated at 175 m^2 with a maximum under-ice depth of .5 m, from recent, unpublished survey data of Peter Barnes. We made the following assumptions:

- 1) The free-floating ice within the bay rises 1.4 m along a sharp boundary following tidal cracks along the 1.1 m isobath.
- 2) The volume of water added to the bay equals the area of free-floating ice x 1.4 m (surge height).
- 3) The rise in water level occurs over an 18-hour period.
- 4) The ice on the relatively narrow entrance channel remains at the normal level, unbroken and rigid.

Based on these assumptions, the flow rate in the entrance channel would be 3.9 m/sec (about 8 knots). Raising the 1.1 m thick ice as proposed would cause flooding of the bottom-fast ice fringing the bay. This would nearly double the amount of water moved through the channel. Such flooding apparently occurred during a storm surge at Babbage estuary in early January, 1974 (Lewis and Forbes, 1975). We did not account for such flooding, as there are many problems with this model. Changing assumption No. 4 above, and allowing the ice canopy above the channel axis to arch upward 1.4 m, would greatly increase flow crosssection and thereby reduce flow velocity to 1 m/sec (about 2 knots). There are numerous other ways in which the ice canopy might behave under loading by such a surge. However, in all the reasonable models we considered, flow velocity through the channel should be considerable and should lead to bed erosion and deepening. We observed no pronounced deepening during the following summer. This could be explained by 1) channel infilling between the time of scour and the time of our observations in August, 2) ice canopy reacting in an unknown, or unpredictable manner, 3) presence of erosion-resistant anchor ice or ice-bonded sediments along the channel floor, among other possibilities.

Knowledge of how a solid ice canopy reacts during a surge with water forced through a narrow entrance into a bay is critical for determining channel flow velocities. Such knowledge is not available to us. There is evidence that in restricted basins, under certain hydraulic conditions, hydraulic pressure increases to a level at which explosive rupture occurs causing ice ejection and water spouting. It is interesting that such observations are either old, or from natives, people living with nature. In spite of the greatly increased activity over the ice in modern times, the unusual events are unlikely to be

noticed. The modern traveler is preoccupied with his narrow objectives, his time is limited, the transit is rapid, he is overpowered by the noise of engines, he is not searching for distant landmarks, and he returns for the night to safe quarters on land. From late November through January there is nobody on the ice. One old report comes from Parry (1826) who observed that large pieces of ice were thrown hundreds of yards as a result of pressure build-up below the ice canopy of a bay. We found another observation on the same subject in E. de K. Leffingwell's field notebook from the period 1906 to 1914, where he recorded an eye witness report from the mouth of the Aichilik River. Pieces of ice were thrown 15 m high with subsequent water spouting to 9 m high for several hours (entry for Dec. 19, 1910).

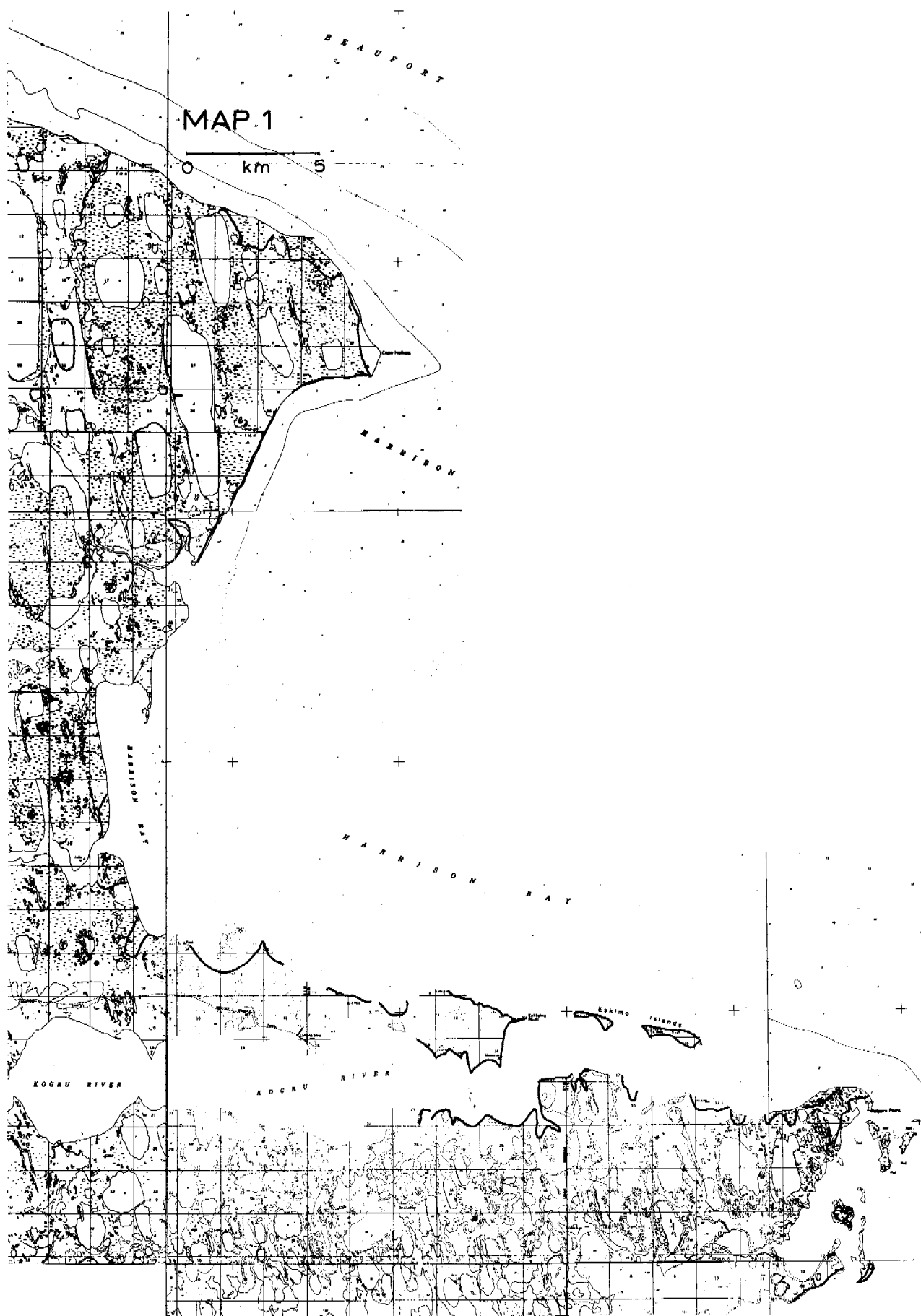
The possible effects of winter surges remains an unsolved problem. Numerous attempts of our own to learn more about this problem using current- and tide-recording packages in shallow waters and tidal inlets below the fast ice have resulted in extensive damage to the equipment or its total loss.

Conclusions

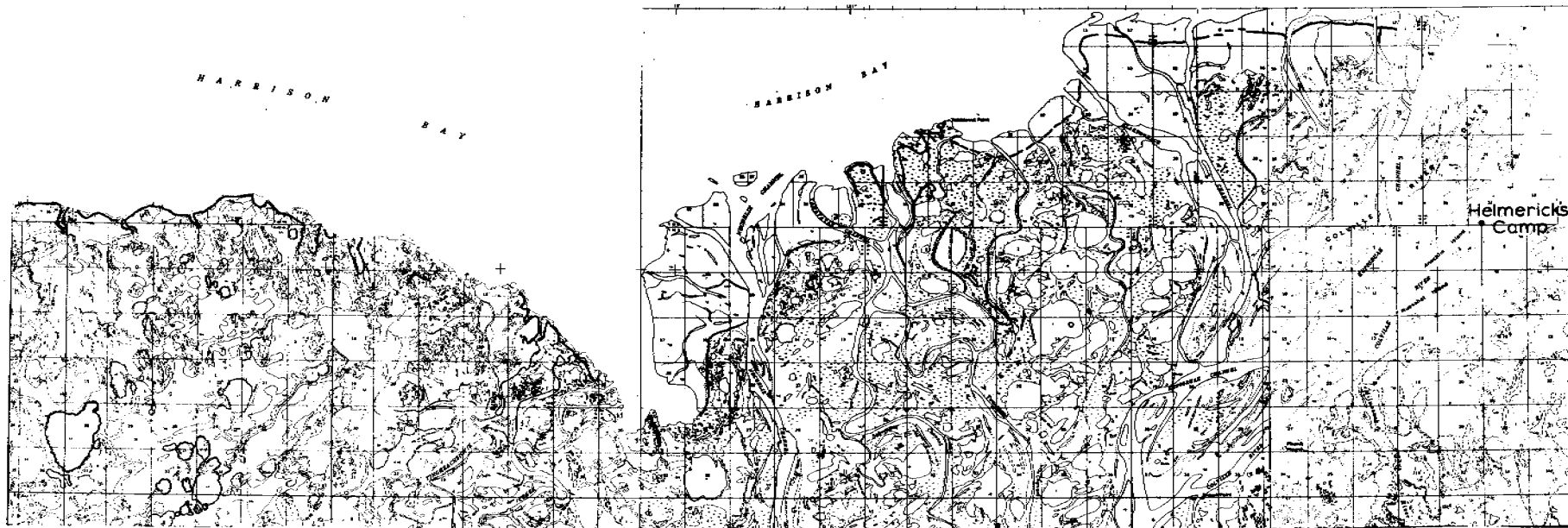
The line of driftwood deposited by the 1970 storm surge ranges in height from about 1.5 to +3 m above mean sea level, and its proximity to the water line ranges from 20 m to 5000 m on low delta plains. The driftwood line today does not coincide with a vegetation boundary resulting from salt water intrusion. Variations in the height of the storm surge follow a predicted pattern, with greatest water pile-up at the end of shallow embayments opening into the direction of westerly wind.

Historical information suggests that storms of similar magnitude to that of 1970 occur at about 25-year intervals, but our findings indicate that the 1970 surge height was not equaled during the last 90 to 100 years and may not have been exceeded in several hundred years.

Large amounts of sediment are supplied to the shelf during such surges from thermo-erosion of the coastal plain. Over long periods of time, westward-facing bluffs of promontories show higher erosion rates than eastward-facing bluffs. This reflects the importance of the short term effects of the rare westerly storms compared to the effects of the dominating easterly winds and waves. Major modification of barrier islands also occurs during the surges. All barrier islands were submerged and under the influence of breakers and currents, and, during late stages, the islands were also affected by gouging and pounding of large ice blocks. The pack ice brought in against the coast during a surge results in intensive ice gouging. If a major surge were to occur during a period of offshore petroleum exploration or production, damage would be extensive.

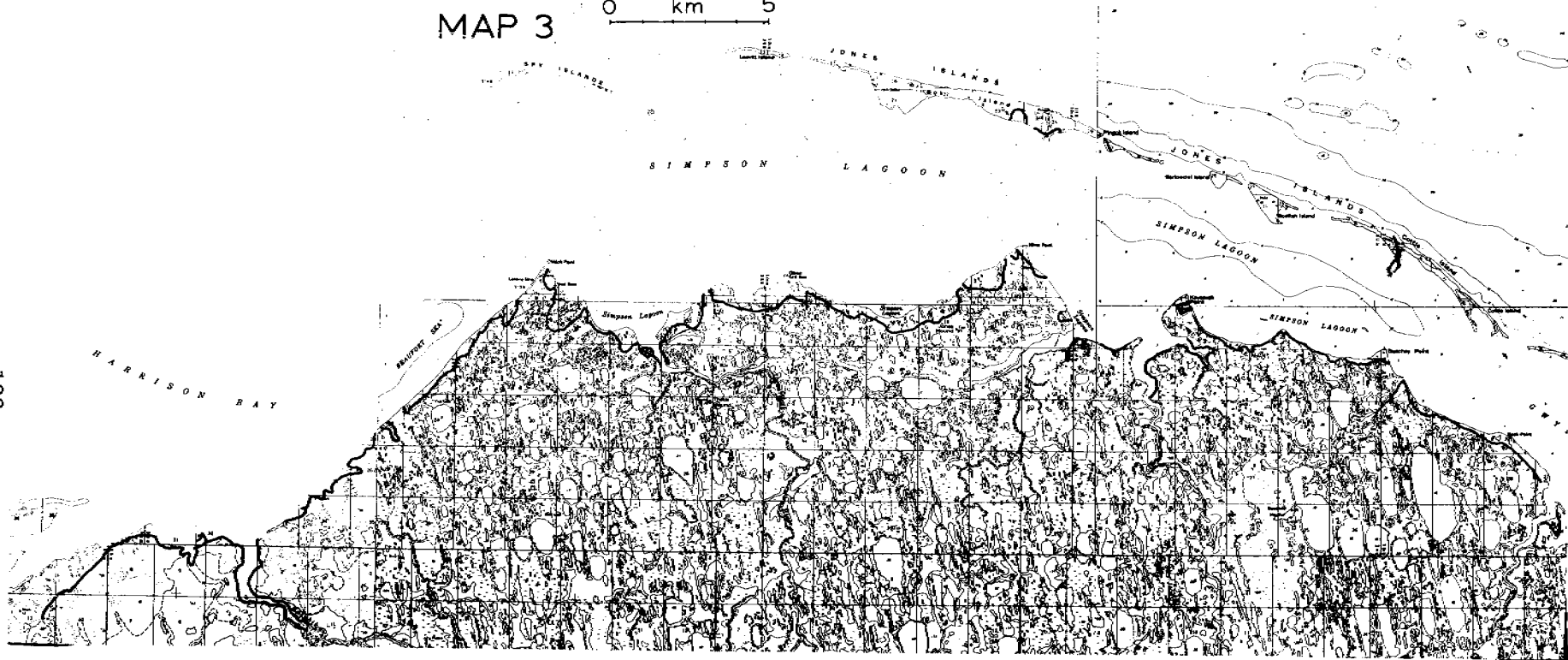


MAP 2 0 km 5

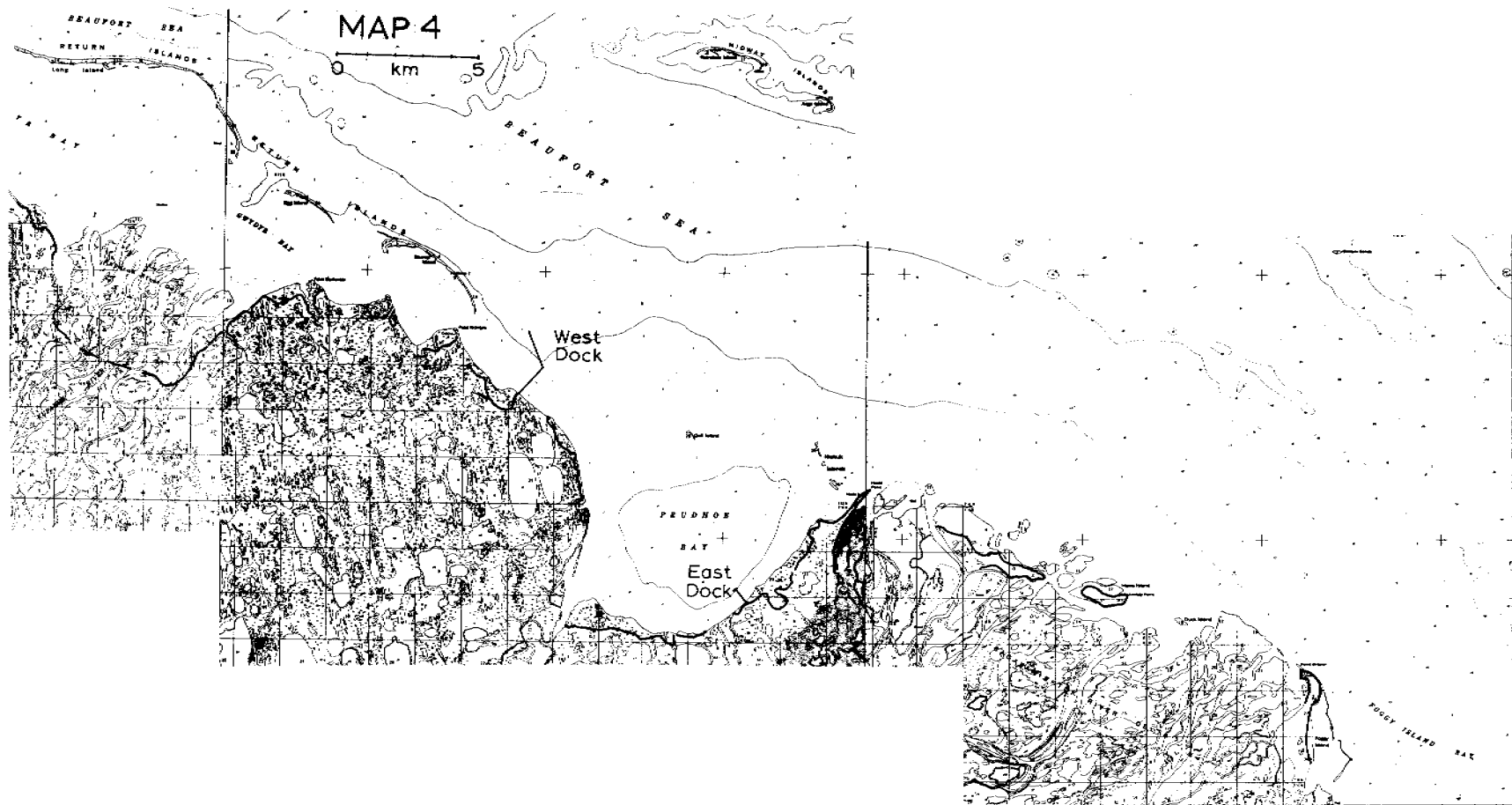


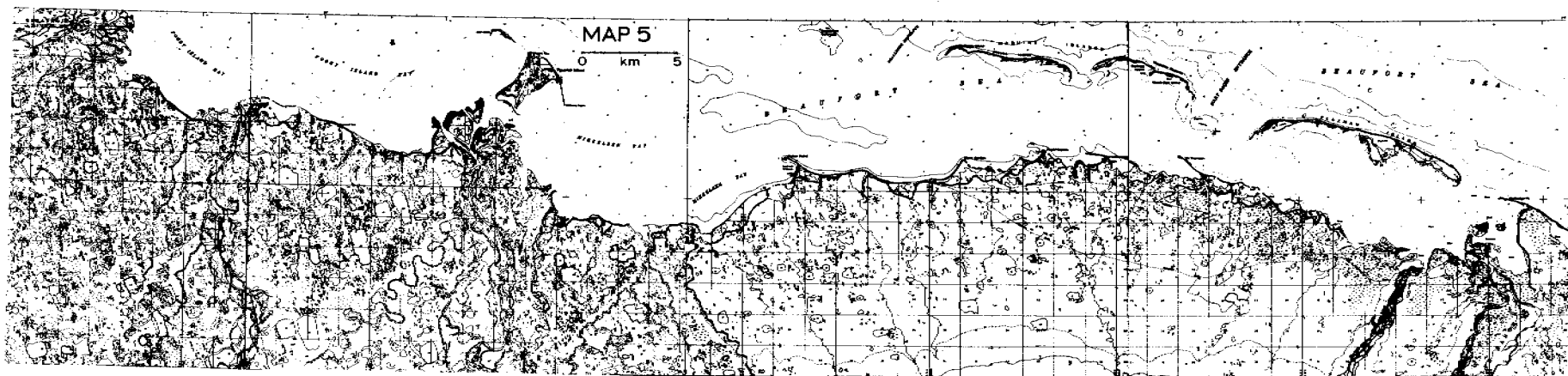
MAP 3

0 km 5



188





REFERENCES

- Anonymous, 1971a, Herschel Island, Feasibility of marine terminal, Department of Public Works, Canada, Unpub. internal rept., 141 p.
- Anonymous, 1971b, Beaufort Sea storm, September 13-16, 1970, Investigation of effects in the Mackenzie Delta region. Dept. Public Works, Eng. Programs Branch, Ottawa, Ont., Canada, 22 p.
- Atmospheric Environment Service, 1972, Ice summary and analysis, 1970, Canadian Arctic, Ann. pub., Toronto, Ont., Canada, p. 60-63.
- Barnes, P.W., and Reimnitz, Erk, 1974, Sedimentary processes on arctic shelves off northern coast of Alaska, in: The Coast and Shelf of the Beaufort Sea. Proc. of The Arctic Inst. of North American Sym. on Beaufort Sea Coast and Shelf Research, Arlington, VA., Arctic Inst. of North America, p. 439-476.
- Burns, B.M., 1973, The climate of the Mackenzie Valley-Beaufort Sea, Climatological studies, No. 24, Atmospheric Environment Service, Toronto, Ont., Canada, 2 volumes.
- Carsola, A.J., 1954, Microrelief on the arctic sea floor, Bull. of American Assoc. of Petroleum Geologists, v. 38, p. 1587-1601.
- Dygas, J.A., and Burrell, D.C., 1976a, Dynamic sedimentological processes along the Beaufort Sea coast of Alaska, Assessment of the Arctic Marine Environment: Selected topics, Inst. of Marine Science, U. of Alaska, Chap. 15, p. 189-203.
- Dygas, J.A., and Burrell, D.C., 1976b, Response of waves and currents to wind patterns in an Alaskan lagoon, Assessment of the Arctic Marine Environment: Selected Topics, Inst. Mar. Sci., U. of Alaska, Chap. 19, p. 263-285.
- Emery, K.O., 1961, A simple method of measuring beach profiles: Limnology and Oceanography, v. 6, p. 90-93.
- Giddings, J.L., Jr., 1952, Driftwood and problems of arctic sea currents, American Philosophical Soc. Proc., Philadelphia, v. 96, p. 129-142.
- Henry, R.F., 1975, Storm surges: Beaufort Sea Project, Tech. Rept. No. 19, Dept. Environment, Victoria, B.C., Canada, 41 p.
- Henry, R.F., and Heaps, N.S., 1976, Storm surges in the southern Beaufort Sea, Jour. of the Fish Res. Board of Canada, v. 33, no. 10, p. 2362-2376.
- Hume, J. D., and Schalk, Marshall, 1967, Shoreline processes near Barrow, Alaska: A comparison of the normal and the catastrophic, Arctic, v. 20, n. 2, p. 86-103.
- Kovacs, Austin, and Mellor, Malcolm, 1971, Investigation of ice islands in

Babbage Bight, Technical Note, N-118, Creare Inc., Science and Technology, Hanover, N.H., 22 p.

Lewellen, R. I., 1972, Studies on the fluvial environment-Arctic coastal plain province, northern Alaska, R.I. Lewellen Publication, Littleton, CO., 282 p.

Lewellen, R.I., 1977, A study of Beaufort Sea coastal erosion, northern Alaska, Environmental Assessment of the Alaskan continental shelf, National Oceanic and Atmospheric Administration, Ann. Repts. for the year ending March, 1977, v. 15, p. 491-527.

Lewis, C.P., and Forbes, D.L., 1975, Coastal sedimentary processes and sediments, Southern Beaufort Sea, Beaufort Sea Project, Dept. of the Environment, Technical Report no. 24, 68 p.

Parry, Sir William Edward, 1826, Journal of a third voyage for the discovery of a northwest pasage, Philadelphia, PA, H.C. Carey and I. Lea.

Reimnitz, Erk, Barnes, P.W., Forgatsch, T.C., and Rodeick, C.A., 1972, Influence of grounding ice on the Arctic shelf of Alaska: Marine Geol., v. 13, p. 323-334.

Reimnitz, Erk, and Barnes, P.W., 1974, Sea ice as a geologic agent on the Beaufort Sea shelf of Alaska, in: The coast and shelf of the Beaufort Sea, Proc. of the Arctic Inst. of North American Sym. on Beaufort Sea Coast and Shelf Research, Arlington, VA, Arctic Inst. of North America, p. 301-353.

Schell, Donald, 1974, Seasonal variation in the nutrient chemistry and conservative constituents in coastal Alaskan Beaufort Sea waters, in: Environmental studies of an arctic estuarine system, Univ. of Alaska, Inst. of Marine Sciences, Report #R-74-1, Chap. 7, p. 233.

Short, A.D., 1973, Beach dynamics and nearshore morphology of the Alaskan Arctic coast, Louisiana State U., (unpub. Ph.D. thesis), 139 p.

Stockton, C.H., 1890, The arctic cruise of the U.S.S. Thetis in the summer and autumn of 1889: The National Geographic Magazine, v. 2, n. 3, p. 174-198.

Zubov, N. N., 1945, Arctic Sea Ice, transl. by Naval Oceanographic Office and American Meteorological Soc. under contract to Air Force Cambridge Rsch. Ctr., 1963, U.S. Naval Electronics Laboratory, San Diego, CA, 491 p.

ATTACHMENT B

Ice Gouging Characteristics: Their Changing Patterns from 1975-1977, Beaufort Sea, Alaska

P.W. Barnes, David McDowell, Erk Reimnitz

Sea ice, in the form of ridges and massive blocks, commonly impacts the sea floor of arctic shelves, scraping, plowing, scoring, scouring and gouging. The characteristics of bedforms have been dealt with at some length (Kex 1955; Kovacs, 1972; Reimnitz and others, 1972; Pelletier and Shearer, 1972; Kovacs and Mellor, 1974; Reimnitz and Barnes, 1974; Reimnitz and others, 1977a and b Lewis, 1977). These bedforms are ubiquitous on the arctic shelves of the Chukchi and Beaufort Seas and are known to be present in many areas of the northern Bering Sea and Norton Sound (Thor and others, 1977). Less well known is the evolution of ice gouges in space and time.

It is important for the design and safety of offshore structures such as pipelines to understand the frequency and character of ice interactions with the sea floor. The rates of sediment reworking by ice can be estimated using ice gouge recurrence intervals coupled with the incision depth of ice keels. Similarly the demise of gouge features in time gives information on the rates of sediment reworking by benthic communities and by currents. Seasonal or annual changes in patterns of ice gouge events and their orientation are a reflection of the ice motion during gouge formation. Furthermore, the orientations and intensities of all gouges are an integration of ice motions dating back many years to the time of complete seabed reworking by ice.

To date there has been considerable disagreement among investigators as to the age of ice gouge features and the relative intensity of contemporary gouging as related to winter ice zonations and seasonal ice patterns (Pelletier and Shearer, 1972; Kovacs and Mellor, 1974; Reimnitz and Barnes, 1974; Reimnitz and others, 1977a,b; Lewis, 1977; and Hnatiuk and Brown, 1977). Much of this has resulted from a general sparsity of data and our lack of understanding of ice-seabed interactions on arctic shelves.

Utilizing data gathered during repetitive surveys of the same area on the inner shelf has allowed us to further define the character of year-to-year ice gouging, the possibility of summer gouging and to assess the variability of gouging from one year to another. Based on these data, the probability of deep gouges and the frequency of ice impacts can be estimated.

In the area of this study (Fig. 1) sea ice can generally be divided into three zones based on bathymetry and ice character (Reimnitz and others, 1977b): 1) a bottom fast ice zone inside the 2-m isobath, where ice at the end of the season of ice growth rests on the sea floor; 2) the zone of floating fast ice; and 3) the stamukhi zone which forms the seaward edge of the floating fast ice, as a series of major grounded ice ridges. The stamukhi zone occurs in 15-20 m water depths, marks the boundary between the quasi-stable fast ice and the moving polar pack. It is an area of shear and pressure ridge formation and an area of intense ridge grounding during the winter. As a result, solidly grounded stamukhi ice ridges may remain grounded

throughout one or several seasons of melting (Kovacs, 1976). The two fast ice zones remain essentially stable once the stamukhi has formed. Prior to this ice in these zones is free to move. During the summer open water season, drifting ice of various drafts is commonly present at all water depths on the inner shelf. The area of this study (Fig. 1) is primarily located in the zone of floating fast ice.

The sea floor in the study area slopes steeply offshore from the islands to depths of about 7 m, then more gradually seaward (Fig. 1). Test line 1 runs northwest from Thetis Island and test line 2 heads just about due north from Spy Island. Along test line 1 no significant bathymetric features are encountered, while on test line 2 several 2 to 4 m high ridges are crossed. (Fig. 1). To the northeast of line 2, several northwest-southeast trending linear shoals are present which apparently have a significant influence on the shelf ice zonation (Riemnitz and others, 1977 and attachment 'D').

FIELD METHODS

In 1973, 1975, 1976, and 1977, a recording side-scan sonar and a precision fathometer were used on carefully navigated test lines to repeatedly obtain records over the same area of sea floor in each year. Test line 1 was surveyed twice during the summer of 1977, once in early August and once in early September. The 1973, 1975, and 1977 side-scan sonar records cover a 125 m swath on each side of the ship track while the 1976 survey flubbed and covered only 100 m on either side. Depending on sea state, bottom reflectivity, and system tuning the sonographs produced by the sidescan can resolve features less than 10 cm high. The fathometer used in this survey utilized an 8° cone in 1975 and 1977 and a narrow beam 4° cone in 1976 and was also capable of resolving bottom relief of less than 10 cm.

Navigation along the test lines was accomplished by ranging on landmarks onshore and by a precision range-range navigation system which reads to the nearest meter and is accurate to ± 3 m. With these techniques the test lines were steered within 50 m from year to year and overlapping sonographs were obtained of the sea floor except in areas where detours were made to avoid ice.

Sonographs from the side-scan sonar were the key data used to define the presence of a gouge feature and to locate and characterize new gouge features from one year to the next (Fig. 2). The analysis of ice gouge character was separated into two parts. First the character of all gouges along the test lines was assessed. The test lines were marked off in 500 m segments from the base of the line on Thetis and Spy Islands seaward (Fig. 1), and the trend, density, maximum incision depth and the maximum disruption width were determined from the 1975 records and again for the longer 1977 tracklines. Secondly, the new gouge features formed between the summers of 1975 and 1976 (Fig. 2) and between the summers of 1976 and 1977 were tabulated for the same characteristics, using the sonographs and fathograms from 1976 and 1977. The techniques used in determining gouge character are given in greater detail along with the results in the section below. A comparison of gouging on test line 1 between 1973 and 1975 has already been reported on (Riemnitz and others, 1977a).

DATA REDUCTION AND RESULTS

An idealized gouge cross section is shown in Figure 3 as an aid in clarifying the terminology used in this report (Reimnitz and others, 1977a). The keel of an ice projection is depicted bulldozing or plowing through the bottom sediments (Fig. 3A) displacing material. The ice keel is presumed to dig below the prevailing sea-floor depth and to pile materials to the side forming flanking ridges. After the ice keel has passed (Fig. 3B), the flanking ridges and the incision remain to the extent that they are modified by slumping, current and biological reworking, and subsequent ice bulldozing and sedimentation. It should be noted that: a) "incision depth" is generally less than the true gouge relief and may be measured less than true depth due to sound-cone geometry of the fathometer, b) the final gouge depression (even from fresh gouges) may be shallower than the incision due to slumping, and c) the "extent of disruption" probably often extended beyond the original incision.

Summary of ice gouge characteristics

The dominant gouge trend, density, maximum incision depth, and maximum disruption width were determined for 1/2 km segments of the test lines. All gouges, new and old, were used for these determinations. We have tried to standardize as many of the admittedly subjective observations (Hnatiuk and Brown, 1977) in an effort to make them comparable from one area to another and from year to year. As the reader proceeds through the various characteristics discussed below, it might be helpful to refer to the 500 m data segment depicted in Figure 4 along with a listing of the characteristics determined from this segment.

Gouge trend: Most ice gouge features are linear. The gouge trend is the orientation of the major portion of the linear features within a given segment. As both the boat speed and paper speed are variable, the sonographs exhibit horizontal exaggeration. By removing the exaggeration and computing the true orientation relative to the ship's course, the gouge trends may be determined (Fig. 4). A dominant trend was computed for each 1/2 km segment. Occasionally subordinate trends were evident, or the variability and non-linearity of orientation were so pronounced that it was not possible to plot a representative trend.

On test line 1 the dominant trend is nearly east-west, which is essentially parallel to the depth contours in this area (Figs. 1 and 5). Furthermore, the trend is uniform on both the inner and outer portions of the survey line and similar on both the 1975 and 1977 data sets. Intervals where no dominant trend was established occur at several locations along the test line but are concentrated on the inner half.

In contrast the dominant orientation of gouges on test line 2 (Fig. 6) swings clockwise from northeast-southwest on the inner 7 km of the line to northwest-southeast on the outer part of the line beyond about 12 km. The submerged ridges and isobaths along this test line also demonstrate the shift in orientation noted in the ice gouges (Fig. 1, see also Attachment D)). The ridge crests are characterized by numerous rather short gouges of various orientations so dominant trend can be determined (Fig. 7).

Gouge density: To determine the density of gouges, every linear feature

resulting from ice contact with the bottom was counted, including each individual scratch produced by multi-keeled ridges, as we wished to assess the effects of ice on the bottom. As more gouges would be seen when the ship track is perpendicular to the trend of gouges over a given distance than when the track is parallel to the features, (due to limited scan width of the sonar), Figure 8, gouge counts were normalized to represent the number of gouges that could be seen if all gouges were at right angles to the ships track using the following equation:

$$N = \frac{i}{i \sin \phi + R \cos \phi} (N_{obs})$$

Where: N = corrected number of gouges in counting interval
 N_{obs} = observed gouges in interval
 R = recorded width of sonograph - meters
 (both sides of record i.e. 125 m scale = 250 m record width)
 i = counting interval length in meters
 ϕ = dominant trend angle of gouges relative to ships' track
 (90° = perpendicular to track).

Utilizing the 1975 and 1977 records, with a sonograph record width of 250 m and a 500 m counting interval, this formula reduces to:

$$N = \frac{500}{500 \sin \phi + 250 \cos \phi} (N_{obs})$$

Thus, a count of 34 gouges in a 1/2 km segment of track, oriented with a dominant trend of 30° to the ships' track, calculates to 36.4 gouges per 1/2 km of track 1/4 km wide (Fig. 4).

Assuming that the distribution and orientation of gouges immediately adjacent to the zone scanned with the sonar is similar to that on the sonograph, the density of gouges per unit area may be calculated. This is only possible because the gouge count has been normalized at right angles to the ship's track and the assumption made that all gouges have the same trend and that they are linear. In this case, the number of gouges calculated for a kilometer segment of trackline should be the same as the number in a kilometer square bisected by that trackline segment (Fig. 8D). Thus, in the above example 36.4 gouges per 1/2 km of trackline, which is equivalent to 72.8 gouges per km of track, which is equivalent to 72.8(73) gouges per km^2 where gouges are at right angles to the track. These assumptions are not strictly correct, of course (Fig. 2 and 4), they simply allow a standardization of the data for comparison.

On both test lines 1 and 2, the gouge densities correlate with bottom slope; portions with steeper slopes have higher density values (Figs. 5 and 6). The highest densities on test line 1 ($88/\text{km}^2$) occur at the upper edge of a slope in the bottom profile ((Fig. 5). The seaward facing slopes of the ridges on test line 2 also show a sharp rise in the density of gouge events (Fig. 6). The longer trackline segment run in 1977 shows that the gouge density tends to increase with increasing water depth although the trend is not clear cut. The increase in gouge density is also very apparent when examining sonographs and fathograms from the outermost portions of the test lines (Fig. 9). The lowest values of gouge densities are associated with areas of low slope, areas inshore of submerged ridges, and in shallow water (Figs. 5 and 6).

Incision depth: Vertical distance to the gouge floor below the surrounding sea bed, exclusive of ridges, is measured as the incision depth rather than the overall vertical relief of the ridges and furrow (Fig. 3). This depth, depending on the gouge history since inception, where slumping, erosion, and/or sediment deposition may have taken place, may or may not be the depth to which ice penetrated below the sea floor. The incision depth is a minimum measure of the depth of sediment reworking. For each 500 m segment the prevailing sea-floor elevation was determined, then the maximum depth of incision below this elevation was scaled from the fathograms. The fathograms represent only a single profile across the area represented in the sonographs. If profiles were taken elsewhere within the sonograph record, chances are good that deeper incision would be noted.

The maximum incision depths shown in Figures 4 and 5 do not correlate with the other summary characteristics. Deep incisions are spread out along the line showing no clear relation to water depth. The deepest gouge (180 cm) was observed at the outer end of line 1, although respectable gouges (50-70 cm) occur on the inner 5 km of both test lines (Fig. 5A and 6A). A greater number of ice bottom interactions is expected in shallow water due to the greater abundance of shallow ice keels. The possibility that one of these many gouges would be deep might be offset by the fact that incision depth would be expected inshore due to the limited size and mass of the cutting tools.

Disruption width: Within each 500 m trackline segment the widest transverse section of the bottom disrupted by a single ice event was measured on the sonographs. This "disruption width" (Fig. 3B) did not necessarily correlate with the deepest keel incision depth. In fact, the reverse may be true. Deep gouges commonly are narrow. The sonographs were used to make width measurement as in some cases the widest feature was not crossed by the trackline and thus not recorded on the fathograms. Furthermore it was easier to identify a single event on the sonographs. The widths measured were graphically corrected for the horizontal exaggeration (the distance along the sonograph record differs from the scale across the record (Fig. 4), see Reimnitz and Barnes, 1974).

In all cases maximum disruption widths tended to increase in an offshore direction (Figs. 5 and 6). Perhaps more significantly, the inner 8-10 km of the test lines show gouge events generally less than 15 m wide. The maximum observed width on test line 1 was 45 m and on test line 2 it was 70 m. Ice gouges more than 15 m wide are almost always the result of the action of multi-pronged ice keels (Reimnitz and others, 1973).

New gouges, 1976, 1977

By comparing the 1975, 1976, and 1977 sonographs for morphologic traits such as intersections of lineations, characteristic angles, and notable debris piles (Reimnitz and others, 1977a), area matches could be made (Fig. 2). Careful analysis of the 1976 and 1977 sonographs revealed new ice gouge features (Figs. 2 and 7).

The 1975 survey was run on 16 September, shortly before freeze-up, whereas in 1976 the reoccupation of the test line took place on 10 August, shortly after sea ice break-up in late July. Thus most of the new gouges seen in the 1976 records probably occurred during the arctic winter when a full ice cover was present. In 1977 two surveys were run. The first was run a year

after the 1976 study on 1 August. Test line 1 was repeated a month later on 3 September, 1977 to find out what changes might have occurred during the open water season.

Using the same techniques and terminology discussed above, the trend, incision depth, incision width and disruption width were determined for each of the new gouges identified in the 1976 and 1977 records. Notes were also made regarding the morphologic character and symmetry of the gouge flank ridges and gouge floor. Gouge densities, maximum incision depths and maximum disruption widths were then determined for the same 500 m intervals used for the summary characterization.

The trend of each new gouge on both test lines was plotted (Figs. 10 and 11) for comparison with the dominant trend noted in figures 5 and 6. On test line 1 the trend of new gouges in 1976 (Fig. 10A) is more onshore than the isobath parallel trend of 1975 (Fig. 5A). Furthermore, most of the 1976 gouges are sub-parallel and very straight, (Fig. 2) suggesting that they may have formed during the same ice movement event when the ice acted as a single unit. This is in contrast to the trend of new gouges in 1977 (Fig. 10A) which show a more random orientation when compared to both the 1975 and 1977 gouge summary data (Fig. 4). This might suggest that the ice conditions and ice movement patterns responsible for the 1976 and 1977 new gouge data sets differed significantly.

On test line 2, the trend of new gouges in 1976 (Fig. 11A) shows essentially the same orientation as the summary characterization (Fig. 6). Although the 1977 new gouge data (Fig. 11B), shows a dominance of east-west gouges. There are more gouges with orientations differing from the summary than in the 1976 data set (Fig. 11A).

When comparing trends of new gouges as yearly data sets, the events which formed the 1976 set were found to be apparently more "normal", i.e., more similar to the summary characteristics, than were those gouges that occurred during formation of the 1977 data set.

The densities of new gouges are remarkably evenly distributed over the length of test line 1 in both years of the study (Fig. 10,). On test line 2, the density appears to be greatest on the line segment seaward of the ridges in 1976 data (Fig. 11A), but concentrated landward of the ridges in the 1977 data (Fig. 11B). The densities do not reflect the character of increased densities offshore suggested in Fig. 9.

As with density distribution, the maximum incision depths of deep new ice gouges on both test lines are rather evenly distributed. Depths tend to increase seaward only on the 1976 data for test line 1. It should be remembered that the maximum incision depth is measured only where the ship crosses the gouge and it would be logical to assume that there is variance in incision depth along the length of a gouge. Thus the maximum values might have been different if the test lines had been run several meters to one side or the other. A scatter plot of incision depths versus water depth for ice gouges (Fig. 12) suggest that there is a concentration of deeper gouges in water depths between 11 and 15 m, although the population between 15 and 20 m may be under-represented because fewer data points were obtained in these water depths (Figs. 10 and 11). The maximum new incision depth on test

line 1 was 120 cm in 1976 and only 60 cm in 1977. Similarly, on test line 2 the 1976 maximum value (80 cm) was greater than that observed in 1977 (40 cm).

The average incision depth of new gouges was computed for each trackline segment. We assumed a depth of 10 cm for those gouges where the gouge did not cross the sonograph centerline and was therefore not recorded on the fathograms, and a depth of 5 cm when the gouge was not crossed but distinguishable on the fathogram. These approximations are further complicated by the problem of distinguishing the quantity and incision depth of small gouges which cannot be detected on the side-scan sonar and the fathometer. Furthermore, furrows formed while ice impacts the flanking ridges of ice gouges will probably not be recorded although they are a part of the gouge population (Fig. 3). As Lewis (1977) pointed out, the smaller gouges are underestimated. Thus, the frequency curve of new gouges (Fig. 13) does not truly represent the distribution of small gouges. Conversely, it is highly unlikely that gouges with incision depths greater than 10 cm will be missed.

The depth averaging of new gouge incisions over the length of the test lines shows a decrease on test line 1 from 37 cm in 1975 (Reimnitz and others, 1977) to 19 cm in 1977 (Table I). On test line 2 the gouges also repeat the decreases from the 1976 to the 1977 data are (Table II) are lower than the respective year values for test line 1. This comparison is significant and suggests that the energy expended by the ice on the bottom was less intense during formation of 1977 data set than it was during formation of the 1976 data set. Furthermore, the energy spent on line 2 was less than that expended on Line 1.

Two width parameters were measured for the new gouge data. The incision width (Fig. 3), as measured on fathograms, was used in calculating the rates of sediment reworking. The disruption width (Fig. 3), measured on sonographs, was used to compare new gouges with the summary gouge characteristics (Figs. 5 and 6). As most gouges were not crossed at right angles, width measurements had to be corrected for gouge trend on both the sonograph and fathogram data.

The maximum disruption width from new gouges on test line 1 in 1976 shows a good correlation with segments where maximum incision widths were observed (Fig. 10A). The new gouges observed in 1977 on test line 1 and in both years on test line 2 do not repeat this correlation. Wider gouges correlated with deeper water depths in 1976 (Figs. 10A and 11A) but not in 1977 data (Figs. 10B and 11B).

Discussion

The above characterization of the two years of data and the two test line environments suggests that the gouging process varies from area to area and from year to year. In an attempt to evaluate the randomness of the processes, the data on new gouges was summarized for 2 km segments of each test line (Tables I and II). Significant differences between test lines 1 and 2 and between the 1975 and 1977 data are: 1) The increase in the number of new gouge events observed on line 1 (from 39 gouges in 1976 to 63 gouges in 1977); 2) The sum of the incision widths on test line 2 has decreased by more than half from one year to the next, whereas on test line 1 the sum has remained unchanged; 3) The average depths of incision on test line 1 are greater by about 10 cm than those computed for

test line 2, although both test lines show a decrease in average depth from 1976 to 1977; and 4) Gouging was apparently concentrated on the inner and outer sections of both test lines in 1976 but was more intense on the central section in 1977 (Tables I and II - Incision Width). However, the range of values for the number of gouges, incision widths, average incision depths are roughly of the same order of magnitude for both the 1976 and 1977 data.

The above discussion suggests that the ice events leading to the gouges recorded by the 1976 data set differed significantly from the events forming the 1977 data set. New gouge data from 1976 regarding the ice events in the winter of 1975-1976 suggest that one or two major ice movements took place in a southwesterly direction which produced straight, deep gouges where keels contacted the sea floor. This gouging tended to follow bathymetric contours. Where shoals were present (Fig. 2) their elongate axes determined direction of movement of the ice keels. In the winter of 1976-1977 ice movements were more random (frequent?) and were less intense, producing shallow gouges with less well-defined orientations. We do not have data available to test this hypothesis, except to note that the ice ridging in the Prudhoe Bay area was less intense in 1977 than in 1976 (RU-88, Kovacs and Weeks). In any event, the widely differing character of gouging during the two periods suggests that gouging is a very sporadic process and perhaps is strongly dependent on storm and ice conditions of the preceding fall and winter.

The abundance of grounded ice in summer has led us to suspect that some gouging must occur during this season. Data from test line 1, taken one month apart in the summer of 1977, revealed that a single gouge event occurred during the month of August (Fig. 14). The gouge (in 12 m water depth) was a straight feature, more than 400 m long, oriented east-west and composed of three furrows on the eastern portion of the sonograph and a single furrow on the west. The incision was 10 cm deep on the fathogram. The direction of ice motion is not apparent on the fathogram. This summer gouge does not differ significantly in orientation, incision depth, length or width from most gouges seen (Figs. 2, 7, and 9, Table I and II). The only unique feature is the wavy character of the gouge and the change from multiple furrows to a single furrow. Most of the ice motion in winter must be rather uniform in direction as ice blocks and ice keels will be "locked" into a larger ice sheet, whereas in summer ice blocks are free to rotate in the currents. Thus the character of the summer gouge described above might be typical of gouges occurring in summertime, where different faces of the ice keel impact the bottom as the ice block swings or rotates in the current field (Reimnitz and others, 1973).

Ice gouge recurrence and rates of sediment reworking

The data from previous surveys described above demonstrates that ice gouging is a modern process on the inner shelf. Questions now arise as to how often gouging occurs and how extensively does gouging rework the bottom sediments. Using data on the incision widths of new gouges, length of test lines, time interval between surveys, the fraction of the bottom impacted within that interval may be calculated. Or:

$$k = \frac{\sum W_i}{L(t)}$$

where: k = fraction of the bottom impacted each year.
 W_1 = incision widths of new gouges (in meters)
 L = total length of test line segments compared for new gouges - less data gaps (in meters)
 t = time interval between compared surveys (in years)

Comparison of the data for test lines 1 and 2 (both test lines and both years) (Tables I and II), indicates that k varies between .011 and .021. In other words, on the average, two percent of the test line was impacted with new gouges each year. Assuming that gouging will proceed in a systematic manner and will not replot¹ any point on the sea floor until the entire sea floor is impacted with new gouges, the fraction of the bottom impacted after T years will be (Fig. 15):

$$G_T = k (T)$$

where: G_T = fraction of the bottom gouged
 T = time in years from some arbitrary T_0

A gouge recurrence interval may also be calculated for any point on the sea floor which would be the time required to completely gouge the segments. We will call this the no-replot recurrence interval, where 100% ($G_T=1$) of the sea floor has been impacted with new gouges since T_0 .

$$\text{No-replot recurrence interval(in years)} = \frac{1}{k} \quad (1)$$

As ice interaction with the bottom does not occur in a systematic manner in our area of study, this approach is not a very good approximation of frequency of new gouges. A better approach, which does not involve rigorous statistics, would be to assume that each year some new gouges will replot portions of gouges extant since the start of the counting interval (T_0). For this projection we will assume that the fraction of the bottom replotted by new gouges is dependent on the area of the bottom that has been impacted by new gouges since T_0 . This can be written:

$$\frac{k_f}{k_g} = \frac{F_T}{G_T}$$

where, $k_f + k_g = k$ and $F_T + G_T = 1$

and where k_f = fraction of new gouges occurring with no replot

k_g = fraction of new gouges reploting

F_T = fraction of bottom not impacted since T_0 at time T

G_T = fraction of the bottom regouged since T_0 at time T

For example: if 10% of the bottom is impacted each year (k), then in the first year 10% (G_T) of the bottom is gouged and 90% (F_T) has not been impacted. In the second year, assuming another 10%, (k), of the bottom is impacted, 1%, (k_g), of these new gouges will occur on the 10% of the bottom impacted the previous year and 9% (k_f) will occur in new areas. Now 19% (G_T) of the bottom is gouged since the first year. In the third year an even larger fraction, (1.9%), of new impacts occurs in areas gouged in the first

¹Replot - Replot occurs when new gouges become superimposed on older gouges. As used here we are referring to those new gouges superimposed on other 'new' gouges that have occurred since some arbitrary time T_0 .

two years. Thus each successive year more and more replot takes place. This relationship can be expressed using the binomial theorem as follows:

$$G_T = 1 - (1-k)^T \quad (2)$$

where G_T = fraction of the sea floor impacted after T years
T = time in years from some arbitrary T_0 initiation of new gouging.
k = fraction of the bottom impacted in 1 year.

Using an average for k computed from 3 years of data on test lines 1 and 2 (Tables I and II) we can determine, based on the above assumptions, the rate at which the bottom will be impacted with new gouges (Fig. 15). This computation suggests that 50% of the bottom will be impacted in less than 40 years and 90% of the bottom will be impacted in about 150 years.

The incorporation of average depth of incision data (Tables I and II), along with the gouge recurrence, makes it possible to estimate the rate of sediment reworking of the sea floor by ice. The average gouge depth of the almost 200 new gouges observed was 21 cm. Assuming a 'no-replot' recurrence interval (Eq. 1), the sea floor was reworked to an average depth of 21 cm in about 50 years. Assuming a proportional replot (Eq. 2), in 50 years only a little over 50% of the bottom would be reworked.

Repetitive sonograph studies in two 14 km² areas of the Canadian Beaufort Sea have been conducted in 15-20 m water depths, slightly greater than our own studies (Lewis and others, 1976). Their data indicates that the fraction of the bottom impacted each year (k) was 0.17% in one case and 2.0% in the other, an order of magnitude difference. The higher value is very similar to the impact rate that we determined for the Alaskan Beaufort Sea in shallower water. No data is given on the incision depths of new gouges. The Canadian workers noted, as we have, that there can be considerable variability between subsequent data sets and record interpretation is often highly subjective. Thus, a rigorous comparison between the Canadian and Alaskan data seems inappropriate at this time.

In considering the rates of sediment reworking incision depths and the amount of bottom disturbed by gouging, our estimates are very conservative. Gouge incision depths do not include the height of the flanking debris ridges, nor do they include a correction for the cone angle of the fathometer which will give conservative depth values for narrow deep gouges (Fig. 3). The "extent of disruption" by ice keels often includes a considerable area on one or both sides of the incision (Fig. 3). Measurement of the 1976 gouges on test lines 1 and 2 indicates that disruption widths were 1 1/2 to 3 times wider than the incision widths. If these widths are used to determine rates of reworking, the values we report above would have to be increased by 30 to 60%.

The rates of sedimentation on the inner shelf in the study area have been estimated at about 10 cm per hundred years (Reimnitz and Barnes, 1974; Reimnitz and others, 1977a). Assuming a no-replot recurrence interval of about 50 years, (Fig. 15), the bottom would be reworked to a depth of 21 cm twice before 10 cm of sediment had accumulated. In this case, sedimentary

structures reflecting hydraulic sedimentation should be almost completely absent due to the intense reworking by ice. Vibrocores taken in the vicinity of test line 1 (Barnes and others, 1977a) are dominated by sedimentary structures related to ice gouging (Barnes and Reimnitz, 1974). However they do show a surprising amount of horizontal bedding one would ascribe to hydraulic sedimentation, suggesting that the rates of sediment reworking are not as rapid as noted above.

The proportional reflow curve for sediment reworking rates (Fig. 15) suggests that in 100 years about 20% of the bottom still remains undisturbed by gouging since T_0 . This suggests that on the average gouges less than 10 cm deep in the 20% of the "undisturbed" bottom would be filled in. Carrying this line of reasoning one step further, in 200 years (Fig. 15), when the average gouge incision (21 cm) would have been filled with new sedimentation (20 cm) there is still a portion of the bottom yet to be gouged (5%). The average gouge occurring in this yet ungouged area in subsequent years would not reach to the bottom of the sediments deposited since T_0 and thus deposition reflective of hydraulic processes would be preserved.

The fact that sediment reworking by ice gouging seen in the vibrocores is not as intense as would be suggested either by the no-reflow or proportional reflow rates of reworking indicates that we do not have a complete understanding of the processes. Our rates of shelf sedimentation might be too low. The pattern of ice gouging may be more systematic in distribution. More likely, local sedimentation rates are high due to the redistribution of materials in the vicinity of a recently formed ice gouge as a function of sediment type, gouge morphology and flank stability, bottom currents, sedimentation, and biologic activity.

The segments of test lines 1 and 2 as reported here are somewhat geographically protected by updrift shoals (Fig. 1 and attachment D) and are located inside of the major stamukhi zone, within the zone of floating fast ice (Reimnitz and others, 1977b). As the stamukhi zone is the site of the most intense winter ice deformation, we would expect rates of gouging and sediment reworking to be greater further seaward along the test lines (see Fig. 9). To date the presence of stamukhi in summer has kept us from obtaining usable repetitive surveys in this area.

Conclusions

Ice gouging has been shown to be the dominant process influencing the sediments in the area of study. Generalities regarding the process are that:

- 1) Higher rates of ice gouging and ice-bottom interaction are related to steeper bottom slopes, local topographic highs such as ridges, the stamukhi zone, and geographic exposure to drifting ice.
- 2) The dominant trend of gouges is parallel to the bottom topography. Submerged ridges tend to 'steer' gouges parallel to their elongate trend.
- 3) The character of gouging can vary significantly from year to year and is probably a reflection of the intensity and direction of motion of local segments of the ice canopy during the previous winter.

4) Ice gouge recurrence data suggest that the bottom is essentially completely reworked to depths greater than 20 cm in less than 200 years and may be reworked in less than 50 years.

5) The intensity of gouging is expected to be much greater within the stamukhi zone when data are obtainable, as this zone experiences the most intense ice deformation.

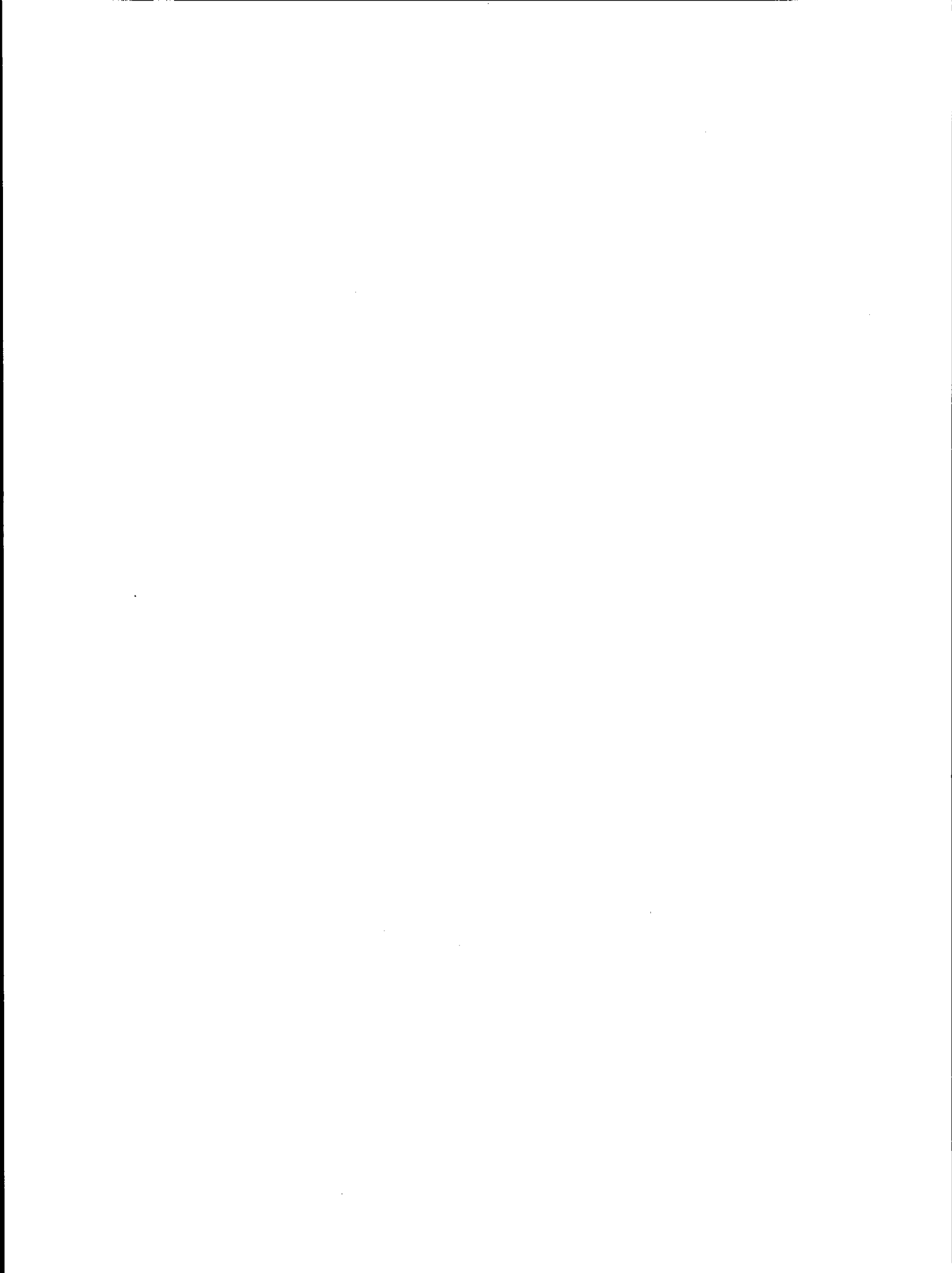
6) In the area studied, the maximum depth of ice gouge incision is less than 2 m and the maximum width of the bottom gouged by a single ice event is less than 100 m.

7) Between 1 and 2% of the bottom is gouged in any one year along the test line.

8) Gouges occur both in the open water and ice-covered periods of the year.

Acknowledgments

The authors would like to express their appreciation to Ralph Hunter for his assistance regarding the statistics of gouge distribution.



REFERENCES CITED

- Barnes, P. W., and Reimnitz, Erk, 1974, Sedimentary processes on arctic shelves off the northern coast of Alaska, in Reed and Sater, eds.: The Coast and Shelf of the Beaufort Sea, The Arctic Inst. of N. Am., Arlington, Va., p. 439-576.
- Barnes, P.W., Reimnitz, E., and Toimil, L.S., 1977. Preliminary results and observations on vibracoring taken on the Beaufort Sea inner shelf. In Oceanic and Atmospheric Adm., Environmental Assessment of the Alaskan Continental Shelf; Quarterly Reports of Principal Investigators, April-June 1977, v. 2, p. 539-569.
- Hnatiuk, J. and Brown, K.W., 1977, Sea bottom scouring in the Canadian Beaufort Sea; in Proceedings of the 1977 Offshore Technology Conference, Houston, Texas, Proceedings v. 3, p. 519-527.
- Kovacs, A., 1972, Ice scouring marks floor of the arctic shelf: Oil and Gas Jour., Oct. 23, 1972, p. 92-106.
- Kovacs, A., 1976. Grounded ice in the fast-ice zone along the Beaufort Sea coast of Alaska; US Army, Cold Regions Research and Engineer Laboratory, Hanover, New Hampshire, CREL Rpt. No. 76-32, 21 p.
- Kovacs, A. and Mellor, M. 1974. "Sea ice morphology and ice as a geologic agent in the Southern Beaufort Sea." In Reed and Sater, Eds. The Coast and Shelf of the Beaufort Sea, Arctic Inst. North America, Arlington, VA., P. 113-161.
- Lewis, C.F.M., Blasco, S.M., McLaren, P., and B.R. Pelletier. 1976, Ice scour on the Canadian Beaufort Sea continental shelf; Poster discussion, Geol. Assoc. of Canada, Annual Meeting, May 1976, Edmonton, Alberta, Canada.
- Lewis, C.F.M. 1977 Bottom scour by sea ice in the southern Beaufort Sea. Marine and Coastal Section, Terrain Sciences Division, Geological Survey of Canada, Technical Report 23, Victoria British Columbia. Beaufort Sea Project.
- Pelletier, B.R., and Shearer, J.M., 1972, Sea bottom scouring in the Beaufort Sea of the Arctic Ocean: Internat. Geol. Cong., Sec. 8, Marine Geology and Geophysics, p. 251-261.
- Reimnitz, Erk, Barnes, P.W., Forgatsch, T., and Rodeick, C., 1972, Influence of grounding ice on the arctic shelf of Alaska: Marine Geology, 13, p. 323-334.
- Reimnitz, Erk, and Barnes, P.W., and Alpha, T.R., 1973, Bottom features and processes related to drifting ice on the arctic shelf, Alaska: U.S. Geol. Survey Misc. Field Studies Map MF-532.
- Reimnitz, Erk, and P.W. Barnes: 1974, Sea ice as a geologic agent on the Beaufort Sea shelf of Alaska; in J. Reed and J. Sater eds., the Coast and Shelf of the Beaufort Sea, Arctic Institute of North America, Arlington, VA. p. 301-351.

Reimnitz, Erk, Barnes, P.W., Toimil, L.J., and Melchior, John, 1977a, Ice gouge recurrence and rates of sediment reworking, Beaufort Sea, Alaska: *Geology*, v. 5, p. 405-408.

Reimnitz, Erk, Toimil, L.J., and Barnes, P.W., 1977b, Arctic continental shelf processes and morphology related to sea ice zonation, Beaufort Sea, Alaska: *AIDJEX Bull.* 36, p. 15-64.

Rex, R.W., 1955, Microrelief produced by sea ice grounded in the Chukchi Sea near Barrow, Alaska: *Arctic*, v. 8, p. 177-186.

Thor, D.R., Nelson, Hans, and Evans, J.E., 1977, Preliminary assessment of ice gouging in Norton Sound, Alaska, Environmental Assessment of the Alaskan Continental Shelf, Ann. Rept. of Principal Investigators for year ending March, 1977, Environmental Research Lab., National Oceanographic and Atmospheric Adm., Dept. of Commerce, v. XVIII, p. 93-110.

Table I - ICE GOUGE DATA - New Gouges

Interval on Test Line 1 (km)

	2-4	4-6	6-8	8-10	10-12	12-14	14-16	<u>Total</u> <u>Average</u>	16-18	18-20	23-25
Water Depth (Meters)	7.6	9.7	10.5	11.3	12.6	13.1	13.7	---	14.0	14.5	16.0
Number of Gouge Events/Yr.											
1973-1975	2	4.5	0	1	0.5	1	1.5	10.5			
1975-1976	5	5	3	10	6	8	3	39			
1976-1977	7	9	13	10	5	12	7	63	1	4	6
Incision Width (M)											
1973-1975	17	79	0	7	45	105	12	263			
1975-1976	13	10	9	40	43	25	24	161			
1976-1977	21	23	15	39	22	27	15	161	3	10	8
Average Incision Depth (CM)											
1973-1975	40	37	0	45	30	45	27	37			
1975-1976	35	12	10	31	40	31	80	31			
1976-1977	14	14	12	21	50	18	22	19	10	29	10
Amount of Trackline Gouged (M/KM/Yr.)											
1973-1975	8	40	0	4	22	53	6	19			
1975-1976	6	5	4	26	21	12	12	12			
1976-1977	11	12	8	20	11	14	8	12			
Fraction of bottom impacted Each Year (K) x10 ⁻³											
1973-1975	8	40	0	4	22	53	6	19			
1975-1976	6	5	4	26	21	12	12	12			
1976-1977	11	12	8	20	11	14	8	12			
Summary Gouge Density "Old and New"											
1975	83	134	77	111	119	110	118	752 - 56.3/km ²			
1977	81	139	99	114	124	112	119	788 - 53.7/km ²			

TABLE II - ICE GOUGE DATA -New Gouges

Interval on Test Line 2 (KM)

	0-2	2-4	4-6	6-8	8-10	10-12	12-14	14-16	<u>Total</u> <u>Average 16-18</u>	
Water Depth (Meters)	7	11.5	12	14	15	15	16.5	18		18
Number of Gouge Events/Yr.					(Data gap 9.1-10.5 km)					
1975-1976	3	2	5	3	1	10	8	9	41	
1976-1977	1	2	10	7	8	3	6	5	42	2
Incision Width (M)										
1975-1976	30	11	21	13	2	7.1	36	81	268	
1976-1977	1	4	27	21	33	11	15	12	124	4
Average Incision Depth (CM)										
1975-1976	3	15	32	17	15	15	24	21	21	
1976-1977	10	10	21	10	9	10	8	12	12	5
Amount of Trackline Gouged (M/KM/Yr.)										
1975-1976	15	7	11	7	2	49	21	41	19	
1976-1977	0.5	2	14	11	17	6	8	6	8	
Fraction of Bottom Impacted Each Year (K) x 10 ⁻³										
1975-1976	15	7	11	7	2	49	21	41	19	
1976-1977	0.5	2	14	11	17	6	8	6	8	
Summary Gouge Density "Old and New"										
1975	47	84	71	65	60	94	72	56	549 - 34.3/km ²	
1977	86	75	100	68	75	107	67	48	626 - 39.1/km ²	

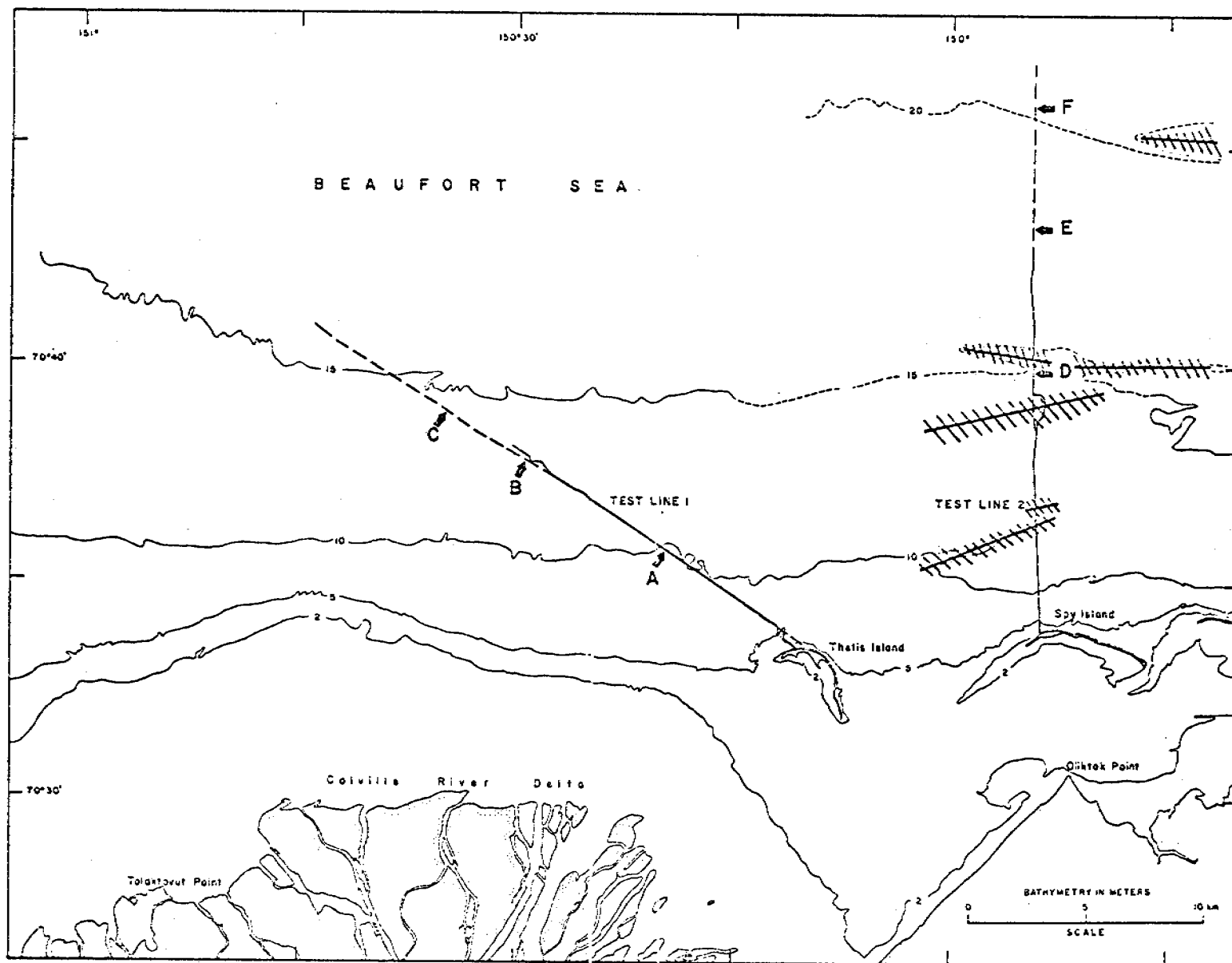


Figure 1. Location map of the study area indicating the location of test lines 1 and 2. Letters A through F designate the location of sonographs and fathograms illustrated in the text. The hachured areas emphasize the location of submerged shoals in the vicinity of test line 2.

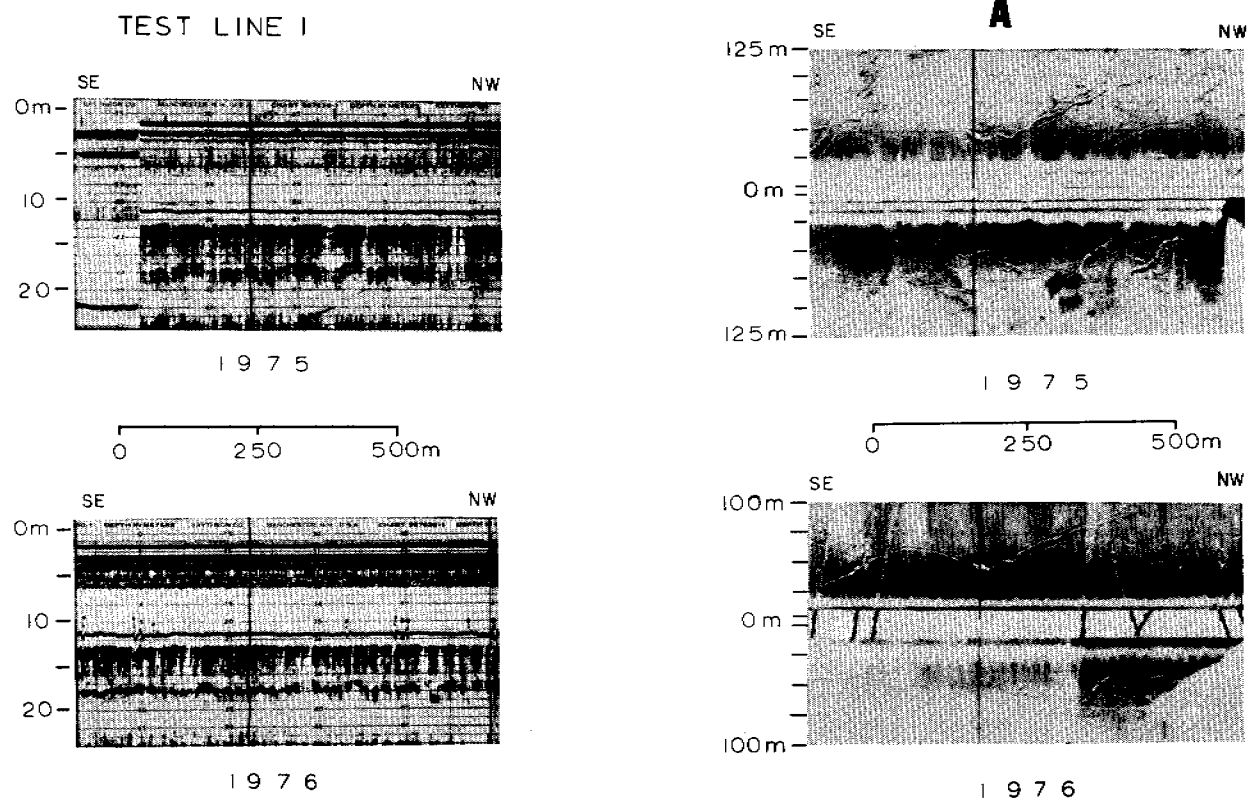


Figure 2. Comparison of 1975 and 1976 sonographs and fathograms at location A (Fig. 1), showing the morphology of new gouges formed between September, 1975 and August, 1976. Three gouge events can be distinguished on the sonographs; a) an event forming the series of 5 parallel gouges seen on the left side of the 1976 record, b) a single gouge which weaves across the record toward the upper right hand corner, and c) the set of three parallel gouges that terminate on the sonograph on the upper part of the trace.

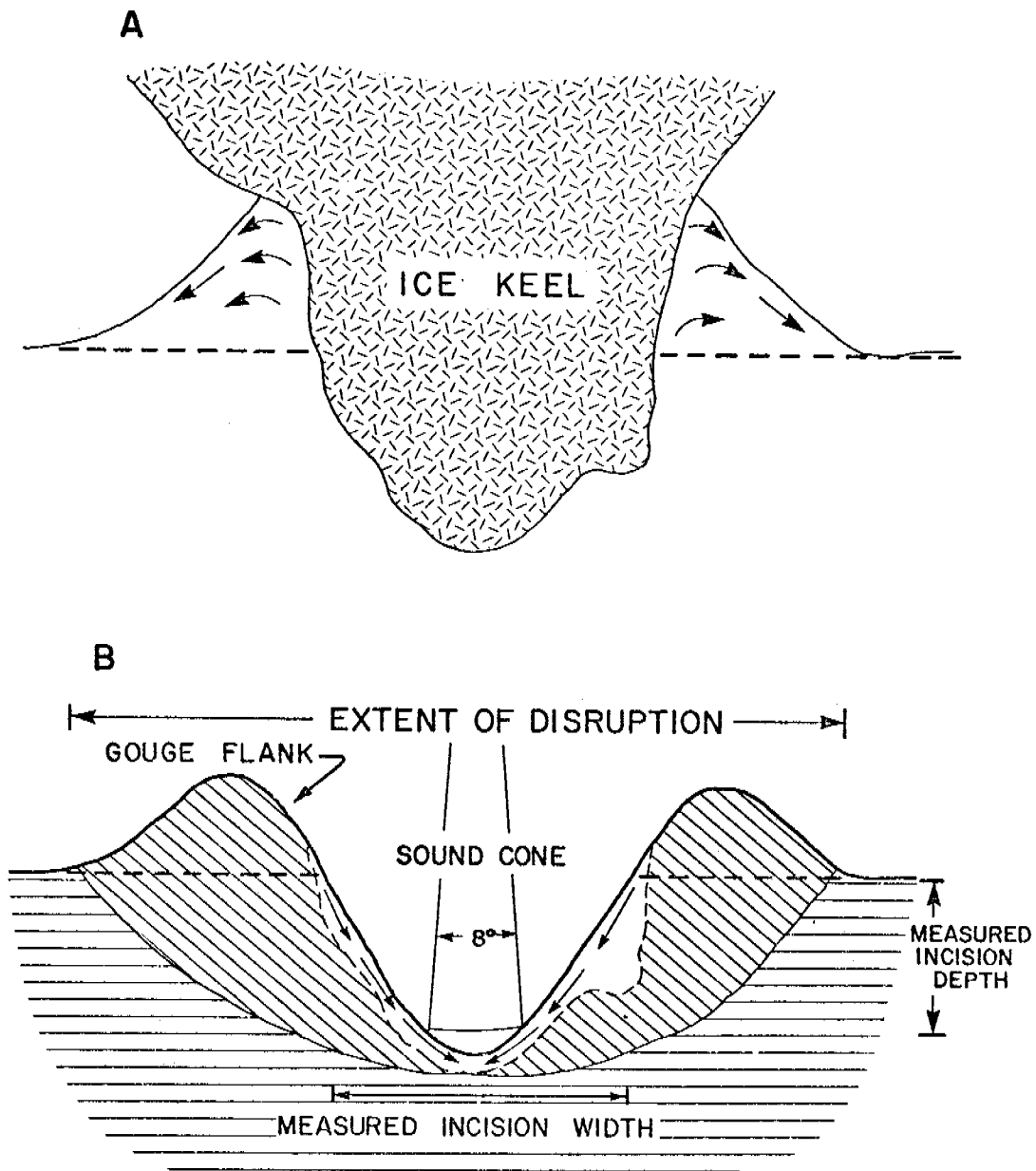
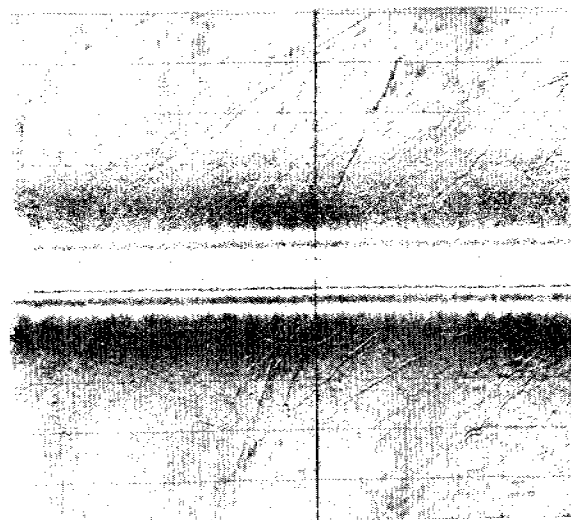


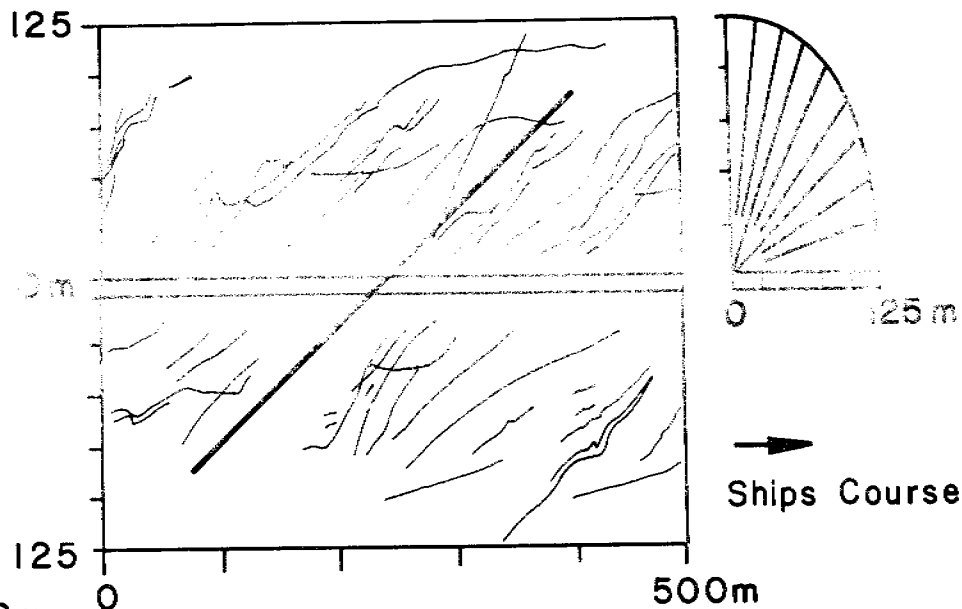
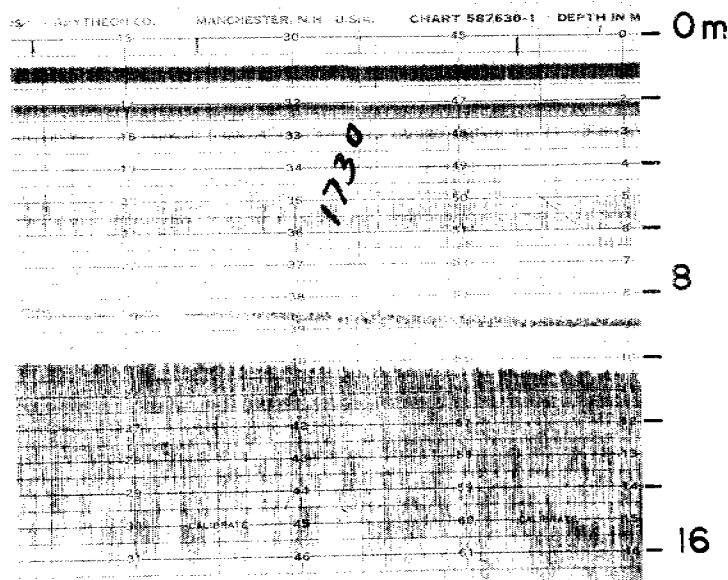
Figure 3. Drawing of an idealized ice gouge cross section with terminology used in this report. A) Gouge being plowed by an ice keel. B) The same gouge after the ice keel has passed and slumping of the flanks of the gouge has occurred (after Reimnitz, and others 1977).

SE

NW



0 500m



LINE 1 1975 3500-4000 m

WATER DEPTH - 8.5m

ORIENTATION:

RELATIVE DOMINANT TREND 30°

SHIPS COURSE 305°

GOUGE TREND 095°-275°T

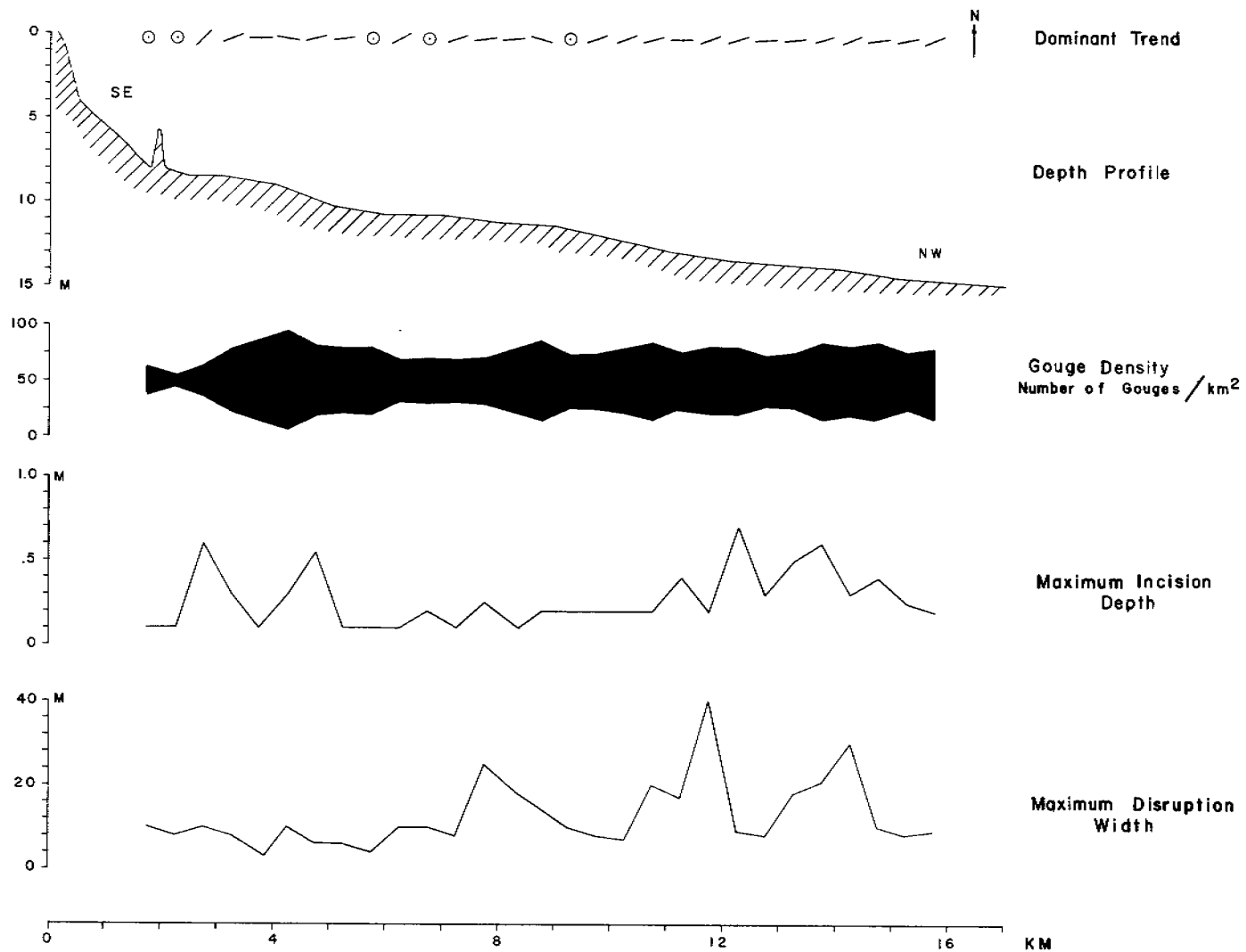
MAXIMUM INCISION DEPTH < .25m

MAXIMUM DISRUPTION WIDTH 3 m

Figure 4. A 500 meter segment on test line one illustrating how ice gouge characteristics were determined from sonograph and fathogram records.

A

SUMMARY OF ICE GOUGE CHARACTERISTICS TEST LINE I



B

SUMMARY OF ICE GOUGE CHARACTERISTICS
TEST LINE 1 1977

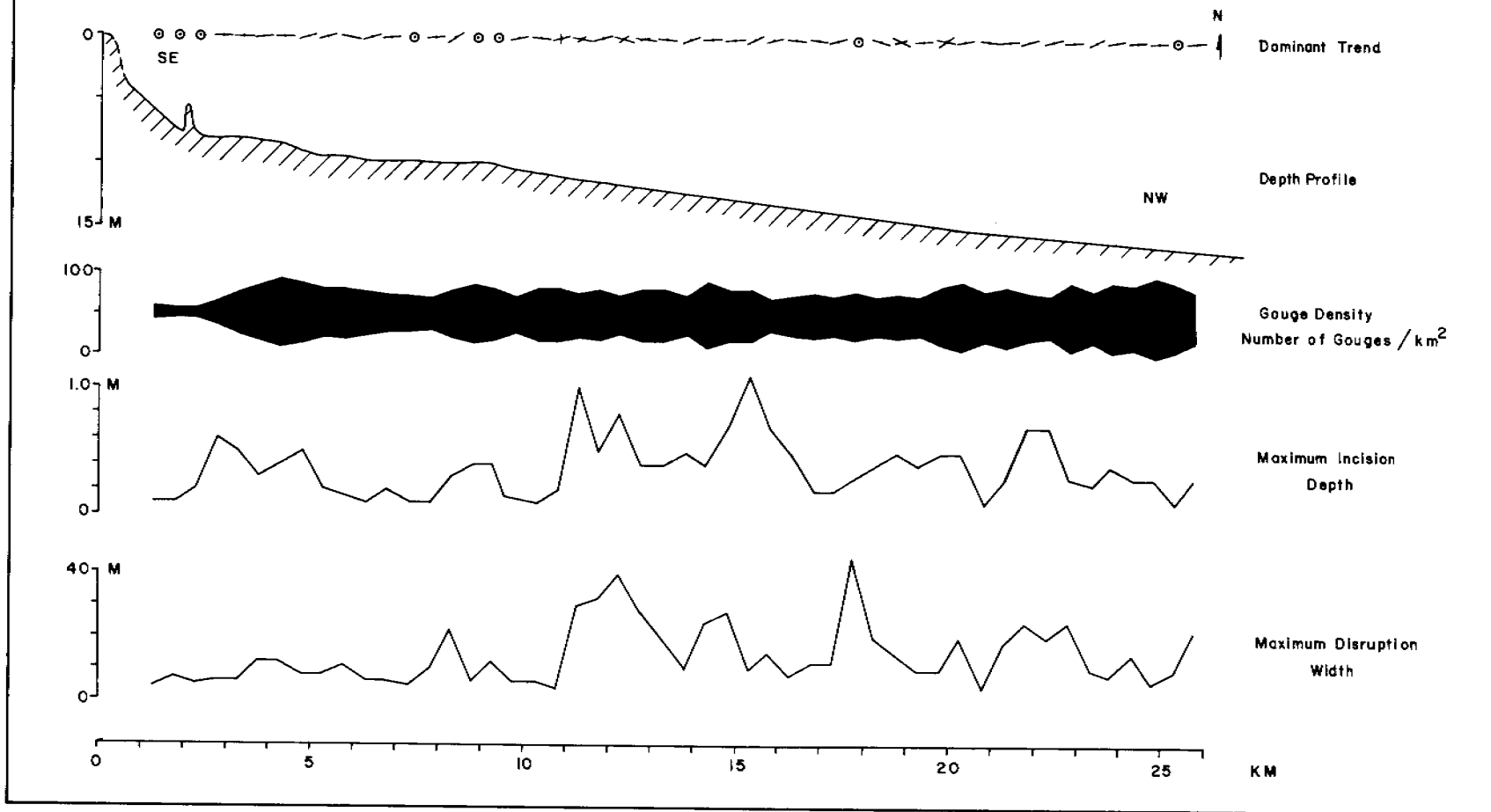
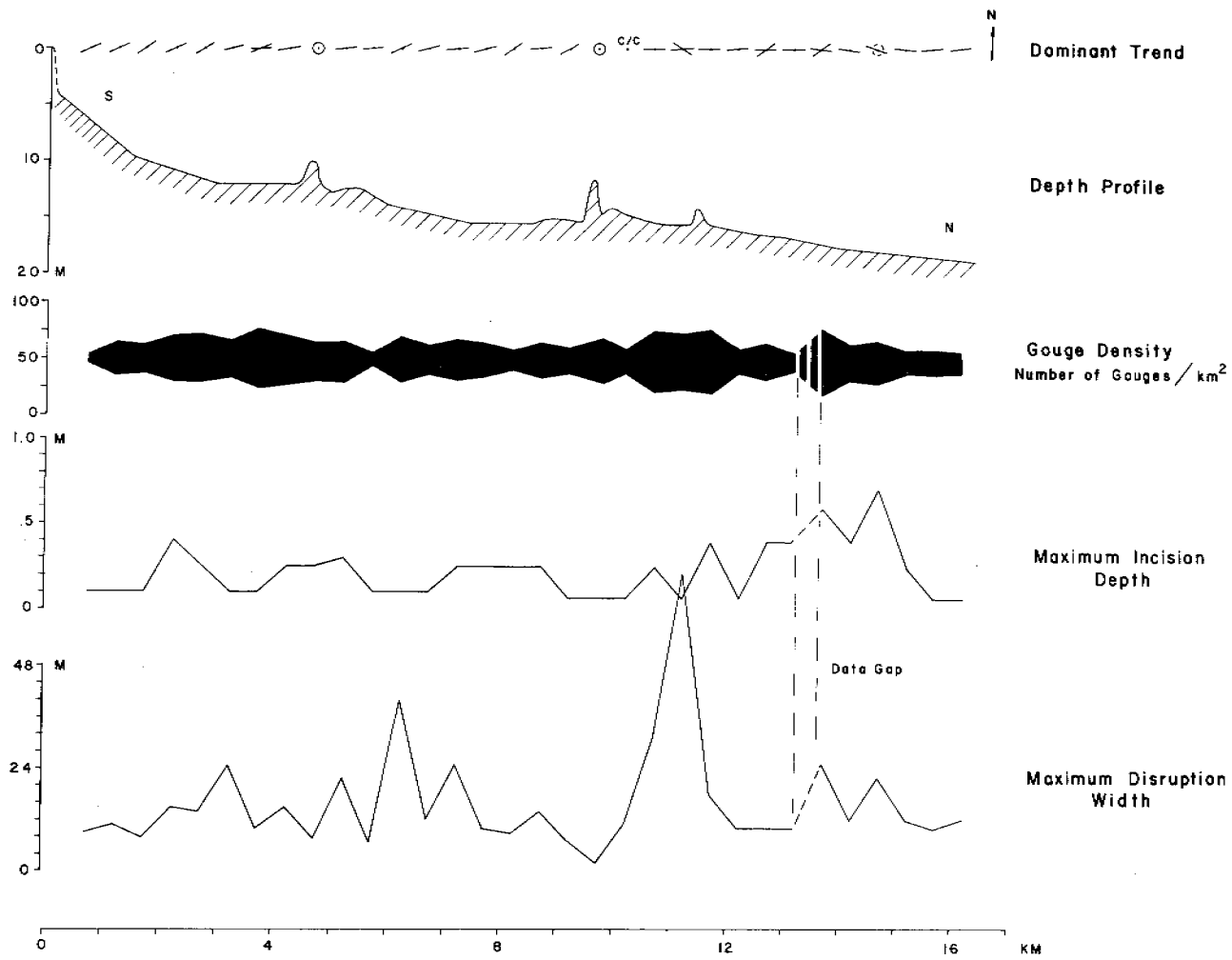


Figure 5. Summary of ice gouge characteristics on test line 1 determined from data taken in 1975 (A) and in 1977 (B). Values were determined from 500 m segments along the test line.

A

SUMMARY OF ICE GOUGE CHARACTERISTICS TEST LINE 2



B

217

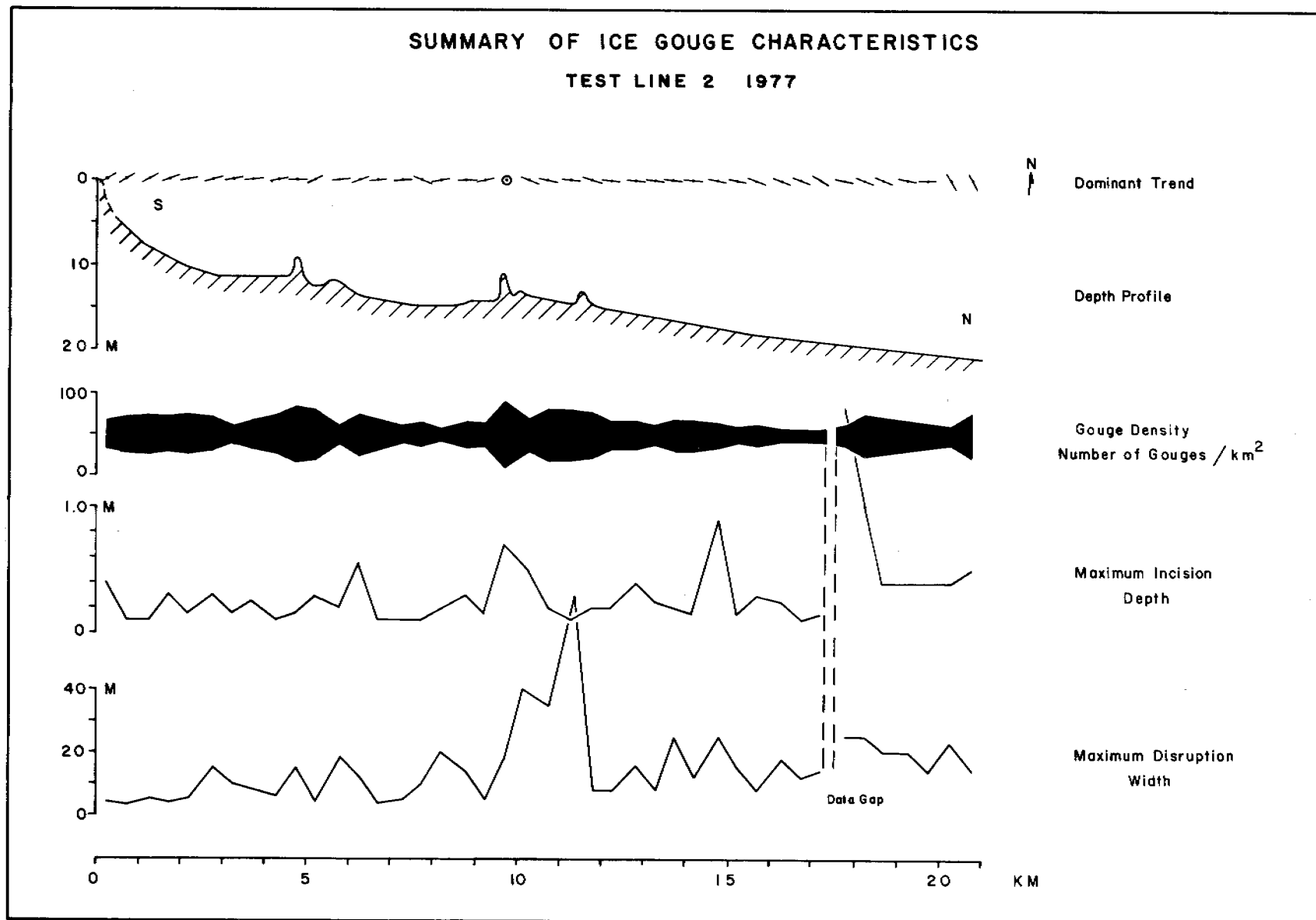


Figure 6. Summary of ice gouge characteristics on test line 2 determined from data taken in 1976 (A) and in 1977 (B).

TEST LINE 2

D

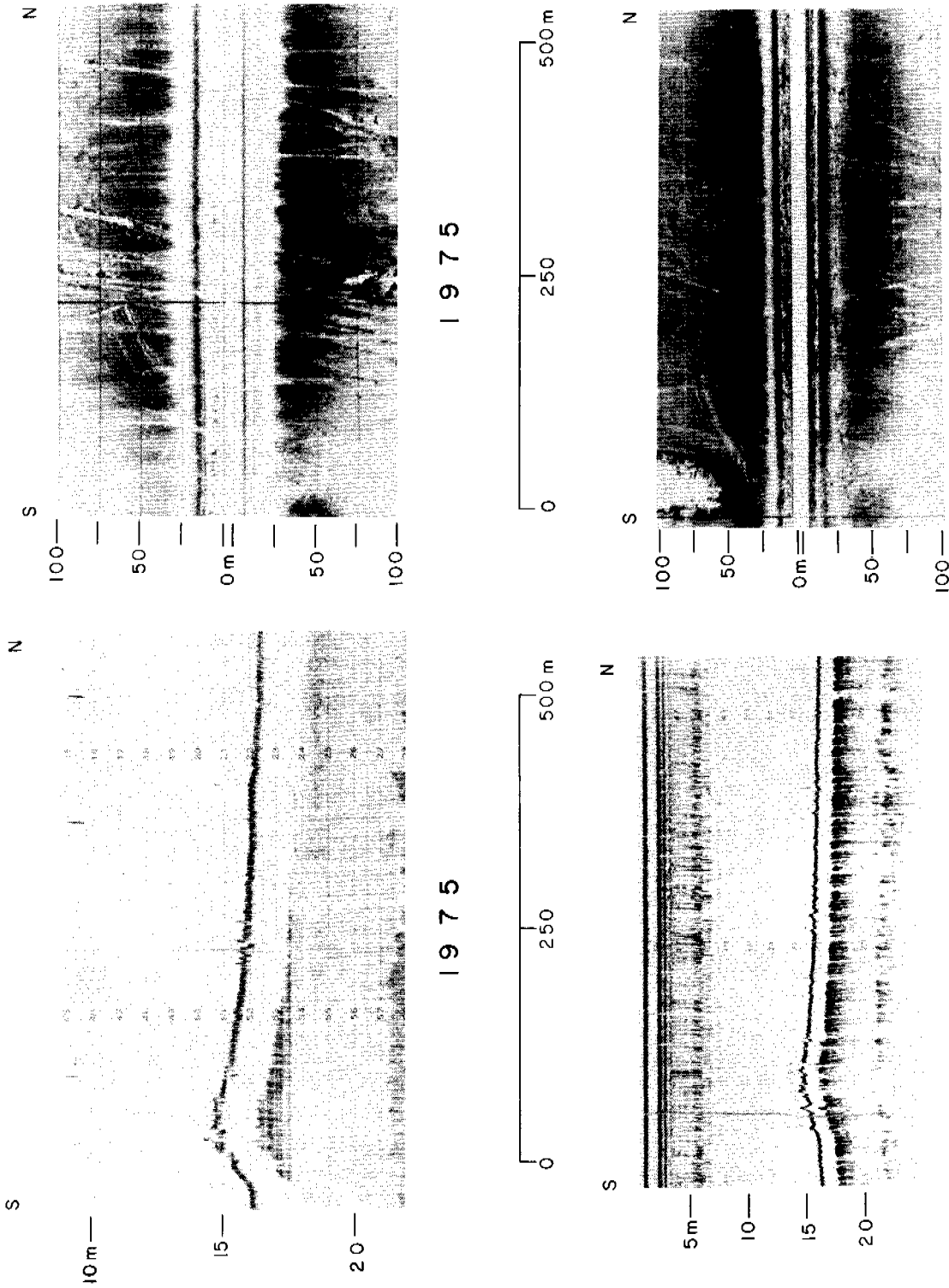
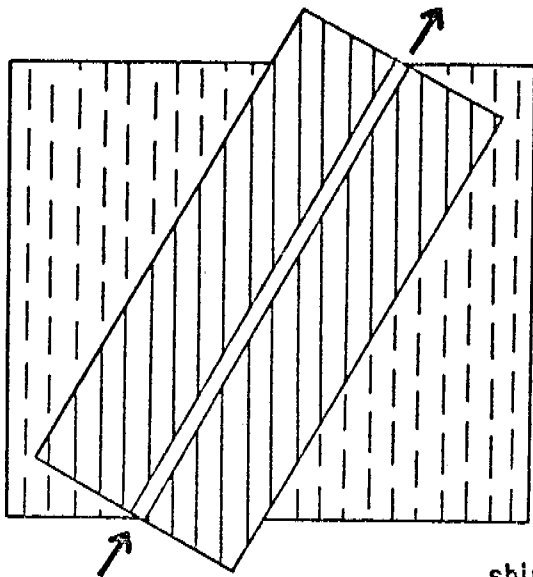
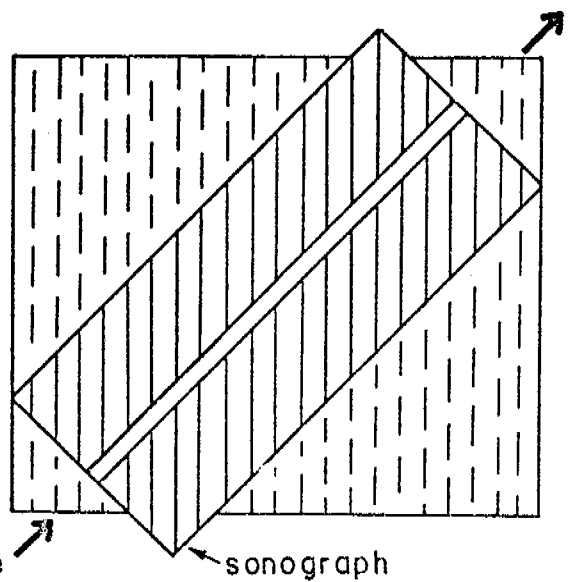


Figure 7. Comparison of 1975 and 1976 sonographs and fathograms at location D (Figure 1) illustrating the change in bottom morphology due to ice gouging. Note vertical scale difference between the 1975 and 1976 fathograms. Of significance is the high density of gouges on the ridge top and seaward flank, and the lack of a dominant trend of the gouging on the ridge crest.



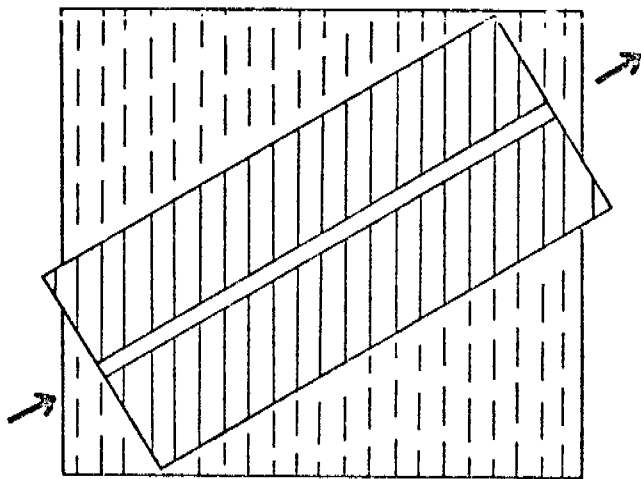
ships course

A. Dominant Trend 30°
to Ships Course

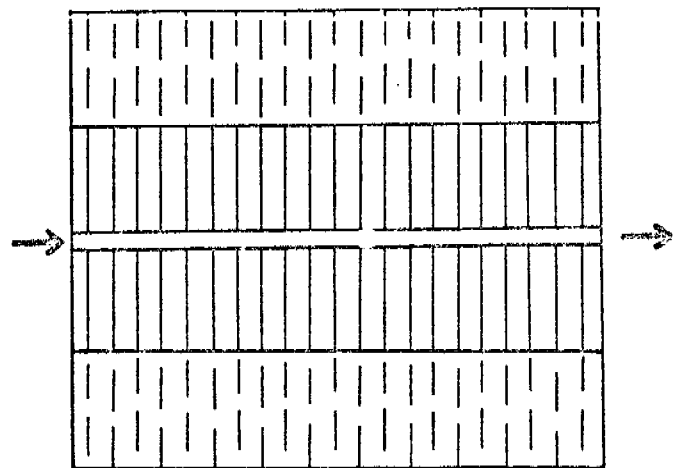


sonograph

B. Dominant Trend 45°
to Ships Course



C. Dominant Trend 60°
to Ships Course



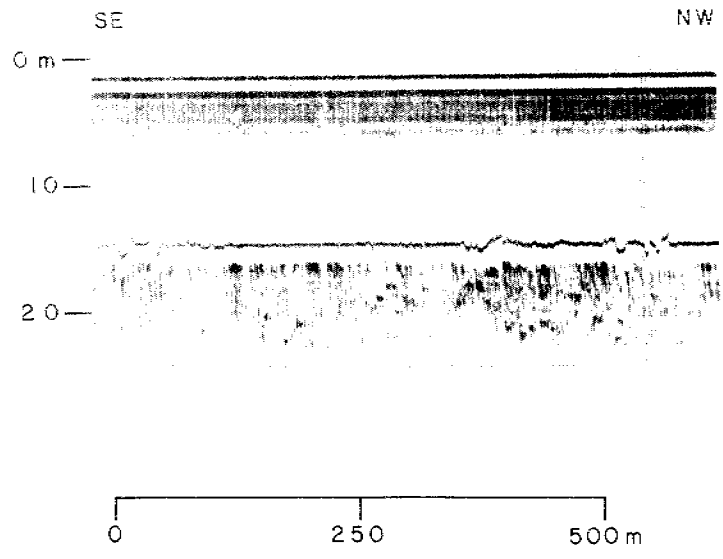
D. Dominant Trend 90°
to Ships Course

Figure 8. Variance in gouge density seen on sonograph records when ships track is not at right angle to the dominant trend. The vertical solid and dashed lines represent ice gouges. If all of the ice gouges in a line segment are assumed to be aligned with the dominant trend as in D, then gouge density may be computed per unit area.

TEST LINE I

1976

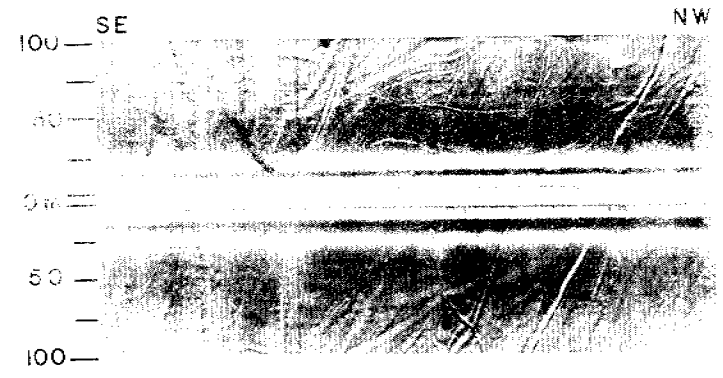
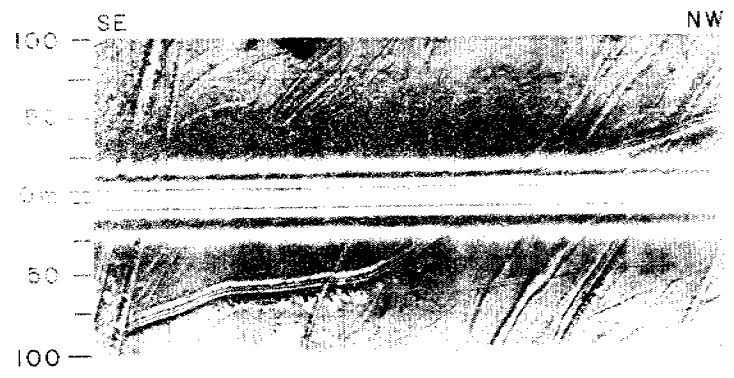
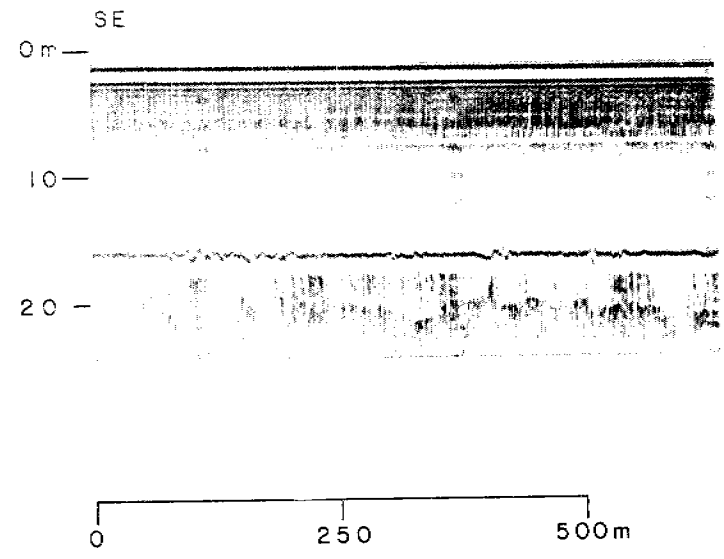
B



TEST LINE I

1976

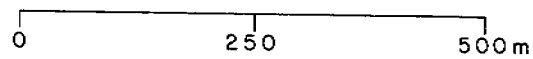
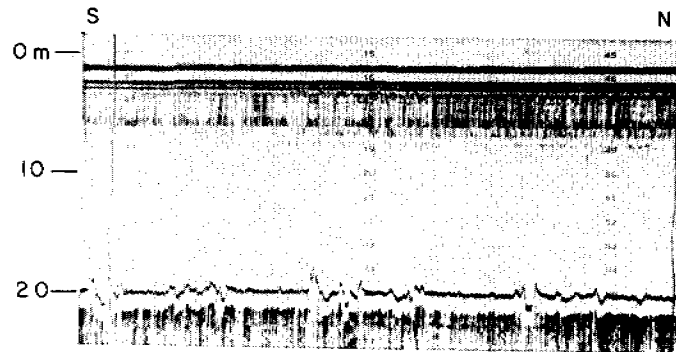
C



TEST LINE 2

1976

E



TEST LINE 2

1976

F

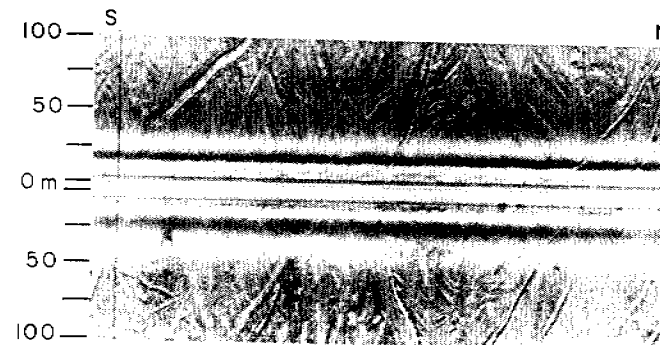
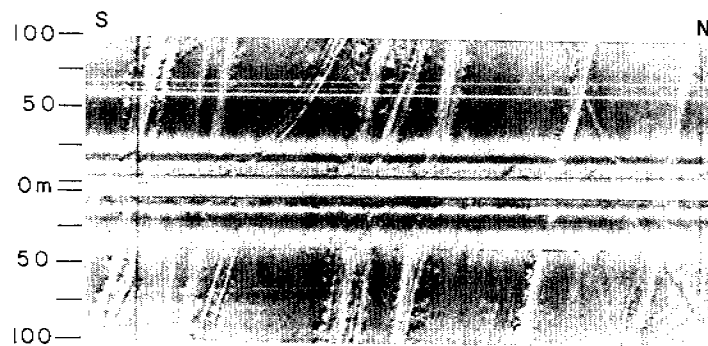
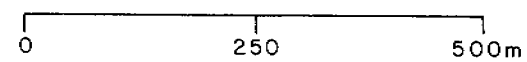
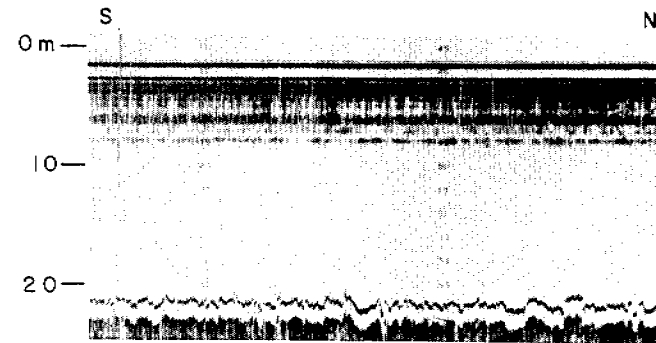
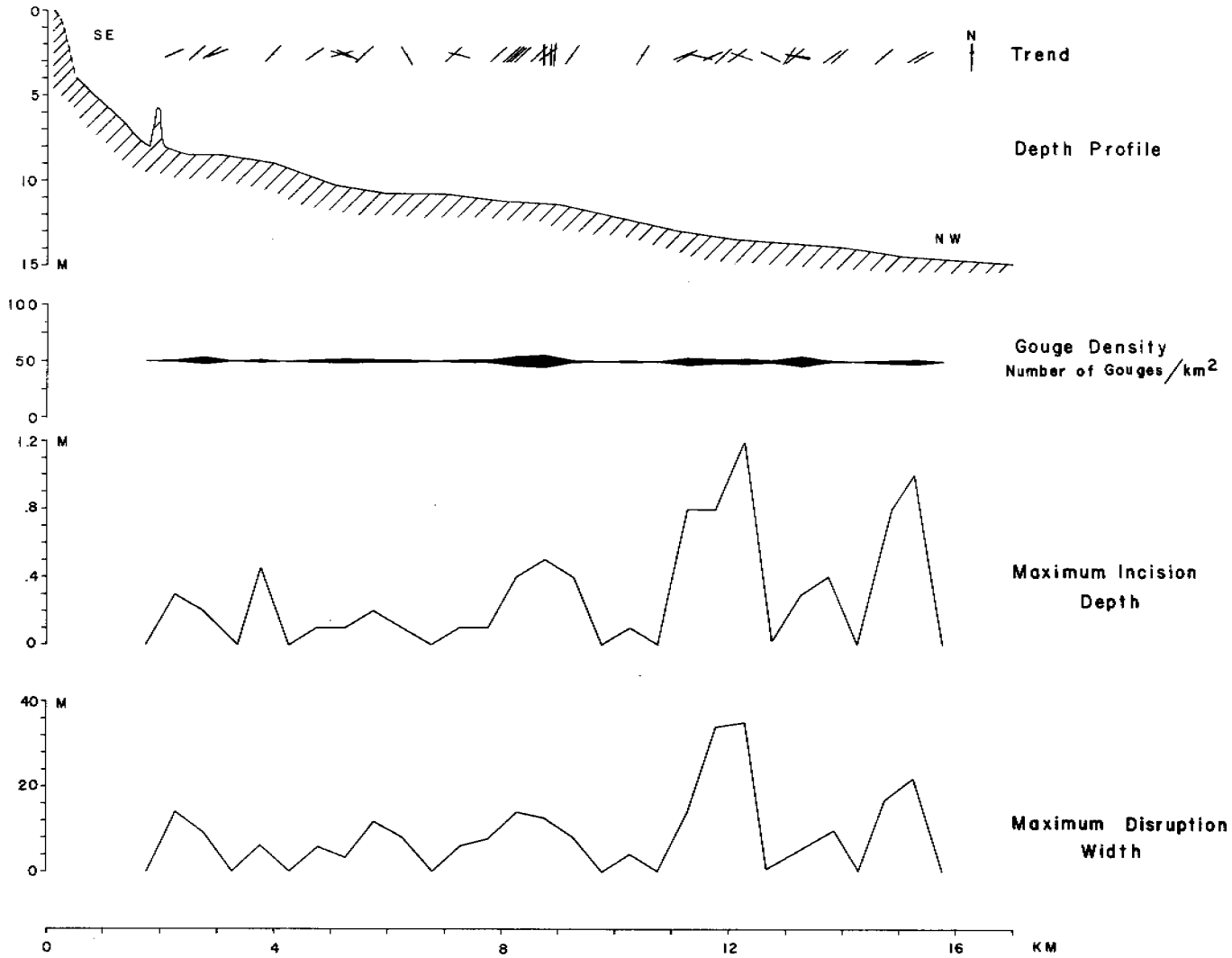
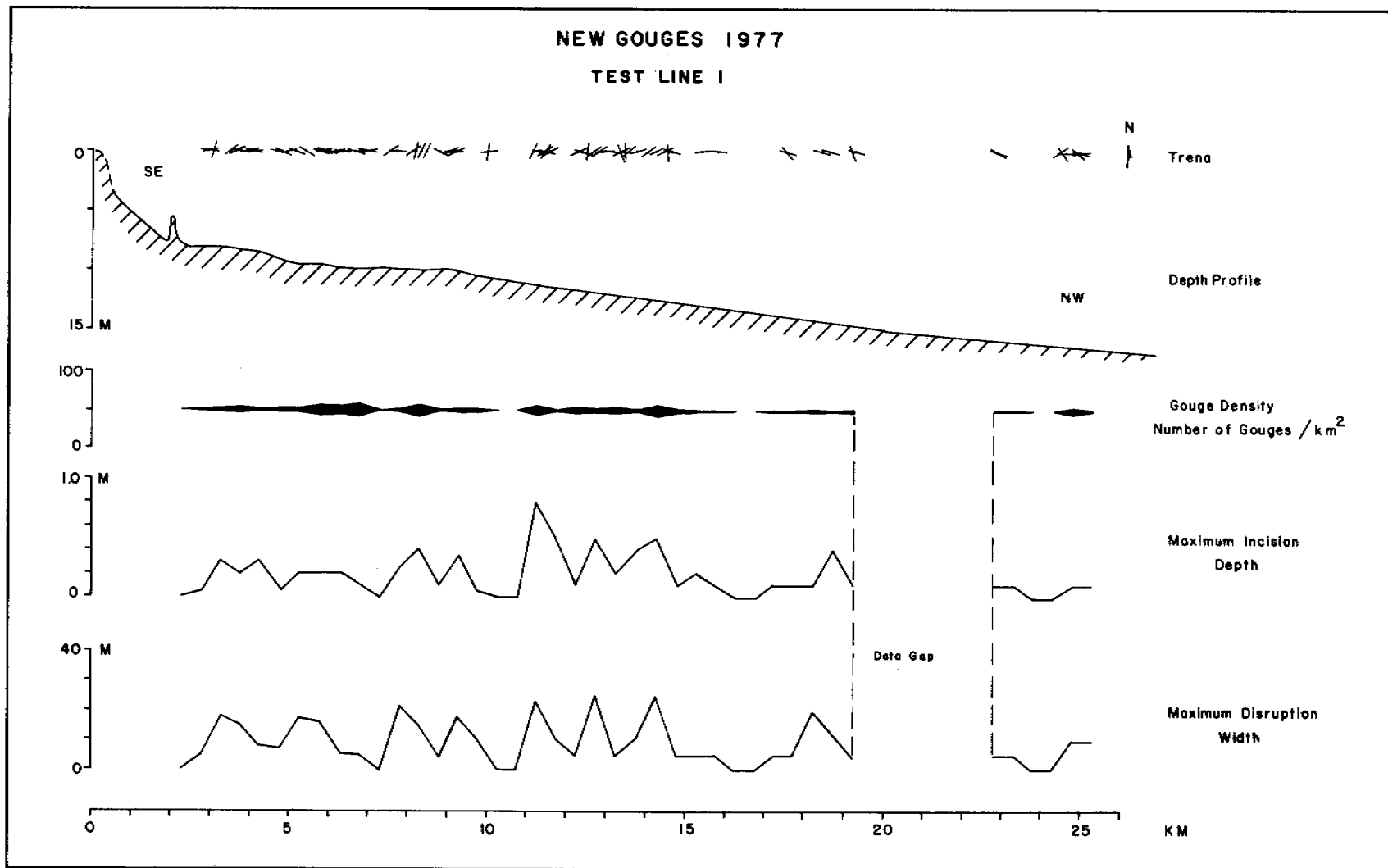


Figure 9. Fathograms and sonographs of 1976 records demonstrating the increase in density of gouging on the outer portions of test line 1 (A) and test line 2 (B). Location of trackline segments shown in figure 1.

A

NEW GOUGES - 1976
TEST LINE I



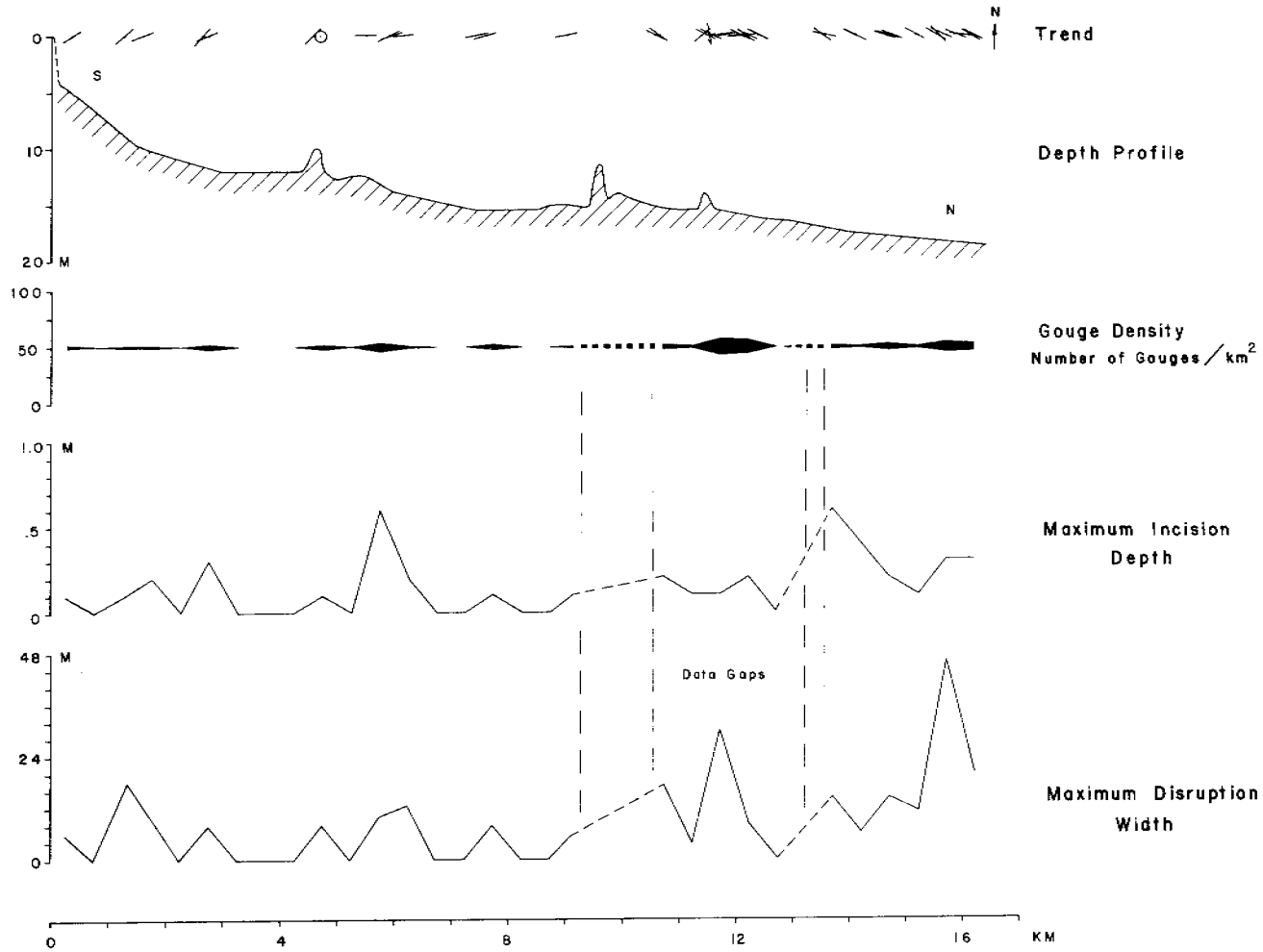
B

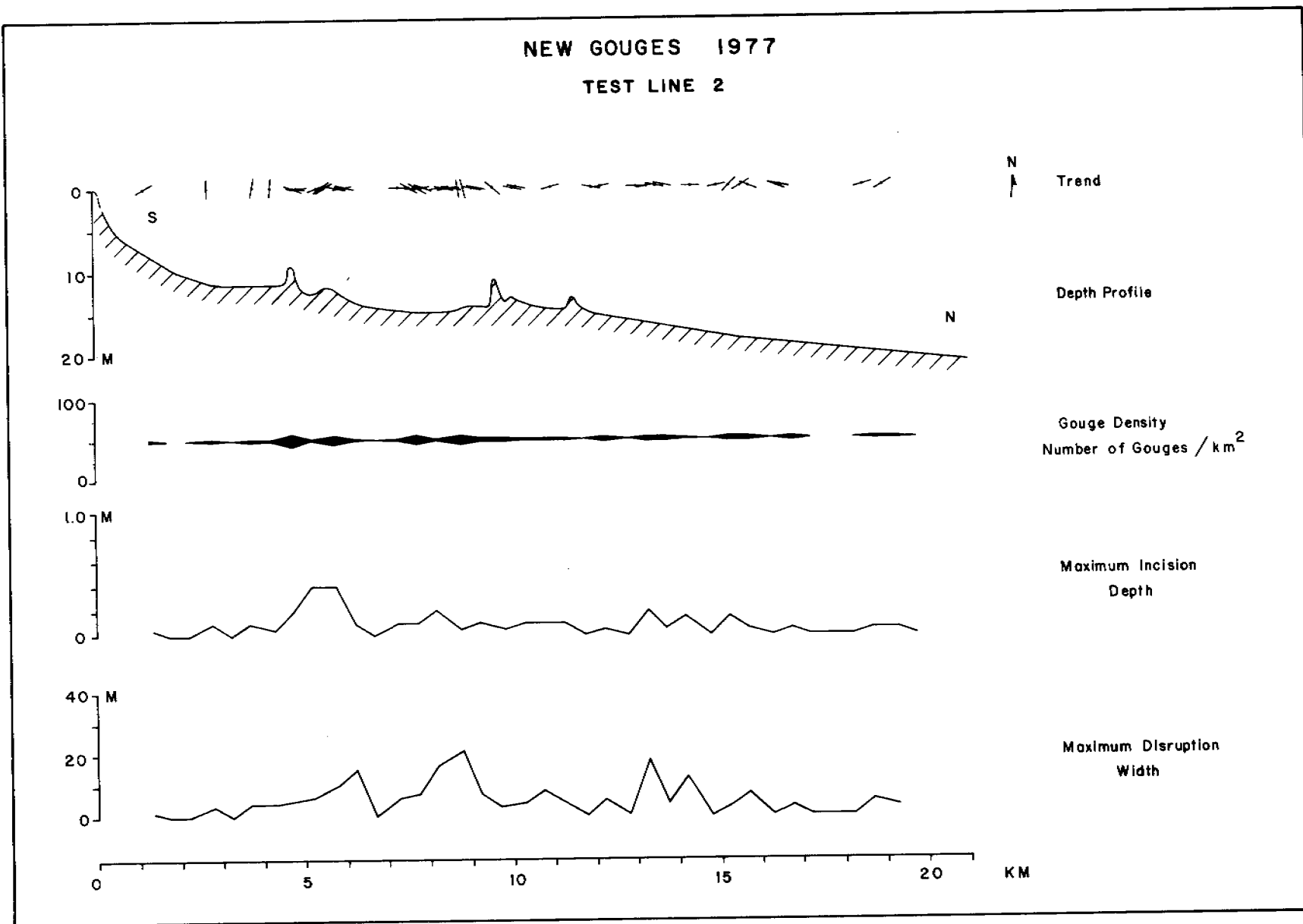
223

Figure 10. New gouge characteristics on test line 1 determined from data taken in 1976 (A) and in 1977 (B). Trend data is shown for each new gouge feature, while density, depth, and width data were determined for 500 m segments of trackline. Data gaps resulted when overlapping records were not obtained due to trackline detours around ice or equipment malfunctions.

A

NEW GOUGES - 1976
TEST LINE 2



B

225

Figure 11. New gouge characteristics on test line 2 determined from data taken in 1976 (A) and in 1977 (B).

SCATTER PLOT
 New Gouges 1976 & 1977
 Test Lines 1 & 2

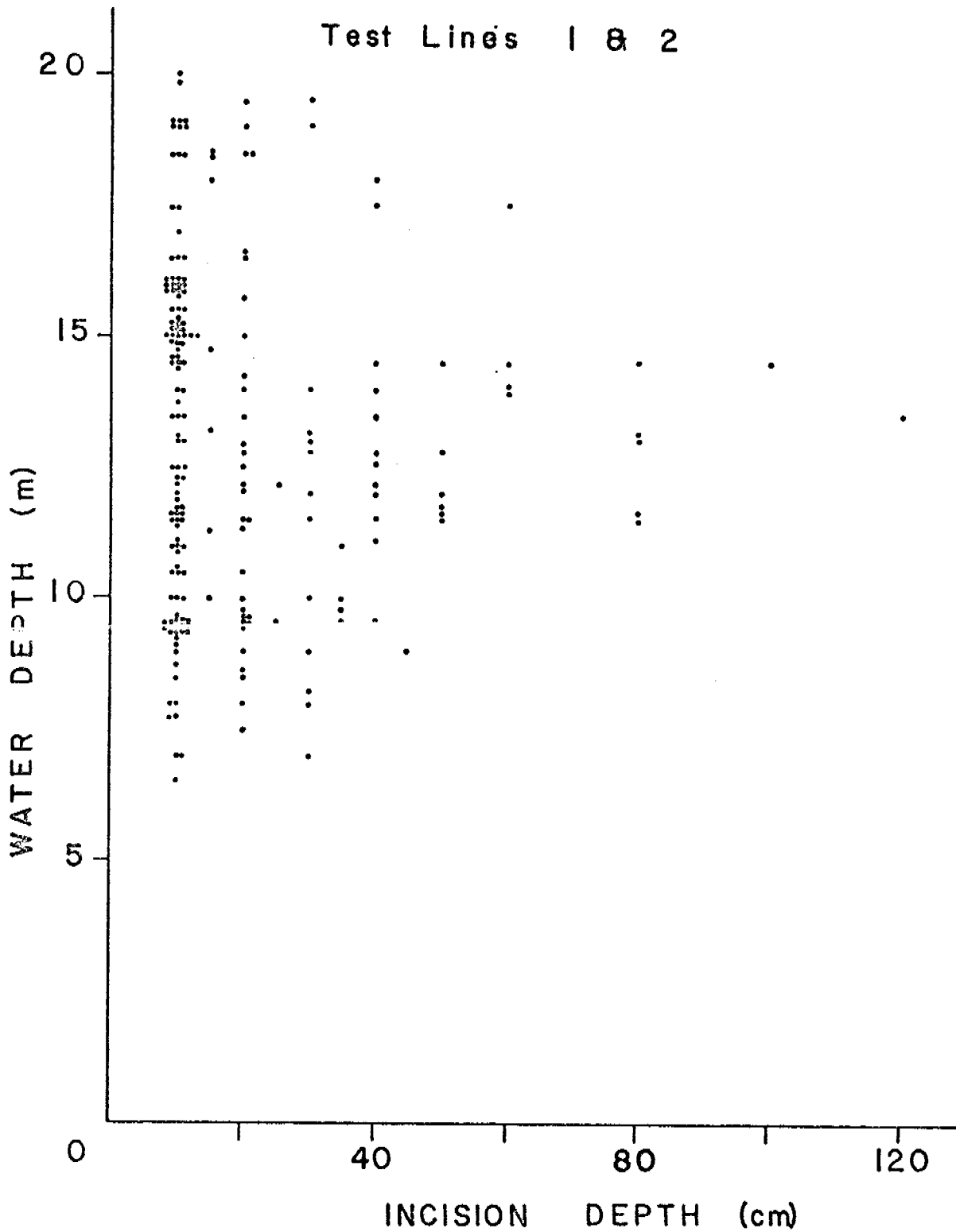


Figure 12. Scatter plot of new gouge incision depths versus water depth. The absence of deep incisions in water depths greater than 16 meters may relate to the fact that this depth interval is under-represented (see figures 10 and 11).

INCISION DEPTH- NEW GOUGES

1976-1977 Test Lines 1&2

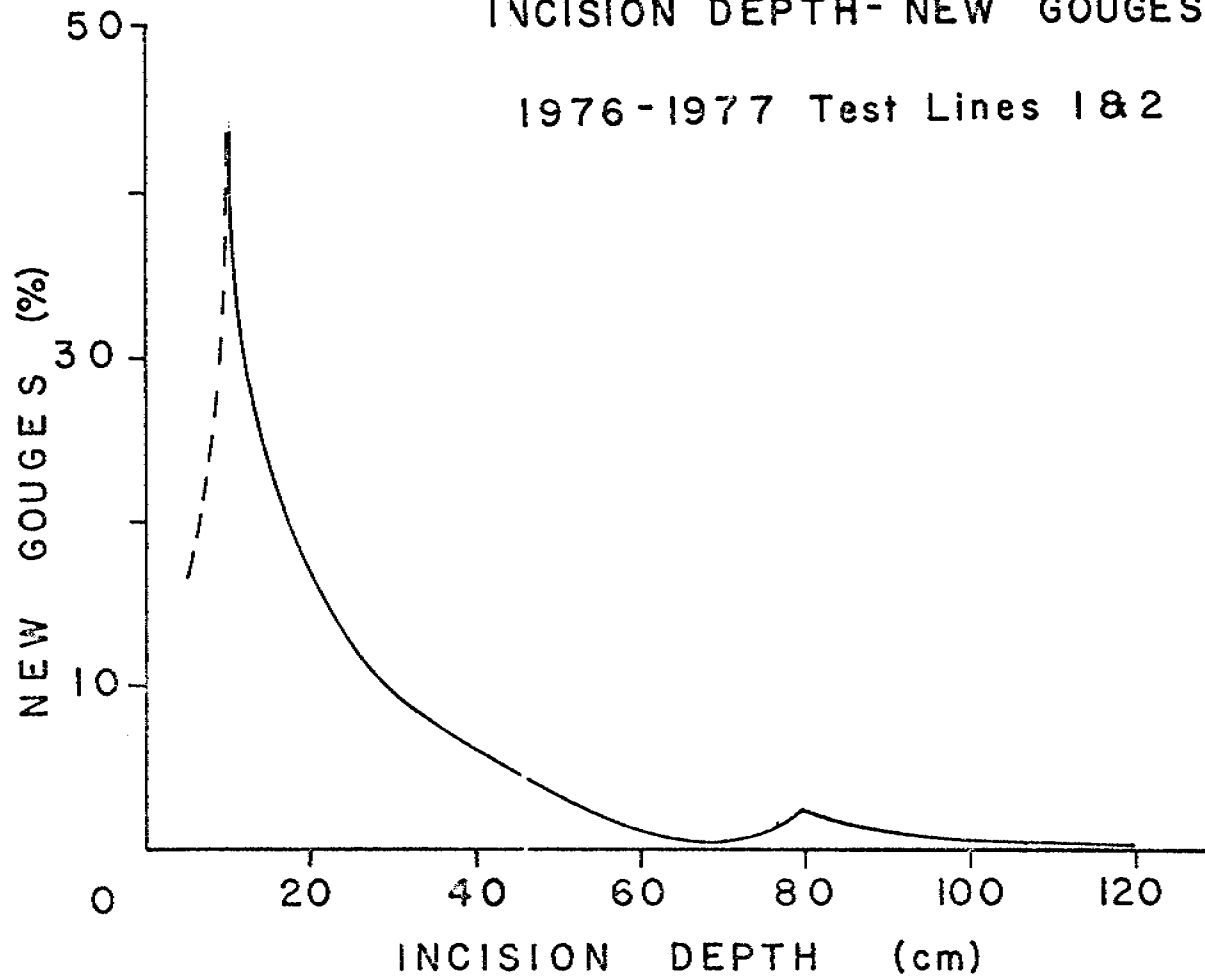


Figure 13. Frequency distribution of new gouge incision depths. Gouges less than 10 cm deep (dashed line) are underestimated due to the resolution limitations of the sonograph and fathogram records.

"SUMMER" GOUGE 1977

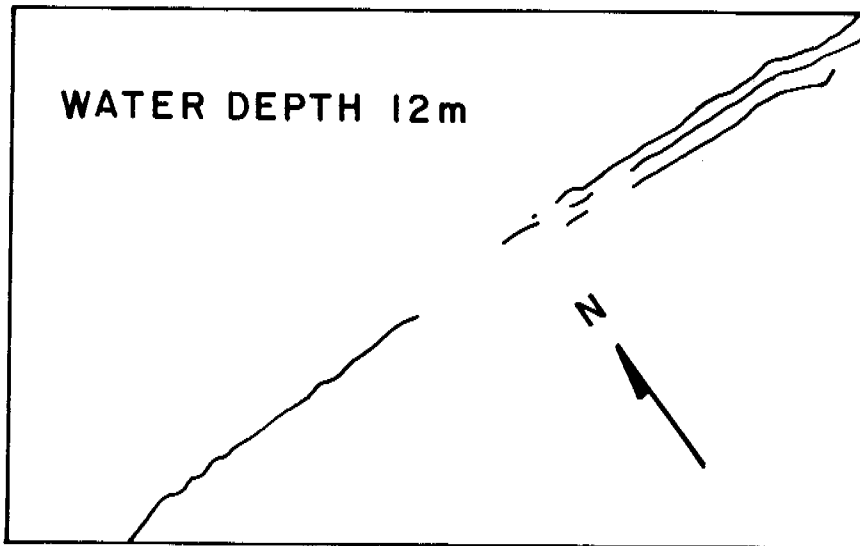
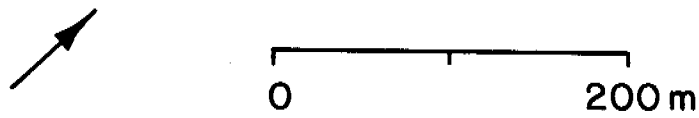
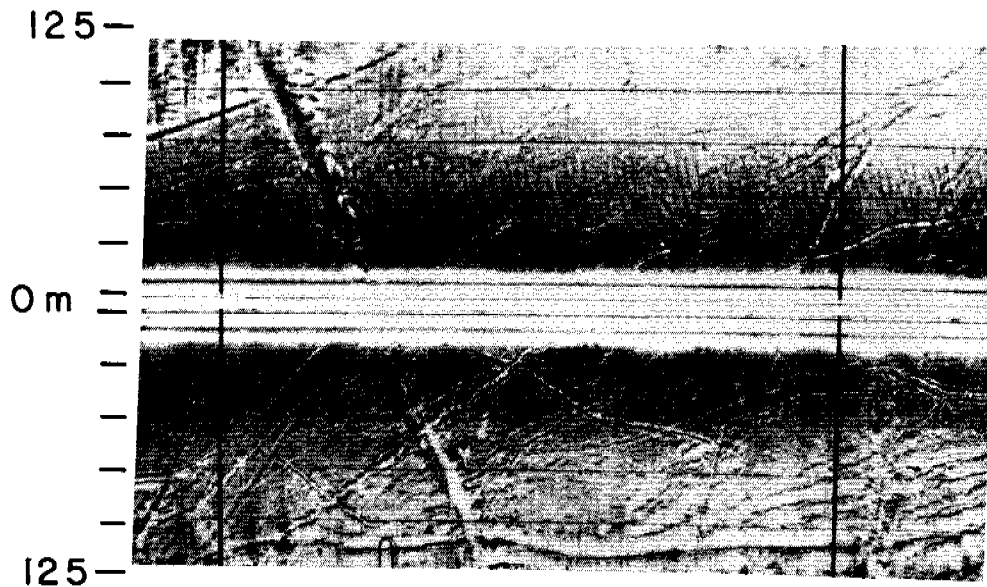


Figure 14. Sonograph and line drawing of a summer gouge event that occurred between 1 August and 3 September, 1977. Compare this gouge with the new gouges in Figure 2.

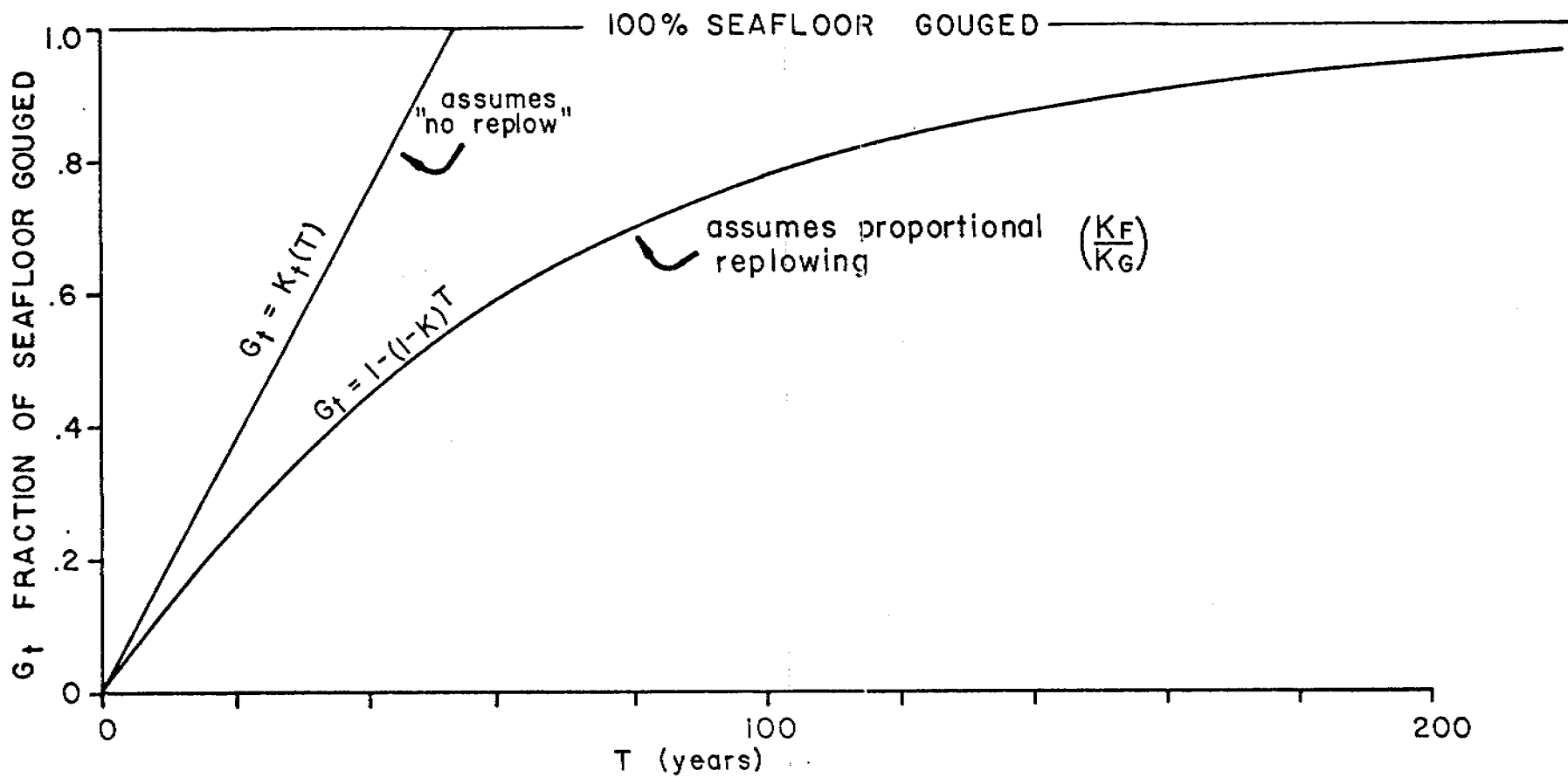


Figure 15. Fraction of the seafloor gouged after T years, assuming a) no-replot of bottom and b) proportional distribution of new gouges in year T (see text). K equal to 0.019 from test line 1 and 2.

ICE-GOUGED MICRORELIEF ON THE FLOOR OF THE EASTERN CHUKCHI SEA
ALASKA: A RECONNAISSANCE SURVEY

By: Lawrence J. Toimil

ABSTRACT

Side-scan sonar and bathymetric records, obtained from 1,800 kilometers of trackline from the eastern Chukchi Sea continental shelf, between water depths of 20 and 70 m, show that the furrow-like linear depressions produced by gouging of the sea bed by ice keels are ubiquitous. These sea bed micro-features are regionally widespread but are not uniformly distributed. Furthermore, the microrelief, texture, and lithologic structure of sea bed sediments have been significantly modified by the disruptive processes associated with ice gouge formation.

An analysis of some 10,200 individual gouges shows that the density of ice gouges increases with increasing latitude, increasing slope gradients, and decreasing water depth. Across the northern half of the shelf few trackline segments were free of ice gouges; in the southern portion numerous segments contained no ice gouges. However, ice gouges do extend at least as far south as Cape Prince of Wales. Densities of over 200 gouges per kilometer of trackline are not uncommon in water depths less than 30 m, but no values higher than 50/km were encountered in water deeper than 50 m. No ice gouges were observed in water depths exceeding 58 m. Saturation ice gouge densities (greater than 300/km) occur along the eastern side of Barrow Sea Valley and the northeast flank of Hanna Shoal.

Maximum gouge incision depths per kilometer of trackline are greatest in water 36 to 50 m deep. A maximum incision depth of 4.5 m was encountered in the 35-40 m depth interval. Individual ice gouge events wider than 100 m, most produced by multi-keeled ice fragments, were found between 31 and 45 m. The dominant linear trend (azimuth) of gouge furrows shows no preferred orientation on the Chukchi Sea shelf; only locally does bathymetric control of the trend of gouges appear.

The occurrence of current-produced bedforms within individual ice gouges suggests an interaction between slow-moving grounded or gouging ice keels and swift currents. In other cases, current-produced bedforms, interpreted as being in equilibrium with existing flow regimes, lie adjacent to ice gouges, suggesting contemporary ice gouging to water depths of at least 43 m.

The character of ice-gouged microrelief in the Chukchi Sea differs from that in the adjacent Beaufort Sea in that: a) ice gouge densities are highly variable or patchy under otherwise uniform conditions; b) preferred orientations of the trend of gouges are poorly developed, c) the process of ice gouging in many instances is associated with and modified by strong current action; and d) the maximum water depth of ice gouge occurrence appears to be shallower in the Chukchi Sea than in the Beaufort Sea. The two areas have similar maximum values of ice gouge densities, ice gouge widths, and incision depths.

INTRODUCTION

During summer 1974 side-scan sonar studies of the eastern Chukchi Sea covered approximately 250,000 km² (Fig. 1). These studies were conducted to test the hypothesis put forward by Grantz (oral commun., 1974) that hyperbolic echo traces in earlier seismic reflection profiles (Fig. 2) of the shelf resulted from the furrow-like, linear depressions produced by gouging of the sea bed by ice keels (Pelletier and Shearer, 1972; Reimnitz and others, 1973). Hyperbolic echo traces can be expected from such features when they lie at an angle to a towed hydrophone array or to a hull-mounted transducer (Hollister and others, 1974), so that sequential reflection points move along the feature and coincide with the sea bed return signal when the feature is crossed.

Nature and Scope of Study

Previous sedimentologic studies of the Chukchi Sea continental shelf have dealt mainly with the nature and textural distribution of sea bed deposits (Creager and McManus, 1967). Processes associated with the disruptive actions of ice keels moving through sea bed materials have been largely ignored (McManus and others, 1969). Such processes include re-suspension, winnowing, and mixing of sea bed sediments, the disruption of lithologic structures and benthic communities, and deformation of the sea bed (Reimnitz and Barnes, 1974). The widespread occurrence of ice-gouged micro-features has important implications for modern depositional and sediment transport mechanisms operating on Arctic shelves.

The sonographs (side-scan sonar records) and bathymetric records obtained during 1974 field operations cover 1,800 km of the shelf in water depths between 20 and 70 m. These records provide a reconnaissance data base from which the significance and general character of ice-gouged microrelief of the eastern Chukchi Sea may be directly analyzed with respect to bathymetry and geographic location. This study involved the examination of some 10,200 individual ice-gouged micro-features for orientation, incision depth, width and relative abundance over the eastern Chukchi Sea. Specific objectives of this study are:

- a) to provide a reconnaissance map showing the extent and areal distribution of ice-gouged microrelief;
- b) to determine the dominant regional trends (azimuth) of ice-gouged micro-features;
- c) to determine whether ice-gouge densities, maximum incision depths, and maximum gouge widths are related to water depth;
- d) to compare the character of ice-gouged microfeatures in the Chukchi Sea with those found in the adjacent Beaufort Sea;

Fieldwork

The records used in this study were collected by members of the Office of Marine Geology of the U.S. Geological Survey in cooperation with the U.S. Coast Guard aboard the U.S.C.G. Cutter BURTON ISLAND. Bathymetric profiles

were obtained with a 12 kHz, hull-mounted transducer coupled to a power transceiver and 47 cm dry paper recorder.

Sonographs were obtained using a dual channel side-scan sonar system consisting of a towed 105 kHz transducer assembly (tow fish) coupled to a double helix wet paper recorder-transceiver. The system transmits short bursts (0.1 millisecond) of sound across the sea bed in fan-shaped beams to both sides of the track surveyed. The return echoes, when processed and graphically recorded, produced a continuous acoustic "shadow" picture of the sea bed. The records allow the detailed study of distribution patterns in sea bed morphology not delineated by vertical echo sounding techniques. Details of the theory of operation have been described by Belderson and others (1972).

During the field survey operations the tow fish was operated 10 to 20 m above the sea bed at speeds of 4 and 7 knots. Slant range (the horizontal distance surveyed to each side of the survey track) was generally set at 125 m.

Ice conditions during the survey allowed freedom of ship movement over all but the northeast sector of the study area (Fig. 1). The location of side-scan sonar Trackline Segment (Fig. 3) was determined by satellite navigation fixes taken by the BURTON ISLAND, which are considered to be accurate within about 0.5 km.

Sea bed sediments were collected at 183 locations to assess the possible correlation between the character of ice-gouged microfeatures seen in sonographs and the texture of sea bed sediments. Of the total, 110 were collected using a modified Van Veen type grab sampler. The remaining sediment samples were collected by the "selective side-scan sonar-based sampling technique" of Newton and others (1972). Surficial sediments were collected by lowering a sampler at points along the survey tracklines where the sonographs indicated the presence of sediment facies boundaries. Such boundaries could often be inferred by the presence or absence of hydraulic bedforms, by changes in the acoustic character of the sea bed, and by changes in the character of individual ice-gouged microfeatures.

Previous Studies

Since the application of side-scan sonar to detailed morphologic studies of high latitude continental margins, numerous authors have presented sonographs to illustrate microfeatures, ascribed to ice keels gouging the sea bed, identical to the features under discussion here. The variety of terms applied to these features has been pointed out by Lewis (1977); these include "ice scours" (Pelletier and Shearer, 1973), "ice scores" (Kovacs, 1972), "plough marks" (Harris, 1974), and "furrow marks" (Harris and Jollymore, 1974). In this paper the term "ice gouge" of Reimnitz and others (1972, 1973) has been used to describe the feature created by an ice keel that has ploughed through the sea bed. The term "ice gouging" has been applied to the interaction of one or more ice keels with the sea bed.

Typically, ice gouges consist of linear or curvilinear depressions having flanking ridges of displaced sea bed materials. They occur as solitary features on an otherwise unmarked sea bed or in groups where sequential ice

gouges may be superimposed. Individual ice gouges may be several kilometers long. They are commonly 0.5 to 2.0 m below the undisturbed level of the sea bed and are tens of meters wide.

According to Reimnitz and Barnes (1974), the appearance of an ice gouge may be related to a) the underwater shape of ice; b) the nature of the materials exposed at the sea bed; c) ice motion during gouging; d) the type of force driving the ice through the sea bed; and e) the relative age of the feature. Broad, flat, and shallow ice gouges are attributed to ice gouging by ice island fragments (i.e. tabular icebergs of glacial origin). The presence of numerous parallel ice gouges is usually the result of gouging by multi-keeled pressure ridges (a line or wall of broken ice forced up and down by pressure) raking the sea bed. Ice gouges formed in cohesive sediments appear rough and irregular on sonographs and are thought to be not easily modified by waves or bottom currents or by slumping of flanking ridges. Ice gouges in soft, unconsolidated materials generally appear smooth on sonographs. Solitary, unstable pieces of ice may wobble or change direction sharply during gouging, producing lines of equally spaced, closed depressions on the sea bed or ice gouges with paths having acute changes in orientation (Reimnitz and others, 1972; Reimnitz and Barnes, 1974).

Repeated ice gouging of the sea bed by ice keels can rotate blocks of sediment, effectively destroy any lateral continuity of sediment beds, and homogenize sea bed materials (Barnes and Reimnitz, 1974). In addition, relatively soft sea bed deposits (30 to 200 kg/m² shear strengths) may become compressed (350 to 700 kg/m² shear strengths) when subjected to ice gouging (Lewis and others, 1977; Reimnitz and Toimil, 1977a).

An idealized ice gouge is shown in Figure 4. The cross-section has been modified after Reimnitz and others (1977b) to illustrate terms applied to ice-gouge morphology. A gouge depression, when observed, is probably narrower and shallower than its initial incision due to slumping of ridge flanks and reworking by sea bed processes. Also, the "extent of disruption" of the sea bed by ice gouging reaches beyond the original incision width of an gouge.

Alaskan Beaufort Sea Studies

Studies of the character of ice-gouged microrelief on the floor of the Alaskan Beaufort Sea between Cape Halkett and Flaxman Island (Fig. 1) have been summarized by Reimnitz and Barnes (1974), who included the complementary studies of Carsola (1954), Skinner (1971), Kovacs (1972), and Brooks (1973). The areas discussed by these authors are of particular interest because of their proximity to the study area and because they lie updrift of the Chukchi Sea. Much of the deep draft ice carried westward within the Pacific Gyre (Fig. 1) and entering the study area probably originates on, or first passes along, the southern Beaufort Sea shelf, leaving a record of its underwater character in the form of ice gouges. Reimnitz and Barnes (1974) find ice gouges to dominate small-scale shelf morphology seaward of the 8 to 10 m isobaths to water depths of at least 75 m, with ice gouges present in water depths in excess of 100 m. A general east-west trend of the orientation of ice gouge paths, parallel to the shore or local water depth contours, is well developed on the open shelf; major exceptions to this pattern are common in nearshore regions with relatively steep bottom slopes and where islands or

irregular coastline configurations affect the westward drift of ice along the shelf (Campbell, 1965). In these regions preferred orientations of ice gouges are largely lacking.

The depth of ice gouge incisions is variable over short distances along a survey track. Zones of relatively deep gouges (greater than 2.0 m) are found adjacent to zones of shallow ice gouges (less than 0.5 m) without intermediate zones. A maximum incision depth of 5.5 m (Reimnitz and Barnes, 1974) was encountered at 38 m of water depth (Reimnitz, oral commun., 1977).

In determining the density of ice gouges per kilometer of ship's track, Reimnitz and Barnes (1974) counted all identifiable gouges revealed in their sonographs for 1-km long, linear, trackline segments. They included every gouge produced by a multi-keeled ice fragment. Corrections were then applied to normalize the ice gouge count to represent numbers that would be counted along a track at right angles to the dominant gouge trend. For a given sea-floor segment more ice gouges will be observed on a survey track heading normal to the dominant ice gouge trend than one run parallel to it. Using this method, ice gouge densities of over 100 per kilometer are reported for a number of regions across the Alaskan Beaufort Sea shelf. Lowest values occur in the shelter of barrier island chains, off major river deltas, and on the shoreward side of bathymetric highs of the central shelf. Highest values occur on the seaward side of bathymetric highs having steep slope gradients and within broad (5 to 15 km wide), roughly east-west trending zones across the central shelf in water 10 to 50 m deep. Ice gouge densities appear relatively uniform over extensive areas of the shelf having similar ice and bathymetric environments.

Evidence suggesting a correlation between zones of the Alaskan Beaufort Sea shelf with high ice gouge densities, great incision depths, and a high degree of disruption of internal sedimentary structures, and sea ice zonation patterns has recently been provided by Reimnitz and others (1977c). Along the boundary between relatively immobile, undeformed fast-ice of the inner shelf and the mobile, polar pack ice, the seasonally recurring development of a zone of shear has long been recognized. Within this zone, sea ice is subjected to the highest compressional and shear stress (Kovacs and Mellor, 1974), resulting in the formation of pronounced, linear, pressure and shear ridges as well as hummock fields stabilized by rounding, generally between the 10 and 20-m isobaths. Solidly embedded ice masses may remain grounded along the central shelf through several melt seasons. Subsequent slippage along the shear boundary is interpreted as occurring at or seaward of initially grounded ridge systems; new grounded ridges thus form in a widening zone, the Stamukhi zone of Reimnitz and others (1977c), which by late winter may extend into water at least 40 m deep. Within the Stamukhi zone the effects of ice gouging are most intense. Using Landsat-1 and NOAA satellite images, together with a variety of sea bed data, Reimnitz and others (1977c) find a causal relationship between the spatial distribution of major ice ridge systems of the Stamukhi zone and that of offshore shoals downdrift of major coastal promontories. Such a relationship implies that ice gouging is not random over given water depth intervals but may be intensified within certain geographic boundaries.

Canadian Beaufort Sea Studies

The character of ice-gouged microrelief on the floor of the Canadian Beaufort Sea shelf in the Mackenzie Bay region (Fig. 1) was first documented with side-scan sonar by Shearer (1971) and Pelletier and Shearer (1972). These authors report ice gouges with incision depths up to 10 m and with fairly constant densities of 14 to 20 per kilometer of ship's track in water 10 to 50 m deep. The approach used in the Canadian studies for determining ice gouge densities differs from that used by Reimnitz and Barnes (1974) in that sets of multiple, parallel furrows are considered as one event. Furthermore, Canadian studies have not presented normalized gouge densities. Thus, the values reported are much lower than those off northern Alaska and are not directly comparable. Ice gouge densities are reported to diminish rapidly below the 50 m isobath, and no ice gouges were observed by Pelletier and Shearer (1972) below the 75 m isobath. Research into the nature of ice gouging in the Canadian Beaufort Sea has been recently stimulated by the joint industry-government assessment program of marine environmental hazards to offshore drilling. This is known as the Beaufort Sea Project operated by the Canadian Department of the Environment. Comprehensive studies by a number of investigators have been summarized by Lewis (1977), and include the observations of Shearer and Blasco (1975), who, using a submersible, found inclinations up to 26° in ice-gouged regions of the sea bed and who attribute high bottom-water turbidity in depths less than 60 m to resuspension of bottom sediments by ice action or to erosion by accelerated bottom currents constricted under an ice canopy.

Measurements based on sonographs and echograms over 1 n. m. trackline segments trending mostly perpendicular to the Canadian coast reveal ice gouge widths from a few meters to hundreds of meters, the widest being multiple gouges (Lewis, 1977), characteristic of those formed by pressure ridges. Incision depths on average are comparable to those reported off northern Alaska, ranging from 0.5 to 1.0 m.

Dominant trends (azimuth) of ice gouges are well developed in all water depths to 55 m and lie oblique to the predominant northeast-southwest trend of bathymetric contours within the Canadian study area. This is fundamentally different from the dominant east-west trend of ice gouges parallel to bathymetric contours and the coast off northern Alaska. In the Canadian study area dominant trends range from 80° and 115° T with mean values between 99° to 107° (Lewis, 1977). Beyond the 55-m isobath, mean orientation of ice gouges decreases and the scattering of values increases.

Contemporary Ice Gouging Estimates

Contemporary ice gouging is occurring in water depths between 6 and 30 m on the Beaufort Sea shelf (Pelletier and Shearer, 1972; Kovacs, 1972; Reimnitz and Barnes, 1974; Lewis, 1977). While ice gouging shoreward of the 6 m isobath is probably frequent, the resulting microrelief is likely to be shallow (0.5 m incision depths) and rapidly smoothed over by wave and current action. Side-scan sonar test lines established off northern Alaska and resurveyed between the years 1973, 1975, and 1976 show that in the depth range of 6 to 14 m about two percent of the sea bed is annually reworked to a depth of 20 cm by ice gouging (Reimnitz and others, 1976c; Barnes and others, 1977). This suggests an ice gouge recurrence interval for a given point on the sea bed of about 50 years. Off northern Canada, in water 15 to 20 m deep, average

ice gouge recurrence intervals are reported from 50 to 500 years (Lewis and others, 1976).

Estimates on the mean age of ice gouges observed on the outer shelf range from a few tens of years to thousands of years (Pelletier and Shearer, 1972; Kovacs, 1972; Kovacs and Mellor, 1974; Reimnitz and Barnes, 1974; Lewis and others, 1976; Hnatiuk and Brown, 1977; Reimnitz and others, 1977). Many of the ice gouges observed in water depths of 30 to 45 m are considered to be relict (over 3,000 years old), i.e. formed at a time of lower sea level (Pelletier and Shearer, 1972). Lewis (1977) places the seaward limit of contemporary ice gouging at the 50 m isobath. Reimnitz and Barnes (1974) and Løken (1974) believe that high age estimates for ice gouges observed on the outer shelf underrate the importance of contemporary ice gouging at depth. They question the validity of applying regional, average sedimentation rates to sediment infilling of individual ice gouges and limited deep-ocean data on the distribution of ice keel depths to shelf areas. Reimnitz and Barnes (1974) consider ice gouges observed at the shelf break to be older than those on the inner and central shelves, but do not rule out the possibility that some of the ice gouges, even at water depths of 100 m, are modern. Reimnitz and others (1977c) point out that the microrelief and configuration of ice gouges in water depths of 100 m within their study area are not strikingly dissimilar to those observed on the central shelf. Additionally, they point out that although bottom current pulses recorded along the shelf edge are sufficient (up to 55 cm/sec) to erode and transport muddy sand sediments of the region, ice gouges are present that have not been markedly eroded or infilled.

Chukchi Sea Studies

Until recently only Carsola (1954) and Rex (1955) had published studies dealing directly with microrelief of the Chukchi Sea continental shelf. Carsola (1954) found micro-relief features almost everywhere on the upper continental slope of the shelf in water depths between 60 and 400 m, and along the northwest flank of the Barrow sea valley. He characterized the relief as a "pit" and "mound" topography having maximum relief to 18 m, but usually only 2 to 10 m over distances of 150 to 300 m. Carsola (1954) attributed the pit and mound topography to mass movement of sea bed sediments on low gradients; after considering several alternatives, including glacial deposition, sea ice melt deposits, relict surface permafrost features, and the grounding of sea ice and icebergs. In examining the latter possibility he points out that, while grounding of sea ice is a common occurrence in all arctic coastal waters, ice of the thickness necessary to ground in 60 to 400 m of water is not known to exist under present conditions within the region. Also, at a lower stand of sea level during the Pleistocene, conditions may have permitted ice grounding to such depths, but post-glacial sedimentation or submarine reworking should have removed traces of these features.

Rex (1955) described bottom irregularities delineated in echograms collected along the inner shelf near Point Barrow; these have relief of 1 to 3 m over distances of 10 to 30 m, which he attributed directly to ice gouging, primarily by the keels of pressure ridges. Rex (1955) noted that the ice-gouged relief is best developed between the 6 and 30 m isobaths; above and below these depths it is much subdued. He recognized an almost exact

coincidence between the distribution of ice-gouged microrelief and the areal distribution of sea ice pressure ridges that annually form adjacent to the coast; this suggests that the microrelief is contemporary.

Evidence for contemporary ice gouging of sediments of the inner shelf is also provided by United States Coast Pilot #9, Seventh Edition (1964), in which changes in water depths over regions of the inner shelf due to ice gouging are noted to extend south of Icy Cape (Fig. 1).

Indirect evidence that sea bed sediments of the shelf have been influenced by ice gouging on a regional basis is provided by Barnes and Reimnitz (1974). These authors state: "in our initial studies in the eastern Chukchi Sea, we thought the chaotic lithologic character of sediments was caused by intense bioturbation, possibly including reworking by walrus tusks (Barnes, 1972). We would now interpret such disturbed structures as resulting from ice bottom interactions, which would suggest that many of the Chukchi Sea sediments are influenced by the ice-related processes we have observed in the Beaufort Sea."

Direct evidence for the widespread occurrence of ice-gouged microrelief is revealed in sonographs from 1974 field operations. A portion of these data has been presented in a report concerning the origin of a recurrent, grounded icefield near the crest of Hanna Sholl (a regional topographic high of the northeast shelf 180 km northwest of Point Barrow) and its influence on the adjacent sea bed (Toimil and Grantz, 1976). Sonographs and bathymetric profiles in a narrow lead along the southwest- to northeast-trending western margin of the grounded icefield show extensive modification of the sea bed sediments by both currents and ice gouging. Water depths along the track varied between 27 and 33 m. Distinct facies changes, defined by sand ripple fields and contrasts in acoustic reflectivity, show the influence of bottom currents and imply a general coarsening of sediments toward the grounded icefield's northern end. Here, disruption of the sea bed by ice gouging was found to be most intense. The ice gouges characteristic of those produced by multi-keeled pressure ridges were more numerous (densities of over 300 per kilometer), wider, and deeper than those observed along the southern portion of the track. Some were more than 100 m wide and were cut as deeply as 1.5 m into the sea bed. Variations in the type of ice gouging along the survey track are attributed to the character and relative age of the adjacent grounded icefield and reworking of the sea bed by bottom currents. Regions in the lee of older, more stable portions of the icefield are considered to have considerable but not total protection from ice gouging that extensively churns the sea bed elsewhere, allowing bottom processes longer periods in which to erode and infill existing gouges. Toimil and Grantz (1976) consider ice gouges observed at the shoal to be modern.

REGIONAL SETTING

The study area, here called the "eastern Chukchi shelf", includes the region between the Alaskan coast seaward of the 20 m isobath and the 169° meridian from Cape Prince of Wales to the Arctic Ocean (about 73°N parallel). Also included are the flanks of Herald Shoal (Fig 1).

The land adjacent to the study area shows the effects of a variety of

marine current patterns, rock types, and sedimentary deposits. From Point Barrow to Cape Beaufort (Fig. 1) the coast transects the Arctic Coastal Plain, a broad province of low relief composed of unconsolidated gravel, sand, and silt deposits of the Quaternary Gubik Formation. This area consists of low tundra bluffs, river estuaries, bays, barrier island chains, and coastal lagoon complexes. The entire onshore region is underlain by permafrost and is subjected to thermokarst erosion. Steep cliffs of Paleozoic and Mesozoic sedimentary rocks of the Brooks Range project into the sea between Cape Lisburne and Cape Krusenstern (Fig. 1). The Noatak and Kobuk Rivers empty into the head of Kotzebue Sound; the deltas and associated alluvial deposits of these rivers are largely responsible for the configuration of the northeastern shoreline. Between Cape Espenberg and Cape Prince of Wales, along the northwest edge of Seward Peninsula, is a low coastal plain composed of sand, silt, and gravel with beach deposits more than 300 meters thick (Creager and McManus, 1966). The peninsula itself is marked by peaks up to 1,450 m in elevation.

Detailed bathymetric data are not available for most of the study area. Existing published data are plotted on a series of 1:50,000 scale charts (numbers 9450 through 9464) compiled by the U.S. Coast and Geodetic Survey, which cover only the nearshore regions of the shelf north of Point Hope (Fig. 1). Bathymetric data from the remainder of the shelf are plotted on 1:700,000 scale, National Ocean Survey chart number 9402. Using this chart and supplementary data from bathymetric measurements made by the U.S. Coast Guard Cutter BURTON ISLAND in 1972 and 1974, together with reconnaissance bathymetric data compiled by Holmes (1975), we prepared a bathymetric map of the study area. The bathymetric contours in Figure 5 depict the major topographic features of the shelf but do not reflect the complexity of the existing bathymetry (Carsola, 1954; Dietz and others, 1964).

The shelf in general is characterized by extremely subtle topographic relief. Regional gradients typically range from 3 m/km to unmeasurable gentle slopes, with maximum local gradients generally not exceeding 6 to 8 m/km (Creager and McManus, 1967). Average water depths are between 45 and 55 m. Among the more conspicuous bathymetric features of the shelf are Hope Sea Valley and Barrow Sea Valley (Fig. 5). Barrow Sea Valley cuts the shelf parallel to the coast and underlies the Alaskan Coastal Current. A detailed bathymetric survey conducted by Lepley (1962) reveals that immediately west of Point Barrow the valley floor is flat over distances of 8 to 20 km, and along this axis depths exceeding 57 m may continue southward to about 159°W. Hope Sea Valley cuts across the southern portion of the study area in a broad s-shaped course trending north-northwest offshore of Cape Thompson (Fig. 5). Along its axis water depths may exceed 60 m.

Herald Shoal and Hanna Shoal, together with a north-south trending extension, are the principal barriers to drifting ice on the open shelf. Herald Shoal occupies approximately 17,000 km². Maximum relief is about 32 m; rising to within at least 20 m of sea level at the crest, with slope gradients ranging from 0.5 to 4 m/km. The crestal ridge is about 25 km in length, trending generally east-west and is marked by irregular relief (Holmes, 1975). The shoal is believed to be a surface expression of a northwest-southeast stratigraphic and structural trend that extends northwest from Cape Lisburne.

Hanna Shoal extends 250 km west from the Barrow Sea Valley, which isolates it from the Alaskan coast. The shoal overlies the seaward extension of the Barrow Arch of northern Alaska (Grantz and others, 1975), a regional geologic structure that brings hard, mildly metamorphosed, early Paleozoic strata to within 1 km of the sea bed beneath parts of the Chukchi Sea. Toimil and Grantz (1977) have suggested that northeast-striking isobaths near the east flank of the shoal's crest may be the physiographic expression of a subsidiary, northeast-striking anticline of the Barrow Arch. During 1976 the U.S. Coast Guard Cutter GLACIER found a narrow shoal that rose to within 17 m of sea level near $72^{\circ}00.5'N$, $161^{\circ}55.0'W$ (Grantz, oral commun.).

Nearshore bathymetry north of Cape Lisburne is irregular due to the presence of numerous isolated shoals (Fig. 5), most common between the 20 and 30 m isobaths. Seaward of Kasegaluk Lagoon and Wainwright these appear as elongate features striking roughly northeast, paralleling the coast, for distances of 10 and 20 km.

Other well-developed spit-like shoals extend from Cape Prince of Wales and Point Hope. On these shoals grounded ice is likely to accumulate (Kovacs and Mellor, 1974). Cape Prince of Wales Shoal strikes north for approximately 150 km, effectively isolating the large embayment along the eastern flank. The shoal is 35 to 55 km wide, with slopes ranging from 1.5 m/km on the eastern flank to more than 6 m/km on the western flank. A similar spit-like shoal, defined by the 30 m isobath, extends northwest from Point Hope for 20 km. Widths range from 2 to 4 km and the steepest slope reaches gradients of 8 m/km along its southern flank.

Extending northeast from Icy Cape 12 to 16 km, Blossom Shoals consist of a series of ridges that parallel the shoreline. Between the ridges, water depth in excess of 10 m allows commercial vessels to navigate the coast within 5.5 km of the Cape.

Because the Chukchi Sea is ice-covered seven to nine months of the year, our knowledge of the oceanographic regime is limited to the relatively short period of summer (July-September). Studies indicate shelf circulation to be strongly influenced by the predominantly northward flow of water from the Bering Sea through the Bering Strait. Current measurements (Fleming and Heggarty, 1966) show that flow is generally barotropic, with speeds and directions fairly uniform from top to bottom. A pressure-induced, north-sloping sea surface probably causes the northward flow from the Bering Sea to the Arctic Ocean (Coachman and Aagaard, 1966).

Along the eastern side of Bering Strait, northward flow may reach speeds up to 200 cm/sec, and may maintain speeds during the summer between 57 and 72 cm/sec (U.S. Navy, H.O. Pub. 705, 1958; Creager, 1967). South-setting currents through the straits have been periodically reported but have not been documented in detail.

The northward-flowing waters entering the southeast Chukchi Sea spread out north of Cape Prince of Wales Shoal, flow east into the embayment headed by Kotzebue Sound along the south shore, and then flow west along the northern shore, parallel to regional isobaths. Average speeds in the central portion of the embayment range from 4-25 cm/sec (Homes, 1975). Beyond Point Hope the flow pattern splits, going northwest toward the central Chukchi Sea and

northeast along the coast in the Alaskan coastal current. Seaward of Icy Cape, flow is again split, part continuing northeast along the coast and part turning north toward the crest of Hanna Shoal (Seaby and Hunter, 1971). During August 1974 the BURTON ISLAND recorded surface currents in a lead along the southwest perimeter of a large, grounded icefield near the crest of Hanna Shoal. Eight of nine determinations revealed current speeds between 25 and 40 cm/sec, flowing in a general northwest direction (Toimil and Grantz, 1976).

Northward flow over the shelf continues to about the 200 m isobath, where it merges with westward- and northward-flowing waters of the Pacific Gyre and transpolar drift system of the Arctic Ocean.

Predominant winds in the eastern Chukchi Sea are from the northwest and may effectively slow the normal, northeast flow of waters along the coast. Occasional winds from the south or southwest increase northward flow along the coast northwest of Cape Lisburne.

Astronomical tides within the study area average about 30 cm in amplitude (Creager and McManus, 1966). Annual fluctuations in sea level of 25 to 30 cm along the coast have been reported by Beal (1968). The highest levels occur in summer (August through September), the lowest in winter (February through March).

Major fluctuations in sea level, in the form of storm surges, have been reported during the summer and fall seasons. On October 3, 1963, a storm at Point Barrow raised sea level 3 to 4 m; upon this were superimposed wind-generated waves 2 to 3 m high (Hume and Schalk, 1967; Matthews, 1970). Along the coast of Kotzebue Sound, storm surges creating cliff retreat of several meters have been observed during the summers of 1961, 1969, 1971, and 1976.

Sea bed sediments collected within the study area consist of palimpsest silts, sands, and gravels (in decreasing order of abundance). Clay particles are generally absent or are found in small amounts. The textural distribution of these deposits (Fig. 6) has been illustrated by Creager and McManus (1966) using Shepard's three end-member classification. The distribution represents a relatively thin blanket of surficial materials, which tend to thicken and mask subsurface topographic irregularities. Sedimentary thickness rarely exceeds 10 m and is more often 3 to 5 m thick (Moore, 1964). In water depths greater than 30 m bedrock is frequently exposed.

The distribution pattern seen in Figure 6 indicates that movement of sediments over the shelf is largely controlled by the predominant northward flow of coastal and offshore waters. Deposition is believed to be localized in depressions and beneath current eddies in the lee of spits and headlands (Holmes, 1975).

The main sediment source for the southern portion of the study area is the northward flow of waters through Bering Strait (Creager and McManus, 1966). During the Holocene (last 12,000 years), one-third to one-half of the sediment load of the Yukon River (96.8×10^6 tons/yr at present) has bypassed the northern Bering Sea and has been deposited in the southern Chukchi Sea (Nelson and Creager, 1977). During the past 18,000 years, sediment has been deposited in the southern Chukchi Basin at an average rate of 70 mg/cm/yr (62 cm/1000 years) (Holmes and others, 1968; McManus and others, 1969). Rates

of sediment accumulation in early Holocene were more rapid (70 mg/cm/yr) than at present (20 mg/cm/yr (Holmes, 1975)).

Secondary sources of sediments introduced into the study area are the cliffs forming the Cape Thompson-Cape Lisburne headland, which provide nearshore gravel in significant amounts to be dispersed by wave action. Other rivers along the coast usually flow into coastal lagoon complexes walled off from the shelf by barrier beaches with narrow openings. Materials introduced by ice-rafting are considered to be relatively insignificant, but the importance of this mechanism may increase in the northern portion of the study area where sediment distribution is diverse (Creager and McManus, 1967).

Radiographs of box-core samples collected on the central shelf reveal sedimentary structures indicating that the sea bed is heavily utilized and reworked by benthic fauna (Barnes, 1972) and subjected to ice gouging (Barnes and Reimnitz, 1974).

There is some evidence of crustal instability during the early middle Pleistocene along both the Siberian and Alaskan sides of the study area (Hopkins and others, 1965; Sainsbury, 1967). However, only small, localized, vertical movements have occurred during and since the Wisconsin (Hopkins, 1959; Ostense, 1963).

Reconstructions of eustatic sea level history of the northern Bering and Southern Chukchi Seas presented by Creager and McManus (1967) and Hopkins (1967) indicate that emergence of the study area would have been nearly total as early as 15,000 years ago. For the next 10,000 years, sea level rose irregularly, submerging the shelf to within a few meters of present sea level 3,000 to 4,000 years ago.

For between 7 and 9 months of the year, the entire eastern Chukchi Sea is ice covered. The inner shelf, out to about the 20m isobath, is covered by floating-fast ice that is attached to the coast and reaches a thickness of 1.3 to 2m by winter's end. Prevailing winter winds cause an overall southward migration of the polar pack ice from its August-September position northwest of Point Barrow to the northern Bering Sea through Bering Strait. By November the polar pack ice has shut down on Icy Cape and by mid-January the entire Chukchi Sea is closed by the polar pack ice. At no time is the sea a solid sheet of ice. Rather, the polar pack ice is continuously undergoing compaction and rarefaction under the influence of winds and currents.

Within the polar pack ice canopy two types of ice have sufficient draft (greater than 20m) to ground within the study area, sea ice ridges, the more abundant type and ice island fragments calved from the floating glacial ice shelves of northern Ellesmere Island and brought westward by the Beaufort Gyre. More than 400 such fragments were observed along the Alaskan Beaufort Sea coast during a reconnaissance flight in spring of 1972 (Hnatiuk and Johnston, 1972), and 27 were found by William S. Dehn in the grounded icefield at Hanna Shoal in 1972 (Kovacs and others, 1975). Ice Island T-3 which grounded on Hanna Shoal in 1960 was about 50m thick (Crary, 1954) and its keel was about 44m below sea level.

Many sea-ice ridges, which are numerous in the polar pack ice, have keels of draft exceeding 20m. Sonar measurements of such keels along 165 km of track in the Chukchi and Beaufort Seas (Weeks and others, 1971) showed that 4 percent were more than 23 m deep and that one was more than 30 m deep. A 47 m keel depth has been reported by Waldo Lyon (in Weeks and others, 1971).

Sea-ice ridges form by compression, or by shear with a component of compression throughout the polar pack ice canopy. The deformation is most intense in the Stamukhi zone (after Reimnitz and others, 1977c), a zone of highly deformed first-year ice that lies between the drifting polar pack ice and the stationary floating-fast ice that develops along both the Beaufort and Chukchi coasts in winter and spring. Ridge heights and keel depths have been found to be 10-20 percent greater in the Stamukhi zone than in the polar pack and ridges and keels are as much as 50 percent more frequent. Belts of heavily ridged ice in the Stamukhi zone may extend parallel to the coast for tens of kilometers (Klimovich, 1972; Hibler and others, 1972; Kovacs and Mellor, 1974).

METHODS

The dominant trend of ice gouges, their density, and maximum incision width ^{were} determined directly from sonographs over 1-km, linear segments of tracklines plotted in Figure 3. Corresponding maximum incision depths and water depths were measured directly from fathograms. The values obtained (Appendix I) were normalized to minimize variations due to differences in record quality, lateral distortions, and trackline orientation relative to the dominant gouge trend of a given segment. The values were then classed according to these parameters and their relative frequency plotted with respect to discrete water depth intervals. Mean ice gouge densities and dominant ice gouge trends over complete trackline segments were also plotted and displayed geographically.

Most ice gouges are linear. The overall orientation (azimuth) along an ice gouge is the gouge trend (Fig. 4). The dominant trend of ice gouges over trackline segments was determined visually and then measured with respect to the navigational heading of the trackline segment. Distortion in the sonographs caused by differences in ship speed versus paper speed was compensated for by using angular correction ellipses (Newton and others, 1973) when measuring gouge trends. Dominant gouge trends could not be determined for all trackline segments because of the high variability of gouge orientation in some regions.

To determine ice gouge densities, all identifiable ice gouges were counted following the method of Reimnitz and Barnes (1974). A correction factor was then applied to normalize the observed values to represent the number of gouges, assuming uniform distribution and trend *which would have been seen on a survey heading run normal to dominant gouge trend, using*

$$N = N_{\text{obs}} (X/X\sin\theta + Y\cos\theta)$$

Where: N = corrected number of ice gouges/(trackline segment)²
 N_{obs} = observed number of ice gouges/trackline segment
 X = length of trackline segment
 Y = 2(slant range of side-scan sonar)
 θ = the angle between the dominant gouge trend over the trackline segment and the trackline azimuth.

The number of observed ice gouges per trackline segment is based on counts made over a rectangular area (in most cases 250 m wide and 1000 m long) whose diagonal length is greater than the length of the trackline segment (Fig. 7). The values obtained are expressed in km².

The maximum incision width (Fig. 4) produced by a single ice gouge event over each trackline segment was measured, again using a correction ellipse to compensate for lateral distortion. In general, ice gouges with incision widths less than 2 m could not be resolved on sonographs. The widest ice gouge event over a particular trackline segment did not always cross the axis of the survey trackline and therefore was not always recorded on corresponding bathymetric profiles.

The maximum gouge incision depth (Fig. 4) over each trackline segment was measured directly from bathymetric profiles with a resolution of about 0.5 m. The values obtained are conservative, since only gouges directly beneath the ship could be measured and true depth could be measured only for gouges that were wide relative to the fathometer sound cone.

RESULTS

Side-scan sonar surveys of the eastern Chukchi Sea shelf, over earlier (1972) seismic reflection tracklines that showed hyperbolic echo traces, confirmed the presence of ice gouges cut into the sea bed. A positive correlation between the occurrence of hyperbolic echo traces and the presence of ice gouges was found, but an inverse relationship was not.

The areal distribution of maximum ice gouge densities over complete trackline segments is illustrated in Figure 8. This shows that within the study area ice gouges are regionally widespread but are not uniformly distributed. South of Cape Lisburne ice gouge densities are generally low, numerous trackline segments are devoid of ice gouges, and in most cases individual gouges appear subdued on sonographs. Along the western flank and more distant portions of Cape Prince of Wales Shoal, maximum ice gouge densities range between 11 km² and 16 km². Ice gouge densities exceeding these values are rare south of Cape Lisburne, but do occur along the north flank of the spit-like shoal extending from Point Hope (trackline segment 33, Fig. 3) and between the 24 and 26 m isobaths southeast of Cape Thompson

(Trackline segment 38, Fig. 3). In these regions maximum densities of 64 km^2 and 26 km^2 , respectively, are encountered.

North of Cape Lisburne, few trackline segments have no ice gouges and the character of individual gouges seen on sonographs is more severe than those south of the cape. Ice gouge densities exceeding 50 km^2 are common along the coast between the 20 and 35 m isobaths, along the north and northeast flanks of offshore topographic highs, and in regions having relatively steep bottom slopes, including the western wall of Barrow Sea Valley, Herald Shoal, and Hanna Shoal.

Over broad, flat regions of the open shelf, few trackline segments reveal densities exceeding 20 km^2 ; none are over 50 km^2 . Individual ice gouges are typically exceptionally long, solitary features.

Figure 8 summarizes ice gouge densities for complete trackline segments that cover large areas of the sea bed. Therefore, the patchiness of areal distribution of gouges seen in the original data base (Appendix I) is not represented. Zones of high gouge densities (100 km^2) are often found adjacent to zones of low densities (20 km^2) without intermediate zones. This can sometimes be related to changes in water depth (e.g. trackline segment 2). Major changes in gouge densities for adjacent zones may also occur without notable changes in water depth (trackline segments 3, 4, 13, and 52).

The variability of ice gouge densities over 1-m water depth intervals, together with corresponding mean density values, is illustrated in Figure 9. The standard deviation of densities over each interval is in general found to exceed mean values and further reflects the wide scatter in ice gouge densities over similar bathymetric settings.

Ice gouge densities, maximum incision depths, and maximum gouge widths over 1-km long segments have been summarized in the form of graphs (Figs. 10, 11, and 12), which show the relative frequency of occurrence of gouge parameters over various water depth intervals. In Figure 10 ice gouge density is shown to decrease rapidly with increasing water depth. Gouge densities of over 200 km^2 are found over about 5% of the total trackline coverage at water depths between 21 and 35 m. Ice gouge densities decrease rapidly at depths greater than 50 m. No values higher than 10 km^2 are found at depths over 56 m. No ice gouges were observed in water deeper than 58 m. Maximum gouge incision depths, as illustrated in Figure 11, are highest in the 36 to 50 m depth range. A maximum incision depth of 4.5 m was encountered in the 36-40 m depth interval (Fig. 13). On a hundred per cent of the gouges in the 21-25 m depth interval have incision depths less than 2.0 m; none of the gouges below 56 m had incision depths of more than 1 m. Maximum gouge widths per trackline kilometer compared to water depth (Fig. 12) show an increase in the occurrence of wide gouges between depths of 31 and 45 m. Gouges wider than 100 m occur within the 36-40 m depth interval. Most of the wide gouges appear to have been produced by multi-keeled ice fragments (Fig. 14).

The dominant trends (azimuth) of ice gouges taken from the data base and plotted over 1 km segments are shown in Figure 15. A wide scatter of dominant gouge trends characterizes the study area. In most cases the dominant trend of gouges lies oblique to regional bathymetric contours; only locally, where slope gradients are relatively steep, is bathymetric control of gouge trends apparent.

DISCUSSION

The distribution of ice gouges indicates that the entire eastern Chukchi Sea shelf has been subject to ice gouging and that the morphologic character and density of existing gouges is highly variable. Two types of ice gouges, each characteristic of particular bathymetric settings, are present. Ice gouges in water less than 35 m deep have narrow widths, shallow incision depths, high density, and no well-developed linear trends (Fig. 16). Gouges in water deeper than 35 m are relatively wide and deep, have low densities, and are linear over long distances (Figs 13, 14). Marked increases in ice-gouge densities are found in shallower water, increasing latitude, and increased slope gradient (Fig. 8). Highest densities occur along the northeast flanks of topographic highs and areas of relatively steep slope gradients. Lowest values occur offshore, over areas of low slope gradients, and along the south flanks of topographic highs.

The distribution of dominant gouge trends plotted over the study area reveals no regionally preferred orientation (Fig. 25). Only locally are dominant gouge trends developed parallel to bathymetric contours, in areas having steep slope gradients, and along the seaward side of elongated, northeast-southwest striking shoals of the inner shelf. Scattering of values increases with distance from the coast. This is fundamentally different from the well developed east-west trend of ice gouges parallel to the coast and the bathymetric contours observed in the Alaskan Beaufort Sea. ^P The distribution of maximum gouge incision depths is patchy. Zones of deep gouge depressions are found adjacent to shallow gouges without intermediate zones and without noted changes in water depth or slope gradient. Maximum values are associated with low slope gradients. The deepest incision depth measured, 4.5 m (Fig. 13), was found in the northernmost portion of the study area (trackline segment 63, Fig. 3). No correlation is apparent between high ice-gouge density and deep incision depths except that maximum values for both parameters are found only north of Icy Cape. Surficial seabed sediments throughout this region are thin, textural distribution is diversified and not related directly to water depth (compare Figs. 5 and 6), and rock is exposed at or near the seabed in water deeper than 30 m. These conditions probably place limits on gouge incision depths unrelated to keel draft; this could explain the wide scatter in gouge incision depth values seen in Appendix I. ^P In the Mackenzie Bay region of the Beaufort Sea Lewis and others (1976), have differentiated active and relict ice gouges according to water depth. They place the limit of active ice-gouging at the 50 m isobath. This limit is based on the premise that gouge incision depths increase with increasing water depth to some relative maximum. Beyond this, incision depths decrease to a point where the deepest ice keels within the ice canopy just brush the seabed and produce no gouges. The premise requires that gouges formed in deep water have incision depths limited only by keel draft and that rates of ice-gouging and gouge infilling be uniform over similar water depth intervals. Such uniformity is not suggested in the sonographs from the eastern Chukchi Sea Shelf.

Increases in gouge densities related to both latitude and slope gradient appear independent of water depth. Gouge incision depth increases with

increasing latitude and decreasing slope gradient. These increases cause a wide scatter in maximum gouge densities (Fig. 9) and maximum gouge incision depths (Appendix I) over similar water depth intervals and suggest pronounced regional differences in rates of both ice gouging and gouge infilling.

In a number of areas rapid infilling and reworking of recent ice gouges is seen in the presence of current-produced bedforms adjacent to or within individual ice gouges (Figs. 17 and 18). In some cases, gouges appear to have been completely filled in and only narrow linear ribbons of rippled bedforms, absent on the surrounding sea bed, mark former gouge flanks. This condition (Fig. 17) suggests an interaction between slow-moving, grounded or gouging ice and swift currents. Rippled bedforms appear most often in water depths less than 30 m in coastal regions south of Icy Cape, but also occur offshore and in deeper water. Rippled bedforms surrounding ice gouges are found near the crest of Hanna Shoal, 180 km northwest of Point Barrow, in water 33 m deep (Toimil and Grantz, 1976). Along trackline segment 24 (Fig. 3) several ice gouges cut across an extensive field of undulating megacurrent ripples in water depths between 43 and 45 m (Fig. 18). The gouges appear subdued and partially filled in.

Seen in Figure 18

The ripples have wave lengths between 3 and 5 m and amplitudes below the 0.5 m resolution of the fathometer. Ripplecrest strike is 150° - 330° T, perpendicular to the axis at the overlying Alaskan Coastal Current, and have slip faces oriented toward the northeast. Surficial sediments in the area of trackline segment 24 have been described by Barnes (1972) as 50 percent sand with grain sizes from 0.62 mm to 2.0 mm. Average surface current speeds in the area of trackline segment 24 have been reported to be from 25 cm/sec to 80 cm/sec (U.S.N.O. Oceanographic Atlas of the Polar Seas - Part II, 1968). Current ripples, consisting of medium grain sands similar to those described, form at current speeds in excess of 65 cm/sec. These conditions suggest that the ice gouges observed cutting the ripple field are recent features. Based on this evidence we believe that ice-gouging is occurring in water at least 43 m deep.

CONCLUSIONS

In previous sedimentologic studies of the Chukchi Sea the physical interaction of ice with the sea bed has been ignored. The reconnaissance data presented here shows that ice gouging plays a dominant role in the sedimentary environment of the shelf.

Existing ice gouges extend as far south as Cape Prince of Wales Shoal, but, the density and morphologic character of gouges is highly variable both locally and regionally.

Ice gouge density increases with increasing latitude, increased slope gradient, and decreasing water depth.

Deepest gouge incision depths (up to 4.5m) and widest gouge widths are found in water depths between 35 and 50m. Maximum incision depths are limited to the area north of Icy Cape.

Preferred regional orientations are lacking, and only locally does bathymetry control the trend of gouging.

The occurrence of fields of current-produced bedforms, adjacent to or within individual ice gouges suggests, a) an interaction between grounded or gouging ice keels and swift currents, b) rapid rates of gouge infilling, and c) contemporary ice-gouging to water depths of at least 43m.

Comparison of ice-gouging in the Chukchi Sea with that of the Alaskan Beaufort Sea shows a number of major differences and some similarities. The Chukchi Sea differs from the Beaufort Sea in that a) ice-gouge density is more variable under otherwise uniform conditions, b) the maximum water depth to which ice gouges are observed is much shallower (58m vs more than 100m), c) rates of gouge infilling and ice gouging are not uniform over similar water depth interval, d) regional orientations of gouge trends not well developed, e) where trends are developed they lie oblique to bathymetric contours, and f) the process of ice-gouging is often associated and modified by strong currents. The two areas are similar in maximum values of ice gouge density, incision depth, and gouge width.

REFERENCES CITED

- Barnes, P. W., 1972, Preliminary results of geologic studies in the eastern central Chukchi Sea. U. S. Coast Guard Oceanographic Report Series, No. 50, pp. 87-110.
- Barnes, P. W. and Reimnitz, E., 1974, Sedimentary Processes on Arctic Shelves off the northern coast of Alaska; in the Coast and Shelf of the Beaufort Sea, eds. J. C. Reed and J. E. Sater; Arct. Inst. North Am., Arlington, Va., p. 439-476.
- Barnes, P. W., Reimnitz, Erk, Melchior, John, Toimil, L. J., 1977, Rates of ice gouging and sediment reworking, Beaufort Sea, Alaska: abs., AAPG Bull. v. 61, p. 764.
- Beal, M. A., 1968, The seasonal variation in sea level at Barrow, Alaska, in Sater, J. E., (Coordinator), Arctic Drifting Station: Washington, D.C.; Arctic Inst. North America, p. 327-341.
- Belderson, R.H., Kenyon, N.H., Stride, A.H., and Stubbs, A.R., 1972, Sonographs of the sea floor; A picture atlas: New York, Elsevier Pub. Co., 185 p.
- Books, L.D., 1973. Ice scour on the northern continental shelf of Alaska. U.S. Coast Guard Report RDCGA-36, 9 pp.
- Campbell, W.J. 1965. "The wind-driven circulation of ice and water in a polar ocean." Journal of Geophysical Research, 70:3279-3301.
- Carsola, A.J. 1954. "Recent marine sediments from Alaskan and northwest Canadian Arctic." Bulletin of American Association of Petroleum Geologists, 38:1552-86.
- Coachman, L.K. and K. Aagaard. (1966). On the water exchange through Bering Strait. Limnol. Oceanogr. 11:44-49.
- Crary, A.P. 1954. Seismic studies on Fletcher's Ice Island, T-3. Trans., American Geophysical Union, 35(2), 293-300.
- Creager, J.S., and McManus, D.A., 1967, Geology of the floor of Bering and Chukchi Seas--American Studies, in The Bering land bridge: Hopkins, D.M., ed. Stanford Univ. Press, p. 7-31.
- Creager, J.S., and D.A. McManus. (1966). Geology of the southern Chukchi SEa. In: Environment of Cape Thompson Region, Alaska. N.J. Wilimovsky, Ed. U.S. Atomic Energy Comm. p. 755-786.
- Fleming, R.H. and D. Heggarty. (1966). Oceanography of the southeastern Chukchi Sea. In: Environments of the Cape Thompson Region, Alaska. N.J. Wilimovsky and J.N. Wolfe, Eds. U.S. Atomic Energy Comm. Oak Ridge, Tenn. p. 697-754.
- Harris I. McK., 1974, Iceberg marks on the Labrador Shelf - offshore geology of eastern Canada Geol. Surv. Can., Paper 74-30, Vol. I.

- Harris, I. McK. and Jollymore, P.G., 1974, Iceberg furrow marks on the continental shelf northeast of Belle Isle, Newfoundland; *Can. J. Earth Sci.*, v. 11, p. 43-52.
- Hibler, W.D., III, W. F. Weeks, and S.J. Mock. 1972. Statistical aspects of sea-ice ridge distributions. *Journal of Geophysical Research*, 77(30), 5954-5970.
- Hnatiuk, John and Brown, K.D., 1977, Sea bottom scouring in the Canadian Beaufort Sea, OTC 2946.
- Hollister, C.D., Flood, R.D., Johnson, D.A., Lonsdale, P., Southand, J.B. Abyssal furrows and hyperbolic echo traces on the Bahama Outer Ridge. *Geology* Vol. 2, #8, 395-400.
- Holmes, M.L. Creager, J.S. and McManus, D.A., 1968, High frequency acoustic profiles on the Chukchi continental shelf (abs.): *EOS (Am. Geophys. Union Trans.)*, v. 49, p. 207.
- Holmes, M.L., 1975. Tectonic framework and geologic evolution of the southern Chukchi Sea continental shelf. Ph.D dissertation, University of Washington.
- Hopkins, David M., 1967. Quaternary Marine Transgressions in Alaska in the Bering Land Bridge. Ed. David M. Hopkins, Stanford University Press, Stanford, Calif.
- Hume, J.D., and Schaik, M., 1957, Shore processes near Barrow, Alaska: a comparison of the normal and the catastrophic: *Arctic*, v. 20, no. 2, pp. 86-103.
- Klimovich, V.M. 1972. Characteristics of hummocks in shore ice. *Meteorology and Hydrology*, 5, USSR (Dept. Commerce Joint Publ. Res. Service JPRS Transl. 56595).
- Kovacs, A. 1972. Ice scoring marks floor of the Arctic shelf; *Oil and Gas J.*, Oct. 23, 1972, p. 92-106.
- Kovacs, A. and Mellor, M., 1974. Sea ice morphology and ice as a geologic agent in the southern Beaufort Sea; *in The Coast and Shelf of the Beaufort Sea*, eds. J.C. Reed and J.E. Sater, *Arct. Inst. North Am.*, Arlington, Va., p. 113-161.
- Kovacs, Austin, McKim, H.L., and Merry, C.J. 1975. Islands of grounded ice. *Arctic*, 28(3), 213-216.
- Lewis, C.F.M., Blasco, S.M., McLaren, P., and B.R. Pelletier: 1976, Ice scour on the Canadian Beaufort Sea continental shelf; Poster discussion, *Geol. Assoc. of Canada, Annual Meeting, May, 1976, Edmonton, Alberta, Canada.*
- Lewis, C.F.M., 1977. Bottom Scour by seaice in the southern Beaufort Sea, Draft Report #23, Beaufort Sea Project, Department of Environment, Ottawa, Ontario.
- Løken, O.H., 1974, Discussion of paper by Mr. Kovacs and Mr. Mellor, in *Symp. on Beaufort Sea Coastal and Shelf Research: Arctic Inst. North America Proc.*, p. 163-164.

- Matthews, J.B., 1970. Tides at Point Barrow: Northern Engineer, v. no. 2, p. 12-13.
- McManus, D.A., Kelley, J.C., and Creager, J.S., 1969, Continental shelf sedimentation in an Arctic environment: Geol. Soc. America Bull., v. 80, p. 1961-1984.
- Moore, D.G., 1964. Acoustic reflection reconnaissance of continental shelves: the Bering and Chukchi seas. In: Paper in Marine Geology: Shepard Commemorative Volume. R.I. Miller, Ed. New York, MacMillan. p. 319-362.
- Nelson, Hans, Creager, J.S. (1977). Displacement of Yukon-derived sediment from Bering SEa to Chukchi SEa during Holocene time; Geology v. 5, p. 141-146.
- Newton, R.S., Seibold and Werner, F. 1973, Facies distribution patterns on the Spanish Sahara continental shelf mapped with side-scan sonar; „Meteor" Forschungsergebnisse Reihe C No. 15, Seite-77, Berlin. Stuttgart.
- Ostenso, N.A., 1968, A gravity survey of the Chukchi Sea region, and its bearing on westward extension of structures in northern Alaska: Geol. Soc. America Bull., v. 79, p. 241-254.
- Pelletier, B.R. and Shearer, J.M. 1972. Sea bottom scouring in the Beaufort Sea of the Arctic Ocean. In: Marine Geology and Geophysics, Proceedings of 24th International Geological Congress, Sect. 8, pp. 251-61.
- Reimnitz, E., Barnes, P.W., Forgatsch, T.C., and Roderick, C.A., 1972. Influence of grounding ice on the Arctic shelf of Alaska; Mar. Geol., v. 13, p. 323-334.
- Reimnitz, E., Barnes, P.W. and Alpha, T.R. 1973. Bottom features and processes related to drifting ice on the arctic shelf, Alaska. U.S. Geological Survey Miscellaneous Field Studies Map, MF-532.
- Reimnitz, E. and Barnes, P.W., 1974. Sea ice as a geologic agent on the Beaufort Sea, eds. J.C. Reed and J.E. sater, Arct. Inst. North Am., Arlington, Va., p. 301-353.
- Reimnitz, E. and Toimil, L., 1977a. In: Dive Site Observations in the Beaufort Sea, Alaska 1976, 84p. Geologic Processes and Hazards of the Beaufort Sea Shelf and Coastal Regions, Quarterly Report to Natl. Oceanic and Atmospheric Adm., Environmental Assessment of the Alaskan Continental Shelf; Principal Investigator's Report, April-June 1977.
- Reimnitz, Erk, Barnes, P.W., Toimil, L.J., and Melchior, John, 1977b. Ice gouge recurrence and rates of sediment reworking, Beaufort Sea, Alaska: Geology, v. 5, p. 405-408.
- Reimnitz, E. Barnes, P. and Toimil, L., 1977c. A word of caution on the age of deep water ice gouges in the Beaufort Sea. In: Barnes, P.W., Reimnitz, E. Drake, D., 1977, Geologic Processes and Hazards of the Beaufort Sea Shelf and Coastal Regions, Quarterly Report to Natl. Oceanic and Atmospheric Adm., Environmental Assessment of the Alaskan Continental Shelf; Principal Investigator's Report, April-June 1977.

- Reimnitz, Erk, Toimil, L.J. and Barnes, P.W., 1977d, Stamukhi zone processes: Implication for developing the arctic offshore area: Offshore Technology Conference. Houston, Tex., Proceedings v. 3, p. 513-518.
- Rex, R.W., 1955. Microrelief produced by sea ice grounding in the Chukchi Sea near Barrow, Alaska; *Arctic*, v. 8, p. 177-186.
- Searby, H.W., and Hunter, M., 1971, Climate of the north slope, Alaska: Nat'l. Oceanic and Atmos. Admin. Tech. Mem. NWS Ar-4.
- Shearer, J.M., 1971. Preliminary interpretation of shallow seismic reflection profiles from the west side of Mackenzie Bay, Beaufort Sea; in Report of Activities, Part B; Geol. Surv. Can., Paper 71-1B, p. 131-138.
- Skinner, B.C. 1971. Investigation of ice island scouring of the northern continental shelf of Alaska; U.S. Coast Guard Acad. Rept. RDCGA-23, 24 p.
- Toimil, L. J. and Grantz, Arthur, 1976. Origin of a Bergfield at Hanna Shoal, Northeastern Chukchi SEa, and its Influence on the Sedimentary Environment: AIDJEX Bull. no. 34, p. 1-42.
- U.S. Coast Pilot #9.1964. Pacific and Arctic coasts. Seventh edition U.S. Dept. of Commerce. Coast and Geodetic Survey. 329p.
- Weeks, W.F., A. Kovacs, and W.D. Hibler III. 1971. Pressure ridge characteristics in the arctic coastal environment. Proc., First International Conference on Port and Ocean Engineering Under Arctic Conditions, vol. 1, Technical University of Norway, Trondheim.

ILLUSTRATIONS

- Figure 1. Location map showing regional geographic features of northwestern Alaska and limits of study area.
- Figure 2. Seismic reflection profile obtained in the eastern Chukchi Sea showing the character of hyperbolic echo traces marked by arrows.
- Figure 3. Location of side-scan sonar survey tracklines as determined by satellite navigation. Individual line segments have been categorized numerically and are keyed to the data base presented in Appendix I. The location of numerals shown corresponds to the initial position fix of each trackline segment.
- Figure 4. Physiographic drawing of typical ice gouge being cut by an ice keel. The idealized cross-section shown has been drawn to express terms applied to ice gouge morphology and also slumping of gouge flanks after ice keel has passed (modified after Reimnitz and other, 1977b).
- Figure 5. Reconnaissance bathymetric map of eastern Chukchi Sea from NOS Chart 9402, bathymetric data compiled by Holems (1975), and U.S. Geological Survey data.
- Figure 6. Textural distribution of sea bed sediments expressed in terms of three-end-member relationship of Shepard (1954). (From Creagar and McManus, 1967)
- Figure 7. For a given trackline segment (a) more ice gouges will be observed on a survey heading running normal to the dominant ice gouge trend than one running parallel to it. In normalizing ice gouge counts with respect to survey heading vs dominant trends consideration was given to the fact that over the rectangular area covered by sonographs the diagonal length is (b) greater than the trackline segment.
- Figure 8. Maximum ice gouge density values over complete trackline segments plotted according to their aeral distribution.
- Figure 9. Normalized maximum ice gouge density values (black dots) and mean ice gouge density values plotted over one meter water depth intervals.
- Figure 10. Summary of ice gouge density values plotted according to their frequency of occurrence within 5 meter water depth intervals.
- Figure 11. Summary of maximum ice gouge depth (incision depth) values plotted according to their frequency of occurrence within 5 meter water depth intervals.
- Figure 12. Summary of maximum ice gouge width values plotted according to their frequency of occurrence within 5 meter water depth intervals.
- Figure 13. A maximum gouge incision depth of 4.5 m was measured from this gouge seen in the northern portion of the study area (trackline segment 64, Fig. 3).

- Figure 14. Widest ice gouges were generally found formed by multi-keeled ice masses characteristic of pressure ridges, as demonstrated in this photo taken of a sonograph obtained in water 37m deep.
- Figure 15. Plotted aeral distribution of dominant ice gouge trends over 1 km segments of side-scan sonar tracklines (Fig.3).
- Figure 16. Sonograph obtained at 25 to 30 m water depth interval. The high density and poorly defined dominant trend of the ice gouges and their narrow, shallow character is typical for gouges observed in water depths less than 35 m.
- Figure 17. The influence of strong currents on ice gouging processes is often recorded by the association of sand ripples along the flanks and troughs of individual ice gouges.
- Figure 18. Sonograph obtained along trackline segment 24 in water depths of 43 to 45 m in which an ice gouge is seen cutting across a sand ripple field which is believed to be active under present day current regimes, suggesting contemporary ice gouging of the shelf to water depths of at least 43 m.

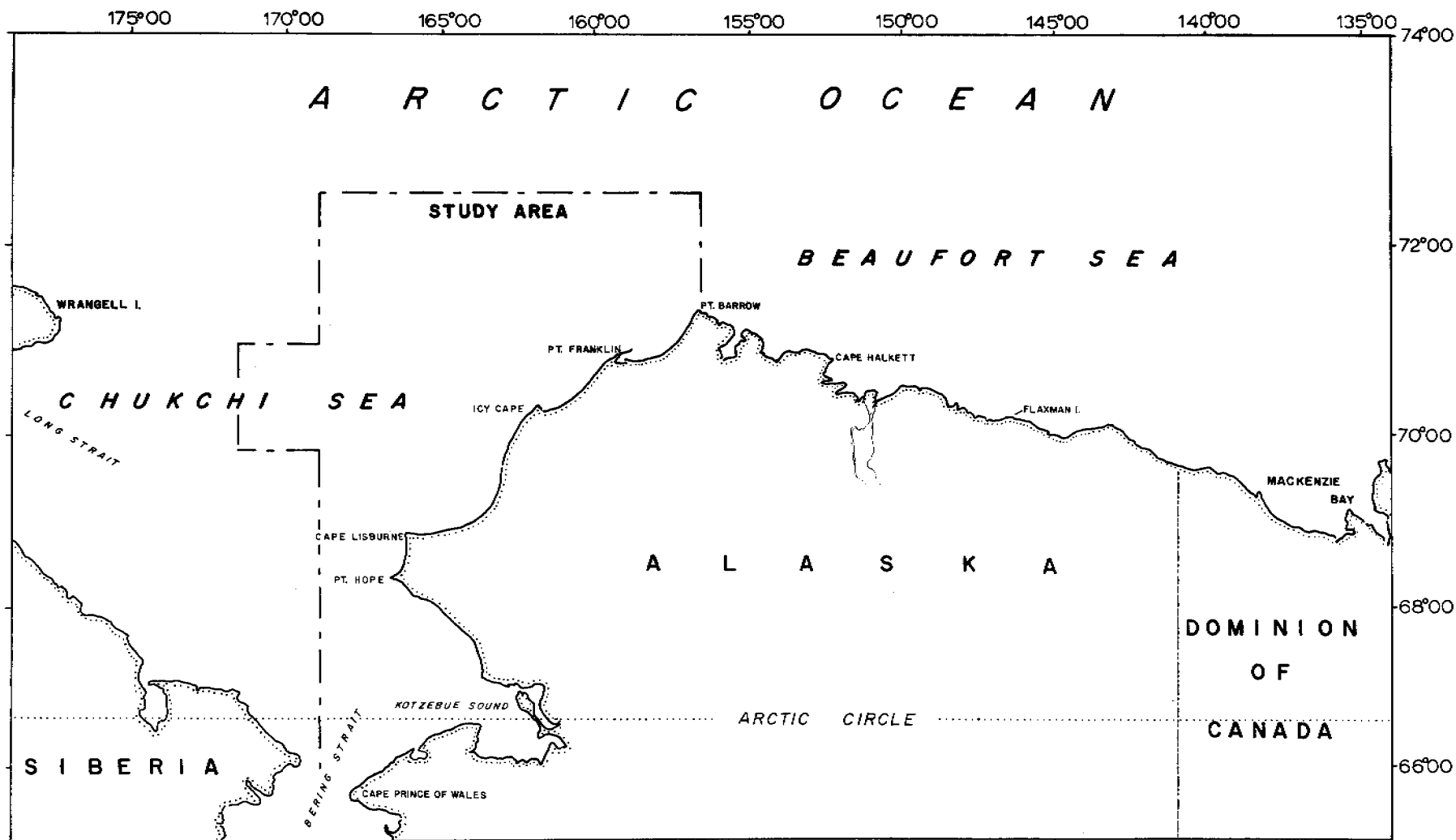


Figure 1.

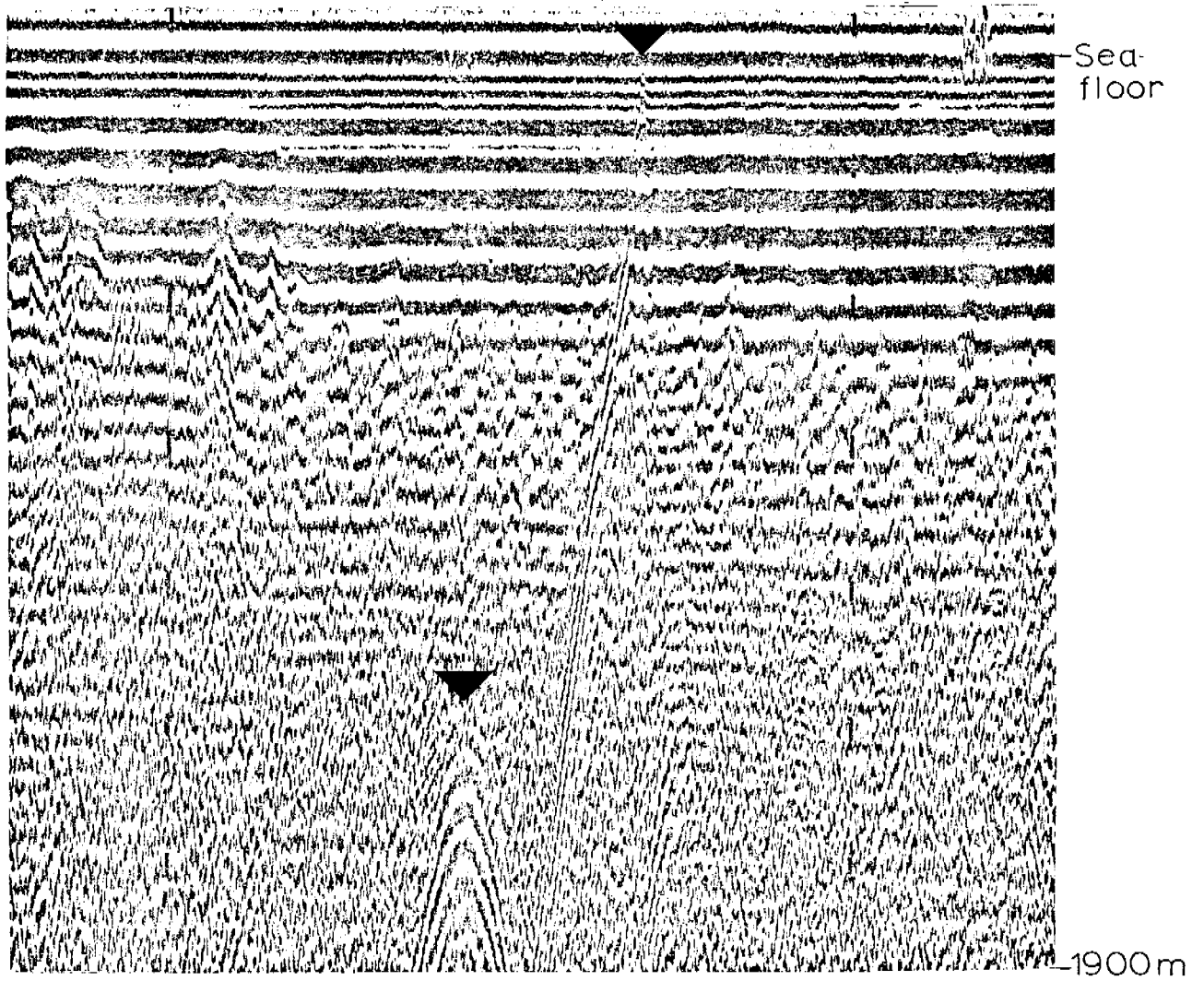


Figure 2.

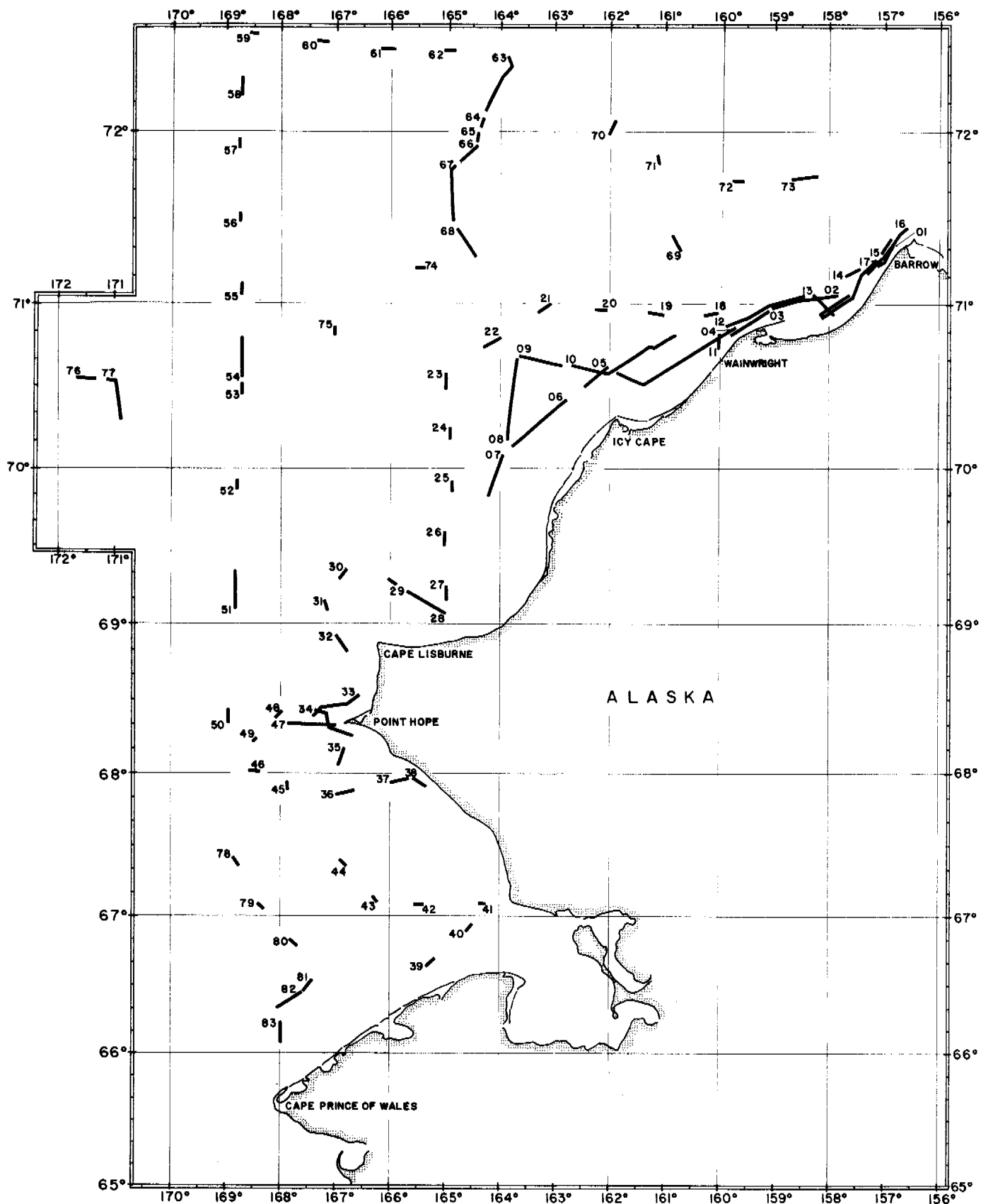


Figure 3

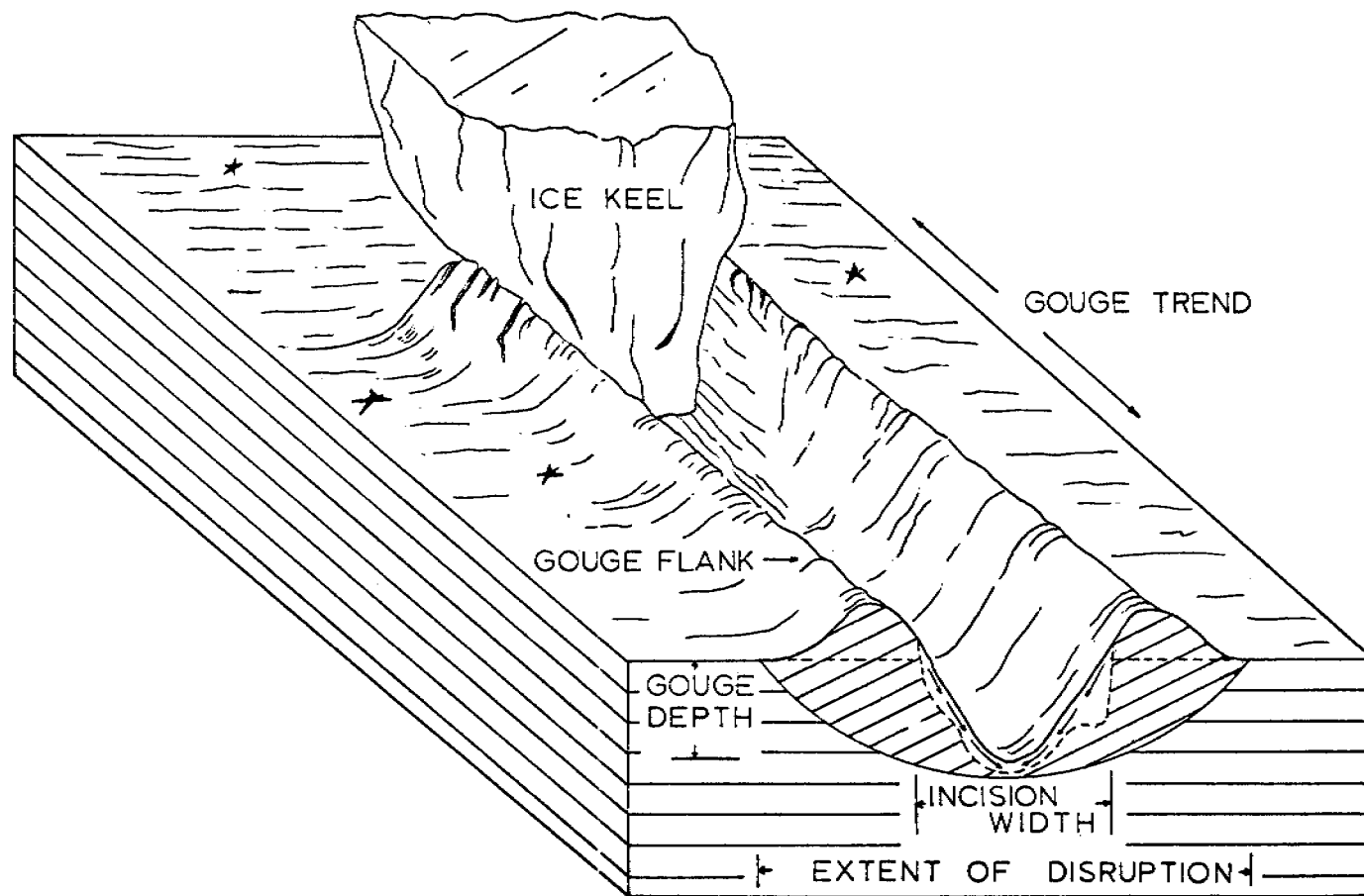


Figure 4

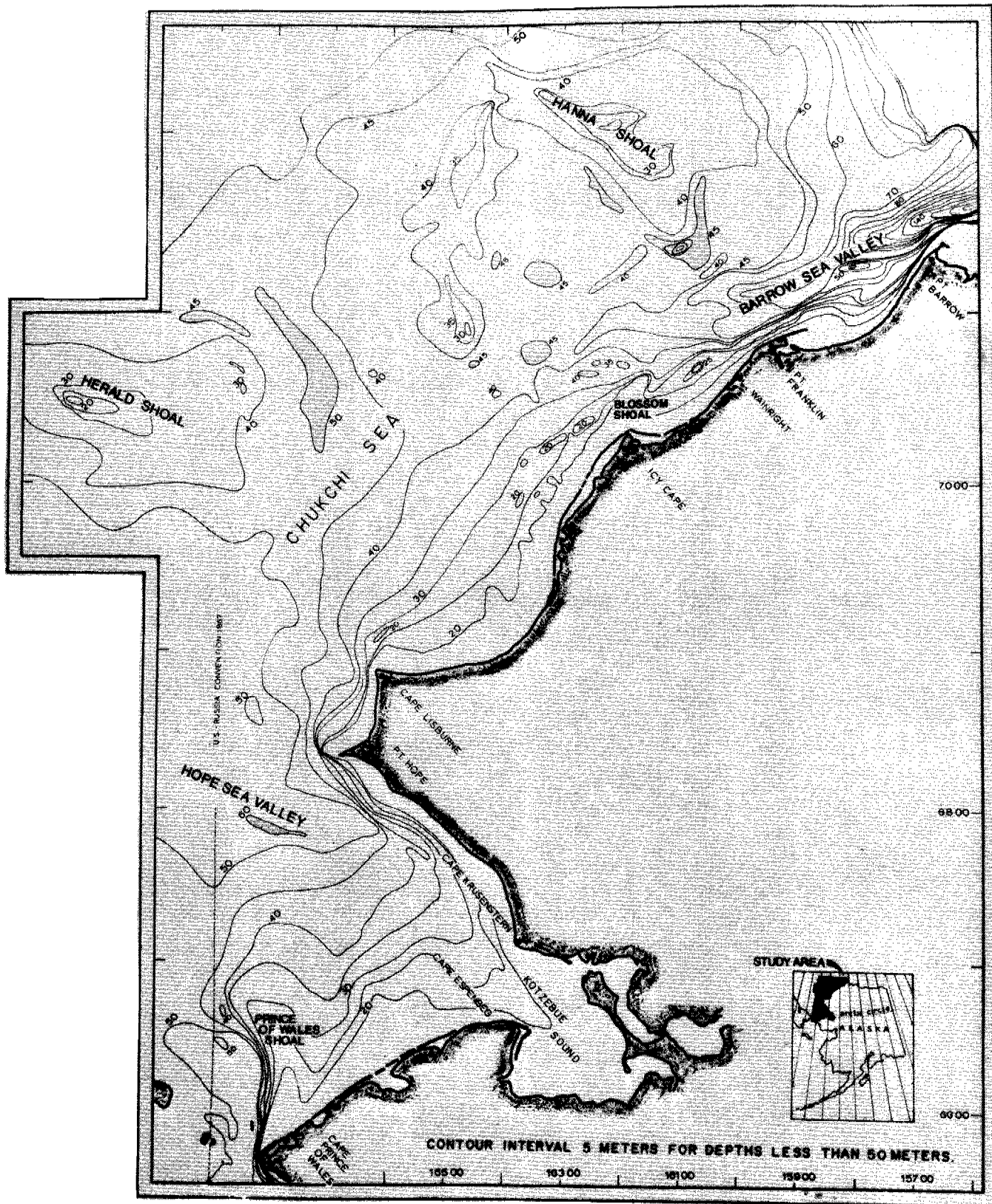


Figure 5

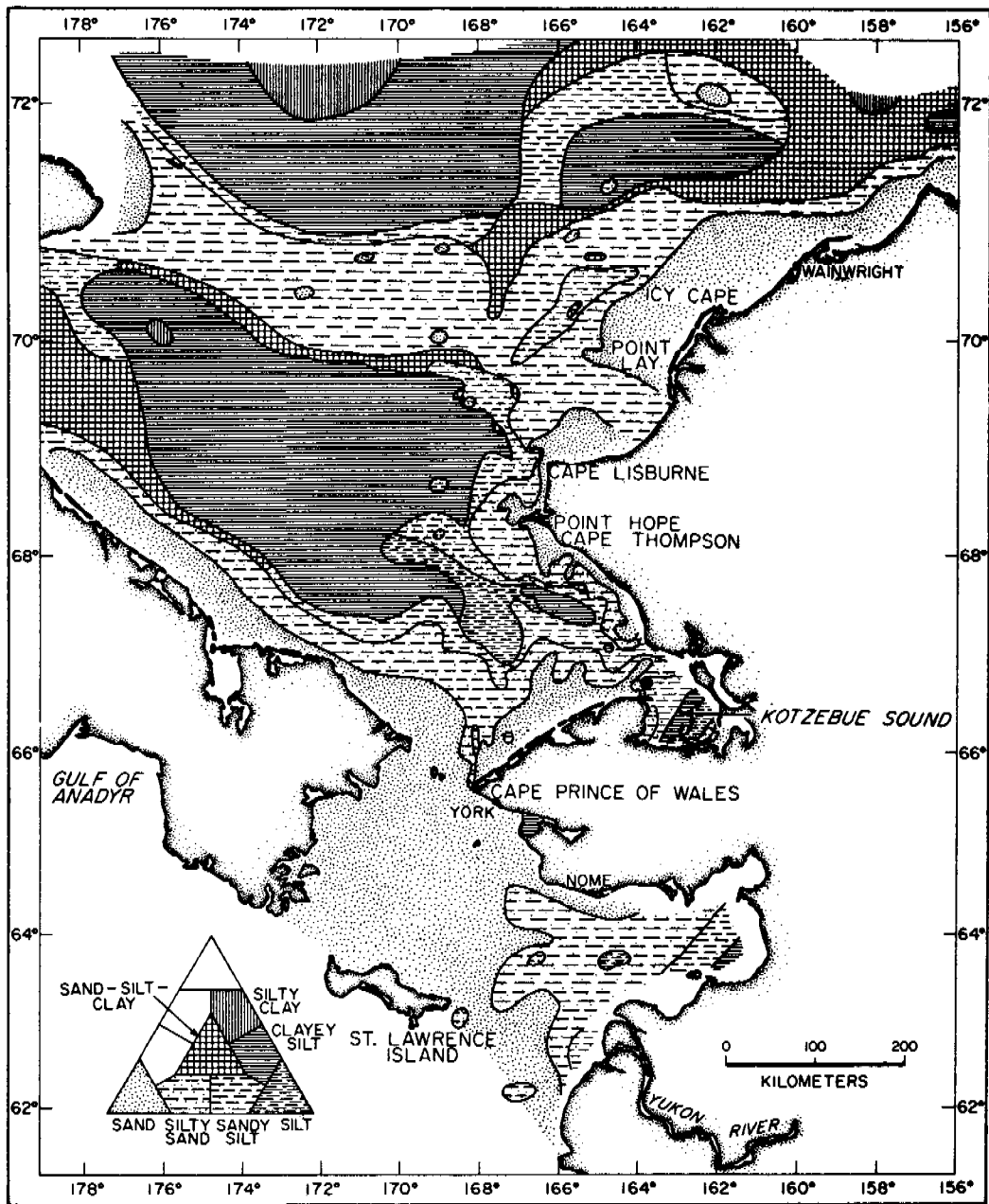
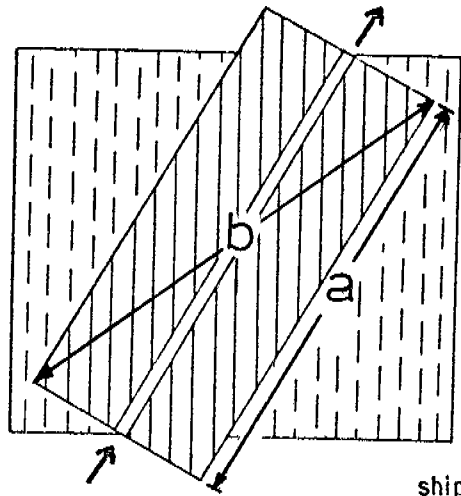
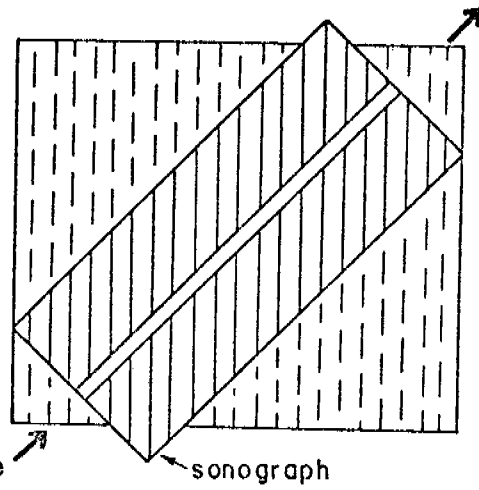


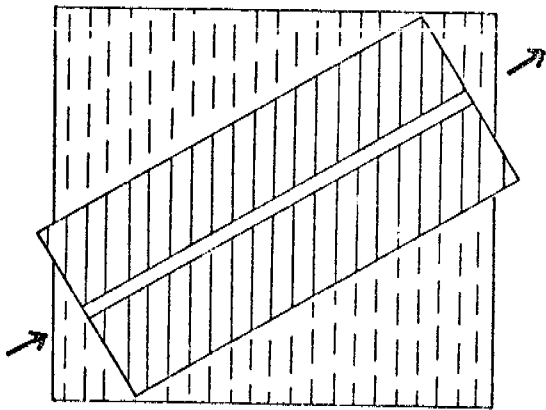
Figure 6



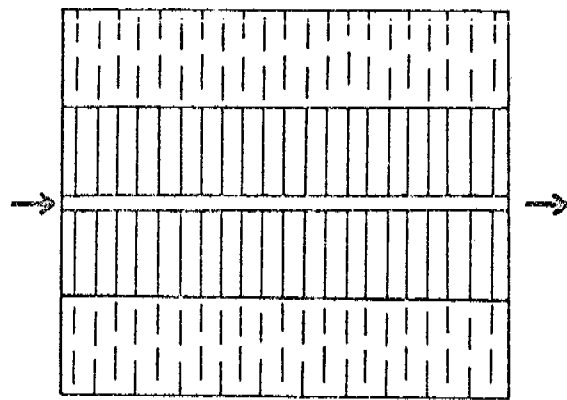
A. Dominant Trend 30°
to Ships Course



B. Dominant Trend 45°
to Ships Course



C. Dominant Trend 60°
to Ships Course



D. Dominant Trend 90°
to Ships Course

Figure 7.

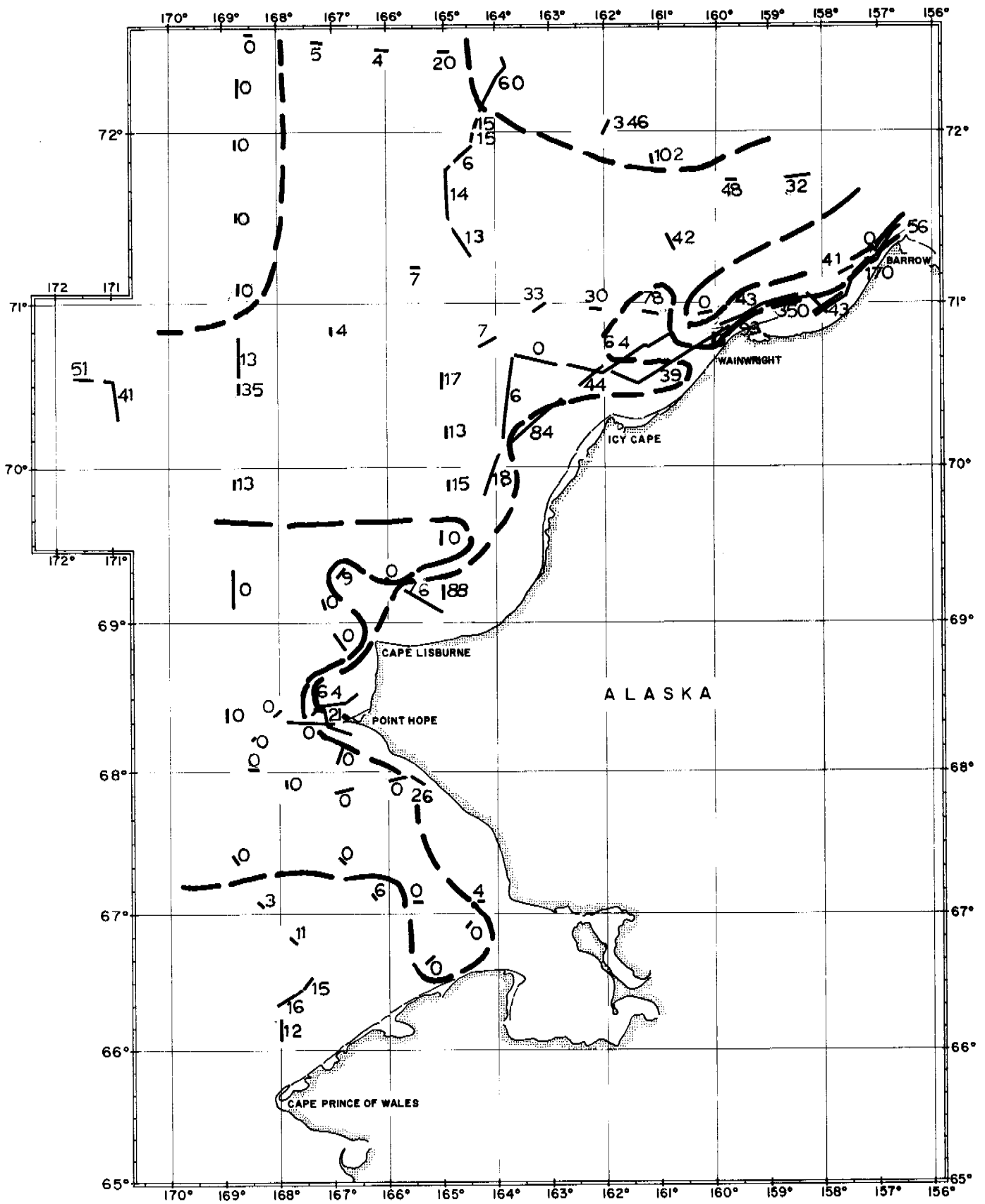


Figure 8

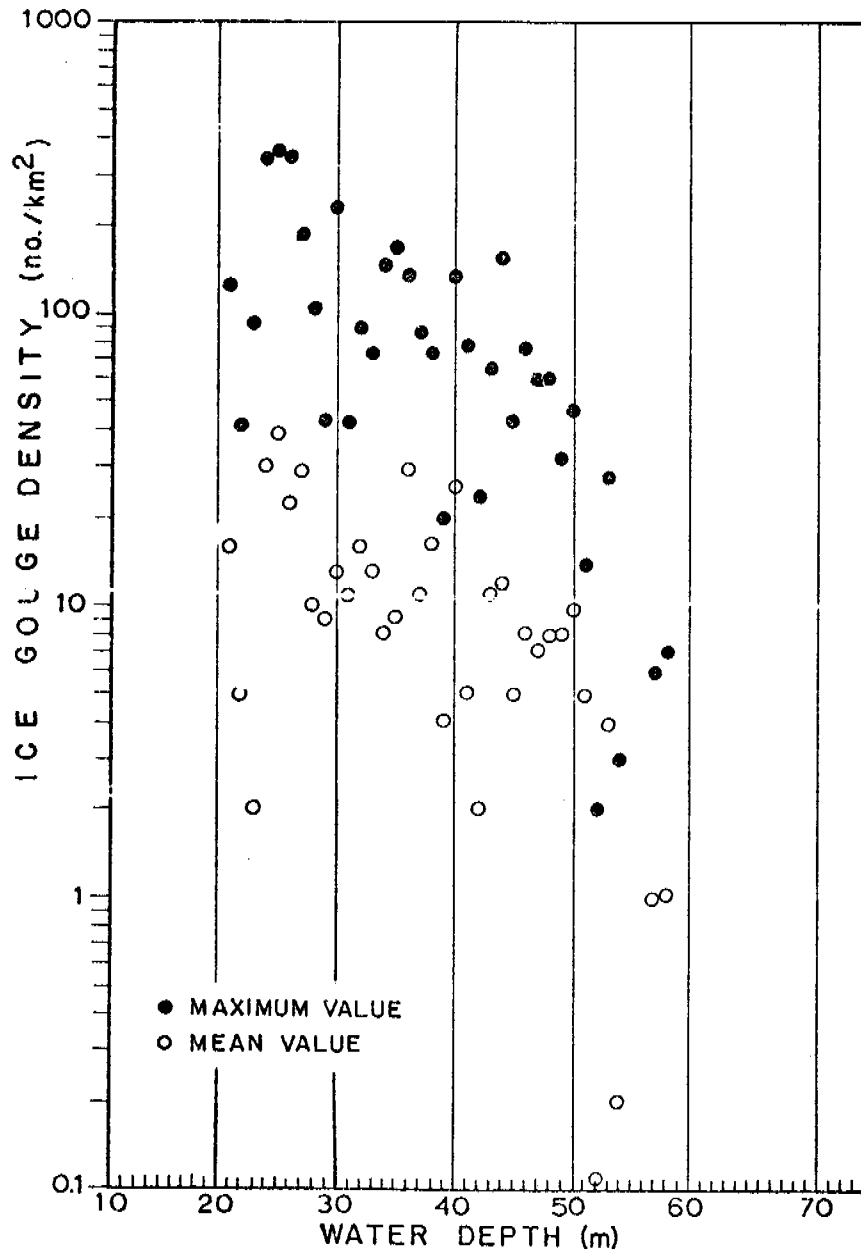


Figure 9

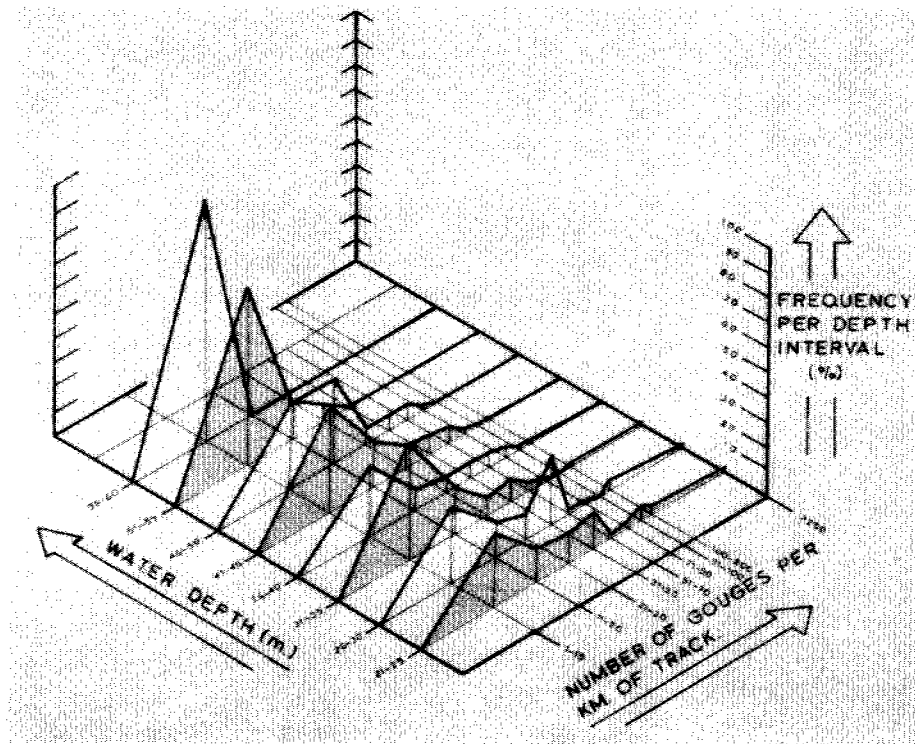


Figure 10

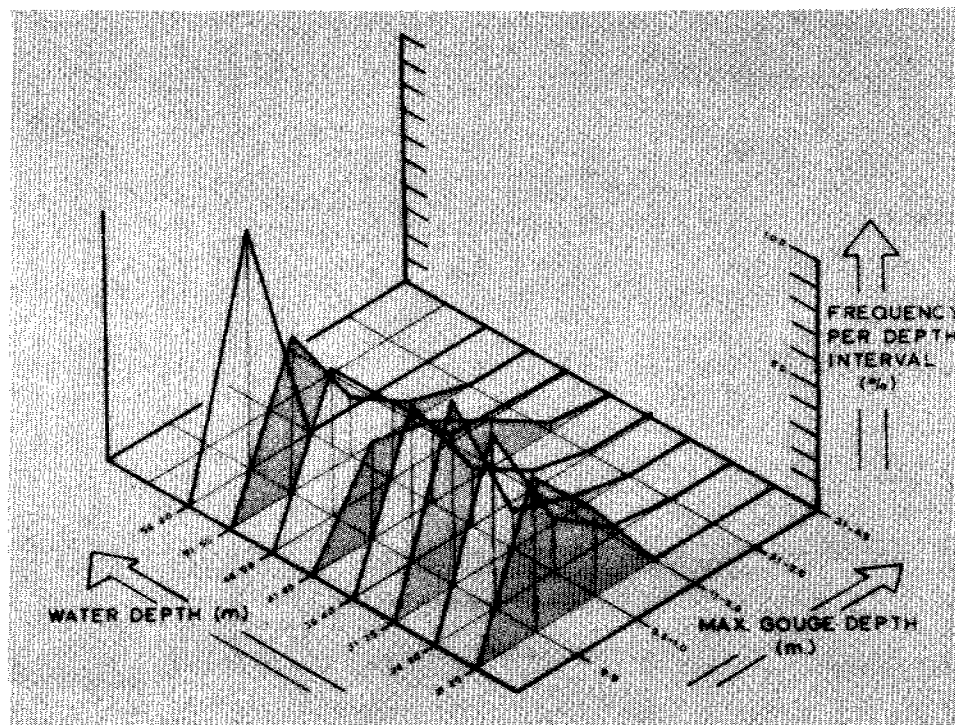


Figure 11

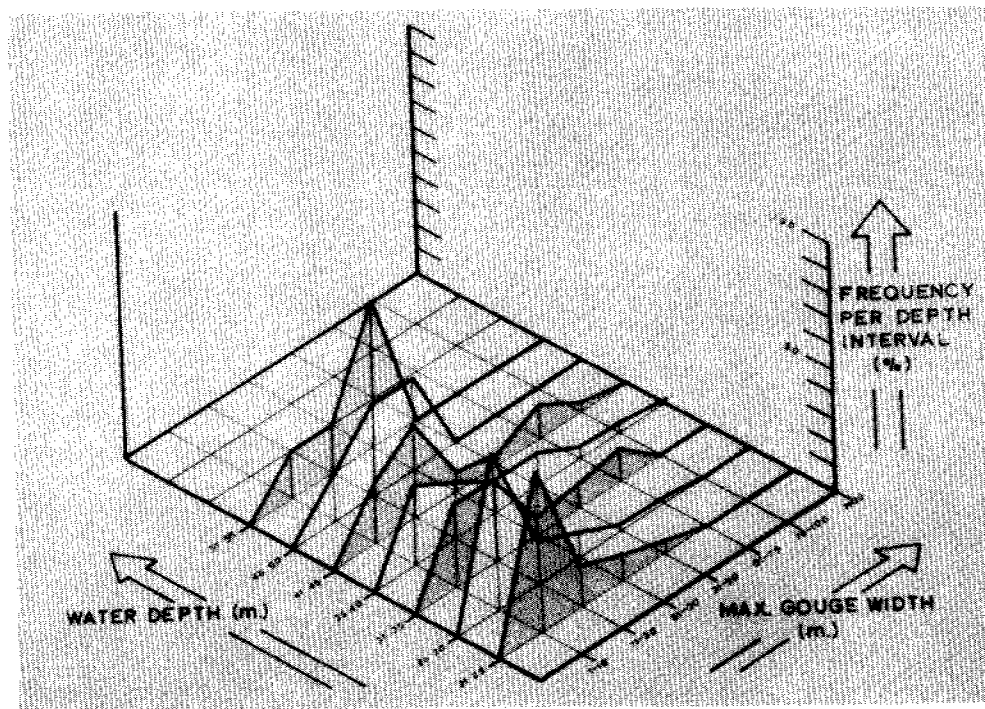


Figure 12

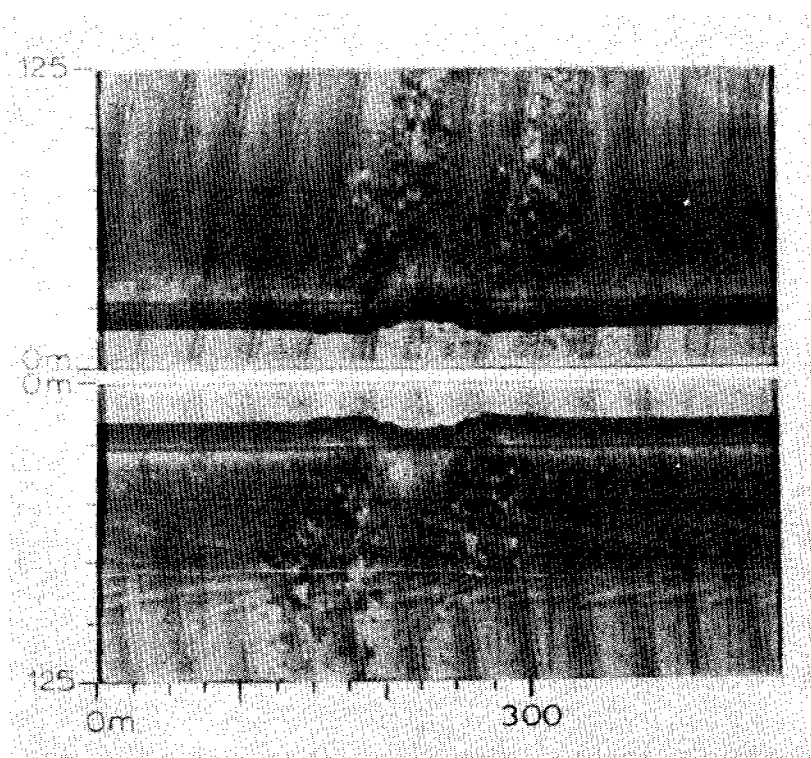


Figure 13

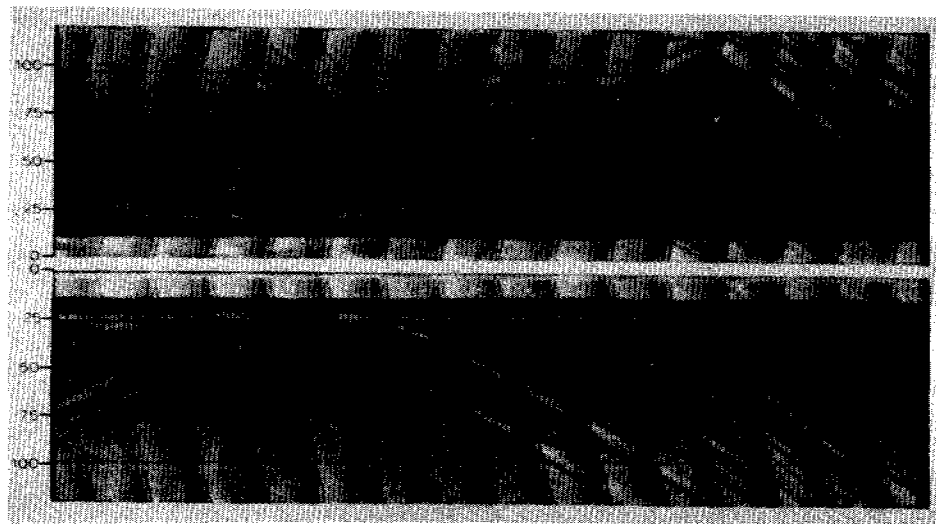


Figure 14

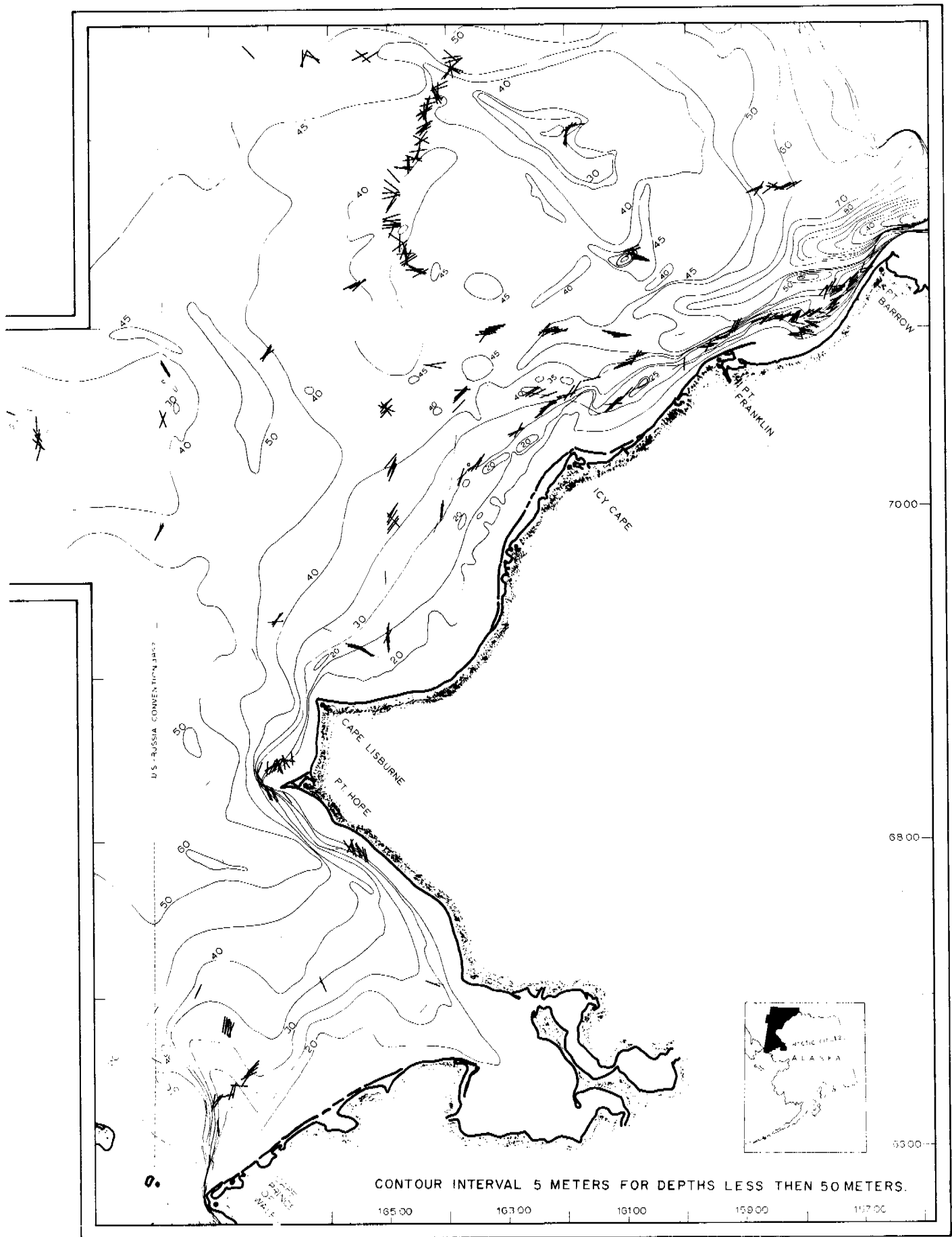


Figure 15

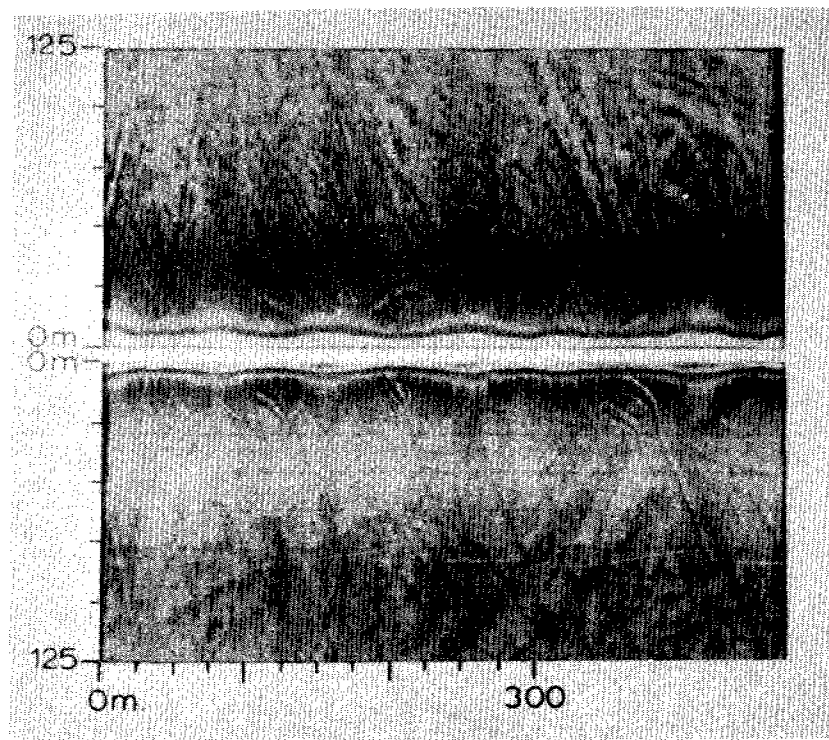


Figure 16

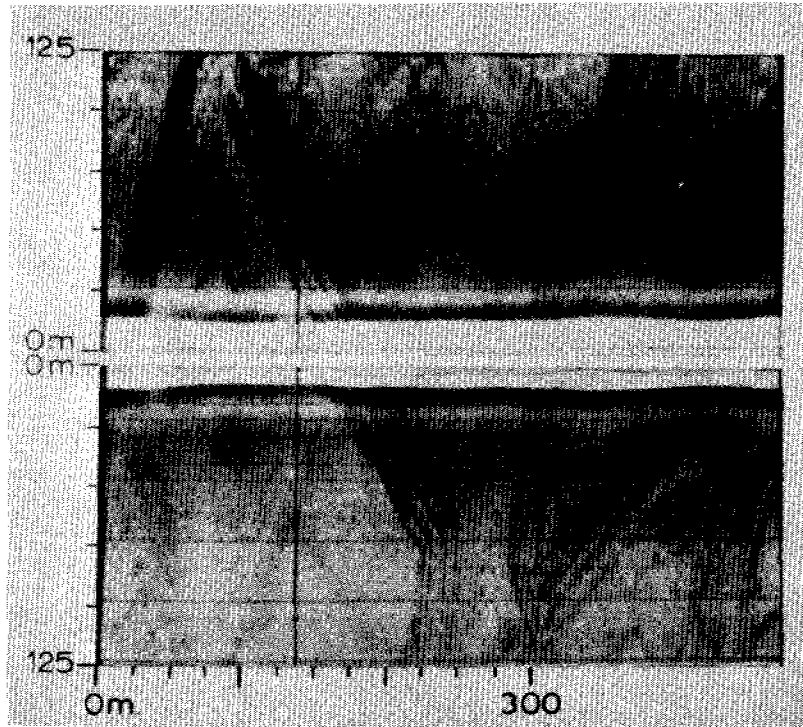


Figure 17

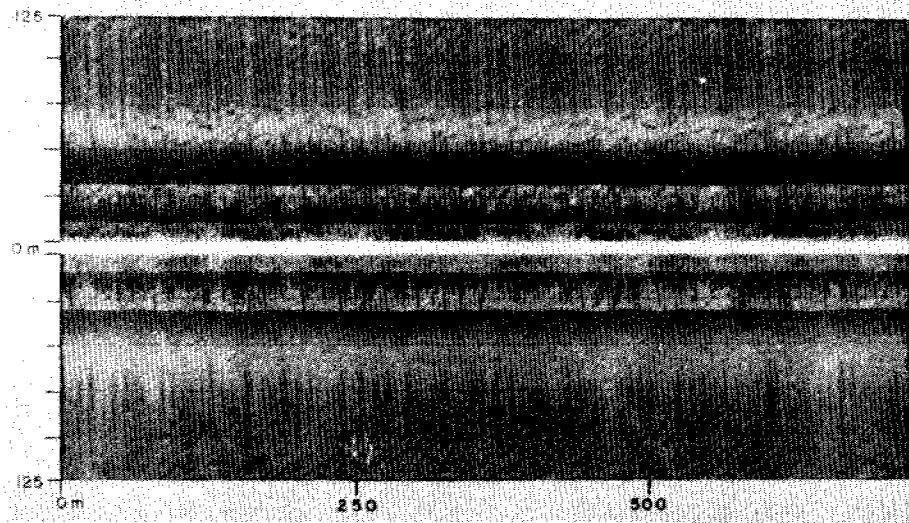


Figure 18

APPENDIX I

Appendix I is presented here only in part. Included are the initial positions of trackline segments plotted in Figure 3. The remaining portion, some 42 pages, includes information on water depth, ship speed, course, dominant gouge trend relative to ships heading, corrected trends, number of observed gouges, correction factors used, maximum incision depths, and maximum gouge width over each 1 km of trackline. The data is available upon request and will be present in a subsequent U.S.G.S. Open File Report.

TRACKLINE SEGMENT	INITIAL POSITION	
	N. LATITUDE	W. LONGITUDE
01	71°21.2'	156°48.2'
02	71°03.8'	157°49.3'
03	70°58.0'	159°06.0'
04	70°51.6'	159°42.1'
05	70°38.0'	162°00.5'
06	70°25.4'	162°43.0'
07	70°06.2'	163°56.5'
08	70°11.4'	163°53.9'
09	70°42.3'	163°39.6'
10	70°38.8	162°41.0'
11	70°44.3	160°00.0'
12	70°52.3'	159°52.1'
13	71°03.2'	158°15.1'
14	71°10.0'	157°47.0'
15	71°12.7'	156°32.5'
16	71°27.6'	156°32.5'
17	71°15.5'	157°07.0'
18	70°57.3'	160°00.0'
19	70°56.5'	161°00.0'
20	70°58.0'	162°03.0'
21	71°00.0'	163°05.5'
22	70°48.2'	163°58.5'
23	70°36.0'	165°00.0'

TRACKLINE SEGMENT	INITIAL POSITION	
	N. LATITUDE	W. LONGITUDE
24	70°15.9'	164°54.2'
25	69°56.0'	165°53.6'
26	69°36.8'	165°02.0'
27	69°16.4'	165°00.0'
28	69°05.5'	169°59.0'
29	69°06.5'	165°53.5'
30	69°22.6'	166°47.0'
31	69°10.9'	167°13.2'
32	68°57.0'	166°59.8'
33	68°33.2'	166°34.1'
34	68°27.0'	167°20.1'
35	68°12.2'	166°49.2'
36	67°53.2'	166°57.5'
37	67°57.1'	166°03.0'
38	67°59.5'	165°37.6'
39	66°39.4'	165°22.5'
40	66°56.9'	164°37.0'
41	67°05.8'	164°14.0'
42	67°06.0'	165°23.5'
43	67°06.3'	166°13.5'
44	67°22.0'	166°13.0'
45	67°54.9'	167°50.0'
46	68°02.0'	168°22.3'

TRACKLINE SEGMENT	INITIAL POSITION	
	N. LATITUDE	W. LONGITUDE
47	68°22.0'	167°45.0'
48	68°26.1'	167°57.2'
49	68°15.6'	168°25.0'
50	68°22.1'	168°56.5'
51	69°07.3'	168°51.0'
52	69°53.2'	168°48.5'
53	70°28.9'	168°44.0'
54	70°34.4'	168°44.8'
55	70°04.2'	168°44.2'
56	71°30.0'	168°45.0'
57	71°55.2'	168°47.2'
58	72°12.9'	168°42.5'
59	72°35.5'	168°33.5'
60	72°32.8'	167°22.0'
61	72°30.0'	166°12.0'
62	72°28.9'	165°01.5'
63	72°26.8'	163°51.0'
64	72°05.5'	164°18.9'
65	72°00.5'	164°24.0'
66	71°55.8'	164°25.5'
67	71°49.1'	164°48.0'
68	71°27.9'	164°46.2'
69	71°19.8'	160°42.2'

TRACKLINE SEGMENT	INITIAL POSITION	
	N. LATITUDE	W. LONGITUDE
70	71°58.5'	162°01.5'
71	71°50.0'	161°04.0'
72	71°44.0'	159°49.5'
73	71°44.0'	158°39.0'
74	71°13.8'	165°23.5'
75	70°52.5'	167°01.5'
76	70°34.5'	171°40.0'
77	70°32.0'	171°10.0'
78	67°26.4'	168°50.5'
79	67°06.9'	168°23.2'
80	66°50.9'	167°50.5'
81	66°32.7'	167°26.2'
82	66°27.0'	167°37.2'
83	66°14.6'	168°00.5'

ATTACHMENT D

STAMUKHI SHOALS OF THE ARCTIC- Some observations from the Beaufort Sea.

by

Erk Reimnitz and Douglas K. Maurer

INTRODUCTION

A number of linear shoals, standing out as pronounced topographic anomalies on the surface of the Arctic shelf, have been studied in the Prudhoe Bay area. These shoals have been referred to in several previous studies. Reimnitz, et al. (1972a), based on seismic reflection records, stated that the shoals are constructional features younger than the post-Wisconsin transgression. Large chunks of grounded ice commonly have been seen on the linear shoals of the inner shelf forming barriers parallel to shore (Reimnitz, et al. 1972b). The lack of gravel concentrations on the shoals was used by Reimnitz and Barnes (1974) as evidence that the stream of pack ice drifting past northern Alaska carries very little gravel today. Lewellen (1977) referred to the linear shoals as submerged barrier islands, while Reimnitz, et al. (1977b) pointed out that, although similar in shape to barrier islands, the linear shoals are very different in composition, and do not appear to represent drowned barrier islands. They show that the shoals localize the formation of major ice shear and pressure events resulting in linear belts of deformed ice, and today appear to be migrating under the influence of ice-bottom interaction. They speculate that the shoals may have formed in response to ice-bottom interaction within the stamukhi zone. Based on the observations that the shoals migrate rather slowly, retain their shapes over periods of 25 years, and control the location of the outer edge of the floating fast ice zone providing shelter for the inner shelf and coast, Reimnitz, et al. (1977b) surmised that similar artificial structures might be used to modify the ice environment on the arctic shelf.

Linear shoals occur along the eastern seaboard of the United States (Field and Duane, 1976), and are similar to those in the Prudhoe Bay region in their general shape, length, and orientation with respect to the coast. Their origin is somewhat in question, but regardless of whether these shoals originated as barrier islands or as nearshore shoals, the processes affecting them today are very different from those found on the Beaufort Sea shelf.

An understanding of the nature and behavior of the shoals, and of their interaction with the ice regime, will be fundamental to an understanding of ice zonation on the Beaufort Sea shelf. A similar interaction between linear shoals, stamukhi, and grounded ridges may control ice zonation along the Siberian shelf. Thus, the shoals are of regional rather than local significance, warranting closer study.

Modern barrier islands along the Beaufort Sea are composed of sand and gravel, a natural resource in high demand for offshore petroleum development. If the shoals under consideration were indeed drowned barrier islands, as proposed by Lewellen (1977), they might also contain valuable materials for offshore construction.

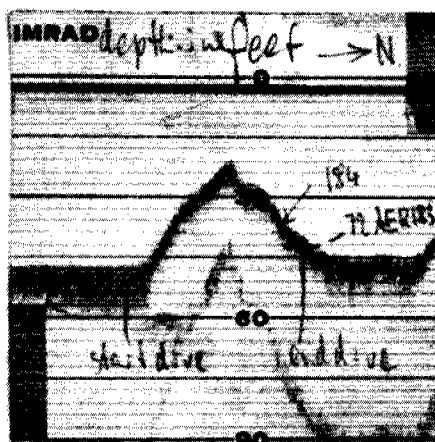
For the above reasons we have made special efforts during the last few years to learn more about the linear shoals of the Arctic shelf, and are presenting some of the data in this report.

REGIONAL SETTING AND MARINE PROCESSES OF THE LINEAR SHOALS

Figure 1 is a contour map of the area of linear shoals under investigation. The outer one, which we surveyed for the first time in 1977, is by far the largest with a length of 17 km. It will be referred to hereafter as Stamukhi Shoal. A 12 km long, broad, and ill-defined, discontinuous shoal forms a southeastward extension of Stamukhi Shoal. Several smaller shoals inshore range in length from 1 to 7 km. The shoals are on the average about 6 m above the surrounding seafloor, and typically are steeper on the landward than on the seaward side.

The frequency and intensity of ice interaction with the shoals has been referred to by Reimnitz, et al. 1972b, Reimnitz and Barnes, 1974, and Reimnitz, et al. 1977. Linear ice ridge elements formed by ice pressure and shearing during the winter within the area of Figure 1 were shown to have a striking correlation with the linear shoals. This was used as evidence that both ice dynamics and ice zonation in this region are perhaps controlled by grounding during ridge formation. From these observations, and the fact that analogous conditions apparently exist on the Siberian shelf, where heaps of ice (stamukhi) form on shoals along the outer edge of the fast ice, and shelter the fast ice, the term stamukhi zone was introduced (Reimnitz, et al., 1977b). At that time a major link was missing to serve as a strong point between Cross Island and Stringer's (1974) ring of grounded ice off Harrison Bay, which apparently also is marked by shoals. The newly surveyed shoal is this link. The Landsat image of early July, 1973, (Figure 2) taken from Reimnitz, et al. (1977b), shows that the Stamukhi Shoal correlates with a major ice boundary. This shoal sets the stage for the ice shear events across Harrison Bay, resulting in further ice grounding there, and also provides the shelter for the formation of the second sheet of undeformed ice in Harrison Bay, discussed in previous reports. The northern tip of the region of white-appearing ice in Figure 2, identified by Stringer (1974) as a hummock field, coincides with the northwestern tip of Stamukhi Shoal. Summer ice distribution is controlled by ice grounding on the shoals as well, as we commonly observe during our offshore work with boats. Figure 3 is a poor quality photograph of the radar screen of the R/V Karluk with Cottle Island close on the right and a linear accumulation of ice along Loon Shoal (described in next section) and smaller shoals inshore. Figure 4 is a Landsat image of July 25, 1977, showing the effects of Stamukhi Shoal as a controlling element in summer ice distribution.

As expected, the ridges are marked by intense and frequent reworking and gouging through the physical action of ice. An abbreviated list of observations taken from a 1972 dive on Loon Shoal will serve to demonstrate the importance of ice related processes: The diving traverse started in the flat trough in the shelter of the ridge, at a water depth of 14.5 m (see ridge cross-section taken after dive on Simrad depth recorder). The bottom was sand, covered by a thin layer of organic ooze, with several obscure, east-west trending gouges. Swimming up the lee-side of the shoal, the ooze disappeared, exposing a surface of clean sand, extremely disturbed by gouging. The trend of the gouges was dominantly parallel to the slope, but they were criss-crossing in irregular patterns, with some trending up-slope. Some of the gouges were multiple types, and many gouges terminated within the field of view, showing that gouges on steep slopes are short.



A 1972 Simrad record of dive traverse on Loon Shoal

Vertical relief across gouges reached up to 2 m, and the width up to 10 m, but the flanks were generally at the angle of repose for the sand. Wave or current produced bedforms were scarce and ill-defined, with ripple structures generally restricted to particular gouges, often transverse to the gouge trend. This observation has been made on other ridge dives. Only few bottom dwelling organisms including isopods and coelenterates, were seen. Shortly after crossing the ridge crest, the layer of organic ooze re-appeared, at first only covering gouge troughs and not their crests, eventually blanketing the entire surface. At a depth of about 11 to 12 m a shelly, gravelly sand was felt about 10 cm below the seafloor. The number of gouges decreased with water depth. At a depth of 13 m, irregular, blocky outcrops of dark, stiff, slightly sandy mud protruded from the sediment blanket.

These observations, including the clean sand bottom, in general apply to all of the shoals landward of the Stamukhi Shoal. Summer sediment accumulation in the upper part of the shoal is less than on the lower flanks and adjacent flat bottom, as currents there are sufficient to effect the distribution of organic (planktonic) ooze. Organisms living on the bottom are scarce so that the dominant reworking process is ice gouging which can often be observed in progress. However, the gouges, being short, irregular, and criss-crossing, with non-cohesive sand lying at the angle of repose, are difficult to record with side scan sonar. Thus, the absolute rate of bottom reworking by ice is not easily monitored by this method, as shown in Attachment B, this report. This is partly due to the presence of stamukhi on the shoals forcing the ship to veer from the comparison base line. However, the shoal north of Spy Island (Figure 1.) does appear entirely different each successive year (See attachment B).

The steering effects of the shoals interacting with ice drift can be seen on a regional scale in the dominant trends of gouges, as shown in Attachment B of this report. North of the linear shoal seaward of Spy Island, the dominant gouge trend is WNW, while south of the shoal it is WSW.

A summary of processes acting on the linear shoals can not be complete without considering the effects of ice rafting as a means of supplying new materials. As pointed out in previous publications, an optimum condition for the concentration of ice rafted sediments on any particular area of the shelf surface is retarded drift of melting ice, as is the case at the shoals. Summer conditions on a shoal are shown schematically in Figure 5. The ridge crests, besides attracting ice rafted debris, should also be sites of enhanced winnowing of sediments by ice contact and currents, when compared to the surrounding seafloor. The presence of clean sand capping the inner shoals, while ice rafting generally is considered to include a wide range of particle sizes including gravel and cobbles; would seem to rule out ice rafting as an important contributor of sediment to the shoals.

BATHYMETRY

Loon Shoal

Methods- Bathymetric data of Loon Shoal obtained by the U.S. Coast and Geodetic Survey in 1950-51 and compiled onto C.&G.S. Hydrographic Sheet #7856, was compared with data obtained in 1976 by the R/V Karluk. The 1950 data was controlled using a combination of Shoran and sextant fixes on shore objects; accurate to ± 100 m. The 1976 data was controlled with a Del Norte range-range navigation system accurate to ± 5 m. Bathymetry was obtained with a 200 Khz narrow beam transducer coupled with a Raytheon RTT 1000 depth recorder. Del Norte ranges were recorded simultaneously with bathymetry on magnetic tape at 10 to 30 second intervals. The data was then plotted by computer at the same scale and projection as C.&G.S. Hydrographic sheet #7856. Where 1976 tracklines coincided with 1950 lines the original 1950 fathograms were used to construct profiles for comparison with the 1976 paper Raytheon records.

Topography-The long shoal about 8 km north of Cottle Island in 13 m of water is called Loon Shoal, after the U.S.G.S. R/V Loon from which the first studies of the shoal were made since 1971. Figure 6 shows 1976 profiles of Loon Shoal, keyed to Figure 1 by letters A' through L'. Profiles G' and K' coincide with 1950 lines and for these the 1950 profiles are shown as dashed lines. Figures 7 and 8 compare 1950 and 1976 bathymetry contoured at 1 m intervals.

Figures 6 and 8 show Loon Shoal as a linear ridge trending approximately 120° T, 6 1/2 km long, and longitudinally asymmetrical, rising 7 m above the sea floor near it's eastern end and gradually diminishing in height toward the west. It is also asymmetrical in cross-section with the landward side characteristically steeper than the seaward side. Profiles D' through K' also show slightly deeper water landward of the shoal than is present at equal distance seaward of the shoal. These characteristics are opposite to the configuration of present day barrier islands which are steeper and deeper on their seaward side.

The seafloor landward of the shoal is generally smoother than it is seaward with major relief features occurring along it's crest. This relief results from deep draft ice grounding.

Comparison of the two bathymetric contour maps show that during the last 25 years changes in the shoals position and configuration have been minor. The flanks of the shoal coincide almost exactly along it's length and the asymmetry

of its longitudinal and axial cross-section has been preserved. Isolated highs near the west end of the shoal and the crest of the shoal have been modified somewhat since the 1950 survey. Also the 8 and 9 m contour west of the shoal's high point have been extended to the west about 1 km showing the most significant deposition along the shoal.

Migration of the shoal's crest is shown in Figure 9. At all points except the extreme west end of the shoal, the crest has either remained stationary or migrated landward. Profile K' shows how the shoal cross-section has changed at the point of maximum migration, approximately 200 m.

Stamukhi Shoal

Methods - The rather rare opportunity to survey the region of Stamukhi Shoal presented itself in 1977, when the area became ice free. Navigation was controlled by Del Norte range-range navigation, and bathymetry recorded with the same system used for Loon Shoal. The Raytheon RTT 1000 was used with a 7 KHz transducer as a sub-bottom profiler. As no previous data exist for the area, comparison with older data could not be made and positions and depths were plotted directly on 1:80,000 scale charts.

Results- Stamukhi Shoal (Figure 1) is the most striking feature on the shelf between Prudhoe Bay and Barrow. Its shape is rather different from that of Loon Shoal, in that it has its highest part on the western, rather than the eastern end. Here it stands about 10 m above the surrounding sea floor. Inshore of Stamukhi Shoal is a broad, lagoon-like depression, that extends seaward with a narrow arm past the southeastern terminus of the shoal. Plotting of additional bathymetry surrounding Stamukhi Shoal will be completed at a later date.

A series of bathymetric and sub-bottom profiles (vertical hatch marks) of Stamukhi Shoal is shown in Figure 10. As with Loon Shoal, these profiles are keyed by letters to Figure 1. It must be noted that profiles I and J were run on a day with rough seas, and therefore the apparent micro-relief is partly due to vertical motion of the ship.

The highest and steepest relief is seen in profile C, where the leeward side is much steeper than the seaward side. This is the case in several other profiles, although less pronounced. Still other profiles show the opposite, with steeper slopes on the seaward side of the shoal. Both ends of the shoal terminate rather abruptly. At the northwestern end the shoal suddenly bifurcates into three distinct arms. It is noteworthy that along the length of the shoal marked changes in profiles occur over short distances, and that the shoal is rather irregular and winding when viewed as a whole.

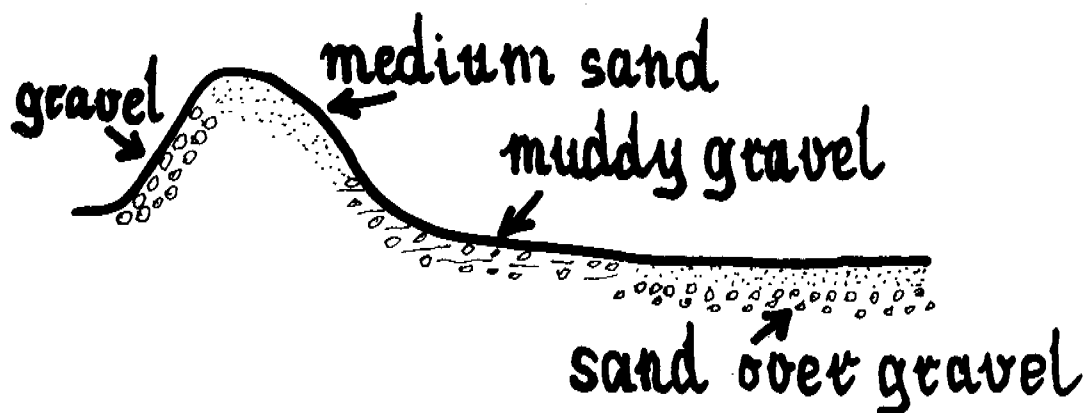
Profiles A through H, run with a calm sea, show very pronounced ice gouging in the form of extremely jagged micro-relief seaward of the crest and rather smooth bottom landward.

SEDIMENTS

Certain textural parameters of surficial sediments from the region under study have been mapped by Barnes and Reimnitz, 1974. However, the patterns show only regional

trends, and are inadequate to portray details of sediment distribution of features like the shoals. Also additional data has been collected in the shoal area since that time. Sampling and observation stations in the study area are shown in Figure 11. The stations represent surface grabs, vibrocores, and dive traverses. Details of one dive were given in our quarterly report for April-June, 1977 (Dive site # 76-18). The diving investigations demonstrate that over much of the area generalizations on sediment types cannot be made because of extreme, short-distance variations. The areas where such variations occur are mapped in Figure 11 as "variable". This area lies seaward of Loon Shoal, and extends seaward through the region of ill-defined shoals forming an extension of Stamukhi Shoal, hereafter referred to as Cat Shoals. All the linear shoals landward of Loon Shoal are made up of well sorted, medium grained sand, and this sand seems to cover the intervening areas, except for a narrow bank of mud along the leeward side of Loon Shoal. The seaward toe of Loon Shoal, below a depth of 11.5 m is underlain by pebbly sand with shells, as observed at three locations along the length of the shoal. Landward of the 10 m isobath the bottom deposits consist of clayey, sandy silt, shown here as sandy mud.

An attempt to make a composite, highly generalized sediment profile from the diving observations cited above and a traverse across the SW shoal in the Cat Shoals area is shown in the following sketch:



Only two diving traverses cover small portions of Stamukhi Shoal and our knowledge on this shoal is very sketchy, with highly differing sediment types occurring on the two dives. Near the center of the shoal, its crest is capped with clean gravel, while near the eastern end we found sand and gravel.

Outcrops of older sediments were seen on two dives in the area of highly variable sediments (Figure 11). One of these, at the seaward toe of Loon Shoal, consisted of angular, blocky outcrops of very dark, overconsolidated, slightly sandy mud in various stages of disintegration from burrowing. This material, containing marine pelecypods (*Serripes Groenlandicus* and *Astarte*), has a C_{14} age of 11,280 years \pm 280 years B.P. (whole sample date). On the lee slope of one of the small shoals about 5 km northeast of Loon Shoal, marked by a dive traverse symbol in Figure 11, we found a different type of outcrop. Here a partly cemented, rusty colored, slightly sandy gravel cropped out in small patches elongated in the north-south direction. These patches were about .5 m across, and one to several meters long. Pounding the surface with a lead weight produced a sharp sound and did not indent the material.

SEISMIC REFLECTION PROFILES

A variety of sub-bottom profiling systems have been used in the study area over the years. For the purpose of this study the RTT 1000, operated at a frequency of 7 Khz, gave sufficient penetration to trace the shallowest sub-bottom reflectors through the area of the shoals. The area is mantled by only 5 to 10 m of Holocene marine sediments with some "windows" exposing underlying deposits of the Quaternary Gubic Formation (Reimnitz, et al. 1972a). Of importance to this study is the fact that the linear shoals are marked by an upward thickening of the surficial unit resting on a flat-lying base. In the case of Loon Shoal and shoals landward of Loon Shoal, this base is probably an old land surface marked with channel-like features. The sub-bottom profiles for Stamukhi Shoal (Figure 10) show that a flat surface extends below the shoal for its entire length. But last years records extending far out onto the shelf, indicate that Stamukhi Shoal and Cat Shoals sit on a different unit than Loon Shoal and shoals landward. More work is required to work out the details of this relationship.

INTERPRETATION AND CONCLUSIONS

The existence of the pronounced linear shoals in the study area is a curious phenomenon, when considering the abrasive powers generally attributed to drifting sea ice. The earth scientist with background from lower latitude shelf studies would initially attempt to interpret the features as barrier islands or offshore bars, left behind on the shelf surface by a rapid transgression and submergence.

Figure 12 shows a profile across Simpson Lagoon, a barrier island, and seaward across Loon Shoal. This comparison shows similarities between a typical modern barrier island and one of the linear shoals. Here, Loon Shoal stands nearly twice as high above the landward shelf surface than the barrier island stands above the adjacent lagoon. Another difference becomes apparent from the detailed profiles of Loon Shoal in Figure 6. These profiles are generally skewed landward, whereas the modern barrier islands are skewed seaward. The overall shape of the ridges also is dissimilar from that of modern barrier islands. Stamukhi Shoal does not have a linear to arched continuous crest, similar to the present barriers. Its crest is instead sinuous and discontinuous.

These difference could be explained in view of the modern ice processes which are now acting on the shoals. As seen from the profiles in Figure 6, G' and K', the tendency through time is toward a steepening of the axial profile on the landward side of the shoal. This process is accomplished by removal of sediment from the seaward side and deposition on the landward side of the shoal. When viewed as a whole, the shoal has not measurably migrated landward during 25 years but has been steepened on its landward side. Thus, the difference in symmetry between the present day barriers and the shoals can be explained by modern processes. Bulldozing action of the ice along the crest of the shoals can easily explain the fact that their crest is now sinuous and discontinuous.

The clean sand composing Loon Shoal and other shoals landward thereof is in sharp contrast with sandy gravels found on adjacent barrier islands and beaches, and on Arctic barrier islands in general. The composition of Stamukhi and

Cat Shoals, on the other hand, is not so dissimilar from that of modern barrier islands and there a case for similar origin could be made. Our new seismic data indicating that the units on which Loon and Stamukhi Shoals sit are different allows for shoal construction from materials available on the adjacent shelf surface. This could result in shoals of different composition being formed from similar processes.

All evidence available to date indicates the linear shoals are depositional features. All observations made on modern processes of the Arctic suggest that anything standing above the general shelf surface will be planned off by the action of ice. Even gently sloping, generally flat surfaces on the inner shelf are reworked by ice at a rate of once every 50 to 80 years (Attachment B this report, and Reimnitz et al., 1977a). The action of ice is focused on the high points, to the extent that ice dynamics, and even the overall ice zonation of the shelf, appears to be controlled by the shoals. As pointed out by Reimnitz, et al., 1977b, a large portion of the available marine energy is expended on the seafloor within the Stamukhi zone on a year-round basis. Linear shoals like the newly found Stamukhi Shoal lying within that zone certainly take the brunt of ice action.

In light of the above, it is difficult to believe that the linear shoals are drowned barrier islands that have survived since submergence, based primarily on lack of chances for survival of such sediment piles for thousands of years under ice processes as we understand them today. However, this possibility is not as yet disproven. As reported previously (Reimnitz, et al., 1977b) and supported by data in this report, the shoals are not stagnant features. The shelly, gravelly sand found at the seaward toe along the length of Loon Shoal support onshore migration, but the processes resulting in the construction of the linear shoals by ice-related processes are not understood. We still concur with a previous statement (Reimnitz, et al., 1977b) that future studies will have to show whether such shoals form by (a) the bulldozing action of ice during one or several major events, (b) the cumulative effects of several thousand years of ice push by grounded ice ridges along the edge of the Pacific Gyre, or (c) winter currents being channeled along major ridge systems tend to concentrate available sediments into sand (or gravel) ridges, or whether several of these processes act together to form the shoals.

Figure 13 gives a regional view of the Beaufort Sea shelf from Prudhoe Bay to Point Barrow. All isolated shoals seaward of the 11 m (6 fm) isobath are circled. The newly surveyed Stamukhi Shoal lies where no major shoal is indicated, and we have evidence that the two shoals to the north and south do not exist today. During the cruises of the Coast Guard Cutter Glacier, several of the indicated shoals on Figure 13 were crossed and not found to be present (Personal Communication with Peter Barnes). Thus the scattering of shoals along the Stamukhi zone from Cross Island to Point Barrow only say that numerous shoals occur in the zone but their true positions and orientations are undetermined in most cases. It may be that many more exist, and we feel that detailed surveys would show the shoals to be more linear, and generally parallel to the coast.

Last summer's ice-free conditions allowed us to run surveys far out to sea NE of Cross Island, and we found no shoals. This lack of shoals up-drift of major promontories is in keeping with the concepts on ice dynamics and zonation proposed previously. We feel that detailed work west of Barter Island and Herschel

Island may well show linear shoals, but do not anticipate the existence of such shoals updrift from these promontories. The concept of linear shoals forming in response to ice-related processes seems to hold for the Alaskan Chukchi coast as well. There the general ice drift direction is southward, and shoals occur south of the Blossom Shoal region, for example, but none are found up-drift.

We feel that shoals similar to those investigated here will play an important role in the future offshore development of the Arctic, but are still far from an understanding of the details of their interaction with the ice.

BIBLIOGRAPHY

- Barnes, P.W. and Reimnitz, Erk, 1974, Sedimentary processes on Arctic Shelves off northern coast of Alaska; in The Coast and Shelf of the Beaufort Sea, Proceedings of the Arctic Institute of North American Symposium on Beaufort Sea Coast and Shelf Research, Arlington, Va., Arctic Institute of North America, p.439-478.
- Field, M.E., and Duane, D.B., 1976, Post Pleistocene history of the United States inner continental shelf: significance to origin of barrier islands. Geol. Soc. America Bull. V. 87, p.691-702.
- Lewellen, R.I. 1977, A study of Beaufort Sea coastal erosion, northern Alaska, Environmental Assessment of the Alaskan continental shelf, National Oceanic and Atmospheric Administration, Ann. Repts. for the year ending March, 1977, V.15, p. 491-527.
- Reimnitz, Erk, Wolf, S.C., and Rodeick, C.A., 1972a, Preliminary interpretation of seismic profiles in the Prudhoe Bay Area, Beaufort Sea, Alaska: U.S. Geol. Survey Open-File Report # 548.
- Reimnitz, Erk, Barnes, P.W., Forgatsch, T.C., and Rodeick, C.A., 1972b, Influence of grounding ice on the Arctic shelf of Alaska. Marine Geology V. 13, p.323-334.
- Reimnitz, Erk, Barnes, P.W., Toimil, L.J., and Melchior, John, 1977a, Ice gouge recurrence and rates of sediment reworking, Beaufort Sea, Alaska. Geology V. 5, p.405-408.
- Reimnitz, Erk, Toimil, L.J., and Barnes, P.W., 1977b, Arctic continental shelf processes and morphology related to sea ice zonation, Beaufort Sea, Alaska. AIDJEX Bull. 36, May 1977, p.15-64.
- Stringer, W.J., 1974, Sea ice morphology of the Beaufort Sea shorefast ice, in The Coast and Shelf of the Beaufort Sea, Proceeding of the Arctic Institute of North America Symposium on Beaufort Sea Coast and Shelf Research, Arlington Va., Arctic Institute of North America, p. 165-172.

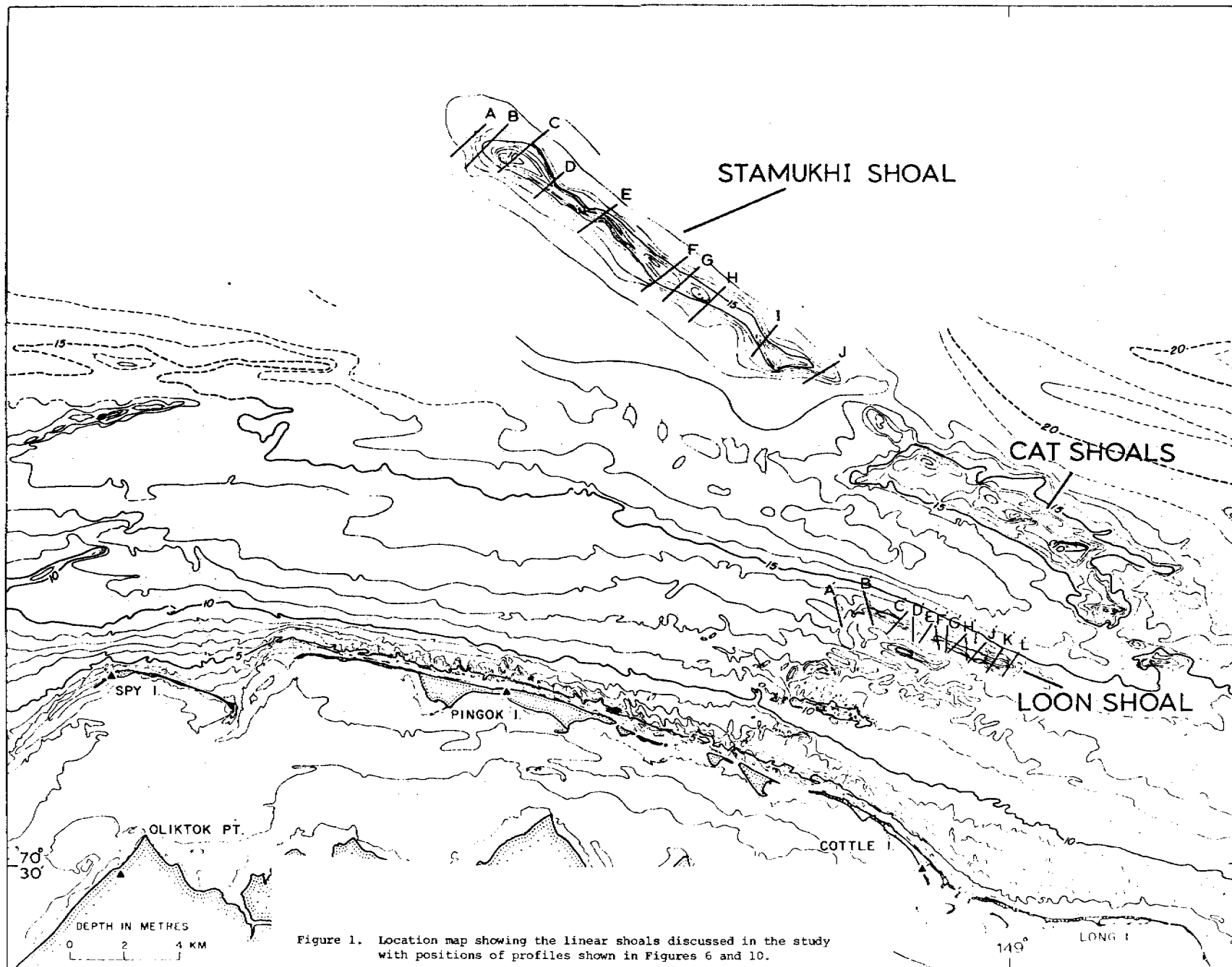


Figure 1. Location map showing the linear shoals discussed in the study with positions of profiles shown in Figures 6 and 10.

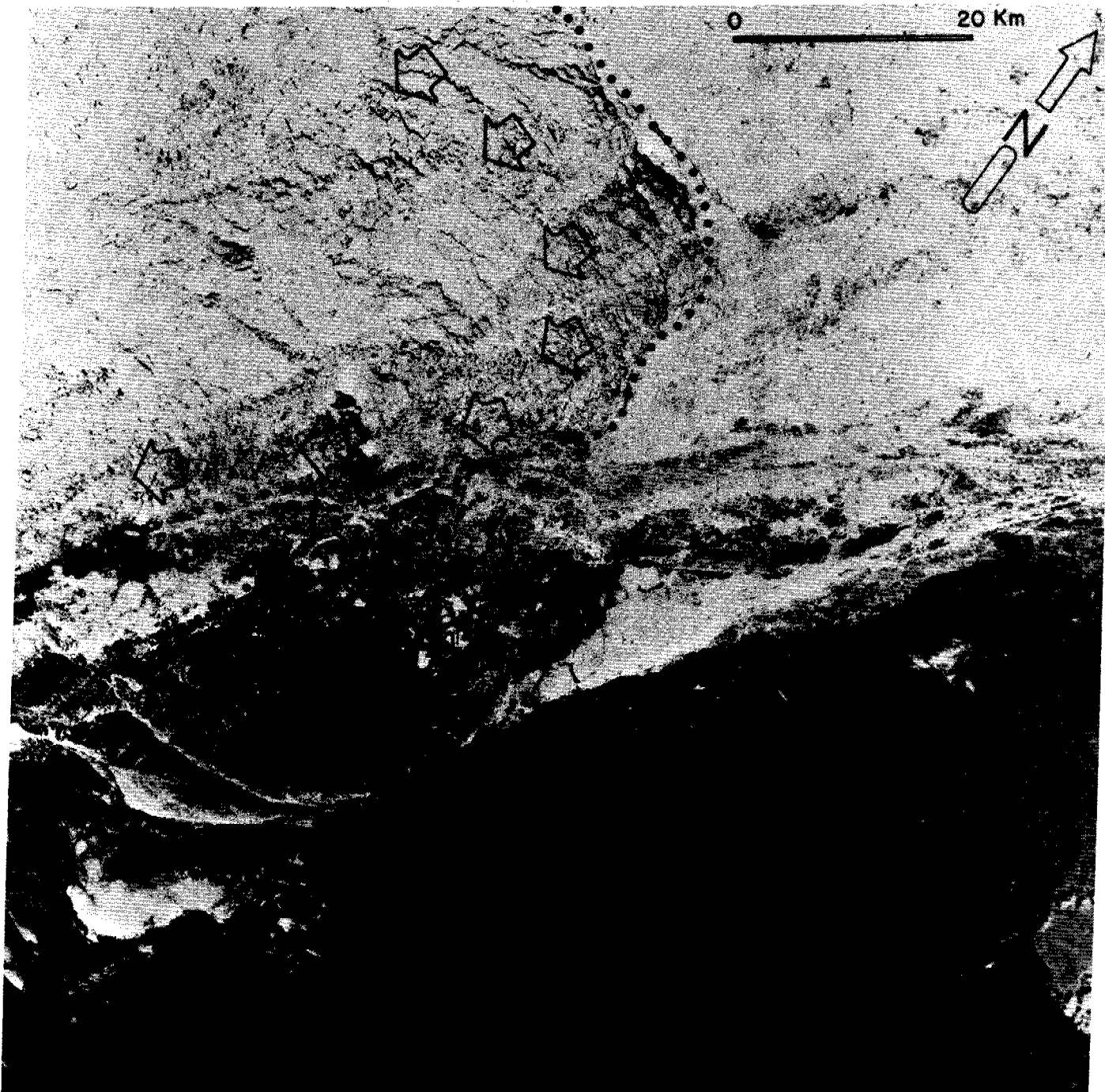


Figure 2. Landsat image of early July, 1973, ice conditions. Stamukhi Shoal corresponds with the northeast boundary of the white appearing ice near the center of photo.

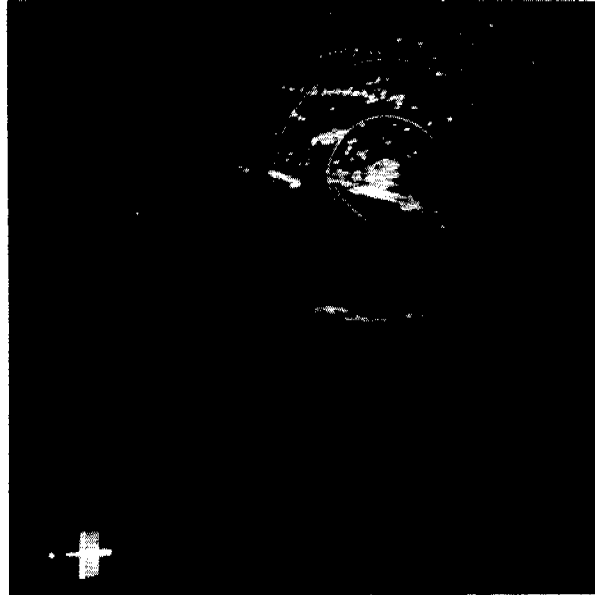
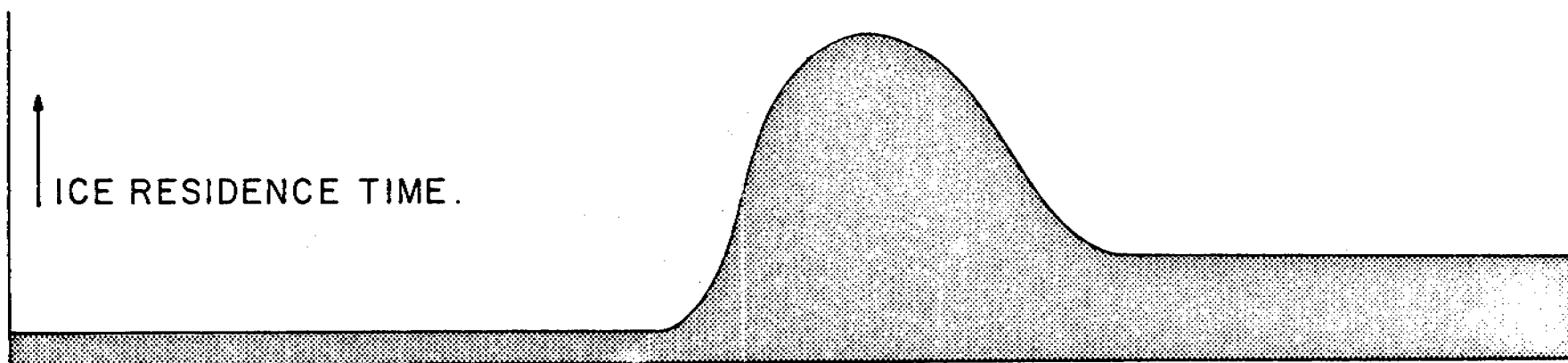


Figure 3. A photograph of radar screen on the R/V KARLUK as it passes just offshore of Cottle Island. Towards the bottom is ice free Simpson Lagoon with Beechy Point being the bottom-most target. Loon Shoal appears as a linear series of targets uppermost in the photo. These targets are stamukhi grounded along the crest of the shoal.



Figure 4. Landsat image of July 25,1977. Northwest end of Stamukhi Shoal is located by leader. The trend of the shoal is closely followed by the landward edge of ice.



291

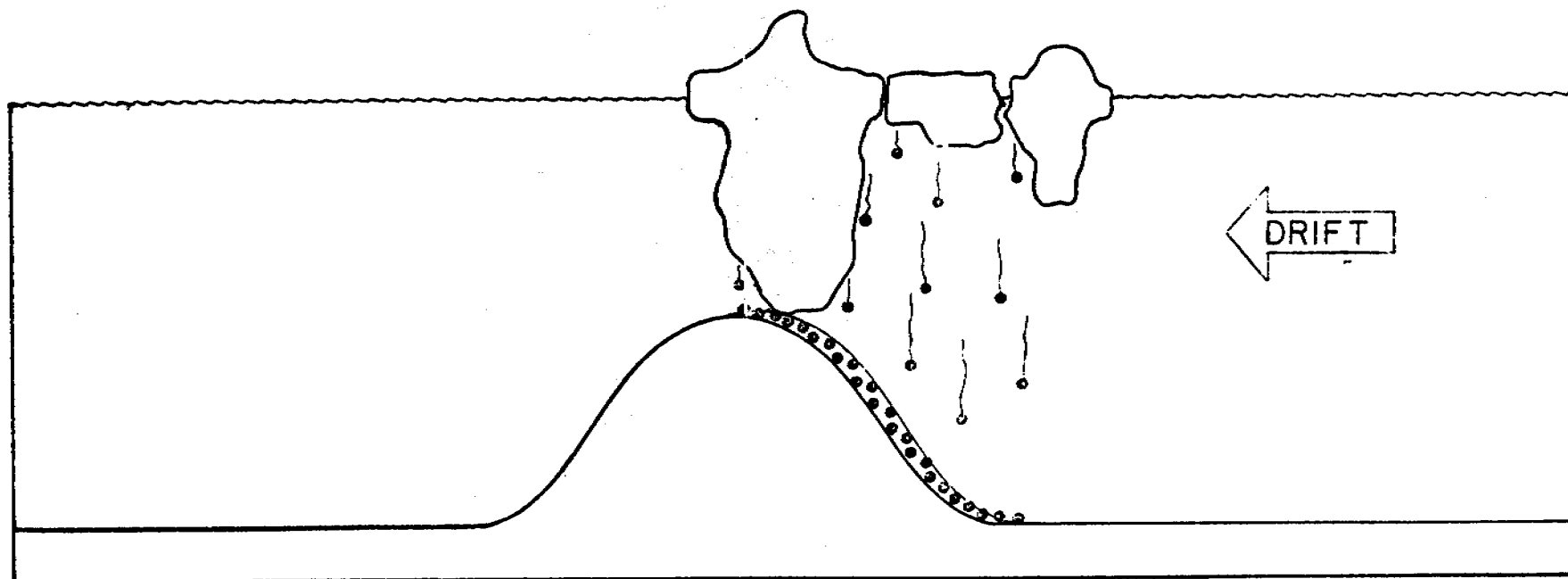


Figure 5. Conceptual diagram showing preferred deposition of ice-rafted materials on shoal during summer conditions.

Landward

Seaward

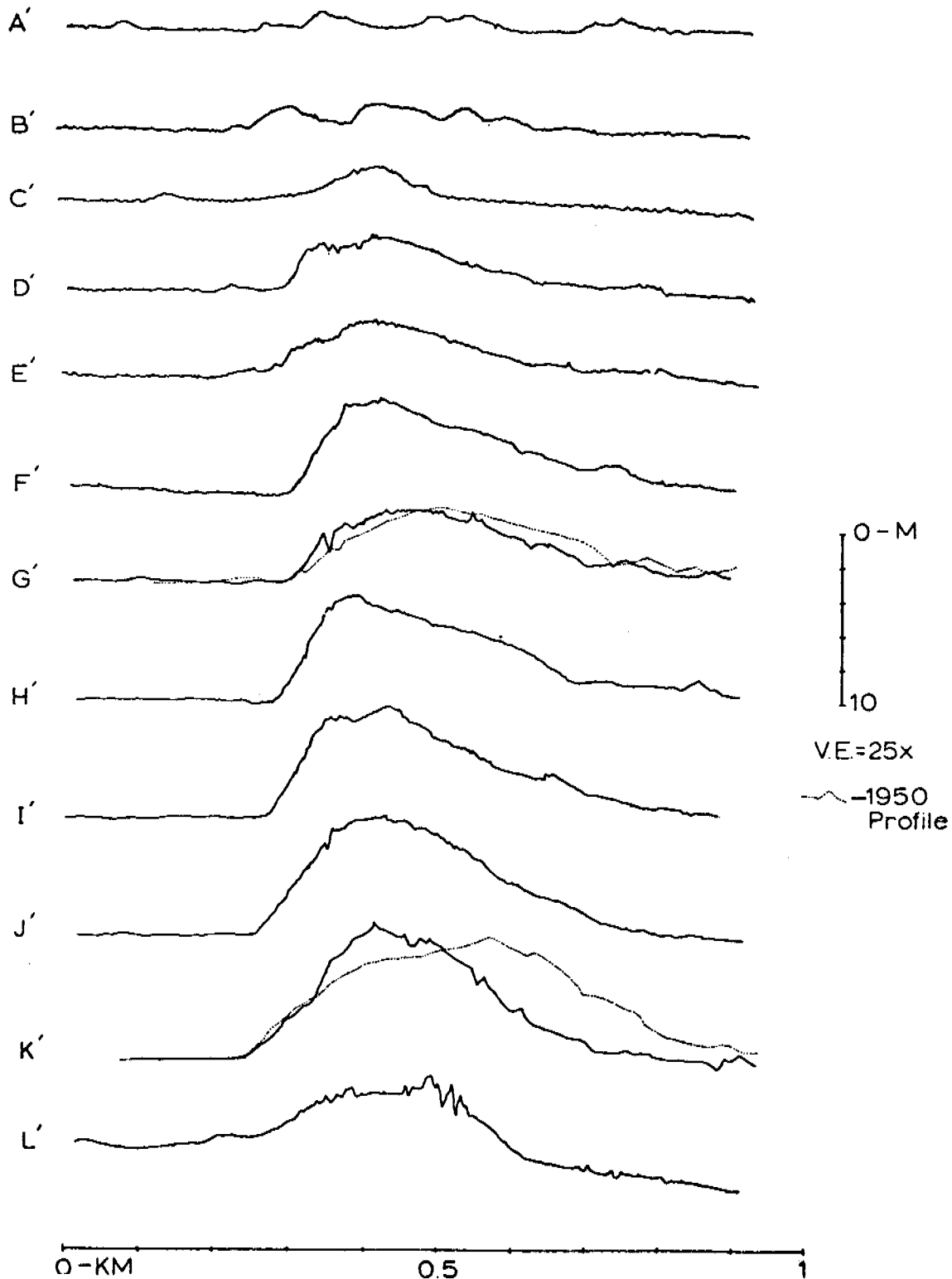


Figure 6. Profiles of Loon Shoal. All profiles were run on calm days so that micro-relief seen is real. Profiles G' and K' are superimposed with 1950 profiles shown as dashed lines.

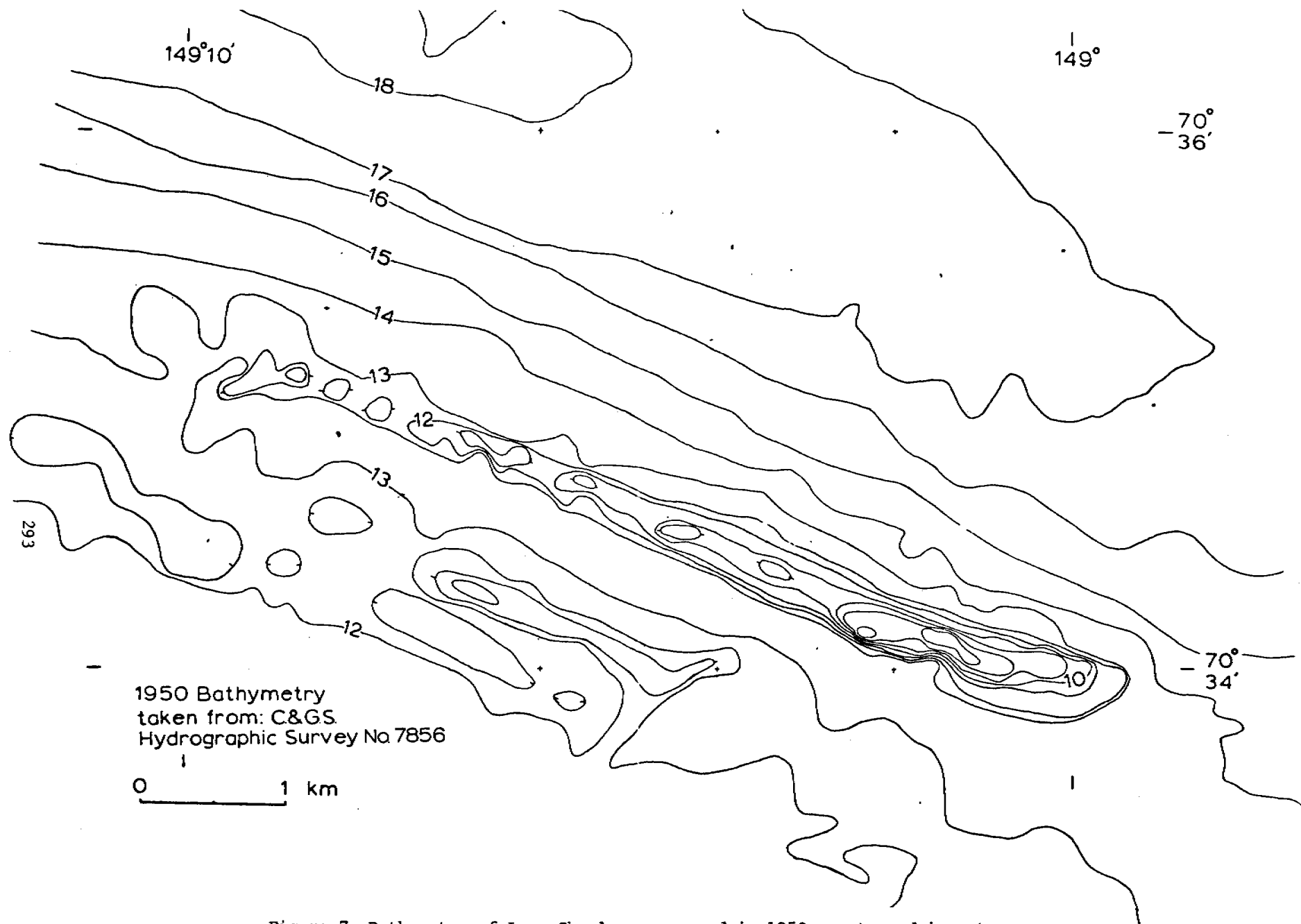


Figure 7. Bathymetry of Loon Shoal as surveyed in 1950, contoured in meters.

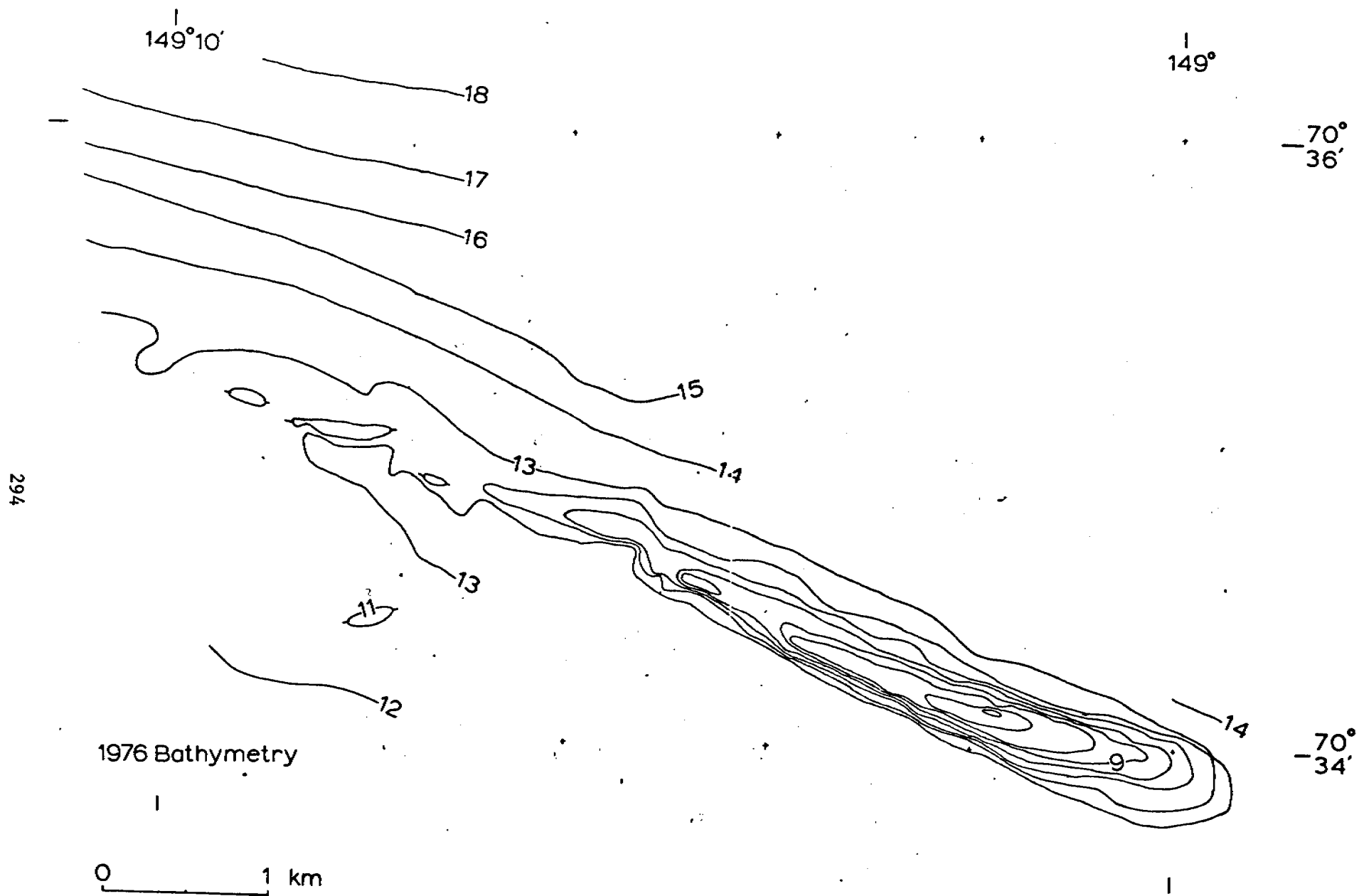


Figure 8. Bathymetry of Loon Shoal as surveyed in 1976, contoured in meters.

149°10'

149°

70°
-35'

70°
-34'

▨ - 1950 Shoal Crest

▧ - 1976 Shoal Crest

0 500m

Figure 9. Superimposed ridge crest from Figures 7 and 8 showing landward migration.

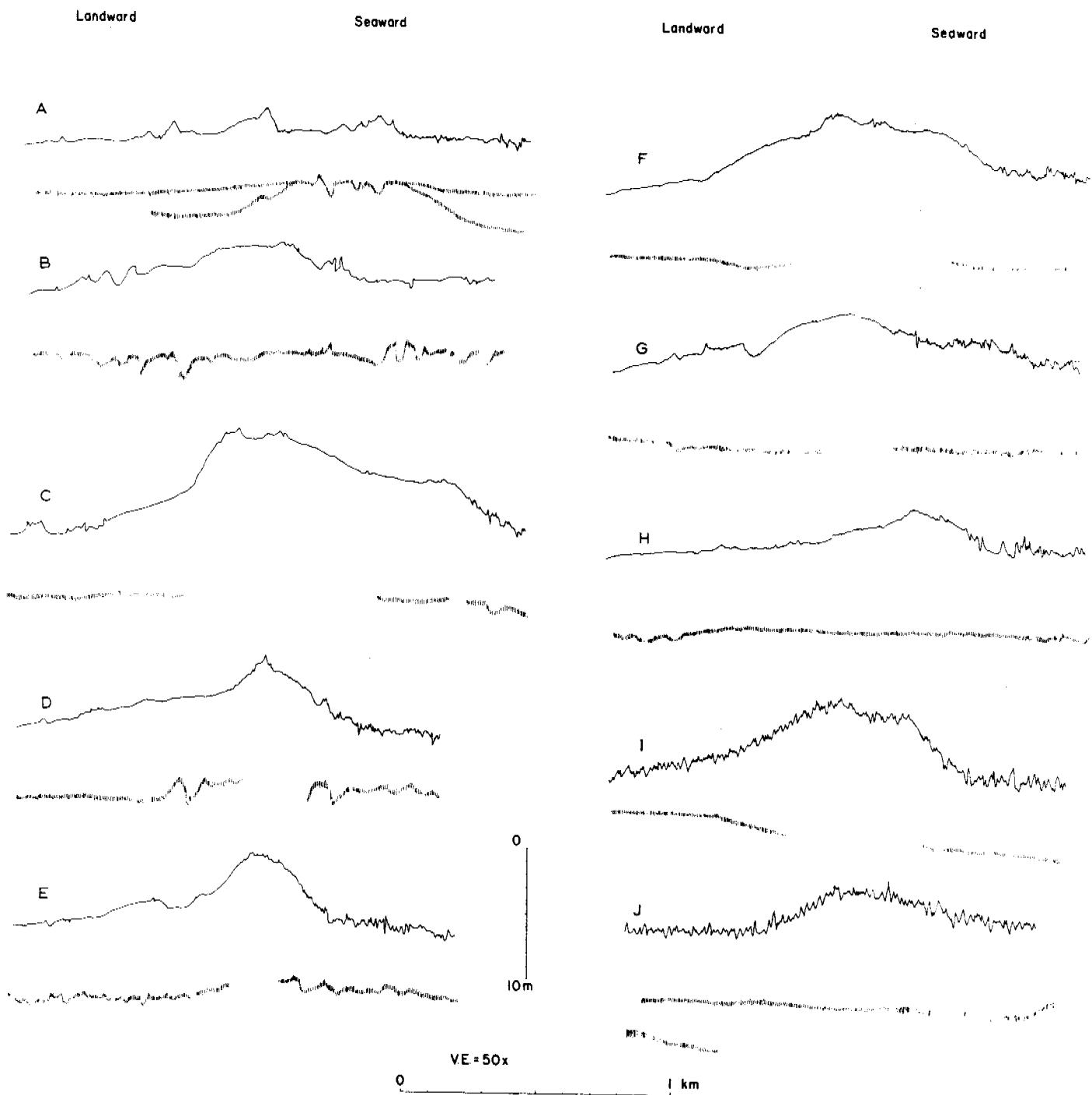


Figure 10. Profiles of Stamuhki Shoal with sub-bottom shown as vertical hatches. Profiles I and J were run with rough seas giving apparent micro-relief. The other profiles show ice gouging, and show the shoal as a boundary for ice processes.

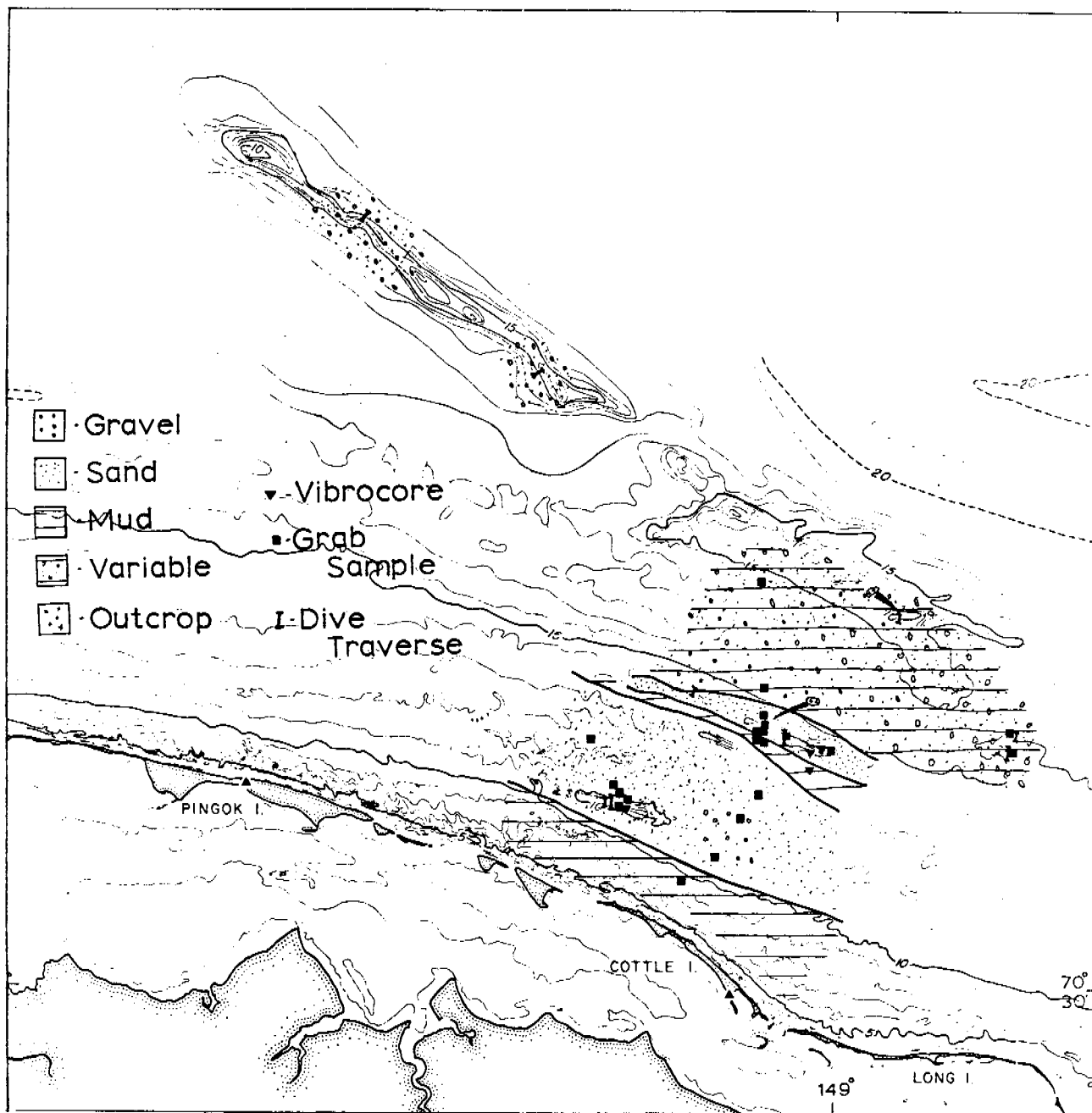


Figure 11. Location of stations in the shoal area and inferred sediment distribution.

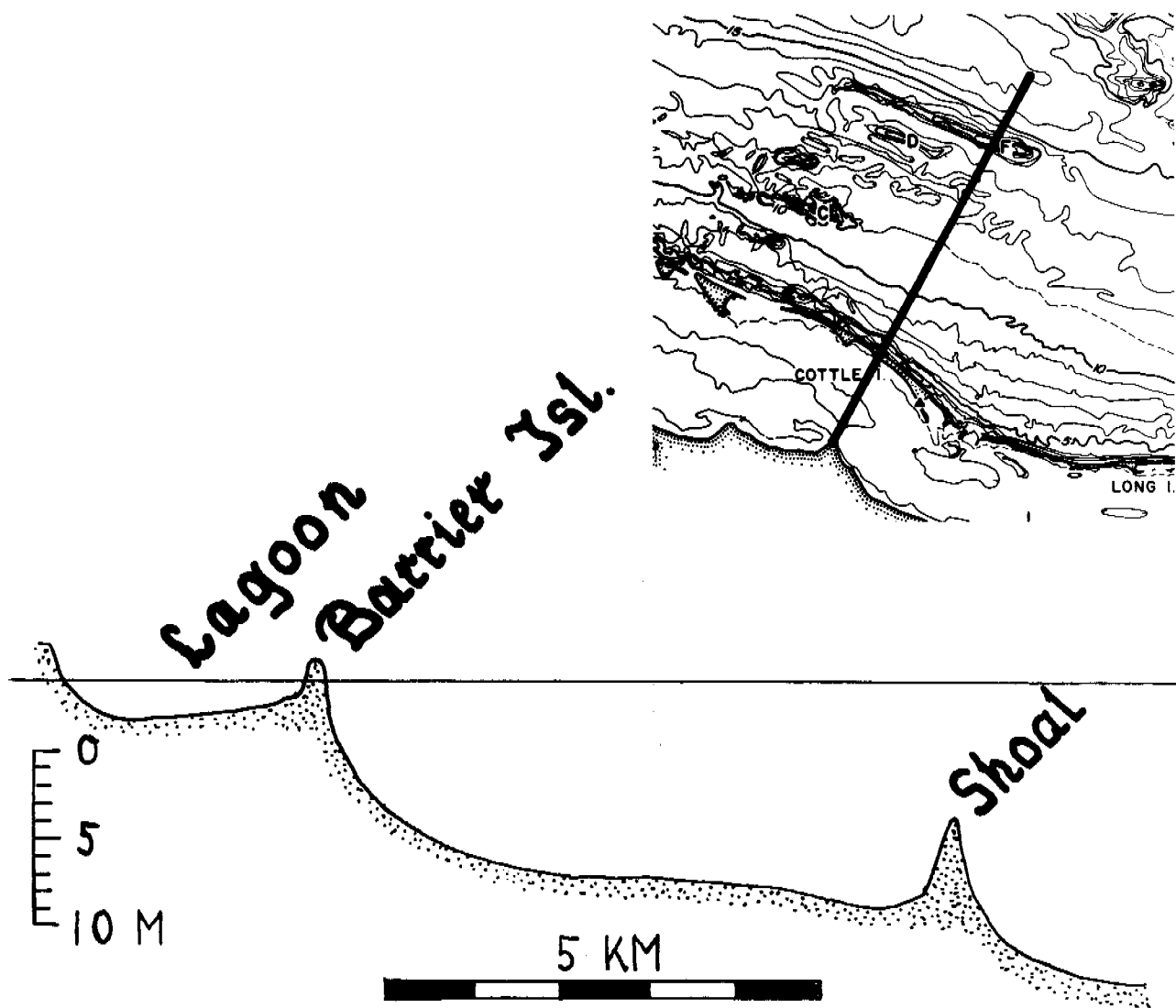


Figure 12.- Comparative profile of a modern barrier island and lagoon and one of the linear shoals. The greater height of the shoal, which should be under the levelling action of ice, is notable.

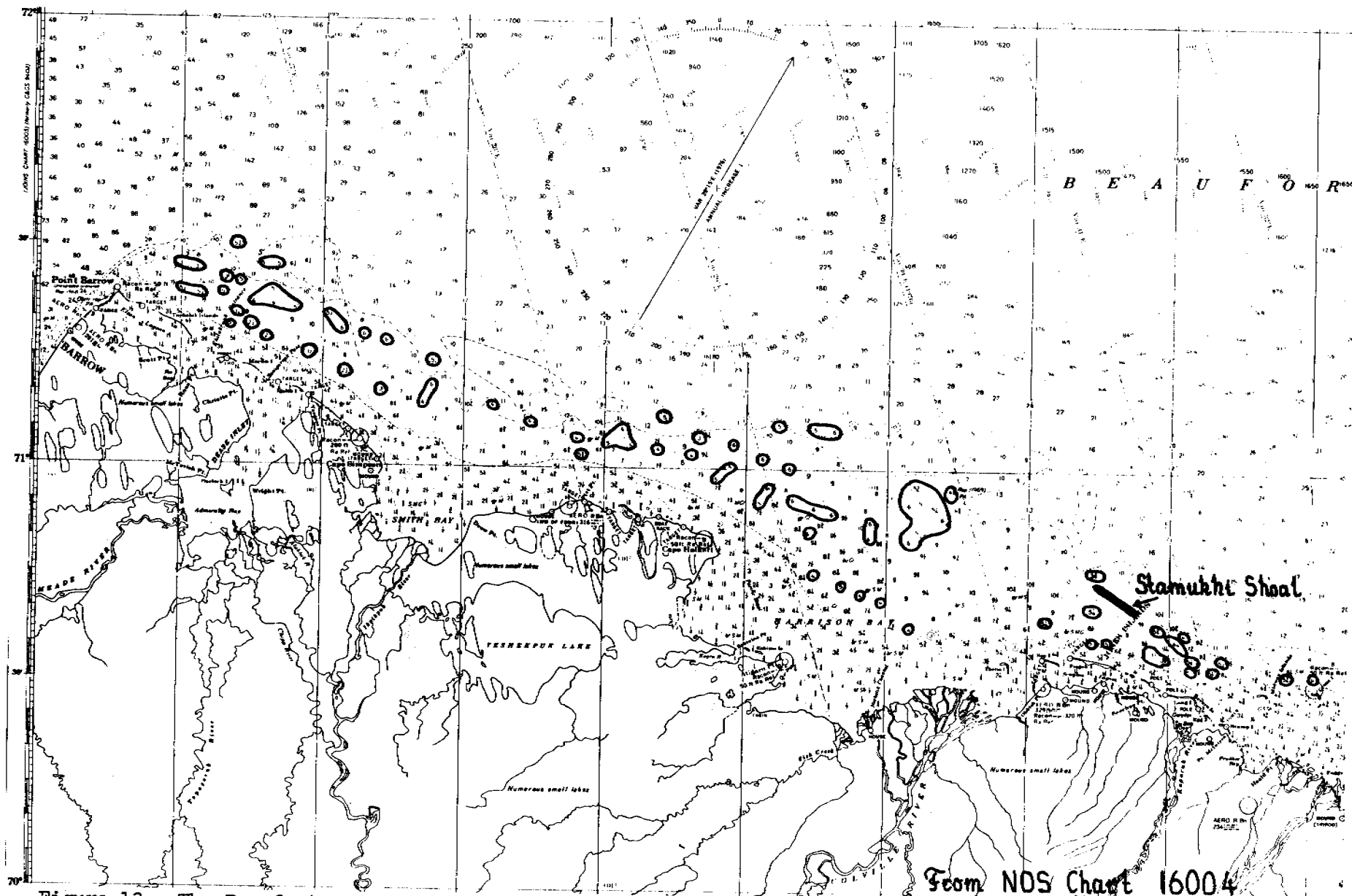


Figure 13.- The Beaufort Sea shelf from Prudhoe Bay to Point Barrow, with all charted shoals cresting shallower than 11 m on the mid shelf circled. Stamukhi Shoal lies where no shoal was indicated, and the two shoals north and south of it apparently do not exist today.

ANNUAL REPORT

Contract #RK6-6074

Research Unit #206 (Gardner & Vallier)

Research Unit #556 (Dean)

Reporting Period: March 31, 1977 -

April 1, 1978

Distributions of Grain Size, Total Carbon,
Heavy and Light Minerals, Clay Mineralogy, and Inorganic
Geochemistry, Outer Continental Shelf, Southern Bering Sea

Principal Investigators:

J. V. Gardner

T. L. Vallier

W. E. Dean

with organic geochemistry section

by K. A. Kvenvolden and G. D. Redden

Reference:

Gardner, J.V., T.L. Vallier, and W.E. Dean (1978) "Grain Size, Total Carbon, Mineralogy, and Inorganic Geochemical Data from Surface Sediments of the Southern Bering Sea Outer Continental Shelf", U.S. Geological Survey Open File Report No. 78-923.

INTRODUCTION

The U. S. Geological Survey and BLM initiated a cooperative program to evaluate potential geologic hazards on the outer continental shelf area of the southern Bering Sea (Figure 1). The principle objectives of this study are to describe the distribution and types of surface sediment, and the processes effecting these distributions.

Results reported here are based on data collected during two cruises (S4-76 and S6-77) aboard the U.S.G.S. R/V SEA SOUNDER. Sampling devices included piston and gravity corers and Sutar Van Veen sampler.

The region covered in this study centers on the St. George Basin (Figure 2) and covers an area bounded by the Aleutian Islands and Alaska Peninsula on the southeast, the shelf break at a depth of about 170m on the southwest, the Pribilof Islands on the north and the 100m isobath on the northeast.

The geologic history and structure of the region have been summarized by Scholl et al. (1958), Scholl and Hopkins (1969), Nelson et al. (1974), Marlow et al. (1975), Scholl et al. (1975), and Marlow et al. (1977). The continental margin of the Bering Sea is thought to have been an active margin during the Mesozoic when the Kula Plate was being obliquely subducted. Subduction ceased along the Bering Sea margin in the late Mesozoic or early Tertiary and jumped to the present Aleutian Trench. Tectonic deactivation of the old margin led to isostatic rebound which resulted in extensive erosion of the Mesozoic margin. Subsequently, the margin collapsed because of relaxed compressional forces and the St. George Basin probably formed as a result of this terminal collapse. Tectonic activity during the Cenozoic included faulting, basin filling, volcanism associated with the Pribilof Islands and Aleutian Island arc, sedimentation along the continental margin, and the formation of submarine canyons. St. George Basin is a surface graben which indicates that the tectonics are continuing today.

Studies of the distribution of sediments on the continental shelf of the southern Bering Sea have concentrated mainly on samples from Bristol Bay, located on the inner shelf (Sharma et al., 1972; Sharma, 1974a; 1974b; 1975). Askren (1972) investigated a broad region northwest of our area but did include 12 samples from within the area of this report.

The oceanographic circulation of the Bering Sea was initially studied by Ratmanoff (1937) who described the exchange between the Bering Sea and the Pacific Ocean. Interpretations through 1974 (e.g. Favorite, 1974; Takenouti and Ohtani, 1974) suggest that a cyclonic gyre or semi-gyre moves water eastward along the north side of the Aleutians-Alaska Peninsula, curves around to the northwest along the Southwestern Alaskan coast, and eventually turns northward and flows through the Bering Strait. The presence of a return flow to the southwest and south over the shelf has not been documented. Recently, Schumaker et al. (in prep.) reported on current-meter moorings deployed to measure long time-series surface and near-bottom currents on the southern Bering Sea outer continental shelf. They report a predominately east-west tidal flow with little net flow. The semi-gyre described above is suggested by their data but the circulation is very sluggish. Pulses of high-velocity flow do occur for a few days during storms, with peak flows up to 40cm/sec but these pulses show no net flow over a season.

METHODS

Sampling

A total of 83 stations were occupied during the 1976 and 1977 field seasons (Figure 3 and Table 1). Samples were obtained by piston corer, gravity corer, or Soutar van Veen grab depending upon the coarseness of the sediment. The tops of gravity and piston cores were soupy and essentially homogeneous to a depth of at least 30cm as a result of mixing with sea water during extraction, handling, and

cutting of the plastic core-barrel liners containing the cores. Therefore, the surface samples from gravity and piston cores represent an average sediment to a depth of at least 30cm below the sediment-water interface. Samples collected by Soutar van Veen grab were undisturbed, and are representative of surface sediment to within a few centimeters below the sediment-water interface. Subsamples for analyses of grain-size, composition of heavy ($\rho > 2.85$) and light ($\rho < 2.85$) minerals, clay mineralogy, and inorganic geochemistry were collected from the top 3cm of van Veen grab samples, and usually from the top 10cm of gravity and piston cores.

Our primary sampling grid during the 1976 field season consisted of 51 stations centered over the St. George Basin and the Pribilof Islands (Figure 3; Table 1). Duplicate (and, at a few stations, triplicate) cores were collected at 30 of these 51 stations. The main purpose of the duplicate cores was for whole-core analysis of organic components. However, subsamples of surface sediment in the duplicate (and triplicate) cores were collected to investigate intra-station variability of sediment composition based on inorganic chemical analyses. Relative locations of cores taken at the same station may vary by as much as several hundred meters, within limits of navigation and station-keeping abilities of the ship. Therefore, samples collected from different cores at each station are measuring variability in sediment composition on the order of several hundred meters, whereas samples collected at different stations are measuring variability in sediment composition on a geographic scale of 30 to 50km.

In addition to samples collected on the St. George Basin grid, 18 samples were collected in the vicinity of the Pribilof Islands, from the continental slope, and Unimak Island in the Aleutian chain (Figure 3; Table 1).

Grain size and Total carbon

Grain size was measured by first splitting samples into $>63\mu\text{m}$ and $<63\mu\text{m}$ size fractions. The $>63\mu\text{m}$ fraction was analyzed using 2-m rapid sediment analyzers

(Thiede, et al., 1976) and the $<63\mu\text{m}$ fractions were analysed with a hydrophotometer (Jordon et al., 1971). Replicate runs and calibration tests show that the rapid sediment analyses have a precision of $\pm 5\%$ and accuracy of $\pm 5\%$. The hydrophotometer has a precision of $\pm 10\%$ and an accuracy of $\pm 1\%$. Total carbon was determined by averaging three runs per sample on a LECO model WR-12. The LECO has a precision of $\pm 2\%$ and an accuracy of $\pm 1\%$.

Heavy and light minerals

Bulk samples of sediment were sieved to retrieve the 63 to $88\mu\text{m}$ fraction. This fraction was floated on diluted tetrabromoethane ($\rho = 2.85$) to separate heavy minerals and rock fragments from light minerals and rock fragments. Random-mounted slides were prepared and over 300 counts were made covering the whole area of each slide using the line method.

Clay mineralogy

All samples used for clay mineralogy, as well as all samples for other studies reported here, were kept moist in air-tight sample vials at 3°C from the time of collection until the time of preparation. The $<2\mu\text{m}$ fraction was used for clay mineralogy following the preparation procedures of Hein et al. (1975), and the semi-quantitative weighted-peak x-ray diffraction technique of Biscaye (1965). A polar planimeter was used to measure the areas under the peaks on the x-ray diffractograms. Barium saturation was attempted on several samples to help differentiate between chlorite and vermiculite. Although a peak at 7.8\AA commonly did appear, it was not well developed and was highly interpretive. Hence, barium saturation was not routinely used. Diffractograms were run from 3° to $14^{\circ} 2\theta$ and measurements of peak areas were taken on the glycolated sample. X-ray diffraction peaks corresponding to d-spacings of 7\AA , 10\AA , and 17\AA were routinely measured for chlorite/kaolinite, illite, and mixed layer clays. A slow scan between 24 and $26^{\circ} 2\theta$ was used to differentiate

kaolinite from chlorite. No internal standards were used in this study. We want to emphasize that the values shown in Appendix A are relative within this study only and should not be taken as absolute percentages of clay minerals present.

Inorganic Geochemistry

A total of 103 samples from the 65 stations in the St. George Basin grid were analyzed for 32 major, minor, and trace elements using a combination of semiquantitative optical emission spectroscopy, x-ray fluorescence, atomic absorption spectrometry, and neutron activation analysis. The details of these analytical methods are described in Miesch (1976). Eighteen of these 103 samples were chosen at random to be duplicated in the analytical laboratories. All 121 analyses were submitted in a randomized sequence. An additional suite of 29 samples from 20 stations in the vicinity of the Pribilof Islands were analyzed for concentrations of 19 major, minor and trace elements by semiquantitative optical emission spectroscopy.

Samples were air-dried and ground in a ceramic mill to pass a 100-mesh (-149 μ m) sieve. Because the samples were air dried, analytical values of Na, S, and Mg will be too high due to Na⁺, SO₄⁼, and Mg⁺⁺ dissolved in interstitial water and left as a residue after evaporation. To correct these values, we assumed that all of the Cl determined by x-ray fluorescence was due to Cl⁻ dissolved in interstitial water, and that the interstitial water contained the same proportions of Na, S, Mg, and Cl as average sea water. Interstitial water contributions of Na, S, and Mg were then subtracted from the analytical values.

RESULTS

Grain Size

Parameters calculated from values of grain size (median grain size, mean grain size, sorting, skewness, and kurtosis) are given in Table 2. Aerial distributions of mean diameters, sorting, sand, silt, clay and lithofacies are shown in Figures 4 through 10.

The salient features of the distribution of grain sizes is the bulls-eye-type pattern of finer grain size over the St. George Basin, and the band of rapid size change around the head of Pribilof Canyon and the northwestern margin of Bering Canyon. The bulls-eye pattern reflects the occurrence of finer silt in the center of the St. George Basin graben with coarser sediment which increases in abundance with distance from the center. The zones of rapid size changes coincide with areas of high topographic relief with coarser sediments at the shallower depths.

The central portion of St. George Basin is very poorly sorted (Figure 10) which reflects the lack of significant winnowing. The northwestern border of the Bering Canyon, the head of Pribilof Canyon and the topographic high of Pribilof Ridge all show moderately-sorted sediments. The size distribution for most of the sediments in the St. George Basin region are leptokurtic to very leptokurtic but in the vicinity of the Pribilof Islands the size distributions are mesokurtic. The sediments are fine- to strongly fine-skewed throughout the region.

Total Carbon

The distribution of total carbon shows a strong negative correlation with grain size (Figure 13) throughout the region. For example, concentrations of total carbon are highest in the fine-grained central region of the St. George Basin and lowest in regions where coarser-grained sand occurs. Our sediments almost completely lack biogenic carbonate and the negative correlation of carbon and grain size is almost universally observed in non-carbonate, fine-grained sediments.

Heavy and Light Minerals

A subset of 32 samples, chosen to represent the whole region under study, were analyzed for heavy and light minerals. Table 3 lists the minerals and classes of rock fragments found in the samples and Appendix A lists the percentages. Unidentifiable minerals and rocks were also recorded in the counting and included in the

subsequent statistics. Table 4 shows the univariate statistics on the percentages of heavy and light minerals and classes of rock fragments.

The heavy minerals and rock fragments (those with a specific gravity > 2.85) fall into two major classes; metamorphic and volcanic. Metamorphic components occur as a rather low-concentration background over the entire area (Figure 14).

The heavy-mineral data are plotted on a ternary diagram (Figure 16) with percentages of amphiboles, pyroxenes, and volcanic-rock fragments as end members. Data from Yukon and Kuskokwim River sediments were also analysed and are plotted for a comparison. There is a suggestion of a Yukon-Kuskokwim-type heavy-mineral assemblage projecting into the region from the north.

The light minerals and rock fragments (those with a specific gravity < 2.85) include quartz, feldspar, volcanic glass, volcanic-rock fragments and non-volcanic rock fragments (Table 3). Relative concentrations within the three-component system of feldspars, quartz and non-volcanic rock fragments, and volcanic glass and volcanic rock fragments is shown in Figure 17. Analyses of samples from the Yukon River are also plotted in Figure 17. An apron of light minerals similar in composition to that of Yukon River sediments extends into the area from the north. The distributions of glass (Figure 18) and volcanic-rock fragments (Figure 19) are similar to the distribution of heavy-mineral volcanic components, decreasing in concentration towards the northwest from the vicinity of Unimak Pass (Figure 15).

Clay Mineralogy

Relative percentages were determined for chlorite, illite, smectite and vermiculite, illite crystallinity, and the expandable and non-expandable percentages of mixed-layer clays. The univariate statistics for chlorite, illite, smectite and vermiculite, and kaolinite are given in Table 5.

The aerial distributions of illite and kaolinite show no distinct gradients or concentrations. Smectite and vermiculite are grouped together because of the

difficulty of separating them on the diffractogram. This grouping is not unreasonable because both clay minerals are the result of weathering of volcanic rocks (Biscaye, 1965). The distribution of smectite and vermiculite (Figure 20) shows a northwest-trending band of values that are greater than the mean. The highest values occur closest to the Aleutians decreasing with a northwest-trending gradient starting in the vicinity of Unimak Pass and Unimak Island. The distribution of chlorite also shows a northwest-trending band (Figure 21), but rather than being a band of higher-than-average values, it represents a zone of lower-than-average values. Chlorite is derived from low-grade metamorphic rocks and is common in high latitude marine sediments (Biscaye, 1965). The belt of lower-than-average values may be the result of dilution within this zone by smectite and vermiculite. The relative percentages of chlorite, smectite and vermiculite, kaolinite, and illite sum to 100 percent for each sample; consequently, an increase in one will result in a decrease in one or more of the others. Kaolinite and illite show an almost random distribution of values suggesting that the trends in chlorite and smectite plus vermiculite may be related.

Inorganic Geochemistry

Summary statistics for each of 30 elements in 103 samples (including 18 analytical duplicates) are given in Table 6 and the actual values are shown in Appendix B. Skewness and kurtosis statistics, histograms of raw and \log_{10} -transformed data, chi-square tests, analysis of variance, and correlation analysis indicate that frequency distributions for most of the 30 elements listed in Table 6 are more closely approximated by a lognormal than a normal distribution. Consequently, all statistical analyses are based on \log_{10} -transformed data.

Estimates of what concentration one might expect for a particular element in outer continent shelf sediments from the southern Bering Sea can be obtained using

the geometric means (GM) and geometric deviations (GD) given in Table 6. The central range of a lognormal distribution is the range in which approximately 68% of the population is estimated to occur and is within the range of GM/GD to GM x GD.

The expected range of a lognormal population is the range in which approximately 95% of the population is estimated to occur, and is defined as GM/GD² to GM x GD².

A three-level, nested analysis of variance was performed on the 30 elements in 103 samples from the St. George Basin in order to determine the relative importance of analytical error and within-station variance on the regional variability in sediment composition. The statistical model we used is as follows (Anderson and Bancroft, 1952):

$$x_{ijk} = \mu + \alpha_i + \beta_{ij} + \epsilon_{ijk}$$

where x_{ijk} is the k^{th} analytical determination of the j^{th} sample from the i^{th} station, μ is the grand mean for the entire population, α_i is the difference between the grand mean and the mean for the i^{th} station, β_{ij} is the difference between the grand mean and the mean of the j^{th} sample from the i^{th} station, and ϵ is the error in the k^{th} determination of the j^{th} sample from the i^{th} station. There are 51 stations ($i = 1$ to 51), a maximum of three samples per station ($j = 1$ to 3), and a maximum of two replicate analyses per sample ($k = 1$ to 2) used for the particular sample design.

The computation of variance components at each of the three levels within the sampling design follows the techniques described by Anderson and Bancroft (1952) using a computer program in the U.S. Geological Survey STATPAC system written by R. N. Eichner. Results of the analysis of variance are presented in Table 7. The variance components at each level are given as percentages of the total logarithmic variance. Those variance components which are significantly different from zero at the 0.05 level of probability are indicated with an asterick (*) in Table 7.

Table 7 shows that most of the geographic variability in surface sediments from the St. George Basin occurs at the station level, with only a few elements exhibiting significant variability at the sample level. This means that there are essentially no chemical differences between samples collected at the same station (i.e. there is no local variability), but there are significant differences between samples collected between stations (i.e. there is a regional component of compositional variability, on a scale of 30 to 50 km). This also means that for future investigations in this area, it would be pointless to collect more than one sample at each station.

The significant variation for most elements at the station level suggests that regional baselines for these elements can be described by maps based on station means. The variance ratio, v , was used to explore this possibility further. A test of variance on the station level, relative to the variances at the other two levels was applied. The variance ratio, v , is defined (Miesch, 1976) as the ratio of the variance among map unit (Stations in this example) to the sum of variances at all levels within a map unit:

$$v = \frac{s_{\alpha}^2}{s_{\beta}^2 + s_{\epsilon}^2}$$

where s_{α}^2 , s_{β}^2 , and s_{ϵ}^2 are respectively the logarithmic variances at the station, sample, and analytical levels. Results of this computation for each element are presented in Table 2.

The variance ratio is a measure of efficiency of the sampling design. Where the variance ratio is large, little sampling is required to describe compositional differences among map units (stations). Where the ratio is small, more sampling and (or) analytical work will be required. For purposes of constructing maps of element concentration in sediments from the St. George Basin, we used an arbitrary

cut-off value of $v = 1$ (i. e. elements for which the variance between stations is at least as large as the sum of the variances within stations). Maps of element concentration for selected elements with values of $v > 1.0$ are shown in Figures 22 to 30.

Elements that exhibit a concentration gradient decreasing from southeast to northwest, similar to the gradient observed in the andesitic components of the light and heavy mineral fractions, include Al, Ca, Mg, Fe, Na, Ti, Co, Cu, Mn, V, and Zn. Maps of concentrations of Si and K exhibit increasing concentration gradients in the same southeast to northwest direction. Maps for U, S, and Li have a bulls-eye pattern centered over the St. George Basin, similar to the pattern exhibited by maps of total carbon and grain size. Local contributions of basaltic material from the Pribilof Islands is suggested by the distributions of heavy minerals. A contribution from the Pribilof Islands is further suggested by relatively high concentrations of Mg, Ti, Co, Cu, Cr, Ni, and V in sediments in the vicinity of the Pribilofs.

DISCUSSION

The present-day continental shelf of the southern Bering Sea is extremely flat and broad. Bottom gradients typically are much less than 0.25° (1:13,000) and the large rivers that feed sediment into the Bering Sea, the Yukon, Kuskokwim, Kvichak, and to a lesser extent the Nushagak Rivers, are all over 500 km away from the St. George Basin area. Sediment is transported from these rivers into Bristol Bay but has almost no opportunity to be advected to the St. George Basin area because of the extremely low topographic gradient and insufficient watermass movement. Structural fronts in the water-column occur paralleling the 50-m isobath (Schumacher, et al., in prep.). These fronts would further impede any horizontal diffusion of detritus toward the outer continental shelf.

The Aleutian Islands and Alaskan Peninsula are potential sediment sources but the Bering Canyon (Figure 2) provides a topographic depression that traps sediment before it can get to the St. George Basin area. The sluggish, semi-gyre cyclonic circulation pattern that characterizes surface flow in the southern Bering Sea (Favorite, 1974; Takenouti and Ohanti, 1974) is only on the order of 2 to 3 cm/sec (Schumacher, et al., in prep.), much too slow to transport even clay-sized particles.

The Pribilof Islands and Pribilof Ridge also are potential sediment sources, but the low relief and small area of the features preclude any large contributions. Lack of a dominant circulation and very low current velocities also eliminates the Pribilof Ridge as a major sediment source.

Consequently, we believe that sediments are not presently being deposited on the outer continental shelf of the southern Bering Sea. This implies that all of the surface sediments are relict. Diatom floras from the bottom of each of our cores all fall within the zone (J. Barron, personal communication, 1976 and 1977), which ranges from 260,000 ybp to present (Koizumi, 1973). Thus, we are dealing with Late Quaternary, but not modern, sediments.

If we accept the relict nature of the surface sediments, then the most reasonable conditions that would allow sediments to be deposited on the outer continental shelf are glacioeustatic lower sea levels. The most reasonable estimate of the lowering of sea level during the Pleistocene glacial periods are all about 130 m (Curry, 1965; Bloom, 1971). We have drawn that shoreline along the present-day 130-m isobath and subtracted 130 m from each of the isobaths to yield a schematic bathymetric map of a low sea-level period (Figure 31). Several features of this map are worth noting. The region landward of the shoreline is featureless and flat with gradients much less than 0.25° . Any streams that flowed across this emerged shelf must have been very meandering with a dendritic distributary system. This is especially important in light of speculations by Scholl et al. (1970) that the Yukon and/or Kuskokwim

Rivers cut the Pribilof Canyon during the Pleistocene. We see no evidence of buried or surface stream channels on more than 10,000 km of high-resolution seismic data (12 kHz, 3.5 kHz, and 1.5 kHz), so we conclude that no rivers cut channels across this portion of the continental shelf during Pleistocene lower sea levels. Streams that debouched into the southern Bering Sea during glacial periods probably were not competent to transport anything but the finest-grained sediment. The heavy mineral, clay mineral, and inorganic geochemical data all support this suggestion. The mainland components are represented by metamorphic minerals and rock fragments, illite and kaolinite, and Si and K. All of these components are distributed as background with relatively low concentrations over the outer shelf.

Superimposed on this background of mainland material are northwest-trending gradients of relatively high concentrations of andesitic components, decreasing away from the Aleutian Islands in the vicinity of Unimak Pass. This Aleutian component is represented by clinopyroxene, orthopyroxene, olivene, volcanic rock fragments, smectite+vermiculite, Al, Ca, Mg, Fe, Ti, Co, Cu, Mn, V, and Zn. Volcanic debris is also distributed as an aureole of local extent around the Pribilof Islands. These northwest-trending gradients reflect a longshore transport of clay- to sand-size material from the Aleutians during periods of low sea levels. The northwest-trending gradients for most compositional variables decrease away from the Aleutians, which strongly suggests that the island arc is the major source of sediments to the outer shelf. Much and perhaps the vast majority of detritus shed off the Aleutians was trapped by the Bering Canyon and funnelled into the deeper regions of the continental rise. However, some material was apparently captured by longshore drift and transported onto and along the narrow shelf. Possibly the head of Bering Canyon periodically filled up, which allowed sediment to be transported across to the shelf before slumping cut off this path. The data also suggest that a relatively

strong, cyclonic, nearshelf, circulation existed that was competent to transport coarse sediment along the shelf.

When sea level rose during periods of glacial to interglacial transition, the shift in the position of the shoreline must have been generally quite rapid because of the very low topographic gradients (Figure 32). If we use the Pleistocene to Holocene transgression as a model, then initially the retreat of the shoreline was slow with a 50-m rise in sea level producing a transgression of about 70 km. Sea level curves (Curry, 1960; 1961; Mörner, 1971, Bloom, 1971) indicate that the first 50-m rise in sea level took about 5,000 years. However, the next 10-m rise in sea level produced a 175-km retreat of the shoreline in only about 1,000 years. The remaining 70-m rise in sea level caused a 250-km transgression in the remaining 6,000 to 8,000 years. The point is, when the shoreline began retreating, it did so rapidly and, in effect, deserted a sedimentation pattern with little modification. The result would be a glacial-period sedimentation pattern and an interglacial-period oceanographic circulation, as appears today.

The present-day oceanographic conditions have modified the distribution and character of the sediments somewhat. Maps of lithofacies and sorting (Figures 9 and 10) show that a tongue of moderately sorted, coarse sediments extends along the shelf break south of Pribilof Canyon and along the northern flank of Bering Canyon. The tongue south of Pribilof Canyon seems to be restricted in extent and this restriction coincides with the steepest portion of the continental slope. Conversely, the poorest sorting and finest grain sizes are found in the center of the St. George Basin region. This distribution of textures can be explained by a combination of long-period storm waves and a gravity potential. Komar *et al.* (1972) show that waves with a 15-second period cause rippling of sandy sediments off the Oregon coast in water depths down to 204 m. Twelve-second period waves affect depths down to 149 m. Thus, high sea states that occur in the Southern

Bering Sea during the late summer and fall can affect the bottom sediments of the outer shelf region. Resuspension of surface sediments by long-period storm wave would increase the density of the shelf-bottom boundary layer with the incorporation of clay and silt. The coarser sediment would probably fall out of suspension quickly. If this dense boundary layer were located in an area closely adjacent to a gravity potential (i.e., a region with a slope of perhaps 2° or more), then the dense boundary layer would flow down slope and out of the area. This mechanism would tend to winnow out the fine-grain sizes and impart a better sorting to the sediment that remains behind. The patterns of textural parameters (Figures 9 and 10) show this result. The broad continental slope north of Bering Canyon has gradients of about 1.5° and apparently is too gentle to provide the critical gravity potential, thus little winnowing is occurring there. However, the slope just south of Pribilof Canyon has gradients in excess of 3° and evidence of winnowing is present.

Sediments in the St. George Basin area also are affected by these long-period storm waves but, because of the lack of a gravity potential, the shelf-bottom boundary layer sloshes back and forth with no significant net transport and the sediment is redeposited in the same general area. The fact that St. George Basin is a surface graben also helps explain the general lack of transport of sediment out of this area. Storm waves mix sediments in the St. George Basin area but the only apparent affect is to obscure the boundaries between the textural provinces and to concentrate finer-grained and more poorly sorted sediment into a bullseye pattern.

Distributions patterns of grain size do not reflect the graded-shelf size distribution described by Sharma et al. (1972). However, their sampling stations stop along the northeastern boundary of the area covered by our data. When the data of Sharma et al. (1972) are joined to our data, the two complement each other very well, yet each tells a different story. Their data are concentrated in the shallow (less than 100 m) reaches of Bristol Bay and reflect a gradual decrease in grain

size with distance from shore. Our data are concentrated in depths greater than 100 m, and show the overprints of the effects of topographic (gravity) controls on the redistribution of sediment. Bristol Bay is persistently affected by storm waves because even the relatively short-period waves can affect the sediment surface. The outer shelf is immune to the normal sea state because of depth and only periodic large storm waves affect the bottom in the sea floor in this region and only for short durations.

REFERENCES CITED

- Anderson, R. L. and Bancroft, T. A., 1952, Statistical theory in research: New York, McGraw-Hill Book Co., 399 p.
- Askren, D. R., 1972, Holocene stratigraphic framework-southern Bering Sea continental shelf: MS Thesis, Univ. of Washington, 104 p.
- Biscaye, P. E., 1965, Mineralogy and sedimentation of Recent Deep-sea clay in the Atlantic Ocean and adjacent seas and oceans: Geol. Soc. Amer. Bull., v. 76, p. 803-831.
- Bloom, A. L., 1971, Glacial-eustatic and isostatic controls of sea level since the last glaciation: in Turekian, K. K. (ed.) Late Cenozoic Glacial Ages, Yale Univ. Press, New Haven, p. 355-379.
- Curry, J. R., 1960, Sediments and history of Holocene transgression, continental shelf, northwest Gulf of Mexico: in Shepard, F. P., Phleger, F. B., and van Andel, T. H. (eds.), Recent Sediments, Northwest Gulf of Mexico, Tulsa, Oklahoma, Am. Assoc. Petroleum Geologists, p. 221-266.
- _____ 1961, Late Quaternary sea level: a discussion: Geol. Soc. Amer. Bull., v. 72, p. 1707-1712.
- _____ 1965, Late Quaternary history, continental shelves of the United States: in Wright, H. E., Jr., and Frey, D. G. (eds.), The Quaternary of the United States, Princeton, N.J., Princeton University Press, p. 723-735.
- Favorite, F., 1974, Flow into the Bering Sea through Aleutian passes: in Hood, D. W. and Kelley, E. J. (eds.), Oceanography of the Bering Sea, Inst. of Marine Science, Univ. of Alaska, Occasional Publ. 2, p. 3-37.
- Folk, R. L., and Ward, W. C., 1957, Brazos River bar: a study in the significance of grain size parameters: Jour. Sed. Petrology, v. 27, p. 3-27.
- Hein, J., Scholl, D. W., and Gutmaker, C., 1975, Neogene clay minerals of the far northwest Pacific and Southern Bering Sea: Sedimentation and diagenesis. in Bailey, S. W. (ed.), AIPEA proceedings, International Clay Conf., Mexico City, p. 71-80.
- Jordon, C. F., Jr., Fryer, G. E., and Hemmen, E. H., 1971, Size analysis of silt and clay by hydrophotometer: Jour. Sed. Petrology, v. 41, p. 489-496.
- Koizumi, J., 1973, The Late Cenozoic diatoms of sites 183-193, Leg 19, Deep Sea Drilling Project: in Creager, J. S., Scholl, D. W., and others, Initial Reports of the Deep Sea Drilling Project, v. 19. Washington, D.C., p. 805-856.
- Komar, P. D., Neudeck, R. H., and Kuhn, L. D., 1972, Observations and significance of deep-water oscillatory ripple marks on the Oregon continental shelf: in Swift, D. J. P., Duane, D. B., and Pilkey, O. H., Shelf Sediment Transport Process and Patterns, Dowden, Hutchinson, and Ross, Inc., p. 601-619.

- Marlow, M. S., Scholl, D. W., and Cooper, A. K., 1975, Structure and evolution of the Bering Sea shelf south of St. Lawrence Island: *Am. Assoc. of Petroleum Geologists Bull.*, v. 60, p. 161-183.
- _____ 1977, St. George Basin, Bering Sea shelf: A Collapsed Mesozoic Margin: *in* Island Arcs, Deep-Sea Trenches, and Back-Arc Basins, v. 1, Amer. Geophys. Union (Ewing Volume), p. 211-219.
- Miesch, A. T., 1976, Geochemical Survey of Missouri, Methods of sampling, laboratory analysis, and statistical reduction of data: U.S. Geol. Survey Prof. Paper, 954-A, 39 p.
- Mörner, N., 1971, Eustatic changes during the last 20,000 years and a method of separating the isostatic and eustatic factors in an uplifted area: *Paleogeography, Paleoclimatology, Paleoecology*, v. 9, p. 153-181.
- Nelson, C. H., Hopkins, D. M., and Scholl, D. W., 1974, Cenozoic sedimentary and tectonic history of the Bering Sea: *in* Hood, D. W., and Kelley, E. J. (eds.), *Oceanography of the Bering Sea*, Inst. of Marine Science, Univ. of Alaska, Occasional Publ. 2, p. 485-516.
- Ratmanoff, G. E., 1937, Explorations of the seas of Russia: *Publ. Hydrol. Inst.* 25, p. 1-175.
- Scholl, D. W., Buffington, E. C., and Hopkins, D. M., 1968, Geologic history of the continental margin of North America in Bering Sea: *Marine Geology*, v. 6, p. 297-330.
- Scholl, D. W., and Hopkins, D. M., 1969, Newly discovered Cenozoic basins, Bering shelf, Alaska: *Amer. Assoc. Petroleum Geologists, Bull.*, v. 53, p. 2067-2078.
- Scholl, D. W., Buffington, E. C., Hopkins, D. M., and Alpha, T. R., 1970, The structure and origin of the large submarine canyons of the Bering Sea: *Marine Geology*, v. 8, p. 187-210.
- Scholl, D. W., Buffington, E. C., and Marlow, M. S., 1975, Plate tectonics and the structural evolution of the Aleutian-Bering Sea region: *in* Forbes, R. B., (ed.), *Contributions to the Geology of the Bering Sea Basin and Adjacent Regions: Geol. Soc. America Spec. Paper 151*, p. 1-32.
- Schumacher, J. D., Kinder, T. H., Pashinski, D. J., and Charnell, R. L., in prep., Structural fronts over the continental shelf of the eastern Bering Sea: submitted to *J. Physical Ocean.*
- Sharma, G. D., 1974, Contemporary depositional environment of the eastern Bering Sea: *in* Hood, D. W. and Kelley, E. J., (eds.), *Oceanography of the Bering Sea*, Inst. of Marine Science, Univ. of Alaska, Occasional Publ. 2, p. 517-540.
- _____ 1975, Contemporary epicontinental sedimentation and shelf grading in the southeast Bering Sea: *in* Forbes, R. B. (ed.), *Contributions to the geology of the Bering Sea Basin and adjacent Regions*, *Geol. Soc. Amer. Spec. Pap. 151*, p. 33-48.

Sharma, G. D., Nardu, A. S., and Hood, D. W., 1972, Bristol Bay: A model contemporary graded shelf: Amer. Assoc. Petroleum Geologists, v. 56, p. 2000-2012.

Takenouti, A. Y., and Ohtani, K., 1974, Currents and water masses in the Bering Sea: A review of Japanese work: in Hood, D. W. and Kelley, E. J., (eds.), Oceanography of the Bering Sea, Inst. of Marine Science, Univ. of Alaska, Occasional Publ. 2, p. 39-57.

Thiede, J., Chriss, T., Clauson, M., and Swift, S. A., 1976, Settling tube for size analysis of fine and coarse fractions of oceanic sediments: Oregon State Univ., School of Oceanography, Reference 76-8, 87 p.

Wentworth, C. K., 1922, A scale of grade and class terms clastic sediments: Jour. Geol., v. 30, p. 377-392.

List of Figures

- Figure 1. Index map
- Figure 2. Bathymetric chart of the outer continental shelf, southern Bering Sea.
- Figure 3. Sample locations from cruises S4-76 and S6-77. See Table 1 for core identifications.
- Figure 4. Map of mean diameters (ϕ values) of surface sediment samples.
- Figure 5. Distribution of sand (in percent by weight) of surface samples.
- Figure 6. Distribution of silt (in percent by weight) of surface samples.
- Figure 7. Distribution of clay (in percent by weight) of surface samples.
- Figure 8. Ternary diagrams showing facies fields (Wentworth, 1922).
- Figure 9. Lithofacies map (see Figure 8 for field, sand-silt-clay).
- Figure 10. Distribution of sorting values of surface samples.
- Figure 11. Sorting plotted against mean grain size.
- Figure 12. Skewness plotted against mean grain size.
- Figure 13. Distribution of total carbon (in percent by weight).
- Figure 14. Distribution of metamorphic components of heavy minerals.
- Figure 15. Distribution of volcanic components of heavy minerals.
- Figure 16. Distribution of heavy mineral components ($\rho > 2.85$). See Figure 8 for fields, pyroxenes-amphiboles-volcanic rock fragments.
- Figure 17. Distribution of major light components ($\rho < 2.85$). See Figure 8 for fields, quartz and non-volcanic rock fragments-feldspars-volcanic rock fragments and glass.
- Figure 18. Distribution of volcanic glass.
- Figure 19. Distribution of volcanic components ($\rho < 2.85$).
- Figure 20. Map showing the distribution of smectite and vermiculite.
- Figure 21. Map showing the distribution of chlorite.

- Figure 22. (a) Distributions of aluminium and (b) calcium.
- Figure 23. (a) Distributions of magnesium and (b) iron.
- Figure 24. (a) Distributions of sodium and (b) titanium.
- Figure 25. (a) Distributions of cobalt and (b) copper.
- Figure 26. (a) Distributions of manganese and (b) vanadium.
- Figure 27. (a) Distributions of zinc and (b) silica.
- Figure 28. (a) Distributions of potassium and (b) uranium.
- Figure 29. (a) Distributions of sulfur and (b) lithium
- Figure 30. (a) Distributions of chromium and (b) nickel.
- Figure 31. Map showing bathymetry, inferred currents and possible sediment transport paths during glacio-eustatic lower sea levels of approximately 130 m.
- Figure 32. Bathymetric profile of the continental margin. Note the extreme flatness between the 130 and 140 m isobaths and the change in slope gradient above 130 m. Each data point on the shelf represents a 5-m isobath.

List of Tables and Appendices

- Table 1. Index of samples to locations on Figure 3.
- Table 2. Grain size statistical phi values (Folk and Ward, 1967).
- Table 3. Heavy and light minerals and classes of rock fragments.
- Table 4. Univariate statistics on percentages of heavy and light minerals and classes of rock fragments.
- Table 5. Univariate statistics for the relative percentages of clay minerals.
- Table 6. Summary statistics for concentrations of major, minor, and trace elements in samples of surface sediments from the St. George Basin.
- Table 7. Analysis of variance of concentrations of major, minor, and trace elements in samples of surface sediments from the St. George Basin.
- Appendix A Analytical results for grain size, total carbon, heavy and light minerals, and clay mineralogy for samples identified in Table 1.
- Appendix B Analytical results of inorganic geochemical parameters for samples identified in Table 1.

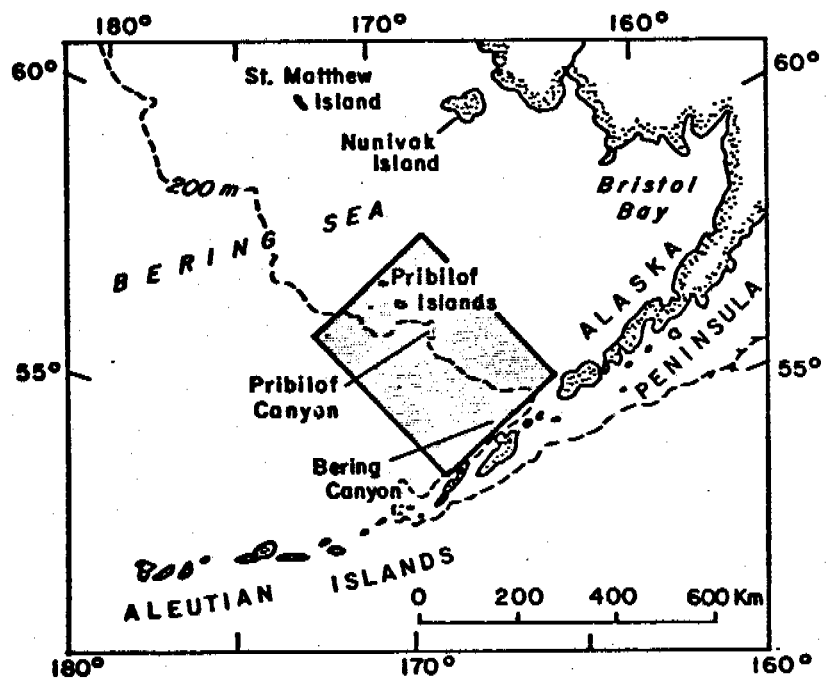
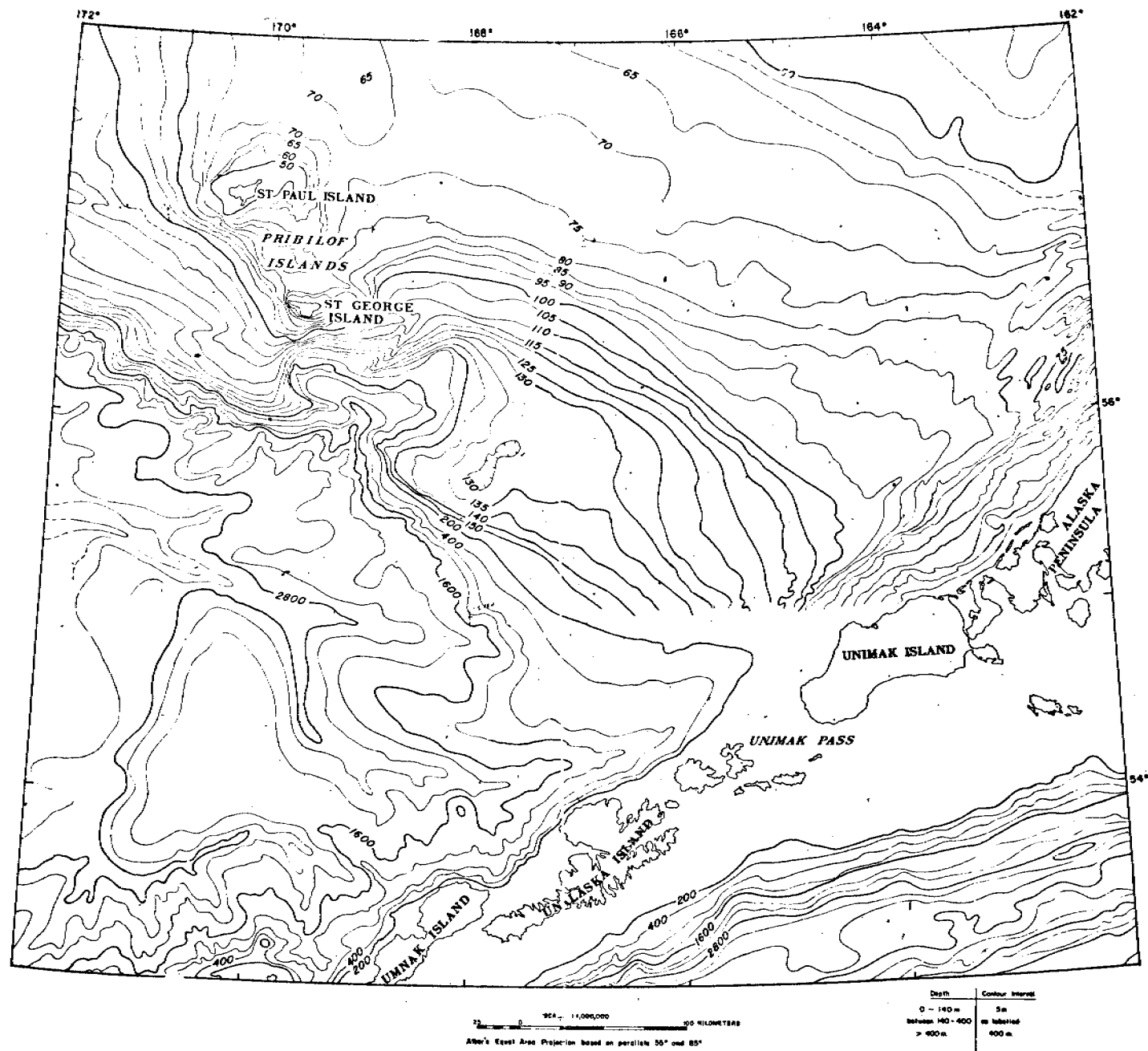


Figure 1



BATHYMETRY OF SOUTHERN BERING SEA REGION

Figure 2

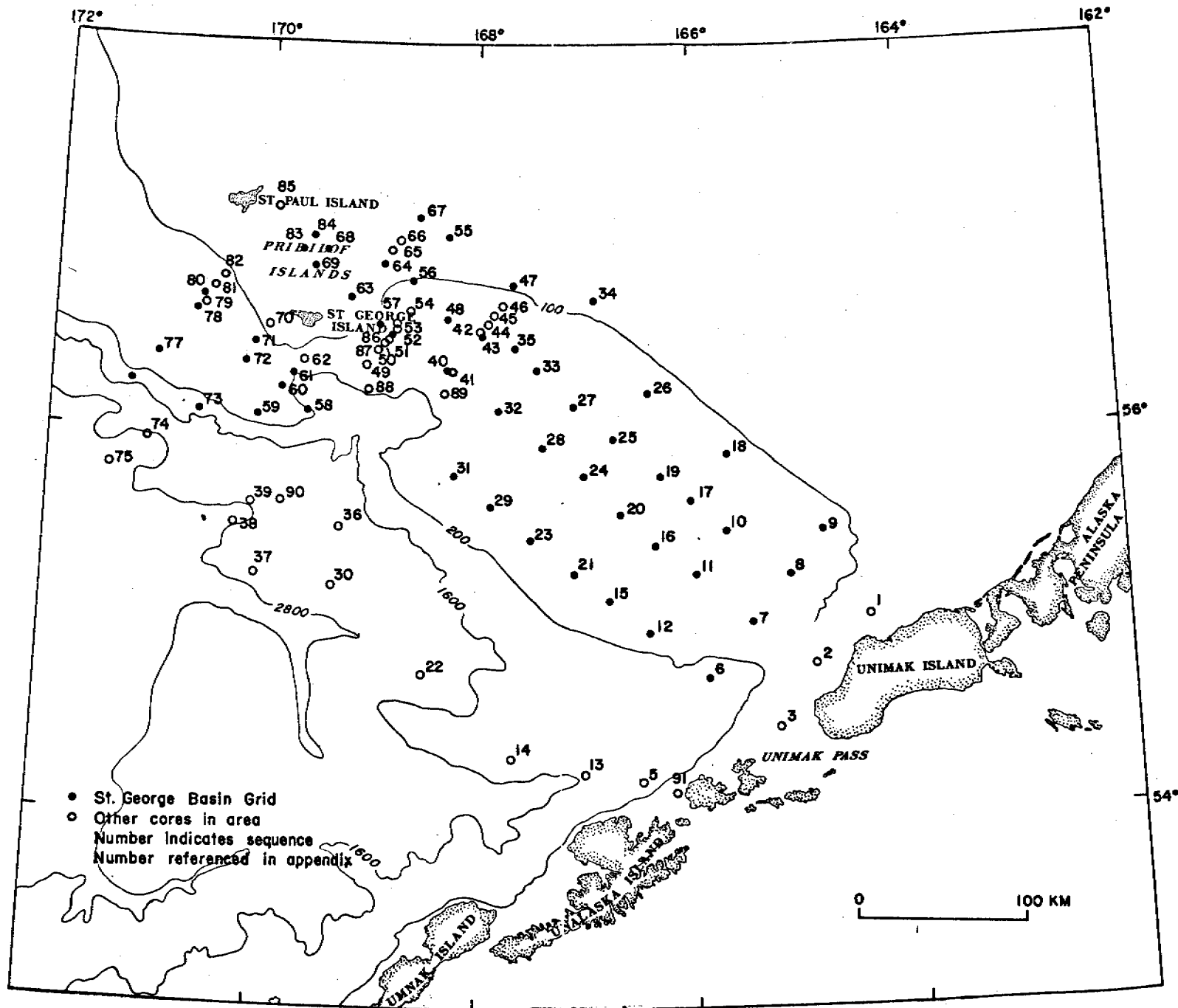


Figure 3

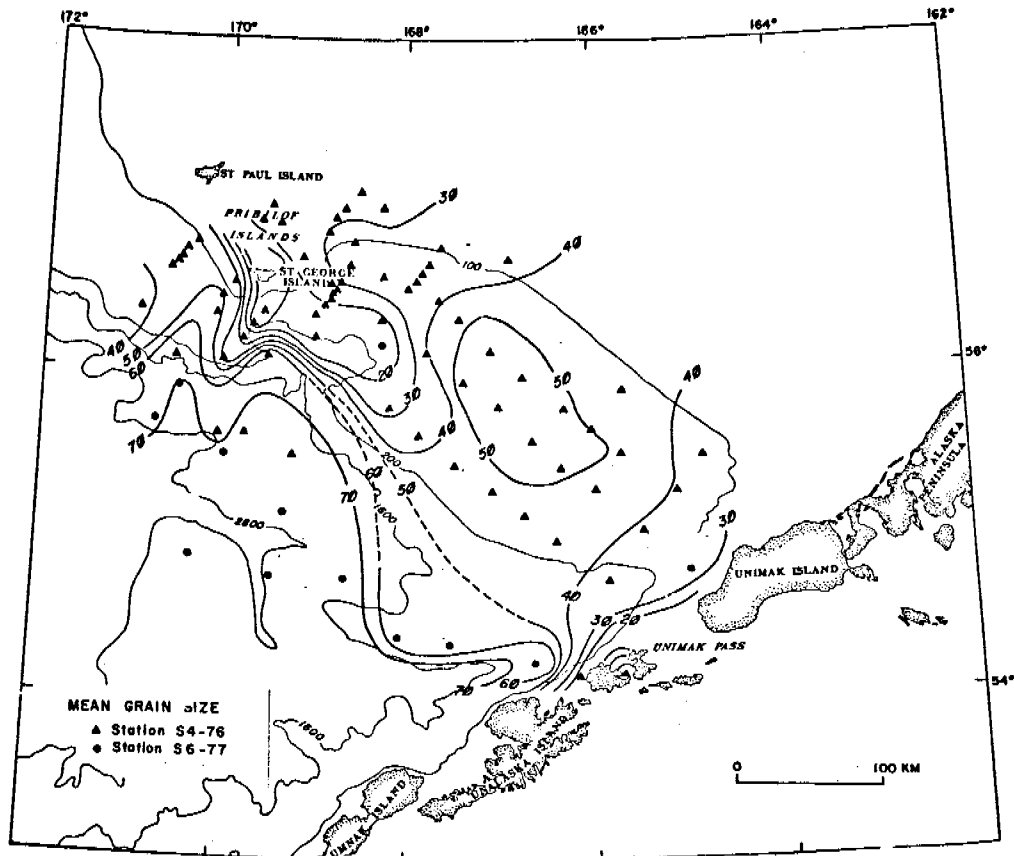
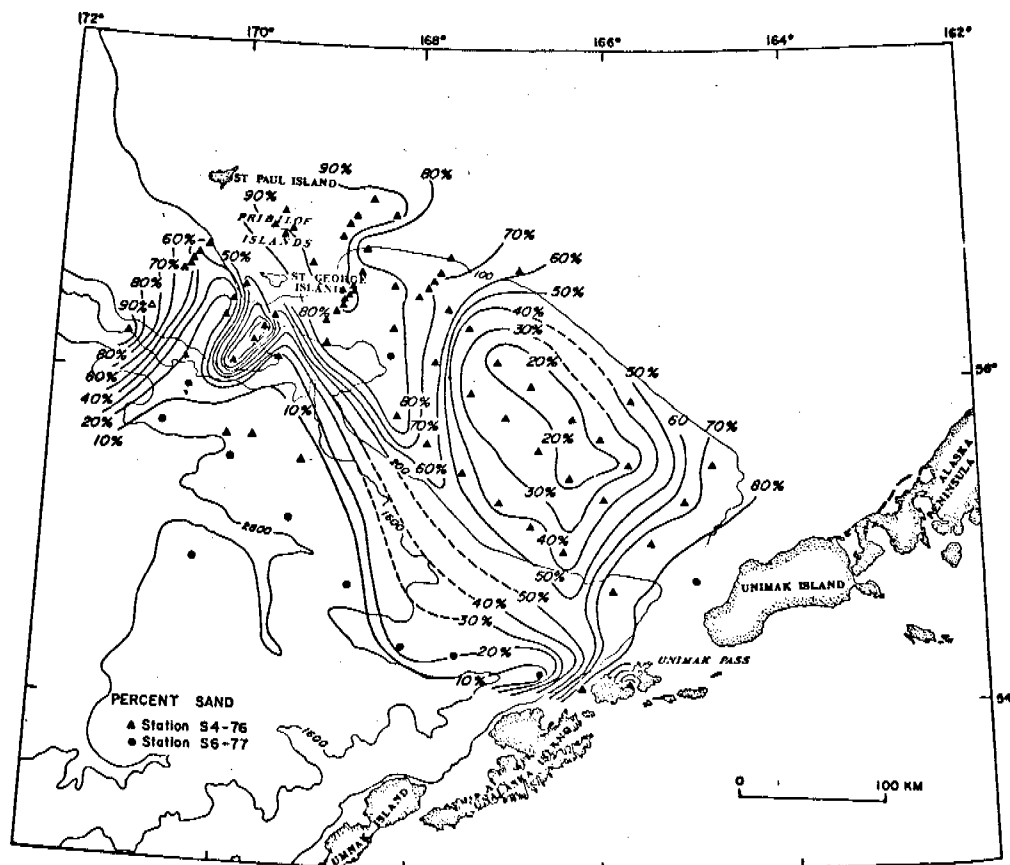


Figure 4



326 Figure 5

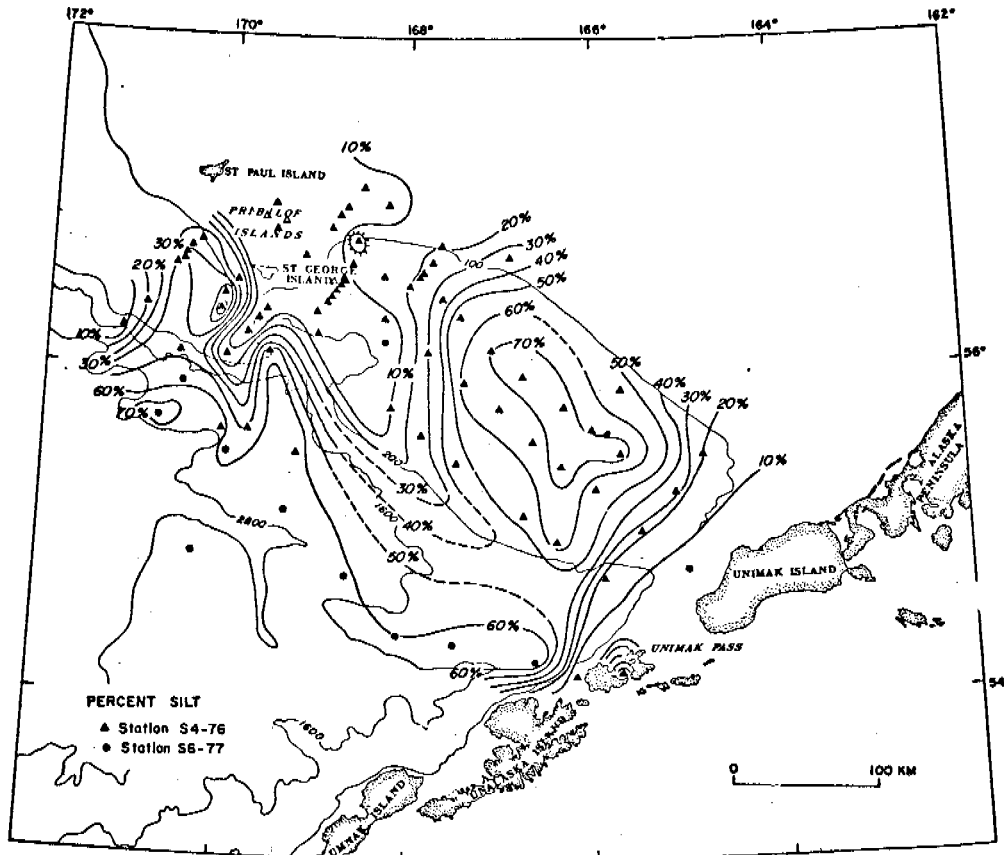


Figure 6

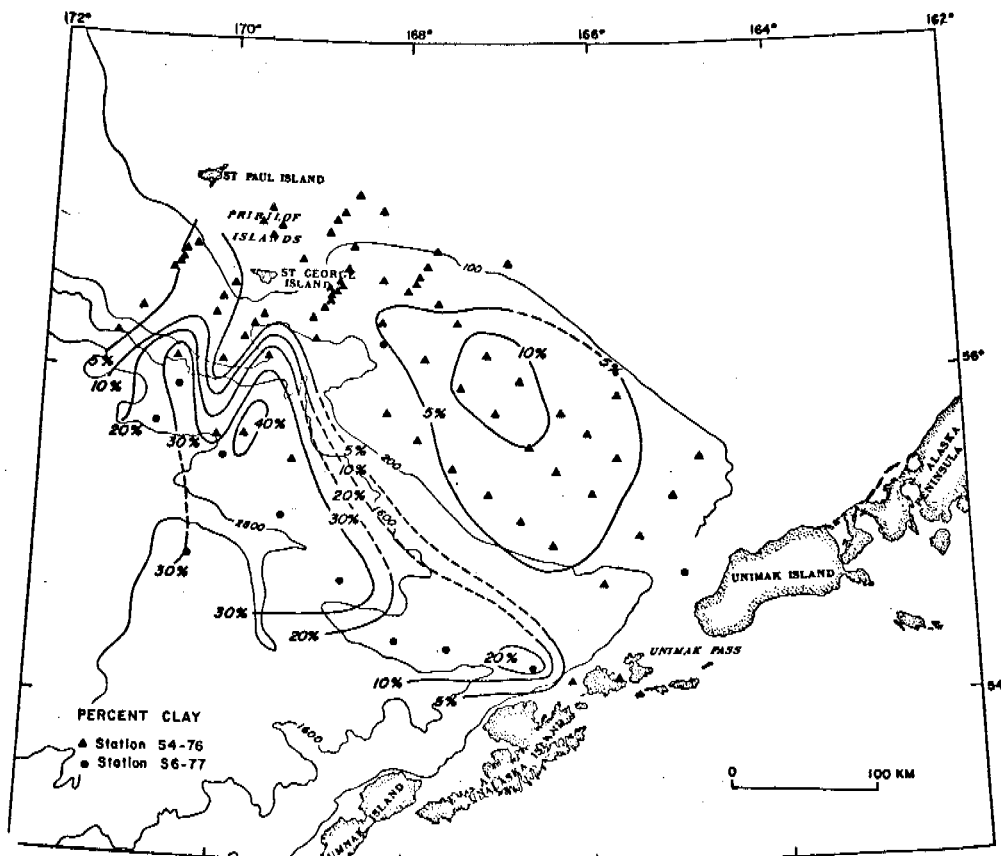


Figure 7 327

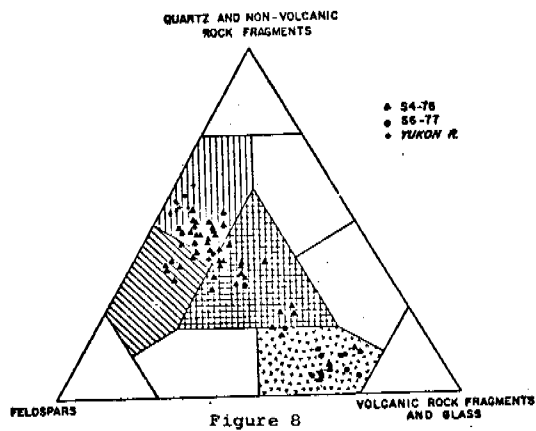
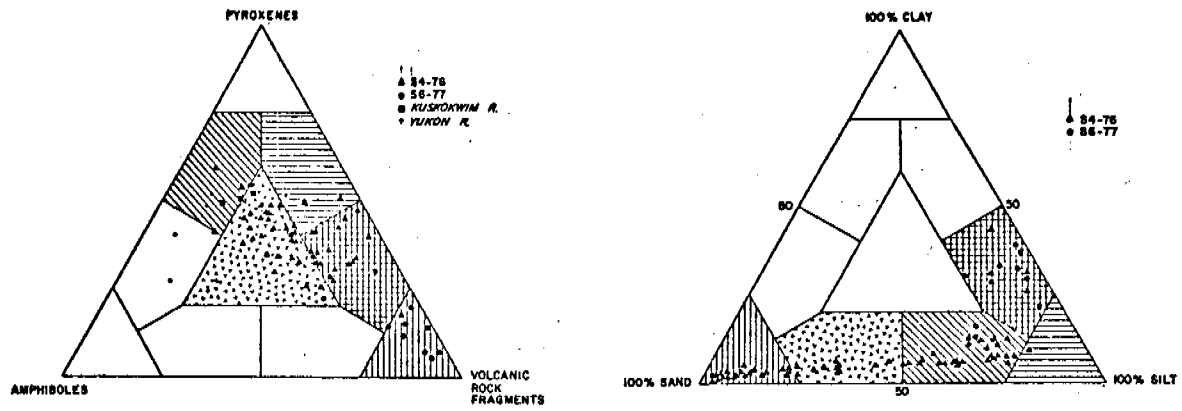


Figure 8

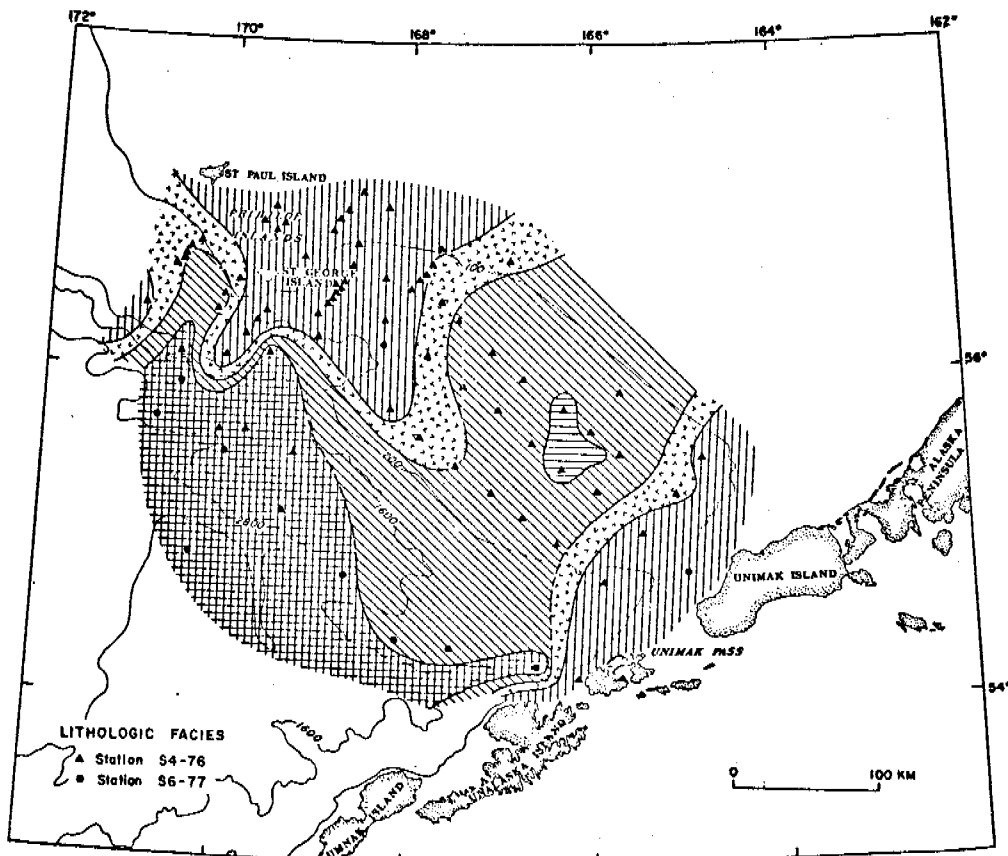


Figure 9 328

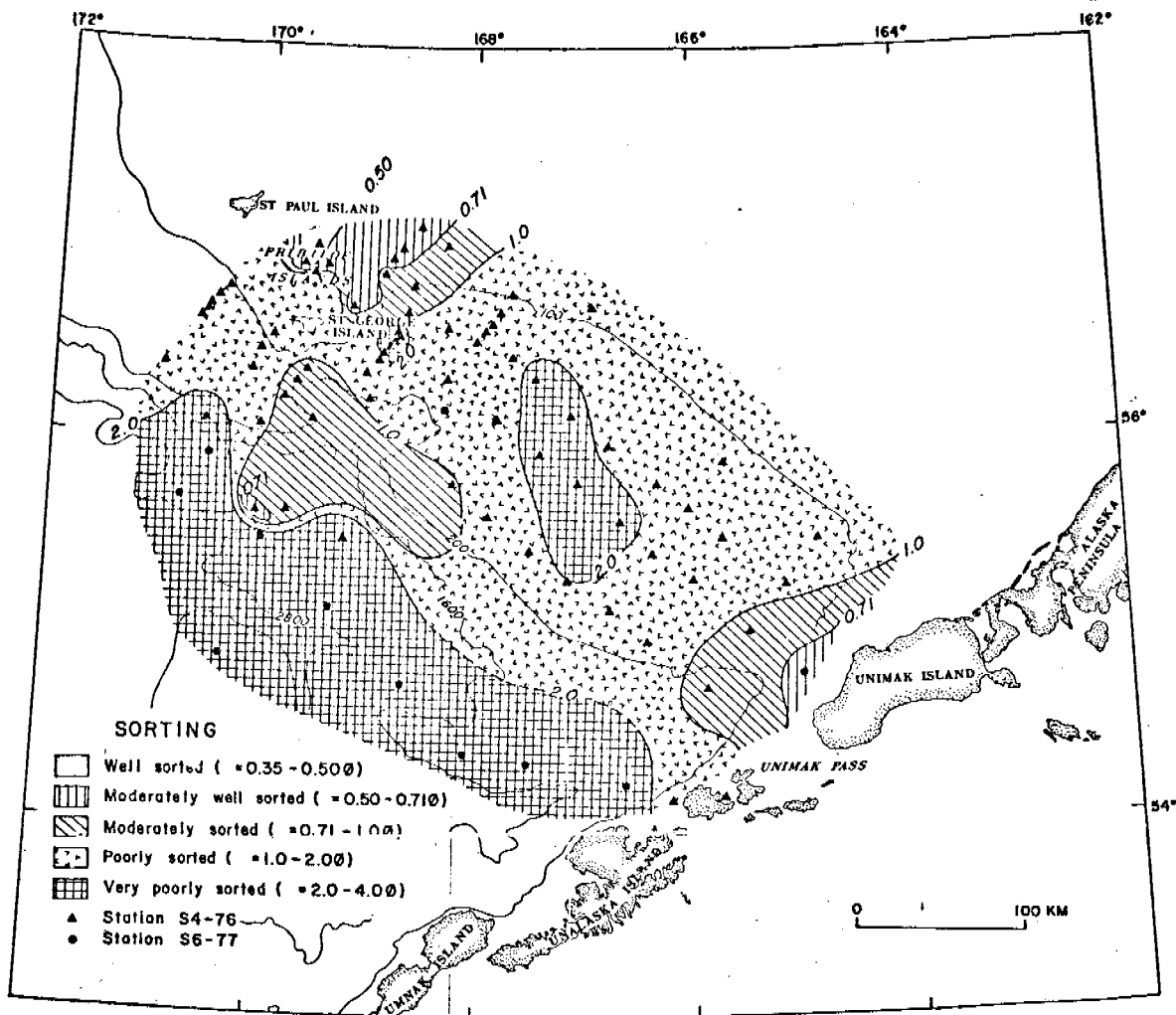


Figure 10

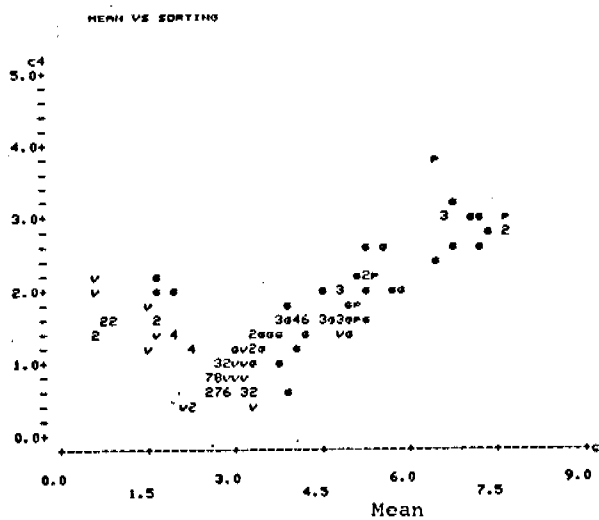


Figure 11

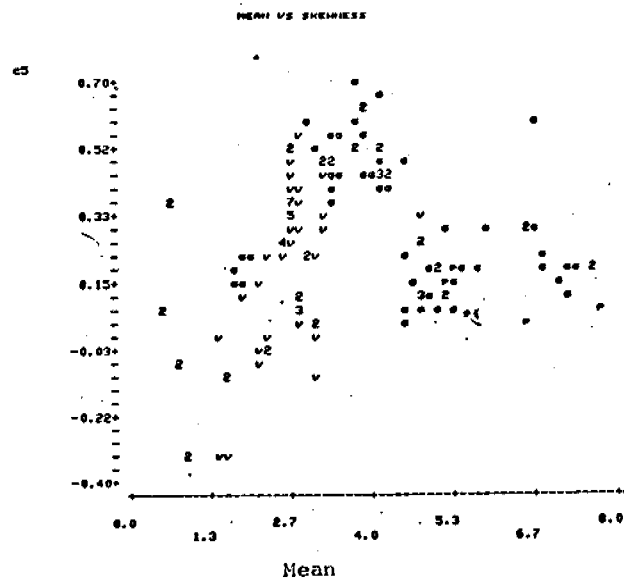


figure 12

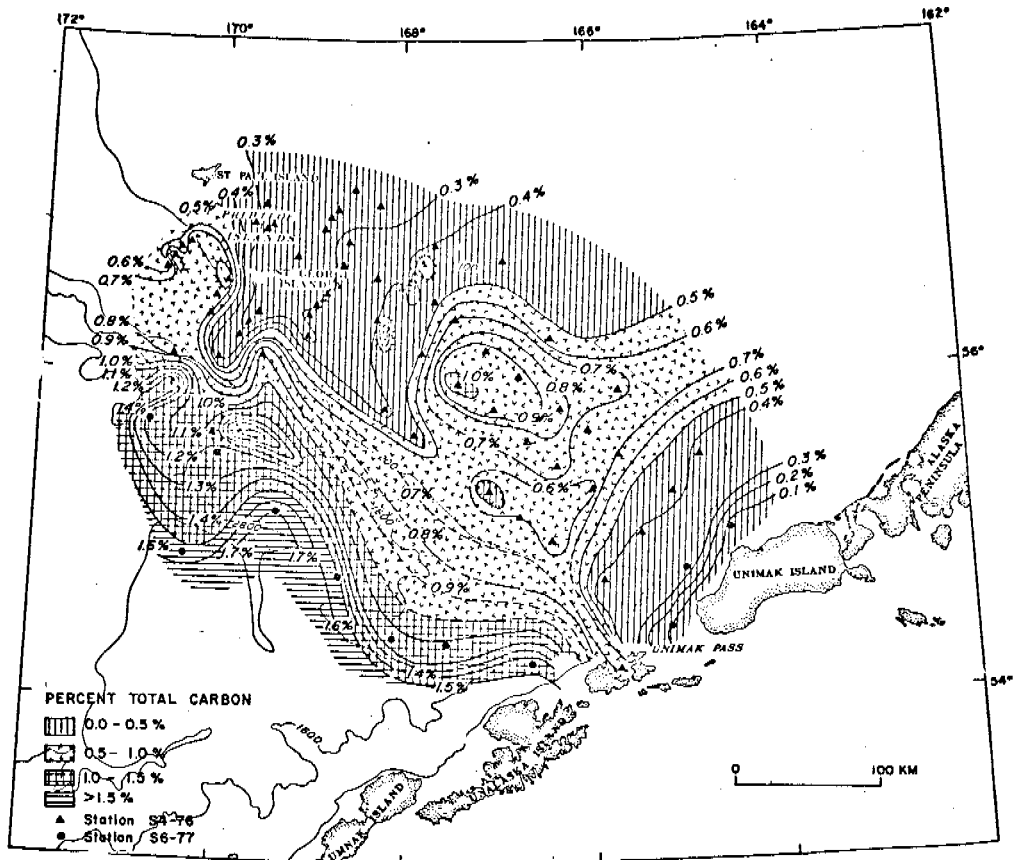


Figure 13

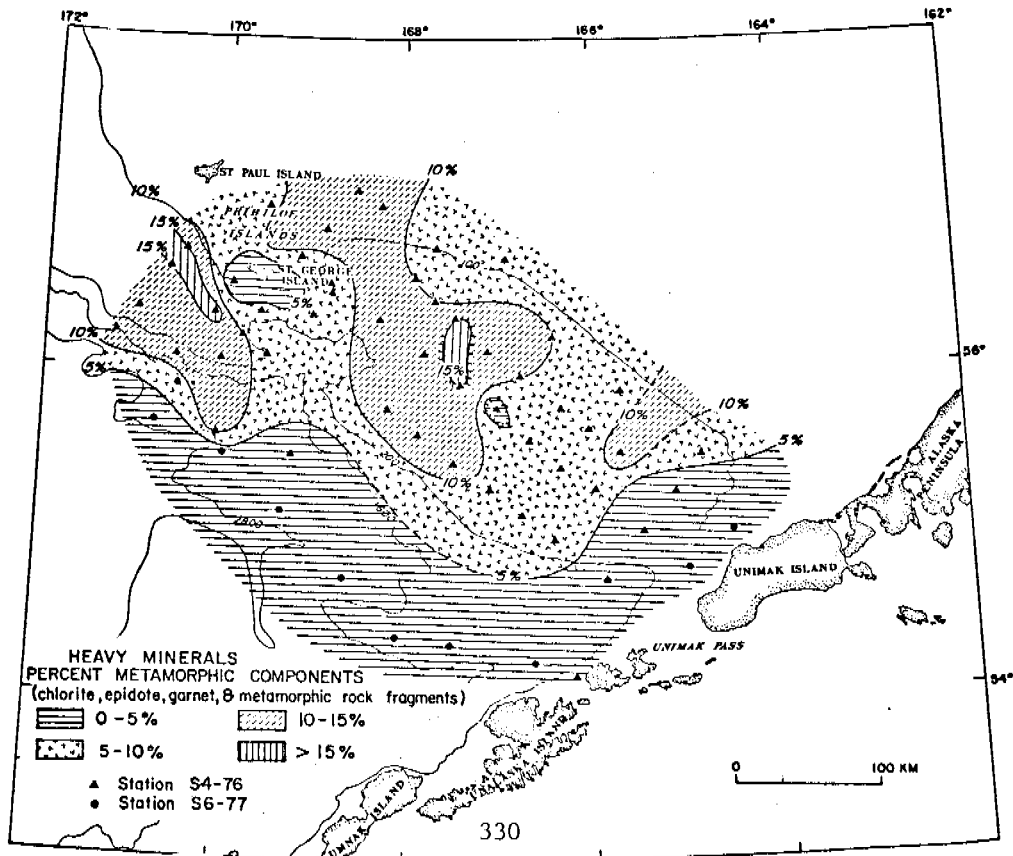


Figure 14

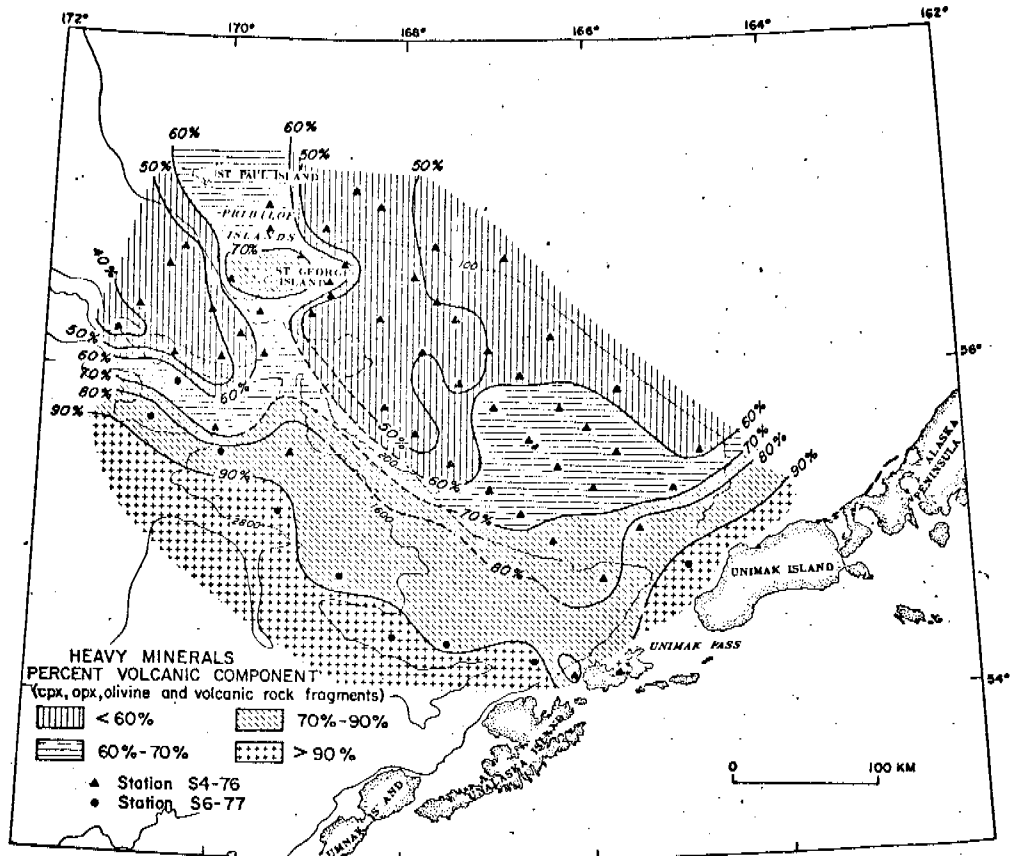


Figure 15

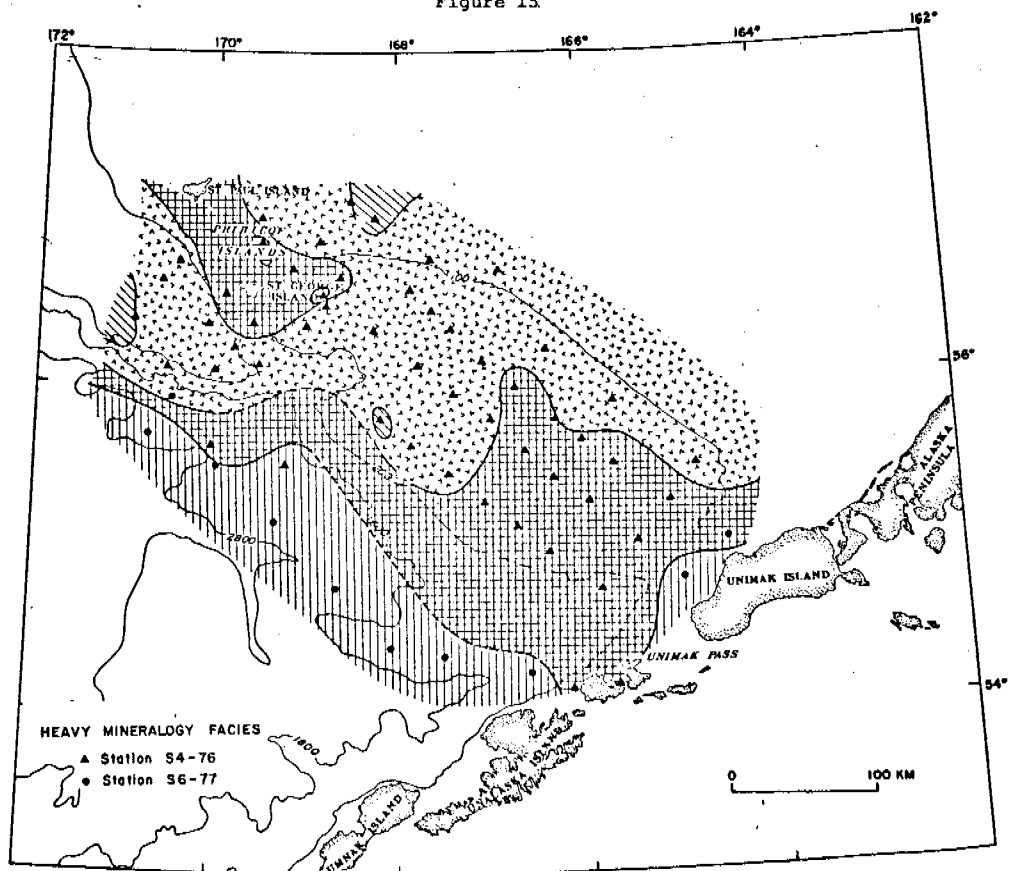


Figure 16

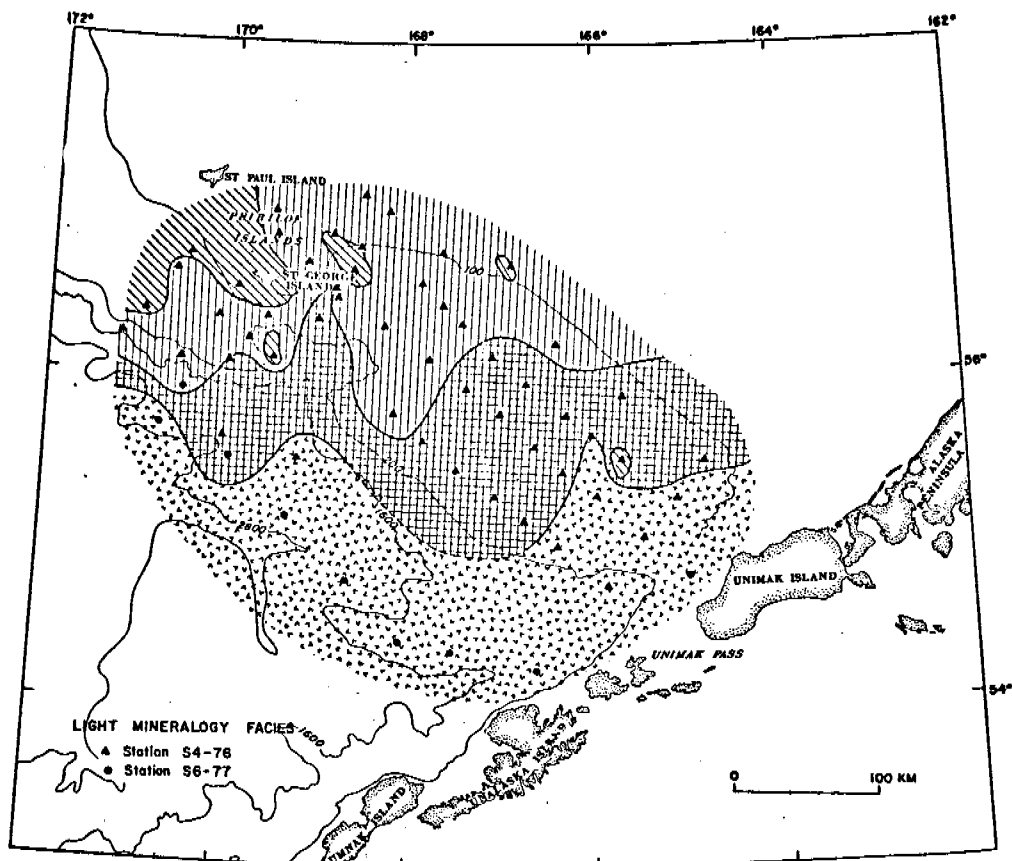


Figure 17

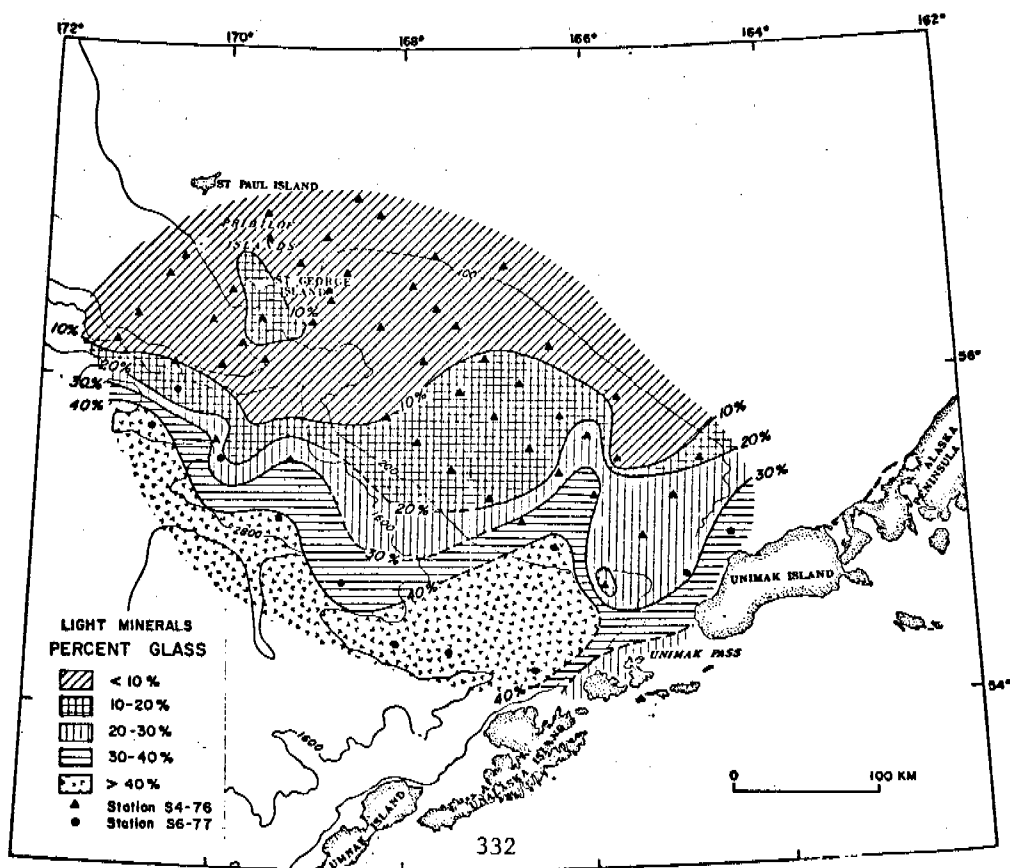


Figure 18

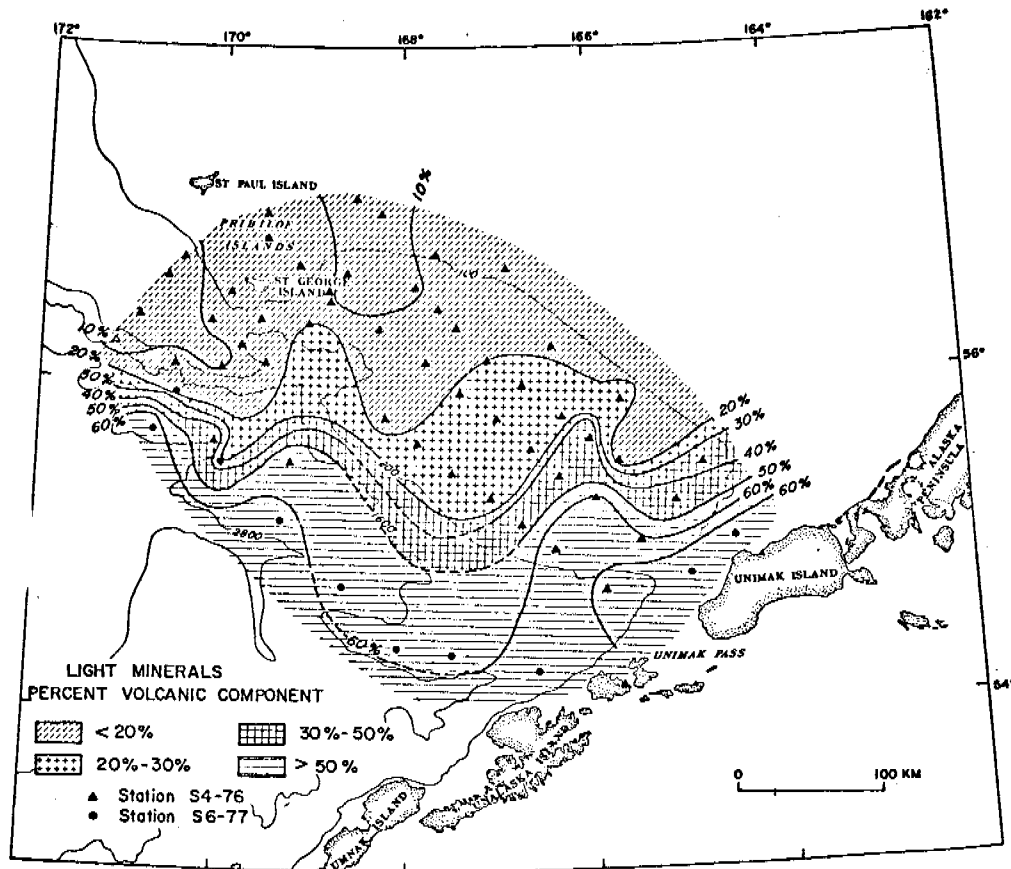


Figure 19

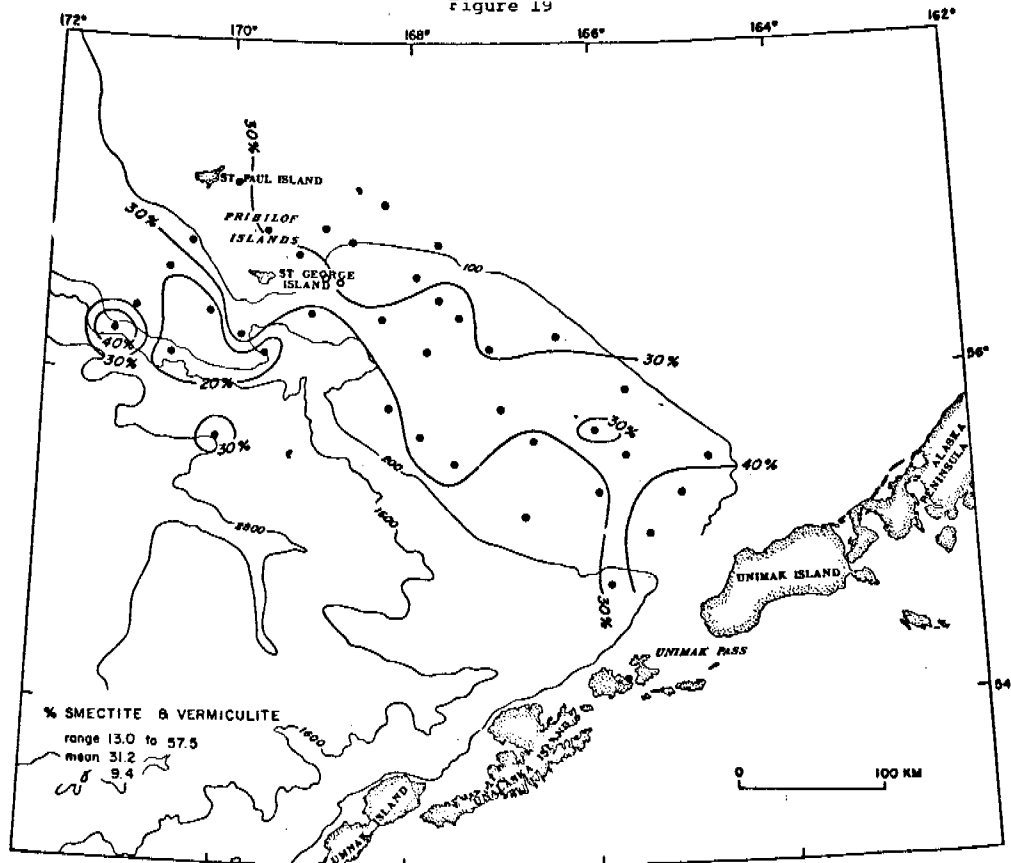


Figure 20

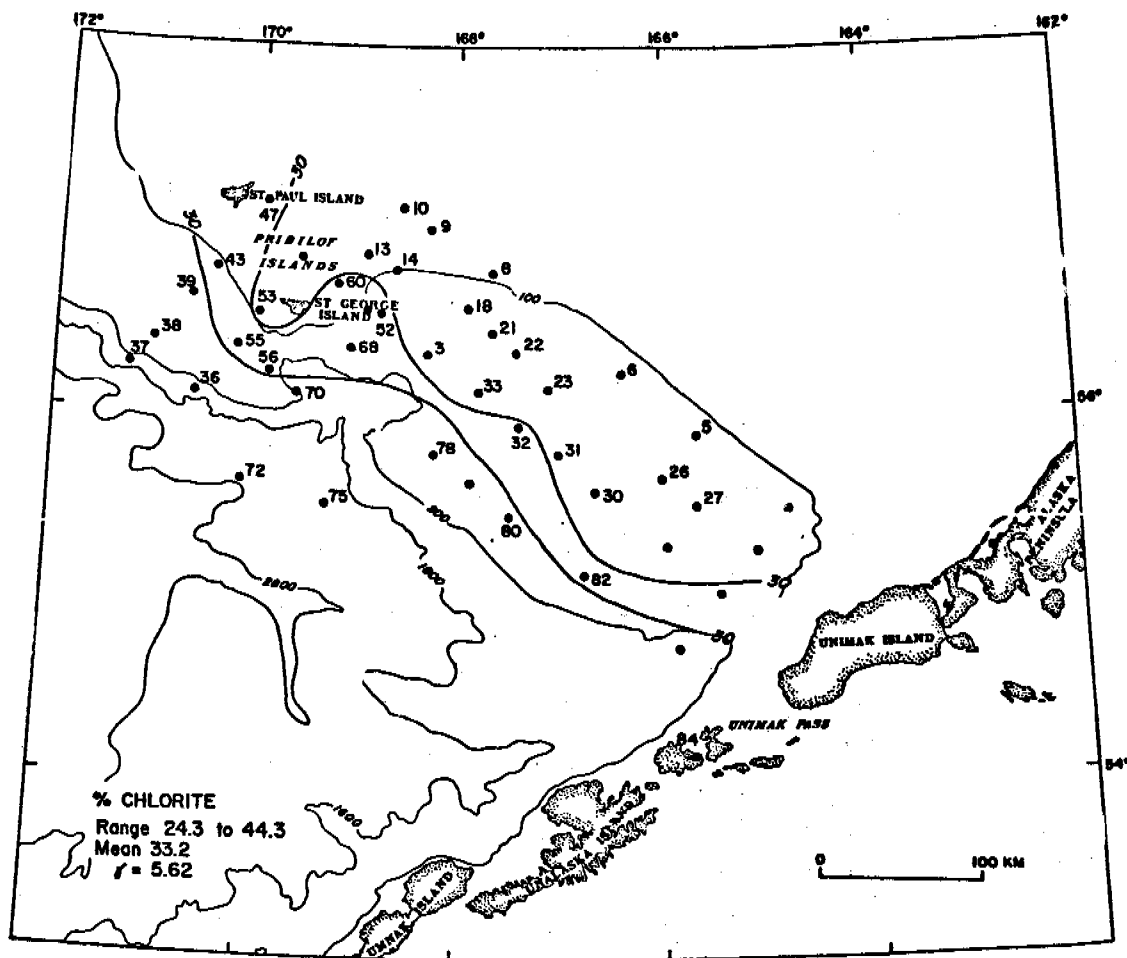


Figure 21

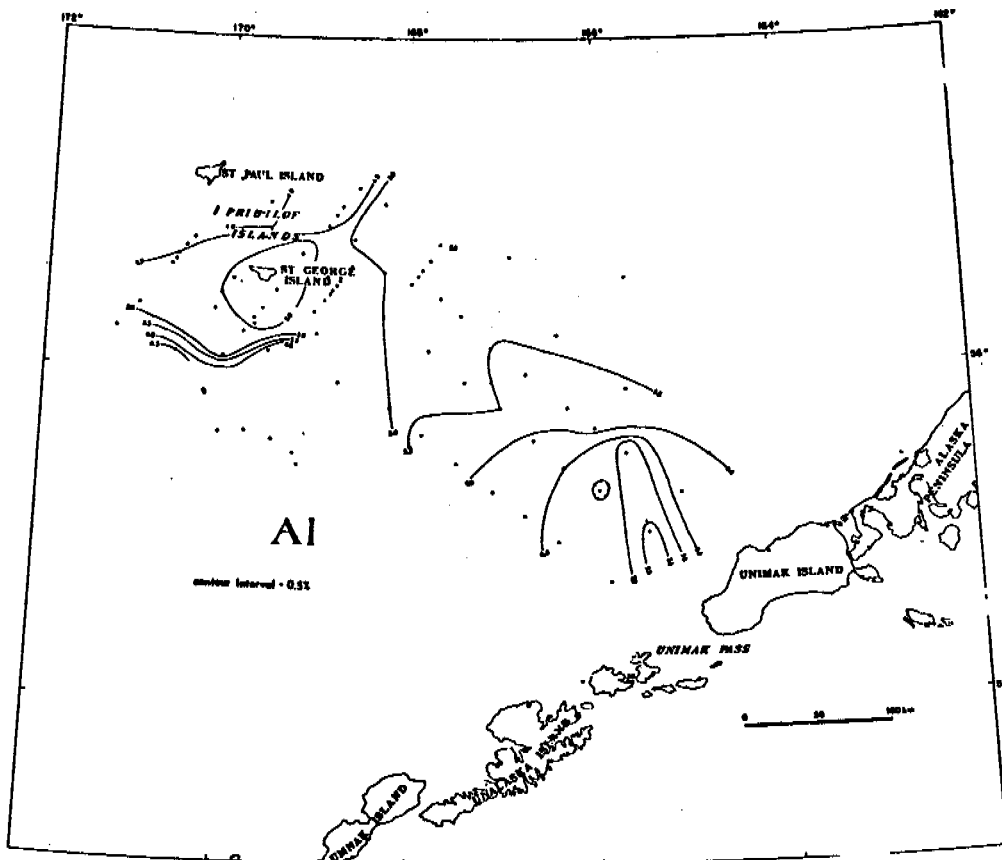
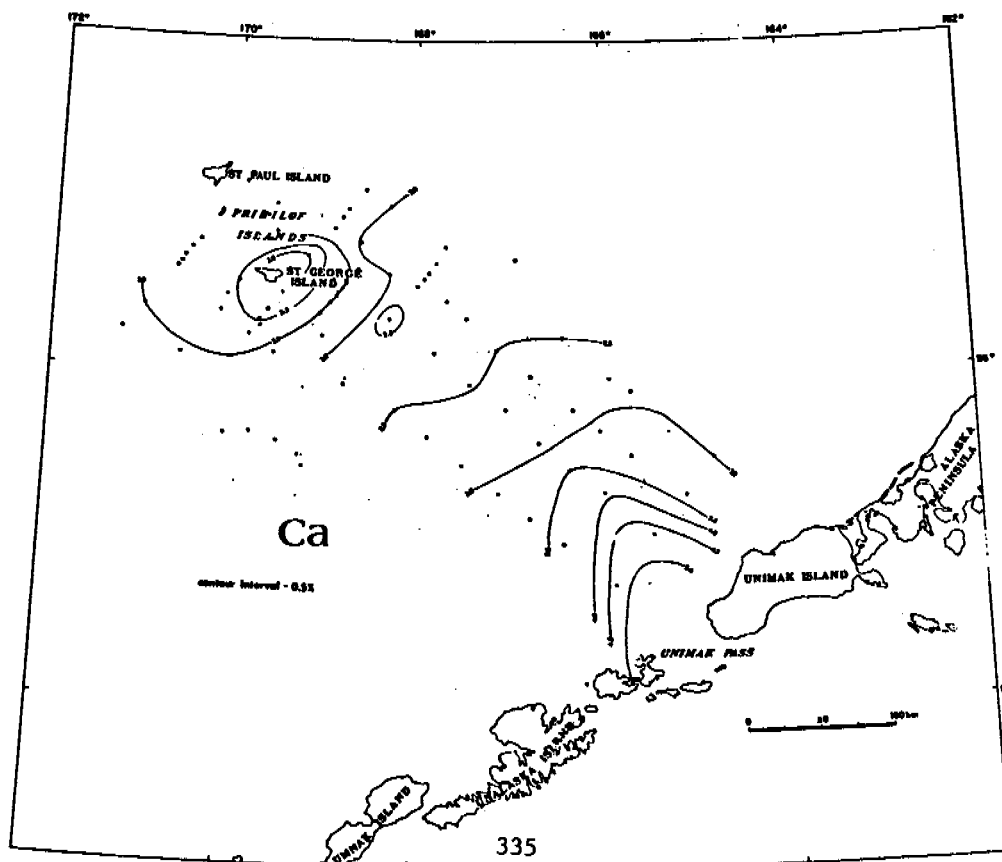


Figure 22a



335
Figure 22b

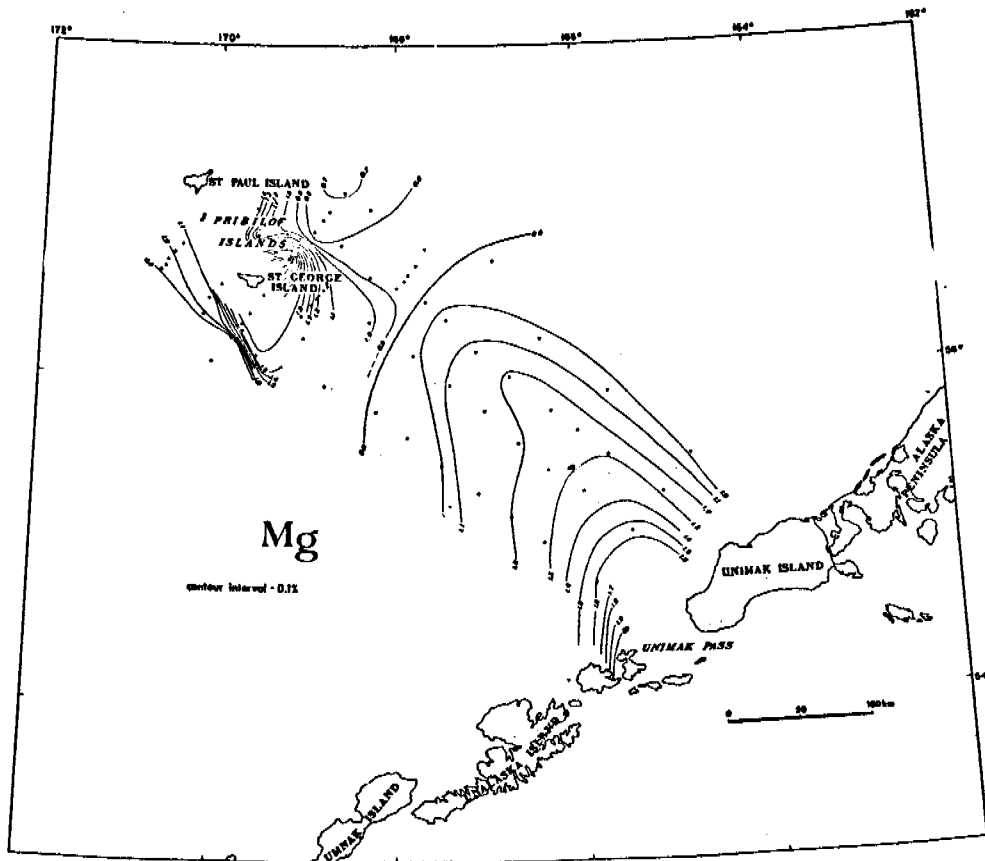


Figure 23a

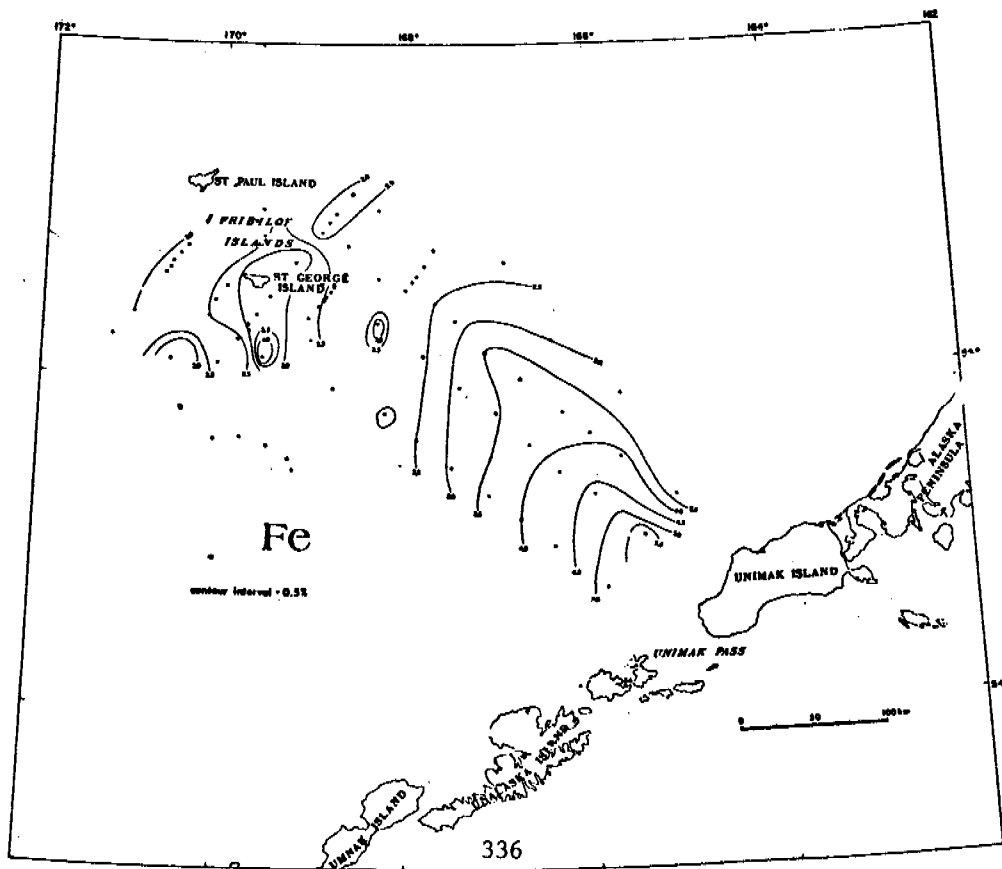


Figure 23b

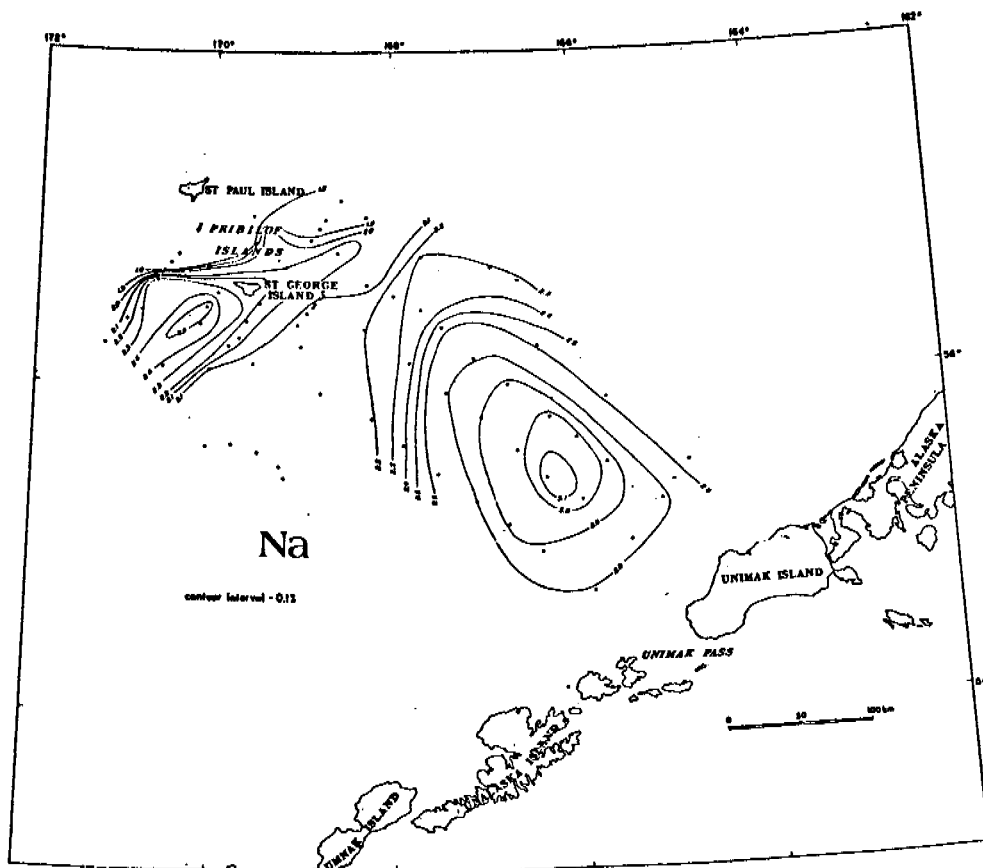


Figure 24a

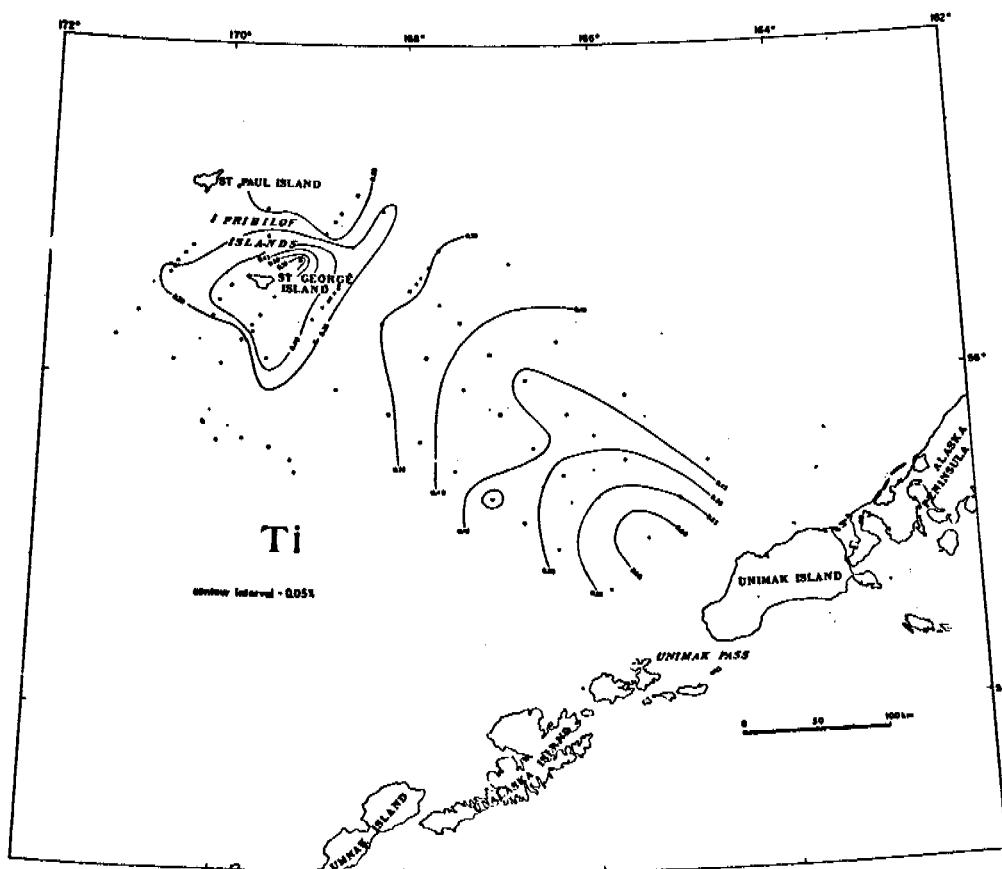


Figure 24b

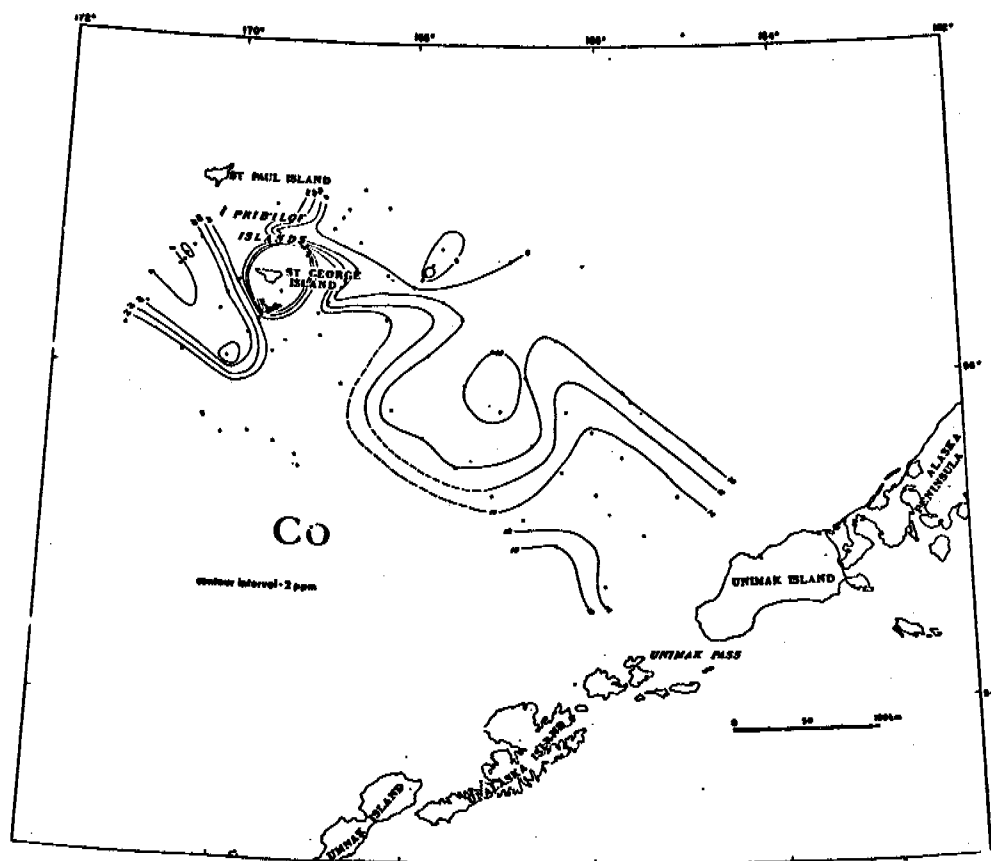


Figure 25a

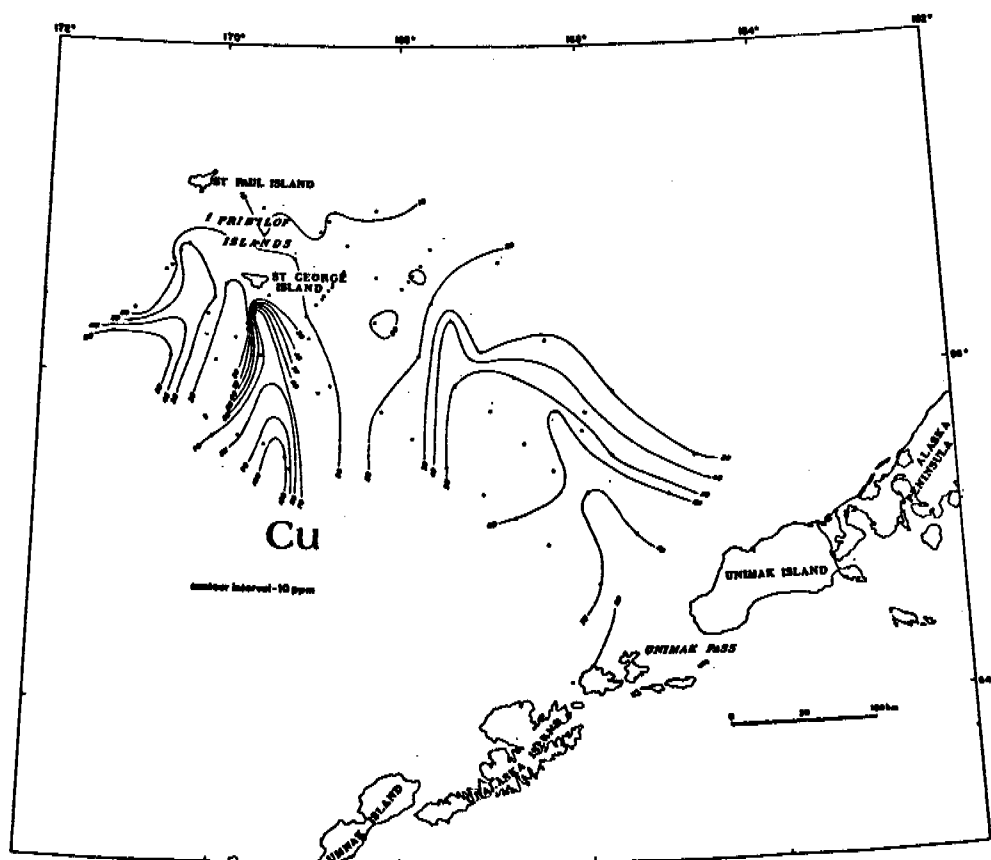


Figure 25b

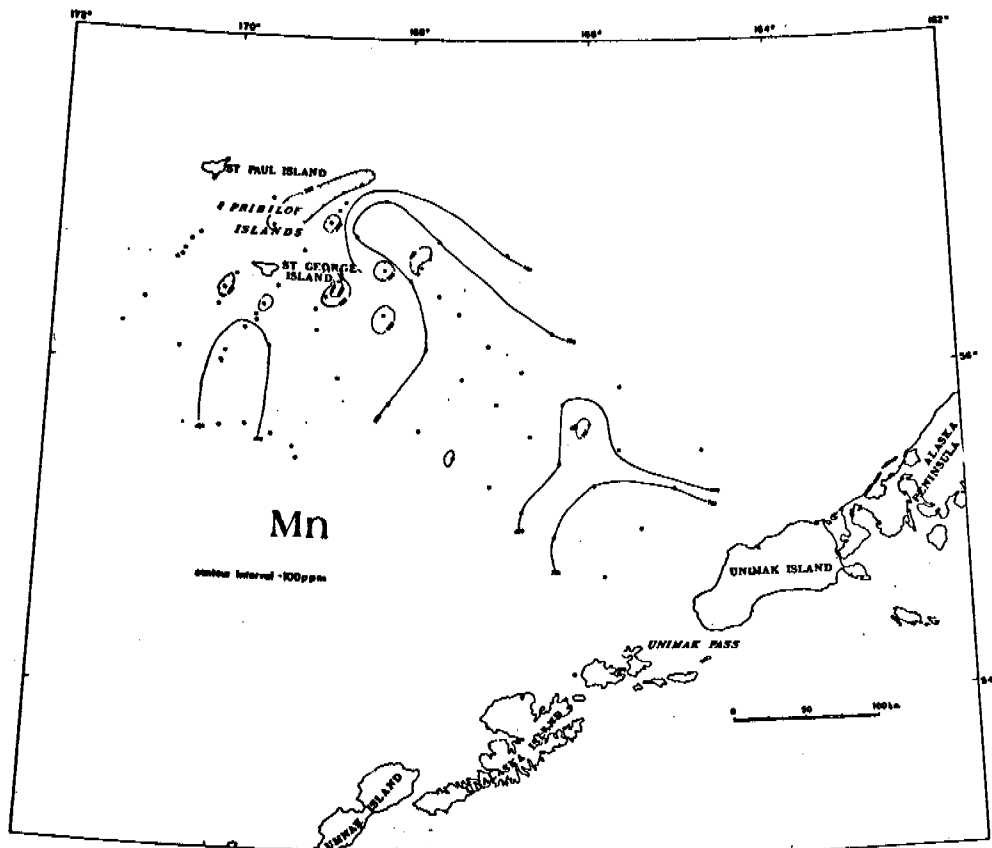


Figure 26a

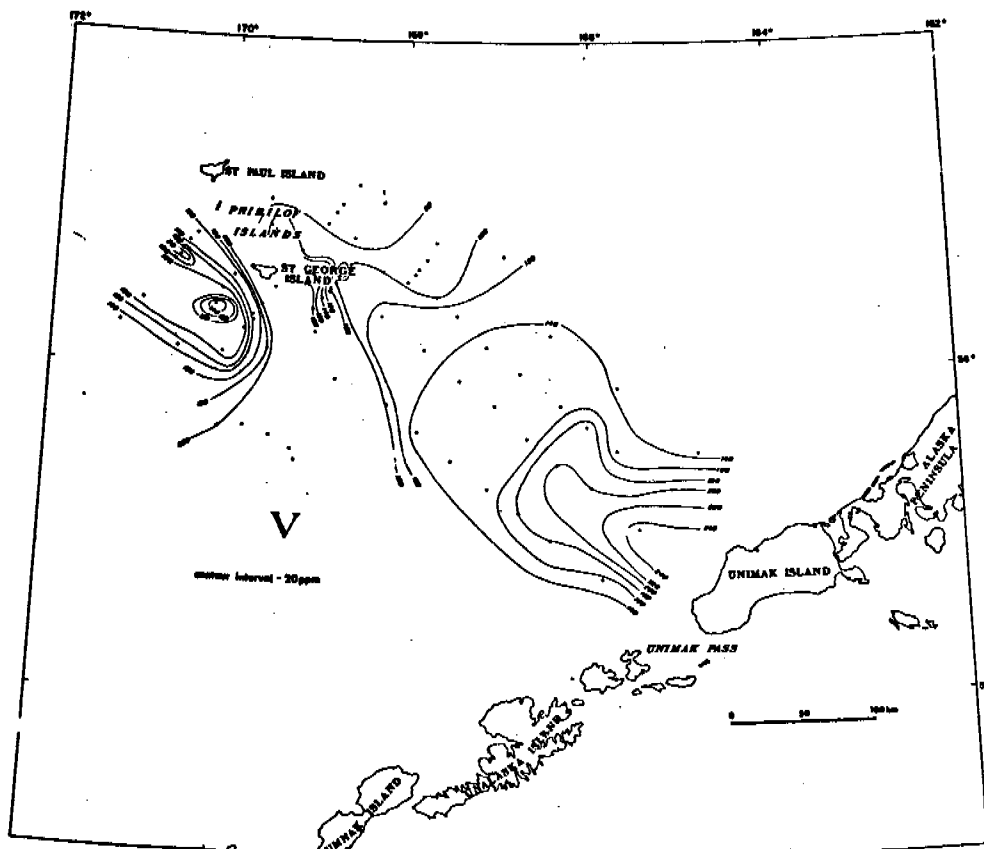


Figure 26b

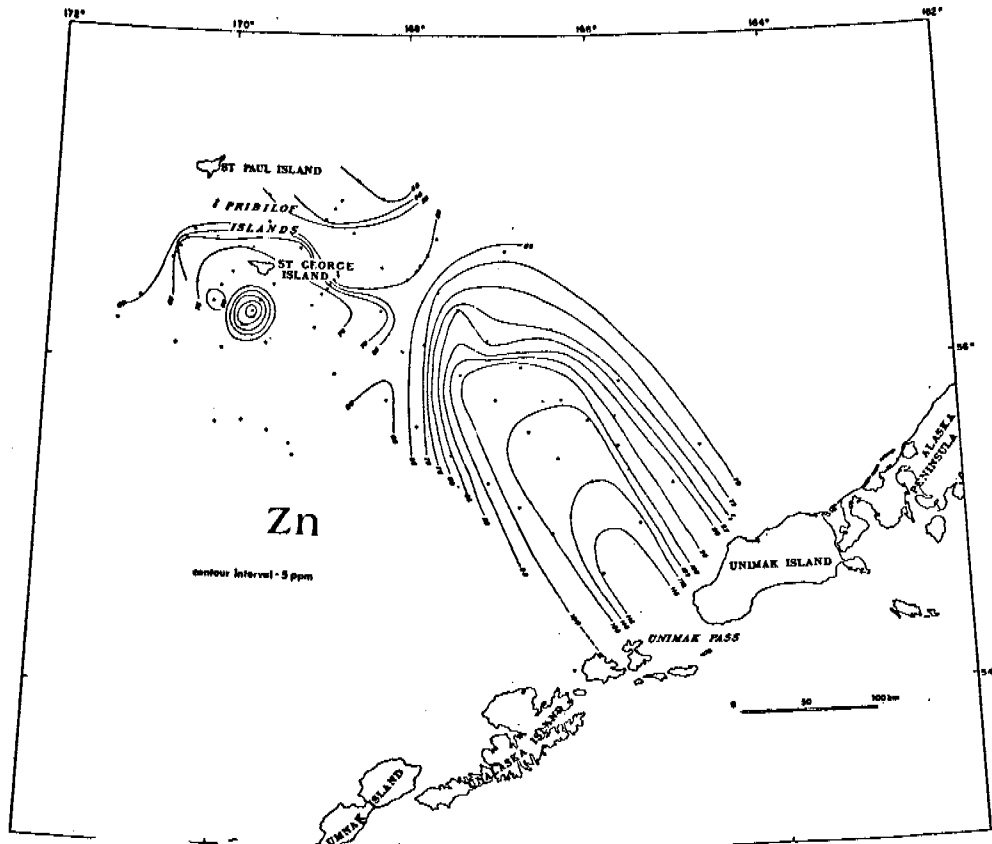


Figure 27a

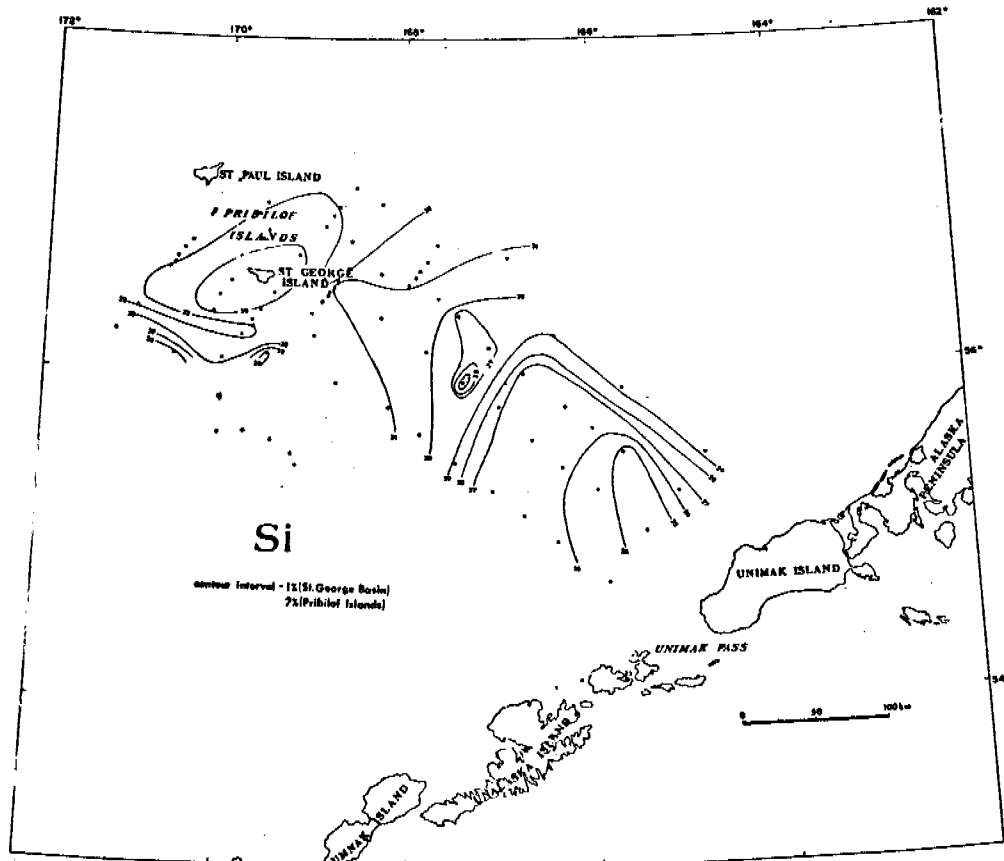


Figure 27b

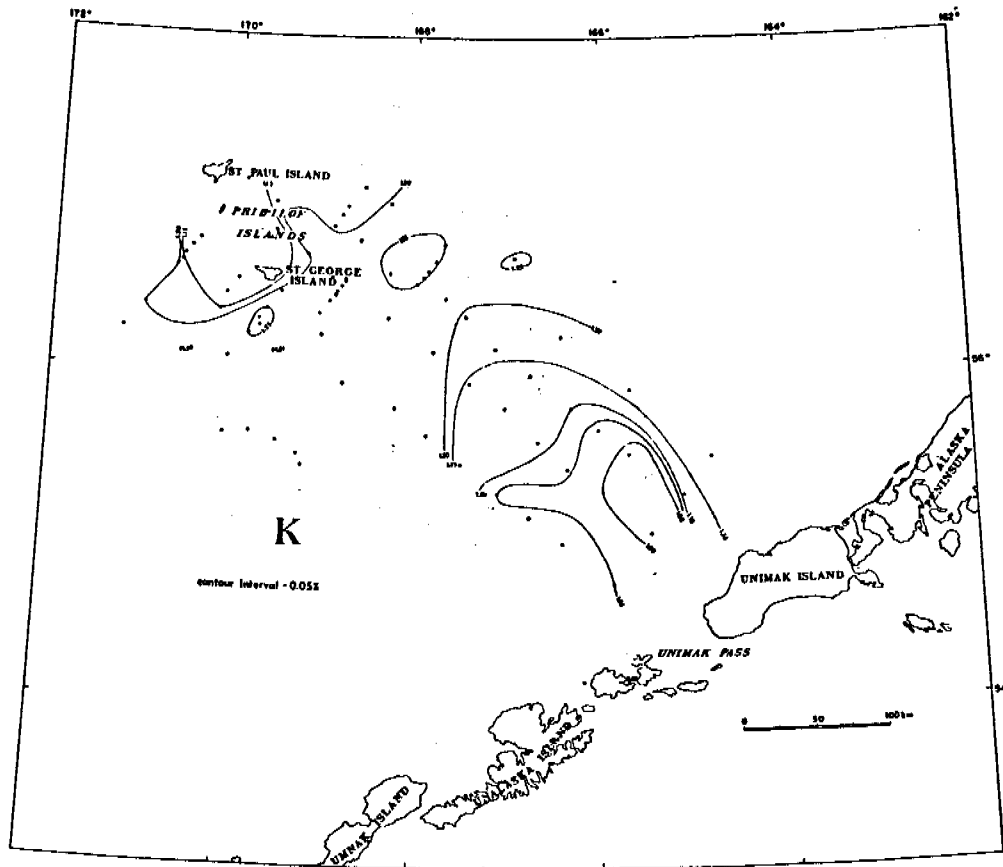


Figure 28a

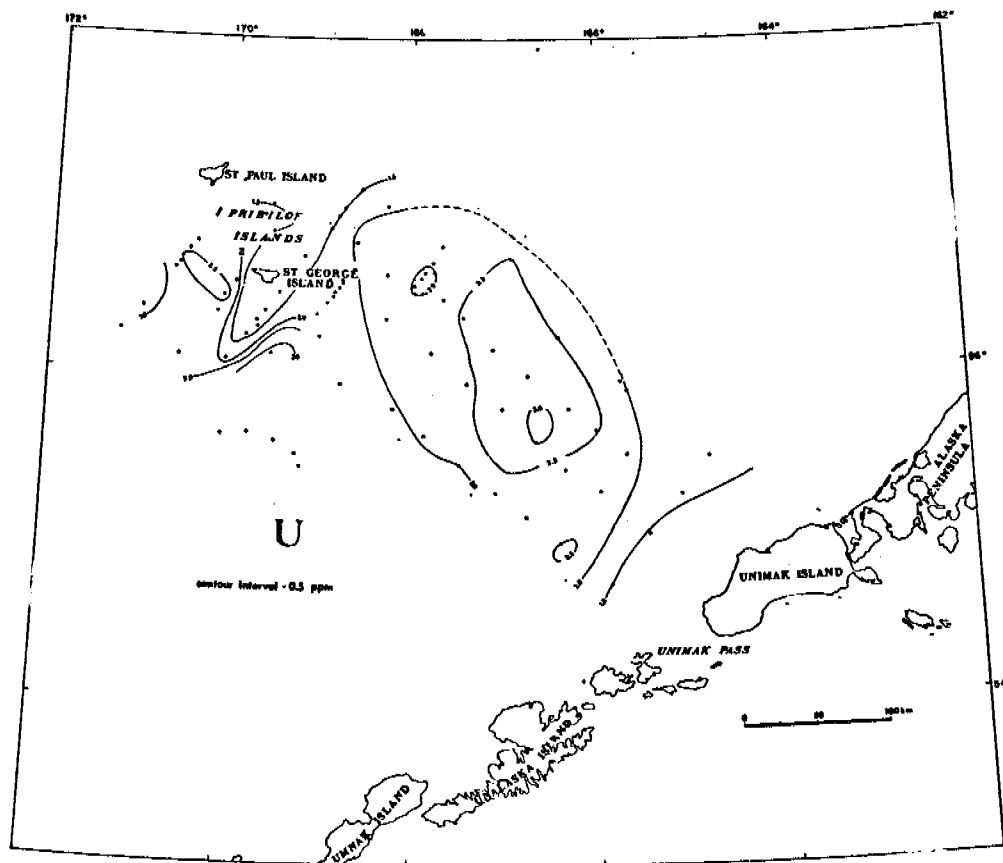


Figure 28b

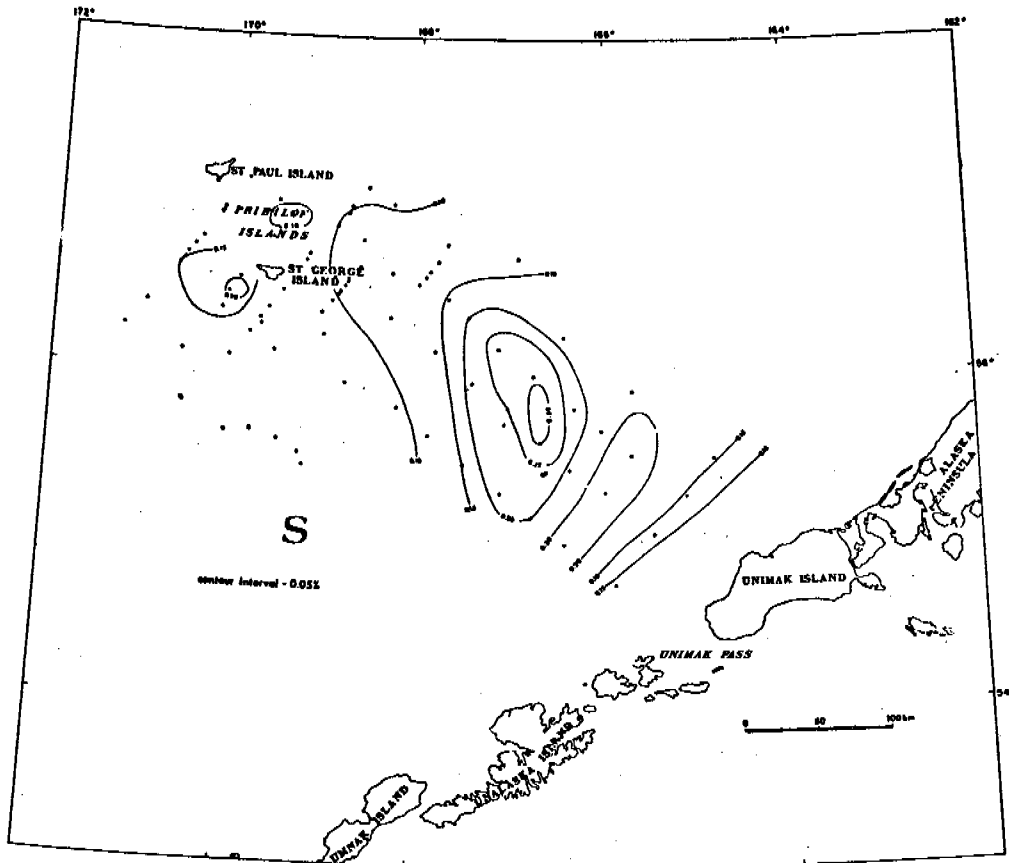


Figure 29a

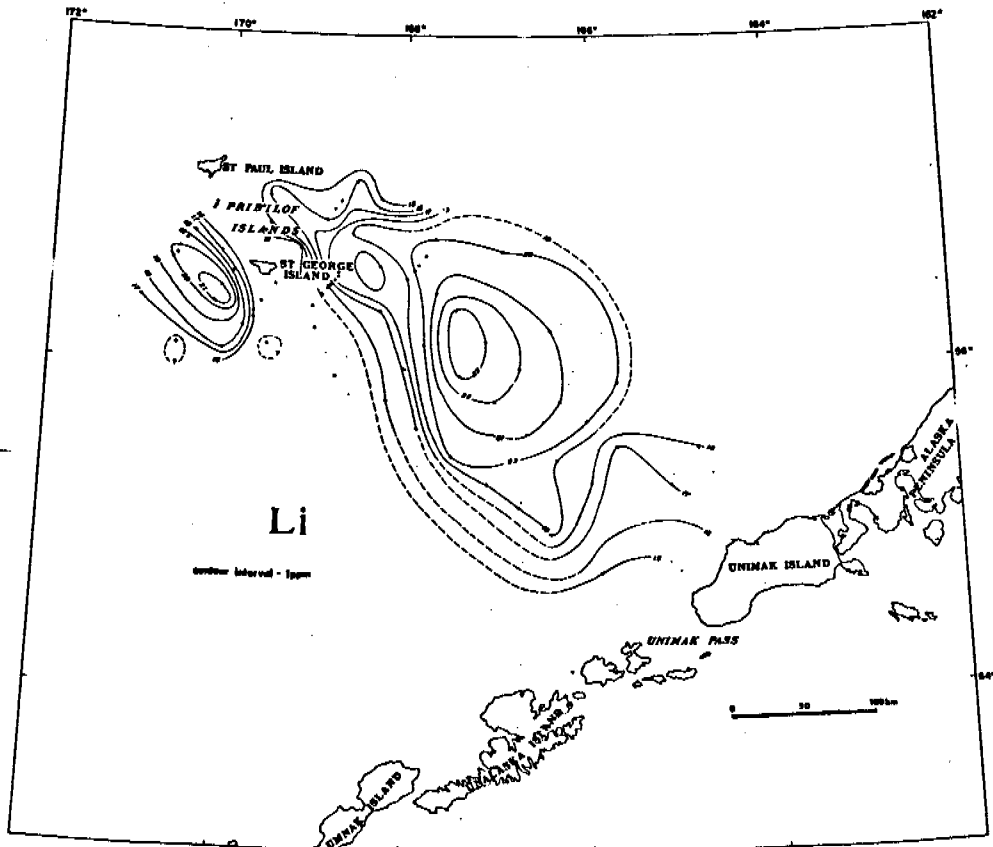


Figure 29b

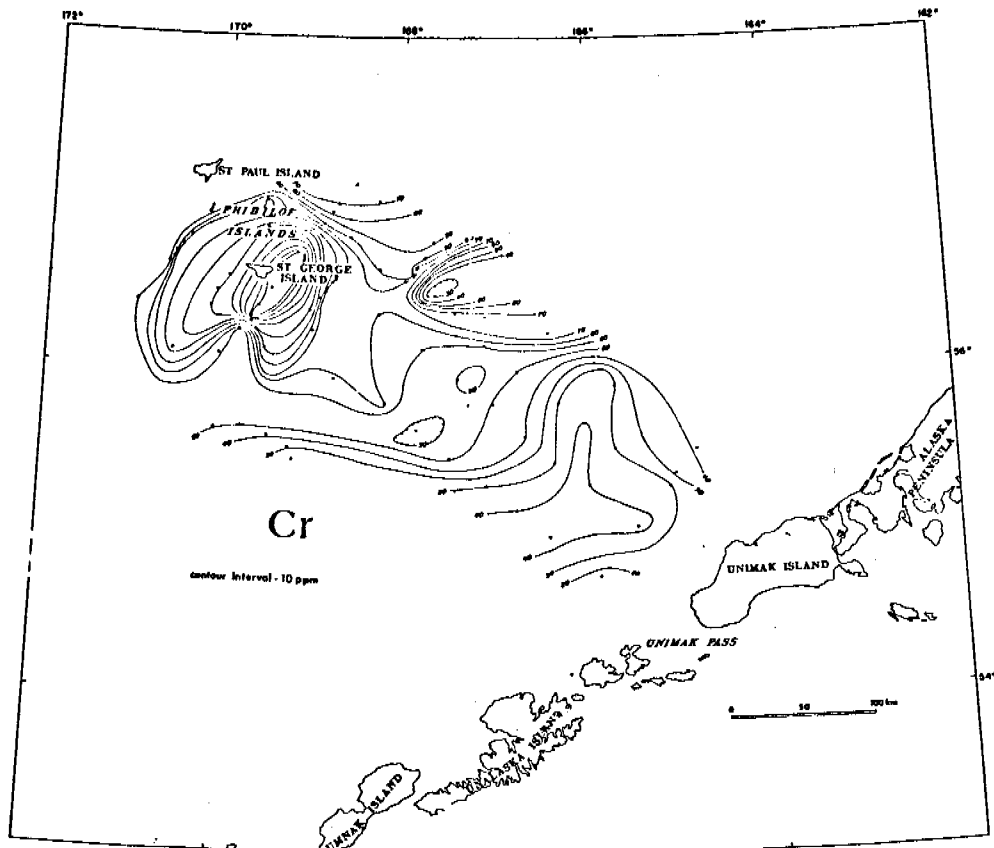


Figure 30a

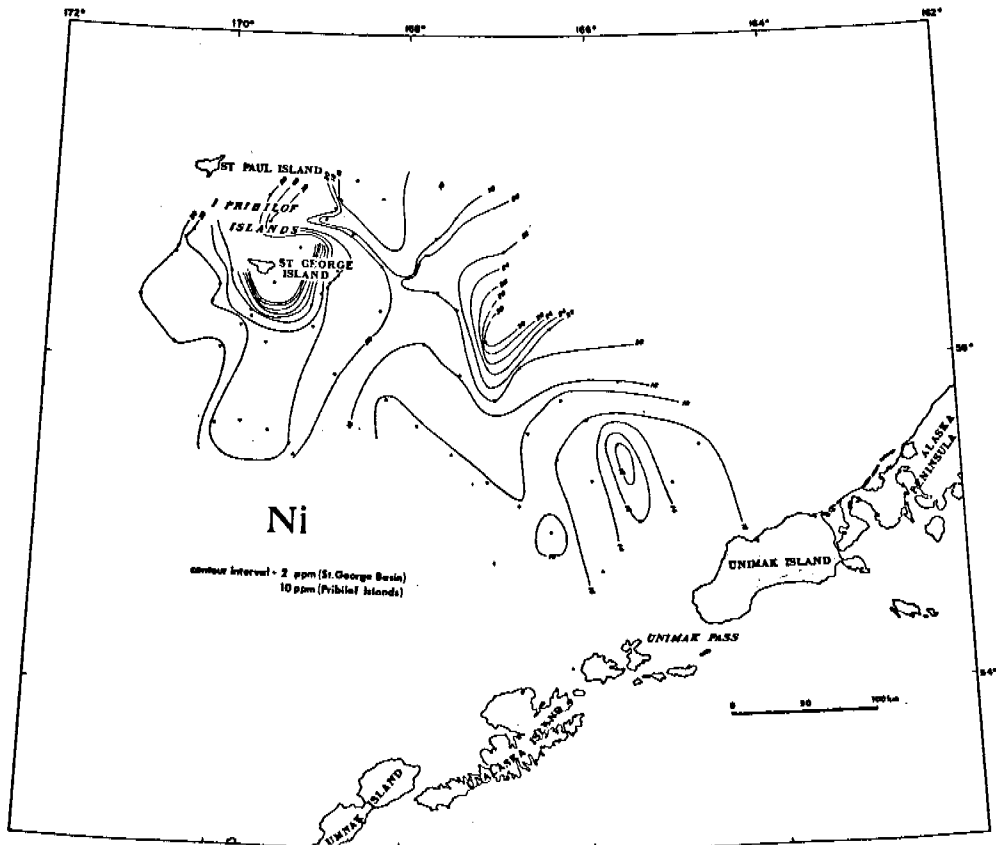


Figure 30b

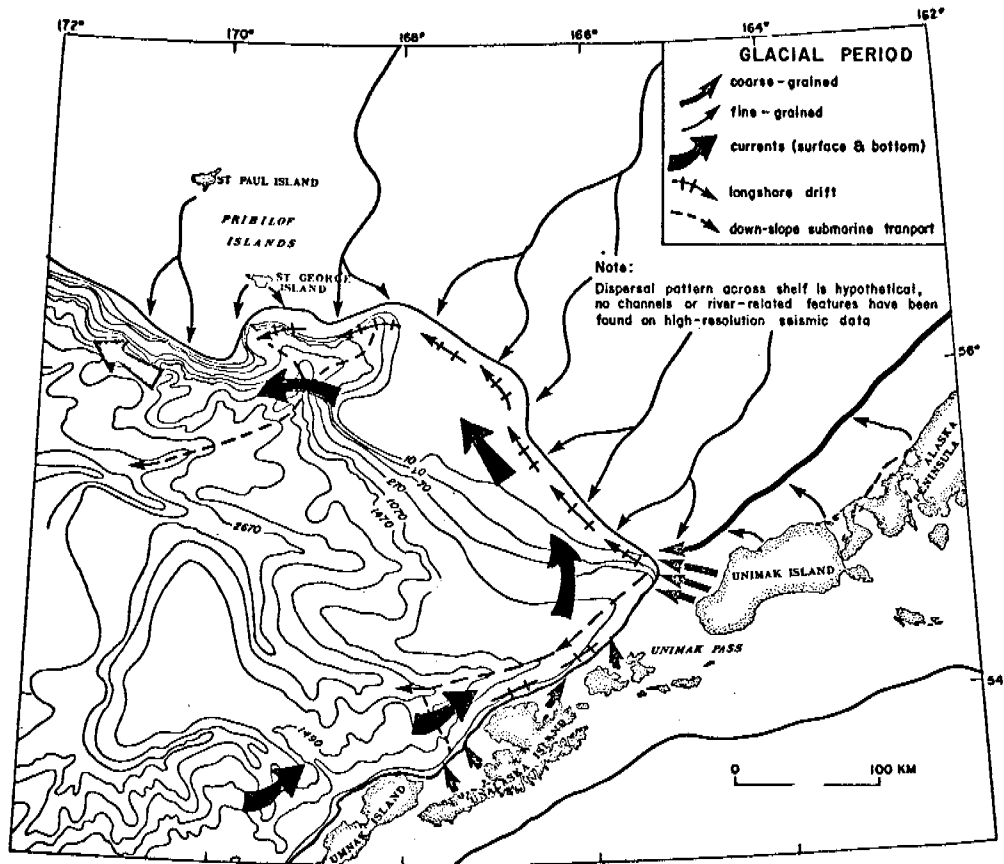


Figure 31

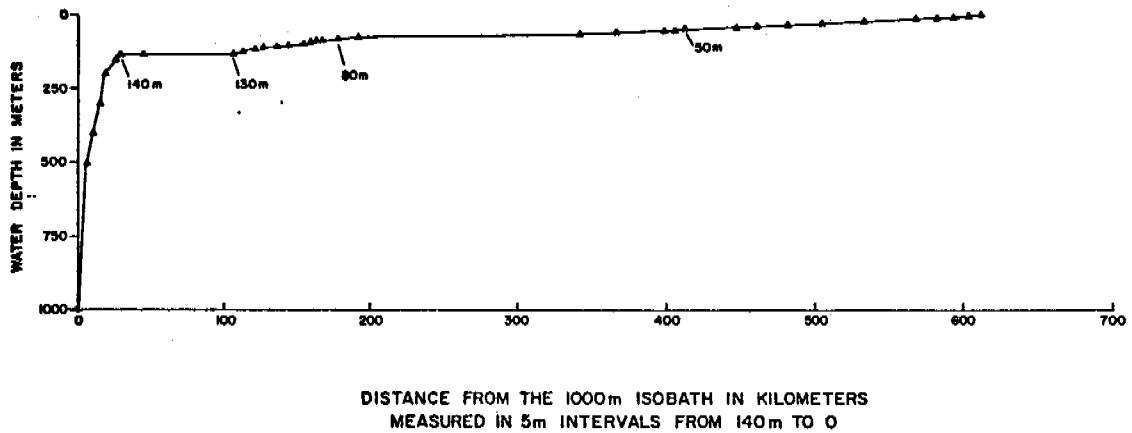


Figure 32

TABLE 1

Map Number	Core		Interval (cm.)	Grain Size	Clay	Heavy Mineral	Light Mineral	Inorganic Geochemistry		Carbon
	year	#						Complete chemistry	6-step spec. only	
1	77	V05	0-3					X		X
2	77	V06	0-3	X		X	X	X		X
3	77	V07	0-3					X		X
4	76	G121	0-5	X	X	X	X	X		X
4	76	V28	0-3					X		
5	77	G014	0-5	X		X	X	X		X
6	76	G002	15-20	X		X	X	X		X
7	76	G005	0-5	X	X	X	X	X		X
7	76	G006	3-4					X		
8	76	G007	0-5							
8	76	G008	7-15	X	X	X	X	X		X
8	76	G009	4-5					X		
9	76	G010	0-10					X		
9	76	G011	13-18	X	X	X		X		X
9	76	G012	4-5					X		
10	76	G052	9-13	X	X	X	X	X		X
11	76	G053	0-1					X		
11	76	G054	0-3	X	X	X	X	X		X
12	76	G119	0-5	X		X	X	X		X
12	76	G120	4-5					X		
13	77	G016	0-5	X		X	X	X		X
14	77	G019	0-5	X		X	X	X		X
15	76	G117	0-1					X		
15	76	G118	6-11	X		X	X	X		X
16	76	G055	4-5					X		
16	76	G056	0-4	X		X	X	X		X
16	76	G057	0-5					X		
17	76	G050	0-1					X		
17	76	G051	6-11	X	X	X		X		X
17	76	P03	3-8					X		
18	76	G013	14-19	X	X	X	X	X		X
18	76	G014	4-5					X		
19	76	G049	0-5	X		X	X	X		X
20	76	G059	5-8	X	X	X		X		X
20	76	G060	0-2					X		
21	76	G115	4-5					X		
21	76	G116	0-5	X		X	X	X		X
??	77	G020	0-5	X		X	X	X		X
23	76	G113	3-8	X	X	X	X	X		
23	76	G114	0-1					X		
24	76	G061	4-5					X		
24	76	G062	0-5	X	X	X	X	X		X
24	76	P05	0-5					X		
25	76	G047	4-5					X		
25	76	G048	0-8	X		X	X	X		X
26	76	G015	4-5					X		
26	76	G016	7-9		X	X	X	X		
27	76	G046	11-16	X	X	X	X	X		X
28	76	G063	15-20	X	X	X		X		X
28	76	P06	6-11					X		
29	76	G111	1-5	X	X	X	X	X		X
29	76	G112	4-5					X		
30	77	G022	0-5	X		X	X	X		X
31	76	G109	3-8	X	X	X	X	X		X
31	76	G110	4-5					X		
32	76	G064	4-5					X		
32	76	G065	10-15	X	X	X	X	X		X
33	76	G042	0-1					X		
33	76	G043	0-6	X	X	X	X	X		X
34	76	G018	4-5					X		
34	76	G019	0-3	X		X	X	X		X
35	76	G041	6-11	X	X	X	X	X		X
36	76	P13	0-2	X	X	X	X		X	X
37	77	G023	0-5	X				X		X
38	77	G024	0-5	X				X		X
38	77	G025	0-10	X			X	X		X
39	76	P10	0-2	X	X	X	X		X	X

TABLE 1 cont.

Map Number	Core		Interval (cm.)	Grain Size	Clay	Heavy Mineral	Light Mineral	Inorganic Geochemistry		Carbon
	year	#						complete chemistry	6-step spec. only	
40	76	G066	4-5					X		
40	76	G067	5-10	X	X	X	X	X		X
41	77	G012	11-12					X		X
42	77	G007	0-1					X		X
43	76	G033	8-13	X				X		X
43	76	G034	4-5					X		
43	76	G036	2-7					X		
44	76	G037	2-8	X		X	X		X	X
45	76	G038	0-5	X				X		X
45	76	G039	0-5					X		
46	76	G040	6-10	X				X		X
47	76	G020	6-11	X	X	X	X	X		X
47	76	G021	4-5					X		
48	76	G032	6-11	X				X		X
49	76	G103	2-7	X	X	X	X		X	X
49	76	V25	0-3					X		
50	76	V23	0-3	X				X		X
51	76	V21	0-3	X				X		X
52	76	V20	0-3	X	X			X		X
53	76	V19	0-3	X				X		X
54	76	G030	1-6	X		X	X		X	X
54	76	G031	4-5					X		
55	76	V02	0-3	X		X	X	X		X
56	76	G027	14-19	X	X		X	X		X
56	76	G028	0-5					X		
56	76	G029	4-5					X		
57	76	V18	0-3	X	X	X	X	X		X
58	76	G105	10-15	X	X	X	X	X		X
58	76	G107	0-5					X		
58	76	P08	3-8					X		
59	76	G069	0-5	X		X		X		X
59	76	V07	0-3	X		X	X	X		X
60	76	V14	0-3	X		X	X	X		X
61	76	V15	0-3	X				X		X
62	76	G094	0-3	X		X		X	X	X
63	76	V17	0-3	X	X	X	X	X		X
64	76	V06	0-3	X	X	X	X	X		X
65	76	V05	0-3	X				X		X
66	76	V04	0-3	X				X		X
67	76	V03	0-3	X	X	X	X	X		X
68	76	V11	0-3	X				X		X
69	76	V12	0-3	X	X	X	X	X		X
70	76	G089	0-3	X	X	X	X		X	X
71	76	G090	2-4	X				X		X
72	76	G091	0-1					X		
72	76	P07	5-10	X	X	X	X	X		X
73	76	G070	0-1					X		
73	76	G071	2-7	X	X	X	X	X		X
74	77	G029	0-5	X		X	X	X		X
75	77	G026	0-5	X		X	X	X		X
76	76	G072	4-5						X	
76	76	G074	0-5		X	X	X			
77	76	G075	6-10	X	X	X	X	X		
78	76	G077	0-5	X	X	X	X	X		X
79	76	G078	0-1						X	
79	76	G079	0-5	X		X			X	X
80	76	G080	0-5	X				X		X
81	76	G081	0-5	X			X		X	X
82	76	G082	0-5	X	X			X		X
83	76	V10	0-3	X				X		X
84	76	V09	0-3	X		X	X	X		X
85	76	V08	0-3		X					
86	76	V22	0-3	X	X	X	X		X	X
87	76	V24	0-3	X					X	X
88	76	V26	0-3	X						X
89	77	V04	0-3	X						
90	76	P11	0-5	X						X
91	76	V29	0-3	X		X				X

TABLE 2
 GRAPHICAL STATISTICS FROM GRAIN SIZE ANALYSIS
 (Folk and Ward, 1957)

SAMPLE	MAP INDEX NUMBER	MEDIAN (Md) (ϕ)	MEAN (M _Z) (ϕ)	SORTING (σ)	SKEWNESS (S _{k_i})	KURTOSIS (K _g)
76-G4	6	3.54	3.81	1.05	0.63	2.71
76-G5	7	3.72	3.88	0.69	0.55	3.02
76-G8	8	3.66	3.98	1.20	0.46	1.27
76-G10	9	3.20	3.52	1.32	0.43	1.66
76-G19	34	3.45	3.85	1.52	0.46	1.16
76-G20	47	3.01	3.33	1.32	0.49	1.44
76-G28	56	3.18	3.53	1.36	0.55	2.06
76-G30	54	3.18	3.29	1.05	0.38	2.38
76-G32	48	3.06	3.29	1.19	0.49	2.12
76-G33	43	3.14	3.71	1.68	0.59	1.54
76-G36	43	3.21	3.83	1.70	0.62	1.20
76-G37	44	3.04	3.32	1.30	0.46	1.48
76-G38	45	3.28	3.70	1.47	0.52	1.42
76-G39	45	3.29	3.75	1.52	0.53	1.35
76-G40	46	3.15	3.39	1.26	0.40	1.25
76-G43	33	4.84	4.80	2.06	0.13	1.08
76-G48	25	5.63	5.80	1.97	0.25	1.71
76-G51	17	4.92	4.81	1.62	0.07	1.37
76-G52	10	4.91	4.89	1.45	0.10	1.61
76-G54	11	4.60	4.52	1.66	0.07	1.30
76-G56	16	4.85	4.89	1.60	0.19	1.56
76-G57	16	5.12	5.26	1.57	0.28	1.72
76-G59	20	5.35	5.32	1.90	0.16	1.48
76-G60	20	5.26	5.11	2.17	0.06	1.16
76-G62	24	5.34	5.25	2.27	0.09	1.15
76-G67	40	2.00	1.93	1.45	0.19	5.24
76-G69	59	2.90	3.05	1.12	0.50	2.45
76-G71	73	6.52	6.76	3.27	0.17	0.93
76-G75	77	2.99	3.37	1.28	0.55	1.68
76-G77	78	3.79	4.15	1.60	0.43	1.16
76-G79	79	3.75	4.16	1.61	0.46	1.15
76-G80	80	4.60	4.64	1.67	0.16	1.05
76-G89	70	3.69	4.19	1.36	0.68	1.63
76-G90	71	4.94	5.01	1.70	0.20	1.44
76-G94	62	0.75	0.65	1.53	0.02	0.63
76-G103	49	1.72	1.77	2.06	0.19	2.27
76-G105	58	6.16	6.60	2.97	0.30	0.86
76-G107	58	5.36	6.66	3.08	0.60	0.97
76-G109	31	2.64	2.87	0.94	0.59	2.90
76-G111	29	3.02	3.71	1.59	0.69	1.06
76-G113	23	4.04	4.50	1.57	0.49	1.21
76-G116	21	4.68	4.80	2.04	0.12	1.34
76-G118	15	4.73	4.57	1.96	0.03	1.04

TABLE 2 cont.

SAMPLE	MAP INDEX NUMBER	MEDIAN (Md) (ϕ)	MEAN (Mz) (ϕ)	SORTING (σ)	SKEWNESS (S_{k_i})	KURTOSIS (K_g)
76-G119	12	4.48	4.57	1.50	0.22	1.27
76-G121	4	4.64	4.75	1.51	0.27	1.13
77-G14	5	6.56	6.77	2.61	0.21	1.14
77-G16	13	5.11	5.18	2.65	0.11	1.43
77-G19	14	5.34	5.48	2.69	0.17	1.32
77-G20	22	7.40	7.58	2.76	0.17	1.09
77-G22	30	7.08	7.30	2.74	0.19	1.13
77-G23	37	7.12	7.25	2.56	0.19	1.38
77-G24	38	7.36	7.61	2.84	0.19	0.85
77-G25	38	7.12	7.24	2.90	0.12	0.97
77-G26	75	6.23	6.51	2.35	0.30	1.19
77-G29	74	6.90	7.01	2.91	0.14	0.99
76-V2	55	2.58	2.59	0.76	0.26	2.41
76-V3	67	2.75	2.75	0.68	0.19	1.94
76-V4	66	2.59	2.66	0.68	0.36	1.79
76-V5	65	2.65	2.71	0.79	0.38	2.10
76-V6	64	2.80	2.99	0.72	0.48	3.34
76-V7	59	3.19	3.19	1.11	0.31	2.41
76-V9	84	2.14	2.13	0.43	0.14	2.22
76-V10	83	2.23	2.22	0.44	0.09	4.58
76-V11	68	2.80	2.80	0.66	0.11	1.66
76-V12	69	2.17	2.20	1.18	-0.03	3.13
76-V14	60	3.00	2.94	0.87	0.22	2.86
76-V15	61	1.42	0.93	1.56	-0.32	0.51
76-V16	62	0.45	0.65	2.10	0.36	1.07
76-V17	63	2.64	2.73	0.64	0.50	2.11
76-V18	57	2.84	2.81	0.64	0.06	1.33
76-V19	53	3.04	3.03	0.91	0.21	2.48
76-V21	51	2.93	2.90	0.89	0.21	2.42
76-V22	86	2.85	2.86	0.97	0.29	2.63
76-V23	50	2.66	2.67	0.93	0.33	2.96
76-V24	87	1.87	1.61	1.57	-0.12	1.86
76-V25	49	1.68	1.43	1.78	-0.01	2.36
76-V26	88	1.96	1.60	1.33	-0.34	2.11
76-V28	4	4.66	4.83	1.48	0.29	1.08
76-V29	91	1.86	1.93	1.33	0.12	3.64
77-V4	89	1.79	1.49	1.23	-0.32	1.94
77-V6	2	3.22	3.25	0.68	0.49	5.47
76-P3	26	5.02	5.06	1.75	0.17	1.56
76-P6	32	5.36	5.36	2.21	0.17	1.14
76-P7	55	5.13	5.14	1.69	0.15	1.16
76-P8	70	6.46	6.47	3.79	0.05	1.32
76-P11	73	7.73	7.72	3.08	0.06	0.89

TABLE 3

HEAVY AND LIGHT MINERALS AND
CLASSES OF ROCK FRAGMENTS

<p>HEAVY MINERALS AND ROCK FRAGMENTS</p>	<p>clinopyroxene volcanic rock fragments orthopyroxene fine-grained rock fragments amphibole plutonic rock fragments garnet metamorphic rock fragments epidote chlorite olivine opaques</p>
<p>LIGHT MINERALS AND ROCK FRAGMENTS</p>	<p>quartz volcanic rock fragments feldspar non-volcanic rock fragments volcanic glass</p>

TABLE 4

UNIVARIATE STATISTICS ON PERCENTAGES OF
 HEAVY AND LIGHT MINERALS
 AND CLASSES OF ROCK FRAGMENTS

MINERAL	MINIMUM	MAXIMUM	MEAN	STANDARD DEVIATION
v clinopyroxene	9.0	35.0	16.8	5.6
v orthopyroxene	5.0	19.0	11.4	3.9
v volcanic rock fragments	6.0	69.0	28.9	13.1
v amphibole	2.0	24.0	15.1	5.4
v olivine	0	7.0	1.1	2.0
opaques	2.0	18.0	7.3	3.8
m chlorite	0	8.0	2.9	2.1
m epidote	0	7.0	2.8	1.8
m garnet	0	4.0	1.2	1.1
m metamorphic rock fragments	0	8.0	3.3	2.2
plutonic rock fragments	0	6.0	1.7	1.6
fine-grained rock fragments	0	8.0	3.1	2.2
quartz	0.3	25.6	15.1	7.0
feldspar	1.6	50.4	36.1	7.0
v volcanic glass	2.9	30.6	11.2	8.3
v volcanic rock fragments	3.3	36.5	11.1	8.4
non-volcanic rock fragments	4.1	34.8	19.7	7.5
v = volcanic origin m = metamorphic origin				

TABLE 5

UNIVARIATE STATISTICS FOR THE
RELATIVE PERCENTAGES OF CLAY MINERALS

MINERAL	MINIMUM	MAXIMUM	MEAN	STANDARD DEVIATION
smectite + vermiculite	13.0	57.5	31.2	9.4
illite	17.0	47.0	29.8	6.9
kaolinite	0	11.8	6.0	3.5
chlorite	24.3	44.3	33.2	5.6

TABLE 6

Summary statistics for concentrations of major, minor, and trace elements in 103 samples or surface sediments from the St. George Basin, Outer Continental Shelf, Southern Bering Sea. N* refers to the total number of samples, out of 103, which contained measured element concentrations greater than the detection limit for that element. For subsequent statistical analyses, values less than the detection limit for a particular element were replaced by a value of 0.7 times the detection limit (e.g., the detection limit for both B and Rb is 20 ppm; values <20 ppm were replaced by $0.7 \times 20 = 14$ ppm). Analytical methods used are: (1) 6-step semiquantitative optical emission spectroscopy; (2) x-ray fluorescence; (3) Atomic Absorption Spectrophotometry; (4) Neutron Activation Analysis.

$\frac{1}{/}$ values for Mg, Na, and S have been corrected for interstitial sea water containing dissolved Mg^{++} , Na^+ , and $SO_4^{=}$.

Element	Method	Observed Range	Arithmetic Mean	Standard Deviation	Coefficient of Variation (%)	(GM) Geometric Mean	(GD) Geometric Deviation	N*
Al (%)	2	3.9 - 7.9	5.6	0.79	14	5.5	1.15	103
Ca (%)	2	1.7 - 5.1	2.7	0.76	28	2.6	1.29	103
Mg (%) $\frac{1}{/}$	3	0.66- 2.1	1.1	0.26	24	1.0	1.24	103
Fe (%)	2	1.7 - 5.6	3.2	0.96	30	3.0	1.34	103
K (%)	2	0.84- 1.9	1.2	0.15	13	1.2	1.12	103
Si (%)	2	22 - 34	29	2.8	10	29	1.10	103
Na (%) $\frac{1}{/}$	3	1.5 - 2.6	2.1	0.26	12	2.0	1.14	103
Ti (%)	2	0.26- 0.70	0.42	0.084	20	0.41	1.21	103
B (ppm)	1	<20 - 70	37	13	34	35	1.42	102
Ba (ppm)	1	300 - 1,500	580	141	24	570	1.24	103
Co (ppm)	1	7.0 - 30	12	3.8	33	11	1.37	103
Cr (ppm)	1	15 - 200	55	29	52	50	1.57	103
Cu (ppm)	1	7.0 - 100	36	21	58	30	1.92	103
Ga (ppm)	1	10 - 30	18	3.8	22	17	1.22	103
Ge (ppm)	2							
Hg (ppm)	3	0.02- 0.11	0.044	0.016	36	0.041	1.36	103
Li (ppm)	3	13 - 48	20	5.9	30	19	1.25	103
Mn (ppm)	1	300 - 700	520	124	24	500	1.30	103
Ni (ppm)	1	10 - 150	22	16	73	20	1.51	103
Rb (ppm)	3	<20 - 90	38	11	29	35	1.40	98
Sc (ppm)	1	7.0 - 30	15	3.9	26	15	1.29	103
Sn (ppm)	2							
Sr (ppm)	1	200 - 700	370	120	33	350	1.39	103
V (ppm)	1	70 - 300	140	46	33	130	1.42	103
Y (ppm)	1	15 - 50	25	6.8	28	24	1.32	103
Yb (ppm)	1	1.5 - 5.0	2.8	0.69	24	2.8	1.28	103
Zn (ppm)	3	45 - 140	83	22	30	80	1.30	103
Zr (ppm)	1	70 - 200	94	27	29	91	1.29	103
U (ppm)	4	1.2 - 3.9	2.2	0.54	25	2.1	1.27	103
Th (ppm)	4	<2 - 7.7	3.5	1.6	46	3.2	1.59	58
S (%) $\frac{1}{/}$	2	0.007 - 0.55	0.14	0.08	57	0.12	1.80	103

TABLE 7

Analysis of variance of surface sample chemistry, St. George Basin, outer continental shelf, southern Bering Sea. Asterick (*) indicates that a variance component is significantly different from zero at the 0.05 probability level; v is the observed variance ratio. See text for explanation.

Element	Total Logarithmic Variance	variance components as percentage of total variance			v
		Between Ship Stations	Between Samples Within Stations	Analytical Error	
Al	0.00393	82*	0	18	4.56
Ca	0.01269	88*	5	7	7.33
Mg	0.00887	97*	2*	1	32
Fe	0.01641	90*	6*	4	9.00
K	0.00292	88*	0	12	7.33
Si	0.00192	79*	0	21	3.76
Na	0.00470	93*	5*	2	13
Ti	0.00719	87*	0	13	6.69
B	0.02336	30*	11	59	0.43
Ba	0.00906	32*	29	39	0.47
Co	0.02041	71*	0	29	2.45
Cr	0.03900	54*	18	28	1.17
Cu	0.08124	90*	6*	4	9.0
Ga	0.00763	41*	46*	13	0.69
Ge					
Hg	0.01758	50*	7	43	1.00
Li	0.00919	96*	1	3	24
Mn	0.01448	58*	0	42	1.38
Ni	0.03239	59*	14	27	1.44
Rb	0.02168	49*	28*	23	0.96
Sc	0.01352	62*	0	38	1.63
Sn					
Sr	0.02053	46*	37*	17	0.85
V	0.02323	74*	4	22	2.85
Y	0.01427	52*	22	26	1.08
Yb	0.01633	42*	0	58	0.72
Zn	0.01633	82*	0	18	4.56
Zr	0.01254	16	9	75	0.19
U	0.01102	61*	33*	6	1.56
Th	0.04087	19	44*	37	0.23
S	0.03932	76*	0	24	3.17

appendix a

SAMPLE	depth	mean	sorting	% gravel	% sand	% silt	% clay	sand+silt	silt+clay	sand/silt
76 g-2	248.0000	3.5750	0.7950	0.0000	51.1200	15.8200	3.0600	96.9400	18.8800	5.1300
76 g-5	118.0000	3.8840	0.6230	0.0000	76.3600	21.0100	2.6300	97.3700	23.6400	3.6400
76 g-8	109.0000	3.6820	1.2010	0.0000	63.9700	32.5400	3.4800	96.5100	36.0200	1.9600
76 g-11	101.0000	3.4350	1.3200	0.0000	75.5300	21.3600	3.0300	96.8900	24.3900	3.9000
76 g-13	109.0000	4.4090	1.2200	0.0000	42.8200	51.8400	5.3400	94.6600	57.1800	0.8300
76 g-16	108.0000	0.0000	0.0000	0.0000	0.0000	0.0000	0.0000	0.0000	0.0000	0.0000
76 g-19	90.0000	3.8470	1.5170	0.2000	73.1900	32.8400	3.7700	96.0300	36.6100	1.9200
76 g-20	95.0000	3.3250	1.3180	0.2600	76.1800	20.2600	2.9500	96.4400	23.2100	3.6900
76 g-27	98.0000	3.6130	1.5270	0.0700	75.5200	19.9900	4.5900	95.4100	24.4800	3.8000
76 g-30	107.0000	3.2860	1.0510	0.0000	52.4300	14.6600	2.7000	97.2900	17.3600	5.6400
76 g-32	107.0000	3.2870	1.1870	0.0000	51.0100	15.0700	3.0200	96.9900	18.0900	5.4400
76 g-33	111.0000	3.7140	1.4500	0.0000	73.6000	21.6400	4.7600	95.2400	26.4000	3.4000
76 g-38	107.0000	3.7010	1.4680	0.0000	70.0300	26.3600	3.6100	96.3900	29.0700	2.6600
76 g-37	107.0000	3.3220	1.3770	0.0000	76.7500	20.4900	2.7600	97.2400	23.2500	3.7500
76 g-40	100.0000	3.3870	1.2610	0.0000	74.4700	23.1800	2.3500	97.6500	25.5300	3.2100
76 g-41	115.0000	3.3690	1.6320	0.0000	63.9900	31.5700	4.4300	95.5600	36.0000	2.0300
76 g-43	121.0000	4.2990	2.0560	0.0000	38.7400	53.0600	8.2000	91.8000	61.2600	0.7300
76 g-46	128.0000	5.5020	2.1770	0.0000	17.8700	60.4700	12.1600	87.5400	81.8300	0.2600
76 g-48	124.0000	5.9190	1.9890	0.0000	13.3500	73.6500	13.0000	87.0000	86.6500	0.1800
76 g-49	126.0000	5.5310	1.7360	0.0000	13.9200	76.8500	9.2400	90.7700	86.0900	0.1800
76 g-51	120.0000	4.3120	1.6940	0.0000	25.4200	68.3400	6.2400	93.7600	74.5800	0.3700
76 g-52	114.0000	4.3950	1.4480	0.0000	21.0600	73.5200	5.4200	94.5800	78.9400	0.2900
76 g-54	122.0000	4.5150	1.4610	0.0000	26.9300	57.4900	5.5800	94.4200	63.0700	0.6400
76 g-56	128.0000	4.8880	1.6040	0.0000	22.4700	70.8500	5.5200	93.4800	77.3700	0.3200
76 g-59	130.0000	5.3180	1.8950	0.0000	19.5100	70.6900	9.7900	90.2000	80.4800	0.2800
76 g-62	135.0000	5.2860	2.2910	0.1800	27.9600	60.7900	11.0700	88.7500	71.8600	0.4600
76 g-63	133.0000	5.3270	1.9890	0.0000	21.0000	68.3700	10.6300	89.3700	79.0000	0.3100
76 g-65	134.0000	3.9970	1.7790	0.0000	63.0400	30.4300	6.3300	93.6700	36.9600	2.0600
76 g-67	152.0000	1.9750	1.4170	1.4200	84.9400	8.5900	5.0600	93.5300	13.6500	9.8900
76 g-69	122.0000	3.0520	1.1180	0.0000	94.7900	11.4400	3.7800	96.2300	15.2700	7.4200
76 g-71	400.0000	6.7560	3.2710	0.0000	20.0200	47.7800	32.2000	67.8000	79.9800	0.4200
76 g-74	310.0000	0.0000	0.0000	0.0000	0.0000	0.0000	0.0000	0.0000	0.0000	0.0000
76 g-75	129.0000	3.3650	1.2920	0.0000	76.8400	20.1600	3.0100	97.0000	23.1700	3.8100
76 g-77	113.0000	4.1520	1.5970	0.0000	54.2000	40.8200	4.9800	95.0300	45.8000	1.3300
76 g-79	111.0000	4.1420	1.4510	0.2300	54.0500	40.7200	4.5000	94.7700	45.2200	1.3300
76 g-80	104.0000	4.6420	1.6660	0.0000	37.9400	56.4700	5.5900	94.4100	62.0600	0.6700
76 g-81	103.0000	4.4880	1.7120	0.0000	45.4200	48.9300	5.6500	94.3500	54.5800	0.9300
76 g-82	97.0000	4.3770	1.0170	0.0000	50.0500	43.9800	5.9700	94.0300	49.9500	1.1400
76 g-80	96.0000	4.1870	1.7570	0.0000	67.1200	31.7300	5.1500	94.8500	36.8800	1.9900
76 g-90	105.0000	5.0000	1.7010	0.0000	44.1500	68.7300	7.1300	92.8800	75.8600	0.3500
76 g-94	123.0000	0.5450	1.4000	77.7300	62.5500	2.4100	1.1200	65.1600	3.7300	24.0100
76 g-103	125.0000	1.4870	1.0270	5.7800	90.3500	10.9500	2.9300	91.3000	13.8800	7.3400

DATE 3/30/78

appendix a-continued

SAMPLE	slt/clay	% carbon	smectone	% illite	% kaolin	chlorite	% cpx	% opx	% vrf	% amphib
76 g-2	5.1700	0.7000	0.0000	0.0000	0.0000	0.0000	27.0000	5.0000	45.0000	2.0000
76 g-5	7.0000	0.4100	43.0400	25.3200	7.1700	34.5100	33.0000	7.0000	44.0000	6.0000
76 g-8	9.3400	0.4300	46.5700	20.4100	1.1300	31.2300	15.0000	8.0000	44.0000	15.0000
76 g-11	7.5700	0.7200	36.5400	25.2500	0.7400	29.4600	26.0000	5.0000	32.0000	18.0000
76 g-13	9.7100	0.7200	39.4400	24.9100	2.3800	34.2500	15.0000	17.0000	24.0000	24.0000
76 g-16	0.0000	0.0000	20.2300	22.3100	7.7500	30.7100	17.0000	14.0000	26.0000	17.0000
76 g-19	8.7200	0.4800	0.0000	0.0000	0.0000	0.0000	17.0000	18.0000	22.0000	19.0000
76 g-20	7.0000	0.4300	30.4000	20.4000	11.7000	33.0100	15.0000	13.0000	29.0000	16.0000
76 g-27	4.7400	0.3900	24.0600	28.2600	5.1700	32.5100	0.0000	0.0000	0.0000	0.0000
76 g-30	5.4300	0.7500	0.0000	0.0000	0.0000	0.0000	14.0000	12.0000	34.0000	15.0000
76 g-32	4.9900	0.3100	0.0000	0.0000	0.0000	0.0000	0.0000	0.0000	0.0000	0.0000
76 g-33	4.5400	0.4600	0.0000	0.0000	0.0000	0.0000	0.0000	0.0000	0.0000	0.0000
76 g-35	7.1000	0.4000	0.0000	0.0000	0.0000	0.0000	0.0000	0.0000	0.0000	0.0000
76 g-37	7.4300	0.3200	0.0000	0.0000	0.0000	0.0000	14.5000	11.0000	16.0000	19.3000
76 g-40	9.9700	0.5400	0.0000	0.0000	0.0000	0.0000	0.0000	0.0000	0.0000	0.0000
76 g-41	7.1200	0.4700	34.4300	27.1700	6.8100	29.6200	11.0000	13.0000	26.0000	20.0000
76 g-43	6.4700	0.4900	35.0500	28.6100	2.1900	34.1400	15.0000	8.8000	19.0000	15.2000
76 g-46	5.7600	0.9700	29.3500	21.7800	4.5600	44.3200	11.0000	12.0000	28.0000	17.0000
76 g-48	5.7600	0.2900	0.0000	0.0000	0.0000	0.0000	11.0000	13.0000	33.0000	13.0000
76 g-49	8.3200	0.3300	0.0000	0.0000	0.0000	0.0000	11.0000	15.0000	35.0000	15.0000
76 g-51	10.9600	0.4700	23.0800	24.6200	10.7100	31.5900	15.0000	9.0000	37.0000	15.0000
76 g-52	13.5500	0.6100	31.4500	27.0100	11.7700	34.7700	13.0000	11.0000	41.0000	6.0000
76 g-54	10.7000	0.5600	28.0200	24.7200	7.1500	28.1100	17.0000	16.0000	35.0000	9.0000
76 g-56	10.5700	0.7500	0.0000	0.0000	0.0000	0.0000	16.0000	9.0000	36.0000	14.0000
76 g-59	7.2200	0.8900	24.0000	27.2400	7.7600	40.1000	12.0000	13.0000	42.0000	13.0000
76 g-62	5.4000	0.9400	34.0800	24.5300	8.5600	29.9700	18.0000	5.0000	46.0000	20.0000
76 g-63	6.4300	0.9900	43.2700	19.2300	11.9300	25.5700	17.0000	11.0000	14.0000	19.0000
76 g-65	4.9400	0.5000	20.2700	22.6200	1.8200	37.5700	14.0000	17.0000	19.0000	19.0000
76 g-67	1.7000	0.3100	30.0900	20.2700	7.1400	33.5100	14.0000	10.0000	21.0000	11.0000
76 g-69	3.0200	0.3400	0.0000	0.0000	0.0000	0.0000	15.0000	13.0000	19.0000	17.0000
76 g-71	1.4800	0.7000	24.2900	22.2900	0.0000	43.4400	9.0000	6.0000	32.0000	15.0000
76 g-74	0.0000	0.0000	44.3700	21.0000	6.5800	27.1100	12.0000	10.0000	10.0000	23.0000
76 g-75	6.7800	0.0000	24.2700	20.2700	8.2700	36.4800	12.0000	12.0000	12.0000	17.0000
76 g-77	8.2100	0.5200	16.8400	36.5100	5.9200	27.7300	13.0000	14.0000	20.0000	23.0000
76 g-79	8.1500	0.7500	0.0000	0.0000	0.0000	0.0000	16.0000	5.0000	2.0000	21.0000
76 g-80	10.1000	0.9200	0.0000	0.0000	0.0000	0.0000	0.0000	0.0000	0.0000	0.0000
76 g-81	8.4600	0.4500	0.0000	0.0000	0.0000	0.0000	0.0000	0.0000	0.0000	0.0000
76 g-82	7.3200	0.7800	25.0300	21.6400	7.5400	25.7000	0.0000	0.0000	0.0000	0.0000
76 g-89	6.1700	0.0000	13.0200	44.0200	0.0000	40.0000	21.0000	6.0000	41.0000	16.0000
76 g-90	5.4500	0.0700	0.0000	0.0000	0.0000	0.0000	0.0000	0.0000	0.0000	0.0000
76 g-94	2.7300	0.2700	0.0000	0.0000	0.0000	0.0000	19.0000	10.0000	31.0000	12.0000
76 g-103	3.7400	0.2400	29.7500	24.4000	6.2800	29.2700	19.0000	9.0000	16.0000	14.0000

appendix a-continued

SAMPLE	% olivin	% opaque	chlorite	% epidot	garnet	% mrf	% pluton	% fn-gr	% unk-hv	% oth-hv
76 g-2	0.0000	17.0000	0.0000	1.0000	0.5000	0.0000	0.0000	0.0000	2.0000	0.5000
76 g-5	0.0000	0.0000	0.0000	0.0000	0.0000	0.0000	0.0000	0.0000	1.0000	1.0000
76 g-7	0.0000	0.0000	1.0000	2.0000	0.5000	0.0000	1.0000	1.0000	2.0000	1.0000
76 g-11	0.0000	6.0000	2.0000	2.0000	1.0000	0.0000	0.0000	0.0000	4.0000	1.0000
76 g-13	0.0000	6.0000	2.0000	2.0000	1.0000	2.0000	1.0000	2.0000	4.0000	1.0000
76 g-16	0.0000	0.0000	4.0000	1.0000	2.0000	3.0000	2.0000	2.0000	3.0000	1.0000
76 g-19	0.0000	4.0000	2.0000	2.0000	2.0000	2.5000	1.0000	2.0000	4.0000	2.0000
76 g-20	1.0000	6.0000	2.0000	2.0000	1.0000	3.0000	1.0000	2.0000	4.0000	4.0000
76 g-27	0.0000	0.0000	0.0000	0.0000	0.0000	0.0000	0.0000	0.0000	0.0000	0.0000
76 g-30	1.0000	5.0000	5.0000	2.0000	2.0000	2.0000	1.0000	3.0000	4.0000	3.0000
76 g-32	0.0000	0.0000	0.0000	0.0000	0.0000	0.0000	0.0000	0.0000	0.0000	0.0000
76 g-33	0.0000	0.0000	0.0000	0.0000	0.0000	0.0000	0.0000	0.0000	0.0000	0.0000
76 g-38	0.0000	0.0000	0.0000	0.0000	0.0000	0.0000	0.0000	0.0000	0.0000	0.0000
76 g-37	0.0000	7.0000	1.6000	2.5000	0.0000	4.5000	5.7000	7.6000	4.7000	2.2000
76 g-40	0.0000	0.0000	0.0000	0.0000	0.0000	0.0000	0.0000	0.0000	0.0000	0.0000
76 g-41	0.0000	6.0000	3.0000	2.0000	1.0000	7.0000	5.0000	2.0000	3.0000	3.0000
76 g-43	0.0000	6.4000	7.6000	7.3000	1.5000	5.5000	2.7000	2.0000	2.7000	4.5000
76 g-46	0.0000	4.0000	5.0000	1.0000	1.0000	5.0000	5.0000	3.0000	4.0000	1.0000
76 g-48	0.0000	4.0000	3.0000	2.0000	1.0000	4.0000	6.0000	2.0000	4.0000	2.0000
76 g-49	0.0000	4.6000	4.0000	2.0000	0.0000	2.0000	2.0000	5.0000	3.0000	1.0000
76 g-51	0.0000	0.0000	3.0000	4.0000	1.0000	1.0000	1.0000	4.0000	2.0000	1.0000
76 g-52	0.0000	4.0000	5.0000	3.0000	0.5000	4.0000	3.0000	3.0000	3.0000	2.0000
76 g-54	0.0000	4.0000	3.0000	1.0000	0.0000	2.5000	3.0000	2.5000	4.0000	1.5000
76 g-56	0.5000	5.0000	3.0000	3.0000	1.0000	3.0000	2.0000	4.0000	4.0000	1.5000
76 g-55	0.0000	5.0000	3.0000	2.0000	1.0000	2.0000	1.0000	3.0000	3.0000	0.0000
76 g-62	0.5000	5.0000	2.0000	1.0000	0.5000	0.0000	0.0000	0.0000	3.0000	1.5000
76 g-63	0.0000	5.0000	4.5000	2.5000	1.0000	4.0000	2.5000	6.5000	4.0000	2.0000
76 g-65	0.0000	0.0000	2.0000	2.0000	2.0000	6.0000	1.5000	2.5000	4.0000	3.0000
76 g-67	0.5000	10.0000	2.0000	2.0000	3.0000	4.0000	2.5000	6.0000	3.0000	3.0000
76 g-69	1.0000	0.0000	3.0000	7.0000	1.0000	2.0000	1.0000	6.0000	3.0000	4.0000
76 g-71	1.0000	6.0000	6.0000	2.0000	0.0000	3.0000	3.0000	7.0000	4.0000	4.0000
76 g-74	2.0000	12.0000	3.0000	4.0000	2.0000	0.0000	1.5000	6.0000	6.0000	0.0000
76 g-75	1.0000	0.0000	5.0000	4.0000	2.0000	7.0000	3.0000	8.0000	5.0000	2.0000
76 g-77	1.0000	2.0000	2.0000	4.0000	1.0000	2.0000	4.0000	6.0000	3.0000	3.0000
76 g-79	0.0000	10.0000	7.0000	5.0000	0.0000	0.0000	1.0000	8.0000	3.0000	0.0000
76 g-80	0.0000	0.0000	0.0000	0.0000	0.0000	0.0000	0.0000	0.0000	0.0000	0.0000
76 g-81	0.0000	0.0000	0.0000	0.0000	0.0000	0.0000	0.0000	0.0000	0.0000	0.0000
76 g-82	0.0000	0.0000	0.0000	0.0000	0.0000	0.0000	0.0000	0.0000	0.0000	0.0000
76 g-85	5.0000	4.0000	3.0000	1.0000	0.1000	1.0000	0.1000	0.1000	2.0000	0.0000
76 g-90	0.0000	0.0000	0.0000	0.0000	0.0000	0.0000	0.0000	0.0000	0.0000	0.0000
76 g-94	5.0000	5.0000	0.0000	2.0000	2.0000	7.0000	0.5000	3.0000	3.0000	0.0000
76 g-103	3.0000	14.0000	1.0000	3.0000	2.0000	3.0000	2.0000	7.0000	4.0000	4.0000

appendix a-continued

SAMPLE	% quartz	% k-spar	% glass	% vol ex	% ron vo	% orb-lt	kaol+chl	illite x	ml (exo)	ml (ilt)
76 g-2	3.2000	27.2000	14.3000	26.5000	1.7000	11.0000	3.0000	0.0000	0.0000	0.0000
76 g-5	2.8000	26.6000	27.2000	32.6000	1.6000	5.3000	31.6500	0.4800	0.7500	0.2500
76 g-8	6.7000	31.1000	26.7000	21.5000	5.2000	10.8000	23.0600	0.5000	0.7200	0.2800
76 g-11	0.0000	0.0000	0.0000	0.0000	0.0000	0.0000	38.2100	0.3600	0.7300	0.2700
76 g-13	10.0000	29.0000	1.0000	12.1000	21.7000	6.4000	36.6700	0.4000	0.6600	0.3400
76 g-16	20.1000	33.7000	5.7000	2.6000	27.1000	8.2000	38.4600	0.5200	0.7100	0.2900
76 g-19	16.9000	38.7000	7.7000	9.3000	25.8000	6.1000	0.0000	0.0000	0.0000	0.0000
76 g-20	19.2000	39.7000	4.0000	9.0000	27.3000	3.2000	44.7100	0.2300	0.7000	0.3000
76 g-22	14.8000	42.7000	1.7000	7.6000	26.6000	6.7000	37.6800	0.3700	0.6000	0.4000
76 g-30	18.4000	46.9000	3.5000	5.4000	18.4000	7.4000	0.0000	0.0000	0.0000	0.0000
76 g-32	0.0000	0.0000	0.0000	0.0000	0.0000	0.0000	0.0000	0.0000	0.0000	0.0000
76 g-33	0.0000	0.0000	0.0000	0.0000	0.0000	0.0000	0.0000	0.0000	0.0000	0.0000
76 g-38	0.0000	0.0000	0.0000	0.0000	0.0000	0.0000	0.0000	0.0000	0.0000	0.0000
76 g-37	20.7000	37.7000	4.4000	4.7000	27.2000	5.7000	0.0000	0.0000	0.0000	0.0000
76 g-40	0.0000	0.0000	0.0000	0.0000	0.0000	0.0000	0.0000	0.0000	0.0000	0.0000
76 g-41	15.8000	35.0000	5.2000	7.7000	26.4000	8.6000	36.4300	0.5500	0.7300	0.2700
76 g-43	14.2000	28.4000	5.5000	9.0000	34.8000	8.1000	36.3400	0.2600	0.7400	0.2600
76 g-46	13.3000	34.2000	10.2000	9.2000	22.1000	10.5000	48.8700	0.4600	0.7300	0.2700
76 g-48	13.1000	24.8000	13.4000	15.7000	21.3000	11.6000	0.0000	0.0000	0.0000	0.0000
76 g-49	11.0000	29.6000	11.0000	12.6000	22.1000	13.7000	0.0000	0.0000	0.0000	0.0000
76 g-51	0.0000	0.0000	0.0000	0.0000	0.0000	0.0000	42.3100	0.6400	0.7000	0.3000
76 g-52	15.6000	41.6000	6.1000	7.3000	22.3000	7.1000	46.5400	0.3600	0.7600	0.2400
76 g-54	1.2000	26.4000	30.6000	29.1000	5.3000	6.4000	45.2600	0.3500	0.7000	0.3000
76 g-56	8.9000	29.4000	20.7000	20.1000	11.6000	7.3000	0.0000	0.0000	0.0000	0.0000
76 g-59	0.0000	0.0000	0.0000	0.0000	0.0000	0.0000	47.8600	0.5200	0.7000	0.3000
76 g-62	14.0000	37.2000	13.4000	7.9000	22.5000	4.4000	38.5400	0.4400	0.7500	0.2500
76 g-63	0.0000	0.0000	0.0000	0.0000	0.0000	0.0000	32.5000	0.3800	0.7300	0.2700
76 g-65	19.7000	33.9000	8.1000	7.1000	25.5000	5.7000	39.4500	0.5900	0.7200	0.2800
76 g-67	22.4000	33.2000	8.2000	6.2000	22.3000	7.2000	40.6500	0.4600	0.7400	0.2600
76 g-69	0.0000	0.0000	0.0000	0.0000	0.0000	0.0000	0.0000	0.0000	0.0000	0.0000
76 g-71	11.6000	35.2000	6.9000	8.0000	25.7000	9.1000	43.4400	0.1300	0.7300	0.2700
76 g-74	22.9000	38.4000	4.0000	4.6000	21.0000	8.2000	33.6900	0.3800	0.7500	0.2500
76 g-75	19.6000	50.4000	3.4000	5.0000	16.8000	4.8000	44.7500	0.2900	0.7300	0.2700
76 g-77	21.4000	41.1000	2.9000	4.9000	23.3000	6.4000	43.6500	0.3500	0.6900	0.3100
76 g-79	0.0000	0.0000	0.0000	0.0000	0.0000	0.0000	0.0000	0.0000	0.0000	0.0000
76 g-80	0.0000	0.0000	0.0000	0.0000	0.0000	0.0000	0.0000	0.0000	0.0000	0.0000
76 g-81	18.9000	46.0000	4.6000	4.6000	15.7000	7.2000	0.0000	0.0000	0.0000	0.0000
76 g-82	0.0000	0.0000	0.0000	0.0000	0.0000	0.0000	33.3300	0.3100	0.7000	0.3000
76 g-89	17.0000	49.8000	5.0000	6.3000	15.1000	6.2000	41.0000	0.0900	0.7000	0.3000
76 g-90	0.0000	0.0000	0.0000	0.0000	0.0000	0.0000	0.0000	0.0000	0.0000	0.0000
76 g-94	0.0000	0.0000	0.0000	0.0000	0.0000	0.0000	0.0000	0.0000	0.0000	0.0000
76 g-103	19.8000	32.0000	0.5000	13.2000	17.1000	5.9000	39.2500	0.6000	0.6400	0.3600

DATE 3/30/78

appendix a-continued

SAMPLE	depth	mean	sorting	% gravel	% sand	% silt	% clay	sand+silt	silt+clay	sand/silt
76 g-105	320.0000	4.5520	2.2610	0.1500	74.1500	47.5000	28.2100	71.6500	75.7100	0.5100
76 g-109	135.0000	2.8140	1.0010	0.4300	87.0400	10.1600	2.3700	97.2000	12.5300	8.5700
76 g-111	132.0000	3.7050	1.5000	0.0000	67.1900	28.5100	4.3000	95.7000	32.8100	2.3600
76 g-113	138.0000	4.5030	1.5710	0.0000	47.1400	47.4500	5.2200	94.7000	52.8700	0.9900
76 g-116	140.0000	4.1450	2.0640	0.2200	54.2200	37.6600	7.3100	92.4300	44.9700	1.4500
76 g-118	144.0000	4.5430	1.0620	0.0000	41.7100	51.9500	5.3400	93.6600	58.2900	0.8000
76 g-119	145.0000	4.5720	1.4900	0.0000	33.5400	61.1200	5.3400	94.6400	66.4600	0.5500
76 g-121	57.0000	4.2510	1.5100	0.0000	72.3300	61.2400	5.8000	94.1700	67.6400	0.5200
76 v-2	90.0000	2.2950	0.2610	0.1600	92.6600	5.6600	1.5300	98.3200	7.1900	16.3700
76 v-3	75.0000	3.0000	0.4000	0.0000	94.0500	4.0000	1.8600	98.1400	5.9400	23.0400
76 v-4	30.0000	2.5500	0.6600	0.0000	83.4400	5.1000	1.4600	98.5400	6.5600	18.3100
76 v-5	31.0000	2.2640	0.2930	0.0000	93.4500	4.7800	1.7700	98.2300	6.5500	19.5500
76 v-6	32.0000	2.4020	0.2200	0.0000	91.7400	6.6100	1.6500	98.3500	8.2600	13.8800
76 v-7	122.0000	2.2000	1.0400	0.0000	66.6200	10.9800	3.4000	96.6000	14.3800	7.8000
76 v-8	52.0000	0.3300	0.0000	0.0000	8.0000	0.0000	0.0000	0.0000	0.0000	0.0000
76 v-9	60.0000	2.1240	0.4320	0.4900	65.3800	3.1900	0.9500	99.5700	4.1400	29.8400
76 v-10	60.0000	2.2020	0.6000	0.2800	92.2800	3.1900	1.6600	95.4700	4.8500	28.9600
76 v-11	68.0000	2.8240	0.6520	0.1300	64.0700	4.3900	1.3500	98.4400	5.7400	21.4000
76 v-12	63.0000	2.2170	1.1330	5.2200	58.2900	4.2500	1.6600	92.5400	5.9100	20.7500
76 v-14	124.0000	2.0450	0.3420	0.0000	51.2400	6.2300	2.5300	97.4700	8.7600	14.6500
76 v-15	145.0000	2.1800	0.2620	0.0000	64.0000	3.3300	1.6900	98.3200	5.0200	28.5000
76 v-16	122.0000	2.6520	2.0900	20.0200	58.4800	6.2200	2.3900	66.9600	8.6000	9.4100
76 v-17	95.0000	2.2320	0.5900	0.5900	62.2700	5.8500	1.3800	98.1200	7.2300	15.7900
76 v-18	100.0000	2.8110	0.6450	0.0000	64.1000	4.9200	1.0800	98.9200	5.9000	19.5100
76 v-19	110.0000	2.0310	0.0950	0.0000	59.7800	8.0600	2.1600	97.8400	10.2200	11.1300
76 v-20	102.0000	2.4900	0.9100	0.0600	61.2200	6.2900	1.9400	98.0000	8.2200	14.6000
76 v-21	101.0000	2.0000	0.8910	0.0000	60.4300	7.7600	1.8100	98.1900	9.5700	11.6500
76 v-22	102.0000	2.9630	0.9700	0.1900	58.4000	8.3600	3.0400	96.7600	11.4000	10.5700
76 v-23	103.0000	2.6710	0.0060	0.0000	61.0400	6.5700	2.3900	97.6100	8.9500	13.8600
76 v-24	108.0000	1.6140	1.5740	10.1300	53.8700	4.1800	1.8100	88.0500	5.9900	20.0400
76 v-26	152.0000	1.5900	1.2250	11.8100	82.2000	3.2300	2.2900	85.9300	5.5200	25.5900
76 v-29	96.0000	1.9330	1.3320	9.4300	64.0600	4.1900	2.3400	88.2400	6.5200	20.1200
76 p-7	110.0000	5.1430	1.6920	0.0000	20.3100	22.3100	5.8000	93.1200	79.2000	0.2900
76 p-10	2850.0000	6.6710	2.6320	0.0000	6.3200	68.0700	25.6500	74.3500	93.6800	0.0900
76 p-11	2770.0000	7.2210	3.0750	0.0000	5.9400	50.5800	43.4700	56.5200	94.0500	0.1200
76 p-13	2090.0000	7.2700	2.6710	0.0000	3.4200	65.2000	31.2300	68.7700	96.5300	0.0500

appendix a-continued

SAMPLE	slt/clay	% carbon	specter	% illite	% kaolin	chloritic	% cpx	% opx	% vrf	% amphib
76 g-105	1.6900	0.9300	17.1900	45.0000	0.0000	37.8000	13.0000	8.0000	40.0000	21.0000
76 g-109	4.2800	0.7400	24.3000	30.0000	9.3600	74.8500	24.0000	13.0000	6.0000	20.0000
76 g-111	6.6200	0.4700	34.5100	21.0500	4.5700	78.9700	13.0000	11.0000	17.0000	23.0000
76 g-113	5.1700	0.0000	36.9700	24.1900	0.7200	29.1600	17.0000	12.0000	27.0000	16.0000
76 g-116	5.1500	0.4100	0.0000	0.0000	0.0000	0.0000	12.0000	9.0000	41.0000	13.0000
76 g-118	8.2000	0.5500	0.0000	0.0000	0.0000	0.0000	14.0000	9.0000	41.0000	9.0000
76 g-119	11.4500	0.5500	0.0000	0.0000	0.0000	0.0000	15.0000	11.0000	47.0000	9.0000
76 g-121	10.6600	0.7500	57.4900	17.0100	0.0000	25.5100	35.0000	8.0000	47.0000	2.0000
76 v-2	3.7100	0.2500	0.0000	0.0000	0.0000	0.0000	18.0000	14.0000	11.0000	17.0000
76 v-3	2.2000	0.2200	15.6700	32.0700	7.4200	41.5700	17.0000	16.0000	12.0000	15.0000
76 v-4	3.4900	0.2200	0.0000	0.0000	0.0000	0.0000	0.0000	0.0000	0.0000	0.0000
76 v-5	2.7000	0.2500	0.0000	0.0000	0.0000	0.0000	0.0000	0.0000	0.0000	0.0000
76 v-6	4.0100	0.0000	22.7000	35.0000	5.4600	35.6700	14.0000	17.0000	16.0000	20.0000
76 v-7	3.2200	0.4000	0.0000	0.0000	0.0000	0.0000	15.0000	13.0000	19.0000	17.0000
76 v-8	0.0000	0.0000	35.6500	34.5600	5.4900	24.0600	0.0000	0.0000	0.0000	0.0000
76 v-9	3.3300	0.2200	0.0000	0.0000	0.0000	0.0000	20.0000	9.0000	27.0000	14.0000
76 v-10	1.9200	0.3700	0.0000	0.0000	0.0000	0.0000	0.0000	0.0000	0.0000	0.0000
76 v-11	3.2500	0.2900	0.0000	0.0000	0.0000	0.0000	0.0000	0.0000	0.0000	0.0000
76 v-12	2.5600	0.2300	16.8500	44.4700	6.0900	32.6200	15.0000	19.0000	26.0000	10.0000
76 v-14	2.4600	0.3100	0.0000	0.0000	0.0000	0.0000	17.0000	17.0000	18.0000	18.0000
76 v-15	1.9700	0.2200	0.0000	0.0000	0.0000	0.0000	0.0000	0.0000	0.0000	0.0000
76 v-16	2.6000	0.0000	0.0000	0.0000	0.0000	0.0000	19.0000	10.0000	31.0000	12.0000
76 v-17	4.0700	0.2900	36.4400	29.0600	8.9100	24.6900	18.0000	13.0000	32.0000	12.0000
76 v-18	4.4600	0.2600	43.0500	26.0500	6.6100	24.7000	23.0000	13.0000	26.0000	11.0000
76 v-19	3.7400	0.3100	0.0000	0.0000	0.0000	0.0000	0.0000	0.0000	0.0000	0.0000
76 v-20	3.2300	0.2900	53.0500	15.2400	9.1700	23.5300	0.0000	0.0000	0.0000	0.0000
76 v-21	4.2900	0.3100	0.0000	0.0000	0.0000	0.0000	0.0000	0.0000	0.0000	0.0000
76 v-22	2.7500	0.2900	38.6400	27.3900	4.1300	29.5400	20.0000	15.0000	21.0000	15.0000
76 v-23	2.7500	0.3300	0.0000	0.0000	0.0000	0.0000	0.0000	0.0000	0.0000	0.0000
76 v-24	2.7100	0.2500	0.0000	0.0000	0.0000	0.0000	0.0000	0.0000	0.0000	0.0000
76 v-26	1.4100	0.2600	0.0000	0.0000	0.0000	0.0000	0.0000	0.0000	0.0000	0.0000
76 v-29	1.7900	3.1900	0.0000	0.0000	0.0000	0.0000	27.0000	15.0000	38.0000	4.0000
76 p-7	10.5000	0.7600	30.2100	35.0000	9.4600	25.2300	13.0000	8.0000	29.0000	16.0000
76 p-10	3.3500	1.1200	38.3700	27.3300	8.4500	25.5500	17.0000	9.0000	36.0000	12.0000
76 p-11	1.1600	1.6500	0.0000	0.0000	0.0000	0.0000	0.0000	0.0000	0.0000	0.0000
76 p-13	2.0000	1.5400	26.6000	31.9100	6.5800	34.9100	11.0000	5.0000	69.0000	6.0000

appendix a-continued

SAMPLE	% olivin	% opaque	chlorite	% epidot	% garnet	% trf	% pluton	% fn-gr	% unk-hv	% oth-hv
76 g-105	1.0000	2.0000	3.0000	3.0000	0.1000	0.0000	1.0000	2.0000	4.0000	1.0000
76 g-109	0.1000	12.0000	2.0000	4.0000	3.0000	5.0000	2.0000	5.0000	3.0000	1.0000
76 g-111	0.1000	10.0000	2.0000	5.0000	2.0000	4.0000	4.0000	7.0000	2.0000	2.0000
76 g-113	0.0000	8.0000	3.0000	4.0000	1.0000	3.0000	2.0000	4.0000	3.0000	2.0000
76 g-116	1.0000	6.0000	3.0000	2.0000	1.0000	3.0000	2.0000	5.0000	3.0000	1.0000
76 g-118	0.0000	5.0000	3.0000	3.0000	1.0000	2.0000	3.0000	4.0000	4.0000	2.0000
76 g-119	0.0000	5.0000	1.0000	4.0000	1.0000	1.0000	1.0000	2.0000	2.0000	0.0000
76 g-121	0.0000	7.0000	0.0000	0.0000	0.0000	0.0000	0.0000	0.0000	1.0000	0.0000
76 v-2	0.0000	14.0000	2.0000	4.0000	4.0000	2.0000	2.0000	5.0000	3.0000	3.0000
76 v-3	0.0000	14.0000	1.0000	6.0000	4.0000	2.0000	1.0000	5.0000	3.0000	4.0000
76 v-4	0.0000	0.0000	0.0000	0.0000	0.0000	0.0000	0.0000	0.0000	0.0000	0.0000
76 v-5	0.0000	0.0000	0.0000	0.0000	0.0000	0.0000	0.0000	0.0000	0.0000	0.0000
76 v-6	1.0000	7.0000	2.0000	2.0000	2.0000	3.0000	1.0000	3.0000	3.0000	3.0000
76 v-7	1.0000	9.0000	2.0000	2.0000	1.0000	7.0000	1.0000	20.0000	3.0000	3.0000
76 v-8	0.0000	0.0000	0.0000	0.0000	0.0000	0.0000	0.0000	0.0000	0.0000	0.0000
76 v-9	6.0000	10.0000	1.0000	2.0000	3.0000	1.0000	0.0000	3.0000	2.0000	3.0000
76 v-10	0.0000	0.0000	0.0000	0.0000	0.0000	0.0000	0.0000	0.0000	0.0000	0.0000
76 v-11	0.0000	0.0000	0.0000	0.0000	0.0000	0.0000	0.0000	0.0000	0.0000	0.0000
76 v-12	2.0000	5.0000	4.0000	5.0000	1.0000	4.0000	0.0000	5.0000	3.0000	1.0000
76 v-14	1.0000	8.0000	2.0000	4.0000	3.0000	2.0000	0.5000	4.0000	3.0000	3.0000
76 v-15	0.0000	0.0000	0.0000	0.0000	0.0000	0.0000	0.0000	0.0000	0.0000	0.0000
76 v-16	5.0000	8.0000	2.0000	2.0000	2.0000	2.0000	0.0000	3.0000	3.0000	0.0000
76 v-17	7.0000	7.0000	2.0000	3.0000	2.0000	0.0000	0.0000	2.0000	4.0000	1.0000
76 v-18	7.0000	4.0000	1.0000	2.0000	2.0000	1.0000	0.5000	5.0000	4.0000	0.0000
76 v-19	0.0000	0.0000	0.0000	0.0000	0.0000	0.0000	0.0000	0.0000	0.0000	0.0000
76 v-20	0.0000	0.0000	0.0000	0.0000	0.0000	0.0000	0.0000	0.0000	0.0000	0.0000
76 v-21	0.0000	0.0000	0.0000	0.0000	0.0000	0.0000	0.0000	0.0000	0.0000	0.0000
76 v-22	4.0000	8.0000	0.1000	4.0000	2.0000	1.0000	0.0000	0.0000	0.0000	0.0000
76 v-23	0.0000	0.0000	0.0000	0.0000	0.0000	0.0000	0.0000	5.0000	4.0000	0.0000
76 v-24	0.0000	0.0000	0.0000	0.0000	0.0000	0.0000	0.0000	0.0000	0.0000	0.0000
76 v-26	0.0000	0.0000	0.0000	0.0000	0.0000	0.0000	0.0000	0.0000	0.0000	0.0000
76 v-29	1.0000	7.0000	0.1000	0.1000	1.0000	1.0000	0.0000	1.0000	3.0000	0.0000
76 p-7	0.0000	6.0000	8.0000	4.0000	1.0000	4.0000	2.0000	4.0000	2.0000	2.0000
76 p-10	0.1000	7.0000	3.0000	4.0000	0.1000	2.0000	1.0000	6.0000	2.0000	0.0000
76 p-11	0.0000	0.0000	0.0000	0.0000	0.0000	0.0000	0.0000	0.0000	0.0000	0.0000
76 p-13	0.0000	3.0000	2.0000	0.0000	0.0000	0.0000	0.1000	3.0000	1.0000	1.0000

appendix a-continued

SAMPLE	% quartz	% k-spar	% glass	% vol rx	% non va	% eth-lt	kaol+chl	illite x	ml (exp)	ml (ill)
76 q-105	11.5000	46.1000	7.4000	5.2000	23.2000	6.4000	32.9000	0.1300	0.6900	0.3100
76 q-109	25.6000	77.3000	6.7000	7.1000	17.9000	6.4000	44.7200	0.4400	0.6600	0.3400
76 q-111	14.1000	47.1000	13.2000	8.5000	15.5000	5.0000	43.5400	0.4200	0.7300	0.2700
76 q-113	15.2000	35.2000	16.7000	6.9000	13.9000	0.0000	38.8800	0.5500	0.7300	0.2700
76 q-116	8.1000	37.6000	17.1000	10.2000	25.5000	5.7000	0.0000	0.0000	0.0000	0.0000
76 g-118	8.9000	26.6000	21.1000	12.9000	15.7000	4.9000	0.0000	0.0000	0.0000	0.0000
76 g-119	2.3000	16.6000	42.1000	21.5000	4.4000	7.2000	0.0000	0.0000	0.0000	0.0000
76 g-121	0.5000	39.9000	22.8000	26.5000	4.1000	5.4000	25.5100	0.5300	0.7700	0.2300
76 v-2	22.5000	42.9000	3.4000	7.1000	24.4000	4.6000	0.0000	0.0000	0.0000	0.0000
76 v-3	22.2000	36.5000	3.9000	3.3000	29.5000	4.6000	49.0000	0.3000	0.7600	0.2400
76 v-4	0.0000	0.0000	6.0000	0.0000	6.0000	0.0000	0.0000	0.0000	0.0000	0.0000
76 v-5	0.0000	0.0000	0.0000	0.0000	6.0000	0.0000	0.0000	0.0000	0.0000	0.0000
76 v-6	20.5000	41.9000	5.6000	9.2000	16.2000	5.5000	41.3100	0.2800	0.7200	0.2800
76 v-7	18.6000	38.1000	5.6000	4.3000	28.8000	4.3000	0.0000	0.0000	0.0000	0.0000
76 v-8	0.0000	0.0000	0.0000	0.0000	0.0000	0.0000	29.7500	0.2900	0.7200	0.2800
76 v-9	22.4000	34.0000	7.4000	5.2000	25.1000	5.2000	0.0000	0.0000	0.0000	0.0000
76 v-10	0.0000	0.0000	0.0000	0.0000	0.0000	0.0000	0.0000	0.0000	0.0000	0.0000
76 v-11	0.0000	0.0000	0.0000	0.0000	0.0000	0.0000	0.0000	0.0000	0.0000	0.0000
76 v-12	25.1000	27.3000	7.9000	7.2000	17.2000	5.3000	38.7100	0.2000	0.6600	0.3400
76 v-14	17.2000	36.2000	6.6000	5.4000	25.1000	5.9000	0.0000	0.0000	0.0000	0.0000
76 v-15	0.0000	0.0000	0.0000	0.0000	0.0000	0.0000	0.0000	0.0000	0.0000	0.0000
76 v-16	21.5000	31.1000	11.5000	4.4000	24.8000	5.3000	0.0000	0.0000	0.0000	0.0000
76 v-17	20.0000	49.2000	8.2000	7.2000	27.3000	3.6000	33.6000	0.2000	0.7400	0.2600
76 v-18	10.9000	35.4000	7.0000	11.5000	20.1000	5.9000	30.9100	0.2200	0.7100	0.2900
76 v-19	0.0000	0.0000	0.0000	0.0000	0.0000	0.0000	0.0000	0.0000	0.0000	0.0000
76 v-20	0.0000	0.0000	0.0000	0.0000	0.0000	0.0000	31.7100	0.0000	0.7500	0.2500
76 v-21	0.0000	0.0000	0.0000	0.0000	0.0000	0.0000	0.0000	0.0000	0.0000	0.0000
76 v-22	25.2000	37.2000	4.6000	5.6000	23.3000	3.6000	33.6700	0.2700	0.7200	0.2800
76 v-23	0.0000	0.0000	0.0000	0.0000	0.0000	0.0000	0.0000	0.0000	0.0000	0.0000
76 v-24	0.0000	0.0000	0.0000	0.0000	0.0000	0.0000	0.0000	0.0000	0.0000	0.0000
76 v-26	0.0000	0.0000	0.0000	0.0000	0.0000	0.0000	0.0000	0.0000	0.0000	0.0000
76 v-29	0.0000	0.0000	0.0000	0.0000	0.0000	0.0000	0.0000	0.0000	0.0000	0.0000
76 p-7	15.6000	26.2000	6.3000	6.0000	27.5000	7.9000	34.7000	0.3800	0.3000	0.3000
76 p-10	7.5000	25.9000	29.8000	14.4000	14.2000	8.2000	33.8000	0.5500	0.7100	0.2900
76 p-11	0.0000	0.0000	0.0000	0.0000	0.0000	0.0000	0.0000	0.0000	0.0000	0.0000
76 p-13	2.5000	15.6000	29.9000	24.5000	8.6000	18.9000	41.4900	0.8100	0.6600	0.3400

APPENDIX B

s4-76 St. George Basin Grid

DATE 3/17/77

CORE	INTERVAL	1	2	3	4	5	6	7	8	9	10
1	(cm)	Si %-xrf	Al %-xrf	Ca %-xrf	K %-xrf	Fe %-xrf	Ti %-xrf	S %-xrf	Mg %-aas	Na %-aas	Hg ppm-a
G002	15-20	26.0000	7.0000	4.0000	1.0500	5.0000	0.7000	0.0200	1.5400	2.3100	0.0300
G005	0-5	24.0244	7.9282	4.6926	0.9747	5.6325	0.6475	0.1160	1.4600	2.5600	0.0400
G006	3-4	24.0945	7.2772	4.8357	1.0012	5.5919	0.6583	0.0670	1.5300	2.5800	0.0300
G008	7-15	31.7937	5.4672	2.1877	1.1643	2.2249	0.3825	0.0860	1.2400	2.4300	0.0400
G009	4-5	26.6231	6.4410	4.0624	1.0834	4.4519	0.5463	0.1210	1.1900	2.4000	0.0300
G010	0-5	30.1806	6.4251	3.0603	1.2005	3.1628	0.4595	0.1390	0.9700	2.3300	0.0500
G011	13-18	28.9928	5.6630	2.8738	1.1947	3.1495	0.4192	0.1460	0.9600	2.1100	0.0400
G012	4-5	28.3333	5.7741	2.9510	1.1540	3.1104	0.4109	0.1220	0.9600	2.1500	0.0400
G013	14-19	28.3011	5.6206	2.9953	1.1756	3.2160	0.4155	0.1100	1.0000	2.1700	0.0300
G014	4-5	28.6984	5.6577	2.8910	1.1947	3.2565	0.4321	0.1410	1.0000	2.0200	0.0400
G015	4-5	29.4651	5.3190	2.5822	1.2411	2.9138	0.4261	0.1410	0.9500	2.2600	0.0800
G016	7-9	27.6187	5.1724	2.4714	1.1158	2.9995	0.4310	0.1300	0.9700	1.9500	0.0500
G018	4-5	30.1847	5.2719	2.2106	1.2760	2.4410	0.3587	0.1540	0.9100	1.9600	0.0400
G018	4-5	31.3298	5.2835	2.2306	1.2677	2.4067	0.3809	0.0620	0.8800	1.9900	0.0400
G019	0-3	29.7649	5.0956	2.3349	1.2403	2.3865	0.3482	0.1310	0.8500	1.8500	0.0300
G020	6-11	30.6427	5.5665	2.0126	1.2503	2.3487	0.3435	0.1180	0.8700	2.0400	0.0600
G021	4-5	32.5123	5.5677	2.2084	1.2750	2.2452	0.3575	0.1230	0.8600	2.0400	0.0400
G021	4-5	30.6334	5.2470	2.0419	1.2229	2.3354	0.3586	0.1070	0.8200	2.0300	0.0300
G027	14-19	31.6617	4.9188	2.0955	1.2710	2.2445	0.3578	0.1630	0.8900	1.8900	0.0300
G028	cc	32.6432	5.1587	2.1934	1.2395	2.0165	0.3637	0.1200	0.7700	1.7900	0.0400
G029	4-5	31.6897	5.0628	2.0226	1.2888	2.0808	0.3133	0.0570	0.8400	1.9900	0.0400
G029	4-5	32.2272	5.5143	2.0921	1.2262	2.0871	0.3593	0.1170	0.8400	1.9000	0.0400
G032	6-11	31.4981	4.9993	1.9783	1.2561	2.1759	0.3276	0.1090	0.8600	1.8200	0.0300
G033	8-13	31.0167	4.8919	2.0904	1.2470	2.3375	0.3399	0.0880	0.8900	2.0900	0.0400
G034	4-5	32.8255	4.8749	2.1591	1.2810	2.2557	0.3459	0.1180	0.8200	1.9500	0.0300
G034	4-5	32.6432	5.4513	2.1834	1.2677	2.2046	0.3693	0.0990	0.8000	1.8400	0.0400
G036	2-7	31.0728	5.0438	2.0812	1.2096	2.2095	0.3303	0.0780	0.8200	1.8400	0.0400
G041	6-11	30.4231	5.1115	2.1227	1.2373	2.5179	0.3577	0.1350	0.8700	1.8600	0.0400
G042	0-1	28.5301	5.1274	2.4514	1.1631	2.9250	0.3950	0.0780	0.9900	1.9400	0.0400
G043	0-6	28.8386	5.7454	2.3020	1.1872	2.9423	0.3927	0.2500	0.9900	2.1100	0.0600
G046	11-16	29.3525	5.4830	2.5222	1.1905	3.4594	0.4282	0.2020	1.0600	2.0000	0.0400
G047	4-5	27.0531	5.8353	2.6408	1.1349	3.7601	0.4595	0.2340	1.1300	2.1100	0.0400
G048	0-3	26.2071	6.0493	2.6094	1.1125	3.7077	0.4553	0.1760	1.0900	2.0000	0.0400
G049	0-5	26.3754	5.7900	2.9510	1.1133	3.8769	0.4724	0.1490	1.1700	2.1700	0.0400
G049	0-5	25.6042	5.9911	2.8724	1.0842	3.7720	0.4586	0.1690	1.1000	2.1500	0.0500
G050	0-1	27.3195	6.0387	3.3376	1.0942	4.0070	0.4878	0.1150	0.9600	2.4300	0.0400
G050	0-1	22.5567	5.1231	2.6351	0.9215	3.2286	0.3651	0.1030	1.1500	2.4700	0.0800
G051	6-11	26.1043	5.8000	3.0954	1.0826	3.8525	0.4743	0.1840	1.2300	2.4600	0.0500
G052	9-13	24.6077	7.1502	3.4220	0.9929	4.2364	0.5161	0.2120	1.2300	2.4300	0.0400
G053	0-1	25.6573	5.9170	3.9556	1.0279	4.6386	0.5457	0.1790	1.2700	2.3900	0.0300
G054	0-3	25.7197	6.2769	3.9444	0.9954	4.5875	0.5463	0.2090	1.2400	2.4200	0.0500
G055	4-5	26.8241	6.6844	3.4977	1.0651	3.9854	0.5163	0.1040	1.2300	2.6000	0.0500
G055	4-5	27.1372	6.7850	3.5443	1.0753	4.1357	0.5435	0.1530	1.1700	2.2800	0.0400
G056	0-4	25.5574	6.4198	3.3049	1.0602	4.4750	0.5237	0.1200	1.1900	2.4100	0.0400
G057	0-5	26.3614	6.0864	3.4792	1.0560	4.2169	0.5055	0.0730	1.1900	2.3500	0.0400
G059	5-8	26.0809	6.1181	2.9103	1.0994	3.7329	0.4381	0.1220	1.0300	2.2100	0.0400
G060	0-2	26.0309	5.0758	2.6315	1.1432	3.6769	0.4272	0.3550	1.1900	2.3200	0.0600
G061	4-5	26.3302	5.3295	2.6844	1.1291	3.4230	0.4294	0.1650	1.0400	1.9700	0.0300
G062	0-5	28.6176	6.0070	2.6287	1.1714	3.3559	0.4609	0.1720	1.0500	2.1100	0.0400
G063	15-20	26.7567	4.8590	2.2835	1.1316	3.1929	0.4268	0.2080	1.0900	2.0600	0.0400

CORE	INTERVAL (cm)										
		1 Si %-xrf	2 Al %-xrf	3 Ca %-xrf	4 K %-xrf	5 Fe %-xrf	6 Ti %-xrf	7 S %-xrf	8 Mg %-aas	9 Na %-aas	10 Hg ppm-a
G064	4-5	29.1050	5.1972	2.0683	1.2071	2.4256	0.3313	0.1000	0.8500	1.8900	0.0500
G065	10-15	31.2130	5.4926	2.2442	1.2403	2.4046	0.3771	0.0930	0.8800	2.0300	0.0400
G066	4-5	29.3060	4.8659	2.7023	1.2470	3.2359	0.3722	0.0870	1.0900	1.9300	0.0400
G067	5-10	39.9325	5.2904	2.5493	1.2146	2.9466	0.3443	0.1000	0.9500	1.8300	0.0400
G069	cc	30.8437	4.7193	2.0105	1.2362	2.1326	0.3215	0.0710	0.8200	1.7400	0.0400
G070	0-1	26.2632	6.3933	2.0419	1.5716	3.8042	0.4244	0.4260	1.3600	1.8100	0.0500
G071	2-7	26.3567	6.5574	1.8211	1.6147	3.7930	0.4220	0.3840	1.2300	1.7500	0.0700
G075	6-10	32.7133	4.6701	2.0169	1.2146	1.9612	0.3150	0.0750	0.8000	1.9400	0.0300
G075	6-10	31.9842	4.9188	1.9926	1.2107	1.9584	0.3375	0.1000	0.7500	1.8200	0.0400
G077	0-5	31.8393	5.1079	2.0926	1.2021	2.0906	0.3843	0.1220	0.8600	1.9000	0.0400
G080	0-5	30.2361	4.5336	2.0769	1.1332	2.2109	0.3418	0.1070	0.9600	1.6600	0.0500
G090	2-4	23.6049	5.0464	2.3221	1.1100	2.7453	0.4318	0.1800	1.0500	1.9000	0.0500
G091	0-1	29.6799	4.9164	2.1613	1.1731	2.7159	0.4191	0.1570	1.0500	2.1400	0.0400
G105	10-15	27.2494	6.1975	1.9382	1.8771	3.9441	0.4496	0.2500	1.4300	1.5600	0.0200
G107	0-5	25.9828	6.2346	1.7903	1.3273	4.0342	0.4437	0.4570	1.5500	1.6000	0.1100
G109	3-8	31.9982	4.8172	2.5043	1.2279	2.4263	0.3363	0.0410	0.9000	2.0900	0.0200
G110	4-5	30.2576	5.1385	2.4121	1.2138	2.7159	0.3449	0.0610	0.9400	1.8800	0.0400
G111	1-5	31.2298	5.7106	2.5579	1.2353	2.5795	0.3576	0.1500	0.8900	2.1000	0.0400
G112	4-5	29.8341	5.4240	2.3957	1.2038	2.4335	0.3680	0.1060	0.8000	1.9700	0.0500
G112	4-5	30.6054	5.7603	2.5372	1.2046	2.4732	0.3800	0.0930	0.8900	2.1000	0.0400
G113	3-8	29.0257	5.9541	2.7766	1.1590	2.9950	0.4289	0.1120	0.9500	2.1100	0.0300
G114	0-1	29.3527	5.4724	2.8917	1.1224	3.1237	0.4095	0.0800	0.9000	2.0700	0.0500
G115	4-5	24.1365	6.9543	4.4876	0.9614	5.1016	0.5941	0.1580	1.1500	2.4000	0.0400
G115	4-5	26.7587	6.0546	3.3705	1.0851	3.9364	0.5098	0.2240	1.1100	2.2200	0.0500
G116	0-5	26.6848	6.2981	2.9939	1.1075	3.5426	0.4546	0.1360	1.0600	2.0200	0.0500
G117	0-1	26.1837	5.7159	3.5814	1.0635	4.0094	0.4976	0.1210	1.1100	2.3800	0.0300
G118	6-11	26.3099	6.6897	3.1726	1.0967	3.9217	0.4708	0.1870	1.1500	2.3700	0.0400
G119	0-5	26.2726	7.2454	3.9566	1.0344	4.6218	0.5705	0.1700	1.2800	2.4000	0.0500
G120	4-5	26.4585	6.4727	3.4649	1.1249	4.1308	0.5243	0.2380	1.2100	2.3400	0.0300
G120	4-5	25.9441	6.3192	3.4277	1.1332	4.1266	0.5227	0.1820	1.2100	2.3700	0.0500
G121	0-5	21.6032	7.0602	4.8028	0.8360	5.6143	0.5087	0.2600	1.8500	2.2500	0.1100
V002	0-3	33.6107	5.1485	1.9819	1.2138	2.0647	0.3939	0.0730	0.7400	1.6500	0.0300
V003	0-3	32.3160	4.8631	1.7603	1.1796	1.7500	0.2638	0.0360	0.6600	1.6300	0.0300
V006	0-3	31.3392	4.1996	1.7467	1.1847	1.8430	0.2901	0.0300	0.7500	1.7000	0.0200
V007	0-3	31.6477	4.6627	2.0998	1.2635	2.2431	0.3218	0.1570	0.8000	1.8000	0.0300
V007	0-3	30.7549	4.5923	2.0305	1.2146	2.1906	0.3391	0.0790	0.8500	1.7500	0.0400
V009	0-3	32.6806	3.9318	1.6924	1.1639	2.2494	0.2767	0.0640	1.4200	1.5200	0.0400
V011	0-3	31.5168	4.3399	2.1219	1.2129	2.5571	0.3903	0.1180	1.0600	1.7000	0.0400
V012	0-3	32.9564	3.9509	1.8060	1.1432	2.1829	0.3100	0.0630	1.0100	1.5500	0.0300
V014	0-3	32.7920	5.3034	2.1470	1.2378	2.2927	0.3352	0.0760	0.8400	1.8100	0.0400
V014	0-3	31.7411	4.5256	2.1348	1.2669	2.2710	0.3307	0.0710	0.8300	1.9000	0.0400
V015	0-3	31.1756	5.2062	2.5872	1.2513	3.3720	0.4710	0.0380	1.5600	1.9200	0.0300
V017	0-3	29.8108	5.2364	2.0860	1.1963	3.6042	0.5651	0.0400	2.1400	1.8700	0.0400
V019	0-3	30.4838	5.0146	2.3192	1.2528	2.7425	0.4252	0.1030	1.3100	1.7000	0.0300
V018	0-3	32.0590	4.7368	2.4214	1.2287	2.7397	0.4330	0.1160	1.2800	1.8400	0.0300
V02	0-3	29.8762	4.8209	2.0133	1.2196	2.3872	0.3559	0.0900	1.0700	1.7900	0.0300
V028	0-3	23.3934	6.9332	5.0879	0.9626	5.6290	0.5179	0.1420	1.9400	2.5400	0.0800
P003	3-8	26.7960	5.8112	3.3941	1.0419	3.9651	0.4990	0.1220	1.0900	2.2500	0.0400
P005	0-5	27.2588	5.1305	2.4843	1.1614	3.4125	0.4364	0.1790	1.0700	2.1300	0.0500
P005	0-5	25.6743	5.5677	2.3992	1.0934	3.3838	0.4098	0.1870	1.0600	2.1700	0.0500
P006	6-	27.0999	5.2655	2.3821	1.0950	3.1279	0.4065	0.1210	1.0400	2.1000	0.0500
P007	5- 0	28.9928	4.6293	2.2291	1.1282	2.5375	0.3770	0.1260	1.0900	1.8400	0.0500
P008	3-8	24.7629	6.3772	1.6738	1.7260	4.7281	0.4518	0.5400	1.6000	1.8900	0.0900

365

s4-76 St. George Basin Grid

DATE 3/17/77

CORE	INTERVAL (cm)	11	12	13	14	15	16	17	18	19	20
		Li ppm-a	Rb ppm-a	Zn ppm-a	As ppm-x	Ce ppm-x	Sr ppm-x	B ppm-s	Ea ppm-s	Co ppm-s	Cr ppm-s
G002	15-20	15.0000	25.0000	116.0000	4.0650	0.6618	0.4058	14.0000	500.0000	15.0000	15.0000
G005	0-5	15.0000	20.0000	107.0000	0.0000B	0.0000B	0.0000B	20.0000	300.0000	20.0000	20.0000
G006	3-4	15.0000	25.0000	119.0000	3.7730	1.4530	1.0250	30.0000	500.0000	15.0000	70.0000
G008	7-15	16.0000	20.0000	91.0000	6.0230	1.8260	1.6030	30.0000	500.0000	15.0000	30.0000
G009	4-5	17.0000	14.0000	97.0000	4.5200	1.2500	1.0340	20.0000	500.0000	15.0000	30.0000
G010	0-5	18.0000	40.0000	72.0000	0.0000B	0.0000B	0.0000B	20.0000	700.0000	10.0000	30.0000
G011	13-18	18.0000	25.0000	71.0000	0.0000B	0.0000B	0.0000B	30.0000	700.0000	10.0000	50.0000
G012	4-5	19.0000	30.0000	71.0000	5.3250	1.5000	1.0170	20.0000	500.0000	10.0000	50.0000
G013	14-19	19.0000	25.0000	83.0000	0.0000B	0.0000B	0.0000B	50.0000	500.0000	10.0000	50.0000
G014	4-5	20.0000	35.0000	79.0000	5.9270	1.4270	1.0270	50.0000	500.0000	10.0000	30.0000
G015	4-5	20.0000	41.0000	77.0000	5.6120	1.2760	1.0000	50.0000	700.0000	10.0000	50.0000
G016	7-9	22.0000	30.0000	82.0000	0.0000B	0.0000B	0.0000B	50.0000	700.0000	10.0000	100.0000
G018	4-5	21.0000	40.0000	70.0000	6.2020	1.6320	1.1570	30.0000	700.0000	7.0000	30.0000
G018	4-5	20.0000	50.0000	68.0000	0.0000B	0.0000B	0.0000B	30.0000	700.0000	10.0000	70.0000
G019	0-3	20.0000	30.0000	65.0000	5.7100	1.3030	1.7700	50.0000	700.0000	7.0000	50.0000
G020	6-11	20.0000	50.0000	63.0000	0.0000B	0.0000B	0.0000B	30.0000	500.0000	10.0000	30.0000
G021	4-5	20.0000	43.0000	63.0000	6.0040	1.6000	0.9185	30.0000	700.0000	7.0000	70.0000
G021	4-5	20.0000	35.0000	63.0000	0.0000B	0.0000B	0.0000B	30.0000	700.0000	10.0000	50.0000
G027	14-19	20.0000	45.0000	62.0000	0.0000B	0.0000B	0.0000B	30.0000	700.0000	7.0000	50.0000
G028	cc	17.0000	43.0000	58.0000	0.0000B	0.0000B	0.0000B	20.0000	500.0000	10.0000	50.0000
G029	4-5	18.0000	40.0000	58.0000	0.0000B	0.0000B	0.0000B	30.0000	700.0000	10.0000	50.0000
G029	4-5	19.0000	39.0000	58.0000	0.0000B	0.0000B	0.0000B	30.0000	700.0000	7.0000	50.0000
G032	6-11	18.0000	45.0000	58.0000	0.0000B	0.0000B	0.0000B	30.0000	700.0000	7.0000	50.0000
G033	8-13	19.0000	41.0000	65.0000	0.0000B	0.0000B	0.0000B	30.0000	500.0000	7.0000	30.0000
G034	4-5	18.0000	44.0000	57.0000	4.6970	1.4040	0.9374	30.0000	700.0000	7.0000	50.0000
G034	4-5	20.0000	45.0000	61.0000	0.0000B	0.0000B	0.0000B	20.0000	500.0000	10.0000	70.0000
G036	2-7	19.0000	40.0000	55.0000	0.0000B	0.0000B	0.0000B	50.0000	700.0000	7.0000	70.0000
G041	6-11	21.0000	55.0000	70.0000	5.7260	1.4700	1.1610	30.0000	700.0000	10.0000	30.0000
G042	0-1	22.0000	40.0000	85.0000	4.5660	1.2020	0.8654	70.0000	700.0000	10.0000	100.0000
G043	0-6	23.0000	35.0000	84.0000	0.0000B	0.0000B	0.0000B	50.0000	500.0000	10.0000	50.0000
G046	11-16	23.0000	40.0000	94.0000	0.0000B	0.0000B	0.0000B	50.0000	500.0000	10.0000	50.0000
G047	4-5	22.0000	43.0000	101.0000	6.2650	1.3220	0.7320	50.0000	500.0000	10.0000	50.0000
G048	0-8	22.0000	38.0000	100.0000	0.0000B	0.0000B	0.0000B	50.0000	500.0000	10.0000	50.0000
G049	0-5	21.0000	35.0000	107.0000	0.0000B	0.0000B	0.0000B	50.0000	500.0000	15.0000	30.0000
G049	0-5	21.0000	33.0000	90.0000	0.0000B	0.0000B	0.0000B	30.0000	500.0000	10.0000	30.0000
G049	0-5	19.0000	31.0000	102.0000	0.0000B	0.0000B	0.0000B	30.0000	500.0000	15.0000	30.0000
G050	0-1	20.0000	25.0000	115.0000	0.0000B	0.0000B	0.0000B	50.0000	500.0000	15.0000	30.0000
G051	6-11	20.0000	20.0000	106.0000	0.0000B	0.0000B	0.0000B	30.0000	500.0000	15.0000	50.0000
G052	9-13	17.0000	35.0000	96.0000	0.0000B	0.0000B	0.0000B	20.0000	500.0000	15.0000	30.0000
G053	0-1	18.0000	20.0000	112.0000	5.1000	1.6600	2.5160	50.0000	500.0000	15.0000	30.0000
G054	0-3	19.0000	14.0000	100.0000	5.0430	1.4060	1.2500	30.0000	500.0000	15.0000	50.0000
G055	4-5	19.0000	20.0000	99.0000	5.5940	1.5160	0.8951	30.0000	500.0000	15.0000	30.0000
G055	4-5	20.0000	25.0000	99.0000	0.0000B	0.0000B	0.0000B	30.0000	500.0000	15.0000	30.0000
G056	0-4	19.0000	33.0000	99.0000	5.7260	1.3050	1.1000	30.0000	500.0000	15.0000	30.0000
G056	0-4	18.0000	26.0000	101.0000	0.0000B	0.0000B	0.0000B	50.0000	500.0000	15.0000	30.0000
G057	0-3	20.0000	30.0000	93.0000	0.0000B	0.0000B	0.0000B	30.0000	500.0000	10.0000	30.0000
G060	0-2	22.0000	45.0000	99.0000	0.0000B	0.0000B	0.0000B	30.0000	500.0000	10.0000	50.0000
G061	4-5	22.0000	30.0000	108.0000	6.0400	1.2730	2.2650	70.0000	500.0000	15.0000	50.0000
G062	0-5	22.0000	40.0000	94.0000	0.0000B	0.0000B	0.0000B	30.0000	500.0000	10.0000	50.0000
G063	15-20	23.0000	35.0000	102.0000	3.4040	0.8798	0.6366	50.0000	700.0000	10.0000	50.0000

CORE	INTERVAL (cm)	11 Li ppm-a	12 Rb ppm-a	13 Zn ppm-a	14 As ppm-x	15 Ge ppm-x	16 Sn ppm-x	17 B ppm-s	18 Ba ppm-s	19 Co ppm-s	20 Cr ppm-s
G064	4-5	20.0000	43.0000	68.0000	4.2730	1.3600	0.5754	30.0000	500.0000	10.0000	50.0000
G065	10-15	20.0000	44.0000	69.0000	0.0000B	0.0000B	0.0000B	30.0000	700.0000	10.0000	50.0000
G066	4-5	17.0000	30.0000	73.0000	4.9450	1.1650	1.0010	50.0000	700.0000	15.0000	70.0000
G067	5-10	16.0000	45.0000	72.0000	0.0000B	0.0000B	0.0000B	50.0000	500.0000	15.0000	50.0000
CC09	cc	13.0000	40.0000	58.0000	0.0000B	0.0000B	0.0000B	30.0000	700.0000	7.0000	50.0000
G070	0-1	42.0000	70.0000	111.0000	3.5400	1.3810	0.9752	50.0000	700.0000	15.0000	100.0000
G071	2-7	44.0000	38.0000	118.0000	0.0000B	0.0000B	0.0000B	50.0000	500.0000	15.0000	70.0000
G075	6-10	17.0000	49.0000	55.0000	0.0000B	0.0000B	0.0000B	30.0000	500.0000	7.0000	50.0000
G075	6-10	17.0000	43.0000	50.0000	0.0000B	0.0000B	0.0000B	30.0000	500.0000	10.0000	50.0000
G077	0-5	20.0000	36.0000	62.0000	4.0650	1.4320	0.7464	30.0000	500.0000	7.0000	50.0000
G080	0-5	20.0000	40.0000	72.0000	0.0000B	0.0000B	0.0000B	50.0000	700.0000	7.0000	70.0000
G090	2-4	21.0000	30.0000	79.0000	0.0000B	0.0000B	0.0000B	50.0000	700.0000	10.0000	100.0000
G091	0-1	20.0000	40.0000	79.0000	4.0400	1.4280	0.7971	50.0000	700.0000	10.0000	100.0000
G105	10-15	43.0000	65.0000	134.0000	18.5300	1.6900	1.4960	70.0000	700.0000	15.0000	100.0000
G107	0-5	45.0000	75.0000	149.0000	13.3100	1.6660	1.4360	50.0000	1500.0000	15.0000	160.0000
G109	3-8	16.0000	43.0000	57.0000	0.0000B	0.0000B	0.0000B	50.0000	700.0000	10.0000	70.0000
G110	4-5	16.0000	40.0000	60.0000	4.9950	1.5620	1.0920	20.0000	500.0000	7.0000	50.0000
G111	1-5	17.0000	40.0000	66.0000	0.0000B	0.0000B	0.0000B	30.0000	700.0000	10.0000	50.0000
G112	4-5	13.0000	35.0000	66.0000	4.0130	1.6690	0.8168	50.0000	700.0000	10.0000	30.0000
G112	4-5	17.0000	25.0000	65.0000	0.0000B	0.0000B	0.0000B	50.0000	500.0000	10.0000	50.0000
G113	3-8	20.0000	33.0000	82.0000	5.6000	1.6280	1.3620	50.0000	500.0000	10.0000	30.0000
G114	0-1	19.0000	14.0000	32.0000	3.8160	1.3790	1.4470	50.0000	700.0000	10.0000	70.0000
G115	4-5	18.0000	30.0000	97.0000	4.8970	1.3140	1.2440	50.0000	500.0000	15.0000	30.0000
G115	4-5	19.0000	20.0000	104.0000	0.0000B	0.0000B	0.0000B	30.0000	500.0000	15.0000	30.0000
G116	0-5	20.0000	40.0000	90.0000	0.0000B	0.0000B	0.0000B	30.0000	500.0000	10.0000	30.0000
G117	0-1	18.0000	14.0000	110.0000	0.0000B	0.0000B	0.0000B	50.0000	500.0000	15.0000	50.0000
G118	6-11	20.0000	25.0000	97.0000	0.0000B	0.0000B	0.0000B	30.0000	500.0000	15.0000	30.0000
G119	0-5	17.0000	25.0000	90.0000	0.0000B	0.0000B	0.0000B	30.0000	500.0000	20.0000	30.0000
G120	4-5	19.0000	25.0000	108.0000	0.0000B	0.0000B	0.0000B	30.0000	500.0000	15.0000	50.0000
G120	4-5	19.0000	35.0000	108.0000	0.0000B	0.0000B	0.0000B	30.0000	500.0000	15.0000	30.0000
G121	0-5	17.0000	25.0000	102.0000	0.0000B	0.0000B	0.0000B	20.0000	300.0000	15.0000	30.0000
V002	0-3	15.0000	40.0000	45.0000	5.1910	1.6670	1.0200	20.0000	500.0000	7.0000	70.0000
V003	0-3	16.0000	35.0000	45.0000	5.4190	1.3980	0.5711	30.0000	700.0000	7.0000	200.0000
V006	0-3	16.0000	45.0000	46.0000	6.3530	1.5700	0.9425	30.0000	700.0000	7.0000	50.0000
V007	0-3	18.0000	35.0000	50.0000	0.0000B	0.0000B	0.0000B	50.0000	700.0000	7.0000	50.0000
V007	0-3	19.0000	45.0000	113.0000	0.0000B	0.0000B	0.0000B	30.0000	500.0000	7.0000	70.0000
V009	0-3	16.0000	48.0000	55.0000	0.0000B	0.0000B	0.0000B	50.0000	500.0000	15.0000	70.0000
V011	0-3	16.0000	30.0000	55.0000	6.7000	1.4220	0.6229	30.0000	700.0000	15.0000	70.0000
V012	0-3	15.0000	30.0000	48.0000	6.9840	1.4360	1.3300	50.0000	700.0000	10.0000	100.0000
V014	0-3	17.0000	20.0000	61.0000	5.2570	1.6520	1.1620	20.0000	500.0000	10.0000	50.0000
V014	0-3	18.0000	40.0000	50.0000	0.0000B	0.0000B	0.0000B	50.0000	500.0000	7.0000	50.0000
V015	0-3	16.0000	44.0000	68.0000	0.0000B	0.0000B	0.0000B	30.0000	500.0000	15.0000	150.0000
V017	0-3	13.0000	33.0000	71.0000	5.6390	1.5530	0.8603	20.0000	500.0000	20.0000	150.0000
V013	0-3	18.0000	40.0000	63.0000	5.5590	1.4630	1.0490	20.0000	700.0000	15.0000	70.0000
V018	0-3	16.0000	43.0000	62.0000	0.0000B	0.0000B	0.0000B	30.0000	500.0000	15.0000	100.0000
V02	0-3	18.0000	40.0000	58.0000	3.4130	1.0500	0.6202	30.0000	700.0000	10.0000	70.0000
V028	0-3	16.0000	23.0000	102.0000	0.0000B	0.0000B	0.0000B	30.0000	300.0000	30.0000	30.0000
P003	3-8	19.0000	14.0000	102.0000	0.0000B	0.0000B	0.0000B	50.0000	500.0000	15.0000	50.0000
P005	0-5	22.0000	25.0000	109.0000	0.0000B	0.0000B	0.0000B	30.0000	700.0000	10.0000	50.0000
P005	0-5	22.0000	35.0000	97.0000	0.0000B	0.0000B	0.0000B	30.0000	500.0000	10.0000	50.0000
P006	6-	23.0000	40.0000	96.0000	0.0000B	0.0000B	0.0000B	50.0000	500.0000	10.0000	50.0000
P007	5-0	21.0000	45.0000	85.0000	0.0000B	0.0000B	0.0000B	70.0000	700.0000	10.0000	100.0000
P008	3-8	48.0000	90.0000	130.0000	8.3310	1.4770	1.4390	30.0000	700.0000	15.0000	70.0000

CORE	INTERVAL (cm)	21	22	23	24	25	26	27	28	29	30
		Cu ppm-s	Ca ppm-s	Mn ppm-s	Ni ppm-s	Sc ppm-s	Sr ppm-s	V ppm-s	Y ppm-s	Yb ppm-s	Zr ppm-s
G002	15-20	70.0000	20.0000	700.0000	15.0000	20.0000	500.0000	150.0000	30.0000	3.0000	70.0000
G005	0-5	70.0000	20.0000	700.0000	10.0000	20.0000	500.0000	200.0000	50.0000	5.0000	100.0000
G006	3-4	70.0000	15.0000	700.0000	15.0000	30.0000	700.0000	300.0000	30.0000	5.0000	70.0000
G008	7-15	50.0000	20.0000	700.0000	15.0000	20.0000	500.0000	200.0000	30.0000	3.0000	70.0000
G009	4-5	70.0000	30.0000	700.0000	15.0000	20.0000	500.0000	200.0000	20.0000	3.0000	100.0000
G010	0-5	30.0000	20.0000	700.0000	15.0000	15.0000	500.0000	150.0000	20.0000	3.0000	70.0000
G011	13-18	30.0000	15.0000	500.0000	15.0000	15.0000	500.0000	150.0000	30.0000	3.0000	100.0000
G012	4-5	30.0000	20.0000	500.0000	15.0000	15.0000	500.0000	100.0000	30.0000	3.0000	100.0000
G013	14-19	30.0000	20.0000	500.0000	20.0000	15.0000	500.0000	150.0000	30.0000	3.0000	100.0000
G014	4-5	30.0000	15.0000	500.0000	15.0000	15.0000	300.0000	100.0000	30.0000	3.0000	150.0000
G015	4-5	20.0000	20.0000	500.0000	30.0000	15.0000	300.0000	150.0000	20.0000	3.0000	100.0000
G016	7-9	50.0000	20.0000	500.0000	15.0000	15.0000	500.0000	150.0000	30.0000	3.0000	150.0000
G018	4-5	20.0000	15.0000	300.0000	15.0000	10.0000	300.0000	70.0000	20.0000	3.0000	100.0000
G018	4-5	30.0000	15.0000	300.0000	20.0000	15.0000	300.0000	100.0000	20.0000	2.0000	200.0000
G019	0-3	15.0000	15.0000	500.0000	30.0000	15.0000	300.0000	150.0000	20.0000	3.0000	100.0000
G020	6-11	15.0000	15.0000	500.0000	20.0000	15.0000	200.0000	100.0000	20.0000	2.0000	70.0000
G021	4-5	15.0000	15.0000	500.0000	20.0000	10.0000	300.0000	70.0000	20.0000	3.0000	70.0000
G021	4-5	15.0000	15.0000	500.0000	15.0000	15.0000	300.0000	100.0000	20.0000	3.0000	100.0000
G027	14-19	15.0000	15.0000	300.0000	20.0000	10.0000	300.0000	100.0000	20.0000	3.0000	100.0000
G028	cc	15.0000	15.0000	500.0000	15.0000	15.0000	200.0000	70.0000	30.0000	3.0000	150.0000
G029	4-5	20.0000	15.0000	500.0000	20.0000	15.0000	300.0000	70.0000	15.0000	1.5000	100.0000
G029	4-5	15.0000	15.0000	500.0000	20.0000	15.0000	300.0000	70.0000	15.0000	2.0000	70.0000
G032	6-11	15.0000	15.0000	300.0000	20.0000	10.0000	300.0000	100.0000	20.0000	3.0000	100.0000
G033	8-13	20.0000	15.0000	500.0000	20.0000	15.0000	200.0000	70.0000	15.0000	1.5000	70.0000
G033	8-13	15.0000	15.0000	500.0000	30.0000	15.0000	300.0000	100.0000	15.0000	2.0000	100.0000
G034	4-5	15.0000	15.0000	700.0000	15.0000	15.0000	300.0000	100.0000	20.0000	2.0000	70.0000
G036	2-7	15.0000	20.0000	500.0000	20.0000	15.0000	300.0000	70.0000	20.0000	2.0000	70.0000
G041	6-11	20.0000	15.0000	500.0000	20.0000	15.0000	300.0000	100.0000	20.0000	3.0000	150.0000
G042	0-1	30.0000	20.0000	500.0000	20.0000	15.0000	500.0000	150.0000	20.0000	3.0000	100.0000
G043	0-6	50.0000	20.0000	500.0000	20.0000	15.0000	300.0000	100.0000	30.0000	3.0000	200.0000
G046	11-16	30.0000	20.0000	500.0000	30.0000	15.0000	300.0000	150.0000	20.0000	2.0000	100.0000
G047	4-5	50.0000	20.0000	500.0000	20.0000	15.0000	300.0000	150.0000	30.0000	3.0000	100.0000
G048	0-3	50.0000	20.0000	500.0000	20.0000	20.0000	500.0000	150.0000	30.0000	3.0000	100.0000
G049	0-5	70.0000	20.0000	700.0000	15.0000	15.0000	300.0000	150.0000	30.0000	3.0000	100.0000
G049	0-5	50.0000	20.0000	500.0000	15.0000	15.0000	300.0000	150.0000	30.0000	3.0000	100.0000
G050	0-1	50.0000	20.0000	700.0000	15.0000	20.0000	500.0000	150.0000	30.0000	3.0000	70.0000
G050	0-1	50.0000	20.0000	500.0000	15.0000	15.0000	500.0000	200.0000	50.0000	5.0000	70.0000
G051	0-1	50.0000	20.0000	700.0000	20.0000	20.0000	500.0000	200.0000	30.0000	5.0000	100.0000
G052	6-11	50.0000	20.0000	500.0000	10.0000	20.0000	300.0000	150.0000	30.0000	3.0000	150.0000
G052	7-13	50.0000	20.0000	500.0000	15.0000	20.0000	500.0000	200.0000	30.0000	3.0000	100.0000
G053	0-1	70.0000	20.0000	700.0000	15.0000	20.0000	500.0000	200.0000	30.0000	3.0000	100.0000
G054	0-3	70.0000	30.0000	700.0000	15.0000	30.0000	700.0000	200.0000	30.0000	3.0000	100.0000
G055	4-5	50.0000	20.0000	700.0000	15.0000	20.0000	500.0000	200.0000	30.0000	3.0000	100.0000
G055	4-5	50.0000	20.0000	500.0000	20.0000	20.0000	500.0000	200.0000	30.0000	3.0000	100.0000
G055	4-5	50.0000	20.0000	500.0000	15.0000	20.0000	500.0000	200.0000	30.0000	3.0000	100.0000
G056	0-4	50.0000	20.0000	700.0000	15.0000	20.0000	500.0000	200.0000	30.0000	3.0000	100.0000
G057	0-5	50.0000	30.0000	700.0000	15.0000	15.0000	500.0000	200.0000	30.0000	3.0000	70.0000
G057	5-8	50.0000	20.0000	500.0000	15.0000	15.0000	300.0000	150.0000	30.0000	3.0000	100.0000
G060	0-2	50.0000	20.0000	500.0000	15.0000	20.0000	300.0000	150.0000	30.0000	3.0000	70.0000
G061	4-5	50.0000	20.0000	500.0000	30.0000	15.0000	500.0000	150.0000	30.0000	3.0000	100.0000
G062	0-5	50.0000	20.0000	500.0000	15.0000	15.0000	300.0000	150.0000	20.0000	3.0000	100.0000
G063	15-20	50.0000	15.0000	500.0000	15.0000	15.0000	300.0000	150.0000	30.0000	3.0000	70.0000

CORE	INTERVAL (cm)	21 Cu ppm-s	22 Ca ppm-s	23 Mn ppm-s	24 Ni ppm-s	25 Sc ppm-s	26 Sr ppm-s	27 V ppm-s	28 Y ppm-s	29 Yb ppm-s	30 Zr ppm-s
G064	4-5	20.0000	15.0000	500.0000	15.0000	15.0000	300.0000	100.0000	30.0000	3.0000	70.0000
G065	10-15	20.0000	15.0000	500.0000	20.0000	15.0000	300.0000	150.0000	20.0000	3.0000	70.0000
G066	4-5	30.0000	15.0000	700.0000	30.0000	15.0000	500.0000	150.0000	20.0000	3.0000	100.0000
G067	5-10	20.0000	15.0000	700.0000	15.0000	15.0000	200.0000	100.0000	20.0000	2.0000	70.0000
G069	cc	15.0000	15.0000	300.0000	15.0000	10.0000	200.0000	100.0000	20.0000	3.0000	100.0000
G070	0-1	50.0000	20.0000	500.0000	20.0000	15.0000	300.0000	200.0000	30.0000	3.0000	100.0000
G071	2-7	50.0000	30.0000	500.0000	20.0000	15.0000	300.0000	150.0000	30.0000	3.0000	70.0000
G075	6-10	15.0000	15.0000	500.0000	20.0000	10.0000	200.0000	70.0000	15.0000	1.5000	100.0000
G075	6-10	15.0000	15.0000	500.0000	20.0000	15.0000	300.0000	100.0000	15.0000	2.0000	100.0000
G077	0-5	15.0000	15.0000	500.0000	20.0000	15.0000	300.0000	100.0000	30.0000	3.0000	150.0000
G080	0-5	20.0000	15.0000	500.0000	20.0000	10.0000	300.0000	100.0000	20.0000	3.0000	100.0000
G090	2-4	30.0000	15.0000	300.0000	30.0000	15.0000	500.0000	100.0000	30.0000	3.0000	100.0000
G091	0-1	20.0000	15.0000	500.0000	30.0000	15.0000	500.0000	150.0000	20.0000	3.0000	100.0000
G105	10-15	70.0000	30.0000	500.0000	50.0000	15.0000	200.0000	150.0000	20.0000	3.0000	70.0000
G107	0-5	70.0000	20.0000	300.0000	50.0000	15.0000	300.0000	200.0000	30.0000	3.0000	100.0000
G109	3-8	30.0000	15.0000	500.0000	15.0000	15.0000	300.0000	100.0000	20.0000	2.0000	70.0000
G110	4-5	15.0000	15.0000	500.0000	15.0000	15.0000	300.0000	100.0000	20.0000	3.0000	100.0000
G111	1-5	30.0000	20.0000	500.0000	15.0000	15.0000	300.0000	150.0000	20.0000	3.0000	150.0000
G112	4-5	20.0000	15.0000	500.0000	15.0000	15.0000	300.0000	150.0000	20.0000	3.0000	70.0000
G112	4-5	20.0000	15.0000	500.0000	15.0000	15.0000	300.0000	150.0000	20.0000	3.0000	100.0000
G113	3-8	50.0000	20.0000	700.0000	15.0000	15.0000	300.0000	150.0000	30.0000	3.0000	100.0000
G114	0-1	50.0000	15.0000	500.0000	15.0000	15.0000	500.0000	150.0000	20.0000	3.0000	100.0000
G115	4-5	50.0000	15.0000	500.0000	15.0000	15.0000	500.0000	150.0000	30.0000	3.0000	70.0000
G115	4-5	50.0000	20.0000	500.0000	15.0000	15.0000	500.0000	150.0000	30.0000	3.0000	100.0000
G116	0-5	50.0000	20.0000	500.0000	15.0000	15.0000	300.0000	150.0000	30.0000	3.0000	100.0000
G117	0-1	70.0000	20.0000	500.0000	15.0000	15.0000	500.0000	200.0000	30.0000	3.0000	70.0000
G118	6-11	50.0000	15.0000	700.0000	15.0000	15.0000	300.0000	150.0000	30.0000	3.0000	70.0000
G119	0-5	70.0000	20.0000	700.0000	15.0000	20.0000	500.0000	200.0000	30.0000	3.0000	70.0000
G120	4-5	70.0000	20.0000	700.0000	20.0000	20.0000	700.0000	200.0000	30.0000	5.0000	70.0000
G120	4-5	50.0000	15.0000	700.0000	15.0000	15.0000	500.0000	150.0000	30.0000	3.0000	100.0000
G121	0-5	70.0000	20.0000	700.0000	15.0000	15.0000	500.0000	200.0000	30.0000	3.0000	70.0000
V002	0-3	7.0000	15.0000	500.0000	15.0000	10.0000	200.0000	70.0000	15.0000	2.0000	70.0000
V003	0-3	7.0000	15.0000	300.0000	15.0000	10.0000	200.0000	70.0000	20.0000	2.0000	70.0000
V006	0-3	7.0000	10.0000	300.0000	15.0000	7.0000	200.0000	70.0000	20.0000	2.0000	70.0000
V007	0-3	15.0000	15.0000	300.0000	15.0000	10.0000	300.0000	100.0000	15.0000	2.0000	70.0000
V007	0-3	20.0000	15.0000	300.0000	20.0000	10.0000	300.0000	70.0000	20.0000	3.0000	100.0000
V009	0-3	7.0000	15.0000	500.0000	50.0000	7.0000	200.0000	70.0000	15.0000	1.5000	70.0000
V011	0-3	15.0000	15.0000	300.0000	30.0000	10.0000	500.0000	100.0000	20.0000	3.0000	150.0000
V012	0-3	10.0000	10.0000	300.0000	30.0000	10.0000	300.0000	100.0000	15.0000	1.5000	70.0000
V014	0-3	15.0000	15.0000	500.0000	20.0000	15.0000	300.0000	100.0000	20.0000	2.0000	100.0000
V014	0-3	15.0000	15.0000	300.0000	30.0000	10.0000	300.0000	70.0000	15.0000	2.0000	100.0000
V015	0-3	15.0000	15.0000	500.0000	50.0000	15.0000	300.0000	150.0000	20.0000	3.0000	70.0000
V017	0-3	20.0000	20.0000	500.0000	150.0000	15.0000	300.0000	100.0000	15.0000	2.0000	150.0000
V018	0-3	15.0000	15.0000	300.0000	50.0000	15.0000	300.0000	150.0000	20.0000	3.0000	70.0000
V018	0-3	15.0000	15.0000	500.0000	30.0000	15.0000	300.0000	150.0000	15.0000	1.5000	100.0000
V02	0-3	15.0000	15.0000	300.0000	30.0000	10.0000	300.0000	100.0000	20.0000	2.0000	100.0000
V020	0-3	100.0000	20.0000	700.0000	70.0000	30.0000	500.0000	200.0000	20.0000	3.0000	70.0000
V020	0-3	70.0000	20.0000	700.0000	15.0000	20.0000	500.0000	200.0000	30.0000	3.0000	100.0000
F003	3-8	50.0000	15.0000	500.0000	20.0000	15.0000	500.0000	150.0000	30.0000	3.0000	70.0000
F005	0-5	50.0000	15.0000	500.0000	15.0000	15.0000	300.0000	150.0000	30.0000	3.0000	70.0000
F005	0-5	50.0000	15.0000	500.0000	15.0000	15.0000	300.0000	150.0000	30.0000	3.0000	70.0000
F006	6-	50.0000	20.0000	500.0000	20.0000	15.0000	500.0000	150.0000	30.0000	3.0000	100.0000
F007	5-0	30.0000	15.0000	500.0000	30.0000	15.0000	500.0000	150.0000	20.0000	3.0000	100.0000
F008	3-8	50.0000	20.0000	500.0000	30.0000	15.0000	200.0000	200.0000	30.0000	3.0000	70.0000

CORE	INTERVAL (cm)	31		32	
		Th	ppm-n	U	ppm-n
G002	15-20	1.9400	1.5300		
G005	0-5	3.5900	1.4600		
G006	3-4	5.1000	1.2300		
G008	7-15	1.9400	1.8300		
G009	4-5	1.9400	1.9200		
G010	0-5	1.9400	2.2200		
G011	13-18	1.9400	1.9700		
G012	4-5	3.2300	1.6200		
G013	14-19	5.7800	1.9400		
G014	4-5	5.7000	2.1600		
G015	4-5	5.1700	2.3700		
G016	7-9	1.9400	2.6400		
G018	4-5	4.9000	2.5900		
G018	4-5	3.7800	2.6900		
G019	0-3	1.9400	2.2600		
G020	6-11	4.9400	2.0900		
G021	4-5	5.8100	2.1900		
G021	4-5	5.4700	2.1500		
G027	14-19	1.9400	2.3700		
G028	cc	4.1700	1.7700		
G029	4-5	4.7300	2.0900		
G029	4-5	3.9200	2.0300		
G032	6-11	3.7500	2.2500		
G033	8-13	3.9700	2.2100		
G034	4-5	5.2600	1.6100		
G034	4-5	1.9400	2.0800		
G036	2-7	4.5300	1.5700		
G041	6-11	1.9400	2.2600		
G042	0-1	5.2700	2.0700		
G043	0-6	5.5200	3.2900		
G046	11-16	6.4300	2.4500		
G047	4-5	1.9400	3.3200		
G048	0-8	4.4900	2.4000		
G049	0-5	1.9400	2.7700		
G049	0-5	1.9400	2.4200		
G050	0-1	1.9400	2.9000		
G050	0-1	1.9400	2.7300		
G051	6-11	1.9400	2.5800		
G052	9-13	1.9400	2.2600		
G052	9-13	5.1300	1.8900		
G053	0-1	1.9400	2.3700		
G054	0-3	4.4100	2.2200		
G055	4-5	1.9400	2.4700		
G055	4-5	1.9400	2.1200		
G056	0-4	4.5000	1.7600		
G057	0-5	1.9400	2.4000		
G059	5-8	1.9400	2.4000		
G060	0-2	1.9400	3.6200		
G061	4-5	4.8800	2.5900		
G062	0-5	1.9400	2.6500		
G063	15-20	1.9400	2.1600		

CORE	INTERVAL (cm)	31		32	
		Th	ppm-n	U	ppm-n
G064	4-5	3.3600		2.0500	
G065	10-15	1.9400		2.3500	
G066	4-5	1.9400		2.6100	
G067	5-10	3.9400		1.6600	
G069	cc	3.6500		1.6300	
G070	0-1	6.6500		2.9100	
G071	2-7	7.7300		3.9400	
G075	6-10	5.7600		1.8400	
G075	6-10	4.3600		1.9200	
G077	0-5	5.6700		2.0300	
G080	0-5	1.9400		2.5200	
G090	2-4	4.5400		2.6000	
G091	0-1	4.9000		2.0900	
G105	10-15	7.1300		3.4000	
G107	0-5	6.9900		2.8200	
G109	3-8	4.3600		1.9000	
G110	4-5	5.4600		1.8100	
G111	1-5	4.6600		2.0900	
G112	4-5	1.9400		2.0900	
G112	4-5	1.9400		1.9800	
G113	3-8	3.9400		1.8000	
G114	0-1	1.9400		2.1900	
G115	4-5	1.9400		2.1300	
G115	4-5	1.9400		2.3500	
G116	0-5	5.2500		2.0100	
G117	0-1	1.9400		1.9900	
G118	6-11	1.9400		2.4200	
G119	0-5	1.9400		2.1900	
G120	4-5	1.9400		2.7000	
G120	4-5	1.9400		2.5700	
G121	0-5	1.9400		1.6900	
V002	0-3	3.6600		1.7600	
V003	0-3	2.7700		1.5100	
V006	0-3	4.9700		1.4700	
V007	0-3	1.9400		1.7900	
V007	0-3	3.7600		1.6500	
V009	0-3	3.5300		1.3300	
V011	0-3	4.8100		1.6700	
V012	0-3	2.8700		1.5200	
V014	0-3	4.5100		1.4200	
V014	0-3	3.5700		1.4300	
V015	0-3	4.4600		1.4200	
V017	0-3	4.4600		1.4300	
V018	0-3	3.6400		1.7400	
V018	0-3	4.2300		1.5900	
V02	0-3	2.0600		1.6900	
V028	0-3	1.9400		1.2100	
P003	3-8	6.1600		2.2200	
P005	0-5	1.9400		2.6600	
P005	0-5	1.9400		3.0300	
P006	6-	1.9400		2.3500	
P007	5- 0	1.9400		2.3200	
P008	3-8	6.3700		3.8100	

AG14
A65

s4-76 Misc. Seds, Pribilof Isl

DATE 3/17/77

CORE	INTERVAL (cm)										
		Ca % - s	K % - s	Fe % - s	Ti % - s	Hg % - s	Na % - s	B ppm-s	Ba ppm-s	Co ppm-s	Cr ppm-s
0020	-6	3.0000	3.0000	5.0000	0.3000	1.5000	2.0000	30.0000	700.0000	10.0000	70.0000
0021	4-5	3.0000	3.0000	5.0000	0.3000	1.5000	3.0000	30.0000	700.0000	10.0000	70.0000
0027	2-7	3.0000	3.0000	3.0000	0.3000	1.0000	2.0000	20.0000	1000.0000	7.0000	50.0000
0037	2-7	3.0000	2.0000	3.0000	0.3000	1.5000	3.0000	30.0000	700.0000	7.0000	50.0000
0038	0-5	3.0000	2.0000	5.0000	0.3000	1.5000	3.0000	20.0000	700.0000	10.0000	30.0000
0039	0-5	3.0000	3.0000	5.0000	0.3000	1.5000	2.0000	50.0000	700.0000	10.0000	100.0000
0040	6- 0	3.0000	3.0000	3.0000	0.3000	1.5000	3.0000	30.0000	1000.0000	7.0000	50.0000
0050	6- 0	3.0000	2.0000	3.0000	0.3000	1.5000	3.0000	30.0000	700.0000	7.0000	50.0000
0072	4-5	3.0000	3.0000	5.0000	0.3000	1.5000	3.0000	30.0000	700.0000	10.0000	50.0000
0072	4-5	3.0000	2.0000	5.0000	0.3000	1.5000	2.0000	30.0000	700.0000	15.0000	100.0000
0070	0-	3.0000	2.0000	3.0000	0.3000	1.5000	3.0000	50.0000	500.0000	15.0000	70.0000
0079	0-5	3.0000	3.0000	3.0000	0.3000	1.5000	3.0000	50.0000	700.0000	10.0000	70.0000
0081	30-35	5.0000	3.0000	5.0000	0.5000	2.0000	5.0000	50.0000	700.0000	10.0000	70.0000
0082	20-25	5.0000	3.0000	5.0000	0.5000	1.5000	3.0000	50.0000	1000.0000	10.0000	70.0000
0089	0-3	5.0000	2.0000	5.0000	0.5000	2.0000	3.0000	30.0000	700.0000	15.0000	100.0000
0094	cc	5.0000	2.0000	7.0000	0.7000	5.0000	2.0000	30.0000	700.0000	15.0000	100.0000
0093	2-7	5.0000	3.0000	7.0000	0.5000	2.0000	2.0000	30.0000	500.0000	30.0000	150.0000
V004	0-3	3.0000	2.0000	3.0000	0.3000	1.0000	3.0000	50.0000	700.0000	7.0000	70.0000
V005	0-3	3.0000	2.0000	3.0000	0.3000	1.5000	3.0000	30.0000	500.0000	7.0000	150.0000
V007	0-3	2.0000	2.0000	3.0000	0.2000	3.0000	2.0000	30.0000	500.0000	15.0000	70.0000
V008	0-3	5.0000	2.0000	3.0000	0.3000	1.5000	3.0000	30.0000	700.0000	10.0000	70.0000
V020	0-3	5.0000	3.0000	3.0000	0.5000	2.0000	3.0000	30.0000	700.0000	10.0000	100.0000
V022	0-3	3.0000	2.0000	3.0000	0.3000	1.5000	3.0000	50.0000	500.0000	10.0000	70.0000
V022	0-3	3.0000	3.0000	5.0000	0.3000	2.0000	3.0000	50.0000	700.0000	10.0000	100.0000
V023	0-3	2.0000	3.0000	3.0000	0.3000	2.0000	3.0000	30.0000	700.0000	10.0000	70.0000
V025	0-3	5.0000	2.0000	5.0000	0.5000	1.5000	2.0000	30.0000	1000.0000	10.0000	70.0000
V025	0-3	3.0000	3.0000	7.0000	0.5000	2.0000	3.0000	50.0000	700.0000	15.0000	100.0000
Z006	07-09	3.0000	2.0000	5.0000	0.3000	1.5000	5.0000	100.0000	1000.0000	10.0000	50.0000
Z003	25-27	5.0000	2.0000	5.0000	0.3000	1.5000	7.0000	100.0000	1000.0000	7.0000	30.0000

CORE	INTERVAL (cm)										
		Ca ppm-s	K ppm-s	M ppm-s	Sc ppm-s	Sr ppm-s	V ppm-s	Y ppm-s	Yb ppm-s	Zr ppm-s	
0020	-6	15.0000	15.0000	30.0000	15.0000	500.0000	100.0000	20.0000	3.0000	200.0000	
0021	4-5	20.0000	15.0000	30.0000	15.0000	500.0000	100.0000	30.0000	3.0000	150.0000	
0027	2-7	10.0000	15.0000	20.0000	10.0000	500.0000	100.0000	20.0000	3.0000	70.0000	
0037	2-7	15.0000	15.0000	15.0000	10.0000	300.0000	70.0000	20.0000	2.0000	100.0000	
0038	0-5	20.0000	15.0000	20.0000	15.0000	300.0000	100.0000	20.0000	3.0000	100.0000	
0039	0-5	30.0000	15.0000	30.0000	15.0000	500.0000	150.0000	30.0000	3.0000	100.0000	
0040	6- 0	15.0000	15.0000	20.0000	15.0000	500.0000	100.0000	20.0000	3.0000	150.0000	
0040	6- 0	20.0000	15.0000	20.0000	10.0000	300.0000	70.0000	20.0000	3.0000	70.0000	
0072	4-5	50.0000	20.0000	50.0000	15.0000	500.0000	150.0000	30.0000	3.0000	150.0000	
0072	4-5	50.0000	15.0000	50.0000	15.0000	300.0000	150.0000	30.0000	3.0000	100.0000	
0070	0-	15.0000	15.0000	20.0000	15.0000	300.0000	70.0000	20.0000	3.0000	150.0000	
0079	0-5	15.0000	20.0000	20.0000	15.0000	500.0000	70.0000	30.0000	3.0000	150.0000	
0081	30-35	20.0000	15.0000	30.0000	15.0000	500.0000	150.0000	30.0000	3.0000	150.0000	
0082	20-25	30.0000	15.0000	30.0000	15.0000	500.0000	150.0000	20.0000	3.0000	100.0000	
0089	0-3	20.0000	20.0000	50.0000	15.0000	500.0000	150.0000	30.0000	3.0000	200.0000	
0094	cc	70.0000	20.0000	100.0000	20.0000	500.0000	200.0000	30.0000	3.0000	150.0000	
0093	2-7	20.0000	15.0000	50.0000	15.0000	500.0000	150.0000	30.0000	3.0000	70.0000	
V004	0-3	10.0000	15.0000	10.0000	10.0000	500.0000	70.0000	20.0000	2.0000	100.0000	
V005	0-3	15.0000	15.0000	20.0000	10.0000	300.0000	70.0000	15.0000	2.0000	100.0000	
V007	0-3	10.0000	15.0000	70.0000	7.0000	300.0000	70.0000	20.0000	2.0000	70.0000	
V008	0-3	15.0000	15.0000	30.0000	15.0000	300.0000	70.0000	20.0000	3.0000	100.0000	
V020	0-3	15.0000	15.0000	30.0000	15.0000	500.0000	100.0000	30.0000	3.0000	70.0000	
V022	0-3	20.0000	15.0000	30.0000	10.0000	300.0000	70.0000	30.0000	3.0000	150.0000	
V022	0-3	15.0000	20.0000	30.0000	15.0000	500.0000	100.0000	10.0000	3.0000	70.0000	
V023	0-3	15.0000	15.0000	30.0000	15.0000	500.0000	70.0000	20.0000	3.0000	70.0000	
V025	0-3	20.0000	15.0000	50.0000	15.0000	500.0000	200.0000	30.0000	3.0000	100.0000	
V025	0-3	70.0000	20.0000	30.0000	15.0000	500.0000	150.0000	30.0000	3.0000	70.0000	
Z006	07-09	70.0000	20.0000	30.0000	15.0000	500.0000	150.0000	20.0000	3.0000	70.0000	
Z003	25-27	100.0000	20.0000	30.0000	15.0000	300.0000	100.0000	20.0000	3.0000	50.0000	

V014
Vc5

s4-76 Misc. Seds, Prifilof Isl

DATE 3/17/77

CODE	INTERVAL (cm)	1		2		3		4		5		6		7		8		9		10	
		Cu % - s	K % - s	Fe % - s	Ti % - s	Mg % - s	Na % - s	B ppm-s	Ba ppm-s	Co ppm-s	Cr ppm-s										
V010	-0	3.0000	3.0000	5.0000	0.3000	1.5000	2.0000	30.0000	700.0000	10.0000	70.0000										
V011	4-5	3.0000	3.0000	5.0000	0.3000	1.5000	3.0000	30.0000	700.0000	10.0000	70.0000										
V012	2-7	3.0000	3.0000	3.0000	0.3000	1.0000	2.0000	20.0000	1000.0000	7.0000	50.0000										
V013	2-7	3.0000	3.0000	3.0000	0.3000	1.5000	3.0000	30.0000	700.0000	7.0000	50.0000										
V014	0-5	3.0000	3.0000	5.0000	0.3000	1.5000	3.0000	30.0000	700.0000	10.0000	70.0000										
V015	0-5	3.0000	3.0000	5.0000	0.3000	1.5000	3.0000	30.0000	700.0000	10.0000	70.0000										
V016	6-0	3.0000	3.0000	3.0000	0.3000	1.5000	3.0000	30.0000	1000.0000	7.0000	50.0000										
V017	6-0	3.0000	3.0000	3.0000	0.3000	1.5000	3.0000	30.0000	700.0000	10.0000	70.0000										
V018	4-5	3.0000	3.0000	5.0000	0.3000	2.0000	3.0000	30.0000	700.0000	15.0000	100.0000										
V019	4-5	3.0000	3.0000	5.0000	0.3000	2.0000	2.0000	30.0000	500.0000	15.0000	70.0000										
V020	0-	3.0000	3.0000	3.0000	0.3000	1.5000	3.0000	30.0000	700.0000	10.0000	70.0000										
V021	0-5	3.0000	3.0000	3.0000	0.3000	1.5000	3.0000	30.0000	700.0000	10.0000	70.0000										
V022	30-35	3.0000	3.0000	5.0000	0.3000	2.0000	3.0000	30.0000	700.0000	10.0000	70.0000										
V023	20-25	3.0000	3.0000	5.0000	0.3000	1.5000	3.0000	30.0000	1000.0000	10.0000	70.0000										
V024	0-3	5.0000	2.0000	5.0000	0.3000	2.0000	3.0000	30.0000	700.0000	15.0000	100.0000										
V025	cc	5.0000	2.0000	7.0000	0.7000	5.0000	2.0000	30.0000	500.0000	30.0000	150.0000										
V026	2-7	5.0000	3.0000	7.0000	0.5000	2.0000	2.0000	70.0000	700.0000	15.0000	100.0000										
V027	0-3	3.0000	3.0000	3.0000	0.3000	1.5000	3.0000	30.0000	700.0000	7.0000	70.0000										
V028	0-3	3.0000	2.0000	3.0000	0.3000	1.5000	3.0000	30.0000	500.0000	7.0000	150.0000										
V029	0-3	3.0000	2.0000	3.0000	0.2000	3.0000	2.0000	30.0000	500.0000	15.0000	70.0000										
V030	0-3	5.0000	3.0000	3.0000	0.3000	1.5000	3.0000	30.0000	700.0000	10.0000	70.0000										
V031	0-3	5.0000	3.0000	3.0000	0.3000	2.0000	3.0000	30.0000	500.0000	10.0000	70.0000										
V032	0-3	3.0000	2.0000	5.0000	0.3000	2.0000	3.0000	30.0000	700.0000	10.0000	70.0000										
V033	0-3	3.0000	3.0000	3.0000	0.3000	2.0000	3.0000	30.0000	700.0000	10.0000	70.0000										
V034	0-3	5.0000	3.0000	5.0000	0.5000	1.5000	2.0000	30.0000	1000.0000	10.0000	70.0000										
V035	0-3	5.0000	3.0000	7.0000	0.5000	2.0000	3.0000	50.0000	700.0000	15.0000	100.0000										
V036	0-3	3.0000	2.0000	5.0000	0.3000	1.5000	5.0000	100.0000	1000.0000	10.0000	50.0000										
V037	07-09	3.0000	2.0000	5.0000	0.3000	1.5000	7.0000	100.0000	1000.0000	7.0000	30.0000										
V038	25-27	5.0000	2.0000	5.0000	0.3000	1.5000	7.0000	100.0000	1000.0000	7.0000	30.0000										

CODE	INTERVAL (cm)	11		12		13		14		15		16		17		18		19	
		Cu ppm-s	Ca ppm-s	Mg ppm-s	Sc ppm-s	Sr ppm-s	V ppm-s	Y ppm-s	Zr ppm-s	Yb ppm-s	Zr ppm-s								
V039	-0	15.0000	15.0000	30.0000	15.0000	500.0000	100.0000	30.0000	3.0000	200.0000									
V040	4-5	20.0000	15.0000	30.0000	15.0000	500.0000	100.0000	30.0000	3.0000	150.0000									
V041	2-7	15.0000	15.0000	20.0000	10.0000	500.0000	100.0000	20.0000	3.0000	70.0000									
V042	2-7	15.0000	15.0000	10.0000	10.0000	300.0000	70.0000	20.0000	2.0000	100.0000									
V043	0-5	20.0000	15.0000	20.0000	15.0000	300.0000	100.0000	20.0000	3.0000	100.0000									
V044	0-5	20.0000	15.0000	30.0000	15.0000	500.0000	150.0000	30.0000	3.0000	100.0000									
V045	6-0	15.0000	15.0000	20.0000	15.0000	500.0000	100.0000	20.0000	3.0000	150.0000									
V046	6-0	20.0000	15.0000	30.0000	10.0000	300.0000	70.0000	20.0000	3.0000	70.0000									
V047	4-5	50.0000	20.0000	30.0000	15.0000	500.0000	150.0000	30.0000	3.0000	150.0000									
V048	4-5	50.0000	15.0000	30.0000	15.0000	300.0000	150.0000	30.0000	3.0000	100.0000									
V049	0-	15.0000	15.0000	20.0000	15.0000	300.0000	70.0000	30.0000	3.0000	150.0000									
V050	0-5	15.0000	20.0000	20.0000	15.0000	500.0000	70.0000	30.0000	3.0000	150.0000									
V051	30-35	20.0000	15.0000	30.0000	15.0000	500.0000	150.0000	30.0000	3.0000	300.0000									
V052	20-25	20.0000	15.0000	30.0000	15.0000	500.0000	150.0000	20.0000	3.0000	100.0000									
V053	0-3	20.0000	20.0000	50.0000	15.0000	500.0000	150.0000	30.0000	3.0000	200.0000									
V054	cc	70.0000	20.0000	100.0000	20.0000	500.0000	200.0000	30.0000	3.0000	150.0000									
V055	2-7	20.0000	15.0000	50.0000	15.0000	500.0000	150.0000	30.0000	3.0000	70.0000									
V056	0-3	10.0000	15.0000	15.0000	10.0000	500.0000	70.0000	20.0000	2.0000	100.0000									
V057	0-3	15.0000	15.0000	20.0000	10.0000	300.0000	70.0000	15.0000	2.0000	100.0000									
V058	0-3	10.0000	10.0000	70.0000	7.0000	300.0000	70.0000	20.0000	2.0000	70.0000									
V059	0-3	15.0000	15.0000	30.0000	15.0000	300.0000	70.0000	20.0000	3.0000	100.0000									
V060	0-3	15.0000	15.0000	30.0000	15.0000	500.0000	100.0000	30.0000	3.0000	70.0000									
V061	0-3	20.0000	20.0000	30.0000	10.0000	300.0000	70.0000	20.0000	3.0000	150.0000									
V062	0-3	15.0000	15.0000	30.0000	15.0000	500.0000	100.0000	30.0000	3.0000	70.0000									
V063	0-3	15.0000	15.0000	30.0000	15.0000	500.0000	150.0000	20.0000	3.0000	70.0000									
V064	0-3	15.0000	15.0000	30.0000	15.0000	500.0000	150.0000	20.0000	3.0000	70.0000									
V065	0-3	20.0000	15.0000	50.0000	15.0000	500.0000	200.0000	30.0000	3.0000	100.0000									
V066	0-3	20.0000	20.0000	30.0000	15.0000	500.0000	150.0000	20.0000	3.0000	70.0000									
V067	07-09	20.0000	20.0000	30.0000	15.0000	500.0000	150.0000	20.0000	3.0000	70.0000									
V068	25-27	100.0000	20.0000	30.0000	15.0000	300.0000	100.0000	20.0000	3.0000	50.0000									

HYDROCARBON GAS IN SEDIMENTS OF THE SOUTHERN BERING SHELF AND SLOPE

Keith A. Kvenvolden and George D. Redden

Studies of hydrocarbon gases in near-surface sediments of the southern Bering shelf and slope have been conducted during the 1976 and 1977 field seasons. The general objectives of this work were (1) to determine the distribution of hydrocarbon gases in surface and near-surface sediments, and (2) to interpret possible sources for the gas. During the 1976 season, 33 stations were occupied where hydrocarbon gases were extracted from 108 sediment samples recovered from gravity cores (maximum depth, 1.4 m), or Van Veen grabs. The stations were part of a network of 85 stations established to evaluate the general geology of the southern Bering shelf between Unimak Island and the Pribilof Islands including the area of the St. George Basin. The gas analysis results from this season will be described in detail (Kvenvolden and Redden, U.S.G.S. Open File Report, in preparation) and are summarized briefly here. Small quantities of methane (C_1), ethane (C_2), propane (C_3), *n*-butane (*n*- C_4), isobutane (*i*- C_4), ethene ($C_2:1$) and propene ($C_3:1$) were found in all samples. C_1 was the most abundant hydrocarbon, having an average concentration of about 5700 nL/L of wet sediment. The concentrations of C_1 usually increased slightly with depth. The other hydrocarbon gases were present at lower concentrations than methane, and these gases showed no identifiable trends with depth. No anomalous distribution or concentrations of hydrocarbon gases were observed that would suggest possible hydrocarbon seeps or potential hazards.

Between the 1976 and 1977 field seasons, examination of multi-channel, seismic profiles across St. George Basin indicated the presence of a number

of acoustic anomalies where reflectors abruptly terminate leaving regions of acoustic turbidity beginning at depths of about 200-300 m. (Marlow, personal communication). Single channel, seismic records also showed these same features, but they were not as well defined. The cause of these anomalies is not known, but it is commonly assumed that they may result from gas occupying a portion of the pore space. Although the features are deep, we reasoned that if hydrocarbon gases are involved, these gases may leak to the surface, giving rise to anomalous concentrations of hydrocarbon gases that would correlate with the acoustic features. The composition of the gases might provide a clue to their sources. A part of the 1977 field season was devoted to testing this idea.

During the 1977 field season two sets of samples were collected for hydrocarbon gas analysis (Fig. 1). The first set consisted of 22 samples from 9 gravity cores. These cores were taken on the southern Bering shelf in a region where acoustic anomalies had been noted on the seismic records. Four of these cores were located over the anomalies, and five were at positions not associated with anomalies. The second set of 22 samples came from 6 gravity cores taken on the southern Bering slope. From these two sets of samples, comparisons were made between the occurrence of hydrocarbon gases from these two regions of the continental margin.

The following procedure was used for gas analysis. The 8-cm internal diameter core liner from the gravity core was cut at intervals (usually 0-10, 50-60, 100-110 cm). The sediment core was extruded from each of these intervals into a preweighed, 1 qt. can. The can had been pre-prepared with two small holes near the top and septa had been fixed over the holes. The can was filled with distilled water that had been purged with helium to remove any dissolved hydrocarbon gases. From the can 100 ml of water was removed. A double friction top was sealed in place, and the 100 ml headspace was purged with helium

through the septa. The cans were shaken for 10 minutes. From the can about 5 ml of gas was removed. Exactly one ml of this gas was injected into a modified Carle 311 Analytical Gas Chromatograph equipped with both flame ionization and thermal conductivity detectors. The instrument was calibrated by means of a standard mixture of hydrocarbon gases prepared by Matheson Gas Company. Calculations of concentrations of gases were determined from chromatograms by measuring the heights of peaks representing the gases. ^{Partition} ~~Position~~ coefficients were used to correct for the varying solubilities of the gases. Concentrations are reported as nL/L of wet sediment.

Results obtained during the 1977 field season are recorded in Table 1 (shelf) and Table 2 (slope). On the shelf, cores G-1, G-4, G-7, and G-10 were obtained in sediments over acoustic anomalies. The remaining cores were taken in areas where no anomalies were evident. There appears to be no correlation between gas concentrations and the presence of acoustic anomalies; that is, no hydrocarbon gas anomalies are associated with acoustic anomalies. If the acoustic anomalies are indeed caused by high concentrations of hydrocarbon gases, our data suggest that these gases do not leak to the surface to produce unusual concentrations of gases. The thick (200-300 m) of sediment cover may obscure or prevent gas migration.

Concentrations and compositions of the gases from the shelf and slope are generally similar. Average concentrations of C_1 differ slightly only because deeper samples with higher C_1 contents were recovered on the slope and are included in the average. For example, on the shelf, the average concentration of C_1 is about 2800 nL/L while on the slope the samples have an average C_1 concentration of about 3400 nL/L. The concentrations of the higher molecular weight hydrocarbons are similar for sediments from both shelf and slope.

Shelf sediments have an average $C_1(C_2 + C_3)$ ratio of 34 in contrast to the

slope sediments with an average ratio of 107. Samples from the slope, however, include deeper intervals with higher C_1 contents and thus higher $C_1/(C_2 + C_3)$ ratios. This ratio has been used in the past to interpret sources of hydrocarbon gases (Bernard, Brooks, and Sackett, 1977, Earth and Planetary Science Letters, 31, 48-54). Ratios less than 50 were interpreted to indicate the presence of thermogenically-derived gases. Ratios greater than 50 suggested mainly biogenically-produced gases. Although this ratio may be a useful guide when high concentrations of gases are being considered, in the present study involving relatively low concentrations of gases, this ratio probably is not indicative of sources of hydrocarbon gases. It is quite likely that most of the hydrocarbon gases measured here are biologically-derived. The fact remains however, that in the first 60 cm of the cores, the $C_1/(C_2 + C_3)$ ratios for southern Bering shelf and slope sediments are generally low as indicated on Table 1 and 2, and as also observed for the samples examined from the 1976 field season.

Two cores show usual concentrations of single components. C_2 is higher in samples from core G-12 than in other cores from both the shelf and the slope. In core G-28, the intervals from 100 cm and deeper show unusually high amounts of $i-C_4$. The significance of these observations is not clear at present.

The data shown in Tables 1 and 2 were obtained from analyses performed on shipboard immediately after core recovery. After gases were analyzed, these samples were frozen. A number of samples were thawed later and reanalyzed. This process tends to increase the amount of hydrocarbon gases that can be extracted. Most of the hydrocarbon gases are probably dissolved in the interstitial water of the sediments, and these are partially removed during the first extraction. Freezing and thawing release additional hydrocarbon gases that are held in the sediment in unknown ways. For these kinds of analyses,

it is evident that comparisons of results can be made only with samples which have been processed in the same way. Because analyses of unfrozen samples recovered immediately after coring involves least sample manipulation, results of these analyses have been given here.

This work has shown that hydrocarbon gases are present in surface and near-surface sediments of the southern Bering shelf and slope. Concentrations of hydrocarbons are about the same in shelf and slope sediments in the interval from 0 to about 60 cm. On the shelf, acoustic anomalies at 200-300 m depth do not produce hydrocarbon gas anomalies in the near-surface sediments above them. The concentrations and distributions of hydrocarbon gases in the sediments examined here do not indicate that gas seeps are active in the areas sampled or that the gas in the sediments constitutes a geologic hazard because of high concentrations.

Table 1. Hydrocarbon Gases - Southern Bering Shelf S6-77

Sta.	Sample	Interval (cm)	Water Depth (m)	Concentrations (nL/L wet sediment)							$\frac{C_1}{C_2 + C_3}$
				C ₁	C ₂	C ₂ : 1	C ₃	C ₃ :1	i-C ₄	n-C ₄	
2	G -1	0-10	136	810	30	34	17	11	-	-	17
	"	50-60		4480	42	28	22	5	6	9	70
	"	92-102		5160	63	44	43	14	9	12	49
3	G -2	0-10	129	890	18	22	13	6	-	-	29
	"	42-52		2150	42	28	24	8	9	9	33
4	G -4	0-10	110	1040	27	34	13	17	-	9	26
	"	55-65		3230	39	31	22	11	-	9	53
5	G -6	0-10	108	1040	27	38	19	11	-	6	23
	"	50-60		3930	48	28	28	8	6	9	52
6	G -7	0-10	109	790	24	22	15	6	-	-	19
	"	27-37		2070	51	50	34	17	12	12	24
7	G-10	0-10	130	750	15	25	9	8	-	2	31
	"	34-44		2300	36	38	24	14	-	-	38
8	G-11	0-10	145	1860	47	45	26	14	6	9	25
	"	50-60		2680	29	18	17	8	6	8	58

379

Table 1. (Cont.)

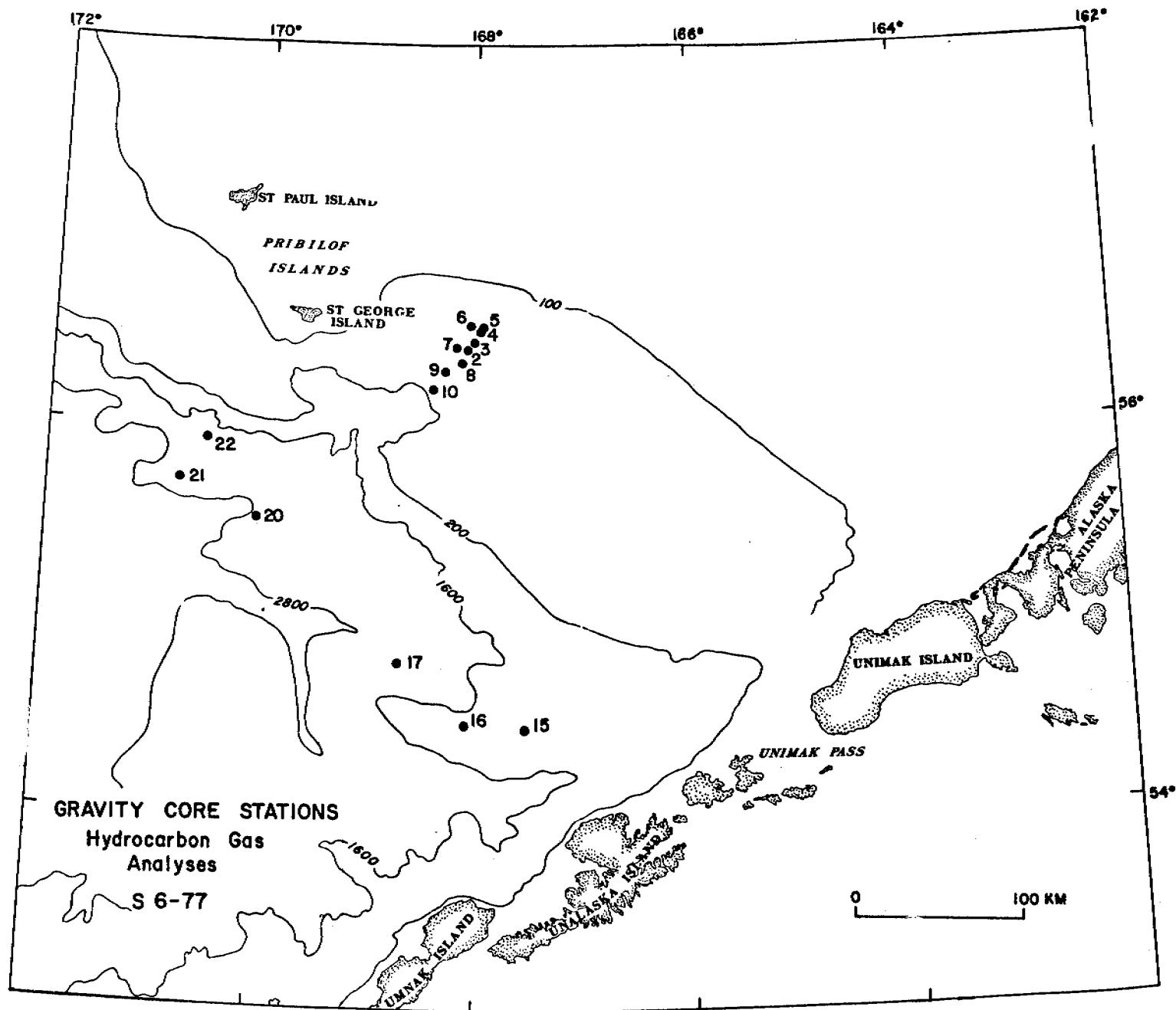
9	G-12	0-10	154	8330	204	75	106	19	29	32	27
	"	50-60		3160	117	6	30	5	-	-	21
	"	100-110		4820	333	6	95	16	15	9	11
10	G-13	0-10	166	1170	47	39	25	14	9	9	16
	"	50-60		3170	35	9	11	11	-	-	69
	"	100-110		3100	79	9	7	27	-	-	36
	"	150-160		3950	158	12	9	49	-	-	24

Table 2. Hydrocarbon Gases - Southern Bering Slope S6-77

Sta	Sample	Interval (cm)	Water Depth (m)	Concentrations (nL/L wet sediment)							$\frac{C_1}{C_2 + C_3}$
				C ₁	C ₂	C ₂ :1	C ₃	C ₃ :1	i-C ₄	n-C ₄	
15	G-15	0-10	825	970	26	47	16	14	6	9	23
	"	100-110		925	43	62	30	26	6	9	13
16	G-18	0-10	1195	815	23	32	16	14	-	6	21
	"	50-60		2880	23	24	14	9	-	-	79
	"	100-110		4090	26	29	14	11	-	6	104
17	G-21	0-10	2224	1290	31	32	25	9	6	9	23
	"	50-60		1610	17	18	9	6	-	-	62
	"	100-110		2090	17	15	5	6	-	-	95
	"	150-160		4070	23	9	9	-	-	-	127
20	G-25	10-20	2900	1010	11	26	9	9	-	-	51
	"	70-80		4600	17	14	7	6	-	-	192
	"	110-120		5330	23	14	9	9	-	-	167
	"	160-170		7730	23	20	9	12	-	-	242
	"	200-210		6650	28	20	9	15	-	-	180
21	G-27	0-10	3158	5120	20	23	9	6	-	-	177
	"	50-60		4740	17	14	5	6	-	-	215
	"	102-112		7920	20	17	7	-	-	-	293

Table 2. (Cont.)

22	G-28	0-10	2630	1140	17	17	12	6	-	-	39
	"	50-60		690	11	17	7	6	-	-	38
	"	100-110		1580	23	20	14	70	455	15	43
	"	150-160		2350	56	75	44	50	203	15	24
	"	200-210		7500	40	17	12	9	55	6	144



ANNUAL REPORT

YUKON DELTA COASTAL PROCESSES STUDY

William R. Dupré

Department of Geology
University of Houston
Houston, Texas

May 30, 1978

Prepared for

U.S. Department of Commerce
National Oceanic and Atmospheric Administration
Environmental Research Laboratories
Boulder, Colorado 80302

Research Unit: 208

I SUMMARY

Objectives

The overall objective of this project is to provide data on geologic processes in the Yukon-Kuskokwim delta region in order to better evaluate the potential environmental impacts of oil and gas exploration and production. The specific objectives of the study include the following:

- 1) Study the processes along the delta shoreline (e.g., tides, waves, sea-ice, river input) to develop a coastal classification including geomorphology, coastal stability, and dominant direction of sediment transport.
- 2) Study the processes active on the delta plain, including river breakup, river bank erosion and sedimentation, and the hydrology of the interconnected lakes and abandoned river channels.
- 3) Make a tectonic map of the delta region, delineating areas of Quaternary volcanism and faulting.
- 4) Make a geologic map of the delta area, emphasizing the delineation of depositional systems, in order to:
 - a) establish a chronology of delta sublobes to serve as a datum by which the relative age of Quaternary faulting and volcanism can be measured.
 - b) establish a chronology of storm-induced erosional events recorded in chenier-like sequences along the coast to estimate the recurrence interval of major storms in the region.
 - c) determine the physical properties of the different geologic units, including the depth and stability of permafrost.
 - d) aid in the definition and extrapolation of biological habitats throughout the region.

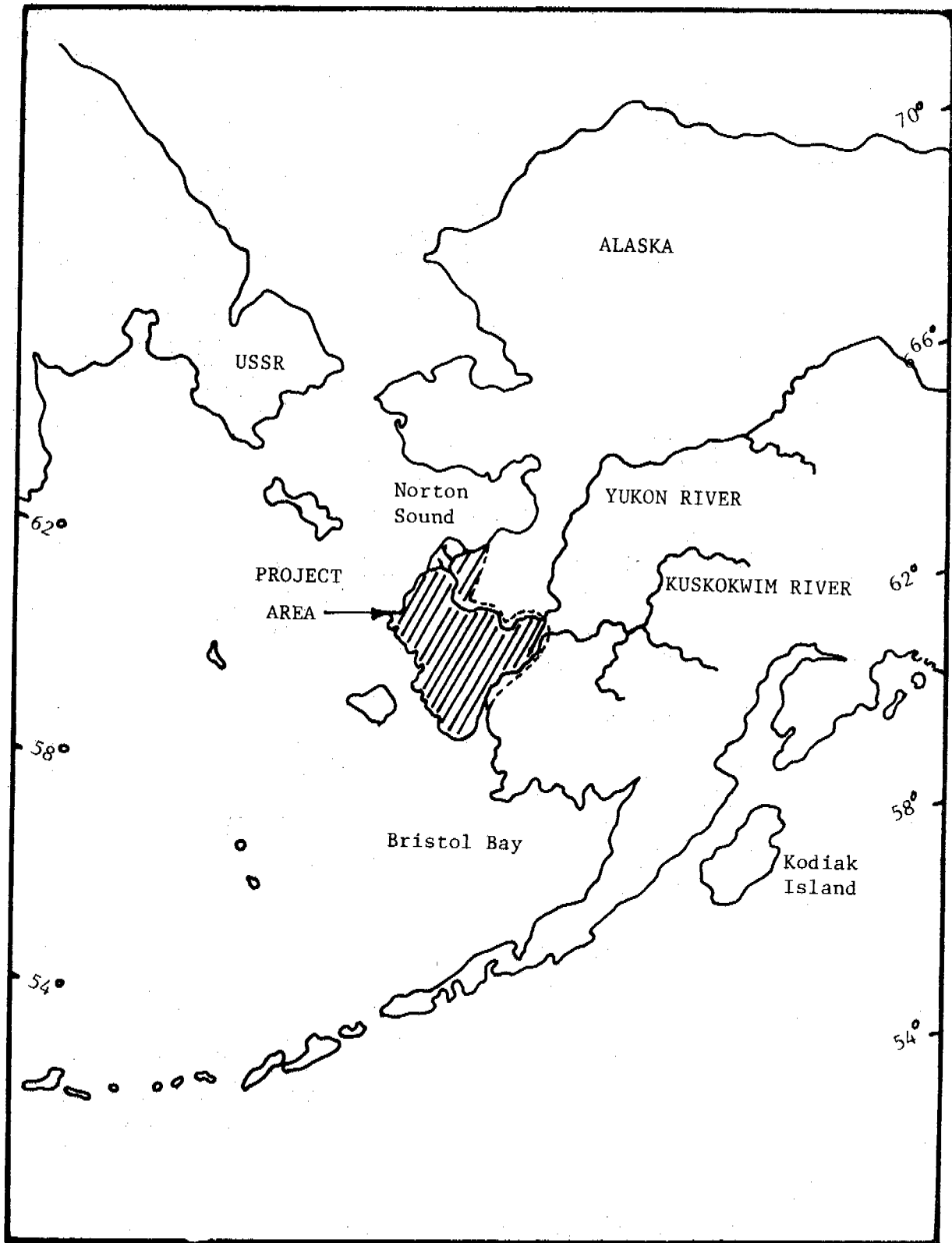


Figure 1: Location of project area - Yukon Delta Coastal Processes Study (R.U. 208).

Conclusions:

The Yukon-Kuskokwim delta region is characterized by widespread Quaternary tectonism. Northwest- and northeast-trending faults and structurally-controlled volcanic vents are mainly restricted to the onland extension of the Nunivak Arch. At least some of these faults appear to have had Holocene movement. Most of the volcanism has occurred within the last 700,000 years, however a 5.5 meter core from a volcanic lake in the region shows no evidence of local volcanism during the last 40,000-50,000 years. Thus, the potential for surface rupture and ground shaking must be considered in site evaluation, however, the risk from volcanism appears slight.

The delta region consists of a complex assemblage of Quaternary deposits of various origins and ages, ranging from Sangamonian (and older) marine terrace deposits to modern deltaic and estuarine deposits. Each is characterized by a variety of physical and hydrologic properties as well as geologic processes which must be considered when evaluating potential environmental impacts.

Permafrost occurs throughout most of the study area. It is most extensively developed in the pre-Holocene deposits where large ice wedges and massive ice are present; the depth of the permafrost in these deposits may locally exceed 200 meters. Widespread thermokarst marks an interval of melting of the permafrost, yet that melting appears to have ceased, at least in the northern parts of the delta region where modern ice wedges are presently forming. Permafrost appears to be present in some degree in most areas except along large rivers, deep lakes, and rapidly prograding coastlines, thereby complicating the selection of potential transportation corridors.

The largest floods along the Yukon River (locally exceeding 1,000,000 cfs) occur during river breakup, however large floods also occur associated with late summer and early fall storms. Extremely large floods may actually divert the entire course of the lower Yukon river, as has already happened at least four times in the last 5,000 years. The most recent of these shifts occurred sometime between 2500 and 1200 years ago, resulting in the formation of the modern Yukon delta.

The coastline is highly variable with respect to its morphology, processes, and overall coastal stability. Of particular importance in determining the relative coastal stability is the proximity of the Yukon River sediment input, the sheltering effects of barrier islands, laterally migrating tidal inlets, and local tectonic patterns. In spite of its heterogeneity, however, the dominant direction of longshore drift is toward the north, coincident with the oceanic and wave-generated currents.

Any study of coastal processes in the Norton Sound/Yukon delta region must take into account the extreme seasonality of coastal processes. In general, the year consists of three seasons: an ice-dominated regime from approximately November to May, a river-dominated regime from May to late summer, and a storm-dominated regime from late summer to freezeup in the fall.

The ice-dominated regimen lasts from freezeup in the fall to breakup in the spring. During that time, shorefast ice extends to approximately the 5-10 meter water depth, where it is terminated by a series of pressure ridges and shear zones formed by the interaction of shorefast and seasonal pack ice. This is a zone of intense ice gouging as well. The pattern:

of ice movement in Norton Sound is quite distinct from that farther to the west.

Breakup marks the end of the ice-dominated processes and the beginning of the river-dominated regimen. During breakup, much of the river water (and sediment) bypasses the nearshore zone by a combination of over-ice flow (c.f. Colville delta) and flow through sub-ice channels which extend from the mouths of major distributaries up to 15 km offshore. These offshore channels continue to be areas of active bedload transport during the summer. In contrast, most of the suspended sediment appears to be transported to the northwest in plumes restricted to the Alaska Coastal Waters.

The storm-dominated regimen begins in late summer, as decreasing river discharge and increasing storm frequency and severity combine to cause significant erosion along much of the coast. Some areas are eroding at rates in excess of 60 meters/year, most of which probably occurs during storms.

In summary, the Yukon delta is strongly influenced by the effects of ice in the ground, on the river, and offshore. Several of the major depositional environments of the Yukon delta appear to be restricted to ice-dominated coastlines. Similarly, the seasonality of coastal processes is dominated by the effects of ice throughout much of the year, thus a careful study of this region may provide insights into sedimentary processes and geologic hazards in other ice-dominated coastal zones as well.

Implications:

The siting of offshore facilities (e.g., drilling platforms, underwater pipelines) must take into account the mobility and deformation of seasonal pack ice, the extent and variability of shorefast ice, the probability of offshore permafrost, and the possible effects of altering offshore bathymetry in changing coastal stability. In addition, the evaluation of possible oil spills must take into account not only the dominant northward drift of water and suspended sediments, and the local and seasonal variability of current patterns, but also the role of sub-ice channels in affecting bedload transport.

The selection of shoreline sites (e.g., docking and pipeline terminals) must take into account the present coastal stability, including the possibility of erosion associated with major storm surges, even in an area of long-term progradation. The effects of shorefast ice for over half of the year must also be considered. The heterogeneity of the shoreline must also be considered in determining oil spill vulnerability.

Much of the delta is underlain by the on-land extension of the Nunivak Arch; this would seem to exclude most of the region for serious consideration for exploration. Nevertheless, the Quaternary faults and volcanoes which characterize the zone constitute geologic constraints on the selection of transportation corridors. The discontinuous permafrost and the complex hydrology of the delta further complicate the location of such corridors, as well as making it difficult to predict the effects of oil spills.

Lastly, an understanding of the geologic processes and products within the delta region will greatly aid in the definition and regionalization of biological habitats, as well as help in the development of depositional models for sedimentation in an ice-dominated coastal environment.

II. INTRODUCTION

The overall objective of this project is to provide data on geologic processes in the Yukon-Kuskokwim delta region in order to better evaluate the potential environmental impacts of oil and gas exploration and production. The specific objectives of the study include the following:

- 1) Study the processes along the delta shoreline (e.g., tides, waves, sea-ice, river input) to develop a coastal classification including geomorphology, coastal stability, and dominant direction of sediment transport.
- 2) Study the processes active on the delta plain, including river breakup, river bank erosion and sedimentation, and the hydrology of the interconnected lakes and abandoned river channels.
- 3) Make a tectonic map of the delta region, delineating areas of Quaternary volcanism and faulting.
- 4) Make a geologic map of the delta area, emphasizing the delineation of depositional systems, in order to:
 - a) establish a chronology of delta sublobes to serve as a datum by which the relative age of Quaternary faulting and volcanism can be measured.
 - b) establish a chronology of storm-induced erosional events recorded in chenier-like sequences along the coast to estimate the recurrence interval of major storms in the region.
 - c) determine the physical properties of the different geologic units, including the depth and stability of permafrost.
 - d) aid in the definition and extrapolation of biological habitats throughout the region.

This project was designed to provide as much information as possible to the problems of petroleum development in the region. A better understanding of the tectonic framework of the delta region should aid in the exploration of oil and gas. Those same tectonic features, to the

extent to which they are active today, also provide serious constraints to the selection of transportation corridors, as does the existence of extensive permafrost and the actively shifting river courses.

A better understanding of coastal processes will aid in the siting of shoreline installations (e.g., docking and transfer facilities), as well as in evaluating the possible impacts of such facilities on coastal stability. The siting of offshore facilities (e.g., drilling rigs, underwater pipelines) must take into account frequency and magnitude of a variety of nearshore processes, including those associated with sea-ice. An understanding of these processes, including their seasonal variability, will also aid in predicting the paths of possible oil spills. An inventory of coastal materials and landforms will also serve as baseline data should spills come onshore.

Lastly, a better understanding of the sub-arctic coastal processes by which the present coastal depositional systems formed, will aid in the interpreting older, potentially oil-bearing units which may have been formed under similar climatic conditions.

III. CURRENT STATE OF KNOWLEDGE

The Yukon River is the 17th largest river in the world providing over 90% of the sediment introduced into the Bering Sea (Lisitzin, 1972), however, relatively little is known of its Quaternary history or of the process by which it was formed.

The ancestral Yukon River emptied into the Pacific in the vicinity of Cook Inlet during early Cenozoic time. Late Miocene uplift of the Alaska Range resulted in the diversion of the drainage system into the Bering Sea, where it has remained to the present (Nelson et al., 1974). Gradual submergence during late Miocene and Pliocene time was followed during the Pleistocene by repeated glacio-eustatic fluctuations of sea-level. River valleys cut into the exposed continental shelf during the last low-stand of sea-level were subsequently filled during rising sea-level with estuarine and marine sediments (e.g., Moore, 1964; Creager and McManus, 1967; Knebel and Creager, 1973). This rise in sea-level was apparently accompanied by a general northward shift of the Yukon River to the north (Knebel and Creager, 1973; Shepard and Wanless, 1971).

Much work has been done on studying the Cenozoic sedimentary and tectonic history of the Bering Sea (e.g., Nelson and others, 1974; Marlow and others, 1976), including studies of the Holocene sediments of the Yukon River at its mouth (Matthews, 1973) and on the Bering Sea shelf (e.g., Moore, 1964; McManus and others, 1974; Nelson and Creager, 1977). However, geologic mapping in the delta region (Hoare, 1961; Hoare and Coonrad, 1959a, 1959b; Hoare and Condon, 1966, 1968, 1971a, 1971b) has largely emphasized the pre-Quaternary history of the region. This study is the first, to deal in detail with the processes and events by which the Yukon-Kuskokwim delta complex was formed.

IV. STUDY AREA

The combined Yukon-Kuskokwim delta complex (Figure 1) is an area of unique natural resources covering over 31,000 square miles. It has a large native population living in large part on a subsistence economy. It provides access to most of the spawning areas for salmon in the region. It is, in addition, one of the most significant breeding grounds for migratory birds in North America.

The delta region is largely a flat, featureless plain consisting of wet and dry tundra, interrupted by innumerable lakes, many of which are oriented. Many of these lakes have coalesced laterally to form very large bodies of water (e.g., Baird Inlet) connected to the sea by a series of ancient river channels. The flatness of the delta complex is interrupted by numerous small Quaternary shield volcanoes, the major uplifted massifs of the Askinuk and Kuzilvak Mountains, and the Quaternary volcanic complex which forms Nelson Island.

The coastline is extremely varied, in part because of the complex geology along the coast, and in part because of the lateral variability of sediment sources and tidal range. For example, broad tidal flats, locally bordered by short barrier islands, flank the macro-tidal Kuskukwim delta, whereas the micro-tidal Yukon delta is fringed by distributary mouth bars and interdistributary tidal flats. Sandy beaches are present near Hooper Bay, where Wisconsinan(?) sand dunes provide the source of sediments, whereas steep gravel beaches and rocky headlands form along the cliffed shorelines at Cape Romanzof, Point Romanof, and Nelson Island. Elsewhere most of the coast consists of low, eroding bulffs cut into poorly consolidated Pleistocene deposits.

V. SOURCES, METHODS, AND RATIONALE OF DATA COLLECTION

Hydrologic data on discharge are available in published form for the Kuskokwim River at Crooked Creek (1951-1965) and for the Yukon River at Kaltag (1957-1965). More recent data are presently unpublished, but are available from the Water Resources Division of the U.S. Geological Station in 1974, providing additional information on suspended and bedload sediment as well as discharge. Additional samples of both the bedload and suspended load of the Yukon and Kuskokwim Rivers are being collected as part of the field work.

Much of the region has been mapped and published at a scale of 1:250,000 by Dr. Joe Hoare and associates at the U.S. Geological Survey. I have been using these maps in conjunction with aerial photography and LANDSAT imagery, to prepare a geologic map of the delta region emphasizing the Quaternary depositional systems.

Field work is providing the ground truth for the mapping as well as samples for textural and mineralogic analyses and radiocarbon dating. Samples for dating are being selected to document the frequency of major shifts in the rivers course as well as major coastal storms. The distribution of permafrost is also being studied, with special emphasis on defining the relationships between geomorphology, vegetation, and extent of ground ice. Hopefully the geologic mapping can be combined with data on morphology, vegetation, and physical properties to aid in the characterization of biological habitats and the definition of resource capability units.

Part of the field work consisted of coring a volcanic lake in the center of the delta region. The cores are presently being analyzed by Dr. Tom Ager (U.S. Geological Survey) to determine frequency of volcanism in the region (via ash content), sources and rates of sedimentation, and evidence of climatic change (via pollen analysis).

Existing imagery is being used in combination with coastal overflights in a light plane and helicopter to develop a coastal classification scheme. Baseline coastal stations were established to characterize homogeneous intervals of the coastline. Approximately twelve such stations were established in 1976; an additional thirty were set up in 1977. All will be reoccupied in 1978. Beach profiles are measured at each station using a modified Emery method - some offshore profiles were obtained in 1976 with a Zodiac and fathometer. Sediment samples and process measurements (e.g., winds, waves) are also collected.

Bathymetric maps (dating back to 1898) are being used in conjunction with aerial photos (1954, 1973, and 1976) and beach profiles to determine rates and directions of shoreline change as well as dominant directions of nearshore sediment transport. LANDSAT imagery is also being used, and has proven invaluable in defining offshore sediment plumes as well as studying the development and mobility of ice in the region. NOAA VHRR(1-2) weather satellite imagery is also being used in combination with synoptic weather data to aid in interpreting ice patterns in the Norton Sound region.

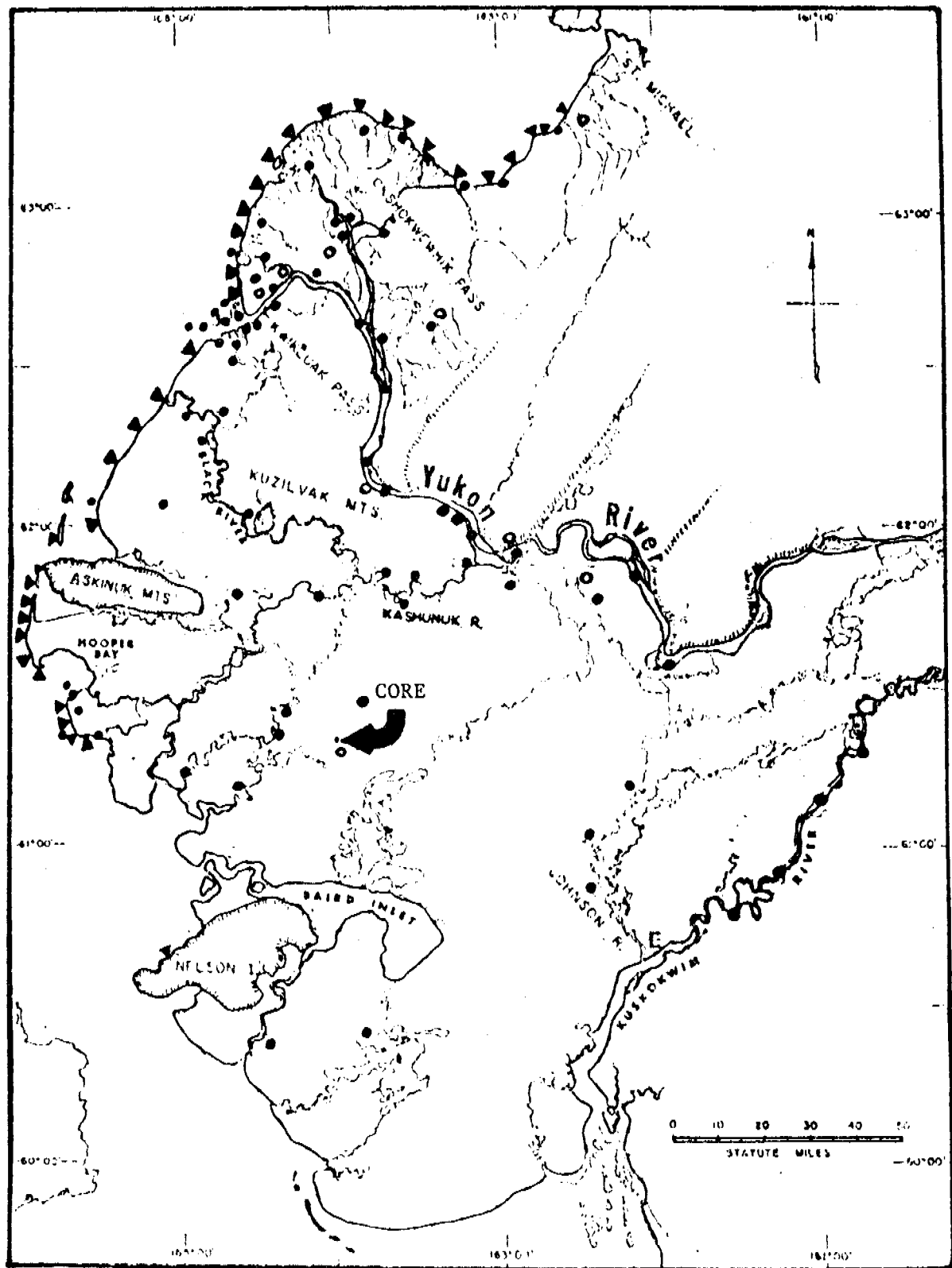


Figure 2: Location of sample stations. Triangle (▼) marks a coastal station with beach profiles, sediment and vegetation samples. Closed circle (●) marks grab samples or short cores for textural analysis or radiocarbon dating (includes some vegetation descriptions). Open circles (○) indicate only vegetation description.

VI. RESULTS

The results to date of this project can best be summarized in a series of illustrations and tables, the significance of which are described in section VII. These include:

- 1) a preliminary tectonic map (Figure 3)
- 2) table of radiocarbon date (Table 1)
- 3) Geologic maps of the Yukon-Kuskokwim delta region (Figures 4, 6, 11)
- 4) Ice wedge chronology (Figure 5)
- 5) Generalized depositional environment of Yukon delta (Figures 8, 9)
- 6) Development of Black River Chenier Plain and role of storms (Figure 12)
- 7) Example of rate of shoreline change (Figure 13)
- 8) Illustration of coastal processes throughout the year (Figures 14-20)

<u>Project No.</u>	<u>USGS No.</u>	<u>Lat.</u>	<u>Long.</u>	<u>Date</u>
II-10	48	62°55'	164°06'	820±90
V-10	49	62°09'	164°59'	1350±80
V-9	50	62°02'	165°14'	734,400
V-4	51	61°32'	164°46'	1200±60
I-4	52	61°36'	166°10'	modern (contaminated)
II-10	53	62°19'	165°12'	1890±85
II-7	213	62°41'	164°37'	600±70
7-13-3B	212	62°32'	164°52'	1430±50
7-12-2B	214	62°37'	164°40'	2420±80
I-6	215	61°36'	166°10'	5070±60
V-5	217	63°23'	164°31'	1930±70
7-12-2a	218	62°37'	164°41'	1800±90
II-9	225	62°18'	164°59'	1550±80
II-8	226	62°29'	164°52'	2570±70

Table 1: Radiocarbon dates of samples from the Yukon delta region (Steve Robinson, U.S.G.S., Menlo Park, Calif.)

VII. DISCUSSION

Tectonic Framework:

The Yukon-Kuskokwim delta complex is located within the Koyukuk volcanogenic province which has been characterized by recurrent faulting and syntectonic volcanic activity throughout Mesozoic and Cenozoic time (Patton, 1973). Most of the major faults in the region (e.g., the Kaltag fault) formed were most active during late Cretaceous and early Tertiary time (Hoare, 1961), presumably in response to large scale oroclinal bending between Alaska and northeastern Siberia (Carey, 1958; Hopkins and Scholl, 1970; Nelson and others, 1974). Many of these structures have remained active, albeit at reduced levels of activity, to the present (e.g., Hoare, 1961; Patton and Hoare, 1968; Grim and McManus, 1970).

Most of the newly recognized faults, photo-linears, and measured joint sets within the Quaternary deposits parallel previously mapped faults. Several of these faults, (e.g., those parallel to the northwest face of the Kuzilvak Mountains) appear to be a continuation of previously mapped faults exposed in the Andreski Mountains. There is no evidence of the Kaltag fault passing through the modern lobe of the Yukon delta, as previously suggested by Hoare and Condon (1971). It is possible that it extends offshore, to the north of the delta; alternatively it may splay into a series of southwest-trending faults which transect the Andreski Mountains and continue across the delta plain.

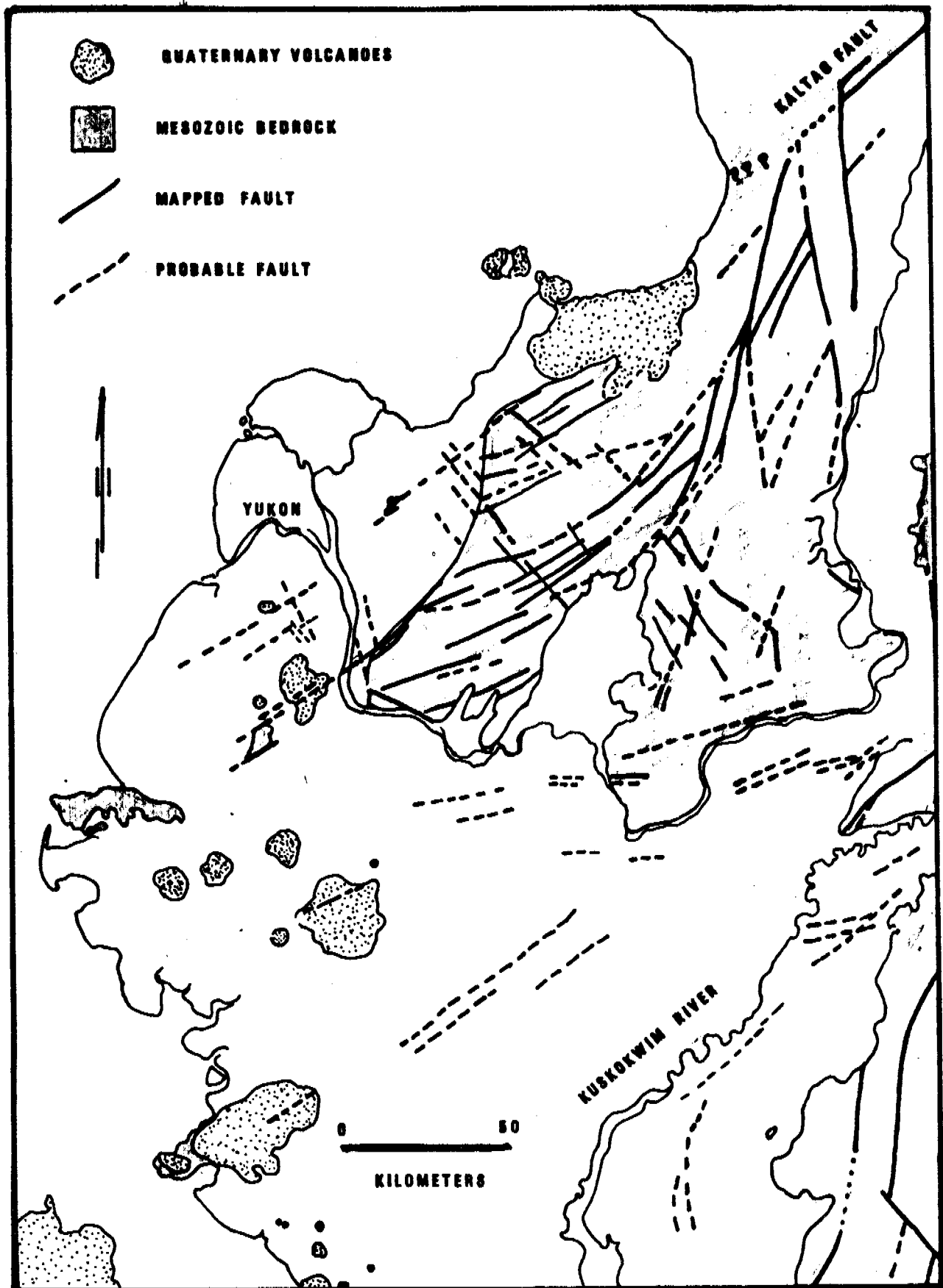


Figure 3: Tectonic map of the Yukon-Kuskokwim delta region (modified after Beikman, 1974).

The age of the most recent faulting remains uncertain, although the scarp near the base of the Kuzikvak Mountains is remarkably well preserved. The exact dating must await more extensive radiocarbon dating of the various sublobes of the delta. Nonetheless, at least some of the faults appear to cut Holocene deltaic and fluvial deposits.

The recentness of fault movement, as based on geologic criteria, is consistent with the recent microseismicity work in progress by Biswas and Gedney (R.U. 483), as well as the abundance of recent faults detected offshore by Johnson and Holmes (in Nelson, 1978). Thus it seems clear that the selection of potential transportation corridors must take into account the possibility of significant ground movement along at least some of the fault zones in the area. In addition, all site investigations must evaluate the potential for ground shaking and liquefaction due to such an event, even though the historical seismicity is relatively low.

The earliest volcanic activity in the region occurred in early Mesozoic time, resulting in the formation of widespread mafic intrusive and extrusive rocks which floor the entire volcanogenic province. These were followed by marine andesitic volcanic rocks, felsic volcanic and intrusive rocks, and most recently, Quaternary alkali basalts (Patton, 1973).

The Quaternary volcanism probably occurred over a wide period of time, as evidenced by the various degrees of weathering and slope modification; however paleomagnetic data indicate that almost all of the basalts are normally polarized, hence are younger than 700,000 years old (Hoare and Condon, 1971b). The age of the most recent volcanism is less clear. A core taken from a volcanic lake in the Ingakslugwat Hills (Fig. 2) contains

an ash deposit which is approximately 3500 years old (based on preliminary radiocarbon dates), however composition of the ash makes a local source unlikely. There is no other evidence of volcanism preserved in the core, which probably records an interval of 40,000 to 60,000 years, suggesting either that the most recent volcanism in the region was far removed from the lake or that it predates the core. The latter seems most likely, however there are some extremely young looking flows near St. Michaels which may be younger than any of the volcanic activity in the delta region. Thus it seems likely that, with the possible exception of the area around St. Michaels, the risk due to volcanic activity should be considered slight.

Yukon-Kuskokwim Delta Complex

The Yukon-Kuskokwim delta complex consists of a complex assemblage of Quaternary depositional systems of various origins and ages (Fig. 4).

These include:

- 1) Pleistocene terrace deposits: highly altered by thermokarst processes; largely covered by patterned ground and polycyclic thaw lakes.
- 2) Abandoned river courses: Pleistocene to Holocene meanderbelt deposits, the oldest of which are progressively altered by thermokarst processes.
- 3) Eolian deposits: mainly Pleistocene sand dunes usually fringing the southern side of abandoned river courses.
- 4) Modern fluvial deposits: including active and recently abandoned meanderbelt deposits, natural levees, and river bars.
- 5) Modern deltaic deposits: including active and abandoned distributaries, interdistributary and coastal marshes, prograding distributary mouth bars and intertidal mudflats (as well as offshore delta margin, delta front, and prodelta deposits).
- 6) Modern bay and estuarine deposits: including large areas of prograding mudflats.
- 7) Sandy beaches and barrier islands: locally bordered by low coastal dunes.
- 8) Gravel beaches and rocky headlands: formed along coastal outcrops of Mesozoic bedrock and Quaternary volcanoes.

Pleistocene terrace deposits: A large portion of the Yukon-Kuskokwim "delta plain" consists of Pleistocene deposits formed under a variety of depositional environments, including alluvial fan, marine, and fluvial. At least three pre-Holocene shorelines can be locally identified, the youngest of which is Sangamon (Dave Hopkins, U.S.G.S., written communication). Unfortunately, these deposits remain largely undifferentiated, in part because of their complexity but mainly because of the pervasive effects of permafrost and associated thermokarst processes.

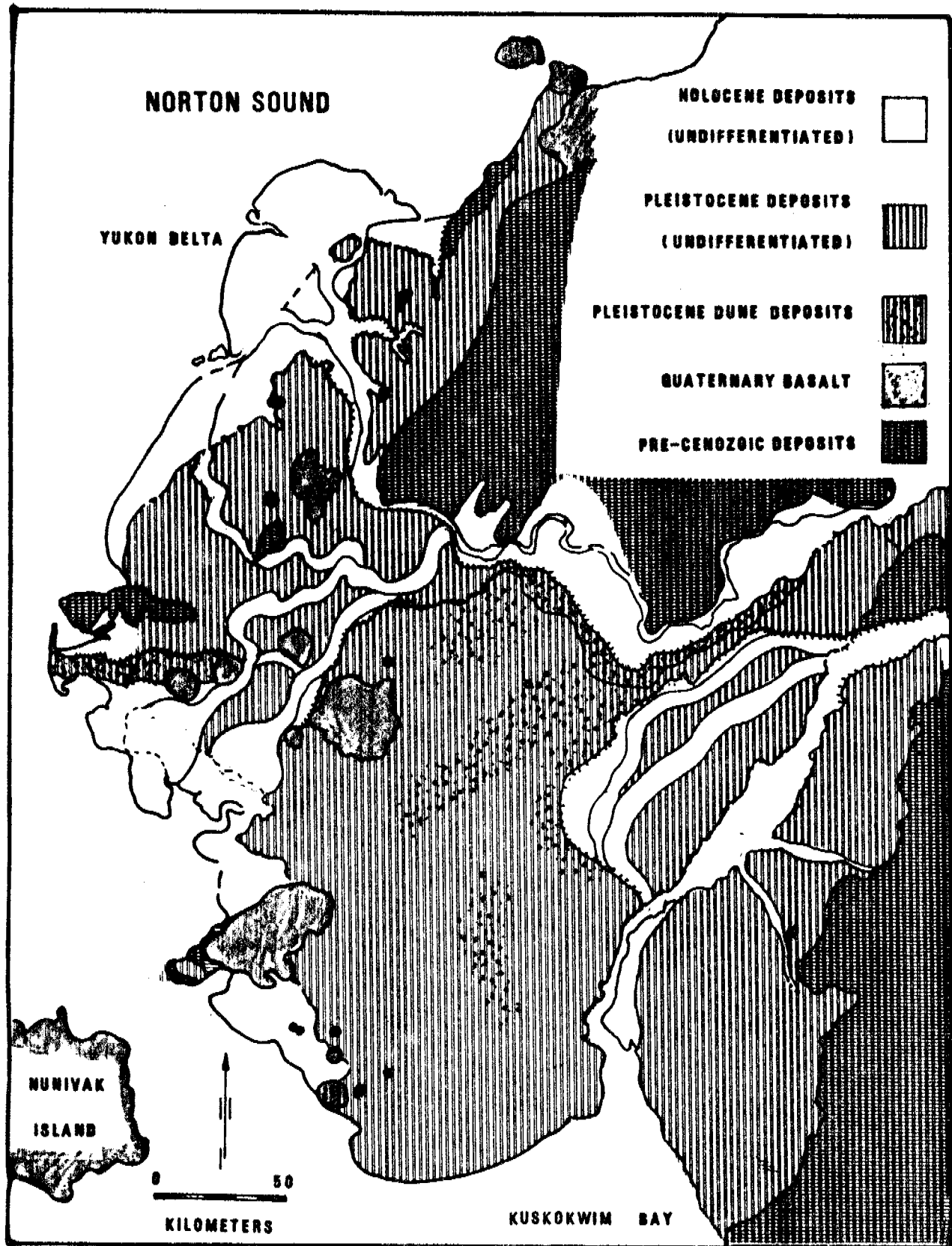


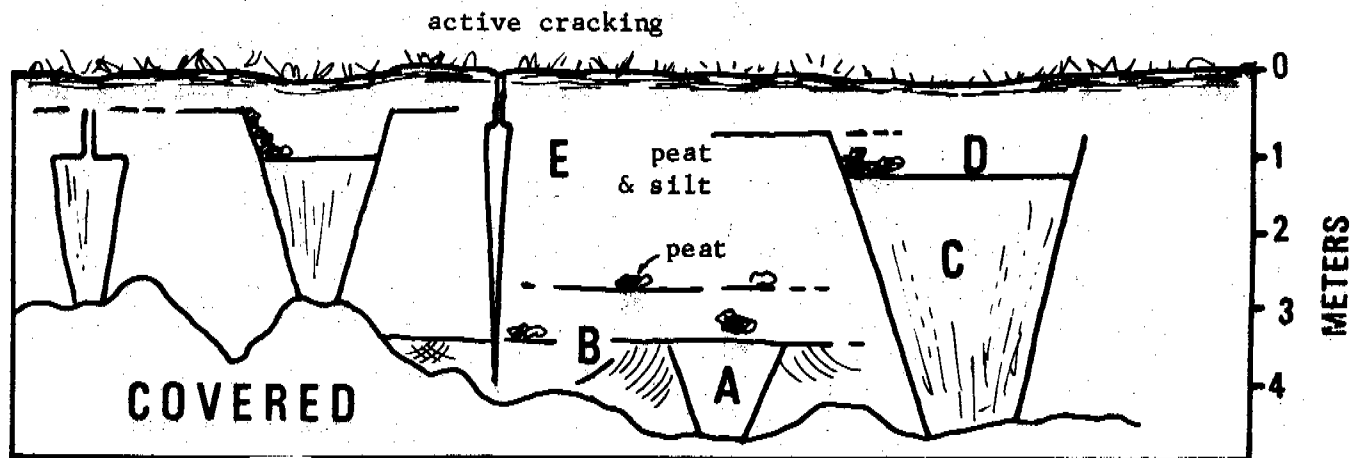
Figure 4: Generalized geological map of Yukon-Kuskokwim delta complex.

The presence of permafrost is well evidenced by an abundance of geomorphic criteria including palsas, patterned ground, thermokarst lakes, solifluction lobes, and stringbogs. Its presence was further substantiated by field studies as well as drillers and engineering reports. The permafrost ranges from thin veins of Taber ice to large ice wedges and massive ice similar to that described by MacKay(1971) in northern Canada; locally the permafrost may be 200 meters thick (Williams, 1970).

One of the most characteristic features of these older deposits is their abundance of lakes, most of which have formed from melting of the permafrost. These lakes, once formed, typically begin to expand laterally by a combination of thermal erosion and wave action. As they expand several may coalesce to form extremely large but shallow bodies such as Dall Lake and Baird Inlet. The lakes are most abundant in the southern part of the delta where most are distinctly oriented, however they are present throughout the region.

It is apparent that many of the older deposits are scarred by polycyclic thaw lakes, i.e., those having gone through several cycles of filling and re-formation. The extent of these polycyclic lakes and the probable age of the deposits makes it likely that they reflect changes between relatively warm intervals, characterized by ice melting and lake formation and cold periods characterized by ice formation and lake infilling.

The exact chronology of these events is not certain, but exposures of ice wedges along the eroding coast between St. Michaels (Fig. 5) may provide a partial answer. Three distinct intervals of ice wedge formation are recorded in these post-Sangamon deposits. The oldest may be early



Possible Chronology:

- A - Formation of large ice wedges (Early Wisconsinan?)
- B - Lowering of the permafrost table (Middle Wisconsinan?)
- C - Formation of large ice wedges (Late Wisconsinan?)
- D - Lowering of the permafrost table (Early Holocene: 11500-8000 BP?)
- E - Formation of modern ice wedges (8000 BP to the present)

Figure 5: Ice wedges exposed along rapidly eroding sea cliff between Point Romanof and the Pigmiktalik River.

Wisconsinan. The younger ice wedges were partially melted, probably during the early Holocene warming trend (11,500-8,000 B.P.) described from the Seward Peninsula by McCullough and Hopkins (1966). This was followed by a subsequent rise in the permafrost table and the formation of modern ice wedges which are actively forming today (at least in the northern part of the delta). Thus it appears that the widespread thermokarst landforms so characteristic of the Pleistocene deposits may be largely relict features.

In summary, permafrost is present, typically with a large ice content, in most of the Pleistocene terrace deposits. The type of permafrost and its stability will vary with the types of deposits, the topography, and vegetation cover, hence it is extremely difficult to predict, however it appears to present the most serious non-tectonic hazard in these deposits.

Abandoned river courses: Several of the rivers which cross the Yukon-Kuskokwim delta plain are clearly underfit, having once marked the location of the Yukon River at some time during the Quaternary. They appear to range in age from early(?) Wisconsinan to perhaps 1250 years old. The older of these abandoned meanderbelt deposits are highly altered by the effects of thermokarst, and their fluvial origin is almost obscured. In contrast some of the younger courses are almost unaltered. In fact, the degree of alteration can be used as a measure of relative age and as a tool for correlation (c.f. Péwé, 1948).

Numerous authors have noted that the Yukon has shifted its course during the Quaternary (e.g., Hoare and Condon, 1966; Shepard and Wanless, 1971; Knebel and McManus, 1973), however the detailed chronology of these river shifts remains less clear. Shepard and Wanless (1971) suggested that the Yukon had shifted progressively to the north based on the relative indentation of the shoreline (i.e., older courses were graded to lower sea-level, hence are now embayed). Unfortunately they did not take into account the local modifications due to tides or the effects of subsequent modifications of the shoreline by erosion and deposition, hence their chronology is in error.

The best approach to unraveling the history of the Yukon is by radiocarbon dates obtained from the delta plain (Table 1). My preliminary interpretation based on available dates is shown in Figure 6. Two things appear worthy of note. The first is that the river has shifted fairly frequently (four times in the past 5,000 years). The second is that the most recent shift, which formed the modern Yukon delta, apparently occurred between 2500 and 1250 years ago (the older date appears more likely).

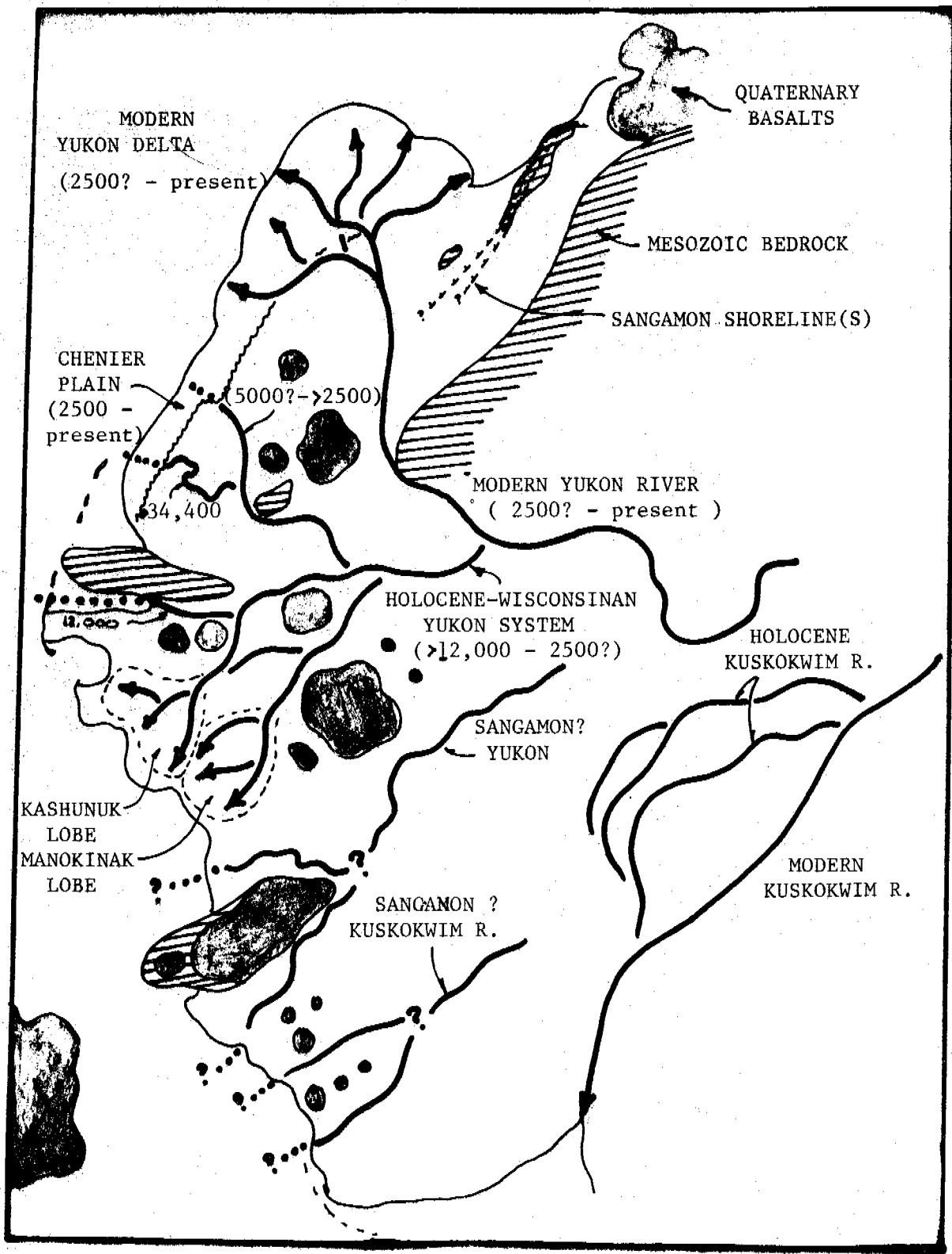


Figure 6: Generalized map of Quaternary river courses (modern and abandoned) in the Yukon - Kuskokwim delta complex. Large areas of pre-Holocene sand dunes and loess have been omitted.

The consequences of such large scale river changes, combined with their relative frequency, marks them as a major geologic hazard to be considered in any plans which might affect the flow characteristics of the Yukon River.

Pleistocene(?) eolian deposits: Large areas of the delta complex are covered with windblown sand and loess. The sand deposits are locally up to 75 feet thick, and have been mapped separately where possible (Fig. 6). No attempt has been made to map loess deposits. Most of the sand deposits are localized along the southern edge of Pleistocene courses of the Yukon River, suggesting they were formed by reworking of fluvial deposits during periods of extensive glacial outwash (Péwé, 1975). Much of the eolian sand may have formed by reworking of glacial outwash associated with the Itkillik II glacial advance approximately 13,000 years ago (Hamilton and Porter, 1975), however both younger and older eolian deposits are present in the delta region.

These extensive sand dune fields were active under conditions different than the present, and are presently stabilized. The dunes can be re-activated, however, if the vegetation cover is disturbed as has happened near Hooper Bay. Therefore special care is needed during construction as these deposits are especially vulnerable to erosion.

Modern fluvial deposits: The most extensive modern fluvial deposits are those associated with the Yukon River where a complex meander schroll topography of point bars, partly abandoned sloughs, and rapidly changing river bars occur. These deposits are prone to flooding, particularly during breakup. Ice scouring can also cause significant damage along the margins of the main river courses. The river is also an area of extremely rapid

erosion and deposition, necessitating bank stabilization techniques for most river sites (or adequate set backs). There is some permafrost in these deposits, however it appears to be discontinuous and relatively thin. The main geologic hazards appear to be those associated with flooding and riverbank erosion: permafrost problems are less significant.

Modern deltaic deposits: The Yukon River has formed a high-constructional, lobate delta which, on the basis of its morphology, might be considered somewhere between a river-dominated and a wave-dominated delta (c.f. Galloway, 1975). A more careful examination of the delta including its offshore components, suggests such a classification is an oversimplification. Wright and Coleman (1973) suggested that deltas could be classified as either wave-dominated or river-dominated based on their subaqueous profile. A comparison of the offshore profile of the Yukon with those of other major deltas (Fig. 7) however suggest it is substantially different from those described by Wright and Coleman. In particular, the presence of an extremely broad offshore (sub-ice) platform owes its origin to the existence of shorefast ice for over half the year. Numerous

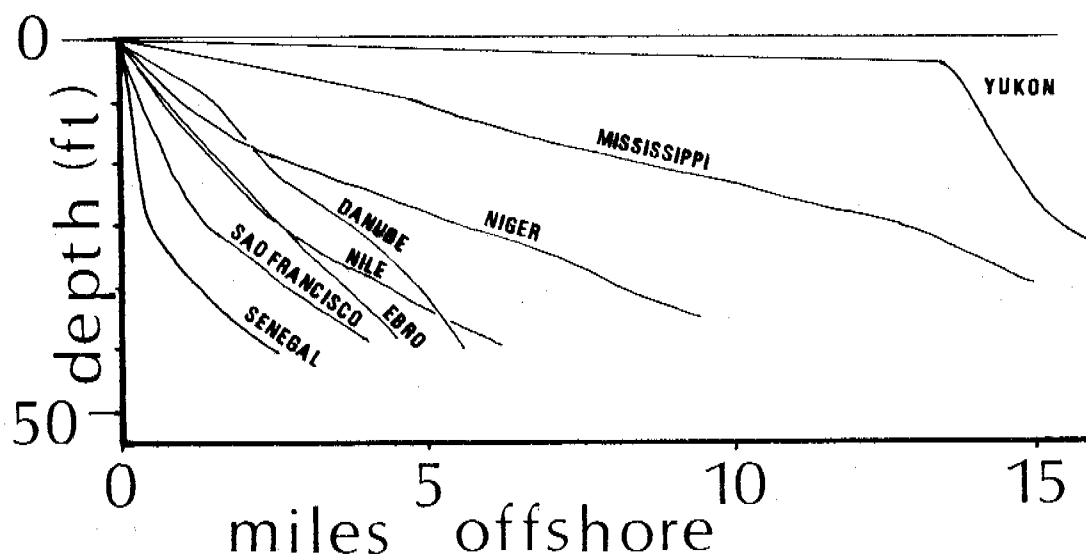


Figure 7: Comparison of the offshore profile of the Yukon delta with those described by Wright & Coleman (1973)

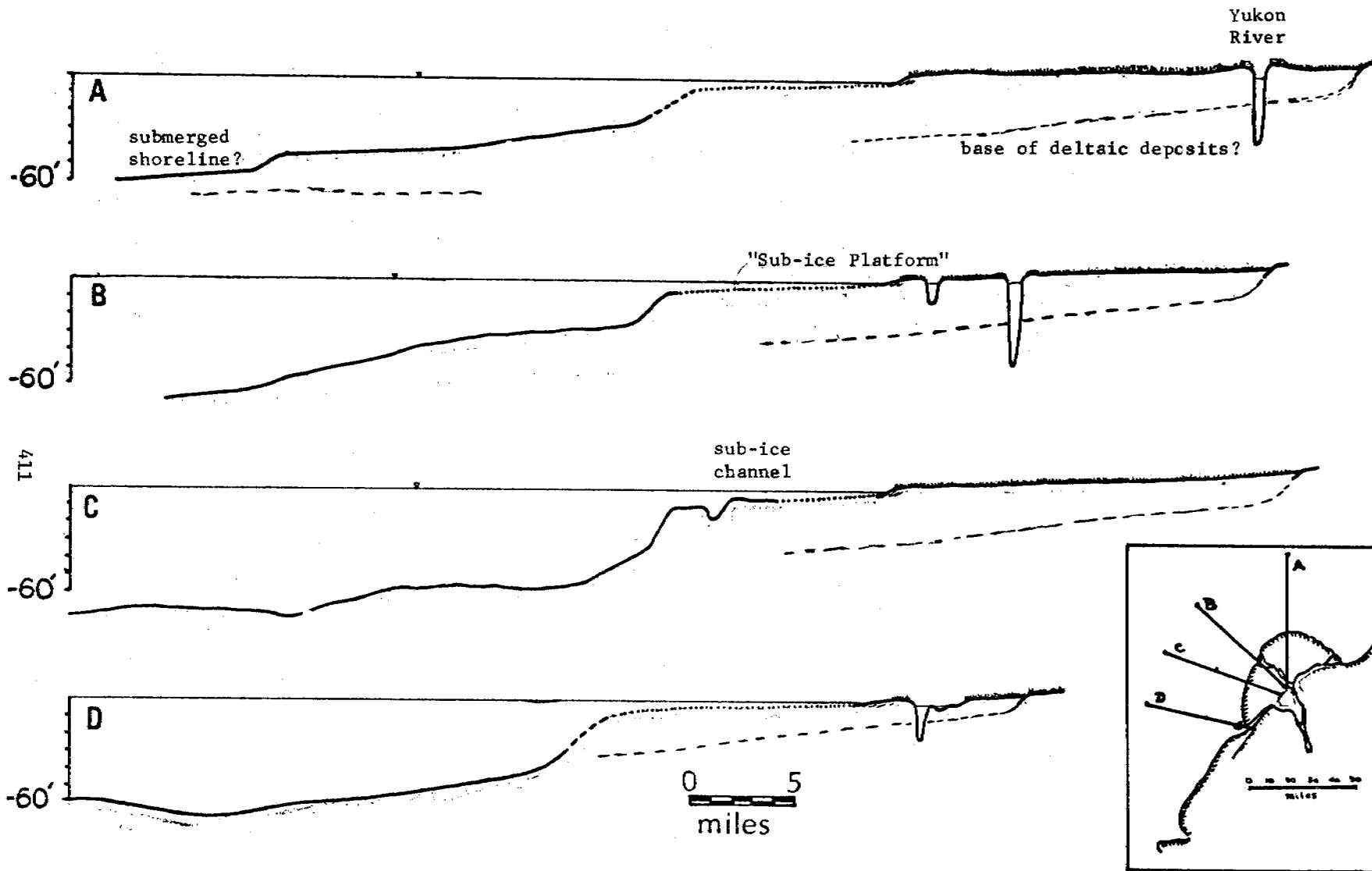
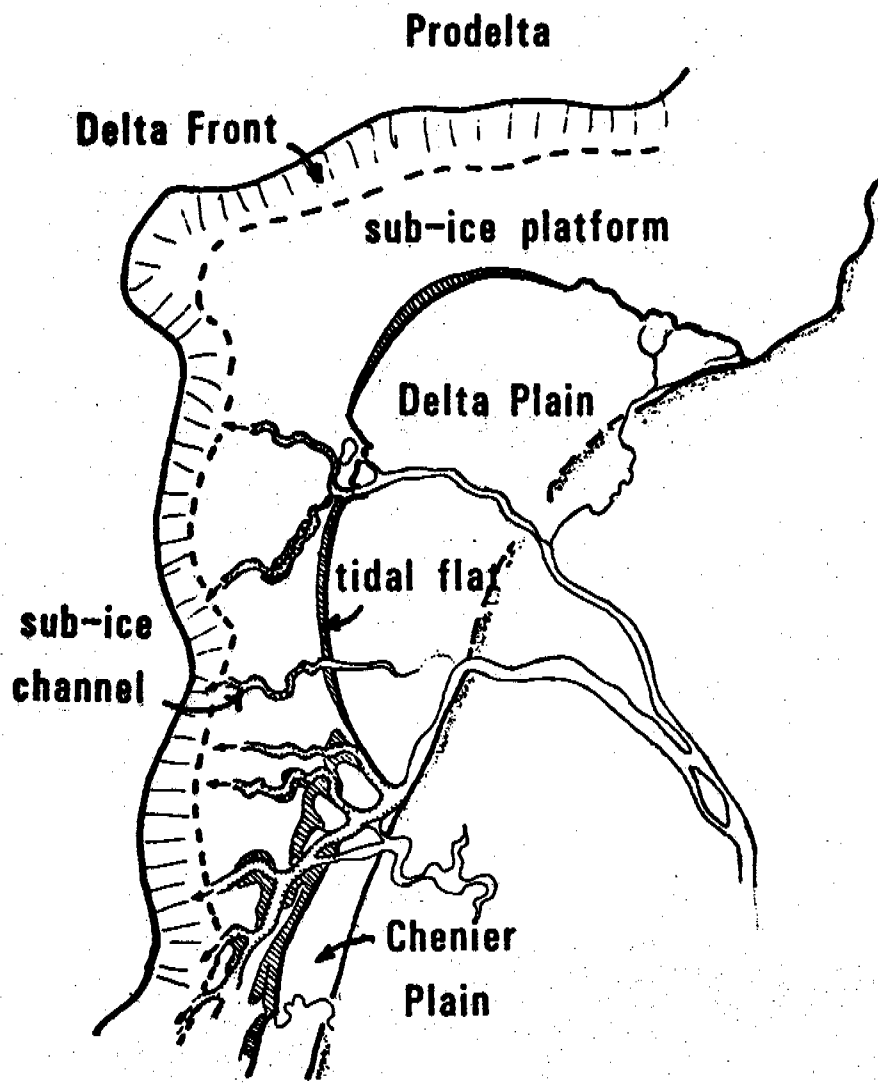


Figure 8: Selected profiles through the modern Yukon delta (from C&GS Chart 9370).

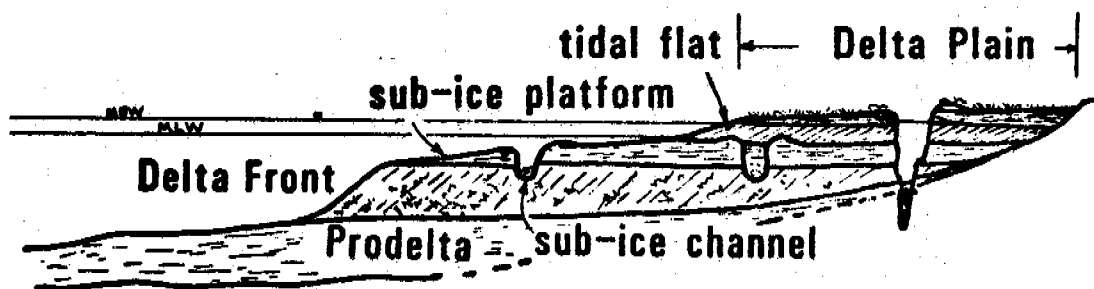
subice channels extend from the mouths of the main distributaries across the sub-ice platform. The delta front is thus separated from the shoreline by up to 30 kilometers (Fig. 8). This is in sharp contrast to most previously described deltas, suggesting that the Yukon delta may represent a type of "ice-dominated" delta, whose morphology differs significantly from the wave-, river-, and tidal-dominated deltas already described in the literature.

The subaerial delta plain consists of a variety of depositional environments including:

- 1) Active distributaries and associated bars: characterized by rapid riverbank erosion and deposition; flooding is common, especially during breakup, as are ice jams and ice scouring.
- 2) Abandoned distributaries and associated bars: characterized by rapid sedimentation and infilling of vegetation; old channels prone to flooding.
- 3) Interdistributary marshes and associated lakes: characterizes older parts of the delta; lakes often formed between natural levees, tend to fill with vegetation; some evidence of permafrost formation (palsas); characterized by high water table and some flooding during extreme events.
- 4) Prograding coastal marshes: characterized by relatively simple assemblage of grasses and sedges; drift lines and old beach ridges form slightly elevated areas; areas of rapid sedimentation (to 40 meters/year); commonly flooded during breakup and late summer/fall storms; may have minor erosion during large storms; some ice scouring during breakup.



A. GEOMORPHIC MODEL OF A SUB-ARCTIC DELTA



B. IDEALIZED PROGRADATIONAL SEQUENCE

Figure 9. Major depositional environments of the modern Yukon delta

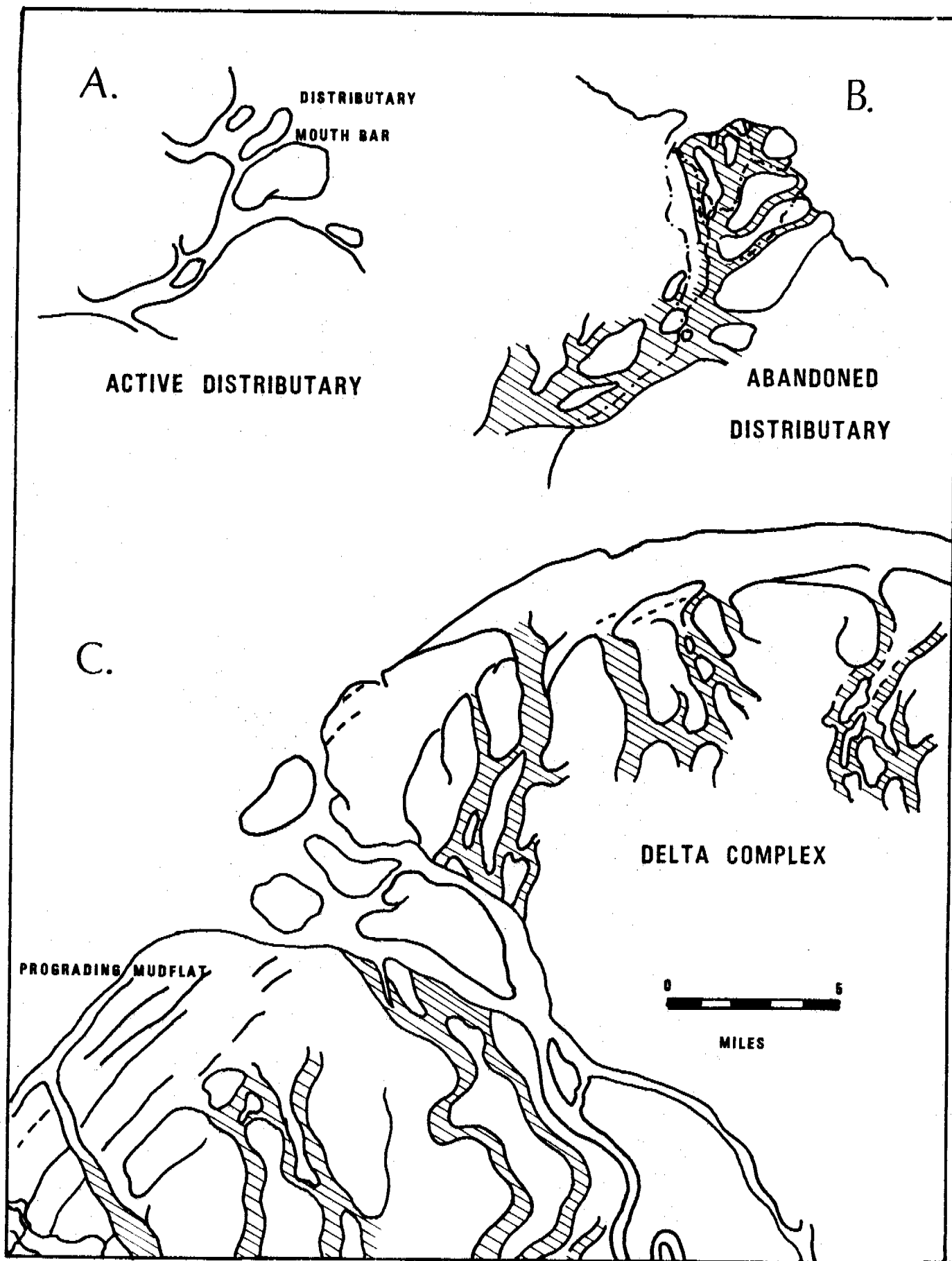


Figure 10: Depositional facies within the modern Yukon delta

- 5) Vegetated distributary mouth bars: characterized by extremely rapid rates of progradation; hazards similar to coastal marshes.

The delta margin consists of the intertidal and sub-tidal depositional environments between the shoreline and the delta front, and includes the following:

- 1) Intertidal mudflats: typical composed of ripple-laminated very-fine sand and silt; characteristic of rapidly prograding areas such as coastal marshes, distributary mouth bars, and aggrading subaqueous levees; ice scouring common, particularly during breakup.
- 2) "Sub-ice platform" (or 2 meter bench): extremely flat, broad bench locally extending over 30 km offshore; average depth probably less than two meters; may have offshore bars or shoals near its outer edge; characteristically covered by shorefast ice (both bottomfast and floating) during much of the year, an area of sediment bypass during breakup and reworking of sediment during the summer and early fall months.
- 3) "Sub-ice channels" and associated subaqueous levees: meandering channels extending up to 20 km offshore from major distributaries, flanked by subaqueous levees which eventually become emergent to form offshore shoals and vegetated islands; Channels are areas of bedload transport during breakup and summer, thereby bypassing much of sub-ice platform; associated levees are areas of deposition from suspension; some flow of water may occur in sub-ice channels throughout the winter; channels are areas of active meandering.

The delta front is an area of rapid sediment deposition off the flank of the delta, however unlike most deltas, it is offset from the shoreline up to 30 km by the broad, sub-ice platform. This suggests that there is a significant amount of sediment bypassing the nearshore zone, as has been demonstrated along the north slope of Alaska (Reimnitz and Barnes, 1974; Walker, 1974). The delta front typically forms to depths of 10-20 meters, and is characterized by relatively steep slopes, rapid deposition, and high rates of ice gouging (as it marks the edge of the shorefast ice and the location of abundant shear zones).

The prodelta is an area of extremely flat slopes, extending for over km beyond the delta front. It is delineated by the presence of modern Yukon sands and silts (McManus and others, 1974), and is an area characterized by advective shelf transport of sediment (Nelson and Creager, 1977). It appears to coincide with sediment plumes and the Alaska coastal waters (Fig. 19). Much of the sediment may actually be reworked from more nearshore areas, having been resuspended either by storms or ice gouging. Clays are relatively uncommon, in part because of the relative paucity of clays being provided from the source areas (Hill and Tedrow, 1961) and in part because of their bypassing the prodelta to be deposited north of the Bering Straits in the Chukchi Sea (Nelson and Creager, 1977).

	DEPOSITIONAL ENVIRONMENT	FLOODING	ICE SCOUR	SEDIMENTATION	EROSION	PERMAFROST
	Pleistocene terrace deposits	Moderate	Low	Low	Low	High
	Abandoned River Courses	Mod-High	Low	Moderate	Moderate	Mod-High
	Pleistocene Eolian Deposits	Low	Low	Moderate	High	Moderate
Delta Plain	Active distributary	High	Moderate	High	High	None
	Abandoned distributary	Moderate	Low	Moderate	High	Low-Mod
	Interdistributary marsh	Moderate	Low	Low-Mod	Low	Low-Mod
	Coastal marsh	High	Moderate	High	Low-Mod	Low
	Vegetated distributary bar	High	Moderate	High	Low-Mod	Low
	Intertidal mudflats	High	Mod-High	High	Low	Low
Delta Margin	Sub-ice platform	N/A	Mod-Low	Low	Low?	None
	Sub-ice channels	N/A	Low	High	Moderate	None
	Delta Front	N/A	High	High	Low?	None
	Prodelta	N/A	Mod-Low	Moderate	Low	None
	Sandy beaches	High	Moderate	Mod-High	Variable	None

Table 2

Summary of non-tectonic geologic hazards associated with specific depositional environments in the Yukon-Kuskokwim delta complex.

Black River Chenier Plain: A significant amount of Yukon sediment is transported to the south by river-induced currents to be deposited in an extensive chenier plain in the vicinity of the Black River. The chenier plain began to prograde approximately 2500 years ago (based on radiocarbon dates of old shoreline deposits), and probably marks the shift of the Yukon River to its present day position and the development of the modern Yukon delta.

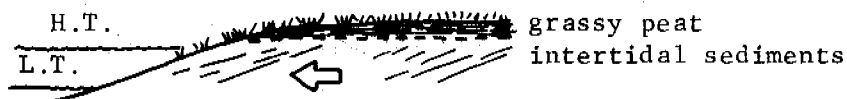
Most of the chenier plain is presently an area of rapid progradation, characterized by broad tidal flats. The dominant processes revolve around the rapid rates of sedimentation and the effect of ice gouging during breakup. Some of the shoreline is eroding, however, particularly where it is farthest removed from the Yukon sediment. In addition, the active chenier plain is marked with numerous erosional shorelines, most of which occurred in response to major storms. Thus any evaluation of the chenier plain (or the modern delta) must take into account the probable effects of such storms.

There are at least three concurrent processes affecting coastal areas during storms (Fig. 11). These include (1) erosion of the shoreline; (2) deposition of a storm berm or washover apron; and (3) flooding due to storm surge. Unfortunately, the inland effects of each process are difficult to predict.

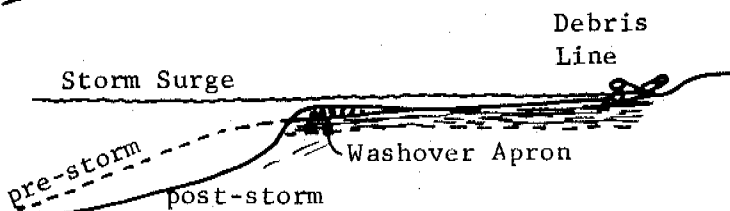
The amounts of erosion are strongly dependent on the type of material being eroded, as well as the storm characteristics. Nonetheless, based on measured rates of erosion from 1954-1975 (from photos) and 1976-1977

DEVELOPMENT OF THE BLACK RIVER CHENIER PLAIN

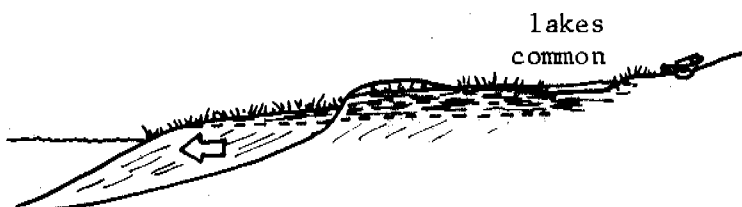
A. PROGRADATION



B. STORM EVENT



C. PROGRADATION



ONSHORE IMPACTS OF A MAJOR STORM

FLOODING* (HIGHLY VARIABLE 10 KM.)

DEPOSITION (10 - 100 M.)

EROSION** (1 - 100 M.)



* Highly dependant on storm characteristics and inland topography

** Highly dependant on the type of material being eroded
(does not include offshore erosion, which may be extensive)

Figure 11

(from beach profiles), low, tundra bluffs will probably erode 10-100 meters, whereas cliffed bedrock will probably erode a meter or less. The amount of deposition (and flooding) will depend both on onshore topography (e.g., low grassflats vs. high cliffs), and the height of the storm surge, which is likely to vary considerably. The width of the washover apron can be determined in the field, in part because of its distinct vegetation assemblage. In low areas, the zone of deposition will probably extend 10-100 meters beyond the point of maximum erosion.

The zone of flooding is most extensive, and will extend at least 15 kilometers inland along parts of the coast. The maximum inland extent of historic flooding is locally marked by debris lines some of which can be easily identified.

Thus, it is necessary to consider geologic hazards in the context of both storm and non-storm periods. The recurrence interval of such storms is somewhat uncertain, however, at least 16 shorelines formed between 1450 and 1850 B.P. suggesting a recurrence interval of approximately 25 years. This figure, based on long-term geologic data, seems consistent with short-term historical data on major storms in the Norton Sound region.

Sandy beaches, spits, and barrier islands: Sandy beaches are relatively uncommon along most of the delta region, however they are quite extensive in the vicinity of Hooper Bay, where coastal erosion of fluvial and eolian deposits provides a ready source of sand. These beaches may form along eroding Pleistocene headlands as well as on spits and nearby barrier islands. Sandy barrier islands also occur south of Nelson Island. The barrier islands tend to form along the mesotidal portion of the coastline,

typically along the outer edge of broad tidal flats. The islands grade laterally into offshore sand shoals along the northern margin of Kuskokwim Bay, where the tidal range approaches macrotidal (c.f. Hayes, 1975). Tidal inlets and associated tidal deltas separate both barrier islands and the sand shoals.

The barrier islands are essentially non-vegetated, hence are characterized by extremely rapid erosion (locally exceeding 60 meters/year). Some islands (e.g. the Sand Islands north of Cape Romanzof) have been drastically changed (Fig. 12C), presumably during storms. There are no dunes on the barrier islands (in contrast to nearby spits). Whether the dunes are absent because of excessive erosion, or the high rates of erosion are because of the lack of dunes remain unclear. In either case, the islands are rarely more than a meter above sea-level, hence are commonly flooded during major storms.

The spits attached to eroding Pleistocene headlands are somewhat more complex. They are typically fringed by coastal dunes, locally exceeding 15 meters in height. These dunes are frequently breached by northeast-trending washover channels formed during major storms. The back part of the spits are formed of broad, washover sand flats which grade into intertidal mudflats. Some spits (e.g. Panawat Spit), are eroding approximately 5 meters per year. Other spits appear to be prograding. Presumably the relatively low rates of erosion are in part because of the stabilizing effects of the dunes, hence their preservation should be a major consideration in any site evaluation in the area.

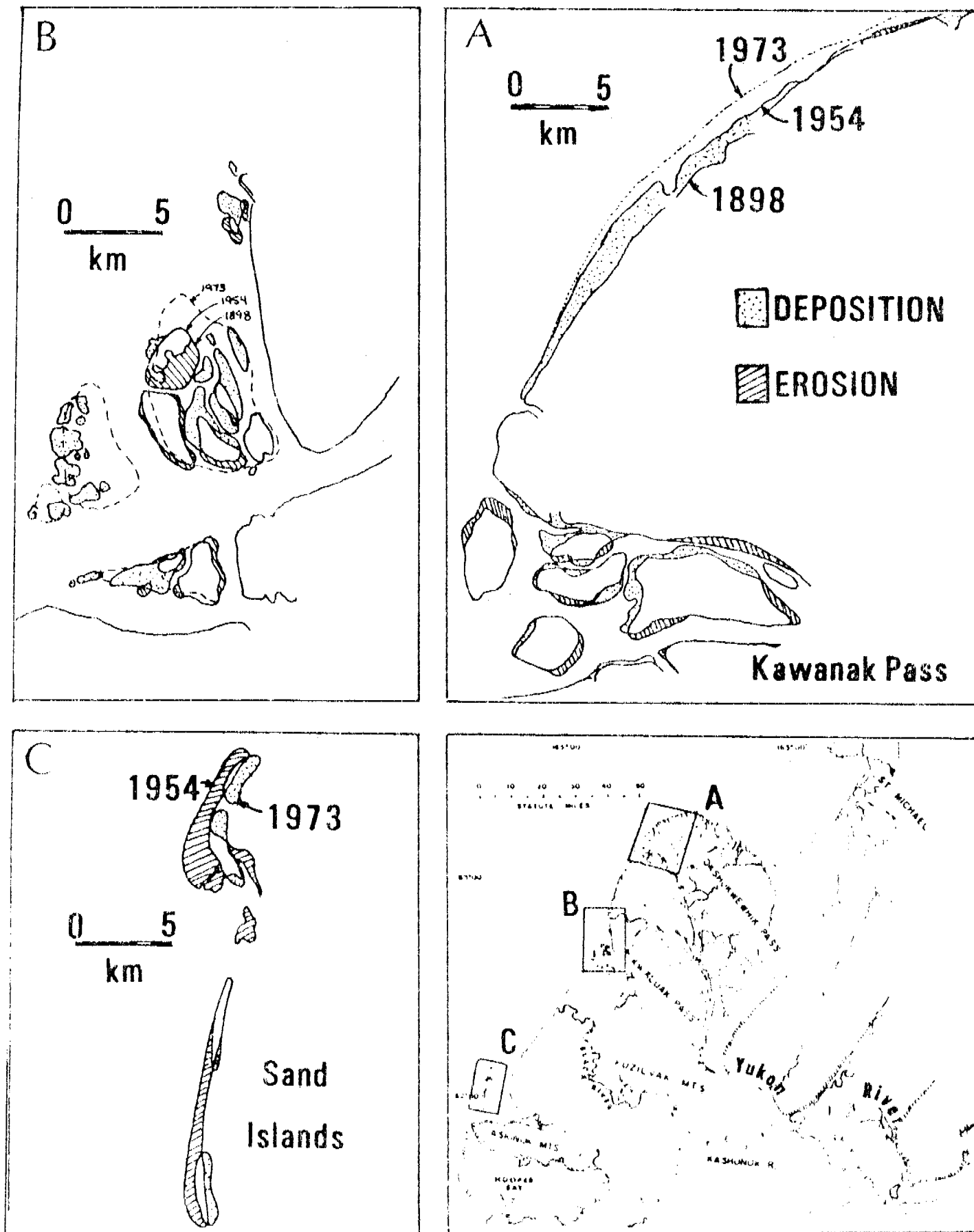


Figure 12. Selected examples of documented shoreline erosion (Dashed areas in A and B indicate net erosion, dotted areas, net deposition from 1898-1954).

Gravel Beaches and Rocky Headlands: Short segments of cliffed coastline form where Quaternary volcanoes or Mesozoic bedrock is exposed along the coast. Rocky headlands and small areas of gravel beaches rim parts of Nelson Island and the Askinuk Mountains. Gravel beaches are relatively continuous in the vicinity of Point Romanof (between the delta and St. Michaels), where wave action has produced a relatively straight, cliffed shoreline.

The gravel beaches are typically steep with multiple berms; beach cusps are common. The steep gravel beach typically grades rapidly offshore to a relatively flat, sandy or muddy substratum.

Low dunes may form where gravel beaches have prograded (e.g. Tanunuk on Nelson Island). Gravels overlie peat just northeast of Point Romanof, where the gravels have been transported via longshore drift during storms. The resultant gravel spits have prograded over adjacent mudflats and completely blocked small coastal streams.

The gravels are obviously areas of high wave energy, however they are not rapidly eroding hence may represent relatively stable coastal sites. They also represent one of the few gravel deposits in the area which might be used for construction purposes. If this is to be considered, more work needs to be done on studying the source of the gravels and their offshore extent.

Coastal Processes

It has long been recognized that coastal morphology is strongly dependent on the coastal processes dominant in the area. This is particularly evident in deltaic regions where river-dominated, wave-dominated, and tide-dominated deltas are defined in large part by the relative importance of shoreline processes (e.g., Fisher and others, 1969; Wright and Coleman, 1973; Galloway, 1975). A problem arises, however, when studying Arctic and sub-arctic coastlines in how to deal with the extreme seasonality of coastal processes, including those associated with ice. This point was strongly made by Barnes and Reimnitz (1974) in their study of ice and sedimentary processes on the north slope of Alaska.

The preceding section on depositional environments demonstrates the extent to which ice-related processes can modify nearshore morphology and sedimentary processes. Yet ice constitutes only part of the system, as river input and storms also play a major role. The relative importance of each process varies systematically throughout the year (Fig. 13), allowing the definition of an ice-dominated, a river-dominated, and a storm-dominated regimen. In as much as each regimen is characterized by its own set of processes and problems, they are best discussed separately.

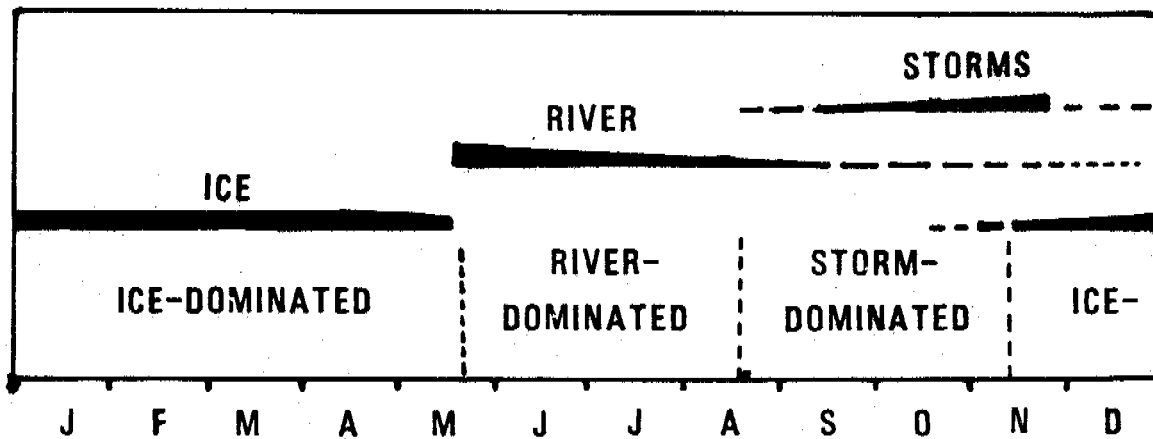


Figure 13: Conceptual model of coastal processes in the Yukon delta region. The width of the bars diagrammatically represents the relative importance of ice-, river-, and storm-related processes, allowing the recognition of three distinct regimens.

Ice-dominated Regimen: The coast of Norton Sound is dominated by the effects of ice for over half the year, yet most of what we know about this extremely important time is from the study of satellite imagery.

Freezeup marks the beginning of this regimen. It typically occurs between October and November. Bottom fast ice forms along the shallow margins of the delta (e.g., on intertidal mudflats and subaqueous levees). Some of the smaller sub-ice channels are soon covered with floating fast ice. The largest sub-ice channels continue to maintain channelized flow of fresh water offshore and are the last of the nearshore areas to freeze.

The shorefast ice continues to expand farther offshore, until it reaches its maximum extent approximately 15-30 kilometers offshore. Most of the shorefast ice is floating fast ice, separated from the bottom fast ice

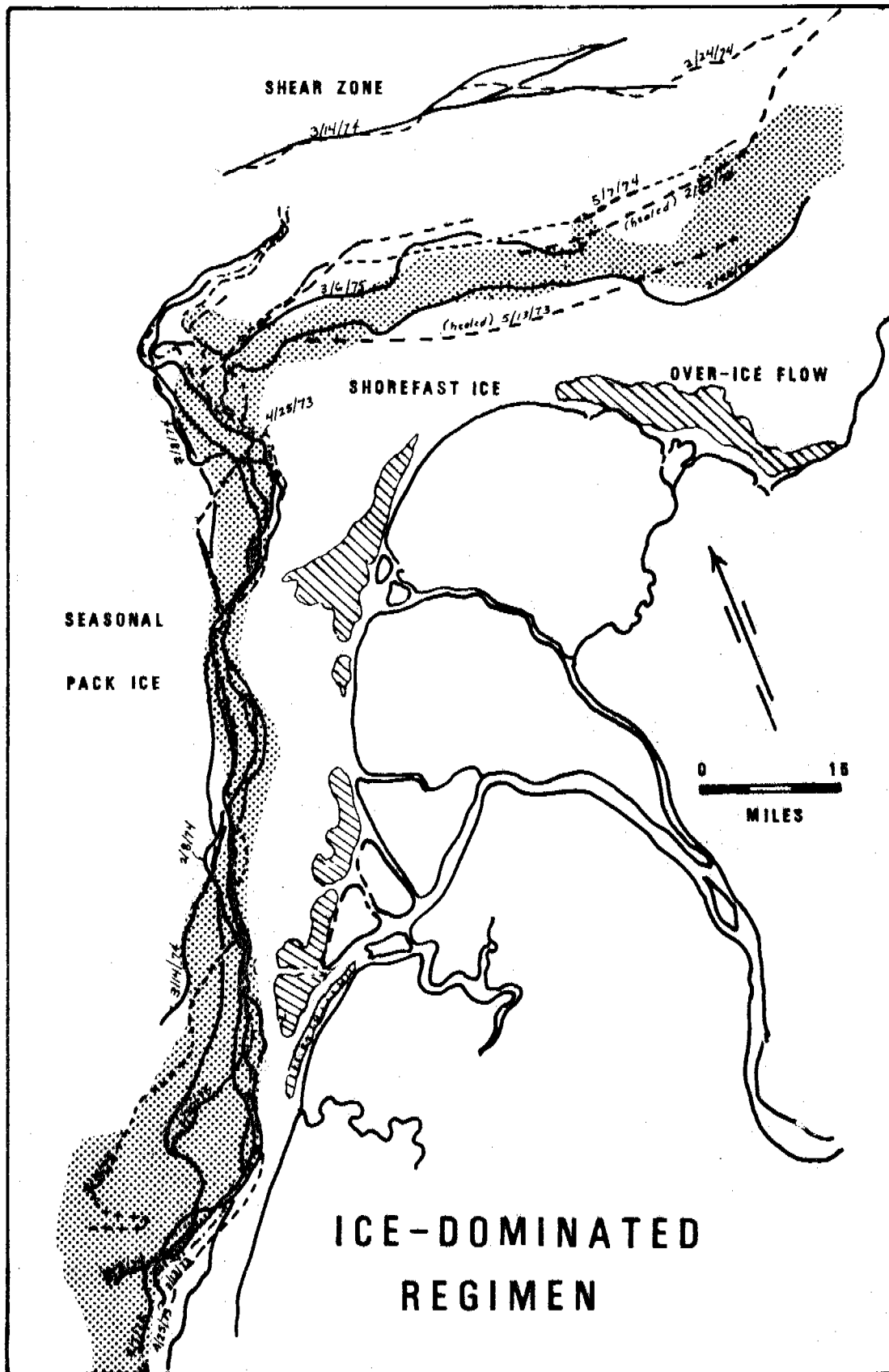


Figure 14. Location of shear zones as determined from LANDSAT imagery, 3/13/73 to 3/6/75. Hatched areas delineate aufeis. Dotted area delineates the 5 to 10 meter bathymetric interval.

by tidal cracks. Much of the bottom fast ice is covered with water repeatedly during the winter. This over-ice flow is probably related to the lifting of the floating fast ice by astronomical or storm tides. This suggests that the area of the sub-ice platform below the floating fast ice may be an area of significant tidal currents, and that the pumping action of the ice may be a significant process in resuspending sediment on the outer sub-ice platform (c.f. Barnes and Reimnitz, 1974).

The seaward edge of the shorefast ice is typically marked by a Stamukhi zone (i.e., a series of accreted pressure ridges and inactive shear zones; Reimnitz and others, 1977). The shear zones mark the zone of deformation between the relatively passive shorefast ice and the highly mobile seasonal pack ice. The location of the shear zones on the west side of the delta coincide extremely well with the 5-10 meter depth interval; their location to the north of the delta is more varied (Fig. 14).

An understanding of the factors controlling the geometry of the Stamukhi zones is extremely important, as they both define the sea-ward extent of the shorefast ice and mark the areas of most intensive ice gouging. The pattern of ice movement and deformation is controlled by the offshore bathymetry and the wind and current patterns. Ice movement is particularly sensitive to wind patterns, hence an understanding of atmospheric conditions is also extremely important. In addition, patterns of ice movement on the western side of the Yukon delta are also strongly affected by ice-deformation events north of the Bering Straits (as described by Shapiro and Burns, 1975).

Most of the ice in Norton Sound appears to be in situ; very little pack ice enters the Sound from the west because of shoals which appear to divert much of the ice to the south. Thus presumably the pack ice on the north

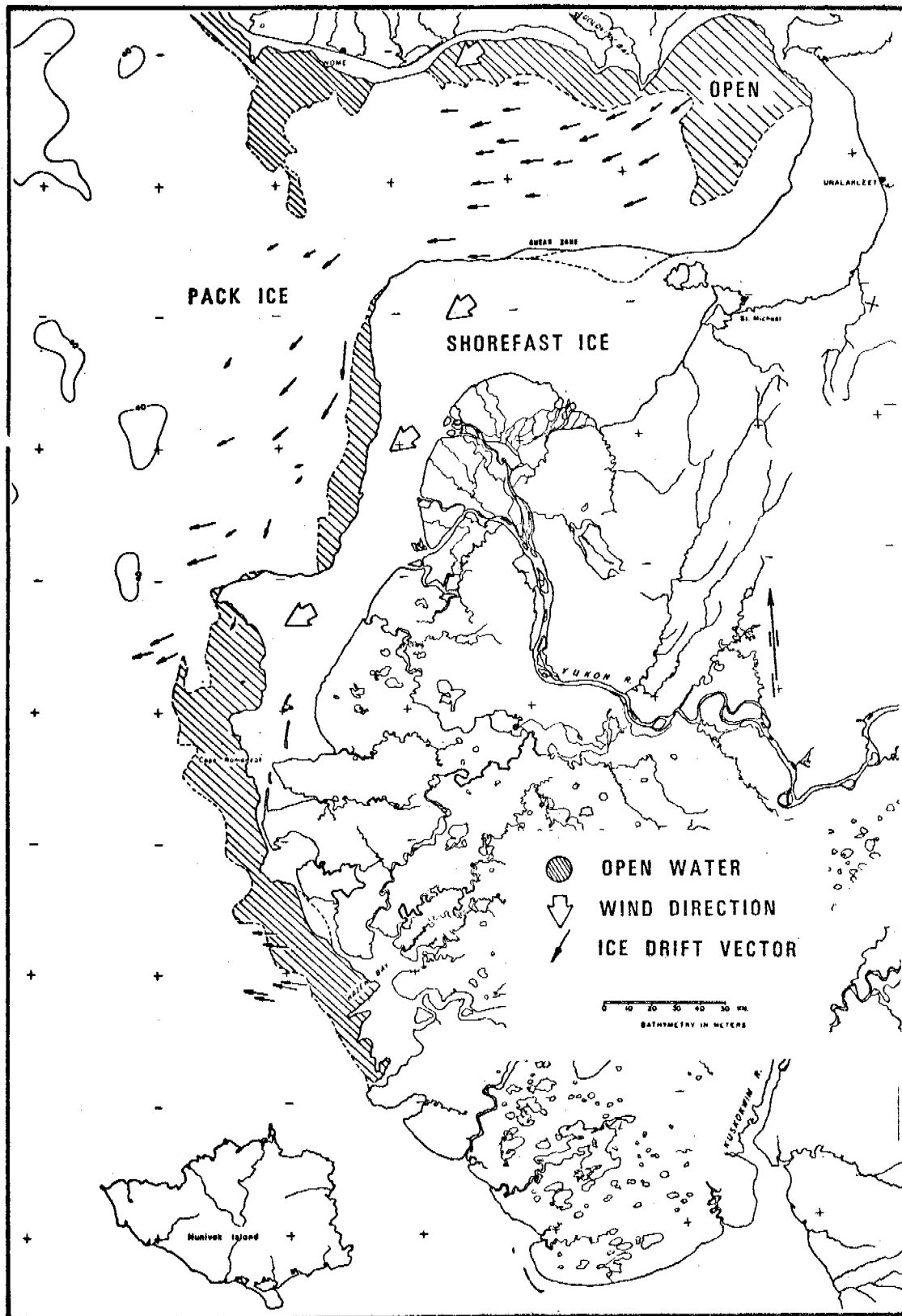


Figure 15. Patterns of ice movement from March 14-15, 1974. Length of ice drift vectors measures distance moved in one day. Dashed lines to north of delta are inactive shear zones.

side of the delta is relatively thin when compared to that west of the delta, much of which is derived from north of the Bering Straits. Nonetheless, the prevailing northeasterly winds cause the northern edge of the Yukon delta to be an area of ice convergence characterized by some of the most intensive ice gouging in Norton Sound (Nelson and others, 1978).

Figure 15 illustrates a relatively typical winter pattern of ice movement and deformation in response to northeasterly winds. Note that whereas the northern edge of the shorefast ice is marked by ice convergence and active deformation, the western side is marked by ice divergence and ice formation.

Figures 16 and 17 illustrate quite different patterns of ice movement and deformation in response to different meteorological conditions. Figure 16 illustrates ice movement from April 25-27, 1973, under the influence of strong northwesterly winds. The western side of the delta under these conditions is becoming an area of ice convergence, although there is some deflection of ice, presumably due to bathymetric ridges. The pack ice to the west of the delta is largely derived from north of the Bering Straits, and is moving relatively rapidly to the south. In contrast, the ice in Norton Sound is largely in situ and is moving rather slowly. There is even some slight evidence of a counterclockwise gyre, suggesting that some of the ice movement may be in response to water circulation patterns.

Figure 17 records the patterns of ice movement from March 13-15, 1976. The wind patterns are somewhat more complex, especially on the northern margin of the delta where easterly winds appear to be driving the pack

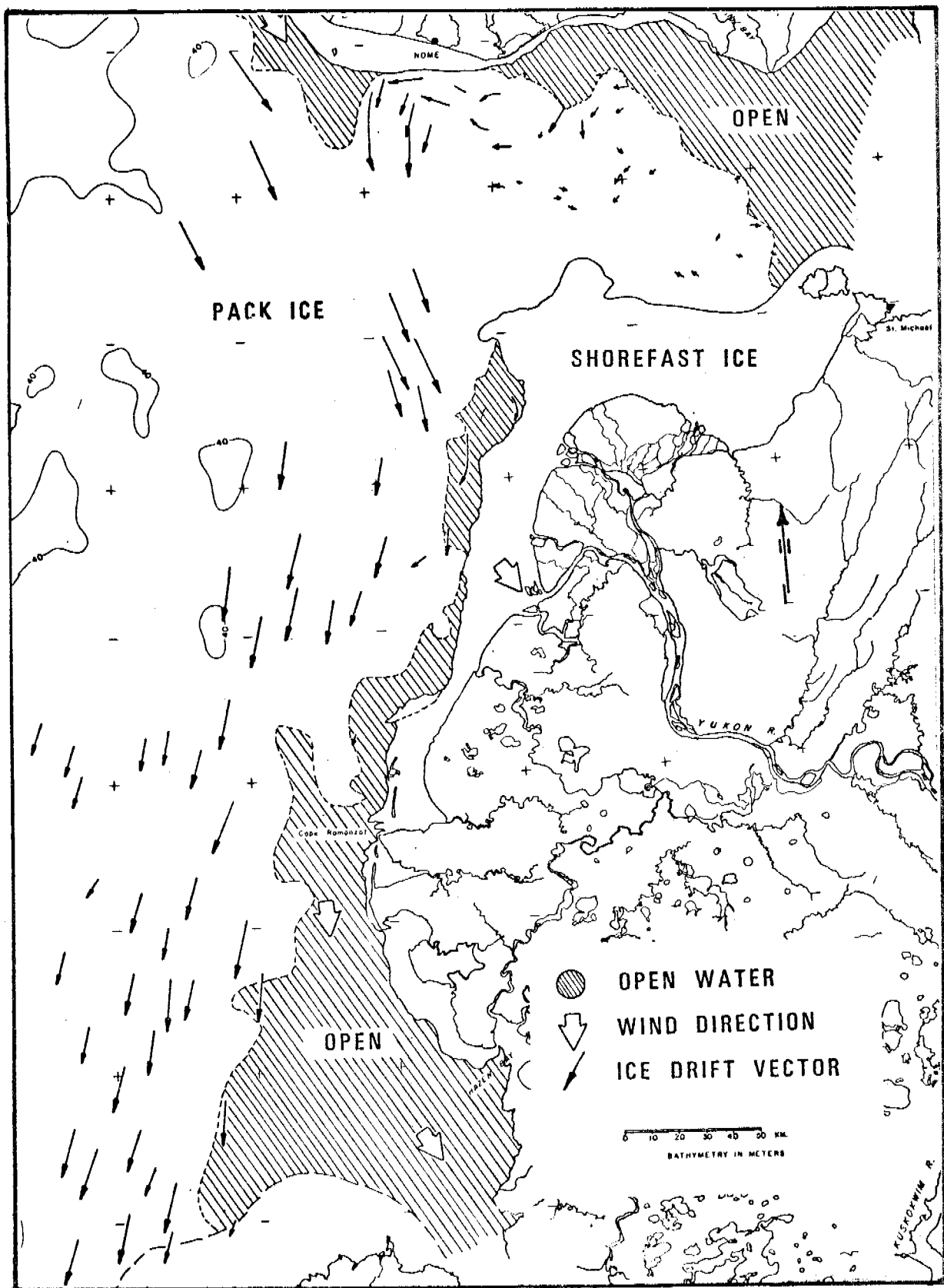


Figure 16: Patterns of ice movement from April 25-27, 1973. Length of ice drift vectors measures distance moved in one day.

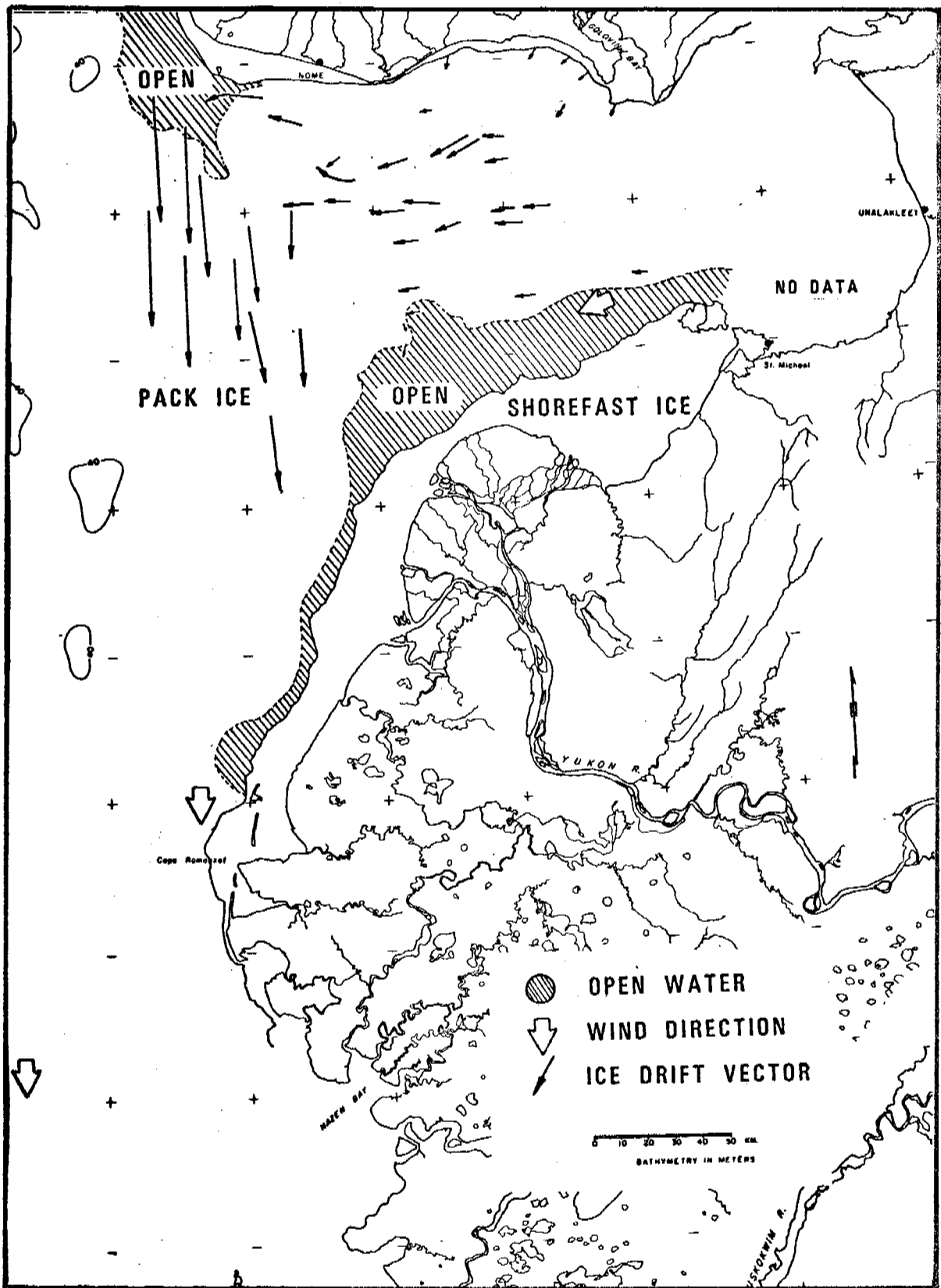


Figure 17: Patterns of ice movement from March 13-15, 1976. Length of ice drift vectors measure distance moved in one day. Maximum rates are approximately 45 km/day.

ice offshore due to the Coriolis effect. The ice to the west of the delta is moving extremely rapidly to the south, however, reflecting a major ice deformation event north of the Bering Straits (c.f. Shapiro and Burns, 1975). Some of the pack ice flows were moving in excess of 45 kilometers/day!

Figures 16 and 17 also illustrate the marked difference between the behavior of pack ice in Norton Sound from that farther to the west. Not only is the origin of the ice different, but the pattern of movement differs as well. Thus the ice-related geologic hazards in the two areas differ significantly. In addition, the patterns of ice-deformation north and west of the delta differ, further complicating an assessment of potential environmental hazards.

The seasonal pack ice begins to move out of the Bering Sea in late April and May due to a shift to southerly winds and a decrease in their intensity. The decreased wind velocities allow the north-flowing oceanic currents to begin transporting the pack ice to the north (Muench and Ahlnas, 1976). There are also short intervals of northward ice transport during the winter months, either due to decreased winds or increased southerly winds. There is very little sediment being transported into Norton Sound during the ice-dominated period. It may be a period of significant reworking of sediment, however, both by the pumping action of the floating fast ice and the gouging of the sediments by ice (c.f. Remnitz and Barnes, 1974). This resuspension of sediment may then allow the finer particles to be transported to the north via oceanic currents (Nelson and Creager, 1977).

Breakup: Breakup along the coast is a relatively brief event which marks the transition between the ice-dominated and river-dominated regimens, however its significance far outweighs its brevity.

River breakup along the Yukon (as with most of the coastal rivers in northern Alaska) occurs due to inland melting of river ice, hence it works its way downstream, preceeding the removal of the shorefast ice. It is marked by a tremendous increase in sediment and water discharge, resulting in ice james, extensive inland flooding and river bank erosion.

As river discharge begins to increase, floating fast ice begins to lift, both in the river and along the coast. The thalwag of the subice channels are especially well delineated by the floating fast ice at this time. The bottom fast ice begins to be flooded by an over-ice flow (Fig. 18) which has been described on the North Slope by Reimnitz and Bruder, 1972; Walker, 1974).

Some sediment is carried onto the ice, thereby effectively bypassing much of the inner sub-ice platform. Much of the sediment appears to remain in the sub-ice channels, which cross the sub-ice the platform. Some of the sediment is probably deposited from suspension on subaqueous levees farther offshore, however much of it probably bypasses the sub-ice platform completely, to be deposited on the delta front or prodelta. The role of sub-ice sediment transport during breakup is particularly intriguing, yet it remains almost unknown.

The floating ice that marks the sub-ice channels soon breaks up and is removed to sea. Much of the over-ice flow may drain through strudel holes (Reimnitz and Bruder, 1972) or causes the bottom fast ice to melt in place.

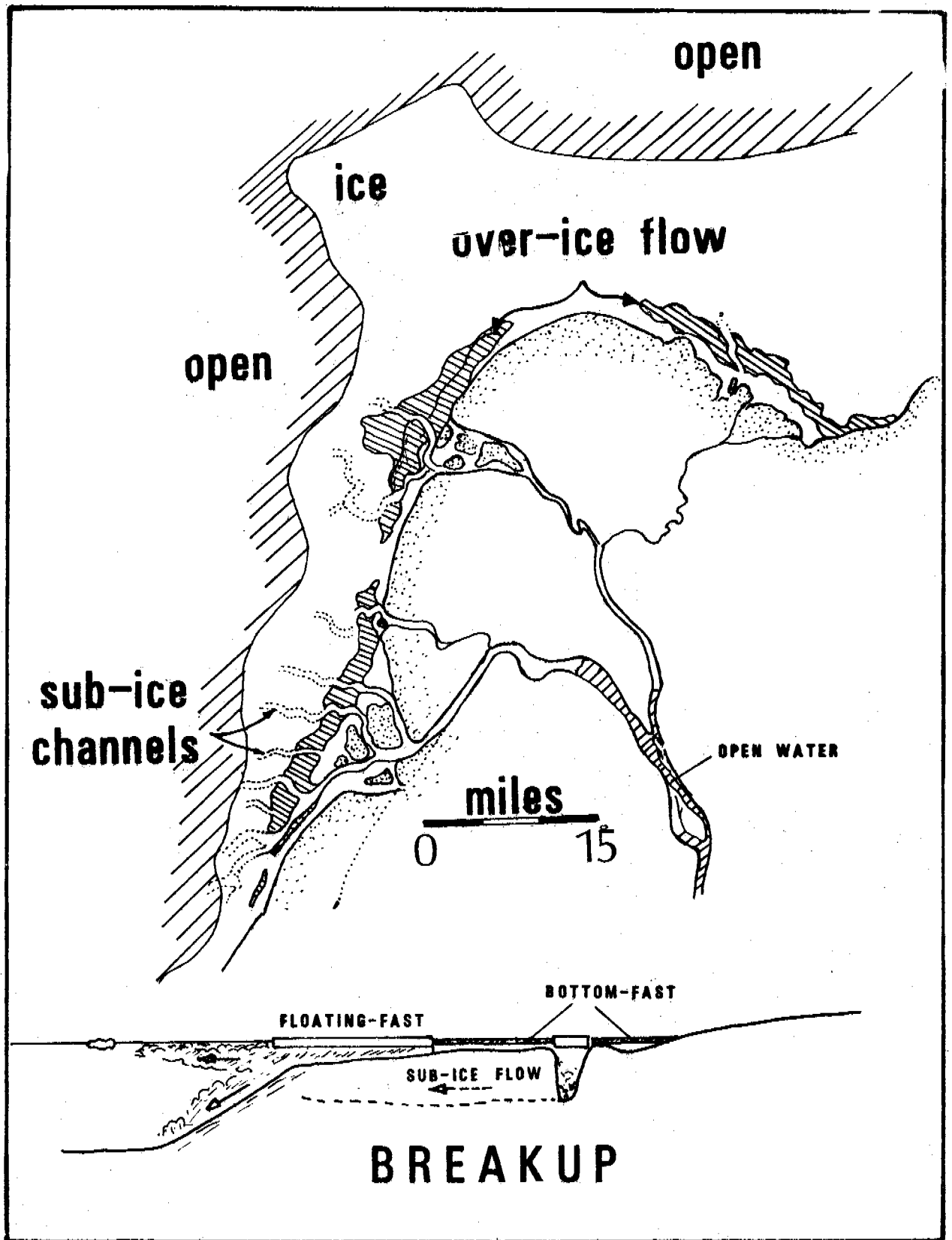


Figure 18

Large pieces of floating fast ice breakoff to be transported farther offshore. Grounded ice may remain in some shallow areas to the northwest of the delta; floating pack ice may remain trapped in the middle of Norton Sound because of the sluggish currents.

River-dominated Regimen: River breakup and the removal of the coastal ice marks the inception of the river-dominated regimen. Early summer is a period of high sediment input and relatively low wave regime, hence it is a period dominated by coastal deposition.

Some of the Yukon sediment is deposited in lakes on or near the delta, some is diverted through older, largely abandoned courses of the Yukon. Most, however, enters Norton Sound via one of the main distributaries of the Yukon delta. Much of this sediment is deposited in rapidly accreting intertidal mudflats, distributary mouth bars, and subaqueous levees. Some parts of the delta are prograding at rates of 40 meters/year (Fig. 12).

Not all of the sediment is deposited near the delta, however. Some of the sediment appears to remain confined to the offshore (sub-ice) channels, presumably as bedload. In addition, large sediment plumes extend for 50 kilometers or more offshore, indicating significant transport of suspended sediment to the northwest. The suspended sediment appears to be confined to the Alaska Coastal Waters (Fig. 19) where some of it may remain to ultimately bypass Norton Sound and be deposited in the Chukchi Sea (Nelson and Creager, 1977).

Storm-dominated Regimen: Late summer marks the continued decrease in sediment and water discharge from the Yukon, coincident with an increase in the frequency and severity of coastal storms. Extremely high southwesterly winds occur during these storms resulting in extensive coastal erosion and

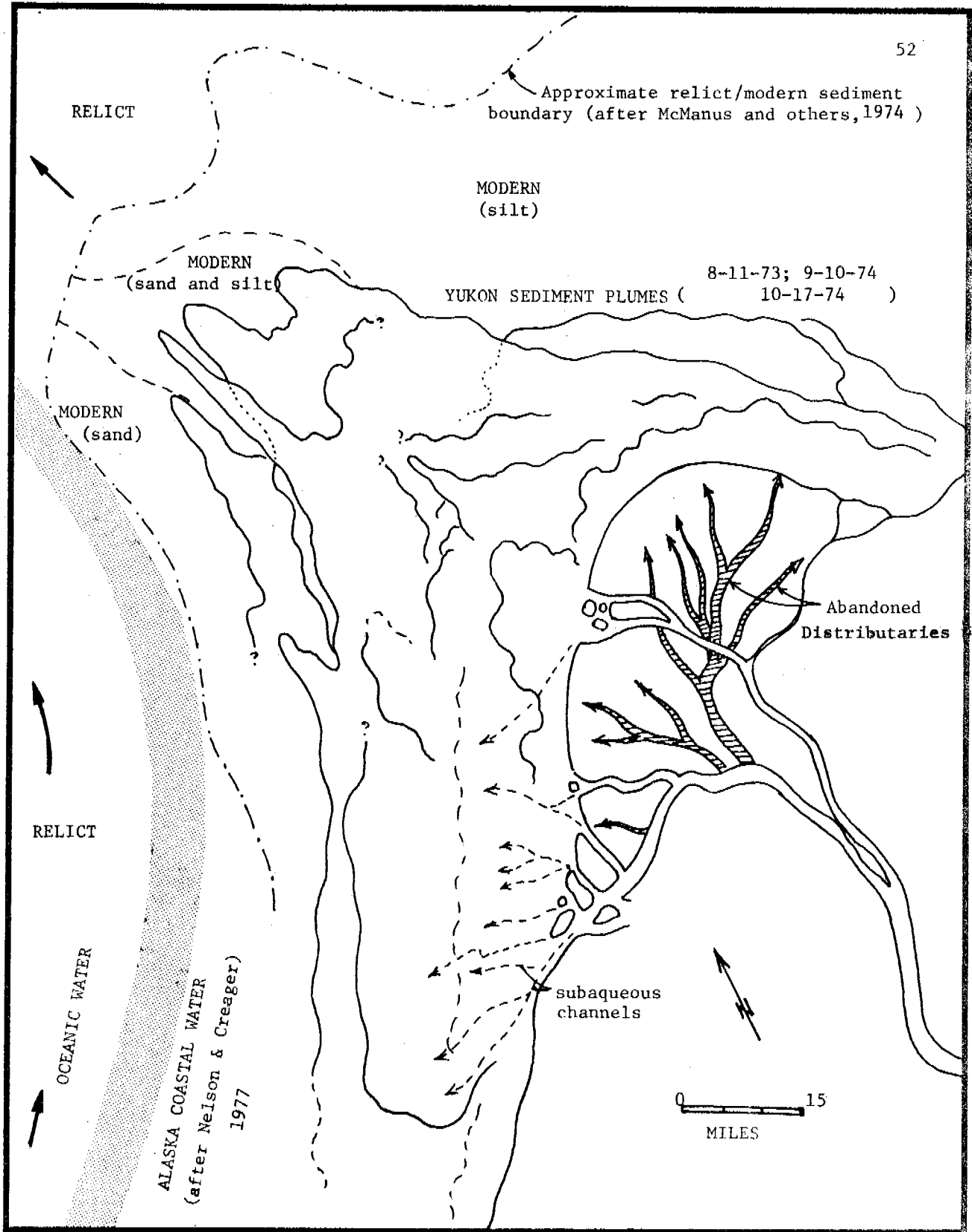


Figure 19. Comparison of offshore sediment plumes, modern and relict shelf sediments, and oceanic currents and water masses off the Yukon delta.

a general northward longshore drift of sediment. Extremely large storms may have a significant storm surge, further aggravating the problem of coastal erosion. Many of the geomorphic indicators of longshore drift (e.g., prograding gravel spits) are probably active only during storms.

With the exception of the modern Yukon delta and adjacent chenier plain, most of the shorelines in the region are erosional. Most of that erosion appears to occur during this storm-dominated period. In addition, even areas that are dominantly stable or prograding may be effected by major storms (Fig. 11).

The formation of shorefast ice tends to dampen the effects of the storms, marking the beginning of the ice-dominated regimen. Especially large storms, however, can lift large areas of newly formed shorefast ice and drive it onshore resulting in significant damage to coastal structures.

VIII. CONCLUSIONS

The Yukon-Kuskokwim delta region is characterized by widespread Quaternary tectonism. Northwest- and northeast-trending faults and structurally-controlled volcanic vents are mainly restricted to the onland extension of the Nunivak Arch. At least some of these faults appear to have had Holocene movement. Most of the volcanism has occurred within the last 700,000 years, however a 5.5 meter core from a volcanic lake in the region shows no evidence of local volcanism during the last 40,000-50,000 years. Thus, the potential for surface rupture and ground shaking must be considered in site evaluation, however, the risk from volcanism appears slight.

The delta region consists of a complex assemblage of Quaternary deposits of various origins and ages, ranging from Sangamonian (and older) marine terrace deposits to modern deltaic and estuarine deposits. Each is characterized by a variety of physical and hydrologic properties as well as geologic processes which must be considered when evaluating potential environmental impacts.

Permafrost occurs throughout most of the study area. It is most extensively developed in the pre-Holocene deposits where large ice wedges and massive ice are present; the depth of the permafrost in these deposits may locally exceed 200 meters. Widespread thermokarst marks an interval of melting of the permafrost, yet that melting appears to have ceased, at least in the northern parts of the delta region where modern ice wedges are presently forming. Permafrost appears to be present in some degree in most areas except along large rivers, deep lakes, and rapidly prograding coastlines, thereby complicating the selection of potential transportation corridors.

The largest floods along the Yukon River (locally exceeding 1,000,000 cfs) occur during river breakup, however large floods also occur associated with late summer and early fall storms. Extremely large floods may actually divert the entire course of the lower Yukon river, as has already happened at least four times in the last 5,000 years. The most recent of these shifts occurred sometime between 2500 and 1200 years ago, resulting in the formation of the modern Yukon delta.

The coastline is highly variable with respect to its morphology, processes, and overall coastal stability. Of particular importance in determining the relative coastal stability is the proximity of the Yukon River sediment input, the sheltering effects of barrier islands, laterally migrating tidal inlets, and local tectonic patterns. In spite of its heterogeneity, however, the dominant direction of longshore drift is toward the north, coincident with the oceanic and wave-generated currents.

Any study of coastal processes in the Norton Sound/Yukon delta region must take into account the extreme seasonality of coastal processes. In general, the year consists of three seasons: an ice-dominated regime from approximately November to May, a river-dominated regime from May to late summer, and a storm-dominated regime from late summer to freezeup in the fall.

The ice-dominated regimen lasts from freezeup in the fall to breakup in the spring. During that time, shorefast ice extends to approximately the 5-10 meter water depth, where it is terminated by a series of pressure ridges and shear zones formed by the interaction of shorefast and seasonal pack ice. This is a zone of intense ice gouging as well. The pattern

of ice movement in Norton Sound is quite distinct from that farther to the west.

Breakup marks the end of the ice-dominated processes and the beginning of the river-dominated regimen. During breakup, much of the river water (and sediment) bypasses the nearshore zone by a combination of over-ice flow (c.f. Colville delta) and flow through sub-ice channels which extend from the mouths of major distributaries up to 15 km offshore. These offshore channels continue to be areas of active bedload transport during the summer. In contrast, most of the suspended sediment appears to be transported to the northwest in plumes restricted to the Alaska Coastal Waters.

The storm-dominated regimen begins in late summer, as decreasing river discharge and increasing storm frequency and severity combine to cause significant erosion along much of the coast. Some areas are eroding at rates in excess of 60 meters/year, most of which probably occurs during storms.

In summary, the Yukon delta is strongly influenced by the effects of ice in the ground, on the river, and offshore. Several of the major depositional environments of the Yukon delta appear to be restricted to ice-dominated coastlines. Similarly, the seasonality of coastal processes is dominated by the effects of ice throughout much of the year, thus a careful study of this region may provide insights into sedimentary processes and geologic hazards in other ice-dominated coastal zones as well.

IX. NEEDS FOR FUTURE STUDY

1) In situ monitoring of fluvial and coastal processes should be planned to characterize the ice-dominated, river-dominated, and storm-dominated regimens. This sampling program should be done to compliment other work being done farther offshore. Hydrologic and STD data should be collected, and be coincident with LANDSAT overpasses when possible.

2) In situ studies of ice dynamics deserves special attention. This should be done in combination with the study of LANDSAT and NOAA(VHRR) imagery, as well as synoptic weather data. The data on ice movement and deformation should then be combined with on-going studies of ice gouging and shelf sediments.

3) Coastal stations should be reoccupied on a regular basis, in order to assess the effects of major storms.

4) A wave-climate model should be made of the Norton Sound region. It should be capable of taking into account the extreme frictional attenuation that occurs on the sub-ice platform off the Yukon delta. This will also necessitate the collection of more up-to-date bathymetric data.

5) Color IR photography should be obtained for the delta region, as it will aid in refining existing geologic mapping and extrapolating biologic habitats.

X. SUMMARY OF FOURTH QUARTER OPERATIONS

No field work or sample collection was done, however I did attend a Principle Investigators Meeting, January 31-February 3, in Menlo Park, California, where I presented a summary of my work to date.

More samples have been sent for radiocarbon dating of the older courses of the Yukon. The textural analyses and interpretations of the sediment samples are still in progress. All of the coastal beach profiles have been placed on magnetic tape, and will be submitted when the textural data have been formatted. Most of the laboratory work has concentrated on studying patterns of ice movement and deformation using LANDSAT and NOAA (VHRR) satellite imagery and synoptic weather data.

BIBLIOGRAPHY

- Beikman, H.M., 1974, Preliminary geologic map of the southwest quadrant of Alaska; USGS open file map (2 sheets).
- Carey, S.W., 1958, A tectonic approach to continental drift, in Continental Drift, a symposium, University of Tasmania, pp.177-355.
- Creager, T.S. and McManus, D.A., 1967, Geology of the floor of Bering and Chukchi Seas - American studies; in Hopkins, D.M. (ed.) The Bering Land Bridge, Stanford Univ. Press, Stanford, Calif., pp. 32-46.
- Fisher, W.L., and others, 1969, Delta systems in the exploration for oil and gas: a research colloquium, Bureau of Economic Geology, Univ. of Texas, Austin.
- Galloway, W.E., 1975, Process framework for describing the morphologic and stratigraphic evolution of deltaic depositional systems: in Broussard, M.L. (ed.) Deltas: Models for Exploration; Houston Geol. Soc., pp. 87-98.
- Grim, M.S. and McManus, D.A., 1970, A shallow-water seismic-profiling survey of the northern Bering Sea; Marine Geology, vol. 8, pp. 293-320.
- Hamilton, T.D. and Porter, S.C., 1975, Itkillik glaciation in the Brooks Range, Northern Alaska; Quaternary Research, vol. 5, pp. 471-497.
- Hayes, M.O., 1975, Morphology of sand accumulation in estuaries: in Cronin, L.E. (ed.) Estuarine Research, vol. II, Geology and Engineering, Academic Press, New York, pp. 3-22.
- Hill, D.E., and Tedrow, J.C.F., 1961, Weathering and soil formation in the Arctic environment: Amer. Jour. Sci., vol. 259, pp. 84-101.
- Hoare, J.M., 1961, Geology and tectonic setting of lower Kuskokwim-Bristol Bay region, Alaska; Am. Assoc. Petroleum Geologists Bull., vol. 45, pp. 594-611.
- Hoare, J.M. and Condon, W.H., 1966, Geologic map of the Kwiguk and Black Quadrangles, western Alaska; USGS Misc. Geol. Invest. Map I-469.
- Hoare, J.M. and Condon, W.H., 1968, Geologic map of the Hooper Bay Quadrangle, Alaska; USGS Misc. Geol. Invest. Map. I-523.
- Hoare, J.M., and Condon, W.H., 1971(a), Geologic map of the St. Michael Quadrangle, Alaska; U.S.G.S. Misc. Geol. Invest. Map I-682.

- Hoare, J.M., and Condon, W.H., 1971(b), Geologic map of the Marshall Quadrangle, western Alaska; USGS Misc. Geol. Invest. Map I-668.
- Hoare, J.M., and Coorad, W.L., 1959, Geology of the Bethel Quadrangle, Alaska; USGS Misc. Geol. Invest. Map I-285.
- Hoare, J.M., and Coonrad, W.L., 1959, Geology of the Russian Mission Quadrangle, Alaska; USGS Misc. Geol. Invest. Map I-292.
- Knebel, H.J., and Creager, J.S., 1973, Yukon River: evidence for extensive migration during the Holocene Transgression; *Science*, vol. 79, pp. 1230-1231.
- Lisitzin, A.P., 1972, Sedimentation in the world ocean; *Soc. Economic Paleontologists and Mineralogists Spec. Pub. No. 17*, 218 p.
- MacKay, J.R., 1971, The origin of massive icy beds in permafrost, western Arctic coast, Canada; *Canadian Jour. Earth Sci.*, vol. 8, no. 4, pp. 397-422.
- Marlow, M.S. and others, 1976, Structure and evolution of Bering Sea shelf south of St. Lawrence Island; *Amer. Assoc. Pet. Geologist*, vol. 60, pp. 161-183.
- Matthews, M.D., 1973, Flocculation as exemplified in the turbidity maximum of Acharon Channel, Yukon River delta, Alaska; Unpublished Ph.D., dissertation, Northwestern Univ., 88 p.
- McManus, D.A., Venkatarathnam, K., Hopkins, D.M., and Nelson, C.H., 1974, Yukon River sediment on the northernmost Bering Sea shelf; *Journal of Sed. Petrology*, vol. 44, pp. 1052-1060.
- McManus, D.A., and others, 1977, Distribution of bottom sediments on the continental shelf, northern Bering Sea; *U.S. Geol. Survey Prof. Paper*, 759-C, 31 p.
- Moore, D.G., 1964, Acoustic reflection reconnaissance of continental shelves: eastern Bering and Chukchi Seas; *in* Moore, R.L. (ed.) *Papers in marine geology*, MacMillan Co., N.Y., pp. 319-362.
- Muench, R.D. and Ahlnas, K., 1976, Ice movement and distribution in the Bering Sea from March to June, 1974; *Jour. Geophys. Research*, vol. 81, no. 24, pp. 4467-4476.
- Nelson, C.H., 1978, Faulting, sediment instability, erosion, and depositional hazards of the Norton Basin sea floor, *in* *Annual Reports of Principal investigators for year ending March 1978*, NOAA-OCSEAP.

- Nelson, C.H., and Creager, J.S., 1977, Displacement of Yukon-derived sediment from Bering Sea to Chukchi Sea during Holocene time: *Geology*, vol. 5, pp. 141-146.
- Nelson, C.H., Hopkins, D.M., and Scholl, D.W., 1974, Cenozoic sedimentary and tectonic history of the Bering Sea; in Hood, D.W., and Kelley, E.J. (ed.), *Oceanography of the Bering Sea*; *Inst. Marine Sci., Univ. of Alaska, Fairbanks*.
- Patton, W.W. Jr. and Hoare, J.M., 1968, The Kaltag fault, west-central Alaska, U.S. Geol. Survey PM Paper 600-D, pp. D147-D153.
- Patton, W.W. Jr., 1973, Reconnaissance geology of the northern Yukon-Koyukuk Province, Alaska; U.S. Geol. Survey Prof. Paper 774-A, 17 p.
- Péwé, T.L., 1948, Terrain and permafrost of the Galena Air Base, Galena, Alaska; U.S. Geol. Survey Permafrost Program Program Rept. 7, 52 p.
- Péwé, T.L., 1975, Quaternary geology of Alaska: U.S. Geol. Survey Prof. Paper 835, 145 p.
- Reed, J.C., and Sater, (ed.), 1974, The coast and shelf of the Beaufort Sea; *Arctic Institute of North America*, 750 p.
- Reimnitz, E., and Barnes, P., 1974, Sea ice as a geologic agent on the Beaufort Sea; in Reed and Sater (ed.), *The coast and shelf of the Beaufort Sea*; *Arctic Institute of North America*.
- Reimnitz, E., and Bruder, K.F., 1972, River discharge into an ice-covered ocean and related sediment dispersal, Beaufort Sea, coast of Alaska; *Geol. Soc. Amer. Bull.*, vol. 83, pp. 861-866.
- Reimnitz, E., Toimil, L.J., and Barnes, P.W., 1977, Stamukhi zone processes: implications for developing the Arctic coast: in *Proceedings of the Offshore Technology Conference, May 2-5, 1977, OTC 2945*, pp. 513-518.
- Scholl, D.W., Buffington, E.C., and Hopkins, D.M., 1968, Geologic history of the continental margin of North America in the Bering Sea; *Marine Geology*, vol. 6, pp. 297-330.
- Scholl, D.W., and Hopkins, D.M., 1969, Newly discovered Cenozoic basins, Bering Sea shelf, Alaska; *Amer. Assoc. Pet. Geol. Bull.*, vol. 53, pp. 2067-2078.
- Shapiro, L.H., and Burns, J.J., 1975, Satellite observations of sea ice movement in the Bering Strait Regions, in Weller, and Bowling, S.A. (ed.), *Climate of the Arctic*; *Geophysical Institute, Univ. of Alaska, Fairbanks*, pp. 379-386.

- Shepard, F.P., and Wankss, H.R., 1971, Our changing coastlines: McGraw Hill, New York, 579 p.
- Smith, M.W., 1976, Permafrost in the Mackenzie delta, Northwest Territories: Geological Survey of Canada, Paper 75-28, 34 p.
- Walker, H.J., 1973, The nature of the seawater-freshwater interface during breakup in the Colville River delta, Alaska: in Permafrost: the North American contribution to the Second International Conference; Nat'l Acad. Sci., pp. 473-476.
- Williams, J.R., 1970, Groundwater in the permafrost regions of Alaska: U.S. Geol. Survey Prof. Paper 696, 83 p.
- Wright, L.D., and Coleman, J.M., 1973, Variations in morphology of major river deltas as functions of ocean wave and river discharge regimes: Am. Assoc. Petroleum Geologists Bull., v. 57, pp. 370-398.

ANNUAL REPORT

Title: Earthquake Activity and Ground Shaking
in and along the Eastern Gulf of Alaska

Report by: Christopher Stephens, Kent A. Fogleman, and John C. Lahr

Principal Investigators: John C. Lahr and Robert A. Page

Office of Earthquake Studies

U.S. Geological Survey

Menlo Park, California 94025

Research Unit: 210

Reporting Period: April 1, 1977 through March 31, 1978

Number of Pages: 27

18 April, 1978

CONTENTS

- I. Summary of objectives, conclusions and implications with respect to OCS oil and gas development.
- II. Introduction.
- III. Current state of knowledge.
- IV. Study area.
- V. Data collected.
- VI. Results.
- VII. and VIII. Discussions and conclusions.
- IX. Needs for further study.
- X. Summary of 4th quarter operations.
- XI. References.

ILLUSTRATIONS

- Figure 1. Plate tectonic relationships in the northeast Pacific.
- Figure 2. Maps of the eastern Gulf of Alaska showing offshore faults and selected onshore faults, and earthquake epicenters from 1899-1975.
- Figure 3. Map of aftershock zones of earthquakes with magnitude greater than 7.3 which occurred in the eastern Gulf of Alaska since 1938.
- Figure 4. Map of earthquake epicenters located by the USGS seismic network in southeastern Alaska, September 1974 through September 1976.
- Figure 5. Map of seismic stations operated by the USGS in southeastern Alaska, 1976-1977.
- Figure 6. Map of strong-motion instruments operated by the USGS in the eastern Gulf of Alaska.
- Figure 7. Map of earthquake epicenters located by the USGS seismic network in southeastern Alaska, October-December, 1977.
- Figure 8. Map of relocated epicenters and composite first motion plots of selected earthquakes which occurred near Icy Bay between 1974-1976.

CONTENTS (continued)

Figure 9. Map of proposed sites for OBS deployment.

Appendix

Appendix I. Catalog of earthquakes located by the USGS seismic network in the eastern Gulf of Alaska from October-December, 1977.

I. Summary of objectives, conclusions and implications with respect to OCS oil and gas development.

The objective of this research is to evaluate the hazards associated with earthquake activity in the eastern Gulf of Alaska and adjacent onshore areas. These hazards may pose a threat to the safety of petroleum development.

Over the past three years, the distribution of seismic activity in the eastern gulf region has been diffuse (Figure 4). Areas of continued high rates of seismic activity have been identified northeast of Icy Bay and northeast of Kayak Island. There does not appear to be any clear association of the seismic activity with mapped faults, although a more detailed study of the seismicity near Icy Bay has revealed an east-west trend in the earthquake epicenters that is parallel to nearby mapped faults. The current seismicity does not necessarily reflect the locations of large historical earthquakes. Large temporal variations in the rate of seismic activity have also been observed.

Continued seismic monitoring will no doubt reveal other areas of activity and delineate other active geologic structures. While the locally recorded earthquake data obtained since September, 1974 provides evidence of active faulting in the Icy Bay region, the general absence of earthquakes elsewhere in the eastern Gulf of Alaska cannot indicate in itself the absence of faults capable of generating potentially damaging earthquakes. For some mapped surface faults, however, sufficient geological and geophysical information may be available or attainable to conclude that the fault is inactive because of the lack of fault movement over a suitably long interval of time.

Three $M > 8$ earthquakes which occurred at the turn of the last century resulted in uplift of up to 14 meters between Cape Yakutaga and Yakutat Bay (Thatcher and Plafker, 1977). Another onshore earthquake such as one of these or a great earthquake associated with low-angle oblique underthrusting of the sea floor beneath the continental shelf (Page, 1975) would be accompanied by strong ground shaking throughout much of the eastern Gulf of Alaska, possibly from Cross Sound to Kayak Island, and could trigger tsunamis, seiches, and submarine slumping, any of which could be hazardous to offshore and coastal structures (Meyers, 1976).

II. Introduction

A. General nature and scope of study.

The purpose of this research is to investigate potential earthquake hazards in the eastern Gulf of Alaska and adjacent onshore areas. This will be accomplished by assessing the historical seismic record as well as by collecting new and more detailed information on both the distribution of current seismicity and the nature of strong ground motion resulting from large earthquakes.

B. Specific Objectives.

The major aim of this research is to develop an understanding of what geologic structures in the eastern Gulf of Alaska have generated or are capable of generating damaging earthquakes.

A second aim of the proposed research is to obtain recordings of strong ground motion close to the zone of energy release in a major earthquake. Currently no such records have ever been obtained within 40 km of a magnitude 8 earthquake. Without such information, there is a disturbing uncertainty in regard to the nature of the ground shaking that causes significant damage in major earthquakes.

C. Relevance to problem of petroleum development.

It is crucial that the potential seismic hazards in the eastern Gulf of Alaska be carefully analyzed and that the results be incorporated into the plans for future petroleum development. This information should be considered in the selection of tracts for lease sales, in choosing the localities for landbased operations, and in setting minimum design specifications for both coastal and offshore structures.

III. Current state of knowledge

The eastern Gulf of Alaska and the adjacent onshore areas are undergoing compressional deformation caused by north-northwestward migration of the Pacific plate with respect to the North American plate (Figure 1). Direct evidence for this convergent motion comes from studies of large earthquakes along portions of the Pacific-North American plate boundary adjacent to the eastern Gulf of Alaska.

The 1958 earthquake on the Fairweather fault in southeast Alaska was accompanied by right lateral slip of as much as 6.5 m (Tocher, 1960). The 1964 Alaska earthquake resulted from dip slip motion of about 12 m (Hastie and Savage, 1970) on a fault plane dipping northwestward beneath the continent from the Aleutian Trench and extending from eastern Prince William Sound to southern Kodiak Island. In the intervening region between these earthquakes, from approximately Yakutat Bay to Kayak Island, the precise manner in which this convergent motion is accommodated is not known. There are some indications that a broad region is involved, extending from the continental shelf inland to the Totschunda and Denali faults. Slip on these faults has been right lateral during Quaternary time as would be expected if the southern margin of Alaska were partially coupled to the Pacific plate (Richter and Matson, 1971). The eastern Gulf of Alaska is bounded to the north by the young Chugach and St. Elais mountain ranges (Figure 2, upper).

The historic record of instrumentally located earthquakes in the vicinity of the eastern Gulf is probably complete only for events larger than magnitude 7-3/4 since 1899, earthquakes larger than 6 since the early 1930's and larger than 5 since 1964. The events contained in the N.O.A.A. Earthquake Data File for 1899 through February 1975 are plotted in Figure 2, lower. Each number corresponds to the decade in which the event occurred. The coordinates of epicenters prior to about 1960 were often rounded to the nearest tenth of a degree. To avoid plotting epicenters on top of one another, the second and subsequent epicenters to be plotted at a given point have been randomly scattered by up to 4 km. The apparent increase in seismicity in the 1960's and 1970's is due in part to aftershocks of the 1964 Prince William Sound earthquake and in part to establishment of seismograph networks in southern Alaska in 1967 by N.O.A.A. (Palmer Observatory) and the Geophysical Institute of the University of Alaska. The seismograph stations closest to the region of study prior to 1972 were located on Middleton and Kodiak Islands and near

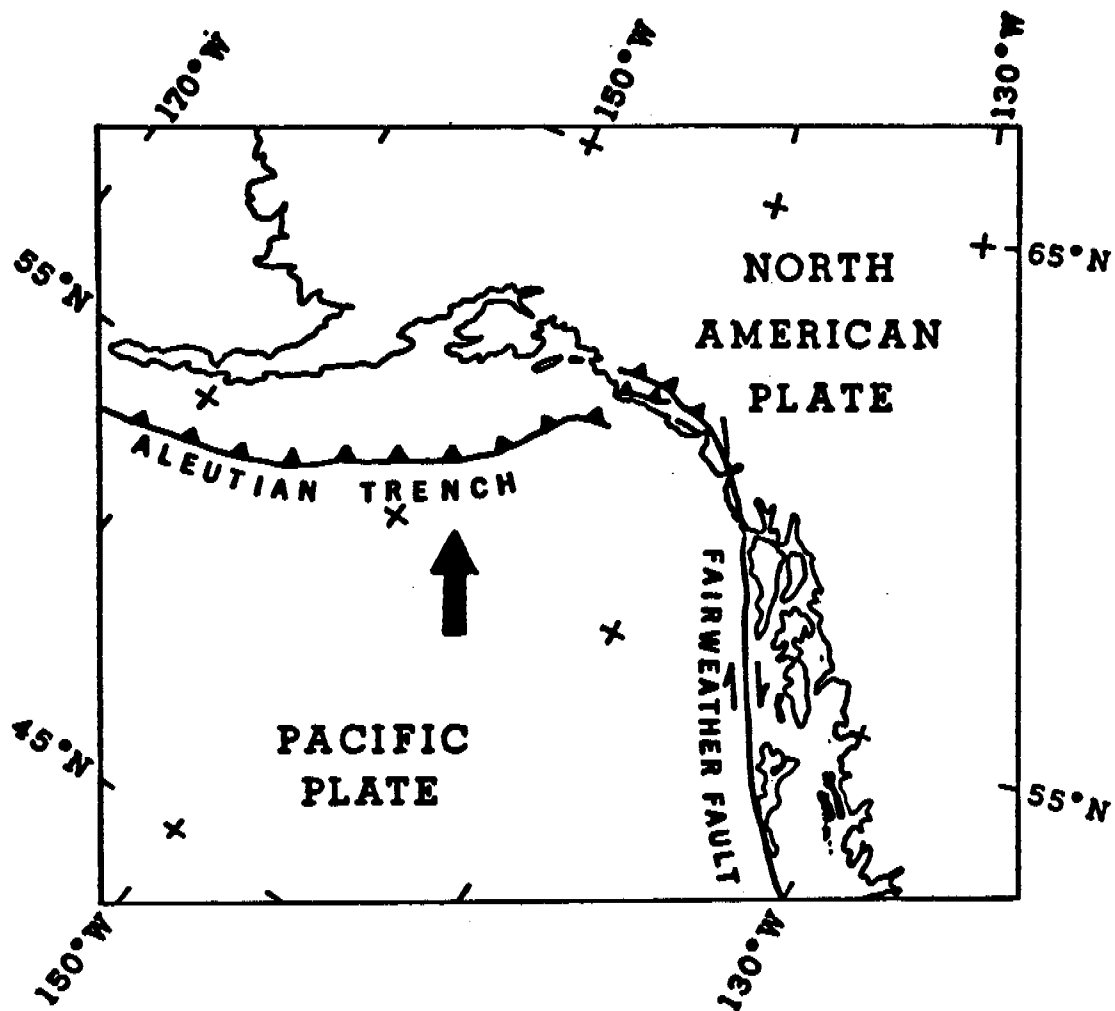


Figure 1. Plate tectonic relationships in the northeast Pacific. Large arrow indicates motion of the Pacific plate relative to a stationary North American plate. Small arrows indicate sense of horizontal slip on faults; barbs are on upper edge of thrust fault.

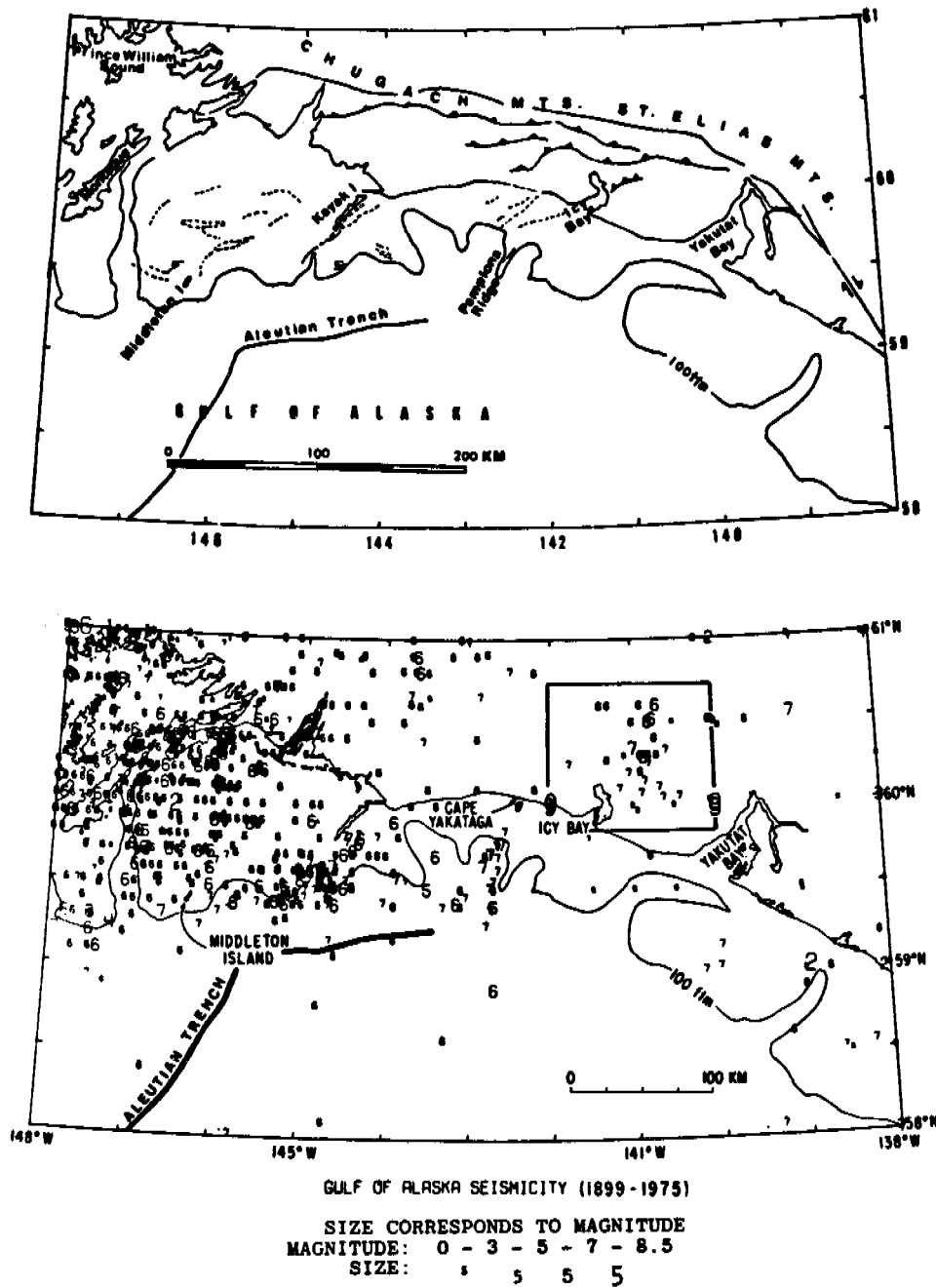


Figure 2. The upper map of the eastern Gulf of Alaska region shows offshore faults and selected onshore faults (from Carlson, 1976). The lower map is a plot of earthquake epicenters in the same area from 1899-1975. Numbers indicate the decade in which the earthquake occurred, for example, 7 indicates 1970's.

Palmer. Prior to 1967 the closest permanent stations were at Sitka and College.

The largest historic earthquakes in the vicinity of the eastern Gulf of Alaska were three magnitude 8 earthquakes in the Yakutat area in 1899 and 1900 (Tarr and Martin, 1912; Richter, 1958), the magnitude 8 Prince William Sound earthquake of 1964 and the magnitude 7.9 earthquake on the Fairweather fault in 1958. Shorelines were uplifted as much as 14 meters in the Yakutat Bay area and about 1 meter at Cape Yakataga during the 1899-1900 earthquakes (Tarr and Martin, 1912). Coastal uplift during the 1964 earthquake ranged from 19 meters at Montague Island to less than 3 meters at Kayak Island (Plafker, 1969). The region between the 1958 and 1964 earthquakes (Figure 3) lies on the Pacific-North American plate boundary and has been identified as a likely location for a magnitude 7 or 8 shock in the next few decades (Kelleher, 1970; Sykes, 1971; Page, 1975). Furthermore, if the 1899-1900 series of earthquakes involved movement on the northern part of the Fairweather fault, as suggested by Thatcher and Plafker (1977), it is possible that at this time the only major seismic gap along the eastern gulf of Alaska could be the area between Kayak Island and Icy Bay (Plafker, et al, 1978).

The Chugach and St. Elias Mountains are bounded on the south and southwest by the Gulf of Alaska Tertiary province. Many north-dipping thrust faults have been mapped in this Tertiary province (Plafker, 1967), but it is not known which are currently active. A few of these faults are indicated on Figure 2, upper.

Available information on the offshore structure has been summarized by Bruns and Plafker (1975) Molnia et al (1976) and Carlson (1976). The location of near-surface offshore faults, interpreted largely from minisparker records, are shown in Figure 2, upper. None of these faults was found to offset Holocene sediments at the sea floor with great certainty, so their current state of activity may best be determined by earthquake investigations.

IV. Study area.

This project is concerned with seismic hazards within and adjacent to the eastern Gulf of Alaska continental shelf area. This is the southern coastal and adjacent continental shelf region of Alaska between Montague Island and Yakutat Bay (Figure 2).

V. Data collected.

The short-period seismograph stations installed along the eastern Gulf of Alaska under the Outer Continental Shelf Environmental Assessment Program as well as the other stations operated by the USGS in southern Alaska are shown in Figure 5. Single-component stations record the vertical component of the ground motion, while three-component stations have instruments to measure north-south and east-west motion as well. Data from these instruments are used to determine the parameters of earthquakes as small as magnitude 1. The parameters of interest are epicenter, depth, magnitude, and focal mechanism. These data are required to further our understanding of the regional tectonics and to identify active faults.

A network of strong motion instruments is also operated by the Seismic Engineering Branch (Figure 6). These devices are designed to trigger during large earthquakes and give high-quality records of large ground motions which are necessary for engineering design purposes.

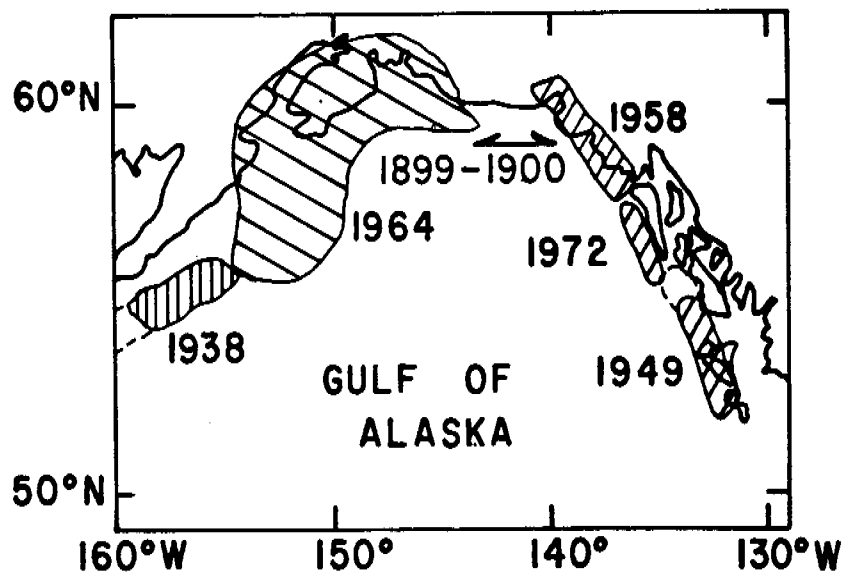


Figure 3. Map showing the aftershock zones for earthquakes of magnitude 7.3 or greater in the eastern Gulf of Alaska since 1938. No large earthquakes have occurred between the rupture zones of the 1958 Fairweather earthquake and the 1964 Prince William Sound earthquake since the 1899-1900 series of great earthquakes near Yakutat Bay, which makes this a likely site for another large earthquake. Modified from Sykes (1971).

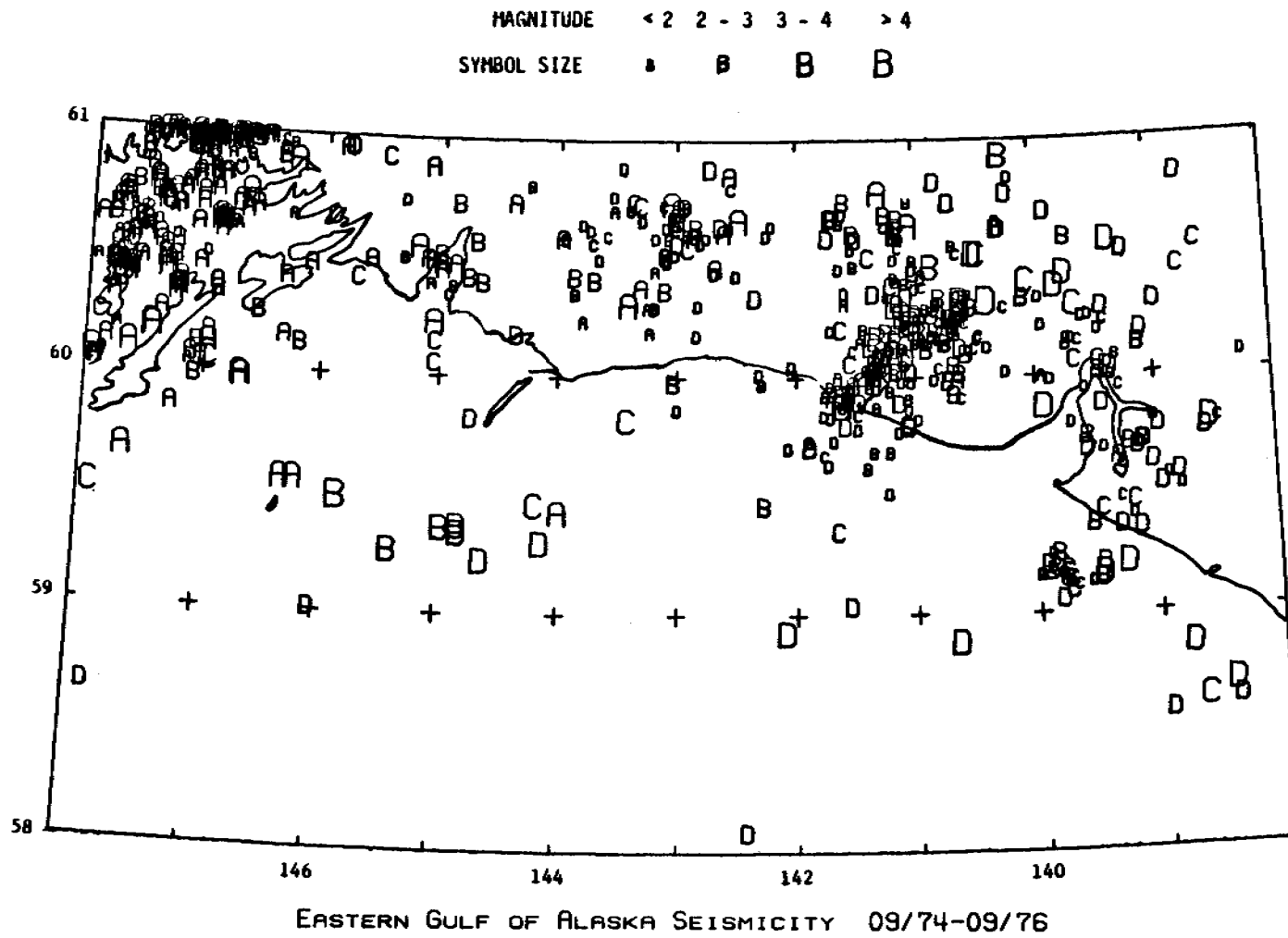


Figure 4. Map of earthquake epicenters located by the USGS seismic network in southeastern Alaska for the two-year period September, 1974-September, 1976. The symbol represents the quality (see Appendix) and the size is proportional to the magnitude.

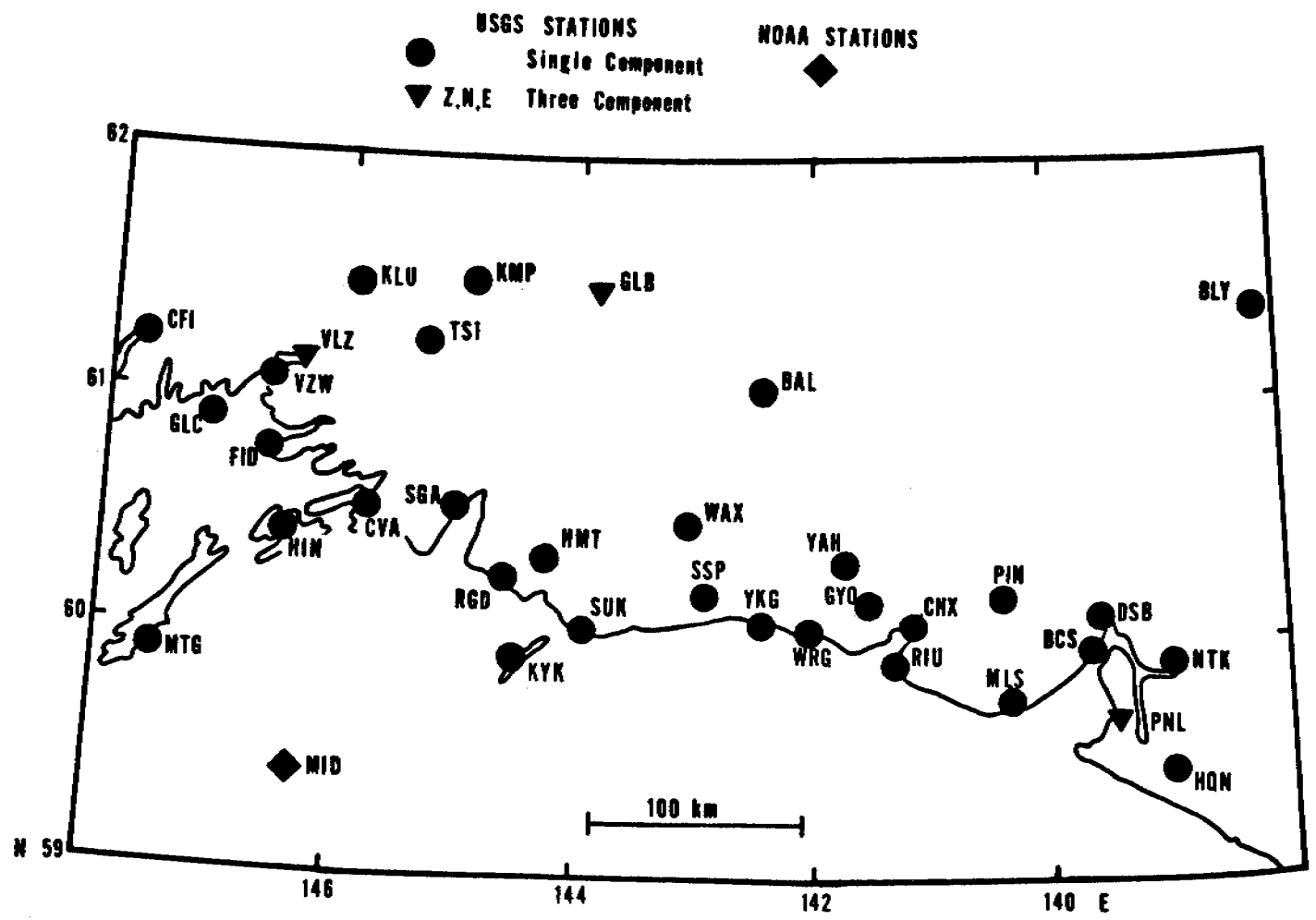


Figure 5. Seismic stations operated by the USGS in southeastern Alaska from 1976-1977.

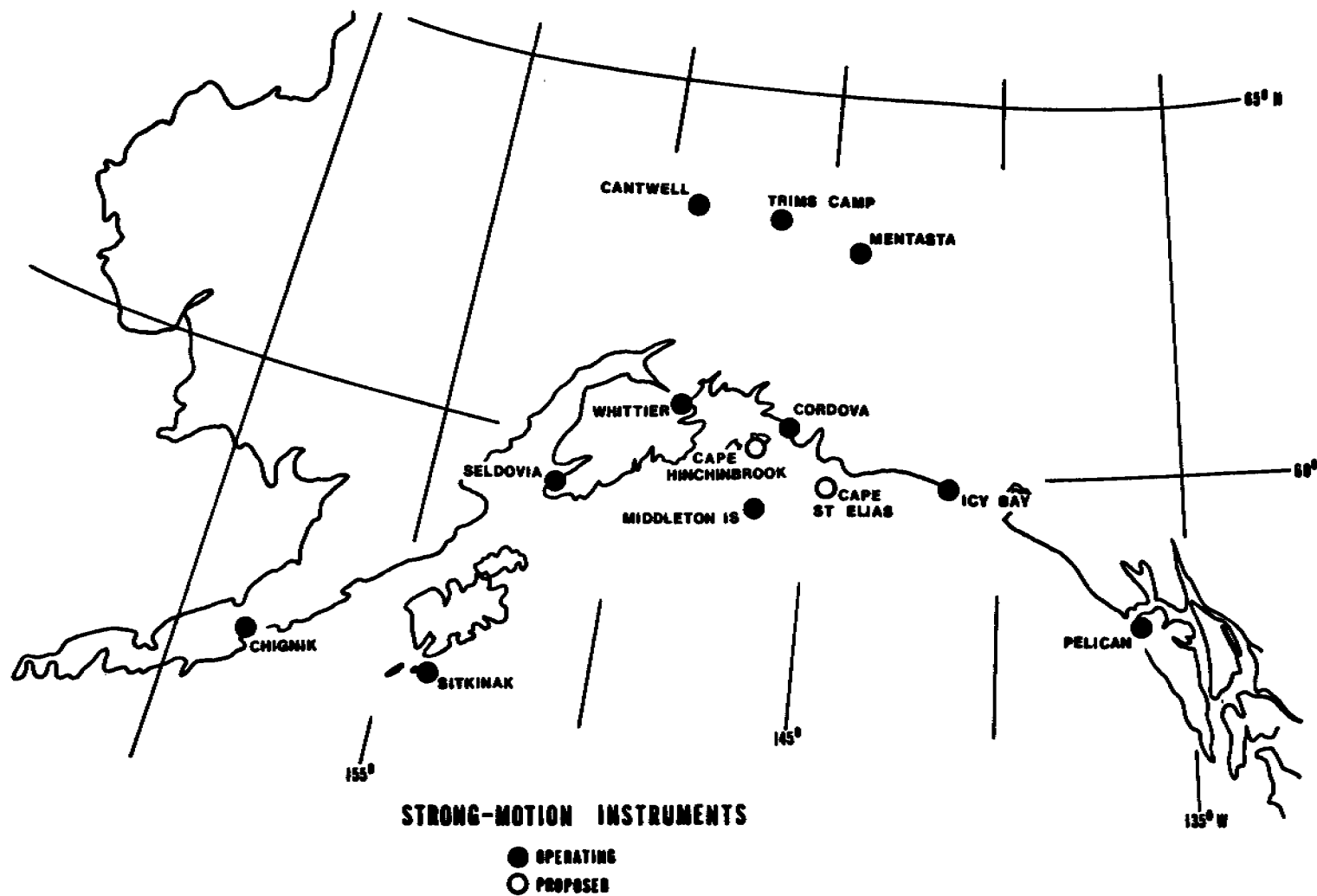


Figure 6. Map showing the locations of USGS operated strong-motion instruments in the eastern Gulf of Alaska and supported by OSCEAP.

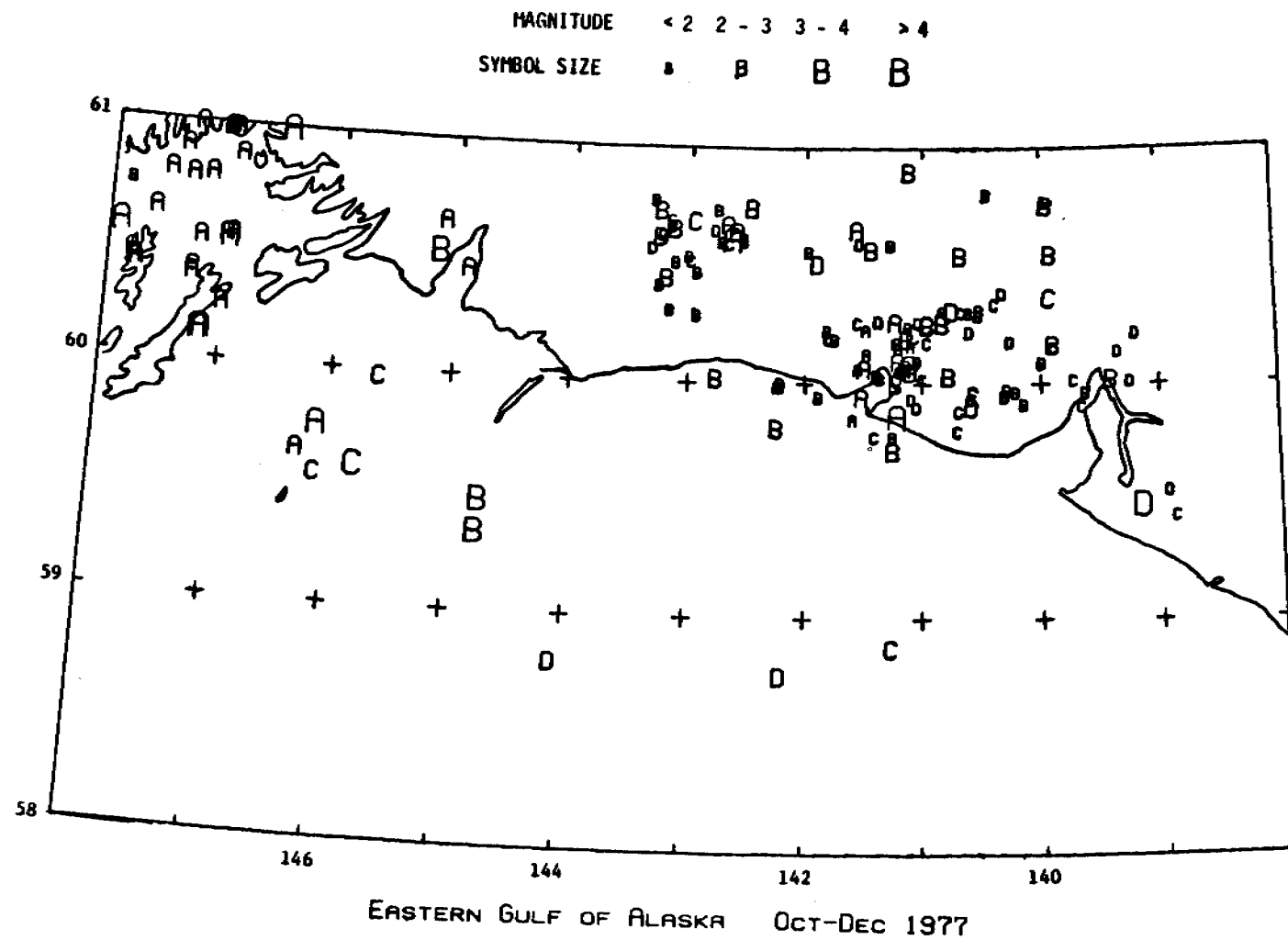


Fig. 7. Map of earthquake epicenters located by the USGS seismic network in southeastern Alaska for the quarter October-December, 1977. The symbol represents the quality (see Appendix) and the size is proportional to magnitude.

VI. Results

Preliminary earthquake epicenters in the eastern Gulf of Alaska region, for the period Oct.-Dec. 1977, are plotted in Figure 7. All earthquakes for which at least four arrivals at three or more stations could be read are included in the map. A catalog listing the earthquakes is contained in the Appendix.

A comparison of the data for this recent quarter and the data for an earlier two year period (Figure 4) shows that many features in the generally diffuse distribution of epicenters have remained the same. The high level of seismic activity northeast of Icy Bay and northeast of Kayak Island is continuing. No earthquakes were located south of Yakutat Bay where a sequence of activity occurred in 1974. Only one earthquake was located within about 20 km of the Pamplona Ridge. Most of the larger magnitude earthquakes which occurred offshore in the gulf were located northeast of Middleton Island and southwest of Kayak Island. Several earthquakes were located near the Copper River Delta and beneath Prince William Sound.

No earthquakes with better control in the solution were located deeper than 40 km.

VII.& VIII. Discussion and Conclusions

A. Icy Bay Region.

Earthquakes which occurred beneath Icy Bay from 1974-1976 were relocated using a master event technique. The earthquakes were selected on the basis of being recorded by at least three of the four closest seismic stations (Figure 8). The velocity model used was simply a linear increase of velocity with depth because the seismic velocity structure of this area is not well known.

The epicenters of the relocated earthquakes have an east-west trend which is parallel to nearby mapped faults. Focal mechanisms determined from single event and composite first motion plots have nodal planes which also strike east-west. Earthquakes with depths less than 10 km have a focal mechanism which is consistent with thrusting on a plane that dips steeply to the north. Slightly deeper earthquakes have nodal planes with similar dips, but the sense of motion is opposite to that of shallower earthquakes. The reason for this reversal of focal mechanism with depth is not yet clear. The focal mechanism of the shallower earthquakes is consistent with focal mechanisms determined for shallow teleseismic earthquakes to the northeast (J. Davies, personal communication, 1977).

The results of this detailed study of the seismicity near Icy Bay suggest that the deformation represented by the broad, northeast-trending zone of seismic activity near Icy Bay may be accommodated by movement on a series of en echelon, east-west trending faults.

IX. Needs for further study.

Employing a master event technique to relocate earthquakes near Icy Bay proved to be useful in helping to improve our understanding of the detailed seismic structure in that area. The seismic structure in other areas along the Eastern Gulf can be better resolved through similar studies. The highly active area northeast of Icy Bay, and the pocket of seismic activity south of Yakutat Bay are two areas where we are planning such studies.

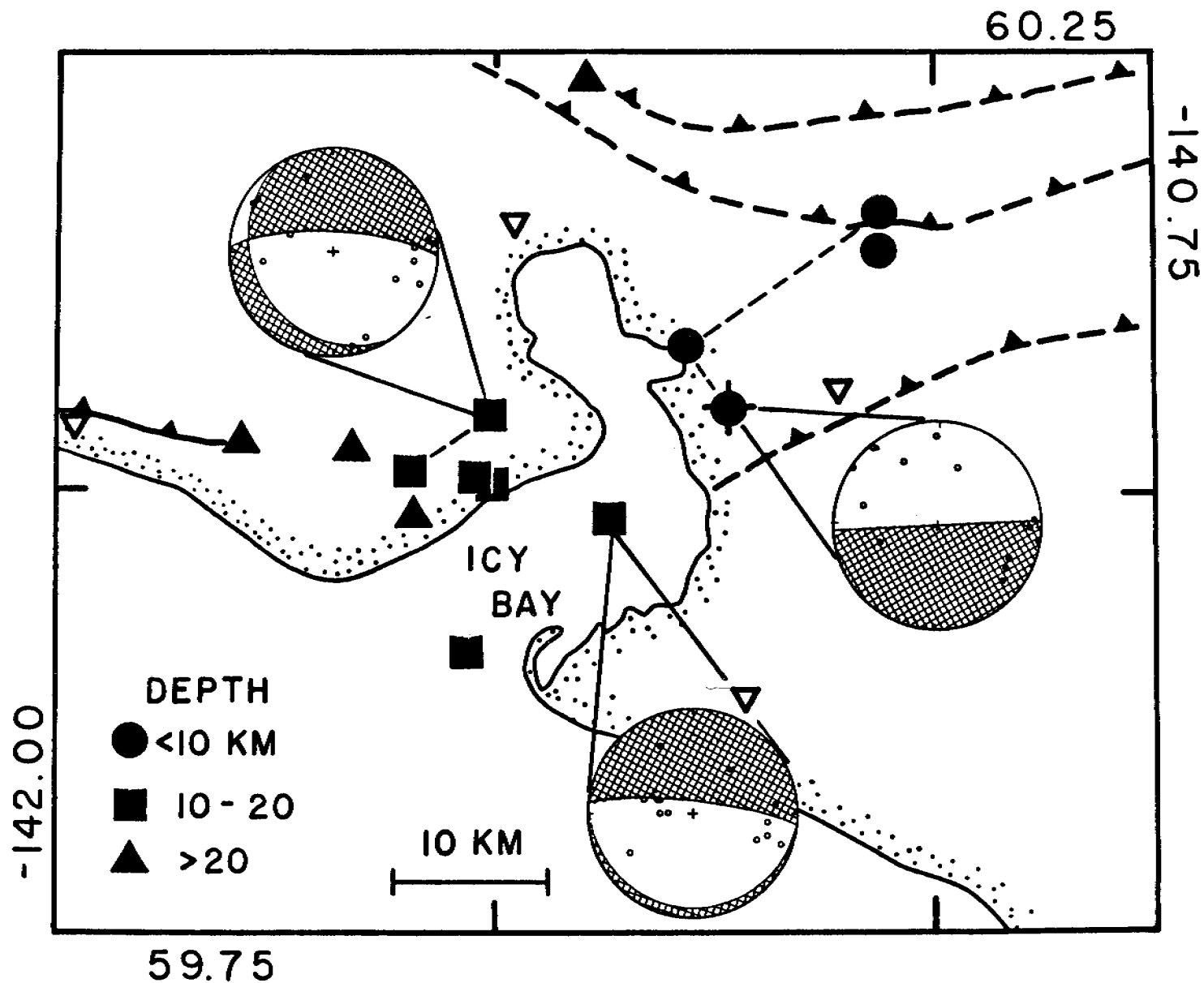


Figure 8. Relocated epicenters of selected earthquakes which occurred near Icy Bay between 1974-1976. Focal mechanisms are lower hemisphere, equal area projections. The light dashed lines join earthquakes used in a composite first motion plot. Heavy dashed lines indicate approximate locations of nearby mapped faults. The master event used in relocating the earthquakes is indicated by a cross.

The seismic velocity structure below a few kilometers depth in the eastern Gulf of Alaska is not well known. Such information is important in understanding the tectonic structure of this region and in helping to improve the accuracy of both absolute and relative earthquake locations. Travel times of refracted arrivals provide some constants on the velocity structure of this region. Active seismic sources with reasonably well located earthquakes are located beneath Icy Bay and in northeastern Prince William Sound. Refracted arrivals from these areas have been observed at distances up to several hundred kilometers. We have been collecting data to construct a reversed refraction profile between these two source areas.

The highly active, northeast trending zone of seismicity near Icy Bay appears to extend only a few kilometers offshore. About 50 km to the southwest lies the fault-bounded Pamplona Ridge, the site of three magnitude 6 earthquakes in 1970. The Pamplona Ridge and the area to the northeast presently appear to be quiet seismically. The land based stations are not ideal for detecting small magnitude earthquakes which occur offshore. Detection of these earthquakes, if they do occur, is important in order to identify any continuity of onshore and offshore structures and to understand the mode of deformation in this area. The use of ocean bottom seismometers (OBS) may improve our detection capability in the offshore area. This summer, in cooperation with the USGS Office of Marine Geology, we are planning to deploy about six OBS units in the area between Pamplona Ridge and Icy Bay (Figure 9).

Several years of recent seismic data for the Prince William Sound area have now been collected. We are studying this data and comparing it with earlier aftershock data from the 1964 earthquake to look for patterns or changes in the seismic activity.

X. Summary of fourth quarter operations.

A. Field and Laboratory Activities.

The operations during the fourth quarter were predominantly concerned with laboratory activities. The major efforts were centered around switching our computer operations from outside sources to the new in-house computing facility, and developing new and more reliable components for field instruments. Each of these will be discussed below in more detail. In addition, limited station maintenance was conducted.

1. Laboratory Activities

Until this quarter many of our computer operations were performed using outside sources. We now have converted these operations to the Honeywell Multics computing facility at the Menlo Park office. All of the seismic data processing from the Alaska network is now being handled by this system. We have almost completed the development and installation of an interactive location system which will improve and speed up the processing of seismic data.

A prototype unit of the newly-designed seismic amplifier voltage-controlled oscillator (VCO) was installed in Alaska. The unit and its automatic gain ranging feature are operating successfully.

In addition to the VCO unit, we are nearing completion of work on

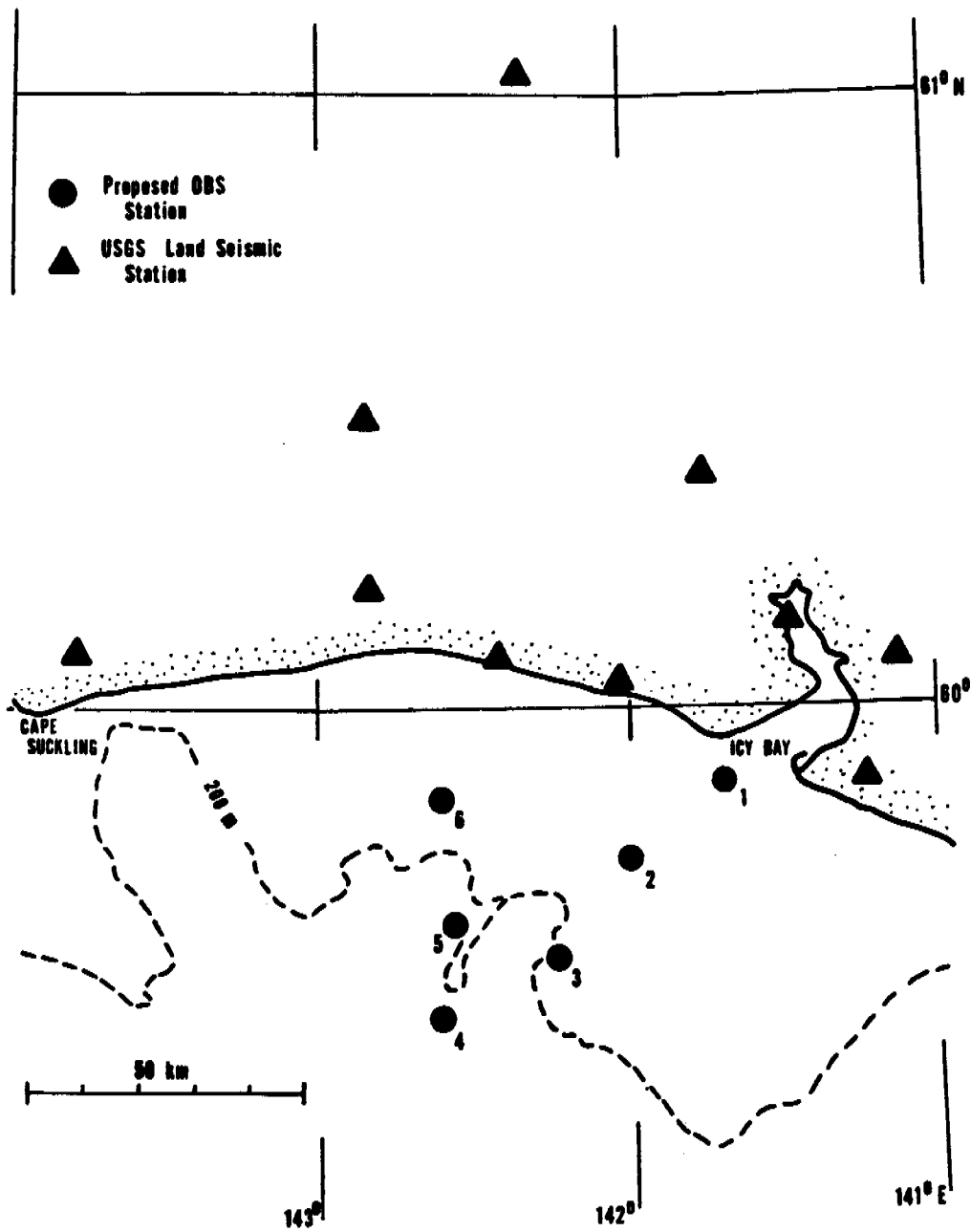


Figure 9. Proposed sites for OBS deployment.

a new filter bridge which will incorporate several new features for monitoring signal levels on telephone lines.

2. Field Operations and Station Maintenance.

Several of the stations in the network were visited during this quarter. The actions taken at the various stations were as follows:

Susitna - teflon-coated antenna was installed to check if this will help to reduce icing problems on the antenna. No results yet.

Valdez - vertical component was repaired.

Cordova - prototype VCO unit was installed.

B. Scientific Party

The scientific party included:

John Lahr, USGS, Project Chief.
Christopher Stephens, USGS, Geophysicist.
Kent Fogleman, USGS, Geophysicist.

The Technical and Field Party included:

Mary Ann Allan, USGS, Physical Science Technician.
Suzanne Helton, USGS, Physical Science Technician.
Kendall Louie, USGS, Physical Science Technician (Mr. Louie left the project in March 1978).
Mark Smetana, USGS, Physical Science Technician (Mr. Smetana joined the project in February 1978).
John Rogers, USGS, Electronics Technician.
Marion Salsman, USGS, Technician
Tom Cleese, Univ. Alaska, Physical Science Assistant.
Lars Gustafson, Univ. Alaska, Physical Science Assistant.

XI. References

- Bruns, T. R. and G. Plafker, 1975. Preliminary structural map of part of the offshore Gulf of Alaska Tertiary province, U.S.G.S. Open-File map 75-508.
- Carlson, P. R., 1976. Submarine faults and slides that disrupt surficial sedimentary units, northern Gulf of Alaska, U.S.G.S. Open-File Report 76-294.
- Hastie, L. M. and J. C. Savage, 1970. A dislocation model for the 1964 Alaska earthquake, Bull. Seism. Soc. Am., 60, 1389.
- Kelleher, J. A., 1970. Space-time seismicity of the Alaska-Aleutian seismic zone, J. Geophys. Res., 75, 5745.
- LePichon, X., 1968. Sea-floor spreading and continental drift, J. Geophys. Res., 73, 3661-3697.
- Meyers, H., 1976. A historical summary of earthquake epicenters in and near Alaska, NOAA Technical Memorandum EDS NGSDC-1.
- Miller, D., 1971. Geologic map of the Yakataga district. Gulf of Alaska Tertiary province, Alaska, U.S.G.S. Miscellaneous Geologic Investigations Map I-610.
- Molnia, B. G., O. R. Carlson, and T. R. Bruns, 1976. Report on the environmental geology OCS area, eastern Gulf of Alaska, U.S.G.S. Open-File Report 76-206.
- Page, R. A., 1975. Evaluation of seismicity and earthquake shaking at offshore sites, Offshore Technology Conference, 7th, Houston, Texas, Proc., v. 3.
- Plafker, G., 1967. Geologic map of the Gulf of Alaska Tertiary province, Alaska, U.S.G.S. Miscellaneous Geologic Investigations Map I-484.
- Plafker, G., 1969. Tectonics of the March 27, 1964, Alaska earthquake. U. S. Geological Survey Professional Paper 543-1.
- Plafker, G., 1972. Alaska earthquake of 1964 and Chilean earthquake of 1960: implications for arc tectonics, J. Geophys. Res., 77, 901.
- Plafker, G. T. Hudson, and M. Rubin, 1976. Late Holocene offset features along the Fairweather fault, The U. S. Geological Survey in Alaska, Accomplishments During 1975, E. H. Cobb, ed., U. S. Government Printing Office.
- Plafker, F., T. Hudson, M. Rubin, and T., Bruns, 1978. Late Quaternary offsets along the Fairweather Fault and crustal plate interactions in southern Alaska, Can. J. Earth Sci. (in press).

XI. References (continued)

- Richter, C. F., 1958. Elementary Seismology, W. H. Freeman and Co., Inc. San Francisco.
- Richter, D. H. and N. A. Matson, 1971. Quaternary faulting in the eastern Alaska range, Geol. Soc. Am. Bull., 82, 1529.
- Sykes, L. R., 1971. Aftershock zones of great earthquakes, seismicity gaps, and earthquake prediction for Alaska and the Aleutians, J. Geophys. Res., 76, 8021.
- Tarr, R. S. and L. Martin, 1912. The earthquakes at Yakutat Bay, Alaska in September, 1899, U.S. Geological Survey Professional Paper 69, 135 p.
- Thatcher, W. and G. Plafker, 1977. The Yakutat Bay, Alaska, earthquakes; seismograms and crustal deformation, Geol. Soc. Am. Abs. with Programs, 9, p. 515.
- Tocher, D., 1960. The Alaska earthquake of July 10, 1958: Movement on the Fairweather fault and field investigations of southern epicentral region, Bull. Seism. Soc. Am., 50, 267.

APPENDIX I

This appendix lists origin times, focal coordinates, magnitudes, and related parameters for earthquakes which occurred in the eastern Gulf of Alaska region. The following data are given for each event:

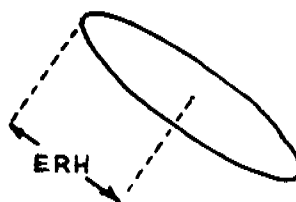
- (1) Origin time in Greenwich Civil Time (GCT): date, hour (HR), minute (MN), and second (SEC). To convert to Alaska Standard Time (AST) subtract ten hours.
- (2) Epicenter in degrees and minutes of north latitude (LAT N) and west longitude (LONG W).
- (3) DEPTH, depth of focus in kilometers.
- (4) MAG, duration magnitude of the earthquake.
- (5) NP, number of P arrivals used in locating earthquake.
- (6) NS, number of S arrivals used in locating earthquake.
- (7) GAP, largest azimuthal separation in degrees between stations.
- (8) D3, epicentral distance in kilometers to the third closest station to the epicenter.
- (9) RMS, root-mean-square error in seconds of the traveltimes residuals:

$$\text{RMS} = \sqrt{\frac{\sum (R_{Pi}^2 + R_{Si}^2)}{NP + NS}}$$

where R_{Pi} and R_{Si} are the observed minus the computed arrival times of P and S waves respectively at the i-th station.

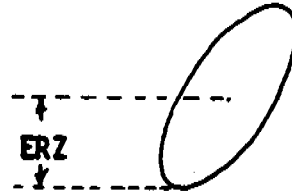
- (10) ERH, largest horizontal deviation in kilometers from the hypocenter within the one-standard-deviation confidence ellipsoid. This quantity is a measure of the epicentral precision for an event. An upper limit of 99 km is placed on ERH.

Projection of ellipsoid
onto horizontal plane:



- (11) ERZ, largest vertical deviation in kilometers from the hypocenter within the one-standard-deviation confidence ellipsoid. This quantity is a measure of the depth precision for an event. An upper limit of 99 km is placed on ERZ.

Projection of ellipsoid
onto vertical plane:



(12) Q, quality of the hypocenter. This index is a measure of the precision of the hypocenter and is calculated from ERH and ERZ as follows:

<u>Q</u>	<u>ERH</u>	<u>ERZ</u>
A	≤ 2.5	≤ 2.5
B	≤ 5.0	≤ 5.0
C	≤ 10.0	≤ 10.0
D	ALL OTHERS	

This quality symbol is used to denote each earthquake on epicenter maps.

EASTERN GULF OF ALASKA EARTHQUAKES

1977	origin hr mn	time sec	lat n deg min	long w deg min	depth km	mag	no	ns	gap deg	d3 km	rms sec	erh km	erz o km			
oct	2	0	39	29.8	60 36.8	142 32.8	8.8	1.9	5	5	109	52	0.83	1.2	2.7	B
	2	3	14	21.1	60 35.9	142 32.8	21.6	1.9	5	5	108	51	0.61	1.7	2.6	B
	2	21	26	21.9	61 20.8	146 49.8	23.1	2.0	11	6	80	52	0.35	1.0	2.2	A
	3	7	32	12.6	60 20.1	140 23.9	15.3	1.5	5	5	227	75	0.24	6.3	2.8	C
	3	13	31	27.1	64 18.8	146 42.7	0.3	3.6	6	3	316	317	0.22	70.9	72.7	D
	3	14	43	50.3	60 8.0	139 21.2	5.3	1.6	4	4	255	61	0.33	4.6	41.2	D
	3	22	35	4.6	60 32.7	139 55.3	12.2	2.1	3	3	231	143	0.41	4.3	2.7	B
	5	18	22	53.6	61 43.6	146 33.8	19.9	2.3	19	13	110	67	0.48	1.0	2.8	B
	6	5	19	18.3	60 10.4	140 58.0	35.8	1.8	3	3	194	122	0.22	7.5	8.2	C
	6	13	12	10.6	60 28.0	142 56.6	0.5	1.7	7	7	173	118	0.50	2.7	2.6	B
	8	20	16	57.8	60 44.5	142 28.7	25.9	2.2	8	7	140	142	0.45	4.4	3.6	B
	10	5	41	58.4	60 30.4	141 54.3	64.1	2.5	3	3	350	261	0.28	69.5	94.7	D
	10	5	41	59.9	60 40.3	142 40.7	6.0	2.5	7	5	97	68	0.67	1.6	2.2	A
	12	6	37	17.7	61 37.7	147 36.3	9.1	2.6	8	6	173	92	0.49	2.5	2.3	A
	14	20	21	22.5	60 33.2	147 54.8	14.4	3.2	28	4	137	70	0.46	1.2	1.2	A
	17	23	24	20.8	61 31.2	146 29.8	26.7	2.3	17	6	86	51	0.32	1.6	2.4	A
	19	2	51	11.6	62 3.2	147 23.0	34.4	3.1	14	9	194	99	0.66	4.3	45.4	D
	22	15	12	38.0	61 42.3	146 35.5	7.7	2.4	23	14	109	65	0.64	0.9	1.2	A
	23	2	33	41.0	61 19.5	146 48.4	20.7	2.0	23	10	77	51	0.36	0.9	2.0	A
	24	11	13	56.3	61 35.4	145 57.8	19.3	2.5	28	11	109	53	0.65	0.9	1.1	A
	24	14	48	7.9	61 23.2	147 12.6	17.8	2.4	27	11	86	67	0.42	1.1	1.2	A
	25	11	2	51.8	60 52.6	146 54.2	20.6	2.3	26	13	104	28	0.50	1.0	1.4	A
	25	23	42	44.6	61 26.2	146 34.3	19.8	2.0	21	11	82	42	0.44	1.2	1.2	A
	27	4	10	16.9	60 27.2	144 54.0	18.0	2.5	21	11	156	109	0.23	2.1	2.0	A
	27	21	1	35.4	60 32.1	143 0.9	2.1	1.7	9	7	120	67	0.31	3.3	4.5	B
	27	12	34	59.1	60 46.7	147 19.1	14.3	2.7	28	10	131	52	0.43	1.2	1.1	A
	28	7	14	39.4	60 11.3	141 8.5	0.1	2.2	17	7	137	39	0.62	2.2	3.3	B
	29	12	13	6.6	63 38.0	147 38.1	10.5	3.7	13	5	274	240	0.25	40.7	41.4	D
	30	10	51	58.8	60 4.3	141 7.0	8.2	3.4	24	2	119	22	0.59	1.3	1.1	A
	30	12	16	7.3	61 24.3	146 56.2	18.0	3.1	32	8	86	55	0.49	1.0	1.1	A
nov	1	2	22	0.1	61 26.9	147 10.8	20.4	2.1	23	13	93	58	0.42	1.0	2.0	A
	1	19	45	0.5	60 48.1	140 27.5	0.3	1.8	8	7	240	92	0.41	1.8	2.5	B
	1	22	0	0.9	60 32.4	146 56.3	20.0	2.4	35	8	80	62	0.49	1.1	1.9	A
	1	22	41	30.0	60 54.0	141 7.4	0.0	2.1	17	4	205	86	0.45	1.7	3.2	B
	2	6	8	47.4	60 13.4	141 48.9	0.0	1.7	10	6	96	24	0.30	1.1	4.2	B
	2	6	48	31.9	61 29.2	147 23.1	20.0	2.3	12	7	97	62	0.29	1.4	4.0	B
	2	10	6	35.1	60 31.3	146 58.0	10.3	3.4	26	7	82	84	0.52	1.3	1.6	A
	2	17	5	33.1	61 24.5	146 51.9	24.0	2.3	10	7	139	54	0.28	1.7	2.2	A
	3	7	12	44.5	61 47.1	147 34.9	20.0	2.6	19	9	151	68	0.36	1.5	3.7	B
	3	9	23	26.1	61 33.7	146 7.5	42.8	2.4	15	13	98	56	0.35	1.7	3.7	B
	3	14	19	1.0	60 31.9	146 59.6	10.7	2.4	22	14	158	82	0.44	1.3	1.4	A
	3	15	39	21.4	60 43.7	143 15.7	0.2	2.0	13	6	76	65	0.46	1.8	3.1	B
	3	20	10	10.4	60 31.3	145 9.1	15.1	3.2	16	7	126	94	0.29	3.0	1.7	B
	4	15	53	13.7	61 6.3	140 39.9	33.0	2.5	3	2	264	116	0.16	5.4	99.0	D
	6	19	11	1.9	62 10.7	145 9.5	1.3	3.4	19	6	224	107	0.55	2.9	2.2	B

EASTERN GULF OF ALASKA EARTHQUAKES (CONTINUED)

1977	origin hr mn	time sec	lat n deg min	long w deg min	depth km	mag	np	ns	gap deg	d3 km	rms sec	erh km	erz q km
nov	7 21 32	47.8	60 35.3	142 40.2	12.5	1.7	5	3	172	53	0.08	9.1	6.4 C
	8 21 8	7.5	60 17.2	140 31.8	17.2	1.9	9	4	185	62	0.17	3.6	2.1 B
	8 21 31	51.6	60 0.1	141 13.8	2.0	2.1	7	2	107	103	0.28	3.8	4.2 B
	8 22 48	18.8	61 37.4	141 51.9	0.5	2.1	7	5	247	141	0.16	4.7	2.6 B
	9 1 35	53.8	60 18.5	140 31.5	15.4	1.9	11	8	179	64	0.24	3.3	1.7 B
	9 12 41	21.3	60 5.7	141 12.8	8.5	2.0	15	5	120	42	0.31	1.4	1.8 A
	10 1 36	32.4	61 2.5	146 31.8	20.2	2.1	12	9	116	68	0.33	1.7	2.0 A
	11 5 59	20.4	60 31.0	147 12.8	8.7	2.0	18	16	154	80	0.63	2.4	1.7 A
	12 2 15	56.8	60 59.6	146 29.5	15.1	3.0	18	10	114	64	0.62	1.2	1.3 A
	12 3 38	48.8	60 3.3	141 12.1	3.2	1.6	8	2	115	46	0.33	2.8	6.1 C
	13 1 47	13.7	61 36.7	146 23.7	32.8	2.2	13	9	90	56	0.30	1.4	5.1 C
	13 13 13	2.5	60 39.1	141 34.2	7.5	2.1	13	4	175	60	0.36	1.7	2.3 A
	13 17 46	49.4	60 58.9	147 1.5	20.0	2.4	18	11	113	41	0.43	1.2	1.4 A
	13 19 43	58.0	60 53.9	147 23.3	29.4	2.6	21	12	141	47	0.44	1.8	1.3 A
	14 2 47	40.1	60 14.4	141 7.7	8.9	1.3	7	6	145	51	0.38	2.3	3.6 B
	14 6 0	7.8	60 59.1	147 1.9	21.7	2.5	21	10	113	41	0.38	1.3	1.8 A
	14 13 18	42.3	61 29.3	141 18.1	1.8	2.2	4	4	252	134	0.21	4.7	6.4 C
	14 15 2	45.8	60 1.2	141 0.2	20.4	1.6	5	3	217	56	0.27	6.0	5.2 C
	14 22 49	43.7	60 41.2	142 58.2	47.4	2.0	6	5	137	81	0.37	3.3	9.9 C
	16 2 30	13.9	61 0.4	147 7.2	20.3	2.0	15	10	118	42	0.43	1.6	2.8 B
	16 9 7	46.4	59 51.7	141 13.0	12.4	3.0	17	1	161	50	0.41	2.1	1.2 A
	16 15 37	43.0	60 47.2	147 9.2	19.8	2.7	24	11	135	55	0.49	1.7	2.0 A
	17 10 6	9.0	61 43.4	142 31.0	51.3	2.1	5	5	271	135	0.35	6.4	8.6 C
	17 10 50	28.2	61 30.3	144 29.7	20.4	1.3	7	4	154	55	0.40	3.5	3.9 B
	17 20 30	11.7	61 43.9	146 33.7	19.6	2.3	18	10	111	68	0.49	1.1	1.7 A
	19 3 10	50.6	60 39.7	143 9.9	0.4	1.6	8	6	94	61	0.38	1.4	4.6 B
	21 5 2	10.9	61 25.3	146 56.3	7.9	2.3	27	11	88	52	0.48	0.8	1.3 A
	21 18 14	24.2	61 2.6	146 24.1	17.2	2.1	18	10	56	37	0.56	1.0	0.9 A
	22 21 6	28.3	60 17.2	142 56.7	10.8	1.5	8	5	90	52	0.32	3.6	3.8 B
	23 1 21	44.3	60 32.6	140 41.3	0.2	2.0	13	6	197	62	0.23	1.8	4.2 B
	23 3 27	14.5	61 21.0	146 49.3	21.1	2.2	19	14	80	51	0.47	0.8	2.0 A
	23 10 28	26.5	60 59.4	147 0.8	22.3	2.3	26	15	58	37	0.41	1.1	1.2 A
	23 15 35	50.3	60 3.3	141 10.2	3.5	1.8	15	6	115	47	0.46	1.3	2.6 B
	23 21 56	10.5	60 3.9	141 9.2	11.8	2.2	16	5	117	47	0.42	1.6	1.5 A
	24 0 41	25.7	61 43.6	147 15.4	14.2	1.8	10	9	134	71	0.36	1.4	2.1 A
	24 1 16	48.4	60 3.7	141 9.2	2.3	1.8	12	8	117	49	0.29	1.5	2.6 B
	24 3 23	48.1	53 29.2	147 32.8	78.7	4.1	17	3	269	226	0.34	17.9	36.1 D
	24 13 47	8.1	60 34.0	143 20.0	0.2	1.4	4	3	258	75	0.11	4.1	99.0 D
	24 22 26	54.4	60 18.4	140 45.7	38.1	2.5	4	4	177	116	0.06	8.8	14.7 D
	25 9 5	50.1	61 11.3	147 14.6	1.0	2.2	17	10	74	40	0.48	1.5	2.3 A
	25 9 57	22.8	60 7.4	147 11.4	3.6	3.2	32	8	119	91	0.44	1.3	1.5 A
	25 14 16	45.4	60 30.6	143 7.6	0.9	1.8	9	8	163	78	0.32	2.4	3.3 B
	26 7 2	39.2	61 13.7	145 32.2	18.0	1.8	13	7	97	44	0.44	1.5	1.1 A
	26 10 45	1.7	60 33.5	141 58.9	25.7	1.5	8	8	139	54	0.23	1.6	2.6 B
	26 12 48	20.7	61 36.6	146 35.7	21.2	2.2	13	14	110	59	0.37	1.5	3.7 B

EASTERN GULF OF ALASKA EARTHQUAKES (CONTINUED)

1977	origin		time	lat n	long w	depth	mag	np	ns	gao	13	rms	erh	erz	q	
	hr	mn	sec	deg min	deg min	km				deg	km	sec	km	km		
nov	26	13	21	48.6	61 36.0	146 15.7	23.7	2.2	14	11	93	62	0.36	1.2	2.3	A
	26	13	56	37.2	61 30.9	139 49.3	0.1	2.9	5	2	281	177	0.47	23.0	28.7	D
	26	21	4	30.0	61 36.1	141 34.9	0.1	2.4	5	5	255	146	0.24	6.0	3.4	C
	27	0	7	2.1	61 33.6	141 44.8	2.2	2.1	2	2	306	137	0.13	10.3	5.6	D
	27	0	10	31.0	61 47.1	146 57.1	11.9	1.9	12	8	137	73	0.32	1.7	2.2	A
	27	12	32	45.6	61 39.7	146 19.9	35.0	3.0	20	6	91	59	0.40	1.5	5.3	C
	27	16	5	48.2	59 56.2	141 5.8	14.2	1.2	3	2	231	113	0.07	20.9	10.8	D
	27	19	53	33.8	60 22.9	140 20.0	32.7	1.4	3	3	229	132	0.09	13.0	29.9	D
	28	4	40	16.2	63 18.1	144 30.5	32.3	3.3	5	3	318	210	0.16	6.9	99.0	D
	28	6	42	23.1	60 43.8	147 50.7	12.3	1.9	7	5	169	68	0.28	2.0	2.7	B
	28	15	11	8.1	59 58.3	145 37.0	17.6	2.7	10	7	203	132	0.28	5.1	5.3	C
	28	21	26	29.0	60 18.1	140 41.1	18.2	1.3	4	4	182	121	0.08	9.0	7.1	C
	29	0	53	54.8	61 33.8	146 28.2	30.2	2.2	14	13	89	56	0.41	1.1	1.1	A
	29	3	14	38.7	60 7.6	147 9.7	4.1	3.2	32	5	118	104	0.35	1.2	1.6	A
	29	12	26	48.3	59 52.9	140 42.0	5.2	1.5	4	2	252	135	0.02	8.7	7.0	C
	29	14	21	52.2	59 59.1	142 14.5	2.9	1.3	11	7	181	40	0.25	2.5	2.2	A
	29	16	22	13.0	60 38.6	142 36.4	0.2	2.9	21	6	97	57	0.47	1.0	1.7	A
	29	16	37	23.1	59 60.0	142 13.0	4.4	1.9	7	6	232	40	0.27	2.6	3.0	B
	29	19	35	0.3	61 29.1	146 34.8	20.6	2.0	14	10	86	72	0.37	1.0	2.7	B
	29	21	6	36.5	61 20.7	146 20.7	24.9	2.4	13	8	70	56	0.30	1.3	1.6	A
	30	5	7	34.4	61 27.2	147 29.9	19.8	2.9	23	4	92	59	0.46	1.3	1.8	A
	30	8	12	10.6	60 1.2	142 46.0	10.7	2.7	7	4	253	41	0.37	3.8	1.8	B
	30	10	25	44.7	61 31.4	146 35.9	19.9	2.3	16	11	90	69	0.43	1.1	1.5	A
	30	13	8	56.3	59 59.1	142 12.7	3.8	1.7	7	3	218	41	0.23	4.9	3.2	B
	30	14	2	26.8	61 26.0	146 6.2	26.2	2.3	17	8	68	47	0.36	1.3	1.5	A
	30	14	9	40.5	59 48.5	142 14.6	19.3	2.6	3	4	286	79	0.32	4.3	2.0	B
	30	17	12	16.1	60 15.2	140 58.2	0.8	2.0	8	4	155	45	0.31	2.2	5.2	C
	30	17	14	27.7	60 5.7	141 2.9	22.7	1.3	4	3	194	49	0.11	10.1	6.7	D
	30	18	44	4.7	60 47.5	147 30.5	22.1	2.8	19	6	152	74	0.35	2.2	2.2	A
	30	22	13	54.9	61 1.6	146 4.2	21.9	3.1	17	5	87	56	0.25	1.4	2.7	B
dec	1	18	45	12.2	58 57.9	137 59.5	23.9	2.0	3	2	357	180	0.07	98.8	8.2	D
	2	16	48	26.4	60 39.2	145 6.4	5.5	2.5	27	6	58	82	0.39	1.1	1.6	A
	2	17	40	18.6	60 15.9	141 22.6	15.6	1.9	4	2	138	65	0.35	10.3	11.6	D
	2	23	29	32.3	60 21.7	139 56.0	0.1	2.4	9	3	272	90	0.49	5.5	4.6	C
	3	1	24	40.5	60 10.5	140 15.9	17.2	1.4	3	1	227	149	0.21	86.8	48.0	D
	3	20	39	29.9	58 45.3	142 11.7	21.3	2.9	14	5	275	147	0.36	24.5	40.7	D
	4	20	3	59.5	59 54.1	139 39.5	2.3	1.4	4	2	153	40	0.18	4.2	7.4	C
	5	0	5	10.5	61 28.6	146 35.8	19.9	2.7	13	6	112	84	0.49	1.6	1.8	A
	5	0	47	1.3	60 36.5	142 38.5	5.3	3.1	16	9	95	50	0.58	1.0	1.6	A
	5	3	24	31.1	59 42.9	141 15.1	11.9	2.0	11	5	183	57	0.33	3.1	2.2	B
	5	6	4	47.0	59 50.8	141 35.6	15.3	1.4	9	8	218	34	0.47	2.4	1.4	A
	5	14	24	31.3	60 41.3	143 10.0	0.5	1.3	10	5	139	59	0.26	1.8	5.3	C
	5	19	7	53.1	60 1.1	139 24.8	1.1	2.2	9	4	234	48	0.47	5.0	3.0	B
	5	20	21	36.2	59 56.8	140 18.7	3.9	1.7	6	2	155	60	0.34	3.0	3.9	B
	5	20	37	24.0	59 58.3	140 17.5	1.2	1.9	3	1	192	68	0.00	9.0	98.7	D

EASTERN GULF OF ALASKA EARTHQUAKES (CONTINUED)

1977	origin		time	lat n		long w		depth	mag	np	ns	gap	13	rms	erh	erz	q
	hr	mn	sec	deg	min	deg	min	km				deg	km	sec	km	km	
dec	6	0	33	52.1	58 52.5	141 15.8		15.0	2.6	12	6	278	138	0.29	6.9	6.1	C
	6	10	56	44.8	61 35.3	146 38.2		31.8	2.2	18	11	98	59	0.36	1.2	2.1	A
	7	9	19	45.9	62 44.5	143 14.2		63.3	3.1	8	1	278	168	0.44	14.2	40.9	D
	7	22	22	27.5	59 56.1	140 35.8		5.3	1.7	4	2	236	128	0.10	7.6	4.2	C
	7	22	42	15.9	59 54.0	140 35.5		3.2	2.1	3	2	259	159	0.07	9.4	12.8	D
	7	22	42	40.1	60 24.6	147 47.2		13.7	2.6	26	11	158	85	0.42	2.0	1.4	A
	7	22	45	44.7	59 45.4	146 6.6		9.0	3.7	36	3	112	90	0.28	1.4	1.7	A
	7	22	50	36.4	59 58.1	140 35.0		13.5	1.7	7	2	159	74	0.33	5.7	4.2	C
	7	22	58	23.9	60 12.6	141 4.8		1.3	2.1	8	2	142	47	0.25	3.8	6.2	C
	8	1	33	54.5	60 35.8	142 43.6		15.7	1.8	7	5	97	53	0.31	2.8	2.5	B
	8	17	27	56.0	63 39.3	147 28.0		4.0	3.8	15	3	275	245	0.56	51.0	64.1	D
	8	22	31	9.1	60 14.4	146 59.8		13.4	2.8	25	5	107	77	0.54	1.4	1.9	A
	11	4	7	42.9	61 31.9	147 25.5		20.6	2.3	21	6	103	57	0.39	1.1	2.0	A
	11	9	52	8.6	60 1.9	140 47.3		7.3	2.0	11	5	153	65	0.45	3.1	2.7	B
	12	8	0	44.5	59 32.8	146 6.6		43.6	2.7	17	4	155	134	0.60	3.5	7.4	C
	12	11	3	48.8	60 13.1	140 36.7		8.2	1.8	5	2	165	63	0.24	24.0	19.5	D
	12	11	7	14.5	59 47.8	140 42.7		13.5	1.8	5	2	243	85	0.25	8.6	3.2	C
	12	18	3	49.0	60 12.7	139 12.0		17.5	1.5	5	2	252	62	0.50	10.4	8.1	D
	12	18	50	45.9	60 35.3	141 16.4		2.2	1.2	7	5	184	77	0.27	1.4	4.3	B
	12	22	27	55.5	61 11.5	147 13.1		12.5	2.5	18	6	97	62	0.60	1.4	1.2	A
	13	11	29	41.7	60 35.6	141 32.8		3.3	1.3	6	6	169	66	0.31	1.8	24.4	D
	13	11	46	11.7	60 24.1	147 46.6		5.8	2.8	31	6	101	86	0.38	1.4	1.6	A
	13	17	1	51.6	59 56.6	141 31.0		13.3	2.2	13	2	153	31	0.35	1.9	1.8	A
	14	8	23	27.6	60 26.2	147 47.7		11.8	2.3	14	11	201	83	0.44	2.2	1.8	A
	14	14	2	47.0	60 58.8	146 58.0		20.6	2.7	16	12	109	38	0.42	1.6	1.8	A
	14	14	5	46.6	59 35.6	145 47.1		0.1	3.2	12	9	217	177	0.23	5.3	3.4	C
	14	14	8	53.1	61 25.8	147 46.3		27.8	2.2	9	6	162	84	0.35	2.9	1.7	B
	14	17	46	24.3	60 59.8	147 16.8		16.0	2.1	8	5	125	53	0.25	2.5	1.6	A
	15	17	0	25.3	62 32.3	147 41.5		0.1	2.9	16	12	228	130	0.60	3.2	1.8	B
	15	23	48	20.1	59 57.7	140 13.1		4.7	1.9	8	5	152	73	0.32	2.4	2.7	B
	16	5	17	1.7	60 39.1	143 8.3		0.4	2.7	14	10	68	61	0.42	1.6	2.7	B
	16	5	47	51.2	61 19.2	143 22.0		18.9	1.2	5	4	180	91	0.26	47.2	10.7	D
	16	14	11	26.2	60 2.9	141 11.4		0.8	1.1	8	4	114	47	0.19	2.1	82.1	D
	16	14	12	45.1	60 1.3	141 21.4		23.1	1.2	4	3	164	62	0.12	4.3	3.9	B
	17	5	20	29.6	60 11.3	141 44.8		18.0	1.3	3	3	137	23	0.04	2.0	4.6	B
	17	5	56	54.5	60 45.2	139 57.2		0.2	2.2	10	8	235	107	0.58	3.2	4.7	B
	17	6	9	46.9	60 23.8	147 45.4		11.6	2.6	17	11	218	87	0.53	2.2	1.3	A
	17	8	13	48.3	61 11.0	147 14.3		13.3	2.4	18	8	85	39	0.45	1.2	1.4	A
	17	15	18	2.5	60 59.1	146 57.8		22.7	2.8	36	11	57	35	0.44	1.0	1.0	A
	17	15	43	19.7	63 32.5	147 33.7		3.9	3.4	16	10	271	232	0.80	25.1	27.3	D
	17	17	1	52.1	57 25.6	139 21.6		32.6	3.5	6	4	325	281	0.25	41.3	99.0	D
	18	5	16	58.6	59 32.7	138 56.1		3.6	1.6	3	1	203	59	0.11	27.8	56.5	D
	18	6	56	44.6	60 3.7	141 33.1		14.2	1.7	16	10	124	27	0.38	1.3	1.1	A
	18	8	16	58.2	60 9.5	141 6.2		17.3	1.5	9	8	133	48	0.33	2.4	1.2	A
	18	9	17	52.3	60 38.8	142 47.2		1.3	1.4	5	3	139	52	0.23	3.0	76.5	D

EASTERN GULF OF ALASKA EARTHQUAKES (CONTINUED)

1977	origin hr mn	time sec	lat n deg min	long w deg min	depth km	mag	np	ns	gap deg	d3 km	rms sec	erh km	erz a km	
dec	18	17 51	57.0	60 15.5	141 2.7	10.4	1.0	6	4	190	47	0.27	7.0	10.7 D
	18	21 52	12.6	60 0.7	139 43.6	17.8	1.3	5	3	211	42	0.26	5.6	1.7 C
	19	8 19	12.5	59 56.6	141 53.1	3.6	1.3	8	6	217	48	0.37	7.7	3.4 B
	19	9 1	0.3	60 21.6	147 16.6	14.1	2.6	27	16	113	86	0.58	1.1	1.3 A
	19	13 53	27.1	60 37.6	147 36.9	14.0	2.0	24	16	144	63	0.59	1.5	1.0 A
	19	19 55	15.5	61 18.3	146 55.6	20.4	2.3	26	16	77	47	0.33	0.9	2.0 A
	20	20 51	45.9	61 35.0	141 57.2	0.0	1.9	8	5	244	135	0.37	4.6	1.1 B
	20	22 26	1.9	60 34.0	141 26.3	8.6	2.0	10	5	172	58	0.31	1.8	2.8 B
	21	7 24	39.5	60 15.3	140 50.5	0.1	2.1	13	5	160	47	0.38	1.8	3.5 B
	21	13 37	2.9	59 54.6	140 8.9	3.1	1.7	6	4	200	78	0.16	4.9	4.6 B
	21	21 3	23.0	61 30.4	146 27.5	25.1	2.3	14	7	84	68	0.39	1.3	2.2 A
	21	22 19	40.8	60 37.1	143 15.7	1.9	2.0	9	7	76	68	0.46	1.6	2.6 B
	22	7 50	3.5	60 14.7	140 57.8	0.2	2.4	7	3	240	104	0.28	3.8	3.3 B
	22	13 21	56.8	59 29.3	139 9.7	25.9	3.3	7	1	317	92	0.37	78.7	11.8 D
	22	16 35	4.5	60 3.0	141 6.3	0.0	2.0	10	6	116	47	0.35	1.3	3.5 B
	22	17 18	0.8	60 46.2	143 18.8	0.8	1.8	5	4	124	79	0.17	1.7	3.3 B
	22	21 31	0.9	60 11.4	141 48.2	24.9	1.9	5	4	226	87	0.14	6.7	3.0 C
	23	0 19	34.9	60 22.9	147 16.2	17.8	2.7	28	12	93	86	0.40	1.2	1.3 A
	23	2 54	12.2	61 35.1	146 35.6	24.4	2.6	21	12	101	62	0.32	1.1	1.8 A
	23	5 10	8.7	62 5.7	146 10.6	17.1	2.5	11	9	135	89	0.40	2.2	1.5 A
	23	15 38	29.1	60 8.9	141 12.2	10.6	1.7	8	5	148	53	0.32	2.5	2.0 B
	23	20 22	49.7	60 9.8	139 54.0	5.5	2.2	11	5	198	69	0.33	4.7	2.8 B
	23	22 50	55.8	61 35.0	146 9.0	27.0	1.9	11	9	98	58	0.42	1.0	1.3 A
	24	0 59	8.2	60 15.6	141 14.2	4.5	2.0	9	6	146	57	0.33	1.6	2.3 A
	24	3 24	14.0	60 3.9	141 30.0	14.5	2.8	23	2	119	26	0.44	1.3	0.9 A
	24	6 48	2.2	59 54.0	141 3.2	3.2	1.3	3	4	189	117	0.18	10.4	13.0 D
	24	10 57	24.1	60 2.3	141 23.3	13.8	1.5	6	3	166	41	0.18	3.9	1.7 B
	24	21 47	21.5	60 30.8	142 59.7	8.9	1.2	4	2	170	68	0.06	8.1	9.0 C
	25	1 11	33.5	59 20.4	144 44.8	14.4	3.1	29	18	188	98	0.34	2.7	1.7 B
	25	3 7	49.1	60 10.4	141 13.6	14.6	1.2	9	7	132	36	0.40	1.8	1.1 A
	25	9 2	14.3	60 45.9	139 57.0	0.5	1.8	9	7	228	126	0.42	2.9	2.4 B
	25	20 53	4.6	60 1.8	141 23.6	19.8	1.3	5	4	181	42	0.17	3.6	1.9 B
	26	5 13	29.8	59 46.4	141 24.5	3.1	1.3	8	5	239	68	0.20	2.9	7.2 C
	26	6 54	23.3	62 7.5	141 6.4	5.4	3.5	17	6	248	209	1.07	21.8	20.6 D
	26	7 33	26.9	60 24.6	143 16.0	0.5	1.8	9	8	173	80	0.37	1.6	3.2 B
	26	7 36	30.8	60 26.6	143 12.4	1.7	2.7	12	9	146	79	0.28	1.6	2.8 B
	27	12 50	50.0	61 2.8	146 28.7	18.2	1.9	18	11	75	36	0.52	1.0	0.6 A
	27	15 19	38.4	61 32.1	146 35.9	24.1	2.3	19	13	105	67	0.38	1.3	1.8 A
	28	4 38	26.0	60 9.0	139 53.9	0.2	1.3	6	5	222	87	0.25	6.1	5.8 C
	28	19 42	54.7	59 38.8	146 16.3	7.0	2.8	24	14	107	112	0.24	1.7	1.5 A
	29	2 23	47.0	58 34.2	137 41.8	13.0	2.3	5	3	344	189	0.07	68.9	16.7 D
	29	6 53	8.7	59 28.5	144 43.7	17.7	3.4	32	9	176	91	0.24	2.9	1.7 B
	29	16 18	3.4	59 26.3	138 52.8	13.0	1.5	4	3	307	70	0.44	9.5	1.3 C
	29	17 12	45.2	60 43.9	142 45.7	4.8	1.1	7	6	107	69	0.36	1.0	2.9 B
	29	18 28	38.7	60 7.5	141 28.7	2.9	1.1	7	4	175	68	0.22	1.6	2.3 A

EASTERN GULF OF ALASKA EARTHQUAKES (CONTINUED)

1977	origin time			lat n		long w		depth	mag	np	ns	gap	d3	rms	erh	erz	q
	hr	mn	sec	deg	min	deg	min	km				deg	km	sec	km	km	
dec	29	20	0	26.0	60 18.0	140 36.8		20.6	1.6	9	5	174	63	0.23	4.0	3.4	B
	29	21	48	18.7	61 41.0	146 26.6		24.0	3.6	31	5	99	62	0.47	0.9	1.5	A
	29	22	18	41.7	61 50.5	147 20.6		18.9	3.2	26	14	150	76	0.45	1.2	1.7	A
	29	23	29	15.6	60 37.5	143 14.6		46.1	1.1	4	3	135	68	0.10	5.5	12.1	D
	30	3	36	55.6	60 0.5	139 15.0		0.4	1.5	4	4	241	57	0.20	2.9	99.0	D
	30	3	37	6.9	58 47.9	144 5.0		32.3	2.5	8	7	265	211	0.16	7.0	99.0	D
	30	4	9	46.3	60 3.2	141 10.0		16.2	1.0	8	7	115	47	0.18	2.7	1.9	B
	30	5	37	35.5	59 46.5	141 15.4		10.2	1.4	3	3	232	153	0.15	4.5	4.8	B
	30	10	30	22.9	60 5.1	139 59.6		6.4	1.6	9	5	189	57	0.22	3.1	2.6	B
	30	16	5	9.8	58 21.6	136 48.5		16.2	3.7	6	1	349	239	0.85	99.0	81.4	D
	30	19	12	2.6	60 15.5	141 33.5		11.7	1.1	3	3	213	175	0.15	7.6	5.6	C
	30	20	58	38.0	60 18.4	143 10.3		0.2	1.8	8	8	157	79	0.44	2.0	2.9	B
	31	3	3	11.3	59 57.5	139 37.7		13.6	0.7	4	4	210	38	0.34	3.9	2.6	B
	31	6	4	58.8	61 25.9	147 49.5		20.6	2.3	22	14	82	50	0.50	1.3	1.8	A
	31	10	37	27.9	60 13.7	141 28.8		15.4	1.3	9	7	130	27	0.24	2.5	1.2	A
	31	17	28	35.9	60 18.3	140 50.4		11.9	1.3	9	8	176	50	0.51	2.1	2.1	A

Annual Report

Contract #03-5-022-55
Research Unit #251
Task Order #C1
Reporting Period: 04/01/77
03/31/78

SEISMIC AND VOLCANIC RISK STUDIES
WESTERN GULF OF ALASKA

H. Pulpan
J. Kienle

Geophysical Institute
University of Alaska
Fairbanks, Alaska 99701

March 20, 1978

TABLE OF CONTENTS

- I. ABSTRACT
- II. TASK OBJECTIVES
- III. FIELD AND LABORATORY ACTIVITIES
- IV. RESULTS AND PRELIMINARY INTERPRETATION

TABLES

FIGURES

APPENDIX I

APPENDIX 2

APPENDIX 3

OCS COORDINATION OFFICE

University of Alaska

Annual Report for Period Ending March 31, 1978

Project Title: Seismic and Volcanic Risk Studies --
Western Gulf of Alaska

Contract Number: 03-5-022-55

Task Order Number: C1

Principal Investigators: H. Pulpan, J. Kienle

I. Abstract

The seismic data gathering system has been performing very well after considerable changes had been made in connection with the annual service trip. Data gathered from the system has permitted to:

- (1) Delineate in detail the Benioff zone of the area.
- (2) Identify seismically several areas of special interest, including:
 - (a) an area of high rate of seismic strain release in the Benioff zone below the area of Iliamna volcano.
 - (b) a seismically active fault previously unmapped on Kodiak Island;
 - (c) an area of high level activity off the southwest coast of Kodiak Island;
 - (d) clusters of shallow seismicity, with high spatial and temporal variability along the volcanic axis;
 - (e) shallow seismic activity with linear trends near the recently formed Ukinrek Maars on the Alaska Peninsula.

Quantitative seismic risk assessments are presently in preparation.

Volcanological field operations included trips to the Ukinrek Maars, Augustine Volcano (collection of gases and rock specimens of the new lava dome), and Redoubt Volcano (geologic-petrologic

studies and studies of ice surface fluctuations).

A fairly comprehensive assessment of the hazard associated with Augustine Volcano is provided, based upon both historical data and detailed studies in connection with the 1976 eruption. A similar, preliminary assessment is provided for the volcanic risk associated with Redoubt Volcano.

II. Task Objectives

It is the purpose of this research to determine the seismicity of the lower Cook Inlet, Kodiak Island, and the Alaska Peninsula and to evaluate the seismic risk to onshore and offshore development, and also to evaluate eruption potential and volcanic risk of Redoubt and Augustine Volcanoes in Cook Inlet.

III. Field and Laboratory Activities

Seismology: Annual service, routine maintenance, and operation of the regional seismic network of 25 seismic stations constituted the largest portion of the field and laboratory activities and a very large portion of the total manpower devoted to the whole project. This was primarily a consequence of the necessity to redesign, reequip and recalibrate portions of the network in order to provide higher reliability and quality of data. However, since the July 1977 annual service trip the seismic network has provided high quality data at a high level of reliability. This is due to:

- 1.) Replacement of every field unit with laboratory tested and calibrated units.
- 2.) Installation of VHF preamplifiers at many VHF telemeter links in order to improve signal to noise ratios.
- 3.) Redesign of portions of the network layout (both physical relocation of stations, rerouting of signals, and elimination of stations).
- 4.) Manning of the Homer recording site during service trips and revisitation of sites until satisfactory signals were received there.

5.) Replacement of two self-installed VHF links with leased commercial telephone circuits.

The Kodiak Island and Alaska Peninsula portions of the network are technically the most difficult ones to operate, owing to the necessity of operating many VHF links in a daisy chain-like fashion with many stations at high altitudes having severe environmental conditions. These portions of the network were the least reliable, so most of the above changes were made in those areas. It will be a major concern of this year's annual service trips to reequip, recalibrate, and update stations of the Cook Inlet regional network.

A total of 185 man-days were expended on field trips, and on the operation and maintenance of the system during the one-year reporting period. Approximately the same amount went into preparation, repair and maintenance work in the laboratory at Fairbanks. We do not expect this to be necessary again; however, we do believe that this unusually high level of effort contributed strongly towards the first very successful operation of the system through a complete Alaskan winter.

From July 4 through July 14, 1977 we operated a three-component short period seismic system near Narrow Cape on Kodiak Island. This station, together with the permanent stations of the Kodiak Island network, provided land based data for the ocean bottom experiment off the south coast of Kodiak, conducted jointly by the United States Geological Survey and Lamont-Doherty Geological Observatory of Columbia University.

In connection with the formation of two maars on the Alaska Peninsula, a seismic station was installed close by in order to better monitor the seismicity associated with these features.

Three strong motion accelerometers (Kinematics SMA-1) were placed near the seismic stations PNM, BMT, and SII, respectively. These strong motion instruments are linked to the conventional short period seismic instrument in such a way that the amplifier output

of the conventional seismometer is grounded for 2.5 seconds whenever the strong motion instrument has completed a recording. This not only allows identification of the particular earthquake which caused the triggering of the strong motion instrument, but also allows absolute timing of the strong motion record.

Table 1 gives the three-letter station code, the coordinates, and altitudes of the seismic stations as presently operated. Figures 1 and 2 show the station layout before and after the 1977 annual service trip, respectively. Tables 2 and 3 give the percentage of station down time during the periods July through September and October through December, respectively. Figure 3 is a schematic diagram of the data flow from a typical remotely located seismic station.

Volcanology: During the past year we conducted field research at the Ukinrek Maars on the Alaska Peninsula and on Augustine and Redoubt Volcanoes in Cook Inlet.

Ukinrek Maars: Following the vent forming eruptions of March 20 to April 9, 1977, a field party from the University of Alaska (Kienle, graduate students Motyka, Carden, Lalla) and from Dartmouth College (Self, Bratton) spent eight days at Ukinrek to conduct reconnaissance geologic-petrologic, gas-chemical, thermal, geodetic and seismologic observations (using portable systems). The effort was sponsored by a Geophysical Institute - State of Alaska emergency fund.

From May 20 to 24, J. Kienle and J. Siwik installed a new seismic station at the maars to achieve better depth control of maar related seismicity. The addition of the new station required visits to adjacent repeaters and slight rearrangement of their telemetry. Logistic costs were covered by a U.S. Geological Survey emergency grant.

A ballistic and geodetic study to obtain energy levels of the vent forming explosions was conducted from August 27 to September 1 by J. Kienle, J.-P. Huot, R. Motyka and V. Ferrell, logistically funded by the State of Alaska.

Augustine Volcano: With U.S. Army helicopter support, J. Kienle and D. Johnston spent two days (July 18, 19) on Augustine's summit to collect gases and rock specimens of the new lava dome.

A helihut shelter, supplied by the Geophysical Institute and equipped with State of Alaska funds, was hauled to Kenai and with U.S. Army support airlifted to Chinitna Bay. It still needs to be moved the final leg to Augustine, where it will replace the base camp destroyed in the recent eruptions.

On September 3, with OCS logistic support, a team of graduate students (Lalla, Pearson, Huot) conducted heat flow measurements on the 1976 pyroclastic flows on the NE side of the volcano.

Redoubt Volcano: With logistic support from the U.S. Army a Geophysical Institute team consisting of a volcanologist (J. Kienle), a glaciologist (C. Benson), one graduate student (D. Johnston) and Sgt. R. Schrupf spent four days (July 14-17) on Redoubt's summit for reconnaissance geologic-petrologic studies and to establish geodetic base lines for follow-up photogrammetric work designed to monitor fluctuations of the crater ice surface in response to volcanic heating.

During these operations OCS supported 34 man-days for the principal investigator (J. Kienle).

IV. Results and Preliminary Interpretation

1. Seismicity

General Remarks: The seismicity of the study area displays the classical features of a plate subduction area. Seismic activity below 50 km depth is exclusively associated with a Benioff zone, which presently appears to be about 30-40 km thick and reaches a maximum depth of about 200 km. There are indications of a kink in the dip of the zone at about 100 km depth, but a more definite statement in this respect will require more than just routine determination of hypocenters. The strike of the dipping plate changes, apparently smoothly, along the arc structure (Figures 4 through 9). The depth to the top of the seismic zone beneath the line of volcanoes is approximately 100 km.

The level of seismic activity in the Benioff zone is not uniform in space. There is an area of intense activity near Iliamna volcano (Figure 10). This is the source area of some of the largest earthquakes that occurred during the past year (Nov. 27, 1977, magnitude 5.3; Dec. 27, 1977, magnitude 6.0) in the study area. There appears, also, to be a definite drop in the Benioff zone seismicity southwest of Becharof Lake on the Alaska Peninsula and southwest of the west coast of Kodiak Island (Figure 11). This boundary, roughly coinciding with the western margin of the 1964 earthquake aftershock zone, might be the expression of the eastern boundary of the Shumigan seismic gap.

The shallow seismicity in the study area is by and large diffuse (Figures 12 and 13), without any apparent preferred association with known major fault systems such as the Bruin Bay fault, the Border Ranges fault, the Castle Mountain fault, or the Homer fault. This does not imply, however, that these faults are seismically inactive, but rather that they do not constitute the sole or prime shallow tectonic features in the area that have to be considered in seismic risk analysis.

Areas of Special Interest

Deadman Bay (Kodiak Island): A linear, shallow seismic trend with all the earmarks of a seismically active fault has emerged near Deadman Bay (near the station DMB on Figure 2). A series of shallow events, with the largest having magnitude 3.7, occurred primarily in August 1977. This series maps as a linear feature (Figure 14). To the best of our knowledge no fault has ever been mapped in this area. Events in this area from February 1976 through December 1977 are listed in Table 4. This cluster does indicate the network's capability to detect seismically active faults.

South Kodiak Offshore Area: Shallow, above magnitude 4 events occur frequently in the area off the southwest coast of Kodiak. The largest of these shallow events during the time span from February 1976 through February 1978 was one with magnitude 4.8. There is presently no clear correlation of these events with faults or slump areas mapped on BLM's Outer Continental Shelf Office map (see Figure 14). We shall investigate any such correlation as soon as the latest results of the submarine fault mapping program of Research Unit 327 are available to us. Since this area of high activity (which can be traced back to times prior to the 1964 Alaskan earthquake) lies in a potential lease area of the OCS it deserves special attention. We shall use special location techniques in order to determine hypocenters in that area, which lies actually outside the seismic network, and thus makes location more error-prone. A list of the events in the area between February 1976 and February 1978 is given in Table 5. However, this list is heavily biased towards the time period from July 1977 through February 1978, as the seismic network in this area was not operating very reliably during the pre-July 1977 period.

Cook Inlet Offshore Areas: Though the shallow seismicity in Cook Inlet is quite diffuse, as can be seen from Figure 12, a few linear seismic trends do appear. Certain of these trends fall close to some of the fault scarps mapped by Bouma and Thompton (Research Unit 327) and are probably associated with them.

Shallow Clusters Associated with Volcanoes: Several clusters of shallow seismic activity with high variability in space and time have been observed. Some of these, located near Snowy Mt., Magiek, and Mt. Katmai, respectively, might be associated with magma chambers inferred by Matumoto (1971) (Figure 15). Though probably not of any consequence with respect to seismic or volcanic risk associated with offshore developments, these clusters do indicate the rather high resolution and low detection threshold of the seismic network.

Volcano associated shallow activity has also been observed at Mt. Douglas, Augustine Island and Iliamna volcanoes.

Seismic Risk Studies

Seismicity data, both historic and from our own network, are now being incorporated into a seismic risk analysis of the study area. This analysis will provide a quantitative expression of the seismic threat risk. The analytical methods follow those of Cornell (1968) and Merz and Cornell (1973). Computer algorithms have been adapted and developed; results will be available during 1978.

2.) Volcanology

Augustine Volcano

We have now compiled a fairly complete eruptive history of Augustine Volcano since its discovery by Captain Cook in 1778. We have determined its structure and plumbing geochemically, magnetically and through a refraction seismic fan shooting experiment. Its cone has a base diameter of 10 km and is 1.3 km high, which corresponds to a volume of about 17 km^3 . Augustine's eruptions typically begin with energetic vent clearing eruptions, a phase which is followed by the arrival of new dacitic andesite melt, usually forming a new dome. The volcanic cone consists now of a central complex of lava domes, mantled by almost exclusively pyroclastic flows, mudflows and rock avalanches, which reflects the high explosiveness of the volcano. In the last 100 years it has erupted four times (1883, 1935, 1963/64, 1976) with an average repose time between eruptions of about 30 years, a time interval that is probably characteristic of the recharge rate of a shallow magma chamber. The 1976 eruption occurred only 12 years after the previous eruption and gave us a unique opportunity to witness one complete eruptive cycle after five years of research on the volcano. We now have two more years of observations following the eruption. The volume of new material ejected in 1976 on the island was about 0.2 km^3 and the regional ashfall, extending north to Anchorage and east to Sitka, amounted to about 0.3 km^3 . Tropospheric ash was observed as far south as Arizona, and stratospheric dust was detected up to five months after the eruption at Moana Loa, Hawaii. The thermal energy released in the 1976 eruption was about 4×10^{24} ergs. In comparison, the pyroclastic debris of the 1963/64 eruption was about 0.1 km^3 (Detterman, 1968). Of the four historic eruptions the 1833 and 1976 eruptions were probably of similar magnitude and considerably more powerful than the 1935 and 1963/64 eruptions. The present cone consists of about 14.7 km^3 debris flows, 1.5 km^3 of plug material concentrated in the center of the volcano and about 1.7 km^3

of uplifted Mesozoic sediments on the south side of the cone. Assuming an average eruption interval of 30 years with typical volumes of fragmental ejecta of about 0.1 to 0.2 km³, one can estimate the age of the volcano from the total volume of the debris flows. We obtain an age range of the volcano from 2,200 to 4,400 years. This very young age may not be as unreasonable as the gross assumptions suggest. At one locality on the south slope of the volcano, at an elevation of 900 feet, we found glacial debris on a surface which truncates Mesozoic sediments. The layer containing glacial erratics is overlain by what we assume to be the oldest Augustine volcanics. The Wisconsin deglaciation was at its peak about 12,000 years ago in Cook Inlet, which means that the volcano cannot be older than 12,000 years and, based on its short eruptive history, is probably much younger, perhaps as young as 4,500 years.

Onshore and offshore hazards posed by Augustine have been summarized in previous reports (e.g. Annual Report of March 31, 1977, tables 1-3, pp. 98-107). Presently, we are preparing a hazard report to be published by the State of Alaska, Department of Natural Resources, Division of Geological and Geophysical Surveys. Because Augustine is so small (5 km radius) there are simply no sites on the island itself that would be safe to erect permanent structures unless they were underground. The principal offshore hazards, as we see it, are pyroclastic flows, one of which produced tidal waves in 1883 that crossed the entire Lower Cook Inlet to the east. Pyroclastic flows or glowing avalanches are always accompanied by subjacent glowing clouds (nuees ardentes). A small glowing cloud was observed on February 9, 1976, by the crew of a University of Washington research aircraft. The cloud travelled at a speed of 50 m/sec (180 km/hr) on the upper slopes, slowing to 6 m/sec (22 km/hr) near the shore where it eventually stopped. Several glowing clouds overran our Burr Point base camp 5 km north of the summit crater during the much more violent vent clearing eruptive phase in late January, 1976. We have, therefore, some documentation of the damage of such clouds to man-made structures. There is geophysical

evidence that in Augustine's past history several glowing avalanches entered the sea and travelled for distances of at least 5 km offshore. Both the 1883 and 1976 eruptions enlarged the island through pyroclastic flows. Unfortunately, very little is known about the mechanism of emplacement of pyroclastic flows and one is forced to resort to accounts of historic eruptions. The famous 1902 eruption of Mt. Pelee in the West Indies produced a glowing cloud of 700 - 1000° C temperature which detached itself from the basal glowing avalanche and overran the city of St. Pierre, 6.4 km (4 miles) from the volcano. Within minutes 30,000 inhabitants died from inhalation of hot dust and gas. Stripping of clothing attests to the force of the blast and opened skull sutures are indicative of a sudden heat intense enough to turn water in human tissues to steam but not of long enough duration to burn fabrics. The ash layer in St. Pierre was only 1 foot thick. The main unanswered problem at Augustine concerns the distances to which larger glowing clouds would travel across the sea and how far the basal glowing avalanche would travel offshore along the sea floor.

Other offshore hazards include regional ashfalls, acid rains, lightning storms, noxious fumes and falling volcanic bombs. Ballistic considerations indicate that large volcanic bombs will generally be restricted to a range of less than 10 km from the volcano.

We observed earthquake precursor activity at least four months prior to the January 1976 eruptions and believe that continued careful geophysical monitoring of the volcano will allow us to at least anticipate, if not predict, future eruptions.

Redoubt Volcano

We have now assembled in some detail the events of the 1965-68, 1933 and 1902 eruptions. In general, the volcano appears to be much less explosive than Augustine as indicated by the predominance of lava rather than pyroclastic flows. It is interesting to observe

that in this century Redoubt tended to erupt within a few years of Augustine, i.e., exhibited a similar periodicity. Redoubt is a much more mature (older) volcano than Augustine, more than twice as high and heavily glaciated. The principle hazard of Redoubt arises from melt water accumulations in the glaciated summit crater (1 x 1.6 km in size, at an elevation of 8,000 - 8,500 ft.). Increased heat flux associated with the 1966 eruptive cycle resulted in two crater outburst floods in January, 1966, which caused a break up of the Drift River in mid-winter and two flash floods in that valley. Such flooding poses a direct threat to the Drift River Tanker Terminal. Presently, the upper Drift River is nearly dammed up by the 1966 ice cored mudslide off Redoubt's summit (Post and Mayo, 1971). A second slide of similar dimensions occurs a few miles upstream. Future slides could easily dam up the valley, creating a lake that could drain catastrophically.

During three days of field work at Redoubt's summit in July 1977, we have surveyed prominent landmarks surrounding the crater and ran several level lines across the crater floor, which will allow us to prepare a high resolution topographic map of the snow surface from aerial photography. This map of Redoubt summit is now being prepared by North Pacific Aerial Surveys in Anchorage. Similar maps will be produced from available photography taken by the U.S. Geological Survey in 1954 and 1957 (i.e., prior to the 1966-68 eruptive cycle). By comparing these maps we will be able to determine the long-term volume changes of the ice in the crater for the past 23 years, and through resurveys in the future. As demonstrated at Wrangell Volcano by the Geophysical Institute's glaciology group and on Mt. Baker (Malone and Frank, 1975), this kind of "calorimetry" yields valuable information about the changing heat flux beneath a glaciated volcano.

Preliminary snow accumulation studies indicate large snow accumulation rates at more than 10 m per year at the summit of Redoubt.

Hand specimen and gases were collected from all outcrops that could be climbed to at the summit of the volcano.

This year we are planning to address this problem in a field study. Clearly, any potential further expansion of the Drift River facility in response to the development of Lower Cook Inlet requires a careful assessment of this obvious volcanic hazard.

Latest Significant Observations

The most significant new discovery in recent months (July-December, 1977) is the detection of shallow earthquake swarms of high temporal and spatial variability beneath the volcanic axis. Clusters of shallow earthquakes have been identified recently with our regional seismic network in the volcanic section extending from Mt. Martin to Snowy Mt., where we located a particularly intense cluster of events. At a first glance, the clusters appear to coincide with the position of shallow magma chambers (less than 10 km deep) located by Matumoto (1971) beneath Martin/Mageik and Snowy Mt. Additional clusters occur near the newly formed Ukinrek Maars near Mt. Peulik (April, 1977) and in the Mt. Douglas- Fourpeaked Mt. area. Presently, we are not sure of the longevity of this seismicity and its significance in terms of future volcanic activity.

Recommendations for Future Research

- 1) Completion of the Redoubt hazard study and focus on the volcanic hazard to the Drift River Tanker Terminal facility.
- 2) Offshore investigation of the submarine extent of Augustine pyroclastic flows and their chronology.
- 3) First stage reconnaissance of Douglas Volcano, the Snowy Mt. - Mt. Martin volcanic section, reactivation of the Katmai seismic station.
- 4) Transition into a monitoring program for Augustine and Redoubt Volcanoes with the goal of eventual eruption prediction.
- 5) Establishment of a volcano warning system, coordinated between industry and the agency involved in volcano monitoring.

References

- Cornell, C. A., 1968. Engineering seismic risk analysis, Bull. Seism. Soc. America, 58(5), pp. 1583-1606.
- Detterman, R. L., 1968. Recent volcanic activity on Augustine Island, Alaska, U.S. Geol. Survey Prof. Paper 600-C, pp. C126-C129.
- Malone, S. D., and D. Frank, 1975. Increased heat emission from Mount Baker, Washington, EOS, 56(10), pp. 679-685.
- Matumoto, T., 1971. Seismic body waves observed in the vicinity of Mount Katmai, Alaska, and evidence for the existence of molten chambers, Bull. Geol. Soc. Am., pp. 2905-2920.
- Merz, H. A., and C. A. Cornell, 1973. Seismic risk analysis based on a quadratic magnitude-frequency law, Bull. Seism. Soc. America, 63(6), pp. 1999-7006.
- Post, A., and R. Mayo, 1971. Glacier dammed lakes and outburst floods in Alaska, U.S. Geol. Survey, Hydrologic Investigations Atlas HA-455.

Ukinrek Maars

A report on our field reconnaissance and the seismicity to date is included as Appendix 3.

UNIVERSITY OF ALASKA
 LOWER COOK INLET, KODIAK ISLAND,
 AND ALASKA PENINSULA SEISMIC NETWORK

STATION NAME	CODE	LATITUDE (NORTH)	LONGITUDE (WEST)	ELEVATION (METERS)	COMPONENTS
AUGUSTINE IS. FLOW	AUF	59 23.27	153 27.45	166	SPZ
AUGUSTINE IS. KAMISHAK	AUK	59 20.05	153 25.62	259	SPZ
AUGUSTINE IS. MOUND	AUM	59 22.26	153 21.17	106	SPZ
AUGUSTINE IS. PINNACLE	AUP	59 21.73	153 25.23	1033	SPZ
BLUE MOUNTIAN	BMT	58 02.8	156 20.2	548	SPZ
CAPE DOUGLAS	CDA	58 57.32	153 31.77	386	SPZ
CHIRIKOF ISLAND	CHI	55 48.5	155 38.6	250	SPZ
CHOWIET ISLAND	CHO	56 02.0	156 42.7	160	SPZ
DEADMAN BAY	DMB	57 05.23	153 57.63	300	SPZ
FEATHERLY PASS	FLP	57 42.7	156 15.9	485	SPZ
HOMER	HOM	59 39.50	151 38.60	198	SPZ
MAARS	MAA	57 51.40	153 04.82	131	SPZ
MCNEIL RIVER	MCN	59 06.06	154 11.99	273	SPZ
MIDDLE CAPE	MMC	57 20.00	154 38.1	340	SPZ
OIL POINT	OPT	59 39.16	153 13.78	625	SPZ
PINNACLE MOUNTIAN	PNM	56 48.3	157 35.0	442	SPZ
PUALE BAY	PUB	57 46.4	155 31.0	280	SPZ
RASPBERRY ISLAND	RAI	58 03.63	153 09.55	520	SPZ
REDOUBT VOLCANO	RED	60 25.14	152 46.32	1067	SPZ
SHUYAK ISLAND	SHU	58 37.68	152 20.93	34	SPZ
SITKINAK ISLAND	SII	56 33.60	154 10.92	500	SPZ, SPE-W
SITKALIDAK ISLAND	SKS	57 09.85	153 04.82	135	SPZ
SPIRIDON LAKE	SPL	57 45.55	153 46.28	600	SPZ
UGASHIK LAKE	UKL	57 24.1	156 51.3	410	SPZ
YELLOW CREEK BLUFF	YCB	56 38.9	158 40.9	320	SPZ

Table 1

Percent Downtime of Seismic Stations

Station	October 1 - December 31, 1977
AUF	0
AUK	0
AUM	0
AUP	100 ¹
BMT	0
CDA	0
CHI	0
CHO	0
DMB	100 ¹
FLP	0
HOM	10 ²
MAA	0
MCN	0
OPT	0
PNM	0
PUB	0
RAI	0
RED	0
SHU	0
SII	0
SKS	0
SPL	0
UKL	0
YCB	0

1. Signal lost late August, 1977.
2. Sensor removed for use as spare during service period. Was reinstalled during October.

Table 2

Percent downtime of seismic stations - October 1 - December 31, 1977

Percent Downtime of Seismic Stations

Station	December 1 - March 15, 1977
AUF	90
AUK	0
AUM	0
AUP	100 ¹
BMT	0 ²
CDA	0
CHI	10 ³
CHO	10 ³
DMB	100 ¹
FLP	0 ²
HOM	0
MAA	0 ²
MCN	0
OPT	0
PNM	0 ²
PUB	0 ²
RAI	10 ³
RED	0
SHU	10 ³
SII	0
SKS	0
SPL	10 ³
UKL	0 ²
YCB	0 ²

1. Signal lost late August, 1977.
2. At these stations, under adverse weather conditions, signals became noisy due to poor VHF transmission. Noise bursts last typically on the order of one minute. Data lost due to these transmission problems are less than 1%.
3. At these stations noisy signal due to poor VHF transmission under adverse weather conditions is more frequent than in (2) above. Data loss is about 5-10 percent in winter time.

Table 3

Percent downtime of seismic stations - December 1 - March 15

DATE	ORIGIN	LAT	LONG W	DEPTH	MAG	NO	GAP	DMIN	RMS	ERH	ERZ	QM	
770621	532	47.99	57-13.02	153-55.13	15.98	0.	15	135	14.7	1.82	15.2	15.1	C1
770719	943	51.06	57- 7.60	153-55.73	35.28	1.74	4	140	4.8	0.	0.	0.	C1
770719	1426	7.87	57-13.63	153-48.26	5.00	1.24	3	176	18.2	0.	0.	0.	C1
770729	1610	15.76	57- 5.91	153-56.66	27.72	1.95	5	112	1.6	0.03	0.5	0.8	C1
770803	1452	44.06	57-11.73	153-46.45	44.94	2.48	4	153	16.5	0.03	0.	0.	C1
770808	1808	39.74	57- 4.59	153-56.00	36.54	3.70	26	115	2.0	0.74	3.4	2.3	C1
770812	1436	57.75	57- 6.21	153-55.46	40.18	1.89	4	148	2.8	0.	0.	0.	C1
770816	1154	30.54	57- 1.70	153-57.57	35.45	2.00	4	120	53.1	0.	0.	0.	C1
770818	1503	11.49	57- 8.58	153-50.09	58.58	2.83	9	111	45.7	0.26	3.0	6.1	C1
770818	1514	22.02	57- 7.07	153-53.92	30.63	1.93	9	112	5.1	0.30	2.4	2.3	C1
770826	1259	41.61	57- 4.81	153-57.17	33.41	1.82	4	114	50.0	0.	0.	0.	C1
770831	159	25.74	57- 4.55	153-56.11	5.00	2.11	3	135	51.1	0.	0.	0.	C1
770901	1226	55.42	57- 2.81	153-57.16	37.31	1.71	4	118	52.1	0.	0.	0.	C1
770913	916	38.73	57- 3.04	153-59.34	32.10	1.92	7	115	50.2	0.19	1.9	2.0	B1
771006	225	20.44	57- 2.09	153-59.47	32.13	1.96	4	118	51.2	0.	0.	0.	C1
771104	642	49.50	57-11.07	153-50.38	0.88	1.49	4	104	46.0	1.88	0.	0.	D1
771105	2033	39.92	57- 5.91	153-57.09	24.82	2.98	15	111	48.9	0.68	3.7	3.7	C1
771112	1126	44.84	57- 7.47	153-54.91	10.87	2.61	7	110	49.3	0.40	3.36	11.2	C1
771218	609	17.72	57- 8.81	153-47.47	10.15	0.69	4	205	43.0	0.14	0.	0.	C1
771220	1819	35.58	57- 0.05	153-59.92	36.01	2.42	7	121	50.4	0.15	1.7	1.4	B1
771221	1458	1.03	57- 2.47	153-56.87	36.58	1.77	5	120	52.8	0.03	0.5	0.6	C1
780117	444	59.44	57- 5.46	153-57.85	25.80	2.41	7	111	48.7	0.27	2.6	3.2	C1
780120	251	54.52	57-10.53	153-59.52	17.45	2.61	6	98	55.1	0.40	5.4	79.7	D1

Table 4. Hypocenter parameter of events in Deadman Bay area between July 1977 and February 1978. For explanation of heading see Appendix 1.

DATE	ORIGIN	LAT	LONG W	DEPTH	MAG	NO	GAP	DMIN	RMS	ERH	ERZ	QM
760322	4 3	3.67	56-49.21	154- 5.83	35.16	0.	4	339240.2	0.73	0.	0.	D1
760805	330	20.25	56- 9.95	154-18.00	27.92	0.	4	343314.1	0.23	0.	0.	C1
760903	1243	57.36	56-46.09	152- 0.91	1.25	3.20	8	335112.814	0.03726	2956.5	0.	D1
760908	252	19.08	56-19.39	153-26.21	5.00	0.	5	336312.7	5.16607	2224.3	0.	D1
761022	1835	24.48	56- 3.76	153- 8.39	26.26	0.	20	267 85.0	0.52	13.1	4.7	D1
761022	1841	39.52	56-19.50	153- 1.57	1.25	0.	12	276 76.0	1.48	33.6	66.1	D1
761025	1727	43.01	56-36.40	153-40.90	33.30	0.	7	235 31.2	0.14	3.3	1.2	D1
770202	714	35.84	56-57.40	152-34.54	33.36	2.09	6	332 88.2	0.02	12.1	2.2	D1
770202	717	12.13	56- 5.48	152-29.78	5.00	3.60	12	305184.5	0.41	21.3	18.8	D1
770202	752	22.82	56- 3.55	152-18.87	28.62	3.55	11	306188.4	0.47	35.75	99.7	D1
770216	428	13.48	56-18.56	151- 7.37	2.50	3.92	4	334353.2	0.73	0.	0.	D1
770219	1615	27.35	56-15.52	153-17.69	7.83	3.05	4	313200.8	0.25	0.	0.	C1
770413	56	53.40	56-31.03	152-38.19	0.08	2.79	12	262 95.313	63287.0603	0.	0.	D1
770530	1541	58.90	56-57.29	151- 1.68	5.00	2.38	3	289178.8	1.99	0.	0.	D1
770530	2302	44.45	56-57.03	151-25.60	2.50	2.58	7	287107.310	56281.7325	2.	0.	D1
770610	1314	9.34	56-57.61	153-38.83	22.00	2.10	5	178 23.7	0.29	11.0	20.9	D1
770615	918	20.79	56- 4.21	152-57.30	10.31	3.61	11	257129.0	0.37	8.9	12.3	D1
770615	1112	47.43	56-44.00	153- 9.28	23.59	2.32	4	289 63.0	0.01	0.	0.	C1
770621	2	40.64	56-31.09	153-25.26	38.70	0.	7	303271.5	3.03302	9.	0.	D1
770709	941	10.83	56-56.75	153- 9.26	32.68	2.57	6	212 51.5	0.19	3.7	3.0	D1
770709	1011	25.57	56-55.79	154- 2.78	29.22	1.22	4	175 18.3	0.	0.	0.	C1
770715	1327	7.91	56-57.86	153-39.65	37.11	2.45	6	158 22.8	0.09	1.3	0.9	C1
770716	9 9	48.26	56-50.20	153-33.22	48.53	1.93	4	193 37.3	0.	0.	0.	C1
770719	1631	46.05	56-19.47	153-57.99	32.47	2.60	5	293 29.4	0.09	6.7	1.2	D1
770728	149	20.55	56-55.53	153-46.57	5.00	1.98	3	154 21.2	0.	0.	0.	C1
770729	2019	5.86	56-36.99	153-17.74	7.54	1.68	4	251 54.8	0.45	0.	0.	D1
770806	1210	23.01	56-56.27	151- 1.57	39.64	3.77	12	290126.3	0.61	30.87	48.7	D1
770810	620	27.16	56-56.88	154-23.09	3.56	1.86	4	177 30.1	0.	0.	0.	C1
770810	935	55.96	56-24.21	152-39.99	32.57	4.84	24	203 88.4	0.57	5.9	3.0	D1
770810	1114	58.95	56-19.89	152-37.49	34.50	3.50	19	250 96.8	0.78	11.0	4.6	D1
770810	1738	26.17	56- 1.38	151-54.93	2.95	2.98	6	275145.8	0.82	24.0	36.9	D1
770811	2147	45.28	56-53.86	153-53.74	5.00	2.28	3	146 21.5	0.01	0.	0.	C1
770827	351	46.28	56-38.05	151-36.28	23.02	4.00	19	236107.6	0.50	7.6	3.6	D1
770830	2045	0.30	56-21.82	152-42.66	31.56	3.81	20	233 92.0	0.42	5.8	2.6	D1
770830	2047	24.04	56- 9.19	152-17.72	7.42	3.60	7	261178.0	0.27	23.2	12.5	D1
770904	440	29.40	56-29.40	154- 6.47	33.82	2.43	7	290 9.0	0.25	6.5	2.4	D1
770905	635	1.03	56-38.91	153-42.86	5.00	1.67	3	217 30.4	0.10	0.	0.	C1
770912	1538	49.21	56-10.01	152-14.17	9.82	2.52	4	275127.9	0.20	0.	0.	C1
770913	1836	48.44	56-53.49	154-24.65	5.00	2.05	3	185 39.5	0.	0.	0.	C1
770919	1007	5.12	56-46.29	153-45.65	38.36	2.83	10	184 34.9	0.34	3.7	1.8	D1
770919	1530	9.10	56-27.44	153-33.27	30.34	2.22	4	266 40.3	0.	0.	0.	C1
770921	1449	53.88	56-25.71	152-43.12	25.10	4.12	23	201 84.9	0.56	5.8	3.0	D1
771018	1648	34.34	56-58.10	153-59.91	29.37	1.89	5	125 46.8	0.25	4.1	5.1	D1
771024	1828	36.09	56-43.08	154-14.65	5.00	2.32	7	144 18.0	2.50	76.81	59.3	D1
771024	1832	2.31	56-26.01	153-48.09	32.26	2.42	7	273 27.3	0.32	9.3	2.5	D1
771103	1133	23.62	56-56.45	152-57.32	6.73	2.91	9	223 26.0	0.96	13.8	9.7	D1
771104	415	45.79	56-49.79	154- 8.93	61.19	2.13	7	247 63.4	0.19	6.1	6.3	D1
771104	859	17.97	56-28.07	153-22.86	32.95	2.29	5	268 50.4	0.10	4.9	1.5	D1
771104	19 5	5.13	56-54.06	153-16.15	5.00	2.07	3	274 28.1	0.04	0.	0.	C1
771105	15 5	57.38	56-53.79	152-39.10	25.28	3.52	21	211 39.6	1.22	12.0	5.7	D1
771107	532	28.88	56-19.19	151-49.57	0.81	3.68	15	255121.4	0.42	9.3	24.6	D1
771111	049	42.90	56-32.41	153- 4.61	28.42	3.43	11	257 67.9	0.49	10.9	3.3	D1
771115	1555	21.35	56-12.03	152-58.60	32.74	3.01	11	285 84.5	0.51	21.8	4.1	D1
771123	533	17.31	56-30.03	152-48.34	25.09	4.20	23	262 75.8	0.53	7.9	2.7	D1
771128	231	23.25	56-27.30	153-24.29	32.50	2.54	5	270 49.3	0.10	5.2	1.6	D1

Table 5. Hypocenter parameter of events in southwest offshore area of Kodiak Island between February 1976 and February 1978. For explanation of heading see Appendix 1.

771128	339	29.97	56- 6.42	153- 5.44	17.72	2.73	5	306	84.3	1.29	181.9	48.6	D1
771205	328	3.20	56-52.75	153-23.24	32.11	4.16	22	203	36.8	0.35	2.8	1.4	D1
771211	1704	15.87	56-47.61	153-13.53	9.00	2.82	4	293	42.2	0.43	0.	0.	D1
771228	549	10.79	56-20.03	152-36.76	23.71	2.77	8	275	96.8	0.55	24.2	6.7	D1
771231	545	14.26	56-15.79	153-10.18	33.78	2.79	10	283	70.7	0.43	18.6	3.3	D1
771231	555	36.13	56-27.23	153-13.24	24.88	3.00	8	264	60.4	0.39	11.5	3.6	D1
771231	617	27.69	56-16.97	153- 8.78	34.73	3.37	8	281	71.0	0.26	11.8	2.3	D1
780101	2116	8.24	56- 1.37	154-20.95	35.42	4.09	13	224	60.7	0.54	8.4	3.1	D1
780105	2100	13.43	56- 3.31	154-23.44	36.99	4.36	14	251	57.7	0.50	8.6	3.2	D1
780108	2213	56.68	56-56.87	153-12.77	31.58	3.90	18	208	25.4	0.33	3.0	1.4	D1
780108	2221	58.42	56-57.16	153-11.94	32.85	3.03	8	208	24.6	0.25	4.1	2.3	D1
780119	1833	42.34	56-29.31	153-26.69	34.96	3.17	12	258	46.1	0.45	11.5	2.8	D1
780204	2044	38.66	56-56.37	153-43.43	2.50	2.11	4	251	46.3	0.73	0.	0.	D1
780209	1418	37.54	56-38.79	154- 2.84	5.00	2.71	3	175	12.7	0.	0.	0.	C1
780212	1400	57.52	56-59.09	153-13.56	33.72	2.99	7	204	21.8	0.11	1.9	1.1	C1
780213	352	59.66	56-12.91	153-19.70	35.97	4.19	8	267	65.2	0.24	9.5	2.1	D1
780213	403	0.75	56-15.34	153-21.77	37.82	3.47	6	274	60.9	0.15	8.2	1.9	D1
780213	1058	24.76	56-27.69	153-34.63	32.84	2.99	7	265	38.8	0.12	3.7	1.0	D1
780218	550	0.09	56-36.99	154-14.50	21.64	1.75	5	172	7.3	0.06	1.7	1.5	C1

Table 5. Continued.

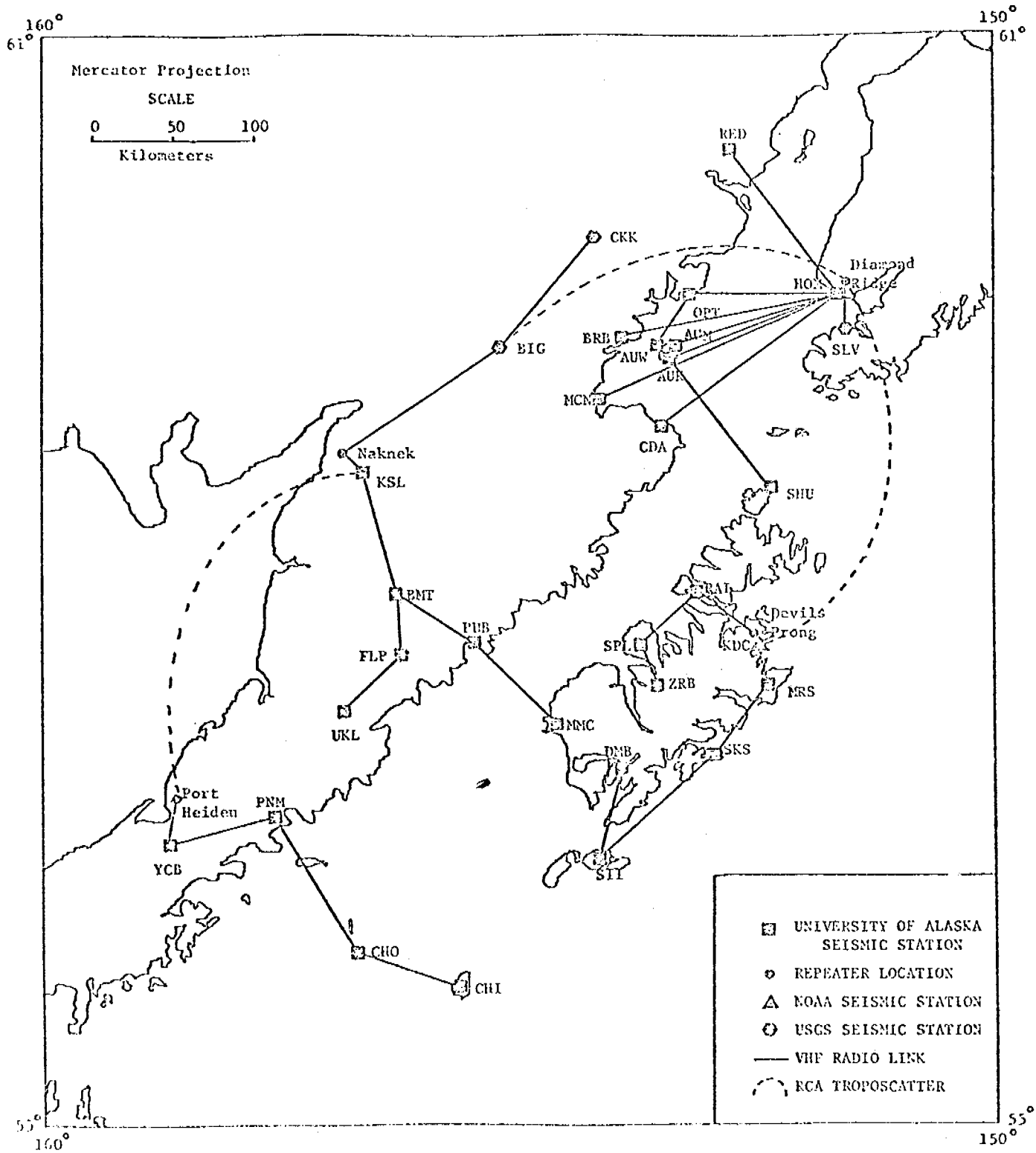


Figure 1. Layout of seismic station before July 1977.

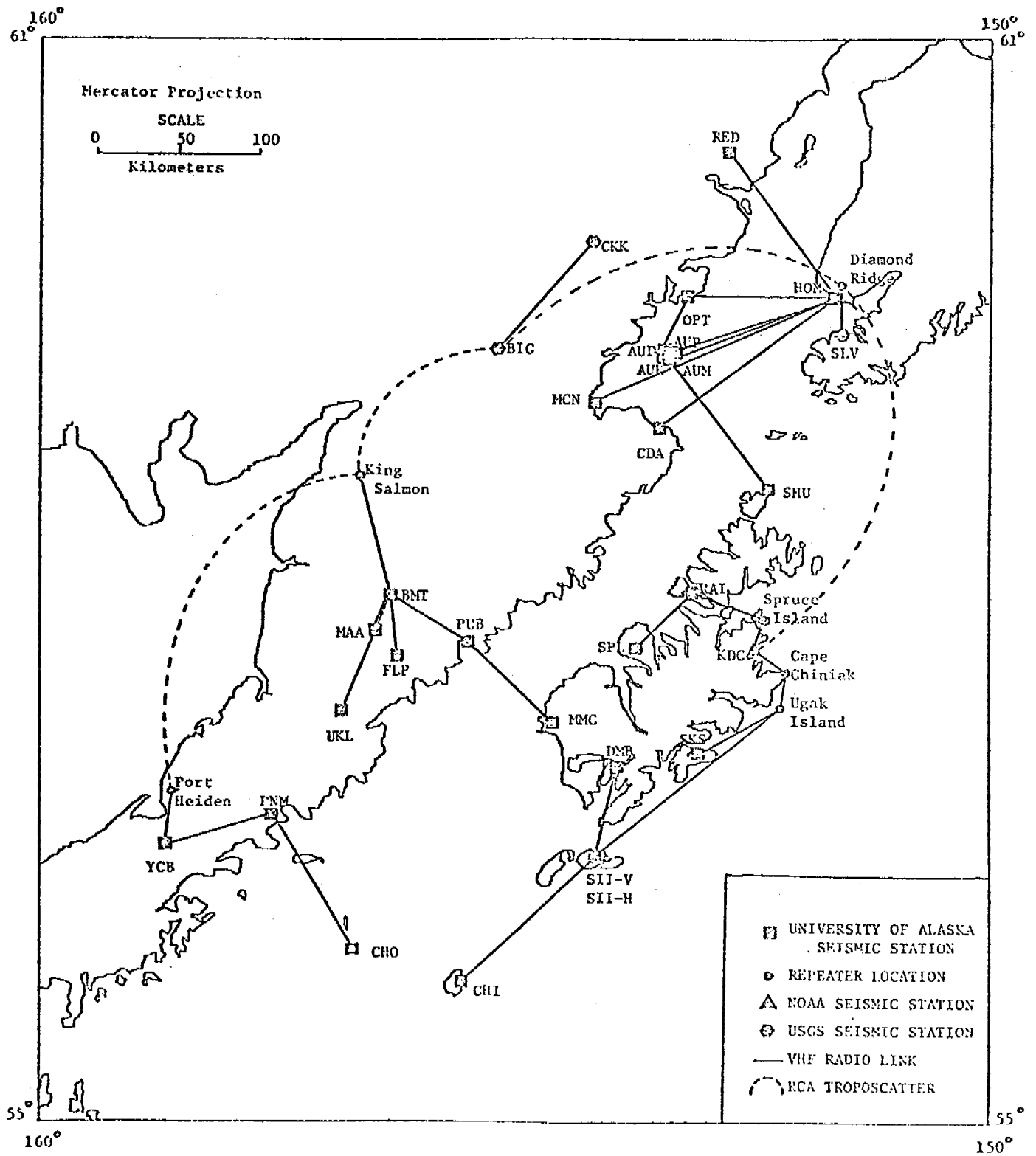


Figure 2. Layout of seismic stations after July 1977.

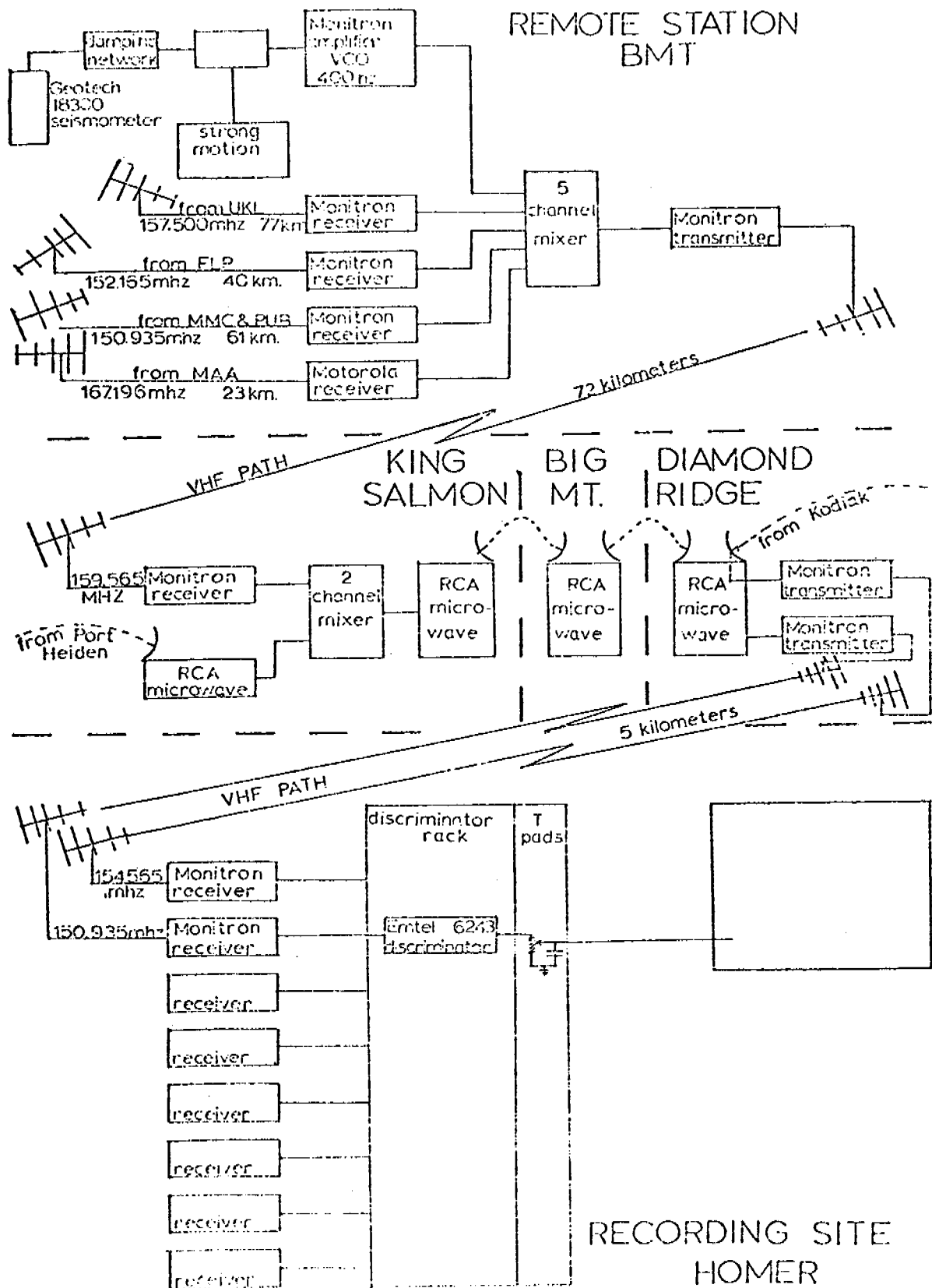


Figure 3. Schematic diagram of data flow from typical remote seismic station.

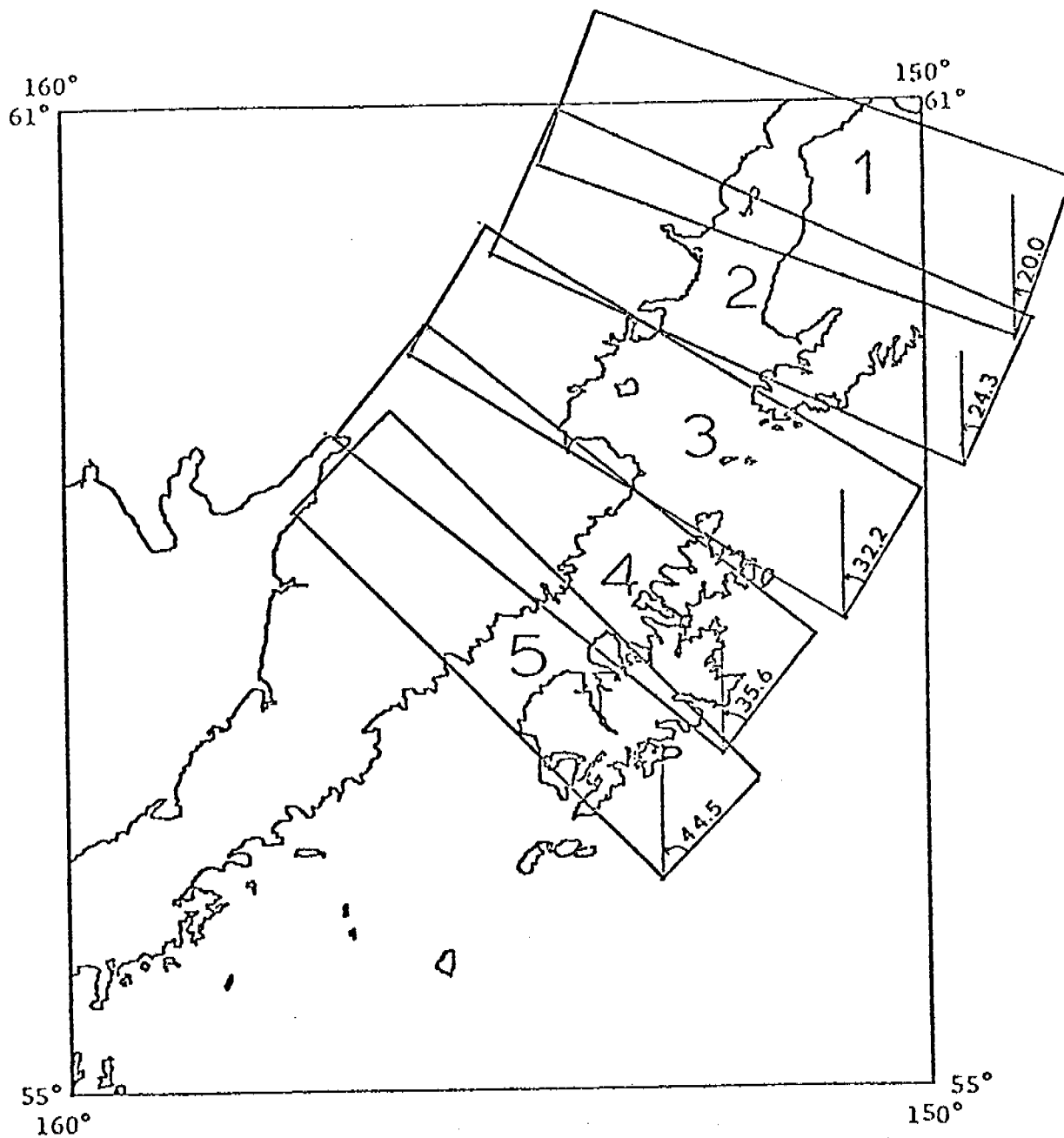


Figure 4. The orientation of five 100-kmwide sections, as determined by a least squares fit, for projection of hypocenters into a vertical plane. The strike of the Benioff zone is perpendicular to the long sides of the rectangles identifying the different sections.

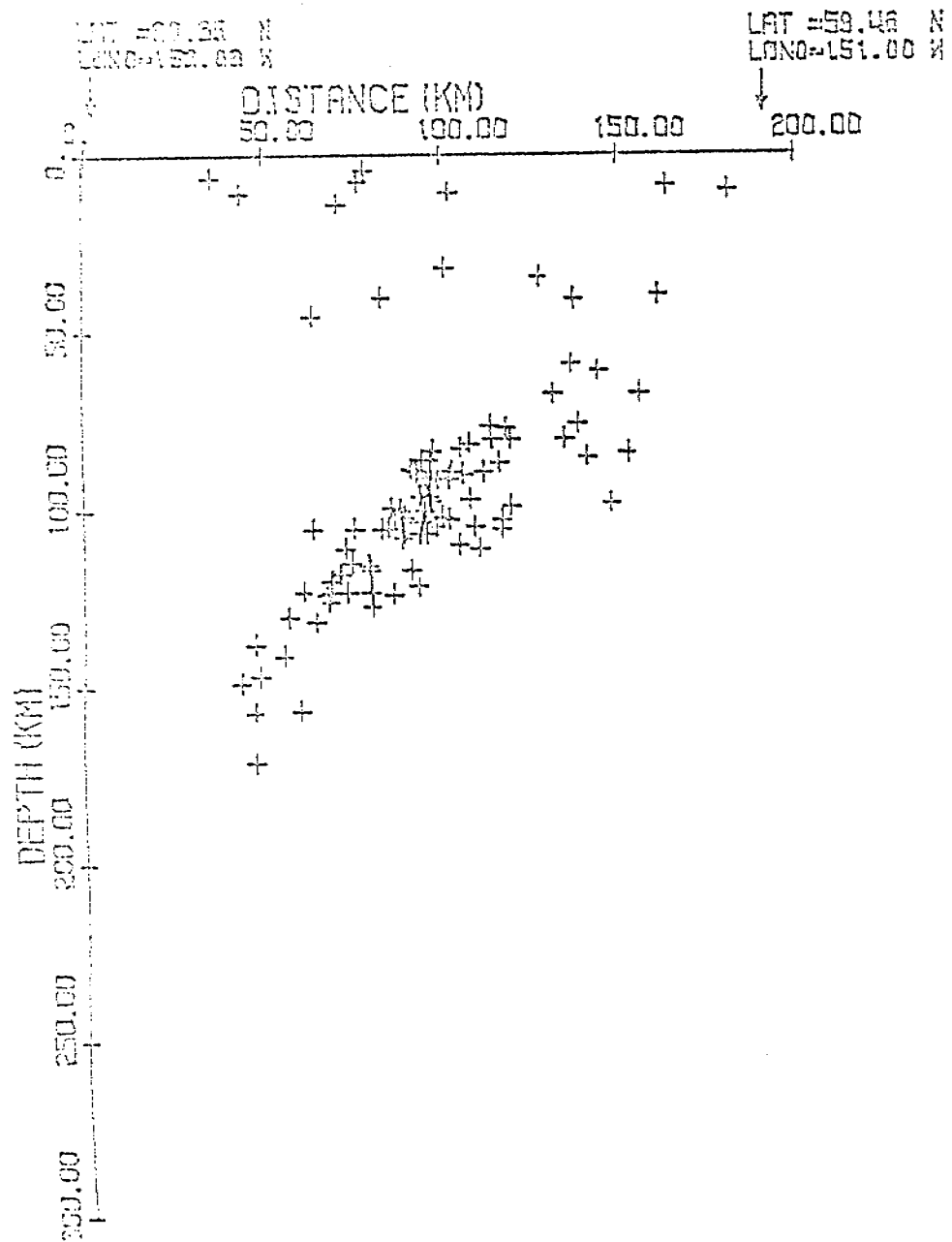


Figure 5. Benioff zone in section 1 of Figure 4. Data used are from February through September 1977.

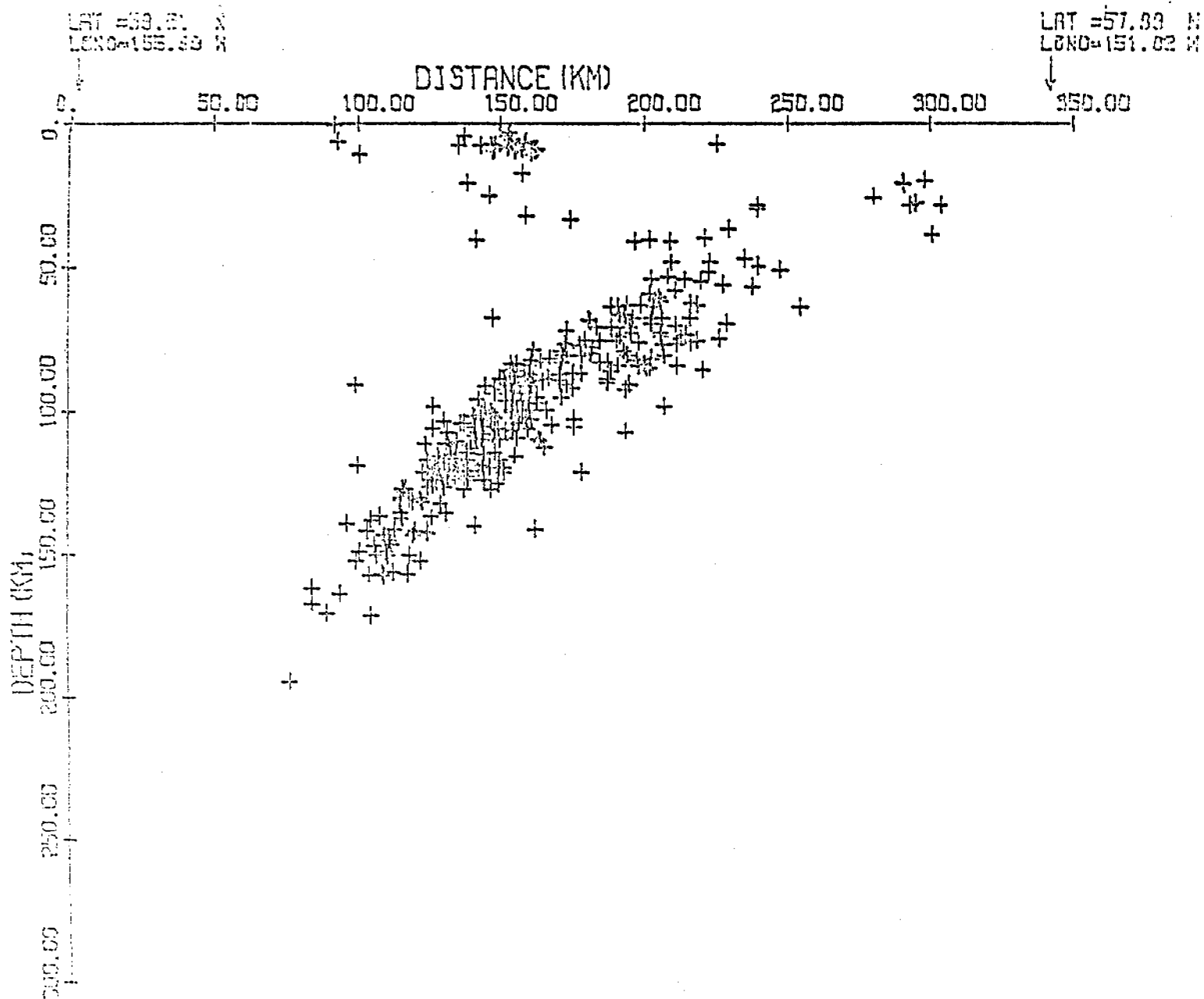


Figure 6. Bonioff zone in section 2 of Figure 4. Data used are from February 1976 through September 1977.

503

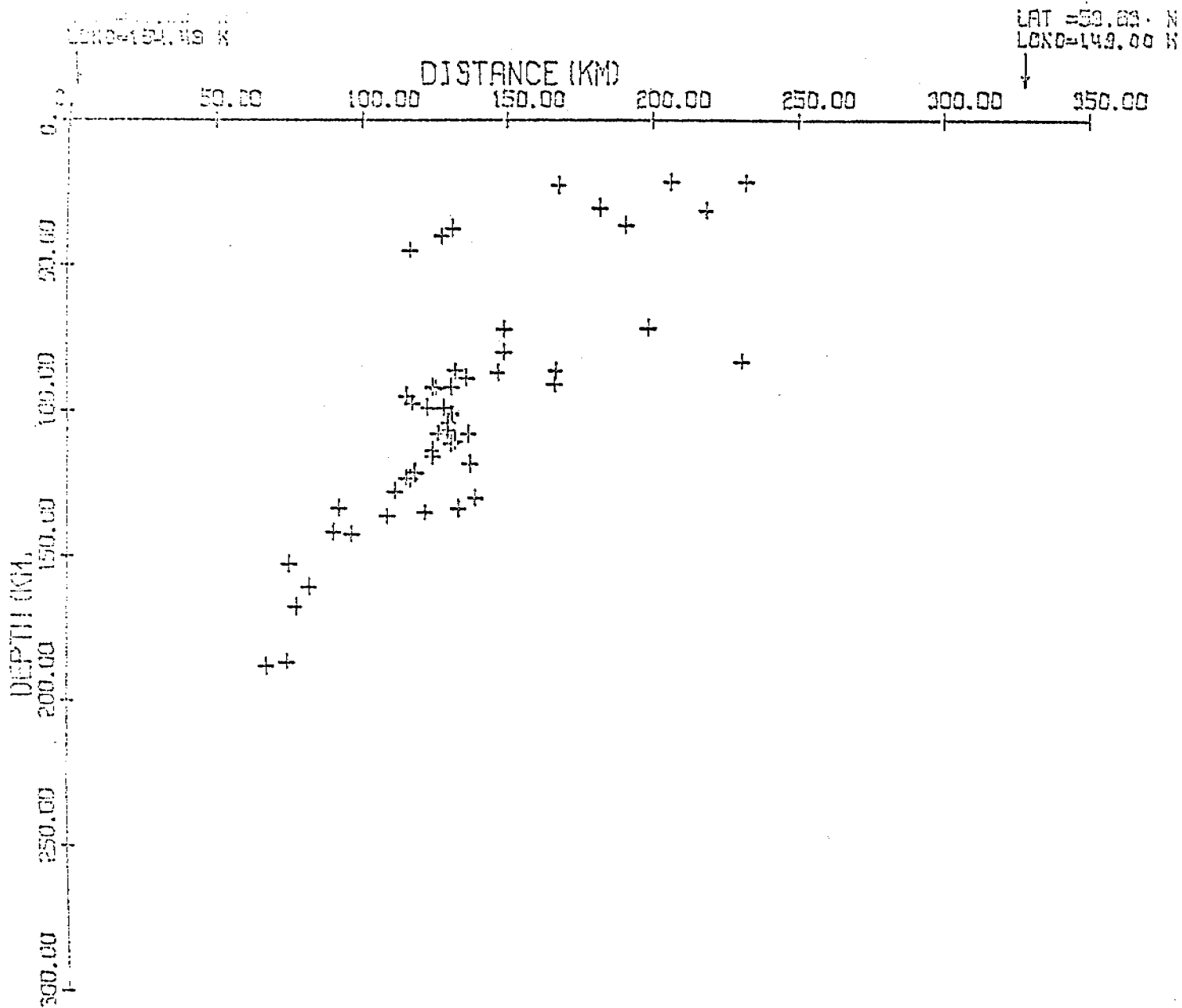


Figure 7. Benioff zone of section 3 of Figure 4. Data used are from February 1976 through September 1977.

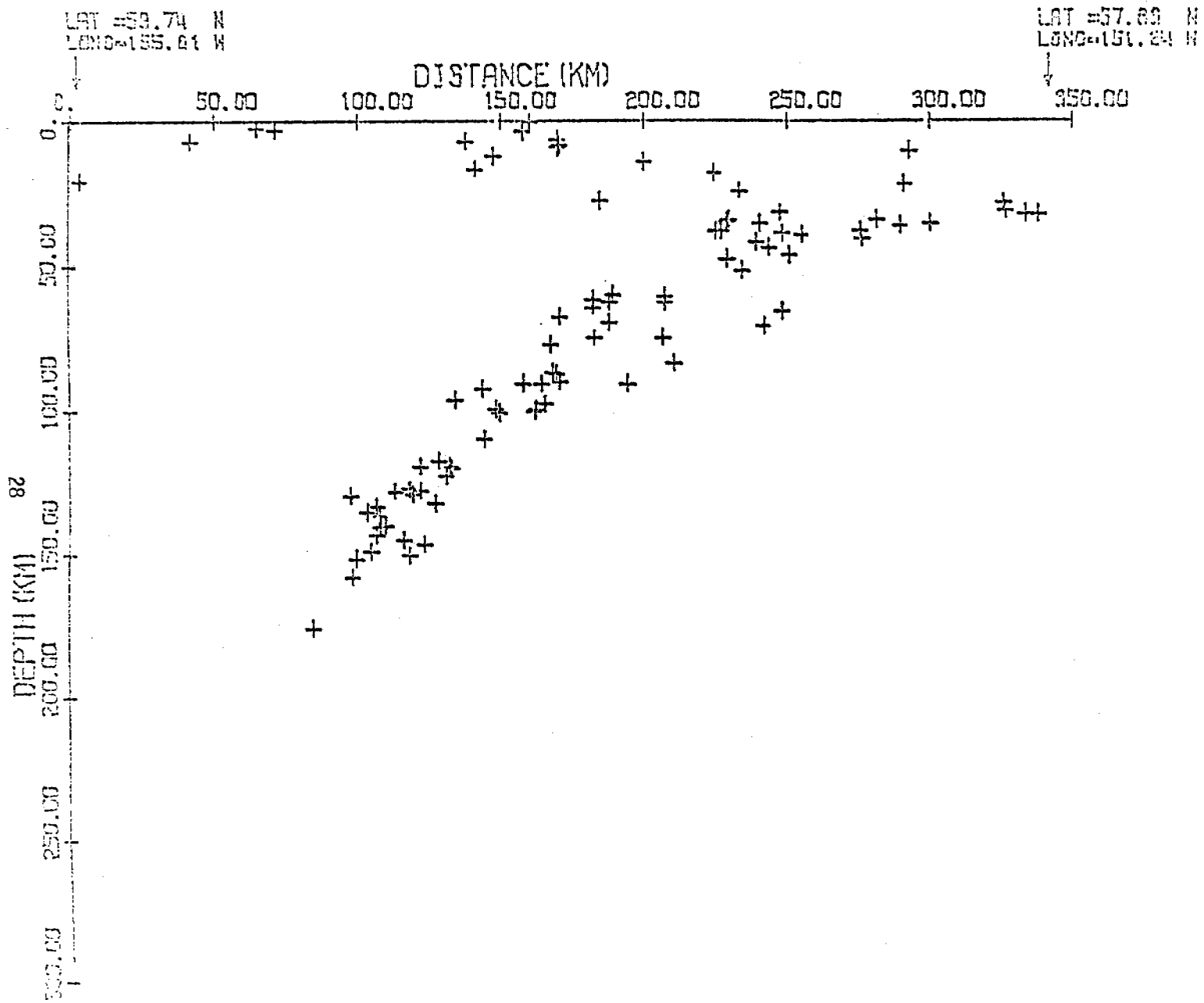


Figure 8. Benioff zone in section 4 of Figure 4. Events used are between February 1976 through September 1977.

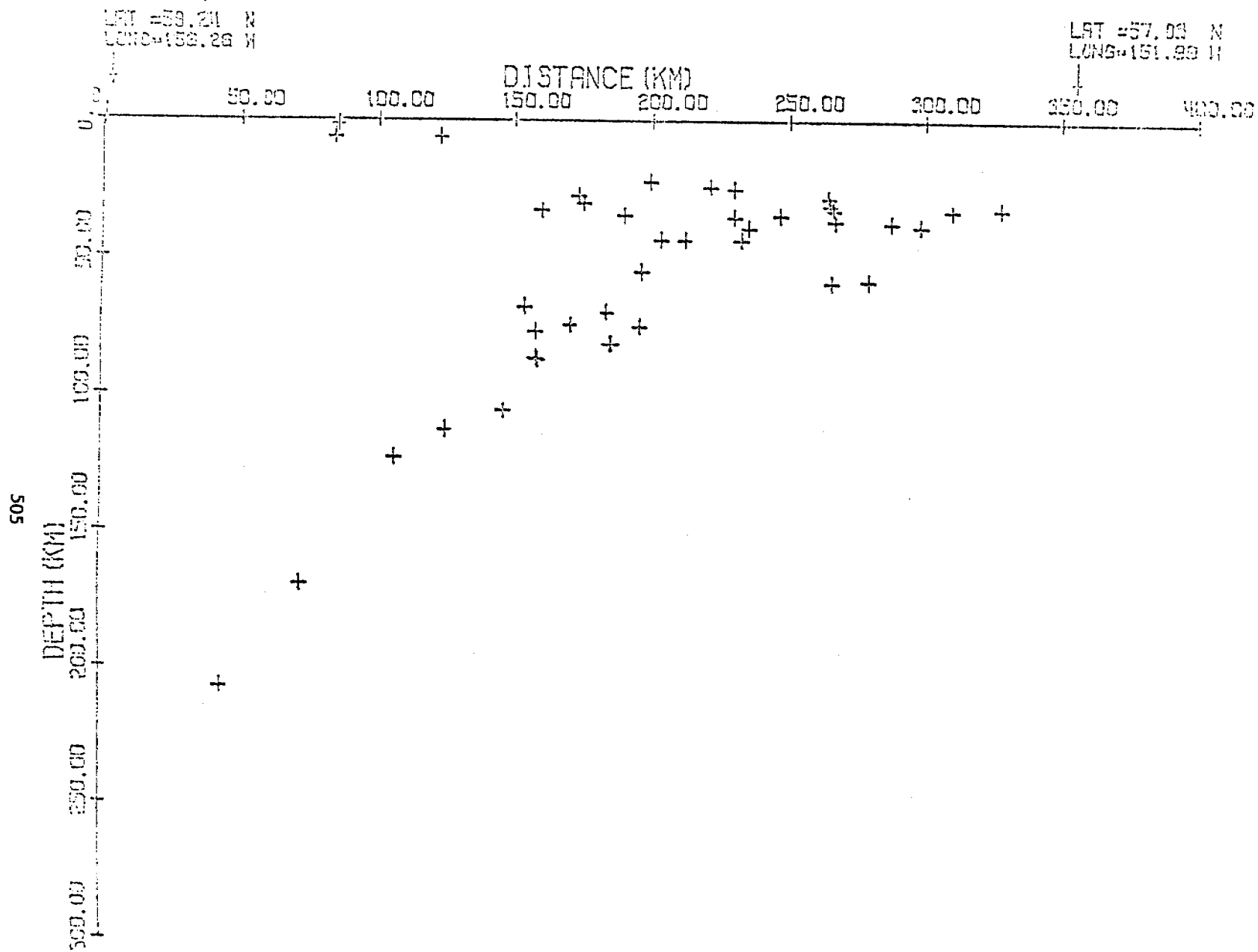


Figure 9. Benioff zone in section 5 of Figure 4. Events used are between February 1976 through September 1977.

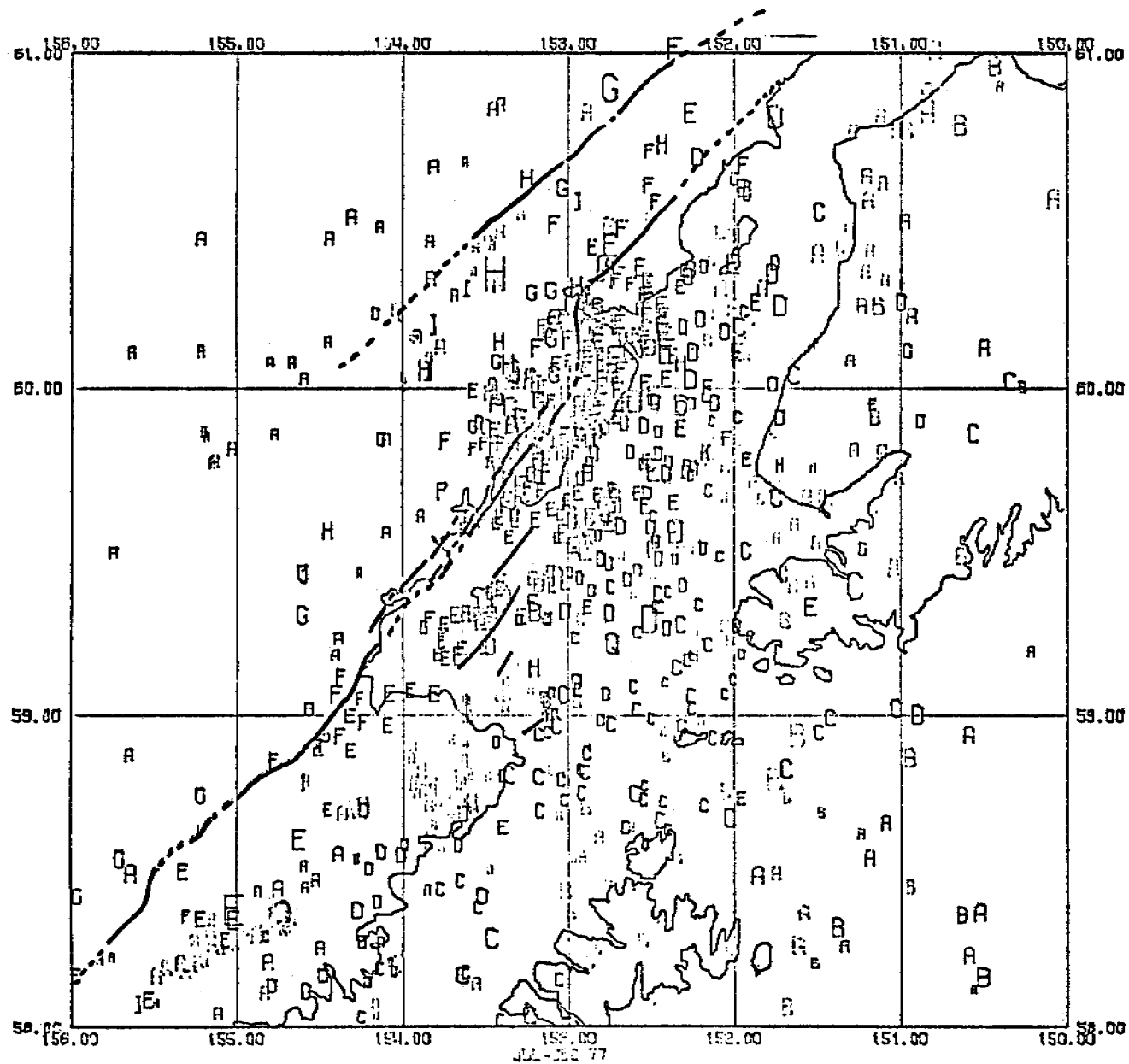


Figure 10. Lower Cook Inlet epicenters for July-Dec., 1977. The depths of the earthquakes are letter-coded: A 0-25 km, B 25-50 km, C 50-75 km, D 75-100 km, E 100-125 km, F 125-150 km, G 150-175 km, H 175-200 km, I 200-225 km.

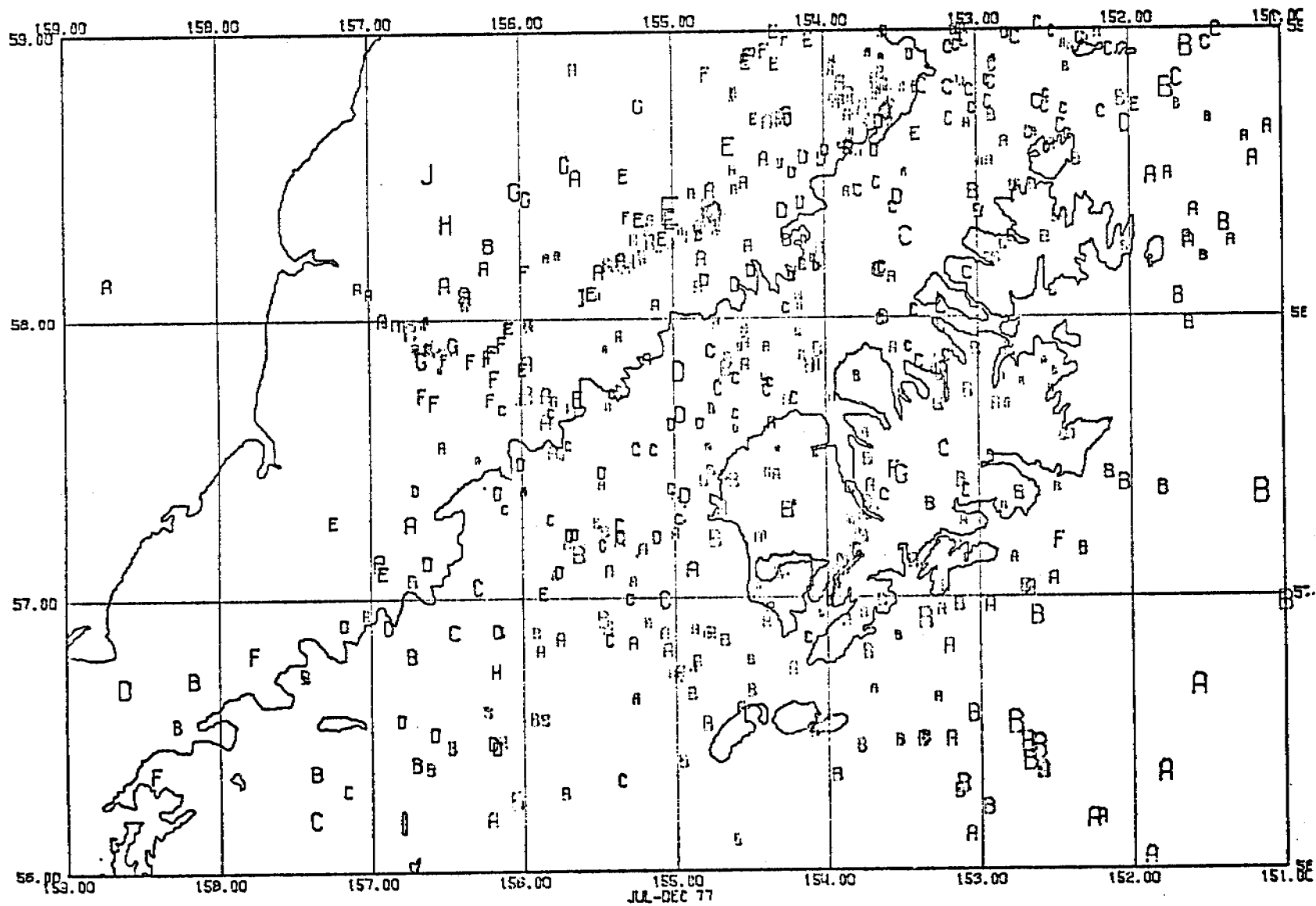


Figure 11. Kodiak-Alaska Peninsula epicenters for July-December, 1977. Symbols are the same as in Fig. 10.

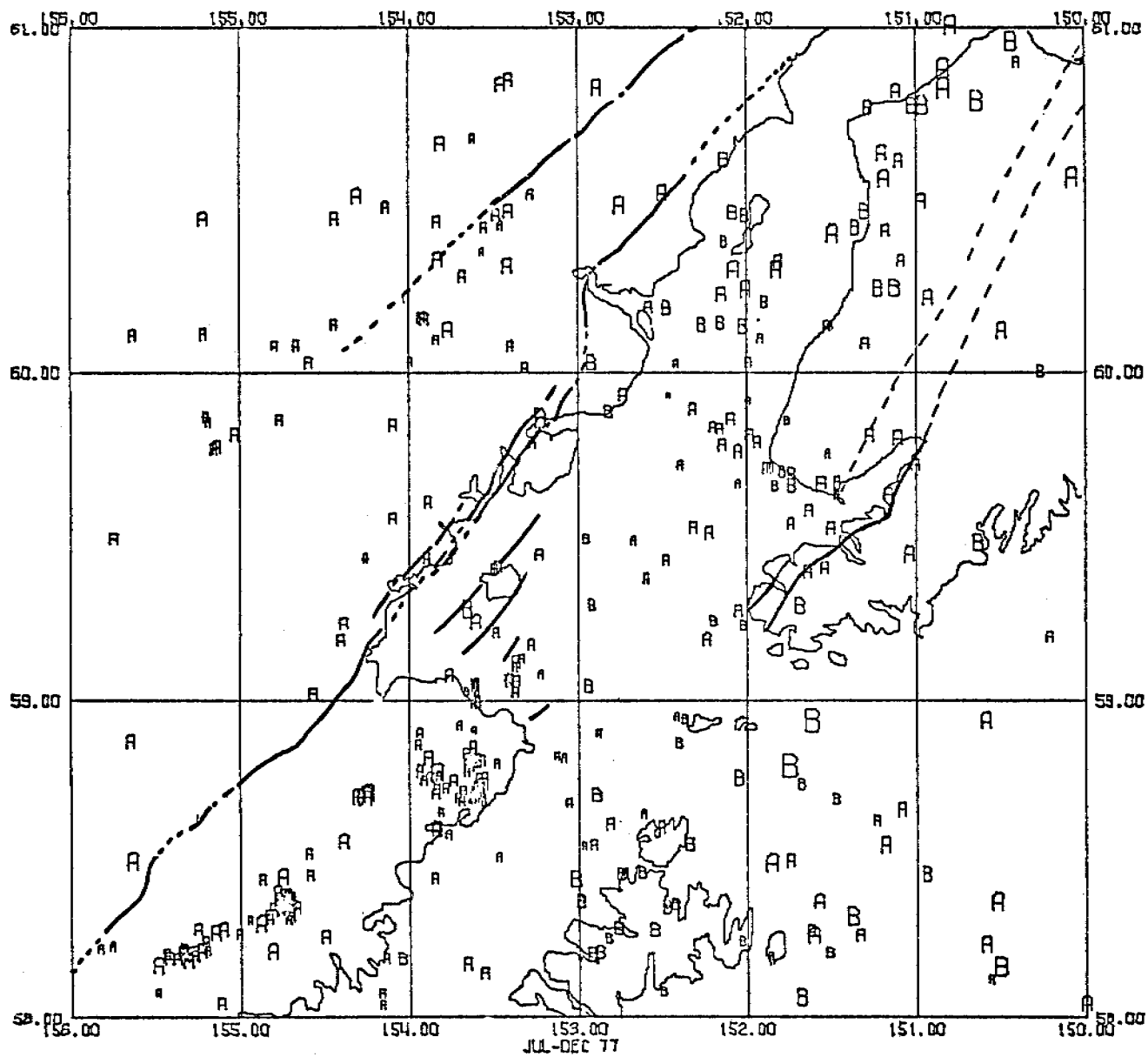


Figure 12. Cook Inlet shallow seismicity, July-December, 1977. Symbols are the same as Fig. 10. Solid lines indicate mapped faults; dashed were inferred.

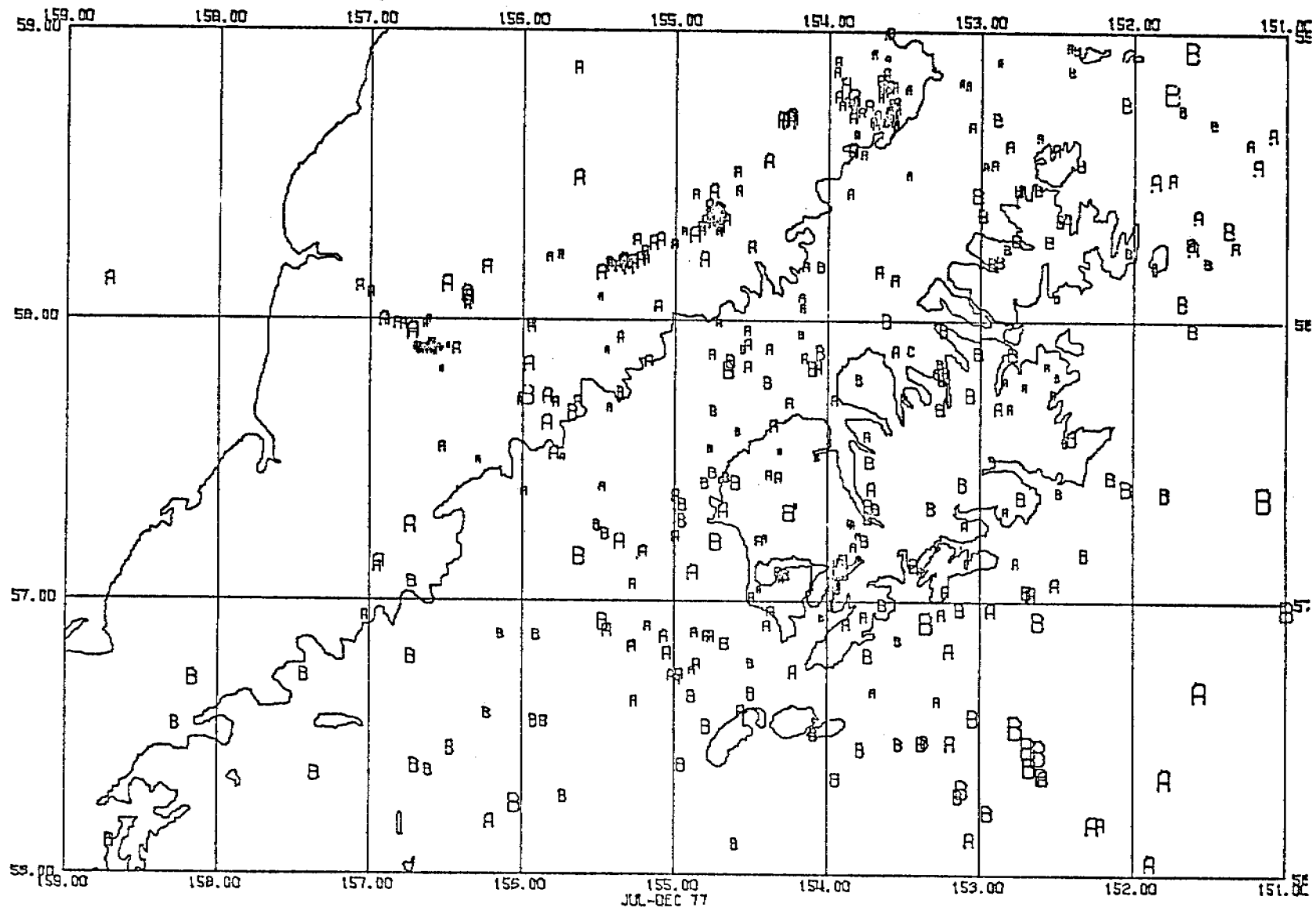


Figure 13. Kodiak-Alaska Peninsula shallow seismicity, July-December, 1977. Symbols are the same as in Fig. 10.

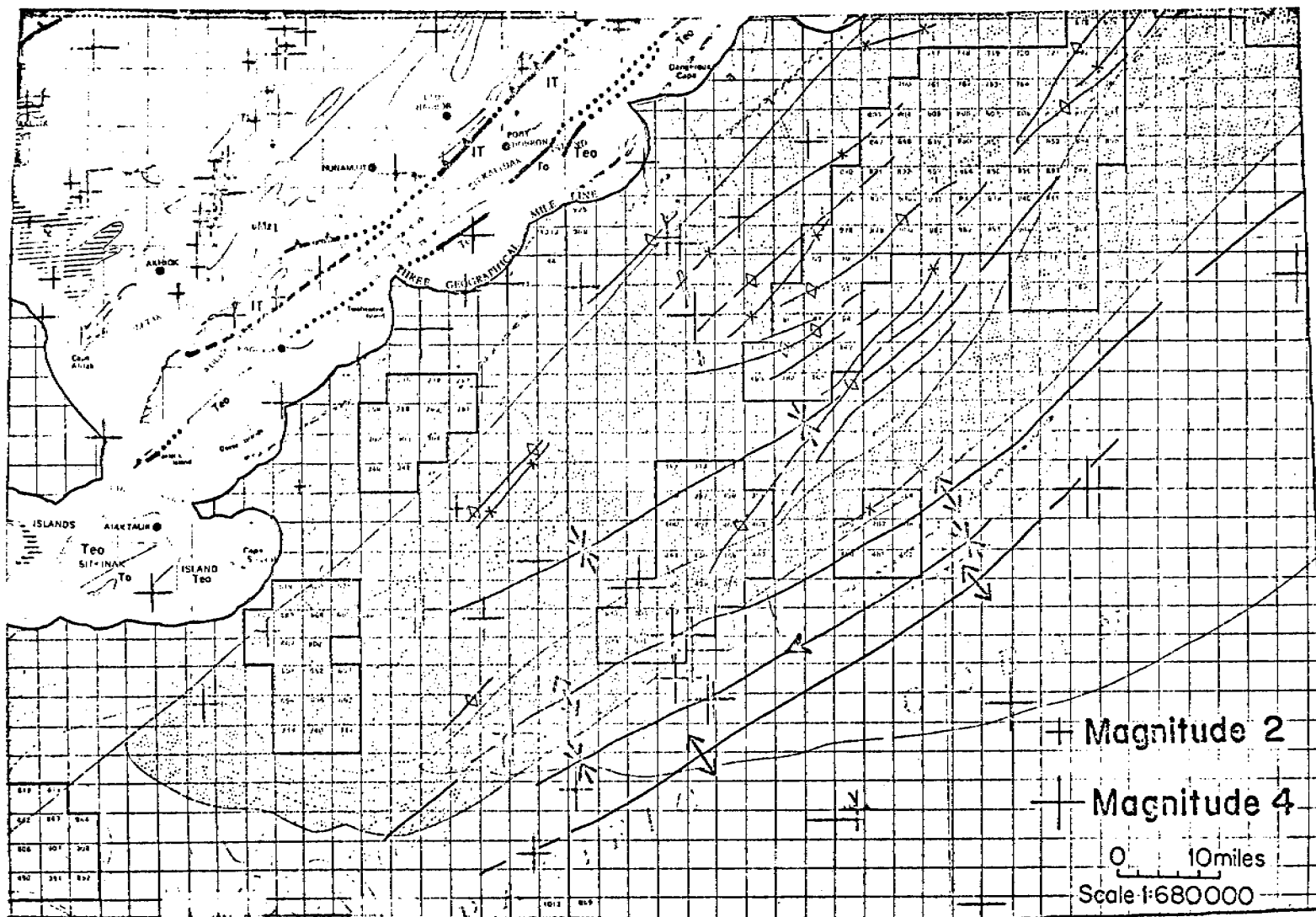


Figure 14. Shallow seismic events in southwestern offshore area of Kodiak Island during July-December, 1977. Linear seismic cluster on upper right hand portion of figure is suspected active seismic fault not previously mapped.

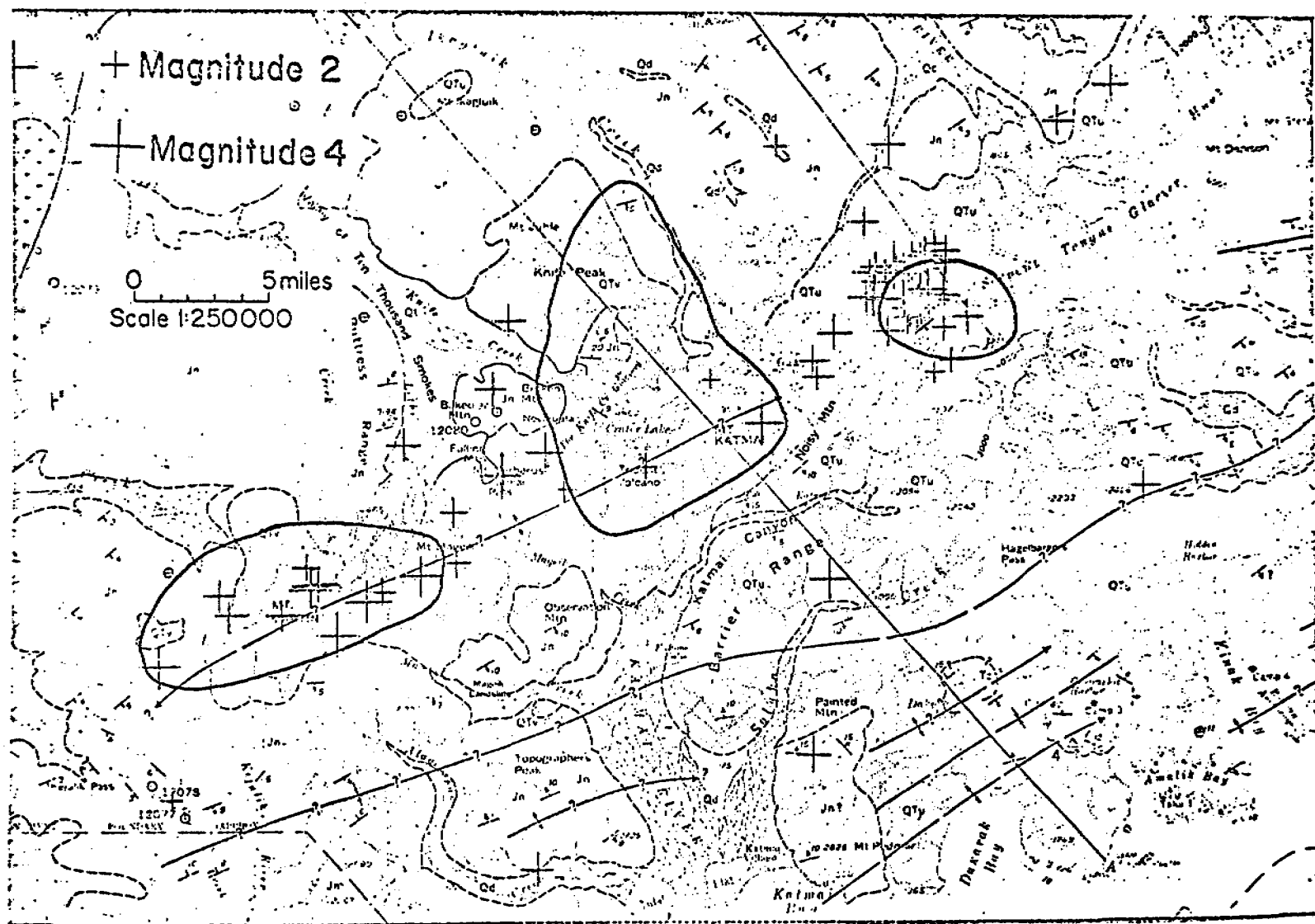


Figure 15. Clusters of shallow seismic activity along the volcanic axis between Mt. Martin and Snowy Mt. The dense cluster to the northeast is located beneath Snowy Mt. The solid contours indicate the loci of magma chambers determined by Matumoto (1971).

Appendix 1

Hypocenter Listings for Cook Inlet,
Kodiak, and Alaska Peninsula

October 1977 through February 1978

Table A1-1 All Events

This appendix lists origin times, focal coordinates, magnitudes, and related parameters for earthquakes which occurred in the lower Cook Inlet, Kodiak, and Alaska Peninsula areas. The following data are given for each event:

- (1) Origin time in Greenwich Civil Time (GCT): date, hour (HR), minute (MN), and second (SEC). To convert to Alaska Standard Time (AST), subtract ten hours.
- (2) Epicenter in degrees and minutes of north latitude (LAT N) and west longitude (LONG N).
- (3) DEPTH, depth of focus in kilometers.
- (4) MAG, magnitude of the earthquake. A zero means not determined.
- (5) NP, number of P arrivals used in locating earthquake.
- (6) NS, number of S arrivals used in locating earthquake.
- (7) GAP, largest azimuthal separation in degrees between stations.
- (8) DM, epicentral distance in kilometers to the closest station to the epicenter.
- (9) RMS, root-mean-square error in seconds of the travel time residuals:

$$\text{RMS} = \frac{\sum_i (R_{Pi}^2 + R_{Si}^2)}{(NP + NS)}$$

Where R_{Pi} and R_{Si} are the observed minus the computed arrival times of P and S waves, respectively, at the i-th station.

- (10) ERH, largest horizontal deviation in kilometers from the hypocenter within the one-standard-deviation confidence ellipsoid. This quantity is a measure of the epicentral precision for an event.
- (11) ERZ, largest vertical deviation in kilometers from the hypocenter within the one-standard-deviation confidence ellipsoid. This quantity is a measure of the depth precision for an event.
- (12) Q, quality of the hypocenter. This index is a measure of the precision of the hypocenter and is the average of two quantities, QS and QD, defined below:

<u>QS</u>	<u>RMS (sec)</u>	<u>ERH (km)</u>	<u>ERZ (km)</u>
A	< 0.15	< 1.0	< 2.0
B	< 0.30	< 2.5	< 5.0
C	< 0.50	< 5.0	
D	Others		

QD is rated according to the station distribution as follows:

<u>QD</u>	<u>NO</u>	<u>GAP</u>	<u>DMIN</u>
A	> 6	< 90°	< DEPTH or 5 km
B	> 6	< 135°	< 2x DEPTH or 10 km
C	> 6	< 180°	< 50 km
D	Others		

The following table is included:

Table A1-1 Cook Inlet, western Gulf of Alaska
All Events

COCK INLET-WESTERN GULF OF ALASKA EARTHQUAKES

1977	ORIGIN HR MN	TIME SEC	LAT N DEG MIN	LONG W DEG MIN	DEPTH KM	MAG	NC	GAP DEG	DM KM	RMS SEC	ERH KM	ERZ KM	Q				
OCT	1	3	22	7.6	58	47.9	153	40.4	0.1	2.0	6	147	19	0.33	4.4	24.5	C
	1	3	28	5.1	59	47.5	153	37.3	0.2	1.7	6	145	18	0.27	4.0	17.4	C
	1	3	32	30.3	59	47.7	153	37.1	2.5	2.2	7	146	18	0.20	2.0	2.6	C
	1	3	55	27.6	58	44.4	153	36.1	0.8	1.8	4	256	24	0.28	0.	0.	C
	1	4	8	13.1	58	43.9	152	4.6	41.7	2.7	6	232	19	0.11	3.4	2.5	D
	1	4	35	42.7	59	46.9	151	7.7	5.0	2.7	4	288	115	0.11	0.	0.	C
	1	5	17	34.3	59	56.6	154	7.1	108.0	2.6	13	79	18	0.30	2.6	4.5	B
	1	6	58	55.8	58	47.8	153	35.2	0.2	2.0	7	149	18	0.29	3.0	13.5	C
	1	7	4	53.1	58	13.6	152	3.0	28.2	1.7	5	264	48	0.42	24.0	7.6	D
	1	7	8	39.7	59	39.7	152	32.4	84.9	1.9	7	183	38	1.45	13.1	15.2	D
	1	8	41	55.2	58	42.5	153	37.2	8.9	1.5	5	138	28	0.03	0.6	0.8	C
	1	9	50	7.2	53	43.8	153	35.3	0.9	1.7	4	297	25	0.34	0.	0.	D
	1	9	57	40.3	52	54.2	154	41.9	5.0	3.8	5	327	372	0.58	318.0	99.9	D
	1	10	7	25.6	59	47.6	153	21.5	143.6	2.2	8	173	17	0.05	1.5	1.7	C
	1	12	16	53.3	56	22.7	154	58.5	42.6	2.5	13	145	52	0.22	1.9	10.4	D
	1	12	28	6.9	59	27.7	152	22.4	90.4	1.7	6	191	52	0.06	1.8	2.2	C
	1	14	32	56.2	59	34.7	152	53.6	116.6	2.2	8	159	20	0.10	2.3	2.9	C
	1	15	58	35.3	57	58.9	156	54.3	4.1	1.7	4	288	28	0.05	0.	0.	C
	1	19	19	34.7	57	57.9	156	50.6	5.9	2.2	8	210	24	0.34	4.8	3.7	D
	1	19	37	5.0	58	46.9	153	39.0	2.8	1.5	4	147	47	0.	0.	0.	C
	1	20	28	47.6	58	47.6	153	37.5	0.6	1.0	6	144	18	0.13	1.1	5.6	C
	2	2	40	5.5	57	20.8	152	45.4	38.6	2.7	5	204	28	0.01	0.3	0.2	C
	2	4	9	32.2	58	19.8	152	30.0	46.3	2.4	6	180	34	0.17	4.1	4.3	D
	2	5	39	41.2	59	58.1	153	49.5	90.3	2.2	4	161	46	0.05	0.	0.	C
	2	6	8	54.0	59	45.8	153	40.3	5.0	1.4	3	162	48	0.01	0.	0.	C
	2	7	19	44.9	56	37.5	154	54.5	39.1	2.3	5	227	45	0.17	5.7	2.5	D
	2	9	17	50.2	59	15.4	155	7.3	1.1	2.5	11	106	58	0.64	3.5	29.8	D
	2	9	51	17.3	53	49.3	153	40.7	5.7	1.7	5	145	43	0.01	0.1	0.2	C
	2	11	13	51.0	59	13.3	154	24.2	5.0	2.0	3	263	82	0.	0.	0.	C
	2	11	43	50.5	59	46.4	154	36.3	5.0	1.8	5	245	94	1.34	53.8	99.9	D
	2	11	58	4.4	59	22.7	152	19.7	77.9	2.2	5	240	59	0.06	5.2	6.0	D
	3	3	4	11.7	59	1.6	152	57.8	45.6	2.3	5	154	43	2.01	47.2	107.9	D
	3	7	13	51.8	60	16.2	153	7.9	173.0	2.9	8	205	25	0.13	6.3	7.0	D
	3	14	39	33.0	59	16.5	153	18.5	89.7	2.0	6	129	9	0.07	1.8	2.6	B
	3	16	49	37.0	56	31.2	153	17.7	45.5	2.3	9	182	27	0.85	41.9	75.5	D
	3	17	19	4.3	59	55.5	151	31.0	57.5	2.4	4	322	116	0.	0.	0.	C
	3	17	56	1.2	60	48.9	153	28.2	9.0	2.3	4	213	58	0.06	0.	0.	C
	3	19	9	20.5	60	1.4	153	15.0	146.3	2.2	8	183	41	0.44	14.1	15.8	D
	3	20	57	21.9	59	45.6	152	33.8	66.4	1.8	4	161	19	0.	0.	0.	C
	4	3	0	52.4	60	12.8	151	57.6	63.9	2.0	6	250	50	0.74	6.7	11.6	D
	4	5	40	54.1	57	49.8	152	34.5	6.1	1.2	5	205	10	0.17	23.1	14.9	D
	4	7	24	24.2	59	22.5	152	11.9	93.8	2.6	17	138	13	0.38	3.3	3.9	C
	4	6	35	37.8	57	1.1	150	3.1	2.3	2.7	15	281	167	0.46	14.1	19.1	D
	4	8	0	10.4	59	54.0	153	37.6	3.2	1.0	4	262	8	0.	0.	0.	C
	4	8	1	47.2	60	3.7	154	40.9	5.0	2.1	3	291	93	0.07	0.	0.	C

COCK INLET-WESTERN GULF OF ALASKA EARTHQUAKES

1977	ORIGIN TIME			LAT N		LONG W		DEPTH	MAG	NO	GAP	DM	RMS	ERH	ERZ	Q	
	HR	MIN	SEC	DEG	MIN	DEG	MIN	KM			CEG	KM	SEC	KM	KM		
OCT	4	10	26	33.1	57	57.7	153	48.1	0.6	2.1	16	172	21	0.84	5.0	13.8	D
	4	11	44	19.9	59	31.9	152	50.1	94.5	2.0	7	223	26	0.11	5.8	8.7	D
	4	15	28	40.6	57	35.6	154	36.3	41.6	1.5	6	129	29	0.13	2.0	1.2	B
	4	20	34	23.7	53	51.9	154	20.1	111.5	2.3	9	191	27	0.39	7.8	11.9	D
	5	2	1	39.3	59	23.4	151	33.4	18.1	2.0	6	273	99	0.23	14.1	6.9	D
	5	3	34	23.4	59	46.8	153	3.6	149.7	2.5	11	304	17	0.17	8.4	8.9	D
	5	6	54	33.7	57	6.8	156	58.0	0.6	2.8	15	128	32	2.32	11.2	44.3	D
	5	8	22	6.2	56	47.2	155	54.1	5.0	2.0	7	161	89	1.09	10.9	99.9	D
	5	9	48	46.8	60	32.0	152	58.1	205.9	2.9	15	206	16	0.40	9.8	10.6	D
	5	12	22	39.0	59	58.8	153	9.4	76.1	1.5	6	133	21	0.26	6.1	7.6	C
	5	13	51	20.2	57	2.7	156	44.8	38.0	2.4	8	264	40	0.70	99.7	46.9	D
	5	14	15	57.1	58	12.2	155	50.5	5.0	1.6	9	161	51	0.34	2.7	4.7	D
	5	14	59	52.5	58	12.9	155	46.0	1.1	1.4	9	158	51	0.66	5.1	30.3	D
	5	15	18	9.0	57	16.1	154	58.5	46.8	2.3	12	103	21	0.29	2.1	3.7	B
	5	15	55	12.5	60	20.1	152	19.3	101.0	2.1	9	250	26	0.42	16.2	17.3	D
	5	17	25	20.3	58	31.6	154	17.7	90.8	1.6	9	101	64	0.35	3.6	10.1	C
	5	17	34	45.2	59	52.3	152	20.4	1.3	2.1	12	202	65	6.65	65.9	320.3	D
	5	18	16	16.6	59	45.3	153	29.2	146.0	1.9	7	279	18	0.08	5.6	7.7	D
	5	19	36	19.2	58	59.8	152	36.9	61.2	2.5	14	185	43	0.45	5.2	6.8	D
	5	20	42	14.1	59	46.3	152	52.1	98.0	2.8	16	242	24	0.44	9.1	7.5	D
	6	2	25	20.4	57	2.1	153	59.5	32.1	2.0	4	118	51	0.	0.	0.	C
	7	6	28	32.5	54	34.9	152	31.8	5.0	2.2	4	244	68	0.24	0.	0.	C
	8	5	53	20.2	59	46.5	152	28.5	94.5	2.4	6	285	44	0.12	13.0	13.7	D
	8	10	36	53.0	59	51.3	153	31.1	153.4	2.8	13	263	27	0.38	14.1	14.8	D
	8	13	13	41.5	57	41.6	155	39.2	4.2	2.0	12	128	12	0.60	3.4	4.9	D
	8	13	27	0.3	57	48.3	153	18.0	5.0	1.5	3	153	28	0.	0.	0.	C
	8	16	23	27.5	58	42.3	153	41.6	0.4	1.6	8	129	29	0.46	3.4	19.5	C
	8	22	57	33.4	59	23.0	153	25.3	121.7	2.6	8	124	2	0.18	4.1	4.2	C
	9	11	30	40.3	55	46.7	155	25.1	29.8	2.8	4	339	12	0.	0.	0.	C
	9	13	22	29.3	57	53.2	156	42.6	2.0	1.5	4	222	13	0.06	0.	0.	C
	9	21	14	50.6	57	46.2	153	16.3	36.6	2.1	6	92	29	0.20	2.5	2.5	C
	10	1	58	20.7	58	27.1	152	44.3	5.0	1.9	3	160	30	0.01	0.	0.	C
	10	3	20	40.5	56	31.9	156	49.6	92.6	2.4	8	104	55	0.17	2.3	5.5	C
	10	6	28	50.6	53	29.0	152	58.1	43.2	1.6	4	197	24	0.10	0.	0.	C
	10	8	3	3.3	59	59.3	152	33.7	110.4	3.0	19	229	53	0.46	6.9	5.0	D
	10	13	58	49.0	56	18.5	155	22.7	70.3	2.2	7	130	53	0.24	5.6	15.3	C
	10	14	55	2.5	54	14.6	155	10.0	24.8	2.9	15	118	56	1.46	7.0	8.7	D
	10	14	56	34.3	53	17.5	155	10.6	5.0	2.1	5	160	61	0.70	16.6	99.9	D
	10	18	38	19.6	54	17.2	157	29.1	37.3	3.9	8	326	349	17.53	99.9	99.9	D
	11	1	37	37.7	55	49.6	155	46.4	5.0	2.4	6	192	89	0.87	12.5	99.9	D
	11	2	16	23.3	59	33.7	152	47.1	113.1	3.3	9	226	27	0.38	8.1	6.3	D
	11	10	42	3.7	57	6.1	155	58.2	4.9	2.2	6	143	34	0.78	8.2	9.3	D
	11	13	4	8.4	59	16.4	154	9.6	5.0	1.8	7	118	51	32.14	325.3	674.1	D
	12	7	33	40.3	60	13.4	151	9.4	46.7	2.9	10	310	132	2.10	101.9	212.5	D
	12	12	55	51.4	60	4.9	152	16.5	89.5	3.0	14	127	71	0.26	2.1	4.1	B

TABLE 11.2 MOORE BUSINESS FORMS, INC. F

COCK INLET-WESTERN GULF OF ALASKA EARTHQUAKES

1977	ORIGIN TIME			LAT N		LONG W		DEPTH	MAG	NO	GAP	DM	RMS	ERH	ERZ	Q	
	HR	MIN	SEC	DEG	MIN	DEG	MIN	KM			DEG	KM	SEC	KM	KM		
OCT	12	17	56	41.9	59	31.2	152	54.4	123.8	2.7	8	259	34	0.29	14.5	13.7	D
	12	20	26	45.7	59	5.5	153	23.3	10.6	1.5	4	178	17	0.	0.	0.	C
	13	1	56	0.3	59	54.6	153	42.9	5.9	1.6	6	141	11	0.11	1.4	1.7	C
	13	3	28	0.0	59	42.2	152	56.8	94.7	2.2	5	297	49	0.09	17.0	14.8	D
	13	15	46	11.6	60	7.1	153	26.2	178.6	2.7	9	319	53	0.08	7.7	8.3	D
	13	22	24	13.1	57	41.6	156	13.7	126.3	2.4	10	94	3	0.22	4.2	6.6	C
	14	17	11	50.5	60	13.1	154	3.5	5.0	2.2	5	249	74	0.50	22.2	99.9	D
	14	17	51	14.7	57	30.3	153	15.2	71.2	2.8	9	105	39	2.68	50.2	87.8	C
	14	19	54	50.5	60	28.0	153	6.7	131.8	2.9	9	168	19	0.27	7.1	9.0	D
	14	20	21	45.0	60	29.6	154	19.5	4.5	2.4	4	278	85	0.49	0.	0.	D
	15	3	25	32.3	59	11.3	154	50.1	19.8	2.6	4	238	90	0.38	0.	0.	D
	15	7	16	57.4	60	20.5	152	48.8	153.6	3.1	11	161	8	0.21	5.6	6.6	D
	15	3	35	36.5	60	19.0	151	48.2	77.7	3.1	12	259	54	0.56	13.9	9.7	D
	15	1	54	22.0	59	31.5	153	3.5	109.0	2.9	10	171	17	0.	4.2	3.8	C
	16	4	25	35.4	60	2.9	152	45.1	123.0	4.6	28	71	41	4.38	24.0	29.9	C
	16	6	42	43.1	59	11.9	152	10.4	61.5	2.2	10	203	64	0.21	3.0	5.0	D
	16	9	24	41.9	59	23.1	153	2.3	109.3	2.4	12	147	22	0.23	2.8	3.4	C
	16	9	53	37.0	60	18.4	151	49.8	5.0	2.0	3	289	53	0.58	0.	0.	D
	16	13	20	43.7	60	18.6	151	6.6	5.0	1.9	3	305	92	0.33	0.	0.	D
	16	16	29	4.9	59	2.3	153	3.4	72.9	3.1	22	90	28	0.37	2.0	2.7	C
	16	17	30	51.6	59	20.4	154	47.3	5.0	2.3	9	117	76	0.60	4.1	809.4	D
	16	21	41	20.2	59	29.1	151	15.4	155.8	2.4	4	301	113	0.	0.	0.	C
	17	18	14	34.3	59	17.5	152	46.3	80.4	2.8	7	162	47	0.06	0.9	1.6	B
	18	7	13	43.4	54	12.8	154	30.0	1.6	0.	20	296	183	0.34	13.6	16.2	D
	18	13	48	34.1	60	47.7	150	52.3	0.1	3.6	16	133	112	0.53	3.8	16.9	D
	18	11	15	6.4	59	3.0	156	23.1	1.5	3.0	16	177	2	0.60	3.4	2.5	D
	18	14	12	33.9	59	2.1	156	22.8	3.3	1.7	7	182	2	0.27	2.8	2.0	D
	18	14	57	43.3	59	2.3	153	9.9	83.1	2.0	9	126	22	0.16	2.3	3.3	B
	18	16	48	34.3	56	53.1	153	59.9	29.4	1.9	5	125	46	0.25	4.1	5.1	D
	18	17	51	8.6	59	59.1	153	6.1	79.8	2.1	14	126	43	0.37	3.2	5.0	C
	18	18	7	47.8	57	39.7	154	45.9	42.4	1.9	6	154	37	0.18	2.8	5.2	C
	18	21	38	43.0	59	25.3	153	54.7	9.0	1.9	9	66	26	0.13	1.0	1.3	C
	18	22	53	42.8	60	24.1	151	23.0	30.1	2.5	11	290	76	0.56	23.3	6.1	D
	19	2	16	16.0	60	51.2	143	41.8	11.2	0.	26	96	63	10.14	71.4	407.0	D
	19	4	23	53.4	57	19.5	156	8.0	63.7	1.8	6	195	44	0.18	5.6	9.2	D
	19	6	7	32.3	59	30.7	152	59.1	107.8	1.8	7	153	20	0.18	4.1	5.2	C
	19	7	48	33.8	59	19.8	154	45.3	2.5	2.0	14	115	76	0.75	3.7	889.6	D
	19	11	4	33.3	59	35.6	153	4.0	117.2	2.0	8	149	11	0.09	2.1	2.5	C
	19	11	16	42.1	59	39.1	143	40.8	4.1	3.1	7	313	166	0.79	58.6	40.6	D
	19	11	25	5.3	57	10.4	152	30.1	133.4	2.8	8	268	35	2.62	133.7	159.7	D
	19	12	3	10.3	60	36.9	151	13.5	5.0	2.6	3	297	87	0.38	0.	0.	D
	19	12	29	35.0	56	44.9	154	52.3	1.9	2.2	4	256	47	0.03	0.	0.	C
	20	5	30	31.0	59	56.0	152	16.4	83.1	2.0	4	158	46	0.	0.	0.	C
	20	5	39	15.1	59	42.4	152	25.0	5.0	1.7	3	166	43	0.	0.	0.	C
	20	19	4	52.4	59	44.6	152	31.6	71.6	2.3	9	111	40	0.50	6.3	10.0	C

1977-1980 WESTERN GULF OF ALASKA EARTHQUAKES, INSET

COCK INLET-WESTERN GULF OF ALASKA EARTHQUAKES

1977	ORIGIN		TIME	LAT N		LONG W		DEPTH	MAG	NO	GAP	CM	RMS	ERH	ERZ	O
	HR	MIN	SEC	DEG	MIN	DEG	MIN	KM			DEG	KM	SEC	KM	KM	
OCT	20	20	30	22.1	59 31.5	151	45.6	5.0	1.9	7	175	16	2.32	17.4	27.1	D
	20	20	41	9.4	59 37.1	152	40.8	55.2	2.4	9	102	19	0.57	17.3	23.6	C
	20	21	12	24.5	59 3.3	153	7.0	90.1	1.9	11	86	42	0.39	3.4	6.5	B
	20	22	29	47.5	59 1.6	153	8.8	82.7	2.1	8	126	37	0.39	5.2	8.1	C
	21	4	51	14.4	59 21.2	154	45.1	5.0	1.6	6	132	78	0.46	4.9	791.4	D
	21	5	37	42.9	59 10.0	152	16.3	64.5	1.6	9	151	60	0.56	6.7	13.4	D
	21	9	28	6.2	59 20.8	154	43.8	2.5	2.1	9	114	78	0.44	2.8	591.4	D
	21	9	34	43.2	58 19.3	154	46.4	2.5	2.0	8	116	75	0.62	4.5	883.7	D
	21	9	37	20.7	58 20.2	154	44.4	0.6	2.8	17	96	77	0.60	2.2	40.1	D
	21	9	40	23.5	58 20.1	154	45.1	0.4	2.4	16	96	77	0.55	2.2	40.6	D
	21	12	41	5.4	58 28.5	155	20.5	119.6	2.7	15	133	75	0.88	7.5	18.4	C
	21	14	2	23.1	59 53.4	152	58.7	107.4	2.2	7	163	30	0.31	7.6	9.7	D
	21	17	44	26.7	57 49.9	154	39.6	48.1	2.6	12	71	51	0.58	3.8	12.6	C
	22	9	46	15.3	59 21.9	152	52.7	87.8	2.1	8	118	77	0.29	3.1	7.7	C
	22	11	9	45.9	55 46.6	155	4.2	30.3	2.9	9	244	32	0.79	21.7	6.4	D
	22	12	45	19.6	60 15.9	153	14.6	164.6	2.5	6	214	31	0.12	7.1	16.2	D
	22	14	33	19.8	59 50.0	153	15.7	140.7	3.0	14	83	38	0.43	4.8	6.6	B
	22	14	35	24.4	59 42.7	152	54.4	99.5	3.0	14	89	19	0.70	6.4	8.0	C
	22	22	14	5.6	60 27.8	152	47.1	7.8	2.8	5	237	5	0.04	1.8	0.8	C
	23	2	30	11.6	59 45.5	151	56.5	114.1	2.3	8	156	20	0.14	3.9	8.7	C
	23	7	23	4.5	59 55.9	151	11.2	104.9	1.9	4	262	39	0.	0.	0.	C
	23	8	28	24.9	60 9.0	151	55.6	5.0	0.	4	221	55	0.57	0.	0.	D
	23	9	21	31.5	60 10.8	152	50.2	121.2	2.4	5	131	26	0.04	2.2	4.2	C
	23	9	28	18.7	60 17.2	152	32.7	112.3	2.9	13	185	19	0.26	3.4	4.5	D
	23	12	37	22.2	59 41.6	151	54.1	2.3	2.2	7	136	15	1.16	58.3	152.6	D
	23	12	58	69.0	60 3.8	153	25.1	5.0	1.8	3	146	46	0.	0.	0.	C
	23	14	14	25.8	57 4.5	155	47.0	76.0	2.2	9	168	74	0.87	10.9	26.0	D
	24	1	38	30.7	58 18.5	156	30.9	189.8	3.2	18	178	30	0.26	3.0	4.5	C
	24	1	23	10.9	60 3.4	153	27.3	158.9	2.6	15	89	44	0.43	5.1	7.2	C
	24	18	28	36.1	56 43.1	154	14.6	5.0	2.3	7	144	18	2.50	76.8	159.3	D
	24	19	32	2.3	56 26.0	153	48.1	32.3	2.4	7	273	27	0.32	9.3	2.5	D
	24	19	55	41.5	60 17.3	152	20.6	111.5	2.1	4	273	27	0.	0.	0.	C
	24	21	9	26.5	57 53.8	156	30.2	5.0	1.1	3	221	4	0.	0.	0.	C
	25	2	9	4.4	59 59.9	148	32.0	5.0	3.2	11	299	178	1.20	38.7	42.5	D
	25	5	33	45.9	59 7.5	149	55.6	60.9	2.8	4	335	101	0.22	0.	0.	C
	25	6	15	25.4	59 14.3	152	35.9	70.2	2.1	5	128	51	0.23	5.0	10.8	D
	25	7	5	17.5	57 38.5	154	36.9	62.4	1.9	4	186	34	0.05	0.	0.	C
	25	9	9	30.1	57 53.3	156	34.0	5.0	1.3	3	260	5	0.04	0.	0.	C
	25	10	54	12.1	59 53.5	151	59.7	62.5	2.1	5	179	32	0.24	8.0	12.2	D
	25	11	10	48.0	59 14.2	155	6.2	2.5	1.6	5	206	75	0.89	22.2	99.9	D
	25	17	41	23.1	57 55.2	155	22.3	24.6	2.0	11	79	18	3.60	21.5	24.2	C
	25	18	1	27.2	59 20.6	154	44.4	2.5	1.5	9	96	78	0.35	2.2	469.2	D
	25	20	36	10.4	58 26.5	152	38.7	45.4	2.1	6	151	27	0.38	9.6	14.5	D
	26	3	4	5.9	60 41.3	152	32.2	128.7	2.5	4	313	32	0.16	0.	0.	C
	26	3	36	50.7	59 46.7	152	11.5	255.9	2.5	4	138	33	0.	0.	0.	C

COCK INLET-WESTERN GULF OF ALASKA EARTHQUAKES

1977	ORIGIN TIME			LAT N		LONG W		DEPTH	MAG	NC	GAP	DM	RMS	ERH	ERZ	Q	
	HR	MIN	SEC	DEG	MIN	DEG	MIN	KM			DEG	KM	SEC	KM	KM		
OCT	26	6	56	51.3	57	19.1	153	45.5	33.3	2.8	9	84	44	0.27	2.0	2.4	B
	26	9	48	30.9	56	27.5	156	9.4	5.0	2.2	10	85	58	0.87	5.1	999.9	D
	26	17	2	53.1	57	46.4	153	48.5	48.5	2.0	8	78	32	0.22	2.3	3.2	B
	27	1	51	27.8	60	8.5	152	36.7	102.0	2.3	6	151	32	0.20	6.4	11.3	D
	27	8	27	6.0	56	49.2	154	41.6	33.1	2.3	6	184	42	0.57	8.6	9.1	D
	27	11	41	50.5	59	7.4	153	13.7	180.3	2.8	4	292	59	0.03	0.	0.	C
	27	14	41	11.3	59	26.6	152	46.4	84.6	2.2	5	174	34	0.25	14.0	32.3	D
	27	23	39	22.9	59	24.6	151	43.4	62.8	2.3	10	148	10	0.36	5.4	6.8	D
	28	4	14	32.3	56	51.1	155	55.6	40.1	2.2	10	129	83	0.29	2.3	370.5	D
	28	5	27	37.4	59	2.4	153	36.8	8.1	1.6	8	131	10	0.17	1.1	1.1	B
	28	6	43	27.0	59	16.4	153	51.7	133.0	2.7	14	89	25	0.34	3.9	5.6	B
	28	15	53	30.9	60	59.9	149	44.5	2.5	3.8	20	83	73	1.22	6.5	20.5	D
	28	15	52	42.3	59	11.3	153	31.8	100.6	2.2	11	144	17	0.33	6.5	4.6	D
	28	17	10	15.7	59	10.5	151	58.1	77.0	1.6	7	163	39	0.31	5.4	8.9	D
	28	19	54	15.9	59	34.8	153	26.1	121.7	2.6	15	157	14	0.30	3.6	3.9	C
	28	21	1	35.9	57	53.6	156	41.7	1.6	1.3	4	221	12	0.04	0.	0.	C
	29	5	30	32.3	58	40.3	151	29.3	36.0	1.8	7	213	50	0.33	7.0	2.9	D
	29	9	40	57.2	60	16.7	152	58.9	188.2	3.3	23	96	19	1.17	14.3	19.1	C
	29	9	15	47.8	60	31.5	149	46.4	27.6	2.6	4	315	142	0.03	0.	0.	C
	29	9	36	13.1	57	1.9	154	27.2	0.2	1.3	5	179	35	0.63	25.1	111.7	D
	29	10	6	0.7	57	23.8	153	8.7	33.8	2.8	17	126	26	0.32	2.1	1.4	C
	29	11	44	27.5	57	11.9	153	23.0	55.3	2.5	14	118	47	0.29	1.9	4.7	B
	29	12	29	23.7	59	29.6	152	12.1	94.7	1.9	4	139	36	0.	0.	0.	C
	29	14	2	50.2	59	10.9	150	13.4	16.0	1.8	4	333	83	0.13	0.	0.	C
	29	15	44	50.4	58	51.2	152	25.4	45.6	1.8	8	135	25	0.25	2.7	4.8	C
	29	20	6	56.2	59	59.2	150	16.6	31.7	1.9	4	303	85	0.	0.	0.	C
	29	21	16	9.6	58	14.0	152	50.7	44.5	2.0	9	153	26	0.53	6.2	8.3	D
	29	21	38	21.5	58	54.7	154	24.5	125.5	2.6	20	90	24	0.35	2.4	5.1	B
	29	21	47	35.7	59	51.2	152	20.9	106.0	2.7	18	139	45	0.62	7.0	8.5	D
	30	0	18	27.4	58	11.1	155	21.6	0.6	2.3	12	108	46	0.43	2.1	14.3	C
	30	1	7	8.9	60	35.0	151	56.4	94.6	2.2	17	283	49	0.31	11.2	9.3	D
	30	2	3	17.8	58	11.7	155	21.8	1.4	1.6	8	110	47	0.58	4.8	30.9	D
	30	9	24	13.6	58	17.8	154	57.2	2.5	1.4	8	111	67	0.59	4.4	830.4	D
	30	9	44	53.6	58	44.7	153	53.7	11.3	1.7	10	149	31	0.50	3.6	650.1	D
	30	10	52	7.4	60	5.9	142	43.6	5.0	3.8	5	318	386	0.43	171.2	954.4	D
	30	11	12	20.1	59	41.9	151	52.5	5.0	1.7	4	225	75	0.19	0.	0.	D
	30	14	59	56.5	59	55.6	152	28.5	5.0	0.7	3	139	52	0.	0.	0.	D
	30	15	42	43.5	58	4.1	155	29.9	5.4	1.2	4	241	32	0.	0.	0.	C
	30	16	31	34.6	60	53.3	150	24.8	1.1	1.9	4	314	139	0.70	0.	0.	C
	30	15	48	26.9	60	47.8	151	8.2	2.5	2.3	4	305	99	0.57	0.	0.	D
	30	18	35	26.5	59	39.3	153	46.8	399.7	3.2	4	294	31	0.01	0.	0.	C
	30	19	50	30.2	60	24.0	152	22.6	114.4	2.4	5	223	6	1.38	148.1	143.6	D
	30	20	53	53.7	60	32.1	152	29.9	130.2	2.6	8	284	19	0.22	10.5	12.8	D
	30	20	41	3.3	59	50.5	151	46.6	36.7	1.5	6	234	84	1.36	86.0	74.6	D
	30	21	37	24.3	59	57.5	153	6.6	5.0	1.6	5	173	57	1.95	43.2	999.9	D

COOK INLET-WESTERN GULF OF ALASKA EARTHQUAKES

1977	ORIGIN TIME	LAT N	LONG W	DEPTH	MAG	NO	CAP	DM	RMS	ERH	ERZ	O	
	HR MN SEC	DEG MIN	DEG MIN	KM			DEG	KM	SEC	KM	KM		
OCT	31 1 9	8.7	60 4.9	152 23.1	112.5	2.1	12	168	43	0.50	8.6	11.5	D
	31 2 25	23.8	57 4.1	154 18.8	1.8	1.4	4	155	35	1.50	0.	0.	D
	31 4 45	45.3	58 27.3	154 32.7	2.5	2.2	14	93	74	0.91	4.1	99.9	D
	31 9 9	55.0	58 45.5	154 37.4	205.2	2.2	6	173	45	2.25	116.5	333.0	D
	31 11 45	15.9	60 11.1	152 13.7	91.5	2.8	20	200	39	0.35	3.7	4.4	D
	31 10 49	39.8	60 35.2	152 32.4	132.0	2.5	11	281	22	0.21	8.1	9.5	D
	31 22 29	44.9	59 37.1	153 25.3	120.1	2.4	18	79	38	2.38	19.7	36.1	C
	31 22 31	12.1	56 49.3	155 27.6	63.2	2.3	10	159	75	0.33	3.3	10.2	D
	31 22 45	15.9	59 3.1	152 4.5	57.9	1.7	6	179	54	0.14	3.4	13.2	D
	31 23 20	44.0	57 18.9	152 50.8	1.9	1.4	4	196	21	0.01	0.	0.	C
NOV	1 1 43	42.3	60 38.7	151 58.2	149.2	2.6	4	290	50	0.15	0.	0.	C
	1 14 22	45.9	59 39.0	153 17.0	119.2	2.7	10	75	3	0.57	7.2	14.1	C
	1 15 30	47.9	58 10.6	152 56.9	45.4	2.5	7	156	18	0.29	4.4	5.0	C
	1 17 44	29.8	57 52.9	156 36.9	9.6	1.9	4	207	24	0.	0.	0.	C
	1 20 28	4.9	58 15.6	152 47.3	41.0	2.5	6	156	31	0.34	6.0	2.9	D
	1 20 57	30.5	58 28.6	151 45.8	24.8	2.3	8	203	94	1.29	22.8	14.5	D
	1 22 31	23.0	57 19.5	154 58.1	48.5	2.3	7	187	20	0.07	1.4	1.4	C
	1 31 3	11.7	57 19.2	154 42.2	10.3	2.7	12	93	5	0.49	2.7	2.2	C
	1 31 39	55.9	58 6.6	158 44.1	5.0	2.5	5	274	136	0.27	17.5	613.0	D
	1 31 22	44.1	59 3.7	153 46.7	8.8	2.2	10	118	18	0.20	1.2	1.2	C
	1 9 53	7.1	58 20.4	150 39.3	37.6	2.6	9	251	103	0.76	18.1	999.9	D
	1 10 6	39.2	60 34.0	147 32.3	39.0	3.2	7	313	256	0.60	83.0	800.5	D
	1 10 57	27.2	60 20.0	152 17.4	88.4	2.8	25	94	28	0.52	3.0	3.9	D
	1 12 4	35.9	59 46.5	151 57.4	5.0	1.8	3	222	73	0.	0.	0.	C
	1 18 30	6.7	60 11.9	152 33.1	110.2	2.5	5	203	27	0.13	6.9	9.3	D
	1 19 14	35.4	59 46.4	153 23.6	144.9	2.4	8	201	16	0.09	4.9	4.6	D
	1 20 3	34.3	60 5.8	153 12.9	145.0	2.9	19	85	43	0.45	4.5	6.0	B
	1 21 40	3.5	59 47.7	153 27.8	149.0	3.3	24	76	20	0.45	3.0	3.8	B
	1 23 44	27.9	59 50.8	153 37.5	0.4	1.8	8	135	27	0.52	4.3	25.6	D
	1 3 6	47.5	57 53.6	156 37.5	11.4	1.6	4	211	24	0.	0.	0.	C
	1 7 21	18.9	59 50.6	152 51.3	92.2	2.8	17	103	30	0.35	3.1	4.5	C
	1 7 33	22.2	60 32.3	150 6.4	21.5	3.3	22	158	130	0.99	6.9	5.2	D
	1 10 38	4.4	57 30.9	155 9.4	64.4	2.1	4	187	35	0.	0.	0.	C
	1 10 53	57.0	59 46.7	153 12.4	64.7	2.6	10	70	27	0.22	1.8	3.1	B
	1 11 33	23.5	56 56.4	152 57.3	6.7	2.9	9	223	26	0.96	13.8	9.7	D
	1 13 20	57.3	58 55.1	153 12.1	74.3	2.3	7	124	19	0.15	2.4	3.4	B
	1 13 39	53.2	57 41.8	156 2.0	0.6	1.7	5	120	13	0.81	11.4	90.3	D
	1 14 14	14.4	57 42.7	156 1.4	1.8	1.5	4	158	14	0.62	0.	0.	D
	1 14 52	25.0	59 39.9	152 10.7	69.4	2.7	7	113	30	0.24	4.0	7.1	D
	1 17 0	26.7	59 9.4	153 41.4	103.1	2.9	14	63	24	0.34	2.9	4.3	B
	1 20 11	3.6	59 23.9	153 14.2	102.5	2.4	10	136	12	0.19	2.9	3.0	C
	1 21 33	56.6	60 21.8	152 9.2	44.7	2.1	4	263	34	0.67	0.	0.	D
	1 22 54	30.3	57 53.0	154 34.3	48.2	1.4	5	186	49	0.18	5.0	9.4	D
	1 23 1	30.7	60 16.7	151 50.9	5.0	2.7	7	243	53	1.01	46.0	56.9	D
	1 4 1	12.4	59 17.5	153 13.5	87.7	3.0	17	80	11	0.55	4.0	5.2	C

14-218 11-2 MODR EUS NISS FORMS, INC F

COCK INLET-WESTERN GULF OF ALASKA EARTHQUAKES

1977	ORIGIN HR MN	TIME SEC	LAT N DEG MIN	LONG W DEG MIN	DEPTH KM	MAG	NO	GAP DEG	DM KM	RMS SEC	ERH KM	ERZ KM	O					
NOV	4	3	0	42.3	53	27.1	153	40.8	68.8	2.1	12	69	53	0.27	2.1	4.9	B	
	4	4	8	12.4	54	11.6	156	51.4	5.0	2.9	6	324	357	0.21	64.0	37	1.4	D
	4	4	15	45.8	56	49.8	154	8.9	61.2	2.1	7	247	63	0.19	6.1	6.3	D	
	4	4	49	14.3	57	53.4	156	37.7	7.5	1.4	5	211	24	0.14	2.9	2.2	D	
	4	5	5	0.2	60	5.0	152	0.9	103.9	3.0	19	205	51	0.37	5.5	6.4	D	
	4	6	14	33.7	57	0.2	152	41.2	18.4	2.8	10	293	29	1.48	75.5	21.0	D	
	4	6	42	49.5	57	11.1	153	50.4	30.9	1.5	4	104	46	1.88	0.0	0.0	D	
	4	7	33	28.7	58	26.2	152	46.3	39.7	2.0	12	119	32	0.64	5.4	3.3	D	
	4	7	58	13.5	58	29.3	154	13.7	92.8	2.1	12	140	65	0.29	2.9	7.3	D	
	4	8	59	18.0	56	28.1	153	22.9	32.9	2.3	5	268	50	0.10	4.9	1.5	D	
	4	9	31	20.8	53	22.0	153	33.9	59.4	2.1	11	80	41	0.26	2.3	5.3	B	
	4	9	45	15.0	60	35.7	152	9.5	46.1	2.5	12	285	39	0.66	23.5	17.1	D	
	4	10	36	24.8	57	31.7	154	19.2	5.0	1.0	3	188	28	0.0	0.0	0.0	D	
	4	11	6	43.2	56	20.1	154	26.3	145.4	2.7	4	334	238	0.15	0.0	0.0	D	
	4	12	26	6.3	59	0.4	154	35.0	3.9	2.0	6	101	24	0.76	8.5	13.0	D	
	4	19	5	5.1	56	56.1	153	16.2	5.0	2.1	3	274	28	0.04	0.0	0.0	C	
	4	19	7	48.1	58	56.9	152	46.0	69.1	2.8	18	97	43	0.29	1.7	3.0	B	
	4	22	28	52.3	57	28.0	156	1.9	97.3	2.9	8	130	46	0.27	5.0	9.4	D	
	4	23	29	41.6	57	19.0	154	25.3	1.3	1.1	5	147	18	0.80	3.7	29.4	D	
	4	23	6	19.8	58	6.8	154	48.8	96.5	2.4	13	113	56	0.22	1.7	4.7	B	
	5	2	22	46.8	57	34.5	153	45.4	5.0	1.8	3	255	59	0.0	0.0	0.0	C	
	5	5	6	51.1	59	59.9	152	17.5	84.5	3.4	28	83	52	0.58	2.8	3.9	D	
	5	7	7	19.5	57	7.3	152	47.1	10.6	2.0	5	268	18	0.22	12.6	3.6	D	
	5	7	32	4.0	57	11.7	153	7.6	5.0	0.3	3	172	4	0.0	0.0	0.0	C	
	5	7	38	13.3	57	2.4	152	31.9	0.4	2.6	8	240	36	0.54	9.5	22.0	D	
	5	8	21	36.0	60	16.7	153	37.9	209.7	2.6	9	254	50	0.16	8.1	12.9	D	
	5	12	35	15.0	58	16.3	154	54.1	2.5	2.9	17	98	66	0.48	1.9	553.4	D	
	5	14	4	1.1	60	9.8	152	19.9	92.7	2.6	12	186	37	0.36	6.7	8.8	D	
	5	15	5	57.4	56	53.8	152	39.1	25.3	3.5	21	211	39	1.22	12.0	5.7	D	
	5	15	35	57.6	58	21.9	154	44.3	5.0	1.9	10	97	80	0.47	2.7	610.1	D	
	5	18	42	16.1	59	49.2	153	17.8	139.0	3.4	35	65	19	0.46	2.3	2.6	B	
	5	18	50	37.3	55	51.3	156	11.3	92.1	2.4	10	161	73	0.67	9.0	24.9	D	
	5	19	10	44.0	57	20.8	153	38.5	64.5	2.3	5	148	39	0.18	5.1	10.9	D	
	5	20	33	32.9	57	5.9	153	57.1	24.3	3.0	15	111	48	0.68	3.7	3.7	D	
	5	20	40	58.1	57	56.7	151	38.2	33.1	2.8	13	238	86	0.40	6.5	2.4	D	
	6	1	52	59.3	56	58.6	155	19.2	66.2	2.0	9	173	57	0.32	3.9	8.5	D	
	6	2	46	32.3	56	52.1	156	54.7	83.7	2.8	8	178	41	0.41	11.2	20.1	D	
	6	7	11	6.2	57	4.2	156	56.4	108.4	2.5	9	320	116	0.50	16.0	100.5	D	
	6	7	13	11.5	57	18.8	153	42.0	37.8	2.2	6	159	41	0.19	2.8	2.2	D	
	6	12	6	29.1	57	30.3	154	4.8	40.9	1.3	4	153	33	0.0	0.0	0.0	C	
	6	15	28	45.0	57	25.7	154	20.5	11.0	2.0	4	166	20	0.83	0.0	0.0	D	
	7	3	31	59.7	53	39.9	154	23.1	5.0	2.4	10	254	98	1.43	28.6	99.9	D	
	7	3	32	28.9	56	19.2	151	49.6	0.8	3.7	15	255	121	0.42	9.3	24.6	D	
	7	6	9	23.5	59	38.8	152	44.4	85.4	2.6	13	90	27	0.63	5.6	8.5	C	
	7	15	16	43.9	60	44.7	152	59.4	33.6	3.2	5	303	104	0.21	245.8	38.2	D	

142718 III 2 MOORE BUSINESS FORMS, INC. 7

COCK INLET-WESTERN GULF OF ALASKA EARTHQUAKES

1977	ORIGI- HR MN	TIME SEC	LAT N DEG MIN	LONG W DEG MIN	DEPTH KM	MAG	NO	CAP DEC	DM KM	RVS SEC	ERH KM	ERZ KM	Q				
NOV	7	21	32	5.4	59	11.3	152	53.5	46.1	2.3	6	121	21	0.13	1.9	3.1	B
	7	23	9	4.8	60	18.5	152	43.6	137.0	3.2	17	152	12	0.37	6.9	8.5	D
	8	6	2	14.1	57	23.6	153	29.4	5.0	1.7	3	273	42	0.04	0.	0.	C
	8	4	15	59.0	57	2.7	153	17.4	6.8	1.8	4	208	82	0.05	0.	0.	C
	8	17	23	12.9	59	45.2	152	25.1	75.5	2.2	10	118	44	0.34	3.9	7.8	C
	8	18	24	41.4	60	20.0	151	13.5	5.0	2.2	6	275	78	0.78	32.2	99.9	D
	8	23	3	26.9	60	9.6	151	59.9	63.4	3.1	24	109	51	0.55	2.7	5.6	C
	9	0	27	14.3	55	57.3	153	10.9	29.8	3.1	8	305	91	1.33	137.8	26.8	D
	9	2	30	54.7	56	26.0	156	29.4	28.8	2.4	5	211	110	0.48	12.2	13.4	D
	9	6	15	31.0	60	7.7	151	31.0	5.0	1.1	3	248	73	0.	0.	0.	C
	9	7	55	26.3	59	57.2	152	11.6	55.1	2.7	14	112	45	0.48	3.5	6.6	C
	9	10	44	9.7	60	12.6	152	10.3	5.0	2.3	5	209	40	1.16	50.9	92.2	D
	9	12	32	33.4	58	40.7	154	18.3	17.3	2.3	10	87	47	0.37	2.3	5.4	C
	9	15	2	1.5	60	9.7	153	10.8	144.5	2.7	7	165	36	0.15	4.6	8.1	C
	9	20	11	13.9	58	41.0	154	16.0	4.5	2.9	11	86	46	0.48	2.6	5.0	C
	9	20	13	17.8	59	40.4	154	19.8	0.3	2.7	6	106	48	0.50	5.6	33.7	D
	9	23	35	27.2	58	41.6	154	15.7	5.7	2.4	12	85	45	0.43	2.3	4.1	C
	10	0	51	19.5	57	52.9	155	27.5	6.7	1.4	5	168	12	0.11	2.5	2.2	C
	10	7	17	53.0	59	5.3	152	39.9	110.5	3.0	13	139	37	0.32	5.1	7.4	D
	10	7	3	15.0	59	40.1	154	17.6	1.8	3.4	18	87	48	0.40	1.6	3.5	C
	10	0	46	35.3	57	56.3	156	6.5	129.1	2.6	8	95	18	0.31	6.3	10.5	C
	10	12	22	53.3	59	55.9	152	29.8	93.3	2.7	11	138	51	0.42	6.2	9.1	D
	10	13	1	36.3	60	1.6	152	49.6	116.3	2.4	7	155	43	0.28	7.6	11.7	D
	10	14	44	46.5	57	10.3	155	29.8	71.9	2.1	8	157	54	0.31	4.0	8.7	D
	10	16	47	43.4	58	43.7	152	56.8	61.0	2.6	14	75	36	0.28	1.9	3.3	B
	10	18	45	6.0	60	4.3	152	0.0	135.2	2.2	4	204	50	0.05	0.	0.	C
	10	19	46	26.5	59	18.4	151	34.0	117.2	2.8	4	295	18	0.01	0.	0.	C
	10	22	34	57.3	57	58.3	153	39.9	62.8	2.2	7	101	24	0.25	3.6	5.3	C
	10	23	5	14.3	59	1.9	154	16.9	125.6	2.2	5	139	9	0.11	5.3	10.8	D
	11	0	25	44.5	59	49.5	152	3.7	147.2	2.3	4	159	29	0.	0.	0.	C
	11	0	49	42.9	56	32.4	153	4.6	29.4	3.4	11	257	67	0.49	10.9	3.3	D
	11	2	6	15.4	57	48.7	156	32.7	5.0	1.0	3	261	6	0.36	0.	0.	D
	11	3	43	50.9	57	50.3	156	14.9	135.2	2.8	8	163	14	0.25	9.4	14.1	D
	11	10	37	59.9	60	22.7	151	31.4	2.5	2.9	4	268	69	0.54	0.	0.	D
	11	11	51	25.9	60	33.5	151	56.8	153.3	2.5	4	279	49	0.15	0.	0.	C
	11	14	20	34.8	58	20.6	154	43.8	5.0	2.3	12	96	78	0.52	2.6	639.0	D
	11	18	18	11.0	57	42.8	153	5.3	38.6	2.7	7	156	38	0.10	1.2	0.7	C
	12	5	24	14.9	59	20.6	154	42.9	2.3	2.2	9	95	79	0.36	2.2	486.0	D
	12	7	23	5.9	58	42.5	153	2.7	65.7	2.2	10	98	39	0.26	2.5	3.9	B
	12	8	46	16.8	59	44.7	153	50.2	4.4	2.1	10	134	29	0.57	3.7	5.4	D
	12	9	9	46.6	58	44.5	153	53.7	10.9	2.0	5	186	31	0.49	9.5	999.9	D
	12	10	56	24.0	60	45.0	151	2.6	41.6	2.7	7	303	101	0.27	27.4	418.0	D
	12	11	26	44.8	57	7.5	153	54.9	19.9	2.6	7	110	49	0.40	3.3	611.2	C
	12	15	35	33.6	59	59.1	153	13.3	146.1	3.1	14	148	37	0.27	2.8	3.5	C
	12	13	50	43.7	59	37.1	152	43.7	83.7	2.6	9	87	28	0.35	4.6	7.2	B

COCK INLET-WESTERN GULF OF ALASKA EARTHQUAKES

1977	ORIGIN HR MN	TIME SEC	LAT N DEG MIN	LONG W DEG MIN	DEPTH KM	MAG	NO	GAP DEG	DM KM	RMS SEC	ERH KM	ERZ KM	Q
NOV	12 17 14	27.7	60 5.4	150 58.9	154.5	2.6	4	276	60	0.03	0.	0.	C
	12 14 35	58.2	59 20.5	152 26.9	43.5	2.2	5	161	32	0.05	1.4	1.7	C
	12 16 17	40.1	60 9.0	153 9.0	164.6	2.9	10	130	36	0.26	5.4	6.2	C
	12 16 20	15.7	59 2.8	153 23.2	9.2	2.0	9	120	13	0.22	1.4	1.3	C
	12 16 23	26.8	59 3.0	153 25.6	18.9	2.0	7	158	11	0.22	2.2	3.4	C
	12 19 36	12.6	59 2.5	153 25.3	8.9	2.4	7	113	32	0.18	1.5	2.3	C
	12 22 13	44.1	59 52.7	153 18.6	126.2	2.9	14	143	25	0.48	5.6	5.3	D
	13 2 2	4.3	57 4.2	155 47.7	5.0	1.8	6	233	74	0.82	17.9	9.9	D
	13 2 31	18.5	59 35.3	153 20.0	91.6	2.1	4	190	9	0.	0.	0.	C
	13 5 54	44.9	60 14.1	151 1.3	82.0	2.7	9	278	73	0.19	9.8	8.9	D
	13 6 5	42.3	59 21.7	152 36.9	21.3	1.8	6	233	41	0.10	3.8	8.4	D
	13 6 52	23.8	59 15.2	152 0.3	54.3	2.4	10	151	34	0.37	4.8	11.0	C
	13 10 25	42.2	60 20.3	152 35.8	120.1	3.0	10	192	13	0.18	5.0	6.8	D
	13 13 7	41.3	59 36.9	153 24.0	126.7	3.7	23	85	10	0.48	3.4	3.5	B
	13 14 36	41.3	56 10.0	155 14.0	23.6	2.8	7	229	109	0.20	4.7	4.9	D
	13 18 24	17.2	60 9.7	152 44.1	121.9	2.7	5	150	28	0.22	13.3	27.3	D
	14 4 42	44.4	59 29.7	152 59.7	106.4	2.6	10	86	22	0.30	3.8	6.5	B
	14 6 47	53.2	57 50.0	153 16.8	147.3	1.8	6	139	26	0.01	0.1	0.1	D
	14 8 10	47.1	56 59.8	155 53.0	101.1	2.2	4	330	84	0.67	0.	0.	B
	14 10 5	20.4	59 30.8	152 56.5	98.2	2.3	7	140	22	0.14	4.2	7.5	C
	14 17 47	10.1	59 38.1	151 6.6	16.5	2.5	5	258	97	0.04	1.5	1.1	C
	15 1 23	20.8	59 11.1	153 39.6	100.6	2.4	8	104	26	0.25	4.3	6.7	C
	15 11 45	50.7	58 57.2	154 15.8	125.5	2.7	8	125	16	0.26	4.4	6.0	C
	15 15 55	21.3	56 12.0	152 58.6	32.7	3.0	11	283	84	0.51	21.8	4.1	D
	15 17 37	55.1	59 14.2	154 30.9	5.0	2.3	9	84	69	0.42	2.5	560.0	D
	15 18 32	40.2	57 40.7	152 49.2	5.0	1.7	3	221	47	0.	0.	0.	C
	15 19 28	20.1	59 35.6	152 49.8	5.0	2.1	3	127	28	0.	0.	0.	C
	15 23 7	42.2	59 46.8	153 23.1	73.0	3.1	20	58	21	0.30	1.5	2.8	B
	16 0 5	43.1	58 3.7	156 23.9	4.7	3.0	9	178	4	0.29	2.6	1.7	C
	16 5 33	33.9	59 22.0	154 44.1	5.0	2.1	5	103	80	0.27	3.7	596.7	D
	16 5 47	56.6	57 51.7	154 46.8	54.2	2.4	7	94	44	0.44	7.9	19.7	C
	16 7 32	17.7	57 11.3	155 23.2	3.1	3.0	13	119	65	4.94	26.7	132.7	D
	16 10 39	0.7	57 51.9	153 2.1	38.3	2.4	6	130	23	0.09	1.5	1.0	B
	16 14 19	0.7	60 15.5	149 34.0	21.8	3.1	6	316	133	0.33	79.2	15.7	D
	16 16 34	5.2	59 49.1	153 5.9	123.8	2.2	4	157	19	0.	0.	0.	C
	16 16 35	47.6	57 52.7	156 27.4	4.8	2.1	5	156	3	0.08	1.3	0.9	C
	16 22 38	52.2	60 2.9	152 59.2	135.7	2.8	13	136	43	0.33	5.4	8.1	D
	16 23 6	31.9	60 2.0	152 39.3	104.4	2.2	6	186	32	0.17	5.6	8.0	D
	17 5 49	10.4	57 58.6	153 38.3	49.3	2.7	6	173	25	0.07	1.5	1.7	C
	17 7 12	35.8	56 45.2	154 30.8	34.2	1.8	5	195	29	0.11	2.8	1.9	D
	18 10 36	32.0	60 0.7	151 40.2	63.4	3.2	26	123	39	0.89	4.1	7.6	C
	18 11 32	25.0	60 3.2	152 20.8	194.6	2.7	4	168	47	0.	0.	0.	C
	18 16 12	2.3	57 39.9	153 17.2	42.7	2.5	9	189	30	0.12	1.0	1.9	B
	18 22 10	55.5	60 9.8	153 50.5	219.6	3.2	6	254	63	0.16	11.2	20.2	D
	19 8 57	25.9	57 15.9	154 59.9	50.4	2.1	6	182	23	0.27	5.7	6.0	D

COOK INLET-WESTERN GULF OF ALASKA EARTHQUAKES

1977	ORIGIN		TIME	LAT N		LONG W		DEPTH	MAG	NO	GAP	DM	RMS	ERH	ERZ	Q
	HR	MIN	SEC	DEG	MIN	DEG	MIN	KM			DEG	KM	SEC	KM	KM	
NOV	19	21	5	40.9	60 49.7	153 25.6	5.0	2.4	4	217	58	0.01	0.	0.	C	
	19	21	40	47.5	58 58.9	153 36.7	19.6	1.7	4	169	5	0.01	0.	0.	C	
	19	23	11	54.3	58 17.5	151 24.6	30.6	3.3	10	231	66	0.45	6.9	3.3	D	
	20	17	10	30.3	59 49.9	153 10.4	122.6	3.5	17	132	52	0.43	3.6	4.1	C	
	20	21	10	34.3	59 35.3	152 47.7	113.1	3.1	10	92	39	0.73	8.9	13.5	C	
	21	13	29	34.2	58 21.7	154 44.8	5.0	2.7	12	97	79	0.52	2.8	640.2	D	
	21	13	34	34.2	59 15.5	152 33.2	90.8	4.4	28	84	47	0.75	3.2	4.7	C	
	21	14	25	2.6	59 54.9	152 21.3	96.6	3.7	26	72	49	0.44	2.2	3.1	D	
	21	15	53	43.2	58 20.4	154 43.8	1.3	2.5	8	139	78	0.45	2.5	25.2	D	
	21	15	53	55.4	56 46.9	155 4.3	5.0	2.6	3	232	66	0.	0.	0.	C	
	21	19	32	22.2	57 51.9	154 4.2	30.5	2.4	6	224	68	0.03	0.8	0.5	C	
	22	00	32	43.4	59 2.6	154 6.6	113.6	2.8	10	112	8	0.22	2.7	3.8	C	
	22	5	10	57.2	57 41.7	154 13.7	59.7	2.4	11	81	28	0.24	2.0	3.7	B	
	22	6	46	43.7	58 21.6	154 42.8	5.0	1.9	8	96	80	0.40	2.7	59.3	D	
	22	6	47	45.6	59 37.6	152 23.1	107.3	2.6	4	163	42	0.65	0.	0.	D	
	22	7	32	7.9	59 0.7	153 23.5	5.9	1.9	6	165	10	0.19	2.2	2.0	C	
	22	9	52	16.5	60 36.3	152 1.4	155.2	2.4	4	285	46	0.07	0.	0.	C	
	22	9	27	46.8	57 58.4	153 56.1	3.9	2.6	7	217	36	0.29	4.8	4.2	D	
	22	11	23	9.4	60 17.3	153 26.2	0.3	2.7	5	130	39	0.28	3.0	14.7	D	
	22	15	11	33.2	59 30.5	151 31.6	9.4	2.4	7	227	5	0.36	7.9	2.6	D	
	22	20	6	56.9	58 5.8	153 31.5	0.1	3.1	13	194	12	0.60	4.5	13.4	D	
	22	22	5	33.4	59 20.5	150 33.0	24.5	3.1	9	265	109	0.82	21.3	7.5	D	
	23	2	11	3.1	60 28.6	150 59.7	2.5	2.5	4	290	98	0.48	0.	0.	D	
	23	5	33	17.3	56 30.0	152 48.3	25.1	4.2	23	262	75	0.53	7.9	2.7	D	
	23	8	26	23.5	60 23.6	151 12.0	2.5	2.1	4	280	85	0.48	0.	0.	D	
	23	9	3	25.8	58 20.5	154 47.8	1.9	2.3	6	211	88	0.97	3.3	11.6	D	
	23	10	48	22.5	59 49.9	150 35.4	60.6	3.1	6	279	62	0.14	9.5	4.4	D	
	23	11	24	22.7	58 58.0	151 27.0	56.9	2.8	7	277	56	0.18	11.9	11.5	D	
	23	13	7	35.2	59 0.3	152 16.7	55.1	2.2	8	148	42	0.17	1.9	4.9	C	
	23	14	3	47.7	57 33.8	152 25.2	47.9	2.7	13	209	21	0.33	4.2	4.2	D	
	23	15	11	15.3	59 7.6	152 22.4	57.8	2.5	10	129	55	0.18	1.6	3.9	B	
	23	20	54	16.9	60 0.4	152 56.7	36.6	2.5	5	172	47	0.57	13.7	18.2	D	
	23	21	11	25.3	57 16.8	153 46.8	11.7	2.5	5	169	44	0.56	10.2	99.9	D	
	24	1	52	37.3	59 16.6	153 33.8	107.1	3.1	15	57	10	0.61	4.9	8.0	C	
	24	3	46	45.6	60 11.7	153 3.6	134.5	2.5	8	159	29	0.22	5.7	10.1	D	
	24	7	21	25.8	56 32.0	155 56.9	33.5	2.5	6	242	104	0.08	2.3	1.9	C	
	24	10	38	5.2	58 19.8	155 9.6	5.0	2.0	6	160	65	2.91	38.3	99.9	D	
	24	13	24	0.2	58 19.5	154 43.0	5.0	1.5	6	153	77	0.08	0.9	132.0	D	
	25	14	15	2.7	59 59.6	150 22.2	65.4	3.1	10	287	80	0.20	9.0	4.8	D	
	25	9	57	21.3	60 5.8	147 19.2	1.3	3.9	17	128	92	1.10	5.6	34.8	D	
	25	10	14	34.1	59 16.6	152 56.4	41.4	2.1	9	111	80	0.35	3.0	466.7	C	
	25	12	29	34.5	59 18.4	154 42.6	5.0	1.6	4	263	76	0.31	0.	0.	D	
	25	12	49	41.6	58 19.8	154 41.5	5.0	2.3	7	217	78	0.32	5.5	48.3	D	
	25	13	12	32.3	59 20.1	154 44.6	2.5	2.4	8	115	77	0.29	6.3	99.9	D	
	25	16	39	53.7	57 12.3	155 43.1	73.3	2.3	5	238	64	0.11	5.7	9.3	D	

COCK INLET-WESTERN GULF OF ALASKA EARTHQUAKES

1977	ORIGI HR	TIME MN	TIME SEC	LAT N DEG	MIN	LONG W DEG	MIN	DEPTH KM	MAG	NO	GAP DEG	DM KM	RMS SEC	ERH KM	ERZ KM	Q	
MOV	25	19	25	25.0	57	53.6	156	36.9	17.3	2.0	5	209	23	0.23	5.9	13.3	D
	25	22	10	44.7	59	52.1	154	32.2	121.9	2.9	13	97	32	0.29	2.5	4.6	C
	26	1	51	25.4	59	36.5	152	48.3	100.5	3.3	17	84	24	0.37	3.1	4.3	B
	26	3	34	59.9	53	5.7	157	5.2	9.7	2.1	5	287	44	0.10	7.9	216.9	D
	26	5	31	56.4	57	4.9	150	41.4	37.5	3.0	6	285	145	0.15	9.4	257.5	D
	26	7	51	47.3	59	34.2	152	59.8	98.9	2.5	5	164	74	0.03	0.8	1.5	C
	26	9	30	24.1	59	21.4	154	45.4	92.5	2.2	8	97	79	0.37	2.5	52	D
	26	17	21	7.4	59	48.9	152	53.7	96.5	2.8	12	98	61	0.31	3.3	6.3	C
	26	19	12	15.0	56	42.3	156	12.2	192.8	2.5	4	314	87	0.05	0.	0.	C
	26	20	48	44.5	57	22.5	152	30.0	36.4	1.9	4	263	42	0.	0.	0.	C
	26	5	22	7.9	60	6.0	152	32.0	90.1	2.9	4	155	38	0.19	0.	0.	C
	26	21	46	54.2	60	5.9	153	54.9	111.6	3.0	11	113	36	0.45	6.0	9.2	C
	26	23	44	32.4	57	1.0	153	14.7	233.5	2.3	15	261	19	0.01	0.4	0.3	C
	27	2	27	40.1	57	40.8	156	36.1	132.8	2.8	13	153	20	0.23	2.5	3.5	C
	27	2	54	5.1	59	58.8	152	49.7	101.5	2.9	13	115	49	0.41	4.2	6.3	C
	27	8	49	15.7	60	7.0	152	17.4	30.2	2.6	4	183	42	0.51	0.8	0.8	D
	27	12	17	19.0	60	13.1	152	1.9	5.0	2.9	9	222	46	1.78	23.8	26.8	D
	27	17	22	28.7	56	15.8	155	44.8	39.4	2.2	4	240	128	0.13	0.	0.	D
	27	15	5	7.3	59	19.8	155	3.7	116.5	3.3	25	107	67	0.29	1.4	3.1	B
	27	18	17	53.0	58	18.9	155	2.9	112.9	3.2	21	107	66	0.29	1.6	3.5	B
	27	18	38	45.5	59	15.5	155	5.4	115.2	2.4	6	232	59	0.24	11.4	16.7	D
	27	20	11	49.2	59	59.1	153	7.7	73.0	2.1	9	124	23	0.30	3.3	4.4	C
	27	21	2	44.9	59	2.7	153	50.1	100.4	2.6	13	82	20	0.33	2.8	4.3	B
	27	21	12	20.4	59	20.5	154	45.4	2.5	2.8	10	97	77	0.48	2.7	621.3	D
	27	21	32	24.3	58	18.0	154	43.6	2.5	1.9	5	213	75	0.12	3.0	273.6	D
	28	2	21	39.4	57	16.8	153	45.3	38.9	2.5	5	169	42	0.	0.1	0.1	C
	28	2	31	23.3	56	27.3	153	24.3	32.5	2.5	5	270	49	0.10	5.2	1.6	D
	28	2	39	30.0	56	6.4	153	5.4	17.7	2.7	5	306	84	1.29	1.9	48.6	D
	28	2	50	21.5	56	53.5	155	30.1	41.8	3.4	16	148	72	0.34	2.1	394.5	D
	28	6	53	30.0	59	21.5	154	46.0	5.0	3.0	13	98	78	0.42	2.0	500.2	D
	28	6	56	20.3	59	21.3	154	47.4	2.5	2.2	7	59	77	0.39	3.3	594.0	D
	28	8	4	2.1	59	36.4	152	49.2	91.5	2.8	6	102	45	0.22	3.6	7.9	D
	28	13	33	56.5	57	48.1	156	0.7	120.8	2.2	4	219	18	0.	0.	0.	C
	28	15	31	51.0	60	0.4	152	44.0	130.9	2.5	10	138	46	1.65	21.7	30.9	D
	28	18	50	2.5	58	21.8	154	44.0	2.5	2.2	10	97	80	0.48	2.8	616.7	D
	28	19	52	34.5	59	20.8	153	0.7	48.6	2.5	7	194	32	0.32	5.8	7.1	D
	28	20	53	24.4	60	6.1	153	47.6	1.1	2.7	8	181	29	0.53	6.2	22.8	D
	29	3	14	40.0	60	1.5	147	7.7	45.8	3.8	19	131	80	1.32	11.1	127.2	C
	29	4	4	3.4	58	3.8	156	22.2	4.1	2.2	4	311	2	0.12	0.	0.	C
	29	10	38	4.4	57	30.9	155	9.4	64.4	2.1	4	187	35	0.	0.	0.	C
	29	10	53	57.0	59	46.7	153	12.4	64.7	2.6	10	70	27	0.22	1.8	3.1	B
	29	13	20	57.3	59	55.1	153	12.1	74.3	2.3	7	124	19	0.15	2.4	3.4	B
	29	17	0	26.7	59	9.4	153	41.4	103.1	2.9	14	63	24	0.34	2.9	4.3	B
	29	23	1	30.7	60	16.7	151	50.9	5.0	2.7	7	243	53	1.01	46.0	56.9	D
	30	0	51	14.8	54	55.8	161	17.8	66.0	3.8	4	341	439	0.45	0.	0.	D

COOK INLET-WESTERN GULF OF ALASKA EARTHQUAKES

1977	OP HR	ORIG MN	TIME SEC	LAT N DEG MIN	LONG W DEG MIN	DEPTH KM	MAG	NO	GAP DEG	CM KM	RMS SEC	ERH KM	ERZ KM	Q		
NOV	30	9	23	59.6	13.4	153	46.7	139.2	2.8	10	71	23	0.09	1.4	2.1	B
	30	9	28	56.1	13.0	151	55.2	60.5	2.5	8	162	34	0.20	3.0	7.1	C
	30	10	10	5.1	5.0	152	58.2	76.3	2.6	12	95	35	0.28	2.3	3.4	B
	30	11	23	53.2	58.4	152	12.7	10.4	1.8	5	203	39	0.45	10.1	999.9	D
	30	11	54	24.7	6.2	156	39.2	87.3	2.7	10	128	35	0.33	3.5	5.2	C
DEC	30	13	51	24.4	49.2	153	5.1	111.4	2.6	9	126	20	0.21	3.0	6.5	C
	30	21	19	59.8	6.7	150	34.3	5.0	1.5	5	320	118	1.22	77.2	48.1	D
	1	3	45	55.7	48.8	154	5.1	5.0	2.5	8	72	62	0.63	4.2	889.9	D
	1	7	31	13.3	59.4	154	15.4	86.6	2.5	9	104	47	0.46	5.5	12.3	C
	1	11	23	48.1	40.6	155	44.0	167.5	3.0	17	157	62	0.55	5.0	9.6	D
	1	11	33	14.3	21.4	154	44.3	5.0	2.5	11	97	79	0.77	4.1	966.0	D
	1	14	20	12.0	30.1	151	31.2	55.5	3.0	13	132	69	0.90	8.0	21.6	C
	1	16	48	45.1	20.7	154	57.5	79.1	2.9	13	98	19	0.55	3.9	7.4	C
	1	17	54	44.7	23.7	152	46.7	122.1	3.8	31	58	2	0.50	2.3	3.5	C
	2	1	26	4.5	16.4	150	46.5	28.0	3.2	15	276	115	0.35	10.1	3.3	D
	2	3	56	15.1	46.7	155	0.4	80.4	3.7	21	81	30	0.27	1.5	2.9	B
	2	5	49	53.6	20.2	154	44.5	5.0	1.6	5	96	77	0.20	2.7	444.9	D
	2	9	7	25.8	52.8	152	9.1	59.0	1.9	5	161	37	0.03	1.0	2.3	C
	2	10	58	12.0	4.0	155	33.4	110.4	2.6	11	143	32	0.24	2.9	3.8	C
	2	13	27	23.0	49.8	153	2.4	104.9	2.6	15	91	22	0.32	2.6	4.1	C
	2	14	9	9.4	55.8	156	45.3	5.4	3.0	12	187	27	0.47	3.6	3.3	D
	2	18	31	49.3	16.1	155	49.9	66.1	1.9	8	150	55	0.40	5.2	9.1	D
	2	18	44	50.3	55.6	152	40.3	115.9	2.8	13	123	43	0.32	4.3	6.1	D
	2	18	36	49.9	14.6	152	32.6	140.0	2.9	9	175	23	0.06	4.7	11.1	D
	3	6	58	23.0	3.7	152	57.9	73.9	2.3	5	139	34	0.13	3.9	4.2	D
	3	7	21	0.5	56.3	156	44.6	7.3	2.8	13	187	17	0.46	3.5	2.6	D
	3	8	20	48.8	17.5	153	45.1	23.2	1.5	4	166	43	0.0	0.0	0.0	C
	3	15	34	53.6	15.8	153	30.0	103.0	2.4	8	144	9	0.27	7.8	6.0	D
	3	18	9	22.0	31.9	154	2.3	77.3	2.6	12	92	55	0.28	2.2	5.9	C
	3	20	23	4.1	26.6	154	46.2	42.0	2.0	7	128	14	0.15	1.7	2.3	B
	3	21	39	11.9	51.6	152	47.5	87.1	2.1	6	134	33	0.22	5.0	8.2	C
	4	4	10	49.3	17.5	153	38.0	120.9	2.5	9	144	12	0.20	4.5	4.5	C
	4	4	47	51.8	18.7	152	28.5	65.3	2.5	10	104	50	0.28	2.5	6.3	C
	4	5	0	22.6	32.3	151	12.9	1.3	2.9	16	134	86	0.36	5.6	31.2	D
	4	11	38	7.9	57.4	155	57.9	6.7	2.5	7	165	24	0.22	2.1	2.2	C
	4	17	46	43.8	20.5	152	46.4	153.1	2.4	8	182	8	0.27	9.7	10.9	D
	4	19	43	30.5	10.1	153	48.3	104.6	2.1	7	213	28	0.13	4.5	3.0	D
	4	19	53	35.1	47.8	152	17.7	101.5	3.2	21	104	49	0.49	2.9	5.0	C
	4	23	55	45.9	27.5	152	28.6	84.6	2.4	6	139	47	0.21	4.3	11.6	C
	5	0	2	52.8	13.2	151	45.3	96.5	3.4	18	242	60	0.38	7.6	7.7	D
	5	3	28	3.2	52.8	153	23.2	32.1	4.2	22	203	36	0.35	2.8	1.4	D
	5	5	19	46.9	21.3	154	46.6	2.5	1.9	6	98	78	0.38	3.6	650.3	D
	5	5	4	19.6	16.6	157	11.0	50.4	2.4	7	226	63	0.19	4.5	9.8	D
	5	7	32	49.8	18.0	152	33.1	101.3	2.6	16	187	17	0.33	3.8	5.0	D
	5	8	47	20.5	36.5	154	50.8	89.8	2.0	5	129	33	0.13	6.3	10.8	D

143278 (11-27) LONE PUBLISHING CO. PMS, INC.

COCK INLET-WESTERN GULF OF ALASKA EARTHQUAKES

1977	ORIGIN TIME			LAT N		LONG W		DEPTH	MAG	NO	GAP	DM	RMS	ERH	ERZ	O	
	HR	MM	SEC	DEG	MIN	DEG	MIN	KM			DEG	KM	SEC	KM	KM		
DEC	5	10	21	23.3	53	15.4	154	9.2	88.9	2.0	6	141	59	0.17	3.0	8.1	D
	5	12	0	27.4	58	21.8	154	44.1	5.0	2.2	7	97	80	0.28	2.2	420.6	D
	5	14	9	12.3	60	12.3	154	10.6	83.4	2.1	5	268	81	0.12	9.7	10.5	D
	5	15	9	15.0	59	39.3	152	57.8	101.1	2.5	15	83	15	0.20	1.8	2.9	B
	5	15	36	25.7	60	11.2	152	48.8	121.7	2.5	7	164	25	0.16	6.2	12.4	D
	5	19	9	59.0	58	10.2	154	23.3	0.2	2.0	7	108	44	0.70	6.3	39.5	D
	6	2	33	24.6	56	33.8	156	15.3	40.9	2.2	8	203	85	0.29	4.6	406.9	D
	6	12	44	29.3	50	42.7	153	16.9	87.3	2.1	5	119	36	0.16	5.0	13.2	D
	6	13	39	29.7	57	52.6	153	28.6	50.0	1.9	4	169	21	0.0	0.0	0.0	C
	6	14	14	2.3	58	19.3	154	49.7	5.0	2.4	9	98	73	0.55	3.4	731.7	D
	6	17	24	10.3	58	17.9	154	50.7	2.5	1.9	6	136	70	0.12	1.2	201.8	D
	6	17	51	17.9	59	45.4	151	47.3	47.7	4.2	26	160	35	0.39	2.0	4.4	C
	6	20	11	19.7	57	25.7	154	40.8	43.6	1.8	6	123	11	0.11	2.2	2.3	B
	6	20	37	36.0	60	13.0	152	35.9	189.8	2.5	4	164	24	0.02	0.0	0.0	C
	6	20	49	30.0	58	47.2	153	24.9	100.4	2.1	6	189	20	0.0	0.3	0.2	C
	7	0	34	42.3	58	58.3	152	31.3	67.1	2.1	7	121	39	0.17	2.2	4.4	B
	7	7	6	39.5	57	28.7	153	44.7	35.6	2.3	5	122	31	0.05	0.8	0.8	C
	7	7	6	50	58	15.2	154	16.0	80.1	2.3	10	94	62	0.31	2.8	8.3	C
	7	7	9	0	58	46.3	153	3.7	59.3	2.2	5	188	33	0.06	3.3	3.9	C
	7	7	9	12	57	26.0	153	30.1	83.8	2.3	10	166	38	0.24	3.3	4.4	C
	7	10	10	0.3	58	20.8	154	43.9	0.6	2.5	13	114	78	0.55	2.6	38.3	D
	7	10	21	51.5	58	21.5	154	47.2	5.0	1.9	8	134	78	0.33	2.6	467.1	D
	7	10	53	24.4	59	21.5	154	45.9	5.0	1.3	5	133	78	0.20	2.8	440.0	D
	7	12	18	44.3	59	21.0	154	47.2	10.8	2.2	7	134	77	0.24	2.2	371.1	D
	7	12	23	50.2	58	56.6	153	6.1	73.6	3.0	19	73	24	0.31	1.7	2.9	B
	7	12	37	22.8	58	55.7	153	9.0	72.1	2.1	5	129	22	0.23	7.2	8.7	D
	7	12	38	14.7	57	32.0	154	46.8	40.9	1.3	6	124	24	0.07	1.0	0.5	B
	7	15	53	27.1	59	2.3	154	25.8	142.4	3.2	13	95	14	0.30	3.4	6.0	C
	7	16	28	55.0	59	55.3	152	50.8	113.8	2.2	10	149	36	0.21	3.6	5.6	C
	7	18	12	46.5	58	53.2	153	57.3	0.2	1.7	5	154	25	0.11	0.1	0.7	C
	7	18	47	40.2	57	0.9	154	19.4	70.9	2.9	16	168	53	0.42	3.3	6.1	D
	7	22	45	42.6	59	36.1	145	49.1	35.9	4.3	18	237	35	0.80	12.2	4.5	D
	8	0	38	12.0	58	15.2	153	29.8	51.4	3.5	21	75	29	0.58	2.9	7.0	C
	8	1	58	5.7	59	21.4	151	18.9	66.0	4.5	31	113	19	0.45	2.0	2.0	C
	8	3	15	12.3	59	57.7	152	52.1	96.3	1.9	7	156	40	0.24	5.1	9.1	D
	8	5	5	6.5	58	4.1	153	31.1	28.9	1.7	7	168	35	0.74	8.6	8.6	D
	8	8	53	47.3	57	58.6	154	43.6	3.0	1.5	5	192	52	0.27	5.3	4.9	D
	8	10	20	3.5	59	52.6	150	54.2	85.7	2.3	4	280	48	0.0	0.0	0.0	C
	8	12	2	41.8	58	0.9	154	16.8	74.1	2.2	5	169	41	0.05	1.4	2.4	C
	8	20	21	39.4	57	53.1	156	28.7	154.7	2.7	9	237	19	0.26	11.1	15.4	D
	8	21	47	6.1	60	42.3	152	27.7	191.3	2.9	6	330	36	0.21	24.8	32.7	D
	9	4	51	50.1	60	7.5	152	26.7	101.3	2.4	6	168	37	0.30	10.6	16.8	D
	9	7	55	11.3	56	13.5	156	5.0	33.3	3.5	11	97	44	0.60	6.1	6.2	C
	9	12	12	40.4	58	19.5	155	14.4	117.0	2.5	9	151	63	0.25	4.3	16.1	D
	9	14	47	51.5	59	36.1	153	27.4	122.1	2.9	14	160	13	0.23	2.7	3.3	C

COCK INLET-WESTERN GULF OF ALASKA EARTHQUAKES

1977	ORIGIN TIME			LAT N		LONG W		DEPTH	MAG	NC	GAP	DM	RMS	ERH	ERZ	Q
	HR	MM	SEC	DEG	MIN	DEG	MIN	KM			DEG	KM	SEC	KM	KM	
DEC	9	18	54	50.4	57	57.0	156	6.0	2.2	6	138	17	0.23	14.1	24.2	D
	9	21	27	14.9	60	58.3	153	51.0	2.7	7	154	31	0.17	5.7	9.8	D
	10	2	1	17.6	59	50.9	152	28.2	2.0	5	129	47	0.13	3.6	6.3	D
	10	4	0	4.3	60	26.7	152	35.8	2.4	5	259	37	0.05	2.7	1.5	D
	10	5	57	4.2	59	15.6	153	45.8	2.3	7	76	20	0.07	1.4	2.9	B
	10	9	1	2.8	60	46.6	151	47.5	4.0	31	112	66	0.86	3.9	8.8	C
	10	10	11	30.9	57	45.6	154	24.9	2.2	5	155	38	0.31	7.4	6.0	D
	10	10	54	57.2	59	55.8	152	8.3	2.7	12	170	41	0.33	4.5	7.1	C
	10	12	28	55.7	59	15.3	152	20.9	2.9	14	119	49	0.29	2.1	4.3	B
	10	13	34	37.3	59	58.8	152	10.9	2.6	4	174	46	0.	0.	0.	C
	11	0	7	25.4	59	16.7	153	8.1	2.2	8	104	42	0.23	2.6	4.6	C
	11	7	43	33.7	57	51.5	152	48.8	2.7	11	105	22	0.49	4.5	2.8	C
	11	9	30	23.5	56	22.1	156	44.1	2.8	10	216	71	0.43	6.9	6.2	D
	11	10	34	53.8	58	26.0	150	57.8	2.4	7	247	83	0.49	12.3	4.5	D
	11	12	16	17.1	59	53.3	153	26.9	2.0	8	102	8	0.21	2.3	3.6	B
	11	17	4	15.9	56	47.6	153	13.5	2.8	4	293	42	0.43	0.	0.	D
	12	9	26	44.2	59	40.9	153	55.0	2.3	7	114	33	0.35	4.1	8.0	C
	12	10	34	17.3	59	25.9	153	47.8	2.3	7	248	61	0.12	3.4	4.0	C
	12	20	44	13.5	59	36.4	151	15.2	1.8	4	283	63	0.04	0.	0.	C
	12	22	14	2.3	60	1.5	153	53.6	3.4	13	95	55	0.28	3.3	5.9	C
	12	22	20	8.0	59	44.5	153	34.0	0.5	5	207	23	0.21	4.2	16.6	D
	12	23	4	2.0	60	11.6	152	26.8	2.7	6	184	31	0.26	9.8	15.8	D
	13	8	46	37.7	60	53.9	153	0.7	2.1	5	184	41	0.14	7.8	19.6	D
	13	10	50	1.6	59	59.4	151	47.3	2.6	8	216	37	0.19	5.1	7.6	D
	13	11	46	2.0	60	50.9	146	29.6	3.9	4	339	314	1.15	0.	0.	D
	14	1	54	4.3	59	34.4	153	51.6	2.5	6	295	46	0.39	37.8	13.8	D
	14	2	33	31.3	59	39.3	152	36.2	2.4	5	116	39	0.01	0.4	0.9	C
	14	6	39	57.1	59	35.3	153	50.9	2.3	5	294	44	0.50	62.3	99.9	D
	14	11	49	43.4	59	34.3	153	51.7	2.3	4	295	46	0.41	0.	0.	D
	14	13	8	15.9	59	29.0	152	31.0	2.8	7	133	44	0.09	1.6	3.9	B
	14	13	10	12.6	59	25.5	151	3.9	2.9	8	290	29	0.19	10.1	4.3	D
	14	14	20	41.7	59	44.3	152	54.3	2.2	5	123	20	0.03	0.9	2.5	C
	14	23	7	46.6	58	41.3	153	51.3	2.0	4	283	35	0.	0.	0.	C
	15	1	0	37.9	60	36.1	153	16.5	2.9	5	302	34	0.16	29.7	55.3	D
	15	3	41	36.6	60	34.2	151	58.7	3.1	6	281	46	0.12	10.1	10.3	D
	15	17	18	30.7	58	44.7	153	52.0	3.4	10	169	30	0.48	3.9	6.2	C
	16	0	48	27.2	57	41.9	155	59.7	3.6	5	285	188	0.17	16.7	389.1	D
	16	6	48	29.1	59	17.7	153	2.7	2.9	11	75	19	0.18	1.7	2.9	B
	16	10	39	18.2	60	40.0	153	14.9	2.8	17	100	39	0.41	3.2	4.6	C
	16	21	24	25.7	59	54.9	152	45.2	2.0	4	150	56	0.64	0.	0.	D
	16	21	49	20.7	59	41.3	153	23.5	4.5	13	69	35	0.21	2.0	3.3	B
	17	1	7	54.2	60	18.0	152	44.3	2.6	8	148	13	0.26	8.7	14.9	D
	17	1	52	57.0	58	32.4	154	9.5	2.5	6	243	58	0.10	4.0	4.2	D
	17	10	31	21.1	59	51.1	152	57.1	2.8	8	154	27	0.24	4.6	10.3	C
	17	17	26	46.3	55	51.9	152	17.6	3.6	6	330	352	0.28	99.4	431.1	D

COCK INLET-WESTERN GULF OF ALASKA EARTHQUAKES

1977	HR	MIN	SEC	LAT N DEG MIN	LONG W DEG MIN	DEPTH KM	MAG	NO	GAP DEG	DM KM	RMS SEC	ERH KM	EPZ KM	Q
DEC 18	0	19	35.4	60 16.6	152 6.2	2.9	2.8	4	226	40	0.50	0.	0.	D
18	0	59	9.0	57 19.9	151 10.9	29.5	4.5	17	205	91	0.45	9.4	4.4	D
18	5	7	17.7	59 57.9	152 59.9	137.4	3.9	35	57	37	0.63	3.0	3.8	C
18	5	9	17.7	57 8.8	153 47.5	10.1	0.7	4	205	43	0.14	0.	0.	C
18	17	20	23.0	60 1.2	153 22.4	159.3	4.0	24	75	41	0.45	3.3	3.6	B
18	17	34	55.4	59 56.6	152 17.7	5.0	2.0	7	172	71	0.96	9.6	99.9	D
19	7	34	0.6	59 18.7	152 29.5	70.8	2.1	8	181	49	0.22	4.5	7.1	D
19	9	56	12.2	59 21.6	152 25.1	71.6	2.1	7	102	49	0.18	2.3	4.6	B
19	11	1	24.0	59 23.7	153 11.2	91.0	2.4	7	139	9	0.07	3.6	4.0	C
19	12	57	48.9	57 58.2	155 58.2	10.5	1.9	4	197	23	0.04	0.	0.	C
19	13	24	33.4	57 54.4	150 15.3	29.6	4.3	20	212	134	0.50	5.7	4.7	D
19	16	37	55.3	60 30.0	152 31.5	7.5	2.6	10	220	16	0.32	3.8	2.5	D
19	21	29	55.2	60 4.2	152 47.2	113.2	2.2	7	170	38	0.17	4.6	7.3	C
20	1	2	47.1	57 40.6	155 26.6	16.7	1.4	4	150	11	0.	0.	0.	C
20	2	4	20.9	59 13.5	155 12.9	0.8	1.7	7	205	53	0.33	4.7	20.4	D
20	3	30	8.1	59 27.4	152 49.5	83.2	2.3	10	87	31	0.20	2.1	3.3	B
20	4	2	14.6	56 25.7	156 12.0	98.1	2.6	11	80	54	0.34	6.2	17.5	C
20	4	5	36.1	57 22.6	156 43.4	80.6	1.9	5	197	8	0.31	20.5	32.1	D
20	9	58	34.5	59 44.5	153 9.4	112.2	2.3	10	156	10	0.29	4.1	5.9	C
20	12	5	32.2	58 11.8	155 12.7	1.1	1.8	6	201	50	0.41	7.6	34.8	D
20	12	29	43.3	59 40.6	152 45.2	85.3	1.8	7	127	70	0.15	2.5	6.3	C
20	12	33	50.4	58 11.4	155 14.9	0.6	2.6	12	105	49	0.55	2.9	20.2	D
20	15	19	35.6	57 0.1	153 59.9	36.0	2.4	7	121	50	0.15	1.7	1.4	B
20	21	13	23.7	59 51.7	153 35.4	169.3	2.2	6	194	77	0.12	5.0	11.9	D
20	21	6	12.4	57 9.1	150 56.0	27.4	3.4	9	260	114	0.21	6.5	2.9	D
21	8	28	15.4	57 20.0	154 13.1	5.0	0.9	3	165	25	0.	0.	0.	C
21	12	40	45.0	53 22.0	154 42.8	5.0	1.9	9	96	81	0.39	2.4	52.0	D
21	13	0	53.4	53 14.9	155 1.2	5.0	1.8	5	228	91	0.12	3.8	274.7	D
21	13	29	4.9	59 22.7	151 39.7	11.9	2.3	5	182	11	0.21	5.2	8.8	D
21	14	58	1.0	57 2.5	153 56.9	36.6	1.8	5	120	52	0.03	0.5	0.6	C
21	15	31	14.5	59 0.1	153 26.4	72.6	2.4	14	55	17	0.26	1.8	3.2	B
21	18	33	1.7	59 36.4	153 47.7	107.5	2.4	7	145	34	0.14	2.8	5.6	C
21	21	13	47.1	57 52.6	156 41.1	0.6	1.4	4	217	11	0.04	0.	0.	C
22	3	16	16.2	59 40.5	153 15.5	134.2	2.2	4	187	81	0.	0.	0.	C
22	11	30	20.6	59 17.7	153 28.8	90.4	2.3	4	155	37	0.	0.	0.	C
22	12	38	13.1	59 23.9	153 5.3	92.2	3.1	13	69	20	0.22	1.8	3.1	B
22	14	55	19.2	59 56.7	153 25.5	99.9	2.0	5	211	64	0.62	4.9	11.2	D
23	0	26	23.5	59 46.8	153 1.6	120.8	3.1	11	121	54	0.36	4.7	8.1	C
23	1	55	48.5	57 32.6	156 0.1	20.4	1.5	4	300	52	0.	0.	0.	C
23	2	2	50.3	57 30.2	155 44.9	23.6	1.2	4	282	33	0.	0.	0.	C
23	5	15	0.3	57 37.9	154 59.1	36.1	3.0	13	139	35	0.20	1.9	3.1	C
23	6	11	25.7	59 15.4	152 0.3	77.6	2.3	6	150	34	0.28	12.9	13.3	D
23	7	5	42.9	58 58.7	154 20.5	123.2	2.4	8	105	46	0.25	3.4	6.8	C
23	10	18	50.4	59 45.4	153 24.5	159.7	3.6	13	73	49	0.47	4.9	9.2	C
24	1	37	5.2	59 51.5	152 54.7	58.6	2.4	9	80	37	0.37	3.3	5.8	B

COCK INLET-WESTERN GULF OF ALASKA EARTH-QUAKES

1977	ORIGI HR	TIME MN	TIME SEC	LAT N DEG MIN	LONG W DEG MIN	DEPTH KM	MAG	NO	GAP DEG	DM KM	RMS SEC	ERH KM	ERZ KM	O	
DEC	24	7	40	24.3	59 59.0	153 11.0	148.2	2.4	7	175	53	0.20	6.5	13.8	D
	24	10	7	27.5	59 53.1	151 44.7	75.2	2.6	6	211	25	0.20	11.0	11.7	D
	24	11	47	53.3	54 41.7	157 27.5	27.3	2.7	7	187	75	0.55	38.9	72.9	D
	24	12	41	3.8	58 11.6	154 5.5	85.1	1.5	6	182	52	0.05	1.3	2.2	D
	24	15	34	57.5	57 7.8	155 39.6	38.9	3.2	11	128	109	0.37	2.7	462.7	D
	25	4	6	46.2	60 19.2	152 49.3	94.4	2.1	4	156	11	0.08	0.	0.	C
	25	4	13	42.3	58 7.7	154 14.0	77.8	2.0	5	214	49	0.26	10.6	18.8	D
	25	6	37	30.3	59 46.8	152 38.8	94.0	2.4	7	133	66	0.14	2.6	4.1	C
	25	13	6	33.7	57 36.2	155 2.3	84.5	2.2	6	161	34	0.04	1.1	1.7	C
	25	23	20	25.0	57 53.1	156 9.1	130.2	2.8	9	101	21	0.11	1.3	2.0	B
	26	10	55	14.4	56 52.0	155 27.8	5.0	2.6	5	119	72	0.39	5.6	881.4	D
	26	12	25	32.7	53 13.5	154 3.0	5.0	2.4	9	71	86	0.64	5.6	999.9	D
	26	2	30	40.5	59 9.3	153 17.9	10.3	1.9	5	218	21	0.01	1.1	0.6	C
	27	9	17	32.2	56 57.8	155 5.8	51.3	3.1	11	132	49	0.30	2.4	5.8	C
	27	12	46	32.0	57 52.4	153 34.2	8.9	1.9	4	138	17	0.	0.	0.	C
	27	15	9	48.8	60 17.5	153 29.7	196.7	6.0	32	80	42	0.51	2.7	3.9	C
	27	22	36	3.5	56 30.9	153 48.9	49.5	2.7	7	249	39	0.20	8.2	9.5	D
	28	1	17	39.3	58 47.1	153 40.4	4.5	2.0	5	204	20	0.01	0.3	0.3	D
	28	5	24	40.0	59 58.4	152 52.7	125.1	2.8	11	155	49	0.33	6.2	9.2	D
	28	5	49	10.9	56 20.0	152 36.8	23.7	2.8	8	275	96	0.55	24.2	6.7	D
	28	6	33	56.3	59 13.2	152 58.8	71.0	2.2	5	233	28	0.16	12.8	14.9	D
	28	6	49	19.0	59 40.2	153 12.2	64.2	2.6	13	82	37	0.32	2.2	4.1	B
	28	7	2	6.5	59 31.5	152 23.6	76.8	4.2	18	83	44	0.34	2.2	3.5	B
	28	7	8	19.2	59 44.6	153 24.9	123.1	2.3	6	302	45	0.16	19.5	17.0	D
	28	7	36	34.2	59 52.2	152 40.9	92.1	2.3	7	140	61	0.14	2.9	5.6	D
	28	9	50	11.4	53 15.6	155 15.9	3.2	2.1	6	166	56	0.43	7.1	13.6	D
	28	12	0	4.8	57 49.8	156 41.2	163.3	2.8	8	272	69	0.15	9.4	10.3	D
	28	15	31	53.9	60 10.5	152 35.9	23.2	1.9	7	156	28	0.55	37.1	29.2	D
	29	1	34	18.7	59 35.2	152 30.3	75.0	2.0	6	184	59	0.16	3.7	7.8	D
	29	9	19	4.3	53 29.7	153 29.1	5.0	1.6	3	199	51	0.	0.	0.	C
	29	10	49	22.5	59 43.3	152 18.9	79.5	2.4	9	119	38	0.26	3.7	6.2	C
	29	15	7	45.9	58 20.7	151 36.0	2.5	2.5	9	218	53	0.45	5.8	6.3	D
	29	17	3	35.3	60 10.0	152 30.1	30.2	2.5	8	168	31	0.51	23.3	16.8	D
	29	19	48	24.5	52 19.3	152 14.0	68.1	2.1	6	119	40	0.26	5.2	8.5	C
	29	22	5	46.2	57 48.3	154 7.3	45.9	2.7	12	73	60	0.48	3.1	16.5	C
	29	23	10	1.4	58 0.6	153 16.3	65.5	3.1	15	96	8	0.27	2.1	3.0	B
	30	1	57	12.0	58 45.3	153 49.9	7.7	1.2	6	133	28	0.56	9.9	13.9	D
	30	7	23	42.1	56 51.1	154 48.7	0.9	2.2	7	241	50	0.55	7.1	11.5	D
	30	7	36	48.2	57 56.2	154 11.4	40.1	1.5	4	180	31	0.02	0.	0.	C
	30	8	7	48.8	58 24.7	153 2.	49.8	2.8	13	97	39	0.42	3.4	7.6	C
	30	15	45	15.4	57 22.5	153 52.5	67.5	2.5	10	76	43	0.12	1.0	1.9	B
	30	21	47	54.0	59 44.6	151 44.6	177.3	2.0	4	187	11	0.01	0.	0.	B
	30	23	43	35.9	59 2.2	152 17.5	64.5	2.7	12	145	45	0.34	2.6	5.3	C
	31	2	49	2.3	56 45.7	155 45.5	38.4	2.8	6	299	135	0.16	17.3	272.6	D
	31	5	40	24.4	55 52.7	152 56.8	38.2	2.7	7	307	108	0.37	47.1	569.6	D

142718 U1-2 MOORE BUSINESS FORMS, INC.

COCK INLET-WESTERN GULF OF ALASKA EARTHQUAKES

1977	ORIG IN	TIME	LAT N	LONG W	DEPTH	MAG	NO	CAP	DM	RMS	ERH	ERZ	Q	
	HR MN	SEC	DEG MIN	DEG MIN	KM			DEG	KM	SEC	KM	KM		
DEC	31	5 45	14.3	56 15.8	153 10.2	33.8	2.8	10	283	70	0.43	18.6	3.3	D
	31	5 55	36.1	56 27.2	153 13.2	24.0	3.0	8	264	60	0.39	11.5	3.6	D
	31	5 17	27.7	56 17.0	153 8.8	34.7	3.4	8	281	71	0.26	11.8	2.3	D
	31	20 22	59.5	60 10.4	153 7.1	150.6	2.6	8	100	33	0.31	6.2	11.7	C
	31	20 36	8.2	57 6.4	153 27.3	36.7	2.7	5	268	75	0.43	33.1	8.9	D
JAN	1	5 13	23.5	60 4.0	151 37.7	36.2	3.0	5	236	45	0.38	91.5	32.1	D
	1	5 59	43.3	59 53.0	152 55.8	103.9	3.0	14	101	60	0.38	3.4	5.8	C
	1	11 15	32.6	60 4.9	152 36.5	189.2	2.3	18	153	38	0.12	3.6	7.1	C
	1	21 16	3.2	56 1.4	154 21.0	35.4	4.1	13	224	60	0.54	8.4	3.1	D
	1	23 28	19.5	58 25.8	146 15.9	5.0	4.4	8	310	326	1.06	136.7	999.9	D
	2	4 23	11.3	60 50.0	151 48.0	83.7	4.1	14	219	70	0.51	6.6	7.3	D
	2	11 13	22.5	59 25.7	151 49.3	62.6	2.5	5	171	14	0.07	5.5	7.2	D
	2	11 47	57.2	59 21.1	154 42.5	5.0	1.9	7	95	80	0.18	1.5	268.2	D
	2	17 2	47.3	59 41.8	151 35.6	58.7	2.6	6	217	5	0.12	5.7	4.5	D
	2	17 59	21.1	54 23.4	158 19.2	108.3	3.0	4	338	400	0.36	0.	0.	D
	2	21 19	29.3	59 53.1	151 49.8	56.1	2.5	7	199	27	0.31	9.9	14.1	D
	3	3 55	42.9	57 48.7	154 36.9	16.5	1.8	4	138	49	0.73	0.	0.	D
	3	13 5	15.9	60 18.2	152 40.3	107.4	2.6	5	165	14	0.24	9.4	11.4	D
	3	13 28	26.8	60 16.3	151 45.6	82.8	3.2	9	240	58	0.23	5.4	6.3	D
	3	22 16	54.5	59 41.5	152 38.6	5.0	2.2	4	122	56	0.39	0.	0.	D
	3	16 37	21.6	57 22.9	153 41.9	33.1	2.9	8	142	44	0.28	3.9	3.3	C
	4	4 6	53.5	60 37.9	151 49.1	63.4	3.3	19	113	57	1.77	9.9	23.0	C
	4	4 10	44.1	59 54.6	153 46.7	15.0	2.5	7	232	15	0.13	2.6	3.4	D
	4	4 44	2.4	59 55.8	152 3.1	77.8	2.8	9	179	38	0.34	7.2	13.1	D
	4	15 12	4.4	58 33.9	152 44.9	48.8	2.5	13	98	24	0.41	2.7	5.3	C
	4	20 40	47.4	60 11.0	153 57.0	204.7	3.3	12	110	29	0.27	3.8	8.1	C
	5	7 46	26.7	60 10.7	152 16.8	28.3	1.5	4	194	38	0.47	0.	0.	D
	5	7 42	23.5	57 50.6	157 9.6	183.3	2.8	5	309	53	0.03	5.9	6.4	D
	5	7 7	15.4	59 26.2	153 37.3	121.9	3.1	14	63	15	0.33	2.6	4.2	B
	5	10 19	41.2	56 9.4	156 24.0	28.4	2.7	5	219	102	0.27	14.6	9.6	D
	5	13 32	53.5	59 17.6	152 26.5	69.5	2.5	6	108	52	0.15	2.5	6.8	C
	5	21 0	13.4	56 3.3	154 23.4	37.0	4.4	14	251	57	0.50	8.6	3.2	D
	6	4 49	42.8	54 30.7	156 47.6	5.0	3.6	7	295	260	0.21	17.3	317.9	D
	6	4 50	58.8	60 59.0	147 7.9	17.6	2.3	4	280	95	0.16	0.	0.	C
	6	5 20	31.2	58 12.8	154 53.9	0.5	2.4	9	94	61	0.30	2.0	15.5	D
	6	5 35	45.2	58 4.0	152 53.6	40.6	2.5	7	119	15	0.29	3.9	2.3	C
	6	11 15	59.9	59 4.5	154 8.5	78.8	2.3	7	128	57	0.11	1.4	4.4	B
	6	15 56	57.3	59 6.2	154 28.1	128.7	2.3	5	160	15	0.05	3.6	5.0	D
	6	18 7	57.8	60 21.6	152 10.2	44.9	2.7	7	238	33	0.49	15.0	19.9	D
	6	18 7	57.8	58 34.2	150 42.5	5.0	2.6	5	297	95	0.31	39.1	697.0	D
	6	20 31	12.3	59 17.9	153 29.7	121.3	2.4	7	94	5	0.15	2.6	4.9	C
	6	22 30	60.3	60 52.9	149 17.4	37.1	4.9	15	174	188	0.48	4.2	557.5	D
	7	11 23	33.5	59 50.6	152 56.9	34.9	2.6	7	148	64	1.01	10.0	9.1	D
	7	11 27	29.2	57 56.6	156 38.2	163.7	2.6	7	195	33	0.24	7.8	12.8	D
	7	19 52	24.9	57 50.3	156 16.8	123.7	3.4	14	124	14	0.66	6.0	8.4	C

COCK INLET-WESTERN GULF OF ALASKA EARTHQUAKES

1978	ORIGIN	TIME	LAT N	LONG W	DEPTH	MAG	NO	GAP	DM	RMS	ERH	ERZ	Q
	HR MN	SEC	DEG MIN	DEG MIN	KM			DEG	KM	SEC	KM	KM	
JAN	8 2 42	45.1	59 31.4	153 13.7	107.2	2.6	6	164	65	0.13	2.8	4.5	D
	8 3 43	55.8	60 4.4	151 36.1	66.1	2.4	6	238	46	0.15	9.1	9.7	D
	8 9 48	17.4	60 50.2	144 50.2	5.0	1.9	3	313	85	0.02	0.	0.	C
	8 12 0	56.7	57 47.8	155 1.0	78.6	2.4	6	146	29	0.20	4.2	6.8	C
	8 18 52	40.2	59 34.9	152 26.9	41.4	2.8	8	187	75	0.33	4.4	47.2	D
	8 22 13	56.7	56 56.9	153 12.8	31.6	3.9	18	208	25	0.33	3.0	1.4	D
	8 22 21	53.4	56 57.2	153 11.9	32.8	3.0	8	208	24	0.25	4.1	2.3	D
	8 22 50	50.4	56 58.4	155 23.4	74.9	2.4	8	181	60	0.26	3.7	7.6	D
	9 9 2	53.6	58 23.1	154 21.5	5.0	2.3	8	84	79	1.24	8.7	9.9	D
	9 9 33	46.5	57 46.9	153 59.1	25.6	3.1	13	76	58	0.44	2.3	3.6	D
	9 11 4	17.8	59 34.5	153 6.4	98.4	2.4	6	170	76	0.18	4.2	9.2	D
	9 9 17	59.2	56 24.6	154 48.5	46.8	2.2	7	218	42	0.25	5.8	9.9	D
	9 9 19	54.0	59 11.4	153 23.4	56.2	2.6	6	123	55	0.25	3.5	8.9	C
	9 9 23	40	57 14.0	155 47.1	91.7	2.2	8	193	60	0.18	3.6	5.0	D
	10 3 58	12.5	56 38.0	156 58.5	57.5	2.3	6	210	41	0.20	5.8	7.4	D
	10 5 17	31.7	56 54.5	155 28.9	61.5	2.4	7	187	69	0.18	3.6	13.0	D
	10 7 7	12.4	59 22.0	153 20.1	104.8	2.5	9	161	66	0.25	3.4	4.2	D
	10 8 19	59.9	56 45.1	153 27.3	76.6	2.4	5	203	80	0.23	8.8	20.0	C
	10 10 21	30.3	60 50.6	152 35.4	36.9	3.0	7	257	48	0.33	2.4	3.4	D
	10 10 13	35.7	56 47.1	154 54.3	0.5	2.5	5	202	50	0.26	1.7	6.2	D
	11 13 13	53.0	59 52.8	150 53.4	39.3	3.4	7	264	48	0.13	4.7	1.2	D
	11 5 44	52.9	59 54.7	152 58.4	5.0	2.3	4	175	57	0.64	0.	0.	D
	11 6 11	41.5	59 40.7	152 58.2	102.7	2.8	10	158	40	0.29	4.1	6.3	C
	11 7 21	33.3	60 12.3	152 46.4	45.2	3.1	8	134	23	0.71	2.1	39.7	C
	11 12 23	27.5	59 53.4	152 53.4	131.4	2.7	8	119	59	0.26	5.8	12.6	C
	11 13 44	34.2	59 30.5	152 56.8	99.8	2.4	5	179	70	0.11	3.2	7.2	D
	11 19 0	54.0	60 7.8	151 46.4	36.1	2.7	7	231	53	0.46	10.0	42.1	D
	11 22 34	33.7	59 52.8	154 41.7	148.6	2.8	4	264	122	0.01	0.	0.	C
	12 3 52	34.3	59 13.4	151 38.9	70.0	2.3	4	269	72	0.	0.	0.	C
	12 5 28	42.9	59 52.2	151 34.2	73.5	2.9	11	228	24	0.44	8.7	9.0	D
	12 6 4	0.4	60 26.4	151 51.9	64.4	2.9	7	264	50	0.55	45.1	39.0	D
	12 10 32	26.9	57 29.1	155 29.4	78.2	2.4	6	155	32	0.18	4.0	5.9	C
	12 10 33	2.4	59 20.5	153 25.0	116.9	2.6	6	162	1	0.28	9.0	7.2	D
	12 12 18	2.0	60 4.3	152 17.5	4.2	2.9	5	176	47	0.33	7.6	7.5	D
	12 13 29	24.7	57 44.7	156 31.4	138.0	3.2	10	171	15	0.24	4.9	6.7	C
	12 16 23	29.4	57 16.0	154 58.5	52.1	2.5	7	182	21	0.33	5.8	5.9	D
	12 16 42	25.6	59 55.5	152 42.9	4.1	1.8	4	153	55	0.50	0.	0.	D
	13 3 24	58.9	58 10.3	155 17.1	6.7	2.5	5	165	47	0.38	10.0	15.3	D
	13 4 19	0.3	59 46.3	153 21.0	5.0	2.1	4	136	78	0.58	0.	0.	D
	13 5 32	31.3	59 55.9	153 35.9	7.8	2.1	9	127	4	0.41	2.6	2.0	C
	13 7 59	22.0	59 43.7	153 16.2	5.0	2.1	4	190	81	0.30	0.	0.	D
	13 9 51	28.2	57 20.0	155 22.5	71.7	3.0	5	185	44	0.07	2.7	7.0	D
	13 12 36	19.7	59 0.0	156 58.5	111.3	2.7	6	174	45	0.16	4.9	8.5	C
	13 13 50	23.2	59 35.3	152 59.2	38.3	2.2	4	136	77	0.01	0.	0.	C
	13 19 36	54.6	57 19.1	155 7.1	74.3	2.3	5	177	29	0.11	4.7	5.0	D

COCK INLET-WESTERN GULF OF ALASKA EARTHQUAKES

1978	ORIGIN			TIME	LAT N		LONG W		DEPTH	MAG	NC	GAP	CM	RMS	ERH	ERZ	O
	HR	MIN	SEC	SEC	DEG	MIN	DEG	MIN	KM			DEG	KM	SEC	KM	KM	
JAN	13	23	33	29.0	60	11.3	152	14.9	30.7	3.0	8	199	38	0.63	8.8	6.3	D
	14	3	33	13.3	57	41.5	152	11.4	23.4	2.3	4	277	70	0.	0.	0.	C
	14	9	27	37.7	57	10.6	155	15.2	19.0	2.1	5	219	41	0.16	9.5	73.1	D
	14	10	56	25.6	59	44.3	153	13.2	5.0	1.9	4	160	79	0.03	0.	0.	C
	14	11	21	26.5	57	54.1	156	28.7	24.8	1.6	4	186	18	0.	0.	0.	C
	14	11	58	55.8	57	53.3	156	29.5	20.5	1.7	4	186	3	0.	0.	0.	C
	14	14	34	22.3	60	14.9	144	35.7	5.0	4.0	5	331	393	0.94	493.2	999.9	D
	14	15	47	17.6	57	29.2	155	1.4	41.6	2.3	7	139	28	0.22	3.1	4.1	C
	14	20	50	51.3	57	45.6	156	9.2	111.8	3.4	15	81	8	0.27	2.2	3.0	B
	14	23	4	35.7	60	8.4	152	42.6	104.1	2.6	5	154	31	0.18	13.9	26.1	D
	15	8	34	50.8	59	9.6	153	4.9	76.6	2.7	15	112	27	0.38	2.8	3.7	C
	15	11	6	27.1	57	53.1	156	41.6	2.3	1.3	5	219	12	0.02	0.4	0.5	C
	15	11	35	33.1	57	9.5	157	1.3	1.6	2.9	7	140	28	0.44	4.6	21.4	C
	15	16	11	11.0	56	37.6	156	30.5	38.1	2.6	11	124	68	0.42	3.4	3.4	C
	15	21	9	27.5	58	55.7	143	47.0	9.0	3.3	10	302	170	0.56	56.2	26.8	D
	16	1	59	35.1	57	51.9	151	56.9	40.3	2.8	4	258	34	0.	0.	0.	C
	16	7	16	19.0	58	11.1	155	20.0	0.6	2.0	8	107	47	0.46	3.2	18.8	C
	16	11	12	27.1	57	31.7	154	38.2	5.0	1.8	3	124	21	1.07	0.	0.	D
	16	12	54	36.7	56	45.4	156	26.3	39.8	2.2	7	188	70	0.36	5.5	4.0	D
	16	13	1	33.3	60	25.4	152	19.7	30.4	2.1	6	247	24	0.77	184.7	59.1	D
	16	13	18	59.6	56	53.1	155	34.1	5.0	2.0	6	228	75	0.36	8.1	626.9	D
	16	14	19	13.0	58	47.5	153	46.6	15.7	1.9	6	142	23	0.56	9.3	34.6	D
	16	23	30	29.9	58	9.9	155	20.6	8.9	1.7	5	198	44	0.38	7.9	847.9	D
	17	2	35	21.2	59	42.9	153	10.3	41.1	2.5	6	164	81	0.63	9.0	999.9	D
	17	4	2	20.6	57	24.8	154	58.5	42.7	2.2	6	153	22	0.10	2.6	2.8	C
	17	4	44	59.4	57	5.5	153	57.8	25.8	2.4	7	111	48	0.27	2.6	3.2	C
	17	7	23	36.2	59	42.6	151	59.3	73.4	2.4	6	135	20	0.19	5.1	7.9	D
	17	7	35	30.9	59	0.4	151	25.0	50.5	2.4	4	278	52	0.08	0.	0.	C
	17	10	50	2.7	60	20.1	151	1.2	68.8	3.1	8	283	83	0.19	13.7	10.6	D
	17	13	12	10.3	58	54.7	153	55.2	95.8	3.0	11	80	23	0.33	3.0	4.5	B
	17	14	16	20.7	57	10.4	155	26.0	5.0	2.3	6	217	51	0.48	29.6	52.3	D
	17	15	7	3.5	58	23.0	152	18.2	39.6	2.3	5	245	61	0.19	8.2	2.7	D
	17	18	33	8.3	60	3.1	152	33.2	9.3	2.9	4	157	33	0.01	0.	0.	C
	17	20	35	54.8	59	7.4	152	31.8	88.0	2.7	6	194	60	0.26	5.5	8.2	D
	17	20	55	36.9	59	53.0	153	7.1	25.9	2.8	4	197	62	0.33	0.	0.	D
	18	12	25	31.2	57	32.6	154	51.4	42.8	3.1	7	117	26	0.23	3.1	4.6	C
	18	13	31	4.1	60	7.6	152	45.4	126.0	2.9	7	139	32	0.08	2.3	4.1	C
	19	13	12	22.3	58	28.5	154	52.0	20.0	3.1	8	289	79	0.39	18.1	7.0	D
	19	14	34	33.9	57	54.1	155	9.2	0.5	3.5	5	125	69	0.12	1.8	272.4	D
	19	14	33	42.3	56	29.3	153	26.7	35.0	3.2	12	258	46	0.45	11.5	2.8	D
	19	22	23	28.4	56	52.8	155	3.5	94.6	2.7	5	192	56	0.62	19.3	38.9	D
	20	2	17	3.5	60	29.8	152	27.2	112.1	2.9	12	223	19	0.41	6.8	8.1	D
	20	2	51	54.5	57	10.5	153	59.5	17.5	2.6	6	98	55	0.40	5.4	79.7	D
	20	3	58	45.2	56	56.7	154	30.6	2.0	2.8	5	135	47	0.09	0.8	2.0	C
	20	7	20	29.2	60	1.9	152	44.3	102.5	2.7	8	151	43	0.26	5.8	11.4	D

COCK INLET-WESTERN GULF OF ALASKA EARTHQUAKES

1978	ORIGIN TIME			LAT N	LONG W		DEPTH	MAG	NO	GAP	CM	RMS	ERH	ERZ	Q
	HR	MIN	SEC	DEG MIN	DEG MIN	KM			CEG	KM	SEC	KM	KM		
JAN	20	12	32	53.2	59 48.7	152 59.1	114.2	2.7	9	93	53	0.21	3.1	7.3	C
	20	13	32	16.4	59 59.9	152 40.9	108.5	3.6	23	87	47	1.37	8.3	9.9	C
	20	17	20	56.8	59 37.0	153 45.7	76.6	2.2	7	150	40	0.06	0.9	1.4	B
	20	23	0	31.7	60 16.6	152 40.3	27.3	2.7	4	160	16	0.47	0.	0.	D
	21	1	22	7.4	56 4.6	156 21.9	20.4	2.6	6	235	110	0.26	6.5	6.7	D
	21	1	35	18.0	57 32.9	152 48.3	0.2	2.9	12	161	29	0.46	3.2	9.4	C
	21	2	26	0.5	59 59.8	153 32.1	182.3	2.7	7	222	63	0.20	8.2	16.4	D
	21	5	30	43.5	60 10.8	153 10.4	166.0	3.3	10	187	34	0.43	10.4	13.7	D
	21	14	32	23.0	56 44.5	155 29.6	5.0	2.3	7	201	84	1.08	14.5	99.9	D
	21	20	31	54.5	59 43.6	153 8.6	108.2	2.6	9	123	46	0.34	4.4	8.8	C
	22	2	2	53.4	60 13.2	152 14.2	119.5	4.7	18	186	37	0.42	4.3	4.9	D
	22	7	49	39.4	59 30.1	152 49.8	93.1	3.1	5	185	33	0.12	3.8	5.2	CC
	22	14	44	13.5	59 12.7	152 26.9	80.8	3.5	12	121	54	0.42	3.7	6.4	CC
	23	13	46	32.2	60 49.9	153 17.6	35.5	4.0	11	315	190	0.36	54.7	10.7	D
	23	14	19	8.2	58 18.9	154 51.4	5.0	2.4	7	107	71	0.39	3.5	603.1	D
	23	19	21	24.5	60 0.5	153 40.1	191.1	3.0	5	211	67	0.11	11.6	26.0	D
	24	7	24	59.9	60 1.4	152 53.7	135.5	3.4	13	127	44	0.43	6.7	9.9	C
	24	16	13	51.7	58 51.3	152 43.3	62.0	2.6	7	140	33	0.29	4.0	4.9	C
	24	17	30	12.7	59 10.3	152 3.1	5.0	2.4	5	231	59	0.21	6.8	473.6	D
	24	22	45	25.2	60 29.8	153 31.7	2.9	2.8	4	244	42	1.17	0.	0.	D
	25	2	4	7.5	57 36.2	154 53.9	53.9	2.4	7	124	34	0.24	3.7	5.9	C
	25	3	8	47.0	57 15.1	153 8.1	60.7	1.9	5	215	31	0.01	0.8	0.4	C
	25	7	12	50.0	57 49.6	155 31.1	112.4	2.2	5	143	5	0.03	1.7	2.7	CC
	25	9	5	27.6	59 51.7	154 23.6	117.5	2.9	12	94	28	0.26	2.6	5.0	CC
	25	11	32	8.7	60 46.3	147 49.9	36.1	4.5	15	194	115	0.61	6.0	714.7	D
	25	12	53	54.9	60 39.3	152 26.5	159.0	3.2	8	291	32	0.35	18.7	21.0	D
	25	17	39	18.3	58 43.6	153 50.9	4.2	1.8	6	162	31	0.24	2.9	3.8	C
	25	18	48	58.7	59 56.3	150 50.4	5.0	2.5	4	258	119	0.05	0.	0.	D
	26	3	10	45.9	53 56.8	156 1.8	5.0	4.8	10	303	344	0.16	10.2	201.4	D
	26	14	36	40.2	59 5.1	154 9.3	124.0	2.8	8	111	3	0.12	1.8	2.8	B
	27	6	54	55.4	56 22.7	156 33.8	32.9	2.9	8	215	78	0.33	6.1	4.2	D
	27	7	49	20.0	53 58.5	153 37.9	16.3	1.5	4	181	5	0.02	0.	0.	C
	27	15	2	1.3	53 56.5	154 37.6	0.1	2.5	6	187	30	0.10	1.1	4.6	C
	27	18	52	53.3	60 20.7	151 3.7	39.9	4.4	21	150	83	0.38	2.2	426.1	D
	27	22	30	53.2	53 9.3	155 17.6	5.0	2.3	5	103	62	0.27	3.8	612.9	D
	28	2	25	0.7	59 9.6	151 7.0	16.4	3.5	6	263	120	0.34	15.2	8.1	D
	28	15	21	0.1	50 50.6	152 53.0	104.7	3.2	13	101	64	0.28	2.8	4.2	C
	28	18	53	7.6	60 12.9	151 18.8	64.1	4.8	16	236	64	0.39	5.8	5.5	D
	29	5	5	29.6	58 59.2	153 1.0	67.7	2.8	7	190	29	0.32	5.9	6.8	D
	29	17	22	46.5	54 35.4	151 7.9	31.2	3.6	8	314	375	0.19	23.3	262.7	D
	29	21	4	42.3	59 35.5	152 55.9	111.7	2.4	8	179	18	0.11	2.3	2.6	C
	30	12	47	5.1	58 20.2	155 59.1	151.8	2.7	6	274	38	0.09	7.2	8.0	D
	30	21	54	27.4	56 44.3	155 51.0	5.0	2.4	7	192	95	0.82	9.9	99.9	D
	31	2	6	6.0	53 53.1	154 32.3	129.9	3.5	17	97	58	0.46	3.2	5.7	C
	31	4	45	6.2	60 2.4	152 56.9	120.7	2.6	6	132	43	0.32	9.2	19.6	C

14-00000-10-7-700000 BUSINESS FORMS, INC. F

COCK INLET-WESTERN GULF OF ALASKA EARTHQUAKES

1978	OP	FIG	TIME	LAT N	LONG W	DEPTH	MAG	NO	GAP	DM	RMS	ERH	ERZ	Q	
	HR	MIN	SEC	DEG MIN	DEG MIN	KM			DEG	KM	SEC	KM	KM		
JAN	31	6	42	40.1	57 46.0	152 41.5	2.9	2.3	5	140	12	0.85	44.8	73.0	D
	31	16	59	0.0	59 47.6	153 15.1	5.0	2.1	4	191	74	1.08	0.0	0.0	D
FEB	1	4	34	14.8	59 49.7	153 31.7	151.1	4.0	15	71	42	0.35	3.9	5.9	B
	1	8	18	8.1	57 52.7	156 31.7	7.9	2.7	8	168	3	0.55	4.9	3.0	D
	1	4	54	51.8	58 54.8	151 14.8	39.2	2.9	7	245	71	0.23	6.8	2.1	D
	1	12	2	26.5	59 44.8	152 22.0	5.0	2.2	4	196	75	1.08	0.0	0.0	D
	1	21	44	13.2	59 59.9	153 2.3	135.9	2.9	5	184	49	0.15	8.9	20.4	D
	2	2	2	37.6	59 43.8	153 5.1	102.2	3.1	7	85	44	0.18	3.0	8.5	B
	2	6	19	43.3	59 57.1	152 54.9	119.0	3.9	14	106	52	0.37	3.8	5.4	D
	2	7	11	33.0	57 58.6	152 38.4	5.6	2.0	5	186	26	0.24	4.4	3.8	D
	2	8	15	21.4	57 0.1	154 11.4	39.2	2.8	7	210	45	0.76	16.9	6.2	D
	2	17	1	58.5	59 51.8	151 47.8	2.5	3.3	9	201	24	0.06	0.0	0.0	C
	2	20	10	43.2	60 5.3	151 29.8	50.0	3.3	4	252	48	0.33	12.8	13.5	D
	2	21	46	15.8	60 9.4	152 43.8	138.4	4.0	15	137	29	0.41	5.2	6.7	D
	3	5	25	35.0	60 11.2	152 48.0	133.1	3.1	7	129	26	0.40	14.8	23.2	C
	3	7	45	15.9	57 42.5	155 41.1	10.7	3.4	11	120	12	0.34	2.1	2.0	C
	3	17	3	21.8	58 28.0	154 47.2	5.0	3.1	5	233	88	0.73	22.9	9.9	D
	4	17	37	56.9	59 28.9	153 57.9	158.4	3.1	7	131	44	0.19	4.1	6.0	C
	4	20	44	33.7	56 28.4	153 43.4	2.5	2.1	4	251	46	0.73	0.0	0.0	D
	5	5	12	21.8	59 46.7	152 37.9	114.1	3.1	7	110	57	0.23	4.7	7.0	C
	5	12	40	25.3	59 4.4	155 13.2	112.5	3.5	17	89	37	0.26	1.7	3.2	B
	6	4	49	53.9	59 28.6	152 15.1	69.2	2.8	5	124	39	0.13	3.3	7.6	D
	6	5	19	27.9	57 59.1	154 39.2	2.5	2.3	4	220	72	0.43	0.0	0.0	D
	6	7	0	49.7	59 50.1	152 54.9	109.9	3.8	14	159	57	0.47	4.7	5.5	D
	6	21	43	0.3	60 0.5	153 28.7	168.6	3.0	6	120	41	0.15	6.1	16.2	C
	7	22	7	26.0	57 52.2	156 37.2	5.0	1.9	3	205	25	0.0	0.0	0.0	C
	7	22	53	33.1	59 2.9	152 29.6	71.3	3.2	9	134	47	0.17	0.2	4.6	B
	8	5	43	19.5	60 22.1	153 7.9	14.5	2.0	4	201	20	0.04	0.0	0.0	C
	8	17	57	56.8	57 20.4	154 37.8	10.0	2.0	4	208	56	0.08	0.0	0.0	C
	9	14	18	37.5	56 38.8	154 2.8	5.0	2.7	3	175	12	0.0	0.0	0.0	C
	9	14	38	46.1	59 44.9	153 0.6	131.6	3.1	9	289	16	0.37	15.5	15.1	D
	9	15	2	18.8	59 26.0	153 13.0	115.3	3.4	14	77	10	0.36	3.4	4.3	B
	10	7	4	44.8	60 0.1	153 0.6	4.0	1.8	4	179	48	0.17	0.0	0.0	C
	10	8	20	5.3	59 10.1	153 39.5	104.6	2.6	6	110	22	0.11	3.6	5.3	C
	10	12	6	35.2	58 2.3	156 6.8	145.4	2.8	6	204	13	0.10	6.8	11.0	D
	11	8	57	57.0	57 5.7	157 19.5	106.8	2.8	7	180	35	0.35	8.9	11.1	D
	11	9	53	2.1	59 39.5	152 10.7	87.8	2.3	4	135	30	0.0	0.0	0.0	C
	11	16	53	56.4	56 16.5	157 12.9	26.8	2.9	8	208	41	0.52	13.3	6.8	D
	11	17	51	58.1	57 38.6	156 7.1	100.0	3.1	1	105	46	0.32	3.1	5.7	C
	11	18	55	44.9	58 18.9	151 52.5	12.0	3.2	9	245	44	0.42	10.5	5.8	D
	12	8	20	37.4	58 28.2	154 0.3	81.0	2.8	12	80	60	0.27	2.3	7.4	B
	12	8	56	32.0	59 17.7	152 21.8	73.4	4.9	32	92	57	0.35	1.5	2.5	C
	12	9	51	15.2	59 10.4	151 45.4	45.2	2.5	4	279	96	0.53	0.0	0.0	D
	12	17	57	37.1	59 15.7	152 21.8	74.0	2.3	4	200	60	0.0	0.0	0.0	C
	12	14	0	57.5	56 59.1	153 13.6	33.7	3.0	7	204	21	0.11	1.9	1.1	C

COCK INLET-WESTERN GULF OF ALASKA EARTHQUAKES

1978	ORIGIN TIME			LAT N		LONG W		DEPTH	MAG	NO	GAP	DM	RMS	ERH	ERZ	Q	
	HR	MIN	SEC	DEG	MIN	DEC	MIN	KM			DEG	KM	SEC	KM	KM		
FEB	13	1	11	36.5	57	25.4	155	22.3	81.3	2.3	4	166	45	0.	0.	0.	C
	13	1	16	53.5	59	40.1	153	35.9	141.4	4.6	24	61	20	0.41	2.4	3.0	B
	13	3	52	59.7	56	12.9	153	19.7	36.0	4.2	8	267	65	0.24	9.5	2.1	D
	13	4	3	0.3	56	15.3	153	21.8	37.8	3.5	6	274	60	0.15	8.2	1.9	D
	13	4	53	0.0	57	31.9	155	49.6	81.0	2.9	13	126	33	0.34	2.8	4.3	C
	13	10	58	24.8	56	27.7	153	34.6	32.8	3.0	7	265	38	0.12	3.7	1.0	D
	13	11	40	12.0	56	20.5	155	33.7	20.0	2.6	6	234	124	0.15	3.9	2.7	D
	13	15	52	23.5	59	38.1	153	5.4	116.6	2.3	7	129	79	0.11	1.6	3.2	B
	14	8	37	41.5	60	21.5	153	15.1	183.8	3.9	11	236	78	0.39	10.3	11.4	D
	14	9	33	43.2	58	10.2	155	17.3	1.0	2.4	6	104	63	0.33	2.6	18.5	D
	14	13	13	2.8	59	38.4	152	43.8	98.6	2.4	4	190	28	0.	0.	0.	C
	15	0	13	35.6	59	29.6	152	43.3	72.6	2.4	6	187	43	0.29	11.6	15.6	D
	15	0	57	12.6	59	10.5	153	41.6	113.8	3.3	16	84	23	0.33	2.4	3.4	B
	15	17	3	53.1	59	41.9	152	50.2	88.4	2.2	7	107	67	0.16	2.6	7.0	C
	15	19	1	25.0	59	56.1	153	14.4	42.4	2.3	5	144	59	1.23	9.8	114.8	D
	16	8	57	55.2	56	20.2	154	59.9	5.0	3.1	5	265	113	0.09	4.7	204.4	D
	16	8	37	39.4	59	43.0	153	12.9	121.6	2.9	7	125	82	0.10	1.9	4.6	B
	16	14	52	44.6	59	36.3	145	52.3	30.5	4.0	11	237	33	0.92	16.6	6.7	D
	17	9	31	53.0	57	51.6	156	29.2	19.0	0.8	4	174	0	0.	0.	0.	C
	17	11	21	45.5	58	43.2	153	53.5	2.8	1.9	5	165	33	0.21	3.6	4.9	D
	17	11	25	25.3	57	52.1	156	31.7	18.9	1.4	5	189	2	0.07	1.5	1.6	C
	17	11	42	27.8	57	52.6	156	29.8	20.6	1.3	4	185	2	0.	0.	0.	C
	17	11	55	33.1	57	52.1	156	28.5	21.2	1.4	4	170	1	0.	0.	0.	C
	17	17	42	46.7	58	12.0	155	15.0	2.5	1.5	6	119	66	0.46	4.7	794.8	D
	17	20	43	59.7	57	51.7	156	30.6	19.4	1.5	4	185	1	0.	0.	0.	C
	18	2	44	42.4	57	15.5	156	6.5	73.3	2.9	8	172	47	0.10	1.5	2.5	C
	18	2	9	35.0	60	11.5	153	3.6	150.6	2.9	9	188	60	0.34	6.0	8.7	D
	18	5	44	13.4	57	34.0	155	16.9	4.6	2.1	5	162	46	0.17	9.1	14.0	D
	18	5	50	0.1	56	37.0	154	14.5	21.6	1.8	7	172	7	0.06	1.7	1.5	C
	18	7	10	56.3	56	53.8	154	32.5	41.3	2.3	7	220	48	0.28	6.6	2.8	D
	18	19	27	51.7	57	29.5	155	11.9	5.0	2.1	5	165	38	0.43	28.4	77.3	D
	18	21	3	10.5	59	55.5	152	49.9	53.0	2.0	3	238	55	0.15	0.	0.	C
	18	22	27	59.3	57	26.4	155	20.8	89.7	2.4	5	162	44	0.12	6.2	21.0	D
	19	5	16	24.5	59	19.0	156	19.5	150.2	3.0	6	191	30	0.12	4.7	8.1	D
	19	5	24	47.5	60	51.6	151	0.6	38.6	2.8	5	275	108	0.64	50.0	999.9	D
	19	6	1	44.3	59	57.7	153	16.4	122.5	2.2	4	180	34	0.	0.	0.	C
	19	10	1	14.8	59	53.7	153	41.6	30.0	2.3	4	143	11	0.01	0.	0.	C
	19	10	34	0.3	59	43.8	153	11.7	5.0	1.6	5	158	80	0.27	4.2	602.1	C
	19	11	48	39.3	60	15.8	152	30.8	143.2	2.2	4	184	22	0.17	0.	0.	C
	19	15	39	23.4	59	24.3	152	37.2	5.0	2.0	4	143	59	0.34	0.	0.	D
	19	15	45	21.4	58	12.3	153	1.3	73.5	2.6	8	194	88	0.26	3.8	9.1	D
	19	15	51	11.5	57	27.0	154	58.7	39.2	2.4	4	173	24	0.01	0.	0.	C
	20	4	59	39.8	57	52.8	155	8.7	39.9	2.4	4	229	68	0.06	0.	0.	C
	20	11	44	45.9	60	35.3	153	27.6	263.8	3.8	6	279	139	0.94	106.2	133.9	D
	20	15	37	57.8	59	21.7	152	25.0	83.8	2.4	10	142	49	0.30	4.2	7.4	C

TABLE 11.2. COCK INLET-WESTERN GULF OF ALASKA EARTHQUAKES

COCK INLET-WESTERN GULF OF ALASKA EARTHQUAKES

1978	OS HR	IGI MN	TIME SEC	LAT N DEG MIN	LONG W DEG MIN	DEPTH KM	MAG	NO	GAP DEG	DM KM	RMS SEC	ERH KM	ERZ KM	O
FEB	20	17	56	59 14.8	153 33.8	101.3	2.7	10	153	12	0.19	3.1	3.8	C
	20	20	53	60 0.1	151 59.6	39.0	3.1	6	263	42	0.46	173.1	98.4	D
	20	20	56	58 58.4	154 26.2	136.2	3.2	14	89	19	0.30	2.5	4.7	B
	21	2	32	57 3.3	156 47.1	109.1	2.7	6	153	38	0.31	12.3	25.2	D
	21	3	39	59 0.9	152 47.6	87.4	2.6	5	195	42	1.33	75.1	86.2	D
	21	7	0	59 33.7	152 10.3	5.0	1.9	3	216	34	0.	0.	0.	C
	21	9	31	59 25.6	152 15.9	19.6	1.9	8	145	39	0.38	3.8	6.4	C
	21	11	26	58 53.7	154 19.8	122.5	3.1	8	186	24	0.45	17.6	39.9	C
	21	12	17	57 50.8	155 34.9	8.5	2.3	3	102	43	0.42	4.1	719.5	C
	21	12	54	57 57.5	155 38.0	103.4	3.0	6	90	42	0.22	3.2	7.8	C
	21	22	54	59 10.6	153 23.5	107.8	2.8	7	251	25	0.12	7.2	7.6	D
	22	10	8	59 19.9	153 56.6	70.9	3.4	10	107	55	0.17	1.5	3.9	B
	22	19	34	57 50.4	153 28.3	6.4	2.5	9	68	20	0.35	2.1	2.6	C
	22	20	35	59 45.8	153 13.2	69.1	2.9	15	57	27	0.54	3.3	6.0	C
	23	17	44	59 51.2	152 58.4	111.3	2.4	8	122	64	0.17	3.1	7.8	C
	23	16	47	57 45.1	154 32.3	5.0	2.0	4	200	103	0.49	0.	0.	D
	23	17	13	60 3.1	151 55.1	22.7	2.5	5	210	46	0.57	85.0	41.7	D
	24	1	24	57 21.7	155 8.3	5.1	3.2	7	151	30	0.15	1.9	2.8	C
	24	6	42	59 11.8	152 19.0	3.6	2.1	4	195	51	0.18	0.	0.	C
	24	7	45	60 31.9	150 45.0	5.0	3.4	12	150	109	0.72	6.0	17.0	D
	24	11	21	59 58.3	152 34.5	10.5	2.5	4	142	51	0.38	0.	0.	D
	24	14	47	57 23.4	152 0.1	83.7	1.9	4	172	25	0.11	0.	0.	C
	24	14	59	60 4.3	152 17.3	30.4	2.9	5	177	47	0.55	9.0	7.1	D
	24	16	59	59 50.3	153 13.9	5.0	1.9	5	168	69	0.35	5.7	783.1	D
	25	0	28	59 46.1	152 19.7	36.4	3.0	7	126	40	0.39	23.9	23.3	C
	25	5	32	60 5.2	153 13.8	200.6	2.7	4	188	44	0.	0.	0.	C
	25	16	49	57 19.6	154 22.3	6.9	2.9	5	201	60	0.06	1.3	131.1	D
	25	21	2	59 46.2	152 49.6	87.3	3.1	9	110	26	0.28	3.7	5.2	C
	26	4	26	59 43.3	152 24.0	73.7	2.8	12	114	43	0.42	4.3	6.6	C
	26	5	40	59 40.0	150 15.0	5.0	2.4	3	306	163	0.01	0.	0.	C
	26	8	22	59 45.2	153 3.3	102.3	2.5	10	86	69	0.24	2.3	5.3	B
	26	10	52	60 4.5	152 52.1	120.8	3.6	20	47	38	0.37	2.1	3.3	B
	27	0	38	59 19.0	152 6.7	5.0	1.9	3	283	34	0.	0.	0.	C
	27	2	12	59 54.2	154 6.4	133.9	2.8	4	230	22	0.01	0.	0.	C
	27	5	36	59 33.9	152 32.1	98.7	2.6	9	119	40	0.19	2.9	5.9	C
	27	11	7	59 52.9	152 6.0	175.1	2.1	4	166	35	0.	0.	0.	C
	27	13	4	59 49.9	152 59.8	33.8	2.2	4	132	66	0.30	0.	0.	C
	27	16	44	59 59.3	153 10.6	140.1	3.7	9	145	37	0.23	4.4	8.3	C
	27	19	3	60 23.9	153 59.5	127.1	1.9	4	250	12	0.23	0.	0.	C
	27	19	8	60 12.2	151 22.6	5.0	2.2	3	261	80	0.10	0.	0.	C
	28	3	36	59 48.1	151 56.6	65.2	2.6	4	185	42	0.	0.	0.	C
	28	12	47	60 15.0	153 24.5	162.2	2.9	8	195	40	0.36	11.0	17.1	D
	28	13	11	59 51.0	152 57.6	32.9	2.0	4	130	64	0.38	0.	0.	D
	28	15	31	59 56.9	153 50.2	109.7	2.0	8	119	52	0.23	5.4	11.1	C
	28	15	48	60 17.4	152 42.9	127.4	3.1	7	152	14	0.22	8.6	13.3	D

1978-1988 DATA BY G. H. HARRIS

COCK INLET-WESTERN GULF OF ALASKA EARTHQUAKES

	ORIGIN TIME			LAT N		LONG W		DEPTH	MAG	NO	GAP	DM	RMS	ERH	ERZ	D
	HR	MM	SEC	DEG	MIN	DEG	MIN	KM			DEG	KM	SEC	KM	KM	
1978																
FEB 28	22	37	42.5	57	52.9	156	37.9	9.0	1.6	5	210	8	0.09	1.9	1.2	C

Appendix 2

Epicenter Location Maps

January 1978 and February 1978

This appendix shows plots of epicenters for January 1978 and February 1978. Triangles with three-letter codes show the locations of seismic stations. The one-letter code shows the epicenter location with the following depth code:

A	0 < 25
B	26 < 50
C	51 < 100
D	101 < 125
E	126 < 150
F	151 < 175
G	176 < 200
etc.	

The size of the letters is proportional to the magnitude of the event.

The following is a list of figures:

<u>Figure</u>	<u>Caption</u>
A2-1	Cook Inlet, all events, January 1978
A2-2	Cook Inlet, all events, February 1978
A2-3	Kodiak-Alaska Peninsula, all events, January 1978
A2-4	Kodiak-Alaska Peninsula, all events, February 1978

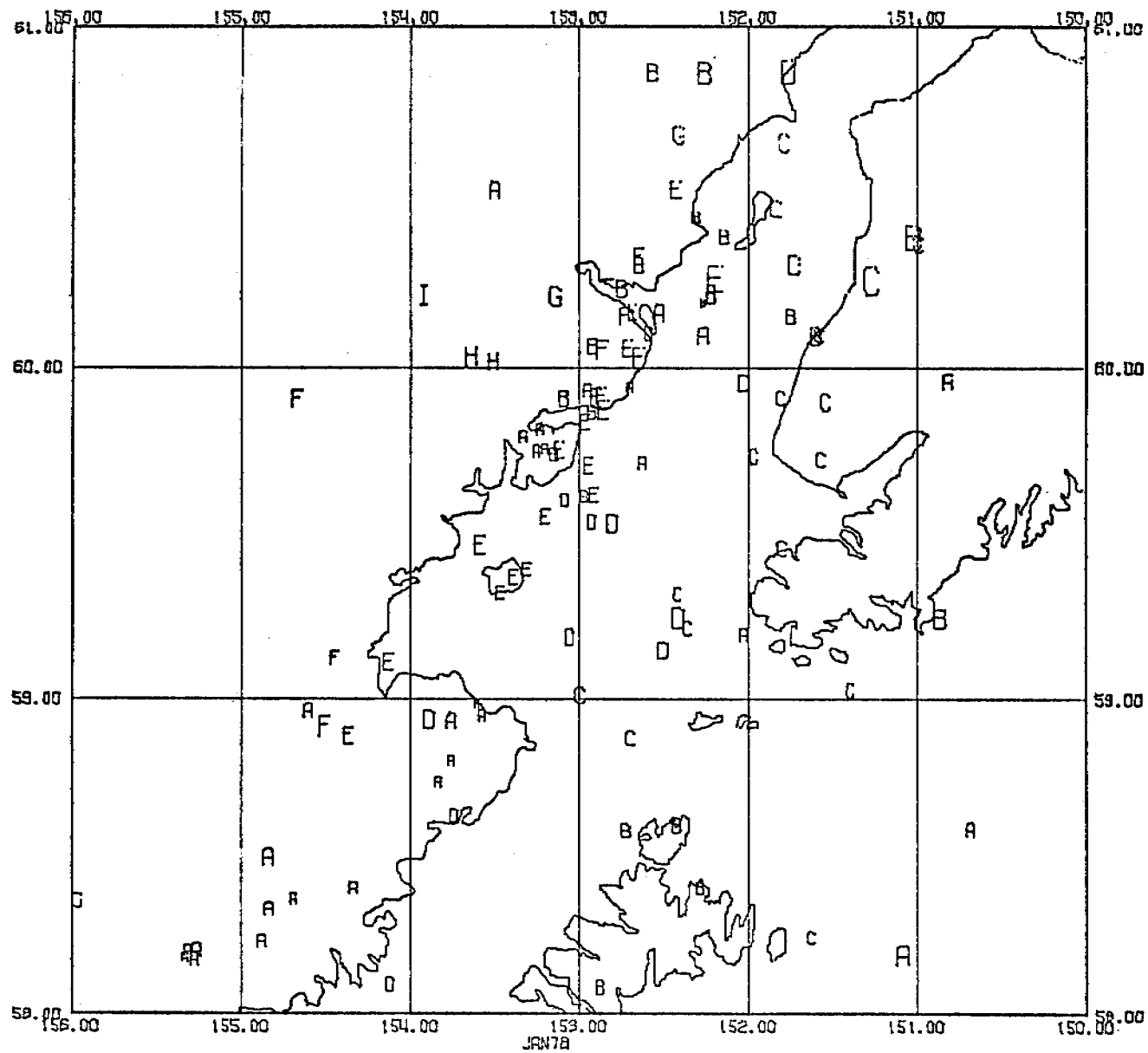


Figure A2-1. Epicenter Map, Lower Cook Inlet, January 1978

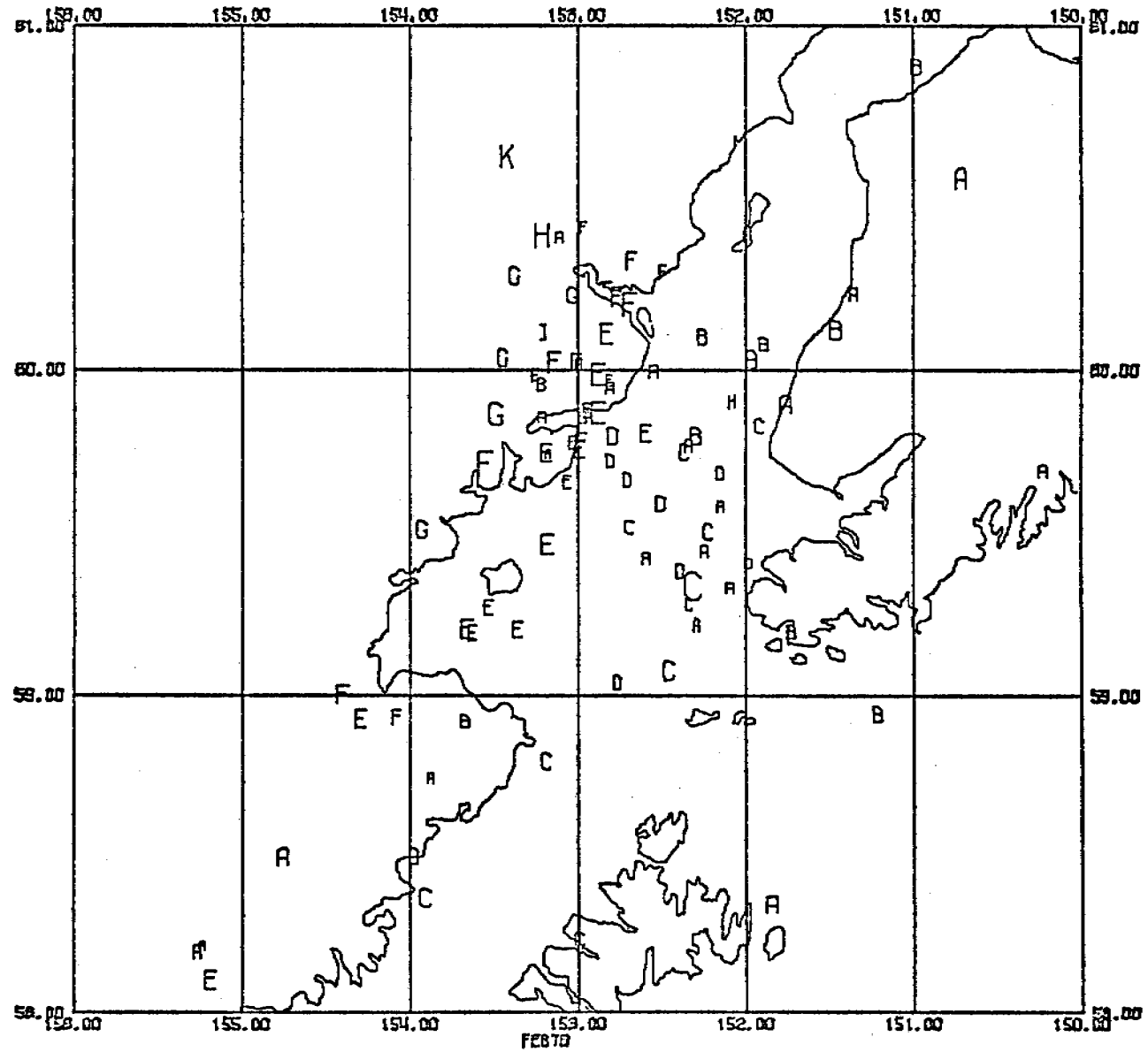


Figure A2-2. Epicenter Map, Cook Inlet, February 1978.

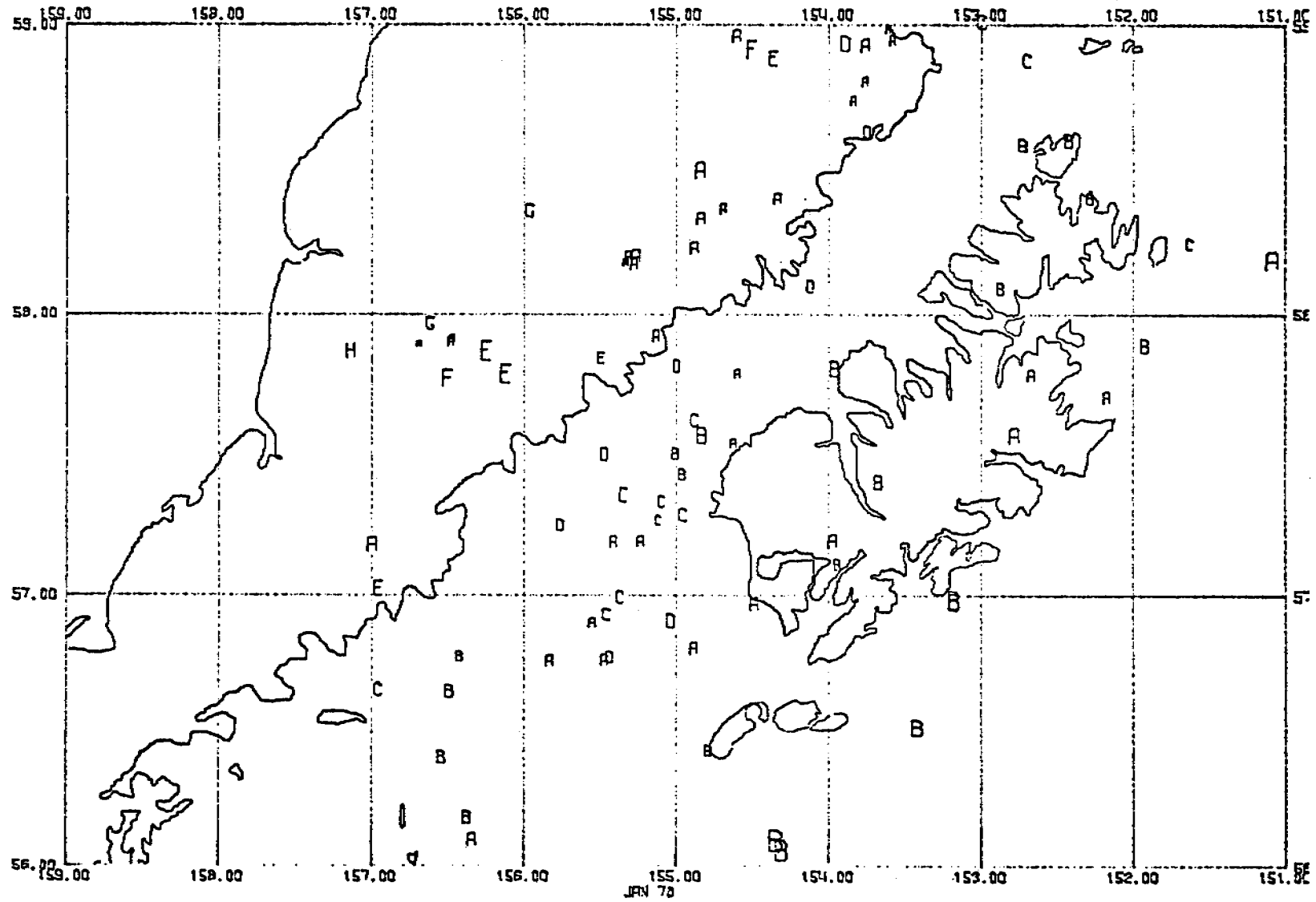


Figure A2-3. Epicenter Map, Kodiak-Alaska Peninsula, January 1978.

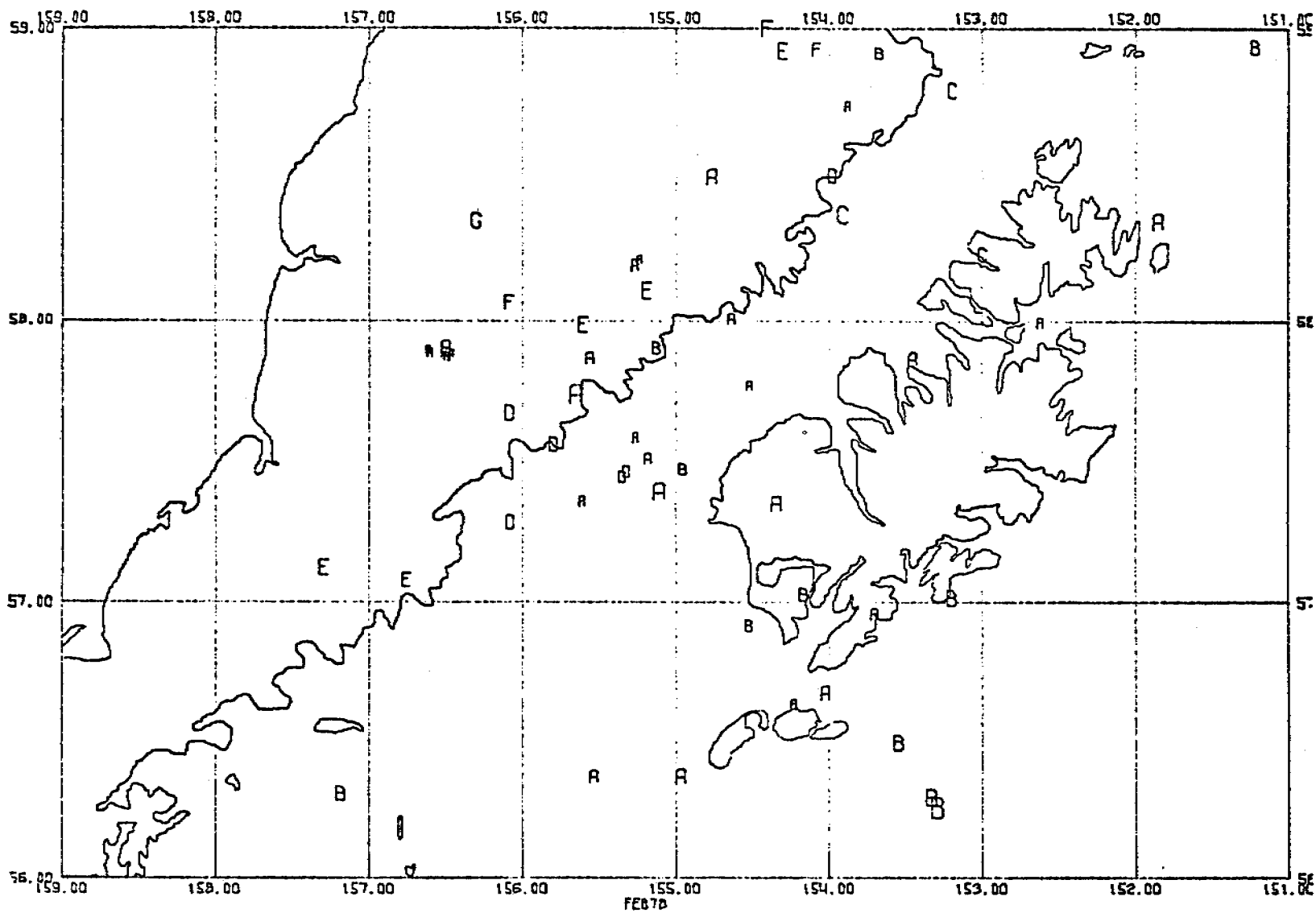


Figure A2-4. Epicenter Map, Kodiak-Alaska Peninsula, February 1978.

Appendix 3

Formation of the Ukinrek Maars

Preliminary Results

DRAFT REPORT

FORMATION OF TWO MAARS BEHIND THE ALEUTIAN VOLCANIC ARC,
ALASKA PENINSULA, APRIL 1977

Preliminary Results: Field Reconnaissance and Seismicity

Juergen Kienle

Geophysical Institute
University of Alaska
Fairbanks, Alaska 99701

Final Version Will Appear
April 1978

Introduction

From March 30 to April 9, 1977, two maars formed on top of a 100 m high hill in generally low-lying glacial terrane at the southern shore of Becharof Lake on the Alaska Peninsula, 3 km south of Gas Rocks. The eruption site lies behind the Aleutian volcanic arc, 13 km northwest of Peulik Volcano, a 1525 m high stratovolcano which erupted last in 1852 (Figure 1). The rims of the two maars are separated by about 400 m. The larger eastern maar is circular, about 300 m in diameter and 70 m deep, and contains a lava dome. The western maar, which actually formed first, is elliptical, with dimensions of about 170 by 105 m and a depth of about 35 m. A shallow lake was present for a few months after formation but drained subsequently, probably through underground waterways, into the deeper eastern maar which was originally dry and is now filling up with water.

The name "Ukinrek Maars" has been proposed by us to the U.S. Board of Geographic Names. Ukinrek in Yupik Eskimo means "two holes in the ground". The name was originally coined by children from the Naknek High School on an excursion to the erupting maars. Peulik in Yupik means "one with smoke". The geographic coordinates of the maars are about 57.75° N and 156.35° W.

Maars form when the earth's crust is initially perforated by phreato-magmatic explosions that result when magma contacts ground water at shallow depth. A rare geologic phenomenon, maars have been seen to form only twice in historic times, once in Chile in 1955 (Illies, 1959), and the second time at Iwo Jima, Japan, in 1957 (Corwin and Foster, 1959). Since the Ukinrek Maars formed near our existing regional Alaska Peninsula seismic network, we saw a unique opportunity to evaluate their tectonic

setting and deep conduit system through seismicity studies. Based on a earthquakes. Based on a rather high level of seismicity observed during our first reconnaissance expedition to the maars from April 14 to 21, 1977, we had good reason to anticipate continued earthquake activity, but in order to assure reasonable depth control of these events we felt that it was essential to install a new short period seismic station close to the maars.

This report summarizes the preliminary observations made during three field trips and the earthquake data up to December, 1977.

Eruptive Phase - March 30 to April 9, 1977

(all times are local = U.T. - 10 hours)

Explosions were first observed on March 30 from a point 70 km SW of the eruption site. Pilots who overflew the eruption at 1725 and 1800 reported a single vent, 20-30 m in diameter, from which first white steam, then a dark ash-laden cloud, rising to 6000-7500 m, were emitted. Fine ash fell at Larsen Bay, 135 km ESE of the vent, and a sulfurous haze lay over Kodiak, 250 km E, all day. More ash clouds were seen on April 1 and 2.

On April 2, the original crater had filled with water and had ceased to erupt. A new vent, 60 m in diameter, had formed half a kilometer to the east. By early afternoon of April 3, the eastern maar had grown to about 100 m in diameter and we received the first report of lava, forming a yellowish-orange lake. Lava fragments up to 1 m across were ejected up to 300 m into the air. Later in the afternoon 15-20 m high lava fountains were observed.

On April 5, an ash cloud rising more than 4000 m deposited trace amounts of ash in King Salmon, 95 km to the north, and over parts of the

Katmai National Monument. By April 6 activity had declined to steam emission and smaller explosions which threw tephra more than 1000 m up from the lava lake (Figure 2). Similar activity and 30 m high orange-red lava fountains were reported on April 7. No further eruptions were observed until the early morning of April 9, when strong explosion columns containing incandescent material were seen from 30 km away. Table 1 summarizes the eruption chronology.

Field Work

1.) April 14-21, 1977

The first reconnaissance landing near the two new maars was made on April 13. A team of volcanologists from the University of Alaska (J. Carden, J. Kienle, D. Lalla, R. Motyka) and from Dartmouth College (J. Bratton, S. Self) investigated the new eruption site on the ground from April 14-21. A University of Washington research airplane, equipped to sample volcanic aerosols and gases, flew several missions over the site from April 8 to 22.

The oblong western maar had nearly vertical walls and was shallowly filled with lukewarm, only slightly acidic water (pH = 6). We were surprised to find very high temperatures of the ejecta within two distinct fallout lobes on the east and west side of this crater, which was the first one to form. The highest temperature we measured was 805°C near its rim at 1.1 m depth. Temperatures on a profile between the two craters decreased from 210°C at 15 cm depth at the rim of the younger maar to 20°C at the same depth at the rim of the eastern maar. These high temperatures can probably be attributed to very rapid accumulation of scoria, cinders, and heated rock bombs during the initial stages of the eruptions, thus trapping the heat contained in the ejecta.

The larger and deeper eastern maar was dry and over one-half of its floor was occupied by a degassing lava dome about 40 m high and coated with sulphur and hematite deposits giving it a greenish overall appearance (Figure 3b). Ground water emerged from the crater walls at 50 m depth and cascaded onto the hot dome, giving rise to a continuous steam plume. Occasional ash puffs were produced when collapsing sections of the steep crater walls collapsed.

The two maars were surrounded by aprons of tan colored ash, black scoria and spatter and lithic ejecta blankets which showed a pronounced grading from fine to coarse as one approached the crater rims (Figure 3a and c). At the rim of the eastern maar the ejecta had accumulated to a depth of 10 m. At a distance of 2 km, at the shore of Becharof Lake, the total ash layer was only a few centimeters thick containing a sprinkling of fist-size scoria bombs probably associated with one of the more violent late eruptions.

A strewn field of exotic blocks and boulders of highly variable composition and some olivine basalt bombs surrounds the two maars (Figure 3d). The bombs decrease in size from 1.5 m in diameter near the crater rims to about 50 cm diameter a few hundred meters away. Stripped branches and bark, and mud plastered against tree trunks 500 m from the vents, indicate at least minor base surge activity during one or more explosions of the eastern maar.

Exotic blocks, the majority of which were not coated with new melt, consisted of a variety of granitic to dioritic igneous rocks, sandstones, shales, cherts, cobble and boulder conglomerates, most likely derived from the underlying Naknek formation, and volcanics, including andesites, rhyolites, and banded pumice.

The new melt found as spatter, scoria and bombs (often with large lithic cores) is vesicular olivine basalt. In thin section the basalt has a hypocrystalline texture. Abundant lath-shaped microlites of plagioclase (An 50) and rare granules of augite, ranging in size from 0.1-0.2 mm in length, enclose large olivine phenocrysts, up to 0.1 mm in diameter, which make up 10% of the rock. The ground mass is composed of a mesostasis of dark glass and small euhedra of magnetite. Augite is conspicuously absent as phenocrysts larger than 0.2 mm. Xenolithic inclusions in the basalt are granitic and basaltic in composition. They make up less than 1% of the more massive samples and over 60% of some of the more scoriaceous varieties.

Using a spectrograph, the Dartmouth group quantitatively measured SO_2 in the plume which continuously rose from the eastern crater but found no detectable quantities of this gas.

From April 15 to 20 the University of Alaska group operated two portable short-period seismograph systems within 2 km of the maars. We found a high level of local microearthquake activity and recorded three distinct earthquake swarms of several hours duration (Figure 4). During these swarms we registered more than one event per minute. Most of the events were shallow (a few km in depth, based on S-P time intervals) and of small magnitude ($M_L = \leq 1$). However, some of the events were large enough to be recorded by a permanent University of Alaska seismic station (BMT), 25 km north of the eruption site.

Geodetic measurements were also begun to locate the maars relative to an existing bench mark on Gas Rocks and to determine the dimensions of the vents and their ejecta aprons.

2.) May 20-29, 1977

From May 20 to May 29, 1977, J. Kienle and J. Siwik from the University of Alaska installed a new short-period seismic station on Gas Rocks (MAA), 3 km north of the maars, field serviced FLP, 35 km south-east of the maars, and also station BMT, 25 km north northeast of the maars, where we had to install a new radio receiver and antenna to receive MAA. We hoped that this new relatively narrow spaced tripartite array, consisting of MAA, FLP and BMT, would allow us to determine fairly rapidly the seismicity and thus the tectonic setting of the maars. Unfortunately, on this trip we did not succeed to establish reliable telemetry for all stations, which we achieved only later, in August, by moving the BMT repeater site to higher ground. In late May we operated the portable seismograph system again, but found that local earthquake activity at the maars had practically ceased. It took another five months of data collection to see a pattern of seismicity emerge.

3.) August 23 to September 1, 1977

With funding from the State of Alaska, J. Kienle, R. Motyka, J.-P. Huot and V. Ferrell returned to the maars in late August for a ballistic study and completion of the geodetic work. We weighed and described well over 100 bombs as to their shape, composition, and distance thrown, and we are now well into the analysis of this data, hoping to obtain estimates of the energy of the eruptions. The portable seismograph station showed again a complete absence of local microearthquakes.

On August 24 and 25, G. McCoy from the Anchorage U.S. Geologic Survey Office, Water Resources Division, collected geochemical samples and determined pH and temperature from a single hot spring left on the

floor of the western maar, which by now had drained completely. He also sampled a series of new gas vents discovered after the eruptions offshore from the Gas Rocks and bubbling up through Becharof Lake. Some of the samples were sent to Ivan Barnes at the U.S. Geological Survey, Menlo Park office, where the analyses are presumably available.

Earthquake Data

Seismic Array: The Kodiak-Alaska Peninsula-Cook Inlet regional seismic network, presently supported by ERDA and NOAA, is shown in Figures 5a and b. The important stations for studies of the seismicity associated with the Ukinrek Maars are MAA, BMT, FLP, PUB, UKL, (KSL), in that order. Figure 5a shows the network before the late May modification. In order to add MAA to the array we had to drop KSL, because we could not multiplex an extra channel onto the RCA telephone line between Big Mountain and Homer. As mentioned before, marginal telemetry necessitated further rearrangement of the system in August, when we leased an RCA telephone link between King Salmon and Big Mountain, and moved the BMT repeater to the summit of Blue Mountain. This allowed direct telemetry from UKL to BMT and improved the MAA-BMT link. The new arrangement is shown in Figure 5b and has worked very well up to now.

Results: Aleutian Range volcanism is the result of the convergence of the Pacific and North American plates. The geometry of the underthrusting Pacific plate in the Upper Alaska Peninsula-Kodiak region is clearly mapped out by the Benioff zone shown in Figure 6 (Estes, 1978). The graph was obtained by projecting all hypocenters in a 150 km wide section onto a plane roughly perpendicular to the volcano line and passing through central Kodiak. Subduction in the section from the

Aleutian trench to the northwestern edge of Kodiak is characterized by a shallow (10 degrees) underthrust. A pronounced knee in the plate configuration occurs at the northwestern edge of Kodiak, where the deeper Benioff zone steepens and plunges at an angle of very close to 45 degrees to a depth of about 200 km. The position of the knee marks the outcrop of the deeper Benioff zone in this area located several hundred kilometers landward of the present trench. The knee coincides with a Lower Cretaceous subduction complex, the so-called Uyak-McHugh melange (Moore and Connelly, 1977), and an adjacent Early Mesozoic blueschist belt, believed to represent earliest subduction in this region (Forbes and Lanphere, 1973). A shallow cluster of earthquakes at Snowy Mountain Volcano in Katmai National Monument marks the position of the volcano line (near 85 km on the distance axis, Figure 6). The depth of the Benioff zone beneath the Katmai volcanoes appears to be about 150 km, a depth that is somewhat greater than, for example, Cook Inlet, where the volcanoes line up above the 120 km depth contour. Based on our limited data, the best estimate of the depth of the Benioff zone beneath the Ukinrek Maars is somewhat deeper than 150 km, since they formed 15 km landward of the Aleutian arc.

Tables 2 and 3 are listings of shallow (less than 50 km) and deep (greater than 50 km) events located near Becharof Lake between February, 1976, and December, 1977. Only since August, 1977, were we able to routinely locate earthquakes near the maars down to local magnitude $M_L = 1$, resulting in a marked increase of events since that time. Figure 7 is an epicenter map of only the July to December portion of the data listed in Table 2, letter coded according to depth and corresponding to better quality data from the new array. Most of these earthquakes

are shallower than 10 km. Intense clustering of epicenters occurs about 8 km west of Gas Rocks at a location where we found earthquake induced scarps on the north-facing bluffs at the southern shore of Becharof Lake. All the deeper events listed in Table 3 are regional Benioff zone earthquakes unrelated to the maars. So far we have no evidence of any seismicity at depths between the surface and the Benioff zone, i.e., associated with the deep plumbing system.

In general, most epicenters locate within a relatively narrow north-westerly trending zone, which is radial to Peulik Volcano. The maars formed at the intersection of this zone with the Bruin Bay fault, a moderate to steeply northwest dipping reverse fault with the northwest side upthrown. It can be traced 515 km to the northeast into the west side of Cook Inlet. On the Alaska Peninsula the fault juxtaposes Early and/or Middle Jurassic intrusive rocks of batholithic dimensions against the Naknek formation of Upper Jurassic age (Keller and Reiser, 1959). The Bruin Bay fault is a likely extension of the Castle Mountain fault, part of which has been active in the Holocene, and because of this association is potentially active (Detterman, et al., 1976).

Nakamura et al. (1977) proposed that the distribution of monogenetic craters at the flank of a polygenetic center indicates a preferred orientation of radial and parallel dike swarms which tend to propagate in a direction normal to the minimum regional stress axis. In an island arc setting this direction would be parallel to convergence. In Figure 7 the arrow indicates the direction of convergence of the Pacific and North American plates using Minster et al.'s pole of instantaneous rotation at 50.9 N and 66.3 W. Convergence agrees within 15° with the orientation of a line radiating from Peulik Volcano and passing through

the maars and the greatest concentration of earthquakes. If this line does indeed indicate a zone of crustal weakness potentially subject to dike injection, flank eruptions could be expected to occur here. The maars formed at the intersection of this potential zone of weakness with the Bruin Bay fault, a major regional fracture which perhaps penetrates the entire lithosphere and could thus provide an avenue for magma ascent from great depth. This hypothesis is of course highly speculative. It remains to be seen whether or not future earthquake data will confirm the northwesterly alignment of epicenters.

There are two other regional tectonic trends that intersect in the vicinity of the maars: (1) the extension of the lineament formed by the Katmai Volcanoes (Figure 1), and (2) the cross-arc southwestern boundary of the great 1964 Alaskan aftershock zone.

Geochemistry

Another test for or against a genetic relationship of the Ukinrek and Peulik lavas is their geochemical affinity. Preliminary data indicates that the Ukinrek lava is a Nepheline normative alkali-basalt, a chemistry which one does not usually see in the tholeiitic basalt-andesite association of typical Aleutian arc volcanism. Selected component bulk chemistry of Ukinrek cinders, scoria, a lava bomb and toothpaste lava shows practically no variance at about 47.6 weight percent SiO_2 , 3.15% Na_2O and 0.85% K_2O . The basalt contains up to 10% forsterite-rich basic olivine and the CPX is quite rich in Al_2O_3 and CaO . The plagioclase is a calcic labradorite. Mt. Peulik, on the other hand, is a dacitic-andesitic stratovolcano. An extensive lava field exists on the Ukinrek facing flank of the volcano. Within this field Tom Miller (personal

communication) collected samples from a lava flow and a dome-like upwelling of lava which turned out to be transitional between basalt and andesite (SiO_2 54%, Na_2O 2.6%, K_2O 1%).

Conclusions

Based on our preliminary seismic and geochemical data, we presently favor a tectonic model for the emplacement of the Ukinrek Maars that does not link the Ukinrek conduit directly to the plumbing system of Peulik Volcano. We feel that the Ukinrek eruptions more likely represent a genetically distinct magmatic pulse originating at asthenospheric depths. The position of the conduit may be controlled by the shear field associated with plate convergence in this region and by the deep Bruin Bay fault fracture, since the maars formed at the intersection of these two tectonic trends.

The question whether or not the Ukinrek basalts genetically belong to the alkaline rock suite found on Kanaga and Bogoslof Volcano not far behind the active arc (Arculus, et al., 1977), will have to be resolved with more geochemical data. DeLong et al. (1975) pointed out that alkaline rocks in island arcs built across oceanic crust tend to occur along lateral edges of subduction zones or where a fracture zone or other linear feature perpendicular to the trench is subducted. For example, the Kanaga alkaline rocks were erupted near the subducted Adak fracture zone. The cross arc boundary of the Alaskan earthquake after-shock zone near the maars may well represent such a lateral discontinuity in the subducting Pacific plate, a setting that would fit DeLong et al.'s (1975) tectonic environment for island arc alkalic volcanism, except that in the Ukinrek case it occurs in continental crust.

Our field investigations and ballistic studies in progress confirm that the Ukinrek vents are true maars which formed in less than two weeks by phreatomagmatic explosions at very shallow depth (few tens of meters), as rising basaltic magma came in contact with ground water.

Acknowledgements

The following individuals have contributed to the field study:

S. Self and J. Bratton from Dartmouth College, and R. Motyka, J.-P. Huot, D. Lalla, J. Siwik and V. Ferrell from the University of Alaska.

A. T. Anderson, University of Chicago, P. R. Kyle, Ohio State University, and R. B. Forbes and C. Nye, University of Alaska, provided preliminary microprobe data and petrographic descriptions of the Ukinrek basalts.

T. Miller, U.S. Geological Survey, Anchorage, provided geochemical analyses of Peulik lavas. I gratefully acknowledge the contribution of these individuals.

References

- Arculus, R. J., S. E. DeLong, R. W. Kay, C. Brooks, and S. S. Sun, 1977. The alkalic rock suite of Bogoslof Island, Eastern Aleutian Arc, Alaska, *J. of Geol.*, 85, pp. 177-186.
- Corwin, G., and H. L. Foster, 1959. The 1957 explosive eruption on Iwo Jima, Volcano Islands, *Am. J. of Science*, pp. 161-171.
- DeLong, S. E., F. N. Hodges, and R. J. Arculus, 1975. Ultramafic and mafic inclusions, Kanaga Island, Alaska, and the occurrence of alkaline rocks in island arcs, *J. of Geol.*, 83, pp. 721-736.
- Detterman, R. L., T. Hudson, G. Plafker, R. G. Tysdal, and J. M. Hoare, 1976. Reconnaissance geologic map along Bruin Bay and Lake Clark faults in Kenai and Tyonek quadrangles, Alaska, U.S. Geol. Survey open-file report 76-477, 4 pp. and map.
- Estes, S. A., 1978. Seismotectonic studies of Lower Cook Inlet, Kodiak Island and the Alaska Peninsula areas of Alaska, M.S. thesis, in preparation.
- Forbes, R. B., and M. A. Lanphere, 1973. Tectonic significance of mineral ages of blueschists near Seldovia, Alaska, *J. Geophys. Res.*, 78, pp. 1383-1386.
- Illies, H., 1959. Die Entstehungsgeschichte eines Maeres in Sued-Chile, *Geol. Rundschau*, pp. 232-244.
- Minster, J. B., T. M. Jordan, P. Molnar, and E. Haines, 1974. Numerical modelling of instantaneous plate tectonics, *Geophys. J. R. Astr. Soc.*, 36, pp. 541-576.
- Moore, J. C., and W. Connelly, 1977. Mesozoic tectonics of the Southern Alaska margin, in *Island Arcs, Deep Sea Trenches and Back-Arc Basins*, edited by M. Talwani and W. C. Pitman III, AGU Maurice Ewing Series 1, pp. 71-82.
- Nakamura, K., K. M. Jacob, and J. N. Davies, 1977. Volcanoes as possible indicators of tectonic stress orientation - Aleutians and Alaska, *Pageoph.*, Birkhäuser Verlag, Basel, 115, pp. 87-112.

TABLE 1. UKINREK MAARS ERUPTION CHRONOLOGY
30 March - 10 April, 1977

<u>DAY</u>	<u>MONTH</u>	<u>LOCAL TIME</u>	<u>ACTIVITY</u>
30	Mar	Morning	Start of eruption. Much explosive activity. Development of first (West) Crater. Ash blown ESE to Kodiak by strong upper west winds.
		17:00-18:00	Phreatomagmatic/vulcanian(?) eruption; plumes to 6500 m, followed by phreatic/strombolian activity.
31	Mar		Poor weather - no observations.
1	Apr	11:00	3000 m high plume sighted. New crater begins to form (?)
2	Apr	17:30	Old vent quiet - new crater active; about 60 m diameter. Mixed phreatic/strombolian activity.
3	Apr	12:00	Second crater increased to 100 m diameter. Strombolian activity.
		14:00-16:00	Yellow-orange magma sighted within second crater. Incandescent fountaining. Ejection of large boulders. Strong strombolian activity.
4	Apr		Poor weather - no observations.
5	Apr	Morning	Ash-laden cloud, 4000 m high. Ash dispersed to 95 km north.
		16:30	Phreatomagmatic/vulcanian(?) eruption from second crater. Spectacular mushroom shaped cloud billowing out at 3000 m, followed by mixed phreatic/strombolian activity.
6	Apr	10:00	Strong phreatic/strombolian activity. Ejection of incandescent debris.
		14:30	Steaming and mild strombolian activity. Second crater, 200-250 m diameter and 70-80 m deep.
		18:00	Strong phreatic/strombolian activity. Plumes to 1500 m.
7	Apr	09:30	Orange-red magma sighted within second crater. 30 m high incandescent fountains. Strombolian activity. Plumes to 1500 m.
8	Apr		Poor weather - no observations.
9	Apr	Early Morning	Violent explosions. Strombolian and phreatomagmatic (?) End of the eruption.
10	Apr		Steaming only. No further activity. Second crater, 300 m diameter and 80 m deep.

Table 2. Listing of shallow (less than 50 km deep) earthquakes February, 1976 to December, 1977. The epicenters have been plotted on Figure 7.

DATE	ORIGIN	LAT	LONG W	DEPTH	MAG	NO	GAP	DMIN	RMS	ERH	ERZ	QM
760224	118	55.80	57-48.05	156-56.95	0.31	0.	5	337	45.5	2.725	63.31	62.7 D1
760226	1820	38.04	58- 1.27	156-24.16	0.54	0.	11	127	4.8	3.30	22.2	19.8 C1
760306	1222	0.83	57-51.74	156-53.03	29.48	4.50	11	145	195.7	0.76	8.99	49.4 D1
760325	333	9.80	58-14.18	156- 6.02	2.50	0.	5	320	139.2	0.54	29.0	22.8 D1
760611	950	19.26	57-59.33	156-51.60	2.25	0.	8	155	80.4	0.96	21.7	56.7 D1
760611	955	1.73	57-59.88	156-51.53	2.50	0.	8	155	79.4	0.91	20.6	53.9 D1
760611	1557	42.49	57-56.74	156-41.03	2.50	0.	11	141	84.4	0.80	9.9	32.9 D1
760626	853	23.74	58- 2.06	156-54.66	30.90	0.	7	156	75.9	0.21	3.9	3.2 D1
760628	1959	1.35	58-10.67	156-22.84	33.23	0.	8	266	150.9	1.24	46.5	750.7 D1
770204	714	18.37	57-46.50	156- 3.14	5.00	0.	3	241	31.9	0.42	0.	0. D1
770217	253	9.10	57-53.61	156-43.84	0.49	2.38	4	175	28.9	0.14	0.	0. C1
770517	1326	3.04	57-52.99	156-51.66	12.79	2.81	4	269	80.9	0.	0.	0. C1
770627	1255	6.99	58- 6.20	156-26.99	5.00	1.78	3	346	9.2	5.05	0.	0. D1
770703	1154	50.75	58-14.17	156-13.98	37.12	2.81	9	252	152.2	0.85	22.4	***** D1
770708	1711	51.37	57-52.34	156-35.32	9.33	1.08	4	201	6.1	0.	0.	0. C1
770722	8 3	21.84	57-59.18	156-38.32	0.02	1.32	4	238	16.9	0.03	0.	0. C1
770722	817	21.35	58- 4.49	157- 0.86	4.65	1.91	5	282	39.4	0.02	1.1	0.4 C1
770802	642	26.72	57-58.24	156-39.18	2.40	1.41	4	235	16.0	0.14	0.	0. C1
770809	216	54.91	57-52.74	156-37.64	8.89	1.51	5	208	8.5	0.05	1.2	0.8 C1
770830	2328	3.26	57-53.21	156-37.22	7.68	1.81	9	191	8.5	0.54	5.5	3.0 D1
770830	2338	22.92	57-52.94	156-40.03	7.05	1.60	6	215	10.9	0.25	4.0	2.5 D1
770831	1838	47.49	57-53.08	156-37.52	8.63	1.55	4	271	8.6	0.11	0.	0. C1
770831	2312	18.00	57-53.17	156-33.17	5.00	0.91	3	257	5.0	0.	0.	0. C1
770901	2134	12.45	57-52.94	156-41.67	3.34	1.07	4	219	12.5	0.	0.	0. C1
770904	1246	18.26	57-53.15	156-38.60	9.10	1.39	4	275	9.7	0.08	0.	0. C1
770913	1124	28.72	57-53.55	156-32.07	5.00	0.35	3	249	4.8	0.	0.	0. C1
770914	647	43.38	58- 9.59	156-15.78	6.35	2.58	11	181	13.3	0.19	1.6	1.6 C1
771001	1558	36.26	57-58.86	156-54.29	4.09	1.66	4	298	28.3	0.05	0.	0. C1
771001	1919	34.66	57-57.89	156-50.62	5.85	2.18	8	210	24.2	0.34	4.8	3.7 D1
771004	1026	38.06	57-57.71	156-48.13	0.63	2.08	16	172	21.9	0.84	5.0	13.8 D1
771009	1322	29.28	57-53.23	156-42.63	2.00	1.46	4	222	13.5	0.06	0.	0. C1
771018	1115	6.43	58- 2.99	156-23.11	1.49	2.96	16	177	2.9	0.60	3.4	2.5 D1
771018	1412	9.91	58- 2.08	156-22.75	3.27	1.71	7	182	2.8	0.27	2.8	2.0 D1
771024	21 9	26.55	57-53.79	156-30.23	5.00	1.14	3	221	4.5	0.	0.	0. C
771025	9 9	30.13	57-53.25	156-34.02	5.00	1.26	3	260	5.7	0.04	0.	0. C
771028	21 1	34.97	57-53.55	156-41.73	1.58	1.33	4	221	12.9	0.04	0.	0. C
771101	1744	28.81	57-52.90	156-36.89	9.65	1.88	4	207	24.7	0.	0.	0. C
771103	655	47.52	57-53.57	156-37.48	11.35	1.56	4	211	24.2	0.	0.	0. C
771104	449	14.27	57-53.43	156-37.72	7.51	1.36	5	211	24.5	0.14	2.9	2.2 D
771111	2 6	15.44	57-48.72	156-32.69	5.00	1.04	3	261	6.0	0.86	0.	0. D
771116	0 5	48.06	58- 3.71	156-23.86	4.70	3.00	9	178	4.0	0.29	2.6	1.7 C
771116	1635	49.56	57-52.65	156-27.37	4.82	2.12	5	156	3.1	0.08	1.3	0.9 C
771122	927	46.81	57-58.37	156-56.08	3.88	2.64	7	217	36.3	0.29	4.8	4.2 D
771122	20 6	56.86	58- 5.83	156-31.52	0.05	3.10	13	194	12.5	0.60	4.5	13.4 D
771125	1925	25.01	57-53.59	156-36.94	17.31	1.96	5	209	23.8	0.23	5.9	13.3 D
771126	334	59.81	58- 5.70	157- 5.23	9.71	2.07	5	287	44.6	0.10	7.92	16.9 D
771129	4 4	8.41	58- 3.75	156-22.15	4.14	2.16	4	311	2.6	0.12	0.	0. C
771202	1409	9.40	57-55.81	156-45.26	5.35	2.97	12	187	27.9	0.47	3.6	3.3 D
771203	721	0.49	57-56.27	156-44.63	7.32	2.83	13	187	17.6	0.46	3.5	2.6 D
771221	2113	47.10	57-52.63	156-41.09	0.63	1.40	4	217	11.8	0.04	0.	0. C

Table 3. Listing of deep (greater than 50 km) earthquakes, February, 1976 to December, 1977.

DATE	ORIGIN	LAT	LONG W	DEPTH	MAG	NO	GAP	DMIN	RMS	ERH	ERZ	QM
770715	334	3.67	57-50.38	156-31.72	133.20	2.08	6	268	3.0	0.70	69.71	06.6 D1
770817	2340	7.78	57-50.74	156-13.03	135.53	3.40	7	214	62.4	0.15	4.0	5.0 D1
770912	2353	57.56	57-49.91	156-21.45	140.37	2.38	7	151	14.5	0.26	11.3	19.3 D1
770913	425	31.71	57-45.91	156-12.20	132.34	2.62	10	81	7.0	0.57	12.4	19.3 C1
771110	946	35.27	57-56.32	156- 6.51	129.06	2.58	8	95	18.1	0.31	6.3	10.5 C1
771111	343	0.02	57-50.29	156-14.85	135.23	2.76	8	163	14.1	0.25	9.4	14.1 D1
771128	1333	56.50	57-48.05	156- 0.72	120.80	2.19	4	219	18.0	0.	0.	0. C1
771208	2021	39.43	57-53.08	156-28.69	154.70	2.70	9	237	19.9	0.26	11.1	15.4 D1
771209	1854	50.44	57-56.97	156- 5.96	124.03	2.18	6	138	17.7	0.23	14.1	24.2 D1
771225	2320	25.04	57-53.10	156- 9.10	130.22	2.83	9	101	21.1	0.11	1.3	2.0 B1
771228	1200	4.83	57-49.78	156-41.21	162.32	2.84	8	272	69.9	0.15	9.4	10.3 D1



Figure 1. LANDSAT mosaic of the Upper Alaska Peninsula and Cook Inlet showing the location of the Ukinrek Maars (arrow) at the southern shore of Lake Becharof. Solid circles denote other volcanoes in this region.

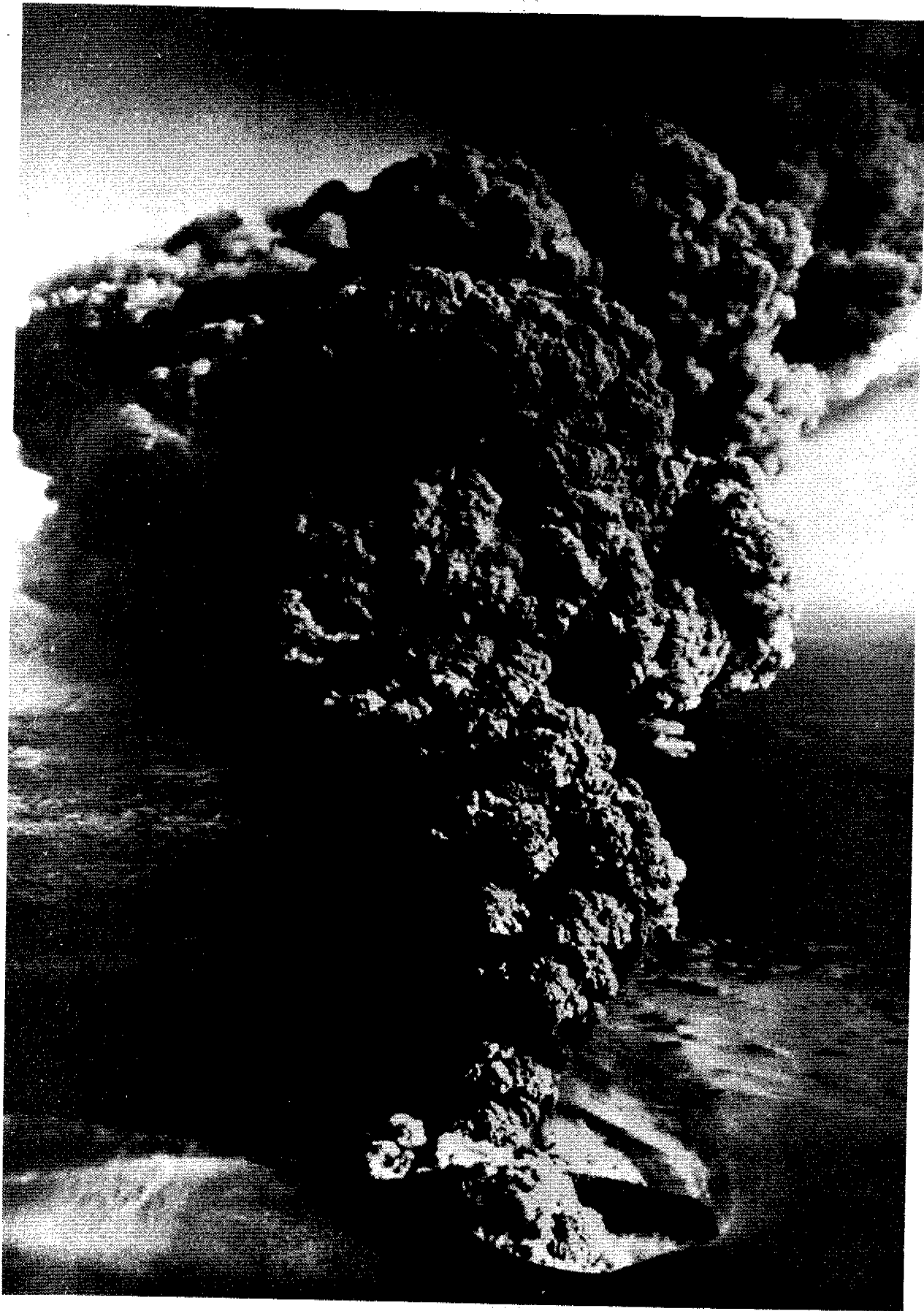


Figure 2. Strombolian activity at the eastern Ukinrek Maar on the evening of April 6, 1977. Photograph by Richard Russell.

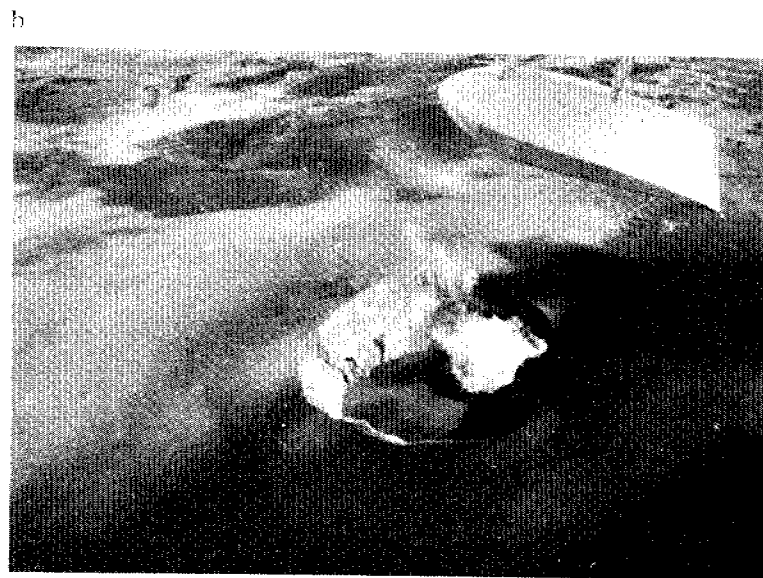
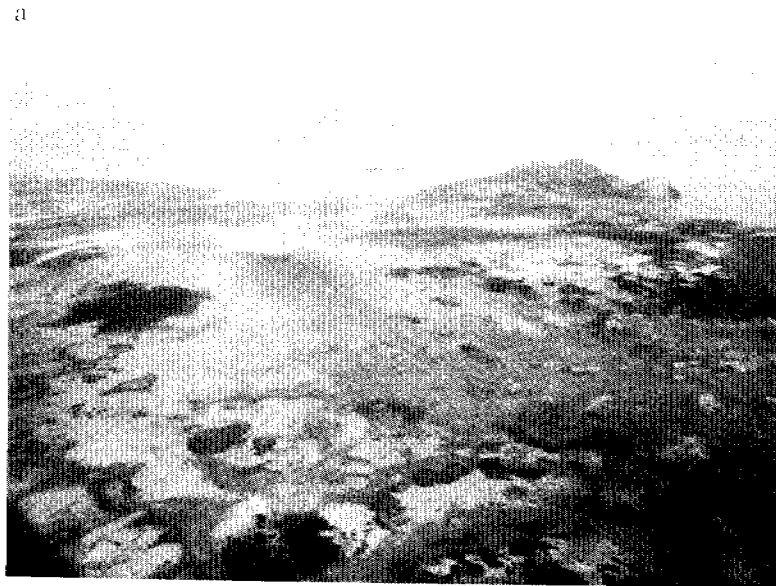
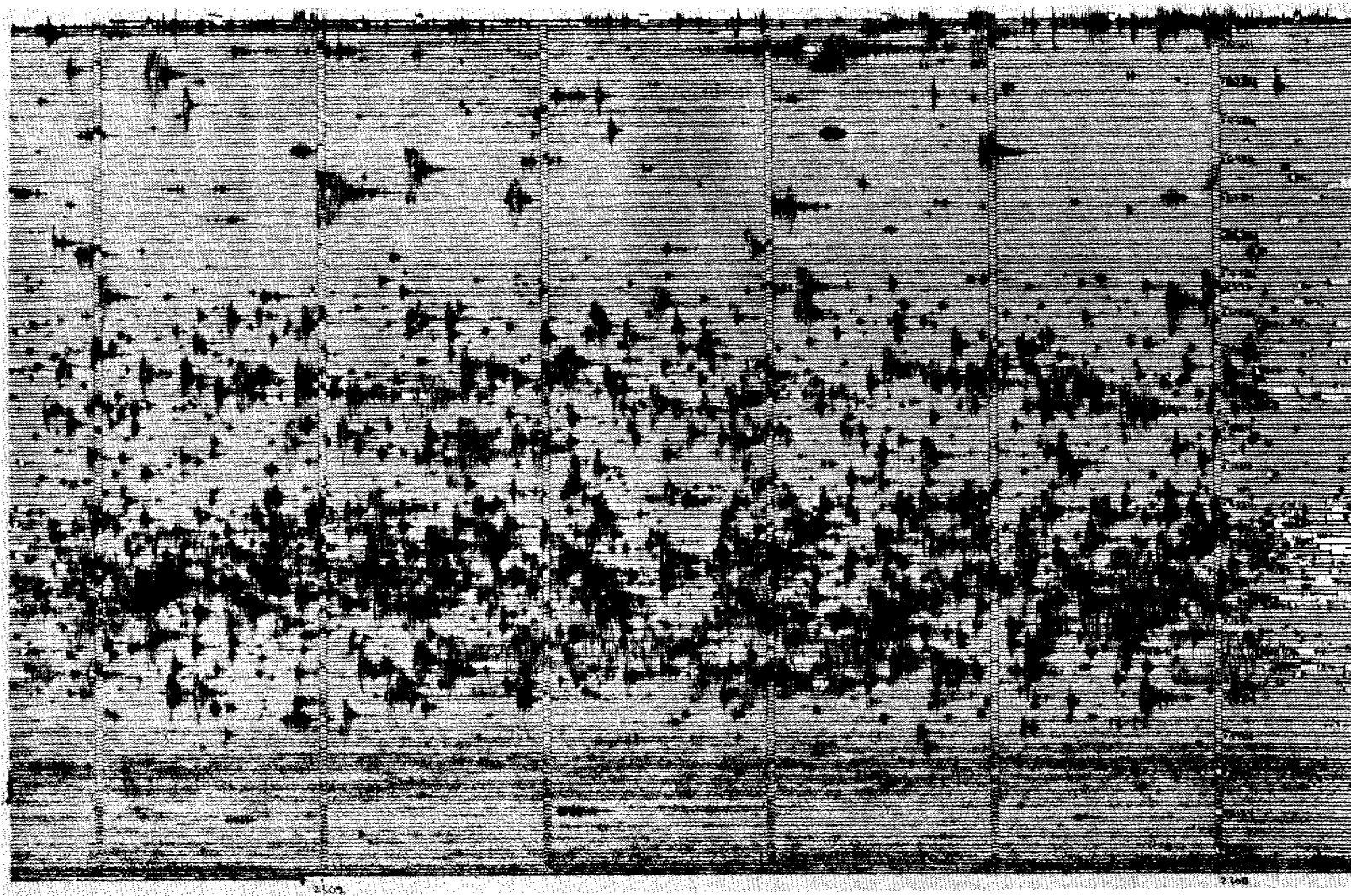


Figure 3. Sequence of photographs showing the location of the Ukinrek Maars (steam column) near Gas Rocks at the southern shore of Lake Becharof (a), a vertical view of the now water-filled eastern maar with its steaming lava dome and exposure of the layered ejecta blanket in its upper wall (b), the smooth ejecta blanket surrounding the maars (c), and a close-up of the strewn field of exotic blocks near the rim of the eastern maar with the Gas Rocks in the background; D. Lalla is kneeling on black scoria (d). Photographs by J. Kienle.



Ukinrek Maars, April 18, 1977, 00:24 - 23:02

Kinematics PS-1A Recorder, Ranger SS-1 Seismometer

($\Delta t = -1.0$ sec, 20/18 DB, 0.033, F5, Vertical)

Figure 4. Local microearthquake swarm, recorded on April 18, 1977, 00:24-23:02 U.T., within a few hundred meters of the Ukinrek Maars. Kinematics PS-1A Recorder, Ranger SS-1 Vertical Seismometer.

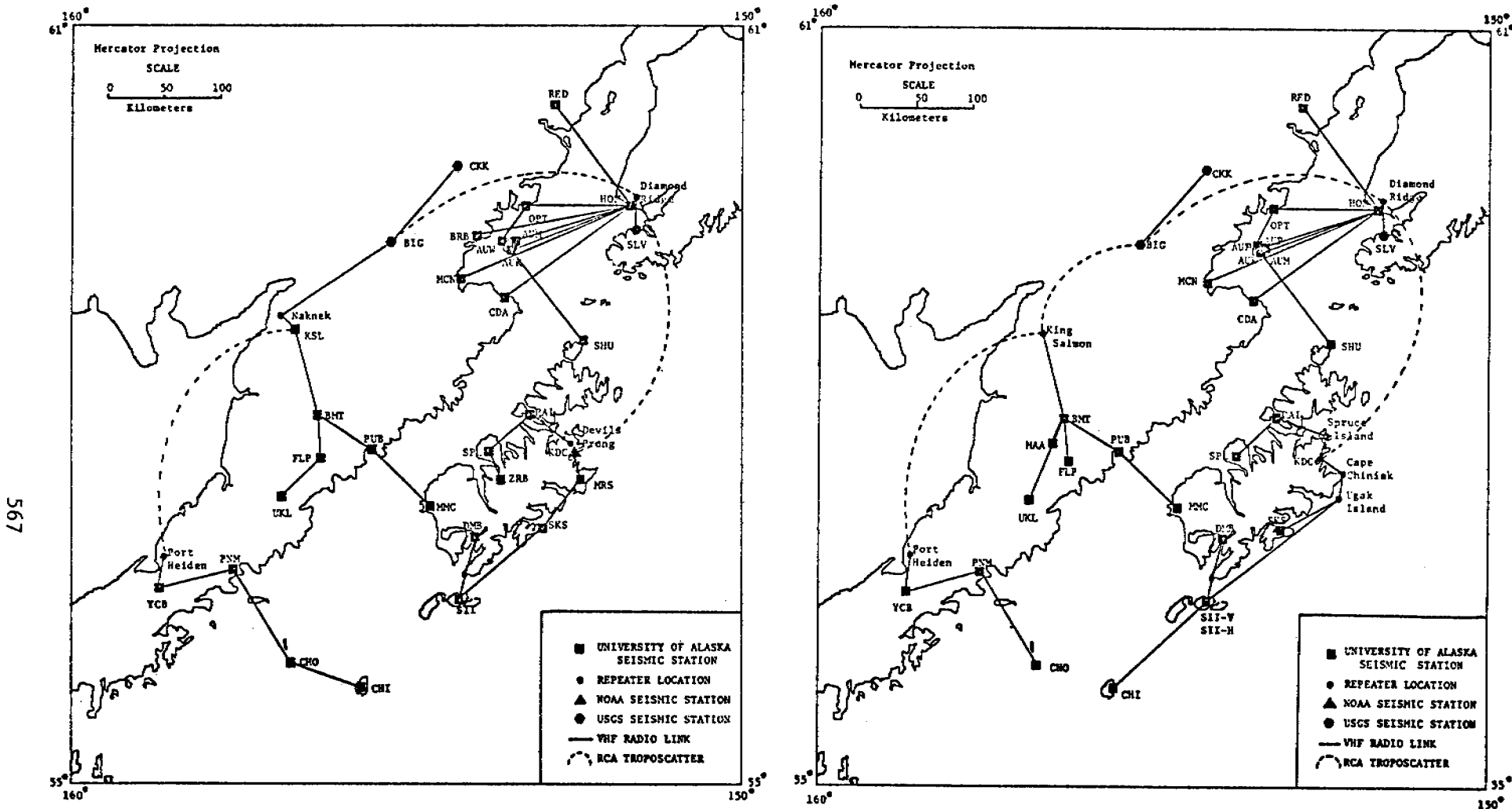


Figure 5. Alaska Peninsula seismic array prior to the late May modification (a) and following it (b).

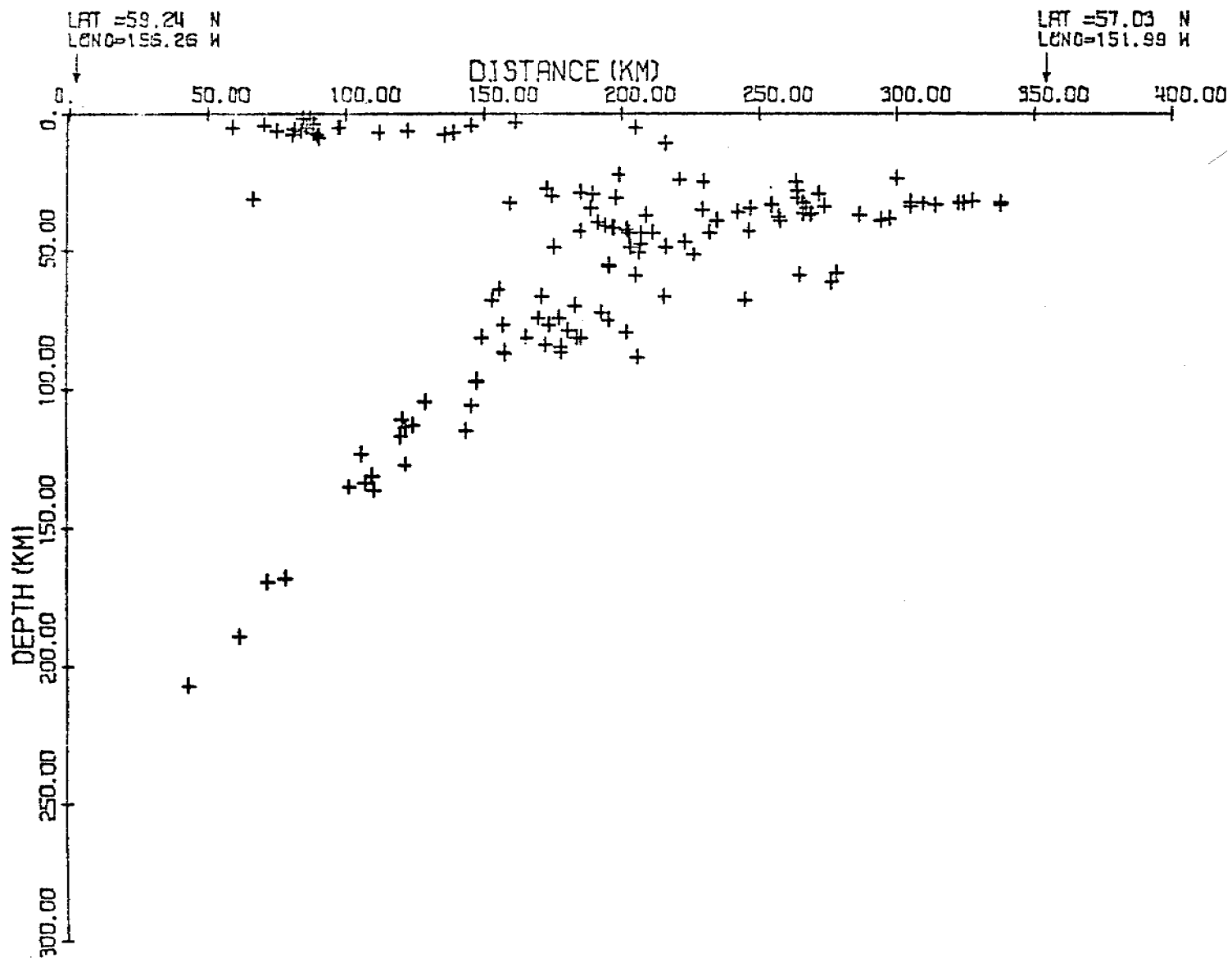


Figure 6. Benioff zone in the Upper Alaska Peninsula-Kodiak region (Estes, 1978), just north of the Ukinrek Maars.

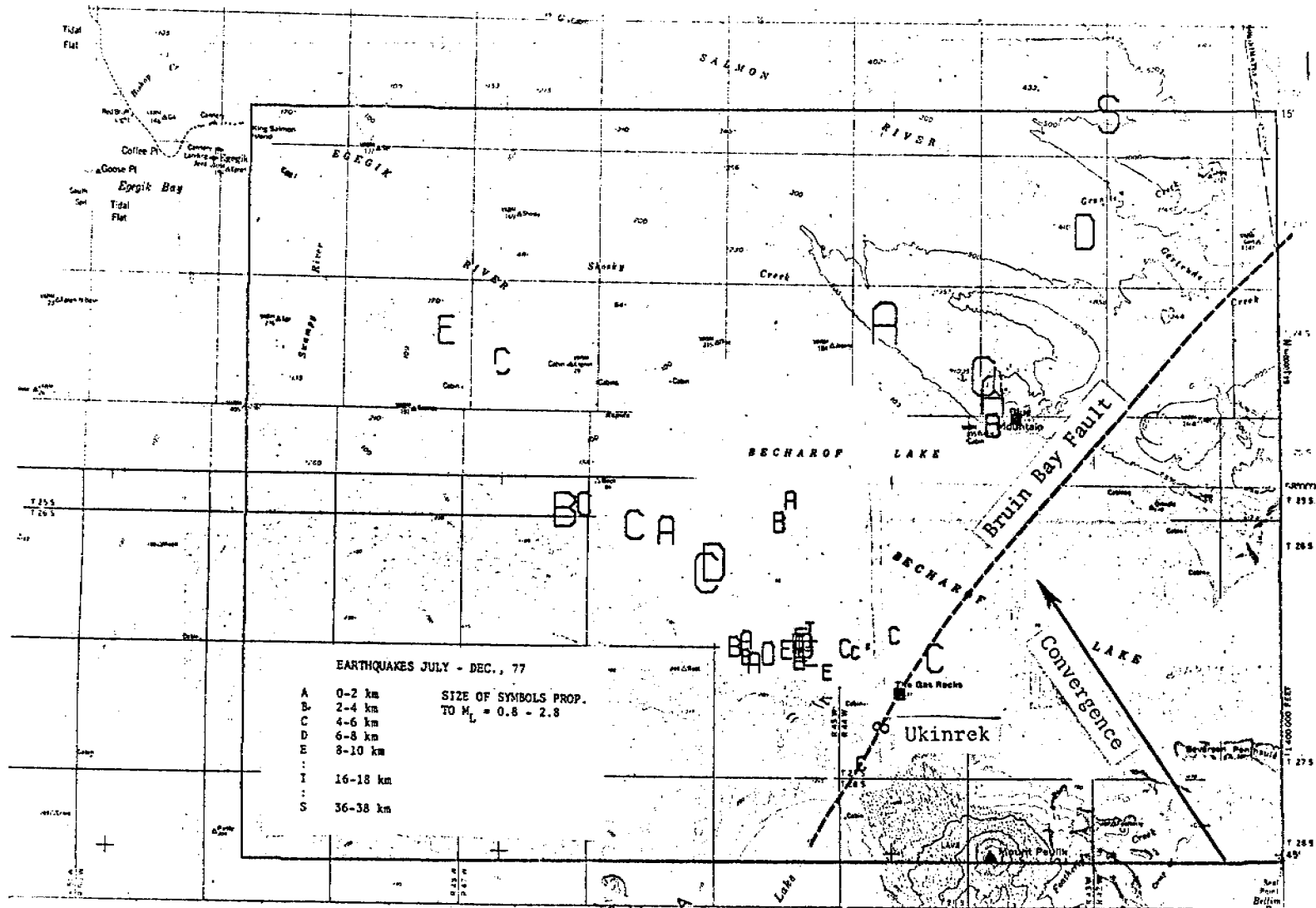


Figure 7. Epicenter map corresponding to the July-December, 1977, portion of the data listed in Table 1. Depths are letter coded; size of symbols proportional to $M_L = 0.8-2.8$. Solid squares denote seismic stations at the Gas Rocks (MAA) and Blue Mountain (BMT). Solid triangle marks Peulik Volcano. Dashed line represents the Bruin Bay fault. Two open circles on the fault trace SW of the Gas Rocks mark the Ukinrek Maars. Arrow indicates the direction of plate convergence after Minster et al., 1974.

ANNUAL REPORT

Contract Number: 03-5-022-55
Research Unit Numbers: 253, 255, 256
OCSEAP Task Numbers: D8 and D9
Reporting Period: April 1, 1977 to
March 31, 1978

SUBSEA PERMAFROST:
PROBING, THERMAL REGIME AND DATA ANALYSIS

T. E. Osterkamp
W. D. Harrison

Geophysical Institute
University of Alaska
Fairbanks, Alaska 99701

March 31, 1978

TABLE OF CONTENTS

- I. SUMMARY OF OBJECTIVES, CONCLUSIONS AND IMPLICATIONS
- II. INTRODUCTION
 - A. General Nature and Scope of Study
 - B. Specific Objectives
 - C. Relevance to Problems of Petroleum Development
- III. CURRENT STATE OF KNOWLEDGE
- IV. STUDY AREA
- V. METHODS AND RATIONALE OF DATA COLLECTION
- VI. and
- VII. RESULTS AND DISCUSSION
- VIII. CONCLUSIONS
- IX. NEEDS FOR FURTHER STUDY
- X. SUMMARY OF FOURTH QUARTER OPERATIONS
- APPENDIX I Near Shore Steady State Temperature
- APPENDIX II Borehole Temperature Data, 1977
- REFERENCES

I. SUMMARY OF OBJECTIVES, CONCLUSIONS AND IMPLICATIONS WITH RESPECT TO OCS DEVELOPMENT

The objectives of this study are to determine the distribution and properties of subsea permafrost in Alaskan waters, in cooperation with other OCSEAP investigators. Besides direct measurements, our program includes an effort to understand the basic physical processes responsible for the subsea regime, as a basis for predictive models.

Work has been carried out in both the Chukchi and Beaufort Seas, and the conclusions are stated separately for each:

A. Chukchi Sea

Observations from 2 boreholes in Kotzebue Sound, one at Rabbit Creek about 3 km north of Cape Krusenstern, and one near NARL, Barrow give direct evidence of permafrost in near shore areas, and in some cases, of ice at depth and shoreline recession. In a broad sense these observations are what is expected from the onshore data, especially the sea level history and shoreline retreat rates, from thermal models, and from onshore boreholes. The question of the larger scale distribution of permafrost beneath the rest of the Chukchi Sea remains open. Existing indirect data and theory indicate it may now be absent from the deeper regions of the proposed Hope Basin lease sale area, although it may exist in regions shallower than 15-30 m.

Water of salinity considerably less than sea water is known to be evident in Kotzebue Sound at times of high Noatak River stage; our observations show that it is also evident off Kotzebue village in late winter, under the ice, when the stage is low.

B. Beaufort Sea

1. Elson Lagoon

Five holes jetted into the sea bed in fine-grained sediment near Tekegakrok Point in Elson Lagoon span the transition from cold, shallow near shore conditions to warmer, deeper conditions where normal sea water salinity is maintained under the sea ice. The presence of ice-bonded, ice-unbonded boundaries in two of the holes, and the temperatures in all of them (which are negative), are the result of rapid shoreline retreat. Interstitial water salinity in at least three of the holes seems to be much greater than that of normal sea water. Permeability values obtained from one hole are 2 or 3 orders of magnitude less than at Prudhoe Bay, indicating that the physical processes that control the evolution of subsea permafrost are probably quite different at the two locations. Thus the physical bases of predictive models, only partially developed so far, are likewise different.

The observations in one of these holes suggest that docks, causeways or islands constructed from local fill material would likely become ice-bonded to 3 or 4 m during the first winter, and therefore resistant to ice forces, although some thawing would of course take place again the following summer. But the high brine concentrations under the ice-bonded layer, which are probably concentrated during the freezing process, will severely reduce the rate of freezing unless some provision is made for their removal.

2. Harrison Bay

Fine-grained sediments were found in Harrison Bay in a hole south of Thetis Island, and sands and gravels offshore SW of Oliktok. A tentative conclusion is that the sands and gravels characteristic of Prudhoe Bay extend at least as far as the Oliktok hole.

3. Prudhoe Bay

Extrapolation of temperature data from 2 more holes along the USGS-CRREL-UA study line, at distances 1252 and 2114 m from shore, suggests that ice-bonded permafrost lies at roughly 30 and 40 m respectively.

II. INTRODUCTION

A. General Nature and Scope of Study

This work is part of a study of the distribution and properties of permafrost beneath the seas adjacent to Alaska. The study involves coordination of the efforts of a number of investigators (RU 204, 271, 253, 255, 256, 473, 102, 407) and synthesis of the results.

B. Specific Objectives

The specific objectives of our particular project are:

1. To investigate the properties and distribution of subsea permafrost at Prudhoe Bay through a drilling, jetting, and probing program and associated interpretation and laboratory analysis.
2. To investigate boundary conditions at the sea bed relevant to the subsea permafrost regime.
3. To study heat and salt transport processes in subsea permafrost, in order to develop models to describe and predict properties and distribution. This work is supported by National Science Foundation although a description of its status and some preliminary results are given here.
4. To extend the area of subsea permafrost field study using simple probing techniques to determine temperature, depth to any ice-bonded boundary, and possibly other quantities.

C. Relevance to Problems of Petroleum Development

(Much of this section was prepared in cooperation with other research units on subsea permafrost.)

Experience obtained in the terrestrial environment has indicated the necessity for careful consideration of permafrost during development activities. Both the National Academy of Sciences review of subsea permafrost problems and Canadian studies suggest that the consequences of errors in planning or design of facilities are potentially greater offshore than on land in terms of loss of human life, environmental damage, and costs.

The primary problem in any new activity in this environment will be lack of data on:

1. The horizontal and vertical distribution of subsea permafrost and the properties of this complex material.

The importance of this information is indicated below in relation to various development activities. This is based on a compilation of data from several sources (Hunter and others, 1976; Osterkamp and Harrison, 1976A; 1976B; OCSEAP reports of Chamberlain and others, 1977 (RI 105) and the National Academy of Sciences Report 1976).

2. Differential thaw subsidence and reduced bearing strength due to thawing of ice rich permafrost.

- (a) Thaw subsidence around well bores causing high down-drag loads on the well casing.
- (b) Differential settlement associated with hot pipelines, silos in the sea bed, and pile and gravity structures causing instability.
- (c) Differential strain across the phase boundary between bonded and unbonded permafrost.

3. Frost Heaving

- (a) Well bore casing collapse due to freeze-back.
- (b) Pipelines - differential movement.
- (c) Gravity structures - local heaving causing foundation instability.
- (d) Pile structures - differential stress in pile founded structures.
- (e) Silos - differential stress on structure.

4. Seismic data interpretation - Data can be misinterpreted and can lead to improper design of offshore production and distribution facilities.

5. Excavation - (dredging - tunneling - trenching)

- (a) Increased strength of material associated with bonded sediment.
- (b) Over-consolidated sediment can influence excavation rates and approach.
- (c) Thaw can be induced in deeper sediment by removal of material at the sea bed.

- (d) Highly concentrated and mobile brines can be found in the bonded sediment.
- (e) Insufficient data on engineering properties for design of excavation equipment and facilities.

6. Gas hydrates

- (a) Blowouts - can result from gas hydrate decomposition during drilling operations.
- (b) Fire danger.

7. Corrosion - Fluids (brines) with concentrations several times normal sea water are common in shallow water (< 3m).

To develop proper precaution against these potential problems, we must obviously develop a better understanding of the horizontal and vertical distribution of subsea permafrost and the processes that control this distribution. This is no easy task in view of the $>2 \times 10^3$ km coast-line subject to potential subsea permafrost problems. It should be emphasized that drilling data exist only near Barrow and Prudhoe Bay in the Beaufort Sea of Alaska and that extrapolations to other areas must be highly speculative.

The exact precautions to take in preventing the above problems (2-7) cannot be specified at present due to a lack of data and the obvious site specific nature of these problems. However, precautions will probably involve:

- (1) An adequate casing seal to drill safely through permafrost.
- (2) A drilling program designed to minimize the thermal disturbance to permafrost and gas hydrates.
- (3) An adequate casing seal to control hydrate decomposition and other high pressure fluids from greater depths.
- (4) Adequate assurance of the structural stability and integrity of silos and other structures.
- (5) Protection against casing collapse should the well be suspended over a season.

For the present the concerns are for the safety of exploratory drilling, but the eventual objective is not only to find, but to produce hydrocarbons. At that stage, permafrost and hydrate conditions will be even more important since hot fluids in the well-bore are unavoidable. Thus, it is very important to maximize the derived

downhole information at the initial stage of exploratory drilling.

Because of the great variability of offshore conditions, extensive preliminary programs will be necessary at each drill site prior to the actual drilling of the well. Without such site specific information it may be difficult to assure a safe drilling program. A partial list of potential accidents is as follows:

- (1) Ruptured well casings
- (2) Ruptured pipelines
- (3) Damage to the drilling structures
- (4) Damage to the production structures
- (5) Casing collapse
- (6) Corrosion and resulting weakening of metals in structures, pipelines, etc.
- (7) Blowouts
- (8) Fires on rigs

These potential accidents could result in the loss of human life, environmental damage and considerable cost to industry in correcting the problems.

III. CURRENT STATE OF KNOWLEDGE

(Much of this section was prepared in cooperation with other research units on subsea permafrost).

Regional details concerning the areal distribution and thickness of permafrost are unknown in the Beaufort Sea, although several local studies have established its existence and local properties (Hunter and others, 1976; Osterkamp and Harrison, 1976A; Lewellen, 1976; Rogers and others, 1975; and the OCSEAP reports of Rogers and Morack, 1976 (RU 271); Chamberlain and others, 1977 (RU 105); Sellmann and others, 1976, (RU 105). These studies have been restricted to three sites in the Beaufort Sea along the $>2.3 \times 10^3$ km coastline from the Bering Straits to the Mackenzie Delta; Elson Lagoon, Prudhoe Bay and the Mackenzie Delta. One borehole also exists in the Chukchi Sea near Barrow (Lachenbruch and others, 1962). Additional studies were performed during the 1977 field season, in Harrison Bay and in the Chukchi Sea near Kotzebue and Barrow. Even though the sites cover a very limited area they are situated in distinctly different geological settings. The Canadian study area off the Mackenzie Delta and the sites in Kotzebue Sound are situated in an area exposed to year around river discharge. The Alaskan Beaufort Sea sites are

distinctly different, with the Barrow area having primarily fine-grained sediments while the Prudhoe Bay area is predominantly coarse-grained material. These contrasts in grain size alone should have a dramatic influence on the distribution of bonded and unbonded permafrost. These differences in material types are anticipated to be somewhat representative of the conditions found along the Beaufort Sea Coast. The Barrow sediments are similar to those between Barrow and the Colville River, while the Prudhoe Bay site would be more like the sediment types found to the east of the Colville River.

Some data are available from direct observations that can help establish some ideas of subsea permafrost limits. The data from the drilling programs supported by NOAA at Prudhoe Bay and the Navy program at Barrow indicate that permafrost (as defined by temperatures colder than 0°C throughout the year) is present in every hole from near the sea bed to depths at least as great as 80 meters, which is the maximum depth of the exploratory holes. However, seismic data indicate the absence of continuous ice bonding in some of these holes (Rogers and others, 1975). One additional industry hole at Prudhoe Bay on Reindeer Island suggests bonded permafrost exists in two zones from 0 to 20 m and 90 to 125 m from the surface, although this hole was never thermally logged. Borehole temperature data available prior to 1977 are given by Lewellen, 1976; Osterkamp and Harrison, 1976, 1977; Lackenbruch and Marshall, 1977; OCSEAP reports of Sellmann and others, 1976. These data indicate permafrost is present 17 km from shore as seen in hole PB-2 at Prudhoe Bay and 11 km at Barrow at B-2.

Considerable data on the extent and distribution of subsea permafrost have been obtained by Canadian government and industry studies in the Mackenzie River region. Drilling and thermal data have confirmed the presence of permafrost, and information on the upper limit of the bonded permafrost was obtained based on a study of industry seismic investigations (Hunter, et al., 1976). Additional information concerning ice-bearing permafrost can be inferred from the thermal data shown earlier. Most of these records have negative thermal gradients, a suggestion of ice-bearing permafrost at depth.

The studies conducted by Osterkamp and Harrison (1976A) and by Sellman and others (OCSEAP reports) near Prudhoe Bay across the land/sea transition established the depth to bonded permafrost along this single line in some detail out to the 2 meter water depth and less detail beyond. These studies, and those of Lewellen (1973) near Barrow, indicate that bonded permafrost is found at a shallow depth beneath the seabed in 2 m of water or less, where the sea ice annually freezes to the sea bed. There is also considerable evidence for a seasonally active layer beneath the sea bed in this region. From Pt. Barrow to Herschel Island the area from the beach to the 2 m water depth is about 3400 km². In this zone the limited data from the two study sites indicate that bonded permafrost will be near the surface, probably within 20 meters. This may not apply to areas near major deltas where the environment is anticipated to be modified by warmer waters during periods of discharge.

Permafrost distribution in areas other than the shallow water environments is implied from results of the drilling and seismic efforts mentioned above as well as from negative bottom water temperatures which would suggest permafrost can exist on most of the Beaufort Sea shelf (Lewellen, 1973).

Recent seismic studies (RU 271) have shown that the top of the ice-bonded permafrost may be quite variable with relief of several tens of meters over short distances and may be near the sea bed at sites far offshore.

Thawing at the sea bed in the presence of negative sea bed temperature has been found by Lewellen (1973) and Osterkamp and Harrison (1976A). This has been attributed to the infiltration of salts into the sea bed. The distribution of these salts in the thawed sediments has been determined by Osterkamp and Harrison (1976A) (RU 253) and by CRREL (RU 105).

Preliminary study of seismic, sea bed temperatures and other data imply that bonded subsea permafrost is probably absent in most of the southern Chukchi Sea in the deeper waters although it may still survive in shallow nearshore waters (OCSEAP 1976 fourth quarterly report of Harrison, Dalley and Osterkamp, 1976 (RU 253, 255, 256)).

IV STUDY AREA

The main study areas have been in the Beaufort Sea at Prudhoe Bay and Elson Lagoon. We have done some work in the Chukchi Sea near Kotzebue and at NARL and in the Beaufort Sea at Harrison Bay. We plan to carry out additional studies at NARL, Elson Lagoon and Prudhoe Bay this spring. The work at Prudhoe Bay will attempt at least one hole farther offshore in about 20 m of water. We also plan a reconnaissance study of at least one offshore island this summer.

V. METHODS AND RATIONALE OF DATA COLLECTION

The basic approach is to make direct observations of subsea soil conditions in holes made with light-weight driving or jetting equipment. The technique does not permit the acquisition of the detailed data that can be obtained with a drill rig, particularly since soil samples are not taken, but it does have the advantages of speed and lightweight. Thus, data can be obtained rapidly and cheaply over a wide area. In the driving technique a portable motorized cathead and tripod set, together with a 64 kg drop hammer, are used to drive EW drill rod into the sea bed. The depth capability depends upon soil type and is optimum for the relatively coarse conditions typical of Prudhoe Bay. There we have achieved a depth of 26 m, which was determined by our available supply of drill rod. In the jetting technique 3/4 inch steel water pipe is jetted into the sea bed using a small water pump and the water from beneath the sea ice. The depth capability depends on soil type and is optimum for the fine-grained soil conditions found at Barrow. There we have achieved a depth of 27 m. The type of data that can be obtained with the driving and jetting techniques is briefly described in the following paragraphs.

Soil Conditions: Some information about soil conditions can be obtained with the driving technique from the blow count data (number of hammer blows to drive the drill rod 0.3 m). Similar information can be obtained from the jetting technique from the drilling rate and "feel" of the string of pipe. Both techniques can detect the presence of firmly ice-bonded soil. With the jetting technique a direct identification of soil type can be made when the cuttings are brought to the sea ice surface. This occurs in shallow water when the sea ice is frozen to the sea bed.

Temperature: Both techniques are well suited to provide access for temperature measurements. In the jetting technique the pipe is left in the hole. To prevent freezing, the pipe is normally run with a check valve at the bottom, and upon hole completion a non-freezing fluid is pumped through it. In the driving technique temperatures are measured inside the drill rod, which is left in place until the temperature measurements are completed. The undisturbed or "equilibrium" temperatures can be accurately estimated after about two days, but for logistics reasons we had to remove the drill rod after 24 hours or so. Some of the resulting problems are discussed later. Temperature was logged inside the pipe or drill rod with a single thermistor. Some problems were encountered with this unit that resulted in a calibration change of about 0.7°C over the field season. Various calibrations permitted most of the change to be accounted for in most but not all cases, and the estimated accuracy is given in the next section. The approach to temperature equilibrium was analyzed as discussed by Osterkamp and Harrison (1976A). The depths on the figures are measured from the sea bed.

Soil Interstitial Water Salinity: Techniques for determining the interstitial water salinity using the driving equipment are under development with NSF support. The water is admitted into plastic tubing run inside the drill rod through a porous metal filter at the bottom. Several

parallel approaches for determining the salinity are under development; these include direct sampling, which has yielded usable data, measurement of electrical conductivity using a cell installed in the bottom of the drill pipe, or a miniature dip type cell run in from the surface. Salinity is as important as temperature in determining presence or absence of ice, and in giving clues to the past history of the subsea soil.

Hydraulic Conductivity: The soil hydraulic conductivity (essentially the permeability) is calculated from the rate at which water from the soil enters the filter, which is determined with a water level sensor. The exact calculation is extremely difficult for some of the geometrically complicated shielded filters that we have used, but we have been able to derive a simple and reasonably accurate approximate method. The hydraulic conductivity has an important effect on the evolution of subsea permafrost.

VI. and VII. RESULTS AND DISCUSSION

A. Chukchi Sea

Although the observations in our holes are the first direct studies of subsea permafrost in the Chukchi Sea outside the Barrow area, other relevant data have been obtained or summarized by Hopkins (1976, 1977) in a coordinated project. Also, the important interaction between onshore and offshore thermal conditions has long been recognized (Lachenbruch, 1957). Our measurements, which apply to near shore areas, are discussed in the context of this existing knowledge. The more global aspects of subsea permafrost distribution in the Chukchi Sea, which we have summarized earlier, are briefly reviewed in a later section.

Although no detailed analysis of the temperature data obtained in our holes is given in the following discussion, the question of whether they can represent equilibrium conditions is considered. To do so it is necessary to take account of the effect of the nearby cold land. This is discussed in Appendix I, where it is shown that the effect of land is significant unless the distance offshore is much greater than a distance L equal to $\frac{\Delta T}{g}$, where ΔT is the difference between sea bed and emergent land temperatures, and g is the geothermal gradient. L is typically on the order of 50 to 150 m. It can also be shown that permafrost, defined by the position of the 0°C isotherm, can exist up to a distance L from shore under positive sea bed temperatures and steady state conditions (Lachenbruch, 1957, and Appendix I).

1. Rabbit Creek

Temperature and blow count data were obtained from a driven hole 75 m offshore near Rabbit Creek, about 36 km north of Cape Krusenstern (Table 1, Figures 1, 2, and 3, Appendix II). Sea bed temperature and depth were also measured in the vicinity. (Figure 4 and Table 2). The site is located between two regions whose onshore surficial geology is described (AEIDC, 1975) as "(1) hard crystalline bedrock overlain with a blanket of frozen silt, sand and gravel 10 to 150 feet thick, and (2) frozen silt, sand and gravel that is more than 150 feet thick". Evidently the sediment thickness is essentially unknown. It evidently contains some coarse-grained material, because an initial attempt to jet this hole was abandoned when the jet was stopped by what appeared to be coarse gravel at about 1 m depth. High blow counts may indicate the presence of ice, as discussed below. According to Hopkins (1976, 1977), the shoreline has retreated something like 0.5 km in the last 3,500 years, and a 2 m retreat was noted during a 1975 storm surge.

The temperature distribution above about 10 m is dominated by seasonal effects. Usually temperature is observed to vary linearly with depth below 10 or 15 m, but this hole shows a pronounced curvature just above 15 m which is probably a larger effect than our errors in estimating the temperature disturbance due to the borehole. The curvature may be due to the presence of ice at this depth, as for example in a hole 481 m from shore at Prudhoe Bay (Osterkamp and Harrison, 1976a). But if this is so, it is a rather different situation from the Prudhoe Bay example, since the blow count data do not indicate a sharp ice-bonded boundary. The blow counts do increase strongly in the vicinity of the temperature curvature, but they decrease deeper and the sediments there cannot be firmly ice-bonded. At the present state of our analysis, the possibility

TABLE 1
CHUKCHI SEA HOLES

HOLE LOCATION	DISTANCE FROM SHORE	DRILLING METHOD	TIME OF DRILLING	DEPTH REACHED BELOW SEA BED	WATER DEPTH	SEA ICE THICKNESS	TEMPERATURE UNDER ICE	DATA OBTAINED
Rabbit Creek	75 m	driving	April 26, 1977 ~09:00-14:00	18 m	4.0 m	1.2 m	-1.88	temperature blow count
Kotzebue	310	jetting	April 28 15:30-17:30	25	1.8	~1.2	-0.94	temperature
Cape Blossom	~300	jetting	April 27 ~16:00	10	1.37	1.07	-1.78	temperature
NARL	705	jetting	May 15	16	6.57	1.63	-1.80	temperature

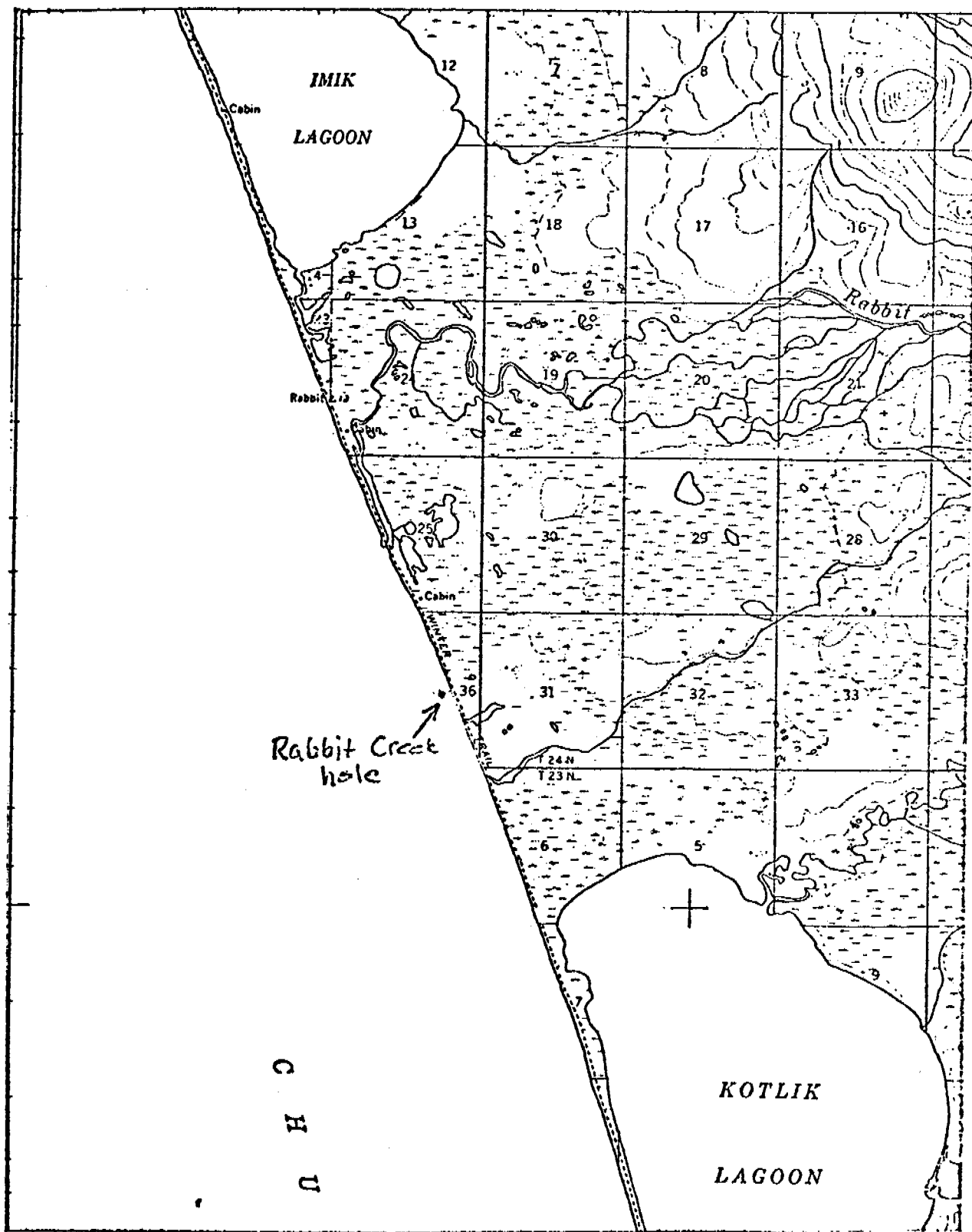


FIGURE 1. Location of Rabbit Creek hole, as determined by tape, Brunton compass, and nearby distinctive features. Distance from shore is 75 m. Map USGS 1:63,360 Noatak (B-4), Alaska.

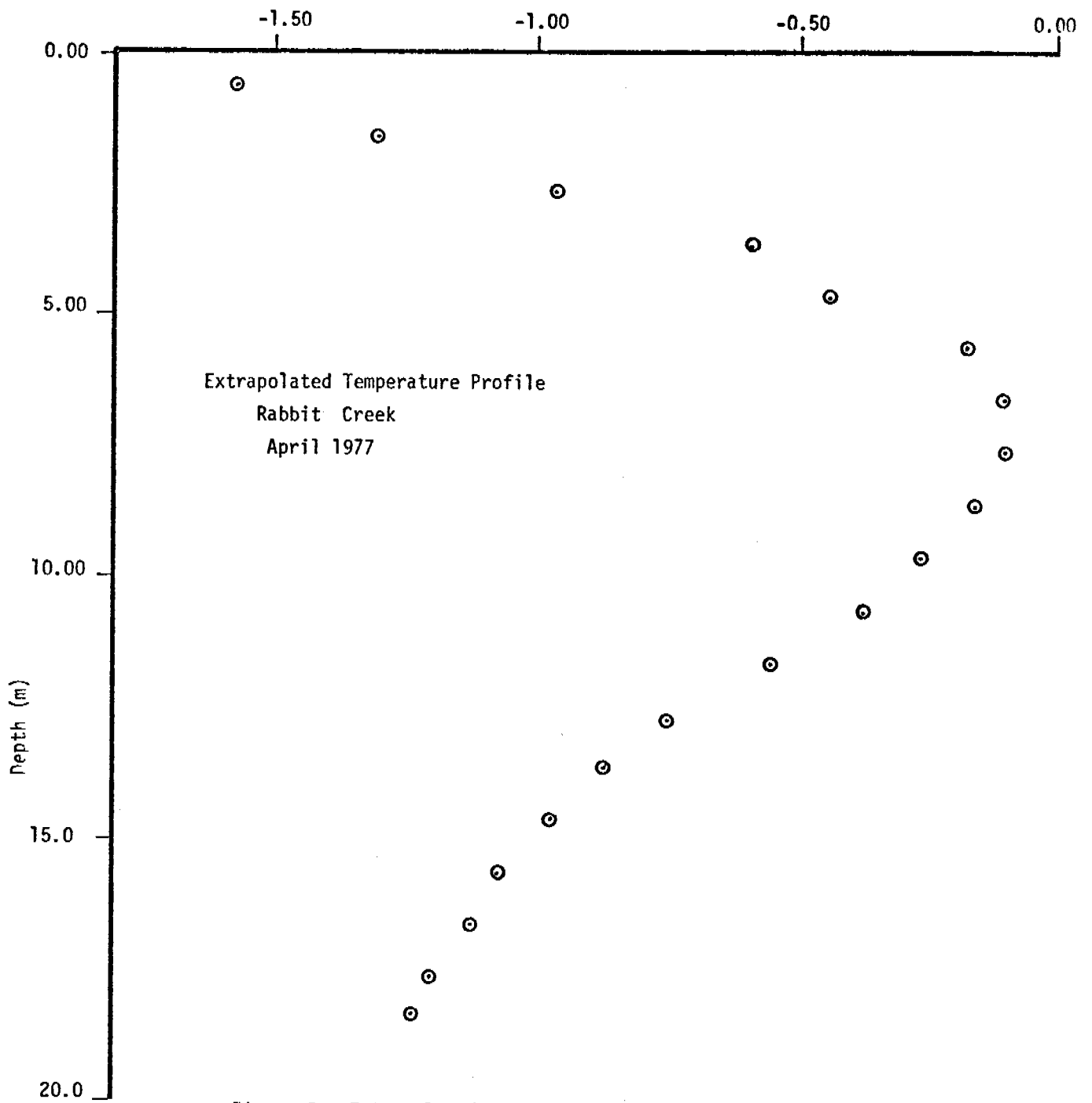


Figure 2: Extrapolated temperature profile for Rabbit Creek hole 75

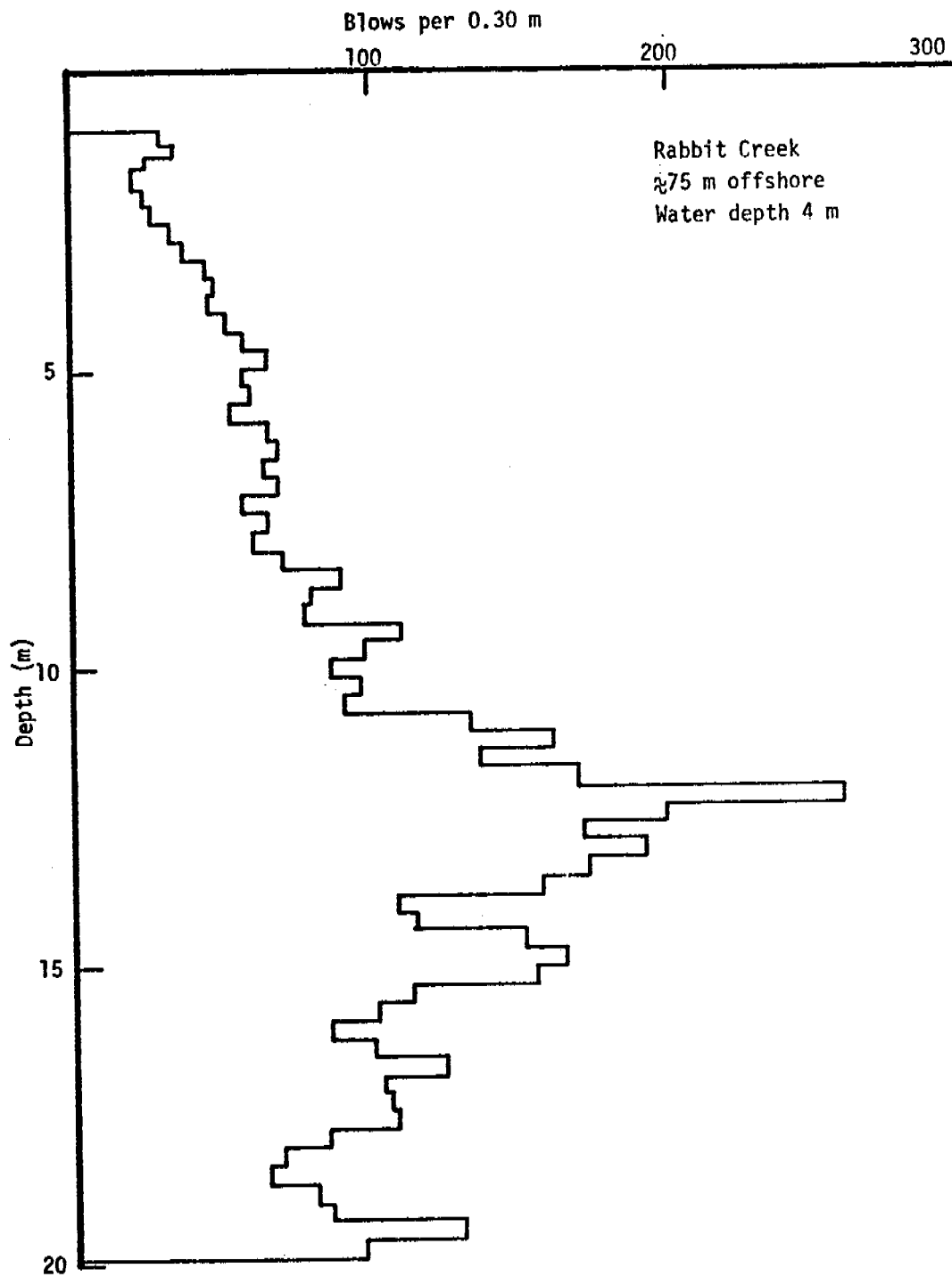
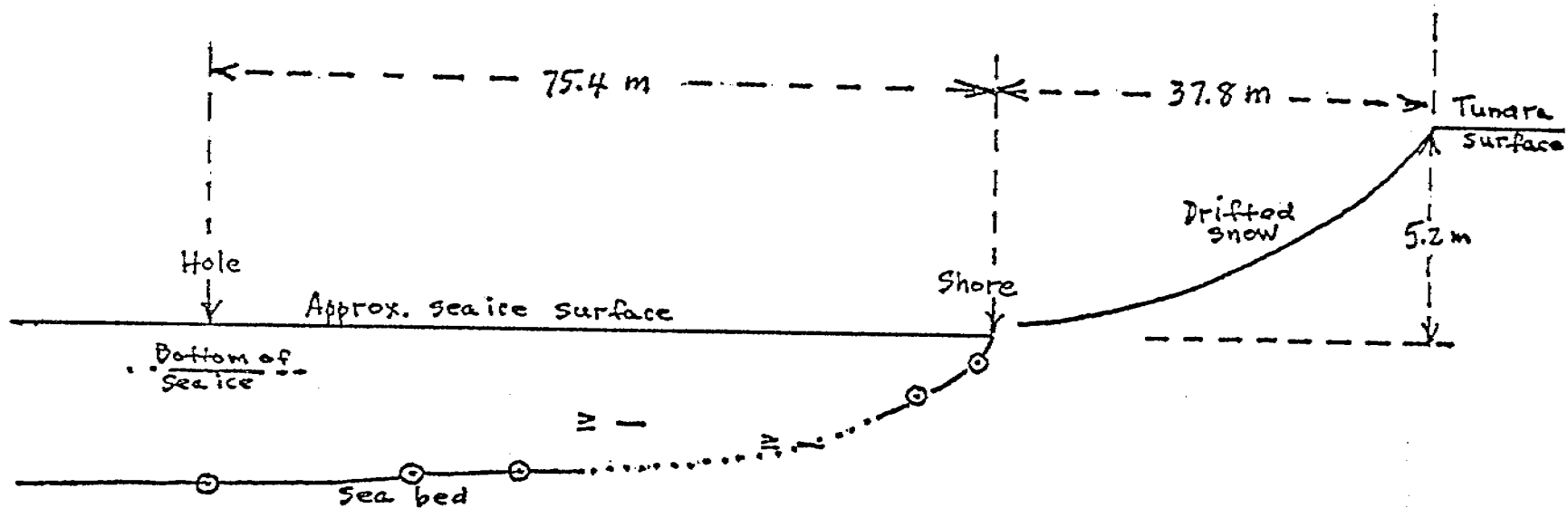


Figure 3: Blow count profile for Rabbit Creek hole 75



587

FIGURE 4. Sea bed, sea ice, and land surfaces near Rabbit Creek hole, with 4 to 1 vertical exaggeration. The sea ice top and bottom surfaces were rough except in the vicinity of the hole. Two water depth measurements, indicated \geq , are minimum values because the ice was rafted in several layers and it was uncertain whether bottom had been reached.

TABLE 2

WATER DEPTH AND TEMPERATURES UNDER SEA ICE NEAR
RABBIT CREEK HOLE, APRIL 26, 1977

DISTANCE FROM SHORE (m)	WATER DEPTH (m)	TEMPERATURE UNDER ICE (°C)
0	0	
1.0	0.6	-2.368
6.4	1.4	-1.877
17.4	≥2.6	-1.880
35.4	≥2.2	-1.890
45.4	3.5	-1.880
55.4	3.8	
75.4	4.0	≈-1.88, 0.34 m above the
125.4	4.4	sea bed in the
175.4	4.8	drill pipe
225.4	4.8	
415.4	6.3	

that the curvature is due to a drastic change in soil type or an anomalously warm sea bed temperature over the past few years cannot be excluded. The first possibility would require a change in thermal conductivity by a factor of 2 or 3, which seems unlikely, and the second possibility seems unlikely in the light of the discussion below. In either of these cases extrapolation of the deeper data suggests a long-term mean sea bed temperature of roughly -0.1°C . The corresponding estimated mean temperature if ice were present would not be well determined, but would be warmer, perhaps in the vicinity of 0.5°C or more. For comparison the mean sea bed temperature off the mouth of Ogotoruk Creek near Cape Thompson about 120 km to the northwest is about 0.7°C , and near Wales at the Bering Strait it is about 0.9°C (see Lachenbruch and others, 1966). These values are representative of the period just prior to 1960 and may have changed slightly. Evidently the assumption of ice in the Rabbit Creek hole gives a value more in line with these others.

For the discussion of steady state conditions it is necessary to estimate the mean annual ground surface temperature. This varies locally, but a representative value from Cape Thompson, discounting the warming trend of the last century, is about -7.1°C (Lachenbruch and others, 1966). We note that the mean air temperature at Cape Thompson is roughly 1.7°C colder than that at Kotzebue (see AEIDC, 1975), and assume it is roughly 0.9°C colder than at Rabbit Creek, which lies midway between these sites. The mean annual ground surface temperature at Rabbit Creek and Kotzebue would then be about -6.2°C and -5.4°C respectively at times prior to the warming of the last century.

The temperature gradient beneath the level of seasonal variations contains some information about shoreline retreat rate, an important parameter in subsea permafrost models, but the analysis has not yet been carried out. Here we merely show that the observed gradient, roughly -0.06 deg m^{-1} if estimated from the deepest data, and more negative if not, cannot represent an equilibrium situation. If ice is present, and a sea bed temperature of 0.5°C is assumed, the parameter L that defines the influence of land (Appendix I) is 68 m; if no ice were present and 0°C were assumed, $L = 63 \text{ m}$. Since the distance from shore is 75 m, the temperatures are strongly influenced by the complicating effect of land. It was not possible to place the hole farther offshore because of sea ice conditions. The corresponding sea bed temperature gradients estimated by the method of Appendix I, are 0.11 and 0.16 of the geothermal gradient or 0.004 and 0.005 deg m^{-1} respectively. Since the observed value is -0.06 deg m^{-1} (or even more negative), steady state conditions do not exist, even considering the uncertainties involved. The estimate of the steady state temperature distribution at this site is probably better than at some of our others, because the sea bed temperature is rather constant with position here. Except for the point 1 m offshore, the sea bed temperatures are essentially constant with distance offshore at about the freezing point of normal sea water (Table 2).

It is also worth noting that the temperature gradient is so negative that it is likely that ice exists within a few tens of m of the sea bed, whether or not it is present near 10 m.

2. Kotzebue

Temperature data were obtained from a jetted hole about 310 m offshore from the Kotzebue runway (Table 1, Figures 5, 6, and 7, Appendix II), and other data were obtained in the vicinity (Table 3). The surficial geology onshore is shown in Figure 5, which is taken from a draft summary of onshore conditions by Williams and Morris (1974). Onshore conditions in the village roughly 2 km northeast of our hole are known from a 100 m deep well (Cederstrom, 1961, and Figure 6). Our jet stopped abruptly at 25 m; this is about the depth at which gravel was encountered in the onshore well, although it should be noted that depths in it are measured relative to the land surface, which is about 3 or 4 m above the sea bed at our site. It is also noteworthy that some gravel was encountered in our hole between 10 and 15 m, and again in the vicinity of 22 m, and penetrated with difficulty by our jet. As noted previously, the jet works best in fine grained materials. According to Hopkins (personal communication) the coast is prograding at Kotzebue.

Equilibrium temperatures are not well determined in this hole. We were delayed by an airline strike in returning to log the hole again and when we succeeded shortly before breakup, it was blocked. The obvious glitch in the data at 21.5 m was caused by loss of water from the jet into the sediments, and was noticed during drilling. The mean annual sea bed temperature seems to be between 2.5 and 3°C (allowing for the fact that the borehole temperatures have not equilibrated). The gradient is roughly -0.06 deg m^{-1} ; this estimate attempts to allow for the apparently greater disequilibrium in the upper part of the hole. The 0°C isotherm is probably at about 50 m depth.

The comparison with steady state conditions is similar to that at Rabbit Creek. The parameter L that represents the effect of land is 83 m; this should probably be decreased because of the large lake near the shore. Since this is much less than the 310 m distance from shore, the land is not very important, and the resulting steady state gradient is 0.73 of the geothermal gradient (or slightly larger.); this is about 0.023 deg m^{-1} . Comparison with the measured value of -0.06 deg m^{-1} indicates that steady state conditions do not exist. The comparison is not as good as the Rabbit Creek case because, although it has not been studied in detail, the sea bed temperature undoubtedly varies inshore from the hole, where sea ice annually freezes to the sea bed (see Table 3).

3. Kotzebue Sound

Temperatures were measured under the sea ice at a number of points in Kotzebue Sound on lines from Cape Blossom to Cape Espenberg to Cape Krusenstern (Table 4). These temperatures are all close to the freezing temperature of normal sea water and indicate little effect, at least in late winter, of the fresh river water evidenced in our Kotzebue observations by temperatures under the sea ice significantly higher than the freezing temperature of normal sea water (Table 3).

4. Cape Blossom

Temperature data were obtained from a jetted hole about 300 m offshore near Cape Blossom, about 18 km south of Kotzebue. (Table 1, Figures 8 and 9, Appendix II). Onshore at this site there are bluffs of unconsolidated sediment of mixed size, which according to AEIDC (1975) fall into the category of "frozen

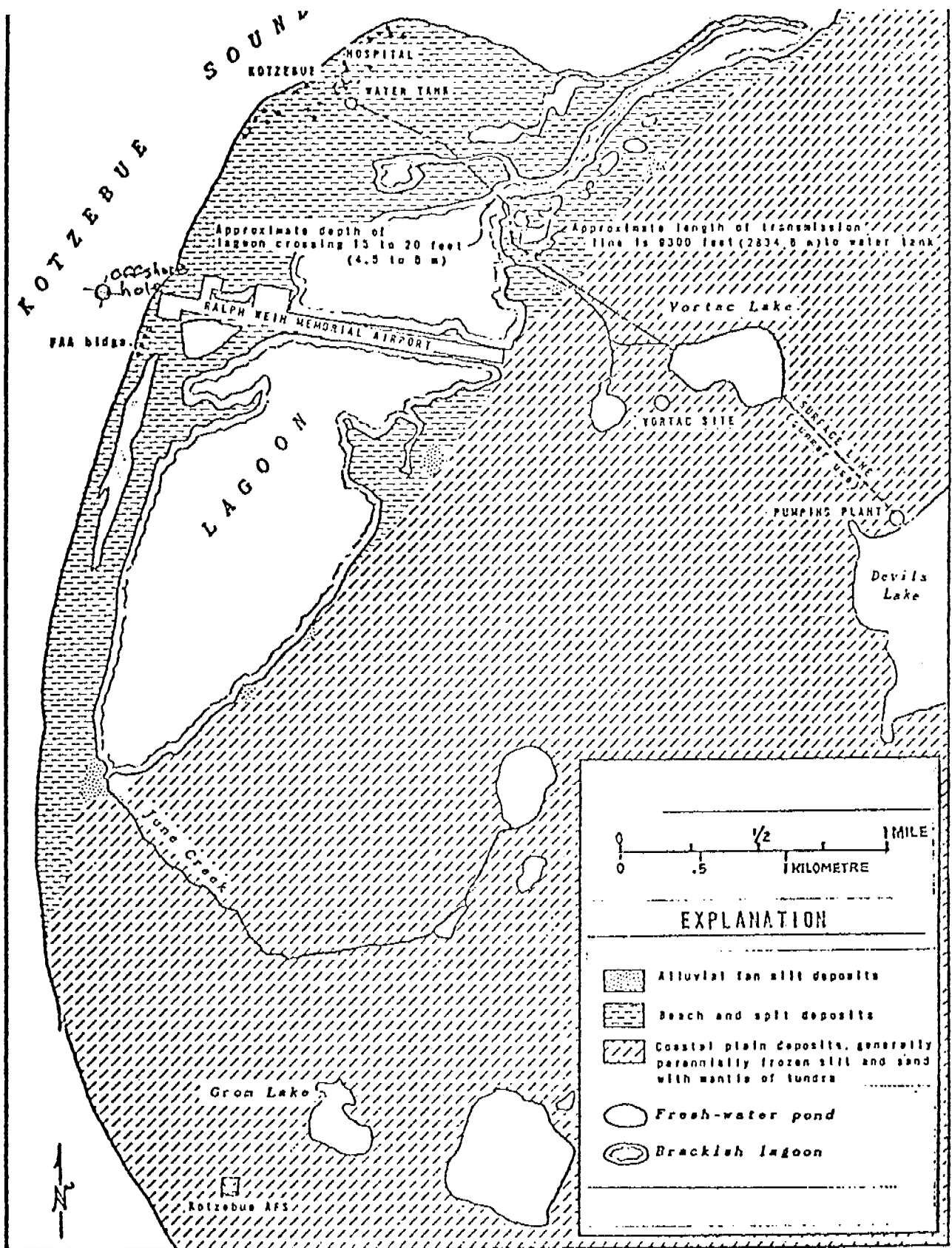
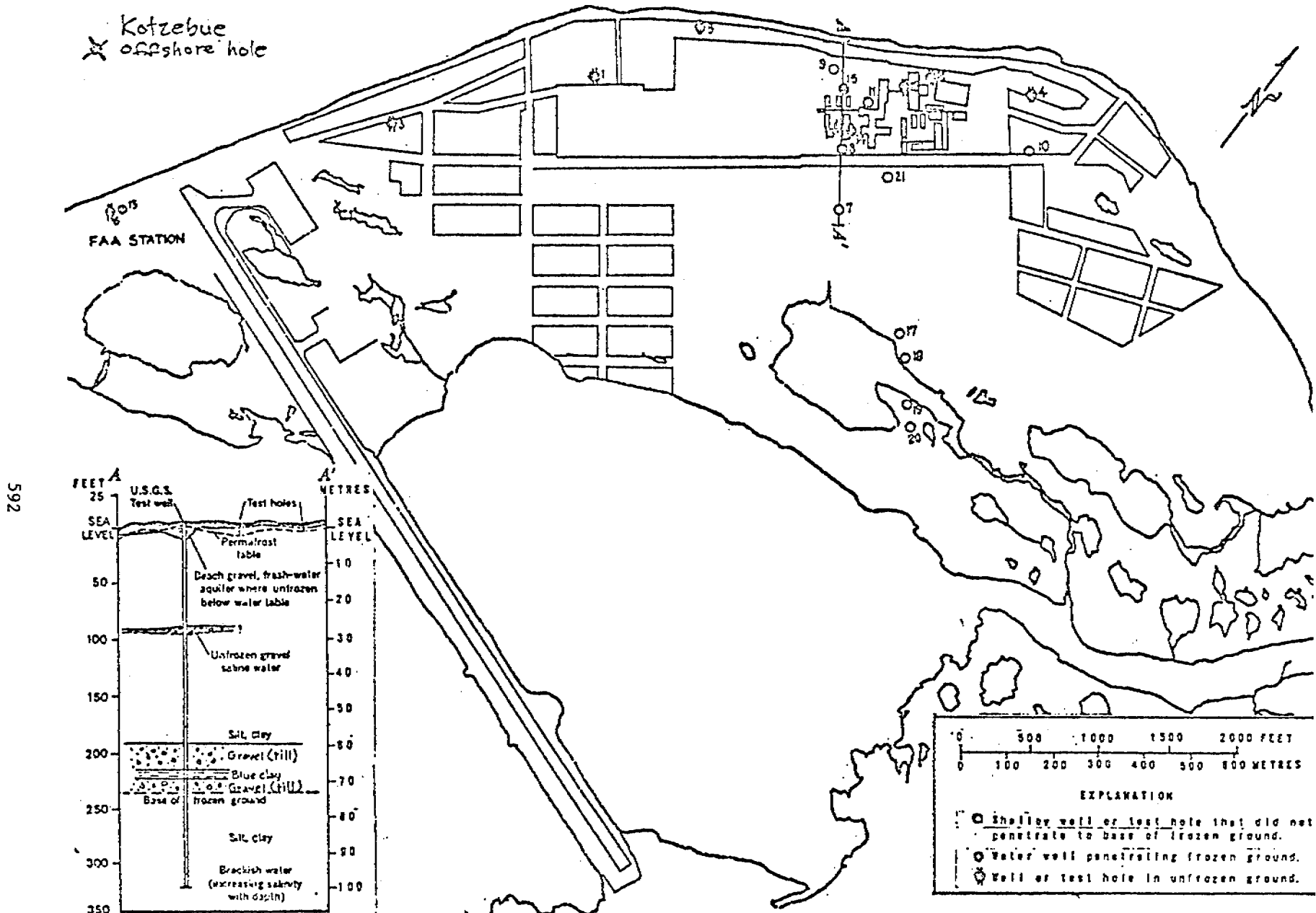


FIGURE 5. Location of Kotzebue offshore hole and surficial geology. The hole is about 310 m from shore, or 372 m from the lights at the end of the runway, and is in line with the runway. Distances were taped.



592

FIGURE 6. Locations of Kotzebue offshore hole (see also Figure 5) and 7 USGS test hole and interpretation (inset).

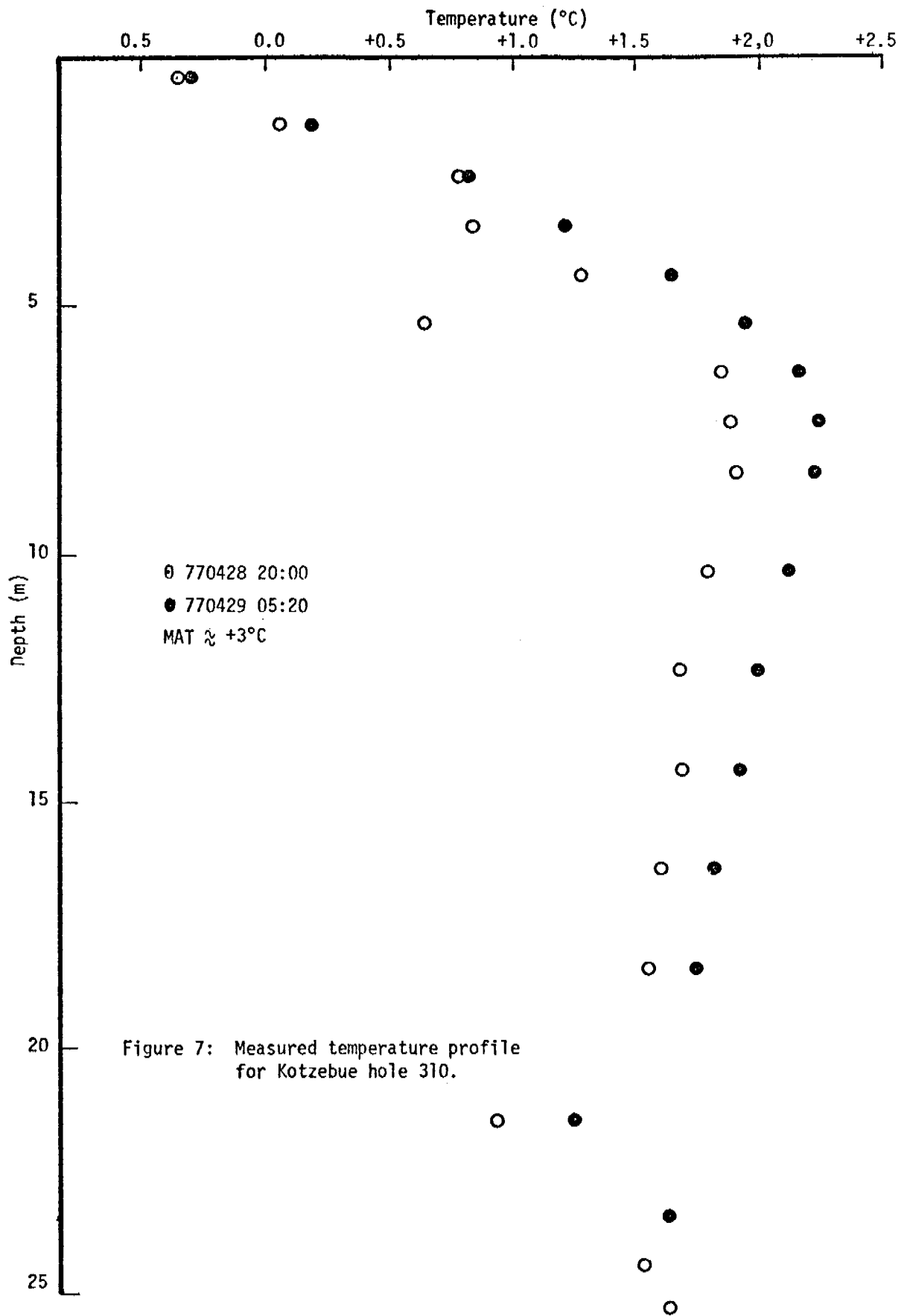


Figure 7: Measured temperature profile for Kotzebue hole 310.

TABLE 3

Water depth, ice thickness, and temperature under the ice on a line between Kotzebue runway and the jetted offshore Kotzebue hole. Distances are paced from the shore, or from the jetted hole 310 m from shore, and are approximate. April 29, 1977.

DISTANCE FROM SHORE	ICE THICKNESS	WATER DEPTH	TEMPERATURE UNDER ICE
150	0.70*		
300	1.45**	1.18	
310	~1.2		
390		6.5	-0.94
450	1.15	6.5	
600	1.00	27	
700	1.00	>20	

* Ice frozen to bottom

** Ice frozen to bottom, but water ran into hole. Ice thickness includes about 0.27 m freeboard.

TABLE 4

Kotzebue Sound - Water temperature at the sea bed

a,b,c - a line from Cape Blossom to Cape Espenberg
 d,e - a line from Cape Espenberg to Cape Krusenstorm
 Roughly equally spaced holes.

WATER DEPTH	THERMISTOR RESISTANCE	TEMPERATURE
(a) 13.7 m	R = 24,274 Ω	-1.785 $^{\circ}\text{C}$
(b) 14	24,321	-1.826 $^{\circ}\text{C}$
(c) 19	24,379	-1.877 $^{\circ}\text{C}$
(d) 2	24,380	-1.878 $^{\circ}\text{C}$
23	24,359	-1.859 $^{\circ}\text{C}$
(e) 14.5	24,333	-1.837 $^{\circ}\text{C}$

* Measurement made just under sea ice.

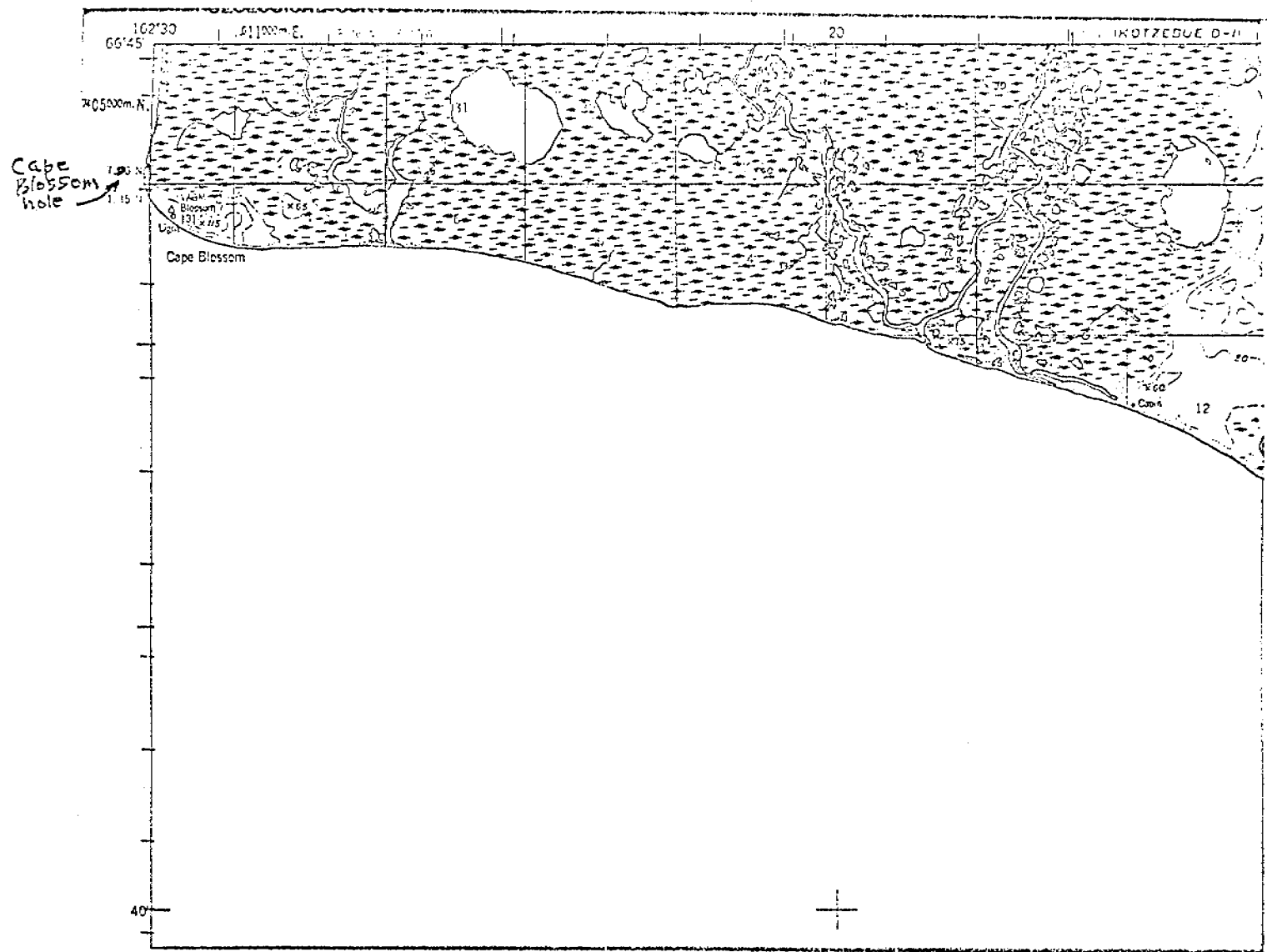


Figure 8. Location of Cape Blossom hole. The hole bears 305° (true) and is 730 ± 20 m distant from Blossom bench mark. The closest land is about 300 m from the hole. Bearings were measured with Brunton compass. Distance to shore was taped and used as a baseline for the determination of the hole-benchmark distance. Map USGS 1:63,360, Kotzebue (C-1), Alaska.

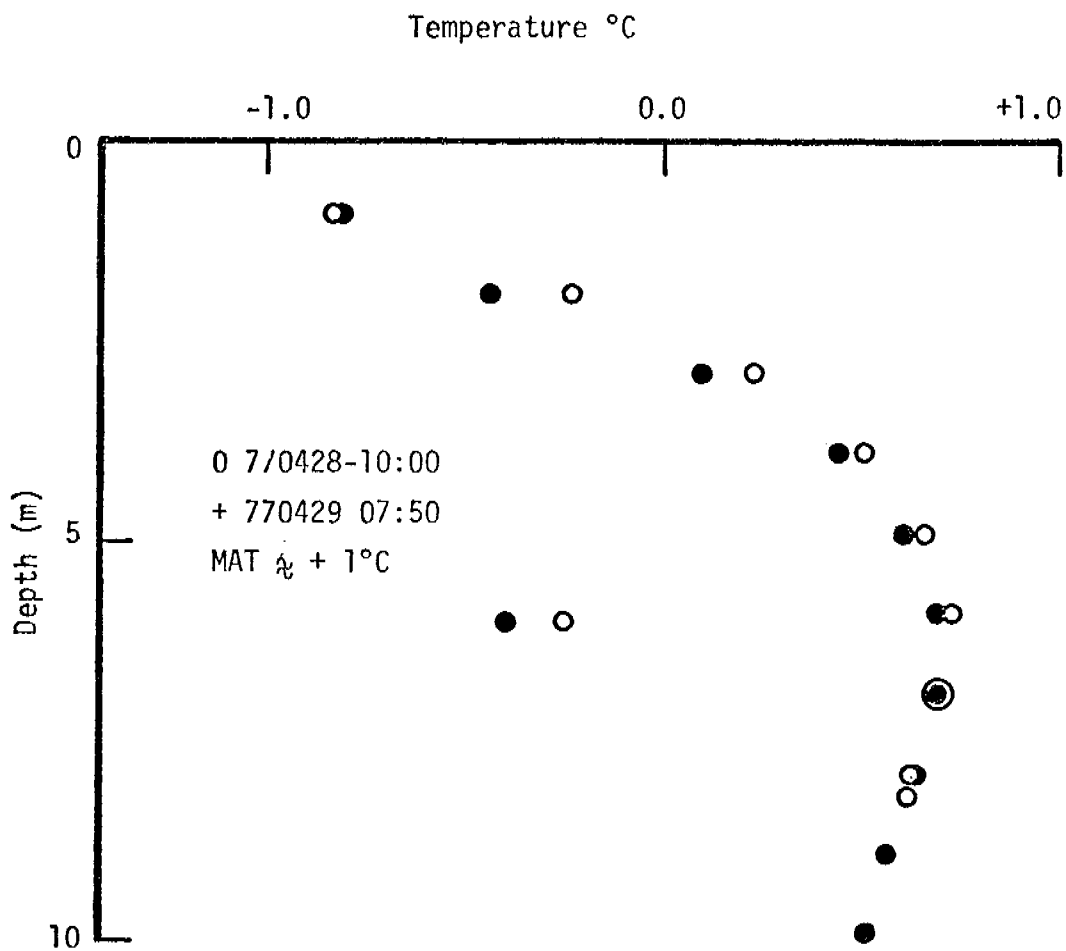


Figure 9: Measured temperature profiles for Cape Blossom hole 300.

silt, sand and gravel that is more than 150 feet thick". Enough gravel was encountered to make jetting inefficient and to prevent a greater depth than 10 m from being reached. The shore line seems to be undergoing rapid retreat (Hopkins, personal communication).

The equilibrium temperatures are not very well determined, except perhaps below 7 or 8 m where the temperature changes on the successive days of logging are small. One feature peculiar to this hole, and evident in Figure 9, is that as the time since drilling increased so did the temperatures above 7 m. We do not understand this behavior, since water at about -1.8°C was used for jetting, which is colder than the sediment. The hole is not deep enough for good estimates of mean annual sea bed temperature and gradient to be made, although values of roughly 1°C or warmer, and -0.06 deg m^{-1} are suggested. The sea bed temperature was -1.78°C at the time of logging.

The parameter L that represents the effect of land is 65 m. Since this is much less than the 300 m from shore, the land is of little importance, and the resulting steady state gradient is 0.78 of the geothermal gradient, or slightly larger because of the 2-dimensionality of the shoreline. This is 0.025 deg m^{-1} , which is to be compared with the estimated value of -0.06 deg m^{-1} above. Evidently the temperature distribution is far from steady state. This is almost certainly true, although it should be noted that as at Kotzebue the sea bed temperature undoubtedly varies in the vicinity of the hole, and is not well known. Hence the steady state gradient is poorly known. The 0°C isotherm is probably at about 20 m depth, and at some greater depth ice is probably present. However, the hole is too shallow for definite conclusions to be drawn.

5. Naval Arctic Research Laboratory

Temperature data were obtained from a jetted hole about 705 m offshore from NARL. (Table 1, Figures 10 and 11, Appendix II). Hard jetting was encountered below 5.5 m and the possibility of some ice bonding, which would be surprising, cannot be excluded. A small curvature in the temperature distribution exists between 10 and 15 m, but unlike the Rabbit Creek case, it may well be due to our errors in estimating the equilibrium temperatures. This is suggested by the data from the last logging, which do not show this effect. The mean annual sea bed temperature seems to be about -0.8°C , and the gradient about 0.014 deg m^{-1} .

The parameter L that describes the influence of land is about 130 m using a mean surface temperature of -12°C (Gold and Lachenbruch, 1973). This should probably be decreased because of the presence of lakes near shore, but the distance of the hole from shore (705 m) is large enough that the difference is unimportant. The steady state gradient should be 0.81 of the geothermal gradient (or slightly larger); this gives 0.026 deg m^{-1} . Since this is somewhat larger than the actual value, estimated to be about 0.014 deg m^{-1} , the temperature may not quite be in steady state, but uncertainties prevent a definite conclusion. At any rate it is closer to steady state than any other offshore temperature profile that we have ever measured (see Lachenbruch and others, 1962). Extrapolation of our data suggests that the 0°C isotherm representing the base of the permafrost probably lies at a depth of roughly 60 m; the estimated steady state depth is about half of this.

The estimated mean temperature of -0.8°C or colder is surprising in the light of measurements by Brewer. Over a four year period, apparently in the 1950's, the mean, said not to vary much locally, was about -0.45°C (see Lachenbruch, 1966). This seems consistent with the value estimated from a borehole described

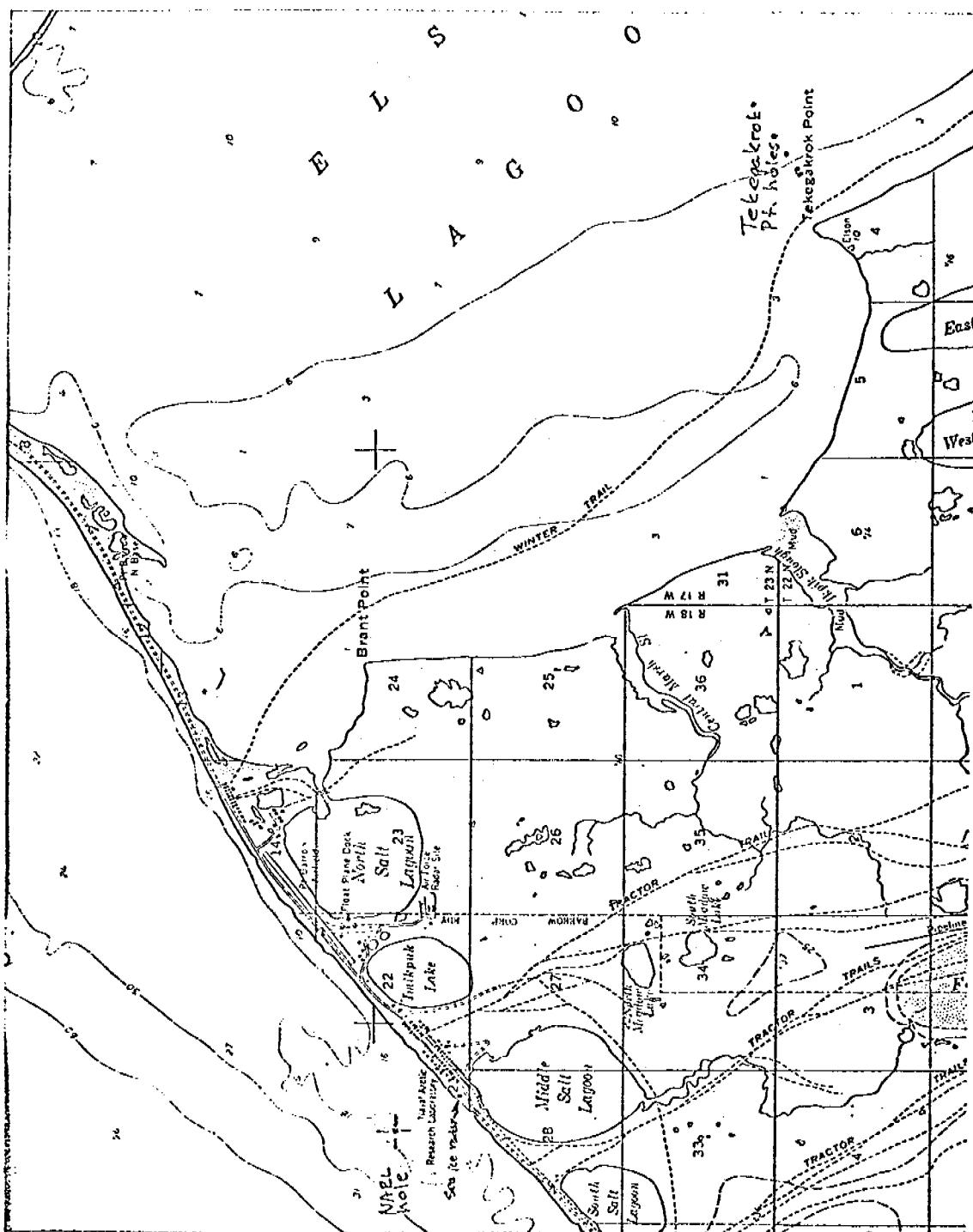


FIGURE 10. Location of NARL and Tekegakrok Point holes. The NARL hole is about 705 m from shore, or 750 m from the sea ice radar mast near the entrance area to the Naval Arctic Research Laboratory. The bearing from the mast to the hole is about 333° (true). Distances were taped and the bearing was measured by Brunton compass.

The distances of the Tekegakrok Point holes from shore, in this case defined to be the seaward edge of the tundra, are 575, 611, 790, 1036 and 1466 m. The distances from the water edge would be a few m less. The line of holes bears 56° (true) from Elson bench mark, which is about 320 m from the edge of the tundra in the direction of the holes. Bearings were measured with Brunton compass and distances were taped.

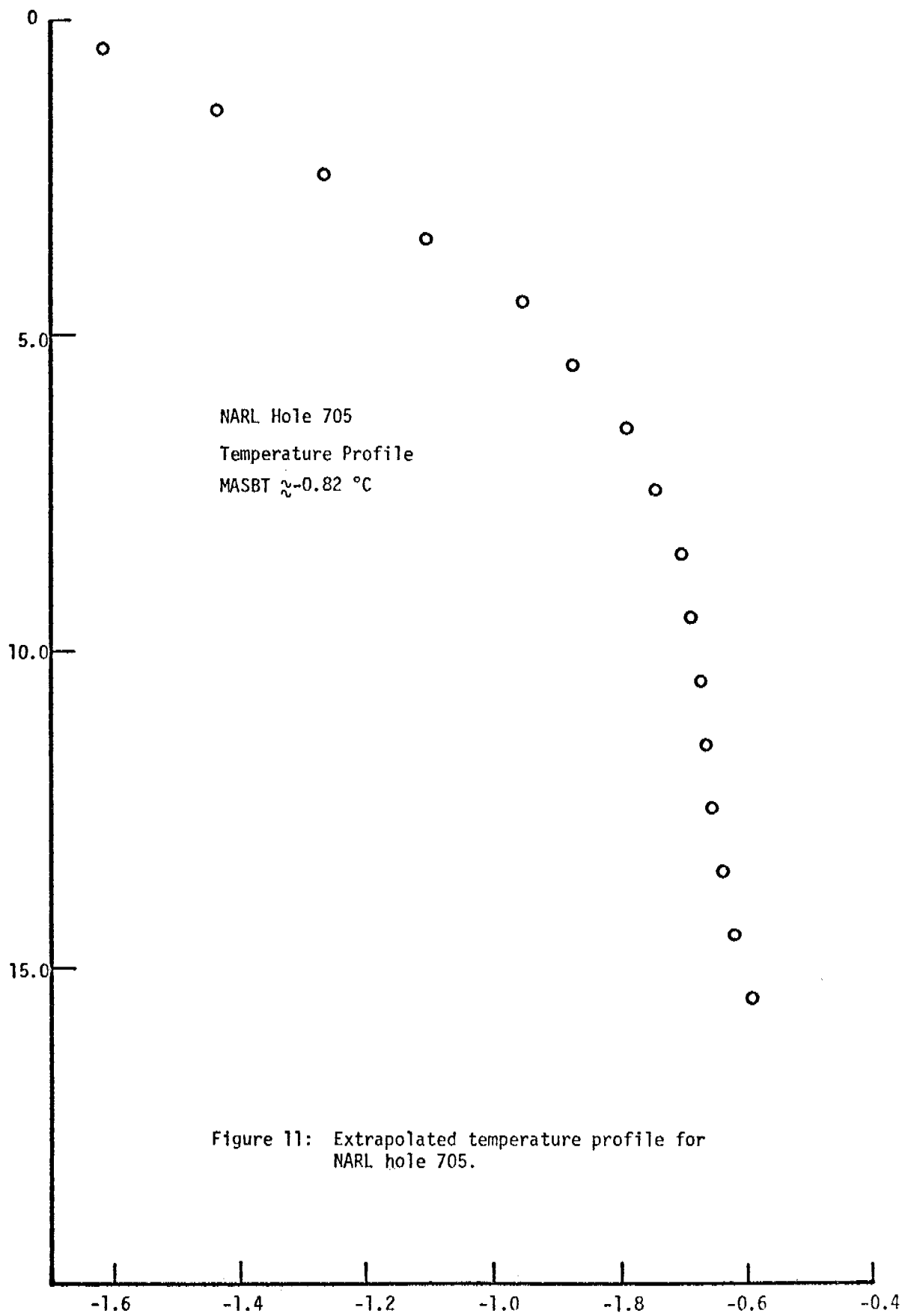


Figure 11: Extrapolated temperature profile for NARL hole 705.

by Brewer (1958). A secular change in mean annual sea bed temperature is therefore suggested.

6. Summary of Chukchi Sea Conditions

These observations give direct evidence, in near shore areas, of permafrost and in some cases ice at depth and shoreline recession. In a broad sense they are to be expected from the onshore data summarized by Hopkins (1976; 1977), especially the sea level history and shoreline retreat rates, from thermal models, and from onshore boreholes (Lachenbruch, 1966). Obviously the subsea permafrost conditions depend on the geologic setting, and will be much different in the bedrock that outcrops at or near the sea bed at Cape Thompson (Scholl and Sainsbury, 1966), and in the sediment, probably thick and frozen at depth, at Rabbit Creek. The latter situation is the more typical (See AEIDC, 1975, Map 2 for the onshore surficial geology.)

The question of the larger scale distribution of subsea permafrost and its properties in the Chukchi Sea remains open, and we have already summarized and discussed the available indirect information (Harrison and others, 1977). Briefly, because the entire present Chukchi Sea was emergent fairly recently, the possibility exists that some of the permafrost which must have formed there under the cold exposed conditions still exists. The most complete information is available from the southeastern Chukchi Sea, the proposed Hope Basin lease sale area. Seismic measurements and crude thermal models using water temperature and sea level data suggest the permafrost may now be absent below the deeper waters of that region, although it may well survive in areas shallower than 15-30 m (see also Hopkins, 1977).

B. Beaufort Sea

1. Elson Lagoon

Measurements were made in a line of five holes off Tekegakrok Point, in Elson Lagoon 12.5 km east of the town of Barrow (Figure 10). This site was chosen because it is the closest to NARL that is not complicated by an offshore bar and that is undergoing rapid shoreline erosion. The holes were chosen to span the transition from cold near shore conditions where the sea ice freezes to the sea bed, to the warmer conditions in deeper water maintained by the presence of sea water of normal salinity under the ice. Measurements at this site, and at others in Elson Lagoon, have been previously made by Lewellen (1973, 1974, 1976) and by Rogers and others (1975). In the Barrow area the top 20 to 30 m of the stratigraphy consists of the Pleistocene Gubik Formation (Black, 1964), and Lewellen (1976) feels that the contact with the underlying Cretaceous (clays with some silts) is consistently at about 30 m throughout the Elson Lagoon area. His studies indicate that the shoreline is retreating about 2.4 m a⁻¹ at Tekegakrok Point, and this is consistent with our own observations, which are based on a comparison of the 1955 USGS map with present conditions.

The data from each hole are presented separately in what follows, and the section concludes with a summary.

Elson Lagoon - Hole 575

Temperature data were obtained from a jetted hole 575 m from shore (Table 5, Figure 12, Appendix II). Hole 575 was the closest of the 5 holes to shore at

TABLE 5
BEAUFORT SEA HOLES

HOLE LOCATION	DISTANCE FROM SHORE	DRILLING METHOD	TIME OF DRILLING	DEPTH REACHED BELOW SEA BED	WATER DEPTH	SEA ICE THICKNESS	TEMPERATURE UNDER ICE	DATA OBTAINED
Elson Lagoon- Tekegakrok Pt.	575 m	jetting	May 15th 16:00-19:15	19 m	1.25 m	1.25 m	-8.3°C	temperature
"	611	jetting	May 13th 09:00-15:30	27	1.7	1.68	-2.3	temperature
"	798	driving and jetting	May 13th-16th		2.22	1.65	-2.0	temperature salinity, blow count, hydraulic conductivity
"	1036	jetting	May 11 16:30-18:15	17	2.5	~1.7	-1.9	temperature
"	1466	jetting	May 12 10:00-11:30	20	2.80	1.8	-1.86	temperature
Harrison Bay- Thetis Island	5.7 km	driving	Apr. 30-May 1	15	2.95	2.0	-2.04	temperature blow count
Harrison Bay- Oliktok	~400 m	jetting	May 2	8	2.4	2.1		temperature
Prudhoe Bay	1252	driving	May 4-5	15	1.97	1.87	-2.37	temperature blow count, hydraulic conductivity
"	2114	driving	May 8 08:45-14:17	26	1.85	~1.9	-2.7	temperature blow count

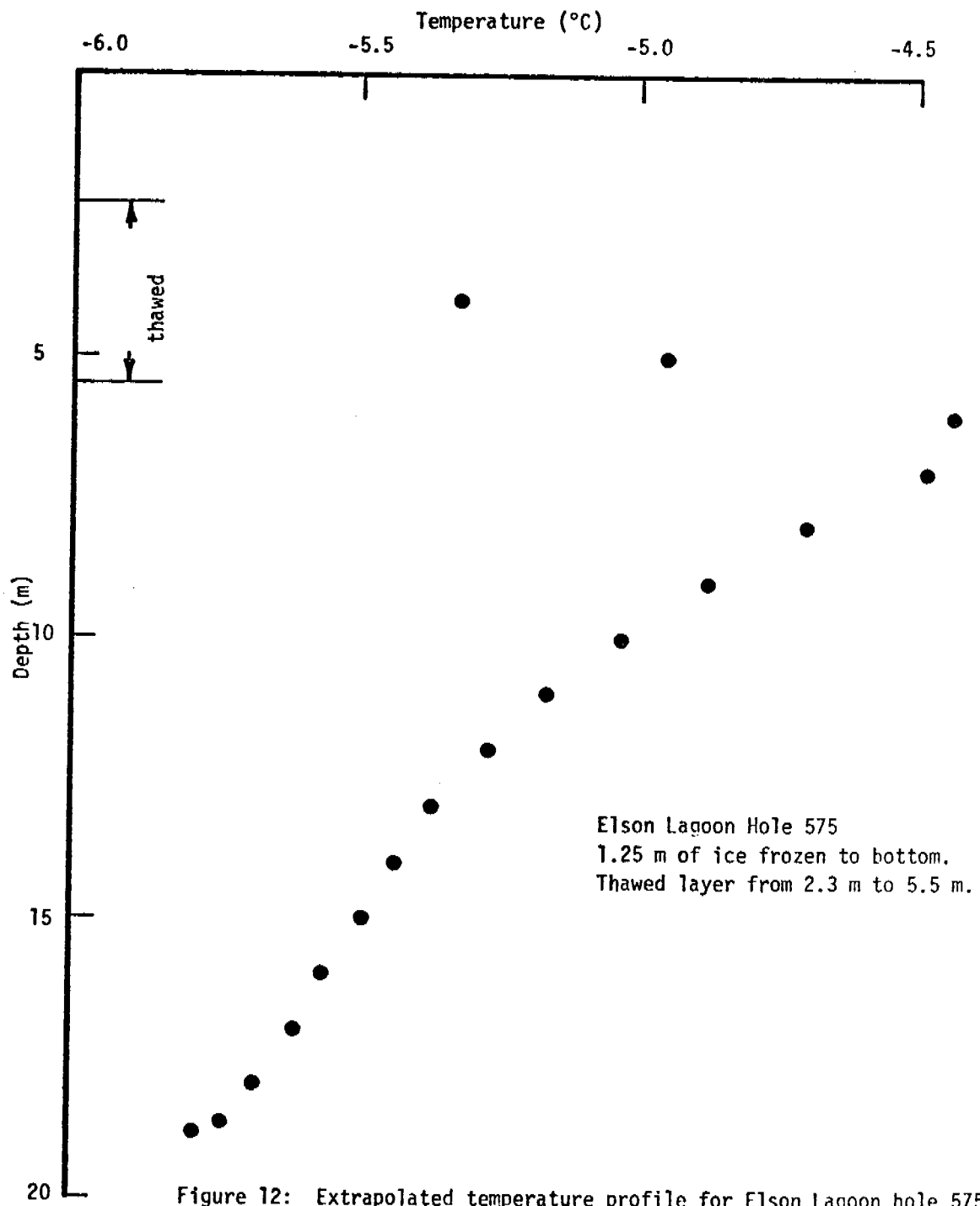


Figure 12: Extrapolated temperature profile for Elson Lagoon hole 575

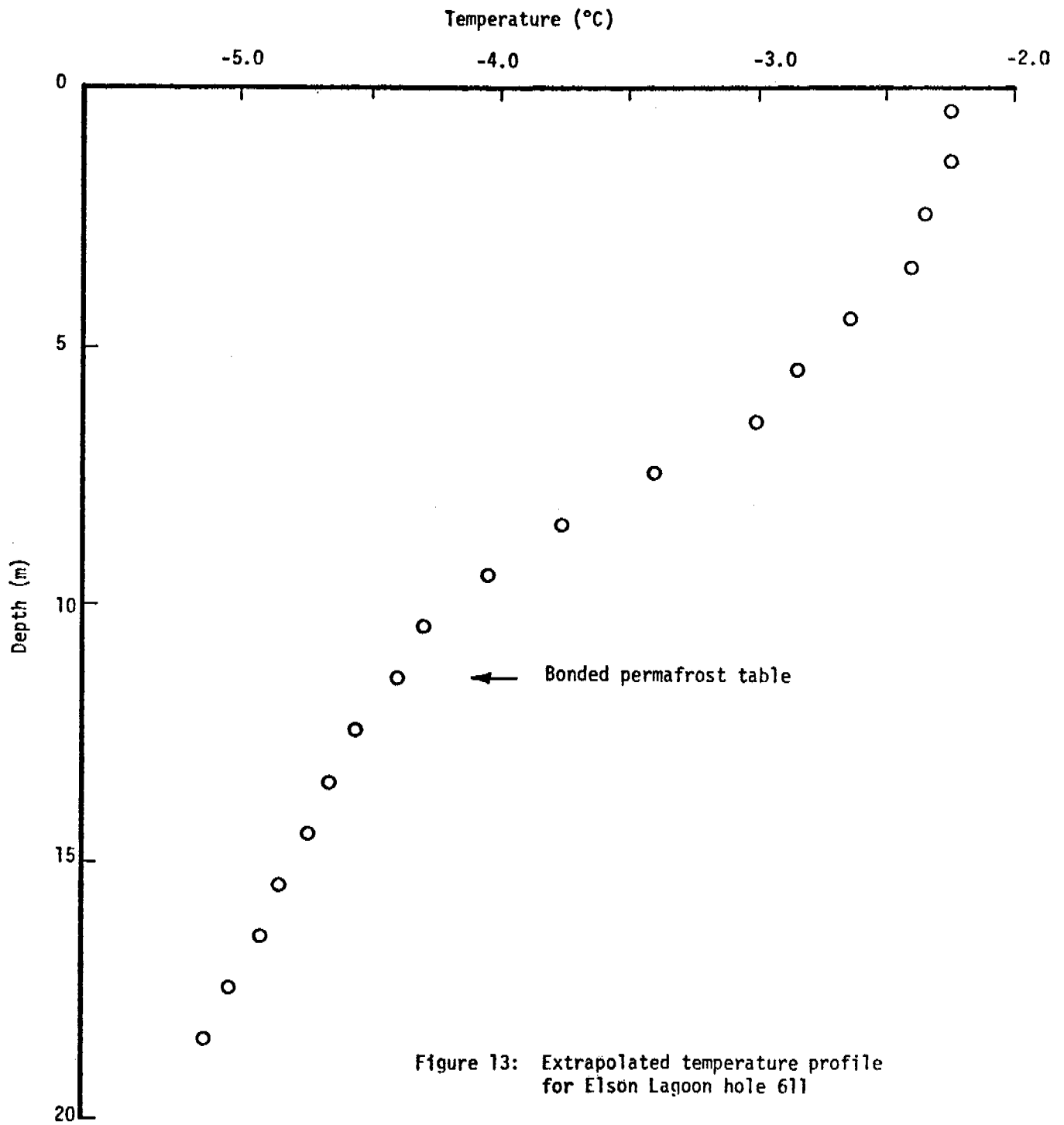
this site. The sea ice was frozen to the sea bed and return flow to the surface from the jet gave a better than usual identification of sediment type. Silts were found throughout most of the length of the hole but some very fine-grained sands and an occasional shell were observed. The sediments were ice-bonded to a depth of 2.3 m below the sea bed, unbonded from 2.3 to 5.5 m, and bonded below 5.5 m. A similar situation has been observed at Prudhoe Bay; the bonding in the top few m is probably a seasonal effect.

The extrapolated temperature profile from the May 18 and 28th data is shown in Figure 12 and the extrapolated data are given in Appendix II. Below the 6 m depth the temperatures on May 28 were probably within 0.1°C of equilibrium. However, it appears that the introduction of relatively warm sea water at depths where the sediments were unbonded caused a major temperature disturbance. The temperatures at the top and bottom of the unbonded layer were about -6.5°C and -4.3°C respectively. Soil particle surface effects complicate the estimation of the corresponding interstitial water salinities, but they are in the vicinity of 3 and 2 times that of normal sea water respectively. At least the first, and probably also the second of these high values seem to be associated with salt rejection during freezing of the sediments below the sea bed. The temperature at the sea bed on May 28 was -8.3°C and appears to show the beginning of a spring warming trend. The mean annual sea bed temperature cannot be estimated very well because of the complicating presence of the two phase boundaries. Extrapolation of the data below 13 m suggests a value of -4.5°C or warmer.

Elson Lagoon - Hole 611

Temperature data were obtained from a jetted hole 611 m from shore (Table 5, Figure 13, Appendix II). The location of this hole was chosen to give information about the changes that occur over short distances from shore. Although only 36 m seaward of hole 575, the slightly greater water depth prevented the ice from freezing to the sea bed and gave rise to a much warmer sea bed temperature. The behavior of the jet during drilling indicates the presence of fine grained sediments, probably silts and fine sands. The sediments were ice-bonded below 11.4 m.

The temperature profile in Figure 13 is the extrapolated temperature from the May 18th and 28th data. The estimated accuracy for these data is about 0.05°C . The temperature at the sea bed was about -2.2°C which is about the same as that found by Lewellen (1973) near the same location. The temperature at the ice-bonded boundary at 11.4 m is about -4.4°C which is almost the same as that at the corresponding boundary in hole 575, although the boundary in hole 611 is almost twice as deep. Given Lewellen's estimated shoreline retreat rate of about 2.4 m a^{-1} , the thawing from 5.5 to 11.4 m may have taken place in about 15 years. As in hole 575 the interstitial water salinity at the bonded-unbonded boundary can only be roughly estimated from the temperature; this gives about twice the value of normal seawater, which is the same as at the corresponding boundary in hole 575. The mean annual temperature at the sea bed is about -1°C . For comparison, a hole 481 m from shore at Prudhoe Bay is in a similar setting with regard to water depth and mean temperature, but a sharp bonded-unbonded boundary there at 19 m depth is at about -2.4°C , or 2 deg warmer.



Elson Lagoon - Hole 798

Temperature, blow count, salinity and hydraulic conductivity data were obtained from a hole driven to 8.2 m and jetted from 8.2 m to 14.6 m (Table 5, Figures 14 and 15, Appendix II). We were unable to hammer the driven drill rod loose, and were forced to run the jet adjacent to it to free it; the jet drilling was then continued. The sediments were evidently fine grained, and were hard below 11.2 m. This could have been due to clay or ice bonding.

The temperatures shown in Figure 14 were obtained by extrapolation of the data of May 18 and 28. A change in slope of the temperature profile just above 11 m seems to correspond fairly well to the depth at which hard sediments were encountered. This may lend some support to the ice-bonding interpretation, but we consider the question to be open. The temperature at the sea bed was -2.0°C indicating slightly greater than normal sea water salinity. It is difficult to obtain a good estimate of mean annual sea bed temperature because of the curvature and possible presence of ice at 11 m. However, it is probably about -1°C .

The sampling techniques which are under development (described in Section V) permitted in situ estimates of hydraulic conductivity at four depths (Table 6), and interstitial water samples to be collected from two depths; the electrical conductivities of the collected samples were measured in the lab (Table 7). The large errors in the salinities are indirectly due to the low hydraulic conductivity, which prevented collection of samples much larger than the probe dead volume (that which cannot be cleared between measurements) of about 25 cm^3 .

The interstitial water salinities at 2.1 and 5.2 m below the sea bed are about twice that of normal sea water, although it should be recognized that the value at the shallower depth has a particularly large uncertainty. It is interesting that this is about the same as that in the vicinity of the bonded-unbonded boundaries in holes 575 and 611. The hydraulic conductivity tends to decrease with depth and is extremely small, typically two or three orders of magnitude less than values we have obtained at Prudhoe Bay. The salinity and hydraulic conductivity are almost as important as temperature, although much more difficult to measure. The results so far seem to indicate that the physics of the heat and mass transport processes that controls the evolution of subsea permafrost is different in Elson Lagoon and at Prudhoe Bay (Harrison and Osterkamp, in press).

Elson Lagoon - Hole 1036

Temperature data were obtained from a jetted hole 1036 m from shore (Table 5, Figure 16, Appendix II). The initial drilling attempt was stopped by what appeared to be a rock of at least cobble size. The next attempt, at a lateral distance of 3 m from the first, was successful. Fine-grained sediments were encountered. Below 15 m they were very hard, perhaps due to clay or ice bonding.

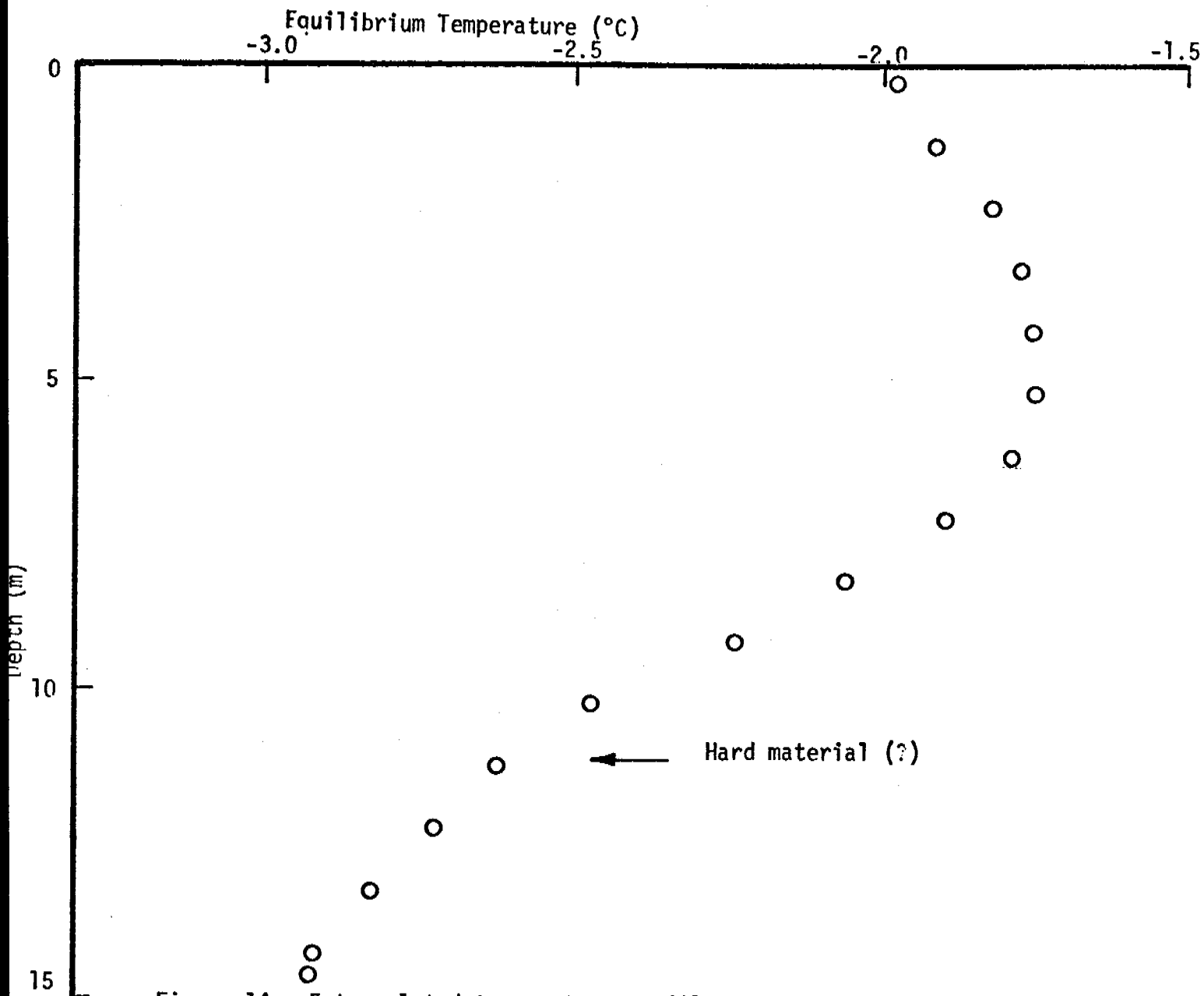


Figure 14: Extrapolated temperature profile for Elson Lagoon hole 798.

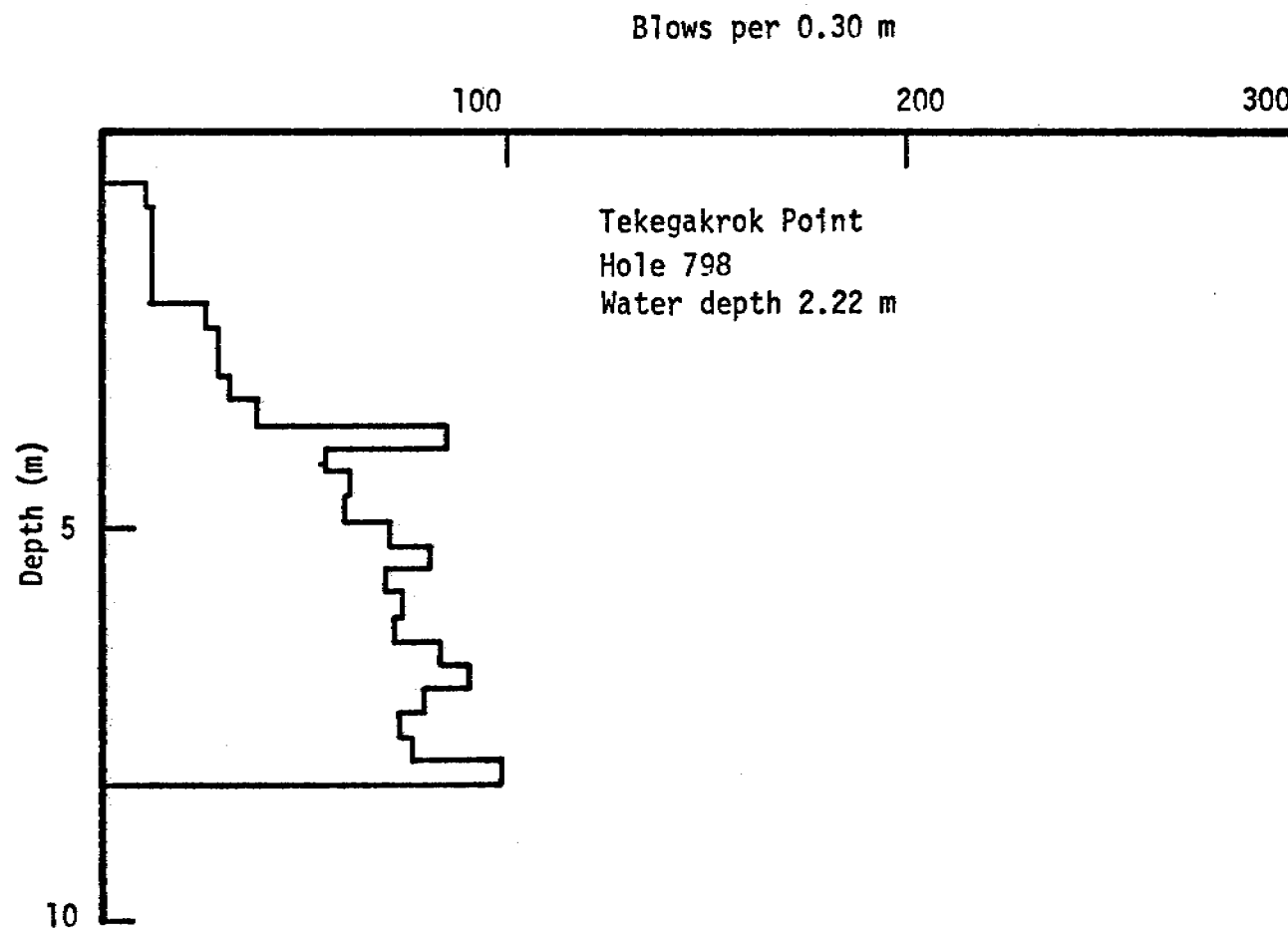


Figure 15: Blow count profile for Elson Lagoon hole 798

TABLE 6

Saturated hydraulic conductivity k of subsea sediments at Elson Lagoon and Prudhoe Bay. ΔH is the change in head during measurement.

DEPTH BELOW SEA BED (m)	$\Delta H(m)$	$k(m\ a^{-1})$	NOTES
Elson Lagoon - 1977 - hole 798 - shielded probe			
2.12	0.015	1.9×10^{-2}	Inflow
2.12	0.16	2.1×10^{-2}	Inflow-under vacuum
3.64	0.040	1.0×10^{-2}	Inflow-under vacuum
5.16	0.80	1.4×10^{-2}	Inflow
8.21	0.45	2.8×10^{-3}	Inflow-under vacuum
Prudhoe Bay - 1975 - hole 3,370			
3.9	?	5.7	Laboratory measurement in Shelby tube-vertical flow
3.9	?	22	Laboratory measurement in Shelby tube-vertical flow
Prudhoe Bay - 1976 - Near hole 481			
1.69	0.44	15	Outflow
3.32	0.62	0.52	Outflow-under pressure
3.32	0.11	1.1	Inflow
3.32	0.35	5.6	Outflow
3.32	0.12	6.7	Inflow
Prudhoe Bay - 1977 - hole 1252			
0.91	0.032	0.88	Inflow
1.68	0.025	0.25	Inflow
2.44	0.29	2.6	Inflow
3.96	0.12	1.1	Inflow
5.49	0.009	6.8	Inflow
7.01	0.005	4.1	Inflow

Table 6 (Cont'd)

DEPTH BELOW SEA BED (m)	$\Delta H(m)$	$k(m\ a^{-1})$	NOTES
Prudhoe Bay - 1977 - hole 1252 (Cont'd)			
7.01	0.279	5.2	Inflow
8.53	0.043	0.40	Inflow
10.06	0.072	2.3	Inflow
15.10	0.054	0.31	Inflow-shielded probe
16.62	0.021	0.14	Inflow- " "
16.62	1.44	0.16	Inflow- " "

TABLE 7

Electrical conductivity of interstitial water at 25°C. For comparison normal sea water is about 5.1 (ohm m⁻¹).

DEPTH BELOW SEA BED (m)	ELECTRICAL CONDUCTIVITY (ohm m ⁻¹)
----------------------------	---

Elson Lagoon - 1977 - hole 798

2.12	10.0 ± 3.5
------	------------

5.16	12.0 ± 2.0
------	------------

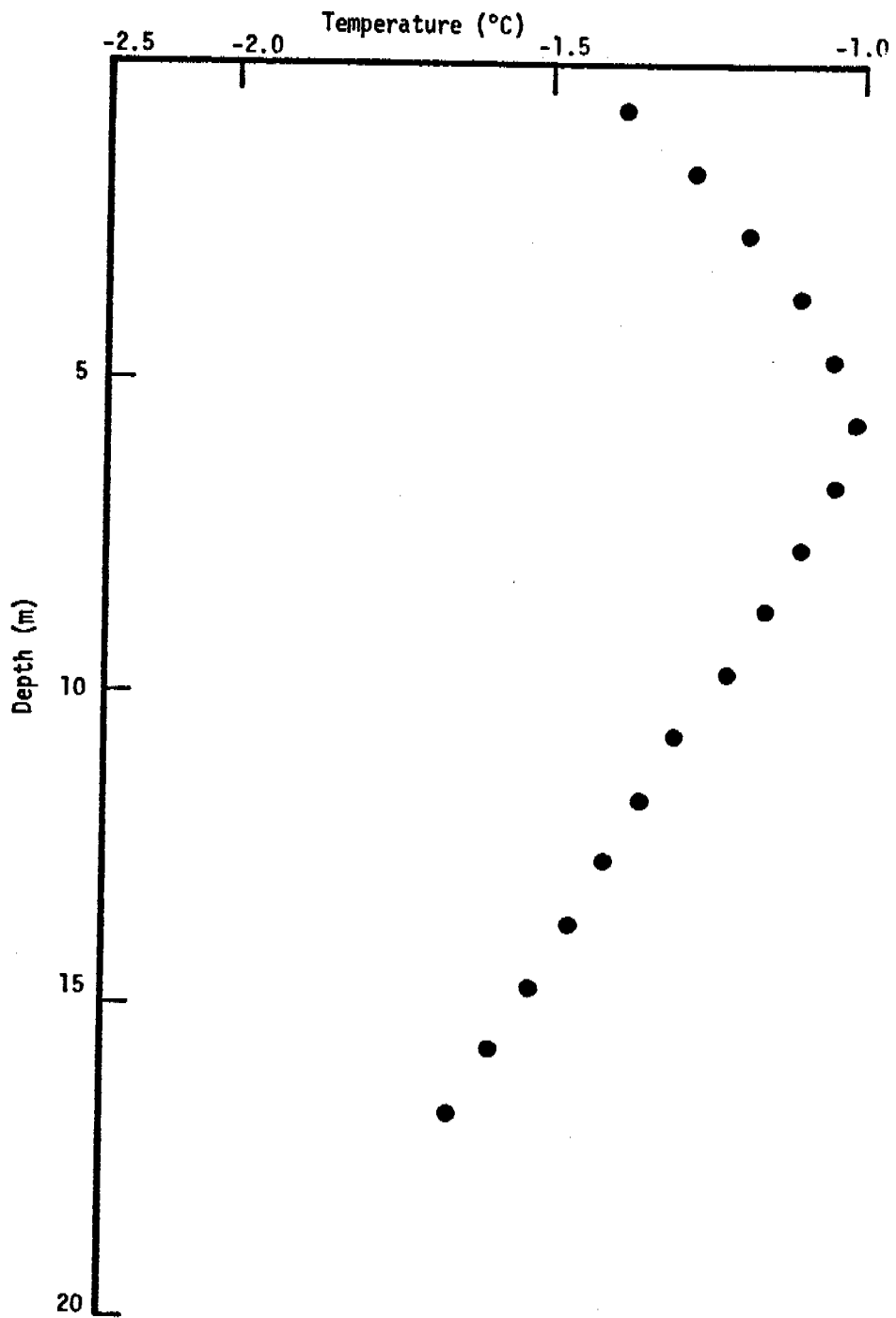


Figure 16: Extrapolated temperature profile for Elson Lagoon hole 1036

The temperature profile in Figure 16 is the equilibrium temperature estimated from the May 18 and 28 data. The sea bed temperature was -1.9°C indicating only slightly greater than normal sea water salinity. The mean annual sea bed temperature seems well determined and is -1.1°C . There is no evidence for the presence of ice at 15 m in the temperature profile, such as a change in slope.

Elson Lagoon - Hole 1466

Temperature data were obtained from a jetted hole 1466 m from shore (Table 5, Figure 17, and Appendix II). This was the farthest from shore of our five holes. The sediments were clay with silt or sand lenses down to 15.7 m where much harder sediments were encountered.

Two temperature profiles are shown in Figure 17. One represents data obtained on May 18 and the other is an "extrapolated" equilibrium profile, which was obtained by subtracting 0.14°C from the May 18 data. This is the average difference between the May 18 and equilibrium temperature in hole 1036. The procedure was necessary because the hole was blocked when logging was attempted on May 28, and it seems fairly well justified by the similar settings and drilling conditions in the holes. The sea bed temperature was -1.86°C , which is characteristic of normal sea water. The mean annual sea bed temperature is -1.0°C . There is no obvious break in slope of the temperature profile at the 15.7 m depth where hard jetting began.

Elson Lagoon - Summary

Five holes were drilled into the sea bed near Tekegakrok Point in Elson Lagoon, where the shoreline retreat rate is estimated to be about 2.4 m a^{-1} (Lewellen, 1973). They span the transition from cold near shore conditions where the sea ice freezes to the sea bed, to the warmer conditions in deeper water maintained by the presence of sea water of normal salinity under the ice. Judging from the behavior of the jet used in drilling, the sediments are fine grained.

The temperature data summarized in Figure 18 are all far from steady state, and, as in the Chukchi Sea cases discussed earlier, are a result of the shoreline retreat. The thawing of the initially ice-bonded sediments downward from the sea bed is still in evidence in the two innermost holes (575 and 611 m from shore) where boundaries between ice-bonded and unbonded sediments are observed. In the first hole the sediments are also bonded to 2.3 m below the sea bed but this is a seasonal effect. Changes in drilling speed were also noted in other holes, but they are not necessarily associated with ice bonding (Figure 19). In the next hole out (798 m from shore) interstitial water salinity measurements at two depths gave values about twice that of normal seawater, which is about the same as those at the lower bonded-unbonded boundary in the inner hole and at that in the next hole. Hydraulic conductivity measurements at three depths in the hole 798 m from shore gave values decreasing with increasing depth, and in the vicinity of 10^{-2} m a^{-1} , two or three orders of magnitude less than those measured at Prudhoe Bay. As a result, the physics of the heat and mass transport processes that control the evolution of the subsea permafrost is probably quite different at the two locations.

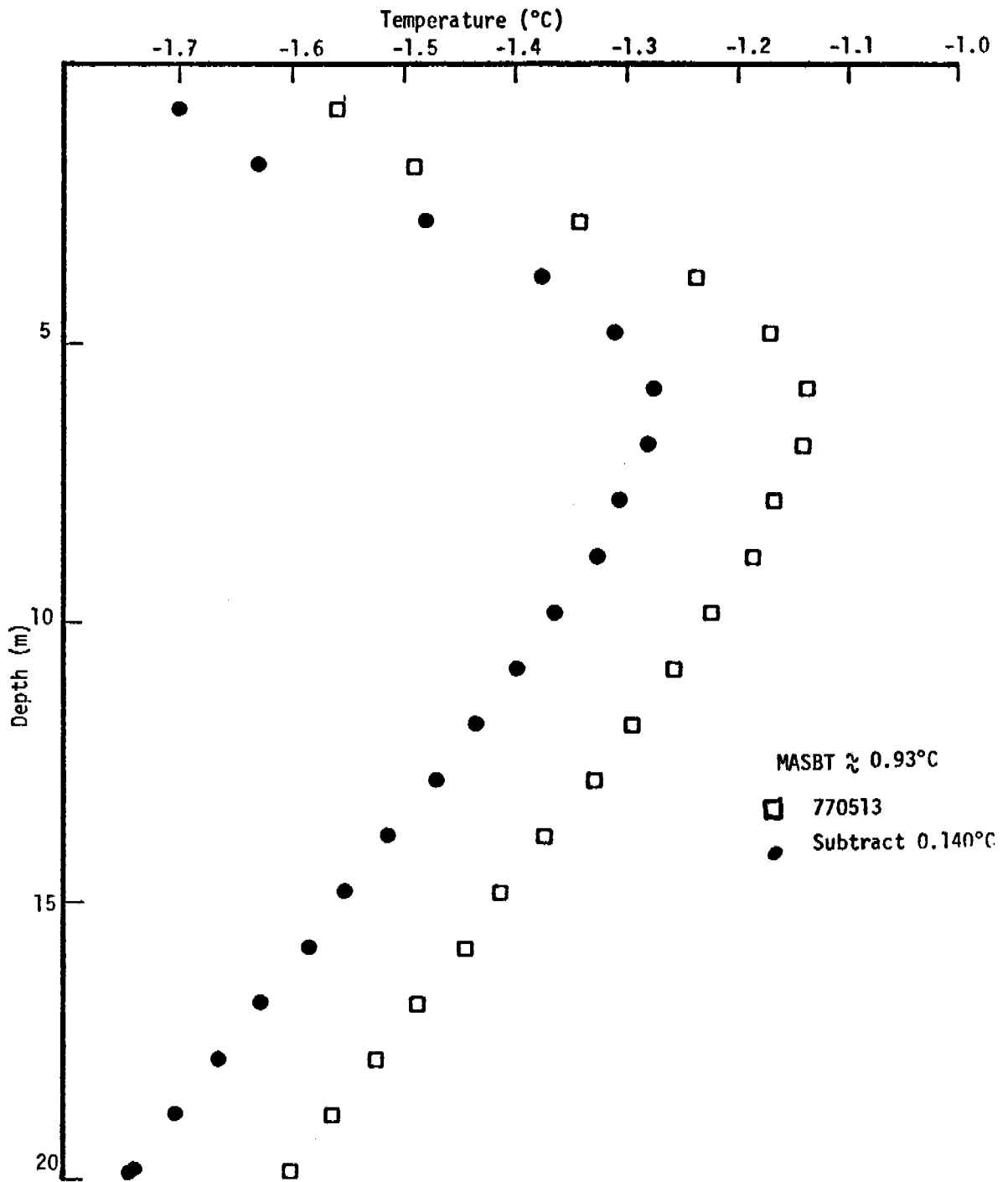


Figure 17: Temperature profiles for Elson Lagoon hole 1466
 Measured profile (□) on May 18. Extrapolated profile
 (●) obtained by subtracting 0.140°C from May 18 profile.

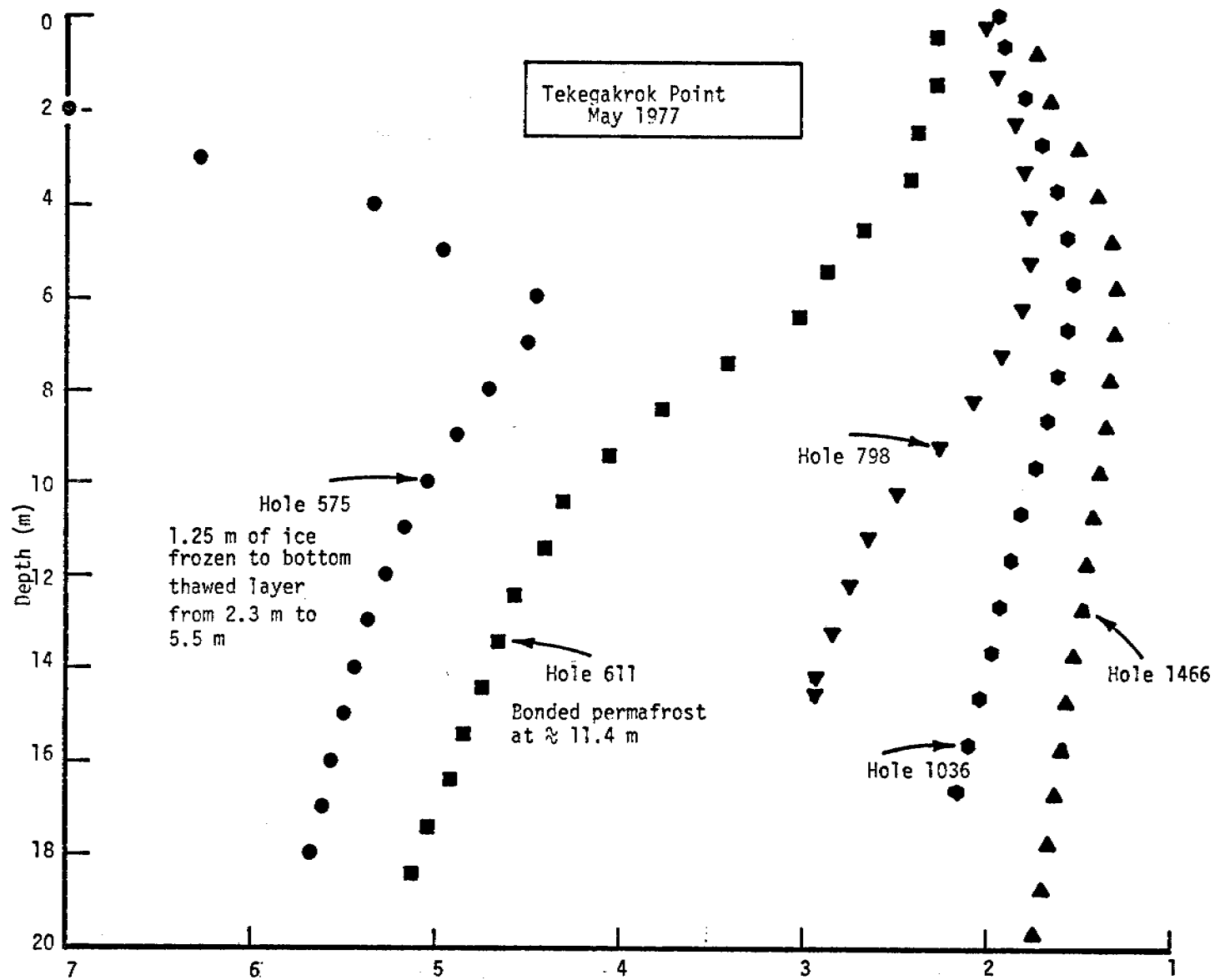


Figure 18: Summary of temperature profiles in Elson Lagoon at Tegegakrok Point during May 1977.

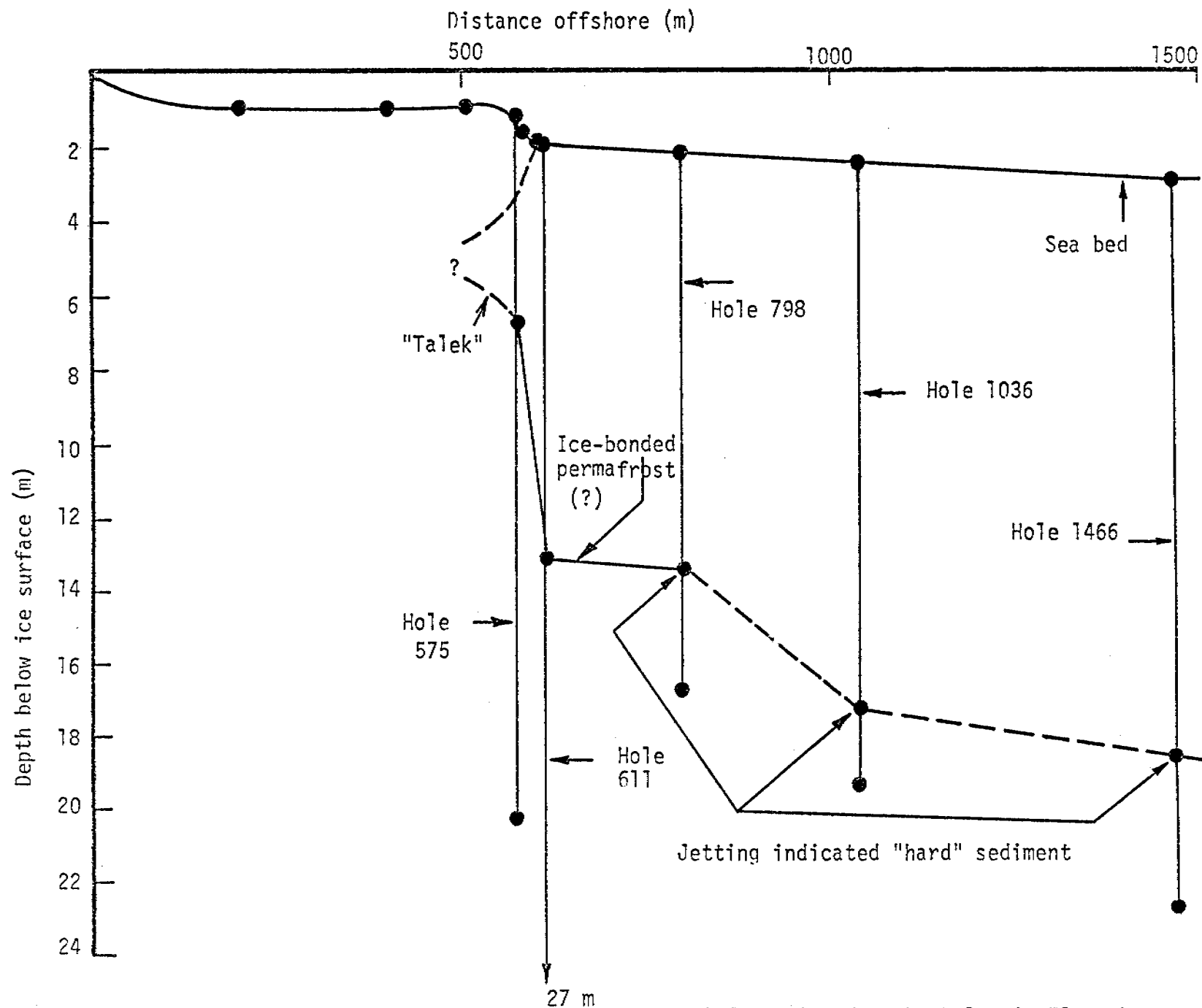


Figure 19: Sea bed profile and sediment information for the holes in Elson Lagoon at Tekegakrok Point.

The observations in hole 575 suggest that docks, causeways or islands constructed from local fill material would likely become ice-bonded to 3 or 4 m during the first winter, and therefore resistant to ice forces, although some thawing would of course take place again the following summer. But the high brine concentrations under the ice-bonded layer, which are probably concentrated during the freezing process, will severely reduce the rate of freezing unless some provision is made for their removal.

2. Harrison Bay

Two holes were made in the sea bed at Harrison Bay (Figure 20). This area is of special interest because it is thought to be the dividing line between the fine grained sediments characteristic of the Barrow area and the coarser grained material characteristic of Prudhoe Bay. It is also of importance because the sedimentation, salinity, and temperature environments should be strongly influenced by a major river, the Colville .

Harrison Bay - Hole South of Thetis Island

Temperature and blow count data were obtained from a driven hole due south of Thetis Island and about 8.5 km west of Oliktok DEW station. (Table 5, Figures 20, 21, 22, and 23, and Appendix II). Judging from the material adhering to the drill rod, the sediments were clays and silts. A blow count profile is shown in Figure 23. Progress was stopped by the extremely hard driving (515 blows per 0.3 m) at 15 m. This suggests ice bonding but the effect could also be due to the soil type.

Temperatures logged at three times are shown in Figure 22. These suggest that the major portion of the disturbance caused by driving disappears the first day. The equilibrium temperatures, although not well-defined, are therefore probably not grossly different from those logged on the last day. The mean annual temperature is about -0.7°C , which is about the same as in a hole 3,370 m from shore at Prudhoe Bay where the water depth was about the same. This site does not seem to be greatly affected by the Colville River.

Harrison Bay - Oliktok Hole

Temperature data were obtained from a jetted hole about 550 m offshore from the point where the Oliktok DEW station runway intersects the coast (Table 5, Figures 20, 21, and 24, Appendix II). The jetting indicated the presence of sands and gravels, and caving prevented penetration below 8 m. This behavior is typical of Prudhoe Bay, and we conclude that the sands and gravels characteristic of that location probably extend to this one as well.

The temperature profile of Figure 24 was obtained on the last logging day. The estimated accuracy is only 0.2°C . The hole is not deep enough to provide a reliable estimate of mean annual temperature.

3. Prudhoe Bay

Two holes were driven along the USGS-CRREL-UA study line bearing about $\text{N}31^{\circ}\text{E}$ from north Prudhoe Bay State #1 Well near the west dock.

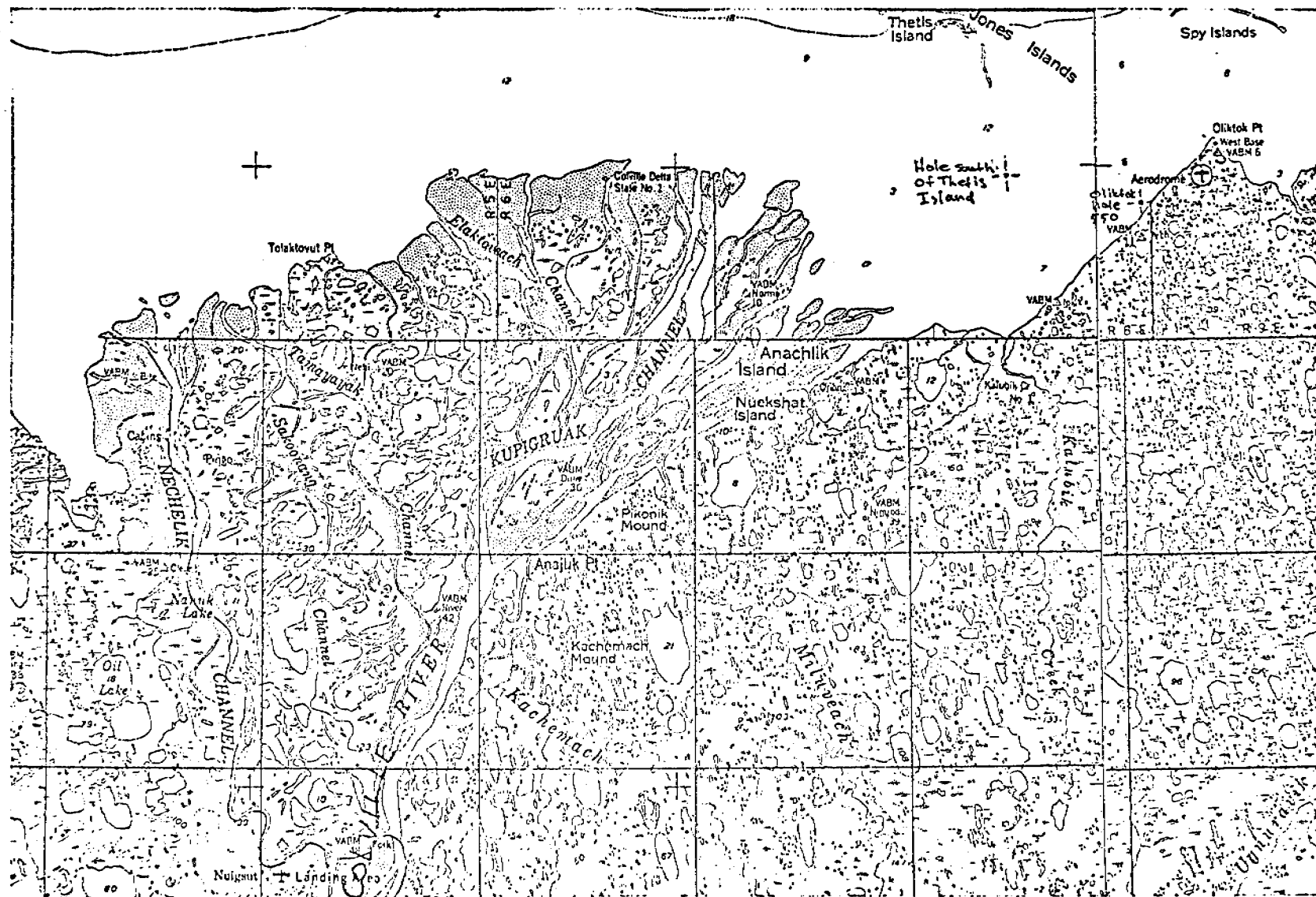


FIGURE 20. Location of Harrison Bay offshore holes with respect to Colville River and its delta. Maps USGS 1:250,000. Harrison Bay, Alaska and Beechey Point, Alaska.

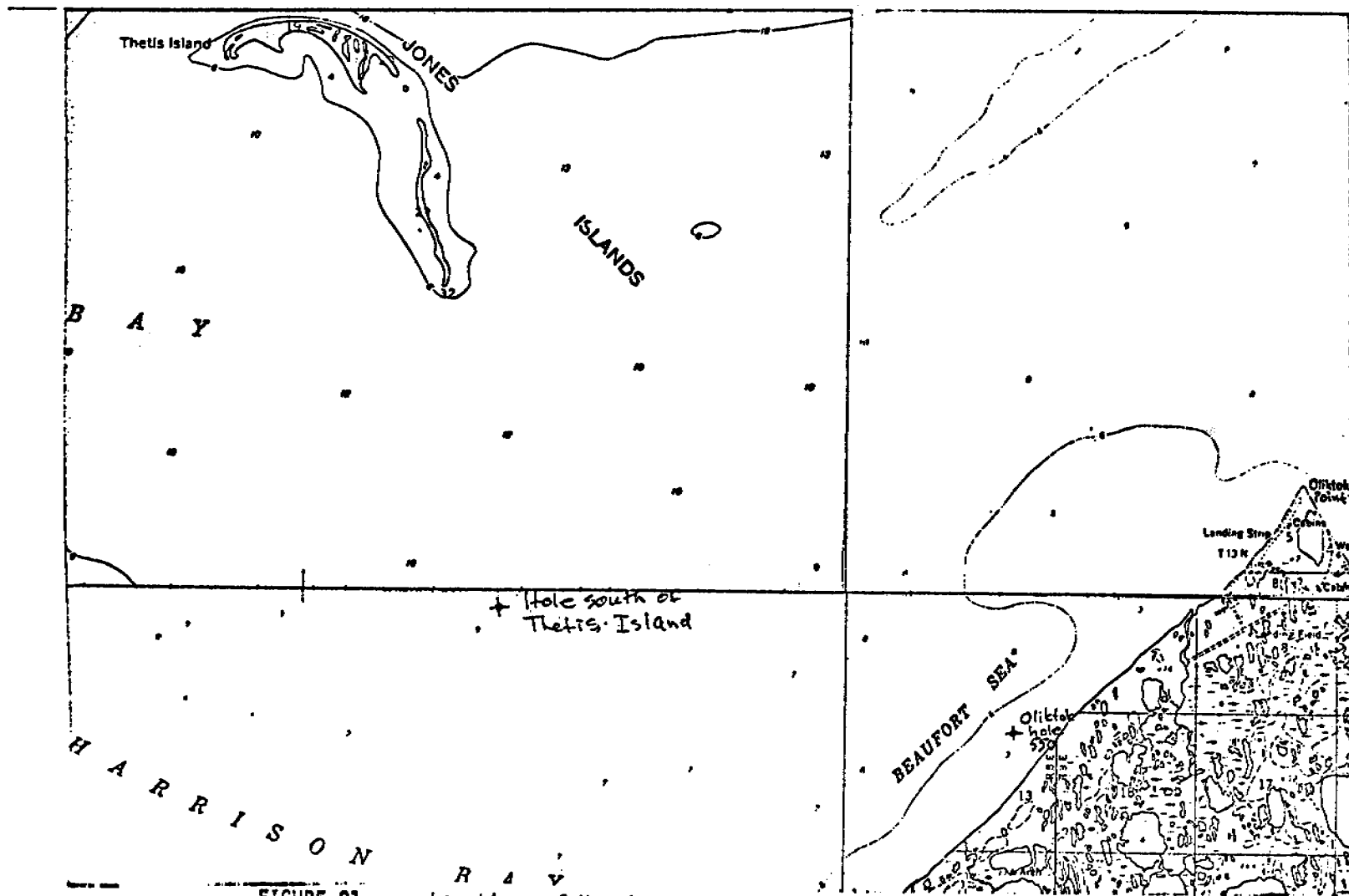


FIGURE 21.

Locations of Harrison Bay holes. The Oliktok hole is about 550 m west of the point where the projection of the DEW station runway intersects the coast. The closest land is about 400 m from the hole. The bearing was measured by Brunton compass. The distance was determined by a combination of taping and pacing, and is subject to considerable error. The location of the Thetis Island hole was determined by the Global Navigation System on board the NOAA Bell 205 helicopter, calibrated on the position of the Oliktok hole. It also is subject to considerable error. Maps USGS L;63,360 Beechy Point (C-5), Beechy Point (B-5), Harrison Bay (B-1), and Harrison Bay (C-1), Alaska.

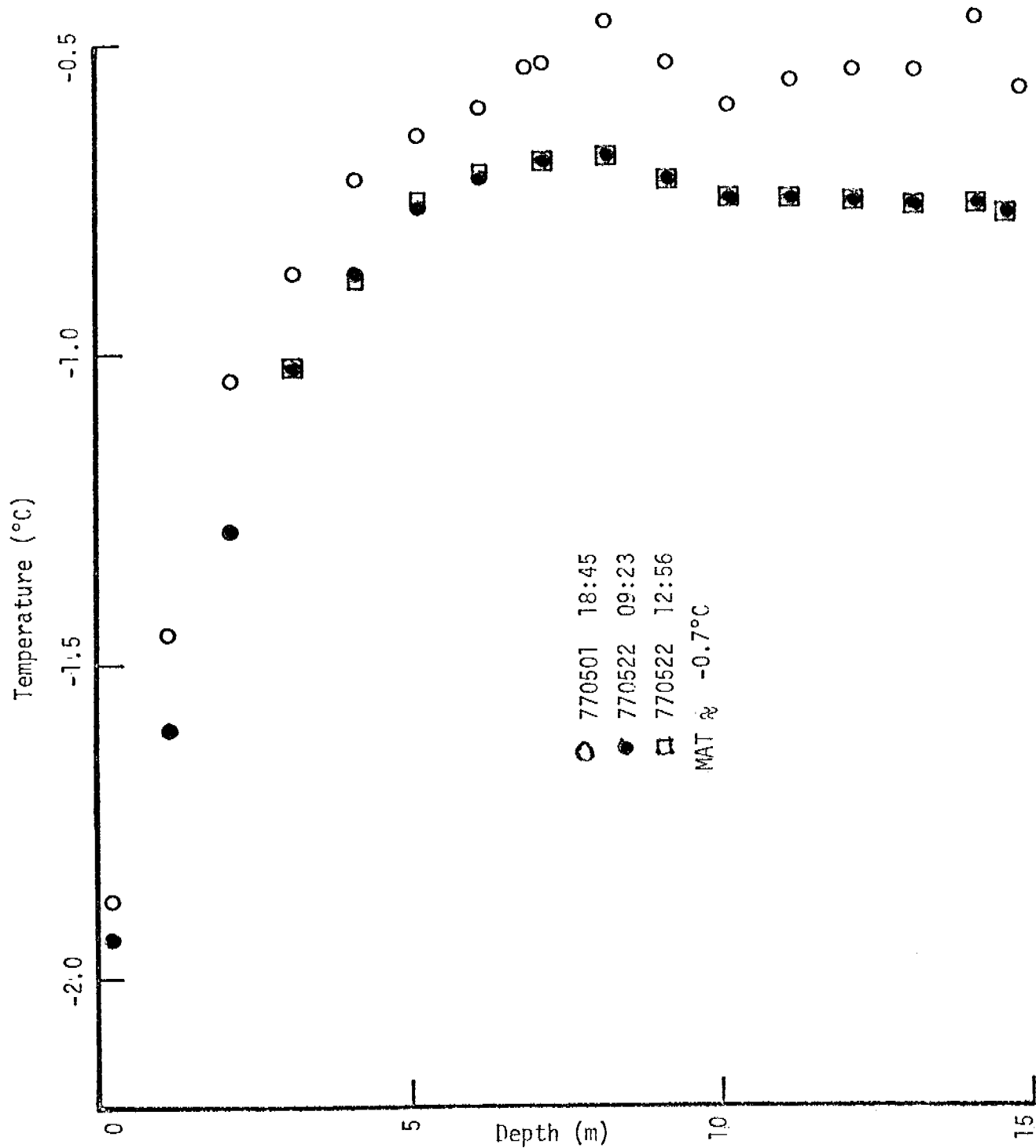


Figure 22: Measured temperature profiles for the Harrison Bay hole south of Thetis Island

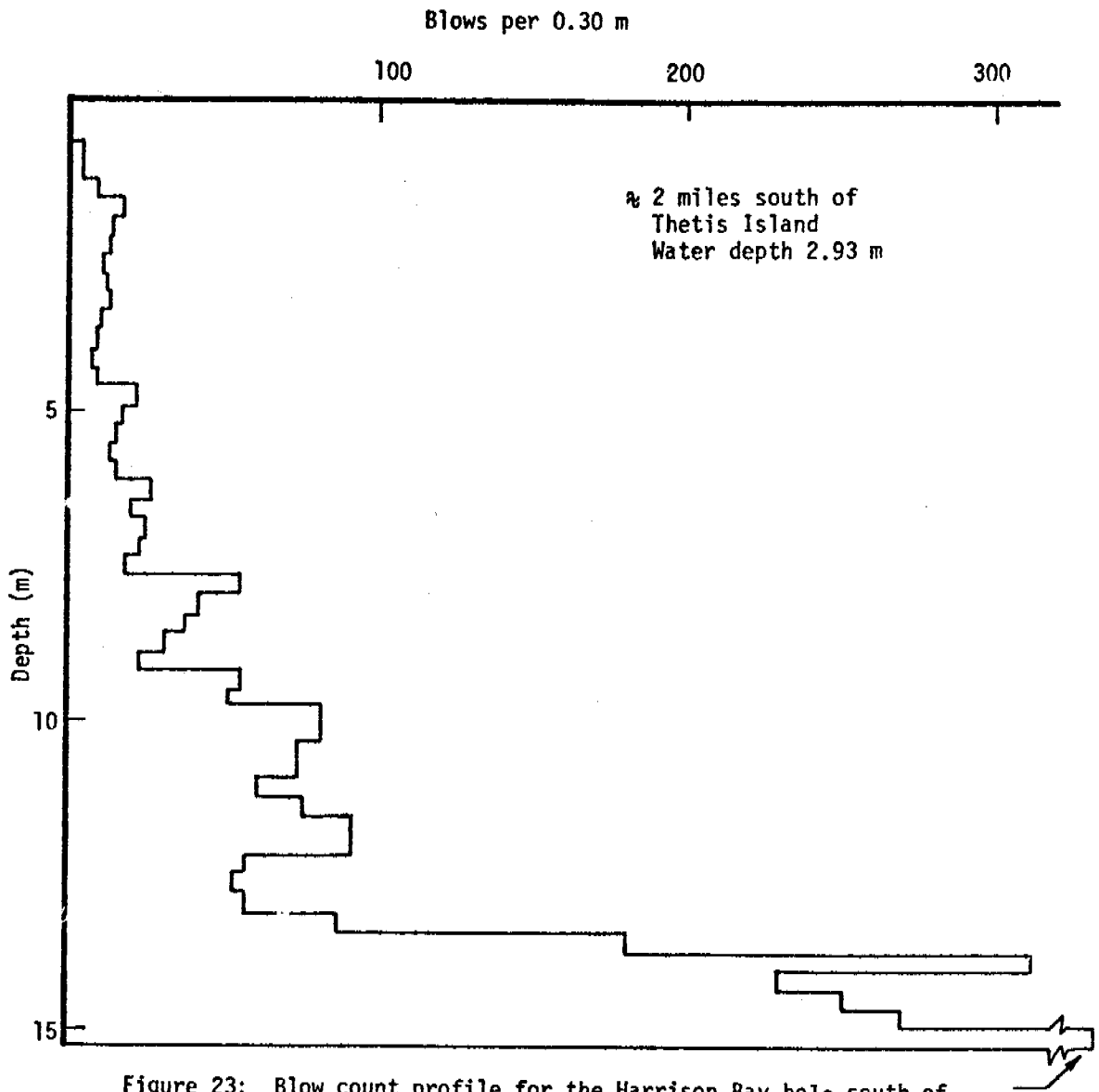


Figure 23: Blow count profile for the Harrison Bay hole south of Thetis Island

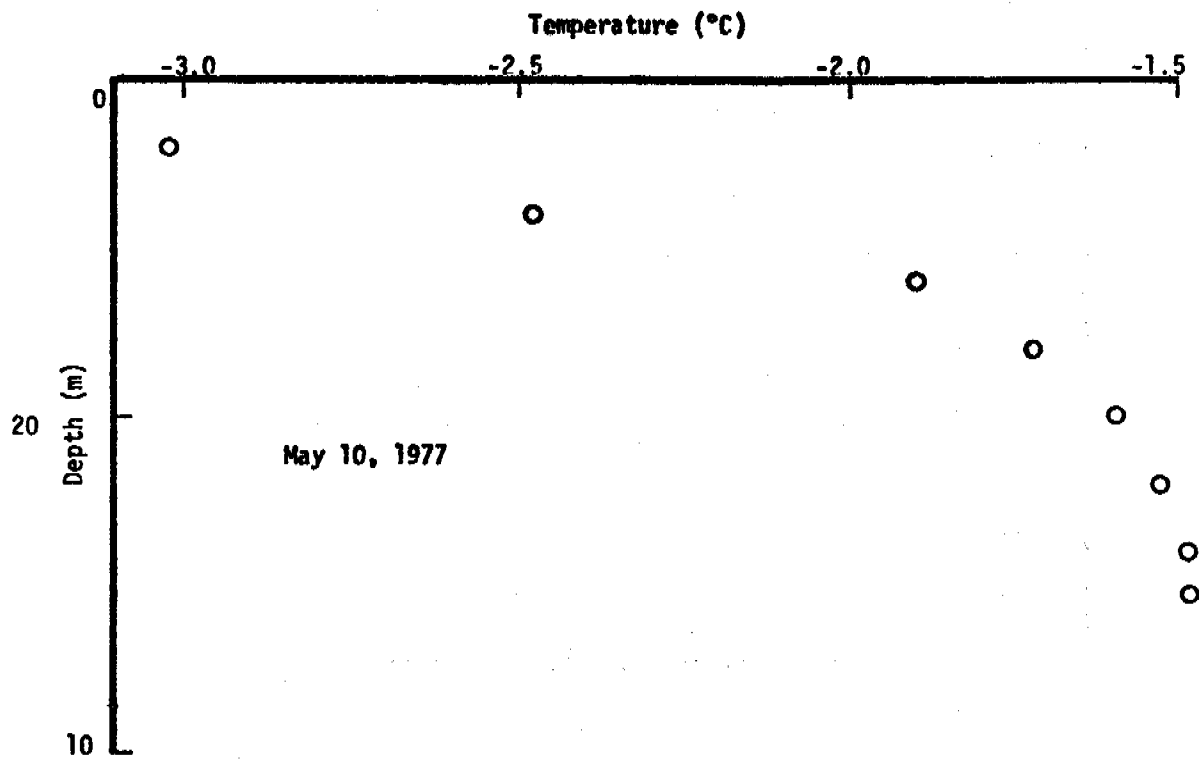


Figure 24: Measured temperature profile on May 10, 1977 for the Oliktok hole

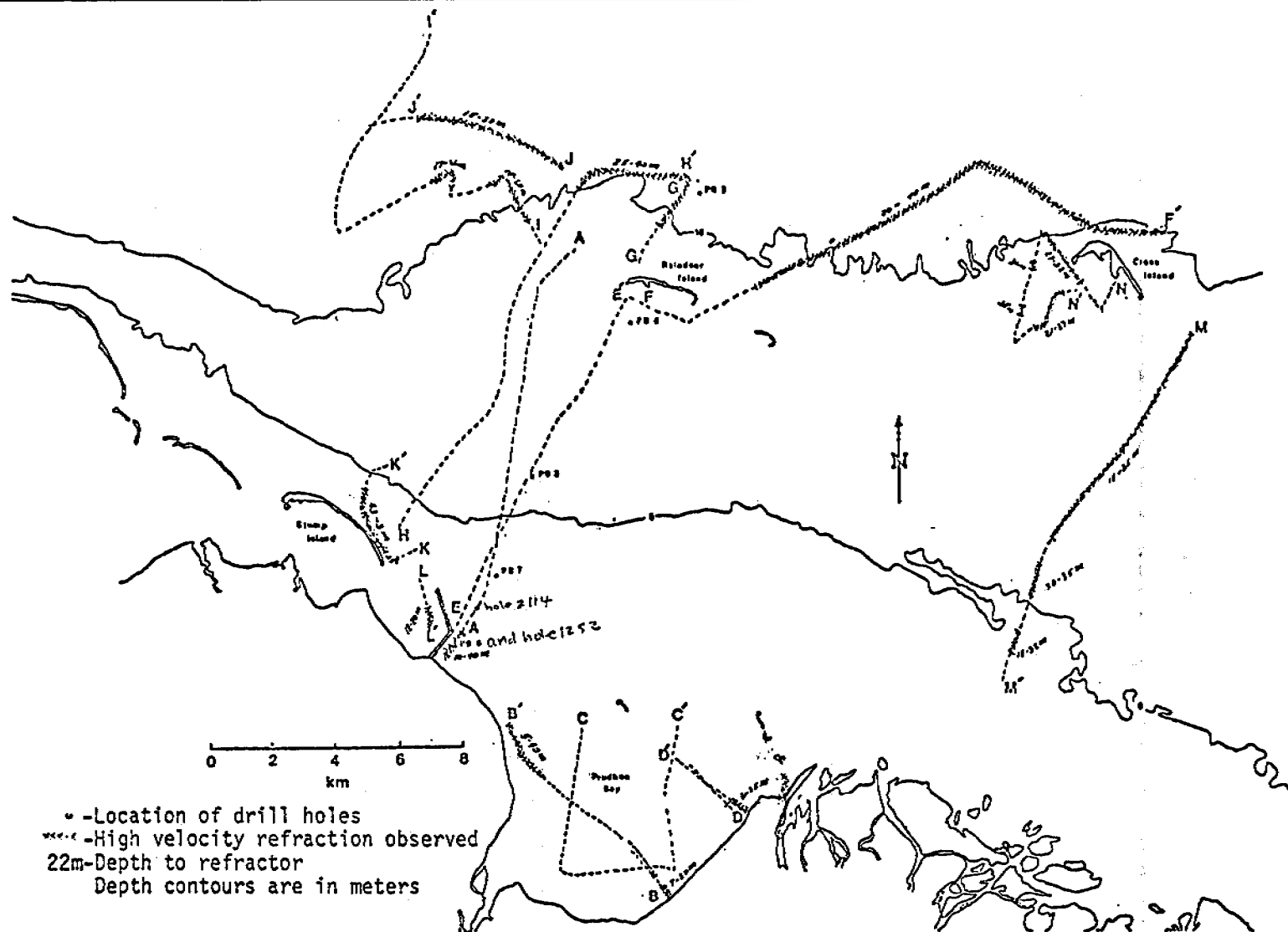


FIGURE 25. Locations of Prudhoe Bay holes. The designations on the two holes, 1252 and 2114, are the distances taped from shore in m. The first hole is 1376.4 m from our reference mark near North Prudhoe Bay State #1 well (Osterkamp and Harrison, 1976). They lie along a line bearing 31° (true) from the well, as measured by Brunton compass. The map is taken from other OCSEAP investigators. Locations of other holes, and of seismic lines, are also shown.

Prudhoe Bay - Hole 1252

Temperature, blow count, and hydraulic conductivity data were obtained from a driven hole 1252 m from shore along the study line described above (Table 5, Figures 25, 26, and 27, Appendix II). The main purpose of the hole was to test our interstitial water sampling techniques by comparison with data obtained from cores at the same site by USGS-CRREL. The hole was terminated when a hard spot in the driving (Figure 27) broke off the special probe-tip at 14 m.

The temperature profiles obtained at the two logging times are shown in Figure 26. Probably the second is not far from equilibrium. The mean annual sea bed temperature is about -1.2°C . Extrapolation of the temperature data below 10 m indicates that the temperature -2.4°C should lie, very roughly, at a depth of about 30 m. Since this is the temperature at a sharp thawed-frozen boundary which was found in a hole 481 m from shore (Osterkamp and Harrison, 1976a, 1977), a similar boundary at roughly 30 m may exist at the site of this hole.

Hydraulic conductivity data were also obtained in this hole; these are discussed in a subsequent paragraph with similar data from other Prudhoe Bay sites.

Prudhoe Bay - Hole 2114

Temperature and blow count data were obtained from a driven hole 2114 m from shore along the study line described above (Table 5, Figures 25, 28, and 29, Appendix II). The purposes of the hole were to fill a gap in previous measurements, and to test the depth capability of our portable driving equipment in Prudhoe Bay soils. Driving was still proceeding normally at a depth of 26 m below the sea bed when we exhausted our supply of drill rod.

The temperatures shown in Figure 28 are estimated equilibrium temperatures obtained by extrapolation of three sets of data taken over a 24 hour period. The accuracy is only about 0.1°C due to the calibration problems noted earlier. Slush formation in the water in the drill pipe and resultant release of latent heat probably complicate the approach to equilibrium. The low sea bed temperature of -2.7°C (and consequent high salinity under the ice), and the low mean annual temperature of about -1.3°C are not surprising since there were only a few centimeters of water under the sea ice. The mean sea bed temperature is colder than that at hole 481 (about -1.1°C) and at hole 3,370 (-0.8°C). Although the temperature has decreased to -2.1°C at the bottom of the hole the blow count data do not indicate any strong ice bonding. However, if as in hole 481 this occurs at a depth corresponding to -2.4°C extrapolation of the data indicates that this would be at about 40 m.

Hydraulic Conductivity at Prudhoe Bay

The hydraulic conductivity measurements made by us at Prudhoe Bay, and those in Elson Lagoon discussed earlier, are summarized in Table 6. The values from hole 3,370 at a depth of 3.9 m were obtained from a lab measurement on a core sample (Osterkamp and Harrison, 1976a). All the others were obtained using a piezometer method in which the rate of inflow or outflow of fluid through a radial porous metal filter near the end of our drill rod was measured under a known head. The measurements in hole 1252 at Prudhoe Bay and at hole 798 in Elson Lagoon are probably the most reliable, since plastic tubing was run inside the drill rod to eliminate the possibility of leakage through joints in the drill pipe from being measured.

Part of the considerable scatter is undoubtedly due to the non-homogeneous and non-isotropic properties of real soils, but despite the scatter it is evident that the Elson Lagoon values are 2 or 3 orders of magnitude less than those at Prudhoe Bay. As noted earlier, this probably leads to important differences in the transport regimes which control the evolution of the subsea permafrost at the two sites (Harrison and Osterkamp, in press).

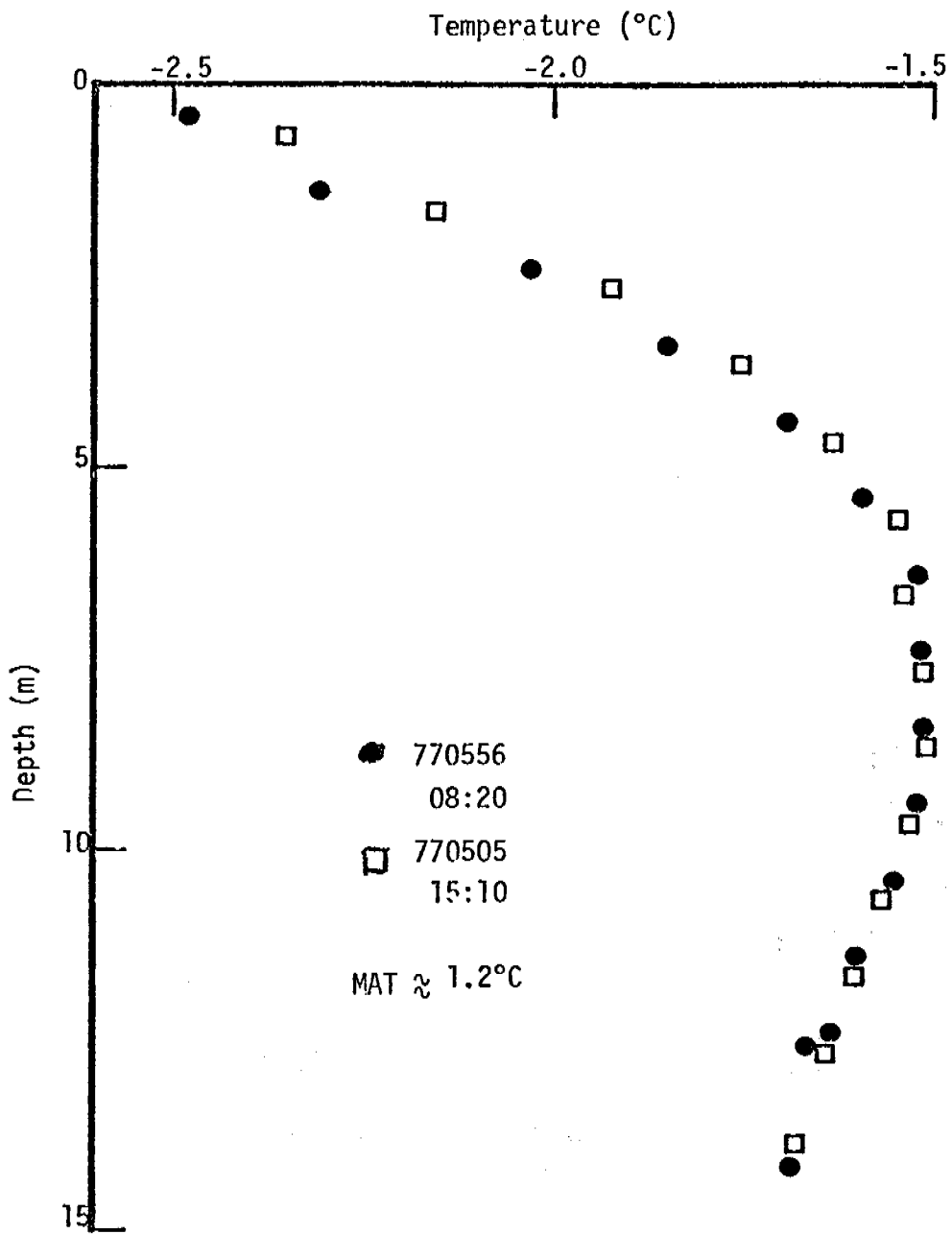


Figure 26: Measured temperature profiles for the Prudhoe Bay hole 1252. (●) measured on May 6 at 08:20, (□) measured on May 6 at 15:10.

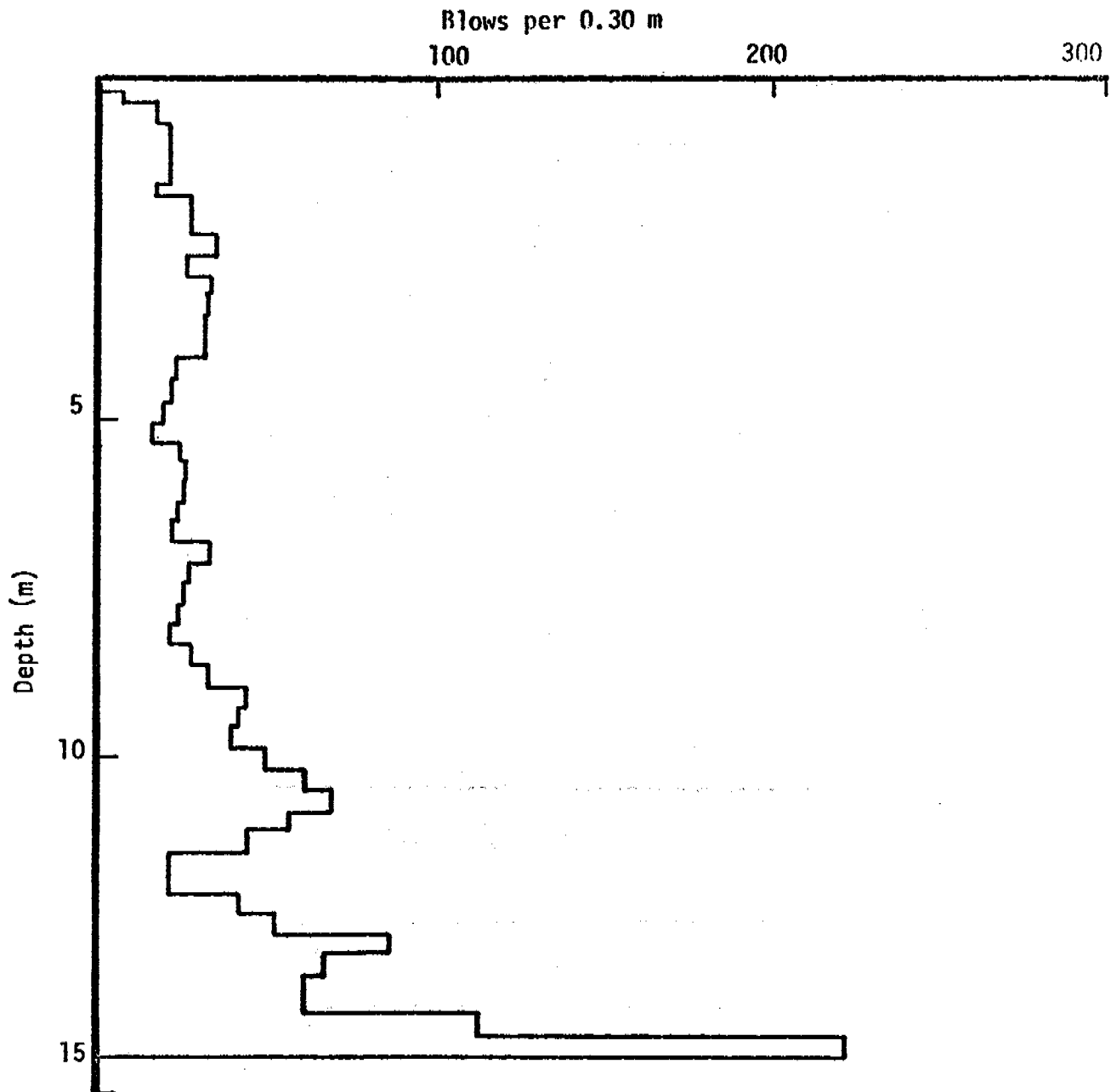


Figure 27: Blow count profile at Prudhoe Bay hole 1252

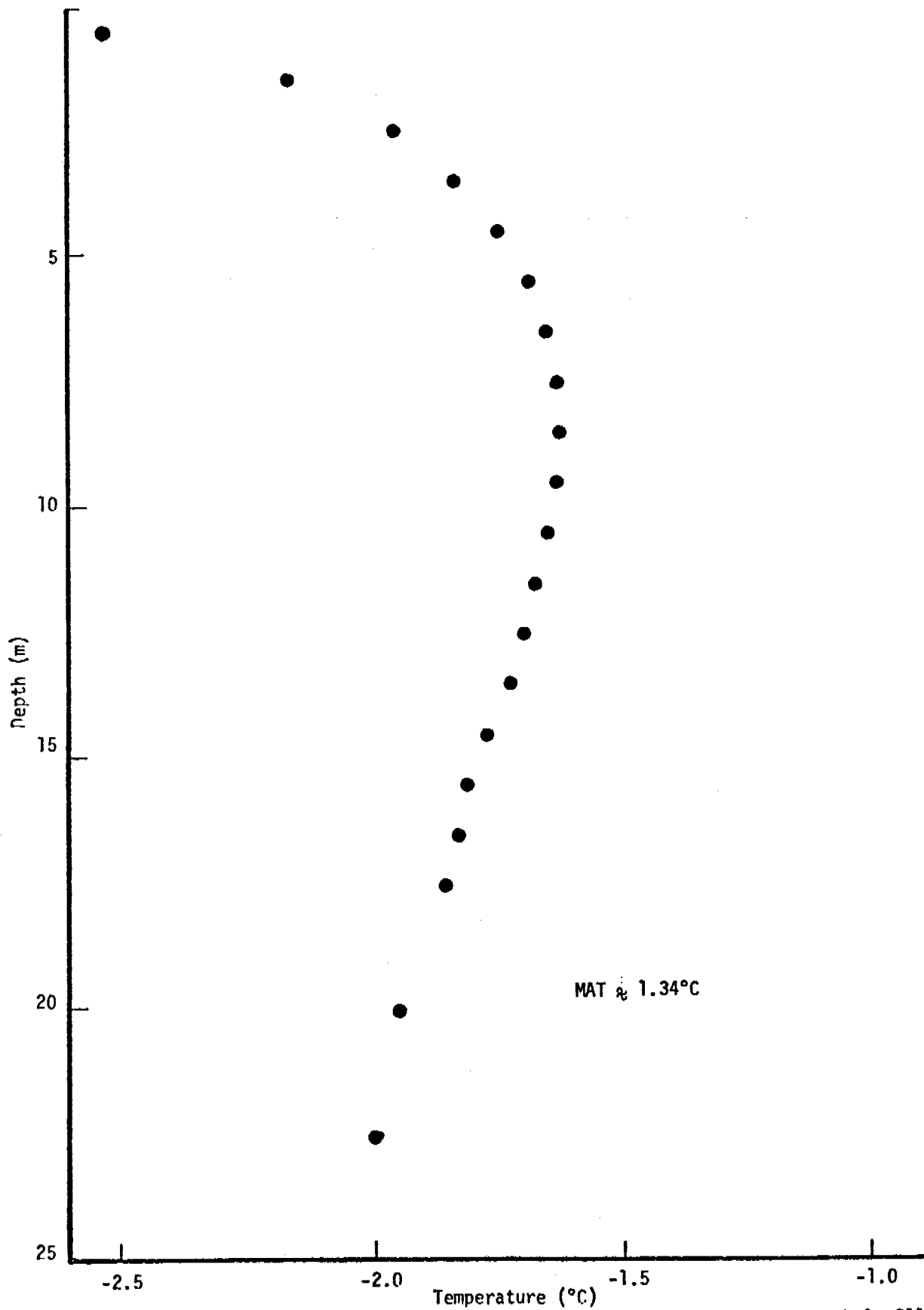


Figure 28: Extrapolated temperature profile for Prudhoe Bay hole 2114.

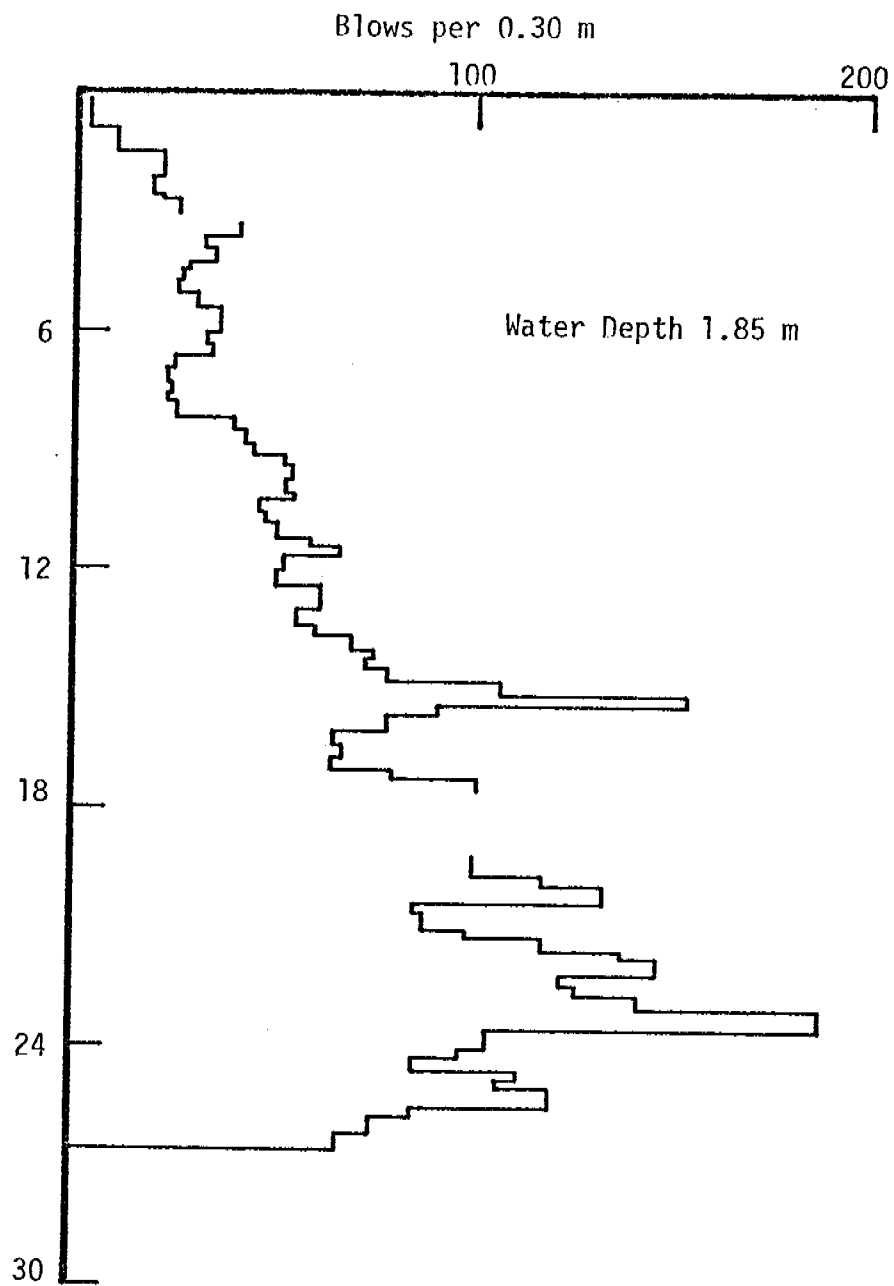


Figure 29: Blow count profile for Prudhoe Bay hole 2114

VIII. CONCLUSIONS

A. Chukchi Sea

These observations give direct evidence of permafrost in near shore areas, and, in some cases, of ice at depth and shoreline recession. In a broad sense they are expected from the onshore data summarized by Hopkins (1976, 1977), especially the sea level history and shoreline retreat rates, from thermal models, and from onshore boreholes (Lachenbruch, 1966). Obviously the subsea permafrost conditions depend on the geologic setting, and will be much different in the bedrock that outcrops at or near the sea bed at Cape Thompson (Scholl and Sainsbury, 1966), and in the sediment, probably thick and frozen at depth, at Rabbit Creek. The latter situation is the more typical. (See AEIDC, 1975, Map 2 for the onshore surficial geology.)

The question of the larger scale distribution of subsea permafrost and its properties in the Chukchi Sea remains open, and we have already summarized and discussed the available indirect information (Harrison and others, 1977). Briefly, because the entire present Chukchi Sea was emergent fairly recently, the possibility exists that some of the permafrost which must have formed there under the cold exposed conditions still exists. The most complete information is available from the southeastern Chukchi Sea, the proposed Hope Basin lease sale area. Seismic measurements and crude thermal models using water temperature and sea level data suggest the permafrost may now be absent below the deeper waters of that region although it may well survive in areas shallower than 15-30 m (see also Hopkins, 1977).

Water of salinity considerably less than sea water is evident in Kotzebue Sound at times of high Noatak River stage (Cederstrom, 1961; Williams and Morris, 1974). Our observations show that it is also evident off Kotzebue village in late winter under the ice when the stage is low.

The mean annual temperature at the sea bed 705 m offshore at NARL and the measured temperature gradient imply a permafrost thickness of ≈ 60 m. This is about twice the thickness predicted on the basis of a stable shoreline model of subsea permafrost (Lachenbruch, 1957).

B. Beaufort Sea

1. Elson Lagoon

Five holes jetted into the sea bed in fine-grained sediment near Tekegakrok Point in Elson Lagoon span the transition from cold, shallow near shore conditions to warmer, deeper conditions where normal sea water salinity is maintained under the sea ice. The presence of ice-bonded, ice-unbonded boundaries in two of the holes, and the temperatures in all of them (which are negative), are the result of rapid shoreline retreat. Interstitial water salinity in at least three of the holes seems to be much greater than that of normal sea water. Permeability values obtained from one hole are 2 or 3 orders of magnitude less than at Prudhoe Bay, indicating that the physical processes that control the evolution of subsea permafrost are probably quite different at the two locations. Thus the physical bases of predictive models, only partially developed so far, are likewise different.

The observations in hole 575 suggest that docks, causeways or islands constructed from local fill material would likely become ice-bonded to 3 or 4 m during the first winter, and therefore resistant to ice forces, although some thawing would of course take place again the following summer. But the high brine concentrations under the ice-bonded layer, which are probably concentrated during the freezing process, will severely reduce the rate of freezing unless some provision is made for their removal.

Harrison Bay

Fine-grained sediments were found in Harrison Bay in a 15 m hole south of Thetis Island, and sands and gravels about 400 m offshore SW of Oliktok. A tentative conclusion is that the sands and gravels characteristic of Prudhoe Bay extend at least as far as the Oliktok hole.

Prudhoe Bay

Extrapolation of temperature data from 2 more holes along the USGS-CRREL-UA study line, at distances 1252 and 2114 m from shore, suggests that ice-bonded permafrost lies at roughly 30 and 40 m respectively.

IX. NEEDS FOR FURTHER STUDY

As noted a year ago, the obvious need of the subsea permafrost assessment program is for more data, considering the 2000 or more km of coast in the Beaufort and Chukchi Seas alone, and the many different geologic settings, oceanographic conditions, and shoreline processes represented. The situation has improved somewhat in the past year with the results described here and those of the other OCSEAP investigators, although several key representative settings remain to be sampled.

A list of some of these settings was given in last year's report. One of the most important is the barrier islands. We hope to probe Stump and Reindeer Islands this summer in close cooperation with the seismic studies of R.U. #271. This should help with the seismic interpretation and extend the meager subsurface data, which so far exists only for Tapkaluk and Reindeer Islands. In 1979 we plan to probe an area of extremely rapid shoreline retreat, probably near Cape Simpson. In our imminent spring 1978 field studies we plan to exploit newly developed probing and jetting techniques in the Barrow and Prudhoe Bay regions, utilizing the latter to obtain information well out on the Beaufort Sea shelf.

Many questions have only been partially studied or not at all. These include the configuration of the ice-bonded subsea permafrost table and base, the ice content of the subsea permafrost, salinity of the ice-bonded subsea permafrost, presence or absence of frozen gas hydrates in the ice-bonded subsea permafrost and the influence of present causeways on the subsea permafrost regime.

The field programs have already supplied enough information that a major effort in interpretation and model development and application is required

beyond the work already accomplished by us and other investigators. We hope to devote more time to this after the 1978 spring and summer field seasons.

Coordination of efforts and synthesis of results with other investigators will continue to be essential. Finally, it should be noted that NSF is now our major source of funding for subsea permafrost research.

X. SUMMARY OF FOURTH QUARTER OPERATIONS

A. Field and Lab Activity and Travel

Dr. Osterkamp attended Barrow synthesis meeting, and both he and Dr. Harrison attended the National Academy of Science permafrost meeting in San Francisco in December.

A paper by Harrison and Osterkamp "Heat and mass transport processes in subsea permafrost I: an analysis of molecular diffusion and its consequences" has been accepted for publication in JGR. Preprints are available upon request.

Our time has been spent in new equipment design, construction and calibration for field use starting in April, and in data reduction and report preparation.

B. Research Administration

No changes anticipated.

C. Funds Expended

\$218,330 as of March 13, 1978.

D. Problems

Coincidence of report and field preparation times.

APPENDIX I

APPENDIX I

Near Shore Steady State Temperature

In the vicinity of a stationary shoreline when the sea bed and emergent land temperatures T_o and T_i are constant in space and time, the resulting steady state temperature distribution T_{ss} is given by

$$T_{ss} = g y + T_i + (T_o - T_i) \left[\frac{1}{2} + \frac{1}{\pi} \tan^{-1} \frac{x}{y} \right] \quad (A-1)$$

where x is the distance from shore, y is the depth below the sea bed, and g is the geothermal gradient (Lachenbruch, 1957). It is assumed that the relief of the sea bed and emergent land surface is small, and that the thermal conductivity is constant. The latter assumption is only a rough approximation in our applications because the sediments on land are frozen, and those near the sea bed are thawed.

A linear approximation of Equation (A-1) is valid for our shallow measurements. It gives

$$T_{ss} \approx T_o + g \left[1 - \frac{L}{x} \right] y$$

where

$$L \equiv \frac{T_o - T_i}{\pi g}$$

The temperature varies linearly with depth y . The term in brackets represents the effect of the nearby land. Evidently it will be negligible for offshore distances x such that $x \gg L$. For $x < L$ the steady state temperature decreases with depth near the sea bed, although at greater depths geothermal heat flow reverses the gradient and temperatures become warmer with depth. Evidently the 0°C isotherm (and therefore by definition permafrost) may be encountered close to shore beneath a sea bed of positive temperature even under steady state conditions. The distance from shore to which permafrost extends under these conditions can be found from Equation (A-1). It will be a maximum when the sea bed temperature is just slightly positive, and will then have the value L . For sea bed temperatures T_o appreciably greater than 0°C this distance will be less than L . Evidently L is a useful parameter for discussing steady state conditions.

g is estimated from a measured value in frozen sediments on shore at Prudhoe Bay of about 0.018 deg m^{-1} (Gold and Lachenbruch, 1973). If the sediment were thawed but the geothermal heat flow were the same, this value would be increased by the ratio of the thermal conductivities of the frozen and thawed sediments, which is about 1.75 (Gold and Lachenbruch, 1973; Harrison and Osterkamp, in press). The resulting value of g is 0.032 deg m^{-1} , which is used in all the applications discussed here.

APPENDIX II

Borehole Temperature Data, 1977

Depths are measured relative to the sea bed. "Extrapolated" or "equilibrium" temperatures are those corrected for the disturbance due to the borehole

Rabbit Creek - Hole 78

Depth (m)	Extrapolated Resistance (Ω)	Extrapolated Temperature ($^{\circ}\text{C}$)
0.66	24,038	-1.576
1.66	23,737	-1.306
2.66	23,360	-0.963
3.66	22,960	-0.591
4.66	22,750	-0.393
5.66	22,520	-0.174
6.66	22,450	-0.106
7.66	22,445	-0.101
8.66	22,505	-0.159
9.66	22,610	-0.260
10.66	22,730	-0.374
11.66	22,920	-0.553
12.66	23,130	-0.750
13.66	23,258	-0.869
14.66	23,360	-0.963
15.66	23,473	-1.066
16.66	23,532	-1.120
17.66	23,618	-1.198
18.36	23,655	-1.232

Cape Blossom - Hole 300

Depth (m)	Measured Resistance (Ω)		Measured Temperature ($^{\circ}\text{C}$)	
	April 28	April 29	April 28	April 29
0.89	23,213	23,205	-0.827	-0.820
1.89	22,583	22,799	-0.234	-0.440
2.89	22,103	22,240	+0.230	+0.097
3.89	21,829	21,888	+0.501	+0.443
4.89	21,665	21,717	+0.665	+0.613
5.89	21,593	21,635	+0.737	+0.693
6.89	21,632	21,631	+0.698	+0.699
7.89	21,705	21,703	+0.625	+0.627
8.19	21,713	-----	+0.617	-----
8.89	-----	21,767	-----	+0.563
9.59	-----	21,820	-----	+0.510

Kotzebue - Hole 310

Depth (m)	Measured Resistance (Ω)		Measured Temperature ($^{\circ}\text{C}$)	
	April 28	April 29	April 28	April 29
0.40	22,703	22.64K	-0.349	-0.030
1.40	22.29K	22,153	+0.048	+0.182
2.40	21,551	21,525	+0.780	+0.806
3.40	21,494	21,126	+0.837	+1.214
4.40	21,064	20,712	+1.278	+1.647
5.40	21,693	20,434	+0.637	+1.943
6.40	20,526	20,242	+1.844	+2.150
7.40	20,494	20,181	+1.879	+2.217
8.40	20.47K	20,174	+1.904	+2.224
10.40	20,575	20,281	+1.792	+2.108
12.40	20,679	20,388	+1.682	+1.992
14.40	20,668	20,453	+1.693	+1.923
16.40	20,752	20,554	+1.604	+1.814
18.40	20,804	20,617	+1.550	+1.747
21.40	21,406	21,094	+0.927	+1.247
23.40	-----	20,726	-----	+1.632
24.40	20,822	-----	+1.531	-----
25.36	20,724	20,718	+1.634	+1.640

NARL - Hole 705

Depth (m)	Extrapolated Resistance (Ω)	Extrapolated Temperature ($^{\circ}\text{C}$)
+ 0.5	24,764	-1.614
1.5	24,560	-1.437
2.5	24,366.5	-1.267
3.5	24,183	-1.105
4.5	24,014	-0.955
5.5	23,929	-0.878
6.5	23,831.5	-0.791
7.5	23,784.5	-0.748
8.5	23,738	-0.706
9.5	23,721.5	-0.691
10.5	23,705.5	-0.676
11.5	23,694.5	-0.666
12.5	23,683.8	-0.657
13.5	23,666.5	-0.641
14.5	23,644.3	-0.621
15.5	23,614	-0.593

Elson Lagoon - Hole 575

Extrapolation of 18 & 28th data

Depth (m)	Extrapolated Resistance (Ω)	Extrapolated Temperature ($^{\circ}\text{C}$)
- 0.02	23.07K	-8.268
+ 0.98	34.22K	-8.358
1.98	32.00K	-6.987
2.98	30.90K	-6.266
3.98	29.52K	-5.319
4.98	29.00K	-4.949
5.98	28,288	-4.429
6.98	28,352	-4.477
7.98	28,643	-4.690
8.98	28,892	-4.871
9.98	29,109	-5.027
10.98	29,294	-5.159
11.98	29,438	-5.261
12.98	29,578	-5.360
13.98	29,672	-5.426
14.98	29,758	-5.486
15.98	29,860	-5.557
16.98	29,929	-5.605
17.98	30,030	-5.675
18.64	30,114	-5.733
18.81	30,185	-5.782

Elson Lagoon - Hole 611

Depth (m)	Extrapolated Resistance (Ω)	Extrapolated Temperature ($^{\circ}\text{C}$)
0.43	25,515	-2.251
1.43	25,517	-2.253
2.43	25,635	-2.351
3.43	25,692	-2.398
4.43	26,010	-2.659
5.43	26,250	-2.854
6.43	26,435	-3.003
7.43	26,932	-3.397
8.43	27,383	-3.747
9.43	27,766	-4.039
10.43	28,103	-4.292
11.43	28,241	-4.394
12.43	28,455	-4.552
13.43	28,586	-4.649
14.43	28,702	-4.733
15.43	28,845	-4.837
16.43	28,949	-4.912
17.43	29,112	-5.029
18.43	29,243	-5.123
19.23		
19.43		
19.95		

Elson Lagoon - Hole 798

Depth (m)	Extrapolated Resistance (Ω)	Extrapolated Temperature ($^{\circ}\text{C}$)
0.23	25,192	-1.980
1.23	25,118	-1.917
2.23	25,009	-1.824
3.23	24,948	-1.772
4.23	24,922	-1.750
5.23	24,919	-1.747
6.23	24,966	-1.787
7.23	25,095	-1.897
8.23	25,286	-2.059
9.23	25,501	-2.239
10.23	25,781	-2.472
11.23	25,971	-2.628
12.23	26,093	-2.727
13.23	26,215	-2.826
14.23	26,330	-2.919
14.58	26,335	-2.923

Elson Lagoon - Hole 1036

Depth (m)	Extrapolated Resistance (Ω)	Extrapolated Temperature ($^{\circ}\text{C}$)
0.68	25,078	-1.918
1.68	24,946	-1.883
2.68	24,843	-1.770
3.68	24,744	-1.682
4.68	24,681	-1.597
5.68	24,641	-1.542
6.68	24,676	-1.507
7.68	24,736	-1.538
8.68	24,802	-1.590
9.68	24,874	-1.647
10.68	24,970	-1.709
11.68	25,034	-1.791
12.68	25,100	-1.845
13.68	25,168	-1.902
14.68	25,240	-1.959
15.68	25,316	-2.020
16.72	25,394	-2.084
		-2.150

Elson Lagoon - 1466

Depth (m)	Measured Temperature (°C) May 18	Extrapolated Temperature (°C)
+ 0.81	-1.561	-1.701
1.81	-1.491	-1.631
2.81	-1.342	-1.482
3.81	-1.237	-1.377
4.81	-1.170	-1.310
5.81	-1.136	-1.276
6.81	-1.140	-1.280
7.81	-1.166	-1.306
8.81	-1.185	-1.325
9.81	-1.223	-1.363
10.81	-1.257	-1.397
11.81	-1.294	-1.434
12.81	-1.328	-1.468
13.81	-1.373	-1.513
14.81	-1.411	-1.551
15.81	-1.443	-1.583
16.81	-1.486	-1.626
17.81	-1.523	-1.663
18.81	-1.562	-1.702
19.81	-1.599	-1.739
19.87	-1.603	-1.743

Harrison Bay - Hole south of Thetis Island

Depth (m)	Measured Resistance (Ω)			Measured Temperature ($^{\circ}\text{C}$)		
	May 1-18:45	May 2-09:23	May 2-12:56	May 1-18:45	May 2-09:23	May 2-12:56
0.16	24.38K	24.45K	24.62K	-1.878	-1.939	-2.087
1.16	23.97K	24.07K	24.05K	-1.453	-1.605	-1.587
2.16	23.45K	23.72K	23.75K	-1.046	-1.291	-1.318
3.16	23.26K	23.43K	23.43K	-0.871	-1.027	-1.027
4.16	23,094	23,263	23,277	-0.717	-0.874	-0.887
5.16	23,017	23,139	23,131	-0.645	-0.759	-0.751
6.16	22,970	23,089	23,085	-0.601	-0.712	-0.708
6.86	22,899	-----	-----	-0.534	-----	-----
7.16	22,893	23,063	23,063	-0.529	-0.688	-0.688
8.16	22.82K	23,055	23,056	-0.460	-0.680	-0.681
9.16	22,893	23,093	23,095	-0.529	-0.716	-0.718
10.16	22,971	23,126	23,126	-0.602	-0.747	-0.747
11.16	22,926	23,129	23,129	-0.560	-0.749	-0.749
12.16	22,908	23,134	23,135	-0.543	-0.754	-0.755
13.16	22,910	23,144	23,148	-0.545	-0.763	-0.767
14.16	22,821	23,140	23,144	-0.461	-0.760	-0.763
14.61	-----	23,157	23,157	-----	-0.775	-0.775
14.84	22,942	-----	-----	-0.575	-----	-----

Harrison Bay - Oliktok hole

Depth (m)	Measured Resistance (Ω) May 10	Measured Temperature ($^{\circ}\text{C}$) May 10
0.97		-3.021
1.97		-2.479
2.97		-1.898
3.97		-1.717
4.97		-1.591
5.97		-1.524
6.97		-1.484
7.62		-1.480

Prudhoe Bay - Hole 1252

Depth (m)	Measured Resistance (Ω)		Measured Temperature ($^{\circ}\text{C}$)	
	May 6-08:20	May 6-15:10	May 6-08:20	May 6-15:10
+ 0.37	25.08K		-2.481	
0.66		24.93K		-2.354
1.37	24.88K		-2.311	
1.66		24,687		-2.154
2.37	24,556		-2.032	
2.66		24,432		-1.924
3.37	24,347		-1.849	
3.66		24,236		-1.752
4.37	24,168		-1.692	
4.66		24,097		-1.629
5.37	24,054		-1.591	
5.66		24,001		-1.544
6.37	23,974		-1.519	
6.66		23,990		-1.534
7.37	23,969		-1.515	
7.66		23,965		-1.511
8.37	23,963		-1.510	
8.66		23,962		-1.509
9.37	23,974		-1.519	
9.66		23,985		-1.529
10.37	24,009		-1.551	
10.66		24,024		-1.564
11.37	24,062		-1.598	
11.66		24,067		-1.602
12.37	24,102		-1.633	
12.57	24,139		-1.666	
12.66				-1.639
12.88		24,108		
13.84		24,156		-1.681
14.16	24,162		-1.686	

Prudhoe Bay - 2114

Depth (m)	Extrapolated Resistance (Ω)	Extrapolated Temperature ($^{\circ}\text{C}$)
- 0.44		
0.56	25,135	-2.527
1.56	24,715	-2.169
2.56	24,476	-1.962
3.56	24,338	-1.841
4.56	24,239	-1.754
5.56	24,167	-1.690
6.56	24,127	-1.655
7.56	24,103	-1.634
8.56	24,095	-1.627
9.56	24,106	-1.636
10.56	24,123	-1.651
11.56	24,152	-1.677
12.56	24,178	-1.700
13.56	24,209	-1.728
14.56	24,263	-1.775
15.56	24,307	-1.814
16.56	24,328	-1.832
17.56	24,358	-1.859
20.06	24,464	-1.951
22.56	24,521	-2.001
24.96	24,596	-2.066

REFERENCES

- Black, R. F., 1964, Gubik Formation of Quaternary Age in Northern Alaska, U.S.G.S. Professional Paper 302-C, p. 59-91.
- Brewer, M. C., 1958, Some results of geothermal investigations of permafrost in Northern Alaska, Transactions American Geophysical Union, Vol. 39, No. 1, p. 19-26.
- Cedarstrom, D. J., 1961, Origin of a salt-water lens in permafrost at Kotzebue, Alaska, Geological Society of America Bulletin, Vol. 72, p. 1427-1432.
- AEIDC, 1975, Chukchi Sea: Bering Strait-Sky Cape. Physical and biological character of Alaskan coastal zone and marine environment, University of Alaska Sea Grant Report, No. 75-10.
- Gold, L. W., and A. H. Lachenbruch, 1973, Thermal conditions in permafrost—a review of North American literature, Proceedings of the research international conference in permafrost, North American contribution, National Academy of Sciences, p. 3-25.
- Harrison, W. D., P. D. Miller and T. E. Osterkamp, 1977, Permafrost beneath the Chukchi Sea—preliminary report, In OCSEAP Annual Report, by W. D. Harrison and W. D. Harrison, 1977, Appendix II.
- Harrison, W. D., and T. E. Osterkamp, in press, Heat and mass transport processes in subsea permafrost I: An analysis of molecular diffusion and its consequences, Journal of Geophysical Research.
- Hopkins, D. M., 1976, Shoreline history as an aid to predicting offshore permafrost conditions, OCSEAP Quarterly Report, Oct. 1-Dec. 31, 1976, R.U. 473.
- Hopkins, D. M., 1977, Coastal processes and coastal erosion hazards to the Cape Krusenstern archaeological site, U.S.G.S. Open file report 77-32.
- Hunter and others, 1976, The occurrence of permafrost and frozen sub-seabottom materials in the southern Beaufort Sea, by J. A. M. Hunter, A. S. Judge, H. A. MacAulay, R. L. Good, R. M. Gagne, and R. A. Burns, Beaufort Sea Project Technical Report *22, Department of the Environment, Victoria, B. C., Canada.
- Lachenbruch, A. H., 1957, Thermal effects of the ocean on permafrost, Bulletin of the Geological Society of America, Vol. 88, p. 1515-1530.
- Lachenbruch and others, 1962, Temperatures in permafrost by A. H. Lachenbruch, M. C. Brewer, G. W. Greene and B. V. Marshall, In "Temperature—its measurement and control in science and industry", Vol. 3, Part 1, p. 791-803, Reinhold Publishing Corp., New York.
- Lachenbruch and others, 1966, Permafrost and the geothermal regimes, by A. H. Lachenbruch, G. W. Greene, and B. V. Marshall, In "Environment of the Cape Thompson Region, Alaska, 1966", Chapter 10, p. 149-165.

- Lachenbruch, A. H. and Marshall, B. V., 1977, Sub-sea temperatures and a simple tentative model for offshore permafrost at Prudhoe Bay, Alaska, U.S.G.S. Open File Report 77-395.
- Lewellen, R. I., 1973, The occurrence and characteristics of nearshore permafrost, northern Alaska, Permafrost: The North American Contribution to the Second International Conference, National Academy of Sciences, Washington, D. C.
- Lewellen, R. I., 1974, Offshore permafrost of Beaufort Sea, Alaska, In "The coast and shelf of the Beaufort Sea", Proceedings of a symposium on Beaufort Sea Coast and Shelf Research, J. C. Reed and J. E. Sater, Editors, Arctic Institute of North America.
- Lewellen, R. I., 1976, Subsea permafrost techniques, Symposium on research techniques in coastal environments, Louisiana State University, Baton Rouge, Louisiana.
- Osterkamp, T. E., and W. D. Harrison, 1976a, Subsea permafrost at Prudhoe Bay, Alaska: Drilling report, University of Alaska Geophysical Institute Report UAG R-245, Sea Grant Report 76-5.
- Osterkamp, T. E., and W. Harrison, 1976b, Subsea permafrost: its implications for offshore resource development, The Northern Engineer, Vol. 8, No. 1, p. 31-35.
- Osterkamp, T. E., and W. D. Harrison, 1977, Sub-sea permafrost regime at Prudhoe Bay, Alaska, U.S.A., Journal of Glaciology, Vol. 19, No. 81, p. 627-637.
- Rogers, J. C. and others, 1975, Nearshore permafrost studies in the vicinity of Point Barrow, Alaska, University of Alaska, Geophysical Institute Report UAG R-237, Sea Grant Report 75-6.
- Scholl, D. W., and C. L. Sainsbury, 1966, Marine geology of the Ogotoruk Creek area, In "Environment of Cape Thompson Region, Alaska, 1966, pp. 787-806.
- Williams, J. R. and D. A. Morris, 1974, Water resources of the Kotzebue area, northwestern Alaska, U.S.G.S. administrative report prepared in cooperation with the State of Alaska Department of Natural Resources, Anchorage, Alaska, Report for administrative release only, Subject to revision.

Annual Report

Contract #03-5-022-55
Research Unit #271
Reporting Annual Report
Period: Period Ending
April 1, 1978
Number of Pages: 38

BEAUFORT SEACOAST PERMAFROST STUDIES

J.C. Rogers and J.L. Morack
Geophysical Institute
University of Alaska
Fairbanks, Alaska 99701
(907) 272-5522

April 1, 1978

TABLE OF CONTENTS

I	Summary
II	Introduction
III	Current State of Knowledge
IV	Study Area
V	Sources and Methods of Data Collection
VI	Results
VII	Discussion
VIII	Conclusions
IX	Needs for Further Study
X	Summary of Fourth Quarter Activities
	References for Annual Report

I. SUMMARY

The objective of this study is to develop an understanding of the nature and distribution of permafrost beneath the ocean and barrier islands along the Alaskan Beaufort Sea Coast. Several general statements can be made regarding the distribution of offshore permafrost on the Alaskan Shelf of the Beaufort Sea. Three principal points discussed at the Barrow Synthesis Meeting in January, 1978, can be listed as bounds on the distribution.

On the basis of bathymetry and sea level history:

(1) Shallow, inshore areas where ice rests directly on the sea bottom are underlain at depths of a few meters by ice-bonded equilibrium permafrost. Ice-rich permafrost must be anticipated where ever the water is less than 2 m deep.

(2) Ice-bonded permafrost was once present beneath all parts of the continental shelf exposed during the last low sea level interval, and consequently relict ice-bonded permafrost may persist beneath any part of the shelf inshore from the 90 m isobath. Observed depths to relict permafrost off the Alaskan coast range from 10 m or less to depths greater than 100 m. Similar depth data gathered along the Canadian coast range from 10 m to 250 m.

(3) Ice-bonded permafrost is probably absent from parts of the Beaufort Sea shelf seaward from the 90 m isobath, although subsea temperatures are probably below 0 C.

In addition to these general guidelines, some specific conclusions resulting from the current studies can be listed along with their possible implication to offshore oil and gas development:

a. From (2) above, we conclude that in some offshore areas, it should be

possible to bury hot oil pipelines beneath the ocean at distances from shore where the depth of ice-bonded and ice-rich permafrost precludes thermal destruction by the pipeline. Such burial could provide protection from ice gouging.

In near shore areas where permafrost can be ice-rich and within a few meters of the ocean bottom, it may be necessary to construct surface causeways for hot oil pipelines to bridge the shallow permafrost zone.

b. Seismic studies outside of the barrier islands have shown that the depths to ice-bonded permafrost are not simply related to their distance from shore. In the Prudhoe Bay area shallow ice-bonded materials have been mapped offshore while nearer to shore these materials are considerably deeper.

c. The barrier islands are not uniformly underlain by ice-bonded permafrost. Areas with no ice bonding have been observed. In these cases, it should be possible for hot oil gathering lines to cross the island areas with no adverse effects from ice-bonded materials.

d. Also from (2) above, we conclude that cold gas lines can be buried in the offshore regions where a non-frozen layer exists but that the problem of freeze-back must be dealt with. The presence of salt brine complicates this problem beyond the onshore freezing problem.

e. Former thaw lakes which contribute to the variability of the upper permafrost surface can be found in subsea permafrost of land origin. It may be possible to utilize these areas for offshore structures and avoid ice-bonded materials if desired.

II. INTRODUCTION

A. General Nature and Scope

The known oil reserves along the Beaufort Sea coast coupled with a national need to develop these resources have focused attention on the distribution and character of permafrost in that area. Of particular concern to this project is the comparatively unknown areas offshore and along the barrier islands. Recently priorities have been established for attacking the problem area and a high priority was established for mapping the distribution of offshore permafrost.

This study of coastal offshore permafrost which utilizes seismic refraction techniques to probe the ocean bottom along the Alaskan Beaufort Sea coast was initiated in April of 1975. It will provide information relevant to task D-8 in NOAA's proposal to BLM.

B. Specific Objectives and Relevance to Problems of Petroleum Development

The most important parameter to be determined in this study is the distribution of offshore permafrost. Also, the depth to the top of the bonded permafrost beneath the ocean floor is to be determined. Using the equipment purchased by the program, data are being gathered which are of immediate practical value in determining the distribution and nature of offshore permafrost. An objective is compilation of the above parameters for use by other principal investigators and appropriate agencies and industries.

The distribution study has focused primarily on the Prudhoe Bay area with secondary emphasis at Point Barrow. The truncation of permafrost beneath the ocean is of interest, particularly the shape of the frozen-nonfrozen boundary.

Thus, the second major objective is the determination of the shape of the boundary. One important facet of this objective is determining the nature and extent of permafrost beneath the barrier islands. These results will provide valuable information for refinement and testing of thermal models as well as for determining operational methods for offshore oil and gas development.

The third major objective is to provide information to support reconnaissance drilling programs including those of the University of Alaska, CRREL, and the USGS. Drilling provides information on bottom conditions only near the drill hole. It is possible, using the seismic technique, to extend such site specific information to areas remote from the drill site, by correlating seismic data at the drill site and at the remote locations. Also, seismic information can be used to suggest areas for future drilling investigations.

Specific and detailed relevance to problems of offshore petroleum development have been addressed in the synthesis document developed by the Earth Science Study Group at Barrow in January, 1977. The reader is referred to the section on permafrost-induced problems from that report.

III. CURRENT STATE OF KNOWLEDGE

Permafrost, which commonly occurs in high latitudes and altitudes on the earth, also exists beneath the sea floor along the Arctic Coast. At this time, although relatively little is known about offshore permafrost properties including its distribution and the dynamics of its formation and destruction, definite progress is being made. Several of the problem areas needing investigation have recently been discussed in "Priorities for Basic Research on Permafrost" and also in a position paper for the National Science Foundation

titled: "Problems and Priorities in Offshore Permafrost."

The existence of offshore permafrost which has long been suspected as the result of ocean transgression upon land permafrost in northern latitudes is now a demonstrated fact. Lachenbruch (1957, 1968) discusses relict permafrost which can take thousands of years to dissipate.

More recently, permafrost has been reported beneath the Canadian Beaufort Sea (Hunter, 1974; Hunter et al., 1976) and beneath the water of Prudhoe Bay, Alaska (Osterkamp and Harrison, 1976, 1977). Some of the physical processes involved in the degradation of relict permafrost are beginning to be understood and it is clear that in addition to temperature, the porosity of the sediments and the salinity of the interstitial liquids are important. Current data are available in the annual reports of research units 253, 255, 256, by Harrison and Osterkamp. Some details of the processes involved are also found in Harrison and Osterkamp (1976). The results reported in this report are in agreement with the drilling results obtained by the Joint USACRREL/USGS drilling program (R.U. 105) as reported by Sellman et al. (1976). Later in this report a close correlation between their drilling and the geophysical results is shown. Also, the geophysical results are in agreement with those of Osterkamp and Harrison. From their records and the seismic records presented in the following sections, it is clear that offshore permafrost which is ice-bonded exists in the Prudhoe Bay area and on some offshore islands. The distribution of this permafrost and the depth of its upper surface are currently known along several transects made both inside and outside of the barrier islands. Aerial distribution and depth information remain to be determined although it is possible to make some general statements regarding offshore permafrost. (See the summary section of this report.)

IV. STUDY AREA

The principal area investigated during the last year is shown in Figure 4. During the summer work season ice conditions were often not favorable to marine work during the available field period. Therefore, the data are somewhat limited in geographical extent and in general the northernmost excursion along the data lines was limited by the presence of ice.

V. SOURCES AND METHODS

Shallow seismic refraction techniques have been documented by Dobrin (1975) and their application to the detection of sub-sea permafrost has also been described (Hunter, 1974; Hunter and Hobson, 1974). The seismic refraction data taken in and near Prudhoe Bay were collected using two 40 cubic inch air guns as an acoustic source and the refracted signal was detected along a 480 m hydrophone line towed behind the USGS vessel "Karluk." The air guns were fired simultaneously and the 24 channels of hydrophone output were recorded in analog form by a chart recorder and on magnetic tape. These data were gathered at several points along the ship transects, scaled and reduced to time-distance plots. Over 200 of these plots were made last season and several of these are shown in a later section.

Refraction data taken on offshore islands near Prudhoe Bay consisted of six channels taken on a digital enhancement hammer seismograph. The data are read from the seismograph and also reduced to time-distance plots.

Finally, the inverse slopes of the time-distance plots are used to determine seismic velocities in the sub-bottom material, depths to the layers, and the velocities are then used to determine whether the bottom materials are frozen. Permafrost velocities are typically between 2500 m/s and 3000 m/s while similar materials in the nonfrozen state typically have velocities

ranging from 1600 m/s to 2000 m/s (Rogers et al., 1975). Significant velocity contrasts such as these, which are typical of coarse sandy materials, allow easy classification of materials into the frozen or unfrozen state.

VI. RESULTS AND VII DISCUSSION

Several kinds of data have been gathered in the study of offshore permafrost including marine seismic refraction and reflection as well as seismic studies on some barrier islands. These data coupled with the results of geophysical investigation by others provide a better understanding of the character and distribution of offshore permafrost than has previously existed.

In this section we distinguish between permafrost as given by the thermal definition: material whose temperature has remained below 0 C for two or more years in succession (Lachenbruch, 1968) and ice-bonded permafrost: material whose physical characteristics are dominated by the freezing and bonding action of interstitial fluid. It also appears useful to introduce the distinction between ice bearing permafrost (material below 0 C with ice and fluid in the interstices) and ice-bonded permafrost. Since the seismic methods used depend primarily on the bonding effects for velocity enhancement, it is possible and indeed seems to be the case, that one can find small amounts of ice during drilling but observe no seismic velocity enhancement.

Offshore Island Studies

Seismic refraction studies were conducted during the summer of 1977 on two offshore islands along the Beaufort Sea coast near Prudhoe Bay. The experimental techniques and equipment used on Cross Island and Stump Island were similar to those used in earlier work (Rogers et al., 1975; Rogers and Morack, 1977). Areas underlain by both frozen and unfrozen material were

located on the islands.

Cross Island

Figure 1, showing Cross Island, indicates the site of refraction studies during August of 1977. Data collected on the island in 1976 was extended to the westward. Approximate locations of seismic lines are shown on the figure. Their orientations, which were established with a compass, are approximate. A summary of the maximum velocities measured is presented in Table I along with calculated values of the depths observed to the high velocity layer.

TABLE I

Line Number	Maximum Velocity m sec ⁻¹	Depth to Maximum Velocity Layer m
1	2448	1.7
2	1478	none
3	1982	none
4	2179	1.1
5	2190	1.0
6	2294	.9
7	2344	1.3
8	3030	1.5
9	3371	1.8
10	1887	none

As in earlier work the lines (8,9) near the grassy area on the island produced high velocities indicative of ice-bonded materials, while the remainder showed lower velocities. A few lines (1,6,7) produced intermediate velocities, that could possibly be attributed to ice-bearing sandy gravels that are not ice bonded, but are perhaps partially frozen. The lines showing ice-bonded materials (8,9) give depths of 1.5 and 1.8 m respectively. These

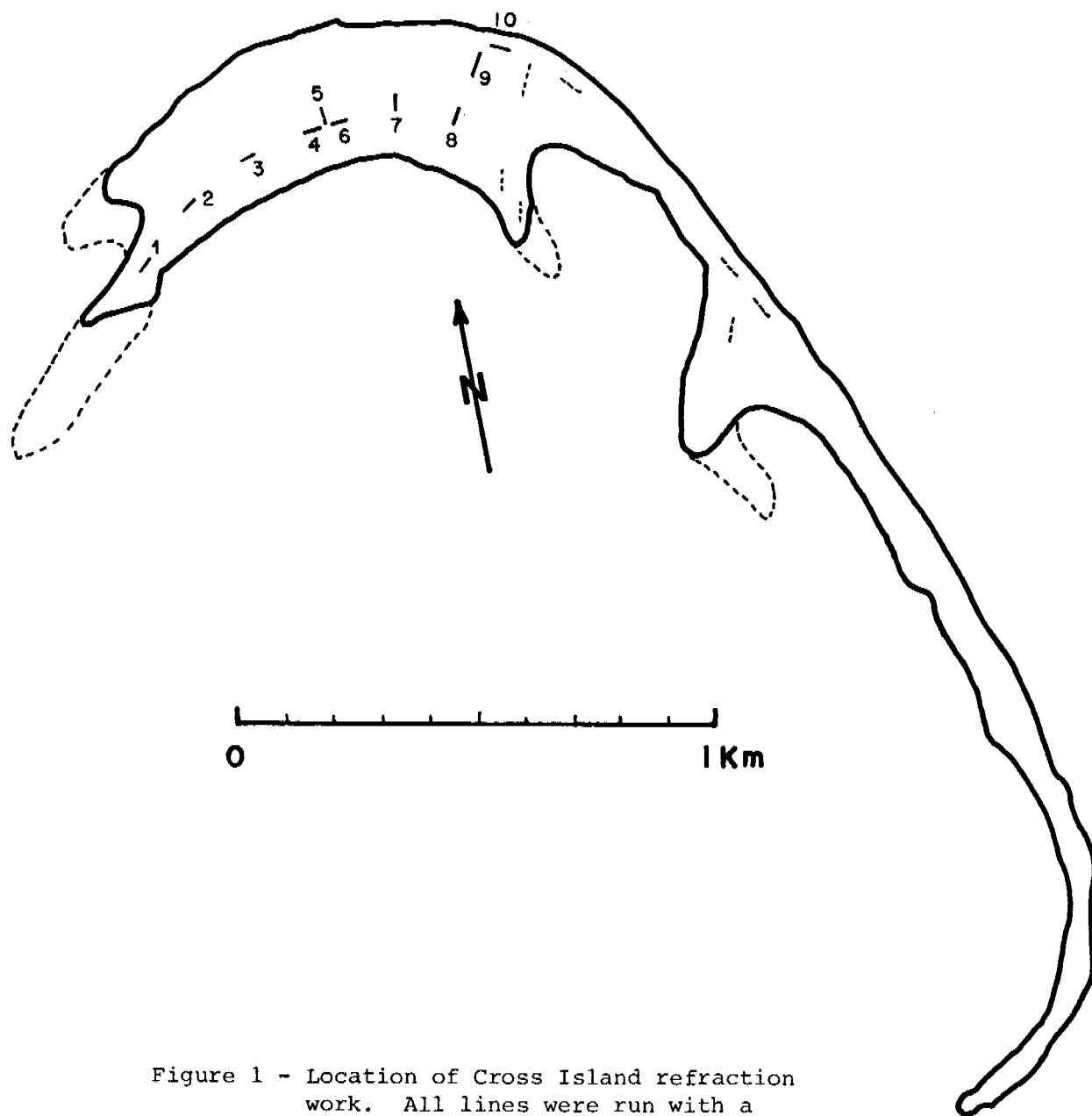


Figure 1 - Location of Cross Island refraction work. All lines were run with a hammer enhancement seismograph. Only lines 8 and 9 displayed high velocities (>3000 m sec $^{-1}$) indicating ice-bonded material. The seismic lines shown as dashed lines in the figure are from the 1977 field season. The lines in the vicinity of lines 8 and 9 also showed high velocity material.

depths are similar to those observed on islands and spits near Barrow as well as to earlier observation on Cross Island. In these cases vegetation is associated with shallow ice-bonded materials and nonvegetated areas considerably removed are found not to be ice-bonded.

In all cases to date the ice-bonded materials observed are at depths considerably less than the 10 to 15 m resolution limit of the hammer seismograph. Materials subject to possible annual freezing and thawing are on the order of a meter or so beneath the island and would easily be observed with the hammer seismograph equipment. Frozen materials that are below the resolution depth of the hammer seismograph are relict in origin and are not associated with annual freezing and thawing. Thus observation of slow velocities on Cross Island indicates the absence of bonded materials over a large portion of the island. This feature is significant from the standpoint of construction on the island.

Stump Island

Figure 2 shows Stump Island which lies about 1 km offshore from Point McIntyre near Prudhoe Bay. Because of its near shore location and the shallow water (less than 2 m deep) between the island and shore, one would expect to find ice-bonded permafrost under the island from earlier times when the island was part of the main land.

A total of 15 seismic lines were taken on the island using the methods discussed earlier. These lines are also shown on Figure 2 and give an excellent coverage of the island. As expected all the lines except one (line 1) give high velocities indicative of ice-bonded materials. Figure 3 summarizes the velocity and depth information found on the island. The velocities shown for lines 6, 10 and 14 are slightly below those expected for

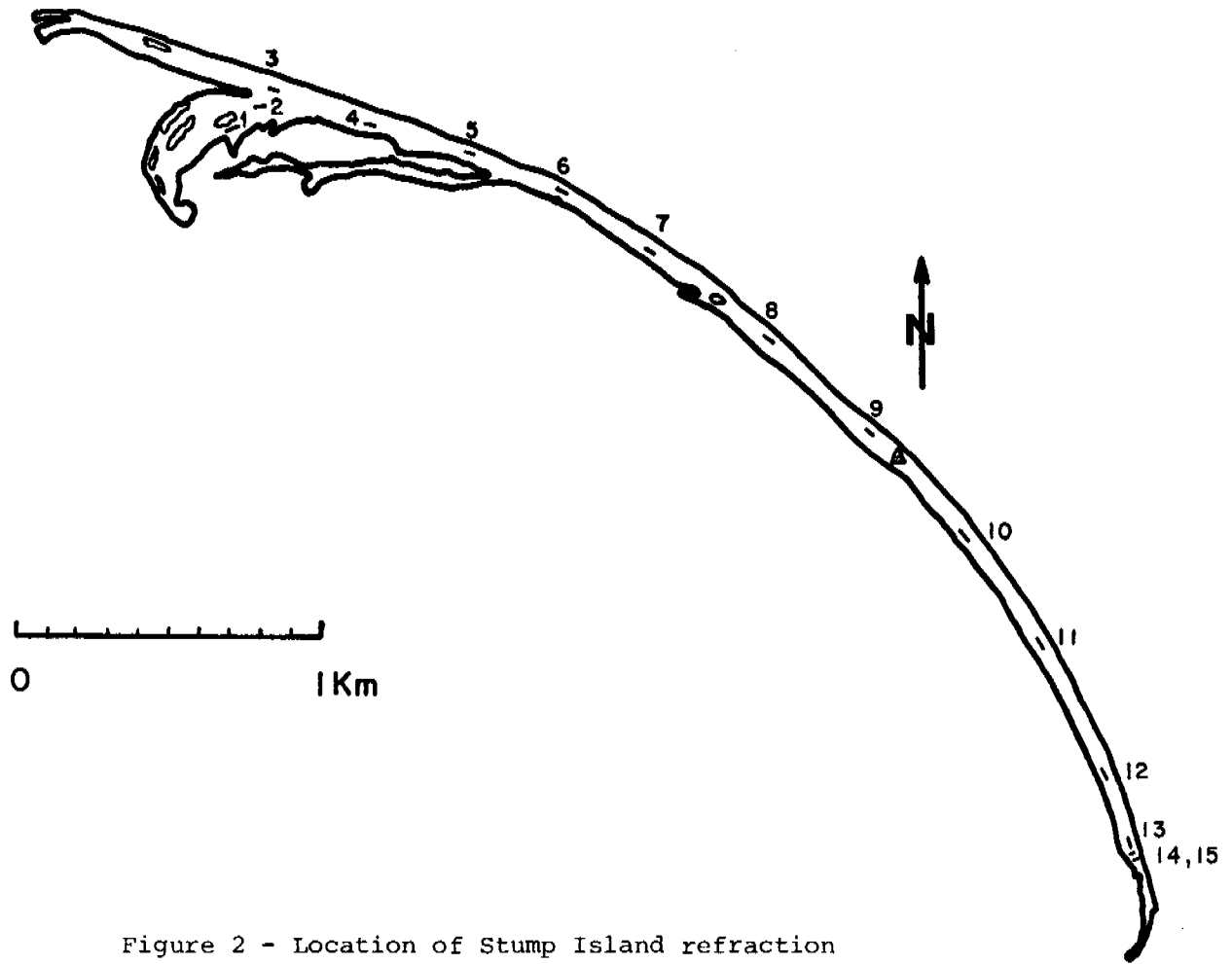


Figure 2 - Location of Stump Island refraction work. All lines were run with a hammer enhancement seismograph. All lines except line 1 showed high velocity material.

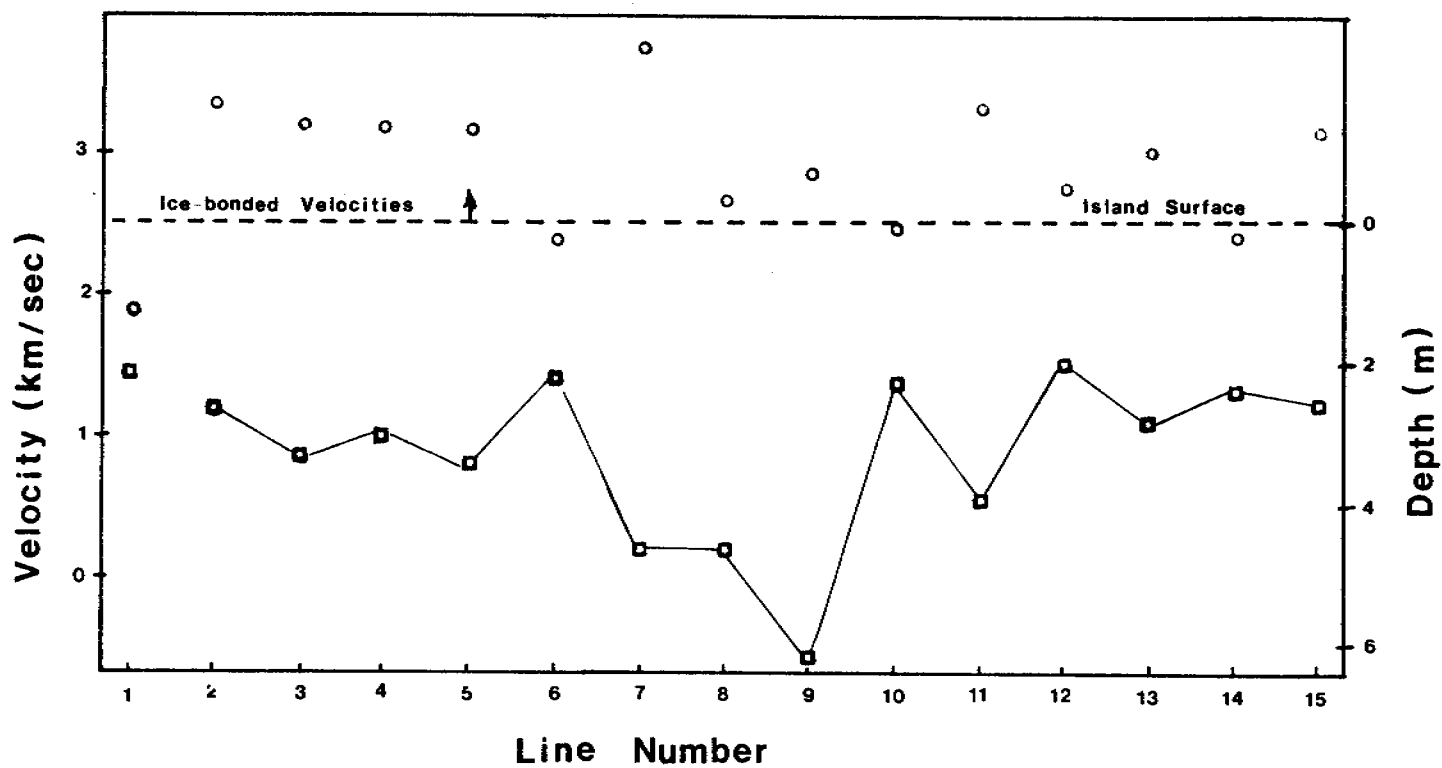


Figure 3 - Velocity and depth data from Stump Island.

The \circ points indicate the velocities of buried layers. Velocities greater than 2.5 km sec^{-1} indicate ice-bonded materials.

The \square points indicate the depth of the ice-bonded surface.

ice-bonded materials, but is easily explained by the layer dipping a few degrees as is the excessively high velocity of line 7. The velocity measured in line 1 is too low to be explained by the layer dipping.

Marine Refraction Studies - Prudhoe Bay Area

Figure 4, a map of the Prudhoe Bay Area, indicates several vessel tracks where the USGS vessel "Karluk" towed the refraction streamer. Approximately 150 km of line have been run in this area. Also shown on the figure are the locations of several drill holes identified as PB-1, PB-8, etc. which were drilled by other OCS investigators (Osterkamp and Harrison, CRREL/USGS).

Several locations of the refraction lines have been cross hatched to indicate location of ice-bonded permafrost identified with the seismic refraction equipment. Depths in meters from the ocean surface to the top of the permafrost are indicated with small numbers by the lines. In general very near shore areas (within one kilometer or so) are underlain by ice-bonded materials from depths of a few meters to depths up to 40 meters, the approximate depth limitation of the refraction equipment. This depth limitation is the result of limited seismic energy from the air gun sources. One line (A-A') which extends from the west ARCO dock to a point just west of Reindeer Island has been used to obtain seismic reflection data on the depth to the top of the ice-bonded layer.

Figure 5 is a vertical section of a line extending from the west ARCO dock to drill hole PB-2. Several data have been plotted on this figure including refraction data, reflection data and drill data. The seismic data were compiled from lines A-A', E-E' and G-G' and were projected onto the vertical section along with the drilling information. There is good general

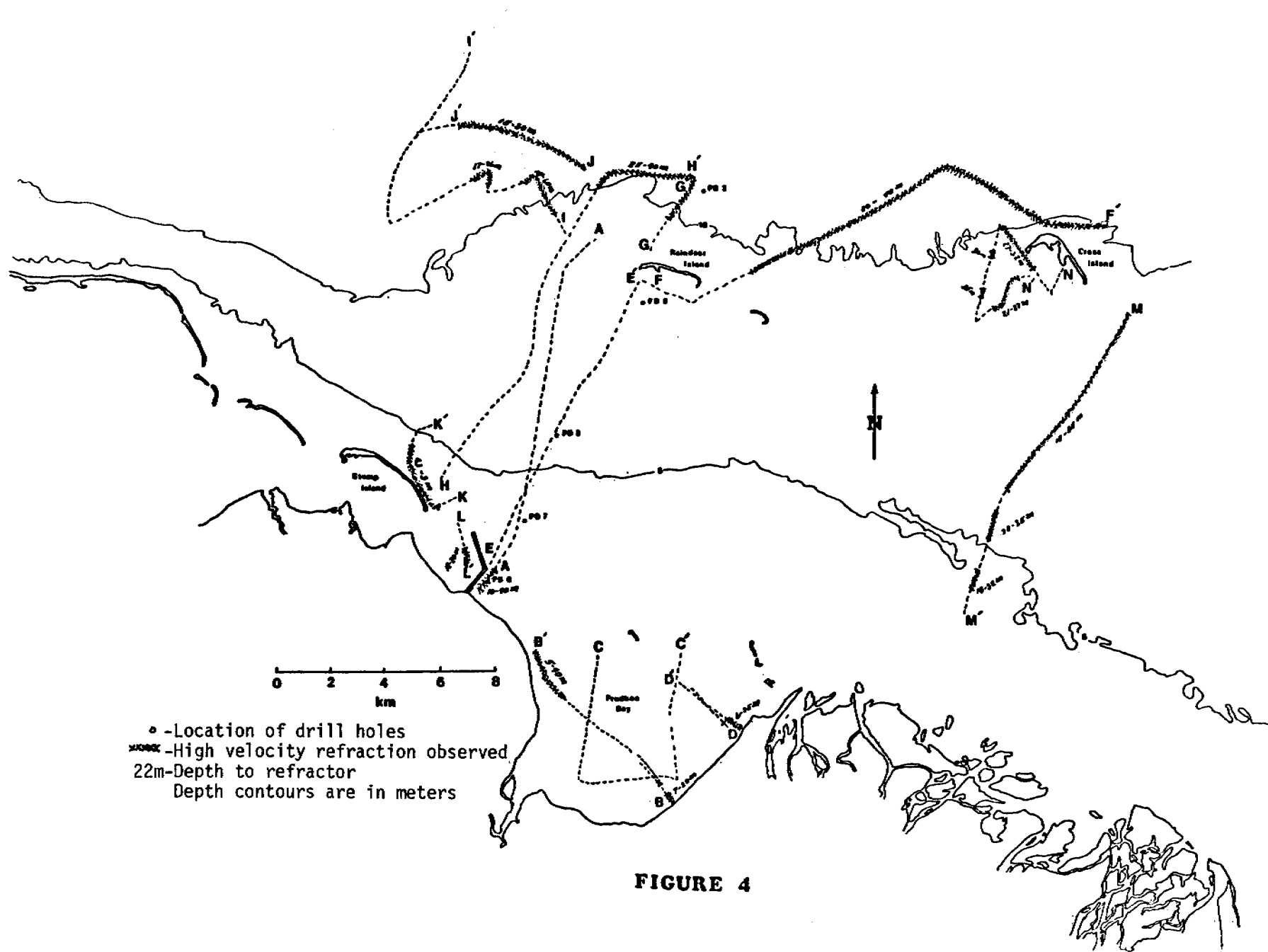


FIGURE 4

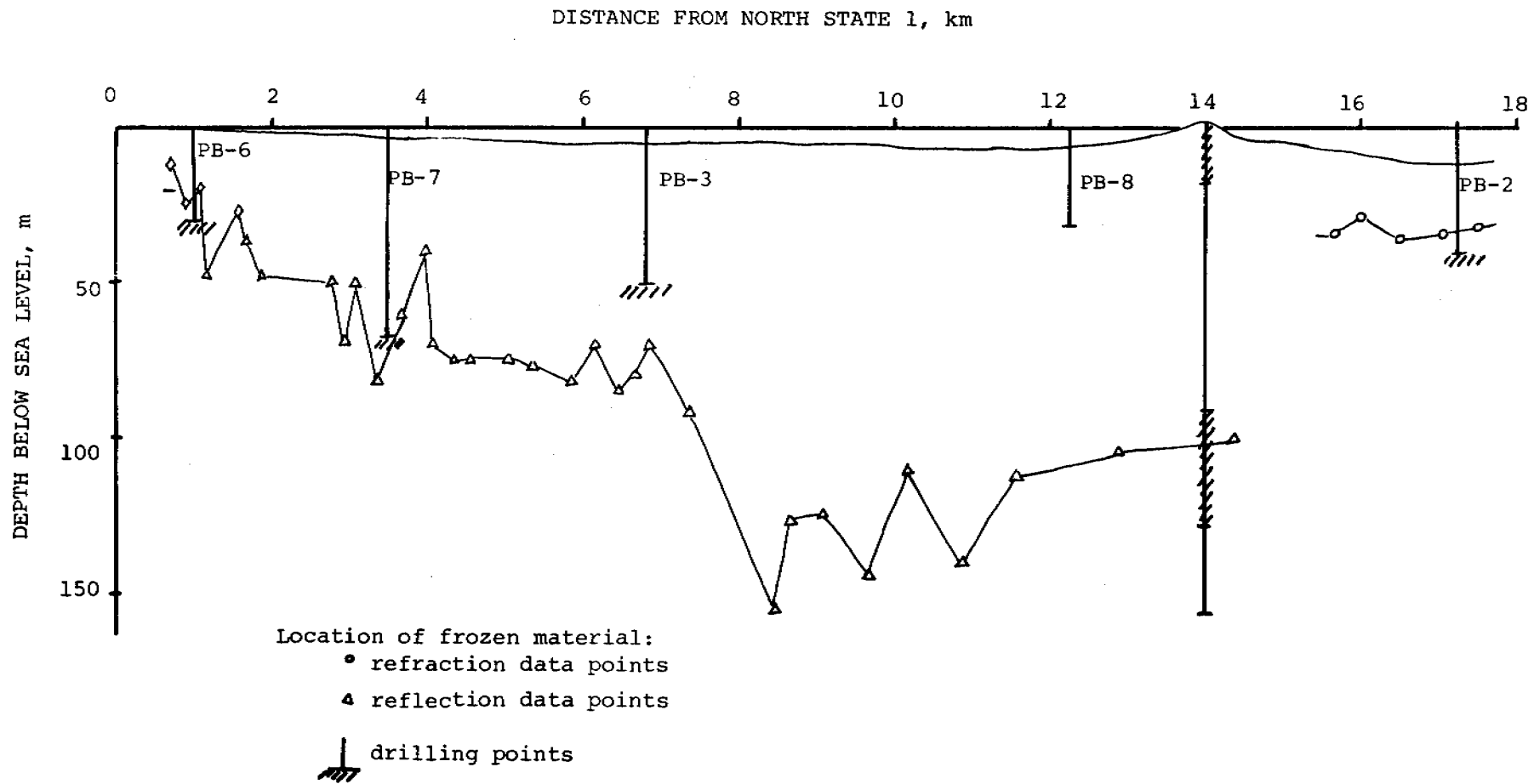


Figure 5 - Vertical section from new ARCO dock through Reindeer Island.

agreement with the drilling and seismic results. Although the depth to bonded permafrost is seen to be approximately 120 m at 10 km from shore the depths at a distance of 17 km is seen to be approximately 35 m. This general characteristic, shallow depths near shore and beyond Reindeer Island is supported by lines K-K', H-H', I-I', and J-J'. Presently no explanation exists for the relatively deep bonded permafrost shoreward of Reindeer Island and for the relatively shallow ice-bonded permafrost seaward of the island. Although there is an apparent sharp discontinuity in the upper boundary of the bonded materials approximately 15 km from shore in Figure 5 the data are supported by drilling information and are believed to be reliable. In addition, this abrupt change in the surface elevation is supported by other lines including lines F-F', H-H', and I-I' where refraction data indicate an abrupt edge of the shallow (20 - 30 m below sea level) permafrost.

One record from near the middle of line A-A' is shown in Figure 6. A reflection event is located on the record approximately 80 ms from the shot point (0 seconds) and corresponds to a reflector at a depth of approximately 80 meters. Several reflection points similar to this have been identified in Figure 2.

A series of time-distance plots are shown in Figures 7-a through 7-t. Each of these plots represents data scaled from refraction records taken along the first 10.3 km of line F-F' in Figure 4. The first 7 records (7-a through 7-g) do not indicate frozen material velocities. However records 7-h through 7-t do present high velocities characteristic of frozen materials. The depth of the frozen materials ranges from about 20 m to 30m below the ocean surface and is noted on each figure where high velocities were observed. The depth information from Figure 7-a through 7-t have been plotted on a vertical section in Figure 8 which indicates the depth to the high velocity

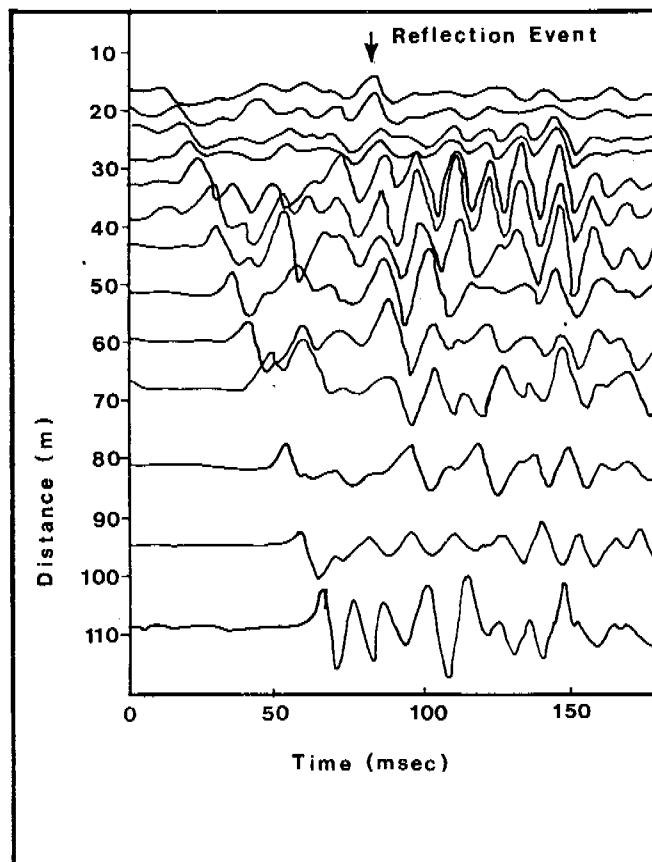
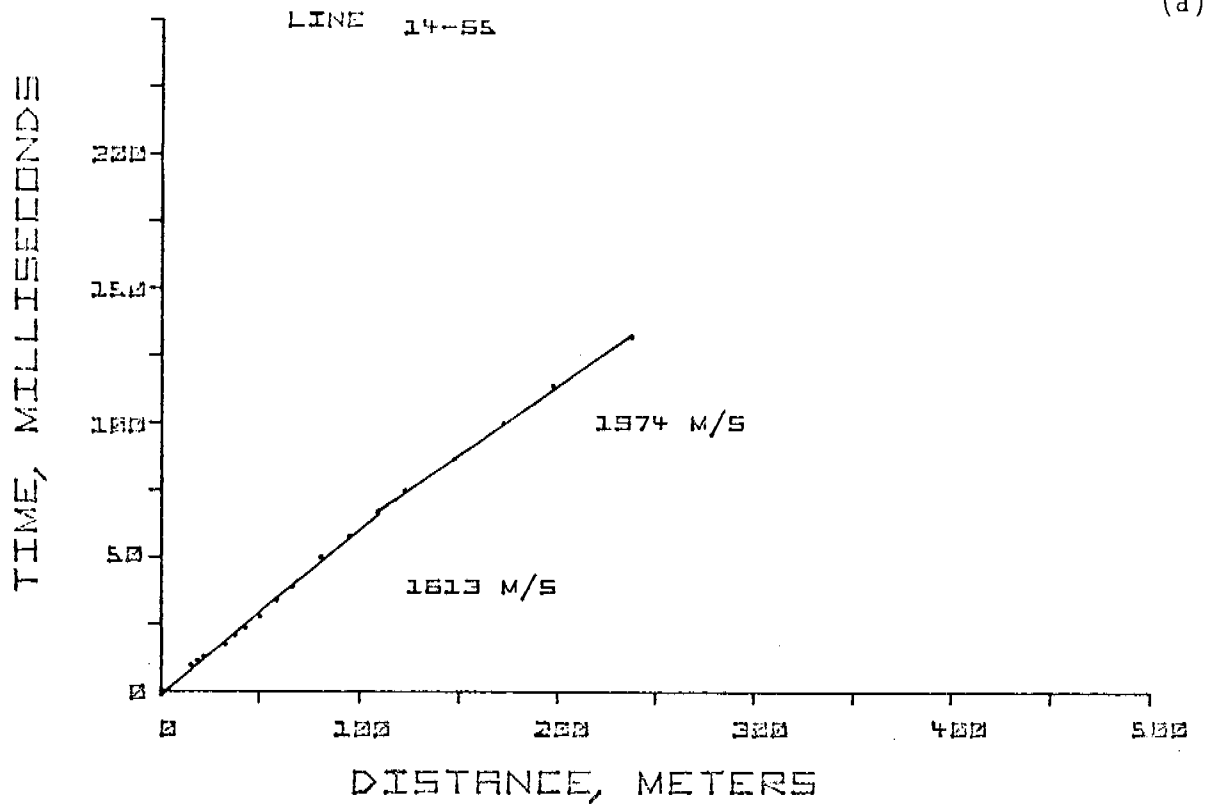
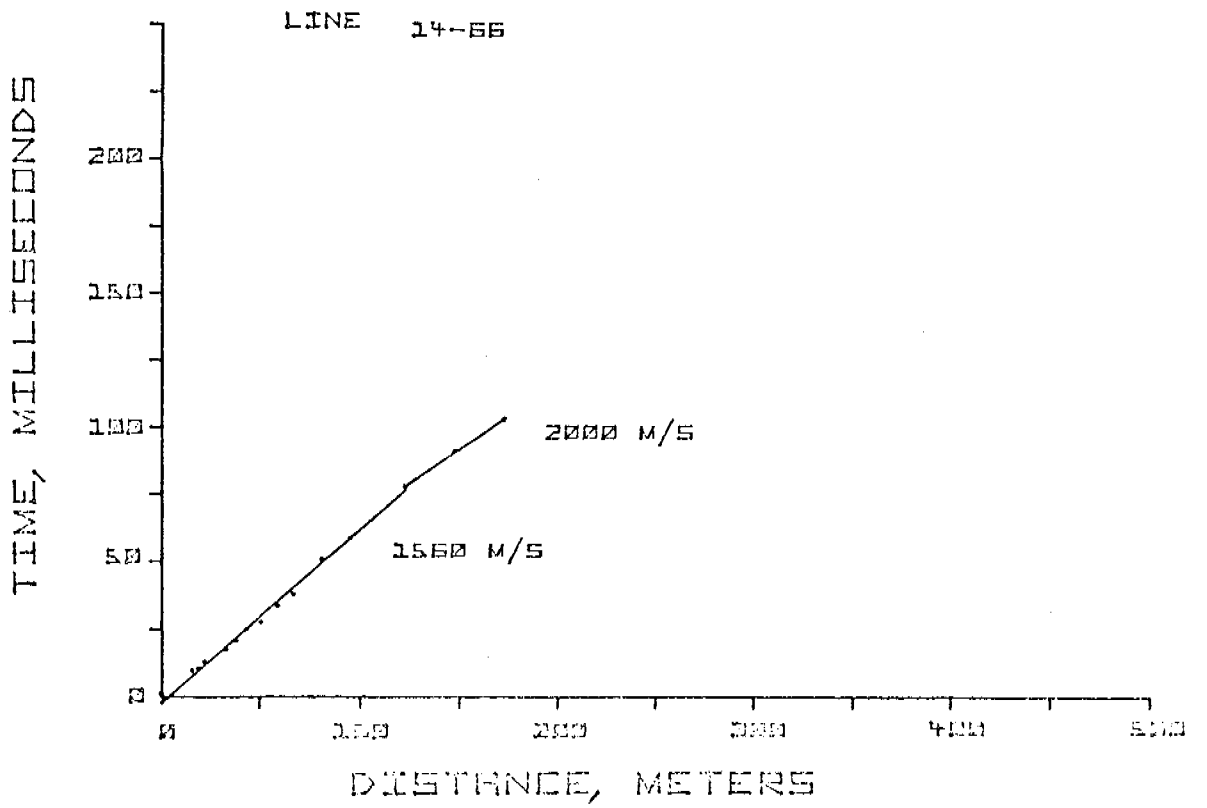


Figure 6 - Marine seismic data taken along line A-A' showing a reflection event. The first arrivals seen in the refraction record give a velocity of 2000 m sec^{-1} in the bottom sediments. A reflection event is seen in the first 10 channels of the record approximately 80 milliseconds after the shot time. Events such as this are plotted as triangles on Figure 5. The reflection data depths have been plotted using an average velocity for the non-frozen material of 2000 m sec^{-1} . As it is not possible to know exactly where the reflection takes place, all reflections are plotted assuming the reflectors were directly beneath the boat. Consequently, points may be plotted too deep. It is not likely that they are plotted too shallow, a feature that would result from using too low a velocity in the non-frozen materials.

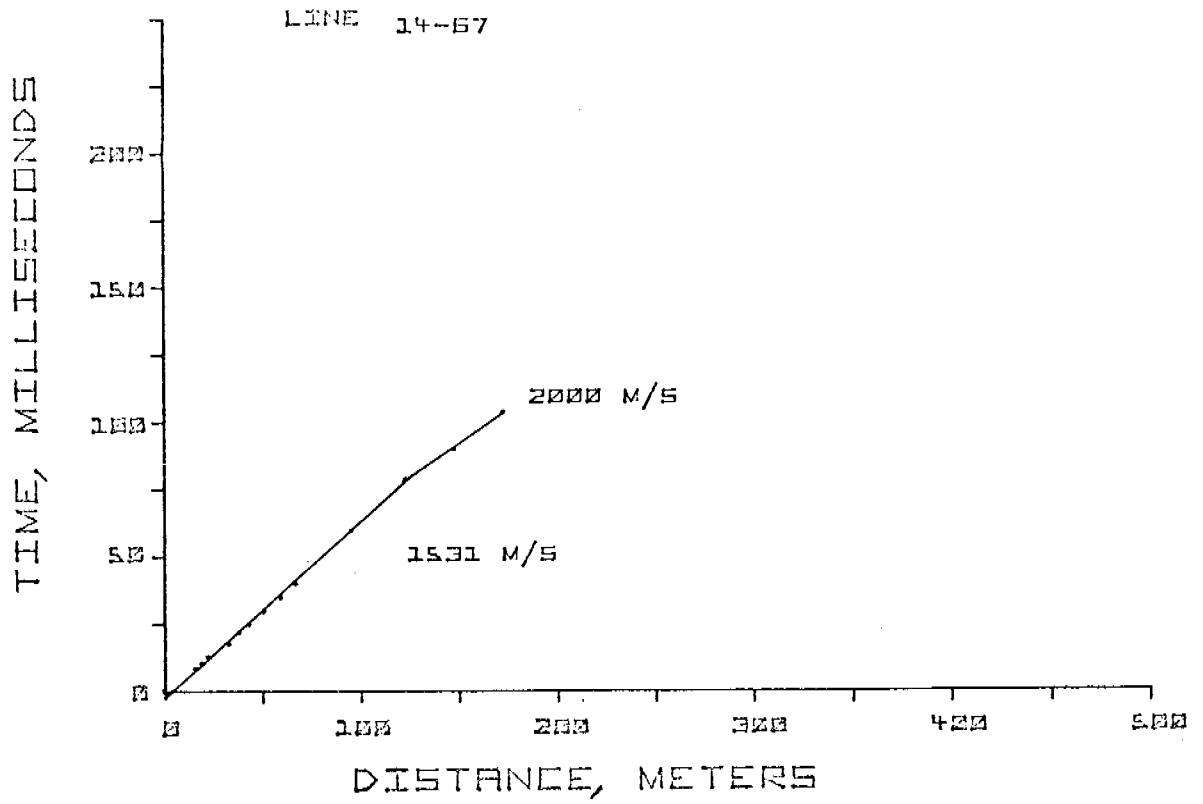
(a)



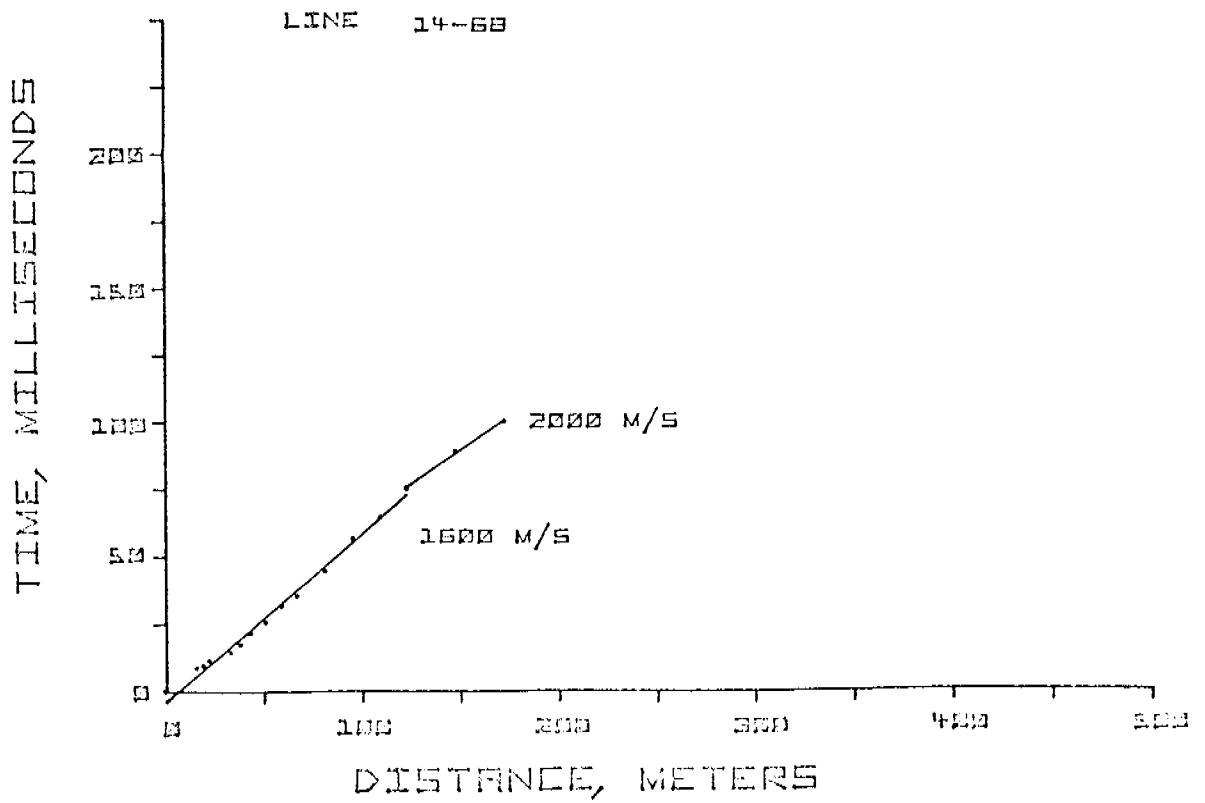
(b)



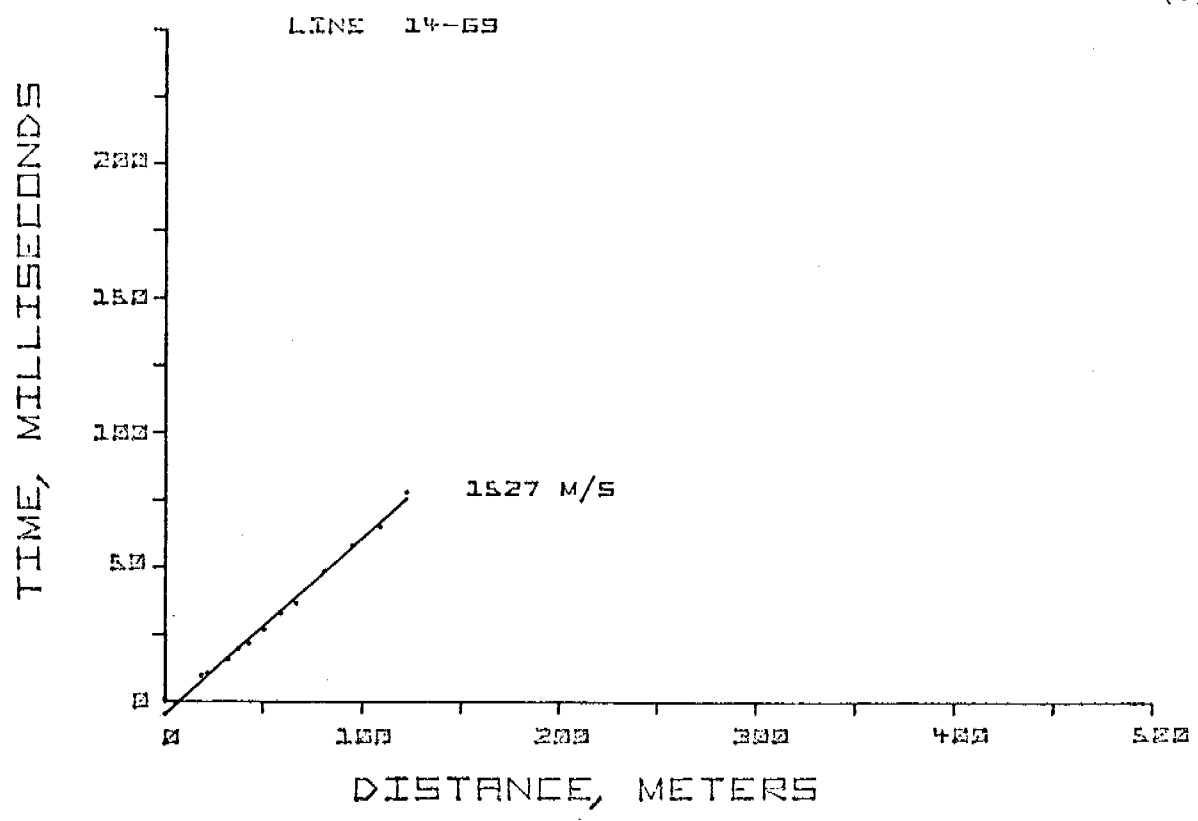
(c)



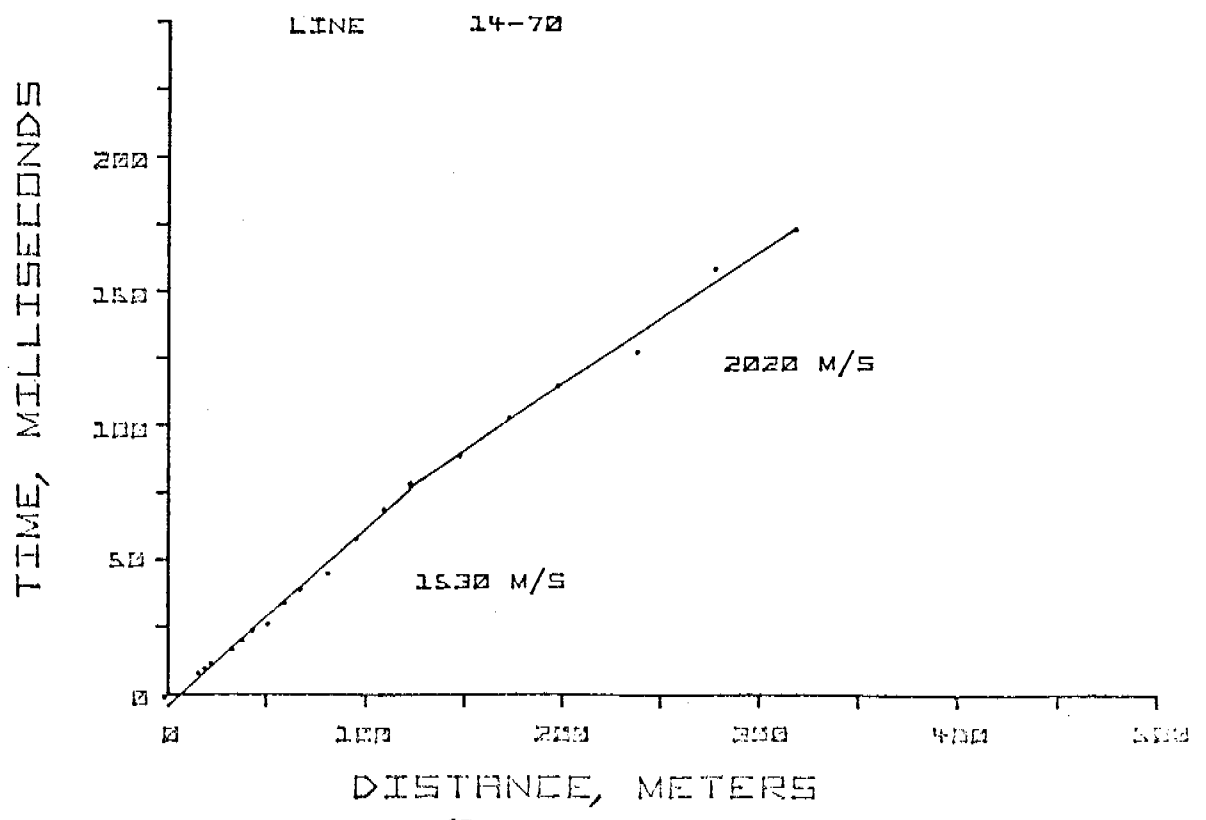
(d)



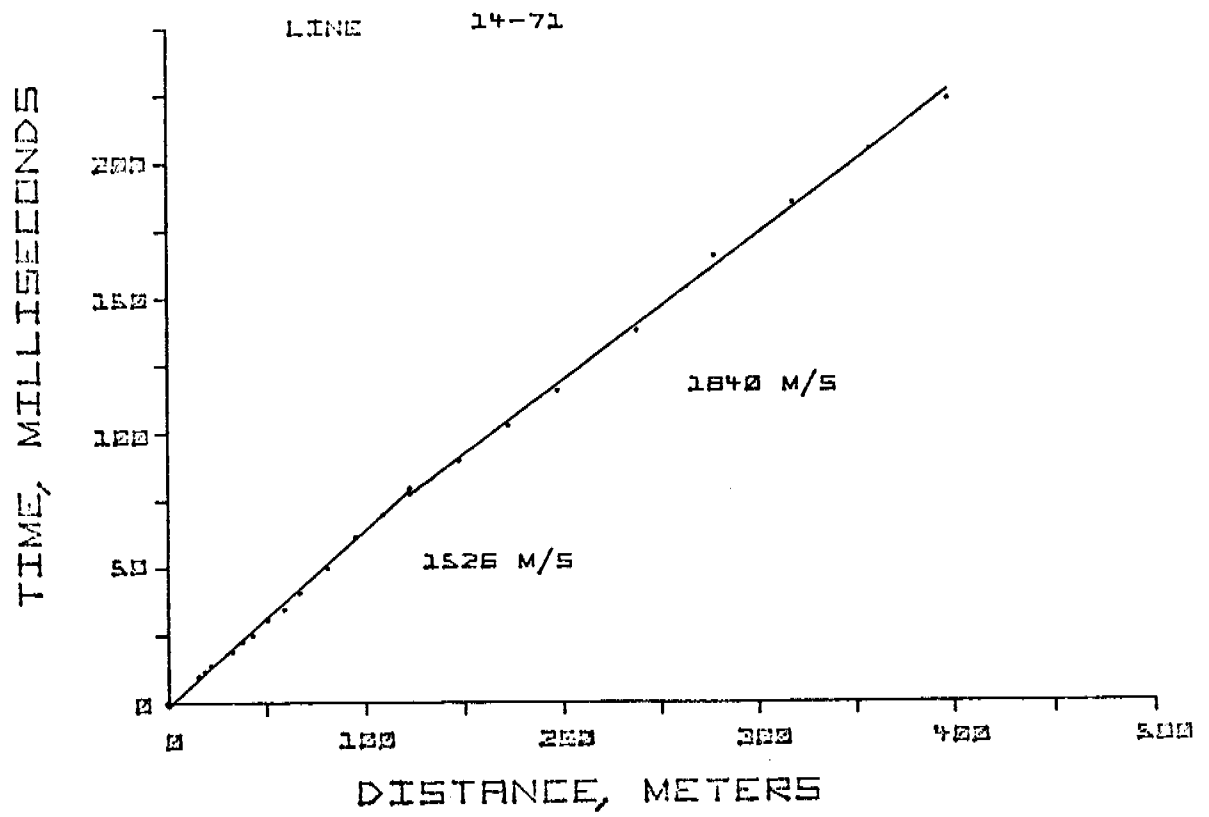
(e)



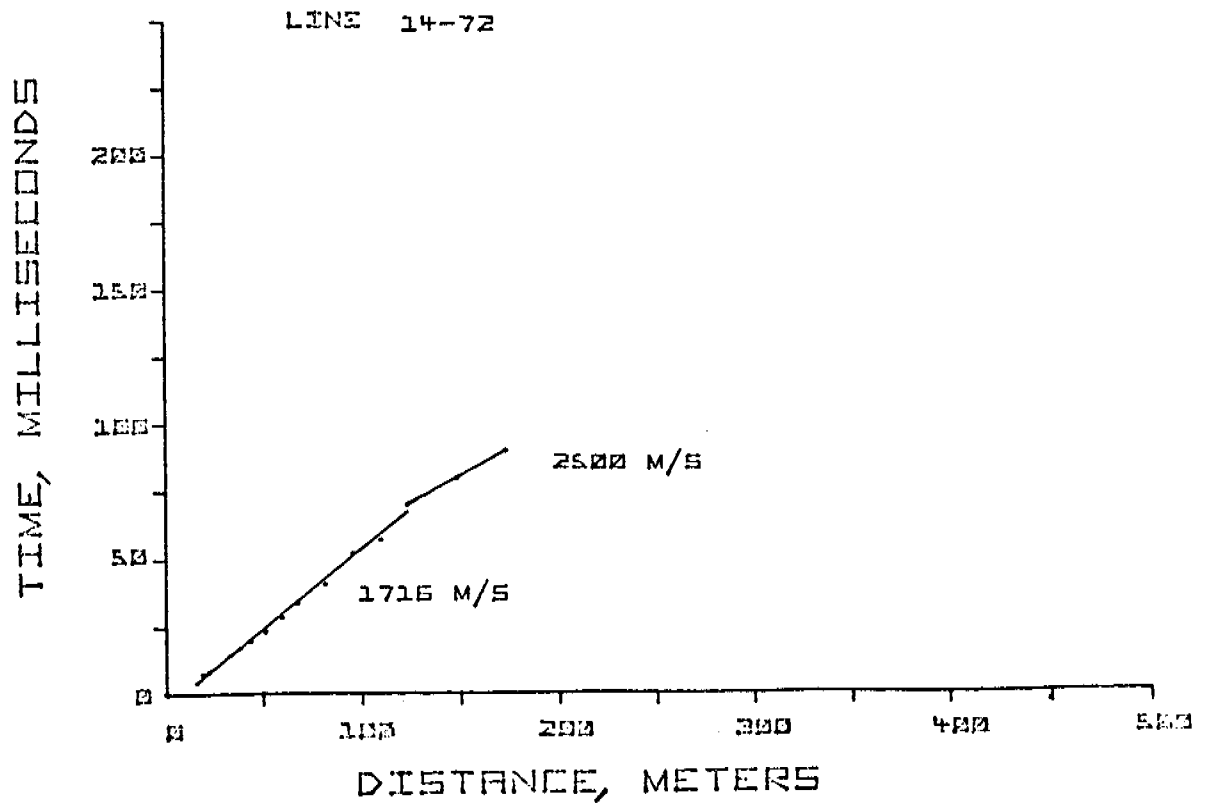
(f)



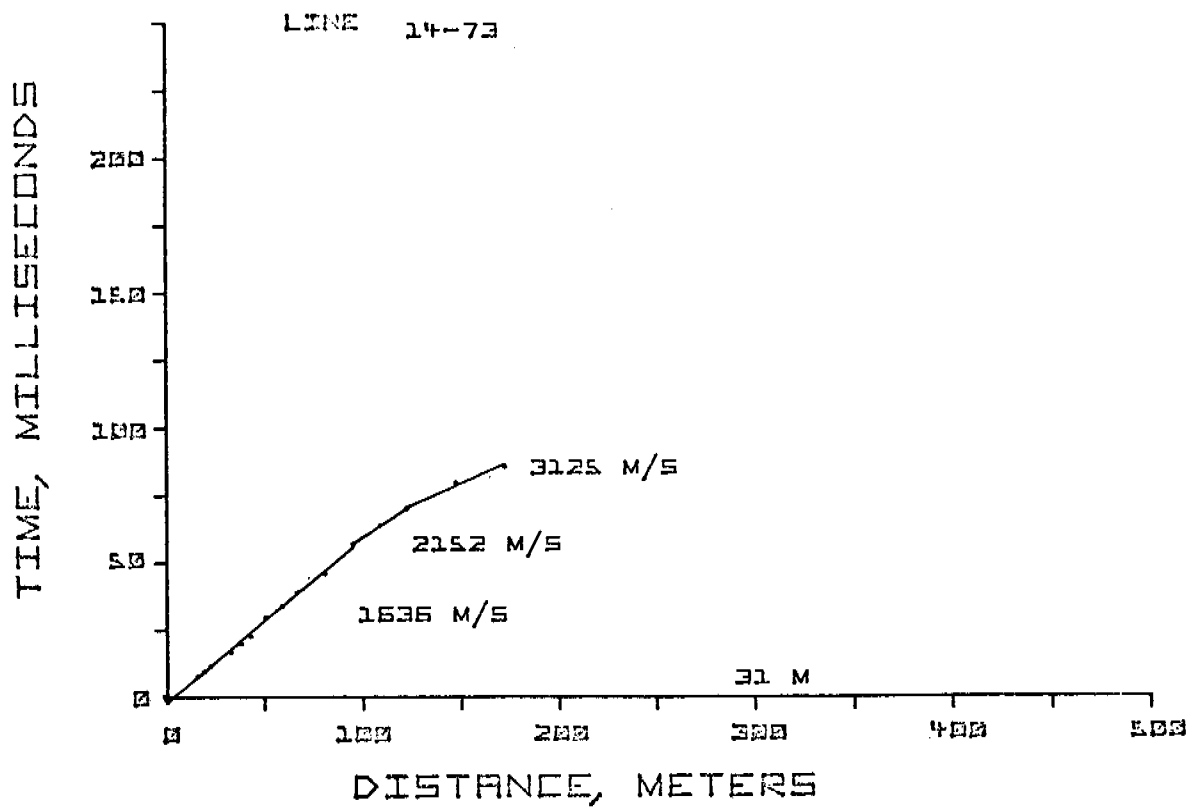
(g)



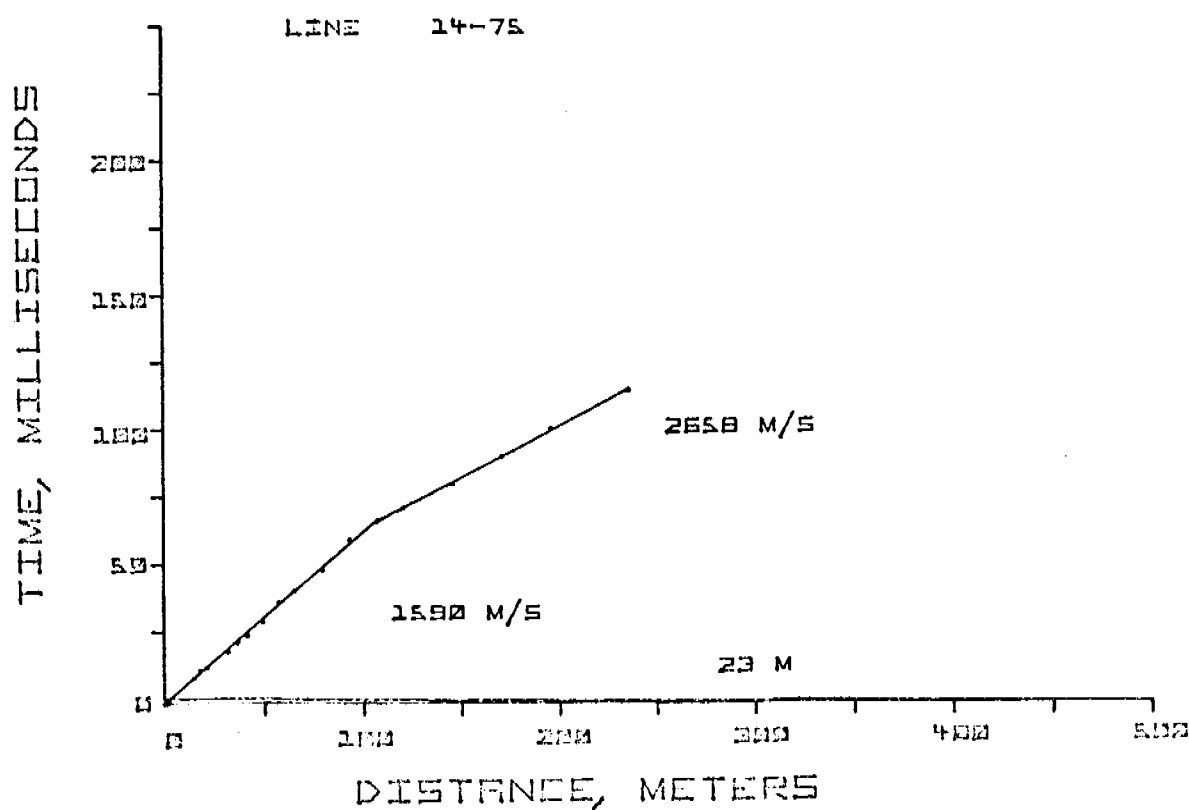
(h)



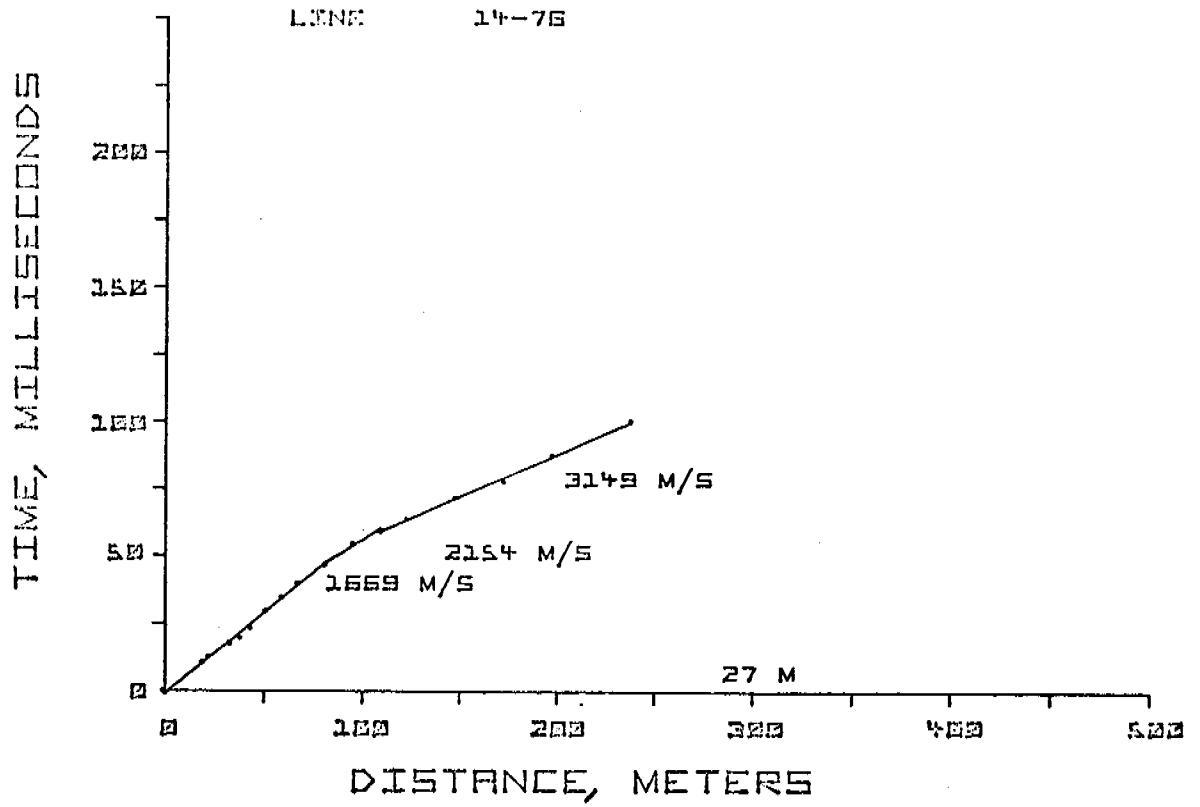
(i)



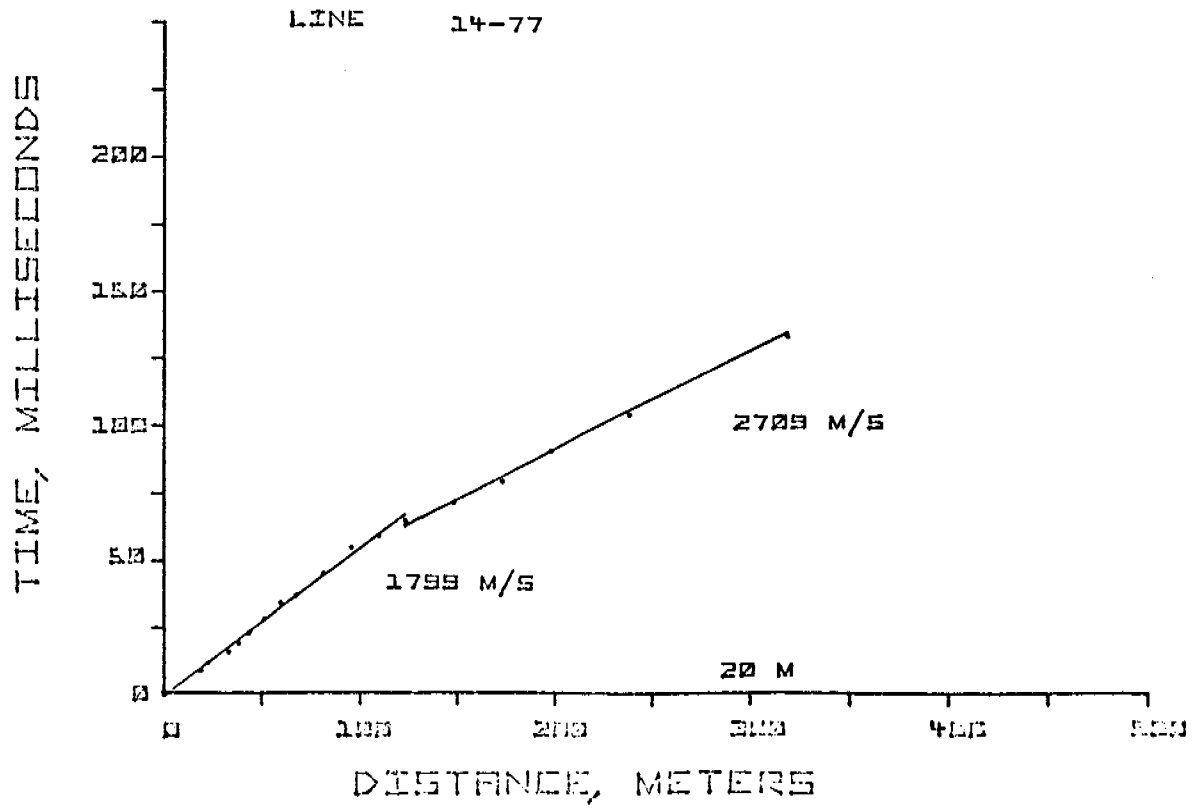
(j)



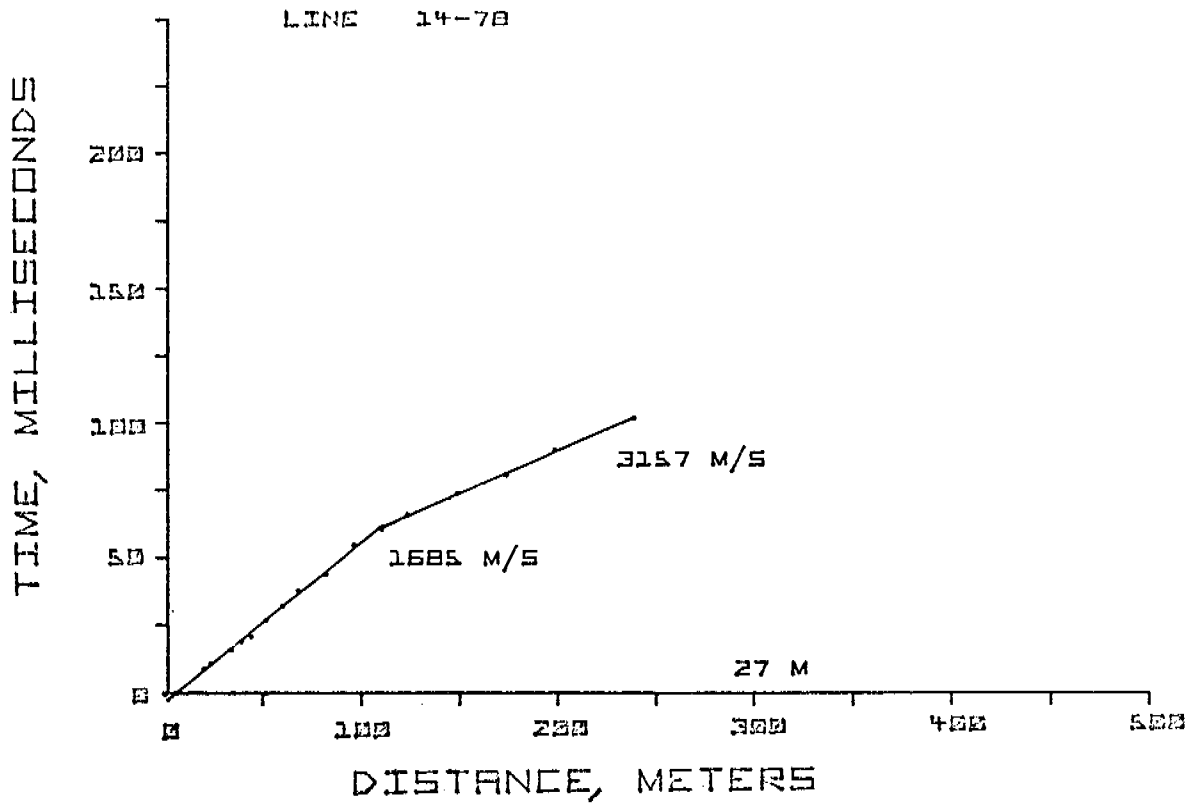
(k)



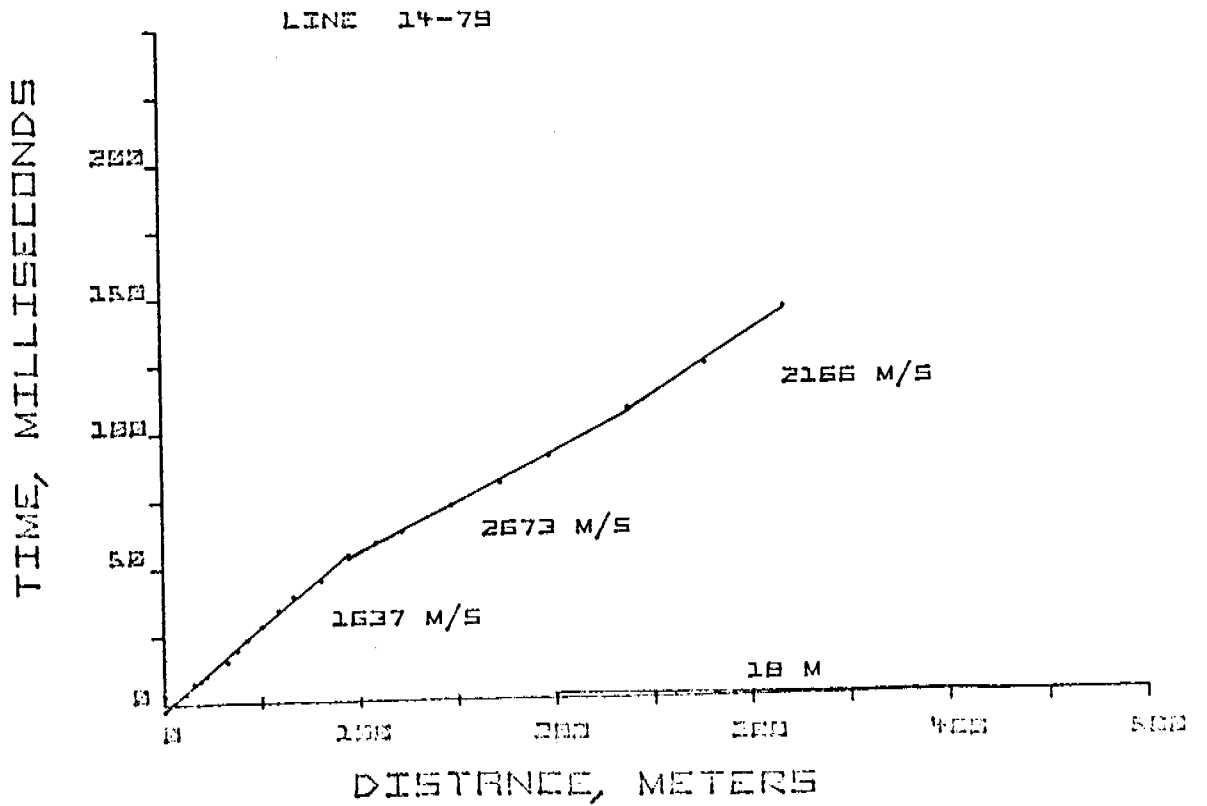
(l)



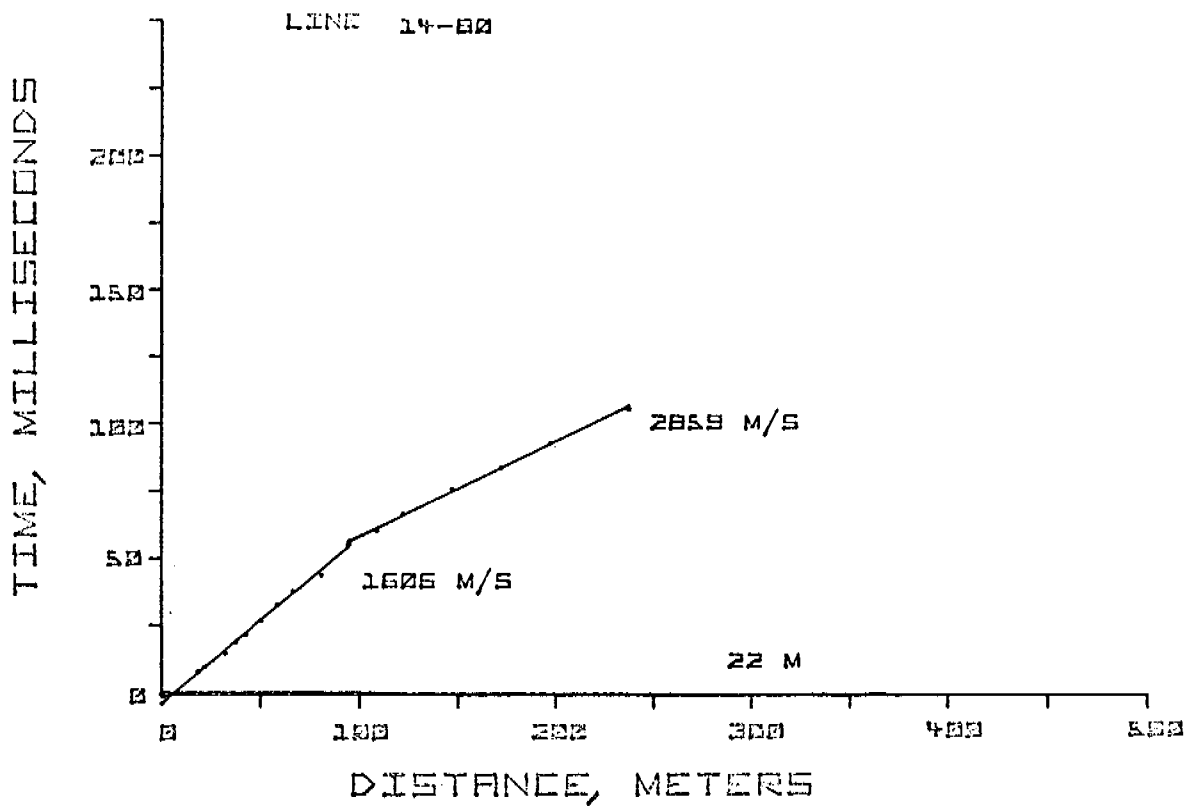
(m)



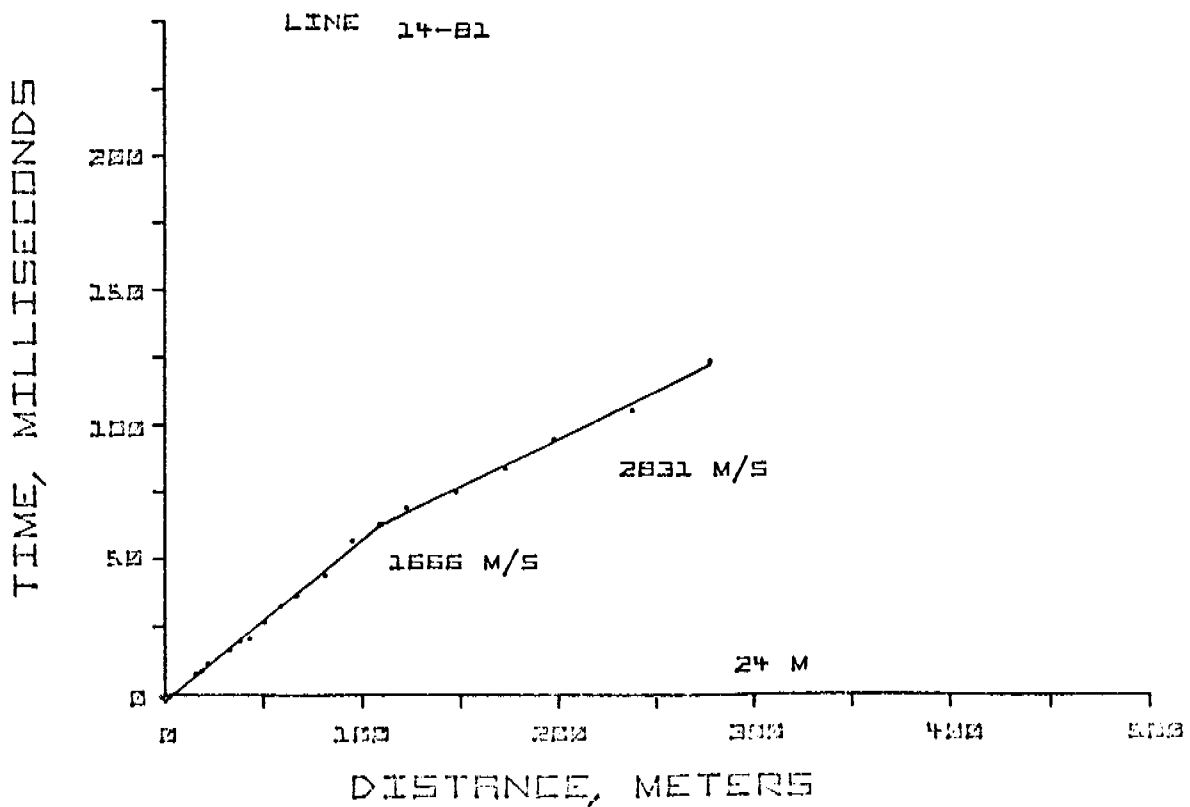
(n)



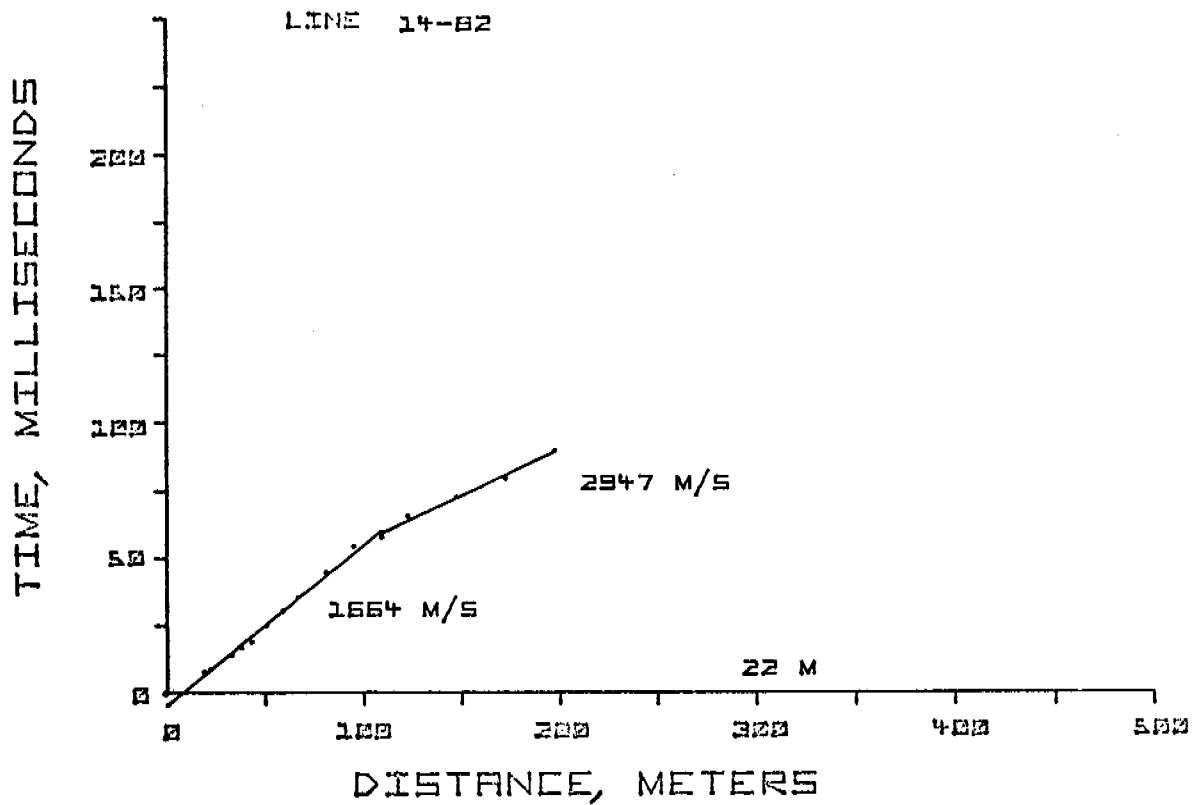
(o)



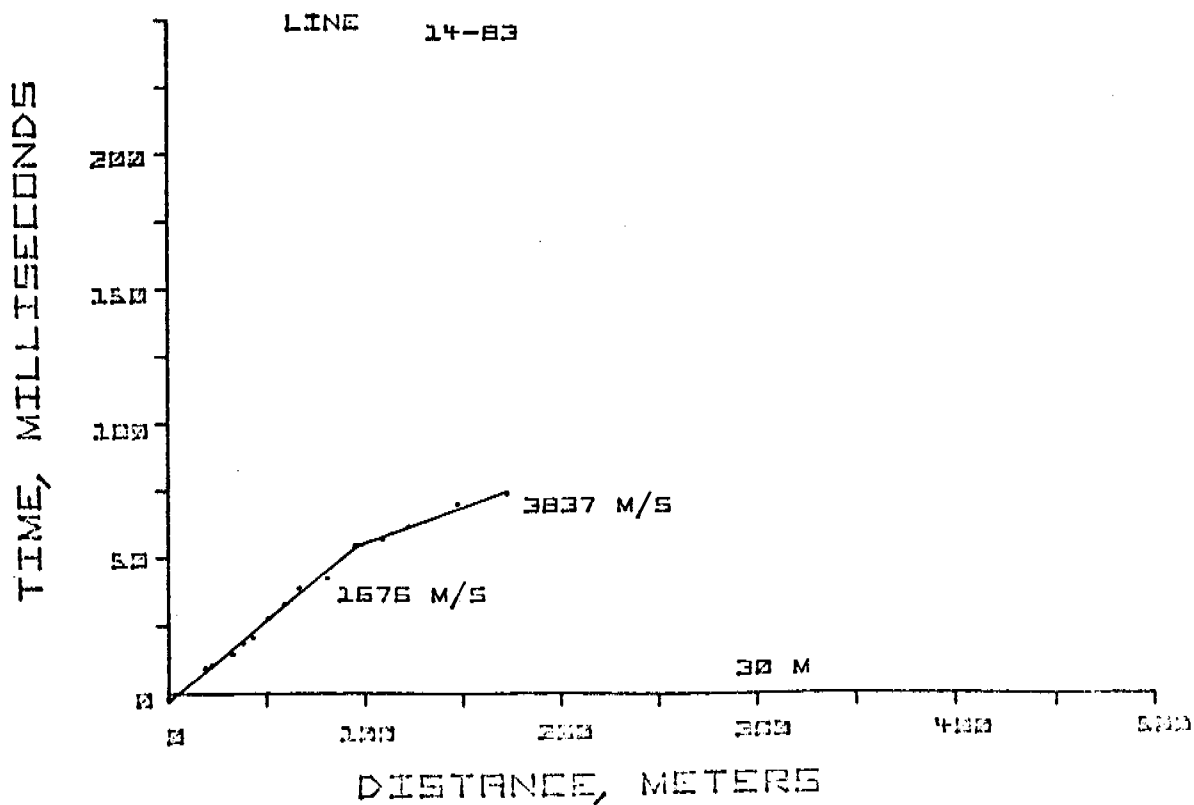
(p)



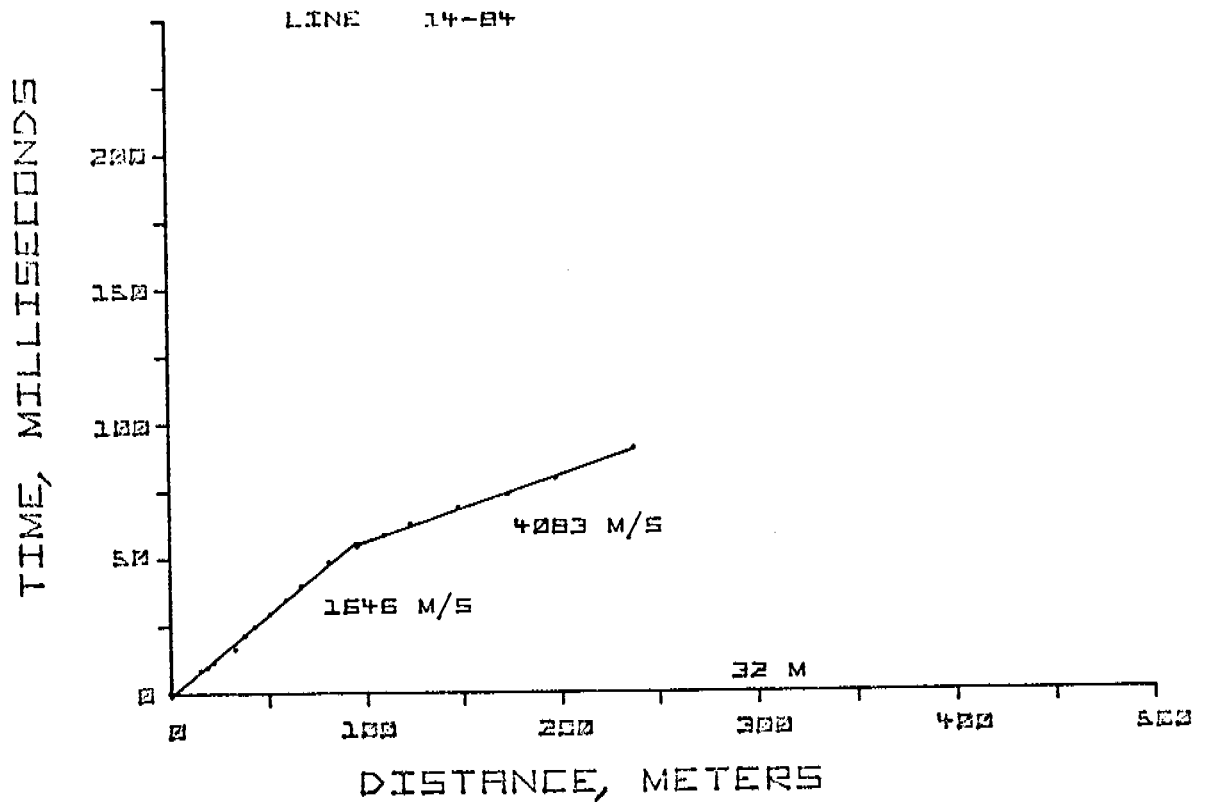
(q)



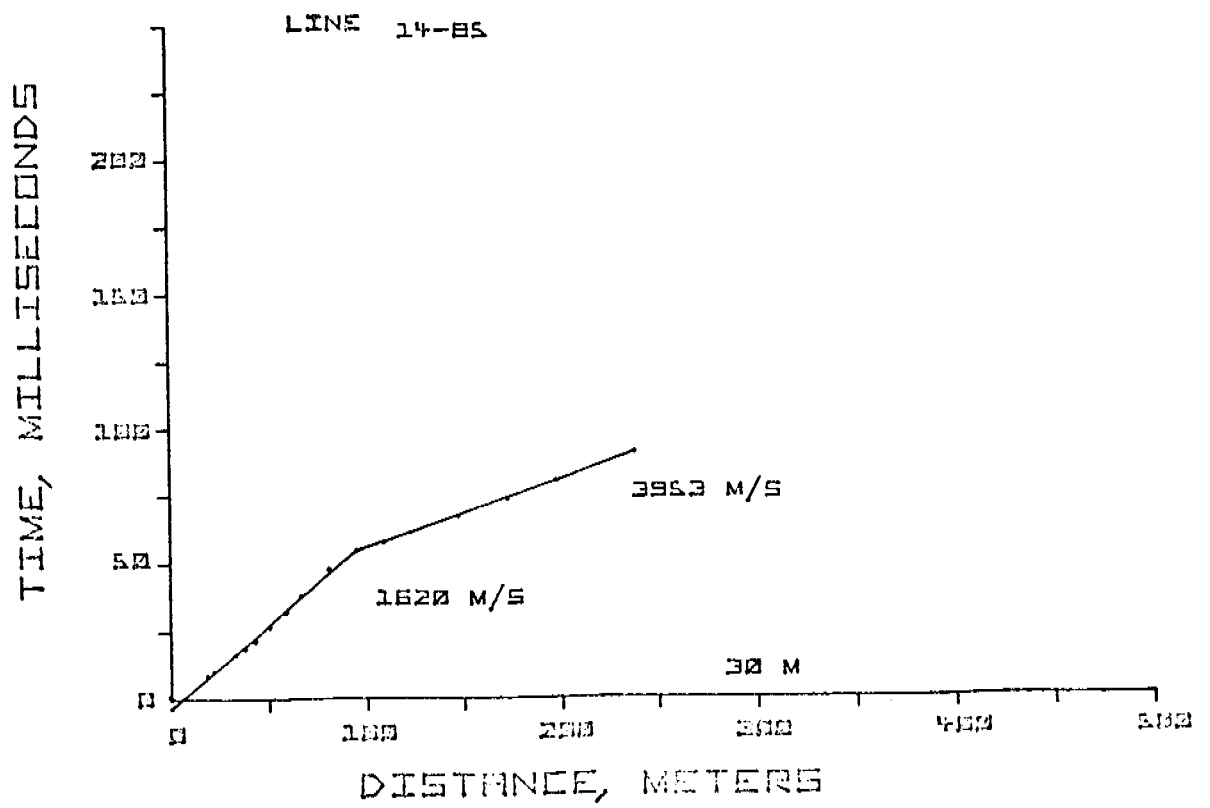
(r)



(s)



(t)



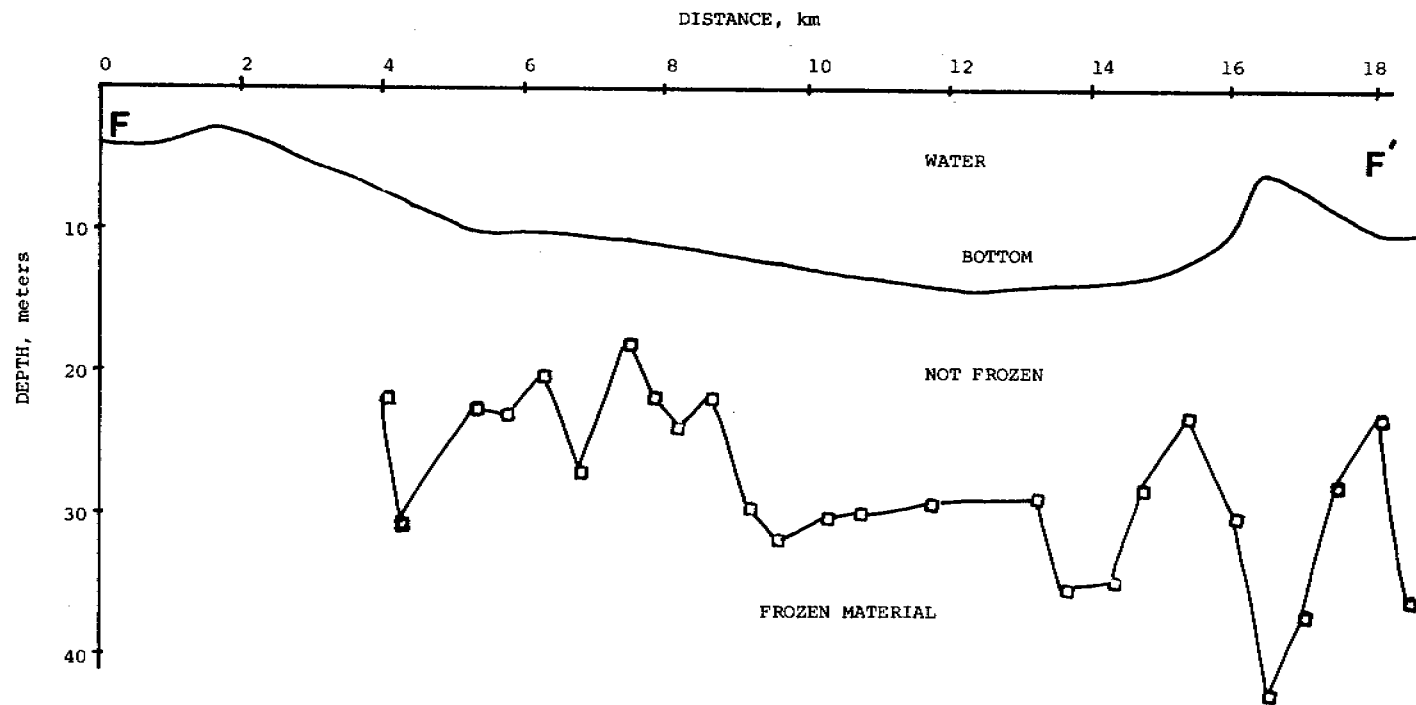


Figure 8 - Vertical section along line F-F'

refractor and the water depth along 10.3 km of line F-F'. Distance is measured from F. The abrupt boundary of shallow permafrost is clear in the figure and corresponds to the start of the cross hatching along line F-F' of Figure 4.

Approximately 7.5 km along the line the ice-bonded materials were observed at a depth of 7 m below the ocean bottom. This is significant in that a buried hot oil pipeline at this location could possibly melt this shallow permafrost and thaw subsidence could occur.

Figure 9 is a vertical section through line M-M' which is east of Cross Island. The upper surface of the high velocity refractors is irregular and varies in depth from 15 to 35m. Near shore the refractor becomes less regular and occurs only sporadically. One major difference between this line and line A-A' of Figure 5 is the relatively shallow depth of the ice-bonded materials over the entire line. The lines are otherwise similar in their length and orientation. At the present time no explanation for the differences between these lines is known.

VIII. CONCLUSIONS

At this time in the project, it is possible to test several conclusions about offshore permafrost. Some of the conclusions are site specific, while others have more general implications. The nature and implications of the conclusions are discussed below.

A. In past reports (last years annual report) we suggested that one possible way to deal with shallow permafrost near shore is to extend a causeway from shore to regions offshore where the ice-bonded permafrost is sufficiently deep so that any thaw bulb from a hot oil pipeline would not

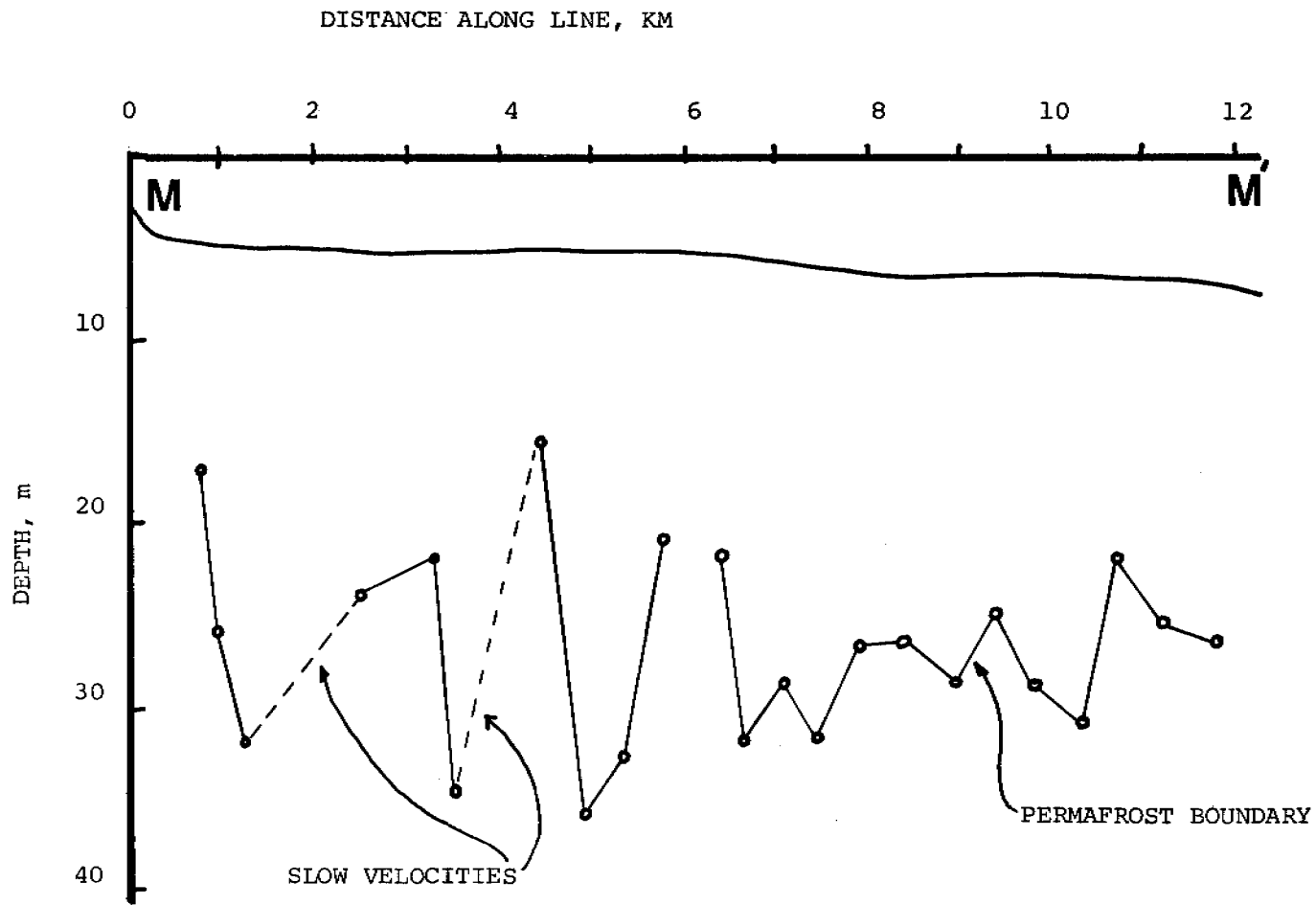


Figure 9 - Plot of approximate depths to the fast refractors versus the distance along line M-M'.

affect the permafrost. Figure 5 is a good example of a case where such a plan might be used. A 2 km long causeway extending from the shore would enable regions with shallow permafrost (less than 30 m below the ocean bottom) to be avoided. However, with more recent data as presented at the extreme right of Figure 5, shallow ice-bonded materials could again present a design problem at distances of 15 km or so from shore. Figure 8 indicates the shallowest offshore ice-bonded permafrost (7m below the ocean bottom) that we have observed in our rather limited reconnaissance program. This observation which is at a distance of approximately 18 km from shore clearly calls for careful consideration of possible effects from subsea permafrost on offshore structures. Based upon our data gathered to date we conclude that the surface of ice-bonded permafrost may often dip downward offshore, this is not always the case and in some cases (line M-M') no dip is apparent.

B. Seismic reconnaissance on three barrier islands indicates that they are not completely underlain by bonded permafrost, but that some may be completely free of ice-bonded permafrost. Certainly this conclusion is dependent upon the history of the island; whether it is a fragment of a former shoreline or whether it is a constructional feature. Also, the width of an island, its migration rate and soil types are important.

From the standpoint of offshore petroleum development, the islands may be useful platforms for drilling purposes. Therefore the condition of the permafrost beneath them is important. Also, oil produced seaward of the islands will probably be brought to shore by buried pipelines which will perhaps cross under the islands. Again, whether or not the islands contain bonded permafrost will be an important consideration.

The fact that all offshore islands are not underlain by near surface bonded permafrost provides an important distinction from the standpoint of their history and formation. A complete understanding of island growth and movement must include an understanding of their different permafrost characteristics.

C. Prudhoe Bay appears to be an old thaw lake (see the 1977 annual report) and therefore presents a large dip or possibly a window in the surrounding bonded permafrost surface. This is site specific information, but it seems unlikely that there are not other old thaw lakes offshore along the Beaufort Sea coast. Knowledge of such sites could provide permafrost free locations for bottom founded structures or, if such locations are not desirable for a particular application, old thaw lakes could be avoided. Whatever their use, knowledge of their existence can be expected to affect offshore construction activities.

D. Several island sites have been studied where seismic velocity data and drilling data seemed not to agree (Tapkaluk Island and Reindeer Island-- see the 1977 annual report). That is, drilling evidence indicated frozen material, but refraction velocities were not high. Our conclusion is that ice-bearing materials should be distinguished from ice-bonded materials. Brine inclusions depress the freezing point of a material and tend to spread the freezing point from a discrete temperature to a range of temperatures corresponding to various stages of freezing. Thus a material may have ice inclusions but may not be ice-bonded and hence present a relatively low velocity compared to the totally bonded material. The distinctions between ice bearing and ice-bonded is important from the standpoint of material properties. For example, an ice-bonded material may have a high resistance to

shear stress, but the same material when not ice bonded may have little shear resistance.

IX. NEEDS FOR FURTHER STUDY

In order to fully understand offshore permafrost characteristics and their importance to offshore oil and gas development, additional work is required in several areas.

As continued efforts are expended on the drill line from the new ARCO dock to and beyond Reindeer Island, it is desirable to continue seismic investigations in close support of that effort. Of particular interest is the relatively shallow ice-bonded permafrost offshore of Reindeer Island. Thus additional lines parallel to the existing seismic lines to Reindeer Island and at right angles are needed. Also, the shape of the upper permafrost surface surrounding Cross Island and Stump Island will aid in determining the feasibility of utilizing such features in offshore development. In addition to this close support work, wide area coverage should be obtained. The most likely technique is probably the use of commercial geophysical data in a manner similar to Hunter (1976).

X. SUMMARY OF 4TH QUARTER ACTIVITIES

A. Laboratory Activities

1. Field work: None conducted
2. Scientific party: John L. Morack and James C Rogers participated in laboratory analyses and report writing.

3. Methods: Seismic reflection and refraction data were scaled and analyzed.
4. Sample localities: Figure 4 of the April, 1978, annual report indicates the location of the lines analyzed.
5. Data analyzed: Approximately 150 total kilometers of seismic data have been scaled and analyzed.

B. Problems Encountered

Limited boat time was available and difficulty was encountered with ice beyond the barrier islands during field work in the third week in July. In order to overcome this difficulty, a boat dedicated to the project for approximately three weeks is being obtained.

REFERENCES FOR ANNUAL REPORT

- Barnes, P. W., Reimnitz E., Gustafson, W., Larsen, B. R. USGS Marine Geologic studies in the Beaufort Sea off Northern Alaska, 1970 through 1972; Data, Type and Location.
- Dobrin, M. B., 1975. Introduction to Geophysical Prospecting, 2nd edition, McGraw Hill.
- Harrison, W. D., Osterkamp, T. E. "Coupled heat and salt transport model for subsea permafrost, University of Alaska, Geophysical Report UAG 247, U of A Seagrant report 76-15.
- Hunter, J. A. M., Judge, A. S., Macaulay, H. A., Good, R. L., Gagne, R. M., Burns, R. A., 1976. Permafrost and Frozen Sub-seabottom Materials in the Southern Beaufort Sea. Beaufort Sea Technical Report #22, Department of Environment, Victoria, B. C.
- Hunter, J. A. M., Hobson, G. D., "A Seismic Refraction Method to Detect Sub-sea Bottom Permafrost", Beaufort Sea Symposium Proceedings, Arctic Institute of North America, San Francisco, J. C. Reed, J. E. Sater, Eds., 1974.
- Hunter, J. A. M., The Application of Shallow Seismic Methods to Mapping of Frozen Surficial Materials, Permafrost, Second International Conference, 1974.
- Lachenbruch, A. H., "Permafrost" In Encyclopedia of Geomorphology, R. W. Fairbridge (ed.), Vol. 3, pp. 833-839, 1968.
- Lachenbruch, A. H., "Thermal Effects of the Ocean on Permafrost", Geological Society of America, Bulletin 68: 1515-29, 1957.
- Lewellen, R. I., Offshore Permafrost of Beaufort Sea, Alaska. The Coast and Shelf of the Beaufort Sea, Arctic Institute of North America, J. C. Reed and J. E. Sater, Eds., 1974.
- Osterkamp, T. E., Harrison, W. D., 1976. Subsea Permafrost at Prudhoe Bay, Alaska: Drilling Report, University of Alaska, Geophysical Institute, Scientific Report, UAGR 245.
- Priorities for Basic Research on Permafrost, National Academy of Science, Committee on Polar Research, Washington, D. C., 1974.
- "Problems and Priorities in Offshore Permafrost Research," A position paper developed by the working group on offshore permafrost, Committee on Permafrost, Board on Polar Research, National Academy of Science, 1975.
- Reimnitz, E. and Barnes, P. W., 1974. Sea Ice as a Geologic Agent on the Beaufort Sea Shelf of Alaska, The Coast and Shelf of the Beaufort Sea. Reed, J. C. and Sater, J. E., editors, Arctic Institute of North America.

Reimnitz, E., Wolf, S. C., Rodeick, C. A., 1972. "Preliminary Interpretation of Seismic Profiles in the Prudhoe Bay Area, Beaufort Sea, Alaska." U.S. Department of Interior Geological Survey, open file report no. 548.

Rogers, J. C., Harrison, W. D., Shapiro, L. H., Osterkamp, T.E., Gedney, L. D., Van Wormer, J. D., 1975. "Near Shore Permafrost Studies in the Vicinity of Point Barrow, Alaska." University of Alaska, Geophysical Institute Scientific Report, UAGR 237.

Rogers, J.C., Morack, J. L., 1977. "Beaufort Sea Coast Permafrost Studies." Environmental Assessment of the Alaskan Continental Shelf, Vol. XVII, pp. 467-510, 1977.

Rogers, J. C., Morack, J. L., 1978. "Geophysical Investigation of Offshore Permafrost, Prudhoe Bay, Alaska." Permafrost Third International Conference, 1978.

Sellmann, P. V., Lewellen, R.I., Ueda, H. T., Chamberlain, E., Blouin, S.E., 1976. "Operational Report 1976 USACRREL-USGS Subsea Permafrost Program Beaufort Sea, Alaska." U. S. Army Cold Regions Research and Engineering Laboratory, Hanover, New Hampshire, SR 76-12.

U. S. Department of Commerce, 1977. Environmental Assessment of the Alaskan Continental Shelf, Executive Summary, 1977.

ADF&G HABITAT LIBRARY



3234500066234